



Parma 16-19 settembre 2019

ABSTRACT BOOK

a cura della Società Geologica Italiana



Congresso
SIMP-SGI-SOGEI 2019

Il tempo del pianeta Terra
e il tempo dell'uomo:
Le geoscienze fra passato e futuro



PRESIDENTI DEL CONGRESSO

Mario Tribaudino (SIMP), Fabrizio Storti (SGI)

COMITATO SCIENTIFICO

Luca Bindi, Angelo Camerlenghi, Piergiulio Cappelletti, Fulvio Celico, Carlo Doglioni, Elisabetta Erba, Francesco Frondini, Guido Giordano, Massimo Mattei, Alessandro Pavese, Stefano Poli, Antonello Provenzale, Elisabetta Rampone, Mauro Soldati, Andrea Zanchi

COMITATO ORGANIZZATORE

Alessandra Montanini (coordinatore)
Domenico Calcaterra, Bernardo Carmina, Lorenza Fascio, Nadia Malaspina, Fabio Massimo Petti, Alessandro Zuccari

COMITATO ORGANIZZATORE LOCALE

Andrea Artoni, Fabrizio Balsamo, Luca Barchi, Danilo Bersani, Cristian Cavozi, Alessandro Chelli, Andrea Comelli, Daniela D'Alessio, Antonietta Di Matteo, Giovanna Gianelli, Paola Iacumin, Giovanni Leonelli, Alessio Lucca, Luciana Mantovani, Paola Monegatti, Davide Peis, Emma Petrella, Davide Persico, Mattia Pizzati, Emma Salvioli Mariani, Arianna Secchiari, Enrico Selmo, Elena Turco, Roberto Valentino, Giuliana Villa

ABSTRACT BOOK EDITORS

Bernardo Carmina, Fabio Massimo Petti, Giulia Innamorati, Lorenza Fascio

*Papers, data, figures, maps and any other material published are covered by the copyright own by the **Società Geologica Italiana**.*

DISCLAIMER: The Società Geologica Italiana, the Editors are not responsible for the ideas, opinions, and contents of the papers published; the authors of each paper are responsible for the ideas opinions and contents published.

La Società Geologica Italiana, i curatori scientifici non sono responsabili delle opinioni espresse e delle affermazioni pubblicate negli articoli: l'autore/i è/sono il/i sol/i responsabile/i.

ABSTRACT INDEX

Sessioni Plenarie	35
Cordier P. - Creeping minerals: new insights from numerical modelling and transmission electron microscopy.....	36
Fantoni R. - The Po Plain - Adriatic foreland from Mesozoic extension to Cenozoic compression.....	37
Iadanza A., Tribuzio R. & CNR Committee “ECORD-IODP and ICDP” - IODP-Italia and the Italian participation in ECORD-IODP and ICDP.....	38
Luguet A. - Mantle Geochronology: Insights from the Re-Os isotopic system.....	39
S1. Integrated mineralogy, petrology and computational modelling to decipher geochemical interactions and tectonic histories recorded by metamorphic rocks from the deep Earth	40
Agrosi G., Tempesta G., Mele D., Caggiani M.C., Mangone A., Della Ventura G.C., Cestelli-Guidi M., Allegretta I., Hutchison M.T., Nimis P. & Nestola F. - Multiphase inclusions associated with residual carbonate shed new light on the origin of super-deep diamonds from Juina (Brazil).....	41
Bonazzi M., Tumiati S., Thomas J., Angel R.J. & Alvaro M. - Elastic geobarometry for Quartz inclusions in garnet: comparison between hydrostatic and isotropic methods to evaluate the entrapment pressures..	42
Cámara F., Lotti P., Belmonte D., Pagliaro F., Merlini M. & Joseph B. - High pressure softening of grossite (CaAl ₄ O ₇).....	43
Campomenosi N., Scambelluri M., Angel R.J., Hermann J., Rubatto D., Mihailova B. & Alvaro M. - Applying Raman-elastic barometry to UHP metamorphic rocks: insights from the Dora Maira Massif (Western Alps).....	44
Capizzi L.S., Stagno V., Andreozzi G.B., Bosi F., Nazzari M. & Scarlato P. - Experimental investigation of the stability of iron-rich tourmaline as a function of pressure, temperature and oxygen fugacity with implications for the release of B-rich fluid during subduction.....	45
Ferrero S., Angel R.J., O’Brien P.J. & Wunder B. - Mineral growth and metastability phenomena in melt inclusions from metamorphic rocks	46
Geddo Z., Mazzucchelli M.L. & Alvaro M. - Combining micro-tomography and finite element analyses for elastic geobarometry on real geological samples	47
Jahn S. - First-principles molecular dynamics simulations of aqueous fluids at high temperatures and pressures	48
La Fortezza M., Campione M., Alvaro M., Scambelluri M. & Malaspina N. - Multiphase inclusions in harzburgites from the Bétic Cordillera (Cerro de Almirez, Spain): growth and orientation of magnetite in olivine	49
Locatelli M., Verlaquet A., Agard P., Pettke P. & Federico L. - Stepwise brittle deformation at 80 km-depth triggered by internal then external fluid circulation (Monviso eclogitic breccias, W. Alps).....	50
Lorenzon S., Nestola F., Thomassot E., Prosperi L., Lorenzetti A., Alvaro M., Salvadego F. & Nimis P. - Super-deep diamond from Central African Republic.....	51
Morana M., Murri M., Girani A., Angel R. J. & Alvaro M. - Characterizing deviatoric stress in mineral inclusions.....	52
Musiyachenko K., Murri M., Prencipe M. & Alvaro M. - Rutile in diamond: the role of elastic anisotropy	53
Nestola F., Zaffiro G., Mazzucchelli M.L., Nimis P., Andreozzi G.B., Periotto B., Princivale F., Lenaz D., Secco L., Pasqualetto L., Logvinova A.M., Sobolev N.V., Lorenzetti A. & Harris J.W. - Diamond-magnesiocromite host-inclusion system recording old deep lithosphere conditions at Udachnaya (Siberia).....	54
Pasqualetto L., Nestola F., Nimis P., Jacob D.E., Oliveira B., Perritt S., Chinn I., Milani S. & Harris J.W. - Crystallographic relationships between diamond and its clinopyroxene inclusions.....	55
Rebay G., Godard G. & Kiénast J.R. - Eclogite-facies coronitic metagabbro and metatroctolite from the Zermatt-Saas ophiolites, Valtournanche, Italy.....	56

Zhong X., Andersen N., Dabrowski M. & Jamtveit B. - Zircon and quartz inclusions in garnet used for complimentary Raman-thermobarometry: application to the Holsnøy eclogite, Bergen Arcs, Western Norway	57
S2. Mineralogical Crystallography and New Minerals	58
Agrosi G., Lacalamita M., Mesto E., Schingaro E. & Tempesta G. - New insights into the crystal chemistry of tourmaline from Busachi (central Sardinia), Italy.....	59
Bersani D., Fornasini L., Zanoni A., Andò S., Gentile P., Salvioli-Mariani E. & Lottici P.P. - Micro-Raman chemical characterization of amphiboles	60
Biagioni C., Bosi F., Cook N.J., George L.L., Makovicky E., Moëlo Y., Pasero M., Sejkora J., Stanley C.J. & Welch M.D. - New nomenclature and classification of tetrahedrite-group minerals	61
Biagioni C., Mauro D., Bindi L., Hålenius U. & Pasero M. - Giacovazzoite and scordariite, two new minerals related to metavoltine.....	62
Bindi L. - Collisions in outer space produced a vacancy-rich, partially inverted tetragonal ringwoodite in several shocked meteorites	63
Bonaccorsi E., Merlino S. & Pasero M. - Superstructure of moraesite: a synchrotron study	64
Bonazzi P. & Bindi L. - Dienerite, Ni ₃ As: a mineralogical species to revalidate	65
Bussolesi M., Zaccarini F., Grieco G. & Tzamos E. - Rare and new mineralogical phases in the Ni-Cu-Sb-As system from the Gomati ophiolite, Northern Greece	66
Carbone C., Audra P., De Waele J., Bentaleb I., Chro?áková A., Krišt?fek V., D'Angeli I.M., Madonia G., Vattano M., Scopelliti G., Cailhol D., Vanara N., Temovski M., Bigot J.-Y., Nobécourt J.-C., Galli E., Rull F. & Sanz-Arranz A. - Phosphate minerals forming in karst environment: a state of art	67
Consani S., Giuli G., Martinelli A., Cardinale A.M., Trapananti A. & Carbone C. - Possible Rare Earth Element-induced structural modification in Layer Double Hydroxides: the case of synthetic woodwardite [Cu _{1-x} Al _x (SO ₄) _{x/2} (OH) ₂ ?nH ₂ O]	68
Della Ventura G., El Moutouakkil N., Boukili B., Lucci F., Conte A. & Talavera C. - Tracking the Ti substitution in biotite by FTIR imaging	69
Della Ventura G., Hawthorne F.C., Waesermann N. & Mihailova B. - The quantitative analysis of the octahedral composition of amphiboles by Raman spectroscopy.....	70
Fantini R., Quartieri S., Arletti R., di Renzo F., Fabbiani M., Morandi S., Martra G. & Vezzalini G. - Dehydration and Thermal stability of High-Silica Mordenite: <i>In-Situ</i> Synchrotron X-Ray Powder Diffraction Study	71
Griffin W.L., Gain S.E.M., Camara F., Bindi L., Toledo V. & O'Reilly S.Y. - Exotic mineralogy in an ultra-reduced magmatic system beneath Mt Carmel, Israel.....	72
Lotti P., Comboni D. & Gatta G.D. - Unusual symmetry of an intermediate scapolite.....	73
Mauro D., Biagioni C., Pasero M. & Zaccarini F. - Coquimbite: a mineral to be redefined?	74
Mesto E., Laurita S., Lacalamita M., Schingaro E., Rizzo G., Sinisi R. & Mongelli G. - Crystal-chemistry and thermal behavior of Fe-carpholite: a case of study from the Pollino Massif (southern Italy).....	75
Mugnaioli E., Gemmi M. & Németh P. - Disorder and modulation in first aragonite precipitates from Obstanser Eishöhle (Austria).....	76
Nazzareni S., Nestola F., Bindi L., Scricciolo E., Pacheco J., Zanon V., Zanatta M. & Giuli G. - Peculiar mineralogy of the Água de Pau syenites (São Miguel, Azores islands, Portugal)	77
Precisvalle N., Martucci A., Ferretti V., Bonadiman C., Bianchini G. & Natali C. - A reexamination of the crystal structure of lorándite	78
Scricciolo E., Nazzareni S., Giura P., Calandrini E. & Giuli G. - IR and Single-crystal XRD characterisation of natural pyrochlores	79
Zucchini A., McCammon C., Comodi P. & Frondini F. - Ex situ study of cation disorder in Fe-rich dolomites	80

S3. Georesources, geomaterials and their synthetic counterparts: occurrence, properties, utilizations/industrial applications	81
Aquino A., Lezzerini M., Pecchioni E., Giamello M., Cantisani E. & Fratini F. - Production of hydraulic binders using Lime from Mt. Morello formation in Florence area (Tuscany, Italy)	82
Ardit M. & Dondi M. - Micronization of ceramic pigments: the mineralogist's viewpoint on comminution rate and amorphisation.....	83
Beltrami G. - Thermal stability of hybrid organic-inorganic metasilicates	84
Boschi C., Baneschi I., Bonini M., Brogi A., Dini A., Gola G., Lelli M., Liotta D., Norelli F., Manzella A., Montanari D., Montegrossi G., Orlando A., Raco B., Rielli A., Ruggieri G., Santilano A. & Trumpy E. - H2020 GECO - Geothermal Emission Control- Project.....	85
Carta R. & Fumanti F. - The Mineral resources database of Italy (GeMMA).....	86
Castagnotto E., Locardi F., Cabella R. & Ferretti M. - Purple hematite: synthesis of the pigment <i>Caput Mortuum</i> through thermal treatment of natural samples	87
Caviglia C., Confalonieri G., Destefanis E., Mandrone G., Pastero L., Boero R. & Pavese A. - Evaluations of the reuse of municipal solid waste incinerator bottom ashes as aggregated materials in civil applications.....	88
Chirico R., Mondillo N. & Boni M. - Preliminary characterization of the Nonsulfide Zn(Pb) ores from the Florida Canyon Project (Northern Peru)	89
Coccatto A., Strocchio A., Finocchiaro C., Fugazzotto M., Occhipinti R., Bersani D., Fornasini L., Mazzoleni P. & Barone G. - Raman spectroscopy of aluminosilicates. What about geopolymers?	90
Columbu S., Comboni D., Gatta G.D. & Sitzia F. - Chemical reactivity of pozzolans from Sardinia for the industrial production of hydraulic limes.....	91
Comboni D., Lotti P., Gatta G.D., Merlini M. & Hanfland M. - Anisotropic compressional behavior of ettringite.....	92
Comodi P., Cavalaglio G., Nicolini A., Cambi C., Vivani R., Zucchini A., Susta U., Frondini F. & Cotana F. - Biomass vs coal ashes: a multi-methodic analysis to assess their hazardousness or reusability	93
Confalonieri G., Arletti R., Di Renzo F., Fabbiani M., Fois E., Haines J., Martra G., Quartieri S., Santoro M., Tabacchi G. & Vezzolini G. - Hydrocarbon Polymerization in Pure Silica Mordenite: The Effects of Structure, Pressure, Temperature and Time.....	94
Conte S., Zanelli C., Melchiades F.G., Hernández-Sánchez M.Y., Boschi A.O. & Dondi M. - Brazilian phyllite as feldspar substitute in ceramic bodies	95
Dondi M., Guarini G., Conte S., Molinari C., Soldati R. & Zanelli C. - A global view at sourcing and composition of fluxes for ceramics.....	96
Ercoli R., Renzulli A., Orlando A., Tassi F., Pagnetti A., Vaselli O., Borrini D., Paris E., Tarantino S.C. & Di Gregorio A. - Enhancing the sustainability of the aluminium production: experimental tests addressed to the inertization of industrial by-products through hydrogen storage for furnace fuel and to the synthesis of foamed geopolymers.....	97
Finocchiaro C., Barone G., Mazzoleni P., Leonelli C. & Rossignol S. - FT-IR study of early stages of geopolymer gel formation of AAMs based on pyroclastic deposits (Mt. Etna, Sicily, Italy) using two different alkaline solutions	98
Fugazzotto M., Coccatto A., Finocchiaro C., Occhipinti R., Strocchio A., Mazzoleni P. & Barone G. - Red brick waste as geopolymeric precursor for a sustainable restoration of ancient masonry	99
Funari V., Mantovani L., Vigliotti L., Dinelli E. & Tribaudino M. - Municipal solid waste incineration (MSWI) ashes: potential impacts and metal resources assessed by environmental magnetic methods..	100
Gaggero L., Ferretti M. & Locardi F. - Assessment of post treatment acceptance for Asbestos-Containing Waste by differential thermal analysis and thermo-gravimetry (DTA-TG).....	101
Galderisi A., Iezzi G., Bianchini G., de Brito J., Paris E., Piattelli V., Casarin A., Cinosi J., Macrini D., Schettino D., Santone S., Rossi M. & Buccieri F. - Petrography of Construction and Demolition Wastes from Abruzzo Region (Italy)	102

Giorno M., Barale L., Bertok C., D’Atri A., Martire L., Piana F. & Rossetti P. - Gorno mining district (Southern Alps): new preliminary data about ore mineral precipitation and multiphase diagenetic evolution	103
Lotti P., Comboni D., Gatta G.D., Pagliaro F., Catizzone E., Migliori M., Giordano G., Milani S., Merlini M., Collings I.E. & Hanfland M. - Methanol intrusion in MFI- Zeolites at High Pressure	104
Mancinelli M., Pompilio A., de Castro E.I., Pasti L., Rosatelli G., Di Bonaventura G., Pedrotti J.J. & Martucci A. - Development of a nanocomposite membrane based on reduced graphene (r-GO) and zeolite 13X for the removal of metal ions with bactericidal actions	105
Mantovani L., Funari V., Tribaudino M., Mazzari C. & Sabatino S. - Bottom ash from Parma WtE plant: mineralogical and chemical characterization	106
Martucci A., Bonadiman C., Zappaterra O., Renna M., Castelli S. & Rodeghero E. - Traceability of Ruby: challenges and opportunities by a combined LA-ICP-MS, UV-VIS and XR diffraction.....	107
Moroni M., Naitza S., Rossetti P., Ruggieri G., Magnani L., Aquino A., Tartarotti P., Ferrari E., Oggiano G. & Secchi F. - Conditions for hydrothermal cobalt and nickel mineralization – suggestions from some little known, historical ore deposits in Italy	108
Moroni M., Sessa G., Tumiati S., Ferrari E. & Langone A. - Hydromagmatic PGE telluride-rich Ni-Fe-Cu sulfide mineralization related to melt-rock reaction processes in presence of carbonated hydrous fluids: examples from sulfide-rich ultramafic intrusions of the Ivrea-Verbano Zone.....	109
Naitza S., De Giudici G.B., Funedda A., Loi A., Meloni M.A., Moroni M., Oggiano G. & Secchi F. - Metallogenesis in Sardinia - the Critical Raw Materials (CRM) perspective	110
Novembre D., Gimeno D., Graziano S.F. & Cappelletti P. - Zeolitization processes at the pyroclastic deposit “Tufo rosso a scorie nere” (Auctorum), Vico Volcano, Italy.....	111
Novembre D., Gimeno D. & Del Vecchio A. - Synthesis and characterization of Li-ABW zeolite using a kaolinitic rock.....	112
Oberto M. & Rossetti P. - The gold mineralization of Rio Cannero (Serie dei Laghi, north-western Italian Alps): first geologic and metallogenic data	113
Occhipinti R., Coccato A., Finocchiaro C., Fugazzotto M., Strocio A., Mazzoleni P. & Barone G. - Natural-fibres-reinforced geopolymers for application in Cultural Heritage	114
Paris E., Grandinetti V., Manzi S., Stabile P. & Bignozzi M.C. - Geopolymer-based Terrazzo tiles with a high-waste content: stepping forward from the laboratory phase to the industrial scale	115
Peroni V., Botter R., Cabella R., Risso L. & Carbone C. - Mineralogical and microstructural characterization of stoneware for wine use.....	116
Polisi M., Fabbiani M., Arletti R., Vezzalini G., Martra G., Di Renzo F. & Quartieri S. - Zeolite as an abiotic environment for amino acid condensation: spatial confinement and high pressure effects	117
Precisvalle N., Martucci A., Bonadiman C., Langone A. & Nobre A. - Topaz characterization: mineralogy and geochemistry at the service of the jewelry market	118
Putzolu F., Abad I., Balassone G., Boni M., Cappelletti P., Graziano S.F., Maczurad M., Mondillo N., Najorka J. & Santoro L. - Genesis of phyllosilicates in the Wingellina Ni-Co laterite deposit (Western Australia).....	119
Rossi G., Gamberi F., Marani M., Mattioli M., Di Gregorio A. & Renzulli A. - The hydrogenetic ferromanganese crusts and hydrothermal massive sulphide deposits in the Tyrrhenian Seafloor: a geological reassessment of the supply of Raw Materials.....	120
Santoro L., Herrington R. & Putzolu F. - Natural Iron oxy-hydroxides from supergene ore deposits: mineralogical, morphological and geochemical characterization	121
Sinisi R., Mongelli G., Perri F. & Khosravi M. - Aluminum Phosphate–Sulfate (APS) minerals occurrence and REEs control in the Darzi-Vali bauxite deposit, Iran.....	122
Stabile P., Abudurehman A., Bello M., Carroll M.R. & Paris E. - Characterization and vitrification of combined waste materials and potential use for reutilization in eco-sustainable building	123
Toffolo L., Nimis P., Tret’yakov G.A., Melekestseva I.Yu. & Beltenev V.E. - What controls metal endowment of massive sulfide deposits on mid-ocean ridges?	124

Ulian G., Moro D. & Valdrè G. - Density Functional investigation of the thermomechanical, electronic and thermodynamic properties of ZnS cubic polymorphs	125
Ulian G., Moro D. & Valdrè G. - Thermal and mechanical properties of phyllosilicates: some case studies from <i>ab initio</i> quantum mechanical investigations.....	126
Zanelli C., Conte S., Molinari C., Soldati R., Guarini G. & Dondi M. - Geomaterials on the edge of the circular economy: the case study of the ceramic tile industry.....	127
S4. Minerals, environment and medical uses	128
Beltrami G., Martucci A., Pasti L. & Chenet T. - Probing the sorption capacity of Y Zeolite towards pharmaceutical compounds: a neutron powder diffraction study.....	129
Belviso C., Belviso S., Ragone P. & Cavalcante F. - Red mud neutralization by layered double hydroxides (LDHs) formation: differences in the synthesis process used	130
Botta S., Avataneo C., Barale L., Compagnoni R., Cossio R., Marcelli I., Piana F., Tallone S. & Turci F. - Petrofacies for the prediction of NOA content in rocks: application to the “Gronda di Genova” tunneling project.....	131
Capella S., Visonà S., Osculati A. & Belluso E. - Occupational and anthropogenic environmental exposure during asbestos-cement production by FIBRONIT in Broni (Pavia): assessment of asbestos lung burden by SEM-EDS	132
Chillieri E., Byrne P., Onnis P., Lattanzi P., Costagliola P., Rimondi V. - Trace metal contents and mobility in mine wastes of the Central Wales mine district: environmental implications.....	133
Croce A., Rinaudo C., Grosso F., Erra S. & Amisano M.F. - Identification of asbestos fibers in tissues of patients affected by important diseases in extra respiratory systems	134
D’Aleo R., Cangemi M., Speziale S., Garabeiti E., Madonia P. & Favara R. - Ash leachates from Yasur volcano (Vanuatu): human and livestock health assessment implications	135
Di Benedetto F., Belluso E., Capella S., Giaccherini A., Romanelli M., Ciuffi B., Montegrossi G., Zoleo A. & Capacci F. - An EPR study of silica radicals in lung tissues with evidence of silicosis.....	136
Fornasaro S., Comodi P., Crispini L., Malatesta C., Zucchini A. & Marescotti P. - Distribution and concentration of potentially toxic elements in ultramafic rocks: a case study from the Voltri Massif (Western Alps, Italy).....	137
Funari V., Toller S. & Costa A. - Human Health vs. Urban Geochemistry during the Anthropic Times	138
Giordani M., Di Lorenzo F., Mattioli M. & Churakov S. - Solubility Assay of the Natural Zeolites Erionite, Offretite and Stellerite	139
Grieco G., Sinojmeri A. & Cavallo A. - Pyrite separation in copper enrichment plants as a key to circular economy driven remediation: a case study from Northern Albania Cu mining district.....	140
Lettino A., Belviso C., Cavalcante F. & Fiore S. - Potential Environmental risk induced by TiO ₂ dispersions in waters and sediments: a case history of the Frido stream deposits (Southern Apennines, Italy).....	141
Mattioli M., Giordani M., Ottaviani M.F., Cangiotti M., Valentini L., Di Giuseppe D. & Gualtieri A.F. - Fibrous ferrierite from the Lessini Mounts, Veneto Volcanic Province, NE Italy.....	142
Medas D., Carlomagno I., Meneghini C., Pusceddu C. & De Giudici G. - Laboratory and synchrotron radiation-based techniques to investigate the soil-plant system in Zn-extreme environments	143
Militello G.M., Gaggero L., La Maestra S., Sanguineti E., Yus González A. & Lavagnino G. - Lower and upper aspect ratio range to consider on quantitative determination of Elongated Mineral Particles (EMP) in bulk samples and in vitro study	144
Moro D., Ulian G. & Valdrè G. - Mechanical properties of calcium apatite-based biominerals: hydroxylapatite (<i>P6₃</i>) and type-A carbonated apatite (<i>PI</i>).....	145
Mousavi Aghdam M., Loi A., Dentoni V., Meloni M.A., Pistis M., Funedda A., Randaccio P. & Da Pelo S. - Can be geogenic radon potential indirectly inferred?.....	146
Parisi F., Sciascia L., Princivalle F., Merli M., Lazzara G. & Milioto S. - Montmorillonite clay for the removal and recovery of metals and dyes from industrial wastewaters.....	147

Pascucci S., Palombo A., Santini F., Pignatti S., Ionca V., Cavalcante F. & Belviso C. - Hyperspectral thermal data to identify natural and manmade asbestos minerals: TASI-600 imagery case studies	148
Pastero L., Curetti N., Ortenzi M.A., Schiavoni M., Destefanis E. & Pavese A. - Non-conventional CCS reaction: Ca-oxalate precipitation via Vitamin C promoted green reaction	149
Placitu S., Fancello D., Medas D., Alisi C., Paganin P., Tasso F., Sprocati A.R., Turnau K. & De Giudici G. - Mineral dissolution enhanced by bacteria can improve sustainability of agricultural practices	150
Rigonat N., De Giudici G., Medas D., Cidu R., Lattanzi P., Podda F., Dore E., Frau F., Marras P.A. & Frau I. - Assessment of environmental impact of mine drainage on the Rio Montevecchio watershed (SW-Sardinia) through hydrologic-tracer techniques and environmental mineralogy	151
Rizzo G. & Sinisi R. - Mineralogical and petrographical assessment of edenite crystals from Southern Apennine (Italy).....	152
Sacchi E. - Unusual (but not too much) particles in forensic soil samples.....	153
Sacchi E. - Facies analysis at the crime scene: a traditional method in a different frame.....	154
Smiljanić D., Daković A., de Gennaro B., Germinario C., Grifa C., Izzo F., Langella A., Spasojević M. & Mercurio M. - Novel zeolite's nanocomposites with a two-tailed cationic surfactant – Arquad® 2HT-75 with increased stability.....	155
Somma R. - The judicial contribution of the Messina University on Forensic Geology and Environmental Crimes.....	156
Tribaudino M., Mantovani L., Solzi M. & Zaccara P. - Environmental monitoring with magnetic minerals on leaves in wintertime: an assessment.....	157
Valdrè G., Moro D. & Ulian G. - Amino acids-chlorite interaction at the nano-atomic scale.....	158
S5. Geosciences in Archaeometry and Cultural Heritage Conservation	159
Beltrame C., Lazzarini L. & Antonelli F. - The marble identification of ancient shipwrecks for an enhancement of the in situ underwater heritage of Italy: the case of the cargo of Punta del Francese (Stintino-Sassari, Sardinia).....	160
Bernabale M., Nigro L. & De Vito C. - Microstructure and chemical composition of Iron Age archaeological objects from the Phoenician-Punic site of Motya (Sicily, Italy).....	161
Borghesi A., d'Atri A., Gambino F., Martire L., Perotti L., Vaggelli G. & Valentino D. - STONE Pietre Egizie: a free mobile application for promoting the knowledge and dissemination of ornamental stones exposed in Museo Egizio of Torino (NW Italy).....	162
Caruso V., Marinoni N., Merlini M., Cantaluppi M., Diella V., Trombino L. & Cattaneo C. - A comparison between the decay of adult and juvenile human skeletons from archeological and contemporary burials using a multidisciplinary approach.....	163
Castagnotto E., Locardi F., Scrivano S., Ferretti M. & Gaggero L. - Chemical and textural fingerprint of natural stones for the use of construction and restoration stakeholders (CatSTONE project).....	164
Coletti C., Maritan L. & Mazzoli C. - “Our Common Future”: a lesson from the past for a renewed responsibility	165
De Francesco A.M., Barca D., Tucci A. & Scarpelli R. - Provenance study of the protohistoric impasto <i>pithoi</i> in the Soverato area (Calabria - Southern Italy) by LA-ICP-MS analysis of individual biotite grains	166
Di Fazio M., Felici A.C., Catalli F., Doménech-Carbó A., Doménech-Carbó M.T. & De Vito C. - Roman orichalcum coins: a deep investigation from patina to core	167
Fioretti G. & Campobasso C. - Petroarchaeometric investigation of building stones and mensiochronological analysis of masonry structures of the St. Maria Veterana archaeological site in Triggiano (Apulia, southern Italy), as multidisciplinary tool for the chronological dating and traditional production technology studies.....	168
Fratini F., Pecchioni E., Cantisani E. & Rescic S. - Pistoia, city of stones.....	169
Germinario C., Cappelletti P., De Bonis A., Di Martire D., Esposito R., Grifa C., Morra V., Rispoli C. & Talamo P. - The Roman villa at the Castle of Baia (Naples, Italy): preliminary investigations on the polychromy of frescoed surfaces by using non-destructive spectroscopic techniques	170

Germinario L. & Oguchi C.T. - Weathering of anthropic caves of soft rock in the Kant? region, Japan.....	171
Giustetto R., Padovan S., Barale L. & Compagnoni R. - The Neolithic <i>greenstone</i> industry from Chiomonte (Turin Province, Northwestern Italy): archaeometric study and comparison with analogous findings ..	172
Manca R., Scrivano S., Manfredi C., Ager Vázquez F. J., Ortega Feliu I., Respaldiza M.A. & Benvenuti M. - Castellani gold jewels: materials characterization by in-situ, non invasive analyses at the Museo di Villa Giulia (Rome)	173
Medeghini L., Botticelli M., De Vito C., Nigro L. & Mignardi S. - Archaeometric analysis on ceramic material from the Khalet al-Jam'a necropolis (Bethlehem, West Bank)	174
Moro D., Ulian G. & Valdrè G. - Monte Carlo SEM-EDS micro- and nanoanalysis in archaeometry and cultural heritage: Thickness, shape/geometry effects and measurement strategy	175
Muntoni I.M., Torre M. & Eramo G. - Setting the technological patterns in the Neolithic pottery production of central Apulia	176
Pancani D., Raneri S. & Gioncada A. - Mineralogical and petrographic evidences of fires at Pisa Cathedral: the case of Panchina Livornese	177
Paris E., Sciarroni G., Virgili S., Abudurehman A. & Antongirolami V. - A newly discovered ceramic production center in Camerino (Marche, Italy)	178
Pellegrini M., Donahue R.E. & Lee-Thorp J.A. - Tracking animal movements with tooth enamel oxygen and strontium isotopes	179
Precisvalle N., Ardit M., Martucci A., Bonadiman C., Bianchini G. & Natali C. - Macedonian ruby: mineralogical and geochemical analysis of a national treasure.....	180
Rispoli C., Cappelletti P., De Bonis A., Di Benedetto C., Esposito R., Graziano S.F., Guarino V. & Morra V. - Historical mortars beyond Pompeii: the example of Villa del Pezzolo (Sorrento Peninsula).....	181
Santi P., Foresta Martin F., Spatafora F., De Vita S., Dell'Aquilano M. & Renzulli A. - Volcanic millstones trade in the Mediterranean during the Hellenistic-Roman period: the impact on the production of manufacts and milling technique evolution at Ustica Island (Southern Tyrrhenian Sea, Italy)	182
Savelli C. - Olduvai Subchron (Pliocene-Pleistocene Transition) In Tyrrhenian Sea and Africa Rift Valley: Geological and Paleoanthropological Implications	183
Scrivano S., Cabella R. & Giannattasio B.M. - Archaeometric contribution to the study of the Small Thermal Baths in the roman town of Nora (Sardinia): mortars and plasters.....	184
Scrivano S., Gambino F., Borghi S., Cabella R. & Giannattasio B.M. - Archaeometric contribution to the study of the Small Thermal Baths in the roman town of Nora (Sardinia): white and coloured marbles	185
Stroschio A., Coccato A., Fugazzotto M., Occhipinti R., Mazzoleni P. & Barone G. - Potentiality of PXRF for the discrimination of altered carbonate rocks in Cultural Heritage.....	186
Testone V., Longo V., Mameli P., Cherchi M. & Milanese M. - Detection of graves and buried walls using ground penetrating radar: the Sant'Antioco di Bisarcio archaeological site (Sardinia).....	187
Tonelli G., Renzulli A., Santi P., Talozzi D., Tramontana M. & Veneri F. - The bricks of the UNESCO historical town of Urbino (Marche, Italy): characterization, provenance of the raw material and archaeometric dating.....	188
Vettori S., Verrucchi M., Di Benedetto F., Gioventù E., Benvenuti M., Pecchioni E., Costagliola P. & Moretti S. - Hyperspectral sensor: a practice tool to evaluate the efficacy of cleaning procedures.....	189
S6. Experimental and theoretical studies of magmatic processes	190
Arzilli F., La Spina G., Burton M.R., Polacci M., Le Gall N., Hartley M., Di Genova D., Cai B., Vo N., Bamber E., Nonni S., Atwood R., Llewellyn E., Heidy M., Brooker R.A. & Lee P. - Highly explosive basaltic eruptions: magma fragmentation induced by rapid crystallisation	191
Buono G., Di Genova D., Fanara S., Palladino D.M., Pappalardo L., Petrosino P., Schmidt B.C. & Sottili G. - The effect of decompression rate and volatile (H ₂ O - CO ₂) content on degassing of trachytic melts ..	192
Buttitta D., Caracausi A., Giannandrea P., Paternoster M., Rizzo A.L. & Rizzo G. - Diffusive fractionation of helium isotopes as a possible process to explain the mantle source feature beneath Mount Vulture volcano (Italy).....	193

Cariddi B., Costamagna L.G., Guarino V., Morra V. & Melluso L. - Petrogenesis of Cenozoic Volcanism in the Cixerri Graben (Southwestern Sardinia)	194
Casiraghi G., Schiavi F., Fumagalli P., Cannaò E. & Tiepolo M. - The effect of chlorine on the incorporation of water in magmatic amphibole in subduction settings: an experimental study at lower crust conditions.....	195
De Cristofaro S.P., Arzilli F., Giordano D., Polo L., Janasi V., Fanara S., Burton M., Polacci M., González-García D. & Masotta M. - Pre- and syn-eruptive conditions of Caxias do Sul silicic magmas (Parana? Magmatic Province, Brazil): Crystallisation kinetics of dacitic melts	196
Di Fiore F., Vona A., Romano C., Sulpizio R. & Mollo S. - The role of undercooling and strain rate on the syn-eruptive rheological evolution of the magma feeding the Pollena eruption of Somma-Vesuvius (Campania; Italy).....	197
Di Genova D. - Volcanic eruptions: a nanoscale perspective	198
Fanara S., Schmidt B.C., Sottili G. & Palladino D.M. - Phase equilibria experiments on a leucitite from the Colli Albani volcanic district (Italy).....	199
Giuliani L., Iezzi G., Davis M., Hippeli T., Vetere F., Elbrecht A.L., Nazzari M., Mollo S. & Scarlato P. - Onset of crystallization in a cooling MORB: an <i>in-situ</i> DSC investigation.....	200
González-García D., Giordano D., Bersani D., Fornasini L., Raneri S., Di Genova D., Dingwell D.B., Russell J.K., Ferrando S. & Lottici P.P. - Raman characterization of natural anhydrous silicate glasses: structure and physical properties of the melt	201
Iacovino K., Giuli G. & Carroll M.R. - Sulfur in alkaline melts: An experimental study.....	202
Milani S., Baratelli L., Comboni D., Maurice J., Lotti P. & Merlini M. - Structure and thermal equation of state of Ca ₃ KNa(CO ₃) ₄ carbonate	203
Romano P., White J.C., Andujar J., Scaillet B., Di Carlo I., Liotta M. & Rotolo S.G. - Experimental and thermodynamic constraints on mineral equilibria in pantelleritic magmas.....	204
Spartà D., Fumagalli P., Merlini M., Borghini G. & Poli S. - Phase relations in hydrous REE-bearing carbonatite at 1 GPa, 700-1000°C	205
Stabile P., Arzilli F., Paris E. & Carroll M.R. - Role of the kinetics of nucleation and crystal growth of alkali feldspar in a peralkaline pantelleritic melt	206
Stabile P., Appiah H. & Carroll M.R. - Water solubility in Pantelleritic melts.....	207
S7. New frontiers in metamorphism and deformation-metamorphism relationships through cutting-edge analytical, experimental, numerical, and theoretical techniques	208
Angel R.J., Murri M., Prencipe M., Stangarone C., Mihailova B.D. & Alvaro M. - Measuring strains with Raman Spectroscopy	209
Carvalho B.B., Bartoli O., Cesare B., Tacchetto T., Gianola O., Ferri F. & Aradi L.E. - Fate of primary COH fluid inclusions in garnet from high-grade rocks.....	210
Cesare B., Nestola F., Mugnaioli E., Della Ventura G., Peruzzo L., Bartoli O., Viti C., Johnson T. & Erickson T. - I was not born cubic, said low-temperature metamorphic garnet.....	211
Corti L., Visalli R., Zucali M., Mancini L. & Sayab M. - Integrating X-ray microtomography with the chemical imaging of EMPA: A robust method to quantify mineral re-crystallization during metamorphism: example for granulite to eclogite in the Western Alps, Italy	212
Corti L., Zucali M., Delleani F., Zanoni D. & Spalla M.I. - 3D reconstruction of fabric and metamorphic domains in a slice of continental crust involved in the Alpine subduction system: the example of Mt. Mucrone (Sesia-Lanzo Zone, Western Alps).....	213
Croce A., Pigazzi E., Rinaudo C. & Zucali M. - Micro-Raman spectroscopy and microstructural thermometers applied for the evaluation of carbonate mylonites deformation temperature.....	214
Ferrero S., Wannhoff I., Darling R., Wunder B., Laurent O., Ziemann M.A., Günter C. & O'Brien P. - Micropetrology of megagarnets: nanogranitoids reveal presence of melt during formation of the giant garnets of Barton Mine (Adirondacks, US).....	215

Gilio M., Alvaro M., Angel R.J. & Scambelluri M. - Elastic geothermobarometry on multiple inclusions in a single host.....	216
Giuli G., Pratesi G., Radica F., Stabile P., Paris E. & Cibin G. - Iron oxidation state in Fulgurite glass	217
Giuntoli F., Vitale Brovarone A. & Menegon L. - High pressure abiotic methanogenesis and strain localization in metamorphosed carbonate rocks.....	218
Malaspina N., Langenhorst F. & Montanini A. - The oxidation state of C-S-bearing garnet clinopyroxenites from External Liguride (Italy) and Beni Bousera (Morocco): a TEM-EELS study.....	219
Marchesini B., Menegon L., Prando F., Schmidt P.K., Garofalo P.S., Schwarz G., Hattendorf B., Günther D., Mattila J. & Viola G. - Evidence of low-temperature plasticity in naturally deformed pyrite: a LA-ICP-TOFMS-EBSD combined approach (Olkiluoto Island, Finland)	220
Mazzucchelli M.L., Angel R.J., Morganti S. & M. Alvaro M. - EntraPT: a GUI program for anisotropic elastic thermobarometry	221
Menant A., Sternai P. & Gerya T. - Magmatic forcing of Cenozoic climate?.....	222
Mitterpergher S. - From aseismic to seismic slip in exhumed seismogenic sources: insights from geochemical and microstructural studies of pseudotachylyte bearing faults in the Adamello massif	223
Piccoli F., Ague J.J., Chu X. & Vitale Brovarone A. - Multistage metasomatism recorded in HP metamorphic unit: a natural example of porosity waves in subduction zones?	224
Schwarzenbach E.M., Li J., John T., Caddick M.J., Petroff M. & Gill B.C. - Sulfur transfer within subduction zones: Evidence from exhumed mafic and ultramafic slab material.....	225
S8. Permo-Triassic geodynamic evolution of the Western Tethys realm: insights from magmatism, tectonics and stratigraphic data	226
Brack P. - Timing of Middle Triassic Magmatism in the Southern Alps.....	227
Brombin V., Bonadiman C., Jourdan F., Roghi G., Coltorti M., Webb L.W., Callegaro S., Bellieni G., De Vecchi Gp., Sedeo R. & Marzoli A. - Deciphering a geological enigma: occurrence of intraplate magmatism at convergent plate boundaries.....	228
Caggiati M. & Gianolla P. - Distribution of Triassic magmatism in the Southern Alps: an updated overview .	230
Casetta F., Ickert R.B., Mark D.F., Bonadiman C., Giacomoni P.P., Ntaflou T. & Coltorti M. - The alkaline-carbonatitic lamprophyres of the Dolomitic Area: Late Triassic precursors of the Alpine Tethys opening	231
Casetta F., Giacomoni P.P., Nardini N. & Coltorti M. - Petrological features of clinopyroxene in lava flows from Cima Pape (Dolomitic Area, Southern Alps): how to unravel the feeding system of a Middle Triassic volcano	232
Curzi M., Gianolla P., Caggiati M. & Carminati E. - Middle Triassic subsidence in the Dolomites (Italy): control of tectonics	233
Ferrari E., Tribuzio R., Bosch D., Bruguier O. & Langone A. - Lower Carboniferous to Upper Triassic evolution of the Ivrea-Verbano Zone: geochronological constraints from the Alpe Morello (Val Strona) rock sequence.....	234
Martin S., Toffolo L., Moroni M., Montorfano C., Secco L., Agnini C., Nimis P. & Tumiatì S. - Early Permian - Early Triassic siderite deposits in the Southern Alps (Italy).....	235
Mazzucchelli M., Giovanardi T. & Cipriani A. - Mantle carbonatites or anatectic carbonatites of crustal origin in the Ivrea-Verbano Zone?.....	236
Molli G., Brogi A., Caggianelli A., Capezzuoli E., Liotta D., Spina A. & Zibra I. - A review of upper Carboniferous-Permian tectonics in Corsica, Calabria and Tuscany	237
Morelli C., Bargossi G.M., Gasparotto G., Mair V., Moretti A., Piccin G. & Trentini T. - Outline of a mega volcanic system: The Athesian Volcanic Group	238
Pecorari M., Gianolla P. & Caggiati M. - The onset of Middle Triassic volcanism in the Dolomites (Southern Alps, Italy)	239
Roda M., Regorda A., Spalla M.I. & Marotta A.M. - What drives Alpine Tethys opening? Clues from the review of geological data and model predictions	240

Succo A., Festa A., Balestro G., Borghi A. & De Caroli S. - Role of Late Carboniferous - Early Triassic structural inheritance in the continental break-up of Pangea and exhumation of the Alpine Tethyan mantle: insights from the Canavese Zone, Western Alps	241
Velicogna M., Venier M., Brombin V. & De Min A. - Comparison among the volcanic complex of Gorski Kotar and lava flows from the Medvednica Mountains with the Triassic magmatism of the Dolomites, first results	242
Zanetti A., Giovanardi T., Morishita T., Hemond C., Dallai L., Langone A. & Mazzucchelli M. - Evidence for subduction-related components in sapphirine-bearing gabbroic dykes (Finero Phlogopite peridotite): Insights into the mantle sources of the Mesozoic magmatism at the Africa-Europe boundary	243
S9. Isotopic tracers and timing of dynamic evolution of subduction zone settings	244
Agostini S., Di Giuseppe P., Manetti P., Savascini M.Y., Doglioni C. & Conticelli S. - Early Miocene to Pleistocene Na-alkaline Volcanism on the North-East Arabian plate (South-East Turkey)	245
Bragagni A., Mastroianni F., Avanzinelli R., Conticelli S. & Münker C. - Extreme HFSE fractionation in Italian magmas: metasomatism vs. different mantle domains.....	246
Cannaò E., Scambelluri M. & Tiepolo M. - Into deep and beyond: carbon and nitrogen subduction recycling by secondary peridotites	247
Cannaò E., Tiepolo M., Sessa G., Deloule E. & Poli S. - Amphibole as carbon fixing mineral at lower crust depth	248
Casalini M., Avanzinelli R., Tommasini S., Garzonio C.A., Cioni R. & Conticelli S. - Genesis and differentiation of a calc-alkaline volcano in syn-collisional continental setting: the Mount Ararat (A?r? Da??, Eastern Anatolia)	249
Di Giuseppe P., Agostini S., Manetti P., Savascini M.Y. & Conticelli S. - Early Miocene to Pliocene magmatic activity in the Sivas-Malatya Volcanic Region (Central-Eastern Anatolia)	250
Elliott T., Freymuth H., Andersen M., Chen S. & Hin R. - Isotopic fractionations between dehydration fluid and descending slab	251
Gilio M., Scambelluri M., Agostini S., Godard M., Pettke T., Agard P., Locatelli M. & Angiboust S. - Fingerprinting and relocating tectonic slices along the plate interface: evidence from the Lago Superiore Unit at Monviso (Western Alps)	252
Malaspina N. & Tumiati S. - Redox processes and the role of carbon-bearing volatiles at subduction zones: natural versus experimental perspectives	253
Narduzzi F., Farina F., Lana C., Teixeira L., Schannor M., Stevens G., Alkmim A. & Nalini Jr H.A. - Long-lived petrological cannibalism and slow cooling rates for the Galiléia batholith (SE Brazil): supporting the “hot” nature of Araçuaí-West Congo orogen.....	254
Natali C., Aghazadeh M., Braschi E., Badrzadeh Z., Bianchini G. & Conticelli S. - Eocene subduction to collision-related volcanism in the Arasbaran area (NW, Iran): evidence for progressive evolution of mantle sources	255
Tamburello G. - The importance of direct gas flux measurements at active volcanoes for understanding the geochemical cycles in the subduction zones	256
Tumiati S. - Dissolution of graphite in high-pressure aqueous fluids: the roles of crystallinity and of coexisting silicates and carbonates	257
Tumiati S. - Decoupling between the carbon isotopic signature of CO ₂ -bearing aqueous fluids and of their graphite+carbonate source at subarc depth.....	258
S10. Metasomatic and refertilization processes in lithospheric mantle: unraveling the heterogeneities in mantle sources and related geodynamic systems	259
Alipour R., Perinelli C., Moeinzadeh H., Ahmadipour H., Bosi F. & Gaeta M. - Mineralogical and petrogenetic characteristics of the peridotites and associated podiform chromitites from Abgarm ultramafic complex (south-eastern Iran).....	260

Andreozi G.B., Bosi F., Conte A.M., Cuccuru S. & Naitza S. - Evaluating the controls on the origin of tourmaline-bearing rocks in peraluminous and metaluminous systems: examples from Late-Variscan magmatism of Sardinia (Italy).....	261
Antoniceili M., Tribuzio R., Wu F.Y. & Liu T. - Origin of the peridotite-pyroxenite association from Rocca di Argimonia, Ivrea Mafic Complex (Ivrea-Verbano Zone).....	262
Bonadiman C., Pelorosso B., Curetti N., Merli M., Coltorti M. & Pavese A. - Phlogopite-pargasite coexistence in spinel peridotite xenoliths from Mount Leura (southeast Australia).....	263
Borghini G., Fumagalli P. & Rampone E. - Peridotite modification via reaction with pyroxenite-derived andesitic melts: an experimental study at 2 GPa.....	264
Casetta F., Giacomoni P.P., Ferlito C., Bonadiman C. & Coltorti M. - From the 600 ka tholeiites to the recent trachybasaltic magmas at Mt. Etna: evolution of a lherzolitic mantle.....	265
Consuma G., Braga R., Giovanardi T., Bersani D., Konzett J., Lugli F., Mazzucchelli M. & Tropper P. - The Carbon pathway through subduction zones: petrological and geochemical constraints on carbonates from garnet-bearing orogenic peridotites.....	266
Conte A.M., Perinelli C., Bigi S., Bosman A., Castorina F., Conti A., Cuffaro M., Di Vincenzo G. & Martorelli E. - New insights on volcanic activity related to the opening of the Central Tyrrhenian Sea: the transitional basalts of the Ventotene Volcanic Ridge (Pontine Islands, Italy).....	267
Correale A., Pelorosso B., Rizzo A.L., Coltorti M., Italiano F., Bonadiman C. & Giacomoni P.P. - The noble gases geochemistry in mantle xenoliths from West Antarctic Rift System.....	268
Faccini B., Coltorti M., Brenna M., Casetta F. & Briggs R. - Multiple subduction-related metasomatic pulses in mantle xenoliths from the Karioi volcano, North Island, New Zealand.....	269
Fumagalli P., Borghini G., Klemme S. & Rampone E. - Major and trace elements distribution during high-pressure melt-peridotite reaction: experiments at 2 GPa.....	270
Giacomoni P.P., Coltorti M., Bonadiman C., Ferlito C., Faccini B., Zanetti A. & Ottolini L. - From mantle to magma: a volatile budget between mantle xenoliths and primary magmas in the Western Antarctic Rift System.....	271
Giovanardi T., Girardi V.A.V., Teixeira W., Mazzucchelli M. & Cipriani A. - Mafic dyke swarms at 1882, 535 and 200 Ma in the Carajás region: an insight on the evolution of the sub- Amazonian Craton mantle.....	272
Giovanardi T., Zanetti A., Langone A., Cipriani A. & Mazzucchelli M. - Dioritic-albititic dykes in the Finero Phlogopite Peridotite: an intrusive event in the Northern Ivrea-Verbano Zone (Southern Alps).....	273
Mazzucchelli M., Bertotto G.W., Giovanardi T., Zanetti A., Ponce A.D., Brunelli D., Bernardi M.I., Hémond C. & Cipriani A. - Xenoliths's evidence for refertilisation of a strongly depleted mantle column in the Patagonian extra-Andean backarc (Paso de Indios, Argentina).....	274
Pellegrino L., Malaspina N., Zanchetta S., Langone A. & Tumiati S. - Eclogite-derived melts-peridotite interaction at HP in the Monte Duria area (Central Alps, N Italy): a proxy for the mafic crust-to-mantle mass transfer in subduction zones.....	275
Rizzo A.L., Coltorti M., Faccini B., Casetta F., Ntaflou T. & Italiano F. - Petrological features and volatile content of ultramafic xenoliths from Eifel (Germany).....	276
Salari G., Rahimzadeh B., Agostini S., Masoudi F. & Lustrino M. - Quaternary ultrabasic volcanic rocks in central Urumieh-Dohkhtar magmatic arc (Central-Northern Iran): melanephelinites in post-collisional setting.....	277
Venier M., Bernardini F., Caldeira R., de Ignacio C., Marzoli A., Mata J., Princivalle F., Boumehdi M.A., Bensaid I.A.A., Youbi N., De Min A. & Lenaz D. - MicroCT rendering of spinel-facies mantle xenoliths.....	278
S11. Mantle Petrology: from observation to calculus.....	279
Belmonte D. - <i>Ab initio</i> thermodynamics of deep mantle phase transitions and seismic discontinuities: the role of MgSiO ₃ polymorphs.....	280
Del Vecchio A., Poe B.T., Cestelli-Guidi M. & Misiti V. - Point defect equilibria in hydrous forsterite synthesized at 1100°C and up to 4 GPa.....	281

Li P., Xia Q.-K., Dallai L., Bonatti E., Brunelli D., Cipriani A. & Ligi M. - H ₂ O Enrichment in Residual Mantle Peridotites at a Mid-Atlantic Ridge Segment.....	282
Merli M., Bonadiman C. & Pavese A. - Earth's non-primitive lower mantle: aluminium recycling	283
Merli M., Bonadiman C. & Pavese A. - Oxidation state of iron in the Earth's lower mantle	284
Moretti R. - Vapor-buffered magmatic activity and the unique CO ₂ -rich source of magmatism in Southern Italy.....	285
Ottonello G., Belmonte D. & Vetuschi Zuccolini M. - Thermochemistry of silicate melts in high-rank simplexes: the new HPA model	286
Papale P. - Why do we need mathematical models in petrology and volcanology?.....	287
Sanfilippo A., Sokolov S., Salters V.J.M., Stracke A. & Peyve A. - Melting an anciently depleted mantle	288
Vetuschi Zuccolini M., Ottonello G. & Belmonte D. - TRIangular DIagram and deSCENT line analysis - a code to generate a computationally manageable liquidus surface of a molten silicate system and a consistent cooling descent line description from modelling	289
S12. Advances in Understanding Geological and Petrological Processes in the Oceanic Lithosphere..	290
Assanelli M., Luoni P., Rebay G. & Spalla M.I. - Structural and metamorphic evolution of Gias Vej serpentinites (Piemonte Zone, Lanzo Valley, Italian Western Alps).....	291
Basch V., Rampone E., Ferrando C., Borghini G. & Zanetti A. - pMELTS modeling of depleted melts evolution in oceanic environment: implications of pyroxenite formation as deep melt segregation	292
Bonatti E. Early days of the plate tectonics revolution - "Geo-data gatherers" versus "Geopoets".....	293
Borghini G. & Fumagalli P - Partial melting experiments on olivine-free pyroxenites at 2 GPa	294
Brunelli D., Maia M., Ligi M., Bonatti E., Briais A., Campos T., Ceuleneer G., Cipriani A., Cuffaro M., Gregory E., Hamelin C., Jbara R., Kaczmarek M.-A., Lombardi F., Moreira S., Mougél B., Petracchini L., Puzenat V., Revillon S., Seyler M., Soltanmohammadi A., Verhoest L., Trivellato T. & Wang Z. - Cold spots at Mid Ocean Ridges help revealing mantle heterogeneity: a summary of the SMARTIES cruise in the Equatorial Atlantic.....	295
Deraco M., Sanfilippo A., Ligi M., Rasul N., Vigliotti L., Jerais A., Tharowi A., Langone A. & Zanetti A. - Formation of a hybrid oceanic crust at the onset of the Red Sea opening (Tihama Asir magmatic complex; Saudi Arabia).....	296
Ferrari E., Montanini A., Secchiari A., Bosch D. & Cluzel D. - Pyroxenite diversity in the New Caledonia mantle sequence: a preliminary study	297
Grammatica M., Fumagalli P. & Borghini G. - The role of melt/rock ratio in olivine-rich troctolite formation via basalt-dunite reaction: an experimental study at 0.5 GPa.....	298
Guerini S. & Tartarotti P. - Listvenites in the western Alps: the case of the Mount Avic massif (Aosta Valley, northwestern Alps).....	299
La Rosa A., Pagli C., Keir D., Sani F., Corti G., Wang H. & Posee D. - Observing oblique slip during rift-linkage processes in Northern Afar	300
Ligi M., Bonatti E., Brunelli D. & Cuffaro M. - Global Seafloor Spreading Variations and the Evolution of Seawater Composition since the Mesozoic	301
Luoni P., Rebay G., Roda M., Spalla M.I. & Zanoni D. - UHP relics in the Zermatt-Saas Zone serpentinites: new puzzle tiles in the geodynamic scenario.....	302
Maino M., Casini L., Sanfilippo A. & Ildefonse B. - From dislocation creep to grain boundary sliding in high-temperature troctolites: insights into shear localization mechanisms in the oceanic crust.....	303
Montanini A., Secchiari A., Bosch D. & Tribuzio R. - Pb isotope composition of recycled mantle pyroxenites: insights into the the HIMU source of oceanic basalts?.....	304
Mosconi A., Sanfilippo A., Liu C.Z., Salters V., Tribuzio R. & Zanetti A. - Isotopic heterogeneity of mantle melts migrating through the Lanzo South Ophiolite: a focus on Re-Os isotopes and PGE.....	305
Renna M.R., Tribuzio R., Sanfilippo A., Armandola S., Becker H. & Wang Z. - Highly siderophile elements and Re-Os isotopes of primitive oceanic troctolites: implications for reactive processes during lower crust formation.....	306

Salvioli-Mariani E., Boschetti T., Toscani L., Montanini A., Petriglieri J.R. & Bersani D. - Multi-stage rodingitization of ophiolitic bodies from Northern Apennines (Italy): constraints from petrography, geochemistry and thermodynamic modelling.....	307
Sani C., Sanfilippo A., Ohara Y., Snow J., Harigane Y. & Yamahshita H. - Mado Megamullion (Shikoku basin): a new window into a backarc lower crust and mantle.....	308
Sani F., Bonini M., Corti G. & Moratti G. - The role of rift width in controlling fault pattern and kinematics in oceanic and continental rifts: examples from Iceland and Ethiopia.....	309
Savelli C. - Oceanization and Hydrography (West Mediterranean)	310
Sternai P. - Surface processes forcing on rift magmatism: insights from numerical modeling.....	311
Verhoest L., Brunelli D., Hemond C., Bonatti E., Ligi M. & Cipriani A. - Mantle source heterogeneity in the Equatorial Mid Atlantic Ridge: a multi-isotopic approach.....	312
S13. A multidisciplinary approach to unravel the evolution of basement geology	313
Bartoli O. - Constraining fluid regime during melting of crystalline basements: experiments vs. thermodynamic modelling.....	314
Benà E., Martin S., Marzoli A., Mazzoli C., Sassi R. & Zattin M. - Apatite (U-Th)/He thermochronometry from trachytes and latites of the Euganean Hills and their exhumation history.....	315
Bonazzi M., Langone A., Zanetti A., Dellarole E., Mazzucchelli M. & Giovanardi T. - Origin of Plumasite dykes intruded in Variscan basement during triassic: new insights from Zircon (Val Sabbiola, Ivrea-Verbano zone).....	316
Carosi R., Montomoli C., Iaccarino S. & Visonà D. - The High Himalayan Discontinuity and the Main Central Thrust in Central Nepal: timing constraints by in-situ U-Th-Pb monazite petrochronology	317
Carosi R. - Partitioned transpressional tectonics in the Variscan Basement of northern Sardinia (Italy).....	318
Casini L., Corvo' S., Maino M., Seno S. & Schenker F. - Numerical modelling of floating P-T conditions in inclusion-matrix systems, with application to the Cima Lunga Unit (Central Alps)	319
Corvo' S., Maino M., Langone A., Piazzolo S., Seno S. & Schenker F. - Determination of P-T-t-d path in a high-grade shear zone: petro-chronological and microstructural study from the Cima di Gagnone (Adula-Cima Lunga nappe, Central Alps).....	320
Cruciani G., Franceschelli M., Massonne H.-J. & Musumeci G. - P-T path of felsic granulite from south-east Corsica (France) and implications for geodynamic setting.....	321
Franceschelli M. & Cruciani G. - Clockwise and anticlockwise P-T path in the axial zone of the Variscan Sardinia-Corsica block	322
Giuntoli F., Menegon L., Warren C., Darling J. & Anderson M. - Protracted shearing at mid crustal conditions in the Scandinavian Caledonides	323
Iaccarino S., Carosi R., Montomoli C., Montemagni C., Massonne H.-J., Jain A.K. & Visonà D. - Geology and tectono-metamorphic history of the Himalayan metamorphic core: insights from the Alaknanda-Dhauli Ganga valleys (NW India).....	324
Möller C., Andersson J. & Rebay G. - High-temperature metamorphism and deformation in the footwall of an eclogite-bearing nappe, Sveconorwegian orogen: metamorphic evolution of the Obbhult Complex, SW Sweden	325
Martini M. & Zepeda-Martínez M. - The Jurassic exhumation history of basement rocks in Mexico preserved in the stratigraphic record of rift basins associated to Pangea breakup	326
Molli G., Vitale Brovarone A., Beyssac O. & Cinquini I. - Thermal architecture and deformation structures in the Alpi Apuane (NW Tuscany Italy): new insights for the metamorphic and tectonic history of the inner northern Apennines.....	327
Montemagni C., Zanchetta S., Montomoli C., Iaccarino S., Visonà D., Villa I.M. & Carosi R. - Geochronology and kinematics of flow of the Main Central Thrust zone in the Bhagirathi valley, NW Indian Himalaya	328
Morelli G., Ruggieri G., Zucchi M., Braschi E., Agostini S., Ventruti G., Brogi A., Liotta D., Boschi C. & González-Partida E. - Characterization and evolution of the paleo-fluids in the Las Minas exhumed geothermal system (Mexico)	329

Nania L., Montomoli C., Iaccarino S., Leiss B., Di Vincenzo G. & Carosi R. - Kinematics and deformation temperatures of the MCTz and the STDS in Central Himalaya	330
Ortolano G., D'Agostino G., Visalli R., Fiannacca P. & Cirrincione R. - Development of vermicular clinopyroxene-amphibole symplectites replacing garnet in amphibolites of the Peloritani Mountain (Northeastern Sicily).....	331
Ortolano G., Visalli R., Fazio E., Fiannacca P., Godard G., Pezzino A., Punturo P., Sacco V. & Cirrincione R. - Unravelling cooling rates of the Calabria continental lower crust from combined microstructural, thermodynamic and diffusion modeling: An example from the Sila Piccola Massif, (Northern Calabria)	332
Petroccia A., Carosi R., Montomoli C. & Simonetti M. - Geochronology and deformation in the Posada-Asinara Line (NE Sardinia basement, Baronia, Italy): timing and shearing constraints in the Southern European Variscan belt	333
Petroccia A., Carosi R., Montomoli C. & Simonetti M. - 1:25.000 structural map of Mamone in the northern of the Sardinian variscan basement	334
Renna M.R., Langone A., Caggianelli A. & Prosser G. - Interaction between migmatite-related melts and amphibole-gabbros: evidence from mineral geochemistry and zircon dating (Variscan lower crust, Palmi area, SW Calabria)	335
Simonetti M., Carosi R. & Montomoli C. - Extension, timing and deformation of the East Variscan Shear Zone	336
Simonetti M., Carosi R. & Montomoli C. - Structural analysis, kinematic of the flow and petrochronology of shear deformation in the Aiguilles Rouges Massif.....	337
Tursi F., Acquafredda P., Festa F., Fornelli A., Langone A., Micheletti F. & Spiess R. - Reworking of felsic rocks in ductile shear zones: an example from the Curinga-Girifalco line.....	338
Van Schroyen Lantman H.W., Langone A., Scambelluri M. & Alvaro M. - Uncovering UHPM garnet growth and dissolution mechanisms using trace elements in metasediments from Lago di Cignana, Western Alps.....	339
Zepeda-Martínez M. & Martini M. - Tectono-sedimentary evolution of the Tlaxiaco Basin, southern Mexico: A key to understand the Jurassic structural history of Proterozoic and Paleozoic basement rocks of Mexico during Pangea breakup.....	340
Zucchi M. - Faults-controlling geothermal fluid flow in low permeability rock volumes: an example from the eastern Elba Island (northern Tyrrhenian Sea, Italy).....	341
S14. Bio-Geo materials for environmental remediation: novel approaches, technologies and case studies	342
Artioli G., Berto D., Dalconi M.C., Gò E., Peruzzo L. & Tateo F. - Occurrence of pararealgam in As-rich aquifer sediments of the Venetian plain (Italy).....	343
Deltedesco E., Zehetner F., Unterfrauner H. & Keiblinger K.M. - Microbiological assessment of lime application to agricultural soils.....	344
Faccini B., Di Giuseppe D., Ferretti G., Galamini G. & Coltorti M. - Effects of natural and NH ₄ -enriched Zeolite on nitrogen leaching from a reclaimed agricultural soil of the Ferrara province (Italy)	345
Ferretti G., Galamini G., Deltedesco E., Gorfer M., Faccini B., Zechmeister-Boltenstern S., Coltorti M. & Keiblinger K.M. - Effects of natural and NH ₄ -charged zeolite amendments and their combination with 3,4-dimethylpyrazole phosphate (DMPP) on soil gross ammonification and nitrification rates.....	346
Ferretti G., Keiblinger K.M., Faccini B., Galamini G., Mentler A., Zechmeister-Boltenstern S. & Coltorti M. - Sorption of 3,4-Dimethylpyrazole phosphate (DMPP) in Soils amended with different chabazite zeolites.....	347
Keiblinger K.M., Maftukhah R., Ngadisih, Murtiningrum, Kral R.M. & Mentler A. - Soil amendments for re-cultivation of formerly mined land on Bangka island, Indonesia	348
Leoncini C., Lo Monaco A., Gagni S., Emiliani R., Riberti R., Forti F., Caridei F., Filippini M. & Gargini A. - Optimal hydrogeological conditions for phytoscreening in sites with chloroethenes subsurface contaminations.....	349

Malferrari D., Bernini F., Bigli B., Borsari M., Brigatti M.F., Castellini E., Mucci A. & Sebastianelli L. - Sulfur bearing and aromatic compound trapping by layered silicates: a great start for innovative technological applications	350
Matteucci F., Curri M.L., Comparelli R., Giannantonio R., Giansante C., Mascolo G. & Giannini C. - Nanomaterials for the abatement of contaminants in water treatment	351
Mentler A., Ottner F., Wriessnig K., Keiblinger K.M. & Kral R.M. - Production potential in central Mozambique: soil analysis and mineralogy	352
Mentler A., Keiblinger K.M., Maftukhah R., Ngadisih N., Murtiningrum M. & Kral R.M. - On the ground or in the ground? Co-learning of farmers and scientists about soil	353
Molinari S., Salviulo G., Magro M., Baratella D. & Vianello F. - Water total arsenic remediation via a new generation colloidal superparamagnetic maghemite nanoparticles	354
Morrone L., Facini O., Mari M. & Rotondi A. - Effects of zeolite and kaolin foliar application in olive trees on photosynthesis and on drupes oil content	355
Morrone L., Mari M. & Rotondi A. - Use of geo materials (zeolites) in the rooting phase for the production of olive plant	356
Neri L., Carriero G., Facini O. & Baraldi R. - Environmental remediation of the historical suburban forest Bosco Albergati	357
Neri L., Monti A. L., Ottoni S., Facini O. & Baraldi R. - Phytoremediation of contaminated sites: the case study of a petroleum refinery in Mantova, Italy	358
Prisa D. - Chabazitic-zeolites and Effective Microorganisms for the qualitative improvement and fertilizers reduction in the growth of Aloe plants	359
Prisa D. - Improvement Quality and Content of Pepper and Chilli Nitrates Influenced by the Effective Microorganisms	360
Rizzo P., Sanangelantoni A., Iacumin P. & Celico F. - Isolation and selection of bacterial strains for aquifer remediation: a case study in Val d'Agri (Southern Italy)	361
S15. Geobiology: Biosphere-Earth interactions	362
Azzarone M., Cheli A., Mancuso A., Stagioni M., Falini G., Goffredo S. & Scarponi D. - <i>Chamelea gallina</i> response to a warming Earth: A case study from the Holocene sedimentary succession of the Po-Adriatic system	363
Berton D., Rodriguez Navarro A., Grenier Romero C., Roman Martinez R., Rodeghero E. & Martucci A. - The precipitation process of the calcium carbonate in <i>Austrorhynchus Psittacus</i> and the role of organic matter: a multidisciplinary study	364
Bonacina G., Sanfilippo A., Previde Massara E., Scotti P., Viaggi P. & Piva A. - The Cretaceous Oceanic Anoxic Event 2: geochemical constraints from a section of the Atlantic margin	365
Bosio G., Bracchi V.A., Malinverno E., Basso D., Collareta A., Gioncada A., Coletti G., Di Celma C. & Bianucci G. - Taphonomic and diagenetic history of a Panopea-rich layer from the Pisco Formation, Peru	366
Bracchi V.A. & Basso D. - Crustose coralline algae: the bioengineers of Mediterranean seafloor at the geological scale	367
Bragato P.L. - Human and geological crises of the last millennium in Italy modulated by the episodes of the Little Ice Age	368
Consani S., Borello A., Vezzulli L. & Carbone C. - Characterisation of prokaryotes and eukaryotes in contaminated extreme environments: preliminary results	369
Leonelli G., Pelfini M. & Maggi V. - Changes in the tree-ring $\delta^{18}\text{O}$ from the Forni Glacier forefield due to glacier stream water inputs and climate change: potential use for environmental and climatic reconstructions	370
Malferrari D., Ferretti A., Mascia M.T., Medici L. & Savioli M. - Integrated strategies for quantifying major element contents in modern and fossil bioapatite	371
Notaro A., Garzarella A. & Raffi I. - Calcareous nannofossils behavior during global warmth intervals of the Neogene	372

Vertino A., Savini A. & Marchese F. - Bio-geosphere interactions in the deep: The important role of cold-water corals.....	373
S16. Planetary evolution: new insights from remote sensing, in-situ, terrestrial analogues and meteorite studies	374
Antonangeli D., Badro J., Boccato S., Morard G., Rivoldini A., Siebert J., Xu F. & the InSight Science Team - InSight, first months on Mars and laboratory experiments to complement planetary observations.....	375
Baioni D., Gutierrez F., García-Arnay A., Luzzi E., Parenti C., Sevil J. & Nesci O. - Two possible episodes of karstification in the equatorial layered deposit within Kotido crater, Arabia Terra, Mars	376
Campanale F., Mugnaioli E., Folco L., Gemmi M., Lee M.R., Daly L. & Glass B.P. - Evidence for direct solid-state quartz-to-coesite transformation in shocked ejecta from the Australasian tektite/microtektite strewn field	377
Carli C., Morlok A., Stojic A., Weber I., Renggli C., Klemme S., Ferrari S., Pratesi G., Hiesinger H. & Capaccioni F. - VNIR reflectance spectra of iron-bearing Mercury-like glasses	378
Fastelli M., Comodi P., Zucchini A., Maturilli A., Balic-Zunic T. & Rossi M. - Reflectance and emissivity spectroscopy of hydrated salts at different temperature: a method to understand icy planetary bodies surfaces composition	379
Folco L. - The near-Earth cosmic dust complex: Perspectives from the unique Transantarctic Mountains micrometeorite collection	380
Galluzzi V., Ferranti F., Massironi M., Giacomini L., Guzzetta L. & Pasquale P. - High-Mg region induced stress field in the Victoria quadrangle of Mercury.....	381
Giacomini L., Galluzzi V., Carli C., Zambon F., Massironi M., Ferranti L. & Palumbo P. - Geological mapping of the Kuiper (H06) quadrangle of Mercury: Integration between morphologic and spectral characteristics	382
Italiano F., Di Bella M., Sabatino G., Barbieri R., Cavalazzi B., Ferretti A., Danovaro R., Romeo T., Andaloro F., Esposito V., Tripodo A., Scotti G. & Quartieri S. - Hydrothermal iron ooids on Earth as homologues of hematite spherules discovered on Mars.....	383
Massironi M., Pozzobon R., Franceschi M. & Penasa L. - From Planetary surface mapping to Planetary subsurface structures.....	384
Miozzi F., Morard G., Antonangeli D., Clark A.N., Baron M.A., Dorn C., Rozel A., Pakhomova A., Mezouar M. & Fiquet G. - Characterization of the Fe-Si-C system at extreme conditions and application to exoplanets interior	386
Moggi Cecchi V., Pratesi G., Giuli G., Nemati M., Di Martino M. & Serra R. - The 2017 Joint Italian - Iranian Lut desert expedition: compositional and textural features of the meteorites recovered.....	387
Mugnaioli E., Gemmi M., Campanale F., Suttle M.D., Folco L. & Pignatelli I. - 3D electron diffraction for the characterization of cryptocrystalline micro-samples: Applications to planetary sciences	388
Nava J., Maturilli A., Zambon F., Carli C., Alemanno G., Helbert J., Genovesi S. & Massironi M. - Laboratory experiments on carbonaceous chondrites: insights into cryovolcanism and hydrothermal alteration on planetary bodies.....	389
Nazzareni S., Pauselli C., Skogby H., Murri M., Domeneghetti M.C., Alvaro M., Stalder R., Petrelli M., De Sanctis M.C., Formisano M. & Federico C. - Pyroxenes as a proxy for thermal history and water content of asteroid 4 Vesta.....	390
Nestola F., Barbaro A., Morana M., Christ O., Brenker F.E., Domeneghetti M.C., Dalconi M.C., Alvaro M., Goodrich C., Fioretti A.M., Leoni M. & Shaddad M.H. - Diamonds in ureilites: how did they form?..	391
Pisello A., De Angelis S., Ferrari M., Vetere F.P., Pauselli C., Kueppers U., De Sanctis M.C. & Perugini D. - A new spectroscopic database for silicate glasses: implications for planetary science.....	392
Re C., Cremonese G., Naletto G. & Tordi M. - HYPSON, Next generation of a stereo camera	393
Suttle M.D., Twegar K., Nava J., Spiess R., Spratt J., Campanale F. & Folco L. - A unique CO-like micrometeorite hosting an exotic Al-Cu-Fe-bearing assemblage – close affinities with the Khatyrka meteorite	394

Tangari A.C., Marinangeli L., Scarciglia F., Pompilio L. & Piluso E. - Genesis and age of clay deposits in Margaritifer Region on Mars using terrestrial soil analogues	395
Tribaudino M., Mantovani L., Bersani D. & Salviati G. - Cathodoluminescence and photoluminescence: combined SEM-EDS and Raman to approach the analysis of anorthite in Ca-Al inclusions	396
Zambon F., Carli C., van der Bogert C.H., Hiesinger H., Altieri F., Giacomini L. & Massironi M. - Spectral variations across Apollo basin on the Moon.....	397
S17. Unveiling the Antarctica: geological, geophysical and sedimentological approaches to the evolution of Antarctica	398
Balestrieri M.L., Olivetti V., Rossetti F., Gautheron C. & Zattin M. - Topography, structural and thermochronological analysis in the Admiralty Block, northern Victoria Land, Antarctica: decoding the Cenozoic evolution of the NE termination of the Transantarctic Mountains	399
Battaglia F., Baradello L., De Santis L., Gordini E., Sauli C., Kovacevic V., Morelli D., Langone L., Colleoni F., Colizza E., Rebesco M. & Accetella D. - High resolution seismo-stratigraphic evidence from the Edisto Inlet fjord, western Ross Sea (Antarctica).....	400
Capponi G., Montomoli C., Casale S., Simonetti M., Musumeci G. & Salvatore M.C. - Geology of the Convoy Range and Franklin Island quadrangle, Victoria Land - Antarctica.....	401
Cornamusini G., Zurli L., Perotti M. & Talarico F.M. - Deformational structures in Paleozoic sandstones of the Transantarctic Mountains: glacial vs tectonic origin	402
Dal Seno N., Lelli L., Millikin L., Smith Lyttle B., Cox S.C., Crispini L. & Burton-Johnson A. - GeoMAP dataset of the Antarctic Peninsula.....	403
Dallai L. & Sharp Z.D. - Continental hydrology and atmospheric circulation during Cenozoic super warm periods	404
De Santis L., Olivo E., Sorlien C., Kim S., Granot R., Sauli C., Busetti N., Wardell N., Rui L., Perez L.F., Colleoni F., Pochini E., Wilson D., Bart O.J., McKay R.M., Kulhanek D. & IODP Expedition Scientific Party - Miocene paleobathymetric reconstruction of the Ross Sea (Antarctica)	405
Federico L., Cianfarra P., Crispini L., Capponi G., Rossi C. & Salvini F. - Reconstruction of multiple tectonic events in the Rennick Geodynamic Belt (northern Victoria Land, Antarctica) through inversion of fault slip data	406
Ferraccioli F., Armadillo E., Crispini L., Läufer A., Ruppel A. & Lisker F. - Crustal architecture of a major pull apart basin in northern Victoria Land, East Antarctica.....	407
Ferraccioli F., Jordan T.A., Forsberg R., Eagles G., Eglington B., Kuszniir N., Olesen A., Matsuoka K., Casal T. & Paxman G. - Aerogeophysical imaging unveils the architecture and basement of the Pensacola-Pole subglacial basin in East Antarctica.....	408
Giacomoni P.P., Coltorti M., Bonadiman C., Ferlito C., Casetta F., Zanetti A. & Ottolini L. - Subduction-related volatiles involved in the genesis of Cenozoic primary alkaline melts in Northern Victoria Land.....	409
Guzzo G., Cattò S., Olivetti V., Zattin M., Balsamo F., Balestrieri M.L. & Rossetti F. - Thermochronological evolution of Transantarctic Mountains in the Mt Murray area.....	410
Iaccarino S., Carosi R., Montomoli C. & Massonne H.-J. - Tectonometamorphic evolution of the Dessent Unit (northern Victoria Land, Antarctica): new data from pseudosection modeling of metasediments .	411
Li X., Zattin M. & Olivetti V. - The detrital apatite fission-track signature of post-LGM sediments in the Ross Sea.....	412
Liberato G.P., Cornamusini G., Zurli L., Conti P., Calver C., Meffre S. & Talarico F.M. - Stratigraphic insights across Permian-Triassic boundary in southern Gondwana: comparison between Victoria Land (Antarctica) and Tasmania (Australia)	413
Liberato G.P., Cornamusini G., Zurli L., Woo J., Corti V., Oh J.-R. & Talarico F.M. - Sandstones provenance study of the Permian-Triassic sequences at Allan Hills (Victoria Land, Antarctica): evidence from petrographic framework	414
Pelorosso B., Bonadiman C., Ntafflos T., Gregoire M., Zanetti A. & Coltorti M. - Ultramafic cumulates from Harrow Peaks, (NVL, Antarctica): the first stages of the Ferrar magmatism.....	415

Rocchi S. & Smellie J.L. - Plutons, dykes and volcanoes as witnesses of lithospheric thinning, faulting and necking in northern Victoria Land, Antarctica	416
Rocchi S., D’Orazio M., Masotta M. & Folco L. - In memory of Pietro Armienti	417
Tolotti R., Caffau M., Colizza E. & Sauli C. - Holocene Antarctic Ice Sheet evolution in the Ross Sea: new evidences from the North-Western Basin	418
Tribuzio R., HenjesKunst F., Gerdes A. & Braga R. - Geochemical, isotopic and geochronological constraints on formation of boninite-type rocks at the Paleopacific margin of Gondwana.....	419
Vignaroli G., Rossetti F., Di Vincenzo G., Balsamo F., Gerdes A., Theye T. & Ghezzi C. - Late Cambrian-Early Ordovician orogenic construction along the paleo-Pacific margin of Gondwana, USARP Mountains, Northern Victoria Land (Antarctica)	420
Zurli L., Cornamusini G., Liberato G.P., Talarico F.M., Woo J., Conti P. & Corti V. - Stratigraphic comparison between Victoria Land (Antarctica) and Tasmania (Australia) Late-Palaeozoic glaciogenic sequences.....	421
Zurli L., Cornamusini G., Liberato G.P., Talarico F.M., Woo J. & Corti V. - Provenance study of Late Palaeozoic Ice Age sequences in Victoria Land (Antarctica): petrography and geochronology.....	422
Zurli L., Perotti M., Talarico F.M., Cornamusini G., McKay R.M., De Santis L., Kulhanek D.K. & the IODP Expedition Scientists - Petrographic characterization of gravel size clasts of the IODP_exp374 cores: implication for Miocene ice flows in the Ross Sea region (Antarctica)	423
S18. Mechanical, chemical and hydraulic interactions in seismogenic fault zones	424
Aben F.M. - Rupture-induced off-fault damage: Laboratory quantification and implications for fault mechanics	425
Cerchiari A., Remitti F., Mittempergher S., Festa A., Lugli F. & Cipriani A. - Interrelated changes in fluid sources and stress field orientation during the seismic cycle reconstructed for an exhumed analogue of the subduction megathrust shallow portion.....	426
Collettini C., Tesei T., Scuderi M.M., Carpenter B.M. & Viti C. - Beyond Byerlee Friction, Weak Faults and Implications for Slip Behaviour	427
Coppola M., Billi A., Stagno V., Cavallo A., Correale A., Fondriest M., Nazzari M., Paonita A., Romano C., Viti C. & Vona A. - Fluid-mediated deformation processes along the seismogenic Mt. Morrone fault zone (Central Apennines, Italy).....	428
Corsi G., Balsamo F., Bezerra F.H.R. & Salvioli-Mariani E. - Structural inheritance, fluid flow and intraplate seismicity along the Samambaia Fault, NE Brazil	429
Fondriest M., Mecklenburgh J., Passelegue F.X., Artioli G., Nestola F., Spagnuolo E. & Di Toro G. - Pseudotachylytes alteration and their loss from the geological record	430
La Rosa A., Pagli C., Molli G., Casu F., De Luca C., Pieroni A. & D’amato Avanzi G. - Growth of a sinkhole in a seismic zone of the northern Apennines (Italy).....	431
Malatesta C., Crispini L., Läufer A., Ildefonse B., Federico L. & Scarsi M. - Microstructural investigation of a prehnite-epidote bearing detachment horizon in granite (northern Victoria Land, Antarctica): influence of hydrothermal fluids on the fault mechanics.....	432
Marchesini B., Garofalo P.S., Menegon L., Mattila J. & Viola G. - Fluid-mediated, brittle-ductile cyclicity at seismogenic depth: Fluid record and deformation history of a fault system of the Svecofennian basement in SW Finland.....	433
Meneghini F., Aretusini S., Spagnuolo E., Harbord C. & Di Toro G. - Weakening mechanisms and rupture propagation along the Hikurangi margin frontal thrust: preliminary results from high speed friction experiments under controlled fluid pressure.....	434
Merico A., Giuliani L., Iezzi G., Pace B., Ferranti L., Cremona M., Scafa M., Nazzari M., Colella A. & Scarlato P. - Texture of tectonised calcite clasts from the San Benedetto-Gioia dei Marsi fault (central Italy).....	435
Mittempergher S., Bistacchi A., Di Toro G., Nielsen S. & Gukov K. - Roughness, off-fault damage and frictional melt distribution in an exhumed seismogenic fault: quantitative high resolution data from a Digital Outcrop Model study.....	436

Pizzati M., Balsamo B. & Storti F. - Influence of accommodated displacement upon microstructural and petrophysical properties of deformation bands and gouges affecting faulted high-porosity siliciclastic sediments (Rocca di Neto fault zone, Crotona Basin, Italy)	437
Raggiunti M., Keir D. & Pagli C. - Seismicity induced by fluid migration in the Main Ethiopian Rift	438
Vadacca L., Rossi D., Scotti A. & Buttinelli M. - Understanding the hydro-mechanical interaction in active fault zones by induced seismicity studies.....	439
S19. The interplay between magmatic systems and tectonics: insights from multidisciplinary approaches.....	440
Acquafredda P., Festa V., Fornelli A., Micheletti F. & Tursi F. - Controlled behavior of anatectic melts in the deep crust by regional tectonics and metamorphic conditions	441
Casini L., Maino M. & Montserrat L. - Frictional-viscous heating in strong elliptical inclusions during simple shear.....	442
Corvo' S., Langone A., Maino M., Cuccuru S., Oggiano G. & Seno S. - Petrological and geochronological constraints of a shallow intrusion into the Variscan medium-grade metamorphic sequence of the Asinara Island (Sardinia).....	443
Cuccuru S., Conte A.M., Naitza S., Oggiano G., Secchi F. & Puccini A. - Application of <i>in-situ</i> gamma-ray spectrometry to mapping intrusive complexes: examples from Sàrrabus igneous massif (SE Sardinia, Italy).....	444
Fazio E., Fiannacca P., Lombardo R., Tomaselli L., Vilardo F. & Cirrincione R. - A combined petro-structural study assisted by UAV-survey of mafic microgranular enclaves hosted by syn-tectonic tonalites at Rovaglioso outcrop (Calabria-Peloritani Orogen)	445
Fazio E., Fiannacca P., Lombardo R. & Cirrincione R. - Interaction between deformation and crustal melt generation at the plastic-brittle transition: a perspective from exhumed pseudotachylyte-bearing mylonites	446
Fazio E., Fiannacca P., Cirrincione R. & Mantani M.A. - A combined petrofabric and AMS approach to reveal the magmatism-tectonics link in a composite batholith: an example from the Serre Massif (Calabria, Italy).....	447
Fiannacca P., Fazio E., Russo D., Cirrincione R. & Pezzino A. - Submagmatic to solid-state shear-related deformation in late Variscan granitoids from a poly-orogenic mountain belt (Peloritani Mountains, southern Italy).....	448
Filippi M., Pulcini G., Rebay G., Zanoni D., Vergani D. & Spalla M.I. - Structure and petrography of mafic dykes from Val Camonica, Orobic Alps, Italy	449
Franceschini Z., Cioni R., Corti G., Sani F., Scaillet S., Isola I., Mazzarini F., Erbello A., Muluneh A., Keir D. & Brune S. - Recent volcano-tectonic evolution of the Ririba rift (southern termination of the Main Ethiopian Rift, East Africa).....	450
Gaggero L., Maino M., Cuccuru S. & Oggiano G. - Bimodal felsic-mafic volcano-plutonic magmatism associated to intramontane basins: the late-Variscan geodynamics recorded in North Sardinia (Italy)..	451
Liotta D., Brogi A. & Dini A. - Pliocene-Quaternary granitoids in the transfer zone of the Larderello geothermal area (Italy).....	452
Lombardo R., Fiannacca P., Basei A.S. & Cirrincione R. - Origin and evolution of post-collisional mafic granitoids (Capo Vaticano Promontory, Southern Calabria): geochemical and geochronological constraints.....	453
Olvera Garcia E., Bastesen E., Bianco C., Brogi A., Caggianelli A., Garduño Monroy V.H., Liotta D., Torabi A., Wheeler W.H. & Zucchi M. - Faults controlling ore deposits distribution in the Las Minas area (Mexico)	454
Roda M. & Zanoni D. - Multidisciplinary approach to test the thermal state of Biella pluton country rocks ...	455
Spieß R., Caggianelli A., Langone A., Stuart F., Bianco C., Zucchi M., Brogi A. & Liotta D. - The cooling, deformation and exhumation history of the late Miocene syn-tectonic Porto Azzurro pluton in a transfer zone (Elba Island, Italy)	456

Visalli R., Fazio E., Ortolano G., Alsop G.I., Pagano M. & Cirrincione R. - Semi-automated fabric analysis of strong rheologically contrasting mylonitic rocks: The example from the strike-slip Palmi shear zone.....	457
Zucchi M., Brogi A., Liotta D., Ruggieri G., Fregola R.A., Matera P.F., Dini A., Morelli G., Ventruti G. & Rimondi V. - Geothermal fluids flow and storage in faulted and folded metasiliciclastics (eastern Elba Island, Italy)	458
S20. Orogenesis and orogenic wedges: a multiscale and multitechnique approach	459
Argnani A., Manzi V., Lugli S. & Roveri M. - The Calabrian Arc orogenic wedge: a Messinian reconstruction	460
Barbero E., Delavari M., Dolati A., Pandolfi L., Marroni M., Saccani E. & Catanzariti R. - The Ganj Ophiolitic Complex reinterpreted as a Late Cretaceous volcanic arc: implications for the geodynamic evolution of the North Makran domain (SE Iran)	461
Barbero E., Delavari M., Dolati A., Pandolfi L., Marroni M., Saccani E., Chiari M., Luciani V. & Catanzariti R. - Preliminary stratigraphic and petrological data on the Durkan Complex (Makran accretionary wedge, SE Iran)	462
Basso J., Artoni A., Torelli L., Polonia A., Carlini M., Gasperini L. & Mussoni P. - The Plio-Pleistocene Bradano basin and the Southern Apennine Orogenic Wedge: evidences of accretion collision and segmentation of Apulian continental plate	463
Berardo G., Bonaccorso L., De Filippis G., Di Carlo L., Di Renzo M. E., Emili E., Gencarelli G., Iammarino C., Lavaroni F., Locchi M.E., Modesti M., Mosconi F., Pardo S., Perrotta V., Pignalberi F., Rinaldi F., Ruggiero G., Solfanelli M., Tedesco C., Valente M., Scuderi M., Curzi M., Marmoni G.M., Mercuri M. & Collettini C. - The M. Tancia regional thrust: geometric, kinematic and mechanical characterization within the Structural Geology course at La Sapienza.....	464
Berio L., Balsamo F., Bistacchi A., Mittempergher S. & Storti F. - Structural and paleofluid evolution during and after the growth of the Parmelan Anticline, Bornes Massif, Western Alps	465
Bitonte R., Bellentani G., Dall'igna M., Livio F., Ciabbarri F. & Scaramuzzo E. - Validation of structural and depositional models for a reservoir study in southern Apennines: uncertainty quantification by means of discrete geological scenarios.....	466
Cerchiari A. & Fagereng A. - Low temperature cyclical switching between brittle and ductile deformation inferred from microstructural analysis of quartz shear veins	467
Curzi M., Carminati E., Aldega L., Berra F., Billi A., Van der Lelij R. & Viola G. - Architecture and evolution of an extensionally-inverted thrust (Monte Tancia thrust, central Apennines, Italy): geological, structural, geochemical, and K-Ar geochronological constraints.....	468
D'Intino N., Scisciani V. & Esestima P. - The superposition of non-coaxial extensional events in rift basins: a case study from the Utsira High	469
Federico L., Maino M., Crispini L. & Capponi G. - Paleo-depth of fault activity: testing a method based on inversion of fault-slip data.....	470
Lacombe O. - Thick-skinned tectonics in orogenic forelands: the external western Alps and the western US Laramide Province case studies.....	471
Lucca A., Storti F., Balsamo F., Clemenzi L., Fondriest M., Burgess R. & Di Toro G. - Out-of-sequence thrusting from marine to phreatic conditions in the Gran Sasso Massif, Central Apennines, Italy	472
Panini F., Bettelli G., Carlini M., Fioroni C., Nirta G. & Remitti F. - A new geological map of the high Sillaro Valley (Northern Apennines, Italy)	473
Rossi F.P., Corrado S., Lugli S., Manzi V., Reghizzi M., Roveri M. & Schito A. - Multiproxy Burial and Exhumation Numerical Modelling of the late Miocene succession of the Eastern Romagna Apennines: implications for Messinian salinity crisis-related deposits diagenetic products	474
Sabbatino M., Vitale S., Consorti L., Corradetti A., Arienzo I., Cipriani A. & Parente M. - Multidisciplinary study of the Miocene forebulge unconformity in central-southern Apennines	475
Sternai P. - Present-day uplift of the European Alps: mechanisms and relative contributions.....	476

Succo A., Mittempergher S., Lucca A., Bistacchi A., Meda M. & Storti F. - From layer-parallel shortening and duplexing to fold tightening and strike-slip compartmentalization in the External Dinarides orogenic wedge: the case of platform carbonates folded in the Pag anticline.....	477
Tavani S., Corradetti A., Sabbatino M. & Mazzoli S. - Geological record of the transition from induced to self-sustained subduction in the Oman Mountains.....	478
Velicogna M., Princivalle F., Petrelli M., Venier M. & Lenaz D. - U-Pb detrital zircon geochronology of Cretaceous-Eocene flysch basins of the N-E Adria plate	479
S21. Active tectonics and seismotectonics between Northern Apennines and Southern Alps as a complex thrust belt - foredeep system	480
Bonadeo L., Frigerio C., Ferrario M.F., Livio F., Michetti A.M., Bitonte R., Scaramuzzo E., Zerboni A., Porat N., Fioraso G., Irace A., Catanzariti R., Da Prato S., Ellero A. & Ottria G. - A multidisciplinary approach to the structural setting and morphotectonics of the Eastern Monferrato Arc: new constraints to the seismic hazard assessment of a slowly deforming area	481
Bragato P.L. - Tectonic cycles over a human lifetime: multi-decadal periodicity of strong seismicity in Italy (Alps-Apennines system)	482
Busetti M., Zgur F., Dal Cin M., Vrabec M., Baradello L., Böhm G., Brancatelli G., Caffau M., Furlani S., Picotti S. & Zampa L.S. - The effects of the Cenozoic Dinaric and Alpine orogenies in the Gulf of Trieste (North Adriatic Sea).....	483
Cheloni D., Giuliani R., D'Agostino N., Mattone M., Bonano M., Fornaro G., Lanari R., Reale D. & Atzori S. - Active seismotectonics of the Northern Apennines: insights from the 2012 Emilia earthquake sequence.....	484
Dal Cin M., Busetti M., Böhm G., Picotti S., Zgur F. & Camerlenghi A. - 3D velocity depth model and seismic imaging of geological structures in the Gulf of Trieste (North Adriatic Sea), at the south-western edge of Dinarides and Alps	485
Galderisi A., Galli P. & Trotta O. - Evidence of surface ruptures along the Norcia fault during the Mt. Vettore fault earthquake. Passive activation induced by Coulomb stress change?	486
Mascandola C., Massa M., Barani S., Albarello D., Lovati S., Martelli L., Poggi V. & Morasca P. - Seismo-stratigraphic model of the Po Plain (Italy).....	487
Mele M., Zuffetti C., Aliverti Piuri E., Bersezio R., Giudici M., Comunian A. & Contini D. - Geophysical imaging of a buried faulted anticline: the San Colombano hill, southern Po Plain of Lombardy (Northern Italy).....	488
Nirta G., Piccardi L., Bonini M., Corti G., Montanari D., Moratti G. & Sani F. - Active normal faulting in the Garfagnana and Lunigiana basins. New geomorphic and geological constraints	489
Patricelli G. & Poli M.E. - Seismotectonic characterization of active faults in the LGM plain between Udine and Pozzuolo (Friuli, NE Italy)	490
Romano M.A., Peruzza L., Garbin M., Priolo E. & Picotti V. - The Montello thrust image obtained with a dense, high-quality seismic network (Southeastern Alps, Italy)	491
Sbarra P., Burrato P., Tosi P., Vannoli P., De Rubeis V. & Valensise G. - A new approach to estimate the depth of historical earthquakes: seismotectonic implications for the Northern Apennines and the southern Po Plain.....	492
Scaramuzzo E., Livio F., Di Capua A. & Bitonte R. - Crustal wedge structure in the Mt. Campo dei Fiori Area (Lugano - Lake Maggiore area): foredeep implication.....	493
Serpelloni E., Anderlini L., Pintori F., Vannucci G., Tolomei C., De Martini P.M. & Pezzo G. - Kinematics and seismic potential of the Eastern Southern Alps from space geodetic data.....	495
Teloni S., Invernizzi C., Costa M. & Pierantoni P.P. - Seismogenic structures in the onshore-offshore Padano-Adriatic foothills between Emilia Romagna and Marche: a tentative modelling for the evaluation of risks in seismically quiet areas	496
Tirincanti E., Roccheggiani M. & Menichetti M. - Geometry and kinematics of the Umbro-Marchean Apennines in the Adriatic foreland.....	497

Zampieri D., Burrato P. & Vannoli P. - The Schio-Vicenza fault system: field and seismological evidences and open questions.....	498
Zanchi A., Deaddis M., De Amicis M., Marchetti M., Ravazzi C. & Vezzoli G. - The Holocene deformed succession of Montodine (Cremona, Italy): evidence of recent tectonic activity?.....	499
Zuffetti C. & Bersezio R. - Late Quaternary sedimentation and tectonics in the Po Basin: field evidences at the Po Plain-Apennines border (Lombardy).....	500
S22. From seismic source to fault using multidisciplinary approaches: the central and southern Apennines as natural laboratory	501
Barreca G., Scarfi L., Gross F., Monaco C. & De Guidi G. - Fault pattern and seismotectonic potential at the south-western edge of the Ionian Subduction system (southern Italy): new field and geophysical constraints	502
Brozzetti F., Mondini A.C., Pauselli C., Mancinelli P., Cirillo D., Guzzetti F. & Lavecchia G. - Mainshock anticipated by intra-sequence ground deformations: insights from multiscale field and SAR interferometric measurements	503
Buttinelli M., Petracchini L., Maesano F.E., Scrocca D., D'Ambrogi C., Di Bucci D., Marino M., Capotorti F., Cavinato G., Bigi S. & RETRACE-D working group,, - The impact of high structural complexity on seismotectonics: hints and lessons learned in the areas of the 2016-2018 central Italy seismic sequence in the framework of the RETRACE-3D project	504
Caporali A., Zurutuza J. & Bertocco M. - A time dependent model of elastic stress in the Central Apennines, Italy	505
Cirillo D., Brozzetti F., de Nardis R., Lavecchia G., Orecchio B., Presti D. & Totaro C. - Multidisciplinary approach for 3D fault geometry reconstruction: an example from Calabrian-Lucanian boundary in the Mt. Pollino area (Southern Apennines-Italy).....	506
Cortinovis S., Balsamo F., Fondriest M., La Valle F. & Di Toro G. - Structural architecture and microstructural properties of the seismogenic Monte Marine fault zone, central Apennines (Italy)	507
De Guidi G., Barreca G., Bella D., Brighenti F., Carnemolla F., Figlioli A., Menichetti M., Roccheggiani M. & Monaco C. - Multidisciplinary survey methods of the Fiandaca-Pennisi fault zone reactivated during the 26th December 2018 coseismic and postseismic event	508
de Nardis R., Pandolfi C., Monachesi G., Cattaneo M., Marzorati S., Cirillo D., Ferrarini F., Brozzetti F. & Lavecchia G. - High-sampling of multi-layered crust-scale seismogenic deformation in Central-Eastern Italy.....	509
Ferranti L., Pepe F., Barreca G., Meccariello M. & Monaco C. - Multi-temporal tectonic evolution of Capo I Granitola and Sciacca foreland transcurrent faults (Sicily channel)	510
Forlano S., Ferranti L. & Milano G. - Recent and active tectonics in the Campanian Plain based on integration of fault kinematics and seismological data: preliminary results	511
Lavecchia G., de Nardis R., Pandolfi C., Monachesi G., Cattaneo M., Marzorati S., Cirillo D., Ferrarini F. & Brozzetti F. - Three-dimensional pattern of lithospheric compression in central Italy – Geodynamic implication.....	512
Maraio S., Villani F., Serri L., Sapia V., Improta L. & Bruno P.P. - Ultra-shallow imaging of a surface rupture fault of the 30 October 2016 Mw 6.5 central Italy earthquake from multidisciplinary geophysical approach	513
Menichetti M., Tirincanti E. & Roccheggiani M. - Earthquake ruptures geometries as tools for seismic hazard assessment.....	514
Montone P. & Mariucci M.T. - The shallow crust in Central Italy depicted by geophysical deep well logs	515
Nappi R., Paoletti V., Gaudiosi G., Luiso P., Cella F., Florio G. & Fedi M. - A multi-method approach to characterize the geometry of the Paganica and Matese seismogenic faults (Central-Southern Apennines, Italy).	516
Porreca M., Fabbrizzi A., Azzaro S., Pucci S., Del Rio L., Pierantoni P.P., Giorgetti C., Roberts G. & Barchi M.R. - 3D reconstruction of the M. Vettore seismogenic fault system (Central Apennines, Italy): cross-cutting relationship with the M. Sibillini Thrust.....	517

Puliti I., Pizzi A., Benedetti L., Di Domenica A. & Fleury J. - Evolution of an active fault system in an extensional context: the case of the Mt. Vettore system in the central Apennines and insights in its segmentation pattern.....	518
Scarpa R. - The southern Italy 1980 earthquake and the rupture processes of large earthquakes in Italy.....	519
Trippetta F., Barchi M.R., Borromeo O., Mastellone D., Rosset G. & De Paola N. - Seismic velocity variations of carbonates across the Apennines	520
Villani F., Maraio S., Bruno P.P., Improta L., Wood K., Civico R., Baccheschi P., Sapia V., Pucci S., Brunori C.A., De Martini P.M., Pantosti P.M., Conti P. & Doglioni C. - High-resolution seismic profiling in the Castelluccio basin: new constraints on the shallow subsurface of the 30 October 2016 Mw 6.5 Norcia earthquake fault (central Italy).....	521
Zambrano M., Corradetti A., Tavani S., Pitts A., Seers T.D. & Tondi E. - Roughness evaluation of the Monte Vettoreto active fault after the massive 2016 seismic sequence of Central Apennines, Italy	522
S23. Analogue and numerical modelling of geological processes: linking observation, interpretation and prediction	523
Cocco F. & Funedda A. - An attempt at modelling the lithosphere of Sardinia block and surroundings: relationships among isostatic disequilibrium, geomorphic features and neotectonics.....	524
Corbi F. - Improving subduction megathrusts seismic hazard assessment: a proof of concept based on analog modelling and machine learning.....	525
Corti G., Nencini R. & Skyttå P. - Modelling the influence of pre-existing brittle fabrics on the development and architecture pull-apart basins	526
Lanzi C., Trasatti E. & Battaglia M. - Unveiling the engine of mid-term deformations at Ischia resurgent caldera (Italy) using remote sensing and in situ data.....	527
Maestrelli D., Bonini M., Corti G., Montanari D. & Moratti G. - Collapsed calderas vs inherited fabrics: insights from analogue modelling	528
Maestrelli D., Bonini M., Corti G., Montanari D. & Moratti G. - Interplay between rift propagation and inherited crustal fabrics: a case study from the Trans-Mexican Volcanic Belt (Mexico).....	529
Massaro L., Adam J. & Jonade E. - New Granular Rock-Analogue Materials (GRAM) for simulation of multi-scale fault and fracture processes.....	530
Regorda A., Lardeaux J.-M., Roda M., Marotta A.M. & Spalla M.I. - How many subductions in the Variscan orogeny? Insights from numerical models	531
Ruch J. - Combining analogue experiments with ground deformation from space to study volcano tectonic processes.....	532
Spreafico M.C., Sternai P. & Agliardi F. - Rock-slope failure after deglaciation: rapid response or progressive long-term evolution? Insights from numerical modelling	533
Zwaan F., Corti G., Keir D. & Sani F. - Factors controlling the structural architecture of continental rift margins: insights from analogue centrifuge models.....	534
S24. Geology-hydrogeology of karst environments and modeling of preferential flow in variably saturated fractures.....	535
Arcari A., Dall'Aglio M., Balsamo F., Menezes D., Bagni F. & Bezerra F.H.R. - Structural control on karst system in folded layered carbonates, Potiguar basin, NE Brazil.....	536
Berardi M., Vurro M. & Portoghese I. - Modeling hydraulic conductivities of an infiltration trench.....	537
Bordoni M., Valentino R., Meisina C. & Bittelli M. - Detailed analysis of soil-atmosphere interactions in two sample sites in Oltrepò Pavese	538
Caputo M.C., Nimmo J.R. & Perkins K.S. - Characterization of Episodic Recharge in a Fractured and Karst Coastal Aquifer by Episodic Master Recession Analysis.....	539
Caputo M.C., De Carlo L., Masciale R., Perkins K.S. & Turturro A.C. - Combined approaches to provide evidence of preferential flow in a layered vadose zone during artificial rainfall	540

Gentile P., Iaia C., Liso I.S. & Parise M. - Occurrence of flash floods in the karst environment of Apulia (Southern Italy).....	541
Liso I.S. & Parise M. - Micro-climatic aspects at the karst system of Vora Bosco (Salento, Southern Italy)....	542
Liso I.S., Masciopinto C. & Parise M. - Hydrogeological model to study natural water flow in karstified and fractured aquifers.....	543
Martinelli G. & Tamburello G. - Influence of tectonic CO ₂ degassing on the occurrence of earthquake precursors.....	544
Nimmo J.R. & Perkins K.S. - Preferential flow dynamics in unsaturated zone hydrology.....	545
Perkins K.S. & Nimmo J.R. - Estimation of Preferential Flow Contributions to Aquifer Recharge Based on Hydrograph Analysis.....	546
Piccini L. & Poggetti E. - Hydrodynamic of karst springs in metamorphic carbonate rocks: the case of Apuan Alps (Tuscany, Italy).....	547
Pintori F., Serpelloni E., Longuevergne L., Belardinelli M.E., Gualandi A. & Scoccimarro E. - Water storage changes and crustal deformation in karst regions: examples from the Venetian Southern Alps.....	548
Turturro A.C., Nimmo J.R., Perkins K.S. & Caputo M.C. - Evidence of No Preferential Flow in Porous Rock by Testing the Validity of the Darcy-Buckingham Law in a Centrifugal Field.....	549
Vigna B. & Fiorucci A. - Conceptual models related to underground circulation in carbonate aquifers ¹	550
Wang X. & Jourde H. - Numerical models of karst processes.....	551
Zucchini A., Cirilli S., Comodi P., Mitillo N., Lanzafame G. & Frondini F. - The influence of the dolomitization process on texture and porosity of carbonates.....	552
S25. Geosciences for disaster risk reduction: problems, solutions and perspective.....	553
Allasia P., Godone D., Wrzesniak A., Notti D., Baldo M., Faccini F., Elter F.M. & Poggi F. - The importance of integrated monitoring approach: the case study of Arzeno (Graveglia Valley - Ligurian Apennine, Italy).....	554
Alvioli M., Guzzetti F. & Marchesini I. - Automatic delineation of slope units and terrain classification of Italy.....	555
Brunetti M.T., Peruccacci S., Rossi M., Marchesini I., Denti B., Solimano M., Martinotti M.E., Balducci V. & Guzzetti F. - Regional landslide early warning systems in Italy.....	556
Buondonno E., Cubellis E., Delizia I., Luongo G. & Ricci F. - Ischia Island: a model for sustainable development and natural risk mitigation.....	557
Cappello A., Ganci G., Bilotta G., Corradino C., Hérault A. & Del Negro C. - Assessing lava flow risk at Etna volcano.....	558
Chiappetta G.D., Gervasi A., Festa R.L. & La Rocca M. - Seismic site effects in the area of Tortora (Northern Calabria).....	559
Fiorucci F., Ardizzone F., Santangelo M., Bucci F., Allasia P., Alvioli M., Baldo M., Bianchi C., Brunetti M.T., Cavalli M., Clerissi F., Crema S., Donnini M., Giordan D., Guzzetti F., Marchesini I., Marchi L., Melillo M., Mondini A.C., Peruccacci S., Reichenbach P., Rossi M., Salvati P. & Cardinali M. - The 2016 Central Italy Seismic Sequence: emergency and post-emergency activities.....	560
Gioia E. & Marincioni F. - Analyzing flood risk perception to connect forecasting and alert agencies with the community: the case of the life primes project.....	561
Gioia E. & Marincioni F. - A comparison between empirical landslide predictive models applied to the Marche region (Central Italy).....	562
Giuffrè M., Benigni M.S., Coltella M., Martelli L., Pietrosante A. & Romani M. - Seismic microzonation and analysis of the Emergency Limit Condition - Useful tools for the seismic risk mitigation.....	563
Grezio A., Ardizzone F., Bucci F., Guzzetti F. & Marzocchi W. - Seismic- and Meteo-induced Landslides in Emilia Romagna.....	564
Marchesini I., Salvati P., Rossi M., Donnini M., Guzzetti F., Sterlacchini S., Zazzeri M., Cappellini G. & Voltolina D. - A statistical procedure used for the flood hazard zonation at national scale.....	565

Martinotti M.E., Marchesini I., Rossi M., Peruccacci S. & Guzzetti F. - Local indexes, based on a nationwide threshold, for rainfall-induced landslides	566
Marzocchi W., Falcone G. & Taroni M. - Progresses and challenges for Operational Earthquake Forecasting in Italy.....	567
Meletti C., Marzocchi W., D'Amico V., Luzi L., Martinelli F., Pace B., Rovida A., Visini F. & MPS Working Group - MPS19: the updated seismic hazard model of Italy as an example of state-of-the-art in PSHA	568
Pepe A., Zhao Q., Kubanek J., Falabella F., Yin J., Yu D., Lin N., Ma G. & Liu M. - Differential Synthetic Aperture Radar Experiments over the Ocean-Reclaimed Lands of Shanghai: Long-term flood Hazard Modeling and Urban Infrastructure Monitoring	569
Peruccacci S., Brunetti M.T., Gariano S.L., Melillo M., Rossi M. & Guzzetti F. - National and regional empirical rainfall thresholds for possible shallow landslide occurrence in Italy	570
Porfido S., Nappi R., Gaudiosi G., Alessio G. & Michetti A.M. - Between ethics and territorial planning: the value of the ESI-2007 scale.....	571
Rossi M., Guzzetti F., Salvati P., Donnini M., Napolitano E. & Bianchi C. - Modelling societal landslide risk in Italy.....	572
Rossi M., Marchesini I., Martinotti M.E., Brunetti M.T., Peruccacci S., Balducci V. & Guzzetti F. - Landslide early warning: lessons learned after 10-year experience in Italy.....	573
Sterlacchini S., Zazzeri M., Cappellini G., Voltolina D., Marchesini I., Salvati P., Rossi M., Donnini M. & Guzzetti F. - A GIS-based application to support decision makers in preparedness and response to flood-related risks	574
Versace P., Capparelli G., Spolverino G. & Galasso L. - Laboratory tests on pyroclastic soil to simulate the infiltration processes responsible of landslide trigger	575
Versace P., Capparelli G., Biondi D., Cruscomagno F., Vacha D. & Galasso L. - People's vulnerability to floods: the EVIL model	576
S26. Approaches for evaluation and protection of groundwater resources.....	577
Apollaro C., Fuoco I., De Rosa R., Vespasiano G., Gabriele B., Mancuso R., Criscuoli A. & Figoli A. - Natural polluted waters in Calabria Region (Italy): preliminary data on arsenic contamination and treatment	578
Barbagli A., Guastaldi E., Giannuzzi M., Borsi I., Lotti F., Basile P., Schembri M. & Sapiano M. - 3-Dimensional geological reconstruction of the Maltese archipelago geology as a tool for a better understanding on the main Maltese groundwater bodies	579
Barbero D., Bucci A., De Luca D.A., Forno M.G. & Lasagna M. - A new thermal model of the shallow aquifer by statistical temperature distribution in the Piedmont Po Plain (NW Italy).....	580
Barbero D., Bucci A., De Luca D.A., Forno M.G. & Lasagna M. - Thermal data as a tool for groundwater flow velocity determination in aquifer recharge areas.....	581
Capizzi P., Martorana R., Favara R., Albano L., Bonfardeci A., Costa N. & Gagliano A.L. - Geophysical and hydrological model of "Barcellona-Milazzo plain" groundwater body	582
Chiaudani A., Di Curzio D. & Rusi S. - The role of snow melting and rainfall on the discharge and physico-chemical characteristics of springs: a statistical analysis in Central Apennines	583
Corniello A., Del Gaudio E., Ducci D. & Stellato L. - The well fields of the Maggiore e Tifata mountains (Campania Region): new hydrochemical and isotopic data	584
Deluca F., Mongelli G., Paternoster M., Sinisi R. & Zhu Y. - Rare earth element speciation in volcanic groundwater: the Mount Vulture aquifer (Southern Italy).....	585
Di Curzio D. & Rusi S. - Stationary and non-stationary geostatistics to model 3-D hydraulic conductivity distribution: a case study in the southern Po river plain.....	586
Ducci D. & Sellerino M. - A Modified AVI Model to Map Groundwater Vulnerability to Contamination: case studies in Southern Italy	587

Iván V., Masetti M., Mádl-Szőnyi J., Pollicino L.C. & Stevenazzi S. - Spatial and statistical analysis of factors influencing groundwater vulnerability on the study area of the Gömör-Torna Karst (Hungary and Slovakia)	588
Petrella E., Chiari A., Segadelli S. & Celico F. - Hydrogeological and isotopic characterization of an ophiolite aquifer (Monte Zirone, Northern Apennines, Italy)	589
Portoghese I., Demichele F., Fidelibus D. & Vurro M. - Infiltration ponds adopted for treated wastewater disposal: a risk-assessment approach in the Apulia region.....	590
Raimondo M., Chelli A., Celico F., Iacumin P. & Petrella E. - Hydrogeological and isotopic investigation to define the hydrological behaviour of a complex landslide: a case study in the Northern Apennines (Italy)	591
Severini E., Pinardi M., Racchetti E., Celico F. & Bartoli M. - Evidences of diffuse water and nitrate input via river-groundwater interactions in a regulated river: flood irrigation as main driver?	592
Stellato L., Allocca V., Arienzo M., Coda S., De Vita P., Di Rienzo B., D’Onofrio A., Ferrara L., Marzaioli F. & Trifuoggi M. - Multi-disciplinary study to characterize groundwater flow processes and quality in an agriculture impacted volcanic-sedimentary coastal aquifer in the archaeological site of Cumae (Phlegraean Fields, southern Italy).....	593
Vespasiano G., Apollaro C., Muto F., Tripodi V., Fuoco I., Dotsika E. & De Rosa R. - Hydrogeochemical, isotopic and geological characterization of the thermal areas in the Calabria region	594
S27. Geologic and geothematic mapping in a dynamic country: maps, database and data dissemination.....	595
Bahrambeygi B., Moeinzadeh H. & Alavipanh SK. - Effect of types of Atmospheric corrections on Hyperspectral processing in lithology mapping, Case study of Iranian S-E Ophiolitic lithology	596
Berti D., Basi M., Bonomo R., Marino M., Pampaloni M.L., Ricci V., Rossi M., Silvestri S. & Urbani A. - Geological mapping and first level seismic microzonation in Abruzzo: case studies in the Aventino basin (southern Abruzzo).....	597
Carta R., Muraro C., Bonomo R., D’Angelo S., Martarelli L., Papasodaro F., Ricci V. & Vita L. - The Lithological Database of the CARG Project	598
Conti P., Cornamusini G. & Carmignani L. - Geological map of the Italian Northern Apennines (Emilia-Romagna, Marche, Tuscany, Umbria regions) at 1:250.000 scale, with GIS vector data	599
d’Atri A., Barale L., Borghi A., Dino G., Favero-Longo S.E., Gambino F., Giardino M., Lombardo V., Martire L., Perotti L. & Piana F. - The Piemonte Ornamental Stones geodatabase compliant with the “GeoPiemonte Map” web-GIS service.....	600
Federico L., Scarsi M., Crispini L., Piazza M. & Capponi G. - Mapping a HP belt and its sedimentary cover: interplay between tectonics and sedimentation (Ligurian Alps, Italy)	601
Funari V., Rizzieri A. & Dinelli E. - SuoliBo-HD: preliminary results of the high-density magnetic mapping of the Bologna topsoils from the public green and other outcropping urban soils.....	602
Montepeloso M., Zanchetta S., Berio L. & Zanchi A. - Geological-Structural map of the Late Carboniferous – Early Permian Orobic basin in the upper Brembana Valley (Orobic Alps, N Italy).....	603
Taussi M., Borghi W., Gliaschera M., Del Moro S., Di Gregorio A. & Renzulli A. - Defining the potential of Ground Source Heat Exchanger (GSHE) through a geological-based thermal modelling: a GIS approach applied to Fano Municipality (Marche region, Italy).....	604
Vennari C., Casarano D., Marchesini I., Salvati P., Parise M. & Lollino P. - A regional geodatabase on landslide, flood and sinkholes for civil protection application.....	605
S28. Geomorphological Hazards and Cartography.....	606
Bonomo A.E., Prosser G., Rizzo G., Bentivenga M. & Acito A.M. - The negative space: a geological journey into an open pit quarry.....	607
Bordoni M., Lucchelli L., Corradini B. & Meisina C. - Reconstruction of lithotechnical terrain units for the assessment of shallow landslides hazard in Oltrepò Pavese (northern Italy).....	608

Bosino A., Bernini A., Botha G., Omran A., Pellegrini L. & Maerker M. - Using web-based applications to enhance traditional geomorphic mapping: a case study of the Upper Mkhomazi River basin, KwaZulu-Natal, South Africa.....	609
Cafiso F., Cappadonia C., Rotigliano E. & Sulli A. - Seismic-induced rockfalls: Correlations between the slope aspect and seismic source.....	610
Conoscenti C., Martinello C., Agnesi V. & Rotigliano E. - Gully erosion susceptibility maps in Sicily through data mining techniques	611
Gemignani C.A., Giacomelli S., Leonelli G. & Chelli A. - Historical maps as source of information on temporal distribution of landslide events in the Northern Apennines	612
Giacomelli S., Lammoglia T. & Sgavetti M. - A SRTM-based geomorphometric analysis aimed at (neo) tectonics activity detection: a case study from an intracratonic area (Mato Grosso, Brazil)	613
Giacomelli S., Sgavetti M., Bertoni D., Rossi V., Lammoglia T., Leonelli G. & Chelli A. - Integrated use of geomorphological and open-access remote sensing data: examples from different case studies.....	615
Guarino P.M., Amanti M., Chiessi V., Fiano V., Guarneri E.M., Marasciulo T., Olivetta L., Pistocchi L., Roma M., Serafini R. & Vitale V. - Landslides in the Sibillini Mountains National Park (Central Apennines, Italy)	616
Guerra C., Guerra V. & Nesci O. - Geomorphological cartography in urban coastal settlements: the Rimini town case history (Emilia-Romagna, Italy).....	617
Ivy-Ochs S., Martin S., Viganò A., Campedel P., Rossato S., Vockenhuber C. & Rigo M. - Historic and pre-historic landslide activity along the lake Garda - Brenta Group channel area (NE Italy)	618
Leonelli G., Celico F., Petrella E., Francese R. & Chelli A. - Integrating GIS and tree-ring techniques for characterizing surface movements of landslides in the Northern Apennines: challenges, strengths and limitations at the Carobbio study site	619
Martinello C., Rotigliano E., Conoscenti C. & Agnesi V. - Investigation of prediction errors in the landslide susceptibility statistical models through multiple nested MARS analyzes: application in the Caldera area of Ilopango (El Salvador, C.A.)	620
Nsengiyumva J.B., Valentino R., Sobio Y., Mizero J., Nsengiyumva F., Bordoni M. & Meisina C. - Site-specific to large-scale landslides susceptibility assessment in Rwanda	621
Rossi M., Santangelo M., Alvioli M., Marchesini I., Cardinali M., Bucci F. & Fiorucci F. - Composite landslide susceptibility maps.....	622
Rotigliano E., Martinello C., Cappadonia C. & Agnesi V. - Integrating pixel analysis into slope units landslide susceptibility mapping: an application to the Imera river basin	623
Valletta A., Cavalca E., Savi R. & Segalini A. - Advantages of innovative automatic inclinometers applied to landslides monitoring for early warning activities	624
S29. Recent advances in fluid geochemistry in active volcanic and geothermal areas: following Mariano Valenza	625
Aiuppa A. - Global trends in volcanic gas composition	626
Bini G., Chiodini G., Cardellini C., Vougioukalakis G.E. & Bachmann O. - Estimating the energetic budget of hydrothermal systems using diffuse emission of CO ₂ : the case of Nisyros (Greece).....	627
Brugnone F., Calabrese S., D'Alessandro W., Li Vigni L. & Parello F. - The impact of Mt. Etna's ash plume on the chemical composition of meteoric deposition	628
Cabassi J., Capecciacci F., Magi F., Vaselli O., Tassi F., Montalvo F., Esquivel I., Grassa F. & Caprai A. - Water and dissolved gas geochemistry at Coatepeque, Ilopango and Chanmico volcanic lakes (El Salvador, Central America)	629
Calabrese S., Li Vigni L., Brugnone F. & Capasso G. - The precious "scientific heritage" of Mariano Valenza: the unknown history of Ludovico Sicardi and the birth of the modern volcanology	630
Cardellini C., Chiodini G., Frondini F., Caliro S., Avino R., Bagnato E., Beddini G. & Rosiello A. - Carbon dioxide diffuse emission in volcanic and hydrothermal areas: monitoring volcanic activity and impact on carbon global emissions.....	631

Chiodini G. & Caliro S. - Magma degassing episodes at volcanoes in hydrothermal activity.....	632
Chiodini G., Beddini G., Caliro S., Cardellini C., Frondini F. & Rosiello A. - Measuring and interpreting CO ₂ and advective heat fluxes at regional scale: the case of Apennines, Italy.....	633
Di Martino R.M.R., Camarda M. & Gurrieri S. - The monitoring of hydrogen and carbon dioxide at Stromboli volcano.....	634
Di Martino R.M.R., Capasso G. & Camarda M. - The on-field measurements of ¹³ C/ ¹² C of the CO ₂ improve the consolidated practices of volcano monitoring.....	635
Falcone E.E., Federico C., Boudoire G., Brusca L., Bellomo S. & Saiano F. - Geochemistry of trace metals and REE in low temperature hydrothermal areas in Vulcano Island (Aeolian Islands, Italy).....	636
Fazi S., Tassi F., Rossetti S., Pratesi P., Ceccotti M., Cabassi J., Capechciacci F., Venturi S. & Vaselli O. - The microbial community structure in a meromictic volcanic lake (Lake Averno, Italy).....	637
Federico C., Bellomo S., Brusca L., Calabrese S., D'Alessandro W., Falcone E.E. & Longo M. - Bioavailability of trace and ultratrace elements in soils in the Mt. Etna volcanic area: the role of the emission source and insights on their mobility in the interstitial solution.....	638
Fuoco I., Apollaro C., Vespasiano G., Timpano A., Cundari F. & De Rosa R. - Chemical weathering rates and CO ₂ consumption in the eastern sector of Sila Massif (Calabria, Italy) inferred from riverine water chemistry.....	639
Gagliano A.L., Daskalopoulou K. & D'Alessandro W. - New perspectives in geothermal CH ₄ output estimation.....	640
Grezio A., Costa A., Rouwet D. & Chiodini G. - Modelling the dynamics of volcanic lakes: Nyos Lake (Cameroon) and Albano Lake (Italy).....	641
Lelli M., Taramaeli M., Ariph K., Sadock J., Pisani P., Pasqua C., Principe C., Mnzava F., Armadillo E., Rizzello D. & Mkangala A. - Relationships between CO ₂ soil degassing and regional/local fault systems in the Kiejo-Mbaka geothermal prospect (Tanzania).....	642
Li Vigni L., D'Alessandro W., Cardellini C., Daskalopoulou K., Calabrese S. & Brugnone F. - Preliminary study on geogenic degassing through the big karstic aquifers of Greece.....	643
Mancini A., Frondini F., Capezuoli E., Galvez Mejia E., Lezzi G., Matarazzi D., Brogi A. & Swennen R. - Travertine masses from western Central Italy and natural Earth degassing: an approach to evaluate the geogenic CO ₂ flux.....	644
Meloni F., Vaselli O., Nisi B., Rappuoli D., Cabassi J. & Bianchi F. - Geochemical features of the shallow aquifer in the former mining area of Abbadia San Salvatore (Tuscany, central Italy).....	645
Moretti R., Moune S.--, Robert V., Bonifacie M., Jessop D.-- & Komorowski JC. - A geochemical reappraisal of the hydrothermal system of La Soufrière of Guadeloupe (French West Indies) with implications for unrest.....	646
Nicodemi L., Brogi A., Capezuoli E., D'Orazio M., Fulignati P. & Zanchetta G. - Unravelling hypogean mineralizing fluids from the geochemistry of epigeal travertines: insights from central-southern Tuscan (Italy).....	647
Procesi M., Cinti D., Cabassi J., Capechciacci F., Caracausi A., Pizzino L., Fazi S. & Casentini B. - Does the anthropogenic lake Ex-Snia, in the centre of Rome, simulate the characteristics of a volcanic lake?.....	648
Randazzo P., Caracausi A., Apollaro C., Cardellini C., Chiodini G., Paternoster M., Rosiello A. & Aiuppa A. - Fluid geochemistry and CO ₂ output in the southern Apennine (Italy): Preliminary results.....	649
Rosiello A., Cardellini C., Chiodini G., Frondini F. & Caliro S. - CO ₂ Earth Degassing in Southern Italy: quantification and source identification of the main regional aquifers of the Southern Apennines and Gargano Promontory.....	650
Rouwet D., Tamburello G., Procesi M., Venturi S., Santi A., Chiodini G., Pecoraino G., Ricci T., Cabassi J. & Tassi F. - Resuming volcanic surveillance at Lake Albano: updates on the dissolved gas content and vertical temperature profiles.....	651
Ruggieri G., Orlando A. & Borrini D. - The synthesis of fluid inclusions: from the lab to geothermal wells...	652
Tamburello G. & Carbonara N. - Distribution of the thermal springs in the world in relation to active volcanic and tectonic areas.....	653

Tassi F. - Past and present of geochemical investigations on meromictic volcanic lakes: hints for the next future.....	654
Tassi F., Inostroza M., Sepúlveda J., Capecchiacci F. & Aguilera F. - Preliminary geochemical investigation of the Colpitas hydrothermal system, northern Chile.....	655
Tassi F., Cabassi J., Andrade C., Callieri C., Silva C., Viveiros F., Corno G., Vaselli O., Selmo E., Gallorini A., Ricci A., Giannini L. & Cruz J.V. - Mechanisms regulating CO ₂ and CH ₄ dynamics in the Azorean volcanic lakes (São Miguel Island, Portugal)	656
Venturi S., Cabassi J., Butturini A., Vazquez E., Pacini N., Tassi F., Vaselli O., Amalfitano S., Crognale S., Rossetti S., Harper D.M., Capecchiacci F. & Fazi S. - Tropical saline-alkaline lakes as a major source of greenhouse gases: evidence from lake Sonachi, Kenya	657
S30. Legacy and new applications of stable-isotope geochemistry.....	658
Boito M., Iacumin P. & Ogrinc N. - The link between groundwater and milk in the Parmigiano-Reggiano cheese production area: validation with the isotopic analysis for food traceability.....	659
Cavazzini G. - Inter-measurement determination of the isotopic composition of Sr (II).....	660
Dordoni M., Pennisi M., Agostini S., Dini A., Di Giuseppe P., Rielli A., Provenzale A., Bianchini G., Natali C., Marchina C. & Cidu R. - First isotopic analyses in fluid samples using MC-ICP-MS (NEPTUNE PLUS™): results on Boron-poor fluvial and rain water (Adige basin)	661
Doveri M., Stenni B., Gianecchini R., Petrini R., Ghezzi L., Dreossi G. & Menichini M. - Characteristics of hydrogen and oxygen stable isotopes in water from an area impacted by past-mining activity in southern Apuan Alps (Italy).....	662
Ghezzi L., Petrini R., Castorina F., Scotti C., Ottria G. & Bartelletti A. - Trace element composition and Sr-isotope ratio in wine, must and soil from a high-altitude vineyard in the Apuan Alps UNESCO Global Geopark (Italy).....	663
Lutman A., Petrini R. & Ghezzi L. - Chromium-isotope systematics, new insights from a contaminated area in the Friuli Venezia-Giulia Region.....	664
Maccelli C., Avanzinelli R., Casalini M., Nisi B., Vaselli O. & Mason P. - Heavy metals in surface waters and suspended solids from the Usciana River (Tuscany, central Italy).....	665
Macri A. & Iacumin P. - Paleoclimate reconstruction using freshwater organisms from prehistoric shell midden	666
Pennisi M., Agostini S., Dini A., Dordoni M., Di Giuseppe P., Rielli A., Provenzale A. & Rodushkin I. - Boron isotopic analyses in fluid samples - PTIMS <i>VERSUS</i> MC-ICP-MS (Neptune PLUS™).....	667
Regattieri E., Zanchetta G., Drysdale R.N., Giaccio B., Isola I., Mannella G., Nomade S. & Hellstrom J.C. - Hydrological significance of δ ¹⁸ O composition of speleothems and lakes carbonates from Apennine sites (Italy): a coherent hydrological framework for the Last Interglacial period.....	668
Rodushkin I., Pallavicin N. & Engström E. - Novel application of MC-ICP-MS for stable isotope measurements	669
Varrica D., Tamburo E., Alaimo M.G., Losno R. & Monna F. - Use of lead isotopic fingerprint in human scalp hair to identify potential sources of pollution in industrial Sicilian sites (Italy).....	670
Vaselli O., Tarchiani U., Nisi B. & Cabassi J. - Geochemical and isotopic investigation on underground waters affected by high sulfate contents.....	671
S31. Geochemistry of mercury: from noble metal to global pollutant.....	672
Acquavita A., Brandolin D., Felluga A., Maddaleni P., Meloni C., Poli L., Skert N. & Zanello A. - Mercury distribution and speciation in soils contaminated by historically mining activity: The Isonzo River plain (NE Italy).....	673
Bianchi F., Rappuoli D., Vaselli O., Nisi B. & Esposito A. - Distribution of mercury, antimony and arsenic in the terrains from the former mining area of Abbadia San Salvatore (Siena, central Italy).....	674

Cabassi J., Rimondi V., Yeqing Z., Vacca A., Vaselli O., Buccianti A. & Costagliola P. - 100 years of high GEM concentration in the Central Italian Herbarium and Tropical Herbarium Studies Centre (Florence, Italy)	675
Cabassi J., Di Bennardo F., Venturi S., Tassi F., Nisi B., Magi F., Ricci A., Picchi G. & Vaselli O. - Gaseous Elemental Mercury (GEM) fluxes from the soil of the hydrothermal area of Monterotondo Marittimo (Grosseto, Central Italy)	676
Covelli S., Langone L., Petranich E., Acquavita A., Giordano P. & Giani M. - Spatial and temporal distribution of mercury in the recent sediments of the Adriatic Sea	677
Fantozzi L., Marziali L., Valsecchi L., Schiavon A., Orrù A. & Guerrieri N. - First investigation of atmospheric mercury pollution around the chlor-alkali plant of Pieve Vergonte (Italian central Alps) ..	678
Magi F., Cabassi J., Capecciacci F., Giannini L., Nisi B., Pandeli E., Rappuoli D., Tassi F., Venturi S. & Vaselli O. - Mercury in groundwater from the Mt. Amiata area (central Italy).....	679
Monaci F., McLagan D.S., Rappuoli D., Huang H., Lei Y. D., Mitchell C.P.J. & Wania F. - Long-term monitoring and modeling of gaseous mercury concentrations around the abandoned mine of Abbadia San Salvatore: the potential of passive sampling for detecting variation patterns and effects of emission-reduction associated with remediation works	680
Pasquetti F., Zanchetta G., Vaselli O., Nisi B., Bianchi S., Mirri S. & Nannucci S.M. - New insight into Hg origin in the Orbetello lagoon (Tuscany, Italy).....	681
Petranich E., Pavoni E., Signore S. & Covelli S. - Mercury mobility in harbour sediments: evidence from selective sequential extraction and short-term microcosm resuspension experiments (northern Adriatic Sea, Italy).....	682
Pirrone N. - What are the major challenges that should be taken on board in supporting nations in the implementation of the Minamata convention on mercury.....	683
Valerio M., Ghezzi L. & Petrini R. - Mercury contamination in soils of an urban setting and the pathways of dispersion.....	684
Vaselli O., Nisi B., Rappuoli D., Cabassi J., Esposito A. & Tassi F. - Discontinuous monitoring of Gaseous Elemental Mercury in the former mining area of Abbadia San Salvatore (Siena, central Italy).....	685
S32. New developments and challenges in volcanology: insights from experimental, analytical and field studies	686
Cubellis E., Pappalardo L. & Petrosino P. - Eruptive dynamics during violent strombolian Vesuvius 1906 eruption.....	687
Del Bello E., Taddeucci J. & Scarlato P. - Investigating the behaviour of volcanic ash using controlled laboratory experiments	688
Di Salvo S., Avanzinelli R., Isaia R., Druitt T.H. & Francalanci L. - The role of new magma recharges and crystal-mush interaction in the Campanian Ignimbrite activity, revealed by geochemical and isotope micro-analyses	689
Frontoni A., Costa A., Vona A., Pistone M. & Romano C. - Rheology of particle-bearing suspensions: preliminary results	690
Frontoni A., Vona A., Giordano G., Viccaro M. & Romano C. - Clastogenic lava flow: the case study from Mount Etna	691
Ganci G., Cappello A., Bilotta G., Corradino C., Héroult A. & Del Negro C. - Monitoring of lava flow hazards: The December 24, 2018 Mt. Etna eruption.....	692
Giuliani L., Iezzi G., Casarin A., Piattelli V., Lanzafame G., Nazzari M., Ferlito C., Mollo S., Scarlato P., Trabucco F. & Colò M. - Textural variations along a vertical section of a distal portion of an Etnean lava flow	693
González-García D., Petrelli M., Behrens H., Vetere F., Morgavi D., Giordano D. & Perugini D. - Diffusive fractionation of trace elements between mixing melts: the experimental approach.....	694
Kazarian A., Cáceres F., Scheu B., Vona A., Misiti V., Dingwell D.B. & Romano C. - An experimental overview on the role of decompression on bubble formation in trachytic magma	695

Monaco L., Giaccio B., Palladino D.M., Gaeta M., Sottili G., Marra F., Castorina F., Nomade S., Pereira A. & Albert P.G. - Early explosive activity at Vico volcano, central Italy: a new perspective from proximal and distal sedimentary archives	696
Morgavi D., Spina L., Cannata A., Musu A., Campeggi C. & Perugini D. - AEOLUS: a laboratory to study bubble-bearing flow dynamics and geophysical signals through analogue volcanic eruption.....	697
Musu A., Morgavi D., Spina L., Corsaro R.A. & Perugini D. - Lava fountaining activity: the Collapsing Foam Layer Model applied to the 2000 – 2013 South-East Crater eruptive period (Mt. Etna, Italy).....	698
Petrelli M. & Zellmer G. - Volcanic plumbing system dynamics: unravelling rates and timescales of magma transfer, storage, and eruption	699
Pisello A., Vetere F.P., Murri M., Alvaro M., Rossi S., Holtz F. & Perugini D. - Viscosity of ultramafic melts during cooling: insights for emplacement of Martian lava flows.....	700
Primerano P., Giordano G., Vona A., De Vita S. & Morgavi D. - Rheological behavior of lava flows from Ischia Island (Campania, Italy).....	701
Rooyackers S., Morgavi D., Perugini D., Petrelli M., Vetere F., Stix J., Berlo K., Barker S. & Charlier B. - Basalt-rhyolite interaction timescales in the caldera-forming Halarauður eruption (Krafla, Iceland) constrained by chaotic mixing experiments	702
Rossi S., Petrelli M., Morgavi D., Vetere F.P., Almeev R.R., Astbury R.L. & Perugini D. - Role of magma mixing in the pre-eruptive dynamics of the Aeolian Islands volcanoes (Southern Tyrrhenian Sea, Italy).....	703
Sacco G., Caltabiano T., Salerno G. & Viccaro M. - SO ₂ flux and eruptive activity at Mt. Etna between the 2015 and 2016	704
Scarani A., Silleni A., Vona A., Romano C. & Giordano G. - Infrared thermography of pyroclast cooling across the glass transition temperature: effect of clast composition, porosity and dimension.....	705
Silleni A., Ryan A.G., Russell J.K., Vona A., Giordano G., Ort M. & Romano C. - The effects of interclast viscosity contrast in the welding ability of pyroclastic deposits	706
Spina L., Morgavi D., Cannata A. & Perugini D. - Experimental investigations on degassing behavior and related seismo-acoustic markers: the effect of complex conduit geometries	707
S33. Geosciences at school 2019	708
Antiga R., Cabella R., Elter F.M. & Massa A. - Design and experimentation of educational activities on Water resources in the underground: development of an experimental protocol to analyze the dynamics of infiltration, accumulation and exploitation processes in incoherent deposits.....	709
Antiga R., Cabella R., Coniglio L., Carpanese M.G., Elter F.M., Lodi C., Massa A., Parola C., Tarella G. & Tsakarisianos M.D. - To know the hydrogeological instability - study methods and its awareness: the case of Val Graveglia - Genova - Eastern Liguria	710
Artoni C., Bollati I.M. & Pelfini M. - Virtual geomorpholabs: simple games for geomorphorisk education....	711
Beccaceci A., Stacchiotti L. & Paris E. - Sustainable city: work together for a more sustainable life style	712
Belluzzo A., Bronzo L., Citron S., Di Stefano G., Favaroni A., Gazzola R., Gazzurra G., Giacomini P., Martella A., Merella M., Nicodemi L., Porta L., Bianucci G., Bosio G., Collareta A., Gioncada A., Landini W., Mollì G., Sarti G. & Borghini A. - ICA-LAB: un laboratorio di ricerca interdisciplinare nel Lagerstätte del deserto costiero di Ica (Perù)	713
Bonaccorsi E., Borghini A., Gioncada A. & Pieraccioni F. - The good, the bad and the ugly: a movie around the geoscience textbooks	714
Boniello A. & Paris E. - The virtual trip of Darwin, the geologist	715
Borghini A., Pieraccioni F., Gioncada A. & Bonaccorsi E. - What are the students' mental models of the Earth's inner structure?.....	716
Caironi V., Regazzola V., Lorenzetti S.C., Berra G., Coltro G. & Fumagalli P. - Project "What a show! Create a geological corner in your high school"	717
Ferretti M., Invernizzi C., Mazzoli S. & Carroll M.R. - Exploring the moon, using Earth's rocks and fossils: an earth science module.....	718

Garzarella A., Valentini A., Pace B., Liguori A., Michelangeli M.A. & Middle School Class B - From Physics to Geology: exploring the time and space”, an outreach and successful project to understand the Earth system and the earthquakes, through the use of the <i>Quakecaster</i> , awarded by Gran Sasso National Laboratory (LNGS), INFN (National Institute for Nuclear Physics), contest “Anch’io Scienziato 2019”	719
Lozar F. & Tonon M.D. - Climate education in the deep time perspective: working with teachers and students	720
Moroni B. - “HAVE YOU GOT A GREEN THUMB?” Hands-on experiences of kids’ and teens’ earth science education by inquiry-based methods	721
Occhioni M. - Earth Science in Opensim-based virtual worlds.....	722
Occhipinti S. - A PBL approach to enhance the sensitivity of students towards natural risks and hazards, in Italian schools	723
Occhipinti S. - a EGU-IGEO European chapter to promote the teaching learning of Earth science in all schools	724
Pauselli C., Musu A., Mancinelli P., Ercoli M., Porreca M., Azzaro S., Carboni F., Samperi L., Giorgetti C., Mirabella F., Barchi M., Minelli G., Moriconi A. & Martorana S. - Il terremoto: impariamo a conoscerlo. The earthquake: let’s get to know it	725
Pelfini M., Apuani T., Artoni C., Conforto A. & Bollati I. - How to exploit geodiversity in geoscience education activities?	726
Pelorosso B., Brombin V., Bertagnon A., Calore E., Forastieri F., Polastri L., Rolando V. & Vinciguerra E. - Alps in a box.....	727
Piangiamore G.L., Trolese P., Frione A. & Cortopassi P. - Social Emotional Learning (SEL) and earthquake: teaching through emotions meets Geoscience.....	728
Placuzzi E., Barbieri G., Berti M., Gasparotto G., Giura E., Rossi V., Squarzoni G., Vaiani S.C. & gli studenti del Liceo E. Ferrari, Cesenatico - Il Piano Lauree Scientifiche come strumento di didattica inclusiva: il contributo delle geoscienze.....	729
Punturo R., Fazio E., Fiannacca P., Ortolano G. & Cirrincione R. - The Floristella-Grottafaldina Mineral Park (Sicily): a geological trip that becomes history, literature and memory of a territory.....	730
Realdon G. & Gravina T. - New opportunities for teacher professional development in Earth sciences: EGU Geoscience Fieldwork Officers Project	731
Scacchetti M. & Chicchi S. - Esperienze didattiche attorno a Valentina, balena fossile di 3.5 milioni di anni .	732
Scapellato B. - La circolazione oceanica	733
Scopesi C., Belmonte D., Briguglio A., Cabella R., Carbone C., Forchielli A. & Doria G. - Geosciences and museum: new frontiers in didactic for high school students	734
Seno S. & Lupi C. - Geoscience laboratory for primary school: an attempt for engaging young people in Earth Sciences.....	735
Stacchiotti L., Beccaceci A. & Paris E. - The scientific method between geology and history.....	736
Tonon M.D. & Caretto A. - The aesthetic approach to teaching geosciences and sustainable education	737
Zaccara Bertolini P., Foglia C., Classe IVF, Groppi E., Classe IIIH, Mantovani L., Tribaudino M., Artesi T. & Solzi M. - Pollution from magnetic minerals in leaves: an “Alternanza Scuola Lavoro” project in secondary schools in Parma and Torino	738

SESSIONI PLENARIE

Creeping minerals: new insights from numerical modelling and transmission electron microscopy

Cordier P.*

Univ. Lille, CNRS, INRA, ENSCL - UMET - Unité Matériaux et Transformations, Lille, France.

Corresponding email: Patrick.Cordier@univ-lille.fr

Keywords: RheoMan project, mantle convection, creeping minerals.

The Earth is an active planet which evacuates its internal heat through large scale convection motions which slowly stir the mantle. Mantle rocks and their constitutive minerals are thus subjected to large strains to sustain this activity. Modelling mantle convection requires understanding of how minerals creep under mantle conditions. In the last decades, a lot of efforts have permitted to extend considerably the pressure-temperature range where deformation experiments can be performed. However, experiments still face the difference in timescales between laboratory and natural conditions.

In this context, we are developing an approach which aims at addressing the elementary deformation mechanisms of some major minerals of the mantle. In the ERC funded RheoMan project we have developed a multiscale numerical modeling approach which has been applied to minerals of the transition zone and the lower mantle. The first step of this approach is to model the atomic structure of dislocations and then their mobility. We show a tendency of pressure to strongly inhibit dislocation glide (with some exceptions however). These calculations have led us to propose that the lower mantle is controlled by the pure climb creep of bridgmanite.

In the upper mantle, conditions are slightly different since some minerals like olivine can be preserved at ambient pressure. Taking advantage of this possibility we design new experiments performed in situ in the TEM based on newly developed nanomechanical testing. The advantage of this technique is to allow experiments directly at the scale of elementary mechanisms which can be directly investigated and quantified. We expect these experiments to yield information which can be linked to numerical modeling.

In this presentation, we will illustrate these two approaches with some recent results.

The Po Plain - Adriatic foreland from Mesozoic extension to Cenozoic compression

Fantoni R.*

Eni Upstream & Technical Services, San Donato Milanese (Milano).

Corresponding email: roberto.fantoni@eni.com

Keywords: Po Plain, Adriatic foreland, Apennines, Southern Alps, Mesozoic extension, Cenozoic compression.

The Po Plain and Adriatic foreland is shared by three partially coeval orogenic belts: the Southern Alps in the north, the Apennines in the west and the Dinarides in the east. Based on the well data and 2D/3D seismic survey achieved during its 60 year long hydrocarbon exploration history, a detailed reconstruction of the area is presented.

As well as in the bordering chains, the Cenozoic compressional architecture of the present day foreland results overprinted on the foreland previous framework produced by the previous Mesozoic extensional cycles (from late Triassic to early Cretaceous).

As well as in the bordering chains, in the foreland area the Alpine/Apennine compressional architecture is overprinted on the remarkable framework produced by the Mesozoic extensional cycles (from late Permian to early Cretaceous). Pre-rift extension followed in the Adria region a eastward polarity and started with progressive westward onlapping of late Permian-Anisian continental to paralic silicoclastics over the cratonized Variscan substratum. It culminated with the highly fragmented kilometric/deca-kilometric platform and basin carbonate system of the Anisian-early Carnian cycle.

The maximum basin widening and deepening were achieved only after the late Triassic-Liassic syn-rift phases related to the Ligurian-Piedmontese cycle that progressively led to the formation of the hundred kilometer wide Jurassic-Cretaceous Lombardian, Belluno and Adriatic basins bounded by long ranging carbonate platforms.

The earliest Alpine effect recorded in the region was the late Cretaceous (Eoalpine) bending of the western Southalpine margin. The foreland flexuring then started with a Paleocene-Eocene (Mesoalpine) inflection of the whole area towards the Dinaric/Albanian chain system; even remaining external to the foredeep depocenters, the inherited Mesozoic platforms and ridges were overpassed and the distal turbidite infilling of the pre-existing basins began. The following flexuring progression went on increasingly compartmented and controlled by both scaled chain segments activation and their coeval competition, as well as by the inherited poorly deformable shields distribution (Trento plateau, Istrian, Dalmatian and Apulian platforms).

From Oligocene to Late Miocene the Po Plain and north Adriatic areas kept anyway marginal to the Apennine flexuring (that involved the presently emerged sector of this chain) while they essentially recorded the Neoalpine inflection towards the Southalpine chain; a 6000 m thick foredeep faced the piling up of the western (Lombardian) chain segment, while only a halved bending responded to the later activation of the eastern (Veneto-Friuli) one. A more than 6000 m foredeep depocenter also accompanied to the SE the coeval flexuring of the Albanian foreland segment in south Adriatic, while the substantial disactivation of the Dinaric one occurred in the north Adriatic area.

The latest Messinian-Quaternary foreland evolution was, on the other hand, marked by the disactivation of the western Southalpine sector and the inflection peak towards the Apennine chain that produced up to 7-8000 m thick foredeep depocenters. The strong Apennine competition substantially inhibited a further consistent bending of both the still active eastern Southalpine and Albanian compartments.

The result is a fragmented post-Eocene tectonic evolution of the Adriatic foreland controlled by both the diachronous chains activity and their coeval competition. The effect of the opposite chain segments interference was a multiple system of differently evolving foredeeps not exclusively ruled by the chains at their back. Time and amount of flexuring were moreover controlled by formation of transversal positive belts that played the role of flexure transfer zones.

IODP-Italia and the Italian participation in ECORD-IODP and ICDP

Iadanza A.*¹, Tribuzio R.² & CNR Committee “ECORD-IODP and ICDP”

¹ CNR-DSSTTA, Dipartimento Scienze del Sistema Terra e Tecnologie per l’Ambiente.

² Università degli Studi di Pavia, Dipartimento Scienze della Terra e dell’Ambiente.

Corresponding email: annalisa.iadanza@cnr.it

Keywords: IODP, ECORD, seafloor environments.

The International Ocean Discovery Program (IODP) is an international marine research collaboration that explores Earth’s history and dynamics using ocean-going research platforms to recover data recorded in seafloor sediments and rocks and monitor seafloor environments through drilling and coring. Italy participates in IODP as a member country of the European Consortium for Ocean Research Drilling ECORD. Thanks to a national funding annually allocated by MIUR since 2013 and managed by the CNR Dept. of Earth System Science and Environmental Technologies (DSSTTA), IODP-Italia regularly operates through a national office, a scientific coordinator and an advisory committee (www.iodp-italia.cnr.it). The CNR Committee “ECORD-IODP and ICDP” replaced the former Advisory Committee IODP-Italia with new members and assignments, in order to implement a joint IODP-ICDP support to the Italian participation in the international scientific drilling, including the International Continental Scientific Drilling Program (ICDP).

IODP-Italy fosters the Italian participation in ECORD-IODP through a funding scheme supporting travel expenses to participate in both cruise/post-cruise activities and ECORD summer schools/training courses. On a national scale, the Committee is currently planning new education and training initiatives for students and young scientists including (1) cycles of seminars in IODP/ICDP thematic areas and (2) guided tours to be held in the institutes of marine sciences CNR-ISMAR and OGS.

IODP-Italy and CNR-DSSTTA have recently awarded three two-years research proposals devoted to post-doc scientists aiming at supporting IODP-related scientific activities. Recent outreach activities have been carried out through an interactive booth with activities dedicated to primary schools and general public on the occasion of the Festival del Mare (Genova, May 16th-18th 2019).

Many Italian geoscientists have been selected through ECORD calls as members of IODP Science Parties during IODP 2013-2023. The shipboard specialties included expertise in micropaleontology, sedimentology, paleomagnetism, petrophysics and petrology. Hard rock petrologists, in particular, were involved in IODP expeditions 357 (Atlantis Massif Serpentinization and Life) and 360 (SW Indian Ridge Lower Crust and Moho). The major objective of IODP expedition 357 was to examine the role of serpentinization in driving hydrothermal systems, sustaining microbial communities, and sequestering carbon. The primary aim of IODP expedition 360 was to recover the lowermost gabbros and crust-mantle transition to understand the processes creating mid-ocean ridge basalt, and to resolve the controversy as to whether the Moho at slow spreading ridges can be a serpentinization front.

Mantle Geochronology: Insights from the Re-Os isotopic system

Luguet A.*

Institute for Geosciences, University of Bonn, Germany.

Corresponding email: ambre.luguet@uni-bonn.de

Keywords: dating mantle peridotites, geochronometer, Re-Os isotopic system.

Dating mantle peridotites is one of the backbones to our understanding of the Earth's mantle dynamics. It provides insights into the formation, evolution and possible destruction of the lithospheric mantle and into the genetic and evolutionary relationships between mantle and crust at regional as well as global scales.

The Re-Os isotopic system is widely seen as the geochronometer of choice to date mantle peridotites. This isotopic system, where both parent and daughter elements belong to the Highly Siderophile Elements (HSE: Os, Ir, Ru, Pt, Pd and Re), is based on the radioactive decay of ^{187}Re into ^{187}Os . The reason behind the Re-Os isotopic system being the geochronometer of choice to date mantle peridotites lies in the compatibility of osmium during partial melting of peridotites (Re behaves incompatibly). This contrasts with the lithophile-element-based element isotopic systems (e.g. Rb-Sr, Sm-Nd), typically used to date crustal lithologies, whose both daughter and parent elements behave incompatibly during partial melting of peridotites (except for Lu in presence of garnet). Additionally, the compatibility of Os may potentially make the Re-Os isotopic system more robust to overprinting/resetting by melt percolations and melt-rock reactions in mantle peridotites when compared for example to the Rb-Sr geochronometer.

Since the late 1980s, the main targets of Re-Os dating investigations on the Earth's mantle have been the whole-rock peridotites, with the Re-Os isotopic measurements being sometimes coupled with the HSE systematics. The identification of the Base Metal Sulfides (BMS) and Platinum Group Minerals (PGM) as the main Os host minerals in mantle peridotites in the mid 1990s opened up the way to Re-Os dating of these micrometric and nanometric Os mineral hosts, either via Laser-Ablation MC-ICP-MS or by mechanical extraction of the minerals followed by wet chemistry, NTIMS, and ICP-MS.

In this lecture, I will review the basic concepts of Re-Os dating, highlight the current state of the art as well as the limits of the Re-Os dating when conducted at the whole-rock, BMS and PGM scales; and show how three decades of research have challenged our understanding of the Re-Os geochronometer, especially its robustness and geological meaning.

S1

Integrated mineralogy, petrology and computational modelling to decipher geochemical interactions and tectonic histories recorded by metamorphic rocks from the deep Earth

CONVENERS AND CHAIRPERSONS

Mattia L. Mazzucchelli (Università di Padova)

Mattia Gilio (Università di Padova)

Marco Scambelluri (Università di Genova)

Donato Belmonte (Università di Genova)

Multiphase inclusions associated with residual carbonate shed new light on the origin of super-deep diamonds from Juina (Brazil)

Agrosi G.*¹, Tempesta G.¹, Mele D.¹, Caggiani M.C.², Mangone A.², Della Ventura G.C.³⁻⁴, Cestelli-Guidi M.⁴, Allegretta I.⁵, Hutchison M.T.⁶, Nimis P.⁷ & Nestola F.⁷

¹ Department of Scienze della terra e Geoambientali, Università di Bari “Aldo Moro”, Bari, Italy.

² Department of Chemistry, University of Bari “Aldo Moro”, Bari, Italy.

³ Department of Science, University Roma Tre, Roma, Italy.

⁴ INFN, Frascati (Rome), Italy.

⁵ Department (Di.S.S.P.A.), Università degli Studi “Aldo Moro”, Bari, Italy.

⁶ Trigon GeoServices Ltd., (Las Vegas, USA).

⁷ Department of Geoscienze, Università degli Studi di Padova, Padova, Italy.

Corresponding email: giovanna.agrosi@uniba.it

Keywords: diamond, Juina, inclusions.

Super-deep diamonds and their mineral inclusions preserve very precious information about Earth's deep mantle. In this study, we examined multiphase inclusions entrapped within a diamond from the Rio Vinte e um de Abril, São Luiz area (Juina, Brazil), using a combination of non-destructive methods: micro-Computed X-ray Tomography (μ -CXRT) to investigate the size, shape, distribution and X-Ray absorption of inclusions and mapping by micro X-ray Fluorescence (μ -XRF), μ -Raman Spectroscopy and micro-Fourier Transform Infrared Spectroscopy (μ -FTIR) to determine the chemical and mineralogical composition of the inclusions. Previous studies revealed that the diamond has nitrogen occurring in clusters of three atoms and a vacancy (Type IaB), has a N-enriched core, is plastically deformed, and contains several syngenetic, Fe-rich ferropericlasite–magnesiowüstite inclusions in its N-rich core (Agrosi et al., 2017; Nimis et al., 2019). In this work we found that four large inclusions, enclosed in the N-H rich core, consist of complex assemblages dominated by ferropericlasite/magnesiowüstite with locally exolved magnesioferrite and carbonates. Compared with other similar diamonds from Juina, this sample was remarkable because it encased an atypical inclusion, which showed a very unusual flask shape resembling a large (ca 100 μ m) fluid/melt inclusion. Based on μ CXRT tomography and μ -Raman mapping, the inclusion is polyphase and consists of magnetite and hematite partly replacing a magnesiowüstite core. μ -Raman spectra reveal local features that could be ascribed to xieite, a polymorph of chromite, stable for $P \geq 18$ GPa. Some spectra show also the presence of huntite, a carbonate with formula $\text{CaMg}_3(\text{CO}_3)_4$ that represents the first known occurrence in diamond.

We interpret the composition of the inclusions as further evidence of ferropericlasite-bearing diamond formation in a carbonate-rich environment, probably under evolving redox conditions. This work shows that a full picture of the significance of diamond inclusions cannot be determined without an accompanying multidisciplinary study that allows a full description of the growth history of occluding diamond.

Agrosi G., Tempesta G., Della Ventura G.C., Cestelli Guidi M.A., Hutchison M.T., Nimis, P. & Nestola F. (2017) - Non-destructive in situ study of plastic deformations in diamonds: X-ray Diffraction Topography and μ FTIR mapping of two super deep diamond crystals from São Luiz (Juina, Brazil). *Crystals*, 7(8), 233.

Nimis P., Nestola F., Schiazza M., Reali R., Agrosi G., Mele D., Tempesta G., Howell D., Hutchison M.T. & Spiess R. (2019) - Fe-rich ferropericlasite and magnesiowüstite inclusions reflecting diamond formation rather than ambient mantle. *Geology*. 47 (1), 27-30.

Elastic geobarometry for Quartz inclusions in garnet: comparison between hydrostatic and isotropic methods to evaluate the entrapment pressures

Bonazzi M.*¹, Tumiati S.², Thomas J.³, Angel R.J.¹ & Alvaro M.¹

¹ Department of Earth and Environmental Sciences, University of Pavia, Italy.

² Department of Earth and, University of Milan, Italy.

³ Department of Earth Sciences, Syracuse University, NY, USA.

Corresponding email: mattia.bonazzi01@universitadipavia.it

Keywords: inclusion, Quartz, elastic geobarometry.

Elastic geobarometry makes use of the contrast in elastic properties between host-inclusion pairs to determine the entrapment conditions of the inclusions. The theoretical basis has been developed extensively in the past few years, but an experimental validation and assessment of the calculated P and T of entrapment is still required. We report the entrapment pressures determined using elastic geobarometry on quartz inclusions trapped in almandine garnet synthesized at eclogitic conditions (Alm-1 at P=3.0 GPa and T=775°C; Alm-2 at P=2.5 and T=800°C) in a piston cylinder apparatus. From the fitted Raman spectra we determined the pressure on the inclusion using the hydrostatic calibration and the mode Grüneisen tensor approach. The use of a hydrostatic calibration of the 464 cm⁻¹ line of quartz leads to a large spread in entrapment ‘pressure’ values that increase with increasing entrapment pressure conditions (i.e. pressure at which the synthesis have been performed). For example, the errors on the entrapment pressure are about 1.4 GPa for inclusions synthesized at 3 GPa and approximately 0.2 GPa those synthesized at 2.5 GPa. These discrepancies arise mostly from the incorrect assumption of perfectly hydrostatic conditions that cannot be applied to elastically anisotropic inclusion trapped in a cubic host. Conversely, the use of the mode Grüneisen tensors for the quartz inclusions enables the full strain state of the inclusion to be determined from which its’ stress state can be calculated (Murri et al., 2018; Angel et al., 2019). Such a procedure leads to a much smaller spread in “pressure” values inferred for the inclusions; the maximum deviation from the experimental synthesis pressures is smaller than ± 0.2 GPa. The entrapment pressures calculated from the residual pressure obtained adopting the mode Grüneisen tensors approach is always higher than those obtained using the hydrostatic calibration. In conclusion our results show that the most significant effect on the calculated entrapment pressures is due to the elastic anisotropy of quartz and the affect of this on the shift of the Raman bands for the inclusion rather than the subsequent calculation of entrapment conditions.

This project received funding from the European Research Council (ERC) under the European Union’s Horizon 2020 research and innovation programme (grant agreement No 714936) by M. Alvaro. MA has also been supported by the MIUR-SIR grant “MILE DEEP” (RBSI140351). JT was supported by the Earth Sciences Division of the National Science through grant number EAR-1447468.

Angel R.J., Murri M., Mihailova B. & Alvaro M. (2019) - Stress, strain and Raman shifts. *Zeitschrift für Kristallographie - Crystalline Material*, 234, 11.

Murri, M., Mazzucchelli, M.L., Campomenosi, N., Korsakov A.V., Prencipe M., Mihailova B.D., Scambelluri M., Angel R.J. & Alvaro M. (2018) - Raman elastic geobarometry for anisotropic mineral inclusions. *American Mineralogist*, 103, 1869-1872.

High pressure softening of grossite (CaAl₄O₇)

Cámara F.*¹, Lotti P.¹, Belmonte D.², Pagliaro F.¹, Merlini M.¹ & Joseph B.³

¹ Dipartimento di Scienze della Terra 'A. Desio', Università degli Studi di Milano.

² Dipartimento di Scienze della terra, dell'ambiente e della vita (DISTAV), Università degli Studi di Genova.

³ GDr Indian Institute of Science-ICTP, Elettra Sincrotrone Trieste.

Corresponding email: fernando.camara@unimi.it

Keywords: grossite, high-pressure single-crystal X-ray diffraction, phase transition.

The elasticity of grossite (CaAl₄O₇) has been investigated by experimental (synchrotron radiation high-pressure single crystal X-ray diffraction, using an ETH-type Diamond Anvil Cell and M.E.W. as pressure-transmitting fluid, at Xpress beamline at Elettra, Trieste, $\lambda = 0.4957 \text{ \AA}$) up to 8.6 GPa and first-principle methods (using a WC1LYP hybrid functional and Crystal program). On compressing, a displacive first order phase transition has been observed between 6.1 and 7 GPa by ca. a 3% change in lattice volume and the violation of *C*-centring extinction conditions. In fact, the symmetry changes by losing the centring of the lattice and the centre of symmetry, passing from *C2/c* to *Pc* space group. A dramatic change on the isothermal bulk modulus (K_0) of grossite accompanies the transition: by preliminary fitting of lattice parameters data using a BM2 EoS we obtain changes from 123(4) GPa in the low pressure regime to 35(8) GPa in the high-*P* phase, which shows a very soft and anisotropic behaviour (linear compressibility changes from 1.19:1.00:1.00 in *C2/c* to 1.74:5.74:1.00 in *Pc*). Intensity data was collected at 17 *P* values (data collected every 0.5-1.0 GPa up to 8.6 GPa). We have been able to solve the structure of the high-*P* phase from experimental data by group theory symmetry reduction and structure refinement of a symmetry relaxed model. The structure has two symmetrically independent AlO₄ tetrahedra in the *C2/c* phase, which become seven symmetrically independent AlO₄ tetrahedra plus one AlO₅ pyramid (the Al(21) site) in *Pc* phase ($d = 1.884(1) \text{ \AA}$, polyhedral volume 5.04 Å³). The change in coordination of the Al atom at the Al(21) site is probably the driving force of the strong compressibility along [010] in high-*P* phase. First principles calculations agree very well with the experimental data. By fitting ab initio energy-volume data with a BM3 EoS in the range $V/V_0 = 0.95 - 1.04$ we obtain $K_0 = 128.8(1) \text{ GPa}$ and $K'_0 = 4.0(1)$ for the *C2/c* phase. The calculated static value of K_0 is, in turn, perfectly consistent with aggregate bulk modulus obtained from static elastic constants by using a Voigt-Reuss-Hill average scheme (i.e. $K_{\text{VRH}} = 129.2 \text{ GPa}$). Ab initio calculation of the full elastic tensor (with 13 independent components) permits to define the shear modulus (i.e. $G_{\text{VRH}} = 52.1 \text{ GPa}$) and seismic anisotropy of this phase, for which no experimental data exist so far. Computed volume and axial compressibilities match the observed trends within 1%, except for c/c_0 which is slightly overestimated by WC1LYP calculations. Further ab initio calculations on both *C2/c* and *Pc* phases are currently in progress in order to characterize the thermodynamic features of the phase transition. The unattended behaviour of grossite implies drastic changes on the mechanical response of this phase that should be accounted for when modelling phase diagrams of the CAS (CaO-Al₂O₃-SiO₂) system and the mechanical response of high alumina cements (HAC).

Applying Raman-elastic barometry to UHP metamorphic rocks: insights from the Dora Maira Massif (Western Alps)

Campomenosi N.*¹, Scambelluri M.¹, Angel R.J.²⁻³, Hermann J.⁴, Rubatto D.⁴, Mihailova B.⁵ & Alvaro M.²

¹ Department of Earth Science, Environment & Life, University of Genoa, Italy.

² Department of Earth and Environmental Sciences, University of Pavia, Italy.

³ Institute of Geoscience and Georesources, CNR of Padova, Italy.

⁴ Institute of Geological Sciences, University of Bern, Switzerland.

⁵ Department of Earth Sciences, University of Hamburg, German.

Corresponding email: nicola.campomenosi@edu.unige.it

Keywords: UHP, elastic-barometry, zircons.

Recent developments in elastic barometric methods allow accounting for the elastic anisotropy in mineral hosts and their inclusions in order to retrieve entrapment P-T conditions in metamorphic rocks (e.g. Murri et al., 2018).

In this study, we applied this technique to three garnet megablasts from the whiteschist lenses of the Brossasco-Isasca UHP unit. First, we combined Raman spectroscopy with cathodoluminescence and trace element analyses on exposed zircons in order to recognize zircons that underwent partial or total metamictization. This enabled us to rely on Raman spectroscopy for selecting the buried zircon grains whose wavenumber variation is solely dependent on the strain acting on the inclusion. Zircon inclusions with almost rounded or ellipsoidal shapes fully buried within the garnet host have been selected on the basis of detailed petrographic analysis. From the measured Raman peak position we determined the strain state adopting the phonon Grueneisen tensor approach (Murri et al., 2018).

We show that selected buried zircon inclusions display a systematic decrease in the phonon frequencies moving from grains entrapped at the core toward those entrapped at the rim of the garnet host and the same is for the calculated residual pressure (P_{inc}). On the other hand, Zr content in rutile inclusions coupled with the host garnet composition suggest a narrow range of increasing T for garnet formation and then zircon entrapment. Therefore, since zircon is stiffer than the host garnet, our results are consistent with increasing entrapment pressure (P_{trap}) from core to rim, and hence with garnet growth on the prograde path (e.g. Chopin, 1984).

This work was supported by ERC-StG TRUE DEPTHS grant (number 714936) and MIUR-SIR Mile Deep grant (number RBSI140351) to M. Alvaro. N. Campomenosi was also supported by the University of Genova.

Chopin C. (1984) - Coesite and pure pyrope in high-grade blueschists of the Western Alps: a first record and some consequences. *Contributions to Mineralogy and Petrology*, 86(2), 107–118, <https://doi.org/10.1007/BF00381838>.

Murri M., Mazzucchelli M.L., Campomenosi N., Korsakov A.V., Prencipe M., Mihailova B.D., Scambelluri M., Angel R.J. & Alvaro M. (2018) - Raman elastic geobarometry for anisotropic mineral inclusions. *American Mineralogist*, 103(11), 1869-1872. <http://doi.org/10.2138/am-2018-6625CCBY>

Experimental investigation of the stability of iron-rich tourmaline as a function of pressure, temperature and oxygen fugacity with implications for the release of B-rich fluid during subduction

Capizzi L.S.*¹, Stagno V.¹, Andreozzi G.B.¹, Bosi F.¹, Nazzari M.² & Scarlato P.²

¹ Department of Earth Sciences, Sapienza University of Rome.

² National Institute of Geophysics and Volcanology - Rome section.

Corresponding email: lucasamuele.capizzi@uniroma1.it

Keywords: high pressure, redox conditions, subduction zones.

The origin and deep cycle of volatile-rich metasomatic fluids at mantle conditions strictly link with the stability at high pressure and temperature of minerals whose crystal structure can host the elements within the C-O-H-S-B-F-N system. Tourmaline from metamorphic assemblages can contain up to ~11 wt.% B₂O₃ (i.e. >80 wt.% of the whole-rock B), ~4 wt.% H₂O and up to 2 wt.% F, representing an important carrier of volatile elements. In addition, tourmalines can also contain variable amount of both Fe²⁺ and Fe³⁺ implying a key role in redox reactions either as oxidising or reducing agent in volatile-bearing rocks. Finally, recent findings of tourmaline along with coesite and diamonds in UHP metamorphic rocks have raised important questions on their stability at upper mantle P-T conditions.

To date, experimental studies have focused mainly on the compressibility of tourmalines at HP and room T (Berryman et al., in press), tourmaline breakdown in B-doped synthetic metapelites (Ota et al., 2008) and P-Trange for the stability of dravite (Dutrow & Henry, 2011), all neglecting the role of fO_2 . However, due the presence of multiple coordination sites and Fe²⁺/Fe³⁺ species, an experimental study at HP-T is needed to shed light on the stability of tourmaline at mantle conditions.

We investigated, for the first time, the structural stability of natural schorl tourmaline from Seagull batholith (Yukon Territory, Canada, [NaFe₃Al₆Si₆O₁₈(BO₃)₃(OH)₃(OH)]), characterized by ~19 wt.% FeO (as Fe²⁺). The experiments were performed using the Walker-type multi anvil press (840t), at a fixed pressure of 4 GPa and temperatures between 450-1000 °C with duration between 2 and 10 hrs. The fO_2 in these experiments was buffered by mixing the schorl starting material with 20 wt.% of I) Re+ReO₂ (1:1 mole ratio) and II) Ag₂C₂O₄. Rhenium and graphite were also used as capsule material. The recovered quenched products were then polished and analysed by FE-SEM and EMPA for both textural and chemical characterization. Our preliminary data shows a partial breakdown of schorl within the investigated experimental conditions, resulting into a gradual increase of Si and Fe with increasing T as consequence of the crystallization of Al-rich phases like kyanite, mullite, corundum and almandine garnet. Additional phases like jadeite might form as result of oxidation of Fe²⁺ to Fe³⁺ of the starting material. The results from this study provide useful tool to interpret the coexistence of similar assemblages in natural metapelites and model the P-T- fO_2 paths for the formation of B-rich fluids.

Berryman E.J., Zhang D., Wunder B., Duffy T.S. In press. Compressibility of synthetic Mg-Al tourmalines to 60 GPa. *American Mineralogist*, <https://doi.org/10.2138/am-2019-6967>.

Dutrow B.L. & Henry D.J. (2011) - Tourmaline: A Geologic DVD. *Elements*, 7, 301-306.

Ota T., Kobayashi K., Katsura T. & Nakamura E. (2008) - Tourmaline breakdown in a pelitic system: implications for boron cycling through subduction zones. *Contribution to Mineralogy and Petrology*, 155, 19-32.

Mineral growth and metastability phenomena in melt inclusions from metamorphic rocks

Ferrero S.^{*1-2}, Angel R.J.³, O'Brien P.J.¹ & Wunder B.⁴

¹ Department of Geosciences, Universität Potsdam.

² Museum für Naturkunde, Berlin.

³ Dipartimento di Scienza della terra e dell'ambiente, Università di Pavia.

⁴ Helmholtz-Zentrum Potsdam, GFZ.

Corresponding email: sferrero@geo.uni-potsdam.de

Keywords: melt inclusions, polymorphs, glass.

Small portions of pristine melt with diameter 2 to 50µm are being increasingly recognized as a rather common occurrence in high grade garnet from high grade metamorphic terranes, and their study delivers crucial chemical information on the anatectic melt at depth. But they are also unique “natural experimental charges” where the behaviour of the silicate melt can be investigated, directly in the natural rocks, under P-T-t conditions which cannot be completely reproduced in the laboratory. Each nanogranitoid case study has consistently shown a H₂O-bearing, silica and alkali-rich melt. Despite this within the inclusions the melt behaviour on cooling is rather surprising as it shows clear evidence of metastability phenomena commonly ascribed to rapid cooling, a phenomenon not recognized in the metamorphic rocks in which they occur.

Different volumes of identical melt in the same mineral may either crystallize completely or remain partially or completely glassy despite having experienced exactly the same slow cooling path. This is possibly the result of the fact that fluids in small pores can maintain higher threshold supersaturation, up to the point that melt crystallization may be completely inhibited.

Even when crystallized, the phase assemblage of these tiny granitoid plutons is often unexpected in nature. Quartz and feldspars are very often absent, replaced by cristobalite and/or tridymite in the case of quartz, and kumdykolite and kokchetavite for plagioclase and K-feldspar, respectively. Other polymorphs of plagioclase, namely svyatoslavite and disteinbergite, have been also recently recognized, making the presence of these phases a feature characteristic of crystallized volumes of melt hosted in isolated pores.

These metastable polymorphs crystallize directly from the melt on cooling, independently from the internal P of the inclusions and from the conditions of melt entrapment. They are likely the result of rapid crystallization due to undercooling of the trapped melt, once again result of the peculiar supersaturated conditions achieved on cooling by a confined melt.

Combining micro-tomography and finite element analyses for elastic geobarometry on real geological samples

Geddo Z.*¹, Mazzucchelli M.L.¹ & Alvaro M.¹

¹ Department of Earth and Environmental Sciences, University of Pavia, Italy.

Corresponding email: zeno.geddo01@universitadipavia.it

Keywords: host-inclusion systems, elastic geobarometry, elastic anisotropy.

Minerals in high-pressure metamorphic rocks may host other minerals as inclusions. During the exhumation that brings the rock to the Earth surface, inclusions develop residual stress and strain fields because of their anisotropic mechanical properties. The strain can be measured with experimental techniques such as Raman spectroscopy or X-ray diffraction. Once the residual strain in the inclusion is known, elastic geobarometry allows us to constrain the entrapment condition of the system providing precious information on geodynamical settings such as subduction zones. We present a new elastic geobarometry method that includes both the geometrical effects and the anisotropic properties of the minerals into the calculation of the entrapment conditions. We built a digital 3D model of the host-inclusion system based on Synchrotron X-Ray microtomography. The residual strain field in the inclusion was obtained with both Raman spectroscopy and X-ray diffraction (Murri et al., 2018) which also allows the determination of the crystallographic orientations of all the minerals involved. The elastic relaxation, including the effects of the morphology of the inclusion and its proximity to the external surface of the host, was evaluated with Finite Element (FE) analyses performed on the realistic 3D model. Finally, thermodynamic calculations considering axial equations of state were computed with EntraPT program to constrain the entrapment conditions. As an example, we show application of this method on quartz inclusions entrapped in a garnet of an eclogite xenolith found in the Mir pipe (Yakutiya, Korsakov et al., 2009). Results point to an elastic re-equilibration occurred under external hydrostatic conditions at P of ~ 3 GPa and temperatures between 925°C and 1000°C. This suggests a metamorphic origin of this eclogite xenolith, providing constraints on the mechanisms of craton accretion from a subducted crustal protolith.

This work was supported by ERC-StG TRUE DEPTHS (grant number 714936) to M. Alvaro. We acknowledge F. Marone at the Paul Scherrer Institut, Villigen, Switzerland for provision of synchrotron radiation beamtime at the TOMCAT beamline of the SLS.

Murri M., Mazzucchelli, M.L., Campomenosi N., Korsakov A.V., Prencipe M., Mihailova B.D., Scambelluri M., Angel R.J. & Alvaro M. (2018) - Raman Elastic Geobarometry For Anisotropic Mineral Inclusions. *Am. Mineral.*, 103, 1869–1872.

Korsakov A.V., Perraki M., Zhukov V.P., De Gussem K., Vandenabeele P. & Tomilenko A.A. (2009) - Is quartz a potential indicator of ultrahigh-pressure metamorphism? Laser Raman spectroscopy of quartz inclusions in ultrahigh-pressure garnets. *Eur. J. Mineral.*, 21, 1313–1323.

First-principles molecular dynamics simulations of aqueous fluids at high temperatures and pressures

Jahn S.*

Institute of Geology and Mineralogy, University of Cologne, Germany.

Corresponding email: s.jahn@uni-koeln.de

Keywords: molecular dynamics, aqueous fluids, speciation.

Aqueous fluids are important agents in many geological processes of the Earth's crust and upper mantle. They facilitate chemical reactions and element transport, modify rock and melt properties, or provide a source of geothermal energy. To quantify and understand the role of fluids in various geological environments, their chemical compositions as well as their equations of state and other physical or thermodynamic properties need to be known or studied. The solubility of mineral components in aqueous solutions and the ability of such fluids to fractionate elements or isotopes during fluid-rock or fluid-melt interactions ultimately depends on the speciation of the solute ions or molecules. Complementary to experimental approaches, first-principles molecular dynamics simulations have become a powerful tool to study the relation between the molecular structure of model fluids and their physical or geochemical properties. In this talk, I will review some of the recent progress in this field and discuss a number of case studies. This will include predictive modeling of metal speciation and its relation to thermodynamic fluid properties, theoretical spectroscopy to link simulations and in situ experimental studies, and preliminary studies to predict the solubility of minerals or element and isotope partitioning during fluid-rock interactions.

Multiphase inclusions in harzburgites from the Bétic Cordillera (Cerro de Almirez, Spain): growth and orientation of magnetite in olivine

La Fortezza M.*¹, Campione M.¹, Alvaro M.², Scambelluri M.³ & Malaspina N.¹

¹ Department of Earth and Environmental Sciences, University of Milano-Bicocca.

² Department of Earth and Environmental Sciences, University of Pavia.

³ Department of Earth Science, Environment, and Life, University of Genova.

Corresponding email: m.lafortezza1@campus.unimib.it

Keywords: subduction, multiphase inclusions, epitaxy.

Magnetite-bearing multiphase solid inclusions hosted in metamorphic olivine found in harzburgites from the Almirez Complex (Bétic Cordillera, Spain) have been interpreted as cavities trapping the dehydration fluid produced by the subduction-zone dehydration of former serpentinites (Scambelluri et al., 2001). In this study we present an analysis of the possible mechanisms of growth and nucleation of the daughter phases from the analyses of the crystallographic orientation relationships (CORs) between the inclusions and the host mineral, to shed light on the crystallization mode and to verify the existence of an epitaxial registry between olivine and magnetite. We performed single-crystal x-ray diffraction (SC-XRD) measurements using OrientXplot program (Angel et al., 2015), from which we determined the CORs between the host and the inclusion indicating possible epitaxial growth. The resulting epitaxial relationship for the magnetite-olivine system demonstrates preferential orientations between magnetite and olivine along magnetite (111)//olivine (100), magnetite $\langle 1\bar{1}0 \rangle$ //olivine $\langle 011 \rangle$. This evidence points to the possible growth of magnetite and olivine by sharing planes along (111) and (100), respectively. Reticular nodes coincidence for the two minerals is observed along $\langle 1\bar{1}0 \rangle$ and $\langle 011 \rangle$ crystallographic direction, respectively. These two planes are both cleavage planes that can promote epitaxial growth minimizing the potential energy. The diffractometer experimental results of the geometric lattice coincidence between olivine and magnetite were modelled by calculating the geometrical misfit between the two lattices in contact as a function of their relative azimuthal orientation. We found an azimuthal orientation ensuring perfect commensurism of the two lattices, i.e. all the nodes of the magnetite lattice coincide with some of the nodes of the olivine lattice. This particular relation represents a unique occurrence, playing a fundamental role in favoring the heterogeneous nucleation of magnetite on olivine.

The stabilizing effect provided by lattice commensurism represents an effective driving force for the heterogeneous nucleation and heteroepitaxial growth of magnetite inclusions. The nucleation, crystallization and growth of the magnetite microinclusions may be therefore attributed to a process involving heterogeneous nucleation and crystallization under near – to – equilibrium conditions, as an alternative mechanism to the chemical precipitation from an oversaturated solution.

Angel R.J., Milani S., Alvaro M. & Nestola F. (2015) - OrientXplot – a program to process and display relative crystal orientations. *Journal of Applied Crystallography*, 48, 1330-1334.

Scambelluri M., Rampone E. & Piccardo G.B. (2001) - Fluid and element cycling in subducted serpentinite: a trace-element study of the Erro-Tobbio ultramafites (Western Alps, NW Italy). *Journal of Petrology*, 1, 55-67.

Stepwise brittle deformation at 80 km-depth triggered by internal then external fluid circulation (Monviso eclogitic breccias, W. Alps)

Locatelli M.*¹, Verlaquet A.¹, Agard P.¹, Pettke P.² & Federico L.³

¹ Istep, Sorbonne Université.

² Geologie Institut, Bern Universität.

³ DISTAV, Università di Genova.

Corresponding email: locatellimichel@me.com

Keywords: Monviso Massif, Western Alps, eclogitic breccia.

Eclogite-facies breccias from the Lago Superiore Unit -LSU- (Monviso metaophiolite complex, W-Alps) preserve a unique record of the HP deformation history of Tethyan oceanic lithosphere metamorphosed during prograde Alpine subduction (peak conditions: 580°C/2.7GPa). Here, the foliation of intact Fe-Ti-rich (Omph + Grt + Rtl ± Lws ± Qtz ± Glp) and Mg-Al-rich metagabbro clasts (Omph + Ep + Rtl ± Qtz ± Glp and locally Grt) cemented by unfoliated Omph ± Grt ± Lws matrices demonstrates pristine brecciation at eclogite-facies conditions. Successive generations of high-pressure veins (omphacite ± garnet ± apatite) and matrices (omphacite ± grenat) reveals multiple brittle rupture events prior to a stage of massive, eclogite-facies fluid ingress marked by a last lawsonite-rich matrix (M3). Trace element composition (on bulk and in-situ) suggests that veins and M1 matrix minerals crystallized in presence of fluids buffered by the metagabbro minerals, i.e. incipient brecciation linked to local fluid production by prograde metamorphic reactions. On the contrary, trace element composition of M3 matrix points to the infiltration of serpentinite-derived fluids. M2 matrix composition suggests a mixing of local fluids with serpentinite-derived fluids, and thus witnesses the opening of the system to external fluids. Both the sharp increase in fluid content (lawsonite content) and shift towards external fluid source from M1 to M3 matrix thus points to (I) local embrittlement due to local reaction-induced fluid release, prior to external fluid ingress throughout stepwise brecciation events reflecting (II) a progressive opening of the system to external fluid sources. Thus, structural and petrographic evidences coupled to geochemical data suggests that the brecciation at eclogite-facies conditions controlled the initial stages of strain localization within the shear zones crosscutting the LSU, likely affecting the evolution of the entire Monviso metaophiolite complex. Its preferential occurrence at the transition Fe-Ti/Mg-Al metagabbro (where strongly focused deformation likely induced transient, anisotropic, high-permeability zones) contributed to rock weakening and promoted preferential pathways for fluid transfer inside the subducting slab.

Super-deep diamond from Central African Republic

Lorenzon S.*¹, Nestola F.¹, Thomassot E.², Prosperi L.³, Lorenzetti A.⁴, Alvaro M.⁵,
Salvadeo F.⁶ & Nimis P.¹

¹ Dipartimento di Geoscienze, Università degli Studi di Padova.

² CRPG-CNRS, Università di Lorraine (Francia).

³ Istituto Gemmologico Italiano.

⁴ Dipartimento di Ingegneria Industriale, Università degli Studi di Padova.

⁵ Dipartimento di Scienze della Terra e dell'Ambiente, Università degli Studi di Pavia.

⁶ Collegio Periti Italiani.

Corresponding email: sofia.lorenzon@phd.unipd.it

Keywords: super-deep diamond, hydrous ringwoodite, subduction.

Diamonds and their inclusions are key geological materials that provide a unique opportunity to directly investigate the deepest regions of our planet.

Based on their depth of formation, diamonds are classified in lithospheric, which formed between about 120 and 220 km depth and represent about 99% of worldwide diamond population, and sub-lithospheric or super-deep diamonds, extremely rare samples which crystallized from about 300 to more than 800 km depth (Stachel et al., 2008).

Here, we have investigated a 1.3 carats diamond, Type IaAB (determined by FTIR), from an alluvial deposit located in Central African Republic, close to the Ubangy river. As far as we know, this is the first study dedicated to diamonds from Central African Republic.

The investigated diamond shows the second world finding of hydrous ringwoodite after the first one found within a Brazilian diamond by Pearson et al. (2014) and thus definitively indicates that our diamond is certainly a super-deep diamond coming from the transition zone between 525 and 660 km depth. The carbon and nitrogen isotopic composition ($\delta^{13}\text{C}$ and $\delta^{15}\text{N}$) of the diamond host was investigated by Secondary Ion Mass Spectroscopy (SIMS) in order to establish the possible source of C and N. Our data show average values of $\delta^{13}\text{C} \sim -2 \text{‰}$ and $\delta^{15}\text{N} \sim +4\text{‰}$ (the nitrogen content is homogeneous over the diamond and in average is 55 ppm). These values match in agreement with those found in super-deep diamonds and reported in previous studies (Stachel et al., 2002). They are consistent with a diamond forming fluid originating from a subducted source (Walter et al., 2011; Cartigny, 2005), which confirms recent studies reporting transition zone and lower-mantle diamonds (Nestola et al., 2018).

Cartigny P. (2005) - Stable Isotopes and the Origin of Diamond. *Elements*, 1, 79-84.

Nestola F., Korolev N., Kopylova M., Rotiroti N., Pearson D.G., Pamato M.G., Alvaro M., Peruzzo L., Gurney J.J., Moore A.M. & Davidson J. (2018) - CaSiO₃ perovskite in diamond indicates the recycling of oceanic crust into the lower mantle. *Nature*, 555, 237-241.

Pearson D.G., Brenker F.E., Nestola F., McNeill J., Nasdala L., Hutchison M.T., Matveev S., Mather K., Silversmith G., Schmitz S., Vekemans B. & Vincze L. (2014) - Hydrous mantle transition zone indicated by ringwoodite included within diamond. *Nature*, 507, 221-224.

Stachel T., Harris J.W., Aulbach S. & Deines P. (2002) - Kankan diamonds (Guinea) III: $\delta^{13}\text{C}$ and nitrogen characteristics of deep diamonds. *Contrib. Mineral. Petrol.*, 142, 465-475.

Stachel T. & Harris J.W. (2008) - The origin of cratonic diamonds -Constraints from mineral inclusions. *Ore Geol. Rev.*, 34, 5-32.

Walter M.J., Kohn S.C., Araujo D., Bulanova J.P., Smith C.B., Gaillou E., Wang J., Steele A. & Shirey S.B. (2011) - Deep Mantle Cycling of Oceanic Crust: Evidence from Diamonds and Their Mineral Inclusions. *Science*, 334, 54-57.

Characterizing deviatoric stress in mineral inclusions

Morana M.*¹, Murri M.¹, Girani A.¹, Angel R. J.¹ & Alvaro M.¹

¹ Dipartimento di Scienze della Terra e dell'Ambiente, Università degli Studi di Pavia.

Corresponding email: marta.morana01@universitadipavia.it

Keywords: XRD, DFT, quartz.

An elastically anisotropic mineral, such as quartz, entrapped in an elastically isotropic host, like garnet, can develop deviatoric stresses. However, the effect of deviatoric stress on crystals is still poorly understood, despite its important role in reconstructive (Richter et al., 2016) and symmetry breaking (Bismayer et al., 1982) phase transitions, and its ubiquitous presence in rocks. Quartz is the ideal starting point to evaluate the effects of deviatoric stress. It has a simple and well-known structure that has been characterised over wide ranges of pressure and temperature and it is one of the most common mineral inclusions in metamorphic rocks. Ab initio hybrid Hartree–Fock/Density Functional Theory calculations were performed as a function of different applied strains (Murri et al., 2019). Simulation results were compared with X-ray diffraction data from a real host-inclusion system: a quartz crystal entrapped in garnet. In this contribution we describe how to deal with the experimental challenges in the collection of intensity data from a host-inclusion system, evaluate the quality of the refinement, and the agreement between the simulation and the experimental data.

Bismayer U., Salje E. & Joffrin C. (1982) - Reinvestigation of the stepwise character of the ferroelastic phase transition in lead phosphate-arsenate, $Pb_3(PO_4)_2 \cdot Pb_3(AsO_4)_2$ J. Phys., 43, 1379-1388.

Murri M., Alvaro M., Angel R.J., Prencipe M., & Mihailova B.D. (2019) - The effects of non-hydrostatic stress on the structure and properties of alpha-quartz. Phys. Chem. Miner., 46, 487-499.

Richter B., Stünitz H. & Heilbronner R. (2016) - Stresses and pressures at the quartz-to-coesite phase transformation in shear deformation experiments. J. Geophys. Res. -Solid Earth, 121, 8015-8033.

Rutile in diamond: the role of elastic anisotropy

Musiyachenko K.^{*1-2}, Murri M.¹, Prencipe M.¹ & Alvaro M.¹

¹ Dipartimento di Scienze della Terra e dell' Ambiente, Università degli Studi di Pavia, Italy.

² V.S. Sobolev Institute of Geology and Mineralogy of the Siberian Branch of the RAS, Novosibirsk, Russian Federation.

Corresponding email: kira.musiyachenko01@universitadipavia.it

Keywords: Rutile, elastic geobarometry, ab-initio calculations.

Rutile stability and abundance in geological environments under a variety of physical and chemical conditions makes it a unique tool for reconstructing rock histories from their crystallization at depth to exhumation to the Earth's surface. Rutile is often trapped as inclusion in garnets and diamonds. On these inclusions, beside chemical barometric methods, elastic geobarometry can be used to determine entrapment conditions for the pair. Elastic geobarometry is based on the evidence that minerals trapped as inclusions within other host minerals can develop non-lithostatic pressures on exhumation as a result of the differences between the thermo-elastic properties of the host and inclusion phases (Angel et al., 2015).

Rutile is much stiffer than garnet, so it is not expected to exhibit any significant residual pressure when trapped at typical metamorphic conditions (Zaffiro et al., 2019). Also, rutile trapped in diamonds within the diamond stability field (e.g. 5 GPa 1250°C) will be under-pressurized ($P_{inc} = -0.997 \text{ GPa}$) at room conditions. While the volume strain of the inclusions cannot be used to infer the entrapment conditions for these pairs, we can use the strains along the two principal crystallographic directions. The entrapment conditions can be calculated from the residual strains on the inclusion using the fully anisotropic elastic geobarometry approach (Mazzucchelli et al., 2018). For example, our calculations for rutile in diamonds assuming entrapment conditions of 5 GPa 1250°C predict that the residual strains should be considerably different from one another ($\epsilon_1 = -0.00111$, $\epsilon_3 = 0.00688$).

The backward process of determining the entrapment conditions requires to calculate the residual strains on the inclusions. These can be obtained from the Raman wavenumber shifts using the concept of phonon-mode Grüneisen tensor. We investigated the elastic and vibrational properties of rutile performing ab initio hybrid HF/DFT simulations under different strain conditions to determine the phonon-mode Grüneisen tensor for rutile following the protocol adopted by Murri et al. (2018). The expected strains ($\epsilon_1 = -0.00111$, $\epsilon_3 = 0.00688$) would develop measurable Raman wavenumber shifts ($>5 \text{ cm}^{-1}$), according to our ab initio calculations.

This project has received funding from the European Research Council under the H2020 research and innovation program (N. 714936 TRUE DEPTHS to M. Alvaro)

Angel R.J., Nimis P., Mazzucchelli M.L., Alvaro M. & Nestola F. (2015) - How large are departures from lithostatic pressure? Constraints from host-inclusion elasticity. *J. Metamorph. Geol.*, 33(8), 801-813.

Mazzucchelli M.L., Burnley P., Angel R.J., Morganti S., Domeneghetti M.C., Nestola F. & Alvaro M. (2018) - Elastic geothermobarometry: Corrections for the geometry of the host-inclusion system. *Geology*, 46(3), 231-234.

Murri M., Mazzucchelli M.L., Campomenosi N., Korsakov A.V., Prencipe M., Mihailova B.D. Scambelluri M., Angel R.J. & Alvaro M. (2018) - Raman Elastic Geobarometry for Anisotropic Mineral Inclusions. *Am. Mineral.*, 103(11), 1869-1872.

Zaffiro G., Angel R.J. & Alvaro M. (2019) - Constraints on the Equations of State of stiff anisotropic minerals: rutile, and the implications for rutile elastic barometry. *Min. Mag.* (in press)

Diamond-magnesiochromite host-inclusion system recording old deep lithosphere conditions at Udachnaya (Siberia)

Nestola F.¹, Zaffiro G.², Mazzucchelli M.L.², Nimis P.*¹, Andreozzi G.B.³, Periotto B.¹, Princivalle F.⁴, Lenaz D.⁴, Secco L.¹, Pasqualetto L.¹, Logvinova A.M.¹, Sobolev N.V.⁵, Lorenzetti A.⁶ & Harris J.W.⁷

¹ Dipartimento di Geoscienze, Università di Padova.

² Dipartimento di Scienze della Terra e dell'Ambiente, Università di Pavia.

³ Dipartimento di Scienze della Terra, Sapienza Università di Roma.

⁴ Dipartimento di Matematica e Geoscienze, Università di Trieste.

⁵ Institute of Mineralogy and Petrography, Novosibirsk, Russia.

⁶ Dipartimento di Ingegneria Industriale, Università di Padova.

⁷ School of Geographical and Earth Sciences, University of Glasgow.

Corresponding email: paolo.nimis@unipd.it

Keywords: host-inclusion system, diamond, magnesiochromite.

Lithospheric diamonds (formed between 130 and 200 km) represent 99% of all mined diamonds. These diamonds may contain mineral inclusions, which can be used to derive inferences on the physical-chemical environments in which their host diamonds were formed. Magnesiochromite (mchr) is one of the most common of these inclusions, representing about 19% of reported inclusions in lithospheric diamonds worldwide, but this mineral is not amenable to conventional thermobarometry. To determine the formation conditions of a mchr-bearing diamond from the Paleozoic Udachnaya kimberlite (Siberia), we adopted an alternative method based on elastic geobarometry. When a mineral is trapped in a host at conditions P_{trap} and T_{trap} and then is exhumed to the Earth's surface, it may develop residual strains as a result of the contrast in elastic properties between the host and the inclusion. If T_{trap} is known independently and the residual strains are measured when the host is at room pressure, P_{trap} can be back-calculated as the condition at which mechanical equilibrium between the host and the inclusion is elastically restored.

FTIR spectra of the diamond host indicated an average N content of 267 ppm and allowed to classify the diamond as type-IaAB. The measured N-aggregation state is compatible with a mantle residence T (assumed to be the same as T_{trap}) of 1125–1140 °C for a diamond age of 3.5–2 Ga, typical for Udachnaya diamonds. A residual pressure $P_{\text{inc}} = 1.073(72)$ GPa was obtained by studying the mchr inclusion by single-crystal X-ray diffraction and by comparing its unit-cell volumes measured before and after its release from the host diamond. Using the obtained T_{trap} , P_{inc} , the appropriate P-V-T Equation of State for mchr and diamond and an elastic model, we obtained the following entrapment conditions: $P_{\text{trap}} = 6.5(2)$ GPa and $T_{\text{trap}} = 1125(32)$ – $1140(33)$ °C. These conditions fall on a ~35 mW/m² geotherm, which is colder than most mantle xenoliths from the same depths, suggesting that cold cratonic conditions persisted for billions of years to at least 200 km in the local lithosphere.

Given the relatively common occurrence of mchr inclusions in diamonds, this method can potentially be applied to a large number of diamonds from worldwide localities. This would in turn allow better insight into the depth distribution of lithospheric diamonds at global scale and, consequently, into the processes that control diamond formation in the Earth's mantle.

Crystallographic relationships between diamond and its clinopyroxene inclusions

Pasqualetto L.*¹, Nestola F.¹, Nimis P.¹, Jacob D.E.², Oliveira B.², Perritt S.³, Chinn I.³,
Milani S.⁴ & Harris J.W.⁵

¹ Department of Geosciences, University of Padova, Italy.

² Department of Earth and Planetary Sciences, Macquarie University, North Ryde, Australia.

³ De Beers Exploration, South Africa.

⁴ Department of Earth Sciences, University of Milano, Italy.

⁵ School of Geographical and Earth Sciences, University of Glasgow, United Kingdom.

Corresponding email: leonardo.pasqualetto@phd.unipd.it

Keywords: diamond, clinopyroxene inclusions.

Inclusions in kimberlite-borne diamonds represent exceptional samples of the deep Earth, which have provided invaluable information on deep mantle processes that occurred up to several billion years ago. Recent work on the crystallographic orientation of inclusions in diamonds has suggested that several inclusions that were previously interpreted to be syngenetic with diamond may actually have formed before the diamond (i.e., they are protogenetic) (Nestola et al., 2014, 2017, 2019; Milani et al., 2016; Nimis et al., 2019). Specific data on clinopyroxene inclusions, however, are still very scarce. In this on-going work, we have studied by single-crystal X-Ray diffraction the crystallographic orientations of 26 clinopyroxene inclusions in 8 diamonds from the Cullinan (South Africa), Voorspoed (South Africa) and Udachnaya (Siberian Russia) kimberlites. The results indicate no specific crystallographic orientations between the clinopyroxenes and their host diamonds. However, three diamonds with multiple inclusions have pairs of clinopyroxenes that are iso-oriented within a few degrees. We interpret these inclusions as portions of pre-existing clinopyroxene monocrystals, which were partially dissolved during entrapment by the diamond host. Therefore, at least these iso-oriented inclusions are probably protogenetic. This interpretation is similar to that given by Nestola et al. (2014, 2019), Milani et al. (2016) and Nimis et al. (2019) for some olivine, garnet and magnesiochromite inclusions in diamonds. The implications of our results for the correct interpretation of thermobarometric and geochronological data based on clinopyroxene inclusions in diamonds will be discussed.

Milani S., Nestola F., Angel R.J., Nimis P. & Harris J.W. (2016) - Crystallographic orientations of olivine inclusions in diamonds. *Lithos*, 265, 312-316.

Nestola F., Jacob D.E., Pamato M.G., Pasqualetto L., Oliveira B., Greene S., Perritt S., Chinn I., Milani S., Kueter N., Sgreva, N., Nimis P., Secco L. & Harris J.W. (2019) - Protogenetic garnet inclusions and the age of diamonds. *Geology*, 47, 431-434.

Nestola F., Jung H. & Taylor L.A. (2017) - Mineral inclusions in diamonds may be synchronous but not syngenetic. *Nat. Commun.*, 8, 14168.

Nestola F., Nimis P., Angel R. J., Milani S., Bruno M., Prencipe M. & Harris J.W. (2014) - Olivine with diamond-imposed morphology included in diamonds. Syngenesi or protogenesis?. *Int Geol. Rev.*, 56, 1658-1667.

Nimis P., Angel R.J., Alvaro M., Nestola F., Harris J.W., Casati N., & Marone F. (2019) - Crystallographic orientations of magnesiochromite inclusions in diamonds: what do they tell us? *Contrib. Mineral. Petr.*, 174, 29.

Eclogite-facies coronitic metagabbro and metatroctolite from the Zermatt-Saas ophiolites, Valtournanche, Italy

Rebay G.*¹, Godard G.² & Kiénast J.R.²

¹ Dipartimento di Scienze della Terra, Università di Pavia, Italy.

² IGP-Paris, France.

Corresponding email: gisella.rebay@unipv.it

Keywords: Valtournanche, eclogitized rocks, metamorphic reactions, oceanic hydrothermal alteration.

Coronitic metatroctolite and metagabbro from scree west of Crépin village, Valtournanche, in the Western Alps, Italy, belong to the Zermatt-Saas ophiolitic Unit. The rocks display a whole range of transformation, from very thin coronitic reactions, giving rise to eclogite-facies minerals, to the complete replacement of igneous minerals by new high-P peculiar, chloritoid-bearing, assemblages.

In incompletely eclogitized rocks, the relics of igneous minerals are rimmed by complex concentric coronas consisting of talc + clinopyroxene + chlorite + garnet between olivine and plagioclase, and by omphacite coronas between augite and plagioclase. The pseudomorphs after plagioclase are made of very fine-grained clinozoisite + garnet ± jadeite ± kyanite.

In fully transformed troctolite, fine-grained jadeitic clinopyroxene and clinozoisite have replaced igneous plagioclase. Progressing towards the former olivine, small kyanite crystals appear around large clinozoisite crystals, together with micas (phengite and paragonite), chloritoid and, finally, garnet, which forms irregular coronas at the former plagioclase-olivine interface. Olivine is mainly transformed into talc. Large tremolite crystals are also common, as well as very fine-grained omphacite, phengite, chloritoid, chlorite, kyanite and rare quartz. The igneous Cr-rich clinopyroxene is partly to completely overgrown by omphacite, which may in turn be overgrown by Cr-rich chloritoid and talc.

The various degrees of development of eclogite-facies metamorphic reactions are related to the intensity of the oceanic hydrothermal alteration that preceded eclogitization and which favoured both the chemical homogenisation of igneous microdomains and the kinetics of the subsequent eclogite-facies reactions.

The observed mineral assemblages (omphacite, garnet, kyanite, chloritoid, talc), together with mineral composition, are consistent with re-equilibration under high-P conditions. Pressure and temperature conditions, inferred from thermobarometric calculations and P-T pseudosection modelling, indicate $P > 2$ GPa for $T \gg 600^\circ\text{C}$.

Zircon and quartz inclusions in garnet used for complimentary Raman-thermobarometry: application to the Holsnøy eclogite, Bergen Arcs, Western Norway

Zhong X.*¹, Andersen N.², Dabrowski M.¹⁻³ & Jamtveit B.¹

¹ Physics of Geological Processes, The Njord Centre, Department of Geosciences, University of Oslo, Norway.

² Department of Chemistry, University of Oslo, Norway.

³ Computational Geology Laboratory, Polish Geological Institute - NRI, Wrocław, Poland.

Corresponding email: xinzhong0708@gmail.com

Keywords: zircon, Raman spectroscopy, Bergen eclogite.

Mineral inclusions entrapped into a host crystal are commonly observed in nature. During tectonic or erosional processes, cooling and decompression may occur that lead to the development of residual pressure within the inclusion. This is because of the differences in thermal expansivity and compressibility between the inclusion and host. By combining laser Raman spectroscopy and experimental data relating pressure and Raman shift, it is possible to estimate the entrapment pressure-temperature (P-T) conditions using an isotropic elastic model. In this study, both quartz and zircon inclusions entrapped in garnet host have been identified in Holsnøy eclogite with laser Raman spectroscopy, and their Raman spectral shifts are measured. Using the published experimental data, the maximal residual pressures for zircon and quartz inclusions are estimated to be ca. 0.6GPa and 0.65GPa, respectively. The equation of state for zircon has been fitted based on experimental measurements and used in a 1D isotropic elastic model to recover the entrapment P-T conditions. The recovered entrapment P-T conditions are ca. 1.7~1.9GPa and 680~760°C, which are generally consistent with previous estimates using phase equilibria techniques. Heating/cooling experiments are performed on a spherical, entrapped zircon inclusion using a specially designed thermostated aluminium box and cryostat. A clear trend is observed between the residual zircon inclusion pressure and the externally controlled temperature from ca. -100 to 100°C. It is confirmed in this study that the residual zircon inclusion pressure sealed in garnet host is very sensitive to the entrapment temperature and can be used as a Raman-thermometer. The effect of laser power has been found out to be significant. A safe laser power is determined to be ca. 10mW, which does not cause any local heating effect. The significance of thermo-elastic anisotropy of zircon inclusion on the residual stress/strain state is investigated using the classical Eshelby's solution and will be discussed.

S2.

Mineralogical Crystallography and New Minerals

CONVENERS AND CHAIRPERSONS

Fernando Camara (Università di Milano)

Cristina Carbone (Università di Genova)

New insights into the crystal chemistry of tourmaline from Busachi (central Sardinia), Italy

Agrosi G. *, Lacalamita M., Mesto E., Schingaro E. & Tempesta G.

Dipartimento di Scienze della Terra e Geoambientali, Università di Bari Aldo Moro.

Corresponding email: emanuela.schingaro@uniba.it

Keywords: tourmaline, crystal chemistry.

Crystal chemical studies of minerals belonging to the tourmaline supergroup require full chemical analyses including light elements and site assignments by crystal-structure refinements (Bosi, 2018). Moreover, the chemical zoning that commonly affect tourmaline minerals needs to be investigated by a multi-analytical approach to provide information also about the evolution of growth environment (Agrosi et al., 2006).

We investigate tourmaline from Busachi (central Sardinia, Italy) via optical observation on thin sections, quantitative chemical analyses, EDS-chemical mapping and structure refinements by SCXRD. The light elements were detected by LIBS (Tempesta & Agrosi, 2016). The studied samples come from rare tourmalinite veins intruded in migmatites and orthogneiss (Matteucci & Zucchetti, 1965) belonging to the Paleozoic Variscan basement (Carmignani et al., 2015)

The preliminary results show that the samples are fractured with a textural and compositional heterogeneity. Two main growth stages are identified: the first exhibits distinctive compositional asymmetry characterized by light and dark green bands; the second exhibit a blue colour and consists of a partially replacing of pre-existing tourmaline and filling of fractures from reactive fluids. The primary tourmaline is ranging from schorl to dravite with highly-variable Mg and Fe contents; the secondary tourmaline is a blue schorl with the highest Fe content.

The average Li₂O amount is below 0.03 wt % with the highest concentration in the secondary blue schorl.

The s.g. is R3m, with unit cell parameters: $15.9679(2) < a < 15.9750(2) \text{ \AA}$, $7.1160(1) < c < 7.1615(1) \text{ \AA}$. Structure refinements converged to R values better than 1.5%. The X site is occupied mainly by Na, with mean atomic numbers (m.a.n., e⁻) varying from 5.94 to 7.71; the Y site is populated by Fe and Mg with m.a.n varying from 18.51 and 20.33 e⁻; in the Z site m.a.n varies from 12.92 and 13.09 e⁻ and, for the T site $13.49 \leq \text{m.a.n.} \leq 13.88$. The B site is stoichiometric. The W site has m.a.n. ranging from 8.31 to 8.53 e⁻.

For the first time we evidence deformation and fracturing of primary Busachi tourmaline and partial tourmaline replacement by reactive fluids with adequate chemical affinity.

Agrosi G., Bosi F., Lucchesi S., Melchiorre G. & Scandale E. (2006) - Mn-tourmaline crystals from island of Elba (Italy):

Growth history and growth marks. *Am. Mineral.*, 91(5-6), 944-952.

Bosi F. (2018) - Tourmaline crystal chemistry. *Am. Mineral.*, 103(2), 298-306.

Carmignani, L. Oggiano, G. Funedda, A., Conti P. & Pasci S. (2015) - The geological map of Sardinia (Italy) at 1:250,000 scale. *Journal of Maps*, 12(5), 826-835. <https://doi.org/10.1080/17445647.2015.1084544>

Matteucci & Zucchetti (1965) - Studio dei sistemi di filoni di Tormalinite di Busachi (Sardegna Centrale). *Boll. Ass. Min. Subalpina*, 3, 381-396

Tempesta G. & Agrosi G. (2016) - Standardless, minimally destructive chemical analysis of red beryls by means of Laser Induced Breakdown Spectroscopy. *Eur. J. Mineral.*, 28(3), 571-580.

Micro-Raman chemical characterization of amphiboles

Bersani D.*¹, Fornasini L.¹, Zanoni A.¹, Andò S.², Gentile P.², Salvioli-Mariani E.³ & Lottici P.P.¹

¹ Università di Parma, Department of Mathematical, Physical and Computer Sciences, Italy.

² Department of Earth and Environmental Sciences, University of Milano-Bicocca, Italy.

³ The Department of Chemistry, Life Sciences and Environmental Sustainability, Parma, Italy.

Corresponding email: danilo.bersani@unipr.it

Keywords: Raman spectroscopy, amphiboles.

Raman spectroscopy is a powerful tool for the identification and characterization of minerals. However, the assessment of the chemical composition of a mineral belonging to a series starting from its Raman spectrum is a difficult task, requiring detailed preliminary calibration work. Here we report on the results obtained on two important families of amphiboles: tremolite-actinolite and glaucophane. In the calcic amphibole series, sometimes called “nephrite series”, tremolite is the magnesian term ($\text{Ca}_2\text{Mg}_5\text{Si}_8\text{O}_{22}(\text{OH})_2$), while ferro-actinolite ($\text{Ca}_2\text{Fe}_3\text{Si}_8\text{O}_{22}(\text{OH})_2$) is the ferric one. The members of the series can be distinguished by $X = \text{Mg}/(\text{Mg}+\text{Fe}^{2+})$ ratio: for $0.9 \leq X \leq 1$ we have tremolite, for 0.5

Glaucophane ($\text{Na}_2\text{Mg}_3\text{Al}_2\text{Si}_8\text{O}_{22}(\text{OH})_2$) is a sodic amphibole, typical component of the “blue schists”. The substitutions, in particular Fe^{2+} for Mg and Fe^{3+} for Al, are frequent. Glaucophane forms a series with ferroglaucophane $\text{Na}_2\text{Fe}^{2+}_3\text{Al}_2\text{Si}_8\text{O}_{22}(\text{OH})_2$ and magnesian riebeckite $\text{Na}_2\text{Mg}_3\text{Fe}^{3+}_2\text{Si}_8\text{O}_{22}(\text{OH})_2$.

18 natural samples of glaucophane and 21 natural samples of tremolite-actinolite, mostly coming from Alps, have been studied. The first part of the characterization was carried out by SEM-EDS, in order to have the elemental composition of the crystals in different points of each sample. Non-polarized micro-Raman spectra have been obtained on the same points with a Horiba Jobin-Yvon LabRam apparatus with excitation at 473.1 and 632.8 nm.

The first important source of information on the chemical composition is the OH stretching vibration, in the high-wavenumber range. The OH-stretching peaks changes in number (1 to 4) and relative intensity, according to the composition. A simple statistic model is presented to estimate the $\text{Mg}/(\text{Mg}+\text{Fe}^{2+})$ molar ratio from the areas of the OH stretching peaks for both sodic and calcic families of amphiboles. At lower wavenumbers, the main Raman feature, at nearly 670 cm^{-1} , attributed to the Si-O-Si symmetric stretching, show a splitting in glaucophane increasing with the relative amount of Mg, useful to estimate the $\text{Mg}/(\text{Mg}+\text{Fe}^{2+})$ ratio. In the case of tremolite-actinolite, the 670 cm^{-1} peak is not splitting but downshifts with increasing the amount of iron and its position can be used to estimate the $\text{Mg}/(\text{Mg}+\text{Fe}^{2+})$ ratio. Further information can be obtained on $\text{Al}/(\text{Al}^{\text{VI}}+\text{Fe}^{3+})$ ratio in glaucophane from the study of the Raman peaks around $\sim 980 \text{ cm}^{-1}$ and $\sim 1040 \text{ cm}^{-1}$, attributed to the Si-Ob-Si asymmetric stretching.

New nomenclature and classification of tetrahedrite-group minerals

Biagioni C.¹, Bosi F.², Cook N.J.³, George L.L.³, Makovicky E.⁴, Moëlo Y.⁵, Pasero M.*¹, Sejkora J.⁶, Stanley C.J.⁷ & Welch M.D.⁷

¹ Dipartimento di Scienze della Terra, Università di Pisa. ² Dipartimento di Scienze della Terra, Sapienza Università di Roma. ³ School of Chemical Engineering, University of Adelaide (Australia).

⁴ Department of Geoscience and Natural Resources Management, University of Copenhagen (Denmark).

⁵ Institut des Matériaux Jean Rouxel, UMR 6502, CNRS, Université de Nantes (France).

⁶ Department of Mineralogy and Petrology, National Museum, Prague (Czech Republic).

⁷ Department of Earth Sciences, Natural History Museum, London (United Kingdom).

Corresponding email: marco.pasero@unipi.it

Keywords: tetrahedrite, nomenclature, classification.

The nomenclature of minerals of the tetrahedrite group has been revised, and the tetrahedrite group has been formally established (voting proposal IMA 18-K approved by the CNMNC). The key-points of the new tetrahedrite-group report are the following:

- A member of the tetrahedrite group is a sulfosalt having a considerably collapsed sodalite-like framework compatible with the general structural formula $M^{(2)}A_6M^{(1)}(B_4C_2)^{X(3)}D_4S^{(1)}Y_{12}S^{(2)}Z$, where A = Cu⁺, Ag⁺, □ (vacancy); B = Cu⁺, Ag⁺; C = Zn²⁺, Fe²⁺, Hg²⁺, Cd²⁺, Mn²⁺, Cu²⁺, Cu⁺, Fe³⁺; D = Sb³⁺, As³⁺, Bi³⁺, Te⁴⁺; Y = S²⁻, Se²⁻; and Z = S²⁻, Se²⁻, □. The occurrence of both Me⁺ and Me²⁺ cations at the M(1) site, in a 4:2 atomic ratio, is a case of valency-imposed double site-occupancy (Hatert & Burke, 2008). Consequently, samples having different pairs of B and C dominant constituents must be regarded as separate mineral species. So far, little attention was paid to the subordinate – yet essential for stoichiometric constraints – C constituents in the definition of the ideal end-member formulae.

- Each different combination of dominant constituents $M^{(1)}B$, $X^{(3)}D$ and $S^{(1)}Y$ deserves a distinct root-name.
- As a rule the dominant M(1)C is included in the mineral name as a hyphenated suffix, e.g., tetrahedrite-(Fe).
- Depending on the Cu⁺/Ag⁺ ratio, if two minerals have $M^{(1)}B = Cu$ and the same dominant constituent at $X^{(3)}D$ and $S^{(1)}Y$, they will be assigned the same root-name. The adjectival prefix “argento” will be added to the root-name if $M^{(2)}Ag > M^{(2)}Cu$ (no prefix when $M^{(2)}Cu > M^{(2)}Ag$). Minerals with $M^{(1)}B = Ag$ deserve a different root-name.
- The tetrahedrite group is divided into series, on the basis of the combination of $M^{(2)}A$, $M^{(1)}B$, $X^{(3)}D$, and $S^{(1)}Y$ constituents. So far five series have been recognized: tetrahedrite series, tennantite series, freibergite series, hakite series, giraudite series. Some unassigned members [goldfieldite, argentotennantite-(Zn), and rozhdestvenskayaite-(Zn)] belong to other three potential series.

The complex situation within the freibergite series will be discussed in detail. Two minerals exist within that series, namely argentotetrahedrite-(Fe), Ag₆(Cu₄Fe₂)Sb₄S₁₃, and kenoargentotetrahedrite-(Fe), Ag₆(Cu₄Fe₂)Sb₄S₁₂□. The latter mineral has (Ag₆)⁴⁺ clusters surrounding the empty $S^{(2)}Z$ site (hence the adjectival prefix “keno”), whereas in the former mineral the S(2)Z is occupied by the 13th sulfur, giving rise to regular S-centered Ag⁺₆ octahedra.

Hatert F. & Burke E.A.J. (2008) - The IMA–CNMNC dominant-constituent rule revisited and extended. *Can. Mineral.*, 46, 717-728.

Giacovazzoite and scordariite, two new minerals related to metavoltine

Biagioni C.¹, Mauro D.*¹, Bindi L.², Hålenius U.³ & Pasero M.¹

¹ Dipartimento di Scienze della Terra, Università di Pisa.

² Dipartimento di Scienze della Terra, Università degli Studi di Firenze.

³ Department of Geosciences, Swedish Museum of Natural History, Stockholm, Sweden.

Corresponding email: daniela.mauro@dst.unipi.it

Keywords: new mineral, metavoltine group, sulfate.

The mineralogical study of secondary mineral assemblages derived from the TI-rich pyrite ore deposits from the southern Apuan Alps allowed the identification of two iron-potassium sulfates structurally related to metavoltine. The studied sulfate assemblage is mainly formed by melanterite, halotrichite, and alum-(K), with accessory römerite, coquimbite, alunogen, krausite, and minor goldichite, voltaite, khademite, and two new iron-potassium minerals, giacovazzoite (IMA 2018-165) and scordariite (IMA 2019-010).

Giacovazzoite, $K_5Fe^{3+}_3O(SO_4)_6 \cdot 10H_2O$, occurs as prismatic crystals, up to 0.1 mm in length, orange-brown in color, with a vitreous luster and {100} cleavage. The empirical formula of this mineral is $K_{5.06}Fe^{3+}_{2.98}O(SO_4)_{6.00} \cdot 10H_2O$. Single-crystal X-ray diffraction study gave the following unit-cell parameters: $a = 9.4797(2)$, $b = 18.4454(5)$, $c = 18.0540(4)$ Å, $\beta = 92.626(2)^\circ$, $V = 3153.5(1)$ Å³. Space group is $P2_1/c$. Giacovazzoite is the natural analogue of the synthetic β -Maus's Salt (Mereiter and Völlenklee, 1978).

The crystal structure was refined, starting from the atomic coordinates of its synthetic counterpart, to $R_1 = 0.0587$ for 10254 unique reflections with $F_o > 4\sigma(F_o)$ and 515 refined parameters. The crystal structure can be described as formed by a structural unit composed by $[Fe^{3+}_3O(SO_4)_6(H_2O)_3]^{5-}$ clusters, identical to those occurring in metavoltine (Giacovazzo et al., 1976), carlsonite (Kampf et al., 2016), and a series of synthetic compounds, e.g., (Scordari et al., 1994), and by an interstitial complex having formula $\{K_5(H_2O)_7\}^{5+}$.

Scordariite has ideal chemical formula $K_8(Fe^{3+}_{0.67}Na_{0.33})[Fe^{3+}_3O(SO_4)_6]_2 \cdot 14H_2O$. It occurs as pseudo-hexagonal tabular crystals, up to 0.5 mm in size, yellowish to brownish in color, with a perfect {0001} cleavage. The empirical formula of this mineral is $(K_{7.48}Na_{0.34})_{\Sigma 7.82}(Fe^{3+}_{6.47}Al_{0.26})_{\Sigma 6.73}O_2(SO_4)_{12.00} \cdot 14H_2O$. Scordariite is trigonal, space group $R\bar{3}$, with unit-cell parameters $a = 9.7509(4)$, $c = 53.525(2)$ Å, $V = 4407.4(4)$ Å³. The crystal structure was solved and refined to $R_1 = 0.0590$ for 3527 unique reflections with $F_o > 4\sigma(F_o)$ and 143 refined parameters. The crystal structure of this phase is layered, with three distinct kinds of layers stacked along c in the sequence ...*ABC*B*ABC*B... Layer *A* has composition $\{K_4(H_2O)\}^{4+}$; layer *B* is characterized by the same cluster $[Fe^{3+}_3O(SO_4)_6(H_2O)_3]^{5-}$ occurring in giacovazzoite and related compounds, and by an interstitial K^+ ion; finally, layer *C* has composition $\{K_2\}[(Fe,Al)_{0.67}(H_2O)_6]^{4+}$. The occurrence of Fe^{3+} as the only oxidation state of iron was confirmed by Mössbauer spectroscopy collected on an intimate mixture of krausite and IMA 2019-010, showing only a negligible amount of Fe^{2+} [$Fe^{2+}/Fe_{tot} = 0.02(1)$].

Giacovazzo C., Scordari F., Todisco A. & Menchetti S. (1976) - Crystal structure model for metavoltine from Sierra Gorda. *Tschermaks Mineralogische und Petrographische Mitteilungen*, 23, 155-166.

Kampf A.R., Richards, R.P., Nash, B.P., Murowchick, J.B. & Rakovan J.F. (2016) - Carlsonite, $(NH_4)_5Fe^{3+}_3O(SO_4)_6 \cdot 7H_2O$, and huizingite-(Al), $(NH_4)_9Al_3(SO_4)_8(OH)_2 \cdot 4H_2O$, two new minerals from a natural fire in an oil-bearing shale near Milan, Ohio., 101, 2095-2107.

Mereiter V.K. & Völlenklee H. (1978) - Die Kristallstruktur von β -Pentakalium- $[\mu_3$ -oxo-hexa- μ -sulfato-triaquatrisen(III)]-Heptahydrat-eine monocline Modifikation des Mausschen Salzes. *Acta Crystallographica*, B34, 378-384

Scordari F., Stasi F., Schingaro E. & Comunale G. (1994) - A survey of $(Na, H_3O^+, K)_5Fe_3O(SO_4)_6 \cdot H_2O$ compounds: architectural principles and influence of the Na-K replacement on their structures. Crystal structure, solid-state transformation and its relationship to some analogues. *Zeitschrift für Kristallographie*, 209, 733-737.

Collisions in outer space produced a vacancy-rich, partially inverted tetragonal ringwoodite in several shocked meteorites

Bindi L.*

Università di Firenze.

Corresponding email: luca.bindi@unifi.it

Keywords: ringwoodite, shocked meteorites, spinel.

A new high-pressure silicate, $(\text{Mg,Fe,Si})_2(\text{Si},\square)\text{O}_4$ with a tetragonal spinelloid structure (space group $I4_1/amd$), was discovered within shock-melt veins in the Tenham and Suizhou meteorites, two highly shocked meteorites (Ma et al., 2019). Relative to ringwoodite *s.s.*, this phase exhibits an inversion of Si coupled with intrinsic vacancies and a consequent reduction of symmetry. Inversion in naturally occurring silicate-spinels is a new observation, so far reported only in this and in one other recent study (Bindi et al., 2018). It carries the potential for supporting constraints on high-pressure geothermobarometry and kinetic effects. Most notably, the spinelloid makes up about 30 to 40 vol% of the matrix of shock veins with the remainder composed of a vitrified $(\text{Mg,Fe})\text{SiO}_3$ phase (in Tenham) or $(\text{Mg,Fe})\text{SiO}_3$ -rich clinopyroxene (in Suizhou); these phase assemblages constitute the bulk of the matrix in the shock veins. Previous assessments of the melt matrices concluded that majorite and akimotoite were the major phases. Our contrasting result requires a reconsideration of the conditions during shock-melt cooling of the Tenham and Suizhou meteorites, revealing in particular a much higher quench rate (at least 5×10^3 K/s) for veins of 100 to 500 μm diameter, thus overriding formation of the stable phase assemblage majoritic garnet plus periclase.

Interestingly, a new high-pressure, Fe-rich, Cr-, Ti-bearing silicate with formula $(\text{Fe,Mg,Cr,Ti,Ca},\square)_2(\text{Si,Al})\text{O}_4$ and with a tetragonal $I4_1/amd$ spinelloid structure has been recently discovered in a shock melt pocket during an ongoing nano-mineralogy investigation of the Tissint shergottite (Ma et al., 2019). Also in this case, the new phase makes up about 30 vol% of the matrix of the shock vein, thus calling for a general revision of the inferred conditions during shock-melt cooling of highly shocked meteorites.

Bindi L., Griffin W.L., Panero W., Sirotkina E.A., Bobrov A.V. & Irifune T. (2018) - Synthesis of inverse ringwoodite sheds light on the subduction history of Tibetan ophiolites. *Sci. Rep.*, 8, 5457.

Ma C., Tschauner O., Bindi L., Beckett J.R. & Xie X. (2019) - A vacancy-rich, partially inverted spinelloid silicate, $(\text{Mg,Fe,Si})_2(\text{Si},\square)\text{O}_4$, as a major matrix phase in shock melt veins of the Tenham and Suizhou L6 chondrites. *Met. & Plan. Sci.*, <https://doi.org/10.1111/maps.13312>

Ma C., Tschauner O. & Beckett J.R. (2019) - Discovery of a new high-pressure silicate phase, $(\text{Fe,Mg,Cr,Ti,Ca},\square)_2(\text{Si,Al})\text{O}_4$ with a tetragonal spinelloid structure, in a shock melt pocket from the Tissint Martian meteorite. 50th Lunar and Plan. Sci. Conf., Abstract #1460.

Superstructure of moraesite: a synchrotron study

Bonaccorsi E. *, Merlino S. & Pasero M.

Dipartimento di Scienze della Terra, Università di Pisa.

Corresponding email: elena.bonaccorsi@unipi.it

Keywords: moraesite, superstructure, berylllophosphate.

Moraesite (Lindberg et al., 1953) is a hydrated berillophosphate with ideal chemical formula $\text{Be}_2(\text{PO}_4)(\text{OH})\cdot 4\text{H}_2\text{O}$. Its structure has been known since 1992 (Merlino & Pasero, 1992) and refined in the space group $C2/c$, $a = 8.553(6) \text{ \AA}$, $b = 12.319(6) \text{ \AA}$, $c = 7.155(8) \text{ \AA}$, $\beta = 97.93(9)^\circ$. The main structural feature of moraesite is the presence of large structural cavities occupied by water molecules. The latter are implicated in a complex system of hydrogen bonds where two possible hydrogen bond schemes are equally possible. Few very weak superstructure reflections were observed (Merlino & Pasero, 1992), indicating that the true unit cell of moraesite was probably three times larger, with a b parameter of 36.96 \AA and space group symmetry Cc . It was suggested by the authors that the ordering of the hydrogen bond system, concerted with minor adjustments of the structure, could be responsible for the triplication of the b axis. X-ray diffraction data, more recently obtained through synchrotron radiation, confirmed the occurrence of superstructure reflections which were indexed on the basis of an unit cell with tripled b axis. The superstructure of moraesite ($a = 8.572(3) \text{ \AA}$, $b = 36.971(8) \text{ \AA} = 3 \times b_{\text{sub}}$, $c = 7.153(2) \text{ \AA}$, $\beta = 97.72(1)^\circ$, space group Cc) was refined up to $R = 0.081$ for 1789 unique reflections with $F_o > 4\sigma(F_o)$ and 0.0906 for all 2088 data. The structural refinement confirmed that the triplication of the parameter b is due to the ordering of the two possible hydrogen bonding schemes.

Lindberg M.L., Pecora W.T. & Barbosa A.L.M. (1953) - Moraesite, a new hydrous beryllium phosphate from Minas Gerais, Brazil. *American Mineralogist*, 38, 1126-1133.

Merlino S. & Pasero M. (1992) - Crystal chemistry of berylllophosphates: The crystal structure of moraesite, $\text{Be}_2(\text{PO}_4)(\text{OH})\cdot 4\text{H}_2\text{O}$, *Zeitschrift für Kristallographie*, 201, 253-262.

Dienerite, Ni₃As: a mineralogical species to revalidate

Bonazzi P.* & Bindi L.

Università di Firenze.

Corresponding email: paola.bonazzi@unifi.it

Keywords: dienerite, nickel arsenide, awaruite.

A mineral with chemical formula Ni₃As was found for the first time by the Austrian paleontologist Professor Carl Diener (1862-1928) in a now abandoned mine near Radstradt (Salzburg, Austria) and its physico-chemical characterization date back to twenty's. According to Ramdohr (1969) no sample of dienerite was collected after the first finding while the whole original specimen was used completely in the chemical characterization. According to Yund (1961), no phase corresponding to dienerite crystallized in the Ni-As system and it was concluded that, if this phase exists, it must be stable only at a very low temperature (<200 °C). In this light, the successive results from the experimental study (Gervilla et al., 1994) were not significant at all owing the experiments carried out only at higher temperatures (450 and 790 °C). Nonetheless, Bayliss (2001) supposed that a typographic error (i.e. an accidental interchange between As and Ni) in the transcription of the original chemical analysis led to describe a sample of nickelskutterudite (As_{3-x}Ni) as dienerite, which indeed had been described as cubes greyish-white in color and with metallic lustre. As a consequence of his article, the mineral went to discreditation (Burke, 2006).

After that time, however, some occurrences of nickel arsenide corresponding to dienerite have been reported in literature.

In this work, we report the discovery of minute Ni₃As inclusions present in an awaruite sample from the Josephine Creek (Oregon, USA). The structural investigation [*a* = 9.6206(9) Å, sp. gr. I-43d; R₁ = 3%] confirmed the original stoichiometry and the cubic symmetry thus requiring a revalidation of dienerite as a mineral species.

Bayliss P. (2001) - Dienerite - a mystification. *Min. Mag.*, 65, 685-687.

Burke E. (2006) - A mass discreditation of GQN minerals. *Can. Mineral.*, 44, 1557-1560.

Gervilla F., Makovicky E., Makovicky M. & Rose-Hansen J. (1994). The System Pd-Ni-As at 790° and 450 °C. *Econ. Geol.*, 89, 1630-1639.

Ramdohr P. (1969) - *The Ore Minerals and their Intergrowths*, 1st edition. Pergamon Press, Oxford.

Yund R.A. (1961) - Phase relations in the system Ni-As. *Econ. Geol.*, 56, 1273-1296.

Rare and new mineralogical phases in the Ni-Cu-Sb-As system from the Gomati ophiolite, Northern Greece

Bussolesi M.^{*1}, Zaccarini F.², Grieco G.¹ & Tzamos E.³⁻⁴

¹ Dipartimento di Scienze della Terra, Università degli Studi di Milano.

² Department of Applied Geological Sciences and Geophysics, University of Leoben.

³ Department of Chemistry, School of Sciences, Aristotle University of Thessaloniki.

⁴ R&D Department, EcoResources PC, Thessaloniki.

Corresponding email: micol.bussolesi@unimi.it

Keywords: new minerals, Ni-Cu-Sb-As system, ophiolite.

The Gomati ultramafic body (Chalkidiki peninsula, Northern Greece) is located in the Serbo-Macedonian Massif, one of the geotectonic terranes composing the Hellenides orogenic belt. Ophiolite occurrences in this domain have an unclear origin, and consist of altered peridotites hosting scattered chromitite bodies with massive, schlieren and disseminated textures. These ultramafic bodies are enclosed in the Vertiskos unit, an alternation of Silurian gneisses and schists, and are sometimes in contact with late Cenozoic granites. The present work focuses on several accessory minerals in the Ni-Cu-Sb-As system, found in a chloritized clinopyroxenite in contact with chromitite. The composition of these accessory minerals was determined through electron microprobe analyses. Well known mineralogical phases are represented by orcelite (Ni₅As₂) and breithauptite (NiSb), while other detected phases have been either not well described or never reported.

The chemistry of the Gomati minerals clusters around the following ideal stoichiometries: (Ni,Cu)₇(Sb,As)₃, (Ni,Cu)₂(Sb,As), (Ni,Cu)₁₁(Sb,As)₈, Ni₃As, Ni₅(As,Sb)₂ and Ni₇(As,Sb)₃. As orcelite (Ni₅As₂) is a non-stoichiometric mineral, (Ni,Cu)₇(Sb,As)₃, Ni₅(As,Sb)₂ and Ni₇(As,Sb)₃ may correspond to Cu and/or Sb-rich terms of this phase. A mineral phase corresponding to the (Ni,Cu)₂(Sb,As) stoichiometry was first described in the Alaskan-type Tulameen complex of Canada as unknown phase by Nixon and Cabri (1990). A phase with stoichiometry Ni₃As is reported by Tredoux et al. (2016), from Bon Accord oxide body (South Africa), and corresponds to the mineral dienerite, known only from one loose crystal found in Austria in 1921 and recently discredited by IMA. (Ni,Cu)₁₁(Sb,As)₈ probably represents a Cu-rich Sb analogue of the mineral maucherite (Ni₁₁As₈).

Such an anomalous mineral assemblage in the Gomati ophiolite is puzzling. While ultramafic rocks contain Ni and As of magmatic origin, the presence of Sb and Cu could be indicative of a metasomatic enrichment, probably linked to the presence of fluids emanating from the granite body in contact with the Gomati ophiolite.

Nixon G.T., Cabri L.J. & Laflamme J.G. (1990) - "Platinum-group-element mineralization in lode and placer deposits associated with the Tulameen Alaskan-type complex, British Columbia." *The Canadian Mineralogist*, 28(3), 503-535.
Tredoux M., Zaccarini F., Garuti G. & Miller D.E. (2016) - Phases in the Ni-Sb-As system which occur in the Bon Accord oxide body, Barberton greenstone belt, South Africa. *Mineralogical Magazine*, 80, 187-198.

Phosphate minerals forming in karst environment: a state of art

Carbone C.*¹, Audra P.², De Waele J.³, Bentaleb I.⁴, Chroňáková A.⁵, Křišťůfek V.⁶, D'Angeli I.M.²,
Madonia G.⁶, Vattano M.⁶, Scopelliti G.⁶, Cailhol D.⁷, Vanara N.⁸, Temovski M.⁹, Bigot J.-Y.¹⁰,
Nobécourt J.-C.¹¹, Galli E.¹², Rull F.¹³ & Sanz-Arranz A.¹³

¹ DISTAV, Università di Genova.

² Polytech³ Lab EA 7498, University of Nice Sophia-Antipolis.

³ BIGEA, Università di Bologna.

⁴ Institute des Sciences de l'Évolution Montpellier, University of Montpellier.

⁵ Biology Centre CAS, Inst. Soil Biology, Czech Republic.

⁶ Dipartimento di Scienze della Terra e del Mare, Università di Palermo.

⁷ Laboratoire EDYTEM, University Savoie – Mont-Blanc.

⁸ Laboratoire TRACES, UMR 5608 / Université Paris.

⁹ Isotope Climatology and Environmental Research Centre, Institute of Nuclear Research, Hungarian Academy of Sciences.

¹⁰ Association Française de Karstologie (AFK).

¹¹ Crespe, 06140 Vence.

¹² Dipartimento di Scienze Chimiche e Geologiche, Università degli Studi di Modena e Reggio Emilia.

¹³ Unidad Asociada UVA-CSIC al Centro de Astrobiología, University of Valladolid.

Corresponding email: carbone@dipteris.unige.it

Keywords: phosphates, cave minerals.

Phosphates are the largest group of cave minerals. The PO₄ radical combines with some 30 elements to form over 300 phosphate minerals, out of which more than 100 have been found in different cave settings (Onac, 2012). Brushite, members of the apatite group, taranakite, and ardealite are the most abundant, all of the other phosphates are rare. Phosphates occur whenever a cave contains fresh or fossil bat or bird guano or significant accumulations of bone breccia. Concentrations of bat guano are found primarily in caves situated in low-latitude humid areas where these organic deposits decompose and form a series of acid fluids and gases that can interact with the minerals, sediments, and rocks present in the cave. Unlike other cave minerals, the phosphates do not form spectacular speleothems, but occur as crusts, nodules, lenses, and earthy or powdery masses. Depending on whether the percolating water passing through guano reacts with carbonate rocks or clay minerals, Ca-rich or Mg- and Al-rich phosphates will be deposited. Less commonly, the reaction of guano with ore-derived metals or spontaneous combustion of guano can produce some rare phosphate minerals.

Using various analytical techniques, seventeen phosphate minerals were recognized as secondary products of guano decay. Among those, some are very rare and result from the interaction of guano leachates with clays, fluvial deposits, or pyrite. This work reports the mineralogical findings of phosphate guano-related minerals in a variety of European caves, from Hungary, Slovak Republic, France, Rep. of North Macedonia, and Italy, and the processes and environmental conditions that control their occurrences.

Onac B.P. (2012) - Minerals. In: White W.B. & Culver D.C. (eds.), *Encyclopedia of Caves* (2nd Edition). Chennai Academic Press, 499-508.

Possible Rare Earth Element-induced structural modification in Layer Double Hydroxides: the case of synthetic woodwardite $[\text{Cu}_{1-x}\text{Al}_x(\text{SO}_4)_{x/2}(\text{OH})_2 \cdot n\text{H}_2\text{O}]$

Consani S.*¹, Giuli G.², Martinelli A.³, Cardinale A.M.⁴, Trapananti A.⁵ & Carbone C.¹

¹ Dipartimento di Scienze della Terra, dell'Ambiente e della Vita (DISTAV), Università di Genova.

² Scuola di Scienze e Tecnologie - Sezione di Geologia, Università di Camerino.

³ SPIN-CNR, Genova

⁴ Dipartimento di Chimica e Chimica Industriale (DCCI), Università di Genova.

⁵ Scuola di Scienze e Tecnologie - Sezione di Fisica, Università di Camerino.

Corresponding email: sirio.consani@edu.unige.it

Keywords: Hydrotalcite Supergroup, Brucite layer, EXAFS.

Woodwardite, a member of the Hydrotalcite Supergroup, is a relatively common secondary mineral related to the alteration of sulphide Cu ore. It is generated by waters with high metal content, low CO₂ activity, and circumneutral pH. The crystal structure of the minerals of the Hydrotalcite Supergroup is composed of brucite-type layers in which a trivalent cation partially substitutes a divalent cation. The net positive charge is balanced by the entrance of an anionic species in the interlayer, and the general formula for these minerals is $\text{M}^{2+}_{1-x}\text{M}^{3+}_x(\text{A}^{z-})_{x/z}(\text{OH})_2 \cdot n\text{H}_2\text{O}$. Both M²⁺ and M³⁺ are in six-fold coordination.

Recently, not negligible concentration (up to 0,1 wt.%) of Rare Earth Elements (REEs) has been observed in some specimens of woodwardite. Despite many trivalent cations are reported in hydrotalcites and their synthetic analogues, REEs are not among them. In order to deepen the knowledge of the relationships between woodwardite and REEs, a synthetic analogue has been obtained and doped with REEs (Consani et al., 2018).

The material obtained from the synthesis had poor crystallinity, turbostratic structure, and consisted of nanoscopic crystallites. The increase of the *a* cell parameter obtained with the Rietveld refinement showed that REEs were incorporated inside the brucite layers. In order to obtain more information on the coordination sphere around the cations of the brucite layer, Extended X-ray Absorption Fine Structure (EXAFS) was performed at the Cu k-edge and at the Y L₃-edge on Y-doped samples. The observed bond distances with O for Cu (1,99 ± 0,02 Å) was compatible with a six-fold coordination, whereas the Y-O distance (2,37 ± 0,02 Å) seemed too big for an octahedral coordination. In particular, the latter bond distance was comparable to the one reported for Ca in synthetic layered structure (analogous to the mineral kuzelite) by Allmann (1977), who found that this element was in VII coordination.

It is therefore possible that the incorporation of REEs modified the structure of woodwardite. Further investigations are needed to solve this issue.

Allmann R. (1977) - Refinement of the hybrid layer structure $[\text{Ca}_2\text{Al}(\text{OH})_6]^{+} \cdot [\frac{1}{2}\text{SO}_4 \cdot 3\text{H}_2\text{O}]^{-}$. Neues Jahrbuch für Mineralogie Monatshefte, 3, 136-144.

Consani S., Balić-Žunić T., Cardinale A.M., Sgroi W., Giuli G. & Carbone C. (2018) - A Novel Synthesis Routine for Woodwardite and Its Affinity towards Light (La, Ce, Nd) and Heavy (Gd and Y) Rare Earth Elements. Materials, 11, 130.

Tracking the Ti substitution in biotite by FTIR imaging

Della Ventura G.^{*1-2}, El Moutouakkil N.³, Boukili B.³, Lucci F.¹, Conte A.¹ & Talavera C.⁴

¹ Dipartimento di Scienze, Università Roma Tre, Roma, Italy.

² INFN-LNF, Frascati, Rome.

³ Dept. Earth Sciences, University Mohammed V, Rabat, Morocco.

⁴ School of Geosciences, University of Edinburgh (UK).

Corresponding email: giancarlo.dellaventura@uniroma3.it

Keywords: Biotite, FTIR imaging, Ti-substitution.

Biotites have a wide physico-chemical stability field; they are ubiquitous in a wide variety of geological environments and their composition covers a wide range of solid-solutions involving numerous mechanisms of ionic substitutions. Their composition thus provides significant information for understanding geological conditions for rock formation. In this work, we studied some mica single-crystals occurring within a lamprophyre minette from Jersey Island (UK) (El Moutouakkil & Boukili, 2015) and showing Ti-rich compositions with a systematic discontinuous inverse zonation. The cores have a Mg# ($Mg\# = Mg/[Mg + Fe_{tot}]$) of ≈ 0.73 with high TiO₂ contents of $\approx 10\%$. They are systematically surrounded by inner rims having Mg# ≈ 0.90 with TiO₂ not exceeding 2% and a more external rims with Mg# ≈ 0.67 and TiO₂ contents in the range $\approx 5.6-5.7\%$. These compositional patterns suggest that uncommon processes occurred during the magma evolution, demanding for novel imaging techniques to be characterized. In the recent years, the advent of modern FTIR microscopes equipped with bi-dimensional detectors (focal-plane-array, FPA) has revolutionized the world of mid-IR spectroscopy (Della Ventura et al., 2014) allowing the imaging of substituting cations/anions at high-resolution. We present here our crystal-chemical results from FTIR imaging of the hybrid phenocrystals from the Jersey minette coupled to direct analysis of the H content by SIMS. The data show that, differently to what observed in other cases (Cesare et al., 2003), the substitution mechanism responsible for the exceptional Ti zoning during the biotite crystallization is the Ti-vacancy mechanism whereby the entry of octahedral Ti in the structure is locally balanced by the creation of empty sites.

Since the Ti-content in biotite has long been considered to be mainly controlled by temperature conditions (e.g. Patiño Douce, 1993), on a wider scale Ti-rich biotite from Jersey minette suggests the necessity to revise our knowledge on primary dark mica crystallization in magmas and recalibrate existing inverse thermometric models based on Ti-substitution mechanisms.

Cesare B., Cruciani G. & Russo U. (2003) - Hydrogen deficiency in Ti-rich biotite from anatectic metapelites (El Joyazo, SE Spain): crystal-chemical aspects and implications for high-temperature petrogenesis. *Am. Min.*, 88, 583-595.

Della Ventura G., Marcelli A. & Bellatreccia F. (2014) - SR-FTIR microscopy and FTIR imaging in the Earth Sciences. *Rev. Min. Geochem.*, 78, 447-479, The Mineral. Soc.

El Moutouakkil N. & Boukili B. (2015) - Interactions chimiques au niveau d'une interface micacée cas des phlogopites magmatiques zonées de la minette de l'île de Jersey. *Bull. Soc. R. Sci. Liège*, 84, 175-193.

Patiño Douce A.E. (1993) - Titanium substitution in biotite: an empirical model with applications to thermometry, O₂ and H₂O barometries, and consequences for biotite stability. *Chem. Geol.*, 108, 133-162.

The quantitative analysis of the octahedral composition of amphiboles by Raman spectroscopy

Della Ventura G.*¹⁻², Hawthorne F.C.³, Waeselmann N.⁴ & Mihailova B.⁴

¹ Dipartimento di Scienze, Università di Roma Tre, Roma, Italy.

² INFN-Laboratori Nazionali di Frascati (Roma).

³ Department of Geological Sciences, University of Manitoba, Winnipeg, Canada.

⁴ Fachbereich Geowissenschaften, Universität Hamburg, Hamburg, Germany.

Corresponding email: giancarlo.dellaventura@uniroma3.it

Keywords: amphiboles, synthetic, Raman spectroscopy.

Amphiboles are geologically important silicates; their crystal-chemistry is the most complex among the rock-forming minerals, due to their very flexible structure consisting of several different cationic/anionic sites, and to the wide chemical substitutions possible at these sites.

There has been significant effort to set-up methods for the crystal chemical analysis of amphiboles, and it is now clear that the complete definition of a sample composition needs the combined use of different analytical techniques, due to the presence of (1) multi-valence elements (notably Fe but also Mn or Ti), (2) light elements, notably H and Li, and (3) the possibility of a partially vacant A-site.

Vibrational spectroscopy in the OH-stretching region has proven to be a very useful tool for addressing both long-range (LR) and short-range (SR) occupancies in amphiboles, however although much effort have been focused on FTIR (e.g. Hawthorne & Della Ventura, 2007), few studies have addressed the use of Raman (Leissner et al., 2015, Sbroscia et al., 2018, Della Ventura et al., 2018) in this spectral range. A recent comprehensive work by Waeselmann et al. (2019) showed that Raman spectroscopy in the framework mode region is indeed a very powerful tool to investigate the amphibole crystal-chemistry; the method has clear inherent advantages over FTIR in that it is totally non-destructive, can be applied on petrographic thin sections and has a spatial resolution much smaller (1 μm vs 20 μm for conventional instruments) than micro-FTIR, implying a great potential also in environmental and biomedical studies (e.g. Della Ventura 2017). However, the observed wavenumber - local chemistry trends still need further validation that is possible by the examination of synthetic systems. In this work we show our recent results obtained for Mg-Co substituted richterites along the $\text{Na}(\text{NaCa})\text{Mg}_5\text{Si}_8\text{O}_{22}(\text{OH})_2$ - $\text{Na}(\text{NaCa})\text{Co}_5\text{Si}_8\text{O}_{22}(\text{OH})_2$ join.

Della Ventura G. (2017) - The analysis of asbestos minerals using vibrational spectroscopies. EMU Notes in Miner., 18, 135–169. Mineralogical Soc. GB & Ireland.

Della Ventura G., Milahova B., Susta U., Cestelli Guidi M., Marcelli A., Schlüter J. & Oberti R. (2018) - The dynamics of Fe oxydation in riebeckite: a model for amphiboles. Am. Min. 103, 1103-1111.

Hawthorne F.C. & Della Ventura G. 2007. Short-range order in amphiboles. Rev. Min. Geochem., 67, 173-222.

Leissner L., J. Schlüter J., Horn I. & Mihailova B. (2015) - Exploring the potential of Raman spectroscopy for crystallochemical analysis of hydrous minerals: I. Amphiboles. Am. Min., 100, 2682-2694.

Waeselmann N., Schlüter J., Malcherek T., Della Ventura G., Oberti R. & Mihailova B. (2019) - Non-destructive determination of the amphibole crystal chemistry by Raman spectroscopy; one step closer. J. Raman Spec., <https://doi.org/10.1002/jrs.5626>.

Sbroscia M., Della Ventura G., Iezzi G. & Sodo, A. (2018) - Quantifying the A-site occupancy in amphiboles: a Raman study in the OH-stretching region. Eur. J. Min. 3, 429-436.

Dehydration and Thermal stability of High-Silica Mordenite: In-Situ Synchrotron X-Ray Powder Diffraction Study

Fantini R.¹, Quartieri S.*¹, Arletti R.², di Renzo F.³, Fabbiani M.⁴, Morandi S.⁴, Martra G.⁴ & Vezzalini G.¹

¹ Dipartimento di Scienze Chimiche e Geologiche, Università di Modena e Reggio Emilia.

² Dipartimento di Scienze della Terra, Università di Torino.

³ ICGM, CNRS, ENSCM, Université de Montpellier.

⁴ Dipartimento di Chimica, Università di Torino.

Corresponding email: riccardo.fantini1@unimore.it

Keywords: High Silica Mordenite, Negative Thermal Expansion, high temperature.

High-Silica Mordenite (HS-MOR s.g. $Cmc2_1$, a 18.0609(2) Å, b 20.2096(2) Å, c 7.4546(1) Å, V 2721.0(1) Å³) was characterized by thermogravimetric analysis (TGA), nitrogen adsorption, laser granulometry and in-situ FTIR spectroscopy. In-situ synchrotron XRPD was performed from room temperature (rT) to 800°C, and after cooling (rev.) at 150°C and rT . All XRPD data were analysed by Rietveld structural refinement.

The average particle size (Dv_{50}) obtained from laser diffraction is 13.3 µm and nitrogen adsorption detected a micropore volume of 0.22 cm³gr⁻¹ and a mesopore volume ($D=$ 6-60 nm) of 0.04 cm³gr⁻¹. The main weight loss (8.3%) from TGA, occurs in the rT -150°C T range, while at 800°C is 10.6%. The weight loss below 150°C can be ascribed to physisorbed and structural, weakly bonded, H₂O molecules. Above 150°C the weight loss (2.3%) is due to the silanols condensation (Martucci et al., 2013), as confirmed by FTIR data. The Rietveld refinement of rT structure was performed in both $Cmcm$ and $Cmc2_1$ s.g. Since the acentric $Cmc2_1$ better fit the HS-MOR framework and extraframework content, the $Cmc2_1$ s.g. was adopted at all investigated temperatures. Some intensity misfits remain due to structural disorder, mesoporosity and silanols. 10.3 H₂O molecules p.u.c. were located spread over seven sites. The H₂O content from XRPD is lower than the TGA one (14.5 H₂O p.u.c. below 150 °C, being physisorbed water and disordered H₂O not detectable by XRPD). All H₂O molecules are weakly bonded to framework and are lost below 150°C. At 200°C only one H₂O site (~1 molecule p.u.c.) is partially occupied and the complete loss is observed at 400°C. Above 200°C a slight but continuous unit cell contraction is observed, leading to a linear contraction of 0.67%, 1.18% and 0.81% for a , b and c respectively. The final volume contraction is 2.64%. This phenomenon is known as Negative Thermal Expansion (NTE), and in HS-MOR is mainly related to the deformation of the 12MR and 8MR channels in the b direction. The a and c directions are indeed stiffened by 4 and 5-membered rings chains running in these directions. Unlike previously reported NTE zeolites (Leardini et al., 2015), HS-MOR deformation is not completely restored after cooling, and unit cell parameters at 150°C (rev) and rT (rev) are approximately those found at 700°C.

Leardini L., Quartieri S., Vezzalini G. & Arletti R. (2015) - Thermal behaviour of siliceous faujasite: Further structural interpretation of negative thermal expansion. *Microporous and Mesoporous Mat.*, 202, 226-233.

Martucci A., Cremonini M. A., Blasioli S., Gigli L., Gatti G., Marchese L. & Braschi I. (2013) - Adsorption and reaction of sulfachloropyridazine sulfonamide antibiotic on a high silica mordenite: A structural and spectroscopic combined study. *Microporous and Mesoporous Mat.*, 170, 274-286.

Exotic mineralogy in an ultra-reduced magmatic system beneath Mt Carmel, Israel

Griffin W.L.*¹, Gain S.E.M.¹⁻², Camara F.³, Bindi L.⁴, Toledo V.⁵ & O'Reilly S.Y.¹

¹ ARC Centre of Excellence for Core to Crust Fluid Systems (CCFS) and GEMOC, Earth and Planetary Sciences, Macquarie University Australia.

² Centre for Microscopy, Characterisation and Analysis, The University of Western Australia.

³ Dipartimento di Scienze della Terra "Ardito Desio", Università degli Studi di Milano, Italy.

⁴ Dipartimento di Scienze della Terra, Università di Firenze, Italy.

⁵ Shefa Yamim (A.T.M.) Ltd., Netanya, Israel.

Corresponding email: bill.griffin@mq.edu.au

Keywords: super-reduced mineral assemblages, Mt Carmel, mantle methane.

Xenocrysts from Cretaceous pyroclastic vents and tuffs on Mt Carmel, N. Israel record progressively decreasing oxygen fugacity (fO_2) in a magmatic system (Griffin et al., 2018). Grains of vesicular wustite record fO_2 near the QFM buffer ($fO_2 = DIW + 3-4$). Large euhedral crystals of magnesian calcite would have crystallized near the EMOD buffer ($DIW + 1.5$); high-Sr cores with $^{87}Sr/^{86}Sr = 0.7033$ indicate a magmatic origin. Balls of quenched Fe oxide-silicate and Ti oxide-silicate melts, many with cores of Fe^0 , indicate fO_2 near IW. Rubies (to 2 mm) with up to 58 wt% Cr_2O_3 (Esk_1Crn_2) and inclusions of Cr^0 and Cr nitrides also require fO_2 near IW.

The most abundant xenocrysts are aggregates of skeletal/hopper crystals of corundum, trapping pockets of Ca-Mg-Al-Si-O melts with high Ti, Zr and REE. The first phenocrysts in these pockets are Mg-Al-Ti spinel, followed by tistarite (Ti_2O_3) and carmelazite ($ZrAl_2Ti^{3+}_4O_{11}$). More evolved melts precipitated REE-rich hibonite ($CaAl_{12}O_{19}$), moissanite and Zr-REE phases. The melt pockets also contain a variety of immiscible carbon-rich Fe-Ti-Zr silicide/phosphide melts, which crystallized TiC, SiC, TiB_2 , Ti nitrides and silicide phases. SiC crystals (up to 4 mm) contain inclusions of Si^0 melts that crystallized Fe-, Ca- and Al silicides. Crystallization of SiC and reduction of Ti^{4+} to Ti^{3+} require $fO_2 = DIW - 7$ to -8 . The most evolved silicate melts produced coarse-grained hibonite+grossite+spinel aggregates with inclusions of V^0 (Griffin et al., 2019) requiring $fO_2 \leq DIW - 9$. These conditions imply a hydrogen-dominated atmosphere, confirmed by the discovery of VH_2 (Bindi et al., 2019) and abundant H_2 in the hibonite crystals.

Paragenetic studies indicate that these xenocrysts formed at ca 1 GPa, close to the crust-mantle boundary. Zircon studies suggest that the CMB was underplated by mafic magmas from ca 285-100 Ma and differentiated enough to crystallize large zircons and typical basaltic sapphire. We suggest that lenses of such residual melts in the underplate were reduced by mantle-derived $CH_4 + H_2$ fluids. Successive stages of immiscibility modified the melts, and they were desilicated by the separation of abundant silicide melts at $fO_2 = ca DIW - 7$, leading to supersaturation of the melts in Al_2O_3 and the rapid crystallization of skeletal corundum.

Bindi L., Cámara F., Griffin W. L., Huang J.X., Gain S.E., Toledo V. & O'Reilly S.Y. (2019) - Discovery of the first natural hydride. *American Mineralogist* 104, 611-614.

Griffin W.L., Huang J.X., Thomassot E., Gain S.E., Toledo V. & O'Reilly S.Y. (2018) - Super-reducing conditions in ancient and modern volcanic systems: Sources and behaviour of carbon-rich fluids in the lithospheric mantle. *Mineralogy and Petrology*, 112(1), 101-114.

Griffin W.L. Gain S.E., Huang J.X., Saunders M., Shaw J., Toledo V. & O'Reilly S.Y. (2019) - A terrestrial magmatic hibonite-grossite-vanadium assemblage: desilication and extreme reduction in a volcanic plumbing system, Mt Carmel, Israel. *American Mineralogist*, 104, 207-217.

Unusual symmetry of an intermediate scapolite

Lotti P.*¹, Comboni D.¹⁻² & Gatta G.D.¹

¹ Dipartimento di Scienze della Terra, Università degli Studi di Milano.

² Dipartimento di Scienze della Terra e dell'Ambiente, Università degli Studi di Pavia.

Corresponding email: paolo.lotti@unimi.it

Keywords: scapolite, unusual symmetry, temperature.

The scapolite series of minerals represents a complex non-binary solid solution, which end members are: marialite [$\text{Na}_4\text{Al}_3\text{Si}_9\text{O}_{24}\text{Cl}$], meionite [$\text{Ca}_4\text{Al}_6\text{Si}_6\text{O}_{24}\text{CO}_3$] and silvialite [$\text{Ca}_4\text{Al}_6\text{Si}_6\text{O}_{24}\text{SO}_4$]. The members which composition falls on the marialite-meionite joint appears to be the most common in natural occurrences (Teertstra & Sherriff, 1997; 2]. The members close to marialite on one side and to meionite on the other side, are usually reported to crystallize in the tetragonal $I4/m$ space group, whereas intermediate scapolites are usually found in the primitive space group $P4_2/n$. In this study, we report a scapolite sample from Madagascar, which composition falls between those of the end-members marialite and meionite: $(\text{Na}_{1.86}\text{Ca}_{1.86}\text{K}_{0.23}\text{Fe}_{0.01}) (\text{Al}_{4.36}\text{Si}_{7.64})\text{O}_{24}[\text{Cl}_{0.48}(\text{CO}_3)_{0.48}(\text{SO}_4)_{0.01}]$. Based on both X-ray and neutron single-crystal diffraction data, an anomalous I -centered lattice ($I4/m$ space group) is observed. This unusual symmetry for an intermediate scapolite may be assigned to the presence of anti-phase domains too small to be detected by diffraction techniques. In situ high- T X-ray diffraction investigations show that the $I4/m$ space group is observed to be stable at least up to 1000 °C.

Teertstra D.K. & Sherriff B. L. (1997) - Substitutional mechanisms, compositional trends and the end-member formulae of scapolite. *Chemical Geology*, 136(3-4), 233-260

Sokolova E. & Hawthorne F.C. (2008) - The crystal chemistry of the scapolite-group minerals. I. Crystal structure and long-range order. *The Canadian Mineralogist*, 46(6), 1527-1554.

Coquimbite: a mineral to be redefined?

Mauro D.*¹, Biagioni C.¹, Pasero M.¹ & Zaccarini F.²

¹ Dipartimento di Scienze della Terra, Università di Pisa.

² Department of Applied Geological Sciences and Geophysics, University of Leoben.

Corresponding email: daniela.mauro@dst.unipi.it

Keywords: coquimbite, crystal-chemistry, sulfate.

Among the iron sulfates found in the TI-rich pyrite ore formerly exploited at the Monte Arsiccio mine, well-crystallized specimens of coquimbite were found: they occur as purple pseudo-hexagonal crystals, up to 3 cm across, closely associated with halotrichite, römerite, melanterite, alunogen, krausite, and, rarely, khademite.

The ideal chemical formula of coquimbite is usually expressed as $\text{Fe}^{3+}_2(\text{SO}_4)_3 \cdot 9\text{H}_2\text{O}$. Whereas the first chemical data on this mineral reported only minor amounts of Al_2O_3 (e.g., Rose, 1833), modern crystallographic investigations pointed out that Al is likely as essential constituent of this sulfate. Indeed, the presence of Al was observed by Fang and Robinson (1970), who proposed the formula $\text{Fe}_{2-x}\text{Al}_x(\text{SO}_4)_3 \cdot 9\text{H}_2\text{O}$. Recently, Yang and Giester (2018) discussed again the crystal-chemistry of coquimbite, pointing out the necessity of a revision of its chemical formula. However, their structural data were not supported by chemical analyses; on the contrary, they reported chemical data showing only minor Al_2O_3 (< 1 wt%).

In order to collect further data on coquimbite, we performed a full crystal-chemical characterization of a specimen from the new Italian occurrence. Chemical data gave (in wt% - average of 20 spot analyses): SO_3 42.88(45), Al_2O_3 4.38(7), Fe_2O_3 22.23(38), $\text{H}_2\text{O}_{\text{calc}}$ 29.10, total 98.59. On the basis of 42 O apfu, the formula of coquimbite is $\text{Al}_{0.96}\text{Fe}_{3.10}\text{S}_{5.97}\text{O}_{24} \cdot 18\text{H}_2\text{O}$, ideally $\text{AlFe}_3(\text{SO}_4)_6 \cdot 18\text{H}_2\text{O}$.

Single-crystal X-ray diffraction study confirmed that coquimbite is trigonal, space group $P\bar{3}1c$, with unit-cell parameters $a = 10.932(1)$, $c = 17.069(2)$ Å, $V = 1766.6(4)$ Å³. The crystal structure was refined to $R_1 = 0.0219$ for 1341 unique reflections with $F_o > 4 \sigma(F_o)$ and 110 refined parameters. Its crystal structure agrees with previous results (e.g., Yang and Giester, 2018 and references therein) and it is based on isolated $[\text{Al}(\text{H}_2\text{O})_6]^{3+}$ octahedra, $[\text{Fe}^{3+}_3(\text{SO}_4)_6(\text{H}_2\text{O})_6]^{3-}$ clusters, and interstitial (H_2O) groups. On the basis of both chemical and structural data, also considering the site multiplicity, the chemical formula of coquimbite should be correctly written as $\text{AlFe}_3(\text{SO}_4)_6(\text{H}_2\text{O})_{12} \cdot 6\text{H}_2\text{O}$ ($Z = 2$).

Fang J.H. & Robinson P.D. (1970) - Crystal structures and mineral chemistry of hydrated ferric sulfates. I. The crystal structure of coquimbite. *American Mineralogist*, 55, 1534-1540.

Rose H. (1833) - Ueber einige in Südamerika vorkommende eisenoxydsalze. *Annalen der Physik und Chemie*, 27, 309-319.

Yang Z. & Giester G. (2018) - Structure refinements of coquimbite and paracoquimbite from the Hongshan Cu-Au deposit, NW China. *European Journal of Mineralogy*, 30, 849-858.

Crystal-chemistry and thermal behavior of Fe-carpholite: a case of study from the Pollino Massif (southern Italy)

Mesto E.*¹, Laurita S.², Lacalamita M.¹, Schingaro E.¹, Rizzo G.², Sinisi R.² & Mongelli G.²

¹ Dipartimento di Scienze della Terra e Geoambientali. Università degli Studi di Bari "Aldo Moro". Bari, Italy.

² Dipartimento di Scienze, Università della Basilicata, Potenza, Italy

Corresponding email: ernesto.mesto@uniba.it

Keywords: Fe-carpholite, crystal-chemistry, thermal behavior.

The carpholite group encompasses hydrated inosilicates with general formula $A_{0-1}M1_2M2_2M3_2[(OH, F)_4(Si_2O_6)]_2$ where $A = [K, Ba \text{ and } Na]$, $M1 = Mn, Mg, Fe, Al, Li \text{ and } Na$, $M2 = Al, V^{3+}, Fe^{3+} \text{ and } Ti$, and $M3 = Al, Mg, V^{3+}, Fe^{3+} \text{ and } Ti$. In the present study the Fe-carpholite from the Pollino Massif, southern Apennines (Liguride Complex, Frido Unit) has been investigated by combining Secondary Electron Microscopy (SEM), Single Crystal X-Ray Diffraction (SCXRD), μ Raman spectroscopy and *in situ* High Temperature X-Ray Powder Diffraction (HTXRPD). Fe-Mg carpholite is known as an index mineral in LT-HP conditions for blueschist facies rocks, but, in metasedimentary rocks may be the main, or locally the only, evidence of LT-HP metamorphism (Pourteau et al., 2013).

The results of SEM analyses on thin sections show that the studied carpholite is embedded in quartz and quartz-calcite veins cross-cutting fine-grained greyish metapelites cropping out close to Viggianello (Potenza, Italy). The mineral usually exhibits a thin, 200-300 μ m long, hair-like, habit. The SCXRD confirms that the studied Fe-carpholite has *Ccce* symmetry, as previously found by Fuchs et al. (2001) and references therein, with $a \sim 13.77 \text{ \AA}$, $b \sim 20.16 \text{ \AA}$, $c \sim 5.11 \text{ \AA}$ and $V \sim 1419 \text{ \AA}^3$. The structure refinements, that converged at R values between 2.3 and 3.1%, provided $\sim 38\%$ Mg and $\sim 62\%$ Fe at M1, that corresponds to $X_{Fe} = 0.6$; the M2 and M3 sites are fully occupied by Al.

Raman spectra, collected on unoriented crystals, evidence, in the high frequency region, two peaks at 3630 and 3593 cm^{-1} which account for the presence of two independent OH groups as also derived from the structure refinement. Similar results were also reported for the Fe-carpholites in Ferraris et al. (1992) *In situ* HT XRD patterns were collected from 30 to 630°C. No modifications are observed in the diffraction patterns collected from 30 to 380°C whereas a splitting of the reflections occurs starting from 405°C. The phase is stable up to 630°C and transforms to a spinel phase at 680°C. All these findings, and especially the *in situ* HT XRPD results, add further constraints on our knowledge of the thermal behaviour of this mineral in relation to the thermometamorphic history of metasediments.

Ferraris G., Ivaldi G. & Goffé B. 1992. Structural study of a magnesian ferrocapholite: Are carpholites monoclinic? N. Jb. Mineral., Mh., 337-347.

Fuchs Y., Mellini M. & Memmi I. 2001. Crystal-chemistry of magnesiocarpholite: controversial X-ray diffraction, Mössbauer, FTIR and Raman results. Eur. J. Mineral., 13, 533-543.

Pourteau A., Sudo M., Candan O., Lanari P., Vidal O. & Oberhänsli R. 2013. Neotethys closure history of Anatolia: insights from 40Ar-39Ar geochronology and P-T estimation in high-pressure metasedimentary rocks. J. Metamorph. Geol., 31, 585-606.

Disorder and modulation in first aragonite precipitates from Obstanser Eishöhle (Austria)

Mugnaioli E.*¹, Gemmi M.¹ & Németh P.²

¹ Center for Nanotechnology Innovation@NEST, Istituto Italiano di Tecnologia, Italy.

² Institute of Materials and Environmental Chemistry, Hungarian Academy of Sciences, Hungary.

Corresponding email: enrico.mugnaioli@iit.it

Keywords: aragonite, electron crystallography, crystal nucleation.

Aragonite is thermodynamically metastable at near-surface conditions, and still it is relatively widespread in marine and terrestrial sediments. In this contribution we propose the detailed chemical and crystallographic analysis of fresh aragonitic precipitates. Wet samples, collected from a dolomitic cold cave in the East Alpine range, were directly taken from underground dripping water and from the surface of aragonite speleothems. Calcium carbonate nano- and microcrystals are always found in association with magnesite and hydromagnesite and incorporate variable amounts of magnesium and possibly hydroxyl groups.

The typical size of the analyzed precipitates ranges from some tens of nanometers to few microns. Advanced electron crystallographic tools were therefore necessary for a proper structural characterization. Indeed, in the last ten years electron diffraction (ED) turned into a robust protocol for phase identification and ab-initio structure determination. Such evolution was mostly propelled by the development of semi-automatic routines for 3D data collection (Mugnaioli & Gemmi, 2018). The concept at the basis of 3D ED is the same as for single-crystal X-ray diffraction, but electrons allow sampling single crystals 10 to 1000 times smaller, despite the presence of surrounding crystals of other mineralogical phases.

3D ED revealed that first calcium carbonate precipitates have a structure strictly related to conventional aragonite. Still, diffuse scattering and satellite reflections appear along aragonite {110} and point to a reduction of symmetry into the monoclinic system (Németh et al., 2018). Following the order-disorder description of aragonite proposed by Makovicky (2012), such disorder can be associated with the same mechanism responsible for the twinning in mature aragonite. The frequent (or systematic) inversion of the stacking vector can be imposed by the incorporation of magnesium in the structure, whose atomic radius and coordination significantly differ from those of calcium. In turn, the necessity to include magnesium and hydroxyl groups in the lattice may be the very factor that favors the crystallization of aragonite in respect to calcite, which should otherwise be the stable mineral phase at near-surface conditions. Such ‘monoclinic-aragonite’ seeds might therefore represent the key step for the formation of large amount of metastable aragonite sediments.

Makovicky E. (2012) - Twinning of aragonite —The OD approach. *Mineral. Petrol.*, 106, 19-24.

Mugnaioli E. & Gemmi M. (2018) - Single-crystal analysis of nanodomains by electron diffraction tomography: mineralogy at the order-disorder borderline. *Z. Kristallogr.*, 233, 163-178.

Németh P., Mugnaioli E., Gemmi M., Czuppon G., Demény A. & Spötl C. (2018) - A nanocrystalline monoclinic CaCO₃ precursor of metastable aragonite. *Sci. Adv.*, 4, eaau6178.

Peculiar mineralogy of the Água de Pau syenites (São Miguel, Azores islands, Portugal)

Nazzareni S.¹, Nestola F.², Bindi L.³, Scricciolo E.*¹, Pacheco J.⁴, Zanon V.⁴, Zanatta M.⁵ & Giuli G.⁶

¹ Dipartimento di Fisica e Geologia, Università di Perugia, Perugia, Italy.

² Dipartimento di Geoscienze, Università di Padova, Padova, Italy.

³ Dipartimento di Scienze della Terra, Università di Firenze, Firenze, Italy.

⁴ IVAR, Universidade dos Açores, Ponta Delgada, Portugal.

⁵ Dipartimento di Informatica, Università di Verona, Verona, Italy.

⁶ Scuola di Scienze e Tecnologie – sez. Geologia, Università di Camerino, Camerino, Italy.

Corresponding email: enrico.scricciolo@gmail.com

Keywords: Syenite xenoliths, Agua de Pau, mineralogy.

Syenite xenoliths frequently occur in pyroclastic sequences erupted during the Holocene volcanic activity of the Azores archipelago (Portugal). In particular syenite xenoliths occurring at Água de Pau volcano (São Miguel island) are characterised by a peculiar mineralogy of minor components: apatite, titanite, aenigmatite, eudyalite, zircon, chevkinite, pyrochlore, and dalyite. Furthermore, several REE and REE-bearing minerals have been also reported and recently new minerals were discovered in the Agua de Pau syenites (chiappinoite, Kampf & Housley, 2015; fogoite Cámara et al., 2017).

In the course of a research project dealing with the mineralogical and petrographic characterization of minerals from Azores rocks (Nazzareni et al., 2019), we carried out a preliminary combined chemical (SEM-EDS) and structural (single-crystal X-ray diffraction) study. During this study, we identified: zircon, pyrochlore, Fe-katophorite, Nb-bearing titanite, zircon, monazite, Zr- and Nb-bearing astrophyllite, chevkinite-(Ce), steacyite, chiappinoite, euxenite, dalyite, wulfenite, moissanite and native Zn.

Here we focused on pyrochlore and monazite, which have a large chemical variation, as well as chevkinite, steacyite and chiappinoite. A still unidentified phase with V,Ti,Fe composition associated to moissanite is under investigation. A detailed crystal-chemical study of the minor phases present in the Agua de Pau syenites may help to understand the processes related to the REE enrichment of the syenitic magma.

Cámara F., Sokolova E., Abdu Y.A., Hawthorne F.C., Charrier T., Dorcet V. & Carpentier J.-F. (2017) - Fogoite-(Y), $\text{Na}_3\text{Ca}_2\text{Y}_2\text{Ti}(\text{Si}_2\text{O}_7)_2\text{OF}_3$, a Group I TS-block mineral from the Lagoa do Fogo, the Fogo volcano, São Miguel Island, the Azores: Description and crystal structure. *Min. Mag.*, 81(2), 369-381.

Kampf A.R. & Housley R.M. (2015) - Chiappinoite-(Y), $\text{Y}_2\text{Mn}(\text{Si}_3\text{O}_7)_4$, a new layer silicate found in peralkaline syenitic ejecta from the Água de Pau volcano, Azores. *Eur. J. Mineral.*, 27(1), 91-97.

Nazzareni S., Nestola F., Zanon V., Bindi L., Scricciolo E., Petrelli M., Zanatta M., Mariotto G. & Giuli G. (2019) - Discovery of moissanite in a peralkaline syenite from the Azores Islands. *Lithos*, 324-325, 68-73.

A reexamination of the crystal structure of lorándite

Precisvalle N.*¹, Martucci A.¹, Ferretti V.², Bonadiman C.¹, Bianchini G.¹ & Natali C.³

¹ Dipartimento di Fisica e Scienze della Terra, Università degli Studi di Ferrara.

² Dipartimento di Scienze Chimiche e Farmaceutiche, Università degli Studi di Ferrara.

³ Dipartimento di Scienze della Terra, Università degli Studi Firenze.

Corresponding email: prcncl@unife.it

Keywords: Lorándite, sulfosalt, neutrinos.

Lorándite is a Thallium Arsenic sulfosalt found in low-temperature mineral assemblages with other Fe, Pb and As sulfides (Fleet, 1973) most common in Allchar deposit (Kavardaci, Rep. of North Macedonia). The genesis is related to hydrothermal fluids in Pliocenic magmatic activity (Amthauer et al., 2012). Lorándite is commonly exploited 1) as ore mineral for Tl extraction and 2) as natural detector for solar neutrinos. The $^{205}\text{Tl} + \nu = ^{205}\text{Pb} + e^-$ decay (Freedman et al., 1976; Stafilov et al., 1994) is triggered by neutrino fluxes and investigated by the LOREX experiment (Amthauer et al., 2012). Determination of ^{205}Pb give useful information about the neutrino activity (Stafilov et al., 1994). Even if Lorándite detector is still used today, the most recent crystallographic characterization of this mineral was made in 1973 (Fleet, 1973). It has been decided to update this information with a new investigation. The structural refinement of lorándite at RT was performed on single-crystal data obtained using a Nonius four cycle diffractometer equipped with a CCD detector and MoK α radiation. The atomic scattering curve of As, Tl and S were used for structure refinement. The DENZO-SMN (Otwinowski et al., 1997) package was used for the refinement of the unit-cell. The SHELXL (Sheldrick, 2015) program was employed for the crystal structure refinement. Systematic extinctions were consistent with the topological monoclinic $P2_1/c$ space group. Positional parameters determined in the present study show marked discrepancies from those reported in the original work (Fleet, 1973). The most evident are significantly shorter bond lengths between Tl and S and longer bond length between As and S. The average Tl-As bond lengths and Volume are different for Tl1 and Tl2 polyhedra (Tl1-As Average bond length = 3.3009 Å; Polyhedral volume = 46.4341 Å³; Tl2-As Average bond length = 3.2166 Å; Polyhedral volume = 38.9519 Å³). The bonds from non-equivalent As atoms to the non-bridge S are different with respect those reported by Fleet, thus suggesting different S environment and distances between adjacent chains.

Amthauer G., Pavicevic M. K., Jelenkovic R., El Goresy A., Boev B. & Lazic P. (2012) - State of geoscientific research within the lorándite experiment (LOREX). *Miner. Petrol.*, 105, 157–169.

Fleet M.E. (1973) - The crystal structure and bonding of lorándite, Tl₂As₂S₄. *Z. Kristallogr.*, 138, 147-160.

Freedman M.S., Stevens C.M., Horwitz E.P., Fuchs L.H., Lerner J.L., Goodman L.S., Childs W.J. & Hessler J. (1976) - Solar neutrinos-proposal for a new test. *Science*, 193, 1117–1119.

Otwinowski Z. & Minor W. (1997) - Processing of X-ray Diffraction Data Collected in Oscillation Method, *Macromolecular Crystallography Part A. Methods Enzymology*, 276, 307-326.

Sheldrick G.M. (2015) - Crystal structure refinement with SHELXL. *Acta Cryst.*, C71, 3-8.

Stafilov T., Aleksavska S. & Jordanovska V. (1994) - Determination of lead in lorándite and marcasite from Allchar by electrothermal atomic absorption spectrometry, *Neues Jahrb. Mineral., Abh.*, 167, 401–408.

IR and Single-crystal XRD characterisation of natural pyrochlores

Scricciolo E.¹, Nazzareni S.*¹, Giura P.², Calandrini E.² & Giuli G.³

¹ Dipartimento di Fisica e Geologia, Università degli Studi di Perugia, Perugia, Italy.

² Institut de Minéralogie, de Physique des Matériaux et de Cosmochimie (IMPMC), Sorbonne Université, Paris, France.

³ Scuola di Scienze e Tecnologia –sez. Geologia, Università degli Studi di Camerino, Camerino, Italy Italy.

Corresponding email: sabrina.nazzareni@unipg.it

Keywords: pyrochlore, IR, REE.

Accessory minerals are able to incorporate trace-elements whose content is affected by factors that include lattice strain, melt polymerization and the water content of the melt. Most of High Field Strength Elements (HFSE) including rare earth elements (REE), yttrium (Y), zirconium (Zr), hafnium (Hf), niobium (Nb), and tantalum (Ta) are used in a vast array of devices such as lasers, electronic screens, permanent magnets, battery alloys, and ceramics. A worldwide increasing demand on HFSE supply raised the interest on exploiting new deposits, improving extraction processes and REE recovery from waste for reuse. In this framework, understanding the physical and chemical properties of REE- and REE-bearing minerals become critically important.

Pyrochlore-group minerals are among the most common HFSE-bearing minerals. In particular they represent the main ore mineral for Nb. Pyrochlore can be found in carbonatites magmas and alkaline magmas as an accessory mineral. Their structure is characterised by a [8]-fold and a [6]-fold cations sites where HFSE cations can enter by a complex substitutions scheme. Na, Ca, Ba, Y, Ce (and other REE) may be hosted in A site, whereas the B site may host Ta, Nb, Ti. The X and Y sites can host OH, F, H₂O and vacancies.

We selected natural Na-pyrochlore and microlite from the Agua de Pau syenites (Azores islands, Portugal), Chelyabinsk Oblast (Urals region, Russia) and Yenisei Ridge (Siberia Russia). Selected samples contain different amounts of Na, Ca, Ta, Nb, Ti, and in minor concentration Ba, Ce, Y, F, that results in a colour span from yellow to orange to red-orange. Infrared microspectroscopy (IR) and single-crystal X-ray diffraction measurements were performed on the same crystals aiming to characterise the influence of cations substitutions on the structure of pyrochlore-group minerals. IR measurements collected in a transmission configuration in an energy range between 80 and 600 meV reveal several bands varying accordingly with samples composition and provide direct access to the chemical coordination of crystal sites. A detailed characterisation of pyrochlore crystals will better define the physical and chemical properties of the pyrochlore-structure type, giving some insights on the mechanisms of HFSE incorporation and eventually their extraction.

Ex situ study of cation disorder in Fe-rich dolomites

Zucchini A.*¹, McCammon C.², Comodi P.¹ & Frondini F.¹

¹ Dipartimento di Fisica e Geologia, Università di Perugia.

² Bayerisches Geoinstitut, Università di Bayreuth, Germania.

Corresponding email: azzurra.zucchini@unipg.it

Keywords: Fe-dolomite, SC-XRD, cation disordering.

The stability of carbonates under mantle conditions is strongly influenced by chemical and structural features of the minerals and shows a wide variation. Calcite transforms to calcite-II at ~1.5 GPa (Harris et al., 1998), MgCO₃ to MgCO₃-II occurs at 82 GPa (Oganov et al., 2008), and dolomite to dolomite-II at ~17 GPa (Zucchini et al., 2014; Merlini et al., 2012). Moreover, disordering and the addition of Fe to carbonates strongly influence the stability of their crystal structure (Zucchini et al., 2017; Cerantola et al., 2017). The present work examines thermal disordering in Fe-dolomite as a function of Fe content. Annealing experiments were performed using a piston-cylinder apparatus at Bayerisches Geoinstitut (University of Bayreuth, Germany) on samples with Fe content from 0 to 0.55 a.p.f.u. in the temperature (T) range 450–1200 °C. The crystal structure of the annealed samples was refined from single-crystal X-ray diffraction data and results show that the critical T for disordering is 1000-1100°C for stoichiometric dolomite and it decreases to 850-1000°C as Fe content ~0.26 a.p.f.u.. In contrast, as Fe content >0.5 a.p.f.u., a continuous disordering process is observed. Moreover, the thermally induced structural disorder in Fe-dolomite is not quenchable. Reordering occurs during quench and twinned and partially disordered domains develop. Analysis of Fe-dolomite data, both ordered and disordered, is still underway to elucidate the influence of Fe content and disordering on the stability field of the mineral.

Cerantola V., Bykova E., Kupenko I., Merlini M., Ismailova L., McCammon C., Bykov M., Chumakov A.I., Petitgirard S., Kantor I., Svitlyk V., Jacobs J., Hanfland M., Mezouar M., Prescher C., Ruffer R., Prakapenka V.B. & Dubrovinsky L. (2017) - Stability of iron-bearing carbonates in the deep Earth's interior. *Nat. Commun.*, 8, 15960.

Harris M.J., Dove M.T., Swainson I.P. & Hagen V. (1998) - Anomalous dynamical effects in calcite CaCO₃. *J. Phys. Condens. Matter*, 10, L423-L429.

Merlini M., Crichton W.A., Hanfland M., Gemmi M., Müller H., Kupenko I. & Dubrovinsky L. (2012) Structures of dolomite at ultrahigh-pressure and their influence on the deep carbon cycle. *PNAS*, 109, 13509-13514.

Oganov A.R., Ono S., Ma Y., Glass C.W. & Garcia A. (2008) - Novel high-pressure structures of MgCO₃, CaCO₃ and CO₂ and their role in Earth's lower mantle. *EPSL*, 273, 38-47.

Zucchini A., Comodi P., Nazzareni S. & Hanfland M. (2014) - The effect of cation ordering and temperature on the high-pressure behaviour of dolomite. *Phys. Chem. Miner.*, 41, 783-793.

Zucchini A., Prencipe M., Belmonte D. & Comodi P. (2017) - Ab initio study of the dolomite to dolomite-II high-pressure phase transition. *Eur. J. Miner.*, 29, 227-238.

S3.

Georesources, geomaterials and their synthetic counterparts: occurrence, properties, utilizations/industrial applications

CONVENERS AND CHAIRPERSONS

Stefano Columbu (Università di Cagliari)

Laura Gaggero (Università di Genova)

Nicola Mondillo (Università di Napoli)

Rossella Arletti (Università di Torino)

Annalisa Martucci (Università di Ferrara)

Production of hydraulic binders using Lime from Mt. Morello formation in Florence area (Tuscany, Italy)

Aquino A.*¹, Lezzerini M.¹, Pecchioni E.², Giamello M.³, Cantisani E.⁴ & Fratini F.⁴

¹ Università di Pisa - Dipartimento di Scienze della Terra.

² Università degli Studi di Firenze - Dipartimento di Scienze della Terra.

³ Università degli Studi di Siena - Dipartimento di Scienze Fisiche, della Terra e dell'Ambiente.

⁴ CNR - Istituto per la Conservazione e la Valorizzazione dei Beni Culturali, Sesto Fiorentino, Firenze.

Corresponding email: andrea.aquino@phd.unipi.it

Keywords: lime, mortars, binders.

From the Roman times to nowadays the exploitation of natural resources has been of primary importance for the expansion and developments of cities and population in general. As long as for more precious natural materials, like gold and silver, even the exploitation of limestones and other lithotypes of stones for building purposes, as the production of quicklime, hydraulic lime and cements, has covered and still has a great importance (Cantisani et al., 2018; Fratini et al., 1994). The limestone exploitation to produce mortar and concrete in the territories of Florence and Prato has been active in the area from the Roman times (Cantini et al., 2017; Raneri et al., 2018). The main goal of this paper is to characterize the different lithotypes useful to the production of cement and limes for mortar production in this area by mean of chemical, mineralogical and petrographic studies and by defining their physical and mechanical properties. This study analyses stone samples from different quarries, one from the province of Prato, Mt. Calvana, and two quarries from the province of Florence, Settimello and Greve in Chianti. A mapping of these quarries and a comparison between the chemical, mineralogical and petrographic characteristics and physical and mechanical properties of these lithotypes are made.

Cantini F., Abriani A., Belcari R., Benedetti F., Carrera F.M.P., Fatighenti B., Gala L.S.D., Lezzerini M., Marani F., Meneguzzi C., Raggi A., Raneri S., Sagliuocolo A., Stiaffini D. & Tumbiolo G. (2017) - La villa dei "Vetti" (Capraia e Limite, FI): archeologia di una grande residenza aristocratica nel Valdarno tardoantico. *Archeologia Medievale*, 44, 9-71.

Cantisani E., Falabella A., Fratini F., Pecchioni E., Vettori S., Antonelli F., Giamello M. & Lezzerini M. (2018) - Production of the Roman Cement in Italy: characterization of a raw material used in Tuscany between 19th and 20th century and its comparison with a commercialized French stone material. *International Journal of Architectural Heritage*. <https://doi.org/10.1080/15583058.2018.1431730>.

Fratini F., Giovannini P., Manganelli D. & Del Fa C. (1994) - La Pietra da calce a Firenze: ricerca e caratterizzazione dei materiali per la produzione di 'calcina forte' e 'calcina dolce', *Atti del Convegno di Studi "Scienza e Beni Culturali n° 10: Bilanci e Prospettive"*, Bressanone 5-8 Luglio 1994, 189-199, Libreria Progetto Editore, Padova.

Raneri S., Cantini F., Belcari R., Baldanza A., Bertinelli A., Lorenzetti G., Legnaioli S., Mazzoleni P. & Lezzerini M. (2018) - Building materials and architectural models in late Roman Tuscany. *Archaeometric studies on mortars, stones and vitreous tesserae from "Villa dell'Oratorio" (Florence)*. *Mediterranean Archaeology and Archaeometry*, 18 (5), 109-129. <https://doi.org/10.5281/zenodo.1285889>.

Micronization of ceramic pigments: the mineralogist's viewpoint on comminution rate and amorphisation

Ardit M.*¹ & Dondi M.²

¹ Dipartimento di Fisica e Scienze della Terra, Università di Ferrara.

² CNR - ISTECC Faenza.

Corresponding email: rdmtt@unife.it

Keywords: Ceramic pigments, Comminution, Micronization.

Since its advent (a decade ago) the Drop on Demand Ink-Jet Printing (DOD-IJP) is increasingly used worldwide to decorate ceramic tiles (Digital Decoration, DD). The introduction of this technique has forced pigment manufacturers towards a paradigm shift: the way colorants are applied onto the ceramic tiles and the technological requirements for pigments and dyes are completely changed. Indeed, the finished product is no longer a powdered colorant, but a micronized pigment dispersed in a carrier, namely an ink. Ceramic inks are produced by means of a high-energy ball milling process to reduce the particles of pigment from micrometric to submicronic size (i.e., *micronization* down to median diameters, d_{50} , of 0.2-0.5 μm). Along with several advantages (non-contact decoration, high-quality images, print on textured surfaces, less wastage of inks and additives, and no need for screens), DOD-IJP also entails strict requirements, among which ensuring that >99% of the pigment particles are less than 1 μm in diameter (Hutchings, 2010). Being mainly dependent on the specific energy input (i.e., on the energy supplied to the grinding chamber in relation to the mass of product), pigment micronization down to the requested particle size proves to be the most energy-consuming *comminution* process per unit weight of product (Wang Y. & Forssberg, 2007). It derives that comminution of ceramic pigments is a key issue for ink production, which has strong repercussions on color strength, mechanical properties and resistance to amorphization of the pigment crystal structure. Based on size-energy relationships in comminution processes, as well as on the concept of pressure-induced amorphization in crystal structures, this contribution is aimed at providing a new viewpoint on the micronization effects during the comminution of ceramic pigments.

Experimental data on the comminution of representative industrial ceramic pigments (with zircon-, rutile-, spinel-type crystal structure) as micronized in a pilot plant have been selected from literature. Besides to confirm the suitability of the Rittinger's law in the submicrometric range of particles size, the energy dissipated by the comminution process is found to be proportional to the number of iterations during the micronization. In addition, different rates of micronization of three spinel-type pigments (CoFe_2O_4 , CoAl_2O_4 , and $\text{Co}_{0.75}\text{Fe}_{0.75}\text{Cr}_{1.5}\text{O}_4$) point out a new relationship between grindability of a ceramic pigment and its density (or bulk modulus). A new interpretation on the degree of ceramic pigments amorphization after prolonged comminution is also conceived.

Hutchings I. (2010) - Ink-jet printing for the decoration of ceramic tiles: technology and opportunities. In: Proceedings of the 12th World Congress on Ceramic Tile Quality, QUALICER, Castellón (Spain). 1-16.

Wang Y. & Forssberg E. (2007) - Enhancement of energy efficiency for mechanical production of fine and ultra-fine particles in comminution. *China Particuol.*, 5, 193-201.

Thermal stability of hybrid organic-inorganic metallosilicates

Beltrami G.*¹

¹ Department of Earth Sciences, University of Ferrara, Italy.

Corresponding email: bltgd@unife.it

Keywords: ECSs, X-ray diffraction, structural characterization.

Eni Carbon Silicates (ECSs) form a new class of crystalline hybrid organic-inorganic metallosilicates synthesized using bridged silsesquioxanes $(R'O)_3Si-R-Si(OR')_3$ (R =phenylene, biphenyl, naphthyl; R' =methyl, ethyl) as the sole silicon source and $NaAlO_2$ or $Ga(i-PrO)_3$ as sources of trivalent element (*e.g.*, Millini & Bellussi, 2016 and references ins.). Several ECS phases have been synthesized so far by slightly varying the composition of the reaction mixture; the structural characterization of many of them evidenced that all the hybrid phases known so far are invariably composed of a regular stacking of covalently bonded organic and inorganic layers, which alternate along the stacking direction (Bellussi et al., 2012a; Bellussi et al., 2012b; Bellettato et al., 2014). The interest towards this class of materials arises from the possibility of combining advantages of both organic (functionality and flexibility) and inorganic (thermal, mechanical and structural stability) components, thus making ECSs attractive for applications in different fields. Based on the wide range of applications, to investigate ECSs thermal behaviour and characterize their structure under operating conditions is fundamental to predict and optimize the working environment. With this purpose, different ECS samples (*i.e.*, ECS-17, Ga-ECS-17 and ECS-14) were analysed through temperature-resolved powder X-ray diffraction. Data were collected at the ID22 Beamline of ESRF from Room Temperature to 590 °C (heating rate = 5 °C/min). Rietveld refinements of diffraction patterns were carried out using the GSAS software package (Larson & von Dreele, 1994). The experimental approach used gave information about the framework flexibility, monitoring framework geometry variations and studying the rearrangement of alkali metal ions and their interactions with the framework oxygen atoms upon heating; moreover, desorption kinetics in real-time conditions were determined, highlighting the influence of dehydration processes on the structural stability of ECSs phases. These informations are crucial to improve efficiency of ECSs as catalysts as well as for applications such as gas-sensor devices, wavelength converters, and antenna systems (Tani et al., 2009), where they are employed as donor.

- Bellettato M., Bonoldi L., Cruciani G., Flego C., Guidetti S., Millini R., Montanari E., Parker Jr. W.O. & Zanardi S. (2014) - Flexible Structure of a Thermally Stable Hybrid Aluminosilicate Built with Only the Three-Ring Unit. *J. Phys. Chem., C* 118, 7458-7467.
- Bellussi G., Montanari E., Di Paola E., Millini R., Carati A., Rizzo C., Parker W.O.Jr., Gemmi M., Mugnaioli E., Kolb U., Zanardi S. (2012a) - ECS-3: A Crystalline Hybrid Organic-Inorganic Aluminosilicate with Open Porosity. *Angew. Chem. Int. Ed.*, 51, 666-669.
- Bellussi G., Millini R., Montanari E., Carati A., Rizzo C., Parker W.O., Cruciani G., De Angelis A., Bonoldi L. & Zanardi S. (2012b) - A highly crystalline microporous hybrid organic-inorganic aluminosilicate resembling the AFI-type zeolite. *Chem. Commun.*, 48, 7356-7358.
- Larson A.C. & Von Dreele R.B. (1994) - General structure analysis system, report LAUR 86-748. Los Alamos National Laboratory Report LAUR, 86.
- Millini R. & Bellussi G. (2016) - Hybrid organic-inorganic zeolites: status and perspectives. *Catal. Sci. Technol.*, 6, 2502-2527.
- Tani T., Mizoshita N. & Inagaki S. (2009) - Luminescent periodic mesoporous organosilicas. *J. Mater. Chem.*, 19, 4451-4456.

H2020 GECO - Geothermal Emission Control- Project

Boschi C.*¹, Baneschi I.¹, Bonini M.¹, Brogi A.¹⁻², Dini A.¹, Gola G.¹, Lelli M.¹, Liotta D.¹⁻², Norelli F.¹, Manzella A.¹, Montanari D.¹, Montegrossi G.¹, Orlando A.¹, Raco B.¹, Rielli A.¹, Ruggieri G.¹, Santilano A.¹ & Trumpy E.¹

¹ IGG-CNR, Institute of Geosciences and Earth Resources, Italy.

² University of Bari, Department of Earth and Geoenvironmental Sciences, Italy.

Corresponding email: chiara.boschi@igg.cnr.it

Keywords: Geothermal assessment, CO₂ sequestration, geological modelling, reservoir simulation.

GECO project, GECO standing for “Geothermal Emission CONTROL”, is an EU funded project through the Horizon 2020 Research and Innovation programme. GECO aims to develop near Zero Emission Geothermal Power Plants. The challenge of the project is to test advanced technologies where gas emissions (mostly steam and CO₂) from geothermal power plant are condensed and re-injected in the geothermal reservoir, or turned into commercial products, throughout CO₂ mineral sequestration. The 18 GECO partners from 9 countries are committed to characterise 4 different demonstration sites located in Iceland, Italy, Germany and Turkey providing a pre-feasibility assessment of the baseline reservoir conditions and to demonstrate the feasibility of the re-injection (including NGC's) of geothermal fluids.

In Italy, the demonstration site is located at Castelnuovo, few kilometres northeast from Larderello geothermal area where a deep, superheated steam reservoir with 8% of expected NGCs (98% CO₂, 2% H₂S) is hosted mainly in the metamorphic units and characterised by temperature ranging between 300° and 350°C and pressure up to 70 bar at depths ranging from 3.5 and 4 km. For the pre-feasibility assessment of the Castelnuovo (Italy) site a structural, geological, geophysical (MT fieldwork) and geochemical (CO₂ diffuse degassing measurements) integrated approach is ongoing, in order to produce different scales and typologies of modelling. A first level of modelling consists of a geological regional model (about 25 Km x 37 Km) and a steady state thermal regional model, where existing data and information from structural geologic, geophysical and geochemical field works are embedded. The geometries from geological regional model and the natural thermal state of the underground are acting as input and boundary conditions for the reservoir modelling. The reservoir modelling is the second level of modelling, i.e. local model, and is carried out to assess the exploitation scenario accounting for injection and production. Moreover, at reservoir scale, geochemical modelling of the gas-water-rock interaction during the exploitation is ongoing to predict the fate of reinjected fluids at depth. Laboratory experiments will also provide some constrains on the fluid-rock geochemical reactions expected in the reservoir as consequence of re-injection. In addition, based on poro-elasticity model, the setting of fully coupled thermo-hydro-mechanical models is furthermore performed to evaluate the stress-strain relationship under injection conditions

The preliminary results of the different kind of modelling will be the used during the project as base to demonstrate the feasibility of the geothermal fluids reinjection. The methodology used in the Castelnuovo site can be easily reused in different plays and context and even for different purpose where natural reservoir behaviour has to be investigate.

The Mineral resources database of Italy (GeMMA)

Carta R.¹ & Fumanti F.*¹

¹ ISPRA-Dipartimento per il Servizio Geologico d'Italia.

Corresponding email: fiorenzo.fumanti@isprambiente.it

Keywords: geodatabase, quarries, mines.

The Geological Survey of Italy (SGI) of ISPRA is developing a geodatabase aiming at collecting all relevant information from available sources (CARG project, historical geological maps, national census of active mines and quarries, data from regional/provincial databases and mining plans, inventory of historical mining sites, network of national parks and mine museums, etc.). Taking advantage of the preliminary results of the Minerals4EU project (Minerals Intelligence Network for Europe), the PostgreSQL database is being designed with an INSPIRE compliant architecture.

The main purpose is to define the national situation of mineral resources from mines and quarries including the geological, environmental and economic aspects, with particular attention to the environmental impact of mining practices and the potential exploitation of the decommissioned mining assets and the extracted waste piled up over time.

So far, all the active quarries and mines within the national territory have been identified and georeferenced. About 90% of the mines opened since 1870 have been located too.

Each coded mining site has associated information related to data sources, type of mining site, state of activities, type of extracted ore, type of management, environmental situation of the site. The estimate of the resources and reserves amount is more problematic.

Due to the partition of competences attributed to the regional authorities by the Italian legislation, it is necessary to establish contacts and make agreements with numerous local bodies, each one with different rules and competences that must be considered and respected.

Therefore, for the success of this project it is essential to build flexible spaces of dialogue and loyal collaboration. Based on that, ISPRA is coordinating a Thematic Table of the Italian Geological Services Network with the participation also of the Regional Offices for Mining, with the collaboration of Istat and Unmig.

Within these areas of dialogue, the Geological Survey of Italy hopes that GeMMA can become a valid support tool for the development of national and regional policies oriented towards the sustainable production and efficient use of primary and secondary mineral resources, in a circular economy perspective.

Purple hematite: synthesis of the pigment Caput Mortuum through thermal treatment of natural samples

Castagnotto E.*¹, Locardi F.²⁻³, Cabella R.¹ & Ferretti M.²

¹ Dipartimento di Scienze della Terra dell' Ambiente e della Vita, Università degli Studi di Genova, Italy.

² Dipartimento di Chimica e Chimica Industriale, Università degli Studi di Genova, Italy.

³ Istituto di Struttura della Materia – CNR, Area della Ricerca di Roma1, Monterotondo Scalo, RM, Italy.

Corresponding email: castagnottoelena@gmail.com

Keywords: pigments, cultural heritage, iron oxides.

Since the prehistoric era earth pigments are widely adopted in art, among them red and yellow ochre are the most common (Hradil et al., 2003). The first owes its colour to the mineral hematite [α -Fe₂O₃] and can be directly collected in nature or obtained through a thermal-oxidative treatment applied to yellow ochre, which is mostly made of the mineral goethite [α -FeO(OH)] (Cornell & Schwertmann 2000). A purple pigment based on hematite, called Caput mortuum, is often reported in wall paintings, even if the term was introduced only in the XVIII century, at the same time as the introduction of the first purple synthetic iron oxide (Mars' violet) (Eastaugh et al., 2008). In this study, different Fe-rich compounds were used as starting material. Specimen of natural origin have been selected and sampled on Italian territory; hematite, goethite and magnetite of synthetic origin have been used as starting and reference materials in regard of their homogeneous particle size and shape. The study of chemical-morphological changes of the synthetic powders lays the foundation for understanding what could happen with natural materials where genesis conditions are not controlled. Moreover, it allows determining the role of impurities, inevitable in nature, and to assess their necessity for achieving the colour purple. The samples were subjected to different thermal-oxidative and mechanical treatments, all available in antiquity. The most encouraging, deemed suitable to obtain the colour of the Caput mortuum, are those with a starting high content of iron oxides: they were analysed through Scanning Electron Microscopy (SEM), X-ray Powder Diffraction (XRD) and Reflectance analyses. It has been demonstrated that the easiest way to obtain Caput mortuum is through grinding of crystalline hematite, but the thermal treatment allows more control on the final hue, that is achieved by heating at T>900 °C. The macroscopic change in optical behaviour was mostly ascribed to a percentage of particles present in a precise dimensional span, that induce the scattering phenomena causing the perception of purple. Besides, a variation in the local crystallographic structure of Fe₂O₂ was hypothesised according to the reflectance spectra behaviour; it shows a shift in the band assigned to the electron pair transition (EPT) between adjacent Fe cations. This information enriches the knowledge on Fe-based pigments and can be used for a more accurate diagnostic identification.

Cornell R.M. & Schwertmann U. (2000) - The Iron Oxides, Structure, Properties, Reactions, Occurrences and Uses. Wiley-Vch, Weinheim

Eastaugh N., Walsh V., Chaplin T. & Siddall R. (2008) - Pigment Compendium - a dictionary and optical microscopy of historical pigments. Routledge, New York

Hradil D., Grygar T., Hradilová J. & Bezdička P. (2003) - Clay and iron oxide pigments in the history of painting». Applied Clay Science, 22(5), 223–36.

Evaluations of the reuse of municipal solid waste incinerator bottom ashes as aggregated materials in civil applications

Caviglia C.*¹, Confalonieri G.¹, Destefanis E.¹, Mandrone G.¹, Pastero L.¹, Boero R.² & Pavese A.¹

¹ Dipartimento di Scienze della Terra, Università degli Studi di Torino.

²Trattamento Rifiuti Metropolitan – TRM SpA.

Corresponding email: caterina.caviglia@unito.it

Keywords: bottom ash, reuse, aggregates.

Nowadays, the availability of the natural mineral resources is not always able to meet the demands and it requires higher and higher energetic and environmental costs. As a consequence of the growth of the population that involves the construction of an increasing number of infrastructures, the sustainable supply of raw materials used for the production of aggregates has become a topic of fundamental importance.

With regard to sustainability, the use of residues from waste-to-energy plants for urban waste is included: after moderate treatments, they can find a role of raw materials in the construction of works, reducing the need to find additional natural resources and related problems for their disposal or storage.

Bottom ashes reuse is a common practice in many countries of Europe, and even in Italy, most of the bottom ashes from MSWI (Municipal Solid Waste Incinerators) is used, depending on the legislation, for the production of aggregates for civil infrastructures.

The aim of the present study is to characterize the bottom ashes taken by a plant located in the Northern part of Italy, applying a multidisciplinary approach. Some inertization techniques, as the natural and the accelerated carbonation, are also tested to reduce the release of polluting substances in the environment. The carbonation process involves the absorption of carbon dioxide by an alkaline material, as bottom ash, decreasing pH and making calcite precipitate (Van Gerven et al., 2005; Nam et al., 2012). The interaction of carbon dioxide with municipal solid waste incinerator (MSWI) bottom ash has been studied to investigate the resulting changes in pH and bottom ash mineralogy and the impact that these changes have on the mobility of dangerous substances, especially heavy metals. This process can be natural, in an open environment, or accelerated, using laboratories reactors to study the variation of time, temperature and humidity to maximize the carbonation process. We have compared these two methods to evaluate the possibility of a reuse of bottom ashes, respecting the European legislation threshold limits.

Van Gerven T., Van Keer E., Arickx S., Jaspers M., Wauters G. & Vandecasteele C. (2005) - Carbonation of MSWI-bottom ash to decrease heavy metal leaching, in view of recycling. *Waste Management*, 25(3), 291–300.

Nam S.-Y., Seo J., Thriveni T. & Ahn J.-W. (2012) - Accelerated carbonation of municipal solid waste incineration bottom ash for CO₂ sequestration. *Geosystem Engineering*, 15(4), 305-311.

Preliminary characterization of the Nonsulfide Zn(Pb) ores from the Florida Canyon Project (Northern Peru)

Chirico R.*, Mondillo N. & Boni M.

Dipartimento di Scienze della Terra, dell' Ambiente e delle Risorse, Università di Napoli "Federico II", Napoli, Italy

Corresponding email: ritachiricounina@gmail.com

Keywords: Zinc, nonsulfide, Northern Peru.

The Florida Canyon Project is located in the Northern Peru in the sub-Andean fold-and-thrust belt in the upper Amazon River Basin. The mineralization is hosted by the dolomitized carbonate rocks of the Chambará Formation (Pucará Group, Upper Triassic to Lower Jurassic), and consists of both Zn-Pb sulfide and nonsulfide ores. The project comprehends several ore bodies named San Jorge, Central, Karen-Milagros, and Sam, mostly developed in correspondence of fault zones or karsts.

The resources of Florida Canyon have been calculated so far at 12.1 Mt, grading 10.7% Zn and 1.2% Pb (Hunt et al., 2017), and are mostly represented by sulfides (especially in the Karen-Milagros area). However, recent explorative drilling has found abundant nonsulfide intersections in other areas of the project, up to 500 m in depth (de Oliveira et al., 2019). These nonsulfide bodies have an irregular distribution, being represented by new-formed minerals in veins or cavities, but also by direct replacements of former sulfides. The primary sulfides mostly consist of low-Fe sphalerite and Ag-bearing galena with less pyrite, and share several characteristics with typical stratabound Mississippi Valley-type deposits. The most abundant nonsulfide minerals are smithsonite and hemimorphite, forming earthy and colloform agglomerates, whilst hydrozincite and cerussite are rare.

From these preliminary observations, it seems that the Florida Canyon nonsulfide mineralization is very similar to nearby Cristal prospect (Arfè et al., 2018). This suggests that the secondary deposits formed at the same time (Miocene to Pliocene) under the same humid tropical climatic conditions. However, more specific analyses are required for confirming these genetic aspects.

Arfè G., Mondillo N., Boni M., Joachimski M., Balassone G., Mormone A., Santoro L. & Medrano E.C. (2018) - The Cristal Zn prospect (Amazonas region, Northern Peru). Part II: An example of supergene enrichments in tropical areas. *Ore Geol Rev.*, 95, 1076–1105.

de Oliveira S.B., Juliani C. & Soares Monteiro L.V. (2019) - Mineral characterisation of the non-sulphide Zn mineralisation of the Florida Canyon deposit, Bongará District, Northern Peru. *Applied Earth Science (Trans. Inst. Min. Metall. B)*, 128, 27–36.

Hunt W., Pennington J.B., Poeck D.H., Osborn J., Gilbertson J. & Tinucci J. (2017) - NI 43-101 Technical Report Preliminary Economic Assessment Florida Canyon Zinc Project Amazonas Department, Peru Inc. SRK, 217 pp.

Raman spectroscopy of aluminosilicates. What about geopolymers?

Coccatto A.*¹, Stroschio A.¹, Finocchiaro C.¹, Fugazzotto M.^{1,2}, Occhipinti R.¹, Bersani D.³, Fornasini L.³, Mazzoleni P.¹ & Barone G.¹

¹ Dipartimento di Scienze Biologiche, Geologiche e Ambientali, Università degli Studi di Catania.

² Dipartimento di Scienze Umanistiche, Università degli Studi di Catania.

³ Dipartimento di Scienze Matematiche, Fisiche e Informatiche, Università degli Studi di Parma.

Corresponding email: alessia.coccatto@hotmail.it

Keywords: geopolymer, Raman spectroscopy, cultural heritage.

Raman spectroscopy has provided, and provides, valuable information on the structural properties of aluminosilicates, such as rock-forming minerals, Portland cement, ceramics, natural and artificial glasses, zeolites. In the field of sustainable tailor-made materials, geopolymers are assuming more and more importance, thanks to their reduced CO₂ footprint and the tunability of their mechanical properties, for large-scale applications as well as for niche applications, such as conservation and restoration of built heritage.

The geopolymer structure, an aluminosilicate gel, apparently offers a straightforward application for Raman spectroscopy. In the framework of the PNR-funded project “Advanced Green Materials for Cultural Heritage”, the literature on aluminosilicates is being reviewed. It appears that Raman spectroscopy, even if widely used in the study of natural and artificial materials, has rarely been applied to geopolymers, for which the preferred technique is Fourier-transform infrared spectroscopy (FT-IR) (Yarwood et al., 2009). It has to be noted that not all the laser sources provide good-quality Raman spectra of aluminosilicates: green and blue lines are preferred over the red ones, as the fluorescence background appears reduced (see, for example, Carter et al., 2009). Nevertheless, it seems possible to study the raw materials and to successfully characterize the geopolymer (Rüscher et al., 2010; Kosor et al., 2016a, 2016b; Arnoult et al., 2018).

In this work, we review the use of Raman spectroscopy for geopolymers study in the literature and we try to apply this analytical methodology to understand the geopolymerization of sustainable formulations based on volcanic ash, volcanic soils, clayey sediments and ceramics, also for cultural heritage applications.

Arnoult M., Perronnet M., Autef A. & Rossignol S. (2018) - How to control the geopolymer setting time with the alkaline silicate solution. *Journal of Non-Crystalline Solids*, 495, 59-66.

Carter E.A., Hargreaves M.D., Kononenko N., Graham I., Edwards H.G., Swarbrick B. & Torrence R. (2009) - Raman spectroscopy applied to understanding Prehistoric Obsidian Trade in the Pacific Region. *Vibrational Spectroscopy*, 50(1), 116-124.

Kosor T., Nakić-Alfirević B. & Gajović A. (2016a) - Geopolymerization index of fly ash geopolymers. *Vibrational Spectroscopy*, 85, 104-111.

Kosor T., Nakić-Alfirević B. & Svilović S. (2016b) - Geopolymer depolymerization index. *Vibrational Spectroscopy*, 86, 143-148.

Rüscher, C.H., Mielcarek, E., Wongpa, J., Jirasit, F., & Lutz, W. 2010. New Insights on Geopolymerisation Using Molybdate, Raman, and Infrared Spectroscopy. In: Kriven M.W., Zhou Y., Radovic M., Mathur S., Ohji T. (eds.), *Strategic Materials and Computational Design: Ceramic Engineering and Science Proceedings*, Volume 31.

Yarwood J., Douthwaite R. & Duckett S. (2009) - Spectroscopic properties of inorganic and organometallic compounds (Vol. 40). Royal Society of Chemistry, Cambridge.

Chemical reactivity of pozzolans from Sardinia for the industrial production of hydraulic limes

Columbu S.*¹, Comboni D.², Gatta D.² & Sitzia F.¹

¹ Dipartimento di Scienze Chimiche e Geologiche, Università di Cagliari.

² Dipartimento Scienze della Terra, Università di Milano.

Corresponding email: columbus@unica.it

Keywords: hydraulic mortar, ignimbrites, glass.

The research is aimed at studying the chemical reactivity between lime and volcanic rocks belonging to different Sardinian outcrops, for a use as raw material in the production of hydraulic / pozzolanic limes. On the basis of preliminary geochemical and mineralogical-petrographic investigations, several volcanic rocks from basic-intermediate to acid in composition (substantially from andesitic, to dacitic, to rhyolitic) have been selected and used for to perform laboratory reactivity tests. These rocks differ in the variable content of glass (from 15% to about 95% in volume), due to the presence of secondary minerals, and to physical properties (density, porosity, water absorption, etc.). The physical characteristics are essentially linked to the different compositional incidence of the crystalline, crystal-clastic, lithic (present in some pyroclastic facies), type and quantity of glass phases, to their different methods of installation (conditioned by temperature, chemical composition, grade welding, etc.), and to the different degree of alteration.

The results of the investigations on the pozzolan materials (by polarized light microscopy, XRD, SEM, EPMA-WDS, Chapelle test) show that following parameters affect the chemical reactivity of the volcanic products with lime: i) quantity and type of amorphous phases (glass), linked to the different emplacement of volcanic rocks (affected by temperature, chemical composition, welding grade, etc.), ii) compositional incidence of the crystalline phases, crystal-clasts, lithics (these latter present in some pyroclastic facies), iii) alteration grade of the rocks and presence of secondary minerals (e.g., zeolites, phyllosilicates, etc.).

Anisotropic compressional behavior of ettringite

Comboni D.^{*1-2}, Lotti P.¹, Gatta G.D.¹, Merlini M.¹ & Hanfland M.³

¹ Dipartimento di Scienze della Terra, Università degli Studi di Milano.

² Dipartimento di Scienze della Terra e dell'Ambiente, Università degli Studi di Pavia.

³ ESRF- European Synchrotron Radiation Facility.

Corresponding email: davide.comboni@unimi.it

Keywords: High-Pressure, Ettringite, XRD synchrotron experiments.

A Portland cement is a complex multi-component system and, to predict its elastic properties, an exhaustive database of the thermodynamic parameters of the main constituents is needed. Ettringite (ideally $\text{Ca}_6\text{Al}_2(\text{SO}_4)_3(\text{OH})_{12}\cdot 27\text{H}_2\text{O}$, with $a=b \sim 11.21$ and $c \sim 21.43$ Å, Sp. Gr. *P31c*) is one of the most important crystalline phases in Portland cements: its crystallization, in the early hydration stages, governs the set rate of the highly reactive “C3A” phase ($\text{Ca}_3\text{Al}_2\text{O}_6$), whereas in aged cements the formation of ettringite is commonly associated with degradation processes (Taylor et al., 2001). The crystal structure of ettringite is significantly complex with a H-bonding net which connects $[\text{Ca}_3[\text{Al}(\text{OH})_6]\cdot 12\text{H}_2\text{O}]$ -columns (in which $\text{Al}(\text{OH})_6$ -octahedra are alternated with triplets of $\text{Ca}(\text{OH})_4(\text{OH}_2)_4$ -polyhedra) to sulphate groups (Gatta et al., 2019). Despite the previous studies at high pressure on this material (e.g., Cuesta et al., 2017, Clark et al., 2008), the linear bulk moduli (K_a and K_c) and a description of the deformation mechanisms at the atomic scale are still missing. In this light, we have investigated the compressional behavior of ettringite up to 4.2 GPa by means of *in-situ* single-crystal synchrotron X-ray diffraction, using a diamond-anvil cell (DAC) and the mix methanol:ethanol (4:1) as *P*-transmitting fluid.

Ettringite shows a marked anisotropic compressional pattern (K_a 21(1) GPa, K_c 47(1) GPa). This anisotropic elastic scheme dramatically changes at $P > 3$ GPa; K_{V0} drops from 26.6(5) to 10.4(8) GPa, which mainly affects the structure on the *ab* plane (K_a drops from 21(1) to 7.3(8) GPa whereas K_c decreases only moderately). Structure refinements reveal that the elastic softening reflects the collapse of the H-bonding network, due an average decrease of the $\text{O}_{\text{donor}} \cdots \text{O}_{\text{acceptor}}$ distances (up to 0.20 Å in some cases), which mainly affect the interaction between the sulphate groups and the $\text{Ca}(\text{OH})_4(\text{OH}_2)_4$ -polyhedra.

Clark S.M., Colas B., Kunz M., Speziale S., Monteiro P.J.M. (2008) - Effect of pressure on the crystal structure of ettringite. *Cem. Concr. Res.*, 38, 19-26.

Cuesta A., Rejmak P., Ayuela A., De la Torre A.G., Santacruz I., Carrasco F.L., Popescu C., Aranda M.A.G. (2017) - Experimental and theoretical high pressure study of calcium hydroxyaluminate phases, *Cem. Concr. Res.*, 97, 1–10.

Gatta G.D., Hålenius U., Bosi F., Cañadillas-Delgado L. & Fernandez-Diaz M.T. (2019) - Minerals in cement chemistry: a single-crystal neutron diffraction study of ettringite, $\text{Ca}_6\text{Al}_2(\text{SO}_4)_3(\text{OH})_{12}\cdot 27\text{H}_2\text{O}$. *Am. Mineral.*, 104, 73-78.

Taylor H.F.W., Famy C. & Scrivener K.L. (2001) - Delayed ettringite formation, *Cem. Concr. Res.*, 31, 683–693.

Biomass vs coal ashes: a multi-methodic analysis to assess their hazardousness or reusability

Comodi P.*¹, Cavalaglio G.², Nicolini A.², Cambi C.¹, Vivani R.³, Zucchini A.¹, Susta U.¹, Frondini F.¹ & Cotana F.²

¹ Dipartimento di Fisica e Geologia, Università di Perugia, Italy.

² Centro Interuniversitario di Ricerca sull'Inquinamento da Agenti Fisici, Perugia, Italy.

³ Dipartimento di Scienze Farmaceutiche, Università di Perugia, Italy.

Corresponding email: paola.comodi@unipg.it

Keywords: biomass, fly ashes, multi methodic-analyses.

Both biomass and coal derived ashes have a high potential environmental impact because of their grain size, which can be a threat in terms of atmospheric pollution, and because of the high concentration of heavy metallic and radioactive elements. According to European law (UNI EN 450) unprocessed biomass ashes cannot be used in cement as aggregate and are hence partially utilized just as fertilizer in agriculture; on the other hand even a third of the total amount of ashes produced by coal power plants are used as such in the cement industry.

The hazardousness may be directly dependent on the fuel that is combusted (Lima et al., 2008). Sometimes fly ashes are very prone to leach metals and chlorides due to their content in soluble salts and high specific surface and so, heavy metal leachability studies are strongly recommended before the reuse of ashes in different environments.

The focus of present work is laid on the characteristics of fly ashes coming from combustion of coal and different types of biomass, to understand the differences from chemical, dimension and structural point of view. A set of samples coming from gasification plants, from biomass combustion (forest chips, grapevine pruning, thistles, olive-tree pruning) and from coal power plants are taken into account. There are characterized in terms of grain size distribution, calorific power and organic components, physical-chemical properties of the bulk and of the single component (crystalline or amorphous). Particle size distribution was determined by Photon Spectroscopy Correlation (PSC), for particle sizes over 1 micron and Single Particle Optical Sensing (SPOS) for particle sizes below 1 micron, X-ray Powder Diffraction coupled with Rietveld refinement, Inductively Coupled Plasma-Optic Spectroscopy, and Thermal Analysis, allowed the bulk analyses. Punctual chemical composition within the grains at a microscopic scale were determined with Laser Ablation Inductively Coupled Plasma-Mass Spectroscopy and Electron Probe Micro Analysis. Optic Microscopy, Scanning Electron Microscopy (SEM) and high definition Field Emission SEM allowed a textural analysis from micro-to nano scale.

The multi-methodic approach intents to point out the existence of dimensional subclasses (particulates or not), chemical composition (presence of heavy metals or radioactive elements), and microscopic structures and to associate heavy metals (Cd, Cr and other dangerous elements) to the mineralogical phases, which impact on the leachability potential and in turn on the possible re-use, for example on soil stabilization or for a correct landfill disposal of wastes

Preliminary results of a study will be presented.

The study is funded by Fondazione Cassa di Risparmio Perugia, project code. N. 2018.0508.026, P.I. Paola Comodi

Lima A.T., Ottosen L.M., Pedersen A.J. & Ribeiro A.B. (2008) - Characterization of fly ash from bio and municipal waste, *Biomass and Bioenergy*, 32(3), 277-282.

Hydrocarbon Polymerization in Pure Silica Mordenite: The Effects of Structure, Pressure, Temperature and Time

Confalonieri G.*¹, Arletti R.², Di Renzo F.³, Fabbiani M.⁴, Fois E.⁵, Haines J.³, Martra G.⁴, Quartieri S.⁶, Santoro M.⁷, Tabacchi G.⁵ & Vezzalini G.¹

¹ Dipartimento di Scienze Chimiche e Geologiche, Università di Modena e Reggio Emilia, Italy.

² Dipartimento di Scienze della Terra, Università di Torino, Torino, Italy.

³ Institute Charles Gerhardt Montpellier, CNRS, ENSCM, Université de Montpellier Montpellier, France.

⁴ Dipartimento di Chimica, Università di Torino, Torino, Italy.

⁵ Dipartimento di Scienza ed Alta Tecnologia, Università dell'Insubria, Como, Italy.

⁶ Dipartimento di Scienze Matematiche e Informatiche, Scienze Fisiche e Scienze della Terra, Università di Messina, Messina S. Agata, Italy.

⁷ Istituto Nazionale di Ottica, INO-CNR, Sesto Fiorentino, Italy.

Corresponding email: giorgia.confalonieri@unimore.it

Keywords: Zeolite, Hydrocarbon polymerization, XRPD.

Conductive polymers, obtained from the polymerization of hydrocarbons (e.g. acetylene, butadiene, ethylene), are exploitable in many different technological applications, such as electronic devices useable in solar energy conversion, optoelectronic and gas sensing. Being very sensitive to humidity, their confinement inside a host matrix is necessary to reduce their instability in air. Pure silica zeolites, thanks to their structure and composition, have been proved to be promising host materials (Scelta et al., 2014). The presence of channels in their frameworks can drive the polymerization along specific directions (Santoro et al., 2013) and their hydrophobic nature allows isolating and protecting the resulting polymers from water vapor present in the air. In this work, we investigated the effect of pressure coupled with temperature, and of time in promoting the polymerization of linear chains of phenylacetylene and hexadiene in a pure silica mordenite (Si-MOR). In situ synchrotron X-Ray Powder Diffraction was used to characterize the resulting materials, unraveling their structure and the host-guest relationships. Further investigations were performed by TGA and IR analyses and DFT calculations. Both molecules were detected in the zeolite porosities. The complete polymerization of hexadiene inside Si-MOR is observed at ambient conditions while the oligomerization of phenylacetylene was achieved at 1.5 GPa and 150°C. In the case of hexadiene, the acid sites present in Si-MOR catalyse the formation of the polymer chain even at ambient conditions, but only when enough time (approximately 1 week) is provided for the reaction. The results here presented, confirming the formation of phenylacetylene oligomers and of polyhexadiene inside Si-MOR, suggest that both systems could be promising for the realization of embedded linear conductive polymers.

Santoro M., Gorelli F.A., Bini R., Haines J. & Van der Lee A. (2013) - High-pressure synthesis of a polyethylene/zeolite nano-composite material. *Nature Commun.*, 4, 1557. <https://doi.org/10.1038/ncomms2564>.

Scelta D., Ceppatelli M., Santoro M., Bini R., Gorelli F.A., Perucchi A., Mezouar M., Van der Lee A. & Haines J. (2014) - High pressure polymerization in a confined space: conjugated chain/zeolite nanocomposites. *Chem. Mater.*, 26, 2249-2255.

Brazilian phyllite as feldspar substitute in ceramic bodies

Conte S.*¹, Zanelli C.¹, Melchiades F.G.², Hernández-Sánchez M.Y.³⁻⁴, Boschi A.O.³⁻⁴ & Dondi M.¹

¹ CNR-ISTEC, Faenza (RA), Italy.

² Centro de Revestimentos Cerâmicos – CRC, São Carlos, SP, Brasil.

³ Programa de Pós-Graduação em Ciência e Engenharia de Materiais – PPGCEM, Universidade Federal de São Carlos – UFSCar, São Carlos, SP, Brasil.

⁴ LaRC, Departamento de Engenharia de Materiais – DEMa, Universidade Federal de São Carlos – São Carlos, SP, Brasil.

Corresponding email: sonia.conte@istec.cnr.it

Keywords: ceramic tiles, sintering behavior, phyllite.

The Brazilian porcelain stoneware tiles production is nowadays largely based on the use of pyrophyllite: a very fine metasedimentary rock primarily composed of sericite, kaolinite and quartz. Due to its chemical and mineralogical composition phyllite shows an ambivalent behavior: it can act either as flux, plastic component and skeleton in a ceramic mixture. For this reason, Brazilian phyllite is widely employed in ceramic production, especially in the São Paulo area, thanks to its relative abundance in the Southern regions. Despite the presence of phyllite in the ceramic body can reach the 50% in weight, there are almost no information about the firing behavior of this material. Moreover, even if phyllite is usually used in substitution of fluxing component, no study on the effect of this substitution are available to date. In order to fill this knowledge gap, the Brazilian University – Materials Engineering Department – started an investigation of different phyllite deposits. In this work, the sintering behavior of four samples were investigated. Three different phyllite typologies were selected and added to three Brazilian porcelain stoneware mixtures in substitution of the feldspatic component (50%wt of the batch), while a classic body with 50% K-feldspar has been taken into account as benchmark. Each mixture was characterized from the chemical point of view and, once fired, its quantitative phase composition were determined by XRD-Rietveld in order to calculate both the amount of crystalline phases and the chemical and physical properties of the vitreous phase. The mechanism governing the sintering by viscous flow of this ceramic materials mainly depends on the physical properties of the liquid phase at high temperature. Therefore, its viscosity was calculated by the predictive model of Giordano, while the effective viscosity of the whole tile has been calculated following the Brinkman equation. The results show the different firing behavior of the mixtures: the benchmark melts quickly producing a large amount of liquid phase and reaching the maximum densification at a relatively low temperature (1150°C); the bodies with phyllite as raw materials are less reactive, a lower quantity of vitreous phase is formed during the firing and a higher amount of residual quartz is present at the end of the cycle. Moreover, they reach the maximum densification at higher temperatures (1190-1200°C). It was possible to observe a correlation between the phase composition and the refractoriness of the samples with different phyllite types: at 1200°C the % ratio between quartz/mullite/vitreous phase passes from a more refractory behavior (33:10:55) to a more fusible behavior with a ratio of 20:5:73. The viscosity of the liquid phases at different firing temperatures were not so dissimilar, between 4.4 and 5 Log10Pa.S for all the samples.

A global view at sourcing and composition of fluxes for ceramics

Dondi M.*, Guarini G., Conte S., Molinari C., Soldati R. & Zanelli C.

CNR-ISTEC, Istituto di Scienza e Tecnologia dei Materiali Ceramici, Faenza.

Corresponding email: michele.dondi@istec.cnr.it

Keywords: ceramic, ore deposits, raw materials.

Feldspathic fluxes are fundamental ingredients of many ceramic products, but a global view at the geological sources actually exploited by industry and the lithologies occurring in these deposits is lacking. This contribution reviews the sourcing and composition of feldspathic raw materials (and additional fluxes based on sericite, talc and further “low-melting” minerals) used by or proposed to the ceramic industry. It follows a previous analysis of production trends and market dynamics (Dondi, 2018). A large set of data (about 1400 deposits in 75 countries and over 1300 chemical analyses) was collected from literature and industrial information, critically assessed and elaborated to get an exhaustive picture of deposits and composition of both raw and beneficiated fluxes. Overall, the main sources are granitic suites, including acid differentiates (pegmatites and aplites) and the corresponding extrusive and hypabyssal terms (rhyolites, porphyries). Leucogranites are the most important resources among granitoids, even though half of all mining operations in the World reside on pegmatites. A few alkaline complexes with silica-undersaturated rocks are supplying the ceramic industry: both nepheline syenite and nepheline phonolite (and related intrusive and extrusive lithotypes). Intermediate igneous rocks (syenite, trachyte) are seldom exploited as fluxes, but the recourse to basic terms (gabbro, anorthosite, basalt, andesite, etc) is common in red firing products. Fluxes of sedimentary origin are obtained from feldspathic arenites, mainly arkoses. Metamorphic and metasomatic rocks are extensively utilized by the ceramic industry, especially albitites (the most important source for the ceramic tile industry) and phyllites. Deposits generated through low temperature hydrothermal (epithermal) alteration provide a set of peculiar fluxes (e.g., eurite and pottery stone) characterized by a significant amount of low melting minerals, such as sericite. Skarn deposits are the main source of non-feldspathic fluxes, represented by ores rich in talc, wollastonite, chlorite, diopside. The compositional variability in the deposits of each source is represented through diagrams accounting for the relevant parameters for the ceramic industry: equivalent amount of feldspars, Na/K (or Ca/Mg) ratio, and concentration of chromophores ($\text{Fe}_2\text{O}_3 + \text{TiO}_2$). Such a global view is intended to foster studies on flux deposits, focusing on crucial aspects for the ceramic raw materials industry, like the existence of geological constraints to the occurrence of given ore types, or the definition of a genetic model for strategic resources, like albitite deposits.

Dondi M. (2018) - Feldspathic fluxes for ceramics: Sources, production trends and technological value. *Resources, Conservation and Recycling*, 133, 191-205.

Enhancing the sustainability of the aluminium production: experimental tests addressed to the inertization of industrial by-products through hydrogen storage for furnace fuel and to the synthesis of foamed geopolymers

Ercoli R.^{*1}, Renzulli A.¹, Orlando A.², Tassi F.³, Pagnetti A.⁴, Vaselli O.³, Borrini D.³, Paris E.⁵,
Tarantino S.C.⁶ & Di Gregorio A.⁷

¹ Dipartimento di Scienze Pure e Applicate, Università di Urbino.

² IGG – CNR Firenze.

³ Dipartimento di Scienze della Terra, Università di Firenze.

⁴ Laboratorio ARCA Srl, Fano.

⁵ Scuola di Scienze e Tecnologie, Università di Camerino.

⁶ Dipartimento di Scienze della Terra e dell'Ambiente, Università di Pavia.

⁷ CRIET, Università di Milano Bicocca.

Corresponding email: r.ercoli@campus.uniurb.it

Keywords: Aluminium, Hydrogen, geopolymers.

Valorization of the so-called “industrial by-products” is of a paramount importance for (i) the sustainability of raw material exploitation and management, (ii) limiting the greenhouse gases emissions and (iii) reducing the amount of waste to landfill. A fundamental principle of circular economy and sustainable development focus on the use of residual products from industrial processes or from end-of-life materials, with the goal to valorize them for new application and minimizing the waste production. For this purpose, the University of Urbino is working on an innovative PhD project, financially supported by the Regione Marche (*Fondazione Cluster Marche*). Its aim is the disposal and re-use of industrial waste from two local industries: *Profilglass SpA* dealing with specific treatments of aluminium profiles, pipes and laminates for different sectors such as construction, automotive, electronics, mechanics and many others, and *Faber vetreria Srl* which is a glassware industry supplier of the most important European companies. Experimental tests firstly involved industrial by-products of *Profilglass SpA*, produced from three main processes of the aluminium recycling: (a) sifting, (b) pyrolysis and (c) melting. To inertize the above mentioned highly water-reactive materials, that release significant amounts of H₂ from metals, the reaction series were tested and monitored in laboratory. Obviously, aluminium is the most abundant metal species and therefore the main source for the release of hydrogen, given by:

- (1) $2\text{Al} + 6\text{H}_2\text{O} + 2\text{NaOH} \rightarrow 2\text{NaAl}(\text{OH})_4 + 3\text{H}_2$
- (2) $\text{NaAl}(\text{OH})_4 \rightarrow \text{NaOH} + \text{Al}(\text{OH})_3$
- (3) $\text{Al}(\text{OH})_3 + \text{Al}(\text{OH})_3 \rightarrow \text{Al}_2\text{O}_3 + 3\text{H}_2\text{O}$

The experiments were performed by mixing industrial waste to an aqueous alkaline solution in a stainless-steel compact reactor (series 5500 HP T316, 25 ml, Parr Instrument Company) equipped with gas inlet and outlet valves, liquid sampling valve and internal thermocouple in addition to the internal magnetic stirrer. In order to synthesize geopolymers through alkaline activation, the aluminium industrial by-products will be mixed to silica-rich waste of the glass industry, which requires the disposal of sludges from the filtration of glass processing, performed by a high-pressure water jet. The production of H₂ will allow to produce foamed geopolymers with pockets of hydrogen trapped in pores throughout the body of a high strength and hardness material, which is suitable not only as insulation material but also for electronic applications. An essential physical characteristic of geopolymers is also the resistance to mechanical, thermal and atmospheric degradation, parameters suitable to trap polluting and toxic substances.

FT-IR study of early stages of geopolymer gel formation of AAMs based on pyroclastic deposits (Mt. Etna, Sicily, Italy) using two different alkaline solutions

Finocchiaro C.*¹, Barone G.¹, Mazzoleni P.¹, Leonelli C.² & Rossignol S.³

¹ Dipartimento di Scienze Biologiche, Geologiche e Ambientali, Università di Catania.

² Dipartimento di Ingegneria “Enzo Ferrari”, Università di Modena e Reggio Emilia.

³ IRCER (Institut de Recherche sur les Céramiques) University of Limoges.

Corresponding email: claudio.finocchiaro@unict.it

Keywords: innovative materials, alkaline activation, restoration.

The huge quantity of volcanic ash and paleo-soils deposits, locally named “ghiara”, of Mt. Etna volcano encouraged us to test them for alkali activated materials (AAM) production. Ghiara paleo-soils is characterized by an intense reddish hue due to oxidation transformations occurred during Etna’s lava flow. It was widely used in XVII-XVIII centuries, as aggregate for mortar and plaster production due to its high hydraulic modulus (Battiato, 1998; Belfiore et al., 2010). However, the use of traditional recipes based on OPC and lime binders caused degradation forms and durability problems in historical Baroque buildings of the city (belonging to UNESCO heritage list).

This research, supported by the AGM for CuHe project (PNR fund), aims to use these volcanic raw materials as aluminosilicate precursors for AAMs production to be applied in Cultural Heritage of Catania architecture. In this way, ghiara paleo-soils can be used in an innovative way, able to overcome durability problems of old mortars and, on the other hand, volcanic ash can become an important resource, so to solve the emergency during explosive eruptions.

In this work, FT-IR analysis with KBr method were carried out on raw materials both room temperature and after thermal treatments (200°C, 300°C and 400°C) to determine their reactivity in order to understand the polycondensation reaction in presence of alkaline solutions. Several formulations were prepared based on sodium or potassium silicate solutions with the addition of metakaolin. The reactive mixture was analysed by in situ following FT-IR measurements to evidence the aluminosilicate network reticulation (Gharzouni et al., 2015). Compressive test at 7 and 21 days were performed on each family to determine the mechanical strength, obtaining good results, especially for those ones with 20% of metakaolin and potassium alkaline solution.

Finally, the proposed methodological approach was useful to determine and validate the feasibility of formulations considered and to compare the reaction behaviour, and so the polycondensation rates of the two different alkali solutions used.

Battiato G. (1988) - Le Malte Del Centro Storico Di Catania. Documenti Dell’Istituto Dipartimentale Di Architettura e Urbanistica Dell’Università Di Catania, 16, 85–107.

Belfiore M.C., La Russa F.M., Mazzoleni P., Pezzino A. & Viccaro M. (2010) - Technological study of “ghiara” mortars from the historical city centre of Catania (Eastern Sicily, Italy) and petro-chemical characterisation of raw materials. *Environ Earth Sci.*, 61, 995-1003.

Gharzouni A., Joussein E., Samet B., Baklouti S. & Rossignol S. (2015) - Effect of the reactivity of alkaline solution and metakaolin on geopolymer formation. *Journal of Non-Crystalline Solids*, 410, 127-134.

Red brick waste as geopolymeric precursor for a sustainable restoration of ancient masonry

Fugazzotto M.*¹⁻², Coccato A.¹, Finocchiaro C.¹, Occhipinti R.¹, Strocio A.¹, Mazzoleni P.¹ & Barone G.¹

¹ Dipartimento di Scienze Biologiche, Geologiche e Ambientali, Università di Catania.

² Dipartimento di Scienze Umanistiche, Università di Catania.

Corresponding email: maura.fugazzotto@gmail.com

Keywords: geopolymers, brick waste, sustainable restoration.

The conservation of archaeological sites, exposed to the current adverse environmental conditions, is nowadays a challenge for the Cultural Heritage policy. The research on new solutions for the ceramic restoration is also encouraged by the limits of compatibility, effectiveness and durability of the traditional lime or organic resin and by their energy-consuming.

In the optic of a sustainable conservation practices a novel class of materials named Alkaline Activated Materials (AAMs) emerges. AAMs, including those called geopolymers, have chemical and mineralogical similitude to the ceramic materials and their tailored designed structural and chemical characteristics make them a good candidate for ceramic restoration (Reig et al., 2013; Ricciotti et al., 2017).

This research, supported by the AGM for CuHe project (PNR fund), aims to investigate the feasibility of reusing red clay brick waste as precursors in the alkali activation process, in order to produce innovative restoration materials for brick masonries.

Bricks were grinded lower than 10 micron size and activated with NaOH and Na₂SiO₃ solution in different proportions. Liquid/solid ratio has been varied in order to modify the workability of the final products. Geopolymer pastes have been cured either at room temperature or in oven at 65°C for 24 hours. After curing time samples were stored in a chamber with RH 99% for 7 and 28 days.

Formulation and chemical parameters have been varied, involving in some case the addition of metakaolin, in order to develop three types of final products: a mortar for repointings, a paste for new blocks useful in replacements and a blend for consolidations.

To evaluate the effectiveness of the red brick-based geopolymers for restoration purpose, the products were tested on archaeological remains and their performance was evaluated. Morphological and chemical analysis has been carried out by means of SEM-EDS, in order to observe the adhesion at the interface between the substrate and the geopolymer. In order to assess their compatibility and efficacy, mechanical tests and porosity analysis were performed on geopolymer samples. The results reveal that geopolymer pastes made with recycled brick waste are an interesting alternative to the most commonly used materials in the field of brick masonry restoration, both in structural and not structural interventions. Moreover it is worthy to note that the possibility to use raw materials with similar chromatic appearance with the substrate to restore allows to reach a very good aesthetic compatibility, essential requisite in the restoration field.

Reig L., Tashima M.M., Borrachero M.V, Monzò J., Cheeseman C.R. & Paya J. (2013) - Properties and microstructure of alkali-activated red clay brick waste. *Constr Build Mater.*, 43, 98-106.

Ricciotti L., Molino A.J., Roviello V., Chianese E., Cennamo P. & Roviello G. (2017) - Geopolymer composites for potenzial applications in Cultural Heritage. *Environments*, 4, 91.

Municipal solid waste incineration (MSWI) ashes: potential impacts and metal resources assessed by environmental magnetic methods

Funari V.*¹, Mantovani L.², Vigliotti L.³, Dinelli E.¹ & Tribaudino M.²

¹ Dipartimento di Scienze Biologiche Geologiche e Ambientali (BiGeA), Università di Bologna, Bologna, Italy.

² Dipartimento di Fisica e Scienze della Terra, Università degli Studi di Parma, Parma, Italy.

³ Istituto di Scienze Marine, Consiglio Nazionale delle Ricerche, Bologna, Italy.

Corresponding email: valerio.funari@unibo.it

Keywords: Municipal Solid Waste Incineration (MSWI), rock magnetic methods, anthropogenic pollution.

Environmental magnetic studies are widely used to trace sources of anthropogenic pollution and have revealed promises for application to the urban waste management system. Here a collection of solid samples from Municipal Solid Waste Incinerators (MSWI) were studied to probe the capability of geochemical and magnetic data integration as a tool for assessing mineralogy, grain-size, and metal enrichment. A data set of room-temperature magnetic parameters was compiled to confront chemical data by X-ray fluorescence and electron microscopy observations. The aim was to validate or reject methods for urban mining purposes, exploiting the powerful correlations that magnetic properties typically experience with iron, heavy metals, and even magnetic grain-sizes (from mm-scale down below 30 nm). The assessment of domain states, i.e., grain-sizes, in MSWI ashes with the room-temperature magnetic data is complicated by the clumping of tiny and large grains displaying similar magnetic properties, so it needs to be supported by optical methods or more advanced magnetic techniques. On the other hand, the integration between magnetic and geochemical data, constrained by the measures of magnetic/diamagnetic extracts, helped in assessing magnetic mineral assemblages and potential metal enrichments.

Assessment of post treatment acceptance for Asbestos-Containing Waste by differential thermal analysis and thermo-gravimetry (DTA-TG)

Gaggero L.*¹, Ferretti M.² & Locardi F.²

¹ Department of Earth, Environment and Life Sciences, University of Genova.

² Department of Chemistry and Industrial Chemistry, University of Genova.

Corresponding email: gaggero@dipteris.unige.it

Keywords: combustion synthesis, ACW neutralisation, acceptance criteria, re-use.

The Italian normative requirements to assess the end of waste status for the combusted products are severe and claim the absence of fibres, in spite of preliminary and post-treatment investigation by SEM-EDS and XRPD analysis of the waste mixtures, to account for the physical and chemical breakdown of the fibrous minerals. In particular, a thermal treatment for asbestos neutralisation, based on the combustion synthesis (Self-propagating High Temperature Synthesis or SHS) was developed from laboratory scale towards industrial scale up. The method efficiently addressed the passivation of natural asbestos fibres and asbestos-bearing artificial materials. The plant acts in a continuous-feeding configuration with an optimal waste: reagents ratio between 60 and 70.

On the whole, the SHS process in comparison with conventional thermal treatments, due to fast reaction time and low activation energy, particularly advantages the asbestos neutralisation, positively reflecting into time and costs of the process. The validation of treated products opens perspective of their re-use, e.g. as abrasive, or refractory material, yielding a second life as secondary raw material. Following the basic characterisation of post-treatment slags with XR PD and SEM-EDS, according to the current normative, combined DTA/TG analysis were therefore applied to the mixtures along all steps of the treatment, in order to demonstrate that post-treatment products comply the normative requirements. No protocol exists, but MD 248/2004 indicates to use the same analytical techniques for asbestos identification in ACW. The main methods have been optical microscopy, XR diffractometry and scanning electron microscopy. In order to demonstrate that the combusted material after SHS treatment can meet the requirements of the European and Italian normative (Commission Regulation No. 1357/2014, 2014; Directive 2008/98/EC, 2008; Directive 91/689/EEC; Directive 75/442/EEC; Italian Environmental Ministry Directive, 2002; Italian Legislative Decree No. 152/2006, 2006) already at pre-industrial scale, thermal analyses on treated waste, after SHS, by TG (thermogravimetry) and DTA (differential thermal analysis) were addressed. The analyses of treated samples were compared with those of untreated starting material.

Petrography of Construction and Demolition Wastes from Abruzzo Region (Italy)

Galderisi A.*¹⁻²⁻³, Iezzi G.¹⁻⁴, Bianchini G.⁵, de Brito J.⁶, Paris E.³, Piatteli V.¹, Casarin A.¹, Cinosi J.¹, Macrini D.¹, Schettino D.¹, Santone S.¹, Rossi M.¹ & Buccieri F.¹

¹ University of Chieti-Pescara “G. d’Annunzio”.

² Istituto di Geologia Ambientale e Geoingegneria, CNR, Rome.

³ University of Camerino.

⁴ INGV of Roma.

⁵ University of Ferrara. ⁶ Instituto Superior Técnico, Lisboa, Portugal.

Corresponding email: a.galderisi92@gmail.com

Keywords: Construction and demolition wastes, analytical petrographic methods, CDWmanagement.

Construction and demolition wastes (CDW) are among the most abundant by weight in EU, which consequently imposed a reuse ratio of at least 70 by weight. These non-hazardous wastes are mainly reused in downcycling applications for road and construction substrates or are disposed of in landfills. This only partly limits the quarrying of further natural raw materials. Instead, an upcycling reusing of CDWs in new constructions would help circular economy, reducing new quarries of virgin rocks and decreasing landfills.

In this research, 18 CDWs sampled in the Abruzzo region were analysed, representative of possible petrographic variation of raw (stones and aggregates) or industrial-treated (tiles, bricks, ceramics, etc.) materials used by the local population in the last decades. Indeed, construction materials are strongly related to petrography of available rocks in an area and their mechanical features. In turn, CDWs can be different in different geological situations.

The samples were first subdivided according to their mesoscopic appearances such as: concrete, ceramics (brick, tile, roof tile, perforated brick), and ornamental stone. Each sample has been also described as a function of mesoscopic textural features, colour, density and qualitative toughness. These features are relevant for possible separation of CDW.

The samples have been then finely grinded, mounted in zero-background Si sample holder and analysed with Bragg-Brentano D5005 Siemens diffractometer. The obtained XRPD (X-ray powder diffraction) patterns allowed determining the crystalline phases and detect the presence of non-crystalline phases. The four concrete samples have density ranging from 1.9 to 2.4 g/cm³ and are made invariably of quartz, calcite and minerals of the melilite group; they appear free of non-crystalline phases. The two natural stones are made entirely of calcite and have both densities of 2.6/2.7 g/cm³. The three bricks have densities from 1.9 to 2.4 g/cm³ and are composed of quartz, cristobalite, mullite, feldspars, pyroxenes and glass. The three perforated bricks have densities varying between 1.8 and 2 g/cm³ and phase assemblages of quartz, calcite, feldspars, pyroxenes and minerals of the melilite group. The three tiles and three roof tiles have density ranges of 1.8/2.3 and 1.7/2.2 g/cm³, respectively; they are invariably made of quartz, plus cristobalite, calcite, feldspars and glasses.

To complement the XRPD data, a representative sub-set of samples were analysed by XRF, and several polished surfaces of CDW slabs have been prepared to show their mesoscopic textural features. All these data allow characterising in detail the petrography of CDW from Abruzzo. These results are a valuable tool for their reuse in several applications.

Gorno mining district (Southern Alps): new preliminary data about ore mineral precipitation and multiphase diagenetic evolution

Giorno M.*¹, Barale L.², Bertok C.¹, D'Atri A.¹, Martire L.¹, Piana F.² & Rossetti P.¹

¹ Dipartimento di Scienze della Terra, Università di Torino.

² IGG - CNR Torino.

Corresponding email: micheleandrea.giorno@unito.it

Keywords: Gorno, MVT, sphalerite.

The lower Carnian succession of the central Southern Alps in the Riso and Parina valleys (Orobic Alps, northern Italy) is represented by the 50-100 metres-thick Breno Formation, made up of light-coloured, thick-bedded peritidal limestones, overlain by a few metres to some tens of metres of dark medium-bedded peritidal limestones of the Calcare Metallifero Bergamasco Formation. Above the latter a sharp lithological change occurs, represented by the Gorno Formation, made up of interbedded limestones and dark shales, and the Val Sabbia Sandstone, composed of lithic sandstones. The Calcare Metallifero Bergamasco Formation and the upper portion of the Breno Formation were affected by a multiphase diagenetic evolution, resulting in the occurrence of different diagenetic products and sulphide ore mineralizations (\pm fluorite and barite), which in the past were intensely exploited in the world-wide known Gorno mining district.

The first results of this study evidenced that:

- Sulphide mineralizations were preceded by dolomitization, growth of authigenic quartz crystals and dissolution phenomena. Locally the silicification completely replaces the original limestone, and is associated to thick breccia bodies. Dolomite occurs both as vein-filling cement and as replacive dolomite within limestones; its saddle habit and the local association with micritic sediments within geopetal structures document a hydrothermal origin in a shallow burial setting. Dissolution resulted in metre-sized irregular cavities locally filled with laminated sediments, composed of detrital dolomite clasts and quartz crystals (representing the insoluble residue of the early dolomitized and silicified limestones), and microsparitic calcite (possibly due to the recrystallization of micritic sediments).
- Mineralizations form irregular orebodies metres to 10's of metres large, concordant with, or discordant to the bedding; e.g., they can fill dissolution cavities, in most cases parallel to the bedding, or they can occur as cement of breccia bodies. The main orebodies are commonly spatially related to mud-rich beds mostly close to the stratigraphic boundary between the Calcare Metallifero Bergamasco and the Gorno Formations.
- Fluorite, the main ore mineral in the western part of the district, is spatially related to sulphide mineralization. Textural and petrographic features clearly prove that fluorite precipitation postdated the main sulphide deposition.

The genesis of the Gorno district was probably linked to a hydrothermal system, in which metal-rich hot fluids flowed upwards possibly through faults and fracture systems. This circulation caused major modifications in the host rocks, such as multi-phase dolomitization and silicification, dissolution and brecciation, associated with the precipitation of abundant ore minerals. Sulphides precipitation could have been triggered by a mixing of hydrothermal metal-rich brines with shallower reducing fluids.

Methanol intrusion in MFI- Zeolites at High Pressure

Lotti P.*¹, Comboni D.^{1,2}, Gatta G.D.¹, Pagliaro F.¹, Catizzone E.³, Migliori M.³, Giordano G.³, Milani S.¹, Merlini M.¹, Collings I.E.⁴ & Hanfland M.⁴

¹ Dipartimento di Scienze della Terra - Università degli Studi di Milano.

² Dipartimento di Scienze della Terra e dell'Ambiente - Università degli Studi di Pavia.

³ Dipartimento di Ingegneria per l'Ambiente e il Territorio e Ingegneria Chimica - Università della Calabria.

⁴ European Synchrotron Radiation Facility - Grenoble.

Corresponding email: paolo.lotti@unimi.it

Keywords: MFI zeolites, methanol adsorption, pressure.

MFI-zeolites are currently used as catalysts in some olefins-production processes, representing an appealing alternative to the high-energy demanding Steam Cracking process, which accounts for 95% of the total worldwide olefins production (Sadrameli, 2016; Arvidsson et al., 2016). More recently, MFI-zeolites have been used in the promising methanol-to-olefins (MTO) synthesis process, which, being able to obtain olefins directly from methanol in place of oil, bears a potential breakthrough industrial impact. At ambient conditions, only the surfaces of the zeolite crystallites are believed to be active in the methanol-to olefins process. However, pressure may favour the intrusion and diffusion of methanol molecules through the zeolitic channels, as observed in other zeolites (Gatta et al., 2018). This phenomenon may bear a significant impact in the industrial applications of MFI zeolites as catalysts, as a “cold” intrusion of methanol into the zeolite cavities might pave the way to increase the efficiency of the MTO conversion process. In this regard, we have synthesized and investigated, by in situ synchrotron powder-XRD, the high-pressure behaviour of six MFI-zeolites with different chemical compositions (framework-Si partially replaced by Al or B and counterbalanced by Na or H as extra-framework cations), by using methanol and silicone oil (as a reference) as P-transmitting fluids, respectively. All the synthesized zeolites are monoclinic (space group P21/n11) at ambient pressure, although a monoclinic-to-orthorhombic phase transition (MOPT) is observed to occur at $\sim P > 0.5$ GPa. Based on the experimental X-ray diffraction patterns and on the high-P evolution of the unit-cell parameters, we ascertain that: i) all the MFI zeolites compressed in silicone oil (acting as non-penetrating fluid) have, overall, the same bulk compressibility, ii) pressure induces the intrusion of methanol through the structural voids and, among the different zeolites, the magnitude of the adsorption phenomenon is different, iii) the MOPT is influenced by both the crystal chemistry and the sorbate (methanol) loading. The experimental findings of this study represent the first step to select the optimal chemical composition of a potential MFI-catalyst for the MTO conversion process operating at high-pressure conditions.

Arvidsson M., Haro P., Morandin M. & Harvey S. (2016) - Comparative Thermodynamic Analysis of Biomass Gasification-Based Light Olefin Production Using Methanol or DME as the Platform Chemical. *Chem. Eng. Res. Des.*, 115, 182–194.

Gatta G.D., Lotti P. & Tabacchi G. (2018) - The Effect of Pressure on Open-Framework Silicates: Elastic Behaviour and Crystal–fluid Interaction. *Phys. Chem. Miner.*, 45, 115–138.

Sadrameli S.M. (2016) - Thermal/Catalytic Cracking of Liquid Hydrocarbons for the Production of Olefins: A State-of-the-Art Review II: Catalytic Cracking Review. *Fuel*, 173, 285–297.

Development of a nanocomposite membrane based on reduced graphene (r-GO) and zeolite 13X for the removal of metal ions with bactericidal actions

Mancinelli M.*¹, Pompilio A.², de Castro E.I.³, Pasti L.⁴, Rosatelli G.⁵, Di Bonaventura G.², Pedrotti J.J. & Martucci A.¹

¹ Department of Physics and Earth Sciences, University of Ferrara, Italy.

² Department of Medical, Oral and Biotechnological Sciences, “GEOMED”, Center of Excellence on Aging and Translational Medicine, “G. d’Annunzio” University of Chieti-Pescara, Italy.

³ MackGraphe - Graphene and Nanomaterials Research Center, Mackenzie Presbyterian University, São Paulo, SP, Brazil.

⁴ Department of Chemistry and Pharmaceutical Sciences, University of Ferrara, Italy.

⁵ Department of Psychology, Health and Territory Sciences, “GEOMED”, Center of Excellence on Aging and Translational Medicine, “G. d’Annunzio” University of Chieti-Pescara, Italy.

Corresponding email: maura.manci@hotmail.it

Keywords: reduced graphene oxide, zeolite, membrane.

In the last decades, adsorption by membranes is considered an economical wastewater treatment method to raise the emerging problem of a clean water shortage (i.e. sea and produced water, industrial waste water etc). Graphene-based composites (GO and r-GOs) are a new emerging class of materials promising applications in water disinfection and the fouling/biofouling membranes. In this work, we manufactured nanocomposite membrane combining reduced graphene oxide (r-GO) and zeolite advantages. Zeolite 13X (UOP) was chosen (Si/Al=1) for its affinity towards metal ions, highly hydrophilic character, high thermal stability. Graphene oxide and the nanocomposite membrane were synthesized from natural graphite (Aldrich) in the MackGraphe Research Center laboratories according with modified Hummers method. All materials were characterized by SEM, AFM, FT-IR, XRD, TG/DTA and WCA.

The proposed synthesis method involved the deposition on a nylon substrate by vacuum filtration starting from a GO and zeolite 13X homogeneous mixture (2:1 ratio) dispersed in aqueous solution. r-GO was obtained by reducing dispersed GO in the resultant homogeneous GO solution using hydrazine, to compact the structure and force the water flow into functionalized pores as well as increase the adsorption/rejection capacity.

Batch tests for r-GO/ZEO13X membrane adsorption highlighted a strong selectivity towards Na⁺, K⁺, Ca²⁺ and Mg²⁺ thus attesting that functional groups exhibited strong metal–ligand interaction ion in aqueous solutions. Finally, the bactericidal properties of the membrane against Gram-positive (*S. aureus* Sa2 and *E. faecalis* ATCC 29212) and Gram-negative (*Escherichia coli* APN1, *Pseudomonas aeruginosa* PaPh32 and AC12a) species suggested that GO/ZEO13X membranes are a promising approach for the development of novel antimicrobial membranes in water purification technologies.

Bottom ash from Parma WtE plant: mineralogical and chemical characterization

Mantovani L.*¹, Funari V.², Tribaudino M.¹, Mazzari C.³ & Sabatino S.³

¹Dipartimento di Scienze Chimiche, della Vita e della Sostenibilità Ambientale, Università di Parma.

²Dipartimento di Scienze Biologiche Geologiche e Ambientali (BiGeA), Università di Bologna, Bologna, Italy.

³Iren Ambiente S.p.A.

Corresponding email: luciana.mantovani@unipr.it

Keywords: MSWI plant, bottom ash, mineralogical characterization.

A considerable progress in the field of the circular economy can be represented by knowledge of the exact composition of the raw materials, what are they made of, if there are potential risks for environment and human health and their behaviour in case of re-use.

Bottom ash (BA) are the main product of the municipal solid waste incinerator and currently are classified by the European Waste Catalogue (EWC) as industrial non-hazardous waste. However, a focal point debated after the European Council Regulation 2017/997 talks about the heavy metals (both glass and minerals) bearing phases, their identification and characterization as well as their weathering behaviour. BA and leaching processes and metallic trace elements content have been investigated by many authors (Piantone et al., 2004) but without examining thoroughly the mineralogical phases. In particular, there is little information about phase composition. This is most true for the amorphous content that is rarely quantified or analysed with regard to chemical composition (Wei et al., 2011). Moreover, literature data of early 2000s plants are at present obsolete and are not comparable with those after 2010 (Bayuseno et al., 2011).

In this work BA sampled from Parma WtE plant were chemically and mineralogically characterized by means of XRF, ICP-MS, XRD, optical microscopy and SEM-EDS.

The particle size distribution of dry BA was determined and compared to other incinerators with similar technology and conditions showing a very similar pattern for all WtE plants considered, with the Fuller curve for concrete. The cumulative particle size distribution shows that the most part of BA (about 60%) lies in the range of 1-8 mm while a 20% of the total weight have a grain size <1 mm and another 20% are >10 mm.

Bulk chemical composition shows a selective enrichment depending on the grain size: the finest grain size has a higher CaO content, due to the presence of carbonates, as shown by in XRD, while SiO₂ is mainly present in the larger grain size with amorphous and glasses phases. Analysis of trace elements shows a higher concentration of S, Cl, and some heavy metals such as Zn, Pb, Cr, Sr in small grain sizes supposing their presence inside the carbonates structure. SEM-EDS maps showed the strong heterogeneity of the samples, composed mainly of a Si-Ca-Al-O vitreous matrix in which some crystalline fractions, metal and alloy are embedded.

Piantone P., Bodéan F. & Chatelet-Snidaro L. (2004) - Mineralogical study of secondary mineral phases from weathered MSWI bottom ash: implications for the modelling and trapping of heavy metals. *Appl. Geochem.*, 19, 1891-1904.

Bayuseno P. & Wolfgang W. (2011) - Characterization of MSWI fly ash through mineralogy and water extraction. *Resour. Conser. Recy.*, 55(5), 524-534.

Wei Y., Shimaoka T., Saffarzadeh A., & Takahashi F. (2011) - Mineralogical characterization of municipal solid waste incineration bottom ash with an emphasis on heavy metal-bearing phases. *J. Hazard Mater.*, 187, 534-543.

Traceability of Ruby: challenges and opportunities by a combined LA-ICP-MS, UV-VIS and XR diffraction

Martucci A.¹, Bonadiman C.¹, Zappaterra O.¹, Renna M.², Castelli S.² & Rodeghero E.*¹

¹ Department of Physics and Earth Sciences, University of Ferrara, I-44123 Ferrara, Italy.

² Custodia Valore Credito (Gemological Laboratory), Palermo, Italy.

Corresponding email: rdglse@unife.it

Keywords: Corundum, LA-ICP-MS, XRPD.

It's well known that the source, or provenance, of gems is one of the factors that contribute to their monetary value, in addition to cut, clarity, color, and carat weight. As a consequence, the provenance of gemstones is a topic of interest to geologists, historians, gemologists, and others in the gem industry for financial, security, and societal reasons. In this study provenance of unknown ruby samples has been determined using a combination of inclusion analysis, trace element geochemistry, structural characteristics, and internal growth features. Firstly, the sample was characterized by traditional methods of observations of optical and mineralogical features i.e. index of refraction; UV-visible; fluid and mineral inclusions; and the presence or absence of crystallographic features unique to a specific deposit. Laser ablation-inductively coupled plasma mass spectrometry (LA-ICPMS) allowed us to determine the chemical composition of the gem, especially the concentration of trace elements. The relative high Cr / Ga ratio has suggested that samples belong to metamorphic suites while the Cr / V vs Fe / V ratio led to African deposits (Sutherland et al., 1998a; Limtrakun et al., 2001). X-ray diffraction patterns pointed out the presence of secondary phases (shortite, rutile, boehmite and chalcopyrite) whereas structural refinement highlighted variations in the unit cell parameters, bond distances and coordination polyhedral volume compared to pure corundum (Lutterotti et al., 1990). In particular, the geometry of octahedra and the distortion index value are related to the presence of Cr, Fe, Ga, Ti, as isomorphic aluminum substituents. All these chemical composition fingerprints give information on the environment in which the mineral crystallized. In conclusion, the combination of multiple trace-element data points of the stone with diffractometric measurements, opens up research directions in finding unique fingerprints for unique stones.

Limtrakun P., Zaw K., Ryan C.G. & Mernagh T.P. (2001) - Formation of the Denchai gem sapphires, northern Thailand: evidence from mineral chemistry and fluid/melt inclusion characteristics. *Min. Mag.*, 65, 725–735.

Lutterotti L. & Scardi P. (1990) - Simultaneous structure and size-strain refinement by the Rietveld method. *J. Appl. Crystallogr.*, 23, 246-252.

Sutherland F., Schwarz D., Jobbings E.A., Coenraads R.R. & Webb G. (1998a) - Distinctive gem corundum suites from discrete basalt fields: a comparative study of Barrington, Australia, and WestPailin, Cambodia, gemfields. *J. Gemm.*, 26-2, 65–85.

Conditions for hydrothermal cobalt and nickel mineralization – suggestions from some little known, historical ore deposits in Italy

Moroni M.*¹, Naitza S.², Rossetti P.³, Ruggieri G.⁴, Magnani L.¹, Aquino A.⁵, Tartarotti P.¹, Ferrari E.¹, Oggiano G.⁶ & Secchi F.⁶

¹ Dipartimento di Scienze della Terra, Università degli Studi di Milano.

² Dipartimento di Scienze Chimiche e Geologiche, Università degli Studi di Cagliari.

³ Dipartimento di Scienze della Terra, Università degli Studi di Torino.

⁴ IGG-CNR, UOS Firenze.

⁵ Dipartimento di Scienze della Terra, Università di Firenze.

⁶ Dipartimento di Chimica e Farmacia, università di Sassari.

Corresponding email: marilena.moroni@unimi.it

Keywords: Co-Ni arsenides, five element-type deposits, brines.

We present ongoing research about three poorly known, historical Ni-Co-bearing hydrothermal deposits in different geological contexts: the Ni-Co-As-Sb-Au-bearing Arburese vein system (SW Sardinia), the Co-As-rich Usseglio vein system (Piedmont) and the small Cu-Ag-Co-Ni-Pb-Te-Se stockwork ore at Piazza (eastern Liguria). These deposits share some similarities to the Five Element Vein-type, Co-Ni-Ag-Bi-As ores but only the first two display km-sized development and were economic for Co and Ni. The Arburese Ni-rich veins occur in Paleozoic basement near two Variscan plutons. The Co-rich Usseglio and Piazza deposits share ophiolitic contexts: the Usseglio veins crosscut metabasalts near the Lanzo peridotite massif, while the Piazza stockwork crosscuts low-grade metamorphic gabbro of the Bracco ophiolite massif. The Arburese and Usseglio deposits share a complex mineral assemblage with early Bi-bearing Ni-Co arsenides-sulfarsenides followed by Ag-base metal sulfides, in siderite-quartz-baryte gangue. The Piazza deposit stands apart with its early Ag-Pb-Bi telluride-selenide stage with Co-Ni sulfides plus bornite replaced by chalcopyrite, in prehnite-albite-chlorite gangue. Piazza shares its Se-rich character with the Arburese veins, which host Se in base metal sulfides. Preliminary geothermometric estimates are provided by fluid inclusion analyses (Usseglio and Arburese) and chlorite composition (Piazza). Co-Ni arsenide precipitation occurred at $\approx 200^\circ\text{C}$ (0.5 kbar) after a vigorous boiling episode depositing baryte, while later base metal sulfide deposition occurred at $80\div 140^\circ\text{C}$. Ore fluids are NaCl-CaCl₂-bearing brines (18÷25 equiv. mass% NaCl). Ore carbonates display stable isotope signatures compatible with such low temperature brines, typical for five element vein-type deposits. Vein-related chlorites at Piazza provide higher temperatures for ore deposition in the range of $200\div 280^\circ\text{C}$ (avg 230°C), and the carbonate-free prehnite-feldspar assemblage is compatible with CO₂-degassed, alkali chloride waters. No data are available on hydrocarbons in the ore fluids, although observed enrichments in Se and negative $\delta^{13}\text{C}$ in carbonates suggest interaction with carbonaceous shales. In their own regional metallogenic contexts the three deposits stand out and open questions about source rocks and controls on Co/Ni: e.g., within the highly mineralized, Ni-free southern Sardinian crust the Arburese Ni-Co-As vein system is unique, as is the Usseglio Co-As vein system within the western Alps rich in ophiolites and post-peak hydrothermal deposits. The northern Apenninic ophiolites, hosting the unique Cu-Ag-Co-Ni-Pb-Te-Se Piazza deposit, may actually have the greatest potential for hydrothermal Co-Ni mineralization as their many oceanic exhalative Cu-Fe deposits are highly anomalous in Co. Piazza ore fluids recycled metals of various provenance, like Co and Ag, but no economic ore was formed. Could the missing arsenic and carbonate components be part of the problem?

Hydromagmatic PGE telluride-rich Ni-Fe-Cu sulfide mineralization related to melt-rock reaction processes in presence of carbonated hydrous fluids: examples from sulfide-rich ultramafic intrusions of the Ivrea-Verbano Zone

Moroni M.*¹, Sessa G.¹, Tumiati S.¹, Ferrari E.¹ & Langone A.²

¹ Dipartimento di Scienze della Terra A. Desio, Università degli Studi di Milano.

² IGG-CNR, Pavia.

Corresponding email: marilena.moroni@unimi.it

Keywords: Ni-Cu-PGE ore, magmatic fluids, carbonates.

The Ivrea-Verbano Complex hosts several ultramafic intrusions which are enriched in volatiles including carbon, like the sulfide-rich Valmaggia pipe and the Campello Monti intrusion. The Valmaggia pipe displays widespread intergrowths between peculiar, coarse nodular Ni-Cu-PGE sulfide mineralization, carbonates and the magmatic silicate-oxide assemblage. The latter bears evidence of melt-rock reaction process between a peridotitic protolith and a volatile-rich, percolating adakite melt (Sessa et al., 2017). The pipe displays progressive reaction fronts where augite, olivine, enstatite and Cr spinel were replaced by pargasite amphibole oikocrysts, enstatite II, phlogopite and Al spinel by reacting with plagioclase-rich hydrous metasomatizing melt at 5–8 kbar and 700–900°C. Both PGE-bearing sulfide mineralization and carbonates are strictly related to the metasomatic assemblage. Dolomite blebs are interstitial to silicates, but most carbonates occur as intergrowths with the sulfide nodules and their peculiar aureoles of sulfide-silicate symplectites. Carbonates often make up bubble-like meniscus aggregates along embayments of the sulfide nodules and vary in composition (Fe-calcite, dolomite, siderite) according to the nearby phase (silicates, sulfide). Ni-Fe-Cu sulfide nodules are often concentrically zoned, with FeS cores and Fe-Ni-Cu sulfide-rich rims. Pt-Pd tellurides only occurs along the nodule rims as well as in the Fe-Ni sulfide blebs of the nearby sulfide-silicate symplectite haloes, especially where sulfides are intimately intergrown with carbonates and hydrous silicates. Textural relationships suggest metal-rich sulfide (\pm telluride) melt segregation ensuing from sulfur saturation during melt-rock reaction and coexisting with immiscible C-bearing vapour. In this context Pt- and Pd telluride deposition appears to be favoured as a late crystallization product of the fluid-drenched sulfide melt blobs in hydromagmatic conditions. The Valmaggia carbonates do not show carbonatite-like trace element composition, but they display C and O isotope mantle-like signatures, as is the case for the carbonates from the pyrossenitic intrusion of, considered for comparison. The Campello Monti intrusion is highly mineralized in Fe-Ni sulfides, but it is low in hydrous silicates. Like at Valmaggia, carbonates are intergrown with sulfides and silicates (including amphibole) and also enclosed in olivine, although the abundant Fe-Ni sulfides are PGE-poor. This further supports the coupling of carbon and hydrous magmatic fluids (Boudreau, 2019) as a key factor for PGE mineralization.

Sessa G., Moroni M., Tumiati S., Caruso S., Fiorentini M. (2017) - Ni-Fe-Cu-PGE ore deposition driven by metasomatic fluids and melt-rock reactions into the deep crust: the ultramafic pipe of Valmaggia, Ivrea-Verbano, Italy. *Ore Geology Review*, 90, 485-509.

Boudreau A. (2019) - *Hydromagmatic processes and Platinum-Group Element deposits in layered intrusions*. Cambridge University Press.

Metallogenesis in Sardinia: the Critical Raw Materials (CRM) perspective

Naitza S.*¹, De Giudici G.B.¹, Funedda A.¹, Loi A.¹, Meloni M.A.¹, Moroni M.², Oggiano G.³ & Secchi F.³

¹ Dipartimento di Scienze Chimiche e Geologiche, Università degli Studi di Cagliari.

² Dipartimento di Scienze della Terra A. Desio, Università degli Studi di Milano.

³ Dipartimento di Chimica e Farmacia, Università degli Studi di Sassari.

Corresponding email: snaitza@unica.it

Keywords: Critical Raw Materials, Variscan metallogenic peak, Sardinia.

Critical Raw Materials (CRM) future supply is a matter of major concern for the EU, so that in several European old and mature districts new studies have begun to evaluate their potential in terms of CRM resources. Sardinia represents one of these areas: despite the technical exhaustion of its main districts the island still retains a metallogenic potential, not only as secondary resources (old mine wastes), but also as primary, still unexploited ores. A further increase in the list of the potentially economic orebodies comes from recent studies that have substantially improved the past knowledges of the Sardinian metallogenesis suggesting new exploration themes, particularly in the CRM's field. Sardinian mineral deposits include a large variety of types, resulting from a multi-stage metallogenesis that mirrors the complex geological history of the island. Since 1960's, ore geology studies recognized in Sardinia different metallogenic periods, from early Paleozoic to Quaternary. Periods of relative metallogenic stasis alternated with metallogenic peaks characterized by massive mobilization, migration and concentration of elements in the Sardinian crust. The main metallogenic peaks are related with: 1) large MVT deposits in Iglesias district (Cambrian: Pre-sardic phase peak); 2) a huge variety of late Variscan hydrothermal deposits hosted in the metamorphic basement or in granitoids (Carboniferous-Permian: Variscan peak); 3) porphyry to epithermal deposits related to the Cenozoic calcalkaline volcanism (Oligocene-Miocene: Cenozoic peak). From CRM's perspective, the hydrothermal deposits and occurrences related to the Variscan peak emerge now as the most promising in different districts. In detail, major themes of recent investigations include: a) the "five elements-type" veins of Southern Arburès district (SW Sardinia), hosting Ni-Co-Bi-Ag and REE minerals; b) the Mo-W-Sn (Re, In, Ga, Ge, REE) vein, greisen and skarn deposits related to ilmenite-series, F-bearing ferroan granites of southern Sardinia (Linas, Sulcis, Sarrabus); c) the structurally-controlled Au-W-Sb veins of eastern and northwestern Sardinia (Gerrei, Nurra), related to early Permian extensional tectonics; d) REE minerals in granite-related fluorite-barite vein deposits (southern Sardinia) and in shear zone-related skarns (central Sardinia). Interestingly, these latter may be a striking example of metallogenic inheritance, as a major source for REE in Sardinian crust has been identified in late Ordovician sedimentary sequences that host extended heavy mineral (zircon, rutile, monazite) paleoplacers. New evidences from eastern Sardinia basement suggest that this first important REE metallogenic peak was highly remobilized during multiphase deformation and granite emplacement in Variscan times.

Zeolitization processes at the pyroclastic deposit “Tufo rosso a scorie nere” (Auctorum), Vico Volcano, Italy

Novembre D.*¹, Gimeno D.², Graziano S.F.³ & Cappelletti P.⁴

¹ Dipartimento di Ingegneria e Geologia, Università d'Annunzio, Chieti, Italy.

² Departament de Mineralogia, Petrologia i Geologia Aplicada, Universitat de Barcelona, Barcelona, Spain.

³ Dipartimento di Farmacia, Università degli Studi di Napoli Federico II, Napoli, Italy.

⁴ Dipartimento di Scienze della Terra, dell'Ambiente e delle Risorse, Università degli Studi di Napoli Federico II, Napoli, Italy.

Corresponding email: daniela.novembre@unich.it

Keywords: zeolites, secondary processes.

This paper focuses on the authigenic mineralizations acting in the “Tufo Rosso a Scorie Nere” (Auctorum) (hereafter TRS), i.e. one of the main pyroclastic units of the Vico Volcanic Apparatus. Vico is a stratovolcano located in northern Latium (Italy) belonging to the potassium-rich Roman Volcanic magmatic province. Vicanian volcanic products show an ultrapotassic character and extremely variable chemical rock composition, from leucite-bearing tefrites, trachybasalts, tephri-phonolites, to trachites. The “Tufo Rosso a Scorie Nere” belongs to the Ignimbrite “C” formation, i.e. the largest pyroclastic flow of the vicanian plateau and one of the most widespread pyroclastic bodies of the Lazio region, extending on a surface of about 1300 Km², also known as “Sutri Formation” of the “Lago di Vico Synthem” (Perini & Conticelli, 2002). TRS is used with profit in animal feeding (de Gennaro & Langella, 1996) and for the synthesis of zeolites for the chemical industry (Novembre et al., 2004). The cation exchange capacity of this material, due to both chabazite and phillipsite presence, ranges around 2 meq/g (Giampaolo et al., 2008).

The pyroclastic deposits appear in general massive and made of “black vitreous vesiculated juvenile scoriae”, immersed inside a lithified ashy matrix after zeolitization processes. The main minerals are chabazite and phillipsite and the zeolitic content is locally variable, reaching peaks of 68 wt %. Zeolites grow replacing the amorphous fraction and occur both inside matrix and scoriae. Concerning scoriae, zeolitization moves from the rim to the core of the scoriaceous fragment as a function of the temperature of the fluids and permeability of water inside the structure. Composition of parental fresh glass and those of zeolitized rocks is referred to trachyte, lightly undersaturated in SiO₂, and the alteration processes modified the parental rock chemical character. The zeolitic genesis is ascribed to a “geoautoclave system”, zeolites displaying a Si/Al ratio similar to that of the parental glasses.

de Gennaro M. & Langella A. (1996) - Italian zeolitized rocks of technological interest. *Mineral Deposita*, 31, 452-472.

Giampaolo C., Mengarelli L., Torracca E. & Spencer C. (2008) - Zeolite characterization of “Vico red tuff with black scoria” ignimbrite flow: The extractive district of Civita Castellana (Viterbo, Italy). *Il Nuovo Cimento*, 123 B 10-11, 1459-1476.

Novembre D., Di Sabatino B., Gimeno D., García Vallés M. & Martínez Manent S. (2004) - Synthesis of Na-X zeolites from tripolaceous deposits (Crotone, Italy) and volcanic zeolitized rocks (Vico Volcano, Italy). *Microporous and Mesoporous Materials*, 75(1-2), 1-11.

Perini G. & Conticelli S. (2002) - Crystallization conditions of leucite-bearing magmas and their implications on the magmatological evolution of ultrapotassic magmas: the Vico Volcano, Central Italy. *Mineral. and Petrol.*, 74, 253-276.

Synthesis and characterization of Li-ABW zeolite using a kaolinitic rock

Novembre D.*¹, Gimeno D.² & Del Vecchio A.¹

¹ Dipartimento di Ingegneria e Geologia, Università d'Annunzio, Chieti, Italy.

² Departamento de Mineralogía, Petrología y Geología Aplicada, Universitat de Barcelona, Barcelona, Spain.

Corresponding email: daniela.novembre@unich.it

Keywords: zeolites, synthesis.

Zeolite Li-ABW is a synthetic low silica zeolite, which possesses the ABW framework topology. Low silica zeolites such as Li-ABW, are widely involved in several technological applications, such as ion exchangers, adsorbents and catalysts, in radioactive-waste water treatments, sewage effluent treatments, agricultural-waste water treatments, as materials for ferroelectric devices (Fois et al., 2001) etc. Synthesis of Li-ABW zeolite was performed in the past by the use of lithium hydroxide, aluminum hydroxide and silica gel (Barrer & White, 1951), or using zeolite NaA and lithium chloride (Norby, 1990; Dong et al., 2007).

The present work deals with the hydrothermal synthesis of Li-ABW zeolite by using kaolinite, (Standard Porcelain by the IMERYS Minerals Ltd) as starting material. Once the thermal calcination of kaolinite is achieved (at 650°C), the synthesis process from kaolinite is rather simple as the reaction of kaolinite with alkali occurs very readily. Metakaolin was mixed with calculated amount of aluminum hydroxide and lithium hydroxide and the experiment was performed at ambient pressure and 180± 0.1°C

Li-ABW was characterised by powder X-ray diffraction, high temperature X-ray diffraction, scanning electron microscopy, inductively coupled plasma optical emission spectrometry, infrared spectroscopy, differential thermal analysis and thermogravimetry. Calculation of cell parameters (through Rietveld Refinement) and density and specific surface were also achieved. The amount of amorphous phase in the synthesis powders was estimated with quantitative phase analysis using the combined Rietveld and reference intensity ratio methods.

Crystallization of zeolite Li-ABW from kaolinite through a conventional hydrothermal treatment is here achieved with a low synthesis temperature when comparing to other similar previous works and the final products do not contain mica or quartz phases as impurities coming from the natural kaolinite sample. The results are discussed in the light of a possible industrial application of the synthesized minerals.

Barrer R.M. & White E.A.D. (1951) - The Hydrothermal Chemistry of Silicates. Part I. Synthetic Lithium Aluminosilicates. J. of Chem. Soc., 1267-1278.

Dong J., Wang X., Xu H., Zhao Q. & Li J. (2007) Hydrogen storage in several microporous zeolites. International Journal of Hydrogen Energy, 32, 4998-5004.

Fois E., Gamba A., Tabacchi G., Quartieri S., Vezzalini G. (2001) - Water Molecules in Single File: First-Principles Studies of One-Dimensional Water Chains in Zeolites. Journal of Physics and Chemistry B, 105, 3012-3016.

Norby P. (1990) - Thermal transformation of zeolite Li-A(BW). The crystal structure of γ -eucryptite, a polymorph of LiAlSiO₄. Zeolites, 10, 193-199.

The gold mineralization of Rio Cannero (Serie dei Laghi, north-western Italian Alps): first geologic and metallogenic data

Oberto M. & Rossetti P.*

Dipartimento di Scienze della Terra, Università di Torino.

Corresponding email: piergiorgio.rossetti@unito.it

Keywords: hydrothermal circulation, Au-Bi-Te-W, Hercynian magmatism.

Along the Cannero river, a small left tributary of Lago Maggiore (Italian north-western Italian), a previously unknown gold mineralization has been recently discovered by Alpine Gold Lodes S.n.c.

Such mineralization crops out in the central part of the Rio Cannero valley, on both sides of the Cannero stream, within the Serie dei Laghi unit of the Southalpine Domain. The rocks cropping out in the area are mostly paragneisses, with minor amphibolites and aplitic bodies. The gold mineralization is related to quartz-rich hydrothermal veins spatially associated with the Rio Cannero overthrust plane (Boriani et al., 1990). The veins can be deformed and parallel to the regional foliation, or undeformed, with crosscutting relationships with the rock foliation. The mineralization records a complex evolution.

The main mineralization stage is related to the emplacement of the earliest hydrothermal veins, mainly composed of arsenopyrite, pyrite and pyrrhotite that often occur as up to decimetre-sized patches embedded by quartz ± calcite. Fluorite, scheelite, titanite and albite are common, while chalcopyrite and sphalerite may also occur. Gold is related to this stage. Such primary assemblage is affected by a strong deformation event, that modified the rock fabric with formation of cataclastic textures.

A subsequent mineralization stage, postdating the deformation event, is represented by a second generation of arsenopyrite, pyrite, pyrrhotite and scheelite – associated with quartz and calcite - along undeformed veinlets which crosscut the earlier assemblage. Native Bi, bismuthinite, Bi-Te sulphosalts and galena also appear along microveins crosscutting pyrite and arsenopyrite of the main stage.

The hydrothermal alteration assemblage related to the main stage is given by sericite + quartz ± chlorite ± pyrite ± arsenopyrite; titanite and pyrrhotite may also occur and can be abundant when the veins crosscut the amphibolites. The alteration associated with the late mineralization stage is given by a millimetre-thick sericite + quartz ± chlorite ± pyrite rim.

The gold mineralization of Rio Cannero are different from the other mineralizations of the Italian western Alps. In spite of some similarities (first of all, the association of the gold mineralization with quartz-rich veins), they show important differences concerning both the vein and alteration assemblages and the tectonic setting. Such characters suggest that the gold mineralization of Rio Cannero may be a magmatic-related deposit, rather than a typical mesothermal gold deposit like the mineralizations of the Monte Rosa Gold District. A relationship with the Hercynian magmatism represents a reasonable working hypothesis.

Boriani A., Giobbi Origoni E., Borghi A. & Caironi V. (1990) - The evolution of the “Serie dei Laghi” (Strona -Ceneri and Scisti dei Laghi): the upper component of the Ivrea-Verbano crustal section; Southern Alps, North Italy and Ticino, Switzerland. *Tectonophysics*, 182, 103-118.

Natural-fibres-reinforced geopolymers for application in Cultural Heritage

Occhipinti R.*¹, Coccato A.¹, Finocchiaro C.¹, Fugazzotto M.^{1,2}, Strocio A.¹, Mazzoleni P.¹ & Barone G.¹

¹ Dipartimento di Scienze Biologiche, Geologiche e Ambientali, Università di Catania.

² Dipartimento di Scienze Umanistiche, Università di Catania.

Corresponding email: roberta.occhipinti@unict.it

Keywords: conservation, restoration, sustainable composites.

Conservation science allows to safeguard Cultural Heritage for future generations. Current practices tend to include modern techniques and innovative materials, taking into account sustainability, compatibility and durability. In this framework, geopolymers have been proposed as an alternative to traditional materials in restoration (Clausi et al., 2016; Tamburini et al., 2017). Although they have emerged as novel engineering material with commercial and technological potential (Van Deventer et al., 2012; Palomo et al., 2014), their brittle behaviour imposes constraints in structural design and affects the long term-durability. To overcome these limitations, organic and inorganic fibres technology has been developed in order to strengthen geopolymers matrix. Natural fibres have attracted much attention thanks to their cheapness, ready availability, lack of toxicity and good tensile strength (Alzeer & MacKenzie, 2013). This research, funded by the PNR “Advanced Green Materials for Cultural Heritage” project, aims to develop natural-fibre-reinforced geopolymers for retrofitting in seismic areas. The dry fibres of Sicilian prickly pear pads were embedded in geopolymer pastes prepared by mixing two local calcined clays ($T < 800^{\circ}\text{C}$) with Na_2SiO_3 as activating solution. Physical-chemical measurements, by means of XRD, SEM/EDS were carried out to check both the amorphous gel formation and the adhesion of geopolymer matrix to the natural fibres net. Morphological investigations have revealed that the aluminosilicates gel is formed and fissures cracking are less evident with respect to the not-reinforced geopolymer composites. The addition of vegetable fibres can enhance the brittle failure mode of geopolymer binders, reducing the shrinkage and leading up to an improvement in terms of durability of the system, which is highly demanded in the delicate question of Cultural Heritage preservation.

Alzeer M. & MacKenzie K. (2013) - Synthesis and mechanical properties of novel composites of inorganic polymers (geopolymers) with unidirectional natural flax fibres (phormium tenax). *Appl. Clay Sci.*, 75, 148-152.

Clausi M., Tarantino S.C., Magnani L.L., Riccardi M.P., Tedeschi C. & Zema M. (2016) - Metakaolin as a precursor of materials for applications in Cultural Heritage: Geopolymer-based mortars with ornamental stone aggregates. *Appl. Clay Sci.*, 132-133, 589-599.

Tamburini S., Natali M., Garbin E., Panizza M., Favaro M. & Valluzzi M.R. (2017) - Geopolymer matrix for fibre reinforced composites aimed at strengthening masonry structures. *Constr. Build. Mater.*, 141, 542-552.

Palomo A., Krivenko P., Garcia-Lodeiro I., Kavalerova E., Maltseva O. & Fernández-Jiménez A. (2014) - A review on alkaline activation: new analytical perspectives. *Mater. Constr.*, 64, 315, 022.

Van Deventer J.S., Provis J.L. & Duxson P. (2012) - Technical and commercial progress in the adoption of geopolymer cement. *Miner. Eng.*, 29, 89-104.

Geopolymer-based Terrazzo tiles with a high-waste content: stepping forward from the laboratory phase to the industrial scale

Paris E.*¹, Grandinetti V.², Manzi S.³, Stabile P.¹ & Bignozzi M.C.³

¹ School of Science and Technology, Geology Division, University of Camerino.

² Grandinetti srl, San Severino Marche.

³ Department of Civil, Chemical, Environmental and Materials Engineering, DICAM, University of Bologna.

Corresponding email: eleonora.paris@unicam.it

Keywords: geopolymers, high-waste content, terrazzo tiles.

Terrazzo Tiles (TT) are considered here as an example of how cement-based building products can affect the environment and that there is an urgent need to overcome (at least partially) the extensive use of cement in the building sector. TT are currently produced using ordinary Portland cement (OPC) based concrete, made of non-renewable raw materials, consuming high energy and water for its production and being responsible of emitting high level of CO₂. Generally, to produce 1m³ of mix for current production of Terrazzo Tiles at least 500 kg of cement is required mixed with 1.6 t of aggregates from quarries and 250 kg of water. Construction in the EU accounts for about 50% of all extracted materials and energy consumption, generating about 1/3 of all waste, whereas the production of OPC, accounts for 5-8% of total CO₂ emissions. EU directives on saving raw materials, reducing CO₂ emissions and landfill, recycling and upcycling waste, improving circular economy, urgently call for studying new and more sustainable building materials.

Successful laboratory studies on the use of geopolymers (e.g. Bignozzi et al., 2014) for possible application in the building sector have already demonstrated the effectiveness of these binders which can also contain waste of different types. The positive scientific results at the lab scale, however, is still insufficient to promote the effectiveness of geopolymers at a larger scale. In this study we tested the possibility to pass from the successful lab scale to the industrial implementation, with the help of a company leader in the TT products.

TT have been made with the collaboration of the Grandinetti company using alkaline solutions and a combination of: crushed CDW coming from the 2016 earthquake occurred in the Marche region, fly-ash from an electric power plant, rock polishing sludges from local companies. The solid mix is therefore composed of 93% of waste materials, whereas in conventional TT it is composed of 100% of raw materials (75% of raw materials and 25% cement), with a huge saving of raw materials. The geopolymer-based TT so produced satisfied the industrial internal test for quality evaluation. Moreover, the physical properties have been tested and, in particular, the mechanical tests results demonstrated to fall within the limits for the UNI EN 13748-1 norms for TT and in a good agreement with the values for conventional TT. These results are determinant for moving forward to the industrial scale, making the geopolymers products entering the TT market. Moreover, to evaluate the environmental impact of the new products, the Global Warming was calculated as about 184 kg CO₂ e/m³ compared to 361 kg CO₂ e/m³ of the conventional TT, demonstrating a decrease of 51% in favor of the geopolymer-based ones, which evidence their environmental effectiveness in CO₂ reduction.

Bignozzi M.C., Manzi S., Natali M.E., Rickard W.D. & Van Riessen A. (2014) - Room temperature alkali activation of fly ash: The effect of Na₂O/SiO₂ ratio. *Construction and Building Materials*, 69, 262-270.

Mineralogical and microstructural characterization of stoneware for wine use

Peroni V.¹, Botter R.², Cabella R.¹, Risso L.³ & Carbone C.*¹

¹ DISTAV (Dipartimento di Scienze della Terra, Ambiente e Vita) Università di Genova.

² DICCA, Dipartimento di Ingegneria Civile, Chimica e Ambientale Università di Genova.

³ Clayver, Vado Ligure (SV).

Corresponding email: carbone@dipteris.unige.it

Keywords: geomaterials, wine, stoneware.

The history of wine production is inextricably linked to that of the materials used to contain it, earthenware was one of the first materials as results from archaeological excavations in the southern Georgia dating back to the 6th millennium B.C. Recently few producers in the world have reconsidered the use of ceramic to build wine barrels, in particular in Italy a producer has chosen to use stoneware, which allows a certain oxygen transfer to the wine, limited and homogeneous, unlike the terracotta, too porous. Moreover stoneware is free of external contributions that can alter the smell and taste as happens using wooden barrels.

The production of wine vessels represents an unconventional use of stoneware, normally utilized for its waterproof characteristics, and requires specific low porosity and permeability in the final product. The permeability and diffusivity of a gas depend on porosity, pore size distribution, tortuosity, connectivity and degree of flooding of the pore structure. In order to produce a stoneware wine barrel with these calibrated and reproducible characteristics it is necessary an accurate control in all the stages of the production process: raw material mixing and characterization, forming, drying and firing.

Mineralogical investigations on the commercial raw material now used for stoneware barrel production were performed using granulometric analysis, X-ray diffractometry (XRD), scanning electron microscope (SEM) analysis and differential thermal analysis (DTA, TG).

Microstructural study in order to characterize density, water absorption, pore size and water vapour permeability was performed on fired material.

The mineralogical and microtextural results highlight the presence in the raw material of kaolinite, illite, quartz, orthoclase and talc, while in the final cooked product only quartz and mullite embedded in a glassy matrix were found. Chemical analyses excluded the presence of toxic elements like Lead, Cadmium, Arsenic and Cobalt.

The results deriving from the microstructural tests show that the water absorption of the sample is linearly correlated to the final density and the water vapor permeability increases with the open porosity measured with the water absorption tests. The final density depends on the firing temperature and for a not negligible part on the local inhomogeneity of raw material

Zeolite as an abiotic environment for amino acid condensation: spatial confinement and high pressure effects

Polisi M.*¹, Fabbiani M.², Arletti R.³, Vezzalini G.¹, Martra G.², Di Renzo F.⁴ & Quartieri S.⁵

¹ Dipartimento di Scienze Chimiche e Geologiche, Università di Modena e Reggio Emilia, Modena, Italy.

² Dipartimento di Chimica, Università di Torino, Italy.

³ Dipartimento di Scienze della Terra, Università di Torino, Italy.

⁴ Institut Charles Gerhardt, CNRS-UM-ENSCM, Montpellier, France.

⁵ Dipartimento MIFT, Università di Messina, Italy.

Corresponding email: michelangelo.polisi@unimore.it

Keywords: amino acids condensation, zeolite mordenite, high pressure X-ray powder diffraction.

Amino acids, a class of organic compounds largely used in pharmaceutical and biomedical fields, are the fundamental building blocks of the protein structures. In this study, Glycine (GLY) and Alanine (ALA) were adsorbed in a Na-mordenite. The obtained hybrids were previously characterized and then compressed at high pressure HP, with the following aims: 1) to test the effectiveness of the zeolite as sorbent for amino acids; 2) to explore the possibility to use pressure to induce amino acids condensation in zeolite pores. This study, from one side, will contribute to shed light on the role of minerals in amino acids polymerization under abiotic conditions - which is a still open issue in prebiotic chemistry (Martra et al., 2014; Whitesides, 2015) - and, on the other side, will open the way to a “green” and solvent-free, peptide synthesis.

$4\text{Al}_{4.3}\text{Si}_{43.9}\text{O}_{96} \cdot 28.2\text{H}_2\text{O}$, s.g. *Cmc2₁*, $a=18.080(1) \text{ \AA}$, $b = 20.380(1) \text{ \AA}$, $c = 7.489(3) \text{ \AA}$, $V = 2759.3 (3) \text{ \AA}^3$] was synthesized at the Institut Charles Gerhardt in Montpellier. The water content of the final product was determined by thermogravimetric (TG) analysis. GLY was loaded from vapor phase at mild temperature (150-160°C) in a previously dehydrated Na-MOR powder sample. Otherwise, both α -ALA and β -ALA were loaded from aqueous phase and then the hybrid materials were dehydrated at 150° C. The Na cations located in the side pocket of Na-MOR are expected to trap the water molecules possibly generated by the formation of the peptide bond during the condensation reaction. The amino acid/zeolite composites were characterized by TG analysis, elemental analysis, IR spectroscopy, synchrotron XRPD at ambient conditions. Moreover, a series of in situ HP synchrotron XRPD experiments were carried out in diamond anvil cell. XRPD data collected on GLY/MOR composite at P_{amb} show that GLY molecules are located inside the 12MR channel on the (100) plane and oriented along the *b* axis. The structural analyses evidenced a not completed filling of the pores by GLY molecules: GLY sites are only partially occupied and about 1.4 GLY molecules p.u.c. were located, in agreement with the results of the elemental analysis. The XRPD HP experiments did not evidence amino acid condensation, at least up to 2 GPa, probably as a consequence of the too partial loading. The analyses of the ALA/MOR samples evidenced a higher amount of amino acid inside the zeolite channels with respect to GLY: 3.8 and 2.4 molecules p.u.c. for β -ALA and α -ALA, respectively. IR spectra of GLY/MOR composite show the presence of a broad absorption band in the 1700-1600 cm^{-1} range which is compatible with a peptide bond moiety inside the composite material already at P_{amb} .

Martra G., Deiana C., Sakhno Y.; Barberis I., Fabbiani M., Pazzi M. & Vincenti M. Angew. (2014) - The Formation and Self-Assembly of Long Prebiotic Oligomers Produced by the Condensation of Unactivated Amino Acids on Oxide Surfaces. Chem. Int. Ed., 53, 4671-4674.

Whitesides G.M. (2015) – Reinventing chemistry. Angewandte Chemie, 54, 3196-3209.

Topaz characterization: mineralogy and geochemistry at the service of the jewelry market

Precisvalle N.*¹, Martucci A.¹, Bonadiman C.¹, Langone A.² & Nobre A.³

¹ Dipartimento di Fisica e Scienze della Terra, Università degli Studi di Ferrara.

² Istituto di Geoscienze e Georisorse-C.N.R. U.O.S. di Pavia.

³ Instituto de Geociências, Universidade de São Paulo.

Corresponding email: prcncl@unife.it

Keywords: Topaz, jewelry market, gemology.

Topaz is one of the principal fluorine-bearing silicates that occurs as accessory mineral in fluorine-rich granitic rocks associated with pneumatolithic/hydrothermal events and in ultrahigh-pressure rocks (Zhang et al., 2002; Alberico et al., 2003). The topaz structure consists of $[\text{SiO}_4]_4$ -groups linking octahedral chains of $\text{Al}[\text{O}_4(\text{F},\text{OH})_2]$ in a zig zag fashion parallel to the c-axis. Four of the six anions surrounding the Al^{3+} ion belong to $[\text{SiO}_4]_4$ -tetrahedra; the remaining two are either F- or OH-groups. The orthorhombic structure belongs to Pbnm space group, but on the basis of Rinne (1926) and Akizuki et al. (1979) natural topaz present pronounced sectoral textures with growth planes $\{hkl\}$ optically triclinic, $\{0kl\}$, $\{k0l\}$, and $\{hk0\}$ optically monoclinic and $\{100\}$, $\{010\}$, and $\{001\}$ as optically orthorhombic. In this work, a selection of gem quality topazes from various localities (Zacatecas-Mexico, Baoshan-PRC and Padre Paraiso-Brazil) were compared in terms of major and trace element compositions. The relationships between structural feature (i.e. OH/F substitution), surface reactivity and environmental conditions has been explored. Major elements composition was almost constant in terms of Si and Al, whereas F varies in topaz of various localities and formation environment. LA-ICP-MS revealed sectoral and intrasectoral zoning of trace elements as a function of growth-surface structure. The smooth time-resolved LAM-ICP-MS signals suggest that trace elements are incorporated in the mineral lattice. Preliminary results show that topazes from Zacatecas are richer in Li (+1) and B (+3) (up to 90 ppm) and U-Th (+6;+4). In turn Baoshan topaz contain anomalously high contents of pentavalent Nb (18 ppm), Ta (2 ppm) and W (up to 5 ppm). XRD differences in lattice are registered, showing larger distortions for samples hosting larger atoms. By means of micro X-ray tomography (micro-CT) it has been studied an inclusions pattern. The analyzed inclusions are both proto-, syn- and epigenetic. On the basis of chemical and structural data, a model to explain the accommodation of these elements in the crystal structure as function of the geological environment, thus possibly to determine the gem identity has been proposed.

Akizuki M., Hampar M.S. & Zussman J. (1979) - An explanation of anomalous optical properties of topaz. *Mineral. Mag.*, 43, 237-241.

Alberico A., Ferrando S., Ivaldi G. & Ferraris G. (2003) - X-ray single-crystal structure refinement of an OH-rich topaz from Sulu UHP terrane (Eastern China) Structural foundation of the correlation between cell parameters and fluorine content. *Eur. J. Mineral.*, 15, 875-881.

Rinne F. (1926) - Bemerkungen ber optische Anomalien, insbesondere des brasilianer Topas. *Z. Kristallogr.*, 63, 236-246

Zhang R.Y., Liou J.G. & Shu J.F. (2002) - Hydroxyl-rich topaz in high-pressure and ultrahigh-pressure kyanite quartzites, with retrograde woodhouseite, from the Sulu terrane, eastern China. *Am. Mineral.*, 87, 445-453.

Genesis of phyllosilicates in the Wingellina Ni-Co laterite deposit (Western Australia)

Putzolu F.*¹, Abad I.², Balassone G.¹, Boni M.¹⁻³, Cappelletti P.¹, Graziano S.F.⁴, Maczurad M.⁵, Mondillo N.¹⁻³, Najorka J.⁶ & Santoro L.³

¹ Dipartimento di Scienze della Terra, dell'Ambiente e delle Risorse, Università di Napoli "Federico II" Complesso Universitario di Monte S. Angelo, Italy.

² Departamento de Geología and CEACTION, Universidad de Jaén, Spain.

³ Earth Sciences Department, Natural History Museum, Cromwell Road, London, UK.

⁴ Dipartimento di Farmacia Università di Napoli "Federico II".

⁵ Metals X Limited, Perth, Australia.

⁶ Core Research Laboratories, The Natural History Museum, London, UK.

Corresponding email: francesco.putzolu@unina.it

Keywords: laterite, Ni-phyllosilicates, Wingellina.

Wingellina is a large Ni-Co laterite deposit, located in Western Australia. The laterite profile formed from the weathering of the Mesoproterozoic mafic and ultramafic intrusions of the Giles Complex, mainly consisting of peridotite and gabbro. The exploitable Ni-Co resources of the deposit are represented by Ni-Co-bearing Fe/Mn-oxy-hydroxides mostly occurring in the more surficial limonite horizon (probable Reserve = 168 Mt @ 0.98% Ni and 0.08% Co). This makes the Wingellina deposit an unusual "oxide-type" laterite. The deeper saprolite horizon has a lower tonnage, but contains higher Ni concentrations (up to ~3 wt%). We have studied the mineralogy of the Ni-phyllosilicates from saprolite samples of the Wingellina deposit collected from two different profiles, overlying a gabbro and a serpentinite (former peridotite) bedrock, respectively.

From mineralogical and petrographic analyses, we determined that the initial alteration stage of the gabbro was characterized by the formation of nontronite and montmorillonite, at the expenses of olivine and pyroxene, respectively. The congruent dissolution of plagioclase played an important role, supplying the Al required for montmorillonite formation. The following stage was represented by the alteration of montmorillonite, resulting in the precipitation of kaolinite. This paragenetic sequence is in agreement with a typical lateritization pathway. The alteration of the serpentinite followed instead a multistage route. During the initial lateritization stage, the original serpentine was altered to a Ni-rich *srp* II, as well as to tri- and dioctahedral smectites (saponite and nontronite). The chemistry of smectites suggests that the saponite-to-nontronite conversion developed through a progressive increase of the Fe content within trioctahedral smectite. In a following stage, in the upper section of the serpentinite-derived saprolite, disordered talc-smectite and chlorite-smectite interstratified clays formed at the expenses of the former serpentines and smectites. This process is not typical of humid lateritic environments, but common under arid climates characterized by circulation of saline and alkaline fluids. In the Wingellina area, the onset of arid climate during the Late Miocene-Pliocene (Anand and Paine, 2002) likely promoted the formation of these interstratified clays. Taking into the nature and the late stage formation of disordered interstratified clays in the Wingellina saprolite, the evaporative-driven clays authigenesis can be considered as a counterpart of the per descensum process that explains the garnierite formation in active margins.

Anand R.R. & Paine M. (2002) - Regolith geology of the Yilgarn Craton, Western Australia: implications for exploration. *Australian Journal of Earth Sciences*, 49(1), 3-162.

The hydrogenetic ferromanganese crusts and hydrothermal massive sulphide deposits in the Tyrrhenian Seafloor: a geological reassessment of the supply of Raw Materials

Rossi G.*¹, Gamberi F.², Marani M.², Mattioli M.¹, Di Gregorio A.³ & Renzulli A.¹

¹ Dipartimento di Scienze Pure e Applicate, Università degli Studi di Urbino Carlo Bo.

² ISMAR - CNR Bologna 3 Centro di Ricerca Interuniversitario in Economia del Territorio (CRIET), Università degli Studi di Milano-Bicocca.

Corresponding email: giadarossi71193@gmail.com

Keywords: mineralogical and geochemical data, sea-floor ore deposits, Aeolian Archipelago.

Although the growing demand for metals is increasingly focused on the supply of non-energy Raw Materials for industrial and technological purposes, in Italy their extraction is almost zero. This implies a strong dependence on imports from abroad and geopolitically unfavourable conditions. The mineral deposits of the seabed of the southern Tyrrhenian Sea could make a significant contribution to the future supply of Raw Materials, even if the assessment of the quantity of deep-ocean metals and their recoverability is demanding. Exploration and potential extraction of seabed minerals prompt many challenges.

Currently, global commercial interest and scientific research are focused on three classes of deep marine mineral deposits: polymetallic nodules of Fe and Mn, Fe and Mn crusts, massive sulphide deposits (Lusty & Murton, 2018). This research project focuses on the mineralogical and geochemical characterization of the mineral deposits of the southern Tyrrhenian seabed, as an overview and new analyses of samples (dredge hauls, gravity cores) previously collected from surveys conducted in 1995 (Gamberi et al., 1997; Marani et al., 1997) and 1998 (cruise MAR-98; Marani et al., 1999) in the sectors of the Aeolian Archipelago. Low-temperature (both hydrothermal and hydrogenetic) Fe-oxyhydroxide-rich red muds and crusts and high-temperature (i.e. hydrothermal) sediment-hosted massive sulphides are the main ore-mineral deposits (Savelli et al., 1999). The critical reassessment of these two classes of deep-ocean mineral deposits in terms of formation environment, mineral associations and key elements for exploration will be carried out through new processing of the available geochemical data, new XRD and SEM-EDS analyses and new isotopic studies.

The results will be compared with worldwide deep-ocean mineral deposits and hydrogenetic vs. hydrothermal mechanisms of metal resource formation also in terms of tectonic setting, sources contributing to the concentration of seawater trace elements, environmental conditions of water and recent to active hydrothermal activity and volcanism.

Gamberi F., Marani M. & Savelli C. (1997) - Tectonic, volcanic and hydrothermal features of a submarine portion of the Aeolian arc (Tyrrhenian Sea). *Marine Geology*, 140, 167-181.

Lusty P.A.J. & Murton B.J. (2018) - Deep-Ocean Mineral Deposits: Metal Resources and Windows into Earth Processes. *Elements*, 14, 301-306.

Marani M., Gamberi F. & Savelli C. (1997) - Shallow-water polymetallic sulphide deposits in the Aeolian island arc. *Geology*, 9, 815-818.

Marani M.P., Gamberi F., Casoni L., Carrara G., Landuzzi V., Musacchio M., Penitenti D., Rossi L. & Trua T. (1999) - New rock and hydrothermal samples from the southern Tyrrhenian sea: the MAR-98 research cruise. *Giornale di Geologia*, 61, 3-24.

Savelli C., Marani M. & Gamberi F. (1999) - Geochemistry of metalliferous, hydrothermal deposits in the Aeolian arc (Tyrrhenian Sea). *Journal of Volcanology and Geothermal Research*, 88, 305-323.

Natural Iron oxy-hydroxides from supergene ore deposits: mineralogical, morphological and geochemical characterization

Santoro L.*¹, Herrington R.¹ & Putzolu F.²

¹ Natural History Museum, London.

² Università di Napoli, Federico II.

Corresponding email: licia.santoro85@postecert.it

Keywords: Fe-oxy-hydroxides, Supergene deposits, goethite.

Iron-oxy-hydroxides (IOH) phases commonly occur in all Supergene Ore Deposits (SOD) where they are regularly associated with economic ores. The most common phase in these environments is limonite, a micro to nano-crystalline crystalline mixture of IOH mainly consisting of goethite sensu strictu (α -FeOOH). Lepidocrocite (γ -FeOOH), ferrihydrite ($5\text{Fe}_2\text{O}_3 \cdot 9\text{H}_2\text{O}$; $\text{Fe}_5\text{O}_7(\text{OH}) \cdot 4\text{H}_2\text{O}$, $\text{Fe}_5\text{O}_3(\text{OH})_9$, $\text{Fe}_4\text{O}_5(\text{OH})_2 \cdot 2.6\text{H}_2\text{O}$)₁₂), hematite (Fe_2O_3) and minor maghemite (γ - Fe_2O_3) can also occur. Natural IOH are rarely chemically pure; they can host cations, isovalent or heterovalent to Fe^{3+} , which can be incorporated into their structure (Cornell and Schwertmann, 2003).

The aim of this work was to establish the geochemical, morphological and mineralogical variations of limonite collected from a diverse range of SOD in order to assess which IOH phases are present and which metals are incorporated in their structure. The samples were collected from the oxidation zones of Ni-laterite deposits (Caldag and Karacam, Turkey; Wingellina, Australia), supergene Zn-nonsulfides (Hakkari, Turkey; Jabali, Yemen) and bauxite (Maiorano and Dragoni, Italy). The analyses were carried out at Natural History Museum (NHM, London, UK) by several analytical methods used for ore characterization: XRD, SEM-EDS, EPMA, ICP-AES, LA-ICPMS and TEM.

The most common IOH phases from Ni-laterite and Zn-nonsulphide deposits mainly consist of goethite with minor maghemite and hematite, while bauxite specimens mainly consist of hematite with minor goethite.

In Ni-laterite deposits the goethite commonly occur as crusts associated to Mn-oxyhydroxides or quartz, boyitridal concretions within rock pores or as needle-like concretions. In some cases it can be pseudomorph of primary phases (olivine or pyrite). The IOH of bauxite deposits, instead, consist of oids having hematitic cores surrounded by bohemite or crusts of hematite associated with goethite.

In all the selected samples Fe, Si and Al are the major elements. The high Al content of the bauxite IOH depends on the presence of bohemite. EPMA analyses revealed that some amount of Al and Si (up to a max. of ~3wt%) is hosted within the goethite itself. Minor elements content changes according to the deposit type: Cr, Ni and Co occur within goethite samples from Ni-laterite; EPMA results revealed they are hosted within the goethite itself with Ni up to ~3wt% and Co up to ~0.3wt%; minor Mg (from lizardite) and Mn (from Mn-hydroxides) can be present in those samples. The IOH selected from Zn-nonsulphide deposits are enriched in Zn and Pb; some Pb amount can come from the cerussite, but EPMA analyses show that both Zn and Pb can amount up to ~6wt.% within goethite. Ti (from rutile) is a common minor element from IOH selected from bauxites.

LA-ICPMS analyses were useful to identify the Sc, Ge, Ga and REE contents hosted within IOH: the content of Sc, Ge and Ga is always negligible for all the studied IOH while REE (up to ~1000ppm) can be hosted within IOH samples from bauxite deposits.

TEM-based analyses revealed that all the signals for all the detected elements (i.e. Ni, Co, Zn, Si, Cr, etc.) derive from the elements widespread in the crystal lattice and not from nano-crystals of other mineral species.

Cornell R.M. & Schwertmann U. (2003) - Front Matter, in *The Iron Oxides: Structure, Properties, Reactions, Occurrences and Uses*, Second Edition, Wiley-VCH Verlag GmbH & Co. KGaA, Weinheim, FRG.

Aluminum Phosphate–Sulfate (APS) minerals occurrence and REEs control in the Darzi-Vali bauxite deposit, Iran

Sinisi R.*¹, Mongelli G.¹, Perri F.² & Khosravi M.³

¹ Dipartimento di Scienze, Università degli Studi della Basilicata (Italy).

² Dipartimento di Ecologia, Biologia e Scienze della Terra, Università della Calabria (Italy).

³ Department of Earth Sciences, Faculty of Sciences, Shiraz University (Iran).

Corresponding email: rosa.sinisi@unibas.it

Keywords: APS minerals, REE, Iran.

Bauxite is the primary source for aluminium production globally and in the West-Azarbaidjan Province, Iran, the Darzi-Vali bauxite deposit represents a high-grade and minable bauxite ore (Khosravi et al., 2017). The deposit is located within the Iran-Himalayan karst-bauxite belt, about 20 km east of Bukan, northwestern Iran. The stratigraphic succession in this area consists of Upper Permian sandstone, shale, and carbonate of the Ruteh Formation, unconformably overlain by Jurassic shale and sandstone of the Shemshak Formation, followed by Lower Cretaceous conglomerates and sandstones, Upper Cretaceous sparitic limestones, and Quaternary alluvial terraced deposits. The bauxite occurs as discontinuous layers and lenses within the carbonate rocks of the Ruteh Formation. The Aluminum Phosphate–Sulfate (APS) minerals occurs in a wide range of geological environments near the Earth's surface, including weathering, sedimentary, diagenetic, hydrothermal, metamorphic and postmagmatic systems. APS minerals have been also recognized in bauxite ores where they may host critical metals including the Rare Earth Elements (REEs). Further, since APS minerals are highly sensitive to their physico-chemical conditions of formation (Eh, pH, activities of constituent metals, P, T), they gained growing interest for tasks dealing with paleoconditions in natural systems (Gaboreau et al., 2005). In this work, for the first time, a detailed study focussed on mineralogical (XRPD, OM, SEM) and microchemical (EDS and WDS) composition of the Darzi-Vali bauxite is shown with the principal aim to investigate the mineralogical control and distribution of REEs throughout the deposit. Beside primary LREE-monazites and apatites, other uncommon REE-bearing APS, such as svambergite and goyazite, have been detected in the studied deposit. Both svambergite and goyazite host REEs in their crystal structure as replacing elements for Sr and have been distinguished each other for their relative contents of S replacing for P in the $(\text{PO}_4)_3^-$ tetrahedron. In the studied bauxite, these minerals mainly concentrate within millimetre to centimetre pervasive veins suggesting a precipitation from secondary REE-rich fluids circulating in the rock after its formation. Currently no more information on the presence of a vein network rich of REEs-bearing mineral phases in the Darzi-Vali bauxite are available making the studied ore worthy of further investigations.

Gaboreau S., Beaufort D., Vieillard P., Patrier P. & Bruneton P. (2005) - Aluminum phosphate–sulfate minerals associated with proterozoic unconformity-type uranium deposits in the east Alligator river uranium field, northern territories, Australia. *Can. Min.*, 43, 813-827.

Khosravi M., Abedini A., Alipour S. & Mongelli G. (2017) - The Darzi-Vali bauxite deposit, West-Azarbaidjan Province, Iran: Critical metals distribution and parental affinities. *J. African Earth Sci.*, 129, 960-972.

Characterization and vitrification of combined waste materials and potential use for reutilization in eco-sustainable building

Stabile P.¹, Abudureheman A.*¹, Bello M.¹, Carroll M.R.¹ & Paris E.¹

¹ School of Science and Technology, Geology Division, University of Camerino.

Corresponding email: ababaik.abudureheman@unicam.it

Keywords: Waste production, reutilization, eco-sustainable building.

Waste production is a daily/common human activity and the construction industry produces in Europe 820 million tons (Mg) of waste, about 35% of all waste. In particular, construction and demolition waste (CDW) can derive from construction, refurbishment or demolition of buildings, roads or public spaces and up to 85% of CDW is made of concrete, ceramics and masonry, reused only as inert materials. Moreover, fly-ash (FA) and bottom-ash (BA) are troublesome wastes to deal with, due to a limited reutilization (only 16% of FA produced in EU is recycled) and lack of uses.

Aim of this study is to approach CDW, FA and BA characterization and behaviour at high T in order to shed light on possible waste reuse for production of new materials for applications in building materials or in the glass industry. To achieve so, vitrification experiments have been performed at ambient pressure, different temperatures (1000 to 1200°C) and for variable duration (from 2 to 8 h). Vitrification is, among the techniques used to treat and homogenize waste products, a valuable process to have volume reduction and immobilization of potentially hazardous elements for further re-utilization of waste, with the possible additional modification of the starting composition with glass forming additives.

Preliminary studies aimed at investigating chemical, morphological and mineralogical properties. BA revealed to be highly inhomogeneous, consisting mainly of poly-crystalline fragments, glass, silicate minerals and many volatile metals, e.g. Ni, Pb, Zn, Co, Cr, Cu (Stabile et al., 2019). The materials produced by vitrification of CDW have been checked for homogeneity (XRD, optical microscopy, SEM) and results show that, even after treatments at the highest temperatures and longest duration, a complete glassy character is not reached. We therefore attempted several mixtures combining CDW BA (from municipal solid waste) with FA (from electrical power plant) in different proportions, to investigate the vitrification process as a function of the components. The preliminary results show that vitrification is best reached by adding FA (30 wt.% of the mix), whereas adding of BA does not improve the vitrification even at the highest concentrations (70%) and can be therefore disregarded as a suitable component in spite of the high amount of silica component.

The large quantity and the potential leachability of high metal concentrations in these waste residues needs to be tested by leaching tests to provide insights into the mobility of heavy metals, which plays an important major role to assess the possibility of use and treatment within regulatory limits. These preliminary results have shown, however, the presence of possible host phases for potentially hazardous elements in the mixes, providing useful information on properties and possibilities for recycling in the building sector.

Stabile P., Bello M., Petrelli M., Paris E. & Carroll M.R. (2019) - Vitrification treatment of municipal solid waste Bottom Ash, Waste management (submitted)

What controls metal endowment of massive sulfide deposits on mid-ocean ridges?

Toffolo L.¹, Nimis P.*¹, Tret'yakov G.A.², Melekestseva I.Yu.² & Beltenev V.E.³

¹ Dipartimento di Geoscienze, Università di Padova.

² Institute of Mineralogy, Miass, Russia.

³ Polar Marine Geosurvey Expedition, Lomonosov–St. Petersburg, Russia.

Corresponding email: paolo.nimis@unipd.it

Keywords: seafloor, massive sulfides, metals.

Mid-ocean ridges ordinarily host hydrothermal systems in which dominantly seawater-derived fluids precipitate metals as massive sulfides (MS) on the seafloor. These MS deposits may have remarkable grades of base (Cu, Zn), precious (Au, Ag) and critical (Co) metals and have therefore gained attention as potential mining targets. Seafloor MS may show significant geochemical variability along the same ridge and even at the deposit or hand-specimen scale, suggesting a complex interplay of regional and local controlling factors. Studying these factors is pivotal for an understanding of the genesis of MS and for developing effective guidelines for the exploration and economic evaluation of present-day seafloor deposits and of their ancient on-land counterparts. We investigated these factors by means of robust principal component analysis and robust factor analysis of published and novel bulk chemical data for MS from worldwide mid-ocean ridges. The interpretation of the statistical factors was supported by thermodynamic modeling of basalt- and peridotite-seawater hydrothermal systems and long-standing observations in modern seafloor hydrothermal fields. We found that most of the geochemical variability (73%) can be explained by three independent factors, which are interpreted to be (in order of importance): (1) the temperature of sulfide deposition, (2) the ridge spreading rate, and (3) zone refining. The first and the third factors are mostly related to processes operating near the seafloor, such as conductive cooling, mixing with seawater and metal remobilization, and effectively control the relative proportions of the main sulfide minerals and of two main groups of anti-correlated elements, i.e., Cu, Se, Co vs. Zn, Ag, Sb, Pb. Therefore, the relative enrichment in these elements mostly reflects the final depositional conditions and evolution of mound and vent structures rather than the original geochemistry of the hydrothermal fluid. The ridge spreading rate controls the structure of the oceanic lithosphere, which in turn controls the length and depth of the hydrothermal circuit and the rock-to-water (r/w) ratios in the reaction zone. The higher r/w at slow-spreading ridges enhances the release of Au and Ag to the fluid, but may limit that of Ni due to the stabilization of Ni-bearing sulfides and silicates at depth. As a consequence, MS on slow-spreading, ultramafic-rich ridges are systematically enriched in Au, but not in Ni, compared with those on intermediate/fast-spreading, mafic-dominated ridges. Despite the obvious role played by substrate rocks as metal sources, their nature does not emerge as a statistically significant independent factor. The composition of the substrate, however, may become relevant in subseafloor mineralization, where sulfides precipitate by reaction of ascending hydrothermal fluids with Ni-poor mafic or Ni-rich ultramafic host-rocks.

Density Functional investigation of the thermomechanical, electronic and thermodynamic properties of ZnS cubic polymorphs

Uljan G.*¹, Moro D.¹ & Valdrè G.¹

¹ Centro di Ricerca Interdisciplinare di Biomineralogia, Cristallografia e Biomateriali, Dipartimento di Scienze Biologiche, Geologiche e Ambientali, Università di Bologna, Bologna, Italy.

Corresponding email: gianfranco.uljan2@unibo.it

Keywords: Zinc sulphide, thermophysical properties, Density Functional Theory.

Zinc sulphide (ZnS) is an interesting mineral phase presenting two cubic polymorphs, namely zinc-blende (sphalerite) and rock-salt. Sphalerite (zb-ZnS) is a stable phase at ambient conditions, whereas the rock-salt polymorph (rs-ZnS) is the result of high compression loads. Zinc sulphide is an important mineral from the geo-mining and industrial points of view, whose properties found various and manifold applications for the exploitation of georesources and also in electronics, optics and photocatalysis. In the present work, we report an extensive and detailed theoretical investigation of thermomechanical, electronic and thermodynamic properties of zb-ZnS and rs-ZnS over a wide range of pressure, by means of *ab initio* Density Functional Theory, Gaussian-type orbitals and the well-known B3LYP functional. The thermodynamic *P-T* stability of the mineral phases was investigated in the pressure range 0 – 25 GPa and between 0 and 800 K. The athermal (0 K) 3rd-order Birch-Murnaghan equation of state (EoS) resulted in $K_{00} = 72.63(3)$ GPa, $K'_{00} = 3.88(1)$ and $a_{00} = 5.5532(3)$ Å for sphalerite, and $K_{00} = 84.39(5)$ GPa, $K'_{00} = 4.13(1)$ and $a_{00} = 5.2167(3)$ Å for the rs-ZnS polymorph. The phase transition was calculated to be about 15.5 GPa and 14.6 GPa from the athermal EoS and elastic constants data, respectively. In agreement with experimental findings (Ono and Kikegawa, 2018), an inverse relationship between the pressure of transition and temperature was observed. The electronic band structure showed a direct band gap for the zinc-blende zinc sulphide ($E_g = 4.830$ eV at equilibrium geometry), which became an indirect one by increasing pressure above 11 GPa. The results compared and discussed with the available experimental (Uchino et al., 1999; Ono & Kikegawa, 2018) and theoretical (Hu et al., 2008; Cardona et al., 2010) data were found to be in good agreement, further extending the knowledge of important properties of zinc sulphide polymorphs, in particular the thermomechanical ones that we extensively explored.

Cardona M., Kremer R.K., Lauck R., Siegle G., Munoz A., Romero A.H. & Schindler, A. (2010) - Electronic, vibrational, and thermodynamic properties of ZnS with zinc-blende and rocksalt structure. *Physical Review B*, 81(7)

Hu C.E., Sun L.L., Zeng Z.Y. & Chen, X.R. (2008) - Pressure and temperature induced phase transition of ZnS from first-principles calculations. *Chinese Physics Letters*, 25(2), 675-678.

Ono S. & Kikegawa T. (2018) - Phase transition of ZnS at high pressures and temperatures. *Phase Transitions*, 91(1), 9-14.

Uchino M., Mashimo T., Kodama M., Kobayashi T., Takasawa E., Sekine T., Noguchi Y., Hikosaka H., Fukuoka K., Syono Y., Kondo T. & Yagi T. (1999) - Phase transition and EOS of zinc sulfide (ZnS) under shock and static compressions up to 135 GPa. *Journal of Physics and Chemistry of Solids*, 60(6), 827-837.

Thermal and mechanical properties of phyllosilicates: some case studies from ab initio quantum mechanical investigations

Uljan G.*¹, Moro D.¹ & Valdrè G.¹

¹ Centro di Ricerca Interdisciplinare di Biomineralogia, Cristallografia e Biomateriali, Dipartimento di Scienze Biologiche, Geologiche e Ambientali, Università di Bologna, Bologna, Italy.

Corresponding email: gianfranco.ulian2@unibo.it

Keywords: Phyllosilicates, thermophysical properties, Density Functional Theory.

Phyllosilicates are important phases in several geophysical and geotechnological applications. Some of them may act as water carriers, bringing H₂O in the Earth's mantle through release of hydroxyls from their structure and subsequent phase transformations. Thus, the knowledge of the high-pressure and high-temperature behaviour of phyllosilicates is very important in minero-petrological and technological/industrial fields for various genetic and thermobarometric issues and for material science applications, respectively. In this context, quantum mechanical simulations of mineral phases can provide an invaluable tool to study the minerals behaviour at P-T conditions that are difficult to obtain during experimental procedures, especially controlled high pressures and temperatures. There are very few theoretical works in literature devoted to the physical-chemical characterization of layer silicates, and water carriers in general, at atomic scale. Phyllosilicates present interesting challenges to computational mineralogists. For example, layered silicate structures are made by tetrahedral-octahedral-tetrahedral (T-O-T) with an empty interlayer or with cations between the TOTs. For this reason, the simulation parameters should be chosen carefully when dealing with layered silicates, because two directions of the mineral are dominated by covalent bonds (within the TOT layers), while the third direction exhibits an interplay of van der Waals forces (between the layers) and strong ionic interactions due to the interlayer cations. In the present study, we report the thermo-chemical and thermo-physical properties of a series of phyllosilicate minerals, namely talc, pyrophyllite and the 2M1 polytype of muscovite in a wide pressure and temperature ranges. The hybrid DFT/B3LYP density functional has been adopted, adding a correction for dispersive forces and employing the quasi-harmonic approximation (Anderson, 1995) to include the temperature effects on the thermodynamics and mechanical properties. The results can be used as a solid basis to investigate and characterize in detail the phase transitions of selected minerals for mineralogical, petrological and geophysical purposes and in technological and industrial applications as well.

Anderson O.L. (1995) - Equation of state of solids for geophysics and ceramic science. 405 pp. Oxford University Press, New York, US.

Geomaterials on the edge of the circular economy: the case study of the ceramic tile industry

Zanelli C. *, Conte S., Molinari C., Soldati R., Guarini G. & Dondi M.

CNR-ISTEC Faenza (Italy).

Corresponding email: chiara.zanelli@istec.cnr.it

Keywords: mineralogical transformations, waste recycling, technological behaviour.

Circular Economy is a “response to the desire for sustainable growth in the context of the increasing pressure that the production and consumption have on the environment and global resources”. Such a regenerative design aims to keep products, components and materials at their highest utility and value at all times. The economy has worked in a linear model of “collection, production and disposal”, where all the products eventually reach an “end of life” status. This leads to an increase in demand for resources, and consequently, to a greater environmental degradation. The main geo-resources are becoming scarce, thus, the continuous application of the linear model that depends exclusively on the extraction of geomaterials with limited availability is no longer feasible. The transition to a circular economy redirects the focus to the reuse, repair, renovation and recycling of materials and existing products, i.e. what was previously seen as a “waste” can be now transformed into a resource. The ceramic tile manufacturing is often seen as an example of linear economy, where the concept of “reduce, reuse, recycle, recover”, is difficult to be carried and all the efforts reside on recycling processing wastes in cannibalistic loops. Unfortunately, the circular economy cannot be easily applied to ceramics, mainly due to usually long and worldwide distributed life cycles. However, an interesting range of residues has already been studied as raw material for porcelain stoneware tiles, but often limited to a feasibility assessment. A detailed analysis of requirements, pre-treatments and industrial behavior of secondary raw materials suitable for ceramics, is still far from being outlined. This contribution wanted to define why and how wastes affect the technological behavior of porcelain stoneware tiles. we evaluated the concept circular economy that transferred to the tiles industry also considering the actually possible supplies in relation to the needs of the ceramic production process. This is a case study on waste valorization, we selected about a dozen of residues, recycled from Emilia-Romagna region, Italy, and suitable as ceramic raw materials (mostly glasses, ashes and sludges). the wastes are introduced as fluxes, to replace feldspathic raw materials in a standard porcelain stoneware batch, contents up to 60% were reached. Bodies underwent a laboratory simulation of the industrial process, stressing on technological obstacles to a large-scale utilization and fully evaluating their behavior. Thus, a waste classification was allowed, and obtained technological profiles summarize preliminary treatments needed, compositional features and the effects on technological behavior of the porcelains stoneware tiles.

S4

Minerals, environment and medical uses

CONVENERS AND CHAIRPERSONS

Claudia Belviso (CNR-IMAA)

Giovanni Grieco (Università di Milano)

Pietro Marescotti (Università di Genova)

Probing the sorption capacity of Y Zeolite towards pharmaceutical compounds: a neutron powder diffraction study

Beltrami G.*¹, Martucci A.¹, Pasti L.² & Chenet T.²

¹ Dept. of Earth Sciences, University of Ferrara, Italy.

² Dept. of Chemical and Pharmaceutical Sciences, University of Ferrara, Italy.

Corresponding email: bltgd@unife.it

Keywords: Y zeolite, pharmaceutical compounds, neutron powder diffraction.

Due to their widespread use and slow natural degradation, pharmaceutical products are among the most common ubiquitous contaminants of waters and wastewaters. At present, pharmaceuticals removing from water systems through adsorption on synthetic microporous zeolites is considered the best compromise in terms of cost-effectiveness and eco-sustainability (Martucci et al., 2015; Rodeghero et al., 2016). In this work, two samples of Y zeolite (*i.e.*, Si/Al ratio=30) loaded with two different pharmaceutical compounds (*ibuprofen*, C₁₃H₁₈O₂ and *atenolol*, C₁₄H₂₂N₂O₃) were studied through neutron powder diffraction to determine zeolite sorption capacity and highlight host-guest interactions. Drug-loaded zeolites were obtained exchanging the as-synthesized form with deuterated ibuprofen and atenolol in aqueous solution for 140 h at room temperature and then washing with D₂O. Diffraction data were collected at the D2B beamline (ILL; Grenoble) at 4 K. Rietveld refinements were performed using the GSAS software (Larson & von Dreele, 1994), whereas extra-framework sites were located by difference Fourier maps and then optimized using EXPO2014 (Altomare et al., 2013) software to obtain reasonable bond lengths and angles and calculate the H atoms position. Results obtained from the cell parameters analysis confirmed the presence of extraframework molecules within the zeolite pores, which were located within the *supercage* through the difference Fourier maps analysis. Contrariwise, no coadsorbed water molecules were detected. Refinement of extraframework occupancies revealed the presence of higher amount of ibuprofen (33.68%) than atenolol (11.55%) within the zeolite pores. According to bond distances analysis, both molecules directly interact with the zeolite framework, thus guaranteeing the molecule immobilization and preventing from uncontrolled release phenomena. The analysis of structural parameters allowed calculating both ellipticity and Crystallographic Free Area (CFA), which highlighted strong differences among the two drug-zeolite systems. Compared to the bare zeolite (unloaded-Y=46.26), CFA values after molecules adsorption increase: *ibu*-Y=56.58 and *atn*-Y=48.16. On the contrary, after loading no evident differences in channel shape and geometry were detected, thus confirming the high flexibility of zeolite framework. Based on the obtained results, the Y zeolite efficiency in ibuprofen and atenolol adsorption has been proved and its possible exploitation as sorbent materials in water remediation treatments can be assumed.

Altomare A., Cuocci G., Giacobozzo C., Moliterni A., Rizzi R., Corriero N. & Falcicchio A. (2013) - EXPO2013: a kit of tools for phasing crystal structures from powder data. *J. Appl. Crystallogr.*, 46, 1231-1235.

Larson A.C. & Von Dreele R.B. (1994) - General structure analysis system, report LAUR 86-748. Los Alamos National Laboratory Report LAUR, 86.

Martucci A., Rodeghero E., Pasti L., Bosi V. & Cruciani G. (2015) - Adsorption of 1, 2-dichloroethane on ZSM-5 and desorption dynamics by in situ synchrotron powder X-ray diffraction. *Micr. Mesop. Mater.*, 215, 175-182.

Rodeghero E., Martucci A., Cruciani G., Bagatin R., Sarti, E., Bosi V. & Pasti L. (2016) - Kinetics and dynamic behaviour of toluene desorption from ZSM-5 using in situ high-temperature synchrotron powder X-ray diffraction and chromatographic techniques. *Catal. Today.*, 227, 118-125.

Red mud neutralization by layered double hydroxides (LDHs) formation: differences in the synthesis process used

Belviso C.*¹, Belviso S.², Ragone P.¹ & Cavalcante F.¹

¹ Istituto di Metodologie per l'Analisi Ambientale – IMAA-CNR, Italy.

² Università della Basilicata, Dipartimento di Scienze and LASCAMM, CR-INSTM, Italy.

Corresponding email: claudia.belviso@imaa.cnr.it

Keywords: red mud, waste, layered double hydroxides.

Red mud (RM) is a waste material formed during the production of alumina when the bauxite ores are subjected to caustic leaching. The mineralogy of this waste is controlled by both treatment processes and bauxite ore composition. RM is generally characterized by the presence of iron oxyhydroxides such as hematite and goethite with minor aluminium hydroxides (i.e., boehmite). The other phases occurring on traces are calcium oxides, titanium oxides, aluminosilicate minerals and sodalite. Layered double hydroxides (LDH) are a wide family of synthetic layered materials with a brucite structure.

The general formula of LDHs is $[M^{II}_{1-x}M^{III}_x(OH)_2]_{x/n} \cdot zH_2O$ where M^{II} are divalent metal ions (Mg^{2+} , Ca^{2+} , Co^{2+} , Zn^{2+} , Cu^{2+} , Ni^{2+}) whereas M^{III} represent trivalent metal ions (Al^{3+} , Co^{3+} , Fe^{3+} , Cr^{3+} , Ni^{3+}). An- is representative of interlayer anions which hold together the positively charged brucite-like sheets through electrostatic attractions.

In this work, the action of the different methods (direct sonication energy or conventional hydrothermal process) in changing the mineralogical composition of RM was investigated. The data indicate that three main factors determine changes in mineralogical composition of RM: seawater solution, NaOH pre-fusion treatment and following sonication or hydrothermal process. However, the results display the higher efficiency of sonication in forming larger amount of layered double hydroxides.

Due to their properties, mainly represented by high specific surface area, catalysis character, ion-exchange capability and swelling abilities, LDHs have been used in many application including adsorption and catalysis. Based on this, LDHs formation in the bauxite residue represents an interesting method to neutralize RM. To confirm this, a preliminary characterization of adsorption properties of the synthetic products was performed testing the efficiency with Reactive Orange 16 (RO16). Tests on catalytic properties have been scheduled.

Petrofacies for the prediction of NOA content in rocks: application to the “Gronda di Genova” tunneling project

Botta S.^{*1-2}, Avataneo C.¹⁻⁴, Barale L.²⁻⁵, Compagnoni R.³⁻⁵, Cossio R.³⁻⁵, Marcelli I.¹⁻², Piana F.²⁻⁵, Tallone S.² & Turci F.⁴⁻⁵

¹ Gi-RES srl, CNR spin-off company, Torino, Italy.

² Institute of Geosciences and Earth Resources, National Research Council (CNR) of Italy, Torino, Italy.

³ Department of Earth Sciences, University of Torino, Italy.

⁴ Department of Chemistry, University of Torino, Italy.

⁵ “G. Scansetti” Interdepartmental Center for Studies on Asbestos and Other Toxic Particulates, University of Torino, Italy.

Corresponding email: serenabotta09@gmail.com

Keywords: Naturally Occurring Asbestos (NOA), meta-ophiolite petrography, asbestos quantitative analysis.

Realization of large geo-engineering projects in rocks containing Naturally Occurring Asbestos (NOA) must address several crucial geo-environmental issues, including the design of the construction site, the enforcement of health protection measures and the environmental-sustainable spoil management. This leads to a compelling need to develop effective and standard procedures to evaluate the distribution and concentration of NOA in rock volumes. To address this issue we introduced an innovative procedure to evaluate the asbestos distribution and concentration in complex geological settings through the definition of the “NOA petro-structural facies” (“NOA petrofacies” in brief). NOA petrofacies are fundamental asbestos-bearing rock types, showing recurrent lithological and structural features controlling asbestos occurrence.

The NOA petrofacies approach was developed and tested in a geo-environmental study for the evaluation of the asbestos content for the “Gronda di Genova” highway by-pass project (Genoa, NW Italy), contemplating the realization of about 54 km of tunnels partly excavated in potentially asbestiferous rocks (meta-ophiolites).

Eight main NOA petrofacies have been defined on the ground of: i) macro and mesoscopic field observations, ii) optical microscopy and micro-Raman spectroscopy analyses, and iii) quantitative determination of fibrous minerals by SEM-EDS. NOA petrofacies were then categorized into four classes depending on their expected asbestos content (very high, high, low, and nil). NOA petrofacies approach was used to predict the distribution and relative abundance of NOA in each excavated lithotype and in each geologically homogeneous tunnel segment.

A recursive integration and refinement of the NOA petrofacies characters will be achieved by applying this approach to other case-studies in asbestos-rich natural settings.

Occupational and anthropogenic environmental exposure during asbestos-cement production by FIBRONIT in Broni (Pavia): assessment of asbestos lung burden by SEM-EDS

Capella S.*¹⁻², Visonà S.³, Osculati A.³ & Belluso E.¹⁻²

¹ Department of Earth Sciences. University of Torino.

² Interdepartmental Center for Studies on Asbestos and other Toxic Particulates “G. Scansetti”, University of Torino.

³ Department of Public Health, Experimental and Forensic Medicine, Section of Legal Medicine and Forensic Sciences. University of Pavia.

Corresponding email: silvana.capella@unito.it

Keywords: asbestos, SEM-EDS, mesothelioma.

Despite the relation between occupational exposure to asbestos and asbestos related diseases (ARD) is well documented, many issues concerning the etiopathogenesis of ARD are still debated. For example, the role of fiber species and dimension (length and thickness), the importance of exposure dose and the dose-response effect are still questioned.

Moreover, the synergic collaboration between mineralogists and pathologists for a multidisciplinary assessment of the diagnosis of ARD helps to investigate the complex pattern of legal, social, and political issue.

The aim of this study is to put together the mineralogical and medical knowledge in order to investigate a cohort of 188 subjects, some of whom worked at Fibronit (Broni, Pavia, Italy), an important asbestos cement factory (active between 1932 and 1993), and others lived in the surrounding area, in order to clarify the role of asbestos in the etiopathogenesis.

Different issues have been addressed: the latency time before the diagnosis, survival time since the diagnosis, effect due to cigarette smoking, relationship between the concentrations of asbestos fibers in lung tissue and ARD, kind of exposure (occupational and anthropogenic environmental), possible gender differences.

To carry out this complementary investigation, a group of 40 subjects was selected from a larger series of autopathic lung samples; specifically: 20 males with occupational exposure (10 died for mesothelioma and 10 for asbestosis), and 20 subjects with anthropogenic environmental exposure (10 men and 10 women died for mesothelioma).

The inorganic residue of a portion of lung tissue of each subject was investigated by scanning electron microscopy with energy dispersion spectroscopy (SEM-EDS). The following information concerning asbestos fibers were detected: length and width, mineralogical species, and concentration per gram of dry tissue (Belluso, 2006). In addition, typical asbestos bodies were also counted, because hallmark of exposure to asbestos.

Most of the asbestos fibers detected have been identified as crocidolite and amosite.

The data show that, a considerable number of subjects with occupational exposure and high burden of crocidolite and amosite (high dose exposure) did not develop mesothelioma; and that there are subjects with anthropogenic environmental exposure and low burden of crocidolite and amosite (low dose exposure) that developed and died owing to mesothelioma. This fact is consistent with a different predisposition between individuals of the series, probably explained by a genetic substrate.

The present data appear to support the hypothesis that even an exposure to a very low amount of asbestos can cause mesothelioma in hypersusceptible subjects.

Belluso E., Bellis D., Fornero E., Capella S., Ferraris G. & Coverlizza S. (2006) - Assessment of Inorganic Fibre Burden in Biological Samples by Scanning Electron Microscopy – Energy Dispersive Spectroscopy. *Microchimica Acta*, 155 (1), 95-100.

Trace metal contents and mobility in mine wastes of the Central Wales mine district: environmental implications

Chilleri E.¹, Byrne P.², Onnis P.², Lattanzi P.*³, Costagliola P.¹, Rimondi V.¹

¹ Università di Firenze.

² Liverpool John Moores University.

³ CNR-IGG.

Corresponding email: pierfrancolattanzi@gmail.com

Keywords: stream sediments, heavy metals, Wales.

Despite the decline of metal mining in the UK during the early 20th century, a substantial legacy of metal contamination persists in river channels and floodplain sediments. Contaminated drainage from mine wastes can severely impact the hydrological and ecological systems.

This study is a part of a larger project aiming to determine extractable metals content and to assess geochemical and mineralogical controls in mine wastes of the Central Wales mine District.

Eight samples were collected from the abandoned mine wastes occurring along the Nant Cwmnewyddion river, at two locations: excavation spoils at the Frongoch Adit and suspected tailings at a location further downstream, described here as Duck Point. Samples were dry-sieved into three size fractions (<63, 64-250, and 251–2000 µm); mineralogy was characterized by XRD.

The different fractions were subjected to a microwave digestion followed by ICP-AES analysis to determine the (pseudo)total contents of Pb, Zn, Cu, Cd, Fe, Mn and Mo, and a BCR three-step Sequential Extraction Protocol to define the solid fractions to which metals are bound. Furthermore, batch leaching experiments at different contact times, grain sizes, pH and liquid/solid ratios were conducted.

All the samples of Frongoch Adit show high total concentrations (mg/kg) of Pb (maximum 6870) and Zn (maximum 10854), and also of Cu (25-663) and Cd (2.6-441) in one sample; otherwise, the highest concentrations of Mn (478-1313) and Mo (0.8-2.6) are detected at Duck Point. For all the metals, the easily exchangeable and carbonate-bound fraction represents a low percentage of the total metal contents: <1% for Fe and Mo, < 15% for Cu, Cd and Mn, with a maximum of 20% and 30% for Zn and Pb. However, this aliquot contains the highest metal concentrations of the three sequential extraction steps: > 50% for most samples, except for samples with a high step 3 aliquot.

The sum of the concentrations detected by the three extractive steps was compared with the environmental quality limit (PEL) suggested by the Environmental Agency of England and Wales. All spoil samples exceed the PEL for Pb, and one sample also for Zn, Cu and Cd; moreover, three samples of Duck Point exceed the PEL for Pb and one for Zn.

In conclusion, the studied sediments are contaminated with potentially harmful metals beyond recommended limits. A significant fraction of metals is considered easily and/or moderately available for aquatic organisms. Therefore, the analysed sediments may represent a threat for the integrity of the surrounding ecosystem, identifying a diffuse source of contaminants in the spoil heaps of Frongoch Adit, and a potential secondary source at Duck Point.

The results of this study support the general concept that dispersed river sediment may store significant amount of metals. Their potential release should be considered in monitoring and remediation strategies.

Identification of asbestos fibers in tissues of patients affected by important diseases in extra respiratory systems

Croce A.*¹, Rinaudo C.¹, Grosso F.², Erra S.³ & Amisano M.F.⁴

¹ Department of Science and Technological Innovation - University of Eastern Piedmont, Alessandria, Italy.

² Mesothelioma Unit – Oncology – SS Antonio e Biagio e Cesare Arrigo, General Hospital, Alessandria, Italy.

³ S. Spirito Hospital, Department of Anatomy and Pathology, Casale Monferrato, Italy.

⁴ S. Spirito Hospital, General Division Surgery, Casale Monferrato, Italy.

Corresponding email: alessandro.croce@uniupo.it

Keywords: Asbestos fibers, GI cancers, Scanning Electron Microscopy.

The relationships between inhaled asbestos fibers and development of important respiratory diseases (asbestosis, pulmonary carcinoma, mesothelioma...) has been demonstrated by many scientific works and therefore the role of the asbestos in these sicknesses is now universally accepted. The International Agency for Research on Cancer recognized also for other malignancies, as larynx and ovary cancers, an association with past exposure to asbestos (International Agency for Research on Cancer, 2012). For others, as gastrointestinal (GI) cancers, the evidence of the correlation is until now not sufficiently sound (Gamble, 1994; Brandi et al., 2013). A way to contribute at the understanding of the asbestos role in the development of GI cancers is to investigate the number, type, and localization of asbestos fibres in the various human organs affected by the diseases. Being our University and Hospitals placed in an area of the Piedmont sadly famous for the high incidence of asbestos related diseases, as consequence of the presence of an Eternit factory working large contents of asbestos until 1986, we tried to define if asbestos fibers may be localized in GI tract in neoplastic or near neoplastic tissues. A previous elaborated methodology, allowing fiber detection in thin sections used for medical diagnosis under Variable Pressure Scanning Electron Microscopy with annexed Energy Dispersive Spectroscopy (VP-SEM/EDS), has been applied. Tissues from patients living in the highly asbestos polluted area and affected by different GI diseases:

- benign biliary tract diseases,
- mesothelioma and important disorders in the gallbladder,
- cholangiocarcinoma,
- neoplasia of colon,
- were analyzed. Asbestos fibers or bundles of asbestos fibers, in particular of crocidolite and chrysotile, were detected in most examined sections. The results obtained during this work will be presented and discussed.

Brandi G., Di Girolamo S., Farioli A., de Rosa F., Curti S., Pinna A.D., Ercolani G., Violante F.S., Biasco G. & Mattioli S. (2013) - Asbestos: a hidden player behind the cholangiocarcinoma increase? Findings from a case-control analysis. *Cancer Causes Control*, 24, 911–918.

Gamble J.F. (1994) - Asbestos and colon cancer: a weight-of-the-evidence review. *Environ. Health Perspect.*, 102, 1038-1050.

International Agency for Research on Cancer (IARC). (2012) - Asbestos (chrysotile, amosite, crocidolite, tremolite, actinolite, and anthophyllite). In IARC (Ed.): *IARC Monographs on the Evaluation of Carcinogenic Risks to Humans*. Vol. 100C, 219–309. IARC, Lyon, France.

Ash leachates from Yasur volcano (Vanuatu): human and livestock health assessment implications

D'Aleo R.*¹, Cangemi M.¹, Speziale S.², Garabeiti E.³, Madonia P.¹ & Favara R.¹

¹ Istituto Nazionale di Geofisica e Vulcanologia, Sezione di Palermo.

² Deutsches GeoForschungsZentrum, Potsdam, Germany.

³ Department of Meteorology and Geohazards, Port Vila, Vanuatu.

Corresponding email: robertodaleo@gmail.com

Keywords: Ash leachates, Yasur volcano, human health implications.

People who live nearby open vent basaltic volcanoes are exposed to numerous risks such as violent eruptions and earthquakes, but either less destructive volcanoes activities could be dangerous for human health. Volcanic ash, gas or aerosol, may be inhaled or ingested by the population exposed to volcano activity. Persistent strombolian activity releases in the volcano's surrounding environment small, but continuous, amount of volcanic ash that represents one of the most important sources of contaminants at global scale. Due to their small size, ash particles are easily mobilized in the atmosphere and can reach areas far from the emission points. The smallest size particles of volcanic ash can be breathed or ingested directly from the atmosphere or by the consumption of food and water that were in contact with. During degassing activity or eruptions, a huge amount of gas, aerosol and metal salts are absorbed on volcanic ash surface, rapidly scavenged if in contact with water and /or organic fluids (gastric fluids). So, long-term exposition to volcanic ash could lead to chronic impacts on human health. Remote and isolated villages often use roof water catchment systems to collect rainwater in PVC tanks. These water storage systems could lead to mix freshly erupted ash with drinking water that can mobilize elements scavenged from volcanic gas by the ash, some of these are dangerous for human health. We report on results of water and simulated-gastric leachate experiments of Yasur volcanic ashes, a volcano situated in Tanna, a small island in the Vanuatu archipelago (South Pacific region) densely populated. Up to 25800 people are potentially exposed to the semi-continuous volcanic activity. Our data show that trace element potentially able to generate concern for human health, in simulated water leachate, are below the Maximum Admitted Concentration established by the World Health Organization. On the other hand, the simulated gastric leachate reveals higher concentration of this pollutant. In order to quantify the potential impact for human health we calculate, for each element, the Tolerable Daily Intake (TAI), related to ash ingestion. This data, compared with Mediterranean volcanoes, shown a low risk for this hazard. The increase of tourism, attracted by the spectacular explosion and by the easy access to the volcano's vents, creates new work figure in the island, the so-called volcanic guide. These guides are daily expose to volcanic gases emitted by Yasur activity as HCl, H₂S and SO₂ that can cause chronic health disease like asthmatic bronchitis, eye irritation, and lung problem due to acid aerosols.

An EPR study of silica radicals in lung tissues with evidence of silicosis

Di Benedetto F.*¹, Belluso E.², Capella S.²⁻³, Giaccherini A.¹⁻⁵, Romanelli M.¹, Ciuffi B.⁶, Montegrossi G.⁴, Zoleo A.⁷ & Capacci F.⁸

¹ Department of Earth Sciences, University of Florence, Florence, Italy.

² Department of Earth Sciences, University of Torino, Torino, Italy.

³ Interdepartmental Centre for Studies on Asbestos and Other Toxic Particulates G. Scansetti, University of Torino, Torino, Italy.

⁴ Institute of Geosciences and Earth Resources, CNR, Unit of Torino, Torino, Italy.

⁵ Department of Industrial Engineering, University of Florence, Florence, Italy.

⁶ Department of Chemistry, University of Florence, Florence, Italy.

⁷ Department of Chemical Sciences, University of Padua, Padua, Italy.

⁸ Dipartimento di Prevenzione, PISLL, Health Agency of Tuscany (USL Toscana Centro), Florence, Italy.

Corresponding email: francesco.dibenedetto@unifi.it

Keywords: Crystalline silica, health effects, EPR spectroscopy.

The study of inorganic radicals associated to the respirable crystalline silica (RCS) is relevant for the definition of the health issues (silicosis, lung cancer and self-immune diseases) related to occupational exposure contexts.

In this study, a continuous-wave (cw) and pulsed Electron Paramagnetic Resonance (EPR) investigation of human lung tissue samples of an individual diagnosed of silicosis has been carried out. This technique, in fact, is able to trace the presence of radicals and of selected paramagnetic metal ions. Both types of paramagnetic species were observed through the cw-EPR survey, but their spectra resulted heavily superimposed. Through the use of an opportune set of pulse sequence and temperature, we were able to discern the two species, attributing the metal ion contribution to Cu(II) and the radical to an inorganic species. From the time-domain patterns, Cu(II) is found to interact with nitrogen atoms, thus supporting its attribution to biological Cu. Preliminary considerations about the radical species suggest its similarity to the inorganic Si· radicals already described in the literature.

Distribution and concentration of potentially toxic elements in ultramafic rocks: a case study from the Voltri Massif (Western Alps, Italy)

Fornasaro S.¹, Comodi P.², Crispini L.¹, Malatesta C.*¹, Zucchini A.² & Marescotti P.¹

¹ Dipartimento di Scienze della Terra, dell' Ambiente e della Vita, Università di Genova.

² Dipartimento di Fisica e Geologia, Università di Perugia.

Corresponding email: cristina.malatesta@unige.it

Keywords: geogenic source, serpentinization, potential toxic elements.

High concentrations of potentially toxic elements (PTEs) in surface and near-surface environment may be attributed both to anthropogenic sources (including industrial, agricultural, and mining activities) and to geogenic sources (e.g., natural weathering of rocks and pedogenesis).

Among the geogenic sources, ultramafic rocks (e.g., dunite, peridotite, pyroxenite, and serpentinite) are the most critical from the environmental point of view because they are invariably characterized by high amounts of Cr, Ni, and Co.

Despite a general similarity in the whole rock chemical composition, the concentration and distribution of PTEs in ultramafic rocks is highly variable. In general, PTEs content can range up to two orders of magnitude, mainly because of heterogeneities in mineralogy and mineral chemistry, textural, and structural features of the ultramafic rocks. All these factors are strictly related to the various local geological settings as well as to the metamorphic and geodynamic evolutions of these rocks.

The aim of the work is to assess the role of local-scale lithological, textural, and structural factors in the distribution of PTEs in different ultramafic rocks occurring in the high-pressure and low-temperature ophiolites from Voltri Massif (Liguria, NW Italy).

The mineralogy, petrography, and crystal chemistry were investigated by means of optical microscopy, XRPD, SEM-EDS, EMPA-WDS, and LA-ICP-MS. Major, minor, and trace element concentrations were analyzed in situ and in laboratory by means of FP-EDXRF, ICP-EOS, and ICP-MS.

The results evidenced that Cr (up to 4183 ppm), Ni (up to 3900 ppm), and Co (up to 334 ppm) are invariably the PTEs with the highest concentrations; in addition, V, Cu, and Zn are systematically found in non-negligible amounts.

Spinel-group minerals (chromium spinel, ferrian chromite, chromium magnetite, and magnetite) are by far the main potential source of the PTEs. Nevertheless, several PTEs are also present within serpentines, olivines, pyroxenes, chlorites, as well as within accessory phases (e.g., ilmenite and Ni-sulphides) and within authigenic minerals formed in the early stages of rock weathering (cryptocrystalline to amorphous Fe-oxides and -oxyhydroxides).

The multidisciplinary approach used in this work allow to evidence that the most important factors controlling the PTEs variability are the degree of serpentinization (from partially serpentinized peridotites to highly deformed and foliated serpentinites) as well as the style and intensity of deformation, which in turn controls the mineralogical assemblage.

Human Health vs. Urban Geochemistry during the Anthropic Times

Funari V.*¹, Toller S.¹ & Costa A.²

¹ Dipartimento di Scienze Biologiche Geologiche e Ambientali (BiGeA), Università di Bologna, Bologna, Italy.

² National Cancer Institute (CRO), Aviano, Italy.

Corresponding email: valerio.funari@unibo.it

Keywords: medical geochemistry, anthropic contamination, incidence of pathologies.

Following the need to deliver innovation in the epoch that can be currently referred to as Anthropocene we have undertaken a joint research on medical geochemistry that combines a flair for methods development deriving from our different scientific background. At the BiGeA Department (University of Bologna) much work has been done on waste management and critical raw materials recovery from incinerators ashes, with the stimulating discussion at the CA15115 (MINEA), especially in working group n. 3. Our research on geochemistry extends to the environmental characterisation and impact assessments of soils and waters (at Ravenna Campus of Environmental Sciences) until the reach of molecular biology and cancer research (at the National Cancer Institute CRO, University of Trieste, Aviano).

Here we report our comparative analysis of environmental processes and human health issues that can serve as a starting point for further studies during the anthropic times. In particular, we explore the linkers between the environmental issues related to municipal solid waste and incinerated residues, anthropic contamination at stream sediments, and the incidence of human health threats. The geographic boundary of the study is the highly urbanised area of the Emilia-Romagna region, Italy. Our final aim is to create a link between different sectors and try to find a common language to work together.

Solubility Assay of the Natural Zeolites Erionite, Offretite and Stellerite

Giordani M.*¹⁻², Di Lorenzo F.¹, Mattioli M.² & Churakov S.¹⁻³

¹ Institute of Geological Sciences, University of Bern, Switzerland.

² Department of Pure and Applied Sciences, University of Urbino Carlo Bo, Italy.

³ Paul Scherrer Institute, Bern, Switzerland.

Corresponding email: matteo.giordani@uniurb.it

Keywords: Zeolite, fibre, Erionite.

Fibrous zeolites assumed in the last years a growing interest in the scientific community because of their effects on human health after inhalation. The International Agency for Research on Cancer (IARC, 1987) established erionite as the most carcinogenic zeolite fibre. Recently, other fibrous zeolites have been suspected to be dangerous for human, such as offretite (Mattioli et al., 2018), due to its structural and chemical similarities with erionite. The toxicity of these minerals is mainly defined by two important parameters: biodegradability and biopersistence. To the best of our knowledge, experimental solubility data for erionite and offretite are still missing. The lack of these data for natural zeolites, even in simple systems (e.g., in water), represents a severe limitation for the understanding of the complex interaction with the biological environments. This study aims to be a starting point for further detailed studies on the dissolution of zeolites. The defined experimental setup potentially allows to figure out the effect of biochemical agents and this could improve our knowledge on the pathways linking fibrous zeolites and health hazards.

Dissolution experiments were performed to assess the aqueous solubility of natural samples of erionite, offretite and stellerite at 25° C, under the effect of atmospheric CO₂ concentration.

The natural crystals were ground and sieved to obtain a relatively homogenous crystal particle size in the range 64 µm - 250 µm. The powders were added to ultrapure H₂O (previously equilibrated with air for 30 minutes under stirring, i.e. in equilibrium with atmospheric CO₂ at pH 5). The dissolution process was followed over time with a conductivity probe equipped on a Metrohm OMNIS system. After 7 days under vigorous stirring (a floating stirrer was used to avoid a milling effect on the crystals), the samples were filtrated and the amount of Ca, Na, K, Mg, Al and Si was determined by ICP-OES (Agilent Varian, 700 ES).

The powders were characterized before and after the interaction period. X-ray powder diffraction was used for the mineralogical characterization. SEM-EDS and EMPA were used for the morphological characterization of the grains and the determination of the elemental formula, respectively.

IARC (1987) - IARC Monographs on the Evaluation of the Carcinogenic Risk to Humans; Overall Eval. Carcinog. Updating IARC Monographs Vol. 1 to 42; IARC: Lyon, France.

Mattioli M., Giordani M., Arcangeli P., Valentini L., Boscardin M., Pacella A. & Ballirano P. (2018) - Prismatic to Asbestiform Offretite from Northern Italy: Occurrence, Morphology and Crystal-Chemistry of a New Potentially Hazardous Zeolite. *Minerals*, 8, 69.

Pyrite separation in copper enrichment plants as a key to circular economy driven remediation: a case study from Northern Albania Cu mining district

Grieco G.*¹, Sinojmeri A.² & Cavallo A.³

¹ Dipartimento di Scienze della Terra “A. Desio”, Università degli Studi di Milano, Milano Italy.

² Department of Earth Sciences, Faculty of Geology and Mining, Polytechnic University of Tirana, Albania.

³ Dipartimento di Scienze dell’Ambiente e della Terra, Università di Milano Bicocca, Italy.

Corresponding email: giovanni.grieco@unimi.it

Keywords: Pyrite, Albania, Circular Economy.

Pyrite has been for a long time a major commodity due to its use for the production of sulfuric acid. In the last decades it has been progressively replaced by elemental sulfur recovered from oil refining. As a result pyrite mining was abandoned as well as its recovery as a by-product from sulfide ores. Nevertheless, a minor pyrite market, related to other uses, survived and is today growing.

Pyrite is a common phase in several classes of ore deposits and is today reported to the tailings. Here pyrite, due to its abundance, high reactivity and high S to metal ratio is the main responsible of Acid Mine Drainage.

The present study aims to ascertain the change in tailings environmental impact due to the transition from double flotation, with separation of pyrite as a by-product, and single flotation, without pyrite separation. The northern Albania Cu mining district was chosen as a case study because, due to its industrial policy, this country was one of the last to abandon sulfuric acid production from pyrite, so the transition can be studied in recent and present day tailings. Moreover, strongly different tailings due to changes in flotation flowsheet have already been described at the abandoned Reps beneficiation plant (Fantone et al., 2017).

The study was developed on Fushe Arrez enrichment plant, still working during sampling. The plant feed comes from a pyrite-rich massive sulfide ore, hosted in andesitic to basaltic lavas belonging to the upper portion of the Mirdita ophiolite crustal sequence.

At Fushe Arrez the separation of pyrite was abandoned in the late '90. Here the old pyrite-poor and the still active pyrite-rich tailings were stacked in the same valley impoundments but in two well distinct areas. Waters flowing out of the tailing system are acidic and very rich in metals.

Acid Base Accounting, leaching and buffering tests were conducted on both pyrite rich and poor tailings. High pyrite tailings are responsible for most of the metal release and the water treatment of these materials is much more complex and expensive, as neutralization and precipitation of metals cannot be achieved via reaction with calcium carbonate as it happens with pyrite-poor tailings.

The results show that pyrite separation is an efficient technique to strongly reduce the environmental impact of tailings. In a circular economy view this technique could be very cost effective to get both important environmental impact reduction and secondary raw material production. Results also show that, due to their very high pyrite content, single flotation tailings could be a urban mining source of pyrite. The increase in pyrite demand is pivotal in this view and an effort should be done to enhance research to increase pyrite industrial applications.

Fantone I., Grieco G., Sinojmeri A. & Cavallo A. (2017) - A quantitative approach to the influence of pyrite separation on Cu-processing tailings: a case-study at Reps, Mirdita District, Albania. *Environ. Earth Sci.*, 76(22), 774.

Potential Environmental risk induced by TiO₂ dispersions in waters and sediments: a case history of the Frido stream deposits (Southern Apennines, Italy)

Lettino A.¹, Belviso C.¹, Cavalcante F.*¹ & Fiore S.¹

¹ Istituto di Metodologie per l'Analisi Ambientale – IMAA-CNR, Italy.

Corresponding email: francesco.cavalcante@imaa.cnr.it

Keywords: Rutile/Anatase, SEM/XRD, Liguride Complex.

Titanium dioxide (TiO₂) exists in nature in three different crystalline forms: rutile, anatase and brookite. Rutile and anatase are the most common phases, which are accessory minerals in different types of igneous and metamorphic rocks and can also be found as mineral grains in clastic sedimentary rocks. Due to its properties, TiO₂ has been used in many industrial products although the increasing demand of this phase has caused some concerns regarding its high presence in the environment and its effects on human health (Shi et al., 2013). In 2010, The International Agency for Research on Cancer (IARC 2010) has classified TiO₂ as minerals potential carcinogenic to humans on the basis of particle size and shape. However, at the present, epidemiological data do not clearly support this hypothesis. Also some literature data have shown that nanometric titanium dioxide minerals are potentially harmful to human health indicating that the toxicity of TiO₂ primarily depends on the size, specific surface and crystalline form. Although the main risk is associated with anthropogenic TiO₂ dispersion, in the last few years increasing attention has also been paid on naturally occurring TiO₂ minerals. In this work, the potential role of rutile and anatase dispersion from natural outcrops on human health was investigated with the aim to determine the amount of these minerals in the rocks as well as their susceptible to be environmentally released (geoavailability and the geoavailability degree, respectively). The studied area is located in the southern Apennines (Italy) and it coincides with the drainage basin of the Frido stream. Geological data indicate that rutile and anatase are the major components of heavy minerals in HP/LT metamorphic slates of the Frido Unit (Liguride Complex); these phases are also present in fluvial sediment that originates from degradation processes. To evaluate the environmental 'contamination' from titanium dioxide in different water–rock–sediment matrices, 14 samples were analyzed by X-ray diffraction (XRD) and scanning electron microscopy (SEM) combined with elemental analysis (EDX). The suspended TiO₂ particle concentration was also calculated for each water sample. The results indicated that the potential risk is correlated not only with the presence of TiO₂ minerals in the source rocks but also with its presence in rock degradation products (i.e., fluvial detritus).

IARC (International Agency for Research on Cancer) (2010) - IARC Monographs on the evaluation of carcinogenic risks to humans, V. 93, Carbon Black, Titanium Dioxide, and Talc. <http://monographs.iarc.fr/ENG/Monographs/vol93/mono93-7>.

Shi H., Magaye R., Castranova V. & Zhao J. (2013) - Titanium dioxide nanoparticles: A review of current toxicological data. *Particle and Fibre Toxicology*, 10–15, 1–33.

Fibrous ferrierite from the Lessini Mounts, Veneto Volcanic Province, NE Italy

Mattioli M.*¹, Giordani M.¹, Ottaviani M.F.¹, Cangiotti M.¹, Valentini L.², Di Giuseppe D.³ & Gualtieri A.F.³

¹ Dipartimento di Scienze Pure e Applicate, Università di Urbino Carlo Bo.

² Dipartimento di Scienze Biomolecolari, Università di Urbino Carlo Bo.

³ Dipartimento di Scienze Geologiche e Chimiche, Università degli Studi di Modena e Reggio Emilia.

Corresponding email: michele.mattioli@uniurb.it

Keywords: Zeolites, ferrierite, fibres.

Ferrierite belongs to the mordenite group and is one of the most siliceous naturally occurring zeolites. It comprises several species with the same crystal structure (ferrierite framework, FER) but different extra-framework cations (Mg, K, and Na). Ferrierite has a general chemical formula $(Mg_{0.5}, Na, K)_6[Al_6Si_{30}O_{72}] \cdot 20H_2O$ and commonly crystallizes in the orthorhombic space group *Immm*.

Ferrierite may have very different crystal habits such as lamellar, flattened prismatic, acicular, fibrous, and asbestiform. A very recent study (Gualtieri et al., 2018) has shown that ferrierite with a fibrous-asbestiform crystal habit may have the same chemical-physical properties (morphometric parameters, specific surface area, and iron content) of carcinogenic fibrous erionite. Therefore, the presence of fibrous ferrierite is of concern for risk to human health, especially if one considers the potential exposure of workers handling this material or populations living nearby ferrierite outcrops.

Ferrierite often has a hydrothermal origin and is related to the presence of fluids arising and heated from below. In this setting, it has mainly been found in voids of volcanic rocks, coexisting with other zeolites (e.g., heulandite, mordenite, analcime, chabazite, harmotome), carbonates, barite and silica. Ferrierite can also have a diagenetic origin, deriving from a variety of precursor materials including tuffaceous sediments, volcanic glass and aluminosilicate minerals that react to form zeolites by dissolution-precipitation processes. Diagenetic ferrierite often coexists with mordenite, clinoptilolite, feldspars, and quartz.

Recently, new occurrences of hydrothermal ferrierite were detected in the Lessini Mounts (NE Italy), where a thick sequence of lava flows of Veneto Volcanic Province extensively crops out. The crystal habit of ferrierite ranges from flattened-prismatic to asbestiform (elongated, thin and slightly flexible fibres). Single fibres appear with a needle-like crystal habit, while some fibrous crystals have a slight degree of curvature. The crystal habit composed of single needles is similar to that of fibrous erionite, and several fibres are often aggregated in bundles. According to the WHO counting criteria, most of the ferrierite fibres can be classified as breathable.

The discovery of fibrous and asbestiform ferrierite in Northern Italy suggests the need for a detailed risk assessment in all Italian areas showing the same potential hazard, with specific studies such as a quantification of the potentially respirable airborne fibres and targeted epidemiological surveillance.

Gualtieri A.F., Bursi Gandolfi N., Passaglia E., Pollastri S., Mattioli M., Giordani M., Ottaviani M.F., Cangiotti M., Bloise A., Barca D., Vigliaturo R., Viano A., Pasquali L. & Gualtieri M.L. (2018) - Is fibrous ferrierite a potential health hazard? Characterization and comparison with fibrous ferrierite. *American Mineralogist*, 103, 1044-1055.

Laboratory and synchrotron radiation-based techniques to investigate the soil-plant system in Zn-extreme environments

Medas D.*¹, Carlomagno I.², Meneghini C.³, Pusceddu C.¹ & De Giudici G.¹

¹ Department of Chemical and Geological Sciences, University of Cagliari, Italy.

² Elettra-Sincrotrone Trieste, Basovizza, Trieste, Italy.

³ Department of Sciences, University of Roma Tre, Italy.

Corresponding email: dmedas@unica.it

Keywords: *Juncus acutus*, biominerals, synchrotron radiation (SR) techniques.

Abandoned mining activities represent a source of pollution of harmful elements that can disperse into the atmospheric, terrestrial and aquatic ecosystems (Passariello et al., 2002). Interactions between living organisms and the geosphere play a fundamental role in controlling metal mobility and their understanding provide the fundamentals to i) elucidate the biogeochemical cycle of elements, ii) develop quantitative biomonitoring tools, and iii) improve biotechnologies as bioremediation, phytoremediation and phytomining.

Phytoremediation and phytomining exploit plants that have naturally developed defense strategies for surviving under elevated metal contents (Caldelas & Weiss, 2017) or genetically modified plants. This work aims to investigate the plant species *Juncus acutus* (Medas et al., 2019) spontaneously grown in three different abandoned mining areas in SW Sardinia (Italy). Samples were investigated by an interdisciplinary and multi-technique approach combining conventional (chemical analysis, X-ray diffraction and scanning electron microscopy) with advanced synchrotron radiation (SR) techniques, such as micro-X-ray fluorescence mapping (μ -XRF) and X-ray absorption spectroscopy (XAS). Zinc, Pb and Fe are the most abundant metals, with Zn ranging between 2 and 8 w/w % in the rhizospheres. In *Juncus acutus*, Zn is mainly accumulated in the root epidermis and its chemical environment is site-dependent and multi-phase (amorphous Zn silicate, Zn apatite, Zn hydroxycarbonate, and Zn sulphate). Also, different Zn-organic complexes (e.g. Zn histidine and Zn cysteine) were mainly detected in the plants collected from the site characterized by the highest Zn concentration, and they were identified as part of a detoxification strategy.

Combination of SR complementary probes revealed novel unexpected biomineralization paths and demonstrated that biogeochemical interactions play a relevant role in the Zn cycle. The accumulation of Zn in the plant roots makes *Juncus acutus* a valuable autochthonous plant employable in the development of phytostabilization techniques. The variation of Zn speciation suggests that *Juncus acutus* has developed its own site-specific molecular processes that have to be carefully considered during the selection and management of phytoremediation techniques.

The authors acknowledge CESA (E58C16000080003) from RAS and RAS/FBS (F72F16003080002) grants.

Caldelas C. & Weiss D.J. (2017) - Zinc Homeostasis and isotopic fractionation in plants: a review. *Plant Soil*, 411, 17-46.

Medas D., De Giudici G., Pusceddu C., Casu M.A., Birarda G., Vaccari L., Gianoncelli A. & Meneghini C. (2019) - Impact of Zn excess on biomineralization processes in *Juncus acutus* grown in mine polluted sites. *J. Hazard. Mater.*, 370, 98-107.

Passariello B., Giuliano V., Quaresima S., Barbaro M., Caroli S., Forte G., Carelli G. & Iavicolic I. (2002) - Evaluation of the environmental contamination at an abandoned mining site. *Microchem. J.*, 73, 245-250.

Lower and upper aspect ratio range to consider on quantitative determination of Elongated Mineral Particles (EMP) in bulk samples and in vitro study

Militello G.M.*¹, Gaggero L.¹, La Maestra S.², Sanguineti E.¹, Yus González A.¹ & Lavagnino G.¹

¹ Dipartimento di Scienze della Terra, dell' Ambiente e della Vita, Università di Genova.

² Dipartimento di Scienze della Salute, Università di Genova.

Corresponding email: gaiamaria.militello@edu.unige.it

Keywords: cleavage fragments, aspect ratio, in vitro test.

The World Health Organization (WHO) established chrysotile, asbestos tremolite and actinolite, crocidolite, amosite and anthophyllite as asbestos belonging to group I carcinogens. The effects on the health of prismatic/acicular analogues (EMP) of asbestiform phases are still debated, as they are not regulated, although their geometric ratios fall within the definition of fibers (length >5 µm, Ø < 3 µm; aspect ratio > 3:1). The comminution of samples is fundamental for the reproducible quantification of fibers. However, the preparation method described in the Italian Ministerial Decree 06/09/1994 is indicative and lacks one coding. Moreover, the comminution can originate artifacts from pristine acicular/prismatic habit classifiable as fibers. Following the Decree all. 1B, for analysis by Scanning Electron Microscopy (SEM), three asbestiform samples of the actinolite-tremolite series and three made of prismatic/acicular ones were addressed. For each sample, three aliquots (3 g each) were mechanically milled for 30", 2 and 5 min respectively, at constant speed. All samples milled for 30" showed that asbestiform amphiboles originate fibers and others break as prismatic. For longer grinding, this distinction is less apparent.

In vitro tests on cell lines were carried out on the two types, on the fraction ≤ 10 µm.

Oxidative stress is the central mechanism involved in the carcinogenicity induced by asbestos. To mimic intra-alveolar environmental conditions were used A549 (human alveolar basal epithelial cell line derived from lung carcinoma) and RAW 264.7 (mouse monocyte cell line). Preliminary to identify sub-toxic fiber doses unable to cause a cell death over 30%, crystal violet was performed. The cells were exposed to 2.2, 6.6, 22, 50, and 100 µg/ml of each sample, and after 24, 48 and 72 h of incubation, the cell monolayers were rinsed, stained with crystal violet, and dried. The dye taken up by the cells was solubilized and absorbance was read at 590 nm using a microtiter plate reader.

The intracellular reactive oxygen species assessment was evaluated by using the molecule 2', 7'-dichlorofluoresceindiacetate (DCF-DA). Cell monolayers were preliminarily loaded with 2 µM DCF-DA and after 3 h the redox state was quantified by spectrophotometer. After, to examine the genotoxicity/clastogenicity effect induced by exposure at the different fibers the micronucleus test was performed in both cell lines.

The results highlight how critical the asbestos comminution phase is in the preparation of the samples.

Thus, the aspect ratio and the morphology of the fibers play a role in the assessment of health risk; it is debatable what aspect ratio is to be considered as lower and upper limits of a range. Instead, it is proved that fibers with > 20:1 ratio, although EMP, are potentially carcinogenic as not easily phagocytosed by macrophages, therefore not removed from the lungs (Addison, 2008).

Addison J. & McConnell E.E. (2008) – A review of carcinogenicity studies of asbestos and non-asbestos tremolite and other amphiboles. *Regul. Toxicol. Pharmacol.*, 52, S187–S199.

Mechanical properties of calcium apatite-based biominerals: hydroxylapatite (P63) and type-A carbonated apatite (P1)

Moro D.*¹, Ulian G.¹ & Valdrè G.¹

¹ Centro di Ricerca Interdisciplinare di Biomineralogia, Cristallografia e Biomateriali, Dipartimento di Scienze Biologiche, Geologiche e Ambientali, Università degli Studi di Bologna, Bologna, Italy.

Corresponding email: daniele.moro@unibo.it

Keywords: Calcium apatites, thermophysical properties, Density Functional Theory.

Calcium apatites biominerals are among the most studied crystalline phases in biomedicine, due to their similarity to the mineral component of hard tissues in animals and humans. Thus, a detailed knowledge of their mechanical and thermal properties plays a relevant role in biomaterial development and applications. In this work, the mechanical properties of hexagonal hydroxylapatite [OHAp, $\text{Ca}_{10}(\text{PO}_4)_6(\text{OH})_2$, $P6_3$ space group] and type-A carbonated apatite [CAp, $\text{Ca}_{10}(\text{PO}_4)_6\text{CO}_3$, $P1$ space group] were investigated by *ab initio* quantum mechanics techniques.

While some data are present in literature about the second order elastic constants (SOECs) of hydroxylapatite, both on the experimental (Katz and Ukraincik, 1971; Gardner et al., 1992) and theoretical sides (Ching et al., 2009; Slepko and Demkov, 2011), no data are available on SOECs and thermodynamics on the completely carbonated type-A Cap. Also, very few results on the equation of state of both OHAp and type-A Cap are available. In the present study, we report the thermo-chemical and thermo-physical properties of the both minerals in a wide pressure range and at temperatures between 0 K and 1000 K. The hybrid DFT/B3LYP density functional in conjunction with Gaussian-type orbitals basis set were adopted, correcting for dispersive forces and employing the quasi-harmonic approximation. The zero-pressure bulk modulus of hydroxylapatite and type-A carbonated apatite were calculated using a 3rd-order Birch-Murnaghan equation of state, obtaining at 0 K 115.9 GPa and 106.2 GPa, and at 300 K 109.5 GPa and 103.0 GPa, respectively. In addition, we provided the second order elastic constants (SOECs) of both OHAp and type-A Cap in athermal conditions. These data could be helpful for experimental researchers involved in mechanical analysis this kind of minerals at physical conditions that are difficult to obtain during experimental procedures, and for guiding researchers interested in quantum mechanical modelling of apatite-based minerals.

Ching W.Y., Rulis P. & Misra, A. (2009) - Ab initio elastic properties and tensile strength of crystalline hydroxyapatite. *Acta Biomater.*, 5(8), 3067-3075.

Gardner T.N., Elliott J.C., Sklar Z. & Briggs G.A.D. (1992) - Acoustic microscope study of the elastic properties of fluorapatite and hydroxyapatite, tooth enamel and bone. *J. Biomech.*, 25(11), 1265-1277.

Katz, J.L., & Ukraincik, K. (1971) - On the anisotropic elastic properties of hydroxyapatite. *J. Biomech.*, 4, 221-227.

Slepko A. & Demkov A.A. (2011) - First-principles study of the biomineral hydroxyapatite. *Phys. Rev. B*, 84(13).

Can be geogenic radon potential indirectly inferred?

Mousavi Aghdam M.¹, Loi A.², Dentoni V.¹, Meloni M.A.², Pistis M.², Funedda A.²,
Randaccio P.³ & Da Pelo S.*²

¹ Department of Civil and Environmental Engineering and Architecture University of Cagliari, Cagliari.

² Department of Chemical and Geological Sciences University of Cagliari, Monserrato.

³ Italian Institute for Nuclear Physics (INFN). E-laboRad. Cagliari.

Corresponding email: sdapelo@unica.it

Keywords: Geogenic Radon Potential, geological Unit, uranium.

Epidemiological findings of radon risk related studies confirm that residential radon represents worldwide an important cause of lung cancer mortality. The ²²²Rn is one of the most abundant of this noble trace element, which can be transported from the source to indoor spaces. Inhalation of radon gas and its solid decay products (i.e., ²¹⁸Po, ²¹⁴Po) can lead to high-energy alpha irritation of bronchial tissues, which can finally cause lung cancer. The concentration of radon in a dwelling is a complicated function of geogenic factors, such as: geological features (accessory minerals bearing uranium in lithology and geological age), geochemical characteristics (²³⁸U, ²³²Th and ²²⁶Ra content), soil permeability, grain size, presence of faults, fractures and karst zone. Uranium/radium contents in igneous, metamorphic and sedimentary rocks can vary in a wide range from low to very high levels. Higher contents typically occur in some organic-rich argillaceous rocks (Hot Shale), heavy minerals placers deposits, reworked igneous or magmatic clastic rocks and, sometimes, in phosphates. When searching for radon prone areas, the influence of the uranium mineralization in vein or stock work should be taken into consideration, as they typically cause radon emission. Actually, the geology is one of the most important factors in controlling the distribution and level of indoor radon, so that the identification of geogenic radon potential of different areas becomes the most important step in the risk assessment procedures.

Direct soil gas radon measurement are scarce and inhomogeneously distributed, especially in Sardinia. Several methods have been proposed by the international literature to produce GRP map where lack of direct soil gas measurements occurs. In some cases, Rn values of regions with sufficient data have been extended to areas with alleged similar geology or geogenic maps of European territories have been produced based on geological units, mainly defined on the basis of lithology and age. The problem with those approaches is the large variability of the Rn potential within the same geological unit, making the methodology sometimes ambiguous. In fact, the geological conditions that controls the enrichment of U (then Rn) in lithotypes are complex and the lithology cannot always represent the real occurrence of U enrichment. In general, lithotypes are classified with textural and compositional criteria. The latter criterion is based on the main and most common minerals in the crust. Therefore, rocks classified as the same category from a lithological point of view may have different compositions of accessory phases, which may have very different U contents. Rocks can hold U enrichments according to geodynamic, stratigraphic, environmental and geochemical features, climatic conditions and, mainly for sedimentary rocks, composition of the source areas which feed the sedimentary basins. Thus, it can be assumed that different geological evolutions related to the paleogeography of the geological regions do not allow to automatically exporting the measurements performed in other geological regions, in the absence of appropriate measurements that define the contents of Rn producing elements. As a matter of fact, a geogenic potential map must be preliminary drawn to take into account the local geological condition and the geodynamic environment from which they derive.

Montmorillonite clay for the removal and recovery of metals and dyes from industrial wastewaters

Parisi F.*¹, Sciascia L.², Princivalle F.³, Merli M.², Lazzara G.¹ & Milioto S.¹

¹ Dipartimento di Fisica e Chimica, Università di Palermo.

² Dipartimento di Scienze della Terra e del Mare, Università di Palermo.

³ Dipartimento di Matematica e Geoscienze, Università di Trieste.

Corresponding email: filippo.parisi@unipa.it

Keywords: clay, wastwwaters, adorption.

The disposal of wastewaters originated from industrial activities represents a serious environmental issue, mainly due to the simultaneous presence of different type of pollutants and involves researchers in different fields ranging from chemistry, biology, medicine, mineralogy. The interest in this issue comes from the twofold objective to decontaminate the effluents and separate and recover the valuable by-products present in wastewaters, thus satisfying the growing need for availability of economic resources for the production of chemicals, materials or fuels. The employment of Montmorillonite clay, readily and inexpensively available, was here proposed as a green sustainable approach for the adsorption (and removal) of two class of pollutants, metals and dyes. The attention was focuses on three “models” pollutants: Pb(II), Ce(III) and crystal violet. The choice is due to the fact that they are widespread in industrial wastewaters of various origin: this characteristics, together with their effect on human health, make them ideal for a study on water remediation. Moreover, when separated from the industrial wastewater, they can be individually recycled in industrial production with no or simple treatment. Clay/pollutant hybrids were prepared under different pH conditions and characterized through the construction of the adsorption isotherms, kinetic studies and XRD measurements. The obtained information was employed to propose the better strategy for the removal and recovery of the different components from aqueous solutions mimicking industrial wastewaters.

Hyperspectral thermal data to identify natural and manmade asbestos minerals: TASI-600 imagery case studies

Pascucci S.*¹, Palombo A.¹, Santini F.¹, Pignatti S.¹, Ionca V.¹, Cavalcante F.¹ & Belviso C.¹

¹ Istituto di Metodologie per l'Analisi Ambientale, CNR, CNR-IMAA (PZ), Italy.

Corresponding email: simone.pascucci@cnr.it

Keywords: hyperspectral thermal infrared, hazardous minerals and materials, spectral classification.

This research study shows the natural and manmade asbestos mapping accuracy retrievable by hyperspectral thermal data and describes some of the classification results tested on the airborne processed data for a rural area in Italy. Lithological and hazardous materials mapping using visible and shortwave infrared hyperspectral data is consolidated and well-known processing chains are available, however there is a lack of such methodologies for hyperspectral thermal infrared data (Kirkland et al., 2002; Black et al., 2016).

An overview of the principal TASI-600 characteristics (Santini et al., 2012), i.e. 32 spectral bands in the 8.0-11.5 μm spectral range, and the retrieved asbestos maps are presented in this study.

Several Natural Occurring Asbestos (NOA) deposits were identified using the emissivity absorption features of the asbestos minerals composing the NOA outcrops. Whereas, for the detection of asbestos-cement roofs, the diminished spectral contrast is significant because it places higher signal-to-noise ratio (SNR) requirements for spectroscopic detection and identification by airborne imagery. Results accuracies both for NOA and asbestos-cement roofs have been validated using available ground truth.

The study highlights that the new generation of multi/hyperspectral thermal sensors e.g., HyTES, TASI-600, SpecTIR, AHI, Hyper-Cam, AisaOWL (Udelhoven et al., 2017), releases challenging opportunities for accurate hazardous asbestos minerals identification and monitoring.

Black M., Riley T.R., Ferrier G., Fleming A.H. & Fretwell P.T. (2016) - Automated lithological mapping using airborne hyperspectral thermal infrared data: A case study from Anchorage Island, Antarctica. *Remote Sensing of Environment*, 176, 225-241.

Kirkland L., Herr K., Keim E., Adams P., Salisbury J., Hackwell J. & Treiman A. (2002) - First use of an airborne thermal infrared hyperspectral scanner for compositional mapping. *Remote Sensing of Environment*, 80(3), 447-459.

Santini F., Palombo A., Dekker R.J., Pignatti S., Pascucci S. & Schwing P.B. (2014) - Advanced anomalous pixel correction algorithms for hyperspectral thermal infrared data: The TASI-600 case study. *IEEE Journal of Selected Topics in Applied Earth Observations and Remote Sensing*, 7(6), 2393-2404.

Udelhoven T., Schlerf M., Segl K., Mallick K., Bossung C., Retzlaff R., Rock G., Fischer P., Müller A., Storch T., Eisele A., Weise D., Hupfer W. & Knigge T. (2017) - A satellite-based imaging instrumentation concept for hyperspectral thermal remote sensing. *Sensors*, 17(7), 1542.

Non-conventional CCS reaction: Ca-oxalate precipitation via Vitamin C promoted green reaction

Pastero L.*¹, Curetti N.¹, Ortenzi M.A.², Schiavoni M.², Destefanis E.¹ & Pavese A.¹

¹ Dipartimento di Scienze della Terra, Università degli Studi di Torino.

² Dipartimento di Chimica, Università degli Studi di Milano.

Corresponding email: linda.pastero@unito.it

Keywords: carbon capture and storage, calcium oxalate, vitamin C.

The increase in the concentration of carbon dioxide in the atmosphere is a relevant and outstanding problem. Many solutions have been set out, none of them being the definitive one. A synergic approach to the problem is needed: many complementary methods of sequestration should be combined with the reduction of production to decrease the total amount of CO₂ in the atmosphere.

In the present work, a direct and green method to convert C(IV) into C(III) and trap CO₂ into a stable crystalline structure other than a carbonate (i.e. calcium oxalate, weddellite) is proposed (Pastero et al., 2019). CO₂ is reduced and precipitated as calcium oxalate through Ca-ascorbate (CaAsc) as a sacrificial reductant. The reaction has been validated. Reaction's kinetics and trapping yield are under evaluation. Weddellite crystals precipitated show very high quality, as demonstrated by single crystal X-ray measurements. Moreover, crystals obtained by different experimental setups exhibit invariably stable flat (F) forms, even if the morphology reflects the crystal growth conditions. The crystal quality of the precipitate reflects on its stability, essential for storage purposes.

It was experimentally demonstrated that the precipitation of weddellite from CO₂ could be described as a two-step process, following two separate reactions: i) a red-ox reaction that involves the reductant (CaAsc); ii) the nucleation of calcium oxalate. The red-ox is the rate-determining step of the process and should be enhanced to increase the overall reaction rate, for example tuning the temperature and the pH to adjust the reducing power of ascorbic acid.

The conversion of carbon dioxide into oxalates doubles the capturing ratio with respect to the carbonation process. Besides, the dissolution of the calcium oxalates does not directly produce CO₂, as happens for carbonates, thus meaning that if dissolved, CO₂ would not be straight released in the environment.

The ascorbic acid degradation cascade has been proven to have no or just feeble interference with the production of calcium oxalate from CO₂, and the products of the degradation are generally considered not harmful.

The reaction rate of the whole process has been experimentally found to be strongly dependent on the extent of the reaction surface: the reaction yield could be increased explosively working with aerosol (very high reaction surface).

Pastero L., Curetti N., Ortenzi M.A., Schiavoni M., Destefanis E. & Pavese A. (2019) - CO₂ capture and sequestration in stable Ca-oxalate, via Ca-ascorbate promoted green reaction. *Science of the Total Environment*, 666, 1232–1244.

Mineral dissolution enhanced by bacteria can improve sustainability of agricultural practices

Placitu S.¹, Fancello D.*¹, Medas D.¹, Alisi C.², Paganin P.^{1,2}, Tasso F.², Sprocati A.R.²,
Turnau K.³ & De Giudici G.¹

¹ Department of Chemical and Geological Sciences, Cagliari University.

² ENEA, Department of Environment, Global Change and Sustainable Development, CR-Casaccia, Italy.

³ Institute of Environmental Sciences, Jagiellonian University, Krakow, Poland.

Corresponding email: darfan@hotmail.it

Keywords: semi-arid soils, bioaugmentation, soil characterization, extraction tests, DGT.

Semi-arid and arid areas in the Mediterranean basin are characterized by the scarcity of productive soils and water. Agricultural practices, mainly based on the intensive use of chemical fertilizers (NPK), produce a further soil impoverishment and water resources overexploitation. Bioaugmentation (Dejonghe et al., 2001) is an alternative, sustainable strategy that aims to select indigenous bacterial and/or mycorrhizal fungi to be used as inocula to speed up mineral dissolution, making macronutrient bioavailable for the plant growth. This strategy requires an integrated biogeochemical approach, based on a detailed knowledge about soil, hydrogeology, soil-root interaction, site microbial community and about the underlying factors in plant-microbe interactions. Soil samples from a Sardinian farm (Italy) were collected in order to characterize their mineralogy (XRD), chemistry (XRF and CHN analysis) and selected bioavailable macronutrients (Ca, Mg, Na, K and P). The latter were evaluated by different methods as ammonium acetate extraction, pore water analyses and diffusive gradient in thin films (DGT).

The study area (Pula, SW Sardinia) lies in an alluvial plain whose sediments come from a weathered leucogranite belonging to the *Villacidro Intrusive Unit*. The soil samples are loamy sand with low amounts of organic matter (avg. C = 1.16 wt.%; N = 2.5 wt.%), and a granite-like mineralogy mainly consisting of quartz, feldspars, biotite and kaolinite. Major oxides contents (SiO₂~72.2, Al₂O₃~15.3, Fe₂O₃~2.7, Na₂O~1.5, K₂O~6.4 wt.%, and CaO and MgO <1 wt.%) suggest that parent-rock is a syenogranite.

Results indicate that:

- i) the bulk soil composition does not reflect the bioavailability of elements;
- ii) Ca is the most bioavailable element;
- iii) macronutrient concentration in solution depends on the extraction method;
- iv) K and P are the most limiting factors in plant growth.

Ongoing researches aim to select microbial inocula suitable for the bioaugmentation strategy. A first attempt has been performed by placing inoculated granite slices in rhizoboxes with growing plants. Slices will be analyzed by microscopic and spectroscopy techniques to observe the biological contribution to the mineral alteration.

This study is in the framework of the SUPREME project (ERANETMED 2) which involves Italian (UNICA, ENEA, AGRIS and CRS4) and international partners of Mediterranean basin (Algeria, Cyprus, Jordan). The final goal is a successful rearrangement of the group of the main microorganisms involved in the energy flows necessary to counteract soil depletion and provide a sustainable productivity.

Zhang H. & Davison W. (1995) - Performance characteristics of diffusion gradients in thin films for the in situ measurement of trace metals in aqueous solution. *Anal. Chem.*, 67, 3391-3400.

Dejonghe W., Boon N., Seghers D., Top E.M. & Verstraete W. Bioaugmentation of soils by increasing microbial richness: missing links. *Env. Microbiol.*, 3, 649-657.

Assessment of environmental impact of mine drainage on the Rio Montevecchio watershed (SW-Sardinia) through hydrologic-tracer techniques and environmental mineralogy

Rigonat N.*¹, De Giudici G.¹, Medas D.¹, Cidu R.¹, Lattanzi P.², Podda F.¹, Dore E.¹, Frau F.¹, Marras P.A.¹ & Frau I.³

¹ Dipartimento di Scienze Chimiche e Geologiche, Università degli Studi di Cagliari, Monserrato (CA) – ITALY.

² CNR-IGG, UOS Firenze, 1 Firenze.

³ Built Environment and Sustainable Technologies (BEST) Research Institute, Liverpool John Moores University, Liverpool, UK.

Corresponding email: nicola.rigonat@icloud.com

Keywords: mine drainage, attenuation processes, tracer techniques.

Rio Montevecchio (Arbus, Sardinia, Italy) is a stream severely affected by the highly impacting mine wastes, hosted in the Piccalinna impoundment, and is characterised by little vegetation and sandy streambed upstream and rocky and pebbly streambed downstream. The application of hydrologic-tracing techniques, in cooperation with the USGS, allowed to calculate large daily loads of mine-related constituents, reaching 1780 kg/day SO_4^{2-} , 340 kg/day Zn, 47 kg/day Fe, and 50 kg/day Mn. Along the study reach, the cumulative loads reached 2080 kg/day for SO_4^{2-} , 421 kg/day for Zn 56 kg/day for Mn and 50 kg/day for Fe.

Instream attenuation processes account for a 14% loss of Zn and SO_4^{2-} , 89% and 77% for Al and Fe loads respectively. Powder X-ray diffraction analysis of stream precipitates, coupled with geochemical modelling, allowed to identify the newly-formed mineral phases responsible for heavy metals abatement but also potential secondary sources of pollution; Fe-oxyhydroxides, K-jarosite ($\text{KFe}^{3+}_3(\text{OH})_6(\text{SO}_4)_2$) and alunite ($\text{KAl}_3(\text{SO}_4)_2(\text{OH})_6$) are regarded as the major players in Fe, SO_4^{2-} and Al attenuation.

Two nearby mining-affected streams (Rio San Giorgio and Rio Naracauli) (De Giudici et al., 2017, 2014) feature loads respectively two and three orders of magnitude lower, thanks to a depositional (rather than erosional) environment that allows the emplacement of effective and resilient biogeochemical barriers.

Compared to the neighbouring Rio Irvi (De Giudici et al., 2018), that has contaminants loads one order of magnitude higher, Rio Montevecchio has pollution source areas widespread along the entire study reach and its flow regime is slower and is more exposed to evaporation processes, leading to the formation of efflorescent salts, which act as temporary sinks for pollutants.

Finally, the discrepancy between discharge measured at the end of the study reach and at a slug injection point downstream suggests that, along that segment, the stream mainly flows in the sub-riverbed volume and might actively recharge underground water reservoirs.

De Giudici, G., Medas, D., Cidu, R., Lattanzi, P., Podda, F., Frau, F., Rigonat, N., Pusceddu, C., Da Pelo, S., Onnis, P., Marras, P.A., Wanty, R.B. & Kimball, B. (2018) - Application of hydrologic-tracer techniques to the Casargiu adit and Rio Irvi (SW-Sardinia, Italy): Using enhanced natural attenuation to reduce extreme metal loads. *Appl. Geochemistry* 96, 42–54.

De Giudici G., Pusceddu C., Medas D., Meneghini C., Gianoncelli A., Rimondi V., Podda F., Cidu R., Lattanzi P., Wanty R.B. & Kimball B.A. (2017) - The role of natural biogeochemical barriers in limiting metal loading to a stream affected by mine drainage. *Appl. Geochemistry* 76, 124–135.

De Giudici G., Wanty R.B., Podda F., Kimball B.A., Verplanck P.L., Lattanzi P., Cidu R. & Medas D. (2014) - Quantifying biomineralization of zinc in the rio naracauli (Sardinia, Italy), using a tracer injection and synoptic sampling. *Chem. Geol.*, 384, 110–119.

Mineralogical and petrographical assessment of edenite crystals from Southern Apennine (Italy)

Rizzo G.* & Sinisi R.

Dipartimento di Scienze, Università degli Studi della Basilicata - Potenza.

Corresponding email: giovanna.rizzo@unibas.it

Keywords: Asbestos-minerals, edenite, Pollino Massif.

Asbestos-like minerals commonly occur in mafic to ultramafic rocks affected by ocean floor metamorphism and/or, more in general, by metasomatic processes. The occurrence of such rocks in Italy was documented in both Alps and Apennines where occasionally they outcrop from Ligurian to Calabrian region. The ophiolitic sequence we investigated is in Southern Apennines, at the Calabria-Lucanian border zone (Pollino Massif area), that during Jurassic time was connect to the Ligurian sector of the western Tethys. Such a ophiolite includes tectonic slices made up of serpentinitic rocks associated with metadolerite dykes and continental crust rocks (mainly granofels, garnet-, garnet/biotite- and biotite-gneisses, and amphibolites). Although the southern Italy serpentinites have been the object of numerous researches and their mineralogical composition largely studied, in this paper we present new and detailed data from SEM-EDS and EMP analyses, on a mineral, the edenite, recently detected in these rocks by Dichicco et al. (2019). Edenite is a double chain silicate of the amphibole group, fairly rare in the ophiolitic sequences where it testifies a medium to high metamorphism (Garcia-Casco et al., 2002; Deschamps et al., 2011). Similarly to the more common asbestos minerals (tremolite, actinolite, and serpentine) find in the studied serpentinites, edenite may present as crystal aggregates, mostly associated with serpentine, diopside and calcite, or as 30 to 80 μm -long single crystals with a fibrous habit. EMPA results reveal (1) a homogeneous chemical composition of crystals regarding contents of major element oxides ($51.32 < 54.3$, $23.62\text{O}_3 < 2.71$, $1.26\text{tot} < 2.85$ wt%) and (2) the occurrence in their structure of some heavy metals such as Cr ($0.012\text{O}_3 < 0.02$ wt%), Mn (0.04 sensu stricto and accordingly it could represent a mineral “potentially harmful” for human health. However, further detailed field and laboratory studies are needed to improve our knowledge on edenite formation in the serpentinitic rocks of the Southern Apennines in order to better constrain the mode of occurrence of this mineral at the Pollino Massif area and to attempt the estimation of the hazard related to it.

Deschamps F., Guillot S., Godar M., Andrean M. & Hattori K. (2011) - Serpentinites act as sponges for fluid-mobile elements in abyssal and subduction zone environments. *Terra Nova*, 23, 171–178.

Dichicco M.C., Rizzo G. & Sinisi R. (2019) - Mineralogical Asbestos Assessment in the Southern Apennines (Italy): A Review. *Fibers*, 7, 24.

Garcia-Casco A., Torres-Roldán R.L., Milla G., Millán, P. & Schneider, J. (2002). Oscillatory zoning in eclogitic garnet and amphibole, Northern Serpentinite Melange, Cuba: A record of tectonic instability during subduction? *J. Metamorph. Geol.*, 20, 581–598.

Unusual (but not too much) particles in forensic soil samples

Sacchi E.*

ENFSI Animal, Plant and Soil Traces Expert Working Group.

Corresponding email: evasacchi70@gmail.com

Keywords: forensic geoscience, soil analysis, anthropic origin particles.

Soil analyses are among the most known and common analyses in the field of forensic geology investigation. The samples usually are constituted by minerals deriving from the alterations of the lithologies of the substrate. These minerals allow a comparison between the reference (samples taken in the victim or at the scene of a crime) and the comparison samples (samples linked to the suspect). Nonetheless, the elements constituting a soil sample are not always derived from the alteration of the substrate lithologies. Often, in fact, there are rare and scattered particles of different origins, especially in heavily populated areas. Such elements, much less frequent in percentage than the mineral portion, sometimes help distinguish the samples more significantly, while their peculiarity and rarity allow to achieve compatibility between reference samples and samples of comparison. In the world of forensic science these “curious”, but obviously not so unusual, components must never be neglected because they can be instrumental in determining the compatibility between the samples. For this reason, a special “Atlas of micro-compounds in soil” has been drawn up, which includes many elements of anthropic origin.

Facies analysis at the crime scene: a traditional method in a different frame

Sacchi E.*

ENFSI Animal, Plant and Soil Traces Expert Working Group

Corresponding email: evasacchi70@gmail.com

Keywords: forensic geoscience, facies analysis, crime scene.

The body of a young woman - Elisa Claps - was found in a church attic, 17 years after her disappearance. The main problem for law enforcement officers, amongst many others, was to determine the location of the primary crime scene. During the homicide investigation, deeply set in the pattern of the rubber sole of one of the victim's shoe, the investigators recovered some minuscule rock fragments.

The initial phase of securing the evidence, and the subsequent sampling of the area where the body had been found searching for a comparison material, was quite a long but necessary process. Subsequently, a typical carbonate rocks facies-analysis by thin-section was performed on both the evidence and the comparison material. This allowed reaching a close match between the evidence and such material.

The positions of carbonate clasts within the shoe, as well as the location in which they were presumably captured by the sole, helped to answer the big question on where the crime actually took place, suggesting the church attic as the primary crime scene.

Novel zeolite`s nanocomposites with a two-tailed cationic surfactant – Arquad ® 2HT-75 with increased stability

Smiljanić D.*¹, Daković A.³, de Gennaro B.², Germinario C.¹, Grifa C.¹, Izzo F.¹, Langella A.¹, Spasojević M.³ & Mercurio M.¹

¹ Department of Science and Technologies, University of Sannio, Benevento, Italy.

² DICMAPI, Università degli Studi di Napoli Federico II, Italy.

³ Institute for Technology of Nuclear and Other Mineral Raw Materials, Belgrade, Serbia.

Corresponding email: smiljanie@unisannio.it

Keywords: clinoptilolite, water treatment, Arquad ® 2HT-75.

Functionalization of natural zeolites (NZ) with cationic surfactants drastically alters the surface chemistry of zeolite and opens new applications possibilities for water treatment: adsorption of pharmaceuticals, pesticides, dyes, etc. The use of surface modified natural zeolites (SMNZs) could be a reliable approach for water treatment, as they can simultaneously remove cations, anions, and/or non-ionized molecules. The main advantages of the NZs, as starting materials, are their abundance in nature, low-cost and good stability. However, the main drawback is a potential instability of surfactant at the zeolite surface. Literature data showed that a certain amount of surfactant can be removed from the zeolite surface depending on experimental conditions, which could have a negative impact on water quality. To increase SMNZs stability and abate possible negative effects on the environment, it is suggested to use different novel types of surfactants (Reeve et al., 2018 and references therein).

For these reasons, a zeolite-rich tuff IZ CLI (Turkey) with clinoptilolite as the main component (79%) has been modified using two cationic surfactants such as Cetylpyridinium chloride (CPyCl) and Arquad®2HT-75 (ARQ), the latter with two hydrocarbon chains. The bilayer composites (B), CPyCl-B and ARQ-B, were prepared using the method of fast functionalization (de Gennaro et al., 2016). To test the stability of composites, 1 g of CPyCl-B or ARQ-B was washed with 2 l of distilled water. Z-potential (Zetasizer Nano ZS90, Malvern Instruments) was measured for unmodified tuff as well as for composites before and after washing.

Z-potential for IZ CLI has shown a negative value (-37.9 mV). The formation of a bilayer was confirmed by the inversion of Z - potential values which turned to positive for both composites CPyCl-B and ARQ-B (+37.7mV and +36.1mV, respectively). After extensive washing of composites, Z - potential of CPyCl-B has dropped to -7.9 mV indicating a significant loss of surfactant molecules. On the other hand, washing of ARQ-B almost did not affect Z-potential indicating great stability of bilayer at the zeolite surface when a two-tailed surfactant was used. These results could open new possibilities for SMNZs applications in fields where surfactant stability is crucial, such as water treatment, thus promoting further research on the use of different novel cationic surfactants.

de Gennaro B., Mercurio M., Cappelletti P., Catalanotti L., Daković A., De Bonis A., Grifa C, Izzo F., Kraković M., Monetti V. & Langella A. (2016) - Use of surface modified natural zeolite (SMNZ) in pharmaceutical preparations.

Part 2. A new approach for a fast functionalization of zeolite-rich carriers. *Micropor. Mesopor. Mat.*, 235, 42-9.

Reeve P.J. & Fallowfield H.J. (2018) - Natural and surfactant modified zeolites: a review of their applications for water remediation with a focus on surfactant desorption and toxicity towards microorganisms. *J. Environ. Manage.*, 205, 253-61.

The judicial contribution of the Messina University on Forensic Geology and Environmental Crimes

Somma R.*

Department of Mathematics, Computer Science, Physical Sciences, and Earth Sciences (MIFT), Messina University, Italy

Corresponding email: rsomma@unime.it

Keywords: geoforensics, forensic geology, environmental crimes.

Specially after the entering into force of the Law 68/2015 on Environmental crimes, to deal with judicial cases regarding environmental crimes may represent a not negligible difficulty, in economic and technical terms.

In the October 2018 an important and unique agreement regarding Forensic Geology and Environmental Crimes, was signed between the Messina Prosecutors and the Messina University. This agreement, if necessary, allows to the scientific referent of the university to coordinate a multidisciplinary team of forensic scientists to assist the Judicial Authority in the solution of serious and environmental crimes.

The available forensic team is actually composed of researchers and professors expert in forensic geology, chemistry, biology, anthropology, legal medicine, etc., authorized to use high technology instruments supplied by the Messina University both in the labs and in the field. In this last case, the georesistivimeter for ERT tomography or the instrument for refraction seismic, the IR thermo-camera, and/or the metal detector are fundamental geophysical instruments to assist the Judicial Authority in cases of suspect environmental disasters. When necessary, the scientific referent may also involve freelance experts or the staff of the regional agency for environment.

Environmental monitoring with magnetic minerals on leaves in wintertime: an assessment

Tribaudino M.*¹, Mantovani L.¹, Solzi M.² & Zaccara P.³

¹ Dipartimento SCVSA, Università di Parma.

² Dipartimento di Matematica, Fisica e Informatica, Università di Parma.

³ Liceo Scientifico Piero Gobetti, Torino.

Corresponding email: mario.tribaudino@unipr.it

Keywords: magnetic minerals, PM10.

A major environmental issue in the towns of the Padan Plain is particulate pollution. This is especially significant in wintertime, when high pressure and dry conditions hinder the dispersion of the polluting particles. Among the different contributions to the particulate matter (PM10), that from minerals is particularly significant. Minerals in PM10 are in part related to vehicular traffic. Although only a fraction of the total PM10, this mineral fraction, mostly composed by magnetite and maghemite, is a significant carrier of heavy metals. Moreover, it is present with a significant fraction of extra fine particles. These minerals are magnetic; their presence can be monitored by the analysis of leaves and PM10 filters, measuring the SIRM and the mass susceptibility. Leaf monitoring has the advantage of low cost and ubiquitous sampling, but in winter-time the fall makes it of lesser use.

Here we sampled, for 7 weeks between 25/1/2019 and 1/2/2019 the leaves of *Hedera helix*, *Parietaria officinalis* and *Rubus caesius*, in Torino and in Parma, which are evergreen commonly found in urban conditions. Mass susceptibility was measured, with the aim to check whether their magnetic response is significant. The ultimate goal for this investigation is to provide a proxy for magnetic pollution readily available for mapping of the polluters at a fine scale. The investigation was done within an “Alternanza Scuola Lavoro” project with secondary schools in Parma and Torino, reported in a separate communication (session Geosciences at school).

The sampling was done near and at the border of a highly trafficked road (Corso Casale, Torino), in a urban park (Campus in Parma, Murazzi-Lungo Po Macchiavelli in Torino), and near a urban highway (Parma). In Torino, in 4 out of 6 sampling days PM10 was higher than 80 mg/m³, with maximum at 122 mg/m³ (8/2/2019)

The leaves were dried and grounded; the susceptibility was measured at the Department of Physics of the University of Parma. In all samples the susceptibility was significantly beyond error.

The main results are: 1) *Parietaria* and *Rubus* are significantly more efficient than *Hedera* in taking up magnetic particles. In Parma, *Rubus* highlights a significant difference between samples ($p < 0.05$), whereas *hedera* doesn't. 2) The susceptibility of samples collected around the highly trafficked urban road (Corso Casale) is significantly higher than other locations, for both *Hedera* and *Parietaria*. 3) In the traffic-free urban sampling in Lungo Po the response from *Hedera* is not different from that from the side of the urban highway (Tangenziale) in Parma, indicating a substantial mobility of the magnetic matter. 4) Also the magnetic response of *Parietaria* and *Rubus*, is not significantly different in Lungo Po and Tangenziale, suggesting that both are suitable for magnetic monitoring. 5) In *Hedera* no significant difference was found between old and young leaves. 6) Differences during sampling days are hardly significant, with a small increase in Parma, and decrease in Torino, at the end of the sampling. This is possibly related to the beginning of the academic period at the beginning of march in Parma, and to decreased urban pollution (17 mg/m³ the last sampling day in Torino).

In conclusion, we foresee future developments in the magnetic analysis to locate pollution spots, and detail the distribution of pollutants by the analysis of *Parietaria officinalis* and/or *Rubus caesius*.

Amino acids-chlorite interaction at the nano-atomic scale

Valdrè G.*¹, Moro D.¹ & Ulian G.¹

¹ Centro di Ricerca Interdisciplinare di Biomineralogia, Cristallografia e Biomateriali, Dipartimento di Scienze Biologiche, Geologiche e Ambientali, Università di Bologna “Alma Mater Studiorum”, Bologna, Italy.

Corresponding email: giovanni.valdre@unibo.it

Keywords: Clinocllore, surface properties, amino acids.

In a wide variety of basic and applied research, including environment, biology, medicine and nanotechnology, there is an urge towards the fundamental knowledge of biomolecules-mineral interaction at a single molecular level. In fact, mineral surface properties, at the micro- and nanometric scale, can control important interaction processes, such as adsorption, alignment, differentiation, coagulation, aggregation, filtration, and ionic transport in porous media. Furthermore, particle size, shape, surface charge and crystal-chemistry may also have important catalytic repercussion.

Here we investigated in detail the specific interaction between the basic amino acids L-alanine and glycine and the (001) clinocllore surface. The interaction process was investigated by cross-correlated scanning probe microscopy (SPM) and quantum mechanics simulations (QM) at the DFT/B3LYP level of theory. In the present work specifically developed SPM-based methods for nano-morphological-physical characterization and nano-chemical FTIR spectroscopy/imaging with nanoscale X-Y and sub-nm Z resolution were effectively applied. Clinocllore is a very particular phyllosilicate whose surface generally presents after cleavage both positively charged hydrophobic micro-nanostructured areas (related to interlayer brucite-like sheet), and negatively charged hydrophilic ones (related to the TOT layer). These areas are atomic flat ($\sim 0.2 \text{ \AA}$ rms), extended from several micrometers to few nanometers, with a typical in-depth separation of $\sim 4 \text{ \AA}$ (the thickness of the brucite-like interlayer sheet). By depositing amino-acids water solutions on the clinocllore surface we generate a hydrophobic environment (on the brucite-like surface) in a water medium. Similarly to the behavior previously observed for DNA, RNA and single nucleotides, the clinocllore surface was found able to condense (the condensation/amplification factor respect to the amino acid dispersion in the water droplet was about 103), organize, and agglomerate amino-acids molecules onto specific regions, the brucite-like ones. The amino acid is stably and not uniformly adsorbed onto the brucite-like surface of clinocllore, organized in dot-like structures, agglomerates, rings and filament-like structures up to about 150 nm long. Single molecules and the different clinocllore layers were discriminated by SPM and nano-FTIR chemical spectroscopy/imaging, with sizes in agreement with QM calculations. Simulations provided also the conformation of the molecule on the surface, the intermolecular bonding scheme and the Brønsted-Lowry basic/acid strength related to $\text{Al}^{3+}/\text{Mg}^{2+}$ substitutions in the brucite-like sheet and to $\text{Al}^{3+}/\text{Si}^{4+}$ in the TOT. The reported findings are useful not only for biotechnological and environmental purposes (from synthesis/use to sequestration of biomolecules), but also for prebiotic chemistry research.

S5.

**Geosciences in Archaeometry and Cultural Heritage
Conservation**

CONVENERS AND CHAIRPERSONS

Marco Benvenuti (Università di Firenze)

Anna Maria De Francesco (Università della Calabria)

Claudio Mazzoli (Università di Padova)

The marble identification of ancient shipwrecks for an enhancement of the in situ underwater heritage of Italy: the case of the cargo of Punta del Francese (Stintino-Sassari, Sardinia)

Beltrame C.¹, Lazzarini L.² & Antonelli F.*²

¹ Dipartimento di Studi Umanistici, Università Ca' Foscari di Venezia.

² LAMA – Laboratorio di Analisi dei Materiali Antichi, Università Iuav di Venezia.

Corresponding email: fabrizio.antonelli@iuav.it

Keywords: Punta del Francese Roman shipwreck, marble cargo, archaeometric study.

The “Ancient Marble Routes” project started in 2009 thanks to a collaboration between the “Ca’ Foscari” and IUAV Universities of Venice and is finalised to systematically study the wrecked marble cargoes, mostly dating to the Roman age, discovered in the coastal seabeds of Calabria, Sicily and Sardinia. Further to archaeological studies, archaeometric analyses were performed to determine the origin of the stone materials carried by these shipments, generally made of white marbles. Such an origin may help reconstructing the ancient sea routes of the ships and since the wrecks are usually lying in shallow waters, in most cases the stones have already had, or will have in future, an underwater museum destination, or will be the subject of a virtual 3D exploration. This paper presents the results obtained from mineralogical and geochemical studies conducted to establish the geographical origin of the white marble blocks composing the Early Imperial shipwreck found at Punta del Francese, off the coast of Stintino, Sardinia. Each of the fourteen marble blocks recorded was sampled and then analysed in thin section under an optical microscope, subsequently powdered for X-Ray diffraction, the determination of the stable carbon and oxygen isotopic ratios by mass-spectrometry and the geochemical analysis by ICP-MS for the evaluation of the concentrations of some trace elements proven to be discriminant between fine-grain marbles. The results of all the archaeometric investigations indicate that the marble shipment of Punta del Francese was composed of marmor lunense quarried in the Carrara valleys and probably directed to a destination in Spain or Gallia.

Microstructure and chemical composition of Iron Age archaeological objects from the Phoenician-Punic site of Motya (Sicily, Italy)

Bernabale M.*¹, Nigro L.² & De Vito C.³

¹ Dottorato di Ricerca, c/o Dipartimento di Scienze della Terra, Sapienza Università di Roma.

² Dipartimento “Istituto Italiano di Studi Orientali”, Sapienza Università di Roma.

³ Dipartimento di Scienze della Terra, Sapienza Università di Roma.

Corresponding email: martina.bernabale@uniroma1.it

Keywords: archaeological bronzes, SEM, EMPA.

The aim of this work was to characterize chemical composition of the alloys and corrosion microstructures of Phoenician bronze weapons from the archaeological site of Motya (western Sicily, Italy). For this purpose, some bronze artifacts were selected and studied by the combined use of different analytical techniques, such as scanning electron microscope (SEM-EDS) and electron microprobe analysis (EMPA). Moreover, X-ray maps on cross section of the artifacts were also performed to obtain information about elemental distribution in the different layers. Quantitative analysis from rim to core sections has been acquired using EMPA in order to estimate different composition of major and minor elements of the original alloy. The results revealed that binary (Cu-Sn) and ternary alloys (Cu-Sn-Pb) with some impurities of As compose the weapons. A common feature of quite all samples is represented by dissolution of copper in outermost layers (i.e., decuprification process) as well as widespread presence of chlorine as the main corroding agent. However, different microstructures of the alloys were observed, i.e., an axe shows a matrix of low tin bronze with large and insoluble Pb globules, which undergo oxidation processes, forming oxidized lead compounds on the patina; other artifacts display complex stratified corrosion layers with a periodicity, recognized as the Liesegang effect (Scott, 2006), which is related to the occurrence of chloride compounds. The study of the microstructures and the stratigraphy of these metal artifacts allow having new insights about corrosion process and the nature of the alloys as well as on metallurgical background of Phoenicians.

Scott D.A. (2006) - Periodic Corrosion Phenomena in Bronze Antiquities. *Studies in Conservation*, 30(2), 49.

STONE Pietre Egizie: a free mobile application for promoting the knowledge and dissemination of ornamental stones exposed in Museo Egizio of Torino (NW Italy)

Borghi A.*¹, d'Atri A.¹, Gambino F.¹, Martire L.¹, Perotti L.¹, Vaggelli G.² & Valentino D.³

¹ Dipartimento di Scienze della Terra, Università di Torino, Italy.

² CNR – Istituto di Geoscienze e Georisorse, c/o Università di Torino, Italy.

³ Museo dell'Antichità Egizie, Torino, Italy.

Corresponding email: alessandro.borghi@unito.it

Keywords: ornamental stones, multimedia application, Cultural Heritage.

Egypt is extremely rich on ornamental stones and its inhabitants have been able to make the most of what nature has offered them. The richness of this wide range of stone materials can be appreciated by visiting any Egyptian collection. The theme addressed in this project concerns the diffusion at the public of the geo-petrographic characteristics of the stone materials used to preserve the finds in the Egyptian Museum of Turin, through the creation of an application for smartphones and tablet, in Italian and English, whose contents are simple and clear both from the point of view of language and of their graphic and structural organization. It represents a tool of innovative communication aimed at promoting, increasing and enhancing the heritage preserved in one of the main Italian museums, thanks to which the visitor can enjoy cultural and scientific aspect at the same time

The application STONE Pietre Egizie has been developed with the purpose to give the greatest freedom to the visitor who can choose to obtain either i) basic and simple Information or ii) insights based on own interests and decide whether to devote himself mainly to the archaeological part or know the raw material and its provenance

Taking into account the requirements of both artistic and scientific representativeness, 50 finds of Egypt Museum were selected and listed in alphabetical order in the application. The form of each find reports the collocation of the selected find, its name, the epoch in which was carved, the site where it was found, the name of the discoverer, the size and a detailed description, which highlights the material value of the rock used and its interaction with the artwork. Each form is completed by a relevant number of photos, that the user can scroll and zoom in. At the bottom of the form an interactive icon addresses to the corresponding rock.

By means of a numbered list of the stones used in all described monuments, the specific data of each rock can be accessed. The form of each rock is organized according to the following fields: three photos of the rock at macro, meso and microscopic scale, the petrographic name, the historic name, a macroscopic and microscopic description and a list of the main uses in the past. At the bottom of the screen a headword allows to access to the quarry of origin, connected to a simplified geological map where the quarrying district is indicated, implemented by a brief geological setting. The button to see the archeological find with the its raw rock is also reported.

The approach followed in the app may be to raise public awareness of the role that Earth Sciences can play in the future even in unconventional sectors such as the enhancement and dissemination of Cultural Heritage and to increase dialogue between earth scientists, humanists, archaeologists and cultural managers.

The application can be downloaded free from the App Store or Google Play for Apple and Android devices, respectively.

A comparison between the decay of adult and juvenile human skeletons from archeological and contemporary burials using a multidisciplinary approach

Caruso V.*¹, Marinoni N.¹, Merlini M.¹, Cantaluppi M.¹, Diella V.³, Trombino L.¹ & Cattaneo C.²

¹ Dipartimento di Scienze della Terra “Ardito Desio”, Università degli Studi di Milano.

² LABANOF, Laboratorio di Antropologia e Odontologia Forense, Sezione di Medicina Legale e delle Assicurazioni, Dipartimento di Scienze Biomediche per la Salute, Università degli Studi di Milano.

³ Consiglio Nazionale delle Ricerche, IDPA, Sezione di Milano.

Corresponding email: caruso.valentina@libero.it

Keywords: buried juvenile skeletons, bone diagenesis, earth science analytical techniques.

The decay of inhumated human remains cannot be predicted, since under the same extrinsic burial conditions an intra individual skeletal variability may occur, depending on intrinsic bone features, such as shape, porosity, hardness and histological structure. Up to now many studies have been published on the decay of human bones recovered both in archaeological and in forensic field. In particular, many researches have been reported on human bone diagenesis of adult skeleton from a macroscopic and microscopic point of view (Caruso et al., 2018; Caruso 2015-2016). On the contrary, few research projects were provided to investigate the diagenesis of juvenile (or subadult) human skeletons (age ranged from 0 to 18 years old). Generally, the juvenile human bones are poorly preserved, compared to adult human bones; this can be ascribed to their smaller size, incomplete mineralization, higher organic and water content and porosity. Therefore, to understand the causes of the lack of juvenile human skeletons in the archaeological and forensic records is important for several anthropological studies, i.e. paleodemography and paleopathology.

It is generally accepted that diagenetic processes act heavily upon juvenile skeletons, even if the way this occurs is still not well understood and explored. Juvenile bone diagenesis could be influenced by the differential treatment of children in funerary practice compared to adults (depth and burial location) in past cultures. Moreover, the modern archaeological techniques are not often able to retrieve the juvenile remains.

In this light, the current research project aims to investigate how archaeological and contemporary juvenile bones, compared to their adult counterparts, degrade at histological and chemico/mineralogical level for quantifying their diagenesis over time.

For the first time, several subadult bones will be investigated by combining conventional and advanced analysis techniques, such as backscattered scanning electron microscope (BSE-SEM), synchrotron X-ray micro tomography (SR- μ CT), X-ray powder diffraction (XRD) and electron microprobe (EMP-WDS).

Caruso V., Cummaudo M., Maderna E., Cappella A., Caudullo G., Scarpulla V. & Cattaneo C. (2018) - A comparative analysis of microscopic alterations in modern and ancient undecalcified and decalcified dry bones. *Am. J. Physical Anthropol.*, 165(2), 363-369.

Caruso V. (2015-2016) - Degradation of organic and mineral phases in buried human remains: the Earth Sciences analytical characterization, Ph.D. Thesis, Università degli studi di Milano, Dipartimento Scienze della Terra Ardito Desio.

Chemical and textural fingerprint of natural stones for the use of construction and restoration stakeholders (CatSTONE project)

Castagnotto E.*1, Locardi F.2-3, Scrivano S.1, Ferretti M.2 & Gaggero L.1

¹ Dipartimento di Scienze della Terra dell'Ambiente e della Vita, Università degli Studi di Genova.

² Dipartimento di Chimica e Chimica Industriale, Università degli Studi di Genova.

³ Istituto di Struttura della Materia – CNR, Area della Ricerca di Roma1, Monterotondo Scalo, RM.

Corresponding email: castagnottoelena@gmail.com

Keywords: DTA/TG GC-MS, heritage, stones.

In spite of its excellent resolution, the conventional MOLP-based petrographic analysis is an operator dependent technique. In order to make the characterization of ornamental and historical stones more accessible, the CatSTONE project presents an integrated approach more based on instrumental data, as a contribution to the European Innovation Partnership (EIP) NATUREUROSTONE Building a harmonised European database on natural stones for the use of construction and restoration stakeholders. The project aims at defining the limits of investigation and the resolution of an original analytical method for natural stone materials and, within the Cultural Heritage setting, to verify the validity of the chemical imprint as a support to historical-artistic stakeholders. It is mostly addressed to the carbonatic rocks of the European database to-be, which encompasses a large amount of the European market and built heritage. It aims at combining Image Analysis (IA) and Differential Thermal Analysis/Thermogravimetry coupled with the Gas Chromatography and Mass Spectrometry (DTA-TG GC-MS). The automatized IA, based on images acquired by Scanning Electron Microscopy (SEM), allows the study of textural features (e.g., grain size, orientation, pore size, etc.); the other is a micro-invasive technique that gives information about the chemical composition of the bulk rock and its impurities based both on the mass loss and on the chemical analysis of the volatilized component. A first cluster of carbonate lithotypes widely employed as ornamental stones was characterized following the designed protocol. While Gatta et al. (2014) demonstrate that chemometrical analysis of DTA-TGA data could assess marble discrimination and identification, our preliminary results highlight that preparation plays a crucial role. Influence of initial particle-size has been further explored, focusing on samples of white Carrara marble, ground and sieved at different granulometric fractions (A: $\varnothing > 1$ mm; B: $200 \mu\text{m} > \varnothing > 120 \mu\text{m}$; C: $120 \mu\text{m} > \varnothing > 90 \mu\text{m}$; D: $\varnothing < 63 \mu\text{m}$). The TG curves obtained show same behavior and same weight loss percentage; according to what was expected, differences have been registered in the onset and in the peak decomposition temperature ($\text{CaCO}_3 \rightarrow \text{CaO} + \text{CO}_2$) and fine ground marble starts to decompose at lower temperature. The significance of an advanced characterization has been demonstrated: the procedure not operator-dependent allows reproducibility of the measurements, and the bearing of a defined protocol for sample preparation has been underlined. Moreover, all the data acquired will be part of a substantial database that can serve as integration to the EN 12407:2007.

The CARIGE Bank Foundation provided a yearly grant to E. Castagnotto

Gatta T., Gregori E., Marini F., Tomassetti M., Visco G. & Campanella L. (2014) - New approach to the differentiation of marble samples using thermal analysis and chemometrics in order to identify provenance. *Chemistry Central Journal*, 8, 1-9.

“Our Common Future”: a lesson from the past for a renewed responsibility

Coletti C. *, Maritan L. & Mazzoli C.

Department of Geosciences, University of Padova, Italy.

Corresponding email: chiara.coletti@unipd.it

Keywords: Cultural Heritage, georesources, sustainability.

The anthropocentrism, from ἄνθρωπος (human being) and κέντρον (center), argues that human beings are the most important entity in the universe. Cultural Heritage and archaeological artefacts are expression of an anthropocentric action: the material has a value for the human activity that created it and not for the intrinsic value of the matter itself. Under this prospective, the material in Cultural Heritage, archaeometry and up to modern art is interpreted as the epiphany of an image, a social structure, a culture. It represents the cultural contribute in terms of future transmission of our genetical cultural code. For this reason, some recent events such as the Palmira destruction or Paris’s cathedral fire call us to meditate in terms of symbol and cultural identity.

The study of the material of the past put us in an extratemporal view:

1. a material created by other human that discloses past societies know-how and skills;
2. a material subjected by human and environmental activity.

The relationship “environment-human identity” is a hot topic. Since ancient times, most of the materials used to build our cultural identity was supplied from geological deposits/formations of various natures, the consumption of which has increased exponentially during the 20th century, prompted by the global industrialization and the development of a wasteful linear economy. Nevertheless, the extraction of georesources is an inherently irreversible and unsustainable activity, since geological materials are non-renewable and finite.

We are urgently called to progress towards an active environmental and societal strategy for sustaining raw materials supply on a circular and clean economy perspective, while maintaining our cultural identity.

The recovery of the past is not just something concerning symbols and artefacts, but also, in some cases, the recovery of habits; the development of a linear economy, for example, is a real historical anomaly in terms of resource use, diffused in the last centuries. While, the values of circular economy are rooted in our past and can be considered as a lesson of recycling and they revolve around sustainability. This important attitude is easily identifiable, for example, when waste materials occur in the ancient ceramic paste, testifying the recycling of pottery or by-products from other production activities and derived from different geographic and cultural contexts.

The battle against resources exploitation arises the “ethics of responsibility” that calls us to a consciousness on long-term effects of our strategies on raw materials and recycling.

Provenance study of the protohistoric impasto pithoi in the Soverato area (Calabria - Southern Italy) by LA-ICP-MS analysis of individual biotite grains

De Francesco A.M.¹, Barca D.*¹, Tucci A.² & Scarpelli R.¹

¹ Dipartimento di Biologia, Ecologia e Scienze della Terra – Università della Calabria, Rende (CS).

² Archeologa, Libera Professionista – Soverato(CZ).

Corresponding email: donatella.barca@unical.it

Keywords: pithoi, petrographic analysis, biotite crystals, provenance study, Calabria.

In the hinterland of Soverato town (CZ) in Calabria, in the territory of Gagliato, on a series of terraced plateaus, remains of an extensive settlement have been identified, that testify to the human presence from the Ancient Bronze Age to the Hellenistic age (Tucci, 2015). The ceramic production of the Final Bronze Age is characterized by both tableware and large impasto pithoi. Impasto pithoi are attested in southern Sybaris area, in central-southern Calabria, in Sicily and in the Aeolian islands, while north to Sybaris, in the Matera area and in Puglia a purified ceramic production prevails.

The settlement area, located in central-southern Calabria, is part of the Serre and Aspromonte Massif. The Serre Massif mainly consists of a crystalline basement made up of Variscan metamorphic and plutonic rocks. The eastern side of the Serre degrades, towards the Ionian Sea, through several terraced surfaces of Pliocene sedimentary successions with clays, sands and sandy conglomerates with granite and metamorphic rock pebbles, on which the human settlements developed.

The petrographic analysis, carried out on 15 pithoi samples, showed an abundant presence of quartz, biotite, K-feldspar, plagioclase, rare muscovite, fragments of granite and metamorphic rocks. In addition, some fragments contain grog and microfossils.

The remarkable compatibility of the mineralogical composition of the studied pithoi with the rocks of the settlement area suggests their local production, despite the fact that similar lithologies are also present in many other areas of central-southern Calabria.

In the first phase of this work, trace elements analyses by LA-ICP-MS were carried out on biotite individual crystals of representative pithoi fragments and on the biotite individual crystals of the sampled sands of the Gagliato archaeological site to validate the hypothesized local production. Successively other sediments of central-southern Calabria will be analyzed.

Useful results have already been obtained by trace elements mineral chemistry of biotite and other individual crystals applied to archaeometric and geological problems (Scarpelli et al., 2015; Sliwinski et al., 2017).

The preliminary data show a good compositional similarity between biotite crystals in ceramic fragments and those analyzed in the sands collected in the settlement area.

Tucci A.M. (2015) - Dolii protostorici di impasto dal territorio di Gagliato (CZ) – 50ma Riunione Scientifica dell'Istituto Italiano di Preistoria e Protostoria. Roma, 5-9 ottobre 2015.

Sliwinski J.T., Ellis B.S., Dávila-Harris P., Wolff J.A., Olin P.H. & Bachmann O. (2017) - The use of biotite trace element compositions for fingerprinting magma batches at Las Cañadas volcano, Tenerife. Bull. Volcanol., 79, 1.

Scarpelli R., De Francesco A, Gaeta M., Cottica D. & Toniolo L. (2015) - The provenance of the Pompeii cooking ware: insight from LA-ICP-MS trace element analyses. Microchemical Journal, 119, 93-101.

Roman orichalcum coins: a deep investigation from patina to core

Di Fazio M.*¹, Felici A.C.², Catalli F.³, Doménech-Carbó A.⁴, Doménech-Carbó M.T.⁵ & De Vito C.¹

¹ Department of Earth Sciences, Sapienza University of Rome, Italy.

² Department of Basic Applied Sciences for Engineering, Sapienza University of Rome, Italy.

³ Independent Researcher.

⁴ Departament de Química Analítica, Universitat de València, Spain.

⁵ Institut de Restauració del Patrimoni, Universitat Politècnica de València, Spain.

Corresponding email: melania.difazio@uniroma1.it

Keywords: microstructure, brass, multi-analytical approach.

A set of Roman orichalcum coins, issued from 88 B.C. to 96 A.D., has been investigated using a multi-analytical approach.

The aim of the study is to explore the corrosion processes of this alloy, with a special attention to the dezincification and decuprification phenomena, from the external layers to the unaltered core of the samples. Indeed, XRF, VIMP methodology and ATR-FTIR were used to obtain information about the elemental composition (qualitative method) of the external layers and to characterize both the patina and the corrosion pattern of the surfaces, allowing also the analysis of samples that could not be sacrificed. SEM-EDS and FIB-FESEM-EDX analysis allowed to investigate the corrosion micro-texture (e.g. segregation micro-domains) in depth and the unaltered metal core of the coins (Doménech-Carbó et al., 2018). In addition, cross-section analyses at high magnification showed cold-working evidences, i.e. deformed grains and strain lines.

Quantitative data of major, minor and trace elements were obtained by means of EMP analysis. Moreover, differences in chemical compositions between the unaltered core and the altered layers of the samples were highlighted. All these techniques revealed the presence of other metal, besides Cu and Zn as the typical elements of orichalcum. Indeed, Tin, Fe, Pb and As are present at different concentrations (from 0.01 to 2.30 % wt). Finally, the interpretation of voltammetric data permitted to group coins, that belong to different monetary emissions, and the discrimination of the issues emitted by different monetary authorities (Di Turo et al., 2017).

Di Turo F., Montoya N., Piquero-Cilla J., De Vito C., Coletti F., Favero G. & Doménech-Carbó A. (2017) - Archaeometric analysis of Roman bronze coins from the Magna Mater temple using solid-state voltammetry and electrochemical impedance spectroscopy. *Analytica Chimica Acta*, 955, 36–47.

Doménech-Carbó M.T., Di Turo F., Montoya N., Catalli F., Doménech-Carbó A. & De Vito C. (2018) - FIB-FESEM and EMPA results on Antoninianus silver coins for manufacturing and corrosion processes. *Scientific Reports*, 8, 10676.

Petroarchaeometric investigation of building stones and mensiochronological analysis of masonry structures of the St. Maria Veterana archaeological site in Triggiano (Apulia, southern Italy), as multidisciplinary tool for the chronological dating and traditional production technology studies

Fioretti G.*¹⁻² & Campobasso C.¹⁻²

¹ Pasquale Battista Foundation, Milano, Italy.

² PUGLIA MIA Association, Bari, Italy.

Corresponding email: giovafioretti@gmail.com

Keywords: building stone, mensiochronology, petroarchaeometry.

The paper introduces a multidisciplinary method based on the correlation between the petroarchaeometric characterisation of building stone and the mensiochronology investigation of blocks, which represents an efficient tool for the chronological dating and the production technologies study in stone masonry.

The multidisciplinary approach was applied on the St. Maria Veterana archaeological site in Triggiano (Bari, southern Italy), a hypogeum including a medieval church (XI-XVI) and successive several environments (crypts, gates, hallways, tomb chambers) and presenting various archaeological stratifications and renovation of some settings, which hinder the correct dating of building phases.

The research aim was both to provide an original contribution to the poor information of this archaeological site, especially in terms of chronological data on different settings, and to enrich the knowledge about the reconstruction of production technology in Apulian contexts.

For this purpose, representative samples were collected from each wall stratigraphic units and their thin sections were observed by means of optical microscope to highlight the petrographic and textural features and to recognise rocks used for production of building blocks.

Moreover, a direct inspection and measurement of stone blocks was carried out following the mensiochronology method, a non-destructive method providing a dating of stratigraphic units, by means of brick measurement. Mensiochronology data were processed by statistical analysis and analogies of blocks, from different settings, were pointed out to create correlation classes.

Petrographical results revealed the carbonate composition of used rocks, namely calcarenites extracted from the surrounding area and local limestones probably from the near production and supply sites. Furthermore, the mensiochronology analysis displayed recurrent block measures and frequent masonry textures also in different settings. The matching of all results obtained by the petrographic and mensiochronological analysis allowed to discover the analogies among employed rock materials and size features of blocks in wall stratigraphic units and then, to provide the relative chronological correlation of the archaeological site settings.

In addition, starting from historical information and since the use of a specific rock variety and recurring of block sizes are indexes of the same building phase, the presented method supported the historical reconstruction of the St. Maria Veterana site, reason why it represents a valuable multidisciplinary tool for the chronological dating and traditional production technology studies.

This research belongs to TRIVIANUM project, designed by “PUGLIA MIA Association for research, promotion and protection of Apulia cultural heritage” in collaboration with “METROPOLIS Association” and financed by the “Pasquale Battista Foundation”.

Pistoia, city of stones

Fratini F.¹, Pecchioni E.^{*1-2}, Cantisani E.¹ & Rescic S.¹

¹ Institute for the Conservation and Valorisation of Cultural Heritage (ICVBC) - CNR, Italy.

² Earth Sciences Department, University of Florence, Florence, Italy.

Corresponding email: elena.pecchioni@unifi.it

Keywords: Pistoia, stone materials, limestone characterization, decay.

Pistoia, bordered to the north by the slopes of the Apennines and to the south-west by Monte Albano, is characterized by its long walled perimeter inside which many gardens and green spaces alternate with buildings in such a way that the urban space preserves the aspect of the pre-industrial city where Romanesque, Gothic and Renaissance forms coexist. In the urban plan, the phases of development between the VIII and XIV century are clearly recognizable. There is little information about the primitive Etruscan settlement of the VI-V century BC when the current Piazza del Duomo was the starting point for the trans-Apennine routes. More certain are the news of the Roman Pistoia, a colony built along the Via Cassia which constituted the decumanus maximum.

The city has a varied stone heritage that reflects only in part the lithological nature of the surrounding hills; mineralogical and petrographical analyses have partially confirmed the origin. The main building material is the Pietra Serena sandstone that is present extensively in the surrounding mountains and has been used as large pebbles, ashlar and architectural decoration. Secondly there are bricks, found in mixed masonry, for the construction of load bearing arches and for the construction of Santa Barbara Fortress. Regarding decoration and cladding, materials close to the city are the serpentinite from Monte Ferrato, near Prato, the travertine of Monsummano, the Rosso di Monsummano present inside Santa Maria dell'Umiltà and the Pietra Alberese from the nearby hills. About this limestone, it is possible that part of this material is not real Pietra Alberese but Calpionelle Limestone or limestone from the Mesozoic nucleus of Monsummano. Micropaleontological analyses on microsamples are in progress in order to verify the exact origin. In some churches there is also the Pietraforte sandstone and this is quite strange because the outcrops of this lithotype are found in the hills south of Florence, therefore quite distant. Another peculiarity is the use of Montagnola Senese marble in the cladding of Baptistery.

The knowledge of the exact nature of the materials is important to learn more about the construction history of the city but also to understand the decay phenomena and to select the most suitable conservation interventions.

The Roman villa at the Castle of Baia (Naples, Italy): preliminary investigations on the polychromy of frescoed surfaces by using non-destructive spectroscopic techniques

Germinario C.¹, Cappelletti P.², De Bonis A.², Di Martire D.², Esposito R.³, Grifa C.¹, Morra V.², Rispoli C.*² & Talamo P.⁴

¹ Dipartimento di Scienze e Tecnologie, Università degli Studi del Sannio, Benevento, Italy.

² Dipartimento Scienze della Terra, dell'Ambiente e delle Risorse, Università di Napoli Federico II, Napoli, Italy.

³ Dipartimento di Scienze Umanistiche, Università di Napoli Federico II, Napoli, Italy.

⁴ MiBAC- Parco archeologico dei Campi Flegrei, Bacoli (NA), Italy.

Corresponding email: piergiulio.cappelletti@unina.it

Keywords: Raman spectroscopy, non-destructive techniques, roman frescoes, Baia, Phlegraean Fields.

During the Roman age, the southern promontory of the gulf of Baia was the perfect location for the construction of Villas. In 1495 AD, during the Aragonese period, a huge military fortress (Castello Aragonese di Baia) was set in the area of one of these Villas. In 1999, during some restoration works inside the fortress, currently hosting the Archaeological Museum of Phlegraean Fields, some ruins related to the residential sector of a Villa were discovered in the so-called "Padiglione Cavaliere".

The Roman Villa, developed in terraces sloping down to the sea and has been the subject of two large building phases which extend chronologically from the Late Republican Roman age to the first Imperial era.

The most representative evidences of the Villa are represented by the outstanding remains in situ of floors with tesserae and decorated plasters and finely frescoed surfaces. The frescoes pertain to a wall of an unidentifiable space decorated according the II style repertoire.

The decoration, of which only the upper part is preserved, represents a perspective depiction of architectural scenes en trompe l'oeil, divided in three areas. The foreground reported a porch with ionic columns whereas the central part of the scene is occupied by a round arch unveiled by a red colored curtain framing a tholos.

The wall was decorated with brilliant colours that were analysed by means of a non-destructive approach for investigating the polychromy of wall paintings.

Micro-Raman (μ RS) and Fourier Transform Infrared (FTIR) Spectroscopy were performed in situ on red, yellow, white, black, pink, purple, green, and blue decorations. A quantitative evaluation of the colour was obtained, instead, by colorimetric measurements. Infrared thermography (IRT) was also performed for a rapid and non-destructive subsurface detection of defects.

The combined use of spectroscopic techniques points out to the use of a characteristic Roman palette, consisting of cinnabar, yellow ochre, calcite, caput mortuum, and organic black pigments. Regrettably, spectroscopic techniques were not be able to identify blue, green and pink pigments; further elemental analyses (e.g. portable XRF spectroscopy) will be performed for assisting in the determination of pigments constituting blue, green and pink paints. Spectroscopic analyses also detected gypsum as weathering product.

Weathering of anthropic caves of soft rock in the Kantō region, Japan

Germinario L.*¹ & Oguchi C.T.¹

¹ Department of Civil and Environmental Engineering, Saitama University, Japan.

Corresponding email: luigi.germinario@gmail.com

Keywords: cave, stone decay, microclimatic monitoring.

Modern Japan is world-renowned for the vertical development and tall skyline of its metropolises, yet keeps a strong cultural bound with the underground landscape. Anthropic caves, galleries, subterranean settlements and quarries have an unquestionable significance in the Japanese social and religious traditions. Our interest dwelled on three among the many hypogeal historical sites in the Kantō region (central Japan), excavated into soft and porous sedimentary rocks, namely volcanic tuffs and tuffaceous mudrocks. They were destined to diverse utilizations: burials for high-ranking aristocrats in the Kofun period (6th-7th c.) and war logistic support during WWII (Yoshimi, Saitama); practice of esoteric rituals by Shingon Buddhist monks, from the Kamakura period (13th c.) onwards (Taya, Kanagawa); stone quarries opened in the Edo period (17th c.) and places of worship (Oya, Tochigi). In this contribution, we introduce the first results of a research aimed at studying the vulnerability of these underground spaces and its relationship with the relevant microenvironmental conditions. Rock decay is explored by characterizing texture, mineralogy, porosity, bulk-geochemical and microchemical features, and combining that with temperature and humidity monitoring and chemical analysis of groundwater and rainwater. Particular attention is paid to the causes and effects of salt weathering. The eventual outcomes are expected to support the adoption of countermeasures for preserving the integrity of those caves and the artifacts enshrined therein.

The Neolithic greenstone industry from Chiomonte (Turin Province, Northwestern Italy): archaeometric study and comparison with analogous findings

Giustetto R.*¹, Padovan S.², Barale L.³ & Compagnoni R.¹

¹ Dipartimento Scienze della Terra, Università di Torino.

² Parco Archeologico del Lago Pistono, Montalto Dora (TO).

³ Consiglio Nazionale delle Ricerche, Istituto di Geoscienze e Georisorse, Torino.

Corresponding email: roberto.giustetto@unito.it

Keywords: Greenstone, Jadeitite, Eclogite.

An in-depth archaeometric characterization, using both mineralogical/petrographic techniques and morpho-typological issues, was performed on the polished stone industry from the archaeological site of Chiomonte – La Maddalena, dating back to the Middle-to-Late Neolithic. Particular care was spent in studying greenstone artifacts, which represents by far the most significant rock types used in the Po plain for the production of prehistoric tools, with the aim of providing information about the supply sources of the raw materials and determining the functionality of the settlement in the prehistoric Western Alps setting. Half of the 132 global tools proved to be made of stricto sensu greenstones (i.e., ‘Na-pyroxene rocks’ and ‘Na-pyroxene + garnet rocks’; Giustetto & Compagnoni, 2014), the rest being formed by serpentinites (25 %) and other lithologies. The combined application, on the Chiomonte greenstone tools, of XRPD, polarizing microscopy and SEM-EDS brought to the detection of specific mineral/chemical ‘markers’, which – when compared to those found on equivalent specimens of known geological origin – point to their feasible provenance from the Monviso ‘massif’. However, other sources – even closer the investigated site (such as the meta-ophiolite units cropping out in the Orsiera-Rocciavré mountain range or in the lower Susa valley) cannot be ruled out. Presence, on the many retrieved greenstone roughouts and broken tools, of raw, yet unpolished surfaces ascribable to pebbles and cobbles from alluvial or glacial deposits, suggests that these rocks might have been picked up from local ‘secondary’ sources – an assumption that is further supported by the small dimensions of the artifacts. The abundance of roughouts and broken tools labels Chiomonte as a second-order/manufacturing site, though it still remains unclear whether such an activity was restricted to the local needs or rather contributed to the circulation of greenstone implements on a wider scale.

Giustetto R. & Compagnoni R. (2014) - Petrographic classification of unusual high-pressure metamorphic rocks. *European Journal of Mineralogy*, 26(5), 635-642.

Castellani gold jewels: materials characterization by in-situ, non invasive analyses at the Museo di Villa Giulia (Rome)

Manca R.*¹, Scrivano S.²⁻³, Manfredi C.⁴, Ager Vázquez F. J.²⁻⁵, Ortega Feliu I.²⁻⁶, Respaldiza M.A.²⁻⁷ & Benvenuti M.¹

¹ Dipartimento di Scienze della Terra, Università degli Studi di Firenze, Firenze (Italia).

² Centro Nacional de Aceleradores, (Universidad de Sevilla-CSIC-J. Andalucía), Sevilla, España.

³ Laboratorio de Rayos X, Centro de Investigación Tecnología e Innovación de la Universidad de Sevilla (CITIUS), Universidad de Sevilla, Sevilla, España.

⁴ Dipartimento di Studi Umanistici, Università degli Studi di Roma Tre, Roma (Italia).

⁵ Departamento de Física Aplicada I. Universidad de Sevilla, Sevilla, España.

⁶ Departamento de Física Aplicada III. Uni. de Sevilla, Camino de los Descubrimientos, España.

⁷ Departamento de Física Atómica, Molecular y Nuclear. Universidad de Sevilla, Sevilla, España.

Corresponding email: m.benvenuti@unifi.it

Keywords: Italian Archaeological Jewellery, Castellani, production practices, gold jewels.

The Castellani were among the most popular goldsmiths of the 19th century. Based in Rome, but internationally admired, they invented the so-called Italian Archaeological Jewellery, i.e. a revivalist style based on the copy, reproduction and reinterpretation of ancient jewels. Their production has been enormous and their creations are present in many important museums all over the world. In addition to this, the Castellani were collectors and antiques dealers and sold to museums a wide range of ancient - or purported ancient - artefacts.

This research is aimed at broadening our knowledge on the production practices and the various technological experimentations made by the Castellani in the attempt of re-discovering and imitating ancient techniques.

We focused on the technical investigation and compositional analysis of the metal alloys and soldering techniques used for the Castellani gold jewels at the Museo Nazionale Etrusco di Villa Giulia (MN-ETRU) in Rome. When present, we also analysed the enamelled decorations.

Due to the impossibility of taking any sample and of moving a large number of jewels, we set inside the museum's laboratories a portable micro-XRF spectrometer. Thanks to polycapillary optics the X-rays beam is focused on a spot of analysis of 30 µm (Scrivano et al., 2017), thus allowing the analysis of single wires, granules, joining areas, etc.

Castellani jewels made in different periods and with different technical details were analysed in order to make a broad comparative study. In some cases, it was also possible to analyse the ancient jewels which were used as model and direct source of inspiration by the Castellani and which are also held at the MN-ETRU to understand how they developed their imitations starting from ancient prototypes.

The set of analytical data so far acquired is a precious tool to deepen our understanding of the Castellani production practices, the use of geomaterials during the 19th century and to shed some light on the role of this important goldsmiths family in restoring and, possibly, faking, ancient jewels.

The authors sincerely thank the Museo Nazionale Etrusco di Villa Giulia for making the Castellani Collection jewels available for this study.

Scrivano S., Ruberto C., Gómez-Tubío B., Mazzinghi A., Ortega-Feliu I., Ager F.J., Laclavetine K., Giuntini L. & Respaldiza M.A. (2017). In-situ non-destructive analysis of Etruscan gold jewels with the micro-XRF transportable spectrometer from CNA. *J. Archaeol. Sci. Reports*, 16, 185-193.

Archaeometric analysis on ceramic material from the Khalet al-Jam'a necropolis (Bethlehem, West Bank)

Medeghini L.¹, Botticelli M.*¹, De Vito C.¹, Nigro L.² & Mignardi S.¹

¹ Department of Earth Sciences, Sapienza University of Rome.

² Department of Oriental Studies, Sapienza University of Rome.

Corresponding email: michela.botticelli@uniroma1.it

Keywords: Bronze Age Ceramics, multi-analytical approach, technological level.

Since 2014 Sapienza-Palestinian MOTA-DACH Expedition has started systematic excavations in the site of Khalet al-Jam'a, a necropolis located South-East of Bethlehem, very close to the well-known Church of the Nativity (Nigro et al., 2015, 2017). The necropolis included at least 100 shaft tombs, used for a very long period of time from the Early Bronze Age up to the beginning of the Iron Age (2300-700 BC), suggesting the importance of the site for the Bethlehem town (Nigro, 2015).

Optical microscopy in thin section (OM), X-ray Powder diffraction (XRPD) and Scanning Electron Microscopy coupled with X-ray Energy Dispersive Spectroscopy system (SEM-EDS) are applied on ceramic materials from the tomb C5, dated in the Middle Bronze Age, to define the raw material used in the production and the technological level reached by this ancient culture.

Preliminary results show that the ceramics were produced with a calcareous clay characterized by the predominant presence of fragments of limestone, crystals of calcite, dolomite, and rare fragments of sedimentary siliceous rocks, quartz and fossils. The extreme variability of the matrix color suggests that the firing process was performed in uncontrolled atmosphere conditions. The mineralogical assemblages and the microstructure analysis allow estimating a variable firing temperature among samples. For some samples, the presence of abundant calcite, clay minerals and the absence of neo-formed minerals, suggests a firing temperature lower than 800 °C (Medeghini & Nigro, 2017), whereas for others the co-occurrence of calcite, gehlenite and wollastonite allows estimating the temperature in the range 850-950 °C (Cultrone et al., 2001).

The results of the study enable a preliminary characterization of pottery and contribute to improve the knowledge about specific ceramic production used in funerary contexts.

Cultrone G., Rodriguez-Navarro C., Sebastian E., Cazalla O. & De La Torre M.J. (2001) - Carbonate and silicate phase reactions during ceramic firing. *Eur. J. Mineral.*, 13, 621-634.

Medeghini L. & Nigro L. (2017) - Khirbet al-Batrawy ceramics: a systematic mineralogical and petrographic study for investigating the material culture. *Period. Mineral.*, 86, 19-35.

Nigro L. (2015) - Bethlehem in the Bronze and Iron Age. A summary in the light of recent discoveries by the Palestinian MOTA-DACH. *Vicino Oriente*, 19, 1-15.

Nigro L., Montanari D., Ghayyada M. & Yasine J. (2015) - Khalet al-Jam'a. A Middle Bronze and Iron Age necropolis near Bethlehem (Palestine). *Vicino Oriente*, 19, 185-218.

Nigro L., Montanari D., Guari A., Tamburrini M., Izzo P., Ghayyada M., Titi I. & Yasine J. (2017) - New archaeological features in Bethlehem (Palestine): the Italian-Palestinian rescue season of 2016. *Vicino Oriente*, 21, 5-57.

Monte Carlo SEM-EDS micro- and nanoanalysis in archaeometry and cultural heritage: Thickness, shape/geometry effects and measurement strategy

Moro D.*¹, Ulian G.¹ & Valdrè G.¹

¹ Centro di Ricerca Interdisciplinare di Biomineralogia, Cristallografia e Biomateriali, Dipartimento di Scienze Biologiche, Geologiche e Ambientali, Università di Bologna “Alma Mater Studiorum”, Bologna, Italy.

Corresponding email: daniele.moro@unibo.it

Keywords: Monte Carlo simulation, SEM-EDS microanalysis, Accurate analytical strategy.

In the field of archaeometry and cultural heritage conservation Scanning Electron Microscopy (SEM) coupled to Energy Dispersive X-ray Spectrometry (EDS) is a very practical and effective methodology to investigate the local morphology and composition of micro- and sub-micrometric samples. However, a careful micro-analytical strategy must be considered when the dimensions of the object in analysis approach those of the electron penetration volume. Many artefacts could arise from the electron and X-ray scattering in the sample and from EDS detector – sample configurations and arrangements, causing large errors in the quantification. The complexity arises from the variable objects shape and small thickness (< 5 µm) compared to the penetration length of the incident electron beam. A reduced X-ray absorption is mainly related to the object shape, affecting both the length of the X-ray absorption path within the object and the take-off angle. A second effect is related to the elastic scattering of electrons in the finite size (mass) of the object, strongly influenced by the average atomic number. This could be the case, for instance, of thin layers in paintings, surface protective treatments, contamination and alteration layers, micro- and sub-microscopic surface inhomogeneity, oxidized metal surfaces, often found in archaeometry and cultural heritage research.

In the present work, Monte Carlo simulation is proposed as an analytical strategy for simulating either electron transport and X-ray generation (characteristic and Bremsstrahlung) and transport, including primary and secondary fluorescence generation in micro- and sub-micrometric samples and to a realistic EDS X-ray detector. Electron trajectories can be modelled considering the elastic scattering and a continuous energy loss (continuous slowing down approximation). Models are implemented for the elastic scattering, the energy loss, the ionisation cross-section, the mass absorption coefficients and the fluorescence yields. This approach is here proposed reporting as an example a case study on the analysis of ultrathin gold leaves (down to about 100 nm) in glass mosaic tesserae, made up of the support glass, the metal leaf (with different Au-Ag contents) and the cartellina glass. The micro-analytical strategy took into account realistic experimental conditions, such as sample geometry, SEM set-up and detector physics. In order to optimize the microanalysis strategy, in this work the effects related to the electron probe size, electron beam energy and intensity, electron elastic/anelastic scattering, element ionization threshold levels, X-ray generation/adsorption/fluorescence and SEM-EDS chamber setups (azimuthal angle of the probe, take-off angle of the sample, orientation of the electron beam) were considered. The reported results could be very helpful to obtain a detailed, accurate quantitative analysis of micro- and sub-micrometric features working with different types of SEMs and EDS detectors.

Setting the technological patterns in the Neolithic pottery production of central Apulia

Muntoni I.M.¹, Torre M.² & Eramo G.*³

¹ Soprintendenza Archeologia, Belle Arti e Paesaggio per le Province di BAT e FG.

² Dipartimento di Storia, Culture e Civiltà, Università di Bologna.

³ Dipartimento di Scienze Geoambientali, Università di Bari Aldo Moro.

Corresponding email: giacomo.erao@uniba.it

Keywords: Neolithic, pottery, petrography.

The results discussed in this paper represent a first overview of Mid-Late Neolithic Serra d'Alto pottery in the Murge Area, where this kind of ware is widely attested in the V millennium BC especially in ritual and/or funerary archaeological contexts.

The frequent occurrence of the same fabrics in different contexts suggests the circulation of technological models.

To understand the technological properties as relating to raw materials, clay preparation and firing technique, a group of 78 samples were subjected to petrographic analysis on thin section.

The principal aim was to identify differences and/or analogies between ceramic materials from different geographical and archaeological sites, such as caves and settlements, or structures related to them, comparing ceramic materials on technological, geological and archaeological point of view in order to verify the existence of technological model exchanges.

The potsherds analyzed belong to figulina (no. 37), fine (no.26) and semi-fine (no.15) paste groups.

Petrological observations allowed to identify nine different fabrics, collected in three sets on the basis of predominant mineralogical phase represented by quartz (Q), calcite sand (K) and spathic calcite (Ks).

All the petrofacies expressed by the samples are compatible with the karst environments of the sites studied and the pastes are mainly associated with residual clays (i.e. terra rossa).

The Q* fabrics are more widespread in the hinterland, close to the lame, the typical broad, shallow valleys covered on the bottom by colluvial terra rossa and calcareous sand eroded from calcarenites; among this first set, the fabric QK is interpreted as the result of this kind of sediment. Fabric KB, by contrast, rich in calcareous sand and bioclasts, is associated with the shoreline. Although the Ks* fabrics are not associated exclusively with caves, the spathic calcite can be considered to be of speleothemic origin. These fabrics were interpreted as tempered, whereas smaller amounts of spathic calcite and/or calcareous sand were more probably part of the clay.

As for the archaeological wares, the figulina pottery, usually brown painted and/or adorned with zoomorphic handles, is associated with quartz-bearing fabrics and with terra rossa, naturally available with the characteristics observed in thin section. The fine and semi-fine wares, usually unadorned or decorated with incised motifs, present more variable relations with fabrics and probable different strategies of clay exploitation and/or processing.

These preliminary results represent an initial overview of Mid-Late Neolithic material culture in the Murge area through the comparison of pottery samples from various contexts, highlighting technological patterns and showing a local production at every archaeological site together with the use of local or proximal raw materials. Ongoing research at a larger number of sites in the same area will confirm/refute these preliminary results.

Mineralogical and petrographic evidences of fires at Pisa Cathedral: the case of Panchina Livornese

Pancani D.*, Raneri S. & Gioncada A.

Dipartimento di Scienze della Terra, Corso di Laurea in Scienze e Tecnologie Geologiche, Università di Pisa.

Corresponding email: pancani.dario12@gmail.com

Keywords: fires, mineralogical changes, calcarenite.

In the last decade, great attention was devoted to evaluate the impact of global changes in monuments, specifically in protecting heritages from natural and anthropogenic hazards. Thus, the in deep knowledge of conservation history of masonry and its resilience to anthropic risk may support the application of better conservation strategies. During restoration works carried out at the Pisa Cathedral, some elements related to the first construction phases have been brought to the light, especially at the matroneum. Here, the occurrence of a coarse yellowish calcarenite has been evidenced under the marble covering slabs, attributable to Panchina Livornese (Bossio et al., 1998; Sarti et al., 2017), a geological Fm. used since Etruscan period through southern and costal Tuscany (Lezzerini, 2005; Lezzerini et al., 2018). The inspection of the matroneum walls evidenced a huge chromatic surface alteration of the lithotype, turning from yellow to deep red, and dark grey coatings. The possibility to sample some specimens from different galleries make it possible to characterize the lithotype and evaluate the possible relation between the alteration forms and the involvement of the structures in the well-known fire occurred in 1595 (Peroni, 1995). The minero-petrographic analysis of samples, coupled with SEM-EDS and micro-Raman spectroscopy allowed identifying textural and mineralogical elements concerning the effects of fire on the stone surface (Martinho & Dionísio, 2018). The study was complemented by laboratory tests on fresh stone to validate the proposed hypothesis and evaluate the effects of fires into the aesthetical and physical properties of the stone.

The authors acknowledge the Opera della Primaziale Pisana for having provided the studied samples.

- Bossio A., Costantini A., Foresi L.M., Lazzarotto A., Mazzanti R., Pascucci V., Salvatorini G., Sandrelli F. & Tersuoli A. (1998) - Neogene-Quaternary sedimentary evolution in the western side of the Northern Apennines (Italy). *Mem. Soc. Geol. It.*, 52, 513-525.
- Lezzerini M. (2005) - Mappatura delle pietre presenti nella facciata della Chiesa di San Frediano (Pisa, Italia). *Atti Soc. toc. Sci. Nat., Mem. Serie A*, 43-50.
- Lezzerini M., Raneri S., Pagnotta S., Columbu S & Gallelo G. (2018) - Archaeometric study of mortars from the Pisa's Cathedral Square (Italy). *Meas. J. Int. Meas. Confed.*, 126, 322-331.
- Martinho E. & Dionísio A. (2018) - Assessment Techniques for Studying the Effects of Fire on Stone Materials: A Literature Review. *International Journal of Architectural Heritage*, 1-25. <https://doi.org/10.1080/15583058.2018.1535008>
- Peroni A. (1995) - *Il Duomo di Pisa*. Franco Cosimo Panini, Modena.
- Sarti G., Bertoni D., Capitani M., Ciampalini A., Ciulli L., Cerrina Feroni A., Andreucci S., Zanchetta G. & Zembo I. (2017) - Facies analysis of four superimposed transgressive-regressive sequences formed during the two last interglacial-glacial cycles (Central Tuscany, Italy). *Atti Soc. Tosc. Sci. Mem., Serie A*, 124, 133-150.

A newly discovered ceramic production center in Camerino (Marche, Italy)

Paris E.*¹, Sciarroni G.², Virgili S.³, Abudurehman A.¹ & Antongirolami V.³

¹ School of Science and Technology, Geology division, University of Camerino.

² L-43 – Corso di laurea in Scienze e tecnologie per la conservazione e il restauro, Università di Camerino.

³ Archeolab.

Corresponding email: eleonora.paris@unicam.it

Keywords: ceramic production center, Camerino-Marche, 3D reconstruction.

Camerino has a long history. It was founded by the Umbrii-Camertii and, after becoming a Roman ally (310 BC), it was a foedus aequum, testifying a pact between Romans and the Umbri-Camertii with conditions equal for both, demonstrating the strategic importance of the town, located along the roads connecting Adriatic and Tyrrhenian coasts. In 1000 Camerino turned itself into a Guelph commune and in 1262 Gentile da Varano started the dynasty which lasted three centuries, promoting a vibrant cultural atmosphere, founding the University in 1336, with a curriculum studiorum present since 1220.

In spite of the long history, the overlapping of episodes of construction and destruction due to earthquakes, made it impossible to clearly understand the architectonic development of the town, hiding also any sign of the economic activities. The ceramic production during medieval age, given the importance of the city for an extended period of time, was certainly present and important but completely obliterated, until the archaeological excavations carried in the period 2004-2014. In the city center (Pino Argentato) a small furnace was recovered with “maiolica arcaica” materials inside, and near the Tempio dell’Annunziata two large ceramic furnaces were recovered, with abundant materials. This second site, studied thanks to the stratigraphy and the ceramic materials, allow to assign the furnaces to the period between XIII century and first part of the XVI. This area has been recognized now as the “industrial area”, located in the periphery of the town, outside the city walls. The Tempio dell’Annunziata (or dei Varano), which was built in the area, is a clear terminus ante quem (1492-1508).

The recovered materials, the so-called “ceramica graffita”, were found mostly in pieces as production waste, at different stages of production, some decorated with green/brown pigments and glazed or only with a white slip and graffiti representing geometrical and floral items, with some characteristic features. The materials, which have been studied by powder XRD, petrographic analyses and SEM, are homogeneous in mineralogical composition (quartz and small amounts of calcite and feldspars) and granulometry of the small aggregates (rounded flint and few chamotte grains). All indicates an attention to the preparation and a well-established tradition in the manufacture of the products and choice of the components, unchanged for a long period of time. The XRF analysed will help to establish the chemical composition for further provenance studies.

The archaeometric study of the materials contributed to give information regarding the ceramic production, as well as shed some light to the artisans’ activity in Camerino at the time. This information, now still preliminary, will be used to complement the exposition in the Civic Museum, when will be reopened to the public, enriching also the knowledge about the Medieval ceramic production in the Marche and Central Italy.

Tracking animal movements with tooth enamel oxygen and strontium isotopes

Pellegrini M.^{*1-2}, Donahue R.E.³ & Lee-Thorp J.A.²

¹ Thermo Fisher Scientific, Italy.

² Research Laboratory for Archaeology and the History of Art, University of Oxford, UK.

³ Department of Anthropology, Michigan State University, USA.

Corresponding email: maura.pellegrini@thermofisher.com

Keywords: animal movements, isotopes, fossil teeth.

The investigation of animal and human movements by means of isotopes has become an established practice in archaeological, palaeontological, and forensic sciences. Particularly successful are the combinations of strontium isotopes, which are inherited by the individual's tissues from the geological background through ingested food and drinks, and oxygen isotopes, similarly acquired from the local environmental and proxies for the climatic conditions.

This paper will present the methods employed and the results of an isotopic study in which $\delta^{18}\text{O}$ and $^{87}\text{Sr}/^{86}\text{Sr}$ were measured sequentially in deer and horse teeth of fossil remains from a Palaeolithic archaeological site in southern Italy. The aim of the study was to assess animal's roaming areas around the archaeological site throughout the year, and therefore humans hunting those animals' subsistence strategies. The study includes samples coming from stadial and interstadial climatic phases of the last Late-Glacial. Because teeth in ungulate species grow with a nearly linear direction, sequential measurements of isotopes in these teeth has the potential to provide timing and locations roamed by those animals during the mineralization of their teeth. Such mineralization, known as amelogenesis, in these species may take from a little less than one to over two years, therefore enough to record yearly/seasonal movements of the animal. Moreover, the analysis of samples from different climatic phases provide information of possible changes in these movements associated to specific climatic conditions.

Overall, this communication will illustrate the potentials of combined stable and radiogenic isotope geochemistry in assisting cultural heritage studies and archaeological research.

Macedonian ruby: mineralogical and geochemical analysis of a national treasure

Precisvalle N.¹, Ardit M.*¹, Martucci A.¹, Bonadiman C.¹, Bianchini G.¹ & Natali C.²

¹ Dipartimento di Fisica e Scienze della Terra, Università degli Studi di Ferrara.

² Dipartimento di Scienze della Terra, Università degli Studi Firenze.

Corresponding email: rdmttt@unife.it

Keywords: Macedonian ruby, diasporescence.

Corundum crystals from Prilep area (Macedonia) are known in the jewelry market since the 1988, when they appeared for the first time at Tržič mineral fair in Slovenia (Jeršek et al.). Commonly referred as “Macedonian ruby”, this stone had its comeback around the 2006 thanks to Dejan Shkartov, and it is considered the national gemstone of North Macedonia. Today, Macedonian ruby jewelry is a common diplomatic gift from North Macedonian Government. Rubies can be found in marbles from Prilep municipality, included in calcite cavities. These marbles are the uppermost part of highly metamorphic rocks which belong to the central part of the Pelagonian Massif, in the SW of North Macedonia (Jeršek et al.). The specimens usually occur with inclusions of oxides, carbonates (e.g., dolomite and calcite), and aluminum hydroxide. This makes these stones more prone to cabochon than to faceted cut. The main characteristics for Macedonians rubies are: 1) presence of diasporite intergrowth, 2) raspberry-pink colour (light, moderately strong, slightly purplish red), and 3) plate-like, barrel-like and prismatic morphology (Barič, 1963). Diasporite grows in rubies following three preferential directions crossing at 60 degrees (Barič, 1963). Described only in these gemstones, the diasporite intergrowths give to the Macedonian rubies a silver glittering effect called “diasporescence” (Dobnikar et al., 2013; Jeršek et al.). The aim of this work is to study the corundum/diasporite phase ratio, in order to better understand the role of diasporite in these rubies, and characterize Macedonian rubies on geochemical and crystallographic basis. Chromophore ions content, quantified by means of LA-ICP-MS, is rather different compared to what reported in analogues samples by Jeršek & Mirtič (1999). In particular, the chromium contents reach the anomalously high value of 586 ppm, twice as much as highest values (267ppm) reported so far for this population (Jeršek et al.). X-ray diffraction measurements at room temperature show that crystals are biphasic, exclusively composed by diasporite (62 wt.%) and corundum (38 wt.%). Looking for a purer ruby gemstone, the structural behavior of a Macedonian ruby has been studied at high temperature by XRD analysis up to 900 °C. Along with a temperature-induced lattice parameters expansion for both phases, the diasporite/corundum phase fraction ratio, stable up to 450 °C, experiences an abrupt drop in the temperature range of 500-550 °C. Above this range, no more diasporite phase is detected.

Barič L. (1963) - Über die orientierte Verwachsung des Diaspors und des Korunds von Sivec in Mazedonien. Beitr. Mineral. Petr., 9, 133-138.

Dobnikar M., Ferme E., Humar M., Simona S., Jeršek M., Mlakar D., Razinger B. & Šturm M. (2013) - Gemološki terminološki slovar. Založba ZRC, ZRC SAZU.

Jeršek M. & Mirtič B. (1999) - Corundum from Prilep dolomitic marble. Scopolia, 41, 1-22.

Jeršek M. (2015) - Diasporescence in rubies from prilep dolomitic marble. Maced. J. Chem. Chem. En., 34, 139-143.

Historical mortars beyond Pompeii: the example of Villa del Pezzolo (Sorrento Peninsula)

Rispoli C.*¹, Cappelletti P.¹, De Bonis A.¹, Di Benedetto C.¹, Esposito R.², Graziano S.F.¹⁻³,
Guarino V.¹ & Morra V.¹

¹ Dipartimento Scienze della Terra, dell'Ambiente e delle Risorse, Università di Napoli Federico II, Napoli, Italy.

² Dipartimento di Scienze Umanistiche, Università di Napoli Federico II, Napoli, Italy.

³ Dipartimento di Farmacia, Università degli Studi di Napoli Federico II, Napoli, Italy.

Corresponding email: rispolit@gmail.com

Keywords: Sorrento Peninsula, mortar characterization, raw materials

Villa del Pezzolo is an example of a Roman villa located in the Bay of Naples, which includes several worldwide known archaeological sites, among which Pompeii represents, by far, an almost unique example of a still-visible ancient town. Nevertheless, minor, but not for importance, sites (villas, cisterns, thermae, necropolis, etc.) are widespread all over the Bay of Naples. Goal of this study is the archaeometric characterisation of the lime-based mortars from Villa del Pezzolo, a Roman villa dated from the 1st century B.C. to 3rd century A.D. Villa del Pezzolo is located in Marina di Equa (modern Seiano) in southern Italy. This patrician Roman Villa is very interesting for both archaeologists and geologists because represents one site, along Sorrento Peninsula coast, where the consequences of the A.D. 79 eruption of Mt. Vesuvius are clearly visible, despite the great distance from the eruptive center. Sampling was designed by gathering all the available information about geology and archaeological history of the site in strict cooperation with the archaeologists from the Superintendence of Archaeological Heritage of Campania, who recognised three building phases of the monument. Therefore, representative and non-invasive samples of each of the three building phases, were collected. A multi-analytical mineralogical-petrographic approach was implemented for the investigation by means of PLM, XRPD, SEM-EDS, TG/DTA, and MIP. The analyses of mortars from Villa del Pezzolo evidenced the use of local geomaterials composed by sedimentary calcareous and volcanic aggregates, but also confirmed the three distinct building phases identified by archaeologists. Volcanic tuff fragments identified in mortars of the 1st building phase are ascribed to the Campanian Ignimbrite formation, widely cropping out in the Sorrento Peninsula. This was confirmed by the presence of glassy shards, partially devitrified and replaced by authigenic feldspar: a typical feature of welded gray Campanian Ignimbrite lithofacies (WGI; Langella et al., 2013). The volcanic aggregates in samples of the 2nd and 3rd building phases show, instead, the presence of leucite-bearing volcanic scoriae and garnet crystals, which are related to the Somma-Vesuvius activity. The study of these mortars allowed us to: 1) understand the different production technologies, 2) highlight the use of materials with hydraulic behaviour, such as pozzolanic materials and fictile fragments, 3) confirm the three building phases from compositional features of mortars and 4) highlight the change over time of the supply area of the volcanic aggregate for mortar mix-design.

Langella A., Bish D.L., Cappelletti P., Cerri G., Colella A., de Gennaro R., Graziano S.F., Perrotta A., Scarpati C. & de Gennaro M. (2013) - New insights into the mineralogical facies distribution of Campanian Ignimbrite, a relevant Italian industrial material. *Applied Clay Science*, 72, 55-73.

Volcanic millstones trade in the Mediterranean during the Hellenistic-Roman period: the impact on the production of manufacts and milling technique evolution at Ustica Island (Southern Tyrrhenian Sea, Italy)

Santi P.1, Foresta Martin F.2-3, Spatafora F.4, De Vita S.5, Dell'Aquilano M.6 & Renzulli A.*1

¹ Dipartimento di Scienze Pure e Applicate, Università degli Studi di Urbino Carlo Bo, Urbino.

² Laboratorio Museo di Scienze della Terra, Ustica, Palermo.

³ Istituto Nazionale di Geofisica e Vulcanologia, Sezione di Palermo.

⁴ Polo Regionale di Palermo per i Parchi e Musei Archeologici, Palermo.

⁵ Istituto Nazionale di Geofisica e Vulcanologia, Sezione di Napoli. 6 Independent Researcher.

Corresponding email: alberto.renzulli@uniurb.it

Keywords: lavas, grinding tools, Ustica.

Ustica Island is located in the southern Tyrrhenian Sea (ca. 60 km to the north of Palermo, Sicily) and represents the subaerial part (248 m above the sea level) of a large submarine volcanic edifice more than 2000 metres deep. The exposed volcanism developed between 750 and 130 ka, the latter age referred to the youngest eruption of the Falconiera Tuff Cone in the NE sector of the island. The volcanic rocks of Ustica (lavas and pyroclastics), belong to the Na-alkaline series, ranging from basalts to trachytes, with a compositional gap only between ca. 56 and 60% SiO₂ (i.e. benmoreite).

Although inhabited from Neolithic Age, an intense occupation of the island only started in the Middle Bronze Age (e.g. Faraglioni village), a period in which Ustica was probably involved in Tyrrhenian commercial routes that affected the northern coast of Sicily and the Aeolian islands. The sudden disappearance of the Faraglioni village marked a period of abandonment of the island, interrupted only by sporadic frequentation. No nucleus of people settled there in a stable manner until the 3rd century BC, in the Hellenist-Roman Period, as testified by some necropolises mainly located on the western slopes of the Falconiera Tuff Cone.

This study focuses on 28 grey to dark-grey lava manufacts with a variable degree of vesiculation, referable to different grinding tools such as large saddle querns (n.2), Morgantina-type rotary millstones (n.5 metae and n.11 catilli), simple rotary mills (n.9), and one small mortar. Thin section petrography and bulk rock geochemical analyses emphasize most of the grinding manufacts belong to the Na-alkaline rocks of Ustica, mainly basalts, hawaiites and mugearites. Nevertheless, some millstone samples do not match, on petrographic and geochemical basis, with lavas erupted at Ustica. Major and trace elements parameters (alkalies, REEs and incompatible elements normalized to chondrites and primitive mantle respectively, LILE and HFSE abundances) clearly point out some millstones not belonging to the Ustica magmatic series: one high TiO₂ Na-alkaline basalt, some tholeiitic basalts and one calcalkaline basaltic andesite. The investigated saddle querns are made of Ustica lavas and we can therefore infer that during the Middle Bronze Age, the production of the grinding stones was entirely addressed to the exploitation of local volcanic rocks. Starting from the 4th century BC in the Mediterranean, the milling technique turn to the more efficient Morgantina-type rotary millstones and some of them arrived to Ustica through the Mediterranean Sea trade, as testified by some metae and catilli made of Na-alkaline and tholeiitic basalts from other volcanic provinces. On the basis of this new milling technology, the Morgantina-type rotary millstones then started to be produced using the local Na-alkaline lavas of the island as well. The simple rotary mill made of a calcalkaline basaltic andesite should be related to commercial trade in modern time.

Olduvai Subchron (Pliocene-Pleistocene Transition) In Tyrrhenian Sea and Africa Rift Valley: Geological and Paleoanthropological Implications

Savelli C.*

Ismar CNR, Bologna (retired).

Corresponding email: carlo.savelli@bo.ismar.cnr.it

Keywords: Olduvai Subchron, Tyrrhenian Sea, Olduvai Gorge

The Tyrrhenian oceanic opening clearly exhibits a concomitance of hyper-extension tectonics and MORB-type volcanism. In the Late Tortonian-Early Messinian, the submerged continental margin of Hercynian Sardinian microplate experienced hyper-extension due to low-angle east-dipping faulting. At about the same time, MORB lavas erupted in Vavilov basin (DSDP Site 373). Such early short-lived oceanization pulse was followed by the tectono-magmatic activity of Latest Pliocene age (Olduvai Subchron; Savelli & Ligi, 2017). In Marsili basin (ODP Site 650; Kastens et al., 1988), deep-seated MORB-type volcanics with positive magnetic imprinting are overlain by microfossil-rich sediment showing Latest Pliocene age and negative magnetization (Matuyama Chron). The Matuyama Chron is followed by forams-bearing sedimentary successions of Pleistocene age (Brunhes Chron). Biostratigraphic and magnetic reversal features indicate Olduvai Subchron age of Marsili basin oceanization (1.9 – 1.7Ma). The N-S trending axial zone of Vavilov basalt plain experienced hyperextensional low-angle east-dipping faulting at the same time of Marsili oceanic opening (Olduvai Subchron).

At the Olduvai Gorge, Rift Valley of Northern Tanzania were found most important skeleton fragments of Early man (*Homo habilis* - Leakey et al., 1961; Evernden et al., 1965). Hominid remains are associated to footprints that are preserved in K-rich, sanidine-bearing volcanoclastic sediment. The continental sediment layers which yielded skeleton fragments of Hominid capable of working the stone to fashion tools at Olduvai Gorge are of suitable nature for accurate age determination. In fact, the paleomagnetic reversal time scale has been used together with K-Ar Ar-Ar and fission track geochronology of K-rich igneous rocks. Radiometric and paleomagnetic dating shows that the *H. habilis* first appearance is respectively about 1.8/1.7 Ma old and related to the Olduvai Subchron (1.9 – 1.7 Ma). Overall, Tyrrhenian Sea and the East Africa Rift Valley appear to be key-areas to investigate the Tertiary - Quaternary (Anthropozoic) boundary.

Evernden J.F., Curtis G.H., Bishop W., Brace C.L., Clark J.D., Damon, P. E., Hay R.L., Hopkins D.M., Clark Howell F., Knopf A., Kretzoi M., Leakey L.S.B., Maude H.E., Richards J.R., Savage D.E. Wright H.E. Jr. (1965) - The potassium-argon dating of late Cenozoic rocks in East Africa and Italy [and comments and reply]. *Current Anthropology*, 6(4), 342-385.1965.

Kastens K., Mascle J. & ODP LEG 107 Scientific Staff (1988). ODP Leg 107 in the Tyrrhenian Sea: Insights into passive margin and back-arc basin evolution. *Geological Society of America Bulletin*, 100(7), 1140-1156.

Leakey L.S.B., Evernden J.F. & Curtis G.H. (1961) - Age of Bed I, Olduvai Gorge, Tanganyika. *Nature*, 191, 478-479.

Savelli C. & Ligi M. (2017) - An updated reconstruction of basaltic crust emplacement in Tyrrhenian sea, Italy. *Scie. Rep.*, 7, 18024

Archaeometric contribution to the study of the Small Thermal Baths in the roman town of Nora (Sardinia): mortars and plasters

Scrivano S.*¹, Cabella R.¹ & Giannattasio B.M.²

¹ Dipartimento di Scienze della Terra, Ambiente e Vita, Università degli Studi di Genova.

² Dipartimento di Antichità, Filosofia, Storia, Università degli Studi di Genova.

Corresponding email: simona.scrivano@edu.unige.it

Keywords: archaeometry, mortars and plasters, Piccole Terme.

The building identified as Small Thermal Baths in the archaeological site of Nora (near Cagliari, Sardinia – Italy) has a long history. The archaeological data acquired during the excavations along with the analysis of the unearthed coins and ceramic fragments allowed identifying several life phases of the complex. Between II century BC and II century AD private houses lied on the area; along the III century AD the structures were converted in thermal building, probably private at first, than public after renovations during the IV century AD. At last, during late antiquity the complex returned to poor housing and artisanal activities before the abandonment of the site (VIII century AD). In order to support archaeologist in interpreting the complex history of the building and in defining chronology and function of the structures, archaeometric analysis of bedding mortars and plasters were undertaken. A selection of 11 samples, mainly from the frigidarium and corridor area, was characterized by polarized light optical microscopy (PLOM) and scanning electron microscopy with microprobe (SEM-EDS).

Mortars show a relative uniformity by means of petrographic composition of the aggregate. Most of the samples are characterized by the presence of quartz, feldspars, limestones, Palaeozoic-basement rocks, volcanic rock fragments and bioclasts in variable amounts. The selection of the aggregates and their grainsize varies along with the function. Samples belonging to structures connected to water retention or humidity insulation present intentional addition of cocchiopesto and, in some cases, abundance of volcanic glass fragments. The differences in the formulation of hydraulic mortars in structures with the same function suggest stepwise constructive phases. Plasters composition limited to lime, quartz, limestones, bioclasts and white marble fragments, along with the fine grainsize of the outermost layer reflect the rules reported in the Vitruvio essay *De Architectura*. Moreover, the absolute absence of coloured aggregates proved to be essential to make the red linear decorations characterizing some of the pieces stand out. The common lack of lumps in the matrix of both mortars and plasters indicates good technical skills in controlling the temperatures inside the furnaces for calcination.

The archaeometric information acquired helped the interpretation of some of the wall structures, and the cross correlation between different samples helped constraining the temporal sequences of the building.

Archaeometric contribution to the study of the Small Thermal Baths in the roman town of Nora (Sardinia): white and coloured marbles

Scrivano S.*¹, Gambino F.², Borghi S.², Cabella R.¹ & Giannattasio B.M.³

¹ Dipartimento di Scienze della Terra, Ambiente e Vita, Università degli Studi di Genova.

² Dipartimento di Scienze della Terra, Università di Torino.

³ Dipartimento di Antichità, Filosofia, Storia, Università degli Studi di Genova.

Corresponding email: simona.scrivano@edu.unige.it

Keywords: archaeometry, marbles, Piccole Terme.

The building of the Small Thermal Baths in the archaeological site of Nora (near Cagliari, Sardinia – Italy) is organized in several rooms, which are clearly the results of subsequent additions. Based on field observations, coins and ceramic findings, archaeologists identified several phases of the complex dating between II century BC and VIII century AD. Amongst them, the thermal bath phases of III and IV century AD took on particular interest for the recovery of several ornamental stone fragments. The pieces were found mainly in 5 of the 10 rooms of the complex: the corridor, the *apodyterium*, the *frigidarium*, the *frigidarium*-pool and the *prae-furnium*. These spaces were probably those mostly affected by the IV century AD renovation of the thermal bath complex.

The study was addressed to 19 fragments of varicoloured and white marbles, to acquire information about material provenance and indirectly learn about the social and cultural milieu of the city at that time. The macroscopic analysis, polarized light optical microscopy (OM) and scanning electron microscopy with microprobe (SEM-EDS) were the basis for the comparative identification for the 16 fragments of coloured marble. For three selected fragments of white marble also grain boundary analysis and maximum grain size assessment were carried out, in association with stable isotope (C^{13} e O^{18}) measure to look for provenance determination. The analysed samples showed a satisfactory match with: *Greco Scritto* marble from Hannaba (Algeria, 2 pieces), *Rosso Antico* marble (Greece), *Cipollino* marble from Styra (Euboea, 2 pieces), *Verde Antico* marble (Greece, 3 pieces), *Giallo Antico* marble (Tunisia, 3 pieces), *Occhio di Pavone Pavonazzo* marble, *Pavonazetto* marble (Turkey), *Bigio Antico* marble (Greece), white *Hymettus* marble (Greece), white *Carrara* marble (Italy) and white *Paros/Docimium* marble (Greece/Turkey). The analysis encompassed also pieces of mosaic *tesserae*, which proved compatible with local limestone formations, and paving stones of minor rooms, which are compatible with locally outcropping effusive rocks.

On the whole the dataset shows how the city of Nora during III and IV century AD had a prosperous market that included ornamental stones from several localities of the Mediterranean basin. The presence of pieces of *Giallo Antico* and *Pavonazetto* marbles suggests a wealthy community who could afford the most precious ornamental stones for public edifices. Finally, the use of local resources for mosaic *tesserae* and slabs indicates that probably the great variety of foreign and multi-textured marbles was mainly employed for cladding.

Potentiality of PXRF for the discrimination of altered carbonate rocks in Cultural Heritage

Stroscio A.*¹, Coccato A.¹, Fugazzotto M.^{1,2}, Occhipinti R.¹, Mazzoleni P.¹ & Barone G.¹

¹ Dipartimento di Scienze Biologiche, Geologiche e Ambientali, Università degli Studi di Catania.

² Dipartimento di Scienze Umanistiche, Università degli Studi di Catania.

Corresponding email: antonio.stroscio@phd.unict.it

Keywords: calcarenite, artificial neural network, portable X-ray fluorescence.

In the last decade, PXRF analysis has become a widely applied method for the in situ direct study of cultural heritage objects, alone or combined with complementary techniques (Mantler & Schreiner, 2001). In fact, PXRF is a useful tool to study ceramics, paintings, and sculptures (Uda et al., 2005, Barbi et al., 2014), including the identification of original materials, old conservation or protective treatments, and possible alterations.

Recently, limestone varieties (calcarenites) sampled in various quarries in the Hyblean area, south-eastern Sicily, as well as museum samples, were chemically characterized by PXRF. The data were statistically treated (principal components analysis (PCA) and linear discriminant analysis (LDA)) (Barbera et al., 2012).

A further step in this respect is the application of artificial neural network (ANN), recently applied to the study of pottery provenance (Barone et al., 2019), to facilitate the discrimination of limestones from Hyblean area, by studying reference samples and historical buildings in Catania. This showed that, in addition to allowing the discrimination between different calcarenites, PXRF can detect trace-elements in situ and non-destructively. These elements are present in the environment, but both natural and anthropogenic processes can produce higher concentrations of specific elements (Schaap et al., 2010; Satsangi & Yadav, 2013). PXRF data allowed to study the spatial distribution of anomalous values of trace elements on degraded calcarenites, which is an interesting aspect for conservation purposes.

The research is supported by the PNR-funded “Advanced Green Materials for Cultural Heritage” project.

- Barbera G., Barone G., Crupi V., Longo F., Majolino D., Mazzoleni P. & Venuti V. (2013) - Nondestructive analyses of carbonate rocks: applications and potentiality for museum materials. *X-Ray Spectrometry*, 42(1), 8-15.
- Barbi N., Alberti R., Bombelli L. & Frizzi T. (2014) - A Non-Invasive Portable XRF System for Cultural Heritage Analyses. *Microsc. Microanal.*, 20, 2020-2021.
- Barone G., Mazzoleni P., Spagnolo G.V. & Raneri S. (2019) - Artificial neural network for the provenance study of archaeological ceramics using clay sediment database. *Journal of Cultural Heritage*.
- Mantler, M. & Schreiner, M. 2001. X-ray analysis of objects of art and archaeology. *J. Radioanal. Nucl. Chem.*, 247(3), 635–644.
- Schaap M., Weijers E.P., Mooibroek D., Nguyen L. & Hoogerbrugge R. (2010) - Composition and origin of Particulate Matter in the Netherlands. Results from the Dutch Research Programme on Particulate Matter.
- Satsangi P.G. & Yadav S. (2014) - Characterization of PM 2.5 by X-ray diffraction and scanning electron microscopy–energy dispersive spectrometer: its relation with different pollution sources. *Int. J. Environ. Sci. Technol.*, 11(1), 217-232.
- Uda M., Demortier G. & I. Nakai (eds.) (2005) - *X-Rays for Archaeology*. Springer, Amsterdam, The Netherlands.

Detection of graves and buried walls using ground penetrating radar: the Sant'Antioco di Bisarcio archaeological site (Sardinia)

Testone V.¹, Longo V.¹, Mameli P.*¹, Cherchi M.² & Milanese M.²

¹ Dipartimento di Chimica e Farmacia, Università di Sassari.

² Dipartimento di Storia, Scienze dell'Uomo e della Formazione, Università di Sassari.

Corresponding email: mamelip@uniss.it

Keywords: Ground-penetrating radar, church burials, Sardinia.

A GPR survey joined with magnetic prospection was carried out in Sant'Antioco di Bisarcio abbey and in the adjacent archaeological area, aiming to identify old indoor church burials and remains of buried walls around the church.

This Romanesque building betrays Pisan and Lombard stylistic influences and probably it was built, in the present form, between the 11th and 13th centuries by workmen from Burgundy. The building lies on an ignimbrite spur, has a central nave with original wooden roof separated by a colonnade supporting arches of two lateral aisles with a ribbed vaults. A medium grade ignimbrite prevails among the employed materials. This ignimbrite outcrops diffusely around the church. A fine-grained greenish epiclastic sandstone, outcropping north of the abbey defines dichromate inserts and decorations. It was employed in a couple of ashlar rows on the church walls and more diffusely in the monastery walls and in the surrounding village (Bisarchium or Guisarchum) ruins.

The GPR surveys were conducted using a monostatic GPR IDS model 'RIS_MF_HiMod Duo', consisting of a control unit working simultaneously with two transmitters operating at frequencies of 400 and 900 MHz, and two receivers.

Four GPR regular grids, running acquisition every 50 cm, allowed the complete indoor coverage of the church; externally the perimeter of the church and some areas close to the archaeological, in progress, excavations were investigated. Outside the church also a fluxgate magnetometer was used to support GPR prospecting.

The GPR data were processed using standard 2D processing with GRED v. 02.01.008 (IDS Ingegneria dei Sistemi, Pisa, Italy) software.

A study of the polarity of the reflected waves, inside of the church, allowed to better understand the radargrams in correspondence of some electromagnetic anomalies. Many reflection traces exhibit reverse polarity that are an index of interface between ground and the void space. The void spaces and the geometry of some electromagnetic anomalies, identified under the floor level of the naves and the altar, suggest the presence of burials, possibly carved in the ignimbrite, which supports the abbey. Amplitude GPR time-slice analysis joined with magnetometric data also indicates that many structural foundations and walls are still well preserved below the surface.

The bricks of the UNESCO historical town of Urbino (Marche, Italy): characterization, provenance of the raw material and archaeometric dating

Tonelli G.*¹, Renzulli A.¹, Santi P.¹, Talozzi D.², Tramontana M.¹ & Veneri F.¹

¹ Dipartimento di Scienze Pure e Applicate, Università degli Studi di Urbino Carlo Bo, (Italy).

² Studio di Ingegneria e Geologia, Urbania (Italy).

Corresponding email: gianluigi.tonelli@uniurb.it

Keywords: historical centre of Urbino, bricks, raw materials.

Man used bricks for buildings for thousands of years, but the greatest breakthrough came with the invention of fired bricks (about 3.500 BC). Due to the use of mobile kilns, the Romans strongly contributed to spread the fired bricks throughout the conquered territories. The historical town of Urbino (in the list of UNESCO World Heritage since 1998) is characterized by a very widespread use of bricks in monumental walls, palaces and churches. A collection of brick samples from buildings of different historical times such as the remnants of the Roman period, the Urbino Cathedral (built in a span time between the XI and the XVIII century), the Renaissance walls and some other monuments (Mazzini, 1982; Luni, 1985; Agnati, 1999; Luni & Ermeti, 2001; Negroni, 2005) will be investigated through a comprehensive archaeometric project. Close to the town of Urbino, several raw materials suitable to make bricks, such as fine-grained clayey soils, are present and ruins of ancient furnaces since the Roman period are also recognizable (Luni, 1986). Concerning the Urbino Cathedral, the bricks are representative of numerous diachronic building phases, mainly due to the reconstructions after the seismic events of the XVII and XVIII centuries.

The aim of the present work will be the mineralogical and chemical characterization of the bricks in order to define the nature and the provenance of the raw materials employed in their manufacture. Standard thin section and powder XRD methods will be used to identify the different mineralogical assemblages and to establish the reached thermal conditions of firing, whereas major-trace elements analyses (ICP-OES-MS) will be of paramount importance for comparisons with raw materials. Physical and mechanical properties of the bricks (dry bulk density, specific gravity, total porosity and, if possible, uniaxial compressive strength) and also physical properties of the raw materials (grain size distribution and Atterberg limits) will be determined. Finally, thermoluminescence will be used as a powerful method to date the original firing of the bricks (Martini & Sibilina, 2001) in order to constrain a chronology of the various building periods of the architectural structures, coupled with the different pyrotechnological processes and raw materials used through the time.

Agnati U. (1999) - Urvinum Mataurense. In: Per la storia romana della provincia di Pesaro e Urbino. L'Erma di Bretschneider, 19-108.

Luni M. (1985) - Urvinum Mataurense. Dall'insediamento romano alla città medievale. In: M.L. Polichetti (ed.), "Il Palazzo di Federico da Montefeltro". Urbino, 11-49.

Luni M. & Ermeti A.L. (2001) - Le mura di Urbino tra tardoantico e Medioevo. Edizioni all'Insegna del Giglio, 1-10.

Martini M. & Sibilina E. (2001) - Radiation in archaeometry: archaeological dating. Radiation physics and chemistry, 61(3/6), 241-246.

Mazzini F. (1982) - I mattoni e le pietre di Urbino. Argalia Editore, Urbino, 609 pp.

Negroni F. (2005) - Appunti su alcuni palazzi e case di Urbino. Accademia Raffaello, Urbino, 198 pp.

Hyperspectral sensor: a practice tool to evaluate the efficacy of cleaning procedures

Vettori S.¹, Verrucchi M.², Di Benedetto F.*², Gioventù E.³, Benvenuti M.², Pecchioni E.²,
Costagliola P.² & Moretti S.²

¹ Institute for the Conservation and Valorization of Cultural Heritage (ICVBC) - CNR, Milan, Italy.

² Earth Sciences Department, University of Florence, Florence, Italy.

³ ISCR, Rome

Corresponding email: francesco.dibenedetto@unifi.it

Keywords: SWIR hyperspectral investigation, sulfation of marble, Loggia di Baccio d'Agnolo.

Atmospheric agents and air pollution play a key role in the degradation of surfaces of historical buildings and monuments. One of the most diffused decay processes affecting both natural and artificial carbonate materials exposed to the urban atmosphere is the formation of sulfate-based deposits (i.e. “black crusts”). Moreover, the cleaning of exposed surfaces represents a crucial step in the restoration procedure of stone monuments and works of art. For the restorers involved in the cleaning of stone surfaces, it is crucial to know in real time the effectiveness of the adopted procedures in order to opportunely optimize and tune their interventions.

The present study focuses on the evaluation of the efficacy of different cleaning methods (i.e. laser, chemical and microbial) for the “black crusts” on marble surfaces belonging to a column of Loggia di Baccio d'Agnolo in Santa Maria del Fiore Cathedral (Florence) employing SWIR (Short Wave Infrared) hyperspectral investigation. The SWIR technique is fully non-invasive and allows to gain spectral information in both the visible (VIS) and near infrared (NIR) regions using a portable spectroradiometer (ASD Fieldspec® 3). The procedure consisted in the detection of gypsum amount still present onto the stone surfaces after partial cleaning steps. The resulting SWIR spectra were modelled through a full profile approach proposed by Suzuki et al. (2018), in order to obtain a reliable and efficient spectral decomposition and an esteem of the amount of gypsum left on the surface after each cleaning step/procedure. With a support of a dedicated software relying on the approach of Suzuki et al (2018), to be implemented in the next future, the acquisition of the spectra and the determination of the gypsum residues submitted the cleaning treatment may be in principle obtained in less than one minute for surface spots having a surface up to ~20 cm².

In the case of the column under study, the best cleaning results were obtained for chemical cleaning and the combined use of laser and biological procedures.

Suzuki A., Vettori S., Giorgi S., Carretti E., Di Benedetto F., Dei L., Benvenuti M., Moretti S., Pecchioni E. & Costagliola P. (2018) - Laboratory study of the sulfation of carbonate stones through SWIR hyperspectral investigation. *J. Cult. Her.*, 32, 30-37.

S6

Experimental and theoretical studies of magmatic processes

CONVENERS AND CHAIRPERSONS

Michael R. Carroll (Università di Camerino)

Fabrizio Arzilli (Università di Manchester)

Paola Stabile (Università di Camerino)

Highly explosive basaltic eruptions: magma fragmentation induced by rapid crystallisation

Arzilli F.*¹, La Spina G.¹, Burton M.R.¹, Polacci M.¹, Le Gall N.², Hartley M.¹, Di Genova D.³, Cai B.⁴,
Vo N.⁵, Bamber E.¹, Nonni S.⁵, Atwood R.⁵, Llewellyn E.⁶, Heidy M.⁷, Brooker R.A.⁷ & Lee P.²

¹ School of Earth and Environmental Science, University of Manchester.

² Department of Mechanical Engineering, University College London.

³ Institute of Non-Metallic Materials, Clausthal University of Technology.

⁴ School of Metallurgy and Materials, University of Birmingham.

⁵ Diamond Light Source, Harwell Science and Innovation Campus.

⁶ Department of Earth Sciences, Durham University.

⁷ School of Earth Sciences, University of Bristol.

Corresponding email: fabio.arzilli@manchester.ac.uk

Keywords: basalt, fragmentation, rapid crystallisation.

The low viscosity of basaltic magmas generally favours effusive and mildly explosive volcanic activity. Highly explosive basaltic eruptions occur less frequently and their eruption mechanism still remains subject to debate (Szramek, 2016; Moitra et al., 2018), with implications for the significant hazard associated with explosive basaltic volcanism. Particularly, highly explosive eruptions require magma fragmentation, yet it is unclear how basaltic magmas can reach the fragmentation threshold (Papale, 1999).

In volcanic conduits, the crystallisation kinetics of an ascending magma are driven by degassing and cooling (Cashman & Blundy, 2000; La Spina et al., 2016). So far, the crystallisation kinetics of magmas have been estimated through ex situ crystallization experiments. However, this experimental approach induces underestimation of crystallization kinetics in silicate melts. The crystallization experiments reported in this study were performed in situ at Diamond Light Source (experiment EE12392 at the I12 beamline), Harwell, UK, using basalt from the 2001 Etna eruption as the starting material. We combined a bespoke high-temperature environmental cell with fast synchrotron X-ray microtomography to image the evolution of crystallization in real time. After 4 hours at sub-liquidus conditions (1170 °C and 1150 °C) the system was perturbed through a rapid cooling (0.4 °C/s), inducing a sudden increase of undercooling. Our study reports the first in situ observation of exceptionally rapid plagioclase crystallisation in trachybasaltic magmas. We combine these constraints on crystal kinetics and viscosity evolution with a numerical conduit model to show that exceptionally rapid syn-eruptive crystallisation is the fundamental process required to trigger basaltic magma fragmentation under high strain rates.

Cashman K. & Blundy J. (2000) - Degassing and crystallisation of ascending andesite and dacite. *Philosophical Transactions of the Royal Society of London A: Mathematical, Physical and Engineering Sciences*, 358, 1487-1513.

La Spina G., Burton M., Vitturi M.D.M. & Arzilli F. (2016) - Role of syn-eruptive plagioclase disequilibrium crystallisation in basaltic magma ascent dynamics. *Nature communications*, 7, 13402.

Moitra P., Gonnermann H.M., Houghton B.F. & Tiwary C.S. (2018) - Fragmentation and Plinian eruption of crystallizing basaltic magma. *Earth and Planetary Science Letters*, 500, 97-104.

Papale P. (1999) - Strain-induced magma fragmentation in explosive eruptions. *Nature*, 397, 425.

Szramek, L.A. 2016. Mafic Plinian eruptions: Is fast ascent required? *Journal of Geophysical Research: Solid Earth*, 121, 7119-7136.

The effect of decompression rate and volatile (H₂O - CO₂) content on degassing of trachytic melts

Buono G.^{1,2}, Di Genova D.³, Fanara S.⁴, Palladino D.M.⁵, Pappalardo L.*¹, Petrosino P.², Schmidt B.C.⁴ & Sottili G.⁵

¹ Istituto Nazionale di Geofisica e Vulcanologia, Osservatorio Vesuviano, Italy.

² University of Naples Federico II, Department of Earth, Environmental and Resources Science, Italy.

³ Clausthal University of Technology, Institute of Non-Metallic Materials, Germany.

⁴ Georg-August University of Goettingen, Institute of Mineralogy, Germany.

⁵ Sapienza University of Rome, Department of Earth Sciences, Italy.

Corresponding email: lucia.pappalardo@ingv.it

Keywords: alkaline magmas, decompression experiments, microtomography.

Volatile exsolution during magma decompression in volcanic conduit induces bubbles “birth, growth and death”, thus providing the driving force for eruptions and controlling magma ascent as well as eruptive style. Although degassing strongly depends on melt and volatile compositions, similar magmas can feed eruptions with different volcanic explosivity index, which in turn appears well-correlated with decompression rate. Degassing during magma ascent can be investigated through decompression experiments and physico-chemical characterization of experimental samples. Particularly, 3D-textural examination is a powerful tool for the quantification of three-dimensional bubble parameters that are strongly reliant on degassing and are not directly provided by 2D-conventional-techniques. In this study we performed isothermal decompression experiments of trachytic melts at 1200°C to investigate the homogeneous bubble nucleation and degassing behavior using an internally-heated-pressure-vessel with a continuous decompression system. We used H₂O-CO₂ bearing melts (initial XH₂O of 1, 0.5, 0 with saturation concentrations for 200 MPa and water-supersaturated conditions) and applied fast and slow (1 and 0.01 MPa/s) decompression rates, from 200 to 25 MPa, examining also intermediate steps every 50 MPa. We analyzed volatile content (FTIR spectroscopy) and 3D-texture (X-ray micro-tomography) of run products. On the basis of our preliminary results we suggest that at specific decompression rates, CO₂ occurrence and water-supersaturated conditions are first-order factors controlling bubble nucleation and evolution as well as degassing style of trachytic melts. These features shed light on the highly explosive behavior of high-risk volcanoes (e.g. in Italy, Azores) involving alkaline magmas, on which few experimental data have been so far provided.

Diffusive fractionation of helium isotopes as a possible process to explain the mantle source feature beneath Mount Vulture volcano (Italy)

Buttitta D.*¹, Caracausi A.¹, Giannandrea P.², Paternoster M.¹⁻², Rizzo A.L.¹ & Rizzo G.²

¹ Istituto Nazionale di Geofisica e Vulcanologia, Sezione di Palermo, Palermo, Italy.

² Dipartimento di Scienze, Università degli Studi della Basilicata, Potenza, Italy.

Corresponding email: buttittadario@gmail.com

Keywords: diffusion, helium isotopes, Mount Vulture.

Mount Vulture is a Pleistocenic volcanic complex located in the southern part of the Apennine chain (Italy). Its last eruption occurred ~140ka ago. Its products have peculiar petrologic characteristics, not least the trace element pattern and isotopic features that are intermediate between intraplate and subduction-related signatures. Hence, its magmatism is different from Italian Quaternary volcanoes that are characterized by affinities related to subduction. Furthermore, it is located at the eastern border of the Apenninic front far from peri-Tyrrhenian volcanoes and its origin and magmatism are matter of debate (Peccerillo, 2017 and references therein). The differences between Mt. Vulture magmatism and peri-Tyrrhenian ones could be justified by different magmatic sources feeding volcanism in the Italian peninsula. Here we are going to discuss about new helium (He) isotope data, together with the Ne and Ar isotopic signature, in fluid inclusion of pyroxenes and olivine phenocrysts of most the Mt. Vulture volcanites, in order to constrain the features of the mantle source during its eruptive history. The $^3\text{He}/^4\text{He}$ ratio of the samples varies from 2.83 to 6.74 Ra (Ra is the $^3\text{He}/^4\text{He}$ in atmosphere, 1.39×10^{-6}) and the $^4\text{He}/^{40}\text{Ar}^*$ ratio varies from 0.63 to 33.16. This variability has been interpreted as subduction-type effect or heterogeneity of the mantle source (Caracausi et al., 2013). Ne isotopic signatures overlap the air composition and some samples show Ar isotopic signature different from air. Magmatic processes (e.g., diffusive fractionation and magmatic degassing) can also explain the variability of the $^3\text{He}/^4\text{He}$ ratio and of the noble gases relative abundance (e.g., $^4\text{He}/^{40}\text{Ar}^*$). Indeed, mass-dependent fractionation, after volatile trapping and during magma residence in the plumbing system prior to eruption, can produce variations in the $^3\text{He}/^4\text{He}$. This can occur during He diffusion through the phenocrysts within sub-solidus magma conditions. Several studies have previously modelled He isotope fractionation due to the faster diffusion of ^3He than ^4He (temperature-dependent process). Assuming an Arrhenius temperature dependence, a slight He isotopic fractionation can be observed (up to 15% at 1200°C; Trull & Kurz 1993). Using the same approach, we calculate the fraction of lost He and the effect on the $^3\text{He}/^4\text{He}$. Calculated values well fit with the typical MORB or HIMU mantle sources values and can explain the high variability of $^3\text{He}/^4\text{He}$ at Vulture volcano.

Caracausi A., Martelli M., Nuccio P.M., Paternoster M. & Stuart F.M. (2013) - Active degassing of mantle-derived fluid: A geochemical study along the Vulture line, southern Apennines (Italy). *Journal of volcanology and geothermal research*, 253, 65-74.

Peccerillo A. (2017) - The Apulian Province (Mount Vulture). In: *Cenozoic Volcanism in the Tyrrhenian Sea Region. Advances in Volcanology*. Springer, Cham

Trull T.W. & Kurz M.D. (1993) - Experimental Measurements of ^3He and ^4He Mobility in Olivine and Clinopyroxene at Magmatic Temperatures. *Geoch.Cosm. Acta*, 57(6), 1313-1324.

Petrogenesis of Cenozoic Volcanism in the Cixerri Graben (Southwestern Sardinia)

Cariddi B.*¹, Costamagna L. G.², Guarino V.¹, Morra V.¹ & Melluso L.¹

¹ Dipartimento di Scienze della Terra, dell' Ambiente e delle Risorse, Università degli Studi di Napoli Federico II.

² Dipartimento di Scienze della Terra, Università di Cagliari.

Corresponding email: bruna.cariddi@unina.it

Keywords: Cixerri graben, Andesitic domes, Sardinia.

The domes outcropping in the Cixerri graben (28-14 My; Beccaluva et al., 1985), in SW Sardinia, are part of the “subduction-related” igneous activity that developed in Sardinia during the Upper Eocene-Middle Miocene age (38-12 My) with calcalkaline and high-K calcalkaline affinity. This activity developed during the formation of the Sardinian Rift, related to the separation of the Sardinia-Corsica microplate from Europe, its counterclockwise rotation and the opening of the Ligurian-Provençal back-arc basin (30-15 My; Lustrino et al., 2009 and references therein).

The investigated rocks are porphyric, with plagioclase + amphibole ± clinopyroxene phenocrysts included in a groundmass composed by the same phases plus feldspar, quartz and oxides. Plagioclase phenocrysts vary in composition between anorthite and andesine, generally from cores (An₇₆₋₈₈) to rims (An₆₃₋₈₆) and to the groundmass (An₄₆₋₈₄). Diopsides and augites have Mg# variable from 0.83 to 0.64. The amphiboles show tschermakite, magnesio-hornblende and rarer magnesio-hastingsite compositions.

The domes have andesitic composition with calcalkaline affinity and subduction-related character, such as the Pb peak and Nb-Ta-Ti troughs in multi-elements diagram normalized to the primitive mantle. The subduction-related character is observed also in the coeval Sardinian igneous rocks, but the Cixerri andesites differ in the high abundance of amphibole, almost absent in the andesites of other districts. This particular character is explained with the high calculated H₂O content (up to 8 wt.%) in the Cixerri magma. Furthermore the magma evolved in a temperature range of ~1100-800°C, with the initial crystallization of clinopyroxene and plagioclase, followed by amphibole at lower temperatures. The crystallization took place in crustal magmatic chambers at 8-13 km of depth (P≈200-350MPa).

The variations of the bulk-rock major and trace elements (e.g. decrease in TiO₂, Al₂O₃, Fe₂O_{3tot}, V, Sr and increase in K₂O, Rb and Zr contents) in the samples of all the districts are consistent with a common evolution mainly driven by fractional crystallization of the observed phases. The high Zr/Nb ratios (18-26) of the Cixerri graben andesites indicate a depleted source in HFSE, these values are similar to that observed in the Narcao district andesites (19-26; Brotzu et al., 1997).

Beccaluva L., Civetta L., Macciotta G. & Ricci C.A. (1985) - Geochronology in Sardinia: results and problems. *Rend. Soc. Mineral. Petrol. Ital.*, 40, 57-72.

Brotzu P., Callegari E., Morra V. & Ruffini R. (1997) - The orogenic basalt-andesite suites from the Tertiary volcanic complex of Narcao, S-W Sardinia (Italy): petrology, geochemistry and Sr-isotope characteristics. *Per. Mineral.*, 66, 101-150.

Lustrino M., Morra V., Fedele L. & Franciosi L. (2009) - Beginning of the Apennine subduction system in the central-western Mediterranean: constraints from Cenozoic “orogenic” magmatic activity of Sardinia (Italy). *Tectonics*, 28, 1-23.

The effect of chlorine on the incorporation of water in magmatic amphibole in subduction settings: an experimental study at lower crust conditions

Casiraghi G.*¹, Schiavi F.², Fumagalli P.¹, Cannaò E.¹ & Tiepolo M.¹

¹ Dipartimento di Scienze della Terra “A. Desio”, Università degli Studi di Milano.

² Université Clermont Auvergne, CNRS, IRD, OPGC, Laboratoire Magmas et Volcans, Clermont-Ferrand, France.

Corresponding email: giulia.casiraghi1@studenti.unimi.it

Keywords: amphibole, chlorine, water.

Amphibole plays an important role in differentiation processes of magmas in subduction setting, where the melts generated by partial melting of the supra-subduction mantle ascend into the deep crustal roots of the magmatic arc. Here, magmas stall and undergo fractional crystallization producing amphibole-rich cumulates that act as a “sponge” controlling the water content of magmas rising through the crust and thus determining the type of eruption that will take place at the surface (Davidson et al., 2007).

Water is incorporated into the structure of amphibole as hydroxyl (OH)⁻ and is hosted in the anion site O(3). The incorporation of water is controlled by several mechanisms, among which the most important is the oxo-substitution $M^{(1)}Ti^{4+} + O^{(3)}O^{2-} = M^{(1)}(Mg, Fe^{2+}) + O^{(3)}(OH)^{-}$ (Hawthorn et al., 2012). The fluids and melts that circulate in subduction systems are enriched in halogens, particularly in chlorine (Cl) that can substitute OH⁻ in the anion site O(3) of amphibole, thus affecting its water budget.

The aim of this study is to evaluate the Cl-effect on the oxo-substitution and the incorporation of water in amphibole. Several experiments were conducted with end-loaded piston cylinder apparatus at pressure and temperature conditions compatible with lower crustal depth (1.4 GPa and 1015-1050°C) in order to favour the crystallization of amphiboles at equilibrium with the coexisting melt. Alkali basalt powder was used as starting material and water doped with different contents of Cl was added to each experiment. The water content in both glass and amphibole from the experimental charges were determined by performing a new Raman technique.

Our results report a positive correlation between the Cl content of amphiboles (0.18-0.88 wt.%) and the exchange coefficient of water between amphibole and glass (0.30-0.52). This effect was ascribed to the incorporation of Cl in the anion sites O(3) that influences the oxo-substitution impeding the entrance of Ti⁴⁺ in the M(1) sites and thus preventing the amphibole’s dehydrogenation.

This Cl-effect within the amphibole crystal structure highlights that high concentrations of Cl in the magmatic system favours the incorporation of water in amphibole rather than in the coexisting melt, influencing the hydration state of magmas evolving in the crustal roots by crystallizing amphibole and, eventually, the volcanic processes taking place at the surface.

Davidson J., Turner S., Handley H., Macpherson C. & Dosseto A. (2007) - Amphibole “sponge” in arc crust? *Geology*, 35, 787–790.

Hawthorne F.C., Oberti R., Harlow G.E., Maresch W.V., Martin R.F., Schumacher J.C. & Welch M.D. (2012) - Nomenclature of the amphibole supergroup. *American Mineralogist*, 97, 2031–2048.

Pre- and syn-eruptive conditions of Caxias do Sul silicic magmas (Paraná Magmatic Province, Brazil): Crystallisation kinetics of dacitic melts

De Cristofaro S.P.¹, Arzilli F.*², Giordano D.¹, Polo L.², Janasi V.³, Fanara S.⁴, Burton M.², Polacci M.², González-García D.¹ & Masotta M.⁵

¹ Earth Sciences Department, University of Torino.

² School of Earth and Environmental Sciences, University of Manchester.

³ Instituto de Geociências, Universidade de São Paulo.

⁴ Institute of Mineralogy, Georg-August-Universität Göttingen.

⁵ Dipartimento di Scienze della Terra, Università di Pisa.

Corresponding email: fabio.arzilli@manchester.ac.uk

Keywords: Paraná Magmatic Province, crystallisation kinetics, dacite.

Brazil hosts the dominant part of the Paraná-Etendeka Magmatic Province (PMPE), one of the largest continental basalt provinces on Earth. The Brazilian part of the Province (PMP, Paraná Magmatic Province) has Eocretacic age (131-134 Ma) and covers an area of approximately 1,200,000 km². PMP magmatism is composed of felsic deposits (Palmas-type sequence), which correspond to ca. 2.5% of the total volume of the PMP magmatism. The Palmas-type sequence is divided into three different silicic sequences (Caxias do Sul dacites, Barros Cassal basaltic andesite to dacites and Santa Maria rhyolites). The Caxias do Sul dacites correspond to the first manifestation of the silicic volcanism in the PMP. The predominant eruptive style of this volcanism still remains subject to debate and the pre-eruptive conditions have not been constrained. The pre- and syn-eruptive conditions of Caxias do Sul volcanism have been poorly investigated from petrological point of view. Particularly, experimental studies on crystallisation kinetics of Caxias do Sul dacitic magmas are lacking in literature. Here, we present the pre- and syn-eruptive conditions of Caxias do Sul volcanism obtained through crystallisation experiments and petrological analysis of experimental and natural samples. This experimental study provides us the estimation of plagioclase and pyroxene crystallisation kinetics at 150 MPa, over a range of temperatures (900 to 1000 °C) and H₂O contents (0 to 5 wt. %). The pre- and syn-eruptive conditions of the Caxias do Sul volcanism were constrained through crystallisation experiments, replicating the mineral assemblage and the mineral compositions of the natural samples. Crystal size distribution studies allowed us to constrain the magma residence time in the reservoir and the timescales of ascent and emplacement.

The role of undercooling and strain rate on the syn-eruptive rheological evolution of the magma feeding the Pollena eruption of Somma-Vesuvius (Campania; Italy)

Di Fiore F.*¹, Vona A.¹, Romano C.¹, Sulpizio R.² & Mollo S.^{3,4}

¹ Dipartimento di Scienze, Università degli Studi Roma Tre.

² Dipartimento di Scienze della Terra e Geoambientali, Università di Bari.

³ Dipartimento di Scienze della Terra, Sapienza-Università di Roma.

⁴ Istituto Nazionale di Geofisica e Vulcanologia, Roma.

Corresponding email: fabrizio.difiore@uniroma3.it

Keywords: rheology, dynamic crystallization.

Subplinian eruptions are generally characterized by unsteadiness in magma discharge due to decoupling between magma supply at depth and magma discharge at the surface. The result is the formation of short-lived, oscillating convective columns, repeated transitions from sustained to collapsing column and time-breaks of days/weeks between different eruptive pulses. The Pollena Subplinian eruption of Somma-Vesuvius (472 CE) is an archetype of this kind of volcanic event. Previous studies recognized three main eruptive phases related to changes in the eruptive processes and/or to relative changes of magma composition (from phonolite to phonotephrite). In contrast with the classical assumption of a direct proportionality between melt silica content (i.e. viscosity) and explosivity, the highest energy event involves the phonotephritic magma. Some authors invoked a dominant role of the rheological evolution of the rising magma along the conduit and in particular microlite crystallization seems to be the pivotal factor controlling the increasing explosivity. In order to model the syn-eruptive evolution of magma rheology (i.e. change in viscosity), we conducted a series of experiments act to investigate the effects of undercooling and strain rate on the crystallization kinetics. The crystal-bearing rheology of the magma was determined by isothermal crystallization experiments in a concentric cylinder set-up. Starting from a superliquidus state (1300 °C) of magma, the experiments were performed under variable degrees of undercooling (120-150 °C) and strain rates (1-10 s⁻¹), the latter reproduced through the stirring of the melt. Preliminary results show that both degree of undercooling and deformation rate strongly control the kinetics of the crystallization process. Shorter incubation time for crystal nucleation and higher nuclei density are observed with increasing undercooling and/or flow conditions, ultimately influencing the solidification ability of the melt. Notably, dynamic conditions enhance the mobility (by diffusional transport) of chemical elements in the melt and their availability at the growing crystal surface, hence promoting crystal growth. The effect of dynamic crystallization is commonly overlooked in the modeling of volcanic conduit dynamics, but could have played a key role on the syn-eruptive rheological change of unsteady subplinian eruptions during the Pollena event.

Volcanic eruptions: a nanoscale perspective

Di Genova D.*¹⁻²

¹ Institute of Non-Metallic Materials, Clausthal University of Technology, Germany.

² School of Earth Sciences, University of Bristol, United Kingdom.

Corresponding email: digenovadanilo@gmail.com

Keywords: volcano, glass, nanoscale.

There are currently ~550 active volcanoes worldwide, with ~500 million people living in the shadow of a smouldering hazard. Recent population growth has dramatically increased the potential impact of a catastrophic eruption, a trend that is likely to continue in the foreseeable future. The distinction between effusive and explosive eruptive styles is of critical importance in volcanology as it determines the threat to human life and our societal and economic activities, as well as the nature and possibility of the emergency response, including evacuation. Consequently, understanding the factors controlling the eruption style remain a prime objective in physical volcanology.

The style of any volcanic eruption is heavily controlled by the physicochemical properties of magmas and their transient evolution during the rise of magma to the Earth's surface. Magma consists of a silicate melt phase containing dissolved gas and variable amount of crystals. The melt structure modulates the physicochemical properties of magma such as viscosity that is the single most important physical parameter controlling the eruption style of a volcanic event. It seems clear, therefore, that the study of the dynamics of melt structure upon eruption is key for understanding the behaviour of volcanoes.

Of particular interest here is the glass formation process from a molten silicate melt during volcanic eruptions. The glass formation is the ultimate act of volcanic eruptions and lies at the heart of the behaviour (i.e. effusive or explosive) of volcanoes. Glass is a noncrystalline, nonequilibrium and nonergodic state of matter and its structure conserves memory of the physicochemical and thermal history as the melt traverses the glass transformation range (i.e. the glass transition interval).

In this contribution recent observations of nanoscale crystal-like domains in volcanic glasses erupted during explosive events will be presented. The potential of both ex situ and in situ analytical and spectroscopic approaches to characterise volcanic glasses from a chemical and structural standpoint will be explored. In particular, the relationship between the viscosity and melt structure as inferred by Raman spectroscopy will be presented together with synchrotron X-ray diffraction measurements of melts during cooling to monitor nanocrystal formation at eruptive temperature. Finally, the effect of nanocrystals on the physical properties of magmas and thereby on eruption style will be discussed.

Phase equilibria experiments on a leucitite from the Colli Albani volcanic district (Italy)

Fanara S.*¹, Schmidt B.C¹, Sottili G.² & Palladino D.M.²

¹ Institute of Mineralogy, Georg-August University Göttingen.

² Dipartimento di Scienze della Terra, Università la Sapienza, Roma, Italy.

Corresponding email: sara.fanara@geo.uni-goettingen.de

Keywords: Colli Albani, explosive eruptions, crystallization experiments, CO₂-dominated volcanic systems.

The Colli Albani volcanic district is a quiescent volcano near Rome (10 km southeast, central Italy) belonging to the ultrapotassic Roman Province. This volcano was characterized by high volume explosive volcanic events induced by the interaction of low SiO₂ ultrapotassic magma with carbonate rocks, representing an anomalous high explosive behaviour of SiO₂-poor magmas on planetary scale. Highly explosive eruptions are driven by the exsolution of volatile components to a separate fluid phase. The presence of crystals facilitates the nucleation of H₂O bubbles in the magmas because of a reduction of the surface tension at the bubble crystal interface. This work is focused on the determination of mineral stability fields in ultrapotassic, SiO₂-poor, H₂O- to CO₂-dominated magmas and is intended to gain knowledge needed to study the bubble nucleation in the CO₂-dominated volcanic systems.

experiments were performed on a synthetic leucititic melt from the Colli Albani volcano at 100, 200 and 300 MPa and at temperatures from 1000 to 1200°C with run durations up to 15 days. Capsules were prepared with an initial mole fraction of water (XH₂O) of 0, 0.25, 0.50, 0.75 and 1 and run in Internally Heated Pressure Vessel (IHPV) at intrinsic redox conditions ($\log f_{\text{O}_2} = \text{NNO}+3$). Run products were analysed by microscope, electron microprobe and spectroscopic techniques.

First results show that the liquidus for the investigated system lays between 1150 and 1200°C. In the H₂O-dominated systems, magnetite is the first crystallizing phase immediately followed by clinopyroxene. The third crystallizing phase is phlogopite appearing at 1000°C, when the crystallization degree is above 70%. In the CO₂-dominated systems (CO₂ > 70%) the first crystallizing phases are leucite and clinopyroxene.

Experiments show that the most common natural phenocrystal assemblage (leucite, clinopyroxene and oxides) could have been formed only in CO₂ dominated systems.

Onset of crystallization in a cooling MORB: an in-situ DSC investigation

Giuliani L.*¹, Iezzi G.¹⁻², Davis M.³, Hippeli T.³, Vetere F.⁴, Elbrecht A.L.³, Nazzari M.², Mollo S.⁵⁻² & Scarlato P.²

¹ Dipartimento di Ingegneria e Geologia, Università “G. d’Annunzio”, Chieti.

² Istituto Nazionale di Geofisica e Vulcanologia, Roma.

³ SCHOTT North America, Duryea, PA, USA.

⁴ Dipartimento di Fisica e Geologia, Università degli studi di Perugia.

⁵ Dipartimento di Scienze della Terra, Sapienza, Università di Roma.

Corresponding email: letizia.giuliani@unich.it

Keywords: DSC, MORB, solidification.

The glass-forming ability (GFA), the critical cooling rate (R_c) and the crystallization behavior of a MORB were determined by ex-situ experiments (Vetere et al., 2015) in the thermal range 1300 - 800 °C, using six cooling rates ($\Delta T/\Delta t$): 9000, 1800, 180, 60, 7 and 1 °C/h. The textural analyses of these experiments depicted the melt solidification path(s) but the onset of crystallization was not quantified. To fill this gap, the same Islandic tholeiitic MORB (B100) has been heated at 420 °C/h in a differential scanning calorimetry (DSC) from ambient T to 1300 °C (superliquidus), at P and fO_2 of air conditions. After a dwell time of 2 h at 1300 °C, the melt was cooled at 7, 60, 180, 1000 and 1800 °C/h and, then, quenched at 600 °C. The in-situ DSC spectra show that T_g (the glass transition temperature) and T_m (the melting temperature), measured on heating, are almost close to 700 and 1200 °C, respectively. On cooling, the increasing of $\Delta T/\Delta t$ causes that the T_x (the onset of crystallization on cooling) progressively decreases. The DSC-spectra of the runs at 1000, 180 and 60 °C/h display a single exothermic band with asymmetric shape, that becomes a two-mode pattern at 1800 °C/h and is more complex for the run at 7 °C/h. The onset of nucleation (T_{xi_CR}) corresponds to the temperature measured on the first peak base (at 10 % of its maximum intensity) for the high-thermal portion of the DSC spectra. As $\Delta T/\Delta t$ increases, T_{xi_CR} is observed to linearly decrease ($R^2 = 0.97$). This trend is better expressed by an exponential regression fit of the data ($R^2 = 0.99$), as T_{xi_CR} strongly decreases in the proximity of R_c at high $\Delta T/\Delta t$ values. Conversely, when $\Delta T/\Delta t$ is moderate or low, T_{xi_CR} gently increases. The plot of T_{xi_CR} versus time shows a classical TTT-like trend. The textures of each run product were quantified ex-situ by image analysis on 130 BSE microphotographs at variable magnifications (from 100x to 5000x). The assemblage consists of clinopyroxene (cpx), spinel (sp) and melilite (mel); plagioclase (plg) appears only at 7 °C/h with tiny sizes and skeletal-like shapes. The increase of $\Delta T/\Delta t$ causes lower crystal contents (area%) and crystal sizes. In contrast, the crystal shape does not change significantly from 7 to 1800 °C/h, since cpx are always dendritic, sp equant and mel are typically “H”- shaped. The attained results provide a rational, quantitative and general overview of the effect of solidification kinetics operating on a complex silicate melt like MOR basalt.

Iezzi G., Elbrecht A.L., Davis M., Vetere F., Misiti V., Mollo S. & Cavallo A. (2017) - Glass Stability (GS) of chemically complex (natural) sub-alkaline glasses. *Journal of Non-Crystalline Solids*, 477, 21–30.

Vetere F., Iezzi G., Behrens H., Holtz F., Ventura G., Misiti V., Cavallo A., Mollo S. & Dietrich M. (2015) - Glass forming ability and crystallization behavior of sub-alkaline silicate melts. *Earth Sci. Rev.*, 150, 25–44.

Raman characterization of natural anhydrous silicate glasses: structure and physical properties of the melt

González-García D.*¹, Giordano D.¹⁻²⁻³, Bersani D.⁴, Fornasini L.⁴, Raneri S.⁵, Di Genova D.⁶, Dingwell D.B.⁷, Russell J.K.⁸, Ferrando S.¹ & Lottici P.P.⁴

¹ Dipartimento di Scienze della Terra, Università degli Studi di Torino, Italy.

² Istituto di Geoscienze e Georisorse, (IGG), Centro Nazionale delle Ricerche (CNR), Pisa, Italy.

³ Istituto Nazionale di Geofisica e Vulcanologia-Sezione di Pisa, Pisa, Italy.

⁴ Dipartimento di Scienze Matematiche, Fisiche e Informatiche, Università di Parma, Italy.

⁵ Dipartimento di Scienze della Terra, Università di Pisa, Italy.

⁶ Institut für Nichtmetallische Werkstoffe, Technische Universität Clausthal, Germany.

⁷ Department für Geo- und Umweltwissenschaften, Ludwig-Maximilians Universität München, Germany.

⁸ Department of Earth, Ocean and Atmospheric Sciences, University of British Columbia, Vancouver, Canada.

Corresponding email: daniло.bersani@unipr.it

Keywords: Raman spectroscopy, melt, glasses.

Raman spectroscopy is an important tool for the study of amorphous materials, allowing the obtaining of structural and, in some extent, chemical information in a quick and non-destructive way. However, the analysis of the broad Raman bands of glasses is complicated and non-straightforward; for that reason, very often only qualitative information was obtained. Here we report the results of the detailed Raman study of 27 natural anhydrous multicomponent glasses with variable contents of SiO₂ (41 – 80 wt%), Al₂O₃ (6 – 21 wt%), TiO₂ (0 – 4.5 wt%), FeO_{tot} (0 – 16 wt%); alkali oxides (2 – 15 wt%), alkaline-earth oxides (0 – 27 wt%), and minor oxides. The selected glasses result from quenching of remelted and homogenized volcanic rocks and synthetic equivalents. The measurements have been carried out with different spectrometers, with very different setups. To have the best reproducibility, only green lasers (with wavelength ranging from 514.5 to 532 nm) were used.

Raman spectra from different spectrometers show variable intensities for the main the Si-O stretching and bending bands and for intensity ratios. We followed a strategy based on the ratios between the low and high wavenumber peaks (R) to standardize the data to normalized Raman ratios (R_n) and thus to remove interlaboratory differences. This normalization allows to make the results independent of the experimental setup (class and manufacturer of spectrometer, kind of detector, optical configuration, space and spectral resolution). Using these advances, we predict melt viscosity solely with the use of Raman spectral measurements of multicomponent silicate glasses, thus demonstrating the potential of the method in describing physical properties of silicate melts.

Sulfur in alkaline melts: An experimental study

Iacovino K.¹, Giuli G.*² & Carroll M.²

¹ Jacobs–NASA Johnson Space Center, USA.

² Scuola di Scienze e Tecnologie-sez. Geologia, Università degli Studi Camerino, Italia.

Corresponding email: gabriele.giuli@unicam.it

Keywords: S solubility, silicate melts, melt polymerization.

We present preliminary results of experiments to establish the solubility and fluid/melt partitioning of sulfur (sulfate and sulfide) in natural alkaline melts (basanite, KI-04; and phonolite, ERE-97018) from Erebus volcano, Antarctica. Melt composition is known to strongly influence S solubility in natural melts, particularly with respect to FeO_{tot} and SiO_2 (Ducea et al., 1994). Although melt polymerization is thought to have a significant effect on sulfur solubility and speciation, it is likely that a number of other factors, including melt alkali and iron content, also play a role in controlling sulfur behavior in melts. This experimental study examines the interplay between alkalis, oxygen fugacity, pressure, Fe and S oxidation state, and Fe and S coordination geometries and their effects on S^{6+} and S^{2-} solubility. Sulfur saturated and undersaturated experiments have been carried out at a range of oxygen fugacities ($\log f\text{O}_2 = -12$ to -6 , ranging from ca. the iron-wustite buffer to $\text{NNO}+3.45$), pressures of 1 bar and 1 kb and at superliquidus temperatures (1030 and 1200 °C for phonolite and basanite, respectively). This range of experimental conditions and analyses of the sulfur contents via electron microprobe and sulfur and iron speciation and coordination geometry via XANES will allow sulfur solubility and partitioning to be evaluated with respect to the above listed experimental parameters.

Preliminary results indicate a marked increase in total S solubility in evolved phonolite melt relative to primitive basanite at similar T- $f\text{O}_2$ conditions. In addition, we have determined the effect of $f\text{O}_2$ on the solubility of total S at 1 kbar in basanite KI-04 based on experimental run products containing sulfur-bearing crystal phases (i.e. sulfate, sulfide). Experiments indicate a steep increase in S solubility at highly oxidizing conditions ($f\text{O}_2 = \text{NNO}+1.53$; ~1000 ppm dissolved S) and minimum solubility at moderately oxidizing conditions ($f\text{O}_2 = \text{QFM}+0.23$; ~200 ppm dissolved S). The strongly non-linear relationship between S solubility and $f\text{O}_2$ has implications for sulfur degassing at Erebus volcano, whose erupted products indicate a distinct decrease in oxygen fugacity during fluid-magma ascent.

Future experiments at higher pressure (1 GPa) and analyses of all experimental products via XANES will elucidate the roles of oxygen fugacity, pressure, Fe and S oxidation state, and Fe and S coordination geometries in controlling S solubility in basanites and phonolites. Comparisons of our results to similar data from more polymerized (low-alkali) melts and incorporation of data from an unpublished experimental study of S in phonolite at conditions below the silicate liquidus (Moncreiff & Carroll, 1999) will further our understanding of the relation between melt polymerization and S solubility and allow us to characterize the behavior of S in lower temperature systems.

Ducea M.N., McInnes B.I. & Wyllie P.J. (1994) - Sulfur variations in glasses from volcanic rocks: effect of melt composition on sulfur solubility. *International Geology Review*, 36(8), 703-714.

Moncreiff D. & Carroll M. (unpublished PhD thesis, 1999).

Structure and thermal equation of state of $\text{Ca}_3\text{KNa}(\text{CO}_3)_4$ carbonate

Milani S.¹, Baratelli L.¹, Comboni D.¹, Maurice J.¹, Lotti P.¹ & Merlini M.*¹

¹ Dipartimento di Scienze della Terra, Università degli Studi di Milano.

Corresponding email: marco.merlini@unimi.it

Keywords: experimental mineralogy, upper mantle, carbonates.

The presence of alkali-carbonates in the Earth's mantle is suggested by the occurrence of these minerals as diamond inclusion. We expect that alkali-carbonates may play a significant role in carbon-related processes (volcanism, mantle metasomatism, diamond formation...) in upper mantle and transition zone. High-pressures and temperatures experiments have recently revealed the possible occurrence of new class of Ca-alkali-carbonates above 4 GPa. We report the crystal structure of $\text{Ca}_3\text{NaK}(\text{CO}_3)_4$ synthesized at 4 GPa. It appears in equilibrium with carbonatitic liquids. It presents a similar topology with the reported $\text{Ca}_3\text{Na}_2(\text{CO}_3)_4$ high-pressure phase (Gavryushkin et al., 2014) but a different unit cell and symmetry. Irregular coordination sites for Ca, K and Na cations and a partially disordered CO_3 group arrangement reveal an anomalous elastic behaviour for the different cation sites, suggesting an interesting capability of trace element incorporation in the structure.

Thermal equation of state of $\text{Ca}_3\text{NaK}(\text{CO}_3)_4$ is determined by single crystal synchrotron X-ray diffraction with resistive heated DAC (ESRF, Grenoble, ID15a beamline) and the results are used to model the possibility for these phases to differentiate from liquids and stagnate in the upper mantle.

Gavryushkin P.N., Bakakin V.V., Bolotina N.B., Shatskiy A.F., Seryotkin Y.V. & Litasov K.D. (2014) - Synthesis and crystal structure of new carbonate $\text{Ca}_3\text{Na}_2(\text{CO}_3)_4$ homeotypic with orthoborates $\text{M}_3\text{Ln}_2(\text{BO}_3)_4$ (M= Ca, Sr, and Ba). *Crystal Growth & Design*, 14(9), 4610-4616.

Experimental and thermodynamic constraints on mineral equilibria in pantelleritic magmas

Romano P.*^{1,4}, White J.C.², Andujar J.³, Scaillet B.³, Di Carlo I.³, Liotta M.⁴ & Rotolo S.G.^{1,4}

¹ Dip. Scienze della Terra e del Mare Università di Palermo.

² Dept. of Geosciences, Eastern Kentucky University.

³ Institut des Sciences de la Terre d'Orleans (France).

⁴ INGV, sez. di Palermo.

Corresponding email: pierangeloromano@gmail.com

Keywords: peralkaline magmas, experimental phase equilibria, petrology.

Peralkaline (mol Na+K > Al) silicic magmas frequently represent the felsic end-member in bimodal magmatic suites that characterize intraplate and extensional tectonic settings, both oceanic and continental. Whatever their origin, the stability of mineral phases crystallizing in silica-oversaturated peralkaline (viz., comenditic to pantelleritic) compositions have been a matter of debate in the petrological community since the first studies in the early 1960s. Petrological characteristics appear similar at different locations worldwide, with typical assemblages of anorthoclase and sodian clinopyroxene with variable fayalite, aenigmatite, and Fe-Ti oxides. Although considerable progress has been made, previous experimental studies were not able to fully clarify the relationship between peralkalinity and the mineral assemblages observed in natural rocks and the role of fO_2 in the equilibrium mineral assemblages of pantellerites. Here, we present the results of a series of crystallization experiments representative of the peralkaline rhyolite of Pantelleria, the type locality for pantellerite. Experiments were performed at 1 kbar with temperature ranging between 750-900°C, and fluid saturation conditions with X_{H_2O} ($=H_2O/H_2O+CO_2$) between 0 and 1. Redox conditions were fixed at, or slightly below, the FMQ buffer. Results show that at temperature of 900 °C pantelleritic magmas are well above the liquidus regardless their water content; we also observed a decrease in liquidus temperature (750°C) with increasingly reducing conditions. Experiments reproduced the mineral assemblages of the natural rocks, particularly the relationship between fayalite and aenigmatite, which appear to be strongly controlled by melt peralkalinity and redox conditions. Experimental results have been compared with the composition of mineral phases as well as with the results obtained from mineral equilibrium, geothermometry, and oxygen barometry studies on pantelleritic lava and tuffs from Pantelleria (Italy), Eburru (Kenya) and Menengai (Kenya). Our work places new experimental and thermodynamic constraints on stability fields for rock forming mineral phases in pantellerites and their relationships with the intensive parameters.

Phase relations in hydrous REE-bearing carbonatite at 1 GPa, 700-1000°C

Spartà D.*¹, Fumagalli P.¹, Merlini M.¹, Borghini G.¹ & Poli S.¹

¹ Dipartimento di Scienze della Terra Ardito Desio, Università Degli Studi di Milano.

Corresponding email: deborah.sparta@unimi.it

Keywords: REEs, carbonatite, experimental petrology.

Carbonatites are important sources of Rare Earth Elements (REEs). These rocks are the result of liquid immiscibility or fractional crystallization at low pressure; they are often extremely enriched in alkali and may contain up to 15.000 ppm of La (Cullers & Graf, 1984). REEs mainly reside in Ca-bearing phases (carbonates, apatites, Ca-Nb oxides, Ca-silicates) and in accessory phases such as monazite, bastnaesite (La, Nd, Ce) CO₃F and hydroxyl-bastnaesite (La, Nd, Ce) CO₃(OH, F).

This study focuses on processes, precursor to the late differentiation, that lead to the formation of hydrous carbonatite melts at high pressure (>1 GPa). In particular we will investigate the stability of REE-bearing carbonates and silicates at near solidus conditions and the distribution of REEs among accessory phases and melt. Moreover, in alkali free systems, the complete miscibility between silicate and carbonate liquids is expected. However, it is widely known that, while silica glasses are experimentally recoverable, calcite is not quenchable. The compositional threshold at which carbonate-silicate liquids might form a glass is still unexplored.

We performed single stage and end-loaded piston cylinder experiments in the model system CaO-SiO₂-La₂O₃-H₂O-CO₂ in the range 700-1000°C, at 1 GPa. Starting materials were prepared as a powder mixture of La₂(CO₃)₃, amorphous SiO₂ and CaCO₃. Three different bulk compositions at fixed La₂(CO₃)₃ = 10 wt.% with SiO₂:CaCO₃ = 0.7, 1 and 1.4 have been considered. Gold capsules of 3 mm of diameter were loaded with starting mixtures, added with approximately 5-10 wt.% of H₂O, and sealed while freezing the capsule in order to avoid the loss of volatile components.

Run products, carefully prepared to avoid any contact with water and polished with diamond paste, are characterized by BSE images, X-ray diffractometry, Raman spectroscopy and chemically analyzed by electron microprobe. At subsolidus conditions all bulk compositions contain calcite and quartz coexisting with a Ca-Lanthanum silicate with up to 66 wt% of La₂O₃, 9.8 wt.% CaO and 23.5 wt% SiO₂. Preliminary X-ray diffraction data suggest that this phase has an apatite-type structure of general formula Ca₂La₈(SiO₄)₆O₂. An additional Ca, La-bearing phase of few μm has been observed in BSE images. Although further investigation is required, microprobe analysis indicate a likely carbonate composition.

Cullers R.L. & Graf J.L. (1984) - Rare earth elements in igneous rocks of the continental crust: intermediate and silicic rocks—ore petrogenesis. Volume 2: Developments in geochemistry, Elsevier.

Role of the kinetics of nucleation and crystal growth of alkali feldspar in a peralkaline pantelleritic melt

Stabile P.*¹, Arzilli F.², Paris E.¹ & Carroll M.R.¹

¹ School of Sciences and Technology, Geology Division, University of Camerino.

² School of Earth and Environmental Science, University of Manchester.

Corresponding email: paola.stabile@unicam.it

Keywords: crystallization kinetics, disequilibrium, pantellerite.

By investigating the nucleation and growth kinetics of alkali feldspars we can gain information on the cooling history and magma transport dynamics for magma compositions where alkali feldspar is a significant phase (mainly phonolites, trachytes, alkaline rhyolites). In fact, magmas undergo decompression and cooling during their ascent through the conduit producing a textural fingerprint that is useful for understanding their rheological behaviour and ascent processes (e.g. Blundy & Cashman, 2008; Chakraborty, 2008; Shea & Hammer, 2013).

In particular, the aim of this study is to investigate the alkali feldspar textures (as abundance, number of density, size and morphology) as a function of undercooling, water content and time, in the framework of a broader study focused on the understanding of pre-eruptive dynamics in the magma chamber along with syn-eruptive processes occurring within the conduit.

Experimental studies consisted of cooling experiments where the crystallization was simulated by decreasing the temperature and thus applying a certain undercooling (ΔT), defined as the difference between liquidus temperature of alkali feldspar (T_{liq}) and the experimental temperature (T_{exp}), below the liquidus curve ($T_{liq} - T_{exp}$).

The starting material is a synthetic composition analogue of a pantellerite (PAN 0113), which belongs to the Fastuca pumice fall eruptive unit of Pantelleria. PAN 0113 presents a peralkalinity index of 1.1 with a silica content of 68 wt%. As in all pantellerites, the FeO_{tot} content is relatively high (7 wt %).

Different experiments have been performed at pressures between 25 and 100 MPa and temperature of 720 °C, under anhydrous and hydrous conditions. Non-equilibrium experiments were conducted at fO_2 ranging from NNO+1 to NNO-1 (meaning one log unit above or below the fO_2 of the nickel-nickel oxide buffer), where the most reduced conditions represent the most reliable and closest conditions to the natural pantelleritic system.

This work will be, thus, useful to provide new and relevant data of disequilibrium crystallization kinetics in pantelleritic compositions, which have not systematically studied yet.

Blundy J. & Cashman K.V. (2008) - Petrologic reconstruction of magmatic system variables and processes. *Reviews in Mineralogy*, 69, 179–239.

Chakraborty S. (2008) - Diffusion in solid silicates: a tool to track timescales of processes comes of age. *Annual Review of Earth and Planetary Sciences*, 36, 153–190.

Shea T. & Hammer J.E. (2013) - Kinetics of cooling- and decompression-induced crystallization in hydrous mafic-intermediate magmas, *Journal of Volcanology and Geothermal Research*, 260, 127-145.

Water solubility in Pantelleritic melts

Stabile P.¹, Appiah H.¹ & Carroll M.R.*¹

¹ School of Science and Technology, Geology Division, University of Camerino, Italy.

Corresponding email: michael.carroll@unicam.it

Keywords: pantellerite, water solubility, experimental petrology.

While there exist abundant data for water solubility in metaluminous (typical calc-alkaline) rhyolitic melt compositions, our knowledge of water solubility in pantellerites (strongly peralkaline rhyolites) remains limited, even though studies of melt inclusions in such magmas show they may be water-rich (Lowenstern & Mahood, 1991; Barclay et al., 1996). To improve our knowledge of water behavior in peralkaline rhyolites we have conducted several series of new experiments at P=50 to 200 MPa and T=800-850°C using a synthetic pantellerite starting composition with (wt%) SiO₂=76.6, Al₂O₃=8.48, FeO*=5.48, K₂O=3.68, Na₂O=4.72, with molar (Na+K)/Al=1.38. Some experiments were H₂O undersaturated (~2 to 6 wt% H₂O) and the products of these experiments were analyzed by Karl-Fischer Titration (KFT) for total dissolved H₂O abundance. The results from these experiments were used to estimate new extinction coefficients for infrared absorption bands at ~4500 cm⁻¹ and ~5200 cm⁻¹, commonly attributed to molecular water and hydroxyl groups, respectively. Preliminary results suggest molar absorptivity values of 1.80 and 1.62 l mol⁻¹cm⁻¹ for the 4500 cm⁻¹ and 5200 cm⁻¹ bands, respectively.

Additional water saturated experiments at 50-200 MPa, 850°C demonstrate water solubilities, on a wt% basis, in our pantelleritic composition that are significantly higher than observed H₂O solubilities in metaluminous rhyolitic compositions (approximately 1 wt% higher at 100MPa, close to 2 wt% higher at 200 MPa). In addition, trying to calculate H₂O solubilities using existing models (e.g. Moore et al., 1998; Ghiorso & Gualda, 2015) consistently underestimates solubilities, whereas the recent model of Papale et al. (2006) reproduces our data within < 0.5 wt%. Current work in progress is attempting to better define observed solubility variation, as well as exploring possibilities to use Raman spectroscopy for total H₂O measurements on the same glasses we have analyzed using KFT and IR spectroscopy.

- Barclay J., Carroll M.R., Houghton B.F. & Wilson C.J.N. (1996) - Pre-eruptive volatile content and degassing history of an evolving peralkaline volcano. *J. Volcanol. Geotherm. Res.*, 74, 75–87.
- Ghiorso M.S. & Gualda G.A.R. (2015) - An H₂O–CO₂ mixed fluid saturation model compatible with rhyolite-MELTS. *Contrib. Mineral. Petrol.*, 169, 53.
- Lowenstern J.B. & Mahood G.A. (1991) - New data on magmatic H₂O contents with implications for petrogenesis and eruptive dynamics at Pantelleria. *Bull. Volcanol.*, 54, 78–83.
- Moore G., Vennemann T. & Carmichael I.S.E. (1998) - An empirical model for the solubility of H₂O in magmas to 3 kilobars. *Am. Mineral.*, 83, 36–42.
- Papale P. Moretti R. & Barbato D. (2006) - The compositional dependence of the saturation surface of H₂O + CO₂ fluids in silicate melts. *Chem. Geol.*, 229, 78–95.

S7

**New frontiers in metamorphism and deformation-
metamorphism relationships through cutting-edge analytical,
experimental, numerical, and theoretical techniques**

CONVENERS AND CHAIRPERSONS

Nadia Malaspina (Università di Milano Bicocca)

Sabrina Nazzareni (Università di Perugia)

Alberto Vitale Brovarone (Università di Torino)

Stefano Zanchetta (Università di Milano Bicocca)

Measuring strains with Raman Spectroscopy

Angel R.J.*¹, Murri M.², Prencipe M.³, Stangarone C.⁴, Mihailova B.D.⁵ & Alvaro M.²

¹ IGG - CNR, Padova.

² Dept Earth & Environmental Sciences, Pavia.

³ Department of Earth Sciences, University of Torino.

⁴ German Aerospace Centre, Berlin. ⁵ Department of Earth Sciences, University of Hamburg.

Corresponding email: rossjohnangel@gmail.com

Keywords: Raman, piezobarometry, inclusions.

The recent developments of piezobarometry to determine the entrapment conditions of single-crystal inclusions inside host minerals provides an alternative method of geobarometry for metamorphic rocks. For anisotropic inclusion crystals the stress state is not hydrostatic. In addition, for faceted inclusions the stress field is not homogeneous but exhibits stress gradients. Piezobarometry requires the full stress state of the inclusion crystal to be determined while it is still embedded completely in its host crystal. Given that it is not possible to directly measure stress in a crystal, we have developed a method to measure and map the strains in crystals by Raman spectroscopy, from which the stresses can be calculated by using the elastic tensor of the mineral.

Raman spectroscopy provides an alternative method of measuring strains ϵ because strains induce a change in the wavenumbers of the phonon modes (and thus the band positions in a measured spectrum). The changes in phonon-mode wavenumbers, $\Delta\omega$ determined by the mode Grüneisen tensors γ by $\Delta\omega/\omega = \gamma:\epsilon$ (e.g. Key, 1967). We have determined the mode Grüneisen tensors of quartz and zircon by ab-initio HF/DFT (Hartree-Fock/Density Functional Theory) calculations under various strain states ($\epsilon_{11} = \epsilon_{22} \neq \epsilon_{33}$) that preserve the crystal symmetries. For small strains (up to 2% linear) the change in Raman shifts of most modes are linear in the strains, and can be used to determine the two symmetry-independent components γ_{11} (γ_{11}) γ_{33} of the mode Grüneisen tensors (Murri et al., 2019; Stangarone et al., 2019). These reproduce the experimentally-observed shifts in Raman modes of quartz and zircon under hydrostatic stress and the limited data with deviatoric stress. In-situ diffraction and Raman measurements of inclusion crystals trapped inside cubic garnets provide further validation of the DFT results. A program Strainman (Angel et al., 2019) has been developed to allow crystal strains to be determined from the measured band positions in Raman spectra

This work was supported by ERC-StG TRUE DEPTHS (grant number 714936) to M. Alvaro.

Angel R.J., Murri M., Mihailova B. & Alvaro M. (2019) - Stress, strain and Raman shifts. *Zeitschrift für Kristallographie*, 234, 129-140.

Key S.W. (1967) - Grüneisen tensor for anisotropic materials, *Journal of Applied Physics*, 38, 2923-2928.

Murri M., Alvaro M., Angel R.J., Prencipe M. & Mihailova B.D. (2019) - The effects of non-hydrostatic stress on the structure and properties of alpha-quartz. *Physics and Chemistry of Minerals*, 46, 487-499.

Stangarone C., Alvaro M., Angel R.J., Prencipe M. & Mihailova B.D. (2019) - Determination of the phonon-mode Grüneisen tensors of zircon by DFT simulations. *European Journal of Mineralogy*, in press.

Fate of primary COH fluid inclusions in garnet from high-grade rocks

Carvalho B.B.*¹, Bartoli O.¹, Cesare B.¹, Tacchetto T.², Gianola O.¹, Ferri F.¹ & Aradi L.E.³

¹ Dipartimento di Geoscienze, Università degli Studi di Padova, Italy.

² School of Earth and Planetary Sciences, Curtin University, Australia.

³ Lithosphere Fluid Research Lab, Institute of Geography and Earth Sciences, Eötvös University Budapest, Hungary.

Corresponding email: bruna.borgescarvalho@unipd.it

Keywords: anatexis, fluid inclusions, granulites.

Fluid regime and the role that fluids may play during high-grade metamorphism and crustal melting are topics largely debated in the literature. On one side, works arguing for a dry lower crust and predominant fluid absent anatexis are mostly based on the very low permeability of the deep crust, and on petrological evidence. The other school of thought argues that fluids (carbonic, aqueous fluids and/or brines) are essential agents in granulite metamorphism and anatexis. Fluid inclusions (FI), particularly CO₂-bearing ones, often reported in rocks from granulitic terranes, represent an important piece of the puzzle to elucidate such controversies. However, it is fundamental to have sound constraints on the timing of entrapment (primary vs. secondary FI) and a good understanding of (possible) post-entrapment changes, otherwise any further interpretation may be flawed.

In this study, we investigate primary multiphase FI in peritectic garnet from three world-renowned high- to ultra-high temperature metamorphic terranes [Ivrea Zone (NW Italy), Gruf Complex (Central Alps) and Athabasca Granulite Terrane (Canada)] to evaluate the fate of COH fluid inclusions in these metamorphic terranes.

Combination of petrography and micro-Raman spectroscopy has shown that multiphase FI and nanogranitoid inclusions (NI) occur together in the same clusters regularly distributed in the core of peritectic garnets. The great majority of FI is composed of fluid and aggregates of solid phases. The latter usually contains siderite, ferroan magnesite, pyrophyllite, calcite, and in some cases kaolinite, corundum, quartz, dolomite and muscovite. In the fluid phase, CO₂ is the most common component and no H₂O has been detected. Methane and N₂ are also present in samples from Ivrea Zone and Athabasca.

The coexistence of NI and FI suggests the presence of COH-bearing fluids during the growth of the host garnet (i.e. during anatexis). The solid assemblage of FI with carbonates and OH-bearing phases cannot have precipitated directly from a simple COH-fluid as daughter phases. These minerals require additional cations (e.g. Fe, Mg, Ca, Al, Si) which are not dissolved into the fluid and yet are abundant in the host. Thus, their presence implies that the initial composition must have been changed by the interaction with the host garnet during cooling. Phase equilibria modelling of such fluid-garnet interaction shows that the assemblages found in FI are metastable and that, whatever retrograde path is followed by the host rock, primary COH FI must change their nature to a multiphase assemblage.

I was not born cubic, said low-temperature metamorphic garnet

Cesare B.*¹, Nestola F.¹, Mugnaioli E.², Della Ventura G.³, Peruzzo L.⁴, Bartoli O.¹, Viti C.⁵,
Johnson T.⁶ & Erickson T.⁷

¹ Dipartimento di Geoscienze, University of Padova, Padova, Italy.

² Center for Nanotechnology Innovation, Istituto Italiano di Tecnologia, Pisa, Italy.

³ Dipartimento di Scienze, University of Roma Tre, Rome, Italy.

⁴ Istituto di Geoscienze e Georisorse, CNR, Padova, Italy.

⁵ Dipartimento di Scienze Fisiche, della Terra e dell'Ambiente, University of Siena, Siena, Italy.

⁶ School of Earth and Planetary Sciences, Curtin University, Perth, Australia.

⁷ Jacobs – JETS, NASA Johnson Space Center, Houston, TX, USA.

Corresponding email: bernardo.cesare@unipd.it

Keywords: garnet, metamorphism, tetragonal.

Garnet is the paradigmatic cubic mineral of metamorphic and igneous rocks, and is generally regarded as optically isotropic. Nonetheless, evident birefringence is observed, particularly in the rare Ca-Fe³⁺ hydrogarnets, which is attributed to the coexistence of two or more cubic phases. A weak birefringence, with rare examples of optical sector zoning, has also been documented in much more common Fe²⁺-Mg-Mn garnets, but an adequate explanation for its cause is, so far, lacking.

Here we show that optically anisotropic garnets are much more widespread than previously thought, both in blueschists and blueschist-facies rocks, as well as in lower greenschist-facies phyllites, but they are frequently overlooked when working with conventional, 30- μ m-thick thin sections.

Utilizing a multi-technique approach including optical microstructural analysis, BSEM, EMPA, EBSD, FTIR, TEM, EDT and single-crystal XRD, we demonstrate here that the birefringence in these garnets is related to their tetragonal symmetry, that it is not due to strain, and that crystals are twinned according to a merohedral law.

We also show that the birefringent garnets from blueschists and phyllites are anhydrous, lacking any hydrogarnet component, and have compositions dominated by almandine (58-79%) and grossular (19-30%) with variable spessartine (0-21%) and very low pyrope (1-7%).

Considering the widespread occurrence of optically anisotropic OH-free garnets in blueschists and phyllites, their common low-grade metamorphic origin, and the occurrence of optically isotropic garnets with similar Ca-rich almandine composition in higher-grade rocks, we conclude that garnet does not grow with cubic symmetry in low-temperature rocks (< 400 °C). The tetragonal structure appears to be typical of Fe-Ca-rich compositions, with very low Mg contents.

Cubic but optically sector-zoned garnet in a lower amphibolite-facies metapelite from the eastern Alps suggests that preservation of tetragonal garnet is favored in rocks which did not progress to T > 500 °C, where transition to the cubic form, accompanied by change of stable chemical composition, would take place.

Our data show that the crystal-chemistry of garnet, its thermodynamics and, in turn, its use in unravelling petrogenetic processes in cold metamorphic environments need to be re-assessed.

Integrating X-ray microtomography with the chemical imaging of EMPA: A robust method to quantify mineral re-crystallization during metamorphism: example for granulite to eclogite in the Western Alps, Italy

Corti L.*¹, Visalli R.², Zucali M.¹⁻³, Mancini L.⁴ & Sayab M.⁵

¹ Dipartimento di Scienze della Terra, Università degli Studi di Milano.

² Dipartimento di Biologia, Geologia e Scienze Ambientali, Università degli Studi di Catania.

³ Department of Earth and Atmospheric Sciences, University of Houston, Texas-USA.

⁴ Elettra-Sincrotrone Trieste S.C.p.A., Basovizza, Italy.

⁵ Geological Survey of Finland.

Corresponding email: luca.corti@unimi.it

Keywords: X-ray microtomography, X-ray chemical maps, pre-Alpine fabrics.

Metamorphic transformations and fabric evolution are the consequence of thermo-dynamic processes, lasting from thousands to millions of years. Relative mineral mode percentages, their grains size distribution, grains orientation, and grain boundary geometries are first-order parameters for dynamic modeling of metamorphic processes. To quantify these parameters, we propose a multidisciplinary approach integrating X-ray computed microtomography (μ -CT) with the EMPA X-ray chemical maps. We used a granulite metapelite sample collected from the Alpine HP-LT metamorphic rocks of the Mt. Mucrone (Eclogitic Micaschists Complex, Sesia-Lanzo Zone, Western Alps). The Sesia-Lanzo Zone consists of a Paleozoic continental rock sequence poly-deformed during Alpine subduction. The heterogeneous Alpine deformation and metamorphism allowed the HT pre-Alpine features preservation. The pre-Alpine fabrics are marked by granulitic mineral association (Grt+Bt+Sil+Pl+Qtz \pm Ilm \pm Kfs \pm Wm) at metamorphic condition of $P = 0.3 \pm 0.05$ GPa and $T = 720 \pm 48$ °C. These volumes show a pervasive static eclogite facies re-equilibration during the Alpine evolution. Different Alpine metamorphic assemblages occur, strongly controlled by the chemistry of microdomains. Wm, Grt and Op grow as coronas of Bt; Omp aggregates and fine-grained Wm completely overgrown Pl; Omp and small Grt rim Grt; Ky aggregates replace Sil. The inferred eclogitic mineral association is: Wm+Omp \pm Ky+Qtz+Grt developed at $T = 500$ – 600 °C and $P \geq 1.5$ GPa conditions. X-ray μ -CT data on centimeter-sized samples have been acquired at the TomoLab station of the Elettra synchrotron facility (Trieste, Italy) setting a pixel size of 17.7 μ m. The reconstruction of the tomographic data permits the 3D visualization, segmentation, and analysis of different mineral species. The SPO for each mineral grain has been calculated along the entire rock volume. By combining gray-scale threshold-based mineral phase segmentation with microstructures (i.e. different grain-size classes for the same phase and morphology of different pre-Alpine microdomains) allowed to distinguish the pre-Alpine mineralogical phases from the Alpine ones and to quantify their ratio. Each sample preserves 100% of the pre-Alpine granulite fabric, which surprisingly corresponds to less than 5% of pre-Alpine metamorphic assemblages, while Alpine eclogitic static assemblage corresponds to $\approx 95\%$. The combined use of X-ray chemical mapping with the μ -CT technique further permits also to dynamically constraint the chemistry of the mineral phases linked to the metamorphic transformation for the granulitic to the eclogitic conditions.

3D reconstruction of fabric and metamorphic domains in a slice of continental crust involved in the Alpine subduction system: the example of Mt. Mucrone (Sesia-Lanzo Zone, Western Alps)

Corti L.*¹, Zucali M.¹⁻², Delleani F.¹, Zanoni D.¹ & Spalla M.I.¹

¹ Dipartimento di Scienze della Terra, Università degli Studi di Milano.

² Department of Earth and Atmospheric Sciences, University of Houston, Texas-USA.

Corresponding email: luca.corti@unimi.it

Keywords: 3D modelling, strain partitioning, metamorphic reaction progress.

Geological mapping, multiscale structural analysis, and estimations of the degree of fabric evolution and of reaction progress allow the construction of a 3D quantitative model of structural and metamorphic heterogeneity in a continental crust volume deeply involved in the Alpine subduction system before the continental collision. The investigated and modelled rocks surface in the surroundings of Mt. Mucrone, in the central Sesia-Lanzo Zone, Western Alps. Polyphase Alpine heterogeneous deformation allowed the preservation of pre-Alpine magmatic features and HT metamorphic relicts in widely eclogitized metagranitoids and metapelites, respectively. Multiscale structural analysis reveals seven groups of superposed Alpine structures developed under eclogite facies (D1 to D3) and successively under blueschist facies (D4) during subduction, to greenschist facies (D5 to D7) throughout the continental collision. D2 structures are dominant at regional scale and are characterized by isoclinal folds associated with a pervasive foliation. The Geomodeller® software allowed a quantitative 3D estimation of domains characterized by homogeneous degree of fabric evolution and metamorphic reaction progress (DFE and DRP, respectively) for the D2-eclogitic and D5-greenschist stages, that are the more pervasive tectono-metamorphic stages at km-scale. The contouring of DFE domains is based on the estimation of volumes occupied by different degree of grain-scale reorganization during the considered stage (planar fabric: 0-20%; 21-60%; 61-100%). The individuation of the DRP domains is determined based on the modal amount of the stage-related mineral assemblages (0-20%; 21-60%; and 61-100%). Such a 3D modelling, clarifying mutual relationships between fabric and metamorphic gradients: i) the DFE and DRP are closely related regardless the rock type; ii) the syn-deformational thermal regime can influence the degree of metamorphic transformation, if the DFE remains below to the 60% threshold; iii) the phase transitions cannot be properly implemented in quantitative geodynamic modelling without considering the heterogeneity of reaction progress and fabric evolution; (iv) this approach is a powerful tool to unravel the variation in size of rock volumes that, while sharing a common subduction-collision-exhumation history, developed homogeneous in structural and metamorphic records.

Micro-Raman spectroscopy and microstructural thermometers applied for the evaluation of carbonate mylonites deformation temperature

Croce A.*¹, Pigazzi E.², Rinaudo C.¹ & Zucali M.²⁻³

¹ Dipartimento di Scienze e Innovazione Tecnologica (DiSIT), Università degli Studi del Piemonte Orientale “Amedeo Avogadro”, Italy.

² Dipartimento di Scienze della Terra “Ardito Desio”, Università degli Studi di Milano, Italy.

³ Department of Earth and Atmospheric Sciences, University of Houston, Texas, USA.

Corresponding email: alessandro.croce@uniupo.it

Keywords: Micro-Raman spectroscopy, carbonaceous materials, mylonites.

In petrographic studies, micro-Raman spectroscopy has been proved to be useful for the characterization of carbonaceous materials (CMs) in metamorphic rocks and, in particular, with the application of fitting process on the two characteristic Raman bands of these particles, it is possible to evaluate their formation temperatures based on their order degrees (Beysac et al., 2002; Kouketsu et al., 2014; Lünsdorf et al., 2014).

In this work, carbonate mylonites from the Central Southalpine Domain (Monte Sodadura) and Central Austroalpine Domain (Braulio Valley) of the Italian Alps were analyzed using CMs characterization by Raman spectroscopy (RSCM) to infer the deformation temperatures associated with the Alpine thrust tectonic. The samples were investigated by means of a 632.8 nm wavelength, comparing different spectral elaborations and different thermometers proposed in literature (e.g.: Kouketsu et al., 2014; Lünsdorf et al., 2014), in order to obtain the best temperature evaluation compared to petrographic information, demonstrating the reliability of this laser source also for low-grade CMs characterization.

From the obtained results, it is demonstrated that micro-Raman spectroscopy, coupled with petrographic data, may be useful to constrain the temperature of deformation along these main mylonitic horizons. Moreover, our report shows that the tectonic evolution is characterized by plastic horizons predating the well-known thin-skinned brittle thrust tectonics. These conclusions suggest to reconsider the geometry and timing of thrust-fault systems, incorporating these new data.

Beysac O., Goffé B., Chopin C. & Rouzaud J.N. (2002) - Raman spectra of carbonaceous material in metasediments: a new geothermometer. *J. Metamorph. Geol.*, 20, 859–871.

Kouketsu Y., Mizukami T., Mori H., Endo S., Aoya M., Hara H., Nakamura D. & Wallis S. (2014) - A new approach to develop the Raman carbonaceous material geothermometer for low-grade metamorphism using peak width. *Island Arc*, 23, 33-50.

Lünsdorf N.K., Dunkl I., Schmidt B.C., Rantitsch G. & von Eynatten H. (2014) - Towards a higher comparability of geothermometric data obtained by Raman spectroscopy of carbonaceous material. Part I: evaluation of biasing factors. *Geostand. Geoanal. Res.*, 38, 73-94.

Micropetrology of megagarnets: nanogranitoids reveal presence of melt during formation of the giant garnets of Barton Mine (Adirondacks, US)

Ferrero S.^{*1-2}, Wannhoff I.¹, Darling R.³, Wunder B.⁴, Laurent O.⁵, Ziemann M.A.¹, Günter C.¹ & O'Brien P.¹

¹ Institute of Geosciences, University of Potsdam.

² Museum für Naturkunde, Berlin.

³ SUNY College at Cortland, New York.

⁴ Helmholtz-Zentrum Potsdam, GFZ, Potsdam.

⁵ Department of Earth Science, ETH Zürich.

Corresponding email: sferrero@geo.uni-potsdam.de

Keywords: giant garnets, nanogranitoids, polymorphs.

The Barton Mine is located on Gore Mountain, Adirondacks (NY State, USA) and is home to the world's largest garnets – ca. 35 cm in average, while garnet diameters up to 1 m were reported in historical record, occurring in garnet hornblendite and in garnet amphibolite. Garnet crystallization occurred at the metamorphic peak (~800-900°C, 0.6-0.8 GPa) in the late Mesoproterozoic (1.05 Ga) during the Grenville Orogeny. Fluid is often invoked in the formation of large crystals, but so far no study has identified clear witnesses for the presence of fluid during garnet formation, e.g. large amounts of fluid inclusions. However, polycrystalline inclusions containing cristobalite were reported by Darling et al. (1997) who interpreted them as possible crystallized melt inclusions.

These polycrystalline inclusions are the main target of our study. All the investigated inclusions occur either in clusters or are randomly scattered in the host, supporting the interpretation that they formed during garnet growth, and their shape ranges from tubular (2-100 µm in length) to negative crystal shape (2-50 µm). Two types of polycrystalline inclusions can be distinguished based on their mineral assemblage. Type 1 inclusions contain cristobalite/quartz, kumdykolite and amphibole. Albite, formerly described by Darling et al. (1997), is now properly identified as kumdykolite. Minor phases such as biotite/phlogopite, enstatite, rutile, ilmenite and a second, Ca-richer plagioclase (or its rare polymorphs dmisteinbergite and svyatoslavite) may be also present. Type 2 inclusions contain instead only quartz/cristobalite plus ilmenite/rutile.

Type 1 inclusions were re-homogenized to a silicate-rich glass via piston cylinder experiments at 925°C and 1.0 GPa under H₂O free conditions, while type 2 inclusions are unchanged after the heating run. Experimental results and phase assemblage prove that type 1 inclusions were originally a silicate melt, i.e. nanogranitoids, trapped in the garnet during growth. This is also supported by the finding of residual glass along with amphibole in one single inclusion before the experimental runs. Few primary CO₂-rich inclusions were also identified in smaller coeval garnets from the garnet amphibolites, testifying for the presence of a CO₂-bearing fluid during garnet-melt formation. The phase assemblage of type 1 inclusions points toward a tonalitic/ trondhjemitic composition, and LA-ICP-MS analyses show a clear enrichment in some HFSE (Ti, Zr, Hf, Pb, Th and U), LILE (Rb, Sr, Ba) and LREE (La, Ce, Pr, Nd) possibly consistent with a TTG-like/ adakitic melts.

In conclusion, our study suggests that the growth of the Barton Mine garnets into crystals of such an unusually large size may indeed have been favored by the presence of a silicate melt generated in the host rocks during peak metamorphism.

Darling R.S., Chou I.M. & Bodnar R.J. (1997) - An Occurrence of Metastable Cristobalite in High-Pressure Garnet Granulite. *Science*, 276, 91.

Elastic geothermobarometry on multiple inclusions in a single host

Gilio M.*¹, Alvaro M.¹, Angel R.J.¹ & Scambelluri M.²

¹ Department of Earth and Environmental Sciences, University of Pavia, Pavia, Italy.

² Department of Earth, Environment and Life Sciences, University of Genova, Genova, Italy.

Corresponding email: mattia.gilio@unipv.it

Keywords: elastic geothermobarometry, quartz in garnet.

The characterization of the pressure and temperature (P-T) histories of subducted rocks is of key importance to unravel geological processes at all scales. Conventional element-exchange geothermobarometers are challenged in ultra-high-pressure metamorphic terranes as the subduction temperatures may exceed their closure temperature and minerals may undergo re-equilibration along their path. Elastic geobarometry applied to host-inclusion systems is a complementary method to determine P and T conditions of metamorphism that does not rely upon chemical equilibrium. Recent development of elastic geobarometry (Angel et al., 2019; Campomenosi et al., 2018; Murri et al., 2018) allows us to retrieve entrapment pressures for host-inclusion pairs from the residual strains acting on the inclusion. Because only a single measurement, the inclusion strain, is made, only a line in PT space of possible entrapment conditions, the entrapment isomeke, can be determined. Thus, the entrapment pressure along an isomeke can only be determined if the entrapment temperature is known.

An alternative is to calculate entrapment conditions for two types of inclusions that are believed, from petrological evidence, to have been entrapped at the same time. In this study we performed micro-Raman measurements on quartz and zircon inclusions trapped in garnets from a garnet-kyanite gneiss and a quartz-garnet vein from the Fjortoft UHP terrane, Norway. From the micro-Raman data, using the program stRAinMAN (Angel et al., 2019), we calculated the strains at room conditions (Murri et al., 2018) and thus the entrapment conditions. The intersection between the two sets of isomeke calculated on multiple quartz and zircon inclusions demonstrates that measuring different inclusion phases trapped inside a single host allows unique P-T conditions for the host rock to be determined.

This work was supported by ERC-StG TRUE DEPTHS grant (number 714936) to M. Alvaro

Angel R.J., Murri M., Mihailova B. & Alvaro M. (2019) - Stress, strain and Raman shifts. *Zeitschrift für Kristallographie-Crystalline Materials*, 234(2), 129-140.

Campomenosi N., Mazzucchelli M.L., Mihailova B., Scambelluri M., Angel R.J., Nestola, F., Reali A. & Alvaro M. (2018) - How geometry and anisotropy affect residual strain in host-inclusion systems: Coupling experimental and numerical approaches. *American Mineralogist*, 103(12), 2032-2035.

Murri M., Mazzucchelli M.L., Campomenosi N., Korsakov A.V., Prencipe M., Mihailova B.D., Scambelluri M., Angel R.J. & Alvaro M. (2018) - Raman elastic geobarometry for anisotropic mineral inclusions. *American Mineralogist*, 103(11), 1869-1872.

Iron oxidation state in Fulgurite glass

Giuli G.*¹, Pratesi G.², Radica F.¹, Stabile P.¹, Paris E.¹ & Cibin G.³

¹ Scuola di Scienze e Tecnologie, Sezione di Geologia, Università di Camerino.

² Museo di Storia Naturale, Università di Firenze, Italy. ³ Diamond Light Source, Didcot, United Kingdom.

Corresponding email: gabriele.giuli@unicam.it

Keywords: Fulgurites, Scanning Electron Microscopy, Iron oxidation state.

Fulgurites are glasses produced by lightnings striking a rock, soil or sand. They can be found as hollow tubes with thin glass walls, as strong glass cylinders, or as glass droplets. Previous studies found shocked high pressure minerals within the glass, as well as reduced mineral phases as metallic Si or Fe-Si alloys (Essene et al., 1986; Wasserman et al., 2002).

Here we show preliminary results on the Fe oxidation state, water content, and mineralogy of four fulgurite glasses: one is a black droplet from Elko County (USA), whereas the second is a glass tube, from Sahara desert, sealed at both ends and containing unmolten sand in its interior, while the third and fourth are open glass tubes coming from Coolidge globe (AZ, USA) and Inyo County (CA, USA).

Preliminary Scanning Electron Microscopy data reveal the presence of rare Fe alloys in only 1 sample, and zirconia nanoparticles in two samples. Fe K-edge XANES data were collected in order to determine quantitatively the Fe oxidation state by careful analysis of the pre-edge peak. The spectra of all fulgurite samples are consistent with Fe being mostly divalent, similar to tektite glasses (Giuli et al., 2002, Giuli et al., 2010a, 2010b). On the other hand, the unmolten sand enclosed in the sealed tube fulgurite does not show any sign of reduction, and the pre-edge peak of the sand sample shows Fe to be mostly trivalent.

Water contents determined by micro FTIR analyses on polished slides are not homogeneous within each sample, and range from 40 to 600 ppm.

Essene E.J. & Fisher D. C. (1986) - Lightning strike fusion: extreme reduction and metal-silicate liquid immiscibility. *Science*, 234, 189–193.

Giuli G., Pratesi G., Paris E. & Cipriani C. (2002) - Fe local structure in tektites by EXAFS and High resolution XANES spectroscopy. *Geochimica et Cosmochimica Acta*, 66, 4347–4353.

Giuli G., Eeckhout S. G., Cicconi M.R., Koeberl C., Pratesi G. & Paris E. (2010a) - Iron oxidation state and local structure in North American tektites. In *Large Meteorite Impacts and Planetary Evolution IV* edited by Reimold W. U. and Gibson R. Geological Society of America Special Paper, 465, 645–652.

Giuli G., Pratesi G., Eeckhout S.G., Koeberl C. & Paris E. (2010b) - Iron reduction in silicate glass produced during the 1945 nuclear test at the trinity site (Alamogordo, New Mexico, USA). In Reimold W. U. and Gibson R. (eds.): *Large Meteorite Impacts and Planetary Evolution IV* Geological Society of America Special Paper, 465, 653–662.

Wasserman A.A., Melosh H.J. & Lauretta D.S. (2002) - Fulgurites: a look at transient high temperature processes in silicates Proc. 33rd Lunar and Planetary Sc. Conf. Abs# 1308 (LPSC, Texas, US).

High pressure abiotic methanogenesis and strain localization in metamorphosed carbonate rocks

Giuntoli F.*¹, Vitale Brovarone A.²⁻³ & Menegon L.⁴

¹ Dipartimento di Scienze Biologiche, Geologiche e Ambientali, Università degli Studi di Bologna, Bologna, Italy.

² Department of Earth Sciences, University of Torino, Torino, Italy.

³ Institut de Minéralogie, de Physique des Matériaux et de Cosmochimie UMR 7590 CNRS-UPMC-IRD-MNHN, Campus Jussieu, Paris, France.

⁴ School of Geography, Earth and Environmental Sciences, Plymouth University, Plymouth, UK.

Corresponding email: francesco.giuntoli@gmail.com

Keywords: High-pressure abiotic methane generation, strain localisation, fluid-rock interaction.

It has been recently discovered that abiotic hydrocarbon-rich fluids can form via carbonate reduction at high pressure condition in subduction zones (Vitale Brovarone et al., 2017). The integration of such a process in our picture of deep metamorphic processes at convergent margins opens to new scientific questions, among which is the interplay between hydrocarbon genesis and migration and deformation.

In this study we investigate how fluid-rock interactions leading to carbonate reduction and abiotic methanogenesis affect strain localization in carbonate-rich rocks. Our study integrates data from the field to the microscale, including petrographic, microstructural and electron backscattered diffraction analysis. Methanogenesis evolves from discrete domains unaffected by ductile deformation into localized shear zones marked by grain size reduction by subgrain rotation recrystallization, and diffusion creep. Creep-cavitation occurred at the mineral grain boundaries, with nucleation of new phases, promoting phase mixing and pinning the grain size. Creep-cavities evolved into creep-cavitation bands due to protracted deformation. The newly formed shear zones show evidence for enhanced carbonate reduction, suggesting a positive feedback between carbonate reduction and strain localization. Finally, a late fracture system formed, allowing further hydrocarbon-rich fluid migration and suggesting that several fluid pulses occurred during the subduction history.

This study provides the first insights on how deep abiotic hydrocarbons can migrate from their source regions towards shallower reservoirs and suggests that these processes can promote strain localization and fluid channelization at great depths.

Vitale Brovarone A., Martinez I., Elmaleh A., Compagnoni R., Chaduteau C., Ferraris C. & Esteve I. (2017) - Massive production of abiotic methane during subduction evidenced in metamorphosed ophicarbonates from the Italian Alps. *Nat. Commun.*, 8, 14134.

The oxidation state of C-S-bearing garnet clinopyroxenites from External Liguride (Italy) and Beni Bousera (Morocco): a TEM-EELS study

Malaspina N.*¹, Langenhorst F.² & Montanini A.³

¹ Dipartimento di Scienze dell'Ambiente e della Terra (Università degli Studi di Milano-Bicocca).

² Institut für Geowissenschaften (Friedrich-Schiller-Universität Jena).

³ Dipartimento di Scienze Chimiche, della Vita e della Sostenibilità Ambientale (Università degli Studi di Parma).

Corresponding email: nadia.malaspina@unimib.it

Keywords: redox melting, Clinopyroxenite, Electron Energy Loss Spectroscopy.

The occurrence of carbon in the mantle, either as diamond or graphite, is mostly confined to peridotite and eclogite xenoliths derived from the subcratonic lithospheric mantle. In non-cratonic areas C-bearing mantle rocks were reported for the orogenic peridotite massif of Beni Bousera (Morocco, Africa) (Pearson et al., 1989), where mm-sized graphite occurs in some garnet pyroxenites as pseudomorphs after diamond. More recently Montanini et al. (2010) found high-temperature graphite as dispersed flakes in garnet pyroxenites from the Northern Apennines (Italy). Both samples from Beni Bousera and Northern Apennines show sulphides in equilibrium with native carbon. These pyroxenite layers may be proxies of deep recycling of subducted crust and may have formed by melt–rock reactions induced by C-S-related redox processes, namely “redox melting”. The redox state of high-pressure peridotites and pyroxenites is traditionally determined from the Fe³⁺ content of garnet in equilibrium with olivine and orthopyroxene. However, several phases besides garnet incorporate ferric iron, particularly clinopyroxene (Malaspina et al., 2012). Also, garnet and clinopyroxene present iron distribution heterogeneities, i.e. zoning, in relation to its partitioning among mineral phases and/or to the occurrence of fluid fluxes at different redox conditions (e.g. CH₄ fluid inclusions). We performed for the first time in-situ Fe³⁺ measurements of garnets and clinopyroxenes pairs in equilibrium with graphite/diamond and sulphides by Electron Energy Loss Spectroscopy with the Transmission Electron Microscope at the University of Jena. Samples were prepared by Precision Ion Polishing System in order to obtain the maximum analysable surface of both clinopyroxenes and garnets and their inclusions/exsolutions.

Preliminary results indicate that clinopyroxene included in garnet cores of Northern Apennine clinopyroxenites preserve relatively low temperature microstructures and contain ≈ 15% of Fe³⁺, while the host garnet has very low ferric iron (≈ 5%). Further investigations may help in understanding if included clinopyroxenes represent the relict phase of a recycled crust before melting, and to model the composition of slab remnants in terms of redox budget and to investigate the role of C and S in the melting of their protolith.

Malaspina N., Langenhorst F., Fumagalli P., Tumiati S. & Poli S. (2012) - Fe³⁺ distribution between garnet and pyroxenes in mantle wedge carbonate-bearing garnet peridotites (Sulu, China) and implications for their oxidation state. *Lithos*, 146–147, 11–17.

Montanini A., Tribuzio R. & Bersani D. (2010) - Insights into the origin of mantle graphite and sulphides in garnet pyroxenites from the External Liguride peridotites (Northern Apennine, Italy). *Geol. Soc. London*, 337, 87-105.

Pearson D.G., Davies G.R., Nixon P.H. & Milledge H.J. (1989) - Graphitized diamonds from a peridotite massif in Morocco and implications for anomalous diamond occurrences. *Nature*, 338, 60-62.

Evidence of low-temperature plasticity in naturally deformed pyrite: a LA-ICP-TOFMS-EBSD combined approach (Olkiluoto Island, Finland)

Marchesini B.*¹, Menegon L.², Prando F.², Schmidt P.K.³, Garofalo P.S.¹, Schwarz G.³, Hattendorf B.³, Günther D.³, Mattila J.⁴ & Viola G.¹

¹ Dipartimento di Scienze Biologiche, Geologiche e Ambientali, Università di Bologna, Italy.

² School of Geography, Earth and Environmental Sciences, University of Plymouth, PL48AA Plymouth, UK.

³ Laboratory of Inorganic Chemistry, ETH Zürich, CH-8093 Zürich, Switzerland.

⁴ Rock Mechanics Consulting Finland.

Corresponding email: barbara.marchesini2@unibo.it

Keywords: chemical map, element mobility, pyrite deformation.

Knowledge of active slip systems and element distribution in deforming minerals is important in understanding deformation processes. Pyrite is such a common mineral in many ore deposits (e.g. auriferous deposits) and in shear zones that a detailed understanding of the mechanisms steering its deformation is necessary. Due to its resistant, pyrite commonly preserves microstructural evidence of both brittle and low-temperature crystal-plastic deformation. The study of intragrain sub-structures within naturally deformed pyrite grains offers the potential, therefore, to investigate the remobilization of chemical elements within the crystal lattice induced by strain. In this study, we combine microstructural observations by electron back-scattered diffraction analysis (EBSD) with pyrite elemental mapping by laser ablation inductively coupled plasma time-of-flight mass spectrometry (LA-ICP-TOFMS) to study crystal plastic deformation and element mobility in pyrite from a naturally deformed quartz-sulphide vein associated with a strike-slip fault that cyclically experienced transient differential stress and pore pressure oscillations. Initially, LA-ICP-TOFMS imaging was used to image sets of otherwise invisible intragrain sub-structures as highlighted by the structurally controlled accumulation of specific elements (e.g. Co, Ni, Cu, Sn, Ag, As, Sb, Pb). EBSD analysis was subsequently performed in the areas analysed by TOFMS with the aim to study the nature of the intragrain sub-structures. EBSD data show that these chemically defined intragrain sub-structures correspond to low-angle boundaries. Cumulative misorientation profiles across pyrite grains suggest that low-angle boundaries are both related to healed fractures and growth features but also indicate a continuous cumulative lattice misorientation up to $>5^\circ$. Boundary trace analysis suggests that fracturing is competing with tilt boundary rotation and pressure-solution to accommodate strain and locally concentrate specific chemical elements.

EntraPT: a GUI program for anisotropic elastic thermobarometry

Mazzucchelli M.L.*¹, Angel R.J.¹, Morganti S.² & M. Alvaro M.¹

¹ Department of Earth and Environmental Sciences, University of Pavia, Italy.

² Department of Electrical, Computer, and Biomedical Engineering, University of Pavia, Italy.

Corresponding email: mattialuca.mazzucchelli@unipv.it

Keywords: elastic thermobarometry, elastic anisotropy, mineral inclusion.

When rocks are exhumed to the surface of the Earth, residual stresses and strains may be still preserved in mineral inclusions. If measured and interpreted correctly through elastic geobarometry, they give us invaluable information on the pressures and temperatures of metamorphism during geodynamical processes such as subduction.

We have developed a new elastic geobarometric approach that exploits the elastic anisotropy of minerals to quantify the stresses at entrapment if no plastic or brittle deformation has subsequently occurred upon exhumation. We combine micro-Raman spectroscopy and X-ray diffraction to determine the residual strain state in the inclusion while still trapped in its host (Murri et al., 2018). The anisotropic elastic relaxation is evaluated with Finite Element analyses carried out on 3D reconstruction of the sample from synchrotron X-ray tomographic microscopy. Finally, a thermodynamic calculation that combines the volume and axial equations of state (EoS) of the host and of the inclusion is adopted to recalculate one unique P and T of entrapment. The solution is encoded into EntraPT, a new web-based GUI program freely accessible at www.mineralogylab.com. This program relies on an internally consistent set of EoS and relaxation tensors. It allows the user to perform geobarometry calculations with anisotropic elasticity on host-inclusion systems typical of HP and UHP metamorphic rocks such as quartz, zircon and diamond in garnets. As an example, we will present an application of this method to quartz inclusions entrapped in a garnet from an eclogite xenolith from the Mir kimberlite pipe (Yakutiya, Korsakov et al., 2009). Results point to elastic re-equilibration under external hydrostatic conditions at P of ~ 3 GPa and temperatures between 925°C and 1000°C. This suggests a metamorphic origin of this eclogite xenolith, providing constraints on the mechanisms of craton accretion from subducted crustal protoliths.

This work was supported by ERC-StG TRUE DEPTHS (grant number 714936) to M. Alvaro.

Murri M., Mazzucchelli M.L., Campomenosi N., Korsakov A.V., Prencipe M., Mihailova B.D., Scambelluri M., Angel R.J. & Alvaro M. (2018) – Raman Elastic Geobarometry For Anisotropic Mineral Inclusions. *Am. Mineral.*, 103, 1869–1872.

Korsakov A.V., Perraki M., Zhukov V.P., De Gussem K., Vandenabeele P. & Tomilenko A.A. (2009) – Is quartz a potential indicator of ultrahigh-pressure metamorphism? Laser Raman spectroscopy of quartz inclusions in ultrahigh-pressure garnets. *Eur. J. Mineral.*, 21, 1313–1323.

Magmatic forcing of Cenozoic climate?

Menant A.¹, Sternai P.*² & Gerya T.³

¹ GFZ Helmholtz Centre, Potsdam, Germany.

² Department of Earth and Environmental Sciences, University of Milano-Bicocca, Italy.

³ Institute of Geophysics, Swiss Federal Institute of Technology (ETH), Zürich, Switzerland.

Corresponding email: pietrosternai@yahoo.it

Keywords: Cenozoic climate, Neo-tethyan tectonics, magmatism.

Established theories ascribe much of the observed long-term Cenozoic climate cooling to atmospheric carbon consumption by erosion and weathering of tectonically uplifted terrains, but pay less attention to climatic effects due to changes in magmatism and associated carbon degassing. Extinction of Neo-Tethyan volcanic arcs following the onset of the India-Asia and Arabia-Asia collision is largely synchronous with phases of atmospheric carbon reduction, suggesting waning degassing as a possible cause of climate cooling throughout most of the Cenozoic. Here, we present numerical geodynamic petro-thermo-mechanical models elucidating on the rates and modalities of partial melting and volcanic arc demise following continental collision/subduction and use the numerical results to constrain plausible perturbations of the geological carbon cycle. Extinction of volcanic arcs during continental collision/subduction occurs jointly with orogenic and surface processes, implying that reduction of atmospheric CO₂ by enhanced erosion/weathering and reduced volcanic outgassing go hand in hand. However, a phase of enhanced melting and arc activity due to subduction of hydrated and carbon rich materials of the accretionary wedge following the onset of continental collision/subduction may explain the ~10 Ma long period of climate amelioration preceding Cenozoic climate cooling since the onset of the India-Asia collision. Because the observed early-Eocene amelioration of global climate cannot be readily explained by theories referring only to enhanced erosion/weathering following the India-Asia collision, we argue that magmatism provides a substantial and currently overlooked contribution to the Cenozoic climate evolution.

Other major geodynamic events than those occurring along the southern Eurasian margin (e.g. Atlantic mid-ocean spreading between Eurasia and Greenland) occur during the Palaeogene and may have conditioned the overall Cenozoic climate evolution through changes in global outgassing. Constraining the possible magmatic forcing of climate at Cenozoic timescales is thus challenging and should involve global-scale multidisciplinary research. Until the magmatic forcing of Cenozoic climate is quantified, however, no conclusive statements regarding long-debated causal relationships between erosion/weathering of uplifted terrains and climate cooling will be possible. Unifying theories relating tectonic, erosional, climatic and magmatic changes across timescales via the carbon cycle offers an opportunity for future research to advance our understanding of the surface-deep Earth processes coupling.

From aseismic to seismic slip in exhumed seismogenic sources: insights from geochemical and microstructural studies of pseudotachylyte bearing faults in the Adamello massif

Mittempergher S.*

Dipartimento di Scienze dell'Ambiente e della Terra, Università di Milano Bicocca.

Corresponding email: silvia.mittempergher@unimib.it

Keywords: faults, fluid-rock interactions, microstructures.

During their activity, faults experience multiple seismic cycles, with failures possibly followed or preceded by episodes of aseismic creep. Natural fault rocks preserve therefore a record of micro and meso-structures resulting from shear at low to high strain rates, with evolving rock strength, permeability and fluid chemistry. In the northern Adamello (southern Italian Alps), several dextral transpressive faults were active during the Oligocene, at depth of more than 8 km and ambient temperature on the order of 250°C. Pseudotachylytes, quenched frictional melts developed during earthquakes, are structurally associated with indurated cataclasites cemented by chlorite, epidote and K-feldspar. We integrated field, geochemical and quantitative microstructural characterization of cataclasites and pseudotachylytes to explore the deformation mechanisms active in these faults during the seismic cycle, and their role in controlling earthquake nucleation and propagation. Major element and hydrogen isotope geochemistry indicate that the onset of brittle faulting in the area was associated with the ingression of an external fluid, which produced a low greenschist facies mineral assemblage in the cataclasites, and significant major and trace element mobility. Coseismic frictional melts involved both wall rock granodiorite and altered cataclasites. Quantification of the grain size distribution of rock fragments in cataclasites indicates that, with increasing finite strain, the average grain size decreases, the fractal dimension increases (from 1.6 to 2.8 in two dimensions) and the faults develop multiple domains of foliated cataclasites and ultracataclasites. Where ultracataclasite is present, faults accommodated high finite strain, suggesting strain localization and potentially unstable slip. In contrast, faults accommodating low finite strain have a less evolved grain size distribution and show a foliation associated with mineral segregation, indicative of stress driven mass transport processes associated with mineral reactions. Our analysis suggests that in the faults in the Northern Adamello, most of the displacement was accommodated within the granular material deriving from cataclasis of the wall rock, with strain localization and coseismic frictional melting. However, viscous creep associated with incongruent pressure solution processes accommodated a minor proportion of the total displacement.

Multistage metasomatism recorded in HP metamorphic unit: a natural example of porosity waves in subduction zones?

Piccoli F.^{*1-2}, Ague J.J.³⁻⁴, Chu X.⁵ & Vitale Brovarone A.⁶⁻²

¹ University of Bern, Institute of Geological Sciences, Bern, Switzerland.

² Sorbonne Université, Muséum National d'Histoire Naturelle, IRD, Institut de Minéralogie, de Physique des Matériaux et de Cosmochimie, Paris, France.

³ Department of Geology and Geophysics, Yale University, New Haven, CT, USA.

⁴ Peabody Museum of Natural History, Yale University, New Haven, CT, USA.

⁵ Department of Earth Science, University of Toronto, ON, Canada.

⁶ Dipartimento di Scienze della Terra, Università degli Studi di Torino, Italy.

Corresponding email: francesca.piccoli@geo.unibe.ch

Keywords: time-integrated fluid fluxes, porosity waves, C fluxes at subduction zones.

Metasomatic rocks preserved in HP-LT metamorphic units are the ultimate evidence for the passage of fluids through rocks during subduction. Yet, how fluids escape from the subducting slab and in which direction has been a long standing issue. Actually, metamorphic devolatilization reactions involve changes in density, porosity, permeability and fluid pressure which influence fluid flow (Connolly, 2010). Therefore, high fluid fluxes are expected in high-permeability regions that may evolve in fluid conduits (e.g., region developed in compacting two-phase flow systems; lithological contacts; Ague, 1994; Connolly and Podladchikov, 2007; Oliver, 1996). Nevertheless, natural example showing the chemical-mechanical feedbacks during fluid flow in HP metamorphic units (i.e., eclogite-facies metasomatic rocks and HP veins) is still very limited (Plümper et al., 2017; Taetz et al., 2018; Locatelli et al., 2018).

The lawsonite-eclogite unit of Monte San Petrone in Alpine Corsica is a perfect natural laboratory to investigate fluid-rock interactions caused by infiltration of externally derived fluids due to the exceptional preservation of metasomatic rocks. Field and petrological observations allow us to recognize two consecutive metasomatic stages occurring close to peak metamorphic conditions. Mass balance analysis strongly suggest that in order to explain the observed mass change, extremely high fluid fluxes are needed (time-integrated fluid fluxes of the order of 10^4 - 10^5 m³_{fluid} m⁻²_{rock}). We propose that the studied lithological boundaries are the first reported natural example of subduction zone permeability channel. Moreover, mass balance analysis allows estimating volume changes during the two metasomatic stages and give important information on the rheological properties of permeability channels in subduction zones. We will demonstrate how not only the type of fluid, but also the mechanism of fluid flow controls the cycling of elements during subduction. Lastly, we will show how the porosity wave model for fluid flow can reconcile the geochemical signature of the studied metasomatic rocks and the estimated fluid fluxes.

Ague J.J. (1994) - Mass transfer during Barrovian metamorphism of pelites, south-central Connecticut; II, Channelized fluid flow and the growth of staurolite and kyanite: *American Journal of Science*, 94, 1061–1134. <https://doi.org/10.2475/ajs.294.9.1061>.

Connolly J.A. (2010) - The mechanics of metamorphic fluid expulsion: *Elements*, 6, 165–172.

Connolly J. & Podladchikov Y. (2007) - Decompaction weakening and channeling instability in ductile porous media: Implications for asthenospheric melt segregation: *Journal of Geophysical Research: Solid Earth*, 112.

Locatelli M., Verlaquet A., Agard P., Federico L. & Angiboust S. (2018) - Intermediate-depth brecciation along the subduction plate interface (Monviso eclogite, W. Alps): *Lithos*, 378-402. <https://doi.org/10.1016/j.lithos.2018.09.028>.

Oliver N.H.S. (1996) - Review and classification of structural controls on fluid flow during regional metamorphism: *Journal of Metamorphic Geology*, v. 14, p. 477–492. <https://doi.org/10.1046/j.1525-1314.1996.00347.x>

Plümper O., John T., Podladchikov Y.Y., Vrijmoed J.C. & Scambelluri M. (2017) - Fluid escape from subduction zones controlled by channel-forming reactive porosity: *Nature Geoscience*, v. 10, p. 150.

Taetz S., John T., Bröcker M., Spandler C. & Stracke A. (2018) - Fast intraslab fluid-flow events linked to pulses of high pore fluid pressure at the subducted plate interface: *Earth and Planetary Science Letters*, 482, 33–43. <https://doi.org/10.1016/j.epsl.2017.10.044>

Tian M., Ague J.J., Chu X., Baxter E.F., Dragovic N., Chamberlain C.P. & Rumble III D. (2018) - The Potential for Metamorphic Thermal Pulses to Develop During Compaction? Driven Fluid Flow: *Geochemistry, Geophysics, Geosystems*, 19, 232–256.

Sulfur transfer within subduction zones: Evidence from exhumed mafic and ultramafic slab material

Schwarzenbach E.M.*¹, Li J.², John T.¹, Caddick M.J.³, Petroff M.³ & Gill B.C.³

¹ Institute of Geological Sciences, Freie Universität Berlin, Berlin, Germany.

² Institute of Geology and Geophysics, Chinese Academy of Sciences, Beijing, China.

³ Department of Geosciences, Virginia Tech, Blacksburg, USA.

Corresponding email: esther.schwarzenbach@fu-berlin.de

Keywords: subduction, sulfur.

Subduction zones impose a major control on the elemental transfer between the surficial and internal reservoirs of the Earth. Subduction of the oceanic lithosphere transports sulfur and carbon together with numerous other elements into Earth's mantle modifying the chemical budget and the redox state of the mantle. Here, we use bulk rock sulfur geochemical data of exhumed mafic and ultramafic slab material and vein systems in blueschists to provide new insights into the sulfur cycle within subduction zones.

Overall, at moderate peak P-T conditions large sequences of obducted ophiolitic sections can retain their carbon and sulfur signature gained from seafloor alteration signatures. Though with increasing P-T conditions dehydration reactions cause mobilization of oxidized (sulfate) and reduced (sulfide) sulfur. The released sulfur is initially channelized within complex vein systems producing pyrite-rich dehydration veins within the subducting slab. These vein systems carry distinct sulfur isotopic signatures that record dehydration of sedimentary sequences, variably altered oceanic crust and serpentinitized peridotite, and are derived from different stages of oceanic slab subduction. Subsequently, the dehydration fluids are transferred along the slab-mantle wedge interface (e.g., within a subduction zone channel). Small bodies of detached slab material are thereby subject to metasomatic processes during exhumation where fluids that are circulating along the plate interface cause sulfur mobilization. Sulfur mobilization is thereby more pronounced within serpentinites compared to mafic blocks. The sulfur isotopic composition of these blocks can serve as an additional tool to track the sulfur chemistry of the subduction zone channel as they track dehydration reactions of the downgoing slab. Our data provides new insights into the sulfur transfer between the slab and the mantle wedge, which may eventually control the formation of arc-related melts and porphyry deposits.

S8

**Permo-Triassic geodynamic evolution
of the Western Tethys realm: insights from magmatism,
tectonics and stratigraphic data**

CONVENERS AND CHAIRPERSONS

Mauro Caggiati (Università di Ferrara)

Federico Casetta (Università di Ferrara)

Corrado Morelli (Provincia Autonoma di Bolzano – Servizio Geologico)

Timing of Middle Triassic Magmatism in the Southern Alps

Brack P.*

Department of Earth Sciences, ETH Zurich.

Corresponding email: peter.brack@erdw.ethz.ch

Keywords: Triassic, magmatism, Southern Alps.

In the Middle Triassic the South Alpine realm and adjacent areas were affected by locally intense magmatic activity during a short time interval of ca. 5 million years. Magmatism was preceded and accompanied by large-scale tectonic instability manifested by areas of surface uplift and zones of rapid subsidence. Deformation and coeval igneous processes possibly occurred in a transcurrent setting but the larger-scale tectonic context remains as yet unclear.

A prerequisite for a better understanding of the Middle Triassic tectono-magmatic processes is an improved knowledge of the temporal and spatial distribution of their elements. Stratigraphic settings throughout the Southern Alps and cross-cutting relationships provide prime constraints for the correlation also of distant tectonic and magmatic features. However, in view of the short duration of this interval, age data useful for calibration must have a sufficiently high temporal resolution.

In the past decades the procedure of CA-ID-TIMS-U-Pb-dating of magmatic zircon has seen substantial improvements. Zircon geochronometry is at present the arguably most adequate tool for an accurate temporal calibration of magmatic features such as those of the South Alpine Middle Triassic. High precision CA-ID-TIMS U-Pb ages on zircons are available for ash layers in pelagic sediments (Mietto et al., 2012; Wotzlaw et al., 2018) and for intrusive rocks (Storck et al., 2019 and work in progress). This information and results from ongoing work should help establishing the desired temporal framework essential for the comparison of volcanic and intrusive products and their geochemical evolution throughout the Southern Alps and beyond. Attempts to trace tephra layers to volcanic sources will possibly help identify also less evident sites of magmatic activity. Finally, the occurrence of coeval magmatic products in the exposed lower crust of the Southern Alps (Ivrea-Verbanò Zone), if confirmed, could reveal deep-seated aspects of the Middle Triassic magmatic system.

Mietto P., Manfrin S., Preto N., Rigo M., Roghi G., Furin S., Gianolla P., Posenato R., Muttoni G., Nicora A., Buratti N., Cirilli S., Spötl C., Ramezani J. & Bowring S. (2012) - The Global Boundary Stratotype Section and Point (GSSP) of the Carnian Stage (Late Triassic) at Prati di Stuares/Stuares Wiesen section (Southern Alps, NE Italy). *Episodes*, 35, 414-430.

Storck J.C., Brack P., Wotzlaw J.F. & Ulmer P. (2019) - Timing and evolution of Middle Triassic Magmatism in the Southern Alps (northern Italy). *Journal of the Geological Society*, 176, 253-268.

Wotzlaw J.F., Brack P. & Storck J.C. (2018) - High-resolution stratigraphy and zircon U-Pb geochronology of the Middle Triassic Buchenstein Formation (Dolomites, northern Italy): precession-forcing of hemipelagic carbonate sedimentation and calibration of the Anisian-Ladinian boundary interval. *Journal of the Geological Society*, 175, 71-85.

Deciphering a geological enigma: occurrence of intraplate magmatism at convergent plate boundaries

Brombin V.*¹, Bonadiman C.¹, Jourdan F.², Roghi G.³, Coltorti M.¹, Webb L.W.⁴, Callegaro S.⁵, Bellieni G.⁶, De Vecchi Gp.⁶, Sedeo R.⁶ & Marzoli A.³⁻⁶

¹ Dipartimento di Fisica e Scienze della Terra, Università di Ferrara, Italy.

² Western Australian Argon Isotope Facility, School of Earth and Planetary Sciences & JdL Centre, Curtin University, Perth, Western Australia, Australia.

³ Istituto di Geoscienze e Georisorse, CNR, Padova, Italy.

⁴ Department of Geology, University of Vermont, Vermont, USA.

⁵ Centre for Earth Evolution and Dynamics, University of Oslo, Norway.

⁶ Dipartimento di Geoscienze, Università di Padova, Italy.

Corresponding email: brmvnt@unife.it

Keywords: intraplate magmatism, Southeastern Alps, poloidal mantle flow.

The convergence of European plate and Adria microplate is considered responsible for the orogenic magmatism that occurred in the Central Alps along the Periadriatic Line (late Eocene–early Oligocene; Dal Piaz et al., 2003; Bergomi et al., 2015) and the anorogenic magmatism that occurred in the Veneto Volcanic Province (VVP) in the Southeastern Alps (late Paleocene–early Miocene; Beccaluva et al., 2007). However, the occurrence of intraplate-related magmatic activities near convergent margins is still matter of debate and interpretations (e.g., Garzanti et al., 2018).

The VVP is formed by dominant basic–ultrabasic (from nephelinites to tholeiites) magmatic products and by localized acid (latitic, trachytic, and rhyolitic) subvolcanic bodies (Beccaluva et al., 2007). In this work new geochemical and geochronological data of magmatic products from the VVP, are provided to (i) constrain the nature and evolution of the mantle source, (ii) reconstruct the history of magmatic activity, and (iii) develop a new geodynamic model explaining the apparently unusual occurrence of intraplate magmatism near convergent margins.

The new trace element patterns and ratios suggest that the mantle source of the VVP alkaline magma types was a garnet lherzolite possibly metasomatised by carbonatitic melts and with residual phlogopite. The biostratigraphic records accompanied with our new ⁴⁰Ar/³⁹Ar ages demonstrate VVP eruptions occurred in several pulses, reflecting the extensional phases experienced by the Eastern Alpine domain. The volcanism started in the late Paleocene in the western sector of the VVP where activity was widespread also during the Eocene (45.21 ± 0.11 Ma – 38.73 ± 0.44 Ma). In the eastern sector eruptions took place in the early Oligocene (32.35 ± 0.09 Ma – 32.09 ± 0.29 Ma) and in the early Miocene (~ 23 – 22 Ma) (Brombin et al., 2019). In literature, these eruptions were related to mantle upwellings through slab window after the European slab break-off at ~ 35 Ma (Macera et al., 2003). However, considering i) new tomographic images evidencing a continuous subvertical (~ 500 km in depth; Hua et al., 2017) slab beneath the Central Alps, and ii) the onset of magmatic activity in the VVP in the late Paleocene (i.e., before the slab break-off), a better suited geodynamic scenario is required. The westward rollback of the European slab caused the retreat and steepening of the subducting plate. As a consequence, sub-slab mantle material escaped and upwelled from the front of the slab and created a poloidal mantle flow, which induced i) the extensional deformation in the overriding Adria microplate, ii) the decompressional melting of VVP mantle source, and iii) the intraplate affinity of the VVP magmatism (Brombin et al., 2019). During these processes, the Adria microplate also rotated counterclockwise allowing the poloidal mantle flow to affect different portions of the overlying lithosphere and to generate up to five magmatic centers in the VVP.

Beccaluva L., Bianchini G., Bonadiman C. & Coltorti M. (2007) - Intraplate lithospheric and sublithospheric components in the Adriatic domain: Nephelinite to tholeiite magma generation in the Paleogene Veneto Volcanic Province, Southern Alps. *Geol. Soc. Am.*, 418, 131–152.

Bergomi M.A., Zanchetta S. & Tunesi A. (2015) - The Tertiary dike magmatism in the Southern Alps: geochronological data and geodynamic significance. *Int. J. Earth Sci.*, 104, 449–473.

- Brombin V., Bonadiman C., Jourdan F., Roghi G., Coltorti M., Webb L.W., Callegaro S., Bellieni G., De Vecchi G.P., Sedeo R. & Marzoli A. (2019) - Intraplate magmatism at a convergent plate boundary: the case of the Cenozoic northern Adria magmatism. *Earth Sci. Rev.*, 192, 355-378.
- Dal Piaz G.V., Bistacchi A. & Massironi M. (2003) - Geological outline of the Alps. *Episodes*, 26, 175-181.
- Garzanti E., Radeff G. & Malusà M.G. (2018) - Slab breakoff: A critical appraisal of a geological theory as applied in space and time. *Earth Sci. Rev.*, 177, 303-319.
- Hua Y., Zhao D. & Xu Y. (2017) - P wave anisotropic tomography of the Alps. *J. Geophys. Res.: Solid Earth*, 122, 4509-4528.
- Macera P., Gasperini D., Piromallo C., Blichert-Toft J., Bosch D., Del Moro A. & Martin S. (2003) - Geodynamic implications of deep mantle upwelling in the source of Tertiary volcanics from the Veneto region (Southern-Eastern Alps). *J. Geodyn.*, 36, 563-590.

Distribution of Triassic magmatism in the Southern Alps: an updated overview

Caggiati M.*¹ & Gianolla P.¹

¹ Dipartimento di Fisica e Scienze della Terra, Università di Ferrara, Italy.

Corresponding email: marcello.caggiati@unife.it

Keywords: Triassic, Magmatism, Southern-Alps.

The revision of the bio- and sequence stratigraphic interpretation of sedimentary successions, favored by advances of analysis techniques and the increasing availability of new field-data in the last decades, allow to define an updated high-resolution chronostratigraphic framework for the Triassic of regions bordering the Western Tethys, particularly the Southern Alps. At the same time, improvements in knowledge on tectonic lineaments and spatial relationships between different nappes led to new paleogeographic scenarios. Therefore, the distribution of petrographic and geochemical data of Triassic volcanic and volcanoclastic products in the Southern Alps need to be updated in terms of space and time, and new remarks can be done about the evolution of magmatism.

The oldest evidences of volcanism are found in the northeastern part of the Southern Alps, where intermediate to acid products can be referred to the early Late Anisian. From this point forward, the magmatism developed widely in the whole eastern part of the region (e.g. Julian Alps) leading to the emplacement of acid ignimbrites, pyroclastics and even subvolcanic products. Similar patterns have been reported in sectors of neighboring regions like the Outer Dinarides and the Adriatic Foreland. Since the (Early?) Ladinian, the magmatism expanded westward in the Southern Alps, originating acid to intermediate volcanic and subvolcanic products (e.g. Vicentian Prealps). During the Late Ladinian, a strong tectono-magmatic phase affected the Dolomites as well as some parts of the central Southern Alps: huge amounts of mafic volcanics spread in the basins and at least three main volcanoes were set. Subaerial, basaltic lava bodies overlapped shallow carbonate successions in the western Dolomites as well as westward to the Adige valley. Limited occurrences of similar magmatic products in the Brescia Prealps have been referred to the Ladinian.

During the Early Carnian, the magmatism shifted almost definitively westward to the central Southern Alps: first witnesses are mainly represented by volcanoclastics related to eruptive centers located in a nearby southern sector. However, intermediate to acid volcanism continued in the Brescia Prealps during the Carnian, producing both subvolcanic bodies and subaerial flows. Younger occurrences of magmatic products recorded in the Southern Alps consist in basic vein-like intrusions affecting the Brescian Prealps, that has been dated to the Norian time. Interestingly, a similar Late Triassic age has been estimated for new discovered lamprophyres intruded in the western Dolomites (Casetta et al., this session).

As regard the western Southern Alps, the age of the magmatic intrusion of the Finero Mafic Complex is still matter of debate and cannot be confidently referred to the Triassic. However, it is interesting to note that part of detected thermal perturbations has been referred to the Anisian to Carnian timespan, matching the central and eastern Southern Alps magmatic activity.

The alkaline-carbonatitic lamprophyres of the Dolomitic Area: Late Triassic precursors of the Alpine Tethys opening

Casetta F.*¹, Ickert R.B.², Mark D.F.², Bonadiman C.¹, Giacomoni P.P.¹, Ntaflou T.³ & Coltorti M.¹

¹ Department of Physics and Earth Sciences, University of Ferrara, Italy.

² Scottish Universities Environmental Research Centre, UK.

³ Department of Lithospheric Research, Universität Wien, Austria.

Corresponding email: estfre@unife.it

Keywords: Carbonatitic alkaline lamprophyre, Dolomitic Area, Triassic magmatism, Southern Alps.

The camptonitic dykes cropping out at Predazzo (Dolomitic Area, Southern Alps) are among the oldest examples of lamprophyric rocks in Italy. In this study, a detailed petrological, geochemical and geochronological characterization of these rocks was put forward to frame them inside the articulated geodynamic evolution of the Southern Alps domain during Triassic. Whole-rock major and trace element content of lamprophyres suggest that their magmatic system was dominated by fractional crystallization, even some complex textures of amphibole phenocrysts could have formed in response to small-scale mixing processes. Additionally, the occurrence of primary carbonate ocelli in the camptonitic rocks suggest that the alkaline and the carbonatitic melts co-existed. Trace element, Sr-Nd isotopes and ⁴⁰Ar/³⁹Ar data show that Predazzo lamprophyres cannot be considered anymore as a late-stage pulse belonging to the orogenic-like Ladinian magmatic phase of the Southern Alps, but instead represent an isolated magmatic pulse generated, ~20 Ma later, by a garnet-amphibole-bearing mantle source interacting with an asthenospheric component. All these features, fostered by a comparison with the main Middle-Late Triassic magmatic occurrences of the Alps and Carpathians regions, suggest that Predazzo lamprophyres belong to the alkaline-carbonatitic magmatic event that intruded the mantle beneath the Southern Alps between 225 and 190 Ma (Stähle et al., 2001; Schaltegger et al., 2015; Galli et al., 2019). In the light of these new findings, Predazzo lamprophyric dykes can be interpreted as the geochemical/geochronological junction between the orogenic-like Ladinian magmatism and the rifting phase related to the opening of the Alpine Tethys.

Galli A., Grassi D., Sartori G., Gianola O., Burg J.P. & Schmidt M.W. (2019) - Jurassic carbonatite and alkaline magmatism in the Ivrea zone (European Alps) related to the breakup of Pangea. *Geology*, 47(3), 199-202.

Schaltegger U., Ulianov A., Müntener O., Ovtcharova M., Peytcheva I., Vonlanthen P., Vennemann T., Antognini A. & Girlanda F. (2015) - Megacrystic zircon with planar fractures in miaskite-type nepheline pegmatites formed at high pressures in the lower crust (Ivrea Zone, southern Alps, Switzerland). *American Mineralogist*, 100(1), 83-94.

Stahle V., Frenzel G., Hess J.C., Saupé F., Schmidt S.T. & Schneider W. (2001) - Permian metabasalt and Triassic alkaline dykes in the northern Ivrea zone: clues to the post-Variscan geodynamic evolution of the Southern Alps. *Schweizerische Mineralogische und Petrographische Mitteilungen*, 81(1), 1-21.

Petrological features of clinopyroxene in lava flows from Cima Pape (Dolomitic Area, Southern Alps): how to unravel the feeding system of a Middle Triassic volcano

Casetta F.¹, Giacomoni P.P.¹, Nardini N.*¹ & Coltorti M.¹

¹ Department of Physics and Earth Sciences, University of Ferrara, Italy.

Corresponding email: nicolo.nardini@student.unife.it

Keywords: Clinopyroxene texture, feeding system, Middle Triassic magmatism, Dolomitic Area

The Cima Pape volcano-plutonic complex, together with Mt. Monzoni and Predazzo ones, represents one of the main expression of the Middle Triassic magmatic event that occurred in the Dolomitic Area (Southern Alps). The intrusive portion is constituted by gabbroic to monzodioritic products, whereas the overlying volcanites are basaltic to trachyandesitic lavas and pillow breccias. The volcanic products have a porphyritic texture characterized by large amounts of clinopyroxene, plagioclase, and (less abundant) olivine phenocrysts embedded in a microcrystalline matrix. Most clinopyroxenes (up to 3 mm in size) have generally homogeneous or simple-zoned texture, with Mg# [$\text{MgO}/(\text{MgO}+\text{FeO}_{\text{tot}})$ mol%] ranging between 71 and 77. Some of them show a peculiar texture, characterized by an intermediate overgrowth with high Mg# (80-84, up to 90), high Cr_2O_3 (up to 1.0 wt%) and low TiO_2 (down to 0.1 wt%) contents, likely resulting from a mixing within the feeding system, where new mafic input of magma could have interacted with differentiated batches. An evaluation of the textural and compositional features of clinopyroxene in the volcanics and their plutonic counterparts enabled us to speculate about the main chemical and physical processes acting in the feeding systems during the Middle Triassic magmatic event in this part of the Southern Alps.

Middle Triassic subsidence in the Dolomites (Italy): control of tectonics

Curzi M.*¹, Gianolla P.², Caggiati M.² & Carminati E.¹

¹ Dipartimento di Scienze della Terra, Sapienza Università di Roma (Rome, Italy).

² Dipartimento di Fisica e Scienze della Terra, Università di Ferrara (Ferrara, Italy).

Corresponding email: manuel.curzi@uniroma1.it

Keywords: depocenter of subsidence, tectonic lineaments, pull apart basin.

In the Dolomites region, Middle Triassic tectonics was associated with fast subsidence rates and a Late Ladinian magmatic event that induced epicrustal intrusions (Monzoni, Predazzo, Cima Pape) and a significant shoshonitic-basaltic volcanism. Contrasting scenarios (from transpressional/transtensional tectonics to subduction backarc extension) were proposed to explain these tectonics and magmatism (Lustrino et al., 2019 and reference therein). In order to contribute to unravel of this issue, we built subsidence curves and maps for different Triassic periods, based on cross sections and well data. In particular, we analysed the thicknesses of four Triassic carbonate systems (represented by Contrin Fm., Sciliar Fm., Cassian Dolomite and Heiligkreuz Fm.) in 21 areas spread on the central-eastern Southern Alps. Subsidence calculations, covering a time span of about 12 Ma (from Illyrian to Tuvanian), provided us the opportunity to quantify local and regional subsidence rates, and to constrain and reconstruct the time-space evolution of subsidence at a regional scale.

From preliminary results, we can observe that: 1) a depocenter of subsidence was persistent in the eastern Dolomites from late Anisian to middle-late Carnian; 2) subsidence migrated toward east and north-east in Julian time; 3) the time-space evolution and migration of the subsidence was controlled by the principal Triassic (strike-slip and extensional) tectonic lineaments; 4) subsidence rates were faster both in the eastern Dolomites and in areas characterized by Ladinian magmatism (central Dolomites), reinforcing the idea of a control of tectonics (i.e. crustal thinning).

Based on our observations, we speculate the occurrence, during Middle Triassic time, of a wide (crustal scale) strike-slip system, associated with magmatism, in which the Dolomites represented a pull apart basin. Within this scenario, in the Dolomites, N70°-90° strike slip tectonics generated transtensional-transpressional faults (associated with local extra subsidence and uplift, respectively).

Lower Carboniferous to Upper Triassic evolution of the Ivrea-Verbanò Zone: geochronological constraints from the Alpe Morello (Val Strona) rock sequence

Ferrari E.*¹, Tribuzio R.², Bosch D.³, Bruguier O.³ & Langone A.⁴

¹ Dipartimento di Scienze Chimiche, della Vita e della Sostenibilità Ambientale, Università di Parma.

² Dipartimento di Scienze della Terra e dell'Ambiente, Università di Pavia.

³ Géosciences Montpellier - Université Montpellier II. ⁴ Istituto di Geoscienze e Georisorse - C.N.R., Unità di Pavia.

Corresponding email: elisa.ferrari@unipr.it

Keywords: Alpe Morello, geochronology, laser ablation, Paleozoic-Mesozoic evolution.

The basement of the South Alpine domain in northwest Italy exposes a nearly complete section of the continental crust. This section includes several mantle lenses, particularly at the deepest crustal levels, near the Insubric Line. The present study focuses on a mantle lens enclosed at mid crustal levels (Alpe Morello, Val Strona), along the tectonic boundary separating the Ivrea-Verbanò Zone from the Serie dei Laghi. This lens is 1.5 km long and up to 400 m thick, and is physically associated with a thin lens made up of amphibolites retaining eclogite facies relics. Amphibolitized eclogites are also present as layers within the Alpe Morello mantle peridotite. The mantle-amphibolite association is enclosed within sillimanite-bearing, amphibolite facies metasediments, and is crosscut by pegmatoid granitoid dykes. To provide new geochronological constraints on the Paleozoic-Mesozoic evolution of the Ivrea-Verbanò Zone, we carried out a geochronological investigation of the Alpe Morello rock sequence. In particular, we dated by laser ablation ICP-MS, U-Th-Pb analyses: (i) monazite from metasediments of both Ivrea-Verbanò Zone and Serie dei Laghi, and (ii) rutile from amphibolitized eclogites.

The monazite dates span from the Upper Carboniferous to the Lower Permian, similar to what was previously reported for the Ivrea-Verbanò Zone and the Serie dei Laghi (Henk et al., 1997; Guergouz et al., 2018). A slightly younger, Rb-Sr muscovite date of 279 ± 10 Ma was acquired for the Ivrea-Verbanò Zone metasediments cropping out in an adjacent area (Pinarelli et al., 1988). Similarly, a Serie dei Laghi amphibolite body exposed at few hundred meters from Alpe Morello gave a $^{40}\text{Ar}-^{39}\text{Ar}$ amphibole date of 271 ± 1 Ma (Siegesmund et al., 2008). Rutile from Alpe Morello amphibolitized eclogites remarkably furnished younger, Upper Triassic dates, which cannot be related to the age of the eclogite facies metamorphism. The U-(Th)Pb system in the rutile is interpreted to have been reset in response to: (i) Permian to Triassic, slow cooling of the middle continental crust, or (ii) a Triassic heating event.

Guergouz C., Martin L., Vanderhaeghe O., Thébaud N. & Fiorentini M. (2018) - Zircon and monazite petrochronologic record of prolonged amphibolite to granulite facies metamorphism in the Ivrea-Verbanò and Strona-Ceneri Zones, NW Italy. *Lithos*, 308-309, 1-18.

Henk A., Franz L., Teufel S. & Oncken O. (1997) - Magmatic Underplating, Extension, and Crustal Reequilibration: Insights from a Cross-Section through the Ivrea Zone and Strona-Ceneri Zone, Northern Italy. *Journal of Geology*, 105, 367-378.

Pinarelli L., Del Moro A. & Boriani A. (1988) - Rb-Sr Geochronology of Lower Permian plutonism in Massiccio dei Laghi, Southern Alps (NW Italy). *Rendiconti della Società Italiana di Mineralogia e Petrologia*, 43, 411-428.

Siegesmund S., Lauer P., Dunkl I., Vollbrecht A., Steenken A., Wemmer K. & Ahrendt H. (2008) - Exhumation and deformation history of the lower crustal section of the Valstrona di Omegna in the Ivrea Zone, southern Alps. *Geological Society, London, Special Publications*, 298, 45-68.

Early Permian - Early Triassic siderite deposits in the Southern Alps (Italy)

Martin S.*¹, Toffolo L.¹, Moroni M.², Montorfano C.³, Secco L.¹, Agnini C.¹, Nimis P.¹ & Tumiati S.²

¹ Dipartimento di Geoscienze, Università degli Studi di Padova, Italy.

² Dipartimento di Scienze della Terra “Ardito Desio”, Università degli Studi di Milano, Italy.

³ Centro Grandi Attrezzature per lo studio e la caratterizzazione della Materia, Università degli Studi dell’Insubria, Como, Italy.

Corresponding email: silvana.martin@unipd.it

Keywords: Siderite, vein deposits, stratabound deposits, Permian-Triassic time, Uranium, Italy.

Siderite occurs in different sites of the Lombardian and Venetian Southern Alps. Usually siderite is present as veins cutting the basement and Early Permian volcano-sedimentary cover (Collio Fm.), and as both veins and conformable stratabound orebodies in the Late Permian (Verrucano Lombardo, Bellerophon Fms.) and Early Triassic (Servino Fm., Werfen Fm.) sequences. All the deposits show similar major- and rare-earth (REE)-element patterns suggesting a common iron-mineralizing event. The composition of coexisting siderite, Fe-rich dolomite and calcite solid solutions, in addition to a coarse grain size and the nature of ore mineral assemblages suggest formation from hydrothermal fluids at relatively high temperature conditions (~250 °C). Geochemical modelling, supported by REE and new $d^{13}\text{C}$ and $d^{18}\text{O}$ isotopic data suggest that siderite formed by precipitation from hydrothermal fluids, derived from fresh water, leaching organic matter and Fe-proto concentrations contained in continental sediments as well as the Lower Permian volcanic rocks of the Southern Alps. On the basis of U-Th-Pb microchemical dating of uraninite associated to siderite in the Val Vedello and Novazza deposits (Lombardian Alps), the onset of hydrothermalism is constrained to Early Permian, contemporaneously to plutonism and to the volcanic-sedimentary cycle reported in the Orobian Basin. The siderite veins and conformable bodies in the Lower Triassic shallow-marine successions were formed by precipitation from similar hydrothermal fluids (in this case likely fed by sea water) interacting with the underlying Permian successions, able to replace the marine carbonates with siderite at temperatures of ~250° C for high water/rock ratios. The conformable siderite bodies predate the Middle Triassic magmatism of the Alps and were formed in a dilational geodynamic scenario preluding the Neo-Tethys opening along the Gondwana margin.

Mantle carbonatites or anatectic carbonatites of crustal origin in the Ivrea-Verbano Zone?

Mazzucchelli M.*¹⁻², Giovanardi T.¹ & Cipriani A.¹

¹ Dipartimento di Scienze Chimiche e Geologiche, Università degli Studi di Modena e Reggio Emilia, Modena, Italy.

² Istituto di Geoscienze e Georisorse - CNR, U.O.S. di Pavia, Pavia, Italy..

Corresponding email: maurizio.mazzucchelli@unimore.it

Keywords: Ivrea-Verbano, carbonatite, marble melting.

Recently, Galli et al. (2019) reported on pipe-like bodies and dikes of carbonate rocks related to sodic alkaline intrusions and amphibole mantle peridotites from the Ivrea-Verbano Zone. They interpret the bulk trace-element concentrations of these carbonate rocks as typical of low-rare earth element cumulates of carbonatite melts. LA-ICP-MS U-Pb analyses on zircons yielded concordant ages of 187 ± 2.4 and 192 ± 2.5 Ma, coeval with the sodic alkaline magmatism in the Ivrea zone. In their opinion cross-cutting relations, ages, as well as bulk and zircon geochemistry indicate that the carbonate rocks are carbonatites, the first ever reported from the Alps.

However, according to the literature, Stähle et al. (1990; 2001) were the first to report the presence in the Alps of a discordant carbonate dike with abundant inclusions, located within the granulitic rocks of the volcano-sedimentary sequence of the Kinzigite Formation in the Val Grande area. The LREE of the dike are enriched by a factor of 100 and the HREE by a factor of 35 when compared to the sedimentary marbles of the Ivrea zone. They interpreted this dike as representative of an alvikite carbonatite with xenoliths of perthitic alkaline feldspars and syenitic metasomatites.

Here, we discuss the alternative possibility that the carbonate rocks of Galli et al. (2019) may represent carbonate anatectic melts of crustal origin generated during high-grade metamorphism of the Kinzigite Formation.

The Authors acknowledge the PRIN MIUR 20158A9CBM project for financial support.

Galli A., Grassi D., Sartori G., Gianola O., Burg J.-P. & Schmidt M.W. (2019) - Jurassic carbonatite and alkaline magmatism in the Ivrea zone (European Alps) related to the breakup of Pangea. *Geology*, 47, 199-202.

Stälhe V., Frenzel G., Kober B., Michard A. Puchelt H. & Schneider W. (1990) - Zircon syenite pegmatites in the Finero peridotite (Ivrea Zone): evidence for a syenite from a mantle source. *Earth Planet. Sci. Letters*, 101, 196-205.

Stälhe V., Frenzel G., Hess J.C., Saupé F., Schmidt S.Th. & Schneider W. (2001) - Permian metabasalt and Triassic alkaline dykes in the Northern Ivrea Zone: clues to the post-Variscan geodynamic evolution of the Southern Alps. *Schweiz. Mineral. Petr. Mitt.*, 81, 1-21.

A review of upper Carboniferous-Permian tectonics in Corsica, Calabria and Tuscany

Molli G.*¹, Brogi A.²⁻³, Caggianelli A.², Capezzuoli E.³, Liotta D.²⁻³, Spina A.⁴ & Zibra I.⁵

¹ Dipartimento Scienze della Terra Università di Pisa Italy.

² Dipartimento di Scienze della Terra e Geoambientali, Bari, Italy.

³ Consiglio Nazionale delle Ricerche – IGG, Pisa.

⁴ Dipartimento di Scienze della Terra Università di Firenze, Italy.

⁵ Dipartimento di Fisica e Geologia Università di Perugia, Italy.

⁶ Geological Survey of Western Australia, Department of Mines and Petroleum, Australia.

Corresponding email: giancarlo.molli@unipi.it

Keywords: Permian tectonics, Corsica-Calabria, Tuscany.

Combining our and literature data we propose a revision of the upper Carboniferous-Permian tectonics as recorded in Corsica, Calabria and Tuscany. In Corsica, the alpine Santa Lucia nappe shows a kilometer-scale relict of a Permian lower to mid-crust similar to the well-known Ivrea-Verbano zone. The two distinct Mafic and Leucogranitic complexes characterizing this crustal domain are juxtaposed by an oblique-slip shear zone i.e. Santa Lucia Shear Zone. Structural and petrological data document interaction between magmatism, metamorphism and shearing during Permian over a temperature range of 800 to 400 °C. In Calabria (Sila, Serre and Aspromonte) a complete pre-Mesozoic crustal section is documented. The lower crust is characterized by granulite and upper amphibolite facies metapelites and subordinate metagreywacke, marble and metabasite. The mid-crustal c.13 km thick section includes granitoids of tonalitic to granitic composition, testifying magmatism which started with quartz-dioritic dykes at 323±5 Ma, until 300 Ma during extensional shearing to end between 295 and 277 Ma, with shallower dykes emplaced in a transtensional setting. The section is completed by the upper crust portion, mainly formed by a Paleozoic succession deformed in the upper crust as a low grade fold and thrust belt, locally overlaying medium grade paragneiss units and therefore as whole reminiscent of the external/nappe zone domains of Sardinia Hercynian orogeny. In Tuscany, following earlier hypotheses, we document how upper Carboniferous/Permian shallow marine to continental sedimentary basins, characterized by unconformity and abrupt change in sedimentary facies (coal-measures, red fanglomerate deposits) and acid magmatism, well fit a transtensional setting with a mid-crustal shear zone linked with a system of E-W trending (in present orientation) upper crust splay faults. As a whole the sedimentary, tectono-metamorphic and magmatic upper Carboniferous-Permian record of the investigated areas supports a tectonic scenario characterized by regional-scale trascurrent fault systems associated to stretched crustal domains in which extensional structures, magmatism and transtensional basins developed. The first-order shear zone network, we propose, includes a westernmost Santa Lucia Shear Zone and an easternmost East Tuscan Shear Zone developed to accommodate Pangea B to Pangea A transformation during Permian.

Outline of a mega volcanic system: The Athesian Volcanic Group

Morelli C.*¹, Bargossi G.M.², Gasparotto G.², Mair V.¹, Moretti A.³, Piccin G.³ & Trentini T.³

¹ Ufficio Geologia e prove materiali Provincia Autonoma di Bolzano.

² Dipartimento di Scienze Biologiche, Geologiche e Ambientali Università di Bologna.

³ libero professionista.

Corresponding email: corrado.morelli@provincia.bz.it

Keywords: volcanism, caldera, Permian.

The Athesian Volcanic Group (AG) constitutes a major part of the Permian magmatism in the central-eastern Southern Alps. The AG volcanic sequence occurred during the Lower Permian in a post-orogenic extensional to transtensional geodynamic context. The deposition of different stratigraphic units has strongly been influenced by an extensive synvolcanic tectonic related to wide calderas of different ages. The widespread uplift and incision of Permian rocks in the Athesian area, linked to the modest tectonic deformation, allows observing exceptional outcrop exposures.

The Permian volcanic sequence is bounded by two first order unconformities. The lower one rests on the Variscan South-Alpine metamorphic basement, whereas Upper Permian continental red beds (Val Gardena Sandstone) mark the upper one, which represents the onset of the Alpine depositional cycle. The AG volcanic activity lasted about 10-15 Ma during the early Permian (289 to 274 Ma), with a deposition rate that increased throughout the eruptive cycle.

In the last 20 years, an extensive geological survey of the CARG sheets Merano, Appiano, Mezzolombardo, Trento and Bolzano has radically changed the stratigraphic picture of the Permian volcanic succession. Although the distinct areas have different stratigraphic sequences, a common magmatic-depositional development can be observed. In particular, two major pyroclastic units that have impacted the entire volcanic district are recognized: the Gragazzone Formation and the Ora Formation.

The magmatic activity in the early phases was dominated by lava flows, mainly andesites to rhyodacites in composition. In the intermediate to late stages the main activity is mostly pyroclastic (ignimbrites) with composition switching from rhyodacites to rhyolites.

Facies, distribution and thickness of the different stratigraphic units have been strongly influenced by an extensive synvolcanic tectonic. In particular, the nature and distribution of the individual volcanic units are closely related to the formation of multiple calderas, formed over a period of a few million years. Generally, the collapses are getting younger towards the centre of the volcanic system. We recognize two mayor caldera-forming eruptions, which deposit huge volumes of ignimbrites over areas of thousands of kilometres. The old one Gargazzone Formation is a rhyodacitic, crystal-rich lapilli-tuff, very homogeneous and extremely welded. It shows typical characters of caldera-forming eruptions, i.e. tabular geometries, large areal extension (i.e. 4000 to 6000 km²), strong compositional homogeneity and great thickness (up to 900 m).

The Ora Formation is the youngest eruptive unit of the AG. It is a welded, rhyolitic, crystal-rich lapilli-tuff, very homogeneous and with minimum preserved volume of about 1300 km³. Exceptional exposures of its base along the Adige valley allow us to define the internal geometry of the caldera and its northern edges in detail.

The onset of Middle Triassic volcanism in the Dolomites (Southern Alps, Italy)

Pecorari M.*¹, Gianolla P.¹ & Caggiati M.¹

¹ Dipartimento di Fisica e Scienze della Terra, Università di Ferrara.

Corresponding email: matteo.pecorari@student.unife.it

Keywords: Triassic, Dolomites, magmatism.

Due to the almost preserved depositional geometries and stratigraphic relationships, the Dolomites region is a key-area for understanding the Triassic geological evolution of the Southern Alps and more generally of the Western Tethys.

This study is focused in the southern Dolomites, where a great variety of sedimentary environments developed during the Middle to Upper Triassic: from alluvial plains to marginal deltaic systems, from shallow carbonate platforms to deep-water basins, as well as mixed sedimentation ramp systems. From Late Anisian to Early Carnian, basinal sedimentation persisted in most of the area (Bacino Cadorino Auct.), originating relatively thick and continuous successions, suitable for biostratigraphic and sequence stratigraphic analysis. Moreover, the basinal successions often contain several tuff layers, that can be used to furtherly constraint the events of Middle Triassic volcanism in the Southern Alps. This has been recently revised as regard the chemistry and timing (Storck et al., 2018 and references therein): during the late Anisian, a first felsic stage is widely recorded by pyroclastic intercalations in pelagic beds, from Ambata Fm. to Buchenstein Fm., whereas effusive products are limited to outcrops in the eastern Southern Alps. Subsequently, the magmatism developed south to the Dolomites, in the Recoaro area, where acid to intermediate products have been attributed to the Ladinian. Intense mafic magmatism strongly affected the western Dolomites region during the Late Ladinian, allowing the emplacement of thick effusive successions both in basin and shallow environments (Fernazza Fm.). This last magmatic stage mainly ceased in the latest Ladinian, even if rare pyroclastic tuffs are found intercalated in Upper Ladinian to Lower Carnian basinal successions (Wengen and S. Cassiano Fm.), testifying for the persisting of magmatism somewhere out of the region. Early Carnian effusive to subvolcanic products are known only from the Brescian Prealps region, denoting a mainly acid geochemistry of magmas.

In order to better constraint the timing and evolution of magmatism in the Southern Alps, here we present new correlations between unpublished (Matten, Val di Zonia) and revised-published stratigraphic sections from the Dolomites and from eastern Lombardy (e.g. Bagolino). Indeed, Upper Anisian tuff layer- intervals have been correlated, and new occurrences of tuff intercalation have been discovered within pelagic carbonate-siliciclastic beds (Dont and Recoaro Fms.), bio-stratigraphically dated to late Pelsonian (Middle Anisian). These represent the oldest witness of magmatism in the Dolomites and suggest to furtherly backdate the onset of volcanism in the Southern Alps to the Pelsonian time.

Storck J., Brack P., Wotzlav J. & Ulmer P. (2018) - Timing and evolution of Middle Triassic magmatism in the Southern Alps (northern Italy). *J. Geol. Soc.*, 176, 253-268.

What drives Alpine Tethys opening? Clues from the review of geological data and model predictions

Roda M.*¹, Regorda A.¹, Spalla M.I.¹ & Marotta A.M.¹

¹ Dipartimento di Scienze della Terra, Università degli Studi di Milano.

Corresponding email: manuel.roda@unimi.it

Keywords: Alpine Tethys rifting, Permo-Triassic high thermal regime, Variscan collision.

Permo-Triassic remnants (300–220 Ma) of high-temperature metamorphism associated with large gabbro bodies occur in the Alps and indicate a high thermal regime compatible with lithospheric thinning. During the Late Triassic–Early Jurassic, extensional tectonics leads to the break-up of Pangea continental lithosphere and the opening of Alpine Tethys Ocean (170–160 Ma), as testified by the ophiolites of the Alps and Apennines. We revise Permian to Jurassic geological data from the Alps and Northern Apennines, focusing on continental and oceanic basement rocks, together with the predictions of existing numerical models of post-collisional extension of continental lithosphere and successive rifting and oceanization. The aim is to test whether the transition from the Permian-Triassic extensional tectonics to the Jurassic opening of Alpine Tethys occurred. We enforce the interpretation that a forced extension of 2 cm/year of the post-collisional lithosphere results in a thermal state compatible with the Permian-Triassic high-temperature regime indicated by pressure and temperature conditions of metamorphic rocks and widespread igneous activity. Extensional or transtensional tectonics is also in agreement with the generalized subsidence indicated by the deposition of sedimentary successions with deepening upward facies that occurred in the Alps from the Permian to Jurassic. Furthermore, a rifting developed on a thermally perturbed lithosphere agrees with a hyperextended configuration of the Alpine Tethys margins and with the duration of the extension necessary to the oceanization. The review supports the interpretation of Alpine Tethys opening developed on a lithosphere characterized by a thermo-mechanical configuration inherited by the Variscan setting and post-Variscan extension which affected Pangea during the Permian and Triassic. Therefore, a long-lasting period of active extension can be envisaged for the breaking of Pangea supercontinent, starting from the unrooting of the Variscan belts, followed by the Permo-Triassic thermal high, and ending with the crustal break-up and the formation of the Alpine Tethys Ocean.

Role of Late Carboniferous - Early Triassic structural inheritance in the continental break-up of Pangea and exhumation of the Alpine Tethyan mantle: insights from the Canavese Zone, Western Alps

Succo A.*¹, Festa A.², Balestro G.², Borghi A.² & De Caroli S.²

¹ NEXT – Natural and Experimental Tectonics research group, Dipartimento di Scienze Chimiche, della Vita e della Sostenibilità Ambientale, Università di Parma, Italy.

² Dipartimento di Scienze della Terra, Università di Torino, Italy.

Corresponding email: andrea.succo@studenti.unipr.it

Keywords: structural inheritance, Alpine Tethys, continental break-up.

The formation of rifted continental margin by extension of continental lithosphere, leading to seafloor spreading, is a meaningful component of the plate tectonic cycle. Nevertheless, the discrimination on the role played by structural inheritances in controlling the tectonic evolution and structural deformation pattern of lithosphere and the onset of rifting stage can be difficult to decipher. In fact, polyphasic tectonic, inherited structures may be commonly (i) reactivated, and/or (ii) masked by thick sedimentary and/or magmatic sequences that prevent detailed observation on pre-rift crustal architectures. Through multiscale, field- and laboratory-based structural studies (from geological map scale to mesoscale and scanning electron microscope scale), and re-definition of the stratigraphic succession, we document the internal architecture, tectono-stratigraphic setting and geological evolution of the Canavese Zone (Western Alps), which represents the remnant of stretching, thinning and dismemberment of the distal passive margin of Adria, occurred during the opening of the Alpine Tethys. We document that the continental break-up of Pangea and tectonic dismemberment of the distal margin of Adria, up to Alpine Tethyan mantle rocks exhumation, did not simply result from the syn-rift Jurassic extension but was strongly favored by older structural inheritances (Late Carboniferous to Early Triassic regional-scale wrench faults; see Festa et al., 2019 for further details), which controlled earlier lithospheric weakness, as also suggested for other sectors of the Southern Alps (e.g., Roda et al., 2018). This should be taken in consideration in models aimed to understand processes and mechanisms of progressive stretching and lithospheric thinning, driving to the sharp decrease in crustal thickness and strong decoupling between upper crust and continental mantle, up to continental breakup and mantle exhumation of the Jurassic Alpine Tethys.

Festa A., Balestro G., Borghi A., De Caroli S. & Succo A. (2019) - The role of structural inheritance in continental break-up and exhumation of Alpine Tethyan mantle (Canavese Zone, Western Alps). *Geoscience Frontiers*, <https://doi.org/10.1016/j.gsf.2018.11.007>

Roda M., Regorda A., Spalla M.I. & Marotta A.M. (2018) - What drives Alpine Tethys opening? Clues from the review of geological data and model predictions. *Geological Journal*. <https://doi.org/10.1002/gj.3316>

Comparison among the volcanic complex of Gorski Kotar and lava flows from the Medvednica Mountains with the Triassic magmatism of the Dolomites, first results

Velicogna M.*¹, Venier M.¹, Brombin V.² & De Min A.¹

¹ Dipartimento di Matematica e Geoscienze, Università degli Studi di Trieste.

² Dipartimento di Fisica e Scienze della Terra, Università degli Studi di Ferrara.

Corresponding email: matteoveli87@gmail.com

Keywords: Triassic, magmatism, REE.

The Dinaric Alps are located in southern Europe, they were formed during the Dinaric-Alpine tectonic movements. They follow a north-west/south-east direction being subparallel to the Adriatic Sea and extending from the Julian Alps (Italy-Slovenia) to the north of Albania. In the Dinarides plutonic and volcanic Late Palaeozoic-Triassic Magmatism is widely present, showing large variability in chemical and morphological features. Despite their huge diversity, it is possible to subdivide these magmatic masses in seven main subprovinces on the basis of their petrologic affinities (Pamić, 1984). Seven chosen samples belong to the basalt-spilite subprovince of Hrvatsko Zagorje and southern Slovenia. Four of these have been collected in Gorski Kotar (Croatia), which is composed by two subvolcanic effusive masses, which originally were a unique body, then split by the last tectonic movements. The intrusions lie between Carboniferous sediments and Lower Triassic dolomites, furthermore the contact between the volcanics and the sediments is dated 242.4 ± 3.7 Ma (Palinkaš et al., 2010). The other three samples have been collected from a lava flow sampled in Medvednica Mountains (Croatia) that could be related to the Triassic magmatic rocks of the Orešje quarry located near Gornja Bistra. These are considered High-Ti tholeiitic metabasalts that could represent the highest level of an obducted Triassic Oceanic Crust (Halamić et al., 1998). Major and Trace Elements have been measured and considered to investigate petrographical and petrological features. The aims of this contribution are mainly two: first, to determine the possible relation of the two magmatisms, and to obtain the first clues about their genesis, as well as the genesis of the Croatian Triassic Magmatism; second, understanding if they originated by a single common geodynamic event together with the Triassic Magmatism of the Dolomites and Karawanke.

Halamić J., Slovenec D. & Kolar-Jurkovšek T. (1998) - Triassic Pelagic Limestones in Pillow Lavas in the Orešje Quarry near Gornja Bistra, Medvednica Mt. (Northwest Croatia). *Geologia Croatica*, 51, 33-45.

Palinkaš L. A., Šoštarić S. B., Palinkaš S. S., Crnjaković M., Neubauer F., Molnár F. & Bermanec V. (2010) - Volcanoes in the Adriatic Sea: Permo-Triassic magmatism on the Adriatic-Dinaridic carbonate platform. *Acta Mineralogica-petrographica, Field Guild Series*, 8, 1-15.

Pamić J.J. (1984) - Triassic Magmatism of the Dinarides in Yugoslavia. *Tectonophysics*, 109, 273-307.

Evidence for subduction-related components in sapphirine-bearing gabbroic dykes (Finero Phlogopite peridotite): Insights into the mantle sources of the Mesozoic magmatism at the Africa-Europe boundary

Zanetti A.*¹, Giovanardi T.², Morishita T.³, Hemond C.⁴, Dallai L.¹, Langone A.¹ & Mazzucchelli M.²

¹ IGG-CNR Pavia-Pisa. ² Dipartimento di Scienze Chimiche e Geologiche, Università di Modena e Reggio Emilia.

³ Faculty of Geosciences and civil Engineering, Institute of Science and Engineering, Kanazawa University (Japan).

⁴ Institut Universitaire Européen de la Mer, Université de Brest (France).

Corresponding email: zanetti@crystal.unipv.it

Keywords: Triassic Magmatism, Southern Alps, subduction components.

A gabbroic dykes swarm containing magmatic sapphirine occur in the mantle Finero Phlogopite Peridotite (Ivrea-Verbano Zone, IVZ). Sapphirine is associated to a peculiar mineral assemblage, including plagioclase, titanian pargasite-sadaganaite, titanian phlogopite-biotite and apatite: the latter is rich of calcite inclusions. The dykes i) cut at high angle the mantle foliation, ii) are bounded by orthopyroxenite layers, and iii) show a symmetric internal banding, represented by two, outer hornblendite selvages and an inner leucogabbro layer. The sapphirine occurs, along with Al-rich amphibole (locally, sadaganaite in composition) and green spinel, in mm-thick irregular patches in both the hornblendite salvages.

Major and trace elements of minerals and bulk rock, as well as the isotope O, Sr and Nd composition of minerals, have been investigated for dykes and host peridotite of two different FPP areas.

The melt migration early developed by porous-flow within cm-thick channels, being characterised by olivine-segregation and orthopyroxene-dissolution. With the progression of percolation and reaction, the melt became silica-saturated and an orthopyroxenite layer was segregated in the centre of the channels. Three different evolution stages, involving opening and enlargement of the conduits, determined the layered internal structure of the dykes. The sapphirine and green spinel segregation took place at $T > 1000^{\circ}\text{C}$ in presence of a melt with transient composition, which interstitially migrated and reacted with the cumulus minerals forming the hornblendite layers. Composition of newly-formed amphiboles indicates that the sapphirine parent melt was Al-rich, depleted to strongly depleted in Hf, Zr, Nb, Ta, MREE and HREE, and characterised by positive Eu anomaly. These observations suggest the presence in the transient melt of significant amounts of plagioclase component. Plagioclase assimilation was not observed in the studied veins: it is thus argued that the addition of plagioclase component occurred in hidden magmatic bodies or in the melt source.

The $\delta^{18}\text{O}$ of vein amphiboles and plagioclase varies from 6.9 to 8.9‰ SMOW, being well above the mantle range. The additional observation that the orthopyroxene from the wall, reactive orthopyroxenites has “normal” mantle $\delta^{18}\text{O}$ values (5.8‰) brings us to conclude that reaction with the host, metasomatised peridotite was not apparently responsible for the heavy isotope O composition argued for parent melt of the dyke minerals: the latter must have been imparted by crustal component sitting at deeper mantle depth. This finding evidences as the Northern IVZ records an extremely prolonged release (lasted from the Variscan orogenic cycle to the Mesozoic exhumation of lithospheric mantle at shallower levels) of K-H₂O-rich mantle-derived melts polluted by subduction-related components, placing valuable insight into the comprehension of the Mesozoic magmatism and the geodynamic environment at the Europe-Africa boundary.

S9

Isotopic tracers and timing of dynamic evolution of subduction zone settings

CONVENERS AND CHAIRPERSONS

Enrico Cannaò (Università di Milano)

Martina Casalini (Università di Firenze)

Federico Farina (Università di Milano)

Early Miocene to Pleistocene Na-alkaline Volcanism on the North-East Arabian plate (South-East Turkey)

Agostini S.*¹, Di Giuseppe P.¹⁻², Manetti P.¹⁻³, Savascin M.Y.⁴, Doglioni C.⁵⁻⁶ & Conticelli S.³⁻⁷

¹ Istituto di Geoscienze e Georisorse, Consiglio Nazionale delle Ricerche, Pisa, Italy.

² Dipartimento di Scienze della Terra, Università degli Studi di Pisa, Pisa, Italy.

³ Dipartimento di Scienze della Terra, Università degli Studi di Firenze, Firenze, Italy.

⁴ Jeoloji Mühendisliği, Munzur Üniversitesi, Tunceli, Turkey.

⁵ Istituto Nazionale di Geoscienze e Vulcanologia, Roma, Italy.

⁶ Dipartimento di Scienze della Terra, Università La Sapienza di Roma, Roma, Italy.

⁷ Istituto di Geoscienze e Georisorse, Consiglio Nazionale delle Ricerche, Firenze, Italy.

Corresponding email: paolo.digiuseppe@igg.cnr.it

Keywords: triple junction, geochemistry, magmatism.

Widespread alkali basaltic activity developed during the Early Miocene to Pleistocene, around the northern termination of the Dead Sea Fault Zone, and in the North-West foreland of the Arabian plate, in south-eastern Turkey.

Volcanism developed in the Pleistocene around the Anatolia-Africa-Arabia triple junction, in Maras, along the Karataş-Osmaniye Fault, and along the termination of the Dead Sea Fault, in the Karasu Valley.

Widespread volcanic activity developed within the Gaziantep Basin during the Early-Late Miocene (21.2-7.0 Ma), and further east, abundant magmatism characterised the Karacadağ Shield Volcano since the Middle Miocene throughout the Pleistocene (12.1-0.01 Ma).

Rocks emplaced in these areas mainly consist of abundant basalts and basanites with subordinate hawaiites and basaltic andesites, mostly showing Na-alkaline affinity, whereas some of the older products rarely show calc-alkaline signature. As a whole, these rocks show LREE/HREE and HFSE/LILE ratios similar to OIB-like magmas. Chemical variations indicate that they may evolve by low pressure crystal fractionation of mineral assemblage consisting of olivine ± plagioclase ± clinopyroxene + Fe-Ti oxides. The isotopic compositions of ⁸⁷Sr/⁸⁶Sr (0.70301-0.7050), ¹⁴³Nd/¹⁴⁴Nd (0.51266-0.51304), ²⁰⁶Pb/²⁰⁴Pb (18.80-19.22), ²⁰⁷Pb/²⁰⁴Pb (15.59-15.74), ²⁰⁸Pb/²⁰⁴Pb (38.77-39.32) show wide variations, suggesting digestion of crustal material during magma ascent to surface. However, among the least crustally contaminated and relatively primitive samples (MgO > 8 wt.%), Sr-Nd-Pb isotopic variations exhibit marked correlations with major and incompatible elements that cannot be explained with simple fractional crystallisation and crustal contamination, and that require melting of a heterogeneous mantle source.

High LREE/HREE (i.e., La/Yb) and MREE/HREE (i.e., Dy/Yb) ratios are consistent with magma genesis involving a large proportion of garnet-bearing peridotite. Some enrichments in Large Ion Lithophile Elements, are detected in the less evolved samples showing calc-alkaline affinity and higher ⁸⁷Sr/⁸⁶Sr values: this indicate that, likely all magmas formed as Na-alkaline and LILE enrichment depend from assimilation of crustal material. However, some isotopic differences are also detected among most primitive samples, implying the occurrence of a heterogenous source. This is also testified by geothermobarometric estimates, which evidence striking differences in temperature and pressure of magma formations: e.g., 1390-1400°C and 16-21 Kbar for the Pleistocene Osmaniye and Karasu Volcanic Fields (South East Anatolia), and 1400-1520°C and 16-33 Kbar for the Early Miocene Gaziantep and Plio-Pleistocene activity of Karacadağ Volcanic Fields (North-West Arabian foreland).

The occurrence of intense and very long-lasting (20 Ma) alkali basaltic activity in the foreland of a convergent tectonic system, is rather uncommon; one possible interpretation is the northeast mantle flow as suggested by the undulated pattern of the relatively “westerly” moving lithosphere. The mantle previously underwent partial melting beneath the Red Sea rift. Local tensional and transtensional tectonics adjacent to the Dead Sea transform fault system may have allowed the mantle melt upraise.

Extreme HFSE fractionation in Italian magmas: metasomatism vs. different mantle domains

Bragagni A.¹, Mastroianni F.², Avanzinelli R.*², Conticelli S.² & Münker C.¹

¹ Institut für Geologie und Mineralogie, Universität zu Köln, Germany.

² Dipartimento di Scienze della Terra, Università degli Studi di Firenze, Italy.

Corresponding email: riccardo.avanzinelli@unifi.it

Keywords: circum-Thyrrhenian area, magma compositional variations, different mantle domains.

The circum-Thyrrhenian area hosts a large variety of volcanic rocks that are mostly related to the subduction of the Adriatic and Ionian plates. Eastward and then south-eastward migration of magmatism with time occurred following roll-back of the subducting plate starting from the Miocene. In Central and Southern Italy magmatism occurred first in the Tuscan region and then shifted in the Quaternary to the Roman Province (Latian), the Neapolitan area (e.g., Vesuvius) and the Aeolian arc (e.g., Stromboli). Overall, the erupted magmas show large chemical variations, from calc-alkaline to ultra-potassic, and variable degrees of silica saturation, from over- to under-saturated. In addition to subduction related magmatism, Na-alkaline, within-plate volcanic rocks are present in the Sicily Channel (e.g., Pantelleria), whilst Vulture and Etna show intermediate character. These compositional, chronological and spatial variations have been explained by different types of slab-derived components (silica-rich vs. carbonate-rich) and different mantle domains (depleted vs. fertile).

In order to further investigate and constrain the processes responsible for the observed geochemical variability we determined HFSE, W, U, Th concentrations by isotope dilution, and ¹⁷⁶Hf/¹⁷⁷Hf on rocks from Tuscan and Roman Provinces, Stromboli, Vulture, Etna, and Pantelleria.

Our results show selective enrichment in W relative to U and Th in Vesuvius magmas, suggesting enhanced W flux from subducted carbonate-rich material released as fluids or melts. Potassium-rich lavas from the Roman Province have the highest Nb/Ta among the studied subduction related rocks (>17), whilst Tuscan potassic and ultrapotassic rocks are close to normal mantle values (ca. 15). Unusually high Nb/Ta (ca. 20) and sub-canonical W/U and W/Th are observed at Vulture and Etna. Tholeiitic magmas from Etna display the most extreme Nb/Ta and W/Th ever found in within-plate rocks. Collectively, this compositional spectrum is explained by fertile mantle domains enriched in Nb/Ta and depleted in W/Th being overprinted by variable amounts of sediment-derived subduction components with lower Nb/Ta.

Into deep and beyond: carbon and nitrogen subduction recycling by secondary peridotites

Cannaò E.*¹, Scambelluri M.² & Tiepolo M.¹

¹ Dipartimento di Scienze della Terra “A. Desio”, Università degli Studi di Milan.

² Dipartimento della di Scienze della Terra, Ambiente e Vita.

Corresponding email: enrico.cannaò@unimi.it

Keywords: carbon cycle, nitrogen cycle, subduction zone.

The progressive dehydration of serpentinites at variable depths during subduction produces chlorite- and garnet-bearing secondary peridotites (i.e., metaperidotites). The uptake of elements at the ocean floor by serpentinites and successive serpentinite interaction with slab fluids during subduction have been recognized as key processes in recycling incompatible elements (e.g., B, As, Sb, Pb, Sr) and volatiles in the Earth's mantle. Here we focus on the carbon (C) and nitrogen (N) content and on the C isotope composition of chlorite harzburgites and garnet peridotites from the Cima di Gagnone mélange (CdG - C. Alps) in order to further evaluate the role of serpentinite dehydration in the global volatiles cycle. Previous studies have documented these ultramafic rocks represent the high-pressure breakdown products of antigorite and chlorite-bearing ultramafic rocks (forming tectonic lenses in a metasedimentary mélange) along the slab-mantle interface. The chlorite- and garnet-bearing metaperidotites contain similar C concentrations ($[C] = 304 - 659$ ppm and $201 - 712$ ppm, respectively), with the exception of one magnesite-bearing chlorite harzburgites showing up to 11000 ppm of C. The garnet metaperidotites display higher N contents ($[N] = 54 \pm 15$ ppm) than chlorite harzburgites ($[N] = 29 \pm 6$ ppm). The $\delta^{13}C$ composition of the Gagnone metaperidotites ranges between -12.2 and -17.8% , with the exception of the magnesite-bearing chlorite harzburgites showing -7.2% . Our results on $[C]$ are comparable with those of serpentinites from present-day and fossil oceanic environments, as well as with high pressure serpentinites. These $[C]$ compositions suggest that the antigorite and chlorite dehydration episodes were not accompanied by significant C loss from rocks into the fluid phase. The $\delta^{13}C$ signatures seem to reflect mixing between seawater-derived carbonate and a reduced carbon source although exchange with the host metasediments (showing $[C] = 301$ ppm; $[N] = 33$ ppm; $\delta^{13}C = -24.4\%$) cannot be excluded. The $[N]$ contents of the CdG metaperidotites are higher than those of oceanic and of subducted serpentinites, and are similar to those of antigorite-serpentinites from wedge derivation. This enrichment is compatible with an exchange with fluids originated from the surrounding metasedimentary rocks during subduction. Our results suggest that significant amount of surficial C and N are recycled into the deep mantle via secondary peridotites. Finally, we speculate that the deep subduction of Gagnone-like metaperidotites characterized by depleted C isotopic composition and high boron (B) content may represent a good candidate able to contribute to the blue B-bearing diamond genesis in the Earth's lower mantle (Smith et al., 2018).

Smith E.M., Shirey S.B., Richardson S.H., Nestola F., Bullock E.S., Wang J. & Wang W. (2018) - Blue boron-bearing diamonds from Earth's lower mantle. *Nature*, 560, 84–87.

Amphibole as carbon fixing mineral at lower crust depth

Cannaò E.*¹, Tiepolo M.¹, Sessa G.¹, Deloule E.² & Poli S.¹

¹ Dipartimento di Scienze della Terra “A. Desio”, Università degli Studi di Milano.

² Centre National de la Recherche Scientifique, CRPG, Nancy.

Corresponding email: enrico.cannaò@unimi.it

Keywords: carbon cycle, amphibole, lower crust.

Carbon (C) cycle and C fluxes on Earth are controlled by shallow and deep processes connected by chemical reactions in both divergent and convergent margins. Recent estimates of C fluxes suggest that although most of the subducted C mostly comes recycled, a significant amount of C is still stored in the lithospheric mantle and crust lying above the subducting plates (Kelemen & Manning, 2015). Current knowledge on C solubility in volatile-free major mantle minerals indicates that less than 1 ppm of C may be stored at 1.5 GPa (Shcheka et al., 2006). Notwithstanding, specific studies have been never carried out on amphibole that is one of the most important repository minerals in the lower crust – upper mantle system for volatile components (F, Cl and H₂O). The crystal structure of amphibole is more versatile with respect to other common mantle minerals and may potentially accommodate the incorporation of C or its compounds.

Here, we have selected kaersutitic amphibole megacrysts from the Hoover Dam camptonite dike (USA, Basu, 1978) in order to determine the potential of amphibole in fixing C in its structure. Petrographic investigation of selected grains free from alteration reveal the presence of pseudo primary fluid inclusions as a potential source of C. In order to avoid the contribution of such fluid inclusions, C was measured in situ by SIMS technique.

Results reveal that analyzed amphibole contains more than one order of magnitude of C than other common mantle minerals ranging between 15 and 20 ppm.

Current data, although preliminary, suggest that kaersutitic amphibole represent a good candidate for fixing carbon in the upper mantle/lower crust.

Basu A.R. (1978) - Trace elements and Sr-isotopes in some mantle-derived hydrous minerals and their significance.

Geochim. Cosmochim. Acta, 42, 659–668.

Kelemen P.B. & Manning C.E. (2015) - Reevaluating carbon fluxes in subduction zones, what goes down, mostly comes up. Proc. Natl. Acad. Sci., 112, E3997–E4006.

Shcheka S.S., Wiedenbeck M., Frost D.J. & Keppler H. (2006) - Carbon solubility in mantle minerals. Earth Planet. Sci. Lett., 245, 730–742.

Genesis and differentiation of a calc-alkaline volcano in syn-collisional continental setting: the Mount Ararat (Ağrı Dağı, Eastern Anatolia)

Casalini M.*¹, Avanzinelli R.¹, Tommasini S.¹, Garzonio C.A.¹, Cioni R.¹ & Conticelli S.¹

¹ Dipartimento di Scienze della Terra, Università di Firenze, Italy.

Corresponding email: martina.casalini@unifi.it

Keywords: syn-collisional magmatism, Mount Ararat, geochemical characterization, isotopic characterization.

Mount Ararat (Ağrı Dağı) is the largest volcanic center of the Eastern Anatolia block resulting from the syn-collisional magmatism related to the Arabia–Eurasia collision zone. Ararat is a polygenetic, compound, stratovolcano, with two well-developed cones: Greater Ararat and Lesser Ararat.

In this study we present a complete geochemical and isotopic (Sr, Nd, and Pb) characterisation on a set of samples collected from Greater Ararat, revealing clues on magma genesis and differentiation.

During field work was possible to recognise a complex volcanic structure, made up by a basal basaltic plateau and at least two volcanic edifices (Old and Young Ararat) superimposed on top of each other. The lavas range from trachybasalts to basaltic andesites in the basaltic plateau and from high-Mg# andesite to rhyolite in Old and Young Ararat. The rocks have calc-alkaline affinity and subduction-related trace element patterns, with less marked HFSE negative anomalies in the plateau basalts. The data suggest a mantle modified by fluids or melts derived from the recycling of subducted basaltic oceanic crust in amphibolite facies, as suggested by the low Nb/Ta of the least evolved products.

The high-Mg# of the andesites can be interpreted as representative of the direct derivation of these magmas from a modified mantle source, or in alternative as due to significant fractionation of Fe-Ti oxides during the early stage of differentiation from parental basaltic magmas.

Major and trace element data define two distinct differentiation trends, characterised by different contents in alkalis and key trace elements such as Y, Nb, Zr and REE, which are likely related to the fractionation of specific phases (e.g., amphibole). These two trends seem to be not strictly related to the different phases of the volcano activity.

Basalts from the underlying plateau show less radiogenic Sr and more radiogenic Nd isotope compositions than the high-Mg# andesite and the more evolved products. The latter show variable isotope composition and no systematic variation between the Old and Young Ararat or with indices of magma differentiation.

Early Miocene to Pliocene magmatic activity in the Sivas-Malatya Volcanic Region (Central-Eastern Anatolia)

Di Giuseppe P.*¹⁻², Agostini S.¹, Manetti P.¹⁻³, Savascin M.Y.⁴ & Conticelli S.³⁻⁵

¹ Istituto di Geoscienze e Georisorse, Consiglio Nazionale delle Ricerche, Pisa, Italy.

² Dipartimento di Scienze della Terra, Università degli Studi di Pisa, Italy.

³ Dipartimento di Scienze della Terra, Università degli Studi di Firenze, Italy.

⁴ Jeoloji Mühendisliği, Munzur Üniversitesi, Tunceli, Turkey.

⁵ Istituto di Geoscienze e Georisorse, Consiglio Nazionale delle Ricerche, Firenze, Italy.

Corresponding email: paolo.digiuseppe@igg.cnr.it

Keywords: Central-Eastern Anatolia, geochemistry, subduction.

Arc-like magmas worldwide have trace elements and isotopic fingerprints that are usually interpreted as reflecting fluid and/or sediment involvement in their genesis. These magmas are generally characterised by high LILE/HFSE and LREE/HFSE ratios, high $^{87}\text{Sr}/^{86}\text{Sr}$, low $^{143}\text{Nd}/^{144}\text{Nd}$, and relatively high $^{207}\text{Pb}/^{204}\text{Pb}$ and $^{208}\text{Pb}/^{204}\text{Pb}$. In addition, magmas which exhibit “subduction” signature can also be generated in post-collisional setting, in which tectonic episodes such as transcurrent shear zone formation, lithosphere delamination, and back-arc extension can facilitate magmas ascent from source modified by previous subduction events.

The convergence and collision of the Eurasian, African, and Arabian plates, from Early Miocene to Recent, evolved from Ocean-Continent subduction to Continent-Continent collision and post-collisional strike slip dynamics. These phases are accompanied by different magmatic episodes, which is characterised by a wide geochemical-isotopic spectrum.

In the Central Eastern Anatolia region, widespread and abundant volcanism developed from the Early Miocene to the Pliocene in the Sivas-Malatya Volcanic Region (18.7-4.0 Ma). Arc-related calc-alkaline volcanic rocks are found in the Yamadağ and Kepez Dağ volcanic complexes, showing the typical geochemical and isotopic signature of subduction-related magmas consisting of high LILE/HFSE ratio, strong Nb-Ta negative anomalies, high $^{87}\text{Sr}/^{86}\text{Sr}_i$ (0.70400-0.70547) and low $^{143}\text{Nd}/^{144}\text{Nd}_i$ (0.51261-0.51288).

In the same time, Na-alkaline basaltic activity emplaced during the Early-Middle Miocene (16.5-13.1 Ma) in the Sivas Volcanic Field, along the Kizilirmak strike-slip fault. These rocks are characterised by LILE enrichment relative to HFSE, high $^{87}\text{Sr}/^{86}\text{Sr}_i$ (0.70416-0.70554) and low $^{143}\text{Nd}/^{144}\text{Nd}_i$ (0.51262-0.51284), which indicated the persistence of a relict subduction-related geochemical signature.

During the Late Miocene (10 Ma), Na-alkaline magmatism developed along the Malatya-Ovacik fault and scattered lava flows emplaced in the Arapgir, Ortulu Pass and Arguvan areas. These rocks show the typical trace element abundances of intra-plate volcanic rocks. The low $^{87}\text{Sr}/^{86}\text{Sr}_i$ (0.70348-0.70385) and high $^{143}\text{Nd}/^{144}\text{Nd}_i$ (0.51278-0.51292) isotopic ratios suggest a contribution from a sub-lithospheric mantle. However, trace element compositions and enrichment in fluid-mobile elements display that also the Arguvan-Arapgir mantle source was affected by a previous subduction event.

During the Pliocene (5.9-4.0 Ma), scattered basaltic lava flows emplaced within the Kangal basin. These rocks are K-alkaline, and they are characterised by high LILE/HFSE ratios, and Nb, Ta, and Ti troughs in Primordial Mantle-normalised trace element plots. Higher $^{87}\text{Sr}/^{86}\text{Sr}_i$ (0.70425-0.70522) and lower $^{143}\text{Nd}/^{144}\text{Nd}_i$ (0.51263-0.51277) ratios with respect to Arguvan basalts suggest the involvement of a crustal component, which derive from Assimilation+Fractional Crystallisation processes during magma uprise.

Isotopic fractionations between dehydration fluid and descending slab

Elliott T.*¹, Freymuth H.^{1,2}, Andersen M.^{1,3}, Chen S.^{1,4} & Hin R.¹

¹ Bristol Isotope Group, School of Earth Sciences, University of Bristol, UK.

² Department of Earth Sciences, University of Cambridge, UK.

³ School of Earth and Ocean Sciences, University of Cardiff, UK.

⁴ Institute of Oceanology, Qingdao, China.

Corresponding email: tim.elliott@bristol.ac.uk

Keywords: subduction zone processes, isotopic measurements, dehydration fluid.

The increasing range of high precision isotopic measurements made possible by multi-collector, inductively coupled plasma mass-spectrometry has provided some interesting new perspectives of subduction zone processes. The ‘fluid’ component from the subducting slab has been characterised by strong elemental fractionations that have increasingly been linked to partitioning behaviour of residual solid phases in the down-going crust (e.g., Hermann, 2002). Isotopic measurements provide a valuable novel perspective to help interrogate the processes by which such a distinctive fluid forms. In particular, Mo isotopic compositions of fluid-dominated arc lavas are anomalously heavy compared to ambient (Freymuth et al., 2015; König et al., 2016) whilst U isotopic compositions are anomalously light (Andersen et al., 2015). The former can be explained by the significant isotopic fractionation of Mo between a fluid and residual rutile, which is supported from qualitative arguments and initial experiments. This argues for significant interaction of a large, oxidised fluid flux (Bali et al., 2012) with the subducted oceanic crust, consistent with the origin of the fluid from dehydration from underlying slab serpentine. Clearly identifying the phase that causes U isotopic fractionation is an important goal, that will help shed new light on the causes of notable U-series disequilibrium (e.g., Avanzinelli et al., 2018), but might be tentatively ascribed to zoisite.

Andersen M.B., Elliott T., H. Freymuth, Sims K.W.W., Niu Y. & Kelley K.K. (2015) - The terrestrial U isotope cycle. *Nature*, 517, 356-359.

Avanzinelli R., Casalini M, Elliott T. & Conticelli S. (2018) - Carbon fluxes from subducted carbonates revealed by uranium excess at Mount Vesuvius, Italy. *Geology*, 46, 259-262.

Bali E., Keppler H. & Audetat A. (2012) - The mobility of W and Mo in subduction zone fluids and the Mo-W-Th-U systematics of island arc magmas. *Earth Planet. Sci. Lett.*, 351-352, 195-207.

Freymuth H., Vils F., Willbold M., Taylor R.N. & Elliott T. (2015) - Molybdenum mobility and isotopic fractionation during subduction at the Mariana arc. *Earth Planet. Sci. Lett.*, 432, 176-186.

Hermann J. (2002) - Allantite: thorium and light rare earth element carrier in subducted crust. *Chem. Geol.*, 192, 289-306.

König S., Wille M., Voegelin A.R. & Schoenberg R. (2016) - Molybdenum isotope systematics in subduction zones. *Earth Planet. Sci. Lett.*, 447, 95-102.

Fingerprinting and relocating tectonic slices along the plate interface: evidence from the Lago Superiore Unit at Monviso (Western Alps)

Gilio M.^{*1-2}, Scambelluri M.¹, Agostini S.³, Godard M.⁴, Pettke T.⁵, Agard P.⁶, Locatelli M.⁶ & Angiboust S.⁷

¹ Dipartimento di Scienze della Terra Ambiente e Vita, Università di Genova, Italy.

² Dipartimento di Scienze della Terra e dell'Ambiente, Università di Pavia, Italy.

³ CNR - Istituto di Geoscienze e Georisorse, Pisa, Italy.

⁴ Géosciences Montpellier, CNRS, Université de Montpellier, Montpellier, France.

⁵ Institute of Geological Sciences, University of Bern, Switzerland.

⁶ Institut des Sciences de la Terre de Paris (ISTeP), Sorbonne Université, France.

⁷ Institut de Physique du Globe de Paris, France.

Corresponding email: mattia.gilio@unipv.it

Keywords: Monviso Unit, serpentinite geochemistry, subduction zone.

The Lago Superiore Unit (LSU) of the Monviso Massif is a section of fossil oceanic lithosphere equilibrated at eclogite facies conditions (550 °C–2.8 GPa; Angiboust et al., 2012) during the Alpine subduction (45–40 Ma; Rubatto & Hermann, 2003). It is cut by two major serpentinite shear zones, the Intermediate Shear Zone (ISZ) and the Lower Shear Zone (LSZ). The lowermost, serpentine-rich, section of the LSU, the Basal Serpentinite, is in contact with the underlying Dora-Maira Unit (Angiboust et al., 2014; Locatelli et al., 2018).

The LSZ is a strongly foliated, olivine-free, antigorite serpentinite embedding magnesite nodules and eclogite metagabbro blocks of various typology and dimension. It shows a homogeneous geochemical and isotopic composition with enrichments in sediment-derived fluid-mobile elements such as As, Sb, Ba, and Cs. The Sr-isotopic signature (0.7072–0.7093) is more enriched in radiogenic Sr than Jurassic seawater ($^{87}\text{Sr}/^{86}\text{Sr} \sim 0.7070$).

The Basal Serpentinite is olivine + antigorite-bearing and hosts widespread olivine + Ti-clinohumite + magnetite veins that either cut massive serpentinite domains, or run parallel to sub-parallel to the olivine + antigorite foliation. The Basal Serpentinite shows a variable and texture-related trace element and isotopic composition. Massive serpentinites are enriched in W and B; their Sr and Pb compositions points to interaction with Jurassic seawater. Conversely, foliated serpentinites and metamorphic veins are enriched in radiogenic Sr and Pb isotopes and in sediment-derived fluid-mobile elements (As, Sb, U, Ba, Cs).

Our study suggests that most retrograde deformation and mineral re-equilibration were localized in the LSZ. In this domain serpentinite has a significant retrograde overprint and the remnants of the eclogite-facies stage are mostly preserved within magnesite nodules and eclogite blocks. Differently, the underlying Basal Serpentinite largely preserves the records of its prograde evolution, from ocean-floor to HP metamorphic conditions. The LSU is thus a prime example of a piece of oceanic lithosphere subducted to 70–80 km depths and its deformation-controlled, fluid-mediated, geochemical evolution during different evolutionary stages of a slice of oceanic lithosphere accreted to the subduction interface.

Angiboust S., Langdon R., Agard P., Waters D. & Chopin C. (2012) - Eclogitization of the Monviso ophiolite (W. Alps) and implications on subduction dynamics. *Journal of Metamorphic Geology*, 30(1), 37–61.

Angiboust S., Pettke T., De Hoog J.C., Caron B. & Oncken O. (2014) - Channelized fluid flow and eclogite-facies metasomatism along the subduction shear zone. *Journal of Petrology*, 55(5), 883–916.

Locatelli M., Verlaquet A., Agard P., Federico L. & Angiboust S. (2018) - Intermediate depth brecciation along the subduction plate interface (Monviso eclogite, W. Alps). *Lithos*, 320, 378–402.

Rubatto D. & Hermann J. (2003) - Zircon formation during fluid circulation in eclogites (Monviso, Western Alps): implications for Zr and Hf budget in subduction zones. *Geochimica et Cosmochimica Acta*, 67(12), 2173–2187.

Redox processes and the role of carbon-bearing volatiles at subduction zones: natural versus experimental perspectives

Malaspina N.*¹ & Tumiatì S.²

¹ Dipartimento di Scienze dell'Ambiente e della Terra (Università degli Studi di Milano-Bicocca).

² Dipartimento di Scienze della Terra (Università degli Studi di Milano).

Corresponding email: nadia.malaspina@unimib.it

Keywords: oxygen fugacity, carbon speciation, subduction zones.

The valence of carbon is governed by the oxidation state of the host system. The subducted oceanic lithosphere contains considerable amounts of iron so that $\text{Fe}^{3+}/\text{Fe}^{2+}$ equilibria in mineral assemblages are able to buffer the (intensive) $f\text{O}_2$ and the valence of carbon. Alternatively, carbon itself can be a carrier of (extensive) 'excess oxygen' when transferred from the slab to the mantle, prompting the oxidation of the sub-arc mantle. As a consequence, at high fluid/rock ratios, such as in subduction mélanges, oxygen is probably transported along fractures and veins and can be considered as perfectly mobile component. Alternatively, at low fluid/rock ratios mass transfer is supported by a gradient in $n\text{O}_2$ and a metasomatic oxidation front probably develops from the oxidised slab to the overlying mantle. Therefore, the correct use of intensive and extensive variables to define the slab-to-mantle oxidation by C-bearing fluids is of primary importance when considering different fluid/rock ratios. The interaction of mantle rocks with carbon-bearing fluids is evidenced by metasomatic assemblages containing carbonates and by carbon-bearing fluid inclusions in mantle minerals. We will present case studies of slices of metasomatised suprasubduction mantle dragged by the continental crust during subduction and/or exhumation from Ulten Zone (Italian Alps), Sulu (China) and Bardane-Ugelvik (Norway), which experienced metasomatism by $\pm\text{C}$ - and alkali-bearing subduction fluid phases up to 200km depth. To relate the oxidation state of metasomatised suprasubduction mantle and the role of COH and alkali components of the crust-derived metasomatic agents, we will report the Fe^{3+} measurements of garnets and the calculated $f\text{fO}_2$ of the metasomatised peridotites. An apparent correlation between the composition of the metasomatic agent (C- and alkali-bearing) and the fluid-induced oxidation of the peridotite mineral assemblage probably exists. Where metasomatism was induced by C-free metasomatic fluids, peridotites do not provide evidence of oxidation and garnets have $\text{Fe}^{3+}/\Sigma\text{Fe} \cong 0$. The composition of COH fluids in equilibrium with elemental carbon (i.e. graphite, diamond) is, on the other hand, dependent on the redox state of the system and on the P–T conditions and can be predicted by conventional thermodynamic models. At redox states fixed by the FMQ buffer, the composition of C-bearing fluids following conventional thermodynamic models is predicted to be a $\text{H}_2\text{O} + \text{CH}_4$ mixture at low T and low P, nearly pure water at low T and high P, and $\text{H}_2\text{O} + \text{CO}_2$ at high-T conditions. The occurrence of carbon species in different oxidation states may not be directly related to a drastic change in $f\text{O}_2$ (i.e. CH_4 reduced conditions– CO_2 oxidized conditions), but all the variables P, T and $f\text{O}_2$ must be considered simultaneously. Graphite/diamond-saturated COH fluids can be indeed methane-bearing at FMQ conditions ('oxidized' condition in the mantle) at UHP and relatively low temperature.

Long-lived petrological cannibalism and slow cooling rates for the Galiléia batholith (SE Brazil): supporting the “hot” nature of Araçuaí-West Congo orogen

Narduzzi F.¹, Farina F.*², Lana C.³, Teixeira L.³, Schannor M.⁴, Stevens G.⁵, Alkmim A.³ & Nalini Jr H.A.³

¹ Universidade de São Paulo (Brazil).

² Università degli Studi di Milano (Italy).

³ Universidade Federal de Ouro Preto (Brazil).

⁴ University of Cambridge (UK).

⁵ University of Stellenbosch (South Africa).

Corresponding email: federico.farina@unimi.it

Keywords: U-Pb geochronology, granitoids, collision.

The Neoproterozoic Araçuaí orogen was formed by the convergence between the Congo (Africa) and São Francisco (Brazil) cratons during the assembly of West Gondwana. The crystalline core of the orogen includes large volumes of magmatic and anatectic rocks crystallized between 630 and 480 Ma. Its central part is mostly represented by weakly deformed, mid-crustal, medium- to high-K calc-alkaline metaluminous tonalites and granodiorites. These rocks form the Galiléia batholith (15.000 km²) and intrude metasedimentary rocks and Paleoproterozoic gneisses. According to the most widely accepted interpretation, these granitoids are emplaced in three magmatic pulses (632 – 605 Ma, 600 – 590 Ma, 585 – 570 Ma) and represent the plutonic roots of a long-lived pre-collisional magmatic arc. To shed light on the origin of the Galiléia batholith we have dated through the U-Pb method zircon, titanite and apatite crystals from nine samples. For each sample, the age variability of magmatic zircon reach up to 50 Ma, spanning the entire lifetime of the batholith (ca. 630 – 580 Ma). However, high-precision CA-ID-TIMS U-Pb dates on eleven zircon grains gave a well-defined weighted mean age at 581 ± 0.4 Ma, which we interpret as the age of emplacement of the granitoids. Zircon ages older than 590 Ma are mostly determined on zircon centres showing magmatic textures and representing grains repeatedly recycled from older magma batches. All magmatic zircon crystals have initial ϵ_{Hf} values spanning from -6.0 to -14.6. We suggest that the oldest zircon grains crystallized from magmatic pulses derived from Paleoproterozoic mafic sources while younger grains formed from magmas produced by the re-melting of former granitic batches. We envision a process in which each new pulse of magma is capable of re-melting previous magma batches until final cooling and crystallization at ca. 581 Ma. This supports the idea that the crystalline core of the Araçuaí orogen is a deep section through a hot orogeny with the 630-580 Ma magmatic phase formed during continental collision. Titanites, having closure temperature at ca. $650 \pm 50^\circ\text{C}$ gave a consistent weighted mean age of 576 ± 2 Ma suggesting that the Galiléia batholith took 5 Ma to cross the solidus. Apatites from rocks cropping out in the centre of the batholith gave an age of 532 ± 17 Ma indicating further ca. 40 Ma to cool down to ca. 550°C ; while granitoids sampled on the easternmost part of the batholith, close to the anatectic domain, yield and age at 510 ± 26 Ma. This age was most likely reset due to the second partial melting event, which occurred in the anatectic domain between 535 - 515 Ma. Overall, these data indicate a slow cooling history (ca. $4^\circ\text{C}/\text{Ma}$) for the Galiléia batholith consistent with models indicating that the Araçuaí orogen is a hot orogeny which experienced limited pre-collisional subduction.

Eocene subduction to collision-related volcanism in the Arasbaran area (NW, Iran): evidence for progressive evolution of mantle sources

Natali C.¹, Aghazadeh M.², Braschi E.³, Badrzadeh Z.², Bianchini G.⁴ & Conticelli S.^{*3}

¹ CNR-IGG, Via G. La Pira, 4, Firenze, Italy.

² Department of Geology, Payame Noor University, Iran.

³ Dipartimento di Scienze della Terra, Università degli studi di Firenze, Italy.

⁴ Dipartimento di Fisica e Scienze della Terra, Università degli studi di Ferrara, Italy.

Corresponding email: sandro.conticelli@unifi.it

Keywords: Arasbaran region, mantle sources evolution, subduction to collision related magmatism.

The Arasbaran region belongs to the hinterland of the Arabia–Eurasia collision zone within the broad Alpine–Himalayan orogenic belt, and it is characterized by an intense Upper Cretaceous–Cenozoic subduction to collision related magmatism. The magmatic activity records two main volcanic episodes describing a progression from deep to shallow marine and subaerial volcanic activity: i) an old Eocene sequence consisting of lava flows and lava-pillows and ii) a recent Upper Miocene–Quaternary phase consisting of lava flows and pyroclastic eruptions.

We focus on the products of the older phase of activity sampled from two main volcanic successions occurring in three distinct areas in the Arasbaran region. They are characterized by mildly alkaline and shoshonitic affinities and by a wide compositional variation from shoshonite to tephrite and phonolite lavas. In detail, major and trace elements allow identifying different mantle sources of magmatic events along with the two successions, characterizing mafic and more evolved lavas, in agreement with their relative stratigraphic position and petrographic features.

Moreover, Pb-isotope ratios show distinct values for the two groups depicting a single trend within the non-HMU type OIBs field. This suggests an evolution with time of the mantle sources with a progressive involvement of components characterised by more radiogenic values.

The importance of direct gas flux measurements at active volcanoes for understanding the geochemical cycles in the subduction zones

Tamburello G.*¹

¹ Istituto Nazionale di Geofisica e Vulcanologia.

Corresponding email: giancarlo.tamburello@ingv.it

Keywords: Volcanic degassing, subduction, geochemical cycles.

Subduction processes not only return oceanic lithosphere into the convecting mantle but represent also zones where elements are transferred from the down-going plate back to the surface through volcanic emissions. Direct gas flux measurements at such active volcanoes are extremely important to understand regional and arc-scale volcanic emissions and the cycling of chemical components through subduction zones. Sulfur dioxide is of most interest due to the relative simplicity of the SO₂ measurement using UV spectroscopy via ground- and satellite-based remote sensing. The derivation of volcanic fluxes for other gas species (e.g. CO₂, halogens) is obtained by scaling the bulk volcano's SO₂ flux by the gas composition obtained in-situ. Here we provide a synoptic overview of such measurements performed all around the world over the past decades, focusing upon the work done at different arc segments. Despite the recent progress in this field, clearly there is still much to be gained by studying current volcanic emissions and that more gas flux measurements are needed to better constrain the role that volcanoes play in the geochemical cycles.

Dissolution of graphite in high-pressure aqueous fluids: the roles of crystallinity and of coexisting silicates and carbonates

Tumiati S.*¹

¹ Dipartimento di Scienze della Terra, Università degli Studi di Milano.

Corresponding email: simone.tumiati@unimi.it

Keywords: COH fluids, CO₂, carbon.

Organic matter, showing variable degrees of crystallinity and thus of graphitization, is an important source of carbon in subducted sediments, as demonstrated by isotopic signature of deep and ultra-deep diamonds and volcanic emissions in arc settings. Estimates of dissolved CO₂ in subduction-zone fluids are based mainly on thermodynamic models, relying on a very sparse experimental data base. We present experimental data on the interaction of aqueous fluids with graphitic carbon in relatively complex systems diverging from the ideal C-O-H model. The redox state of the experiments was always constrained, using double capsules and either fayalite-magnetite-quartz (FMQ) or nickel-nickel oxide (NNO) buffers. Experiments have been performed at pressures up to 3 GPa and temperatures up to 800°C to retrieve the dissolution susceptibility of elemental carbon in aqueous fluids: 1) in the COH system, using amorphous carbon instead of crystalline carbon; 2) in silicate-bearing systems, investigating the systems SiO₂-COH (graphite + quartz/coesite) and MgO-SiO₂-COH (graphite + forsterite and enstatite); 3) in carbonate-bearing systems, investigating the CaCO₃-COH (graphite + aragonite) and the CaCO₃+SiO₂-COH (graphite + aragonite + coesite) systems. At 1 GPa and 800°C, carbon dioxide produced by oxidation of amorphous carbon shows higher fluid concentrations (+16–19 mol%) compared to crystalline graphite, meaning that amorphous carbon is more prone to oxidation. In contrast, fluids interacting with amorphous carbon at the higher pressure of 3 GPa show only a limited increase in CO₂ ($f_{H_2}^{NNO}$) or even a lower CO₂ content ($f_{H_2}^{FMQ}$) with respect to fluids interacting with crystalline graphite. At the same P–T conditions, the CO₂ content of fluids interacting crystalline graphite and silicates exceeds the amounts measured in the pure COH system by up to 30 mol%, as a consequence of a decrease in water activity probably associated with the formation of organic complexes containing Si–O–C and Si–O–Mg bonds. On the other side, the dissolution susceptibility of graphite seems to be unaffected by the presence of calcite at 3 GPa, 700°C. The contemporaneous presence of calcite and quartz, however, induces an increase of the dissolved graphite, confirming the important role of silica in enhancing the solubility of graphite (Tumiati et al., 2017). The interaction of deep aqueous fluids with silicates and with “disordered” graphite are novel mechanisms for controlling the composition of subduction COH fluids, promoting the deep CO₂ transfer from the slab–mantle interface to the overlying mantle wedge.

Tumiati S., Tiraboschi C., Sverjensky D. A., Pettke T., Recchia S., Ulmer P., Miozzi F. & Poli S. (2017) - Silicate dissolution boosts the CO₂ concentrations in subduction fluids. *Nat. Commun.*, 8, 616.

Decoupling between the carbon isotopic signature of CO₂-bearing aqueous fluids and of their graphite+carbonate source at subarc depth

Tumiati S.*¹

¹ Dipartimento di Scienze della Terra, Università degli Studi di Milano.

Corresponding email: simone.tumiati@unimi.it

Keywords: experimental petrology, mass spectrometry, high pressure.

Subduction zones play a direct role in returning surface carbon to the mantle. Subducted limestones and carbonate-bearing sediments can be very rich in organic matter, for instance those formed during anoxic events or located in near-shore environments with highly productive overlying waters. Once they are subducted, portions of their organic carbon content can be transported down to upper mantle depths, as suggested by the ¹²C-enriched isotopic signature of diamonds from the upper mantle, the transition zone and the lower mantle. On the other side, some organic carbon (graphite) is removed from the down-going slab, transported to the overlying mantle wedge, and eventually released back as ¹²C-enriched CO₂ in the atmosphere by arc magmatism.

In this experimental study, we studied the kinetics of the carbon isotopic exchange among graphite, calcium carbonate (aragonite) and CO₂-bearing aqueous fluids at subarc conditions (P = 3 GPa, T = 700°C), with and without the presence of SiO₂ (coesite). The redox state of the experiments was constrained using double capsules and the fayalite-magnetite-quartz (FMQ) buffer. In the investigated model system, we chose as starting materials: 1) crystalline graphite ~ 99% ¹²C; 2) CaCO₃ ~ 99% ¹³C; 3) ultrapure water; 4) quartz powder. The isotope ratios and the quantitative analysis of the volatile phase in runs quenched to room pressure and temperature has been accomplished by quadrupole mass spectrometry. The isotope ratios of solids (graphite, aragonite) has been performed by means of laser-ablation ICP-MS and secondary ion mass spectrometry (SIMS).

Results show that, while the initial isotopic ratio of graphite remains unchanged in quenched products, the isotopic ratio of aragonite becomes lighter, gaining ~ 20% of ¹²C even after only a few hours, and it is almost independent on run duration. This isotopic lightening of aragonite is enhanced when SiO₂ (coesite) is present in the system, where aragonite contains 40–50% ¹²C. The isotopic ratio of the fluid phase is always comparable to that of aragonite. Results suggest that ¹³C aragonite reacts at high-pressure/temperature conditions with CO_{2(aq)} produced mainly by oxidation of graphite, which is enhanced by the presence of silica. CO₂ evolves rapidly towards ¹³C-rich ratios, due to the isotopic exchange with the dissolution products of aragonite (mainly CaHCO₃⁺ at the investigated P–T–pH conditions). Aragonite continuously undergoes dissolution/precipitation, the higher the amount of dissolved graphite, the higher the ¹²C/¹³C final ratio.

The isotopic signature of volatiles released at subarc conditions is therefore controlled by carbonates, even if the major process underlying the CO₂ formation is the oxidation of graphite. Our results challenge the conventional assumption that the isotopic signature of a devolatilising carbon source and the isotopic signature of the corresponding COH fluid are coupled in a straightforward manner.

S10

Metasomatic and refertilization processes in lithospheric mantle: unraveling the heterogeneities in mantle sources and related geodynamic systems

CONVENERS AND CHAIRPERSONS

Barbara Faccini (Università di Ferrara)

Tommaso Giovanardi (Università di Modena e Reggio Emilia)

Cristina Perinelli (Università di Roma)

Mineralogical and petrogenetic characteristics of the peridotites and associated podiform chromitites from Abgarm ultramafic complex (south-eastern Iran)

Alipour R.*¹, Perinelli C.², Moeinzadeh H.¹, Ahmadipour H.¹, Bosi F.² & Gaeta M.²

¹ Department of Geology, Shahid Bahonar university of Kerman, Islamic Republic of Iran

² Dipartimento di Scienze della Terra, Sapienza Università di Roma (Italy)

Corresponding email: alipour_raziyeh@yahoo.com

Keywords: Abgarm Ophiolites, SE-Iran, peridotites and chromitites.

Abgarm ultramafic complex is a part of the Esfandagheh-Hajiabad coloured melange belt and located in the south east of Iranian segment of Alpine-Himalayan orogenic belt. In the north and north-west sides, the complex has faulted contacts with flysch type sediments of upper cretaceous ophiolite melange complex. The Abgarm ultramafic complex is mainly composed of incipient to widespread serpentinitized peridotites with dominance of the harzburgite but dunites and lherzolites also occur in lesser extents. Some dunites contain massive chromitite pods or bands. The peridotite samples selected for the present study show protogranular to porphyroclastic textures with the high temperature-pressure deformational evidences such as primary minerals orientation, kink band in olivines and undulose extinction in orthopyroxenes. Besides, they have different generations of olivines and orthopyroxenes and show some features suggesting their re-equilibration processes in the crust.

The coarse-grained porphyroclasts of orthopyroxenes are enstatite in composition ($Wo_{1-3}En_{88-91}Fs_{8-10}$) with the Mg# and Cr# values in the range 91-94 and 4-15, respectively. Smaller olivine grains have Fo contents varying from 88.9 to 93.5 with the highest values belonging to dunites. NiO contents range from 0.27 to 0.50 wt% and their CaO are 0-0.08 wt%. Secondary, interstitial and undeformed olivines (Fo_{86}) have also been observed in harzburgites. Clinopyroxenes are diopside type ($Wo_{49-51}En_{45-48}Fs_{3-4}$) with Mg# = 88-90 and have relatively low Al_2O_3 (1.97-4.80 wt%), TiO_2 (0.07-0.39 wt%) and Na_2O (0.2-0.5 wt%) contents. Reddish to dark brown anhedral spinels in peridotites show the Cr# and Mg# values vary between 12 to 44 and 59 to 79, respectively. The TiO_2 and Al_2O_3 contents are from 0.05 to 0.15 wt% and from 21.46 to 55.14. With respect to the peridotitic spinels, the black euhedral ones from massive chromitite pods and bands show higher Cr# values (73-76) and lower Mg# values (50- 65).

The mineral compositional variations of the Abgarm peridotites and tectonic discrimination diagrams indicate that they belong to the fore-arc peridotites. This, along with geothermometric (816–992°C and 708–840°C based on pyroxene porphyroclasts and olivine-spinel assemblages, respectively) and fO_2 estimates (from -0.2 to +1 log-bar units with respect to fayalite–magnetite–quartz buffer) suggest a multi-stage history of melting, deformation and sub-solidus re-equilibration within the spinel stability field (1.2-2 GPa) for Abgarm peridotites. Finally, as pointing out from Cr-spinel compositions of Abgarm massive chromitites, they formed as the first crystallizing phase by fractional crystallization of a mafic melt with boninitic affinity.

Evaluating the controls on the origin of tourmaline-bearing rocks in peraluminous and metaluminous systems: examples from Late-Variscan magmatism of Sardinia (Italy)

Andreozzi G.B.*¹, Bosi F.¹, Conte A.M.², Cuccuru S.³ & Naitza S.⁴

¹ Dipartimento Scienze della Terra, Sapienza Università di Roma.

² CNR-Istituto di Geologia Ambientale e Geoingegneria, Sede Secondaria di Roma, Sapienza Università di Roma.

³ Dipartimento Chimica e Farmacia, Università degli Studi di Sassari.

⁴ Dipartimento di Scienze Chimiche e Geologiche, Università degli Studi di Cagliari.

Corresponding email: gianni.andreozzi@uniroma1.it

Keywords: tourmaline, metaluminous systems, Sardinia.

In magmatic systems, intensive and compositional parameters are commonly invoked to account for tourmaline saturation in the melt. To model the frequent occurrence of tourmaline-bearing rocks associated with peraluminous intrusions, a large emphasis is typically given to Al_2O_3 saturation index of magmas (ASI > 1.2). However, a major role played by partial melting processes of B-bearing protoliths has been recently proposed to control the B saturation of anatectic melts.

In Sardinia, a B-bearing rock series is documented by tourmaline occurrence in the late-crystallization stages of Late-Variscan intrusives related to the older magmatic peak (305-300 Ma). Conversely, intrusives related to the younger magmatic peak (290-280 Ma) are almost made up of F-bearing granites and lack in tourmaline. The controls on the origin of tourmaline were investigated by comparing mineral assemblages from Mandrolisai (central Sardinia) and Arbus (SW Sardinia) igneous massifs, both emplaced at shallow depths in the frontal zone of a nappe edifice.

Mandrolisai igneous massif results as a single pulse of a granodioritic metaluminous magma, while Arbus is a composite pluton made of several pulses reaching a peraluminous character in leucogranitic rock-units (ASI < 1.16). Arbus magmas belong to a true ilmenite *series* while the Mandrolisai straddles the ilmenite/magnetite field *series*. In Mandrolisai, tourmaline occurs in layered aplite/pegmatite dikes and in thin tourmalinite veins in roof pendants of metamorphic rocks, close to the western contacts of the intrusion. In Arbus, tourmaline occurs in pegmatitic layers, in granophyric dykes and within metamorphic country rock.

The inclusive crystal-chemical study of tourmaline samples from pegmatites of both plutons highlights a comparable evolution from shorlitic to foititic composition; in addition, crystals from tourmalinite veins of Mandrolisai and dispersed within the country rock of Arbus show a dravitic composition, mostly related to magma-country rock interaction. The main differences regard the Mg-richest and Al-poorest composition of Mandrolisai tourmaline, which reflect a different composition of granodioritic magma, more magnesian and less aluminous (ASI = 0.93-0.95). The whole data sets of the two plutons allow the reconstruction of the same crystallization path: T = 650-400 °C, P ≤ 2.2 kbar and redox conditions reaching NNO buffer in the Mandrolisai massif.

The uncommon occurrence of tourmaline-bearing rocks in a metaluminous intrusion such as Mandrolisai may be an evidence of the limited control exerted by Al_2O_3 saturation on the origin of tourmaline. Conversely, a more important role of B contents, likely coming from crustal sources, may be invoked for tourmaline saturation in the magma.

Origin of the peridotite-pyroxenite association from Rocca di Argimonia, Ivrea Mafic Complex (Ivrea-Verbano Zone)

Antonicelli M.*¹, Tribuzio R.¹⁻², Wu F.Y.³ & Liu T.³

¹ Dipartimento di Scienze della Terra e dell'Ambiente, Università degli Studi di Pavia (Italy).

² Istituto di Geoscienze e Georisorse - C.N.R., Unità di Pavia (Italy).

³ Institute of Geology and Geophysics - Chinese Academy of Sciences, Beijing (China).

Corresponding email: marta.antoniceili01@universitadipavia.it

Keywords: peridotite-pyroxenite sequence, O-Nd-Hf isotopes, metasomatism.

We present a petrological-geochemical investigation of the Rocca d'Argimonia peridotite-pyroxenite sequence, which is exposed in the lowermost continental crust of the Ivrea-Verbano Zone (South Alpine domain). This sequence is up to 400 m thick and is enclosed within Upper Carboniferous-Lower Permian gabbro-norites from the southern-western sector of the Ivrea Mafic Complex. The main purpose of this study is to unravel the evolution experienced by primitive magmas intruding the lower continental crust. The Rocca d'Argimonia peridotites are amphibole-bearing dunites to harzburgites. Associated pyroxenites are also amphibole-bearing, and range from olivine websterites to plagioclase-bearing websterites, with orthopyroxene modally prevailing over clinopyroxene. Hornblende gabbro-norite dykes (up to 25 cm thick) crosscut the peridotites and show amphibole-bearing orthopyroxenite reaction zones (mm-scale thick) along the contact with host rocks. Peridotites, pyroxenites and gabbro-norite dykes typically display nearly polygonal structure, which most likely reflects slow cooling and recrystallization in the lower continental crust. However, structures and micro-structures of primary magmatic origin are typically preserved, as for instance shown by the local occurrence of poikilitic orthopyroxenes in the peridotites. The whole-rock Mg# [$Mg/(Mg+Fe^{2+}_{tot})$] decreases from the peridotites to the pyroxenites and the gabbro-norite dykes (90 to 75), and these Mg# variations are paralleled by olivine, pyroxene and spinel compositions. The decrease of olivine forsterite proportion (90 to 85 mol%) is associated with $\delta^{18}O$ increasing from +5.8 to +6.6 ‰. Taken as a whole, the peridotites, the pyroxenites and the hornblende-gabbro-norite dykes show substantial variations in incompatible trace element signature and Nd-Hf isotopic compositions. The gabbro-norites enclosing the ultramafic sequence have low Mg# of 56-37 and are geochemically distinct from the hornblende-gabbro-norite dykes intruding the peridotites. In particular, the gabbro-norites enclosing the ultramafic sequence show LREE-enriched chondrite-normalized patterns and low initial ϵ_{Nd-Hf} values. We propose that the peridotite-pyroxenite Rocca di Argimonia sequence formed by injection of primitive mantle melts into gabbro-norites of the Ivrea Mafic Complex. These melts most likely experienced: (i) fractional crystallization driven by olivine + accessory spinel \pm clinopyroxene, and (ii) assimilation of crustal material released by pre-existing gabbro-norites, which promoted the development of orthopyroxene. The geochemical fingerprint of the peridotites is inferred to vary in response to a late-stage process of reactive melt migration, but it concurs to the idea that the mantle melt sources underwent metasomatism in conjunction with the Variscan subduction.

Phlogopite-pargasite coexistence in spinel peridotite xenoliths from Mount Leura (southeast Australia)

Bonadiman C.*¹, Pelorosso B.¹, Curetti N.², Merli M.³, Coltorti M.¹ & Pavese A.²

¹ Department of Physics and Earth Sciences, University of Ferrara, Italy.

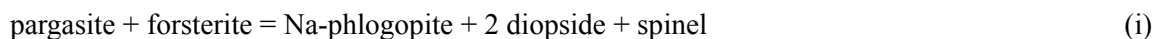
² Department of Earth Sciences, University of Torino, Italy.

³ Department of Earth and Sea Sciences, University of Palermo, Italy.

Corresponding email: bdc@unife.it

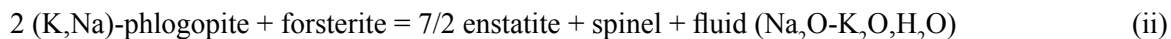
Keywords: mantle xenoliths, volatile contents, phase equilibrium.

Two spinel peridotite xenoliths hosted in Cenozoic basanites from Mount Leura in southeast Australia show coexisting amphibole phlogopite apparently texturally equilibrated with the peridotite matrix. The presence of amphibole and/or phlogopite minerals in *quasi*-anhydrous mantle system is basically due to the interaction, at various levels and stages, between a Na-K-OH rich “fluids” and variably depleted peridotites. This study is aimed to understand the chemico-physical properties of circulating fluids that stabilized these hydrous phases in the mantle ambient. To explore the hydrous phase forming process, we model two fundamental reactions that account for our findings i) to determine the P-T conditions of formation of the related assemblages, and ii) to infer H₂O-activity, for this latter to be used to infer the further geochemical and petrological information. The first reaction (i) accounts for the occurrence of pargasite, and phlogopite in the peridotite assemblage is written as ideal terms:



By means of (i) we estimated P-T equilibrium for the assemblages at the right-hand and left-hand side of (i), the key-equation governing the classic equilibrium relationships between co-existing phases that participate in a reaction, changing into each other: $\sum_j \nu_j \mu(P, T)_j = \sum_k \nu_k \mu(P, T)_k$

Calculations were carried out using the path integrations discussed by Curetti et al. (2018) of the output of tests performed using supercells to model cation order-disorder by means of semi-empirical potentials and lattice dynamics via the GULP code (Gale, 1997). The obtained results confirm that actual assemblage bearing both Na-rich phlogopite and pargasite to be reasonably approximated by (i) in terms of static and vibrational energy contributions. We complemented our modelling introducing configuration contributions stemming from the occurrence of complex solid mixings, and using crystal-chemical data determined by chemical analyses and single crystal diffraction for phlogopite and pargasite, and chemical composition for olivine, clinopyroxene and spinel. The P-T locus obtained (1.5-3.0 GPa – 1412-956 K) were used to constrain the pressure-temperature range on which the second assemblage bearing Na-rich phlogopite, stabilized, according to the following simplified reaction



The model suggests that in spinel bearing peridotites, at increasing pressure, the equilibrium amphibole-phlogopite needs lower temperature (out of geological meaning). The intersection with the geotherm allows to establish the mantle region where the amphibole-phlogopite are formed: 2.1 GPa - 1260 K. Moreover in this P-T region, the fluids (K, Na OH) cannot be stabilized as independent phase (i.e. fluid inclusions), in the peridotite assemblages.

Gale J.D. (1997) - GULP - a computer program for the symmetry adapted simulation of solids. *JCS Faraday Trans.*, 93, 629.

Curetti N., Bonadiman C., Compagnoni R., Nodari L., Corazzari I. & Pavese A. (2018) - Phengite megacryst quasi-exsolving phlogopite, from Sulu ultra-high pressure metamorphic terrane, Qinglongshan, Donghai County (eastern China): New data for P-T-X conditions during exhumation. *Lithos*, 314–315, 156-164.

Peridotite modification via reaction with pyroxenite-derived andesitic melts: an experimental study at 2 GPa

Borghini G.*¹, Fumagalli P.¹ & Rampone E.²

¹ Dipartimento di Scienze della Terra “Ardito Desio”, Università di Milano, Italy.

² DISTAV, Università di Genova, Italy.

Corresponding email: giulio.borghini@unimi.it

Keywords: melt-rock reaction, pyroxenite, mantle heterogeneity.

High-silica andesitic melts can be produced by partial melting of an olivine-free pyroxenite or an eclogite-peridotite mixed source (Mallik & Dasgupta, 2012). Within an upwelling mantle they are expected to react with the surrounding peridotite creating hybrid rocks (i.e. refertilized peridotites and secondary-type pyroxenites). The resulting veined mantle has been diffusely invoked as a suitable source of oceanic basalts (e.g. Lambart et al., 2012). We experimentally investigated the reaction between a fertile lherzolite and andesitic basalts produced by partial melting of the olivine-free pyroxenite Px-1 (e.g. Sobolev et al., 2007) at 2 GPa, 1300-1450°C. We carried out piston cylinder reaction experiments juxtaposing pyroxenite Px-1 on a powdered fertile lherzolite, previously synthesized at the same P-T conditions of reaction experiments. This allows a direct comparison between the modal and mineral compositions in the fertile lherzolite and in the peridotite modified after reaction with pyroxenite-derived melt. At 1300 and 1350°C, partially molten pyroxenite interacts with the subsolidus lherzolite producing a thin (about 50-100 µm) orthopyroxene-rich reaction zone at the pyroxenite-peridotite interface. Chemical profiles along the capsules show that X_{Mg} and Cr_2O_3 content in pyroxenes decreases, and TiO_2 increases, across the pyroxenite-peridotite boundary, with intermediate values in the reaction zone. Remarkably, in the subsolidus lherzolite spinel records X_{Mg} and X_{Cr} decrease and TiO_2 increase going toward the molten pyroxenite, with spinel X_{Cr} variation increasing with temperature. Similar chemical gradients are observed in some natural pyroxenite-peridotite sequences. Experimental results suggest that element diffusion across the two starting layers is able to modify the mineral compositions of subsolidus peridotite. At 1380 and 1400°C, interaction of basaltic-andesite melt produced by extensive melting of the pyroxenite layer with low-degree molten peridotite resulted in a larger glass-bearing websterite layer (about 650µm). Relatively high- TiO_2 contents in pyroxenes and spinel suggest that pyroxenite-derived melt percolated into and refertilized the peridotite layer profiting of the porosity created by low-degree melts in the peridotite matrix. At 1450°C, pyroxenite is almost completely melted. Fluxing of pyroxenitic melt into molten porous peridotite further enhances peridotite melting creating a melt-bearing dunite associated to a refractory harzburgite.

Lambart S., Laporte D., Provost A. & Schiano P. (2012) - Fate of pyroxenite-derived melts in the peridotitic mantle: thermodynamic and experimental constraints. *J. Petrol.*, 53, 451-476.

Mallik A. & Dasgupta R. (2012) - Reaction between MORB-eclogite derived melts and fertile peridotite and generation of ocean island basalts. *Earth Planetary Science Letters*, 329-330, 97-108.

Sobolev A.V., Hofmann A.W., Kuzmin D.V., Yaxley G.M., Arndt N.T., Chung S.L., Danyushebsky L.V., Elliott T., Frey F.A., Garcia M.O., Gurenko A.A., Kamenetsky V.S., Kerr A.C., Krivolutskaya N.A., Matvienkov V.V., Nikogosian I.K., Rocholl A., Sigurdsson I.A., Sushchevskaya N.M. & Teklay M. (2007) - The amount of recycled crust in sources of mantle-derived melts. *Science*, 316(5823), 412-417.

From the 600 ka tholeiites to the recent trachybasaltic magmas at Mt. Etna: evolution of a lherzolitic mantle

Casetta F.*¹, Giacomoni P.P.¹, Ferlito C.², Bonadiman C.¹ & Coltorti M.¹

¹ Department of Physics and Earth Sciences, University of Ferrara, Italy.

² Department of Biological, Geological and Environmental Sciences, University of Catania, Italy.

Corresponding email: cstfrc@unife.it

Keywords: Mt. Etna mantle source, Primary magmas, H₂O- and K-enrichment after 1971 eruption.

The paucity of primitive magmas and the absence of mantle-derived xenoliths make the discussion on the nature and evolution of the Mt. Etna mantle source/s extremely controversial, especially because of the spatial and temporal proximity of the volcano to the Hyblean Plateau and the Aeolian slab. An overview of the geochemical features of the products emitted by Mt. Etna from 600 ka ago to present days and a comparison with the Hyblean magmatic domain enabled us to infer the composition of the Etnean tholeiitic to alkaline primitive magmas as well as the nature and composition of the mantle source/s from which they segregated. According to our model, tholeiitic and alkaline primitive magmas at Mt. Etna were generated by two distinct amphibole + phlogopite-bearing spinel lherzolites at different partial melting degree. The LILE, ⁸⁷Sr/⁸⁶Sr, Rb- and H₂O-enrichment of magmas emitted after 1971 with respect to the pre-1971 ones (Tanguy et al., 1997; Métrich et al., 2004; Di Renzo et al., 2018) could be instead explained by a differential behavior of amphibole and phlogopite during melting, in a modally and compositionally homogeneous lherzolite, at comparable partial melting degrees. A variable H₂O/CO₂ activity in the mantle source could be identified as the principal driving force for the preferential melting of the hydrous phases, and in turn could be linked to the heat/fluxes supply from the upwelling asthenosphere beneath Mt. Etna. In the light of these new findings, some speculations about the geodynamic evolution of eastern Sicily were made to interpret the relationships between Mt. Etna and Hyblean Plateau magmatism.

Di Renzo V., Corsaro R.A., Miraglia L., Pompilio M. & Civetta L. (2018) - Long and short-term magma differentiation at Mt. Etna as revealed by Sr-Nd isotopes and geochemical data. *Earth-Science Reviews*, 190, 112-130.

Métrich N., Allard P., Spilliaert N., Andronico D. & Burton M. (2004) - 2001 flank eruption of the alkali- and volatile-rich primitive basalt responsible for Mount Etna's evolution in the last three decades. *Earth and Planetary Science Letters*, 228, 1-17.

Tanguy J.C., Condomines M. & Kieffer G. (1997) - Evolution of the Mount Etna magma: Constraints on the present feeding system and eruptive mechanism. *Journal of Volcanology and Geothermal Research*, 75, 221-250.

The Carbon pathway through subduction zones: petrological and geochemical constraints on carbonates from garnet-bearing orogenic peridotites

Consuma G.*¹, Braga R.¹, Giovanardi T.², Bersani D.³, Konzett J.⁴, Lugli F.⁵,
Mazzucchelli M.² & Tropper P.⁴

¹ Dipartimento di Scienze Biologiche, Geologiche e Ambientali, Università di Bologna.

² Dipartimento di Scienze Chimiche e Geologiche, Università di Modena e Reggio Emilia.

³ Dipartimento di Scienze Matematiche, Fisiche e Informatiche, Università di Parma.

⁴ Institute of Mineralogy and Petrology, University of Innsbruck.

⁵ Dipartimento di Beni Culturali, Università di Bologna.

Corresponding email: giulia.consuma@unibo.it

Keywords: orogenic peridotite, carbon cycle, metasomatism.

Exposure of garnet-bearing orogenic peridotites in the Eastern Italian Alps affected by metamorphism during and after the Variscan subduction, provides an excellent opportunity to investigate the elements mass transfer between crustal and mantle reservoirs. The occurrence of diverse carbonates in different textural positions suggests several infiltrations of carbon-rich aqueous fluids at different P and T. Based on petrography, major and trace elements concentrations and *in-situ* isotopic analyses of carbonates we document the fate of carbon during the downwards transport of the Ulten Zone peridotites until reaching eclogite-facies conditions and afterwards during exhumation. Trace elements analyses of interstitial dolomite show enrichment in La, Ba, Sr and Pb compared to HREE, consistent with its textural equilibrium with garnet, pargasitic to hornblende amphibole and Cl-apatite. Relatively un-radiogenic $^{87}\text{Sr}/^{86}\text{Sr}$ present day values (av. 0.70487 ± 0.00010) of these dolomites are clearly distinct from the higher radiogenic Sr isotope values of the associated migmatites, considered for long as the sources of fluids that metasomatized the Ulten Zone peridotites. Petrographic evidences for local injection of carbon-rich fluids in veins texturally in equilibrium with different silicates (i.e. magnesite + dolomite + tremolite + serpentine; dolomite + chlorite + tremolite) indicate that carbonation proceeded during retrogression. The variable trace elements patterns and wide range of Sr isotope signatures of a dolomite vein ($^{87}\text{Sr}/^{86}\text{Sr} = 0.70360 \pm 0.00007$ up to 0.71184 ± 0.00026) reflect an efficient elements diffusion and lack of isotopic homogenization, consistent with a complex crust-mantle mélange formed during this exhumation stage. Peridotites suffered also serpentinization during their ascent towards shallow levels: lizardite mesh rims and bastites acted as preferential flow paths at the micro-scale and provided dolomite dissolution with following precipitation of calcite and brucite intergrowths. This reaction releases CO_2 , attesting further mobilization of carbon through the lithospheric mantle. The mantle wedge is therefore capable to store carbonates, representing a complex metasomatic evolution from eclogite-facies conditions to very shallow structural levels, giving us more information on the fate of carbon during its journey through the Earth's upper mantle and surficial reservoirs.

New insights on volcanic activity related to the opening of the Central Tyrrhenian Sea: the transitional basalts of the Ventotene Volcanic Ridge (Pontine Islands, Italy)

Conte A.M.¹, Perinelli C.*², Bigi S.², Bosman A.¹, Castorina F.², Conti A.², Cuffaro M.¹, Di Vincenzo G.³ & Martorelli E.¹

¹ IGAG-CNR Roma.

² Dipartimento di Scienze della Terra, Sapienza Università di Roma.

³ IGG-CNR Pisa.

Corresponding email: cristina.perinelli@uniroma1.it

Keywords: Ventotene Volcanic Ridge, transitional rock-series, ⁴⁰Ar-³⁹Ar geochronology.

High-resolution geophysical data and ROV dives collected along the eastern margin of the Tyrrhenian back-arc basin, in the Pontine Islands area, led to the exploration and mapping of the Ventotene Volcanic Ridge (VR; Cuffaro et al., 2016). The latter is a NW-SE-oriented, and partially buried morphological high, located 25 km north of Ventotene Is. (Eastern Pontine Islands, EPI), whose volcanic origin is linked to the local and regional fault patterns. The VR is considered part of the alignment of volcanoes developed from NW to SE in the central-eastern area of Tyrrhenian Sea, from Western Pontine Islands (WPI) to Campanian Volcanic Region. Here we report the petrographic/geochemical (including Sr-Nd isotopes) and new ⁴⁰Ar-³⁹Ar age data of samples dredged along the VR in December 2015 from National Research Council Vessel Minerva Uno. We discuss the results in the light of tectonic setting of the VR, in the context of the extensional deformations related to the opening of the Tyrrhenian back-arc basin, which drove the magmatism from the WPI to the east Tyrrhenian margin during Plio-Pleistocene. The magmatism developed in the WPI covers a time span of 4.5-1.0 Ma and includes differentiated products of three distinct rock-series, namely, High Potassium-Calc Alkaline (HK-CA), Transitional (TR) and K-alkaline (KA). The parental products of HK-CA and KA series were mostly erupted eastward, in the Campania Plain subsoil (~2 Ma), and in the EPI up to Campania Plain (0.9 Ma to present), respectively. VR samples are basalt to trachybasalt belonging to the transitional-series and then suitable parental melts of the WPI transitional peralkaline rhyolites (1.6-1.1 Ma). This means that the 2.7 Ma age determined for VR basalts significantly enlarges the time interval of transitional magmas emplacement in the area. Moreover, a partial temporal overlap between HK-CA (4.5-2.0 Ma) and transitional (2.7-1.1 Ma) magmatism occurs and an almost continuity with the KA rock-series ones (~1.0 Ma to present). Based also on geochemical signatures of VR samples, we suggest that between ~4.5 and ~2.0 Ma in the area between WPI through the central Tyrrhenian Sea (VR) up to the subsoil of Campi Flegrei a HK-CA/TR magmatism, with typical orogenic signatures originated from similar thought heterogeneous supra-subduction sources, due to crustal components variously recycled in the mantle via subduction. The change towards the more typical KA products with orogenic signatures, which started to erupt at Ponza Is. and continued south-eastwards through La Botte neck, the EPI up to Procida and Ischia Islands, is probably correlated with changes in regional tectonic activity in the area.

Cuffaro M., Martorelli E., Bosman A., Conti A., Bigi S., Muccini F., Cocchi L., Ligi M., Bortoluzzi G., Scrocca D., Canese S., Chiocci F.L., Conte A.M., Doglioni C. & Perinelli C. (2016) - The Ventotene Volcanic Ridge: a newly explored complex in the central Tyrrhenian Sea (Italy). *Bull. Volcanol.*, 78, 86.

The noble gases geochemistry in mantle xenoliths from West Antarctic Rift System

Correale A.^{*1}, Pelorosso B.², Rizzo A.L.¹, Coltorti M.², Italiano F.¹, Bonadiman C.² & Giacomoni P.²

¹ Istituto Nazionale di Geofisica e Vulcanologia, Palermo, Italy.

² University of Ferrara, Physics and Earth Sciences, Ferrara, Italy.

Corresponding email: alessandra.correale@ingv.it

Keywords: Antarctic Rift, Mantle xenolith, noble gases.

We investigated the noble gas content (He, Ne, Ar) in fluid inclusions from mantle xenoliths sampled at three localities in Northern Victoria Land (Baker Rocks, Greene Point and Handler Ridge), in order to investigate the characteristics of the lithospheric mantle beneath this area. The studied rocks include anhydrous and hydrous spinel-bearing lherzolites and harzburgites. The geochemistry of major and trace elements together with the noble gas content highlighted that melting processes variably interested this mantle portion. In detail, the $^4\text{He}/^{40}\text{Ar}^*$ ratios (0.004–0.39) measured in olivines, pyroxenes and amphiboles, much lower than those typical of fertile mantle (1–5), support this hypothesis. The $^3\text{He}/^4\text{He}$ ratios are highly variable (from 2.30 to 19.79 Ra) and evidence the post-eruptive accumulation of radiogenic ^4He and cosmogenic ^3He . By filtering the data for these secondary effects, we constrain the $^3\text{He}/^4\text{He}$ signature of the subcontinental lithospheric mantle below this area to 7.1 ± 0.4 Ra (mean \pm standard deviation). This isotopic helium signature, compatible with mantle metasomatism by MORB-type asthenospheric melts, is in accordance with previous measurements in mantle xenoliths and lavas from other localities of the WARS evidencing a homogeneous He-isotope signature beneath the entire rift.

Multiple subduction-related metasomatic pulses in mantle xenoliths from the Karioi volcano, North Island, New Zealand

Faccini B.*¹, Coltorti M.¹, Brenna M.², Casetta F.¹ & Briggs R.³

¹ Dipartimento di Fisica e Scienze della Terra, Università di Ferrara, Italy.

² Department of Geology, University of Otago, New Zealand.

³ Department of Earth Sciences, University of Waikato, New Zealand.

Corresponding email: fccbbr@unife.it

Keywords: calc-alkaline metasomatism, mantle xenoliths, New Zealand.

Calc-alkaline and alkaline magmatism generally occur separate in space and time at convergent margins. Alkaline magmatism usually post-dates the calc-alkaline event and is generally related to slab retreatment inducing asthenospheric upwelling and/or to the onset of post-orogenic trans-tensional regimes. Alternatively, the formation of a slab window may favor the rise of deep, fertile mantle material. Irrespective of the mechanism, how this succession is reflected in the mantle sources is still largely unknown. Some clues may come from ultramafic xenoliths found in pyroclastic deposits of the Alexandra Volcanics in the North Island (New Zealand), where calc-alkaline and alkaline eruptive products are randomly intercalated in the volcanic sequence of the Pliocene-Quaternary Karioi and Pirongia stratovolcanoes (Briggs and McDonough, 1990).

The xenoliths include typical mantle lithotypes (Iherzolites and harzburgites, characterized by medium to coarse-grained protogranular, porphyroclastic and equigranular textures) but is mainly composed by olivine-clinopyroxenites, dunites and wehrlites. For these latter, the textures vary from cumulitic to a mixed type that, however, have predominant protogranular features. Amphibole is present as traces in few peridotitic samples but is more abundant in some olivine-clinopyroxenites and dunites. Reaction textures with formation of secondary, newly-generated phases and glass are widespread in all nodules but especially in the cumulates, where distinct metasomatic episodes have been recognized even within a single sample.

The lithospheric section represented by Karioi peridotites underwent partial melting (F%) between 5 and 15%, as confirmed by spinel, olivine compositions and clinopyroxene HREE contents. Samples showing the highest F% degree are characterized by orthopyroxenes and clinopyroxenes with the highest LILE, LREE and MREE enrichment. Indeed, a metasomatic event occurred after depletion, due to the interaction with a calc-alkaline melt similar in composition to arc lavas found in the Alexandra Volcanic Group. On the other hand, mineral compositions in the olivine-clinopyroxenites and dunites speak in favor of their origin as deep fractional crystallization products of those calc-alkaline magmas, which most probably also repeatedly infiltrated all lithologies giving rise to multiple metasomatic pulses.

The Karioi ultramafic xenoliths are embedded in tuffs, preventing the identification of the magmatic affinity of the host basalt but, so far, no traces of alkaline metasomatism was found. Thus, the contemporaneous emission of both calc-alkaline and alkaline magmas suggests the presence of different mantle domains with peculiar petrological features below the Alexandra Volcanics area, but only one is represented in the xenolith collection.

Briggs R.M. & McDonough W.F. (1990) - Contemporaneous convergent margin and intraplate magmatism, North Island, New Zealand. *Journal of Petrology*, 31, 813-851.

Major and trace elements distribution during high-pressure melt-peridotite reaction: experiments at 2 GPa

Fumagalli P.*¹, Borghini G.¹, Klemme S.² & Rampone E.³

¹ Dipartimento di Scienze della Terra “Ardito Desio”, Università di Milano, Italy.

² Westfälische Wilhelms Universität Munster, Munster, Germany.

³ DISTAV, Università di Genova, Italy.

Corresponding email: patrizia.fumagalli@unimi.it

Keywords: melt-rock reaction, mantle heterogeneity, experimental petrology.

Melt-rock reactions triggered by deep melt infiltration into the peridotite is thought to strongly affect the mineralogy and chemistry of the upper mantle. The interaction of interstitial melts percolating via reactive porous flow within mantle peridotite is usually assumed to change the major and trace element composition of clinopyroxene. In particular, through chemical exchange with a reactive melt, clinopyroxene can reset its trace element (e.g. REEs) composition changing its chemical and, over time, isotopic signature (Borghini et al., 2013). However, the efficiency of melt-rock reactions in resetting the composition of mantle clinopyroxene has been poorly experimentally investigated.

We are performing piston cylinder experiments of melt-peridotite reaction at 2 GPa to define the style of reactions, the role of temperature and melt composition on this process at lithosphere-asthenosphere boundary. Starting material is a mixture of mantle minerals and glass. Peridotite is modeled as a mix of clinopyroxenes, separated from External Liguride ophiolitic peridotite, and San Carlos olivine (Fo₉₀). Initial reacting melt is a tholeiitic basaltic glass sampled at the Romanche Fracture zone, with a relatively low X_{Mg} (0.60), high alkali (Na₂O = 3.48 wt%, K₂O = 0.81 wt%) and enriched-MORB signature (La_N/Yb_N = 5.49).

Preliminary experiments at 1300-1350°C, 2GPa on the selected enriched-MORB glass indicated that clinopyroxene is its liquidus phase. We performed experiments on different basalt:clinopyroxene:olivine proportions, i.e. 2:1:1 at 1350°C and 1:1:1 at 1300°C. Both runs resulted in clinopyroxene, olivine and glass. At 1300°C glass fraction is significantly lower as compared with run at 1350°C, suggesting a relevant crystallization. Olivine is chemically homogeneous, shows X_{Mg} higher than San Carlos olivine at 1350°C, but lower at 1300°C, and Ca content always higher than San Carlos olivine. In both charges, clinopyroxene consists of large relicts preserving the composition of the starting material with rather large (80-150 μm) reacted rims. These display X_{Mg}, Cr and Ca contents lower and Al, Na higher than the unreacted core. Preliminary results indicate that newly crystallized olivine and clinopyroxene, with significant changes in major element composition, form through basalt-peridotite reaction.

Borghini G., Rampone E., Zanetti A., Class C., Cipriani A., Hofmann A.W. & Goldstein S. (2013) - Meter-scale Nd isotopic heterogeneity in pyroxenite-bearing Ligurian peridotites encompasses global-scale upper mantle variability. *Geology* 41, 1055-1058.

From mantle to magma: a volatile budget between mantle xenoliths and primary magmas in the Western Antarctic Rift System

Giacomoni P.P.*¹, Coltorti M.¹, Bonadiman C.¹, Ferlito C.², Faccini B.¹, Zanetti A.³ & Ottolini L.³

¹ Department of Physics and Earth Sciences, University of Ferrara, Italy.

² Department of Biological, Geological and Environmental Sciences, University of Catania, Italy.

³ National Research Council, IGG-CNR, Pavia Section, Italy.

Corresponding email: gcmppl@unife.it

Keywords: melt inclusions, Antarctica, volatiles storage in the mantle.

The petrological study of olivine-hosted melt inclusions (MI) from the Cenozoic lavas of Northern Victoria Land and of xenoliths entrained in them, allows to compare the volatile composition of the mantle source and that measured in the MI.

In the Paleo-Pacific margin of Gondwana subduction proceeded from 550 to 100 Ma, partially overlapping with the supercontinent break up which was accompanied by the Karoo and Ferrar LIPs magmatism (182 Ma). The onset of the West Antarctic Rift System was at about 80 Ma while associated alkaline magmatism started at about 48 Ma.

The simultaneous occurrence of mantle xenoliths and olivine-phyric lavas allow us i) to constrain the melting processes and the geochemical features of the mantle source/s and ii) to investigate the complex relationships between the migrations of metasomatic fluids and the volatile storage in the mantle after prolonged subduction.

MI range in composition from basanite to basalt, and come from Shield Nunatak (Mt. Melbourne), Eldridge Bluff and Handler Ridge. Host-olivines range from Fo₈₉ to Fo₈₂. Inclusions have been analyzed for major, trace and volatile species (CO₂; H₂O, F, Cl and S) after HT (1300°C) and HP (6 kbar) re-homogenization.

The H₂O content ranges from 0.70 to 2.64 wt% and CO₂ from 25 to 3905 with a H₂O/(H₂O+CO₂) varying between 0.88 and 1). F and Cl content varies from 1386 ppm to 10 ppm and from 1336 ppm to 38 ppm respectively.

The volatile content measured in amphiboles and NAMs from Baker Rocks mantle xenoliths (Bonadiman et al., 2014) has been used to estimate the bulk volatile content of the lithospheric mantle. About 800ppm of H₂O are necessary to explain the MI water content (2.64 wt%) in a basanite and in an alkali basalt with a melting degree of 3 and 6.8% respectively. Similarly, using the CO₂ estimate in the same basanitic and alkali basaltic MI would result in a CO₂ content in the mantle source of slightly less than 300 ppm. The Cl and F content of the amphiboles however result higher than that found in the MI at comparable partial melting degree. These higher values may indicate a link with past subduction events.

Bonadiman C., Nazzareni S., Coltorti M., Comodi P., Giuli G. & Faccini B. (2014) - Crystal chemistry of amphiboles: implications for oxygen fugacity and water activity in lithospheric mantle beneath Victoria Land, Antarctica. *Contributions to Mineralogy and Petrology*, 167, 984.

Mafic dyke swarms at 1882, 535 and 200 Ma in the Carajás region: an insight on the evolution of the sub-Amazonian Craton mantle

Giovanardi T.*¹, Girardi V.A.V.², Teixeira W.², Mazzucchelli M.¹ & Cipriani A.¹

¹ Dipartimento di Scienze Chimiche e Geologiche, Università di Modena e Reggio Emilia, Italy.

² Instituto de Geociências, Universidade de São Paulo, Brazil.

Corresponding email: tomaso.giovanardi@gmail.com

Keywords: Amazonian Craton, mantle evolution, basaltic dykes.

The Carajas region is the eastern part, together with the Rio Maria domain, of the Central Amazonian province, near the margin of the Amazonian Craton with the Araguaia belt. In this region several basaltic dyke swarms were recognized and related to the Uatumã SLIP event. However, recent dating of Carajas dyke swarms highlighted the occurrence of several intrusive events. Currently, three major events are recorded at 1882, 535 and 200 Ma. New geochemical and isotopic data (Sr and Nd) were obtained for the different groups of the Carajas dykes in order to constrain i) the mantle source composition beneath the Carajas region and its evolution through time and ii) the geodynamic setting of the intrusive events.

The oldest 1882 Ma swarm is coeval to the Uatumã SLIP event which is one of the main events of the amalgamation of the Amazonian craton. Trace elements and isotopic values suggest that the dyke parent melt have a crustal component derived from a sedimentary source similar to GLOSS. This is consistent with the emplacement of the dykes in a supra-subduction setting (suggesting that the Uatumã SLIP event developed through a flat-subduction migrating geodynamic setting) or in a post-collisional setting reflecting the beginning of the taphrogenesis of the Columbia supercontinent. Trace and isotopic values of the 535 Ma dyke swarm are consistent with an enriched mantle source from an EMII component. These geochemical features suggest an enrichment of the mantle from an oceanic lithosphere poor in sediments, different to that of the 1882 Ma source. The age of this swarm links the dykes intrusion during a post-collisional extensive-transpressive event mainly recorded in the near Araguaia belt after the amalgamation of the Amazonian Craton to the Western Gondwana during Neoproterozoic. Lastly, the 200 Ma dyke swarm is coeval to the CAMP (Central Atlantic Magmatic Province) magmatism and the opening of the Atlantic Ocean. Dykes trace element composition is similar to Atlantic E-MORB and the isotopic values suggest an enriched mantle source with EMII component. These particular geochemical features suggest that the plume activity responsible for the CAMP near the rifting zone has not affected the mantle beneath the Carajás region.

The Authors acknowledge CNPq and the PRIN MIUR 20178LPCPW project for financial support.

Dioritic-albititic dykes in the Finero Phlogopite Peridotite: an intrusive event in the Northern Ivrea-Verbano Zone (Southern Alps)

Giovanardi T.*¹, Zanetti A.², Langone A.², Cipriani A.¹ & Mazzucchelli M.^{1,2}

¹ Dipartimento di Scienze Chimiche e Geologiche, Università di Modena e Reggio Emilia.

² IGG, CNR Pavia.

Corresponding email: tommaso.giovanardi@gmail.com

Keywords: mantle refertilization, Finero, dyke intrusion.

The Finero Phlogopite-Peridotite (FPP) is a mantle massif completely recrystallized through several events of melt migrations. These events have enriched the FPP in hydrous phases (Amphibole and Phlogopite) and crustal components, being commonly interpreted as related to subduction/post orogenic geodynamic settings. One of the latest melt-migration events developed via hydraulic fracturing through the FPP crystallizing composite Al-rich sapphirine-bearing gabbroic dykes.

In this contribution we present a new type of dykes recognized for the first time in the FPP. These dykes crosscut at high angle the peridotite foliation, suggesting that they intruded after the main metasomatic event. They have a composite structure, similar to the sapphirine-bearing gabbroic ones, formed by melanocratic zones in contact with the peridotite and a leucocratic zone in the centre. The melanocratic zones are formed by green Amphibole and relict Orthopyroxene at the contact with FPP. This association is recrystallized by secondary glimmeritic intrusions, which enrich the melanocratic zone in Phlogopite. The leucocratic zone is formed by Plagioclase (Albite up to 80%) with subordinate Phlogopite, Apatite and relicts of green Amphibole. Accessory phases are Zircons, Monazites and Ca-Betafite. The dykes show sin- to post magmatic deformation, testified by fine-grain recrystallization, occurrence of immiscible batches of both melanocratic and leucocratic associations and the glimmeritic intrusion. The petrographic and mineralogical features of dioritic-albititic dykes suggest possible relationships with the sapphirine-bearing gabbroic dykes of the FPP. However, compared to them, minerals from the dioritic-albititic dykes show lower Mg# and Al, suggesting a more evolved parental melt. This is consistent with the absence of Sapphirine and other Al-rich phases. Amphiboles are enriched in LREE with respect to HREE, with flat LREE trend. Amphibole relicts in the leucocratic zone show variable LREE content suggesting a post-magmatic re-equilibration with Plagioclase. The low U and Th content, associated to high Nb and Ta concentrations, point to different sources with respect to other known metasomatic events in the FPP. The relatively low radiogenic isotopic Sr composition of Amphibole and Plagioclase suggest a mantle-derived source for the dioritic-albititic dyke parent melt. However, the Sr isotopes disequilibrium among minerals indicates that the parent melts of the melanocratic, leucocratic and glimmeritic intrusions was produced by different mantle sources.

Funds provided by PRIN 2015 in the frame of project 20158A9CBM_005 and the Programma Giovani Ricercatori Rita Levi Montalcini to A.C.

Xenoliths's evidence for refertilisation of a strongly depleted mantle column in the Patagonian extra-Andean backarc (Paso de Indios, Argentina)

Mazzucchelli M.^{*1-2}, Bertotto G.W.³, Giovanardi T.¹, Zanetti A.², Ponce A.D.³, Brunelli D.¹, Bernardi M.I.³, Hémond C.⁴ & Cipriani A.¹

¹ Dipartimento di Scienze Chimiche e Geologiche, Università degli Studi di Modena e Reggio Emilia, Modena, Italy.

² Istituto di Geoscienze e Georisorse - CNR, U.O.S. di Pavia, Pavia, Italy.

³ CONICET-Universidad Nacional de La Pampa, Instituto de Ciencias de la Tierra y Ambientales de La Pampa (INCITAP), Santa Rosa, Argentina.

⁴ Laboratoire Géosciences Océan, UMR6538, Institut Universitaire Européen de la Mer, Université de Brest & CNRS, Plouzané, France.

Corresponding email: maurizio.mazzucchelli@unimore.it

Keywords: Mantle Xenolith, Patagonia, Paso de Indios.

The Eocene basalts from the Paso de Indios region (Chubut-Argentina) are some of the various manifestations of Cenozoic basaltic magmatism with ultramafic xenoliths of Patagonia. In this area, located in the extra-Andean back-arc, basaltic necks and dikes outcrop between 43° 36' – 43° 50' S and 68° 53' – 69° 02' W, along with remnants of lava flows, being divided in two groups of Paleocene and Eocene age. The studied samples are mantle xenoliths hosted in Eocene basalts belonging to the Matilde lava flow, the Leon volcano and the Chenque dike. They are mainly spinel-facies harzburgites and clinopyroxene (Cpx)-poor lherzolites, with some dunites. The Chenque xenoliths mainly display porphyroclastic to equigranular texture, whereas those from Matilde and Leon volcanoes have coarse-granular to porphyroclastic textures. The equilibrium temperatures range from 782 to 1067 °C and the estimated pressures are between 1.4 and 1.96 GPa, indicating a provenance of xenoliths from 50 to 75 km in the mantle. The overall refractory character of the mineral assemblages is matched by the major element mineral compositions, which are mostly Al-poor and Mg-and-Cr-rich, and are consistent with melt extraction from 8 to 24% (according to spinel composition). However, the occurrence of melt-related open-system processes is suggested by local trends of positive correlation between Na and Cr# in Cpx, being fully confirmed by the trace element compositions.

In particular, the Matilde harzburgites ubiquitously show Cpx with transient U-shaped REE patterns. The HREE level content (LuN down to 1xCI) is consistent with 20-23% fractional melting of spinel DM. V-to-U-shaped REE patterns are also shown by Chenque lherzolites and harzburgites. Their M/HREE fractionation suggests an onset of the partial melting process at garnet facies conditions. Other Chenque lherzolites experienced a more pronounced refertilisation process led by LREE-enriched to LREE-depleted melts. A refertilised geochemical composition is also shown by the Leon samples, with harzburgite Cpxs resulting enriched in highly-incompatible elements such as U, Th, Sr and LREE.

The data presented in this study, in combination with those from the literature, allow us to conclude that the shallow mantle column beneath Paso de Indios was strongly refractory in origin, being successively affected by multiple events of melt migration. These latter, however, were able to produce only an incomplete refertilisation of the depleted protoliths, which still record geochemical gradients developed during the interaction with both LREE-enriched and LREE-depleted migrating melts. These petrochemical features make the Paso de Indios mantle column a unique study case in the Patagonian region, where the composition of the shallow mantle is usually completely overprinted by multiple stages of melt/fluid migration.

The Authors acknowledge the PRIN MIUR 20178LPCPW project for financial support.

Eclogite-derived melts-peridotite interaction at HP in the Monte Duria area (Central Alps, N Italy): a proxy for the mafic crust-to-mantle mass transfer in subduction zones

Pellegrino L.*¹, Malaspina N.¹, Zanchetta S.¹, Langone A.² & Tumiatì S.³

¹ Dipartimento di Scienze dell'Ambiente e della Terra, Università degli Studi di Milano Bicocca.

² Istituto di Geoscienze e Georisorse-C.N.R. U.O.S. Pavia.

³ Dipartimento di Scienze della Terra, Università degli Studi di Milano.

Corresponding email: l.pellegrino3@campus.unimib.it

Keywords: slab melting, websterite, Adula nappe.

In the Monte Duria area (Adula-Cima Lunga unit, Central Alps, N Italy) Grt-peridotites occur in direct contact with migmatized orthogneiss (Mt. Duria) and eclogites (Borgo). Both mafic and ultramafic rocks share a common HP peak at 2.8 GPa and 750 °C and post-peak static equilibration at 1.2 GPa and 850 °C.

Grt-peridotites show abundant amphibole, dolomite, phlogopite and orthopyroxene after olivine, suggesting that they experienced metasomatism by crust-derived agents enriched in SiO₂, K₂O, CO₂ and H₂O. Peridotites also display LREE fractionation (La/Nd = 2.4) related to LREE-rich amphibole and clinopyroxene grown in equilibrium with garnet, indicating that metasomatism occurred at HP conditions. At Borgo, retrogressed Grt-peridotites show low strain domains characterised by garnet compositional layering, cut by a subsequent low-pressure chlorite foliation, in direct contact with migmatized eclogites. Kfs+Pl+Qz+Cpx interstitial pocket aggregates and Cpx+Kfs thin films around symplectites after omphacite parallel to the Zo+Omp+Grt foliation in the eclogites suggest that they underwent partial melting at HP.

The contact between garnet peridotites and associated eclogites is marked by a tremolitite layer. This rock also occurs as layers within the peridotite lens, showing a boudinage parallel to the garnet layering of peridotites, indicating that the tremolitite boudins formed when peridotites were in the garnet stability field. Tremolitites also show Phl+Tc+Chl+Tr pseudomorphs after garnet, both crystallized in a static regime postdating the boudins formation, suggesting that they derive from a Grt-bearing precursor. Tremolitites have Mg#>0.90 and Al₂O₃=2.75 wt.% pointing to ultramafic compositions but also show enrichments in SiO₂, CaO, and LREE suggesting that they formed after the reaction between the eclogite-derived melt and the garnet peridotite at HP. To test this hypothesis, we calculated a log aH₂O-X pseudosection at fixed P=3GPa and T=750°C to model the chemical interaction between the garnet peridotite and the eclogite-derived melt. Our results show that the interaction produces a Opx+Cpx+Grt assemblage + Amp+Phl, depending on the water activity in the melt, suggesting that tremolitites likely derive from a previous Grt-websterite with amphibole and phlogopite.

Both peridotites and tremolitites also show a selective enrichment in LILE recorded by amphiboles in the spinel stability field, indicating that a fluid-assisted metasomatic event occurred at LP conditions, leading to the formation of a Chl-foliation post-dating the garnet layering in peridotites, and the retrogression of Grt-websterites in tremolitites.

The Monte Duria area is a unique case study where we can observe eclogite-derived melt interacting with peridotite at HP and relatively HT, and could thus represent a proxy for the crust-to mantle mass transfer at great depths in subduction zones.

Petrological features and volatile content of ultramafic xenoliths from Eifel (Germany)

Rizzo A.L.^{1,2}, Coltorti M.*², Faccini B.², Casetta F.², Ntaflou T.³ & Italiano F.¹

¹ Istituto Nazionale di Geofisica e Vulcanologia, Sezione di Palermo, Palermo, Italy.

² Department of Physics and Earth Sciences, University of Ferrara, Ferrara, Italy.

³ Department of Lithospheric Research, Universität Wien, Wien, Austria.

Corresponding email: clt@unife.it

Keywords: Eifel mantle xenoliths, Noble gases, European SCLM.

This work focuses on mantle xenoliths sampled from five localities of the Eifel volcanic field, both from the western and eastern side of the rift system, aiming at improving the knowledge of the local SCLM. Together with the petrology of the xenolith suite, which include major and trace element of whole rock and primary mineral phases, fluid inclusion (FI) analyses (He, Ne, Ar, CO₂) were also carried out via single-step crushing.

A remarkable difference exists between eastern and western outcrops. In the former xenoliths are embedded in lava, sills or necks, while in the latter they are found in scoria cone or in pyroclastic deposits.

The xenoliths are lherzolitic, harzburgitic, and wehrlitic in composition with the exclusive modal presence of both amphibole and phlogopite in the western localities. Few ol-clinopyroxenites and one ol-websterite are also present. Texture varies from protogranular, porphyroclastic and equigranular in most of the xenoliths, to cumulitic in some samples.

Mg# [$\text{MgO}/(\text{MgO}+\text{FeO}_{\text{tot}})$ mol%] varies from 83 to 92 for olivine, from 84 to 92 for orthopyroxene, and from 84 to 94 for clinopyroxene. Al₂O₃ content of orthopyroxene and clinopyroxene ranges from 0.5 to 6.5 wt% and from 0.7 to 8.2 wt%, respectively. Spinel is characterized by Cr# [$\text{Cr}_2\text{O}_3/(\text{Cr}_2\text{O}_3+\text{Al}_2\text{O}_3)$ mol%] ranging between 10 and 82, and by Mg# varying from 40 to 78. Xenoliths from the eastern localities are characterized by the highest Mg# for clinopyroxene and Cr# for spinel, together with the lowest Al₂O₃ contents for both pyroxenes. Based on these petrographic and geochemical features, an origin for these xenoliths via cumulitic or melting processes can be proposed.

In terms of CO₂ and noble gas concentration, clinopyroxenes and most of the orthopyroxenes show the highest gas content, while olivines are gas-poor. This variability in FI concentration seems not related to the variations observed in the He, Ne, and Ar isotopic compositions. In detail, ³He/⁴He varies between 5.5 and 6.9 Ra, where Ra is the ³He/⁴He ratio of air that is equal to 1.39×10^{-6} . These values are within the range proposed for European SCLM (6.3 ± 0.4 Ra), and slightly below that of MORB (Mid-Ocean Ridge Basalts; 8 ± 1 Ra), being comparable to previous measurements, which were developed only in western Eifel. The Ne and Ar isotope ratios fall along a binary mixing trend between air and MORB-like mantle. He/Ar* in FI and Mg# and Al₂O₃ content in minerals indicate that variable extents of partial melting occurred in the local SCLM, followed by metasomatic processes. The ongoing carbon isotopic measurements in the most CO₂-rich mantle xenoliths, coupled to the noble gases systematics in FI and mineral chemistry, will help in shedding light on the local mantle composition and the volatile recycling within the European SCLM, adding new clues to the present knowledge. An additional benefit of this type of studies is the possibility of better constraining the composition of fluids rising through the crust, that are usually monitored for volcanic or seismic hazard.

Quaternary ultrabasic volcanic rocks in central Urumieh-Dohktar magmatic arc (Central-Northern Iran): melanephelinites in post-collisional setting

Salari G.*¹, Rahimzadeh B.², Agostini S.³, Masoudi F.² & Lustrino M.¹

¹ Dipartimento di Scienze della Terra, Sapienza Università di Roma (Italy).

² Department of Geology, Shahid Beheshti University, Tehran (Iran).

³ Istituto di Geoscienze e Georisorse - CNR, Pisa (Italy).

Corresponding email: giulia.salari@uniroma1.it

Keywords: melanephelinites, post-collisional, carbonates.

Here we present results of a petrologic study on 21 samples from young (likely <1 Myr) and small volume lava flows produced by volcanic centers near the town of Nowbaran, ~180 km SW of Tehran (central-northern Iran), belonging to the Urumieh-Dokhtar Magmatic Arc (UDMA). The volcanism of the UDMA is related to the NE-ward subduction of the Neotethys Ocean beneath the Iranian plate that began in the Early Cretaceous, prior to the continental collision between Arabia and Iran in the early Cenozoic. The lava flows consist of ultrabasic plagioclase-free rocks, essentially melanephelinites. Diopside is the most abundant microphenocryst in the lavas, followed by Mg-rich olivine (Fo₈₀₋₉₂) and Mg-rich mica (phlogopite-eastonite with TiO₂ up to ~7.3 wt%). Calcite largely occurs as large plaques (often including opaque minerals and diopside). Nepheline is the most abundant phase occurring in the groundmass along with minor Ti-magnetite and cancrinite-sodalite group minerals. The investigated rocks show anomalous mineral paragenesis and whole-rock chemical compositions compared to the other Cenozoic Iran igneous rocks. Their low SiO₂ content (down to 35.4 wt%) is coupled with high CaO (up to 18.3 wt%). The variable MgO content (8.7-13.3 wt%) is associated to generally high Mg# (0.69-0.74), compatible with magmas in equilibrium with peridotitic matrix. The rocks have the sum of K₂O + Na₂O between 2.2 and 6.2 wt%, and a high Na₂O/K₂O ratio (up to 11.8).

Primitive mantle-normalized patterns show marked troughs at K, Rb and Pb and strong LREE enrichment, resembling mixed features between HiMU-OIB and subduction-related compositions, a characteristic that is also confirmed by isotopic data (⁸⁷Sr/⁸⁶Sr = 0.70519-0.70564, ¹⁴³Nd/¹⁴⁴Nd = 0.51263-0.51269, ²⁰⁶Pb/²⁰⁴Pb = 18.54-18.66). The great variability of the trace elements distribution coupled with the strongly sodic character leads to the hypothesis that lithospheric Na-rich amphibole likely contributed to the partial melting process that formed the lavas. Moreover, their low SiO₂ content, the feldspar-free paragenesis and the high CaO/Al₂O₃ ratios point to a CO₂ enrichment in the source region in the form of carbonate mineralogy. The presence of ultrabasic magmas is a rare occurrence in subduction zone settings and in the UDMA in particular. The source of the Nowbaran magmas likely experienced extensive metasomatism by CO₂-rich fluids derived from the lithospheric mantle.

MicroCT rendering of spinel-facies mantle xenoliths

Venier M.*¹, Bernardini F.^{2,3}, Caldeira R.⁴, de Ignacio C.⁵, Marzoli A.⁶, Mata J.⁷, Princivalle F.¹, Boumehdi M.A.⁸, Bensaid I.A.A.⁸, Youbi N.⁸, De Min A.¹ & Lenaz D.¹

¹ Dipartimento di Matematica e Geoscienze, Trieste, Italy.

² Centro Fermi, Museo Storico della Fisica e Centro di Studi e Ricerche “Enrico Fermi”, Italy.

³ Multidisciplinary Laboratory, The “Abdus Salam” International Centre for Theoretical Physics, Trieste, Italy.

⁴ Laboratório Nacional de Energia e Geologia (LNEG), Amadora, Portugal.

⁵ Department of Petrology and Geochemistry, Complutense University of Madrid, Spain.

⁶ Department of Geosciences, Padova, Italy.

⁷ Instituto Dom Luiz, Universidade de Lisboa, Portugal.

⁸ Department of Geology, Cadi Ayyad University, Marrakech, Morocco.

Corresponding email: marco.venier@phd.units.it

Keywords: MicroCT, Mantle Xenoliths, Spinel.

The petrographic studies of mantle rocks and their minerals, in combination with chemical characterization and trace elements abundances, is essential in the comprehension of the lithospheric mantle evolution. In such view, mantle xenoliths present textures that reflect temperature, pressure, stress conditions and possibly depletion or metasomatism experienced before they were sampled by their host magma. Mercier and Nicolas (1975) classified mantle peridotites by their textural type, distinguishing three main structural groups: protogranular, porphyroclastic and equigranular. The observable textures in mantle rocks depend not only by the grain size and shape but even by the contact relationships between different phases (Tabor et al., 2010). Indeed, the geological marker that allows to define the textural type is the spinel-silicates relation, such as the presence of spinel-pyroxene clusters (SPCs).

The X-ray computed micro-tomography (microCT) is an analytical technique applied in different fields that recently is experiencing a widespread development in geosciences. Being a 3-dimensional non-destructive technique, microCT systems offer applications in 3D pore characterization, 3D grain analysis, fracture analysis, ore analysis, fluid flow analysis, etc. (Cnudde and Boone, 2013). It has the advantage of giving a new depth of information that has not been available with two-dimensional based microscopy analysis. As a matter of fact, conventional petrographic studies are based on thin sections observation, but distribution of crystals in two dimensional sections is affected by the random sectioning plane. Thus, extending mantle xenoliths texture analysis to three-dimensional scale may be a powerful tool in petrography and petrology (Bhanot et al., 2017).

This study presents the first microCT investigation for a set of different mantle xenoliths. The 3D rendered volumes provide clear shapes of both melt channels and spinel-pyroxene clusters, along with grain relationships between pyroxenes and olivines and differences in SPCs sizes, shapes and textures.

Bhanot K.K., Downes H., Petrone C.M. & Humphreys-Williams E. (2017) - Textures in spinel peridotite mantle xenoliths using micro-CT scanning: Examples from Canary Islands and France. *Lithos*, 276, 90-102.

Cnudde V. & Boone M.N. (2013) - High-resolution X-ray computed tomography in geosciences: a review of the current technology and applications. *Earth-Sci. Rev.*, 123, 1-17.

Mercier J.-C.C. & Nicolas A. (1975) - Textures and fabrics of upper mantle peridotites as illustrated by xenoliths from basalts. *J. Petrol.*, 16,454-487.

Tabor F.A., Tabor B.E. & Downes H. (2010) - Quantitative characterization of textures in mantle spinel peridotite xenoliths. *Geol. Soc., London, Spec. Public.* 337, 195-211.

S11.

Mantle Petrology: from observation to calculus

CONVENERS AND CHAIRPERSONS

Enrico Bonatti (CNR-ISMAR)

Giulia Ottonello (Università di Genova)

***Ab initio* thermodynamics of deep mantle phase transitions and seismic discontinuities: the role of MgSiO₃ polymorphs**

Belmonte D.*¹

¹ Dipartimento di Scienze della Terra, dell'Ambiente e della Vita (DISTAV), Università di Genova.

Corresponding email: donato.belmonte@unige.it

Keywords: *ab initio*, mantle, thermodynamics.

Although seismic discontinuities between 410 and 660 km depth are usually attributed to solid-state phase transitions within the olivine component of the mantle, there's growing geochemical and geophysical evidence that MgSiO₃ polymorphs with the garnet, pyroxene, ilmenite and perovskite structure play a key role in controlling phase equilibria and seismic velocity gradients in this part of the mantle. Yet, thermodynamic data are still poor for these mineral phases and their extrapolation at high pressure and temperature conditions is affected by large uncertainties. In particular, laboratory measurements do not constrain well the Clapeyron slopes of mineralogical phase transitions and seismological observations are not more precise due to technical limitations.

In this work, *ab initio* thermodynamic and seismic properties of stable MgSiO₃ polymorphs at deep mantle conditions (tetragonal majorite, Mj; HP-clinoenstatite, HP-CEn; akimotoite, Ak; bridgmanite, Brg) have been fully characterized in a broad range of P-T conditions by phonon dispersion calculations with the hybrid B3LYP density functional method and in the framework of quasi-harmonic approximation.

The calculated heat capacities are in good agreement with the relatively few calorimetric investigations made so far on these minerals in the low- to medium-T range. However, the high-temperature extrapolation of calorimetric results may suffer from physical unsoundness, so that their use in phase equilibria calculation deserves great care. The calculated Gibbs free energies permit to constrain the Clapeyron slopes of phase transition boundaries in the MgSiO₃ phase diagram, which turn out to be equal to +2.2, +8.3, -4.0 and -3.6 MPa/K for Mj-Brg, Mj-Ak, Ak-Brg and HP-CEn-Mj reactions, respectively. A general feature of first principles calculations is that the predicted Clapeyron slopes are remarkably accurate, robust and roughly insensitive to the exchange-correlation term, at variance with P-T location of the univariant phase boundaries. Seismic wave impedance and velocity jumps across the MgSiO₃ phase changes have been computed accordingly and then compared to those inferred by seismological observations. A relevant outcome is that the computed values of $D\rho$, DV_p , DS and $D\rho V_s$ across the seismic discontinuities in the Earth's mantle can be different from that inferred by geophysical models: this suggests either incomplete dissociation reactions or the occurrence of multiple phase changes in deep mantle aggregates. The global-scale implications concerning the role of non-olivine mineral phases in mantle dynamics, seismic discontinuities, density change and slab stagnation at mantle depths are briefly outlined and discussed.

MIUR PRIN 2017KY5ZX8 "Oceanic Megatransforms: a new Class of Plate Boundaries"

Point defect equilibria in hydrous forsterite synthesized at 1100°C and up to 4 GPa

Del Vecchio A.*¹, Poe B.T.¹, Cestelli-Guidi M.² & Misiti V.³

¹ Dipartimento INGEO Ingegneria e Geologia Università G. D'Annunzio Chieti - Pescara.

² INFN-LNF Istituto Nazionale di Fisica Nucleare - Laboratori Nazionali di Frascati (Roma).

³ INGV Istituto Nazionale di Geofisica e Vulcanologia - Roma.

Corresponding email: alessandro.delvecchio@unich.it

Keywords: Forsterite, FTIR, spectroscopy, Point defects.

Water distribution in the deep Earth represents one of the most important topic in the field of geodynamics due to its large impact on the physical and chemical properties of the Earth's mantle. In order to study the mechanisms of hydrogen incorporation in nominally anhydrous minerals, in this work we synthesized polycrystalline samples of hydrous forsterite at 1100°C and up to 4GPa, with either piston cylinder and multianvil apparatus. As starting material we used synthetic forsterite, unbuffered by SiO₂, obtained by thermo-mechanical activation of talc and magnesium carbonate. Hydration was carried out using liquid H₂O as hydrogen source.

FTIR microimaging and point-by-point analyses allowed us to observe the spatial distribution of H₂O in each sample and the complexity of the FTIR spectra in the OH stretching region. This complexity may be related to several factors 1) incorporation of hydrogen as different chemical species such as 4H_{Si} and 2H_{Mg}, 2) multiple topological configurations of individual chemical specie (e.g. 4HSi¹, 4H_{Si}², 4HSi³, 4HSi⁴, with different positions of protons respect to the tetrahedral polyhedron), 3) individual chemical species containing multiple H atoms can exhibit multiple bands in the OH stretching region and 4) we acquired unpolarized spectra of a polycrystalline sample of orthorhombic symmetry.

Multiple absorption bands are found in a frequency range between 3400 – 3700 cm⁻¹, identifying through a deconvolution process, at least 9 peaks in all samples. Except the two overlapping bands at about 3700 cm⁻¹ probably due to the presence of brucite Mg(OH)₂, the stronger OH stretching peaks can be attributable to vibrational modes associated with the hydrogarnet defect 4H_{Si}^x in which four protons occupy a vacant tetrahedral site. Absorption peaks at 3566, 3578 and 3612 cm⁻¹ are strongest and assigned to the fully protonated 4H_{Si} chemical defect species. With increasing total H₂O concentration, the relative intensities of these peaks decrease, and may be explained by the dissociation process of the 4H_{Si}^x species into other chemically distinct defect species. Here, we propose that the 4H_{Si} defect is in equilibrium with an associate defect consisting of a 3H_{Si}⁻ species and a proton occupying an adjacent interstitial site, bonded to an oxygen that is not associated with the vacant tetrahedral site.

It is important to note that the chemical environment in experimental studies plays a key role in defect chemistry at high pressure and high temperature, particularly for nominally anhydrous minerals such as forsterite and olivine. A more complete understanding of H₂O incorporation can be achieved by the high precision, accuracy and attention required in experimental studies and development of increasingly more sophisticated techniques that benefit the study of the physical – chemical characteristics of mantle minerals at depth, with attention to the roles of H₂O and other volatile components.

H₂O Enrichment in Residual Mantle Peridotites at a Mid-Atlantic Ridge Segment

Li P.¹, Xia Q.-K.¹, Dallai L.², Bonatti E.^{3,4}, Brunelli D.^{4,5}, Cipriani A.^{3,5} & Ligi M.*⁴

¹ School of Earth Sciences, Zhejiang University, Hangzhou 310027, China.

² Istituto di Geoscienze e Georisorse-CNR, Pisa, Italy.

³ Lamont-Doherty Earth Observatory of Columbia University, Palisades, New York, USA.

⁴ Istituto di Scienze Marine-CNR, Bologna, Italy.

⁵ Dipartimento di Scienze Chimiche e Geologiche, Università di Modena e Reggio Emilia, Modena, Italy.

Corresponding email: marco.ligi@bo.ismar.cnr.it

Keywords: peridotites, water content, MOR processes.

The mantle degree of melting beneath Mid Ocean Ridges may be affected not only by mantle temperature, but also by its H₂O content and elemental composition. Water causes melting of the upwelling mantle to occur at greater depths and in greater extents acting as an incompatible component and with a strong tendency to be enriched in the melt (Ligi et al., 2005), thereby lowering the Gibbs free energy of the melt. How H₂O is distributed within the oceanic upper mantle remains poorly constrained. We determined the H₂O content of orthopyroxene (opx) and clinopyroxene (cpx) in mantle derived peridotites sampled along a continuous lithospheric section created during a 26 Ma interval at a Mid Atlantic Ridge segment, and exposed along the Vema Fracture Zone at 11 N. The H₂O content of opx ranges from 119 to 383 ppm; that of cpx from 407 to 1018 ppm (Li et al., 2018). Although H₂O is assumed to be incompatible during melting, we did not find an inverse correlation of peridotite H₂O content versus degree of melting. Moreover, we found an inverse correlation of peridotite H₂O content with Ce, another highly incompatible element. Here we report on the highest H₂O contents of pyroxenes ever found in abyssal peridotites. Among several possible mechanisms, we propose post-melting processes above the melting region, i.e., melt-rock interactions and diffusive fractionation of H from other trace elements, as the best explanation of our findings.

Li P., Xia Q.-K., Bonatti E. & Brunelli D. (2018) - Water content of abyssal peridotites: implications for melt transports beneath mid-oceanic ridges. *Goldschmidt Abstracts*, 1487.

Ligi M., Bonatti E., Cipriani A. & Ottolini A. (2005) - Water-rich basalts at mid-ocean-ridge cold spots *Nature*, 434, 66-69.

Earth's non-primitive lower mantle: aluminium recycling

Merli M.¹, Bonadiman C.*² & Pavese A.³

¹ Department of Earth and Marine Sciences, University of Palermo, Italy.

² Department of Physics and Earth Sciences, University of Ferrara, Italy.

³ Department of Earth Sciences, University of Turin, Italy.

Corresponding email: bdc@unife.it

Keywords: MORB component, Al bearing perovskite, open system.

The mantle is the Earth's volumetrically largest division, originally marked by a planetary Siderophile/Lithophile element fractionation. Refractory Lithophile Elements (RLE) condensed from a gas of solar nebula composition at the highest temperature (>1400 K at 10⁻⁴ atm) compatible with the nebula's physical constraints (Davis and Richter, 2005). RLEs' chemical behaviour prevented metal and sulphide phases from entering in metallic cores during the planetary differentiation (Mahan et al., 2018). Aluminium is a purely refractory lithophile element and thus an effective "probe" among the major elements to assess if and how the actual Earth's lower mantle is affected by large scale recycling processes of crustal fragments. Such point requires an understanding of the Al incorporation mechanisms taking place in the lower mantle. The incorporation mechanisms and distribution in the lower mantle (from 24 to 80 GPa) are investigated using quantum mechanics in combination with statistical thermodynamics. The mechanism of incorporation is such that the perovskite's capacity to uptake aluminium decreases as a function of pressure; this is offset by an increase of Al-bearing perovskite amount, with respect to Al-free perovskite. In particular, the Al-bearing perovskite composition changes on average from 0.13 to 0.11 Al₂O₃ per formula unit, at 24 and 80 GPa, respectively. Yet, the ratio between phase proportions of Al-bearing perovskite over Mg-perovskite increases from 0.71 to 0.94, in the same pressure range. Results show that the perovskite-like structure accounts for an accommodation of Al₂O₃ ranging from 4.2 to 4.8 wt.% of lower mantle mass. This range is even consistent with the estimates of a non-primitive composition of the Earth's lower mantle, resulting from the incorporation of a MORB-component up to 5 wt.%. In this light, our study shows that there is no need of phases other than perovskite to account for Al-hosting. The probability to find perovskite with an Al₂O₃-content up to 0.15 fraction per formula unit is 28% at 24GPa/1919 K and increases to 43% at 80 GPa/2550 K. Conversely, the occurrence probability of Al-rich perovskite (alumina contents in the range 0.19-0.30 molar fraction) dramatically decreases from 9.8% to 2.0%, over the same P-T interval. Approaching 80 GPa, the occurrence of a sort of "Al-incorporation saturation" looks like a prelude to instability, possibly leading to the formation of other phases (i.e. structural change to post-perovskite) to host Aluminium, in keeping with earlier equilibria modelling of the MgSiO₃-Al₂O₃ system, at P-T conditions relevant for the Earth's deepest mantle (80-140 GPa/2000-4000 K). Altogether, perovskite can account for an amount of alumina in line with a hypothesis of deep plunging of large portions of crustal material into the lower mantle.

Davis A.M. & Richter F.M. (2005) - Condensation and Evaporation of Solar System Materials. In: Davis A.M. ed. Meteorites, Comets and Planets. Treatise of Geochemistry (vol. 1).

Mahan B., Siebert J., Blanchard I., Borensztajn S., Badro J. & Moynier F. (2018) - Constraining compositional proxies for Earth's accretion and core formation through high pressure and high temperature Zn and S metal-silicate partitioning. *Geochim. Cosmochim. Acta*, 235, 21-40.

Oxidation state of iron in the Earth's lower mantle

Merli M.¹, Bonadiman C.² & Pavese A.*³

¹ Università degli Studi di Palermo, Dipartimento di Scienze della Terra e del Mare.

² Università degli Studi di Ferrara, Dipartimento di Fisica e Scienze della Terra.

³ Università degli Studi di Torino, Dipartimento Scienze della Terra.

Corresponding email: alessandro.pavese@unito.it

Keywords: Fe oxidation state, lower mantle, modelling.

The ratio Fe(III)/Fe(II) in the Earth's lower mantle is still a matter of relevant uncertainty, although it plays an important role as it affects both physical properties (for instance, radiative heat transfer; Goncharov et al., 2008) and chemical processes (for instance, bridgmanite stability; Ismailova et al., 2016; Mao et al., 2015) taking place in the depth of our planet (Lin et al 2013). In the present work we estimated the trend of the oxidation state in the lower mantle, assuming that bridgmanite as the sole phase accommodating ferric iron. Four

REDOX reactions were explored: $(\text{Mg}_3\text{Fe})\text{Si}_4\text{O}_{12} + \text{H} = (\text{Mg}_3\text{Fe})\text{Si}_4\text{O}_{12}\text{H}$; $(\text{Mg}_3\text{Fe})\text{Si}_4\text{O}_{12} + \text{N} = (\text{Mg}_3\text{Fe})\text{Si}_4(\text{O}_{11}\text{N}) + \text{O}$; $(\text{Mg}_3\text{Fe})\text{Si}_4\text{O}_{12} + \text{Al} = (\text{Mg}_3\text{Fe})(\text{AlSi}_3)\text{O}_{12} + \text{Si}$; $(\text{Mg}_3\text{Fe})\text{Si}_4\text{O}_{12} + \text{C} = (\text{Mg}_3\text{Fe})\text{Si}_4(\text{O}_{11}\text{C}) + \text{O}$. Bader theory atomic basin charges were used to infer the iron oxidation state from electron density functions obtained by quantum mechanics calculations. The global Fe oxidation state throughout the lower mantle was then predicted using energy calculations coupled with chemical equilibrium principles and geochemical estimates of elemental abundance. In so doing, we observe that the $\text{Si} + \text{Mg} + \text{Al} + \text{Fe}$ is the most effective reaction to oxidizing iron, among those investigated. Such reaction has an absolute probability of occurrence of some 60% at 90 GPa, in comparison with some 40%, in the case of nitrogen, ($\text{N} \hat{=} \text{O}$), and a few percent, if carbon is involved ($\text{C} \hat{=} \text{O}$). Altogether, preliminary inferences lead us to state that in bridgmanite the $\text{Fe}^{3+}/\text{Fe}^{2+}$ potentially changes from 1:1, 24 GPa, to 1:2, at 90 GPa. Most of the Fe oxidation is governed by the competition between the following replacements: $2 \text{Al} \hat{=} \text{Si} + \text{Mg}$ versus $\text{Al} + \text{Fe} \hat{=} \text{Si} + \text{Mg}$.

Goncharov A.F., Haugen B.D., Struzhkin V. V., Beck P. & Jacobsen S. D. (2008) - Radiative conductivity in the Earth's lower mantle *Nature*, 456, 231–234.

Ismailova L., Bykova E., Bykov M., Cerantola V., McCammon C., Boffa Ballaran T., Bobrov A., Sinmyo R., Dubrovinskaia N., Glazyrin K., Liermann H-P., Kuppenko I., Hanfland M., Prescher C., Prakapenka V., Svitlyk V., Dubrovinsky L. (2016) - Stability of Fe, Al-bearing bridgmanite in the lower mantle and synthesis of pure Fe-bridgmanite. *Sci. Adv.* 2016; 2: e1600427.

Mao Z., Lin J. F., Yang J., Inoue T., Prakapenka V. B. (2015) - Effects of the Fe^{3+} spin transition on the equation of state of bridgmanite, *Geophysics Research Letters*, 42(11), 4335-4342. <https://doi.org/10.1002/2015GL064400>.

Vapor-buffered magmatic activity and the unique CO₂-rich source of magmatism in Southern Italy

Moretti R.*¹⁻²

¹ Université de Paris, Institut de Physique du Globe de Paris, CNRS, Paris (France).

² Observatoire Volcanologique et Sismologique de Guadeloupe, Institut de Physique du Globe de Paris, Gourbeyre (France).

Corresponding email: moretti@ipgp.fr

Keywords: volatile-melt saturation, redox, mantle carbonation.

The Italian territory is heavily invested by widespread deep degassing characterized by huge emissions of carbon dioxide. The pery-thyrrhenian area of southern Italy is the place where these emissions are accompanied by active volcanism, with magmas displaying alkalic affinity and covering a wide compositional spectrum. It has long been debated whether such a production of CO₂ is related to decarbonation of crustal limestones or to other deep source features. However, an overall look at melt inclusions and plume data from southern Italian volcanoes suggests that magmas are produced under CO₂-rich and fluid buffered conditions that initiate in the lithospheric mantle. Nevertheless, what we can heuristically “see” when “looking at” these data depend on the reliability of multicomponent saturation models for the volatile-melt systems. The adoption of a multicomponent saturation model for the H₂O-CO₂-SO₂-H₂S-melt system allows us to infer that source regions of considered volcanic plumbing systems are deeply infiltrated by CO₂-rich fluids and point to a unique fluid-rich deep source evolving under pressure conditions variable in space that determine variable H₂O/CO₂ gas ratios and also oxidation states.

Even though carbon and oxygen isotopes on magmatic products are still too sparse to validate this scenario, volcanic volatiles and the ensemble of petrologic evidences promote the prevailing hypothesis involving the subduction of a continental crust and/or oceanic sediments carrying both pelagic and non-pelagic fractions.

Thermochemistry of silicate melts in high-rank simplexes: the new HPA model

Ottonello G.*, Belmonte D. & Vetuschi Zuccolini M.

Dipartimento di Scienze della Terra, dell'Ambiente e della Vita, Università di Genova.

Corresponding email: giotto@dipteris.unige.it

Keywords: thermodynamics, melts, polymers.

We present here the last formulation of the Hybrid Polymeric Approach (HPA), and show some preliminary application to CMAS, a 3rd-rank simplex of paramount importance in mantle petrology. The Gibbs free energy of mixing of multi-component melts is seen in HPA as a sum of discrete contributions arising from different forms of interaction, namely a dominant chemical interaction taking place among polymeric units (structons) and cations, a (subordinated) interaction taking place in the cation matrix, and a strain energy contribution arising from medium range disorder of the various structons within the anion matrix. The chemical interaction between network formers (NF) and network modifiers (NM) constitutes by far the main form of energy gained (or lost) by the liquid in the mixing process. In the light of the principle of equal reactivity of co-condensing units, the polymerization constant (K_p) cannot be expected to be affected by the length and conformation of the structons. Moreover, its value is shown to be directly related to the electronegativity difference between network former and network modifier. This represents an added value of the polymeric models with respect to the usual Flory-Huggins and Quasi-Chemical approaches. The excess Gibbs free energy of mixing in the cation matrix is approximated by sub-regular (Van Laar) expansions. A Hookian strain contribution representing the energy spent (or gained) in conforming the relative arrangement of the various polymers in the anion sublattice is added. This amount of energy is greatly subordinated with respect to that one arising from chemical interaction, and important only in quantifying the observed unmixing phenomena at high acidity content in the system. Finally, high order interactions are introduced for 2nd and 3rd-rank simplexes in order to account for minor topological effects associated to non-linear polarization of charges.

The ab-initio assisted model parameterization is carried out in a progressive fashion increasing progressively the ranking of the simplex from zero (T-P melting curve of the pure liquid oxides), to one (binary interactions; liquidus and solvi), then 2 (cotectic lines and invariant points) and 3 (primary phase fields).

The Lux-Flood properties of NM are combined in terms of electrically equivalent fractions to achieve consistency with the requirements of the Flood-Grjotheim thermochemical cycle. The Lux-Flood properties of NF are combined in terms of molar proportions. This is a Toop's projection having as pivotal point the adjoined network formers. Strain energy terms follow the same combinatory rules, while cationic interactions are seen to rapidly disappear when NF are introduced in the system.

Why do we need mathematical models in petrology and volcanology?

Papale P.*

Istituto Nazionale di Geofisica e Vulcanologia, Sezione di Pisa

Corresponding email: paolo.papale@ingv.it

Keywords: mathematical modelling, numerical simulations, magma dynamics.

Mathematical models based on the solution of the fundamental laws governing the physical world are today common practice in virtually any field of human investigation, including apparently distant disciplines like biology, sociology, and politics. Geology offers an immense suite of problems, most of which quite complex from a physical and mathematical perspective. When dealing with processes occurring at depth below the Earth surface, further complication comes from the difficulty in obtaining direct data on the conditions, the properties, and the dynamics. Geological and geophysical observations, and laboratory experiments, constrain such processes and represent a (or “the”) primary source of information; however, they are hardly conclusive as i) with very few valuable exceptions, geological observations do not include the P-T conditions of interest; ii) geophysical inversions have limited resolution and most often do not have unique solutions; and iii) lab experiments only partly reproduce the space-time scales of the relevant geological processes. Mathematical modeling and numerical simulations offer unique complementary understanding of the geological processes, that are best approached through multi-disciplinary investigation, by adding the mechanistic perspective through which the forces operating in the system are explored in terms of the processes and dynamics they produce. The fundamental physics are reduced to first principles, basically the two laws of thermodynamics, Newton’s second law of dynamics, and mass conservation, which normally take quite complex forms when referred to the multiphase, multi-component geological systems and to the wide range of space-time scales over which the geological processes develop. As a consequence, the solution of such complex systems of equations often requires simplifications that limit the investigation to specific aspects, and that must be carefully operated and taken into account. Here I provide a few examples related to multiphase multi-component thermodynamics, to multi-component magma thermo-fluid dynamics, and to fluid-structure (magma-rock) interaction dynamics, and show how rigorous physical and mathematical modelling is increasingly providing new understanding of deep (volcanic system scale) processes and their relationships with geological and laboratory observables, as well as to geophysical records and investigation.

Melting an anciently depleted mantle

Sanfilippo A.*¹, Sokolov S.², Salters V.J.M.³, Stracke A.⁴ & Peyve A.²

¹ Dipartimento di Scienze della Terra e dell'Ambiente, Università di Pavia.

² Geological Institute, Russian Academy of Sciences.

³ Department of Earth, Ocean and Atmospheric Science and National High Magnetic Field Laboratory, Florida State University.

⁴ Institut für Mineralogie, Westfälische Wilhelms-Universität, Münster.

Corresponding email: alessio.sanfilippo@unipv.it

Keywords: Nd-Hf isotopes, peridotites, depleted mantle.

The use of combined radiogenic isotope systematics (e.g., Os, Nd, Hf, Sr, Pb) on mantle peridotites and erupted melts reveals an extreme heterogeneity of the asthenospheric mantle, which is nowadays considered to consist of portions re-enriched in fusible elements and portions an old, refractory mantle survived from re-homogenization in the asthenosphere (Stracke et al., 2011). This isotopically depleted material has an important, yet underestimated, contribution on chemistry of the melts erupted on the surface, as testified by scattered compositions of oceanic basalts in the Nd-Hf isotopic space (Salters et al., 2011). Knipovich ridge, a ~550-km long oblique supersegment in the Arctic region, has basalts with the highest Hf isotope compositions amongst Mid Ocean Ridge basalts worldwide (Blichert-Toft et al., 2005). Here we propose that this likely due to a quaternary ridge jump (Sokolov et al., 2014), which results in re-melting the present-day Knipovich lithosphere. Anciently depleted mantle is a common feature in the asthenosphere, albeit its contribution is partly obscured by preferential melting of enriched lithologies.

Blichert-Toft J., Agraniar A., Andres M., Kingsley R., Schilling J.G. & Albarède F. (2005) - Geochemical segmentation of the Mid-Atlantic Ridge north of Iceland and ridge-hot spot interaction in the North Atlantic, *Geochem. Geophys. Geosyst.*, 6, 1-19. <https://doi.org/10.1029/2004GC000788>

Salters V.J., Mallick S., Hart S.R., Langmuir C.E. & Stracke A. (2011) - Domains of de-pleted mantle; new evidence from hafnium and neodymium isotopes. *Geochem. Geophys. Geosyst.*, 12(8). <https://doi.org/10.1029/2011GC003617>

Sokolov S.Y., Abramova A.S., Zaraiskaya Y.A., Mazarovich A.O. & Dobrolyubova K.O. (2014) - Recent tectonics in the northern part of the Knipovich Ridge, Atlantic Ocean. *Geotectonic*, 48, 175-187.

Stracke A., Snow J.E., Hellebrand E., Von Der Handt A., Bourdon B., Birbaum K. & Günther D. (2011) - Abyssal peridotite Hf isotopes identify extreme mantle depletion. *Earth Planet. Sci. Lett.*, 308, 359-368.

TRIangular Diagram and deSCENT line analysis - a code to generate a computationally manageable liquidus surface of a molten silicate system and a consistent cooling descent line description from modeling

Vetuschi Zuccolini M.*, Ottonello G. & Belmonte D.

Dipartimento di Scienze della Terra, dell'ambiente e della Vita - Università di Genova.

Corresponding email: zucco@dipteris.unige.it

Keywords: phase diagrams, descent path, liquidus surface.

The package TRIDISCENT is a tool created to visualize an isobaric ternary phase diagram stemming from the information generated by the code TERNARY (see some computational detail in Ottonello et al., 2013; Belmonte et al., 2017). HERNARY is itself a simplified, user friendly, version of NKCMAS (unpublished), a thermochemical package able to compute all thermodynamic properties of solids and melts and returning divariant, univariant and invariant loci defined through application of the Gibbs free energy minimization and equality of potential rules coupled with simplicial mesh techniques (Attene & Ottonello, 2011; Natali et al., 2011, 2013). NKCMAS is (until now) the unique code able to work with 4 component systems (and at whatever P, T of interest in planetary physics (see an illustrative application in Ottonello, 2018).

TRIDESCENT reduces the numerical noise which perturbs the univariant loci, through an adaptive simplicial mesh (densified around cusps, cotectics and invariant points.). It generates the thermal landscape, the liquidus surface represented by thermal contours and segmented by tessellation in discrete areas representing the Primary Phase Fields (PPF). It is able also to determine Alkemade points thanks to the adaptive sampling routine. It returns (through various subroutines) the cooling path of a liquid from a selected position within a PPF, toward a cotectic line and finally down to an invariant point. Along the path, TRIDESCENT recovers the relevant thermodynamic informations (enthalpy, entropy, heat capacity, density, latent heat of crystallization of solids and liquids, molar phase proportions at all T), down to the last evolutionary point. Data are collected in form of tables or as graphs to follow the behavior of solid/liquid and solid/solid ratios and thermochemical data vs T. Although the main diagram reflect the original output of the TERNARY code (pure oxides at P, T of interest as components) it is possible to plot separately various sub-systems of widespread utilization in petrology (i.e. petrological phase diagrams). These may be expanded at wish, to observe some cryptic details of areas. TRIDESCENT is applicable to a wide range of systems up to hundreds of GPa and could be of great help in deciphering the complex open-system paths followed by ascending diapirs and/or the fractional crystallization processes acting on stationary magma chambers.

Attene M. & Ottonello G. (2011) - Computational geometry meets material science. *ERCIM News*, 84, 43-44.

Belmonte D., Ottonello G., Vetuschi Zuccolini M. & Attene M. (2017) - The system MgO-Al₂O₃-SiO₂ under pressure: A computational study of melting relations and phase diagrams. *Chem. Geol.*, 461, 54-64.

Natali M., Attene M. & Ottonello G. (2011) - Eurographics Italian Chapter Conference.

Natali M., Attene M. & Ottonello G. (2013) - Steepest descent paths on simplicial meshes of arbitrary dimensions. *Computers & Graphics*, 37, 687-696.

Ottonello G., Attene, M., Ameglio, D., Belmonte, D., Vetuschi Zuccolini, M. & Natali M. (2013) - Thermodynamic investigation of the CaO-Al₂O₃-SiO₂ system at high P and T through polymer chemistry and convex-hull techniques. *Chem. Geol.*, 346, 81-92

Ottonello G. (2018) - Ab initio reactivity of Earth's materials. *La Rivista del Nuovo Cimento*, 41, 225-289.

S12

**Advances in Understanding Geological and Petrological
Processes in the Oceanic Lithosphere**

CONVENERS AND CHAIRPERSONS

Giulio Borghini (Università di Milano)

Camilla Palmiotto (ISMAR Bologna)

Alessio Sanfilippo (Università di Padova)

Structural and metamorphic evolution of Gias Vej serpentinites (Piemonte Zone, Lanzo Valley, Italian Western Alps)

Assanelli M.*¹, Luoni P.¹, Rebay G.² & Spalla M.I.¹

¹ Dipartimento di Scienze della Terra “A. Desio”, Università degli Studi di Milano, Italy.

² Dipartimento di Scienze della Terra e dell’Ambiente, Università degli Studi di Pavia, Italy.

Corresponding email: matteo.assanelli@studenti.unimi.it

Keywords: Eclogitized ophiolites, Alpine subduction, multiscale structural analysis.

Thin slivers of metabasites and serpentinites, quartzite, calcschist, fine-grained gneisses (metasediments and metagranitoids) mark the boundary between Piemonte Zone (PZ) metaophiolites and the Sesia-Lanzo Zone (SLZ - Austroalpine Domain), extending from Santanel klippe to Lanzo Massif, over a distance of 50 km. In the upper Tesso valley, in the surroundings of P.ta Gias Vej, numerous slices of serpentinites occur in this subduction-related tectonic mixing. These serpentinites together with the other rocks of SLZ and PZ underwent four episodes of deformation, giving rise to a complex regional tectono-stratigraphy. The earliest deformational structures are represented by up to ten meter-scale isoclinal rootless folds. The metamorphic mineral assemblages marking successive foliations indicate that all rock units (Spalla et al., 1983; Gosso et al., 2015) experienced an early eclogite-facies imprint, followed by re-equilibration under blueschist-facies conditions, and that they were finally widely retrogressed under greenschist-facies conditions during the last two deformation stages (D3 and D4 structures). To refine the tectono-metamorphic history of ultramafites a microstructural and mineral-chemical investigation has been performed to integrate the meso-structural analysis, both on Ol-, Ti-Chu- and Di-bearing serpentinites and Di-bearing chloritic schists. Variations in chemical compositions of mineral phases underlying superposed fabrics, developed under different metamorphic environments, will be explored and compared with those from Zermatt-Saas eclogitized serpentinites (Rebay et al., 2012; Luoni et al., 2018).

Gosso G., Rebay G., Roda M., Spalla M.I., Tarallo M., Zanoni D. & Zucali M. (2015) - Taking advantage of petrostructural heterogeneities in subduction-collisional orogens, and effect on the scale of analysis. *Per. Mineral.*, 84, 779-825.

Luoni P., Rebay G., Spalla M.I. & Zanoni D. (2018) - UHP Ti-chondrodite in the Zermatt-Saas serpentinite: Constraints on a new tectonic scenario. *Amer. Miner.*, 103, 1002–1005.

Rebay G., Spalla M.I. & Zanoni D. (2012) - Interaction of deformation and metamorphism during subduction and exhumation of hydrated oceanic mantle: Insights from the Western Alps. *J. Metam. Geol.*, 30, 687-702

Spalla M.I., De Maria L., Gosso G., Miletto M. & Pognante U. (1983) - Deformazione alpina e metamorfismo nel settore esterno della Zona Piemontese e il Massiccio di Lanzo (Alpi Occidentali). *Mem. Soc. Geol. Ital.*, 26, 499-514.

pMELTS modeling of depleted melts evolution in oceanic environment: implications of pyroxenite formation as deep melt segregation

Basch V.¹, Rampone E.*¹, Ferrando C.², Borghini G.³ & Zanetti A.⁴

¹ DISTAV, Università di Genova, Italy.

² CRPG Nancy, France.

³ Dipartimento di Scienze della Terra, Università di Milano, Italy.

⁴ IGG-CNR, Pavia, Italy.

Corresponding email: betta@dipteris.unige.it

Keywords: pyroxenite, melt-rock reaction, oceanic lithosphere.

Pyroxenites are diffuse in fertile mantle peridotites and considered an important component in the mantle source of oceanic basalts. They are rarely documented in abyssal and ophiolitic peridotites representing residual mantle after melt generation, and few studies defining their origin are to date available. We present a field-based microstructural and geochemical investigation of the pyroxenite layers associated to depleted peridotites from the Mt. Maggiore ophiolitic body (Corsica, France). Pyroxenites are mostly spinel websterites and occur as parallel layers preserving the same orientation throughout the whole peridotite massif. They are affected by multiple episodes of melt-rock interaction, as previously documented in the associated peridotites.

In places, pyroxenite layers are partially dissolved by spinel-facies reactive melt migration, with pyroxene porphyroclasts partly replaced by interstitial olivine. Subsequent plagioclase-facies melt impregnation leads to [orthopyroxene + plagioclase] intergrowths crystallized at the expense of olivine and clinopyroxene. Field and petrographic evidence thus indicate that pyroxenite emplacement preceded the melt-rock interaction history that affected this mantle sector during Jurassic exhumation. In the pyroxenites, pyroxenes show major element compositions similar to abyssal pyroxenites from slow-spreading ridges, indicative of magmatic segregation at pressures higher than 7 kbar. Accordingly, geothermometric estimates on orthopyroxene-clinopyroxene pairs prior to exsolution (using areal analyses as primary pyroxene composition) yield magmatic equilibrium temperatures of 1200-1300°C. In the pyroxenites, both primary spinel-facies clinopyroxene and plagioclase crystallized by impregnating melts exhibit low Na₂O contents and significant LREE depletion. Such mineral compositions indicate a depleted signature of pyroxenite parental melts as well as impregnating melts, corresponding to single melt increments formed after 6% mantle fractional melting. We performed pMELTS thermodynamic modeling of DMM decompressional melting producing such depleted melt, followed by its evolution during deep segregation of pyroxenite layers, spinel-facies reactive porous flow and plagioclase-facies impregnation. These models show that the percolation of depleted single melt increments from spinel-facies to plagioclase-facies depths can account for the observed melt-rock interaction microstructures and major element mineral compositions analyzed in the Mt. Maggiore peridotitic body. Major element modeling also shows that the early process of pyroxenite formation at depth is of utmost importance in the chemical evolution of the percolating melts.

Early days of the plate tectonics revolution: “Geo-data gatherers” versus “Geopoets”

Bonatti E.*¹⁻²

¹ Istituto di Scienze Marine, CNR, Bologna.

² Lamont Doherty Earth Observatory, Columbia University, NY (USA).

Corresponding email: enrico.bonatti@bo.ismar.cnr.it

Keywords: plate tectonics, sea floor spreading.

The scientific revolution that led to the construction and acceptance of Plate Tectonics took place in the years 1960-1970. The success of the revolution was due in good part to the activity of two types of geoscientists. One type includes the “data gatherers”, i.e., scientists with the ability and stamina to collect new data that modify old paradigms. The other type includes a few “geopoets”, who possess intuition and imagination leading to new ideas and interpretations. A leading example of a “data gatherer” in those years is Maurice Ewing, founder and director of Columbia’s University Lamont Earth Observatory, with a small research vessel, the Vema, that sailed continuously across the oceans gathering a wealth of geophysical and geological new data. A foremost example of “geopoet” is Harry Hess of Princeton University, who in 1962 proposed the concept of “sea floor spreading” leading the way to the Plate Tectonics break through. The combined contribution of these two types of scientists led to the success of the theory.

Partial melting experiments on olivine-free pyroxenites at 2 GPa

Borghini G.*¹ & Fumagalli P.¹

¹ Dipartimento di Scienze della Terra “Ardito Desio”, Università di Milano, Italy.

Corresponding email: giulio.borghini@unimi.it

Keywords: partial melting, mantle pyroxenite, experimental petrology.

Mafic heterogeneities are thought to be incorporated into the Earth mantle as recycled oceanic crust. At depth, high-silica melts produced by partial melting of mafic rocks might interact with peridotites and form hybrid olivine-free pyroxenites ($P > 2$ GPa, Mallik & Dasgupta, 2012). However, their role in the decompressional evolution of a heterogeneous mantle is still poorly known due to the lack of experimental data at lower pressure. The phase relation and melting behavior of olivine-free lithologies are essential for understanding how their partial melts impact on the chemistry of primitive magmas or create further mantle heterogeneities by the reaction with mantle peridotite.

We carried out piston cylinder experiments on the olivine-free pyroxenite Px1 (Sobolev et al., 2007) to study its melting behavior and the composition of partial melts at 2 GPa. Px1 bulk composition results from interaction of a peridotite with eclogitic melt until complete consumption of olivine; it is characterized by a relatively high X_{Mg} (0.81) and SiO_2 content (52.9 wt%), moderate Al_2O_3 (11.3 wt%) and low CaO abundances (7.6 wt%).

At 1250°C, subsolidus Px1 is a garnet websterite formed by 51% clinopyroxene, 30% orthopyroxene and 19% garnet. At 2 GPa, the solidus of Px1 is located between 1250 and 1280°C, at about 70°C lower than a fertile lherzolite. At increasing melt fraction, the sequence of mineral phase disappearance is garnet-clinopyroxene-orthopyroxene. Across the solidus, partial melting of Px1 is controlled by reaction garnet + cpx = liq + opx, and above 1300°C, once garnet is completely consumed, by reaction cpx + opx = liq. Orthopyroxene is the liquidus phase and at 1480°C Px1 is completely molten indicating a melting interval of about 200°C. Isobaric melt productivity is similar to garnet clinopyroxenites and it is more than three times that of fertile lherzolite at 1400°C. Px1 partial melts cover a wide range of X_{Mg} (0.57-0.84), with SiO_2 , Al_2O_3 and Na_2O decreasing and Cr_2O_3 increasing with degree of melting. CaO content in partial melts increases until clinopyroxene is involved in melting reaction and decreases after its exhaustion. At 2 GPa and for melting degrees higher than 10%, Px1 produces MgO-rich basaltic andesites. These melts have high silica-activity and therefore they are expected to potentially react with peridotite as confirmed by pyroxenite-peridotite reaction experiments (Borghini et al., this conference).

Borghini G., Fumagalli P. & Rampone E. (2019) - Peridotite modification via interaction with basaltic-andesite melts: pyroxenite-peridotite reaction experiments at 2 GPa. This conference.

Mallik A. & Dasgupta R. (2012) - Reaction between MORB-eclogite derived melts and fertile peridotite and generation of ocean island basalts. *Earth and Planetary Science Letters*, 329-330, 97-108.

Sobolev A.V., Hofmann A.W., Kuzmin D.V., Yaxley G.M., Arndt N.T., Chung S.L., Danyushevsky L.V., Elliott T., Frey F.A., Garcia M.O., Gurenko A.A., Kamenetsky V.S., Kerr A.C., Krivolutskaya N.A., Matvienkov V.V., Nikogosian I.K., Rocholl A., Sigurdsson I.A., Sushchevskaya N.M. & Teklay M. (2007) - The amount of recycled crust in sources of mantle-derived melts. *Science*, 316, 412-417.

Cold spots at Mid Ocean Ridges help revealing mantle heterogeneity: a summary of the SMARTIES cruise in the Equatorial Atlantic

Brunelli D.^{*1-2}, Maia M.³, Ligi M.², Bonatti E.²⁻⁴, Briais A.⁵, Campos T.⁶, Ceuleneer G.⁵, Cipriani A.¹⁻⁴,
Cuffaro M.⁷, Gregory E.⁸, Hamelin C.⁹, Jbara R.⁵, Kaczmarek M.-A.⁵, Lombardi F.¹, Moreira S.⁶,
Mougel B.¹⁰, Petracchini L.⁷, Puzenat V.⁸, Revillon S.³, Seyler M.¹¹, Soltanmohammadi A.⁵, Verhoest L.¹⁻³,
Trivellato T.³ & Wang Z.⁸

¹ DSCG, Università di Modena e Reggio Emilia, Italy.

² ISMAR-CNR, Bologna, Italy.

³ Laboratoire Géosciences Océan, Institut Universitaire Européen de la Mer, France.

⁴ Lamont Doherty Earth Observatory, Columbia University, New York, NY, USA.

⁵ GET (CNRS/INSU-UPS-IRD), Obs. Midi-Pyrenees, Toulouse, France.

⁶ Departement of Geology, Federal University of Rio Grande do Norte, Brazil.

⁷ IGAG-CNR, Roma, Italy.

⁸ Laboratoire de Géosciences Marines, IGP, Paris, France.

⁹ University of Bergen, Department of Earth, Norway.

¹⁰ Centro de Geociencias, UNAM, Campus Juriquilla, Querétaro, México.

¹¹ Laboratoire d'Océanologie et de Géosciences, UFR des Sciences de la Terre, Lille, France.

Corresponding email: daniele.brunelli@unimore.it

Keywords: mantle heterogeneity, Mid Atlantic Ridge, mantle potential temperature.

The heterogeneity of the suboceanic mantle source is usually defined based on MORB lateral geochemical variability. However, tackling short-scale variability is partially hampered by the large extent of mixing occurring during melt extraction and magma chamber processes. We identified a singular region of the Mid Atlantic Ridge at the eastern Romanche Ridge-Transform Intersection (Equatorial Atlantic) characterized by an extreme lateral thermal gradient. Cooling of the upwelling mantle is here induced by heat transfer to a ca. 50 Ma old plate fronting the ridge-transform intersection. Cooling of the plate edge affects the upper mantle for the whole range where melting usually occurs (30-80 km bsl). The resulting ridge axis consequently shows a lateral gradient in magma productivity and composition (Bonatti et al., 2001 and references therein). MORBs erupted at the ridge centre give rise to a “normal” 5 km thick magmatic crust. Moving to the axial tip magmatism diminishes in volume till zero and progressively increases its alkaline character along with the compositional variability revealing the short-scale heterogeneity of the mantle source (Ligi et al., 2005). This thermal and tectonic configuration represents a regional scale natural experiment where to test the effect of varying mantle potential temperature on a given mantle source. Melting a heterogeneous mantle has profound implications on the km-scale heat transfer because of the differential onset of melting of variably fertile lithologies (Brunelli et al., 2018). Here, we will present the results of the upcoming French-Italian SMARTIES expedition, taking place in July-August 2019. We will present a new high-resolution bathymetric coverage of the RTI and peculiar tectonic features where magma is nearly absent accompanied by direct submarine observations and sampling from Nautilite dives.

Bonatti E., Ligi M., Carrara G., Gasperini L., Turko N., Perfiliev S., Payve A. & Sciuto P.F. (1996) - Diffuse impact of the Mid-Atlantic Ridge with the Romanche transform: an ultracold ridge-transform intersection. *Jour. Geoph. Res.*, 101, 8043-8054.

Ligi M., Bonatti E., Cipriani A. & Ottolini, L. (2005) - Water-rich basalts at mid-ocean-ridge cold spots. *Nature*, 434, 66-69.

Brunelli D., Cipriani A. & Bonatti E. (2018) - Thermal effects of pyroxenites on mantle melting below mid-ocean ridges. *Nat Geosci.*, 11, 520.

Formation of a hybrid oceanic crust at the onset of the Red Sea opening (Tihama Asir magmatic complex; Saudi Arabia)

Deraco M.*¹, Sanfilippo A.¹⁻², Ligi M.³, Rasul N.⁴, Vigliotti L.³, Jerais A.⁴, Tharowi A.⁴,
Langone A.² & Zanetti A.²

¹ Dipartimento di Scienze della Terra e dell'Ambiente, Università di Pavia, Italy.

² CNR-Istituto di Geoscienze e Georisorse, U.O. Pavia, Italy.

³ CNR-Istituto di Scienze Marine, Bologna, Italy ⁴ Saudi Geological Survey, Jeddah, Saudi Arabia.

Corresponding email: matteo.deraco01@universitadipavia.it

Keywords: oceanic crust, continental break-up, Tihama Asir Complex, Saudi Arabia.

The role of magmatism during the continental break-up and the birth of a new ocean is still debated. Recent studies on magma-poor passive margin developed at slow to ultra-slow plate separation velocity suggest that the MORB-type melt forms isolate magmatic intrusions within an exhumed sub-continental mantle, whereas volcanism is nearly absent. On the other hand, at higher magma production rates, gabbros may be emplaced within the lower continental crust, promoting continental rupture and the birth of a new ocean. This study explores the geochemical signature of a crustal sequence located in the south-western Saudi Arabia, the Tihama Asir Magmatic Complex (McGuire and Coleman, 1986). Previous K-Ar determinations on these gabbros constrained the age of formation at 20 to 24 Ma (Coleman et al., 1979), coeval with the syn-rift gabbroic intrusions drilled on the western side of the northern Red Sea (borehole QUSEIR B-1X) and exposed on the Brothers Islands (Ligi et al., 2018). Here we use new major and trace element determinations on bulk rock and mineral phases to constrain the origin of the melt fractionating the gabbros and their conditions of emplacement. Clinopyroxene (Cpx) in the gabbros are progressively enriched in LREE at increasing degree of fractionation ($La_N/Sm_N = 0.21-0.43$) and have low Nd_N/La_N ratios (3.48-1.60) compared to Cpx in equilibrium with MORB. The calculated liquid in equilibrium with the most enriched Cpx have a transitional affinity, similar to the melt forming the overlying dyke complex. These data indicate that the melt originating the gabbros was progressively contaminated by crustal material likely deriving from the host continental crust. Selective enrichments in LREE also characterize the Cpx from other syn-rift gabbros from the northern sector of the Red Sea (i.e., Quseir and Brother Islands; $La_N/Sm_N = 0.10-0.22$). If confirmed, our data indicate that the production of abundant MORB-type magmatism in the Red Sea occurred before the continental rupture, leading to a substantial thermal erosion of the thinned continental crust and generating an embryonic oceanic crust with a hybrid geochemical signature.

Coleman R.G., Hadley D.G., Fleck R.G., Hedge C.T. & Donato M.M. (1979) - The Miocene Tihama Asir ophiolite and its bearing on the opening of the Red Sea. In: Al-Shanti, A.M. (ed) *Evolution and Mineralization of the Arabian Shield*. Pergamon Press Ltd, Oxford, pp. 173–186.

McGuire, A.V. & Coleman R.G. (1986) - The Jabal Tif layered gabbro and associated rocks of the Tihama Asir complex. SW Saudi Arabia. *J. Geol.*, 94, 651–665.

Ligi, M., Bonatti E., Bosworth W., Cai Y., Cipriani A., Palmiotto C., Ronca S. & Seyler M. (2018) - Birth of an Ocean in the Red Sea: Oceanic-type Basaltic Melt Intrusions precede continental rupture. *Gondwana Research*, 54, 150-160.

Pyroxenite diversity in the New Caledonia mantle sequence: a preliminary study

Ferrari E.*¹, Montanini A.¹, Secchiari A.¹, Bosch D.² & Cluzel D.³

¹ Dipartimento di Scienze Chimiche, della Vita e della Sostenibilità Ambientale, Università di Parma.

² Géosciences Montpellier - Université Montpellier, France.

³ Université de la Nouvelle-Calédonie, New Caledonia.

Corresponding email: elisa.ferrari@unipr.it

Keywords: New Caledonia, ophiolitic sequence, pyroxenites.

The New Caledonia ophiolitic sequence consists of mantle rocks (harzburgites and minor lherzolites) locally overlain by mafic-ultramafic cumulates. The harzburgites are highly refractory residues which underwent fluid-assisted melting in a fore-arc setting (e.g. Secchiari et al., 2019), whereas the moderately depleted lherzolites show an abyssal-type affinity (Secchiari et al., 2016). In this study we report the first petrological data on pyroxenites associated with the peridotites. The pyroxenites were collected in the harzburgites from the central part of the island (Bogota Peninsula) and in the northern lherzolites (Poum Massif). The Bogota mylonitic harzburgites record deformation along a paleotransform fault (Prinzhofer and Nicolas, 1980; Teyssier et al., 2016). The pyroxenites (~5-15 cm thick) generally cut at variable angles the peridotite foliation but concordant layers, locally boudinaged, also occur, thus suggesting emplacement during and after HT shearing deformation (Titus et al., 2011). Pyroxenites display textures ranging from cumulitic to porphyroclastic or granoblastic-polygonal. They include orthopyroxenites (Opx+Cr-Spl ±Ol) and websterites, (Opx+Cpx ± Cr-Spl± Edenite). The pyroxenites commonly have refractory assemblages characterized by Opx and Cpx with high Mg# (91-92 and ~93, respectively), Cr-rich spinel (Cr# = 50-61) and Fo-rich olivine (91-93 mol%), whereas Cpx and Opx with higher Fe contents and negligible Cr₂O₃ occur in the amphibole-bearing rocks. The Poum lherzolites contain cm-thick concordant orthopyroxenites characterized by exsolved Opx (Mg# ~91-92), Fo-rich Ol (91-92 mol%), Spl with variable Cr# (25-52) and small amounts of Cpx. Equilibration T calculated employing conventional pyroxene geothermometers for the Bogota pyroxenites (930-1040°C) are comparable with those obtained for the enclosing harzburgites (~950°C). The Poum pyroxenite yields higher T (~1000-1100°C) in the range of those determined for the porphyroclastic assemblage of the host lherzolites (Secchiari et al., 2016).

Prinzhofer A. & Nicolas A. (1980) - The Bogota Peninsula, New Caledonia: A possible oceanic transform fault. *J. Geol.*, 88, 387-398.

Secchiari A., Montanini A., Bosch D., Macera, P. & Cluzel D. (2016) - Melt extraction and enrichment processes in the New Caledonia lherzolites: evidence from geochemical and Sr-Nd isotope data. *Lithos*, 260, 28-43.

Secchiari A., Montanini A., Bosch D., Macera, P. & Cluzel D. (2019) - Sr, Nd, Pb and trace element systematics of the New Caledonia harzburgites: Tracking source depletion and contamination processes in a SSZ setting. *Geosci. Front.*, in press.

Teyssier C., Chatzaras V. & Von Der Handt A. (2016) - Microfabrics in depleted mantle paleotransform (New Caledonia). *Geophys. Res. Abstr.*, 18.

Titus S.J., Maes S.M., Benford B., Ferré E.C. & Tikoff B. (2011) - Fabric development in the mantle section of a paleotransform fault and its effect on ophiolite obduction, New Caledonia. *Lithosphere*, 3, 221-244.

The role of melt/rock ratio in olivine-rich troctolite formation via basalt-dunite reaction: an experimental study at 0.5 GPa

Grammatica M.*¹, Fumagalli P.¹ & Borghini G.¹

¹ Dipartimento di Scienze della Terra “Ardito Desio”, Università di Milano, Italy.

Corresponding email: michela.grammatica@unimi.it

Keywords: melt-olivine reaction, troctolite, high-pressure experiments.

Microstructural and chemical evidence supports the origin of olivine-rich troctolites through multistage interactions between a precursor mantle dunite and an infiltrating basalt (Drouin et al., 2010). Borghini et al. (2018) recently performed reactive dissolution and crystallization experiments juxtaposing MORB-type glasses on a melt-bearing dunite at 1300°C and then cooling to 1150°C at constant pressure (0.5 and 0.7 GPa). Their results showed that olivine-rich troctolites might form through dunite infiltration followed by reactive crystallization of interstitial melts resulting in textural relations and mineral chemistry comparable with natural rocks. Significantly they suggested that the initial melt/rock ratio strongly influences the extent of interaction and, thus, the final mineral abundances and chemistry. However, the reaction couple strategy used in their experiments did not allow a quantification of the role of melt/rock ratio. At this purpose, we are performing piston cylinder experiments at 0.5 GPa using a mixture of San Carlos olivine (Fo₉₀) and a reacting MORB-type melt at variable proportions olivine:melt (9:1, 3:1 and 1:1). For each mixture, we perform at 0.5 GPa both isothermal run at 1300°C for 24 hours and crystallization experiment step cooled at a rate of 1°C/min from 1300°C down to 1100°C. Specific aims are to define and quantify how the melt/rock ratio controls the amount of olivine dissolution, the lithology produced by reaction, and the final mineral chemistry. Preliminary results of the isothermal experiment run at 0.5 GPa and 1300°C with 25 wt% of initial basalt powder in the starting mix (olivine:melt 3:1) show run products made of olivine and glass. Olivine occurs both as large subhedral crystals with straight and lobate curvilinear rims against the interstitial glass or as smaller rounded grains. Mineral chemistry indicates that after the high-temperature interaction reacted olivine has slightly lower X_{Mg} and higher CaO contents. Remarkably, NiO content is significantly lower than that of the starting San Carlos olivine and it is still lower than NiO content in olivine from reaction experiments with lower melt/olivine ratios. Compared to the initial melt, final glass composition is characterized by higher X_{Mg}, SiO₂ and NiO contents and lower FeO, Cr₂O₃ and Al₂O₃ abundances.

Borghini G., Francomme J.E. & Fumagalli P. (2018) - Melt-dunite interactions at 0.5 and 0.7 GPa: experimental constraints on the origin of olivine-rich troctolites. *Lithos*, 323, 44-57.

Drouin M., Ildfonse B. & Godard M. (2010) - A microstructural imprint of melt impregnation in slow spreading lithosphere: olivine-rich troctolites from the Atlantis Massif, Mid-Atlantic Ridge, 30°N, IODP Hole U1309D. *Geochem. Geophys. Geosyst.*, 11, 1-21.

Listvenites in the western Alps: the case of the Mount Avic massif (Aosta Valley, northwestern Alps)

Guerini S.*¹ & Tartarotti P.¹

¹ Dipartimento di Scienze della Terra “Ardito Desio”, Università degli Studi di Milano.

Corresponding email: sara.guerini@unimi.it

Keywords: listvenite, carbonation, Mount Avic massif.

Within the Western Alps, listvenites are closely linked to the presence of fragile structures pertaining to the Oligocene Aosta-Ranzola fault system (AR). Evidences of hydrothermal circulation along the AR fault system and related structures, are represented by gold-bearing mesothermal veins and by fault rocks strongly affected by hydrothermal alteration (listvenites). The formers occur in the Ayas Valley, in the Arcesa-Brusson area, inside the Monte Rosa and Gran Paradiso basement, the latter are found along the AR, Ospizio Sottile and Rocca di Verra faults. Listvenitic breccias display spatial-temporal links with quartz veins, pointing to the existence of various hydrothermal pulses of Late Oligocene age.

In the southernmost part of the Mt. Avic ultramafic massif, listvenites crop out along an E-W fault surface, possibly related to the Oligocene AR fault system, exposed within Atg-Mag-Ti-Chu-bearing serpentinites. Detailed field mapping and petrological studies document the listvenitization processes occurring in serpentinites, allowing to interpret the origin of the fluids which drove the metasomatic reactions. According to Rose (1837), listvenite is composed of carbonates (magnesite, ankerite, breunerite), quartz and Cr-rich mica (fuchsite or mariposite) and disseminated sulphides. Based on the average mineralogical assemblage, the analysed samples pertain to the epilistvenitic type of listvenites (*sensu* Kashkai and Allakhverdiev, 1965). In fact, these are made of a cryptocrystalline foliated matrix composed of Qz+Mgs+Fuchsite which envelopes trails of opaque minerals (Mag and Cr-rich Mag), marking S_2 foliation planes and relict D_2 fold hinges, and accessory minerals (such as sulfides, Chl, Srp, Ab and Na-Amp).

EMPA analyses revealed that Mgs ($MgCO_3$, 79.52-98.60 wt.%) is the only type of carbonate. Mgs is intergrown with Qz or chalcedony that shows high Fe, Mg and Al contents (0.00-8.00 wt.%). Cr_2O_3 content inside Fuchsite ranges from 2.96 to 11.10 wt.%. Opaque minerals are dominantly Mag (Fe_3O_4 : 59.30-96.10 wt.%) with Cr-rich cores (Cr_2O_3 : 16.80 to 25.60 wt.%).

The apparent absence of gold mineralizations within the analysed samples from the Mt. Avic ultramafic massif, allow to consider the role of the brittle structures associated with the AR system in remobilizing Au and concentrating it in distal areas such as the Ayas Valley, the Arcesa-Brusson area, the Monte Rosa Massif and the Gran Paradiso basement, which pertain to different tectonic domains.

Kashkai M.A. & Allakhverdiev Sh.I. (1965) - Listvenites, their origin and classification. (Listvenity, ikh genezis i klassifikatsiia: Akad. Nauk Azerbaidzhanskoi SSR, Institut Geologii im. akad. I.M. Gubkina; Izdat. Akad. Nauk Azerbaidzhanskoi SSR, Baku, 142pp.

Rose G. (1837) - Mineralogisch-geognostische Reise nach dem Ural, dem Altai und dem Kaspischen Meere. Volume 1: Reise nach dem nördlichen Ural und dem Altai. Berlin, C.W. Eichhoff (Verlag der Sanderschen Buchhandlung), 641pp.

Observing oblique slip during rift-linkage processes in Northern Afar

La Rosa A.^{*1-2}, Pagli C.², Keir D.¹⁻³, Sani F.¹, Corti G.⁴, Wang H.⁵ & Posee D.³

¹ Università di Firenze.

² Università di Pisa.

³ University of Southampton.

⁴ Consiglio Nazionale delle Ricerche.

⁵ Guangdong University of Technology.

Corresponding email: alessandro.larosa@unifi.it

Keywords: Rift-linkage, InSAR, Afar.

Mid-ocean ridges are segmented and offset along their length. However, the processes leading to growth of the segments and linkage of deformation between offsets are still debated. The continental rift of Afar offers an opportunity to observe these processes, showing tectonic and magmatic features similar to that observed at slow-spreading mid-ocean ridges. The Afar depression results from the divergence of the Nubian, Arabian and Somalian plates along the Red Sea, Gulf of Aden and Main Ethiopian rift arms during the last 30 My. Along the Erta Ale ridge in Northern Afar the extension along the plate boundary is ~N60°E and is focused in ~20km-wide, ~70km-long en-echelon magmatic segments. The surface morphology of the segments is dominated by NNE striking cone fields, and fractures cutting Holocene basaltic lava flows. Here we used InSAR, seismicity, and structural data from analysis of satellite imagery and field measurements to study the deformation in the area connecting the Erta Ale and Tat Ali segments of northern Afar. Modelling of InSAR measurements from co-seismic deformation of a $M_L \sim 5.0$ earthquake in October 2007 shows mainly oblique left-lateral slip along ~N-S-oriented faults, similar to the source mechanism achieved from seismic moment tensor inversion. Structural analysis and field measurements of left-lateral shear, such as horsetail-type fault tips and lozenge-shape structures were also observed, in agreement with geodetic observations. However, orientation of faults planes based on analysis of satellite imagery combined with local earthquake focal mechanisms during 2011/2012 shows evidence for right-lateral slip on conjugate NW-SE striking faults in the same region (Illsley-Kemp et al., 2018). Both InSAR and structural data indicate a local extension with direction ~N50°E in the region connecting the two rift segments, hence oblique to the faults. Our observations are consistent with a model of rift linkage through a dextral oblique transfer zone, causing counter-clockwise rotation of the extension direction. We conclude that oblique slip occurs on a conjugate fault set in the offset zone connecting the Erta Ale and Tat Ali segments.

Illsley-Kemp F., Bull J. M., Keir D., Gerya T., Pagli C., Gernon T., Ayele A., Goitom B., Hammond J.O.S. & Kendall J.M. (2018) - Initiation of a Proto-transform Fault Prior to Seafloor Spreading. *Geochemistry, Geophysics, Geosystems*, 19(12), 4744–4756. <https://doi.org/10.1029/2018GC007947>.

Global Seafloor Spreading Variations and the Evolution of Seawater Composition since the Mesozoic

Ligi M.*¹, Bonatti E.¹⁻², Brunelli D.¹⁻³ & Cuffaro M.⁴

¹ Istituto di Scienze Marine, CNR, Bologna, Italy.

² Lamont Doherty Earth Observatory, Columbia University, Palisades, New York, USA.

³ Dipartimento di Scienze Chimiche e Geologiche, Università di Modena e Reggio Emilia, Italy.

⁴ Istituto di Geologia Ambientale e Geoingegneria, CNR, Rome, Italy.

Corresponding email: marco.ligi@bo.ismar.cnr.it

Keywords: seawater composition, Mg/Ca increase, seafloor spreading, mantle hydration.

There is strong evidence that the seawater composition has not been at steady state over geological time scales. Global cycles, such as sea-level changes, the carbon cycle, and seawater chemistry, are assumed to be partly due to temporal variations of the rates of ocean-floor spreading. Several studies have modelled the evolution of seawater composition during Phanerozoic, or have estimated changes from fluid inclusions; from pore fluid chemistry; from marine biogenic carbonates; from ridge flank hydrothermal carbonate veins; and from Mg, B and S isotope composition. While there is disagreement over the causes of seawater compositional changes, there is a general consensus that the Mg and Ca concentration in seawater has varied during Phanerozoic; in particular, that Mg/Ca has risen over the past 80 Ma as a consequence of both an increase of seawater Mg concentration and a decrease of Ca concentration. It appears that the Mg/Ca ratio of the Mesozoic ocean was 3 to 5 times lower than that of modern oceans. We show here that reactions of mantle-derived peridotites with seawater along slow spreading mid ocean ridges contributed to the post-Cretaceous Mg/Ca increase (Snow and Dick, 1995; Ligi et al., 2013). The amount of hydration of the oceanic mantle depends directly on the amount of cold fluids brought down into the mantle during hydrothermal circulation at ridges. Mantle rocks-seawater reactions can release to modern seawater roughly 20% of the yearly Mg river input. A corresponding decrease of hydrothermal seawater/basalt reactions lowers Ca input to and Mg extraction from the ocean. However, no significant peridotite-seawater interaction and Mg release to the ocean occur in fast spreading, East Pacific Rise-type ridges.

We modelled the effect on Mg, Mg isotopes and Ca seawater concentration of (a) variations through time of oceanic crustal production and (b) volume of low-temperature mantle hydration related to changes in spreading rates and accretionary plate boundary geometry. Model results suggest that three important processes have affected temporal variations of seawater composition during the last 150 Ma: (1) hydrothermal circulation in basalts; (2) low-temperature MORP/seawater reactions; and (3) dolomite formation. Given that the calculated oceanic crust production was higher during the Cretaceous than in the Cenozoic, we estimated a greater hydrothermal Mg-uptake by the crust and Ca-release in the Cretaceous than in the Cenozoic.

Snow J.E. & Dick H.J.B. (1995) - Pervasive magnesium loss by marine weathering of peridotite. *Geochim. Cosmochim. Acta*, 59, 4219-4235.

Ligi M., Bonatti E., Cuffaro M. & Brunelli D. (2013) - Post-Mesozoic rapid increase of seawater Mg/Ca due to enhanced mantle-seawater interaction. *Scientific Reports*, 3, 1-8.

UHP relics in the Zermatt-Saas Zone serpentinites: new puzzle tiles in the geodynamic scenario

Luoni P.*¹, Rebay G.², Roda M.¹, Spalla M.I.¹ & Zannoni D.¹

¹ Università degli Studi di Milano, Dipartimento di Scienze della Terra “A. Desio”.

² Università degli Studi di Pavia, Dipartimento di Scienze della Terra e dell’Ambiente.

Corresponding email: pietro.luoni@unimi.it

Keywords: Piemonte zone, Ti-chondrodite, numerical modelling.

Ti-chondrodite (Ti-Chn) and Ti-clinohumite (Ti-Chu) assemblages in the eclogitized serpentinites indicate that UHP conditions are attained, in other localities of the Zermatt-Saas Zone (ZSZ) besides Cignana Unit. This finding changes the tectonic scenario of the north-western portion of the Alpine ophiolites. This recognition has been possible by multiscale structural analysis and detailed mapping (1:20 scale) integrated with petrological investigation of serpentinites at Créton (upper Valtouranche, north-western Italy). Polyphasic ductile deformation transposed original lithostratigraphy of serpentinites comprising magnetite-rich layers, rare veins of Ti-chondrodite + Ti-clinohumite, olivine-rich and pyroxenite layers and lenses. S2 is the dominant fabric in the region and at Créton; it preserves relics of earlier foliation or isoclinal rootless folds (pre-D2) and is crenulated and intersected by shear zones. Pre-D2 mineralogical and textural relicts are preserved regardless the pervasive development of S2 HP-UHP foliation in serpentinites. Pre-D2 mineral assemblages consist of Cpx or Ol + Ti-Chn + Spl + Atg ± Chl. Ti-Chn + Ti-Chu polygonal aggregates (with minor Chl + Ilm + Mag + Atg + Cpx or Ol) can be interpreted as either predating S2 or synkinematic with the early stages of S2 development (pre- to early-D2). The occurrence of Ol + Ti-Chn + Spl implies recrystallization under UHP conditions ($P = 2.8\text{--}3.5$ GPa, $T = 600\text{--}670$ °C), similarly to those recorded by the nearby Cignana Unit rocks, where coesite and microdiamond have been found. Furthermore, the P-T conditions for D2 assemblages at Créton are similar to those estimated for D2 in the surrounding serpentinites, which were dated at 65 ± 5.6 Ma. These results, coupled with P-T peak condition proposed in this work, lead to consider that the ZSZ was already buried at depth before 70 Ma and dramatically widen the subduction time span under which ZSZ recorded P-T peak conditions. Such observations support the idea that ZSZ is a mosaic of ophiolitic tectono-metamorphic units, which recorded P-peak conditions in different times, and that were coupled during Alpine exhumation, as suggested by quantitative geodynamic modelling.

From dislocation creep to grain boundary sliding in high-temperature troctolites: insights into shear localization mechanisms in the oceanic crust

Maino M.*¹, Casini L.², Sanfilippo A.¹ & Ildefonse B.³

¹ Dipartimento di Scienze della Terra, dell'Ambiente, Università di Pavia, Italy.

² Dipartimento di Chimica e Farmacia, Università di Sassari, Italy.

³ Géosciences Montpellier, Université Montpellier 2, CNRS, Montpellier, France.

Corresponding email: matteo.maino@unipv.it

Keywords: ultramylonite, shear localization, grain boundary sliding.

At high temperature grain size is a fundamental parameter for the evolution of microstructure in mylonite and the rheology thereof. One of the consequences of this microstructural change - i.e., grain-size reduction - is the transition from grain size insensitive (dislocation creep, DC) to grain size sensitive mechanism (grain boundary sliding, GBS), yielding to strain localization in mylonite. GBS is typically associated with a large drop in effective viscosity, and typically characterizes oceanic ultramylonites, which record temperature <800°C. GBS requires the boundaries between grains are extremely weak; thus, it is promoted by fine grain size, large stress and strain rates, and the presence of intergranular fluids. In this contribution, we investigate the effectiveness of this deformation mechanism through a microstructural and petrological study of a troctolite sample collected from the 16.5°N Oceanic Core Complexes of the Mid-Atlantic Ridge. This sample shows a clear transition from proto-mylonite to ultramylonite, which reflects a sharp change in mineralogy (from olivine+plagioclase±clinopyroxene±orthopyroxene±amphibole to amphibole+plagioclase assemblages), texture (plagioclase/clinopyroxene/amphibole CPO), and grain size. The ultramylonite bands has distinctive characteristics suggestive of a switch from dislocation creep to GBS. On the other hand, the ultramylonite records an increase of temperature with respect the mylonite (from 900 to 1000 °C). Taken all together, these evidences rises several questions about the origin of shear localization during the initial, very high-temperature (T>900°C), rifting stages.

Pb isotope composition of recycled mantle pyroxenites: insights into the the HIMU source of oceanic basalts?

Montanini A.¹, Secchiari A.*¹, Bosch D.² & Tribuzio R.³

¹ Dipartimento di Scienze Chimiche, della Vita e della Sostenibilità Ambientale, Università di Parma.

² Géosciences Montpellier - Université Montpellier, France.

³ Dipartimento di Scienze della Terra e dell'Ambiente, Università di Pavia.

Corresponding email: arianna.secchiari@unipr.it

Keywords: Recycled mantle pyroxenites, HIMU, Pb isotope systematics.

Recycled mantle pyroxenites are believed to play a key role in the magma genesis contributing to the radiogenic Pb signatures within the sources of oceanic basalts. In particular, a garnet pyroxenite component derived from recycling of aged oceanic crust is widely advocated to explain the HIMU end-member in the OIB sources. However, natural examples of recycled pyroxenites are rare and the known examples do not meet the required Nd-Hf-Pb isotope characteristics of this component (e.g., Varas Reus et al., 2018). Here, we present Pb isotope systematics of garnet clinopyroxenites and websterites enclosed in fertile mantle sequences of the External Ligurian ophiolites (Northern Apennine). The garnet clinopyroxenite layers have gabbroic crustal precursors that experienced a long-lived evolution of recycling into the mantle (1.5-1.0 Ga), as inferred from Sm-Nd and Lu-Hf isotope systematics, which in addition point to a HIMU affinity (Montanini & Tribuzio, 2015). The garnet clinopyroxenites originated by crystallization of melts produced by partial melting of gabbro-derived eclogites, whereas the websterites were interpreted as secondary pyroxenites with a crustal geochemical fingerprint and a peridotite contribution.

Highly radiogenic present-day Pb isotope compositions were obtained for bulk rocks and clinopyroxene separates from garnet clinopyroxenites. In Pb isotope diagrams, samples exhibit a good positive correlation, with $^{206}\text{Pb}/^{204}\text{Pb}$ extending from MORB field toward the most extreme HIMU components (i.e., St. Helena and Mangaia hotspots). In particular, the pyroxenites and the clinopyroxene separates display somewhat higher $^{207}\text{Pb}/^{204}\text{Pb}$ and lower $^{208}\text{Pb}/^{204}\text{Pb}$ for a given $^{206}\text{Pb}/^{204}\text{Pb}$ than HIMU-type basalts. The less radiogenic values are shown by the websterites containing a peridotite component. Age-corrected Pb isotope compositions of clinopyroxene separates, assuming a melting event at 220 Ma as inferred from Nd-Hf isotopes, are strikingly similar to the most extreme HIMU-type basalts. High-precision LA-ICP-MS analyses of elemental Pb were also performed on the primary HP assemblage of the garnet clinopyroxenites (Al-rich clinopyroxene, garnet and Fe-Ni-Cu sulfides). The results show that clinopyroxene is the main carrier of Pb, whereas Pb is typically below detection limits in sulfides, in contrast with recent measurements on sulfides from abyssal peridotites and pyroxenites (e.g. D'Errico et al., 2019).

The Pb isotope compositions of studied pyroxenites require a long-term evolution of recycled MORB-type gabbros with high and variable U/Pb and Th/Pb ratios. We conclude that these rocks represent a special and rare combination of age and composition of subduction-modified recycled oceanic crust.

Montanini A. & Tribuzio R. (2015) - Evolution of recycled crust within the mantle: constraints from the garnet pyroxenites of the External Ligurian ophiolites (northern Apennines, Italy). *Geology*, 43(10), 911-914.

Varas-Reus M.I., Garrido C.J., Marchesi C. Bosch D. & Hidas K. (2018) - Genesis of ultra-high pressure garnet pyroxenites in orogenic peridotites and its bearing on the compositional heterogeneity of the Earth's mantle. *Geochimica et Cosmochimica Acta*, 232, 303-328.

Isotopic heterogeneity of mantle melts migrating through the Lanzo South Ophiolite: a focus on Re-Os isotopes and PGE

Mosconi A.*¹, Sanfilippo A.¹, Liu C.Z.², Salters V.³, Tribuzio R.¹ & Zanetti A.⁴

¹ DSTA, UNIPV, Pavia, Italy.

² IGGCAS, 19 Beitucheng W Rd, Beijing, China.

³ EOAS and MagLab, FSU, Tallahassee, FL, USA.

⁴ Istituto Geoscienze Georisorse, CNR, Pavia, Italy.

Corresponding email: angelica.mosconi01@universitadipavia.it

Keywords: mantle, ophiolite, Re-Os, PGE.

The Lanzo South ophiolite is a lithospheric mantle section exhumed during the opening of a Jurassic basin akin to the modern slow to ultraslow spreading ridges. The peridotites are mainly constituted by Pl-bearing depleted harzburgites with evidence for refertilisation by MORB-type melts (Piccardo et al., 2007). Here, we found two generations of replacive bodies, in turn, produced by melt with an extreme geochemical variability (Sanfilippo et al., 2019). The first type, concordant to the foliation of the host-rock, is constituted by Px-free dunites and it is related to the migration of melts with a MORB-like geochemical affinity. The second type consists of Px-poor harzburgites that are clearly discordant and geochemically depleted. With this contribution, we show that the whole-rock Re-Os isotopes and PGE compositions of two types of replacive rocks found in the Lanzo South ophiolite agree with a formation by melts with different geochemical affinities.

The host Pl-peridotites have nearly flat PGE patterns and initial $^{187}\text{Os}/^{188}\text{Os}$ ratios (at 165 Ma) of ~ 0.124 , in agreement with an event of refertilization by MORB-type melts. Compared to the host rocks, the MORB-type dunites result preferentially enriched in Pd and Re, though having similar initial $^{187}\text{Os}/^{188}\text{Os}$ ratios (~ 0.123 - 0.126), thereby confirming the formation by MORB-type melts at very high melt flux. Differently, the replacive harzburgites are depleted in Pd and Re and have initial $^{187}\text{Os}/^{188}\text{Os}$ ratios extending towards highly unradiogenic compositions (down to 0.117). The variation in Al_2O_3 initial Os/Os in these rocks agree with the radiogenic Hf compositions of the clinopyroxenes from the same rocks and recall those of the depleted harzburgites from 15.20 FZ in the Atlantic (Harvey et al., 2006; Marchesi et al., 2013) and Gakkel Ridge peridotites (Liu et al., 2008). Our data substantiate the idea that the replacive harzburgites from Lanzo South formed through an incomplete reaction with an ultra-depleted melt originated by an anciently depleted (>1 Gy) portion of the asthenosphere (Sanfilippo et al., 2019).

Liu C.Z., Snow J.E., Hellebrand E., Brüggmann G., Von Der Handt A., Büchl A. & Hofman A.W. (2008) - Ancient, highly depleted heterogeneous mantle beneath Gakkel ridge, Arctic ocean. *Nature*, 452, 311-316.

Piccardo G. B., Zanetti A. & Müntener O. (2007) - Melt/peridotite interaction in the Southern Lanzo peridotite: Field, textural and geochemical evidence. *Lithos*, 94, 1-4.

Sanfilippo A., Salters V., Tribuzio R. & Zanetti A. (2019) - Role of ancient, ultra-depleted mantle in Mid-Ocean-Ridge magmatism. *Earth and Planetary Science Letters*, 511, 89-98.

Highly siderophile elements and Re-Os isotopes of primitive oceanic troctolites: implications for reactive processes during lower crust formation

Renna M.R.*¹, Tribuzio R.²⁻³, Sanfilippo A.²⁻³, Arandola S.⁴, Becker H.⁵ & Wang Z.⁵

¹ Dipartimento di Scienze Matematiche e Informatiche, Scienze Fisiche e Scienze della Terra, Università di Messina.

² Dipartimento di Scienze della Terra e dell'Ambiente, Università di Pavia.

³ IGG-CNR Pavia.

⁴ Department of Applied Geology, Western Australian School of Mines, Curtin University.

⁵ Freie Universität Berlin Institut für Geologische Wissenschaften Arbeitsbereich Geochemie.

Corresponding email: mrenna@unime.it

Keywords: Os isotopes, highly siderophile elements, lower oceanic crust.

The olivine-rich troctolites are the most primitive rocks of the lower oceanic crust. Their petrogenesis is typically related to reaction between an ultramafic protolith and a migrating MORB-like melts crystallizing plagioclase and clinopyroxene. This study reports whole-rock highly siderophile (HSE: Os, Ir, Ru, Rh, Pt, Pd, Au and Re) and chalcogen (S, Se and Te) element compositions, and Re-Os isotopes of olivine-rich troctolites included within lower crustal sequences from the Jurassic Alpine ophiolites. The olivine-rich troctolites have Primitive Mantle (PM)-normalized HSE-Te-Se-S patterns showing a gradual increase from Os to Au, similar to those inferred for primitive mantle melts. Initial γ_{Os} (160 Ma) values range from 5.9 to 0.2, thereby extending to supra-chondritic values that are uncommon in the Jurassic Alpine mantle peridotites. Although some of these olivine-rich troctolites were previously attributed to a process of replacement of former mantle peridotites, their HSE and Os isotopic signatures do not reveal any geochemical signatures that may be attributed to an inherited mantle material, rather indicating a crustal origin. The latter may be envisaged by the crystallization of primitive melt batches within a forming gabbro sequence, followed by hybridization of the residual melt, by an exotic melt rich in incompatible elements, silica and volatile. The supra-chondritic Os/Ir, Pd/Ir, S/Se (1.8-1.3, 47-5.5, 2.8-1.0), variable Au contents (7.6-2.0 ng/g) and radiogenic Os isotopic compositions shown by the olivine-rich troctolites are consistent with this idea and may be related to the addition of S, Os, Pd and Au by the hydrous exotic melt. The most plausible origin for this hydrous melt is that of a melt residual from a process of reactive porous flow in the underlying gabbroic framework.

Multi-stage rodingitization of ophiolitic bodies from Northern Apennines (Italy): constraints from petrography, geochemistry and thermodynamic modelling

Salvioli-Mariani E.*¹, Boschetti T.¹, Toscani L.¹, Montanini A.¹, Petriglieri J.R.² & Bersani D.³

¹ Dipartimento di Scienze Chimiche, della Vita e della Sostenibilità Ambientale, Università di Parma.

² Dipartimento di Chimica, Università di Torino.

³ Dipartimento di Scienze Matematiche, Fisiche e Informatiche, Università di Parma.

Corresponding email: emma.salviolimariani@unipr.it

Keywords: rodingite, hydrothermal alteration, Raman spectroscopy.

The investigated mantle bodies (Gruppo di Gorro and Mt. Rocchetta) from the External Ligurides have undergone a very complex and articulated evolutionary history, determined by an early high temperature metasomatism due to percolating melts of asthenospheric origin and a later low temperature polyphasic metasomatism by hydrothermal fluids. Mantle decompression and concomitant interaction with fluids of asthenospheric origin produced the crystallization of plagioclase at the expense mainly of Cr-spinel and clinopyroxene. The hydrothermal metasomatism caused serpentinization and a multi-stage rodingitization of variable intensities and mineralogical assemblages according to the different protoliths (peridotites and pyroxenites) and physico-chemical conditions of the circulating hydrothermal fluid. At Gruppo di Gorro, the serpentinization and chloritization processes obliterated totally the pyroxenite protolith. The following rodingitization gave an initial garnet plus calcite assemblage and produced a diopside plus vesuvianite assemblage in the advanced stage. At Mt Rocchetta rodingitization preserved relics of the peridotite and pyroxenite protoliths and the mineral assemblage is dominated by garnet whereas diopside and vesuvianite are scarce. The variable intensity of rodingitic alteration in the two investigated sites of Gruppo di Gorro and Mt. Rocchetta can be explained in term of different lithology of the protolith and the duration of the process of fluid-rock interaction. Possibly the rodingitization lasted longer at Gruppo di Gorro than at Mt. Rocchetta. Fluid inclusion measurements show that rodingitization occurred at relatively high temperatures (264-334 °C at 500 bar and 300-380 °C at 1 kbar). Thermodynamic modeling under these conditions and considering fluids of marine and meteoric origin shows that the reaction path is independent by the different origin of the fluid and that Ca, Mg, aqueous silica activities and the pH of the hydrothermal solution are fundamental to enhance the progress of the reactions forming the rodingite mineral associations. The addition of silica, calcium, magnesium and iron and some trace elements, as shown by mass balance calculation, suggests multiphase fluid infiltrations and the fluctuations in the compositions of hydrothermal fluids. This feature is also suggested by the oscillatory zoning of garnet from Mt. Rocchetta, with rhythmic variations from grossularia to andradite. We propose that the rodingite formation could be related to different pulses of hydrothermal activity mainly occurring in an ocean-continent transitional setting and, locally, in a accretionary prism associated with intra-oceanic subduction.

Mado Megamullion (Shikoku basin): a new window into a backarc lower crust and mantle

Sani C.*¹, Sanfilippo A.¹, Ohara Y.², Snow J.³, Harigane Y.⁴ & Yamahshita H.⁵

¹ Dipartimento di Scienze della Terra, Univesità di Pavia.

² Hydrographic and Oceanographic Department of Japan Japan, Agency for Marine-Earth Science and Technology.

³ University of Houston.

⁴ Geological Survey of Japan, Japan, National Institute of Advanced Industrial Science and Technology.

⁵ Kanagawa Prefectural Museum of Natural History.

Corresponding email: camilla.sani01@universitadipavia.it

Keywords: OCC, gabbro.

The Mado Megamullion (MM) in the Shikoku Basin represents an important tectonic window to understand the accretionary processes of the backarc oceanic lithosphere. Due to the easy accessibility (only ~1300 km from Tokyo) this oceanic core complex (OCC) is unique compared to the others well-studied OCCs worldwide. The rocks sampled during the 2007 and 2018 expeditions are mainly peridotites and gabbros, locally associated with minor basalts. The gabbros are deformed and undeformed varieties, the latter including varitextured and microgabbros. Most of these gabbros are fairly evolved consisting of olivine-free to oxide-rich gabbros locally intruded by felsic material resembling, whereas primitive lithologies are missing. Microtextural and chemical data are here used to show that the association of varitextured to fine-grained gabbros with felsic material resemble those of the gabbros formed at the dike-gabbro transition. Hence, we preliminarily propose that the MM exposes a portions of a crustal sequence intruded into the shallow mantle.

Finally, our data indicate that covariations in plagioclase anorthite (An) versus clinopyroxene Mg/(Mg+Fe) of the Mado MM gabbros form a trend notably steeper than those of abyssal oceanic gabbros. This trend mirrors that of the lower crust from the Godzilla Megamullion, a largest OCC in the Parece Vela backarc basin (Ohara et al., 2001), suggesting that the so far considered peculiar composition of the Godzilla gabbros (Sanfilippo et al., 2013) can be instead typical of the crust formed in backarc basins.

Ohara Y., Yoshida T., Kato Y. & Kasuga S. (2001) - Giant megamullion in the Parece Vela backarc basin. *Marine Geophysical Research*, 22, 47–61.

Sanfilippo A., Dick H.J.B. & Ohara Y. (2013) - Melt-rock reaction in the mantle: Mantle troctolites from the Parece Vela Ancient back-arc spreading center. *J. Pet.*, 54, 861–855.

The role of rift width in controlling fault pattern and kinematics in oceanic and continental rifts: examples from Iceland and Ethiopia

Sani F.*¹, Bonini M.², Corti G.² & Moratti G.²

¹ Dipartimento di Scienze della Terra, Università di Firenze, Italy.

² Consiglio Nazionale delle Ricerche (CNR), Istituto di Geoscienze e Georisorse, UOS Firenze, Italy.

Corresponding email: federico.sani@unifi.it

Keywords: Oblique rifting, structural analysis, analogue modeling.

Rifting is an important geodynamical process that leads to separation of a continental plate and eventually to the development of a new oceanic crust. Orthogonal rifting occurs when the direction of spreading is normal to the trend of the rift axis, or to the trend of the major faults delimiting the rift valley. However, this condition is rarely verified. More common are conditions of oblique rifting, which imply a shear component along the rift zone between the two diverging plates. Typically, fault systems generated during oblique rifting show an en-echelon arrangement with different fault segments oriented not perpendicular to the direction of relative motion. Whatever the causes for rift obliquity, the stress within the rift valley is partitioned and faults show a general dip-slip kinematics, with a re-orientation of the stress between the boundary and the internal faults.

With the aim to illustrate similarities and differences between continental and oceanic rifts, we show the results of a field structural study performed at selected key areas along the emerged oceanic ridge system of Iceland, and compare them with data collected in the last years in the continental Main Ethiopian Rift (MER).

Iceland offers a unique opportunity to investigate the geometry and the kinematics of rifting in an oceanic context. In particular, ridge segments with different orientation have been analyzed in terms of fault kinematics and related stress field. The extension directions are roughly orthogonal to the strike of the faults in all the investigated sectors. Extension shows an overall southward increase in divergence from the regional directions indicated by GPS vectors.

Studies in the continental MER show a re-orientation of the extension direction between the rift margins and the internal sectors, resulting in a divergence between local and regional extension directions. Moreover, the MER shows tectonic features that can be compared with those of the Icelandic rifts, such as along-axis variations in the orientation of the rift trend, fault pattern and related stress fields. However, this continental rift also shows complexities not observed in the oceanic rifts of Iceland.

Aimed at investigating the causes of these differences, we performed a new series of analogue models by varying different parameters such as rift obliquity and width. Our findings suggest that rift width exerts a primary control on the boundary-axis variation of the extension direction. In particular, significant differences in fault orientation and local direction of extension between the margins and the rift axis are observed in wider rift valleys (e.g., continental rift of Ethiopia). Conversely, fault orientation and local extension direction are much more homogeneous in narrower rift valleys (e.g., rifts of Iceland), where variations in the direction of extension from the margins to the rift axis are not observed.

Oceanization and Hydrography (West Mediterranean)

Savelli C.*

Ismar CNR (Bologna) - retired

Corresponding email: carlo.savelli@bo.ismar.cnr.it

Keywords: West Mediterranean, oceanic crust, hydrography.

Since Early Oligocene, West Mediterranean basins opened in Alpine Age Orogen and in Hercynian Lithosphere (European plate). After orogenic accretion, the South Tyrrhenian and North Algerian basins experienced rifting and emplacement of oceanic-type lithosphere, whereas the North Tyrrhenian and Alboran rest on rifted continental crust. In Hercynian area, the basement geology of Valencia and Sardinia-Provence basins shows respectively continental (Valencia) and oceanic nature (Sa-Pr), depending on location with respect to deep-seated shear faulting of NNW-SSE trend. The Catalan-Tunisian shear zone (known also as the “Paul Fallot” transform fault) separates the west segment of Hercynian lithosphere and Orogen of Alpine Age from that to the east. Counter-clockwise (C-CW) and clockwise (CW) rotation of continental margin is found to the east and west of faulting, respectively. The tectono-magmatic lineament running along 41° parallel approximately divides the North Tyrrhenian stretched continental crust from the oceanic lithosphere to the South. Correspondingly, Tyrrhenian basin opening is linked to C-CW and CW rotation of North & South Apennines. West Mediterranean geology experienced past East-directed flat-slab subduction linked to crustal thickening (double verging accretion of Orogen of Alpine Age above the lower plate). Subsequently, West-directed steep-slab (still ongoing) lithosphere plunging accompanied hyper-extension tectonics, volcanism and basin formation in the upper plate. Overall, such asymmetric evolution is considered to be consequence of lithosphere westward drift above eastward flow of asthenosphere (Doglioni et al., 1999; Savelli, 2015). Lithosphere and asthenosphere geodynamics appears to be linked to earth rotation.

Along the West Mediterranean continental margins, seawater circulation shows main C-CW trend due to earth rotation. Part of the E-W current of Provence margin changes direction at the northern tip of the Catalan-Tunisian shear zone to parallel the shear’s NNW-SSE trend. Also deep waters from Lions Gulf appear to take such trend (Pinardi & Masetti, 2000). In the Tyrrhenian at the eastern tip of 41° parallel deep-seated lineament, part of the N-S trending current bordering the Hercynian microplate of Corsica-Sardinia attains W-E trend. So, in addition to earth rotation certain West Mediterranean hydrographic features appear to be linked also to marine geology. In prospect, lithosphere and hydrosphere geodynamic aspects ought to be issue of comparative examination.

Doglioni C., Gueguen E., Harabaglia P. & Mongelli F. (1999) - On the origin of W-directed subduction zones and applications to the western Mediterranean. *Geol. Soc. Spec. Publ.*, 156, 541–561.

Pinardi N. & Masetti E. (2000) - Variability of the large scale general circulation of the Mediterranean Sea. *Palaeo.*, 158, 153-173.

Savelli C. (2015) - Fast Episodes of West-Mediterranean-Tyrrhenian oceanic opening and revisited relations with tectonic setting. *Sci. Rep.*, 5, 14271.

Surface processes forcing on rift magmatism: insights from numerical modeling

Sternai P.*¹

¹ Department of Earth and Environmental Sciences, University of Milano-Bicocca, Italy.

Corresponding email: pietro.sternai@unimib.it

Keywords: Continental rifting, surface processes, magmatism.

Continental rifting involves subsidence and uplift of the surface topography and recent research has shown that erosion and sedimentation involve mechanical and thermal effects on the lithosphere rheology, which condition the structural evolution of continental rifts. Whether and how the rheological implications of surface processes may also affect the magmatic history of continental rifting, however, is still largely unknown. Here, I use coupled thermo-mechanical geodynamic and landscape evolution numerical modeling to investigate the first order relationships between erosion, sedimentation and magmatism in extensional settings. A detailed parametric study on plate extension and erosion/sedimentation rates as well as on the lithospheric and upper mantle structure, thermal regime and composition allows defining the extent to which and the mechanisms through which surface processes may affect the magmatic evolution of continental rifts and possible effects on oceanization. Results suggest that efficient surface processes may enhance crustal melting by thermal blanketing and Moho lowering. Efficient surface processes also inhibit mantle decompression melting by lithospheric loading due to sedimentation into the rift basin, thereby delaying continental breakup and oceanization. The surface processes forcing on rift magmatism appears particularly pronounced when the continental crust is thinner than ~40 km, the extension rate is slower than ~2 cm/a and the asthenosphere potential temperature is below 1230 °C. Thus, surface processes may have conditioned the magmatic history of several volcanic rifts and passive margins worldwide, which involves an additional means of linkage between plate tectonic and climatic changes throughout the Earth's history. Feedbacks between surface processes and the structural evolution of continental rifts through magmatism and a contribution from surface processes to establishment or abortion of volcanic and non-volcanic rifts also appear plausible, although these possibilities require further investigations.

Mantle source heterogeneity in the Equatorial Mid Atlantic Ridge: a multi-isotopic approach

Verhoest L.*¹⁻², Brunelli D.¹⁻³, Hemond C.⁴, Bonatti E.³⁻⁴, Ligi M.³ & Cipriani A.¹⁻⁴

¹ DSCG, Università di Modena e Reggio Emilia, Italy.

² Laboratoire Géosciences Océan, Institut Universitaire Européen de la Mer, France.

³ ISMAR-CNR, Bologna, Italy.

⁴ Lamont Doherty Earth Observatory, Columbia University, New York, NY, USA.

Corresponding email: lana.verhoest@unimore.it

Keywords: Equatorial Mid Atlantic Ridge, Romance fracture zone, basalt compositional variability, mantle heterogeneities.

The equatorial portion of the Mid Atlantic Ridge represents an end member of the whole mid-ocean ridge system characterized by extremely low mantle temperatures and a bundle of extremely long fracture zones. Three fracture zones cumulate more than 2000 km offset across the Equator, the longest being the Romanche (offset ~950 km) bounded by the St. Paul FZ to the north and the Chain FZ to the south. The axial, near-zero age topographic level of the equatorial region is deeper than normal, and crustal thickness, inferred from geophysical data, is anomalously low throughout the area. In addition, mantle-derived peridotites are exposed in large areas and the chemistry of zero-age basalts and of mantle-derived peridotites both suggest that the degree of melting undergone by the upper mantle below the MAR is exceptionally low. The ridge axis approaching the eastern Romanche RTI is controlled by a strong lateral thermal gradient resulting in a continuous decrease of the magmatism toward the RTI. The axial tip presents a purely amagmatic steady-state spreading regime. Basalt chemistry shift from N-MORB to alkaline affinity approaching the cold region with the concomitant increase in water and incompatible element contents. We present a preliminary Sr-Nd-Pb and Hf isotope study of the basalts recovered from the center of the ridge segment to the tip of the eastern RTI of the Romanche fracture zone. It appears that the basalt compositional variability is controlled by the thermal state of the decompressing mantle significantly increasing by decreasing the mantle potential temperature. Basalts from the axial tip, where the degree of melting goes to nearly zero, allow discerning the presence of diverse compositional heterogeneities dispersed in a DMM mantle screen.

S13

**A multidisciplinary approach to unravel the evolution of
basement geology**

CONVENERS AND CHAIRPERSONS

Antonio Langone (IGG-CNR Pavia)

Chiara Montomoli (Università di Torino)

Salvatore Iaccarino (Università di Torino)

Constraining fluid regime during melting of crystalline basements: experiments vs. thermodynamic modelling

Bartoli O.*¹

¹ Dipartimento di Geoscienze, Università di Padova.

Corresponding email: omar.bartoli@unipd.it

Keywords: fluid regime, H₂O-fluxed melting.

The nature of fluid regime during high-temperature metamorphism and crustal anatexis is a matter of current debate. The growing list of occurrences where H₂O-fluxed melting is postulated has raised the need of finding geochemical criteria to identify this process. Results of melting experiments have been often used as a benchmark to which natural occurrences (compositions of granitoid rocks) have been compared to infer the nature of fluid regime. Previous experimental studies suggested that trondhjemitic crustal melts are the products of H₂O-fluxed melting (e.g., Patiño Douce & Harris, 1998). Here a comparative study of phase equilibria modeling and melting experiments is presented. Modelling results do not support the existence of a clear link between fluid regime and melt composition. In particular, the formation of trondhjemitic melts via H₂O-fluxed melting reactions does not seem a general rule under equilibrium conditions. The potential causes of this discrepancy (e.g., persistence of metastable phases during experiments, limitations of models for minerals and melt, disequilibrium melting reactions under H₂O-present conditions) will be evaluated and discussed. The nanogranitoid compositional dataset will be interrogated to determine the possible role of water-fluxed melting in the formation of peculiar melt compositions.

Patiño Douce A.E. & Harris N. (1998) - Experimental constraints on Himalayan anatexis. *Journal of Petrology*, 39, 689-710.

Apatite (U-Th)/He thermochronometry from trachytes and latites of the Euganean Hills and their exhumation history

Benà E., Martin S., Marzoli A., Mazzoli C., Sassi R.* & Zattin M.

Dipartimento di Geoscienze, Università di Padova.

Corresponding email: raffaele.sassi@unipd.it

Keywords: Euganean Hills Volcanic District, Apatite thermochronometry, (U-Th)/He thermochronometry.

The Euganean Hills Volcanic District (EHVD) belongs to the wider Venetian Volcanic Province, which covers an area of ~2000 km² in NE Italy. The most representative rock types of the EHVD are Late Eocene latites and basalts to Oligocene trachytes and rhyolites. Alkali trachytes and rhyolites are the dominant magmatic products, whereas latites and basalts occur in minor amounts. Geochemical and geophysical data are consistent with extensional geodynamics. This agrees with the widespread occurrence of extensional tectonic faults with NE–SW and NW–SE directions genetically related to the volcanic activity.

An Apatite (U-Th)/He thermochronometry study from trachytes and latites of the Euganean Hills was carried on to describe their exhumation history.

Preliminary results obtained from different bodies are broadly consistent with, although generally younger than, emplacement age. Samples from the northern area provide values ranging from 21 to 23 Ma. Also the southern bodies part give similar ages (21–23 Ma).

The whole age dataset ranges between 21 and 23 Ma (average value 22.115 ± 0.84 Ma) with the only exception of Monte Merlo body which suffered further exhumation at 15 Ma.

The different models here tested show a number of solutions that give a fundamental constraint to the geologic evolution. For the first time, we are able to trace the thermal path of these rocks from their emplacement to the surface. On one hand, the modeling procedures show that these data are compatible with an intrusion of different shapes and at different depths. On the other hand, the amount of erosion needed to fit the data is not always compatible with observed field and petrographical features that point to a very shallow intrusion. If we consider the model with the lowest exhumation, the igneous body intruded into a sedimentary succession at a depth of less than 2 km at about 33 Ma. It reached thermal equilibrium with ambient country rocks at about 31 Ma and it approached the surface more or less at the same time. Since that time, the cooling of the magmatic bodies was mainly controlled by the process of exhumation until the present day. In terms of cooling rates, the first stage of magmatic cooling (from intrusion to when both the igneous body and country rocks reach a final thermal equilibrium state) was of 730°C/Ma whereas the subsequent erosion cooling rate was of 3°C/Ma.

Origin of Plumasite dykes intruded in Variscan basement during triassic: new insights from Zircon (Val Sabbiola, Ivrea-Verbano zone)

Bonazzi M.^{*1}, Langone A.², Zanetti A.², Dellarole E.³, Mazzucchelli M.^{2,4} & Giovanardi T.⁴

¹ Dipartimento di Scienze della Terra e dell' Ambiente, Università di Pavia, Italy.

² Istituto di Geoscienze e Georisorse-C.N.R. U.O.S. of Pavia, Italy.

³ Sesia Val Grande UNESCO Global Geopark.

⁴ Dipartimento di Scienze Chimiche e Geologiche, Università degli Studi di Modena e Reggio Emilia, Italy.

Corresponding email: mattia.bonazzi01@universitadipavia.it

Keywords: plumasite, zircon, Ivrea-Verbano zone.

Plumasite is a pegmatitic rock consisting of sodic plagioclase (typically oligoclase), corundum (>16%vol.), zircon, biotite, hercynite ± K-feldspar.

The occurrence of plumasite was documented in Val Sabbiola (Bertolani, 1957) and in Val Cannobina (Langone et al., 2017) as small dykes discordantly intruding both magmatic and metamorphic rocks of the Adria lower crust (Ivrea-Verbano Zone). We recognized two plumasite dykes in Val Sabbiola: one crosscuts mafic intrusives (Mafic Complex) and shows mylonitic deformation; the other one intrudes granulites (Stronalite), preserving pegmatitic texture. Petrogenetic models reported in literature suggest a hybrid nature for the plumasite parent melt, resulting by the interaction of silica-undersaturated melts and felsic rock. We present new constraints on the petrologic origin of plumasite by petrographic and geochemical characterization of zircons. BSE-CL images revealed the same internal zircon structures in both dykes: a broad banding zoning, typical of zircons segregated by melts, is commonly overprinted by irregular structureless domains. Trace elements, U-Pb and Lu-Hf surveys on zircon performed by LA-(MC)-ICP-MS suggest a Triassic intrusion age for both dykes, pointing to a pronounced Depleted Mantle geochemical signature for the parent melts. This magmatic activity post-date the youngest intrusion of mafic-ultramafic pipes of mantle origin intruded within the lower crustal levels of the IVZ (Locmelis et al., 2016); it is coeval or slightly older than alkaline dykes reported in the northern sector of the IVZ (e.g. Schaltegger et al., 2015) and pre-date the intrusion of carbonatites during Jurassic time (Galli et al., 2018).

Funds provided by PRIN 2015 in the frame of project 20158A9CBM_005.

- Bertolani M., (1957) - La posizione petrogenetica di alcuni filoni corindoniferi della Val Sabbiola (Valsesia). Rend. Soc. Geol. It., 13, 120-130.
- Galli A., Grassi D., Sartori G., Gianola O., Burg J.-P. & Schmidt M.W. (2019) - Jurassic carbonatite and alkaline magmatism in the Ivrea zone (European Alps) related to the breakup of Pangea. *Geology*, 47, 199-202.
- Locmelis M., Fiorentini M.L., Rushmer T., Arevalo R. Jr., Adam J., Denyszyn S.W. (2016) - Sulfur and metal fertilization of the lower continental crust. *Lithos*, 244, 74-93.
- Langone A., Padrón-Navarta J.A., Ji, W.Q., Zanetti A., Mazzucchelli M., Tiepolo M., Giovanardi T. & Bonazzi M. (2017) - Ductile-brittle deformation effects on crystal-chemistry and U-Pb ages of magmatic and metasomatic zircons from a dyke of the Finero Mafic Complex (Ivrea-Verbano Zone, Italian Alps). *Lithos*, 284-285, 493-511.
- Schaltegger U., Ulianov A., Muntener O., Ovtcharova M., Peytcheva I., Vonlanthen P., Vennemann T., Antognini M. & Girlanda F. (2015) - Megacrystic zircon with planar fractures in miaskite-type nepheline pegmatites formed at high pressures in the lower crust (Ivrea Zone, southern Alps, Switzerland). *The American Mineralogist*, 100, 83-94.

The High Himalayan Discontinuity and the Main Central Thrust in Central Nepal: timing constraints by in-situ U-Th-Pb monazite petrochronology

Carosi R.*¹, Montomoli C.¹, Iaccarino S.¹ & Visonà D.²

¹ Dipartimento di Scienze della Terra, Università di Torino, Italy.

² Dipartimento di Geoscienze, Università di Padova, Italy.

Corresponding email: rodolfo.carosi@unito.it

Keywords: Tectonics, petrochronology, Himalaya, metamorphic units, exhumation, shear zones, P-T-t paths.

The mid-crust of the Himalaya is exposed in the Greater Himalayan Sequence (GHS), one of the major tectonic units of the Himalayan belt cropping out for nearly ~ 2500 km along strike. GHS is regarded as coherent tectonic unit, bounded by the South Tibetan Detachment to the top and the Main Central Thrust to the bottom. Integrated studies by different techniques allowed to recognize several high-temperature shear zones in the core of the GHS, with top-to-the S/SW sense of shear (High Himalayan Discontinuity: HHD, (Montomoli et al., 2013, 2015) U-Th-Pb in situ monazite petrochronology provides ages older than the Main Central Thrust, along the same structural profile. Data on P-T evolution testify that these shear zones, acting for ~ 5-10 Ma, affected the tectono-metamorphic history of the belt and different P-T conditions have been recorded in the hanging-wall and footwall of the HHD. This tectonic feature, running for several hundreds kilometers, is documented in several sections of the belt. We present the results of some transects of the GHS in the Annapurna-Manaslu massif (Central Nepal). Close to the transition between sillimanite-bearing gneiss and kyanite-bearing gneiss, we identified a high-temperature ductile shear zone with kinematic indicators pointing to a top-to-the S sense of shear.

U-Th-Pb in situ analysis on monazite, joined with chemical compositional maps, on samples from the shear zone and its footwall provided ages ranging from ~ 8 to 43 Ma. The age of the HHD in central Nepal is constrained between ~ 27/26 and 18 Ma, in very good agreement with the ages of the HHD detected along strike in the GHS (Carosi et al., 2018) older than the Main Central Thrust along the same section (Catlos et al., 2001; Gibson et al., 2015) constrained at ~ 17-13 Ma.

The occurrence of the HHD in Central Nepal allows us to fill a gap in the recognition of the HHD in the Himalayan belt.

Carosi R., Montomoli C. & Iaccarino S. (2018) - 20 years of geological mapping of the metamorphic core across Central and Eastern Himalayas. *Earth Sci. Rev.*, 177, 124-138.

Catlos E.J., Harrison T.M., Kohn M.J., Grove M., Ryerson F.J., Manning C.E. & Upreti B.N. (2001) - Geochronologic and thermobarometric constraints on the evolution of the Main Central Thrust, central Nepal Himalaya. *J. Geoph. Res.*, 106, 16177-16204.

Gibson R., Godin L., Kellett D.A., Cottle J.M. & Archibald D. (2016) - Diachronous deformation along the base of the Himalayan metamorphic core, west-central Nepal. *GSA Bull.*, 128, 860-878.

Montomoli C., Carosi R. & Iaccarino S. (2015) - Tectonometamorphic discontinuities in the Greater Himalayan Sequence: a local or a regional feature? *Geol. Soc., London, Sp. Publ.*, 412, 25-41.

Montomoli C., Iaccarino S., Carosi R., Langone A. & Visonà D. (2013) - Tectonometamorphic discontinuities within the Greater Himalayan Sequence in Western Nepal (Central Himalaya): insights on the exhumation of crystalline rocks. *Tectonophysics*, 608, 1349-1370.

Partitioned transpressional tectonics in the Variscan Basement of northern Sardinia (Italy)

Carosi R.*¹

¹ Dipartimento di Scienze della Terra, Università di Torino, Italy

Corresponding email: rodolfo.carosi@unito.it

Keywords: Variscan Basement, Sardinia, Transpression.

The Variscan basement of northern Sardinia (Italy) underwent a HP event followed by prograde Barrovian-type metamorphism associated to polyphase deformation during Variscan orogeny (Cruciani et al., 2015).

The D1 collision-related deformation was responsible of S and SW tectonic transport of the nappe (nearly orthogonal to the belt), S and SW-verging F1 folds and top-to-the S and SW shear zones during the thickening stage of the belt (Carmignani et al., 1994). During the D1 phase, the basement was deeply underthrust recording the highest pressures (Cruciani et al., 2013).

The D2 deformation marked a change in the tectonic transport of the belt from perpendicular to parallel to the orogen, associated with non-coaxial shearing along the Posada-Asinara Line. D2 is characterized by a dextral transpressional deformation partitioned in sectors mainly affected by F2 folds and sectors affected by ductile shearing at ~ 320-300 Ma (Carosi & Palmeri, 2002; Di Vincenzo et al., 2004; Carosi et al., 2012). D2 transpression affected the Barrovian index minerals from biotite, garnet, staurolite up to kyanite, caused telescoping and bending of the Barrovian isograds. The component of pure shear, perpendicular to the shear belt, enhanced the telescoping of the isograds and the exhumation of the deep-seated rocks.

New structural geological mapping and structural analysis joined with modern U-Th-Pb petrochronology on monazite allowed to better assess the tectonic and metamorphic history of the Posada-Asinara Line and surrounding units and its role in the tectonic evolution of the belt. After the D1 HP event the inner tectonic units underwent exhumation perpendicular to the belt (late-D1) causing the inversion of the isograds. The inner units underwent initial stages of decompression in the sillimanite stability field during late-D1. The D2 transpressional event caused partitioned ductile dextral shearing and NE-verging folding of the Barrovian isograds.

Recent data point to a regional-scale occurrence of a D2 transpressional deformation in the Southern Variscan belt along a steep belt, the so called East Variscan Shear Zone (Corsini & Rolland, 2009).

Carosi R. & Palmeri R. (2002) - Orogen parallel tectonic transport in the Variscan belt of northeastern Sardinia (Italy): implications for exhumation of medium-pressure metamorphic rocks. *Geol. Mag.*, 139, 497-511.

Carosi R., Montomoli C., Tiepolo M. & Frassi C. (2012) - Geochronological constraints on post-collisional shear zones in the Variscides of Sardinia (Italy), Italy. *Terra Nova*, 24, 42-51.

Corsini M. & Rolland Y. (2009) - Late evolution of the southern European Variscan belt: Exhumation of the lower crust in a context of oblique convergence. *CR Geosci.*, 341, 214-223.

Cruciani G., Montomoli C., Carosi R., Franceschelli M. & Puxeddu M. (2015) - Continental collision from two perspectives: a review of Variscan metamorphism and deformation in northern Sardinia. *Period. Mineral.*, 84, 657-699.

Numerical modelling of floating P-T conditions in inclusion-matrix systems, with application to the Cima Lunga Unit (Central Alps)

Casini L.*¹, Corvo S.², Maino M.², Seno S.²⁻³ & Schenker F.³

¹ Dipartimento di Chimica e Farmacia, Università di Sassari, Italy.

² Dipartimento di Scienze della Terra, dell'Ambiente, Università di Pavia, Italy.

³ Istituto Scienze della Terra, Scuola Universitaria Professionale della Svizzera Italiana, Lugano, Swiss.

Corresponding email: casini@uniss.it

Keywords: Finite Differences, tectonic overpressure, shear heating.

One of the major challenge in structural and petrological studies is to understand the feedbacks of deformation on metamorphism. This contribution presents numerical models with the aim to quantifying the magnitude of the stress- and composition-dependent pressure and temperature variations in a shear zone. A classical inclusion-in-matrix system is simulated in 2D space with evp2d, an elasto-visco-plastic thermo-mechanical code (Casini & Maino, 2018). The algorithm adopt an implicit conservative finite difference scheme based on a fully-staggered Eulerian grid and marker-in-cell method that allow to simulate multiphase flow of material with large viscosity contrast (Gerya & Yuen, 2003). The incompressible continuity equation along with the Stokes equations are solved for velocity and pressure, taken as the mean normal stress $P = s_{ii}/2$. Viscous shear heating is computed from the stress and strain rate tensors as $H_s = s_{ii} e_{ij}^2 + 2s_{ij} e_{ij}$, before solving the Lagrangian form of the heat equation. This continuum-mechanics formulation implies either deviations from an equilibrium lithostatic pressure and local overheating, in response to localization of deviatoric stress and strain-rate.

The experimental setup reproduce a 1 km-thick mid-crustal (20-30 km-depth) shear zone composed of a weak layer and multiple strong inclusions characterized by dry peridotite rheology. A free-slip boundary condition is combined to a gradient of horizontal velocity applied to lateral boundaries. We assume three initial configurations using differently sized inclusions and different geometrical arrangements, as single small inclusion (SSI), single large inclusion (SLI) and multiple inclusion (MI). All experiments were conducted for variable shear rates between 1×10^{-12} and 1×10^{-9} m/s until a finite shear $\gamma = 7$ was achieved. The inclusions record a positive deviation of dynamic pressure in almost all experiments and develop moderate to strong shear heating around the inclusions. This behaviour is taken to extremes in some experiments of group MI whereby multiple inclusions allow the development of complex geometries yielding to stress and strain-rate localization. Here, inclusions record peak dynamic pressure which transiently double the lithostatic condition, and localized shear heating within high strain-rate channels developing between inclusions. The experimental results are finally compared to the P-T-t paths and geological constraints of the Cima Lunga Unit in Central Alps, one of the key-localities to test Alpine subduction models.

Casini L. & Maino M. (2018) - 2D-thermo-mechanical modelling of spatial PT variations in heterogeneous shear zones.

Italian Journal of Geosciences, 137(2), 272-282. <https://doi.org/10.3301/IJG.2018.13>

Gerya T.V. & Yuen D.A. (2003) - Rayleigh–Taylor instabilities from hydration and melting propel ‘cold plumes’ at subduction zones, Earth and Planetary Science Letters, 212(1-2), 47-62.

Determination of P-T-t-d path in a high-grade shear zone: petro-chronological and microstructural study from the Cima di Gagnone (Adula-Cima Lunga nappe, Central Alps)

Corvo S.*¹, Maino M.¹, Langone A.², Piazzolo S.³, Seno S.^{1,4} & Schenker F.⁴

¹ Dipartimento di Scienze della Terra, dell'Ambiente, Università di Pavia, Italy.

² Istituto di Geoscienze e Georisorse, C.N.R., Pavia, Italy.

³ University of Leeds, Leeds, United Kingdom.

⁴ Istituto Scienze della Terra, Scuola Universitaria Professionale della Svizzera Italiana, Lugano, Swiss.

Corresponding email: stefania.corvo01@universitadipavia.it

Keywords: Shear zone, HP-HT metamorphism, P-T-t-d path.

The Cima Lunga Unit in the Central Alps consists of continental basement rocks (orthogneisses, paragneisses and metapelites) hosting small inclusions of oceanic crust (limestones, amphibolites and peridotites). The (ultra-)mafic boudins have been extensively studied as they record extreme metamorphic conditions during the Alpine phases (pressure and temperature up to 2.5 GPa and 750 °C, respectively; Heinrich, 1982). The metamorphism of the surrounding gneiss complex is instead constrained at considerably lower conditions (up to 0.8 GPa and 660 °C; Grond et al., 1995). Several models have been proposed to explain the coupling between ultrahigh- and middle- pressure rock pairs resulting in a large uncertainty in the adopted subduction-exhumation models.

Our research consists in a petro-chronological and micro-structural study to characterize the link between metamorphism and deformation. The aim is to understand the role of deformation for the heterogeneous distribution of P-T records within peridotite inclusions and gneissic matrix.

In order to define the P-T-t-d path, a comprehensive study integrating petrologic-geochemical, and microstructural (SEM- EBSD) analyses were performed on selected samples from the Cima di Gagnone locality. The resulting pressure-temperature paths are temporally constrained with U-Th-Pb dating of monazite and allanite. Our preliminary results suggest that felsic and ultramafic rocks deformed together sharing similar P-T conditions.

Grond R., Wahl F. & Pfiffner M. (1995) - Mehrphasige alpine Deformation und Metamorphose in der nördlichen Cima Lunga-Einheit, Zentralalpen (Schweiz). Schweiz. Mineral. Petrogr. Mitt., 75, 371-386.

Heinrich C.A. (1982) - Kyanite-eclogite to amphibolite facies evolution of hydrous mafic and pelitic rocks, Adula Nappe, Central Alps. Contrib Miner Petrol., 81, 30-38.

P-T path of felsic granulite from south-east Corsica (France) and implications for geodynamic setting

Cruciani G.*¹, Franceschelli M.¹, Massonne H.-J.² & Musumeci G.³

¹ Dipartimento di Scienze Chimiche e Geologiche, Università degli Studi di Cagliari, Italy.

² School of Earth Sciences, China University of Geosciences, Wuhan, P.R. China.

³ Dipartimento di Scienze della Terra, Università degli Studi di Pisa, Italy.

Corresponding email: gcrucian@unica.it

Keywords: Granulitic gneiss, P-T path, Variscan Corsica.

The Solenzara-Fautea unit is made up of Variscan rocks outcropping between the villages of Fautea and Solenzara in SE Corsica (Faure et al., 2014). The unit consists of migmatites and garnet-kyanite granulitic gneiss with pyroxenite and pyrigarnite boudins (Rossi & Faure, 2012). To better understand the metamorphic evolution of this series we studied a gneiss exposed at the seashore south of the village of Tarcu. This foliated leucocratic rock, characterized by the alternation of quartzofeldspathic and biotite-rich layers, consists of quartz, mesoperthitic plagioclase, perthitic K-feldspar, garnet, biotite, kyanite, and subordinate muscovite and chlorite. Garnet occurs as millimetre-sized porphyroblasts or as small crystals in the matrix or included in kyanite. The porphyroblasts are rich in quartz, plagioclase, apatite and rutile inclusions and show an asymmetric compositional zoning with a Ca-rich core surrounded by an Fe-rich rim. The P–T path of the gneiss was reconstructed on the basis of garnet compositional zoning and isochemical phase diagrams. The garnet core formed at *ca.* 1.6 GPa and 700–750°C and, thus, at clearly lower temperatures than previously reported. These peak P-T conditions were followed by an almost isothermal decompression to pressure conditions of 0.8 GPa at *ca.* 700°C. The inferred clockwise P-T path is in agreement with estimations obtained with the Zr-in-rutile thermometer (730–740°C). The P-T conditions derived from the garnet rim (650–750°C; 0.7–0.9 GPa) are similar to those reported for paragneiss of the Porto Vecchio unit (Giacomini et al., 2008), 40 km south of the Fautea-Solenzara unit. The P-T path of the garnet-kyanite granulitic gneiss from Tarcu area is discussed in the framework of the Variscan Corsica geodynamic setting.

Faure M., Rossi P., Gaché J., Melleton J., Frei D., Li X. & Lin W. (2014) - Variscan orogeny in Corsica: new structural and geochronological insights, and its place in the Variscan geodynamic framework. *Int. J. Earth Sci.*, 103, 1533–1551.

Giacomini F., Dallai L., Carminati E., Tiepolo M. & Ghezzo C. (2008) - Exhumation of a Variscan orogenic complex: insights into the composite granulitic–amphibolitic metamorphic basement of south-east Corsica (France). *J. Metam. Geol.*, 26, 403–436.

Rossi P. & Faure M. (2012) - The Variscan Corsica. Field trip guide. *Géol. France*, 1, 11–23.

Clockwise and anticlockwise P-T path in the axial zone of the Variscan Sardinia-Corsica block

Franceschelli M.*¹ & Cruciani G.¹

¹ Dipartimento di Scienze Chimiche e Geologiche, Università degli Studi di Cagliari, Italy.

Corresponding email: francemar@unica.it

Keywords: P-T path, Variscan belt, Sardinia – Corsica block.

Recent petrological studies on the Axial Zone of the Variscan chain have revealed the occurrence of anticlockwise P-T trajectories in metamorphic rocks from Corsica and Sardinia. These new findings, at first glance, appears to be in contrast with the clockwise P-T paths classically described for several high-pressure metamorphic rocks from the Variscan Sardinia - Corsica block in the last decades. For the first time in Variscan Corsica, Massonne et al. (2018) described the anticlockwise P-T path of micaschists from the Porto Vecchio region. These rocks underwent prograde metamorphism starting at 3 kbar/600° C and then reached peak metamorphic conditions at 7 kbar/600-630°C. The Porto Vecchio micaschists are bordered to the north by the Solenzara-Fautea metamorphic rock unit that is, in turn, characterized by migmatites and granulites that underwent a clockwise P-T loop related to burial of continental crust to high-pressure (1.8–1.4 GPa) followed by high- to ultrahigh-temperature conditions (900–1000 °C; Giacomini et al., 2008). In the neighbouring Variscan terrains of north-eastern Sardinia, Scodina et al. (2019) reconstructed the P-T history of an amphibolite body whose burial path started at 0.8 GPa and was then followed by a slight increase in temperature up to peak metamorphic conditions of 1.3–1.4 GPa/690–740 °C. These amphibolites are hosted by migmatites for which a clockwise P-T path, related to a nearly isothermal exhumation, is widely accepted in the literature and confirmed by recent studies (Massonne et al., 2013 and references therein). In conclusion, it thus appears that during the Variscan collision, rock slices of different crustal levels were brought together and metamorphic rocks from upper and lower plates were involved in a particle path along an exhumation channel.

Giacomini F., Dallai L., Carminati E., Tiepolo M. & Ghezzo C. (2008) - Exhumation of a Variscan orogenic complex: Insights into the composite granulitic–amphibolitic metamorphic basement of southeast Corsica (France). *J. Metam. Geol.*, 26, 403–436.

Massonne H.-J., Cruciani G. & Franceschelli M. (2013) - Geothermobarometry on anatectic melts - a high-pressure Variscan migmatite from northeast Sardinia. *Int. Geol. Rev.*, 55, 1490–1505.

Massonne H.-J., Cruciani G., Franceschelli M. & Musumeci G. (2018) - Anticlockwise pressure–temperature paths record Variscan upper-plate exhumation: example from micaschists of the Porto Vecchio region, Corsica. *J. Metam. Geol.*, 36, 55–77.

Scodina M., Cruciani G., Franceschelli M. & Massonne H.-J. (2019) - Anticlockwise P-T evolution of amphibolites from NE Sardinia, Italy: geodynamic implications for the tectonic evolution of the Variscan Corsica-Sardinia block. *Lithos*, 324–325, 763–775.

Protracted shearing at mid crustal conditions in the Scandinavian Caledonides

Giuntoli F.*¹, Menegon L.², Warren C.³, Darling J.⁴ & Anderson M.²

¹ Dipartimento di Scienze Biologiche, Geologiche e Ambientali, Università degli Studi di Bologna.

² School of Geography, Earth and Environmental Sciences, Plymouth University, UK.

³ Department of Environment, Earth and Ecosystems, Centre for Earth, Planetary, Space and Astronomical Research (CEPSAR), The Open University, Walton Hall, UK.

⁴ School of Earth and Environmental Sciences, University of Portsmouth, UK.

Corresponding email: francesco.giuntoli@gmail.com

Keywords: strain localisation, grain size reduction, fluid-rock interaction.

The basal thrusts of mountain belts localize much of the tectonic transport associated with crustal shortening and mountain building processes. These are often the results of protracted shearing from higher to lower metamorphic grades, but several open questions remain regarding the timing, the mineralogical behaviour and the rheology of these shear zones.

In the Lower Seve Nappe of the Scandinavian Caledonides (central Sweden), a main mylonitic foliation is visible in the mid-lower portions (from 1.6 to 2.5 km of depth) of the COSC-I drill core and is overprinted by a younger, discrete, brittle-to-ductile fabric.

Amphibole and plagioclase thermobarometry in mafic amphibolites suggests that the mylonitic foliation developed under epidote-amphibolite facies conditions (~600°C, 0.8-1 GPa) due to fracturing and fluid flow that triggered coupled dissolution-precipitation and dissolution-precipitation creep processes (Giuntoli et al., 2018). EBSD analysis of titanite grains located in pressure shadows indicates that such grains are strain-free and were growing during deformation, probably due to ilmenite destabilization and dissolution and titanite reprecipitation. *In-situ* LA-ICP-MS U-Pb ages of titanite grains constrain the development of this mylonitic fabric at around 418 ± 9 Ma.

The later brittle-to-ductile fabric is particularly well developed in micaschists as C-type and C'-type shear bands, a few tens of microns wide, that are invariably defined by new grains of chlorite and white mica. Locally, these C and C' planes are extremely sharp and cut the surrounding minerals. Chlorite and white mica thermobarometry highlights that this younger fabric developed at much shallower conditions of 300-400 °C and ~0.3 GPa. Deformation mechanisms responsible for this fabric development include progressive grain size reduction of quartz grains, due to dynamic recrystallization by subgrain rotation in proximity to the C and C' planes. Chlorite and white mica display slip on the {001} plane.

The results suggest that these fabrics formed due to protracted shearing from epidote amphibolite to greenschist facies conditions during the Scandian collision and, presumably, during the exhumation of the Lower Seve Nappe.

Giuntoli F., Menegon L. & Warren C.J. (2018) - Replacement reactions and deformation by dissolution and precipitation processes in amphibolites. *Journal of Metamorphic Geology*, 36(9), 1263-1286.

Geology and tectono-metamorphic history of the Himalayan metamorphic core: insights from the Alaknanda-Dhauliganga valleys (NW India)

Iaccarino S.*¹, Carosi R.¹, Montomoli C.¹, Montemagni C.², Massonne H.-J.³, Jain A.K.⁴ & Visonà D.⁵

¹ Dipartimento di Scienze della Terra, Università di Torino, Italy.

² Dipartimento di Scienze dell'Ambiente e della Terra, Università degli Studi di Milano Bicocca, Italy.

³ School of Earth Sciences, China University of Geosciences, Wuhan, P.R. China.

⁴ CSIR-Central Building Research Institute, Roorkee, India.

⁵ Dipartimento di Geoscienze, Università di Padova, Italy.

Corresponding email: salvatore.iaccarino@unito.it

Keywords: Himalaya, P-T-d-t paths, metamorphisms, shear zone.

In the Alaknanda-Dhauliganga valleys (Garhwal Himalaya, NW India) a nearly complete crustal- structural section of the Himalaya crops out (Jain et al., 2014). In this contribution we present field observations, as well as, microstructural, petrological and geochronological data from the Lesser Himalayan Sequences up to the Tethyan Himalayan Sequence from this area.

The pressure-temperature-deformation-time history (i.e. the P-T-d-t path) of selected samples from the Main Central Thrust zone (MCTz) and the up to ductile-sheared portion of the South Tibetan Detachment System (STDS) has been reconstructed with the aid of equilibrium assemblage diagrams, coupled with multi-equilibrium and trace-element based thermobarometry after detailed electron microprobe analytical work and microstructural analysis have been performed.

U-Th-Pb *in situ* monazite geochronology from selected samples of key-structural positions (MCTZ up to STDS) allowed us to put an absolute temporal constraint both on the prograde metamorphic history and on the exhumation-related overprint. These data, joined with the geological literature (e.g. Thakur et al., 2015; Hunter et al., 2018), shed light on the tectono-metamorphic evolution of the Himalayan metamorphic core in this portion of the belt. Moreover, these new P-T-d-t paths could be quite well compared with data from other portions of the belt located in Central and Central-Western Nepal (e.g. Iaccarino et al., 2017), since the same approach was followed.

Hunter N.J.R., Weinberg R.F., Wilson C.J.L., Luzin W. & Misra S. (2018) - Microscopic anatomy of a “hot-on-cold” shear zone: Insights from quartzites of the Main Central Thrust in the Alaknanda region (Garhwal Himalaya). *GSA Bulletin*, 130, 1519-1539.

Iaccarino S., Montomoli C., Carosi R., Massonne H.-J., Visonà D. (2017) - Geology and tectono-metamorphic evolution of the Himalayan metamorphic core: insights from the Mugu Karnali transect, Western Nepal (Central Himalaya). *J. Metam. Geol.*, 35, 301-325.

Jain A.K., Shreshtha M., Seth P., Kanyal L., Carosi R., Montomoli C., Iaccarino S. & Mukherjee P.K. (2014) - The Higher Himalayan Crystallines, Alaknanda – Dhauliganga Valleys, Garhwal Himalaya, India. *J. Virtual Explorer*, 47, Paper 8.

Thakur S.S., Patel S.C. & Singh A.K. (2015) - A P-T pseudosection modelling approach to understand metamorphic evolution of the Main Central Thrust Zone in the Alaknanda valley, NW Himalaya. *Contrib. Mineral. Petrol.*, 170, 1-26.

High-temperature metamorphism and deformation in the footwall of an eclogite-bearing nappe, Sveconorwegian orogen: metamorphic evolution of the Obbhult Complex, SW Sweden

Möller C.¹, Andersson J.² & Rebay G.*³

¹ Department of Geology, Lund University, Lund, Sweden.

² Geological Survey of Sweden, Uppsala, Sweden.

³ Dipartimento di Scienze della Terra e dell'Ambiente, Pavia, Italy.

Corresponding email: gisella.rebay@unipv.it

Keywords: HT metamorphism, dating of metamorphism, structural analysis, thermodynamic modelling.

A section of deep crust is exposed in the Eastern Segment of the Sveconorwegian orogen. Here, a 50 x 75 km eclogite-bearing nappe, which proves deep burial of continental crust and subsequent exhumation by extrusion of partially molten crust, indicates that this was a formerly deep section beneath a frontal part of a Himalayan-Tibetan type plateau (Möller et al., 2015; Möller & Anderson, 2018). This contribution aims at characterizing the P-T-t-d evolution of the footwall beneath the eclogite-bearing nappe, investigating a composite meta-igneous sequence known as the Obbhult complex.

The Obbhult complex underwent polyphasal deformation, involving isoclinal folding, E-vergent shearing, and refolding, and rocks have been heterogeneously mylonitized at high temperature. The igneous assemblage (andesine plagioclase + orthopyroxene + Fe-Ti oxide) of coarse-grained leuconorite–andesine anorthosite was recrystallized to a metamorphic assemblage comprising garnet + orthopyroxene + plagioclase + kyanite + biotite + cordierite + quartz + hemoilmenite. Si-poor, Mg-, Al-rich host rocks formed symplectite of sapphirine + garnet + corundum + hemoilmenite + plagioclase. Thermodynamic modelling using THERMOCALC suggests PT conditions at c. 11.0 kbar and 800 °C for the assemblage observed in mafic rocks.

U-Pb SIMS zircon analysis (performed at the NordSIM Laboratory, Stockholm) dates the intrusion of anorthosite–leuconorite at 1.39 Ga, and the primary crystallization of intermediate–basic host rocks at 1.41 Ga. Thin secondary 0.98 Ga zircon rims formed in sapphirine-bearing and other deformed rocks, confirmed also by in situ monazite EMP and SIMS data.

The 1.4 Ga Obbhult complex demonstrates a distinct deformational and metamorphic event within the footwall beneath the eclogite-bearing nappe, involving high temperature recrystallization (800 °C) and polyphasal deformation, at c. 40 km depth. This event was related to the tectonic emplacement of the eclogite-bearing nappe and associated - however limited - H₂O infiltration.

Möller C., & Andersson J. (2018) - Metamorphic zoning and behaviour of an underthrusting continental plate. *J. Metam. Geol.*, 36, 567–589.

Möller C., Andersson J., Dyck B., & Lundin I.A. (2015) - Exhumation of an eclogite terrane as a hot migmatitic nappe, Sveconorwegian orogen. *Lithos*, 226, 147–168.

The Jurassic exhumation history of basement rocks in Mexico preserved in the stratigraphic record of rift basins associated to Pangea breakup

Martini M.*¹ & Zepeda-Martínez M.¹

¹ Instituto di Geologia, Universita Nazionale Autonoma del Messico.

Corresponding email: mmartini@geologia.unam.mx

Keywords: southern Mexico, Proterozoic-Paleozoic terranes, Jurassic rift basins.

The backbone of Mexico is composed of Proterozoic and Paleozoic terranes that were assembled during the final consolidation of Pangea. By Jurassic time, these rocks were largely exhumed along lithospheric faults that accommodated the regional-scale transtension associated to NW-SE divergence between North and South America (Goldhammer, 1999; Martini & Ortega-Gutiérrez, 2018). However, the Jurassic exhumation history of pre-Mesozoic rocks is poorly known, and the identification of the main faults that were active during Jurassic rifting is made difficult by the complex overprinting of Late Mesozoic and Cenozoic deformation events. A practical way to reconstruct the Jurassic exhumation history of Proterozoic and Paleozoic rocks of Mexico is analyzing the depositional architecture of Jurassic rift basins, giving special attention to major changes in provenance of clastic rocks. In fact, Proterozoic and Paleozoic terranes in Mexico consist of metamorphic rocks characterized by different protoliths, metamorphic grades, and mineral assemblages (Ortega-Gutiérrez et al., 2018). Therefore, the exhumation of different terranes during Jurassic time can be monitored by identifying major provenance changes in the clastic stratigraphic record of rift basins. In this work, we present sedimentological and provenance data from two major rift basins in southern Mexico. Our preliminary results suggest that, during Early and Middle Jurassic time, Proterozoic, granulite-facies metamorphic rocks of the Oaxacan Complex were exhumed along a major NNW-trending, dextral normal fault system, forming a major relief that dominated the Mexican landscape and supplied alluvial fans and major rivers with a main direction of sediment transport to the W. During Middle Jurassic time, greenschist-facies metamorphic rocks of the Paleozoic Acatlán Complex and Totoltepec Pluton were exhumed along major WNW-trending, sinistral normal faults, which temporarily produced local topographic highs bounded by prograding alluvial fans with a main direction of sedimentary transport to the south and to the north. Available data indicate that the Jurassic exhumation of Proterozoic and Paleozoic rocks was mainly controlled by a conjugate system of NNW-trending, dextral normal and WNW-trending, sinistral normal faults.

Goldhammer R.K. (1999) - Mesozoic sequence stratigraphy and paleogeographic evolution of northeast Mexico.

In Bartolini C., Wilson J.L. & Lawton T.F. (Eds.): Mesozoic Sedimentary and Tectonic History of North-Central Mexico. Geological Society of America, Special Paper, 340, 1–58.

Martini M. & Ortega-Gutiérrez F. (2016) - Tectono-stratigraphic evolution of eastern Mexico during the break-up of Pangea: A review. *Earth-Science Reviews*, 183, 38–55.

Ortega-Gutiérrez F., Elías-Herrera M., Morán-Zenteno D.J., Solari L., Weber B. & Luna-González L. (2018) - The pre-Mesozoic metamorphic basement of Mexico, 1.5 billion years of crustal evolution. *Earth-Science Reviews*, 183, 2–37.

Thermal architecture and deformation structures in the Alpi Apuane (NW Tuscany Italy): new insights for the metamorphic and tectonic history of the inner northern Apennines

Molli G.*¹, Vitale Brovarone A.²⁻³, Beyssac O.² & Cinquini I.¹

¹ Dipartimento Scienze della Terra, Università di Pisa, Italy.

² Sorbonne Université, Muséum National d'Histoire Naturelle, Institut de Minéralogie, de Physique des Matériaux et de Cosmochimie, Paris, France.

³ Dipartimento di Scienze della Terra Università di Torino, Italy.

Corresponding email: giancarlo.molli@unipi.it

Keywords: RSCM temperatures, deformation, Alpi Apuane.

A Raman spectroscopy study on carbonaceous material (RSCM) has been applied in the Northern Apennines with particular focus on the Alpi Apuane (NW Tuscany, Italy) and surrounding areas in order to constrain peak metamorphic temperatures and their variability in the different continent-derived units of the nappe stack. Peak temperatures in the range of ~ 530–320 °C were found in the Alpi Apuane, whereas in the nearby metamorphic core of the Monte Pisano and Punta Bianca lower peak temperatures of 305–315 °C and 350 °C were found, respectively. The Tuscan Nappe in La Spezia area (west of Alpi Apuane) shows temperatures in the range of 295–246 °C, whereas the same unit in the Lima Valley (east of the Alpi Apuane) shows temperatures lower than 230 °C.

Using the presented data will discuss the thermal architecture of the inner northern Apennines and the relationships with regional-scale deformation structures to provide new constraints for the thermo-mechanical evolution and exhumation history of the inner Northern Apennine and its geodynamic setting. In particular we support the interpretation of the Alpi Apuane as a cold metamorphic core complex in which the preserved paleothermal structure and part of the exhumation are related with crustal thickening while the final exhumation stages (depth ≤ 15 km and ambient crustal temperature ≤ 350 °C) are associated with crustal thinning still ongoing in the area.

Geochronology and kinematics of flow of the Main Central Thrust zone in the Bhagirathi valley, NW Indian Himalaya

Montemagni C.*¹, Zanchetta S.¹, Montomoli C.², Iaccarino S.², Visonà D.³, Villa I.M.^{1,4} & Carosi R.²

¹ Dipartimento di Scienze dell'Ambiente e della Terra, Università degli Studi di Milano Bicocca.

² Dipartimento di Scienze della Terra, Università di Torino.

³ Dipartimento di Geoscienze, Università di Padova.

⁴ Institut für Geologie, Universität Bern.

Corresponding email: c.montemagni@campus.unimib.it

Keywords: MCTz, geochronology, vorticity.

The Himalayan belt has been long studied to deduce large-scale tectonics of shear zones regarding both their kinematics and the age of their timing, especially in the frame of exhumation of the Greater Himalayan Sequence (GHS), the metamorphic core of the orogenic belt. The GHS is delimited at its bottom by an orogen-scale shear zone, the Main Central Thrust zone (MCTz), a top-to-the-SW km-thick zone of intensively sheared rocks. As quantitative vorticity analyses in deformed rocks and isotope dating are fundamental in the study of the kinematics of flow and time of activity in shear zones, four samples have been investigated to infer these parameters along the two tectonic boundaries of the MCTz in the Bhagirathi valley: the Munsiri (lower) and the Vaikrita Thrust (upper).

To constrain the timing of deformations recorded within the Munsiri and Vaikrita Thrust rocks we undertook ⁴⁰Ar/³⁹Ar dating. We prepared biotite and muscovite separates with different degrees of purity in order to quantify the bias given by fine-grained impurity phases, which make 100% mica purity unattainable. Combining Argon Differential Release Plots (DRP) with EPMA and Ca-Cl-K signatures of each mica populations we identified the step ages dating deformation. Microstructures of the Munsiri Thrust show the occurrence of a main disjunctive foliation defined by biotite and minor muscovite. ⁴⁰Ar/³⁹Ar stepheating coupled with correlation diagrams constrains biotite growth on the main foliation at c. 5 Ma.

The microstructures of mylonitic micaschists from the Vaikrita Thrust include three different textural generation of micas: a relict foliation, a main mylonitic foliation, and a late generation of static muscovite and chlorite overprinting the relict foliation. ⁴⁰Ar/³⁹Ar dating constrains muscovite growth on the main foliation around 10 Ma and the growth of large, static muscovite at c. 8 Ma. In the study area, Bhagirathi valley (NW India), our results support an in-sequence shearing from Vaikrita to Munsiri Thrust from c. 10 to c. 5 Ma.

Adding information about the kinematic of flow to the age of the bounding shear zones of the GHS is a key purpose for its exhumation models. The use of stable porphyroclasts analysis used for vorticity estimates can suffer from severe limitations, because of the reduction to two dimensions of motion of rigid clasts that is a complex 3D problem. We propose an alternative method to acquire data based on the use of X-ray micro computed tomography that allows to considerably decrease the limitation of the method. We selected the mylonitic orthogneisses from the Munsiri Thrust containing K-feldspar porphyroclasts in order to estimate the kinematic vorticity, which ranges between 0.49 and 0.57. We stress here the importance of a multidisciplinary approach based on detailed meso and microstructural, chemical and geochronological investigations of pervasively sheared rocks from shear zones having multiple generations of fine-grained foliations.

Characterization and evolution of the paleo-fluids in the Las Minas exhumed geothermal system (Mexico)

Morelli G.*¹, Ruggieri G.¹, Zucchi M.², Braschi E.¹, Agostini S.³, Ventruti G.², Brogi A.²⁻³, Liotta D.²⁻³, Boschi C.³ & González-Partida E.⁴

¹ IGG-CNR, Institute of Geosciences and Earth Resources, Firenze, Italy.

² University of Bari, Department of Earth and Geoenvironmental Sciences, Bari, Italy.

³ IGG-CNR, Institute of Geosciences and Earth Resources, Pisa, Italy.

⁴ UNAM, Universidad Nacional Autónoma de México, Mexico City, Mexico.

Corresponding email: guia.morelli@igg.cnr.it

Keywords: geothermal system, hydrothermal fluids, fluid inclusions.

The evolution and origin of the hydrothermal fluids circulating in the exhumed geothermal system of Las Minas area (Central Mexico) were investigated by i) structural and mineralogical studies and, ii) fluid inclusion and isotope analyses carried out on skarn and hydrothermal alteration minerals. Different stages of fluid flow in the system related to the emplacement of intrusive rocks and their interaction with the andesitic and carbonatic reservoir in the Las Minas area were recognized from fluid inclusions found in mineral assemblages (e.g. quartz, calcite, garnet) associated with skarn deposits. Fluid inclusions recorded the circulation of: 1) high-temperature (up to 650°C), high-salinity (up to 60 wt.% NaCl equiv.) fluid of magmatic origin; 2) high-temperature (470-650°C) aqueous-carbonic fluid produced during fluid-rock interaction with carbonate basement rocks and 3) relatively low-salinity (up to 2 wt.% NaCl equiv.) fluid of meteoric origin. A general evolution from high- to low-temperature fluid circulation characterized the geothermal system. Stable and radiogenic isotopes analyses also showed that fluids with different origins interacted in the system. The circulation of these geothermal fluids was strictly dependent from two main fault systems NNW- and SW-trending, recognised in the study area. Indeed, the fault zones played the role of main conduits favouring the uprising of the fluids from deep to shallower structural levels. Furthermore, fracture networks characterising the fault zones enhanced the geothermal fluid circulation as shown by hydrothermal veins localised in the damage zones.

The integration of structural, geochemical and fluid inclusion analyses allowed to i) characterize the physical-chemical properties of the paleo-fluids stored in the exhumed reservoir of Las Minas; ii) define the fluid-rock interaction processes promoted by the geothermal fluids circulating through the reservoir rocks; iii) characterize the structural control on the fluids circulation. Finally, the information obtained from the paleo-fluids in Las Minas, were used to better characterize and predict the P-T conditions of the deep fluids circulation in the analogue active geothermal field located in Los Humeros (Central Mexico).

The research leading to these results has received funding from the GEMex Project, funded by the European Union's Horizon 2020 research and innovation programme under grant agreement No. 727550.

Kinematics and deformation temperatures of the MCTz and the STDS in Central Himalaya

Nania L.*¹, Montomoli C.², Iaccarino S.², Leiss B.³, Di Vincenzo G.⁴ & Carosi R.²

¹ Dottorato Regionale in Scienze della Terra Pegaso, Università degli Studi di Firenze.

² Dipartimento di Scienze della Terra, Università di Torino.

³ Geoscience Centre, Georg-August University of Göttingen.

⁴ IGG-CNR Pisa.

Corresponding email: laura.nania@unifi.it

Keywords: Himalaya, non-coaxial flow, microfabric.

The Himalayan Belt is one of the most impressive examples of collisional orogen where crustal shortening has been accommodated by major shear zones with a southward imbrication of north-dipping litho-tectonic units (Hodges, 2000). Over the decades, several studies provided more and more detailed tectonic models; however, understanding how the deformation path evolved in Himalaya is not a simple task (Carosi et al., 2018).

In this contribution, we compared different N-S structural transects along the Greater Himalayan Sequence (GHS), the metamorphic core of the belt, in Central Himalaya. The GHS is bounded by two syn-convergent regional shear zones showing opposite kinematics: the top-to-the-S Main Central Thrust zone (MCTz) at the base, and the top-down-to-the-N South Tibetan Detachment System (STDS) at its top. A strong deformation affects the GHS with important variations in styles and P-T conditions from the MCTz to the STDS.

The heterogeneous deformation along different structural transects has been deeply investigated via structural and textural analyses, focusing on the crystallographic preferred orientation (CPO) of quartz, calcite and dolomite in several lithotypes. Textures have been coupled with paleopiezometric analyses and further structural investigations (e.g. hot-cathodoluminescence image analyses), pointing out a complex deformation history for the exhumation stages.

Within the MCTz, structures and CPO of quartz, feldspar, and dolomite in impure marble, quartz-rich mylonite, mylonitic paragneiss and micaschist, highlight high-temperature deformation regimes in structurally higher-located samples, supporting a northward increasing of deformation temperature from the base to the core of the GHS. Moving up to the STDS, the GHS consists of calcsilicates-rich marble tectonically below low-metamorphic grade impure marble of the Tethyan Himalayan Sequence (THS). Calcite and quartz fabrics support low-to-medium temperatures of deformation followed by lower deformation temperatures mechanisms within the high-strain zones. An associated non-coaxial flow is linked to an important pure shear component in the STDS. Moreover, both deformation temperatures and flow vorticity increase approaching the contact between the GHS and the THS within the shear zone.

The end of the ductile deformation of the STDS is constrained in some key areas by the presence of post-tectonic sub-millimetric biotite. This mineral has been investigated through ⁴⁰Ar-³⁹Ar laserprobe analyses coupled with electron microprobe microanalyses, which point out a late thermal event post-dating the ductile activity of the STDS

Carosi R., Montomoli C. & Iaccarino S. (2018) - 20 years of geological mapping of the metamorphic core across Central and Eastern Himalayas. *Earth-science reviews*, 177, 124-138.

Hodges K.V. (2000) - Tectonics of the Himalaya and southern Tibet from two perspectives. *GSA Bulletin*, 112(3), 324-350.

Development of vermicular clinopyroxene-amphibole symplectites replacing garnet in amphibolites of the Peloritani Mountain (Northeastern Sicily)

Ortolano G., D'Agostino G.*, Visalli R., Fiannacca P. & Cirrincione R.

^UUniversità degli Studi di Catania – Dip. Sc. Biol. Geol. Amb. – Sez. Scienze della Terra.

Corresponding email: rvisalli@unict.it

Keywords: Image analysis, CPO, coronas.

The metamorphic history of a rock can be very difficult to be unravelled if a careful analysis of the sample microstructures is not performed. These microstructures, that are the end product of the metamorphic evolution experienced by crystalline basements, can be the result of complicated chemical reactions and often also deformation events, which provide useful information to infer the PT path followed by the rocks.

One of the most peculiar microstructures which can be observed in metamorphic rocks is given by the formation of symplectites. This last can be described as a particular worm-like structure constituted by mineral intergrowths which develop simultaneously in a solid-state reaction (Vernon, 2004). Such reactions are often incomplete as due to slow diffusion rates in growing in crystalline grains, offering, in turn, the chance to observe and study both reactant minerals and solid products allowing realistic chemical equations to be written.

In this work, a detailed petrographic and mineralochemical study was carried out on an amphibolite sample coming from the high-grade metamorphic unit cropping out in the Peloritani Mountains (i.e. Aspromonte Unit), with the aim to preliminarily bracket the PT evolution of the analyzed rock. The metamorphic history of this sample can be traced back to prograde metamorphism developed under granulite facies conditions, as highlighted by a relict assemblage given by the first generation of garnet, amphibole, plagioclase, and pyroxene. The subsequent metamorphic evolution is testified by the widespread presence of clinopyroxene-amphibole-plagioclase symplectites grown as coronas around the relict garnet, as a result of retrograde transformations occurred under amphibolite facies conditions. Six microdomains containing vermicular symplectites were opportunely selected and x-ray elemental maps were processed by using the Q-XRMA software (Ortolano et al., 2018) for obtaining mineral modal abundancies and chemical compositions. Obtained results from image processing were then used to isolate the effective bulk chemistry operative during the development of symplectites, allowing to preliminarily define a PT range of P = 6.8-7.3 Kbar at T = 615-635 °C for the retrograde amphibolite facies metamorphism.

Ortolano G., Visalli R., Godard G. & Cirrincione R. (2018) - A new GIS-based statistical approach to Mineral Image Analysis. *Computers & geosciences*, 115, 56-65.

Vernon R.H. (2004) - A practical guide to rock microstructure. Cambridge University Press, 606 pp.

Unravelling cooling rates of the Calabria continental lower crust from combined microstructural, thermodynamic and diffusion modeling: An example from the Sila Piccola Massif, (Northern Calabria)

Ortolano G.¹, Visalli R.*¹, Fazio E.¹, Fiannacca P.¹, Godard G.², Pezzino A.¹, Punturo P.¹,
Sacco V.¹ & Cirrincione R.¹

¹ Università degli Studi di Catania – Dip. Sc. Biol. Geol. Amb. – Sez. Scienze della Terra, Italy.

² Institut de Physique du Globe de Paris. Centre National de la Recherche Scientifique & Université Paris Diderot, France.

Corresponding email: rvisalli@unict.it

Keywords: grain size analysis, CPO, geospeedometry.

Understanding the temporal evolution of metamorphic processes and how fast these can occur is one of the most fascinating goals of the earth scientists. Evidence of a rapidly exhumed basement is given by metamorphic rocks where mineral assemblages and compositionally-zoned crystals preserve the prograde growth history (e.g. Zhang et al., 2010). Conversely, a slow exhumation can involve long-lasting high-T processes which can destroy evidences of the early PT path, by erasing the growth mineral zoning (e.g. Spear, 2014). In this context, the study of compositional changes due to diffusion provides a valuable tool for outlining how long zoned minerals in chemical disequilibrium with the surrounding matrix can retain their pre-existing zonings before being homogenized by diffusion mechanisms (Chakraborty, 2008).

In this work, a detailed structural and petrological study was focused on a mylonitic horizon affecting granulite facies rocks cropping out in the Sila Piccola Massif, to obtain new constraints about the exhumation rate-meter of the lower portion of a Variscan basement fragment of the northern Calabria Peloritani Orogen. In particular, an Alpine metamorphic shearing overprint on earlier high temperature Variscan relics was recognized. These pre-mylonitic relics are given by a first generation of garnet, plagioclase, biotite, sillimanite and quartz in which garnet shows a flat compositional profile. The subsequent mylonitic cycle can be subdivided into two metamorphic stages. The first one, ascribable to a late-Variscan extensional shearing, generates a syn-kinematic growth of the second generation of garnet, plagioclase, biotite and quartz. The second one is characterized by a syn-shearing growth of chlorite, white mica, plagioclase and quartz, here interpreted as an early Alpine mylonitic re-activation in compressional regime. In this context, quantitative image analysis was adopted to extract the effective bulk rock chemistries to be used in PT pseudosections computation. This step was useful for constraining the PT range (P=5-6 Kbar; T=610-650 °C) of the early mylonitic stage. In this case, diffusion modeling of garnet compositional relaxation along the equilibrated rims allowed to derive a maximum timescale of ~ 5 Ma for a cooling rate of ~ 25 °C/Ma. Furthermore, a detailed microstructural study for paleopiezometer purpose, consisting in the quartz c-axis pattern analysis accompanied by grain-scale distribution analysis of the syn-mylonitic recrystallized quartz, permitted to obtain shearing temperature of 400-450 °C for a strain-rate of $7,58 \times 10^{-11}$ (1/s). Finally, the mylonitic cycle evolved to an asymmetrical folding stage at shallower conditions as proved by structural evidences, probably ascribable to the staking stages of the Alpine-Appennine tectonic activity in the central Mediterranean area.

Chakraborty S. (2006) - Diffusion modeling as a tool for constraining timescales of evolution of metamorphic rocks. *Mineralogy and Petrology*, 88(1-2), 7-27.

Spear F.S. (2014) - The duration of near-peak metamorphism from diffusion modelling of garnet zoning. *Journal of Metamorphic Geology*, 32(8), 903-914.

Zhang Y. (2010) - Diffusion in minerals and melts: theoretical background. *Reviews in Mineralogy and Geochemistry*, 72(1), 5-59.

Geochronology and deformation in the Posada-Asinara Line (NE Sardinia basement, Baronie, Italy): timing and shearing constraints in the Southern European Variscan belt

Petroccia A.*¹, Carosi R.¹, Montomoli C.¹ & Simonetti M.¹

¹ Dipartimento di Scienze della Terra, Università di Torino.

Corresponding email: alessandro.petroccia@edu.unito.it

Keywords: mylonites, shear zones, Variscan basement, East Variscan shear zone.

The Variscan belt is the result of the Lower Carboniferous continent-continent collision between Laurentia-Baltica and Gondwana (Matte, 1986). The European Variscan belt is characterized by a composite orocline (Matte, 1986; Matte, 2001) made by two main branches: the western Ibero-Armorican arc and an eastern branch delimited by a system of regional-scale dextral transpressive shear zones known as the East Variscan Shear Zone (EVSZ; Corsini & Rolland, 2009; Carosi et al., 2012). We performed a geological-structural mapping, meso- and microstructural analysis, kinematic vorticity and finite strain analysis and U-Th-Pb geochronological study on monazites in the southeastern part of the dextral shear zone, known as the Posada-Asinara Line (Baronie). Vorticity analysis confirmed the occurrence of a ductile transpression characterized by variation in the percentage of pure shear and simple shear along a deformation gradient (Carosi & Palmeri, 2002; Iacopini et al., 2008). U-Th-Pb analyses on monazites were performed on three samples of staurolite-garnet bearing micaschists. The oldest ages of ~ 350 Ma were obtained in monazites inside the inter-kinematics staurolite, whereas ages of ~ 324 Ma were found in monazite inside the mylonitic foliation. Ages of ~ 320 Ma obtained in this work, and the ones by Di Vincenzo et al. (2004) and Carosi et al. (2012) are in agreement with the ages of the dextral transpressional shear zones linked to the EVSZ: in the Maures-Tanneron Massif (Corsini & Rolland, 2009; Schneider et al., 2014), in Corsica (Giacomini et al., 2008) and in the Argentera Massif (Western Alps; Simonetti et al., 2018). These results better constrain the correlation to a network of dextral Late Carboniferous shear zones and show that shearing along the different strands of the EVSZ is diachronous. The different sectors of the EVSZ are affected by dextral transpression at different time because of the progressive change of orientation of the belt with respect to the regional stress field (Carosi et al., 2012). This is also supported by the increase of the simple shear component with time, recognized both in Sardinia (Carosi et al., 2009) and in the Argentera-Mercantour Massif (Simonetti et al., 2018).

- Carosi R., Frassi C. & Montomoli C. (2009) - Deformation during exhumation of medium- and high-grade metamorphic rocks in the Variscan chain in northern Sardinia (Italy). *Geol. J.*, 44 (3), 280-305.
- Carosi R., Montomoli C., Tiepolo M. & Frassi C. (2012) - Geochronological constraints on post-collisional shear zones in the Variscides of Sardinia (Italy). *Terra Nova*, 24, 42-51.
- Corsini M. & Rolland Y. (2009) - Late evolution of the southern European Variscan belt: Exhumation of the lower crust in a context of oblique convergence. *CR. Geosci.*, 341, 214-223.
- Di Vincenzo G., Carosi R. & Palmeri R. (2004) - The relationship between tectono-metamorphic evolution and argon isotope records in white mica: constraints from in situ ⁴⁰Ar-³⁹Ar laser analysis of the Variscan basement of Sardinia. *J. Petrol.*, 45, 1013 – 1043.
- Giacomini F., Dallai L., Carminati E., Tiepolo M. & Ghezzo G. (2008) - Exhumation of a Variscan orogenic complex: insights into the composite granulitic-amphibolitic metamorphic basement of South-East Corsica (France). *J. metamorphic Geol.*, 26, 403–436.
- Iacopini D., Carosi R., Montomoli C. & Passchier C.W. (2008) - Strain analysis and vorticity of flow in the Northern Sardinian Variscan Belt: recognition of a partitioned oblique deformation event. *Tectonophysics*, 221, 345-359.
- Matte P. (1986) - La Chaîne varisque parmi les chaînes paléozoïques péri-atlantiques, modèle d'évolution et position des grands blocs continentaux au PermoCarbonifère. *B. Soc. Geol. Fr.*, 8, 4-24.
- Matte P. (2001) - The Variscan collage and orogeny (480–290 Ma) and the tectonic definition of the Armorica microplate: a review. *Terra Nova*, 13, 117–121.
- Schneider J., Corsini M., Peila A., Lardeaux J. (2014) - Thermal and mechanical evolution of an orogenic wedge during Variscan collision: an example in the Maures-Tanneron Massif (SE France). *J. Geol. Soc. (Lond.)*, 405, 30-37.
- Simonetti M., Carosi R., Montomoli C., Langone A., D'Addario E. & Mammoliti E. (2018) - kinematic and geochronological constraints on shear deformation in the ferriere-mollières shear zone (Argentera-Mercantour Massif, Western Alps): implications for the evolution of the Southern European Variscan Belt. *International Journal of Earth Sciences*, 107, 2163 – 2189.

1:25.000 structural map of Mamone in the northern of the Sardinian variscan basement

Petroccia A.*¹, Carosi R.¹, Montomoli C.¹ & Simonetti M.¹

¹ Dipartimento di Scienze della Terra, Università di Torino

Corresponding email: alessandro.petroccia@edu.unito.it

Keywords: geological map, structural geology, Sardinian basement.

Sardinia consists of a Paleozoic Basement, intruded by Permo-Carboniferous granites and covered by Permian-Mesozoic sediments. The rotation of nearly 90° of the tectonic transport in Sardinia during collisional and post-collisional stages could be related to the paleo-position of the Corsica-Sardinia block close to southeast France (Maures-Tanneron Massif) (Corsini & Rolland, 2009). In northern Sardinia two metamorphic complexes occur, recording similar deformation histories but different metamorphic evolution: the Low to Medium-Grade Metamorphic Complex (L-MGMC) and the High-Grade Metamorphic Complex (HGMC).

The Posada Asinara Line (PAL) is a Carboniferous regional-scale transpressional shear zone (Carosi & Palmeri, 2002) that crops out in northern Sardinia, separating the two latter complexes, playing an important role in the exhumation of the metamorphic complexes (Carosi & Palmeri, 2002). The survey's area near Mamone (NE Sardinia), in the southeastern part of the PAL, allowed to refine previous geological maps available in the neighboring areas (Carosi *et al.*, 2005). A structural-geologic survey has been carried out in an area about 80 km² and a new geological map (1:25000 scale) has been realized. The structural analysis highlighted four deformation phases. The D1 phase has been observed only inside the microlithons of S2 foliation. The prominent deformation phase, D2, is associated with isoclinal and N-vergent F2 folds. The S2 axial plane foliation strikes N70-120° with variable dips but generally steeply dipping. A2 fold axes trend nearly E-W with a variable shallow plunge. Mineral and aggregate lineations, trending nearly E-W and plunging between 5° and 20°, occur on the S2 foliation. Mantled porphyroclasts with sigmoidal and delta-type geometry, S-C and S-C' fabric and shear bands boudin with a dextral top-to-the NW normal sense of shear and top-to-the SE inverse sense of shear have been observed parallel to the lineation and orthogonal to the foliation plane (XZ). The D3 phase is often associated with a crenulation cleavage (F3), parallel to the axial plane of chevron folds. D2 and D3 folds are generally coaxial, but with perpendicular axial planes. The D4 phase is associated with open folds F4 with sub-horizontal axes and axial planes, almost oriented SSE-NNW, but with a considerably axial dispersion, without the formation of an axial plane foliation. These folds cause the change of dip from S to N of the S2. Thanks to this detailed survey, associated to a microstructural study, it has been confirmed that the isograds, marked by the blastesis of the main Barrovian minerals (albite, oligoclase, garnet and staurolite) are deformed during the D2 deformation (Carosi & Palmeri, 2002). Isograds are telescoped approaching the high-strain zone due to the combined effect of simple and pure shear acting during D2 (Iacopini *et al.*, 2008).

Carosi R & Palmeri R. (2002) - Orogen-parallel tectonics transport in the Variscan belt of northeastern Sardinia (Italy): implications for the exhumation of medium-pressure metamorphic rocks. *Geol. Mag.*, 139, 497-511.

Carosi R., Frassi C., Magi S. & Montomoli C. (2005) - Analisi strutturale dell'antiforme di lodè-mamone (sardegna nord-orientale): un esempio di interferenza complessa a scala chilometrica nel basamento ercinico sardo. *Atti Soc. tosc. Sci. nat., Mem., Serie A*, 110, 23-29.

Corsini M. & Rolland Y. (2009) - Late evolution of the southern European Variscan belt: Exhumation of the lower crust in a context of oblique convergence. *CR. Geosci.*, 341, 214-223.

Iacopini D., Carosi R., Montomoli C. & Passchier C.W. (2008) - Strain analysis and vorticity of flow in the Northern Sardinian Variscan Belt: recognition of a partitioned oblique deformation event. *Tectonophysics*, 221, 345-359.

Interaction between migmatite-related melts and amphibole-gabbros: evidence from mineral geochemistry and zircon dating (Variscan lower crust, Palmi area, SW Calabria)

Renna M.R.^{*1}, Langone A.², Caggianelli A.³ & Prosser G.⁴

¹ Dipartimento MIFT, Università di Messina.

² IGG-CNR, Pavia.

³ Dipartimento di Scienze della Terra e Geoambientali, Università di Bari.

⁴ Dipartimento di Scienze, Università della Basilicata.

Corresponding email: mrenna@unime.it

Keywords: mineral geochemistry, U-Pb zircon dating, Variscan lower crust.

The Palmi area (SW Calabria) exposes a portion of the Variscan lower to intermediate crust mainly consisting of tonalite and migmatitic paragneiss. The latter shows a peak metamorphic assemblage of biotite, K-feldspar, garnet and sillimanite. The migmatites include layers of calc-silicate-bearing marble and orthogneiss. Amphibole-gabbros occur as foliated, decimeter-thick layers within the migmatites and as a decametric main body (known as Pietre Nere outcrop) adjacent to the paragneiss. No contacts are exposed between the migmatites and the gabbro body, which is mainly unfoliated and fine-grained, even though coarse-grained portions rarely occur. The gabbros overall contain subhedral to anhedral An-rich plagioclase (An₈₉₋₈₀) frequently developing triple junctions, anhedral amphibole and subhedral biotite, accessory zircon + ilmenite ± allanite also occur. Minor quartz is present in gabbro interlayered within the paragneiss. Amphibole consists of cummingtonite grading into hornblende on the rims and retains some relic cleavage from a pyroxene predecessor.

Here we combine mineral major and trace element data with U-Pb zircon dating of the gabbros in order to understand the interaction among HT metamorphism, migmatization and emplacement of mafic magma at lower crustal levels.

In the main gabbro body the amphibole shows decreasing Mg#, increasing Al and lower LREE in the passage from the coarse-grained to the fine-grained portions. The LREE-depleted patterns likely reflect crystallization of a LREE-rich phase (i.e., allanite) simultaneously with amphibole in the fine-grained portions. Plagioclase and amphibole from the gabbro layers within the paragneiss show a highly evolved REE and incompatible elements geochemical signature. Parallel patterns and increase of REE and incompatible trace elements contents indicate that the transition from cummingtonite to hornblende stability field did not involve reaction with other minerals or exotic agent, but reflects variations of temperature and/or pressure conditions. We propose that a chemical exchange between gabbros and migmatites produced a geochemical gradient within the gabbros. Therefore we suggest that the coarse-grained portions in the gabbro body most likely preserve the pristine composition. U-Pb dating of sector-zoned, magmatic zircon cores from the gabbro body yielded a Carboniferous age of intrusion. Rare thin, homogeneous zircon rims gave Lower Permian ages, which could be related to recrystallization under amphibolite-facies conditions during the regional-scale HT metamorphism.

Extention, timing and deformation of the East Variscan Shear Zone

Simonetti M.*¹, Carosi R.¹ & Montomoli C.¹

¹ Dipartimento di Scienze della Terra, Università di Torino

Corresponding email: matteo.simonetti@unito.it

Keywords: East Variscan Shear Zone, transpression, monazite petrochronology.

Recent models of the Southern European Variscan Belt propose the occurrence of a regional-scale rightlateral strike-slip fault known in the literature as East Variscan Shear Zone (EVSZ, Matte, 2001; Corsini & Rolland, 2009) that involved Corsica-Sardinia block, southern France and the future Alpine External Crystalline Massifs. Several evidences of the activity of the EVSZ are reported in the Sardinian Variscan Basement where the well-known Posada-Asinara Shear Zone (PAL) is interpreted as the southern branch of the EVSZ (Carosi & Palmeri, 2002; Carosi et al., 2012). Toward the northern sectors the evidence and the extension of the EVSZ are less clear. We investigated in detail the kinematic of flow, finite strain and the timing of the deformation of several regional-scale shear zones in the Variscan basement of the Maures Massif (southern France) and of the Alpine External Crystalline Massifs. In the Maures Massif we focused on the Cavalaire Fault while in the Western Alps we focused on two ductile shear zones: The Ferriere-Mollieres shear zone in the Argentera Massif and the Emosson-Val Berard shear zone in the Aiguilles Rouges Massif. Our investigations revealed that, similarly with the PAL, all of them are Variscan transpressive shear zones with variable percentage of simple shear acting together with pure shear. They also initiate during similar high-temperature conditions as the PAL in northern Sardinia nearly at the same time and with the same kinematics. The new data obtained in this work allow to establish that the Aiguilles Rouges Massif, the Argentera Massif, the Maures Massif and the Corsica-Sardinia block underwent very similar transpressional deformation during Variscan time (between ~330 and ~310 Ma) because these sectors were in lateral continuity and they were part of the same system of anastomosing dextral shear zones connected to the development of the EVSZ.

Carosi R., Montomoli C., Tiepolo M. & Frassi C. (2012) - Geochronological constraints on post-collisional shear zones in the Variscides of Sardinia (Italy): Post-collisional shear zones in the Variscides of Sardinia. *Terra Nova* 24:42–51. <https://doi.org/10.1111/j.1365-3121.2011.01035>.

Carosi R. & Palmeri R. (2002) - Orogen-parallel tectonic transport in the Variscan belt of northeastern Sardinia (Italy): implications for the exhumation of medium-pressure metamorphic rocks. *Geological Magazine* 139, <https://doi.org/10.1017/S0016756802006763>.

Corsini M. & Rolland Y. (2009) - Late evolution of the southern European Variscan belt: Exhumation of the lower crust in a context of oblique convergence. *Comptes Rendus Geoscience* 341, 214-223. <https://doi.org/10.1016/j.crte.2008.12.002>.

Matte P. (2001) - The Variscan collage and orogeny (480–290 Ma) and the tectonic definition of the Armorica microplate: a review. *Terra Nova* 13, 122-128.

Structural analysis, kinematic of the flow and petrochronology of shear deformation in the Aiguilles Rouges Massif

Simonetti M.*¹, Carosi R.¹ & Montomoli C.¹

¹ Dipartimento di Scienze della Terra, Università di Torino

Corresponding email: matteo.simonetti@unito.it

Keywords: Aiguilles Rouges Massif, kinematic vorticity, monazite petrochronology.

Two sectors of the Aiguilles Rouge Massif, the Emosson Lake area and the Val Berard area, were studied. Here rocks are strongly sheared along a mylonitic belt developed at the expense of metasediment and orthogneiss. Alpine deformation is weak. Our aim is to clarify the kinematics of the flow and to directly constrain the age of the deformation to verify if there are similarities with the tectonic evolution of the other fragments of the Variscan basement in the Mediterranean area. We carried out structural and microstructural analyses of sheared rocks combined with a kinematic vorticity analysis and a U-Th-Pb petrochronological study on syn-kinematic monazites. Quartz c-axis fabric was analysed in order to constrain deformation temperature. The main foliation has a sub-vertical attitude and strike NE-SW. Mineral lineation is gently plunging toward the NE. Kinematic indicators point to a top-to-the-SW dextral sense of shear. Quartz c-axis fabric analyses are generally intermediate between Type-I and Type-II crossgirdles, suggesting flattening deformation close to plane strain condition. The asymmetry of the fabrics is indicative of a dextral top-to-the-SW sense of shear. The opening angles are indicative of temperature of deformation between ~660° C and ~600° C. Vorticity analysis revealed a transpressional deformation with a prevalent component of pure shear acting together with simple shear. Monazite petrochronology constrain the onset of transpression at ~320 Ma. Transpressional Variscan deformation in the Aiguilles Rouges Massif is similar to that outlined in the Argentera Massif (Simonetti et al., 2018), in the Maures Massif and in Sardinia (Carosi & Palmeri, 2002; Carosi et al., 2012) in accordance that all these sectors of the belt should have been in lateral continuity during Variscan time and they were part of the same regional-scale dextral shear zone known as East Variscan Shear Zone (Corsini & Rolland, 2009).

Carosi R., Montomoli C., Tiepolo M., Frassi C. (2012) - Geochronological constraints on post-collisional shear zones in the Variscides of Sardinia (Italy): Post-collisional shear zones in the Variscides of Sardinia. *Terra Nova*, 24, 42–51.

Carosi R. & Palmeri R. (2002) - Orogen-parallel tectonic transport in the Variscan belt of northeastern Sardinia (Italy): implications for the exhumation of medium-pressure metamorphic rocks. *Geological Magazine*, 139.

Corsini M. & Rolland Y. (2009) - Late evolution of the southern European Variscan belt: Exhumation of the lower crust in a context of oblique convergence. *Comptes Rendus Geoscience* 34, 214-223.

Simonetti M., Carosi R., Montomoli C., Langone A., D'Addario E. & Mammoliti E. (2018) - Kinematic and geochronological constraints on shear deformation in the Ferriere-Mollières shear zone (Argentera-Mercantour Massif, Western Alps): implications for the evolution of the Southern European Variscan Belt. *International Journal of Earth Sciences*.

Reworking of felsic rocks in ductile shear zones: an example from the Curinga-Girifalco line

Tursi F.*¹, Acquafredda P.¹, Festa F.¹, Fornelli A.¹, Langone A.², Micheletti F.¹ & Spiess R.³

¹ Dipartimento di Scienze della Terra e Geoambientali, Università degli Studi di Bari “Aldo Moro”, Bari, Italy.

² Dipartimento di Scienze della Terra e dell’Ambiente, Università degli Studi di Pavia, Pavia, Italy.

³ Dipartimento di Geoscienze, Università degli Studi di Padova, Padova, Italy.

Corresponding email: fabrizio.tursi@uniba.it

Keywords: ductile shear zones, mineral assemblage reworking, Serre Massif.

In the northern Serre Massif, Alpine tectonics juxtaposed the Castagna unit orthogneisses (below), representative of the Hercynian intermediate crust, to mafic and felsic granulites and granulite facies migmatitic paragneisses of the Hercynian lower crust (above), along the Curinga-Girifalco ductile shear zone.

The detailed microstructural study of progressively sampled ductilely sheared orthogneisses from their host, highlighted mineral assemblage variations from i) Kfs + Pl + Qz + Bt + Mu + Ep + Tnt ± Ilm in weakly deformed orthogneisses to ii) Kfs + Ab + Qz + Phe + Czo + Tnt + (Grs-rich) Grt ± Ep ± Chl ± Bt and iii) Kfs + Ab + Qz + Phe + Czo + Tnt ± (Grs-rich) Grt ± Chl in mylonitic orthogneisses.

Phase diagram calculations in the MnNCKFMASHTO model system highlight that the progressive replacement of pre-Alpine mineral phases (e.g., plagioclase, biotite and ilmenite) by new Alpine ones (i.e., garnet, albite, titanite, epidote and clinozoisite) is related to different amount of external fluid infiltration, promoting partial to total renovation of the pre-Alpine mineral assemblage. On the basis of the garnet $X_{\text{Grs}}_{(0.47-0.54)}$ and $X_{\text{Sps}}_{(0.08-0.22)}$ isopleth intersections, the reworked Castagna orthogneisses record a prograde, stepwise, Alpine P – T evolution in the amphibolite facies, with peak metamorphic conditions at ca. 0.9 GPa. Further, the subsequent exhumation stage, characterized by decompression and cooling, occurred in the stability field of sin-kinematic clinozoisite, accounting for an overall anticlockwise P – T path.

The results of this work clearly show that continental crustal rocks from the intermediate nappe underwent hydration when underthrust during the Alpine subduction in Calabria, recording the highest P – T conditions with respect to the juxtaposed other lithologies due to complete mineral assemblage reworking. Therefore, the Curinga-Girifalco shear zone developed during Eocene nappe stacking and prolonged its activity during Oligocene extensional tectonics.

Uncovering UHPM garnet growth and dissolution mechanisms using trace elements in metasediments from Lago di Cignana, Western Alps

Van Schrojenstein Lantman H.W.*¹, Langone A.², Scambelluri M.³ & Alvaro M.¹

¹ Dipartimento di Scienza della Terra e dell'Ambiente, Università di Pavia.

² Istituto di Geoscienze e Georisorse, CNR, U.O.S. di Pavia.

³ Dipartimento di Scienze Della Terra, Ambiente e Vita DISTAV, Università di Genova.

Corresponding email: hugo.vanschrojenste01@universitadipavia.it

Keywords: garnet, growth, dissolution.

Garnetite lenses are a common occurrence in the ultra-high pressure metamorphic grade metasediments from Lago di Cignana. Petrological and microstructural analysis of garnets in the garnetite and the host quartzite suggests a common origin, with the evolution of the garnet types decoupling due to localized fluid influx interrupting metamorphic processes. Trace elements in garnet were analysed to study the similarities and differences between both types of garnet.

Two main differences are observed between analysed garnets in the host rock garnets and the garnetite. Although both show the typical REE pattern for garnet, Y+HREE levels are significantly higher in the host rock. Additionally, garnetite garnets show an enrichment in LREE+MREE. In the host rock, garnets were large enough to measure core and rim separately, which showed only minor differences. Because major element zoning of the garnetite and host rock garnets show great similarity up to the metamorphic decoupling, we considered processes beyond regular element fractionation during metamorphism to explain the different REE concentrations.

Unlike the garnetite, garnets from the host rock show several phases of dissolution-growth, with new growth being enriched in Mn. An element map of Y shows the same trend, so some degree of the Y+HREE enrichment in the host rock is the result of resorption. The LREE+MREE enrichment in the garnetite shows a linear trend with Ti. This enrichment also goes alongside an enrichment of elements commonly found in rutile, and matches rutile-contaminated host rock garnet measurements. The presence of sub-micron size rutile inclusions in garnet is suggested, which are also present in the inner core of host rock garnets. We interpret this as the result of a garnet forming reaction at the cost of titanite. As Ti is fairly immobile, it formed sub-micron size rutile crystals at the site of the titanite breakdown. As garnet dissolved in the garnetite due to pulses of undersaturated fluids, the rutile inclusions were freed and accumulated along fluid pathways.

Tectono-sedimentary evolution of the Tlaxiaco Basin, southern Mexico: A key to understand the Jurassic structural history of Proterozoic and Paleozoic basement rocks of Mexico during Pangea breakup

Zepeda-Martínez M.*¹ & Martini M.¹

¹ Istituto di Geologia, Università Nazionale Autonoma del Messico.

Corresponding email: mildredzm@gmail.com

Keywords: southern Mexico, Tlaxiaco basin, basement rocks exhumation.

The backbone of Mexico consists of a set of metamorphic blocks of different nature, age, and metamorphic grade that were amalgamated during the Late Paleozoic assembly of Pangea (Ortega-Gutiérrez et al., 2018). By Jurassic time, these metamorphic rocks were located in the western equatorial margin of Pangea, at the nascent rift boundary between North and South America. Therefore, the Jurassic tectonic evolution of Mexico was influenced by the activity of major faults that generated extensional to transtensional basins (Martini & Ortega-Gutiérrez, 2016). Because of the complex overprinting of Late Cretaceous and Cenozoic deformation events, it is difficult to identify the major faults that formed during the rifting episode and produced the exhumation of metamorphic rocks during Jurassic time. Considering that sedimentary environments and composition of clastic rocks are very sensitive to topographic changes caused by the activation or deactivation of major faults, the sedimentological and provenance analyses of the Jurassic successions exposed in rift basins of southern Mexico could be a powerful tool for the reconstruction of the Jurassic structural history of basement rocks. In the framework of the PAPIIT IN104018 project, we carried out the sedimentological and provenance analyses of the Jurassic stratigraphic record exposed in the Tlaxiaco Basin, southern Mexico. This record is composed of clastic successions deposited in two different sedimentary environments: 1) an alluvial fans system, with main sedimentary transport to the south, associated with the exhumation of Paleozoic, greenschist-facies metamorphic rocks of the Acatlán Complex along a WNW-trending major fault system; 2) a wandering river, flowing from east to the west, dominantly fed by Proterozoic, granulite-facies metamorphic rocks of the Oaxacan Complex, which were exhumed by a major NNW-trending faults system. Therefore, the depositional architecture of the Tlaxiaco Basin and the provenance analysis of its stratigraphic record document that the Proterozoic and Paleozoic rocks of the basement of southern Mexico were exhumed by a conjugated system of NNW-trending normal-dextral faults and WNW-trending normal-sinistral faults during the Jurassic rifting associated to Pangea breakup.

Martini M. & Ortega-Gutiérrez F. (2016) - Tectono-stratigraphic evolution of eastern Mexico during the break-up of Pangea: A review. *Earth-Science Reviews*, 183, 38–55.

Ortega-Gutiérrez F., Elías-Herrera M., Morán-Zenteno D.J., Solari L., Weber B. & Luna-González L. (2018) - The pre-Mesozoic metamorphic basement of Mexico, 1.5 billion years of crustal evolution. *Earth-Science Reviews*, 183, 2–37.

Faults-controlling geothermal fluid flow in low permeability rock volumes: an example from the eastern Elba Island (northern Tyrrhenian Sea, Italy)

Zucchi M.*

Department of Earth and Geoenvironmental Sciences, University of Bari, Italy.

Corresponding email: martina.zucchi@uniba.it

Keywords: extensional tectonic, contact metamorphism, geothermal fluid.

Geothermal fluids circulation and storage within rock volumes are essential conditions for an effective geothermal system. Although several studies have been addressed to the analysis of the fluid migration through permeable rock volumes, few papers are dealing with fluid flow and fluid-rock interaction within the cap rocks of geothermal systems. This work illustrates the result of an integrated study focused on the circulation of geothermal fluid and fluid-rock interaction in cap rocks (mostly made up of clayey sedimentary rocks) on an exhumed geothermal system located in the south-eastern Elba Island (Acquarilli-Norsi areas, Tuscan Archipelago). Structural and kinematic data highlight that the geothermal fluid was mainly controlled by NE-trending normal faults. These structures played the role of main conduits for the fluid flow. Fe-amphibole+quartz+calcite±chlorite±epidote±titanite mineral assemblage filled the fracture networks associated to two different fault generations. Fluid-rock interaction gave rise to skarnoid, characterised by three distinct mineralised zones that result locally crossed by the faults. Fluid inclusions data on quartz (coexisting with the amphibole in the first faults generation) and calcite (coexisting to the amphibole in the first faults generation, and related to the last geothermal fluid circulation, in the case of the second faults generation) suggest that at least three paleo-geothermal fluids permeated through the fault zones, at a maximum P of about 0.8 kbar: (i) the first H₂O-rich fluid enriched by a volatile phase mainly made up of CO₂ derived from the decarbonation reaction of the hosting metacarbonate rocks; (ii) the second fluid, devoid of CO₂ and characterised by a progressive decrease of temperatures; (iii) the third one, related to the last fluid circulation event. The main conclusion is that: (i) geothermal fluids crossed the cap rocks of the paleo-geothermal system along fault zones; (ii) circulation of fluids occurred within restricted damaged volumes associated to fault zones, developed in an extensional setting.

The research leading to these results has received funding from the European Community's Seventh Framework Programme under grant agreement No. 608553 (Project IMAGE).

S14

**Bio-Geo materials for environmental remediation: novel
approaches, technologies and case studies**

CONVENERS AND CHAIRPERSONS

Giacomo Ferretti (Università di Ferrara)

Lucia Morrone (CNR-IBIMET)

Domenico Prisa (CREA – Centro di ricerca Orticoltura e Florovivaismo)

Occurrence of pararealgar in As-rich aquifer sediments of the Venetian plain (Italy)

Artioli G.¹, Berto D.¹, Dalconi M.C.¹, Gò E.¹, Peruzzo L.² & Tateo F.*²

¹ Dipartimento di Geoscienze, Università degli Studi di Padova.

² Istituto di Geoscienze e Georisorse - CNR, c/o Dipartimento di Geoscienze, Università degli Studi di Padova.

Corresponding email: tateo@igg.cnr.it

Keywords: arsenic, pararealgar, groundwater.

Groundwater with strong As contamination is known in the Venetian plain in the Brenta river domain (up to about 400 ppb, Carraro et al., 2015) and in the Adige river one (up to about 650 ppb, ARPAV, 2009). In the Brenta river plain the variation of groundwater As within a few kilometres or less is accounted for by the redox conditions, that can change within short distances. In oxidizing to slight reducing conditions (Eh > -50 mV) As is adsorbed on Fe-hydroxides and the soluble amounts are very low. For negative Eh values (-50 to -250 mV) soluble As reaches the maximum concentrations, and at very negative redox conditions (< -250mV) soluble As strongly decreases (2-14 ppb). The occurrence of micrometric to sub-micrometric As-S phases observed by SEM-EDS in the aquifer sediments suggests that reductive conditions enable the precipitation of As sulfides which scavenge soluble As. Although the formation of As-sulfides at low temperatures agrees with theoretical computations their documented occurrence is quite rare or inferred according to the X-ray spectroscopy of the bulk sediment.

The experimental study focused on peaty sediments cored in the Brenta plain (2 sites, about 5.4 Km apart), which have been analysed by SEM-EDS to identify mineral phases that concentrate As. Despite the diffuse occurrence of pyrite in all samples no signal of As was found in Fe sulfides and in phosphates. On the contrary, rare micrometric grains composed only by As and S have been found in 5 samples from the 2 cores, over the 16 samples analysed. Some As-S masses are blocky, other are irregular and also fibrous morphology can be seen. μ -Raman spectra were collected on 3 micrometric red-orange crystals from 3 different samples from the 2 cores, ensuring a significant occurrence of the findings.

The Raman spectra collected are almost identical, with broad bands, which fit rather well the realgar and pararealgar references in the RRUFF database (rruff.info).

A sample of true realgar was analysed by XRD and later on by μ -Raman using the same instrumentation. A successive exposure to strong UV-radiation for 6 hours produced additional XRD peaks of As-oxide (arsenolite) and pararealgar. Optical observation revealed the occurrence of different coloured aggregates (red, orange, yellow, green and whitish), and the corresponding μ -Raman spectra differs only in subtle details. The μ -Raman spectra of As-S material taken from Brenta plain and from the exposed realgar crystals are similar and the matching is improved considering areas of green and yellow colours rather than the reddish ones. Even though realgar, pararealgar and other possible polymorphs of As-S do not show marked differences in their Raman spectra, the closer matching between pararealgar reference sample and Brenta sediments samples confirms the occurrence of pararealgar in the Brenta sediments.

Carraro A., Fabbri P., Giaretta A., Peruzzo L., Tateo F. & Tellini F. (2015) - Effects of redox conditions on the control of arsenic mobility in shallow alluvial aquifers on the Venetian Plain (Italy). *Science of the Total Environment*, 532, 581-594.

Microbiological assessment of lime application to agricultural soils

Deltedesco E.*¹, Zehetner F.¹, Unterfrauner H.² & Keiblinger K.M.¹

¹ Institute of Soil Research, University of Natural Resources and Life Sciences, Vienna, Austria.

² TB Unterfrauner GmbH, Rochuspark Erdbergstraße 10/33, Vienna, Austria.

Corresponding email: evi.deltedesco@boku.ac.at

Keywords: Soil compaction, quicklime, limestone, microbial activity.

Soil structure and pore space can be negatively affected by high inputs of mechanical energy in mechanized agriculture. Soil structural degradation further impairs the water and air permeability, and restricts the habitat of soil organisms. A promising approach to improve soil structure is the addition of polyvalent ions like Ca^{2+} , which can be added in the form of quicklime (CaO) or limestone (CaCO_3). While quicklime has been recommended for rapid improvement of soil structural stability, it may raise soil pH to alkaline levels, which could affect the soil microbial activity.

To this end we conducted a greenhouse pot experiment using CaO , CaCO_3 and a control for comparison, in order to examine their effect on soil microbial parameters over time. Silty and clayey soils from three locations in Austria were incubated for three months. Soil samples were analysed 2, 30 and 86 days post lime application for functional enzyme activities, microbial biomass C and N. Besides, different soil parameters, such as pH, dissolved organic C and N, nitrate and ammonium were measured to link them to shifts in soil microbial parameters.

Initially, soil pH and dissolved organic carbon were strongly increased by quicklime. However, after one month, the pH values of all tested soils returned to levels comparable to the soils treated with limestone while the dissolved organic carbon levels declined continuously with incubation time. An immediate inhibition effect of quicklime on potential hydrolytic enzyme activities and an increase in oxidative enzyme activities was observed. These effects seem to cease in the medium-term. We conclude that the application of quicklime has only short-term impact on most microbial activity parameters.

Effects of natural and NH₄-enriched Zeolite on nitrogen leaching from a reclaimed agricultural soil of the Ferrara province (Italy)

Faccini B.*¹, Di Giuseppe D.², Ferretti G.¹, Galamini G.¹ & Coltorti M.¹

¹ Dipartimento di Fisica e Scienze della Terra, Università di Ferrara, Italy.

² Dipartimento di Scienze Chimiche e Geologiche, Università di Modena e Reggio Emilia, Italy.

Corresponding email: fcbbbr@unife.it

Keywords: natural zeolites, nitrate, agriculture.

The impact of agriculture on water quality is a worldwide problem and a matter of concern for the European Union (EU) since the early nineties. Fertilizer-N inputs are generally inefficiently exploited by crops, resulting in widespread nitrogen (N) losses in the environment (Dawson et al. 2008). Agricultural systems characterized by low fertilizer use efficiency (FUE) are responsible for altering the equilibrium of natural ecosystems; in addition, high NO₃ and P levels in waters lead to eutrophication phenomena. Thus, in order to make modern agriculture a sustainable activity, fertilization reductions must be combined with FUE improvements. With the implementation of Nitrates Directive (91/676/EC) and the Water Framework Directive (2000/60/EC) the EU aimed at preventing the negative effects linked to the excess of NO₃ by promoting the use of good and innovative farming practices.

In this study we report an overview of the main outcomes of a three-years experimental cultivation carried out in a reclaimed agricultural field amended with different types of zeolites (rock containing > 50% of zeolites), under cereals cultivation (*Sorghum vulgare Pers*, *Zea mais* and *Triticum durum*). The experimental field was located in the Ferrara Province, declared as Nitrate Vulnerable Zone “NVZ” in 2006 after the implementation of the Nitrate Directive by the Emilia-Romagna Region in central-north of Italy. The aim of the experiment was to exploit the properties of zeolites for reducing the excessively high NO₃⁻ content in the soil and in waters outflowing the sub-surface drainage system (SSDS) of the field and flushing into the surface water system, reducing concomitantly N inputs from chemical fertilizers (up to 50 %). Zeolites were tested both in their natural state and in an NH₄-enriched form, obtained through an enrichment process with zootechnical effluents (pig slurry). NO₃⁻ content in soils and in waters discharged through SSDS were periodically monitored during the experimentation and crop yield quantified. Results showed that, for three consecutive cultivation cycles, the overall NO₃⁻ concentrations in soil (measured in H₂O-extracts) was reduced by 45 % in the zeolite treated soils, while in SSDS waters the reduction reached the 64 %. Notwithstanding the lower N input from chemical fertilizers, crop yield was not negatively affected in the zeolite amended soils, with respect to the control. Zeolite addition probably influenced several pathways of N losses, allowing a better FUE by plants and a reduction of the overall NO₃⁻ concentrations in the surface waters.

Dawson J.C., Huggins D.R. & Jones S.S. (2008) - Characterizing nitrogen use efficiency in natural and agricultural ecosystems to improve the performance of cereal crops in low-input and organic agricultural systems. *Field Crop Res.*, 107, 89-101.

Effects of natural and NH₄-charged zeolite amendments and their combination with 3,4-dimethylpyrazole phosphate (DMPP) on soil gross ammonification and nitrification rates

Ferretti G.*¹, Galamini G.¹, Deltedesco E.², Gorfer M.³, Faccini B.¹, Zechmeister-Boltenstern S.², Coltorti M.¹ & Keiblinger K.M.²

¹ Department of Physics and Earth Science, University of Ferrara.

² University of Natural Resources and Life Sciences Vienna (BOKU).

³ Austrian Institute of Technology (AIT).

Corresponding email: frgcm@unife.it

Keywords: gross N transformation rates, Nitrogen cycle, natural zeolites.

The use of zeolitites (rocks with > 50 wt% of zeolites) at natural (NZ) and NH₄-enriched state (CZ) as soil amendments is recognized as a valuable management practice to improve agricultural sustainability. Zeolites are known to influence the nitrogen (N) dynamics in soils because of their very high cation exchange capacity.

However, their influence on soil N transformation processes is mostly unknown, especially concerning their effects on gross rates of mineralization and nitrification. Recent studies demonstrated that NZ has limited influence on soil microbial biomass activity in the short-term period, while CZ is responsible for a priming effect on soil microbial biomass, which stimulates net NO₃⁻ production and NH₄⁺ consumption. In this optic, the high NO₃⁻ concentrations induced by CZ suggests that the application together with a nitrification inhibitor (NI) would improve Nitrogen Use Efficiency (NUE) and reduce N losses.

With this work we aimed at unveiling the mechanisms for different N availability after zeolite amendments, by measuring gross N mineralization and nitrification rates in zeolite amended soils both with and without the addition of a NI.

Gross nitrification and mineralization rates were evaluated using the ¹⁵N pool dilution technique in soils amended with NZ and CZ, with and without a commonly used synthetic nitrification inhibitor 3,4-dimethylpyrazole phosphate (DMPP).

The experiments were performed on a slightly alkaline soil with silty-clayey texture, amended with ten wt% of NZ and CZ in comparison to an unamended soil. Fertilizers were added at a ratio of 170 kg N ha⁻¹. At time 0 and after 24 h, we measured NH₄⁺ and NO₃⁻ concentration and N isotopic signature. The total evolved N₂O during the incubation as well as total DNA and functional genes involved in the N cycle (*amoA*, *BamoA*, *nirS*, *nosZ*) through qPCR were also determined.

Results show that the addition of NZ to soil had no effects on NH₄⁺ and NO₃⁻ production and consumption rates in this soil. On the other hand, CZ amended soil showed a significantly higher gross NH₄⁺ production as well as high N₂O emissions. The latter were corroborated with a significantly lower content of *nosZ* and *nirS*. The lower expression of N₂O reductase genes likely resulted in higher N₂O emissions.

Concerning the DMPP, it generally lowered the NH₄⁺ consumption, favoring the preservation of this pool. The efficiency of DMPP was not affected by the presence of zeolites at natural state but showed synergic effects with CZ. Additionally, DMPP application reduced by more than 90% the total amount of evolved N₂O in all the treatments. These results suggest that the addition of DMPP to soils can mitigate N₂O losses to a large degree, while the NUE for CZ amendments can be sharply improved via reduced gross nitrification and can thus reduce N losses to the water bodies.

Sorption of 3,4-Dimethylpyrazole phosphate (DMPP) in Soils amended with different chabazite zeolites

Ferretti G.*¹, Keiblinger K.M.², Faccini B.¹, Galamini G.¹, Mentler A.², Zechmeister-Boltenstern S.² & Coltorti M.¹

¹ Department of Physics and Earth Science, University of Ferrara.

² University of Natural Resources and Life Sciences Vienna (BOKU).

Corresponding email: frrgcm@unife.it

Keywords: adsorption, nitrification inhibitor, natural zeolites.

The use of rocks containing more than 50% of zeolites (natural zeolites, ZTs) as a soil amendment is recognized as a valid method to increase soil properties. ZTs are usually used both at the natural state and/or in the pre-enriched form with specific cations (e.g., NH_4^+) to improve the plant N use efficiency (NUE) and soil physic-chemical properties. However, while it has been shown that ZTs at natural state can significantly reduce gaseous N losses and increase crop yield, NH_4^+ -enriched ZT has shown quick NO_3^- production and high gaseous N losses (Ferretti et al., 2017; Faccini et al., 2018). The use of nitrification inhibitors (NIs) could certainly mitigate these losses, constituting an exciting possibility to increase NUE when NH_4^+ -enriched ZTs are employed.

The purpose of this work is, therefore, the description of the adsorption characteristics of a synthetic NI (3,4-dimethylpyrazole phosphate, DMPP) on natural and NH_4^+ -enriched ZTs and different soil-ZTs mixtures. The introduction of new binding sites with the addition of zeolites may, in fact, influence the sorption of NI, which can reduce its availability to soil microbial biomass and therefore its inhibitory effect.

To this aim, we conducted a sorption experiment where different soil-zeolite textures, pure soil and zeolites, have been mixed with DMPP solutions at various concentrations (from 1 to 500 mg L⁻¹). Adsorption isotherms were built using the Langmuir model and other parameters, like organic carbon, cation exchange capacity, pH, and hydrophobicity degree, were measured during the experiment.

Results show that pure ZTs had a deficient capacity for DMPP sorption and thus decreased the possibility to retain DMPP once applied to the soil. The sorption capacity strongly positively correlated to soil organic C content, supporting that sorption was mainly driven by soil organic matter and hydrophobic interaction (reduced by ZTs addition) (Keiblinger et al., 2018). These outcomes indicate that the combined use of natural and NH_4^+ -enriched ZTs with DMPP may result in a good strategy for increasing nitrogen use efficiency since its inhibitory effect will likely not be influenced by sorption processes.

Ferretti G., Keiblinger M.K., Zimmermann M., Di Giuseppe D., Faccini B., Colombani N., Mentler A., Zechmeister-Boltenstern S., Coltorti M. & Mastrocicco M. (2017) - High resolution short-term investigation of soil CO_2 , N_2O , NO_x and NH_3 emissions after different chabazite zeolite amendments. *Appl. Soil Ecol.*, 119, 138-144.

Keiblinger M.K., Zehetner F., Mentler A. & Zechmeister-Boltenstern S. (2018) - Biochar application increases sorption of nitrification inhibitor 3,4-dimethylpyrazole phosphate in soil. *Environ. Sci. Pollut. Res.*, 25, 11173-11177.

Soil amendments for re-cultivation of formerly mined land on Bangka island, Indonesia

Keiblinger K.M.¹, Maftukhah R.², Ngadisih², Murtiningrum², Kral R.M.³ & Mentler A.*¹

¹ University of Natural Resources and Life Sciences Vienna, Austria, Institute of Soil Research.

² Universitas Gadjah Mada, Yogyakarta, Indonesia, Department of Agricultural Engineering.

³ University of Natural Resources and Life Sciences Vienna, Austria, Centre for Development Research.

Corresponding email: axel.mentler@boku.ac.at

Keywords: Re-cultivation, soil amendment, mining, metal contamination, Indonesia.

Bangka Island lies East of Sumatra, in the South East Asian tin belt. Tin is extracted from the near-surface through physical separation using water and floatation; but the formerly mined land suffers from extraction, that leaves behind large deposits of either quartz sand or kaolinite. The former soil is now unsuitable for agriculture, but this livelihood option is strongly needed for the local population.

In this setting, we tested several locally available soil amendments for their potential to improve soil structure and physico-chemical parameters. The experimental area was set up in the field of local farmers, together with these farmers. We tested five treatments or combinations thereof, against a control: (i) lime (10t/ha), (ii) compost (10t/ha), (iii) charcoal (10t/ha), (iv) charcoal + compost (10t/ha each, total of 20t/ha), (v) charcoal and wood chips (10t/ha each, 20t/ha in total), in four replicates. As the main crop, we planted cassava, as cover crop, we used *Centrocema pubescens*. Soil samples were taken before and after harvest to analyse pH, Ct, Corg, Nt, C/N, DOC, and ultrasonic soil aggregate stability (USAS). Samples of the cover crop were taken at harvest time, yield was determined.

Tin in the area is present in caserite, other metals are present in a silica-zirkon matrix. Associated metals are arsenic, selene and lead. The presence of these materials can possibly be an issue for food safety. These metals should not mobile the present silica matrix. However, it is strictly necessary to test the uptake in plant material before promotion of agriculture on formerly mined land can be judged to be safe and fully supported.

While the results from amending soil with the mentioned additives gave encouraging results and underlined the potential of Bangka's soils for agricultural production, the soil samples and especially the plant material need to be monitored for presence of heavy metals. The results have to be analysed in relation to European regulation and standards for safe production.

Optimal hydrogeological conditions for phytoscreening in sites with chloroethenes subsurface contaminations

Leoncini C.*¹, Lo Monaco A.², Gagni S.², Emiliani R.², Riberti R.², Forti F.², Caridei F.³, Filippini M.¹ & Gargini A.¹

¹ Department of Biological, Geological and Environmental Sciences, University of Bologna.

² Agenzia Regionale per la prevenzione, l'ambiente e l'energia dell'Emilia-Romagna (Arpae).

³ Ecosurvey® - 3000 s.r.l.

Corresponding email: carlotta.leoncini2@unibo.it

Keywords: phytoscreening, chloroethenes.

Phytoscreening is a hydrogeological application that has proven to be effective in reflecting the extent and severity of subsurface contamination by chlorinated ethenes (Limmer et al., 2013), being advantageous as time-saving and inexpensive. Volatile organic compounds (VOCs) are absorbed by the roots (directly from groundwater or soil gas/water) and carried through the xylem of the plants. By drilling tree trunks, micro-cores can be obtained and analysed. Moreover, it is possible to insert detector tubes in the residual holes to assess the “in vivo” gaseous phase concentrations of a specific compound directly on-site (Luchetti & Diligenti, 2014).

Former literature proves phytoscreening is a valid tool in various climates, seasons, and with different water table depths (Yung et al., 2017; Duncan & Brasseau, 2017). Still, a systematic analysis about the optimal hydrogeological conditions for the application of phytoscreening is missing (e.g. aquifer hydraulic conductivity, vadose zone porosity). Besides, in most of previous publications, the occurrence of the degradation products of the chlorinated ethenes series in tree core samples is rare. The detectability of the dechlorination products of tetrachloroethene (PCE) and trichloroethene (TCE) –i.e. dichloroethene (cis-DCE) and vinyl chloride (VC)– requires more investigations.

Three hydrogeologically different unconfined aquifers have been surveyed. In the first site, situated in an industrial zone, a poplar grove grows over a shallow (<2 m b.g.l.) silty-sandy aquifer mainly contaminated by PCE and TCE. The second case study, an urban area with a variety of tree species, is underlain by a gravelly-sandy deep aquifer (>8 m b.g.l.) where all the chlorinated ethenes series can be found. Lastly, in a former dump, a shallow (<2 m b.g.l.) sandy aquifer with peaty lenses is heavily contaminated by VC.

Chloroethenes concentrations from tree core and “in vivo” sampling were integrated with site-specific hydrogeological features aiming to improve the applicability of phytoscreening as a new technique for the characterization of sites contaminated by chloroethenes.

Duncan C.M. & Brasseau M.L. (2017) - An assessment of correlations between chlorinated VOC concentrations in tree tissue and groundwater for phytoscreening applications. *Science of the Total Environment*, 616-617, 875–880.

Limmer M.A., Shetty M.K., Markus S., Kroeker R., Parker B.L., Martinez C. & Burken J.G. (2013) - Directional Phytoscreening: Contaminant Gradients in Trees for Plume Delineation. *Environ. Sci. Technol.*, 47, 9069–9076.

Luchetti L. & Diligenti A. (2014) - Individuazione in tempo reale della contaminazione da solventi clorurati nel sottosuolo attraverso l'utilizzo in vivo di fiale colorimetriche negli alberi. *BEA Il Bollettino degli esperti Ambientali*, 4, 51-62.

Yung L., Lagron J., Cazaux D., Limmer M. & Chalot M. (2017) - Phytoscreening as an efficient tool to delineate chlorinated solvent sources at a chlor-alkali facility. *Chemosphere*, 174, 82-89.

Sulfur bearing and aromatic compound trapping by layered silicates: a great start for innovative technological applications

Malferrari D.*¹, Bernini F.¹, Bigli B.¹, Borsari M.¹, Brigatti M.F.¹, Castellini E.¹, Mucci A.¹
& Sebastianelli L.¹

¹ Dipartimento di Scienze Chimiche e Geologiche, Università di Modena e Reggio Emilia.

Corresponding email: daniele.malferrari@unimore.it

Keywords: montmorillonite, gas-trapping, sulfur.

Sulphur-containing compounds (e.g., hydrogen sulphide and thiols), and monocyclic and polycyclic aromatic molecules (e.g., benzene, naphthalene and their chloro-derivatives) are produced by several industrial and human activities, including food processing, bio-composting, combustion processes of vehicles, etc. In many circumstances their removal is an obliged process in consequence of their toxicity even in low amounts or due to the highly corrosive behaviour. In other conditions, for example when they do not represent a health problem (e.g., thiols), their removal (or decrease) is strongly advised both for their bad smell and for the products they can originate in the medium to long term (e.g., acid rains).

Currently, scientific research at the academic level has been strongly focused on carbon dioxide trapping, leaving other research to industrial labs. As a result, many methods currently used for the removal of these gases (Galadima & Muraza, 2015; Özekmekci et al., 2015) still refer to methodologies developed in the past and, therefore, not completely meeting the modern requirements of the circular economy.

In this work we propose an innovative and efficient method for removing and trapping sulfureted and aromatic molecules using the layer silicate montmorillonite intercalated with the μ -oxo Fe(III) phenanthroline complex (Bernini et al., 2015). The process takes place easily also at room temperature, is reversible, does not require pre-treatment of both gaseous and the adsorbent material, and is efficient also when partial pressures of the target gas is very low. Therefore, even extremely low levels of gasses can be removed easily and quickly through redox reactions (sulfureted compounds) or strong interactions with the aromatic moiety of the iron complex (aromatic molecules). Experimental results, previously planned also applying molecular modeling, were confirmed through chemical analyses, spectroscopic techniques (included synchrotron radiation X-ray absorption spectroscopy), X-ray powder diffraction, and thermal methods.

This research will be under the contribution of PRIN2017 “Mineral Reactivity, a Key to Understand Large-Scale Processes: from Rock Forming Environments to Solid Waste Recovering/Lithification” Code 2017183s77-004

Bernini F., Castellini E., Malferrari D., Borsari M. & Brigatti M.F. (2015) - Stepwise structuring of the adsorbed layer modulates the physico-chemical properties of hybrid materials from phyllosilicates interacting with the μ -oxo Fe³⁺-phenanthroline complex. *Micropor. Mesopor. Mat.*, 211, 19-29.

Galadima A. & Muraza O. (2015) - Role of zeolite catalysts for benzene removal from gasoline via alkylation: A review. *Micropor. Mesopor. Mat.*, 213, 169-180.

Özekmekci M., Salkic G. & Fellah M.F. (2015) - Use of zeolites for the removal of H₂S: A mini-review. *Fuel Process. Technol.*, 139, 49-60.

Nanomaterials for the abatement of contaminants in water treatment

Matteucci F.*¹, Curri M.L.², Comparelli R.³, Giannantonio R.⁴, Giansante C.¹, Mascolo G.⁴ & Giannini C.⁵

¹ CNR Nanotec.

² Department of Chemistry, University of Bari.

³ CNR IPCF.

⁴ CNR IRSA.

⁵ CNR IC.

Corresponding email: francesco.matteucci@nanotec.cnr.it

Keywords: environmental nanotechnology, water treatment, photocatalysis.

New emerging pollutants like pharmaceuticals, pesticides, cosmetics, etc. are resistant to conventional biological treatment processes used by municipal wastewater treatment plants (WWTPs) and are subsequently found globally in treated wastewater effluents in concentrations from low ng l⁻¹ to µg l⁻¹. To minimize the presence of emerging pollutants, attention has turned to different techniques such as advanced oxidation processes (AOPs) that form powerful oxidizing species (e.g. hydroxyl radicals). Such species readily and non-selectively attack organic compounds present in effluent waters and accelerate the rate of contaminants oxidation, preferably resulting in their complete mineralization. Among AOPs, photocatalytic processes promoted by nanostructured catalysts are particularly promising due to their high surface-to-volume ratio, leading to a high density of active sites for adsorption and catalysis, and to the possibility to tune band gap and redox potential as a function of their size and shape. Wide band gap semiconductors (e.g. TiO₂, ZnO) activated by UV light are potential valuable photocatalysts as the redox potential of •OH/H₂O pair falls in their band gap, thus photogenerated electron-hole (e⁻/h⁺) pairs can react with dissolved oxygen or water, respectively, to generate •OH. The challenge is to increase the photocatalytic performance of such nanomaterials with different approaches such as coupling them to single- and multi-walled CNT-based systems or to dope them with different metals. In this presentation, it will be discussed the synthesis and the physico-chemical and photocatalytic characterization of different nanocatalysts performed within the project TARANTO which is financed with PON R&I funds. In particular, we will disclose the development of novel photocatalytic reactors to be used for pilot tests of emerging pollutants degradation in real WWTPs.

Production potential in central Mozambique: soil analysis and mineralogy

Mentler A.*¹, Ottner F.², Wriessnig K.², Keiblinger K.M.¹ & Kral R.M.³

¹ University of Natural Resources and Life Sciences Vienna, Austria, Institute of Soil Research.

² University of Natural Resources and Life Sciences Vienna, Austria, Institute of Applied Geology.

³ University of Natural Resources and Life Sciences Vienna, Austria, Centre for Development Research.

Corresponding email: rosana.kral@boku.ac.at

Keywords: lixisol, granite, production potential, nutrient cycling, Mozambique.

Agriculture is the dominant livelihood activity in Central Mozambique. The climate is semi-arid and challenging; meteorological and soil physical data at high spatial and temporal resolution are scarce. This situation makes it difficult to support farmers with qualified information in their decision making. Local farming systems in Marara district in Central Mozambique integrate extensive goat and cattle farming with crop production. Inputs are hard to come by and if available, the prices are prohibitive. Increasing soil fertility and optimizing nutrient cycling is therefore of paramount importance not just from an ecological, but also from an economic point of view. Slash-and-burn practices are very common, as is using wood to produce charcoal, thus hampering water storage and exacerbating erosion through wind and water.

We wanted to elucidate the production potential in the region and therefore analysed soils from 58 fields in Marara district for basic physico-chemical soil parameters (pH, Ct, Corg, Nt, C/N, DOC, electrical conductivity, CEC). The present soils are lixisols, but also show other influences. Organic carbon content and CEC were in a medium to high range, higher than expected and in contrast with soil taxonomy. These findings can be explained by taking into account the specific local geology and geochemistry, where granite and gneiss rocks supply weathered material, as well as through the presence of vertisols and fluvisols.

Minimizing for production potential in this area are the nitrogen and the phosphorus content of local soils. In a first measure it is strictly necessary to increase nitrogen and phosphorus stocks. In this low-input system, the farmers can only achieve this by taking advantage of their animals' manure and by increasing the share of legumes in their cropping systems.

We conclude that the production potential of the investigated soils is better than could be assumed. This potential could further be improved by increased cycling of nutrients. However, soils are extremely sensitive to erosion by wind and water. There is a serious threat for water logging leading to erosion and increased greenhouse gas emission. Slash-and-burn practices and deforestation further add to the risks in the present environment.

On the ground or in the ground? Co-learning of farmers and scientists about soil

Mentler A.¹, Keiblinger K.M.¹, Maftukhah R.², Ngadisih², Murtiningrum² & Kral R.M.*³

¹ University of Natural Resources and Life Sciences Vienna, Austria, Institute of Soil Research.

² Universitas Gadjah Mada, Yogyakarta, Indonesia, Department of Agricultural Engineering.

³ University of Natural Resources and Life Sciences Vienna, Austria, Centre for Development Research.

Corresponding email: rosana.kral@boku.ac.at

Keywords: soil education, outreach, training, participation, Mozambique, Indonesia.

Agricultural research is often worried about acceptance of propositions and uptake of suggested measures by farmers, especially when working in the Global South. We argue based on our experiences in field work with farmers in Mozambique and Indonesia that this need not be the case. Soil is a unique entry point for establishing collaborative work that can take all involved parties far beyond the original project goals. Learning spaces that are created jointly can not only serve for capacity development and support scientific investigation; they can also spur innovation.

In the present work, we revisit experiences from two projects. In Mozambique, we set up a soil health training (SHT) for farmers, extension agents and government representatives, in order to create learning opportunities about local challenges, mitigation measures and to complement farmers' observations with scientific evidence; in Indonesia, we jointly set up a field experiment with farmers to test locally available soil amendments for re-cultivation of former mining land and to derive recommendations for extension. In both cases we used video for documentation to make the implementation of these activities available also to others.

In Mozambique, the SHT complemented previous measures like technical trainings and personalized recommendations based on physico-chemical analysis of soil samples and individual farm walks. The SHT spurred deep discussions on soil fertility measures and erosion control, as well as reflections on current practices. In the case of the Indonesian project, while setting up the experimental site together, farmers interviewed researchers about the scientific method and reasoning behind test plot schemes, and thereby set their own agenda for capacity development.

A relational approach proved successful in stimulating learning on both sides, the farmers' and the scientists' sides. We therefore strongly advocate for partnership-like approaches that facilitate joint experimentation, discussion and exchange.

Water total arsenic remediation via a new generation colloidal superparamagnetic maghemite nanoparticles

Molinari S.*¹, Salviulo G.¹, Magro M.²⁻³, Baratella D.² & Vianello F.²⁻³

¹ Department of Geosciences, University of Padova, Italy.

² Department of Comparative Biomedicine and Food Science, University of Padua, Italy.

³ Regional Centre of Advanced Technologies and Materials, Department of Physical Chemistry, Palacky University in Olomouc, Czech Republic.

Corresponding email: simone.molinari@phd.unipd.it

Keywords: adsorption, arsenic removal, surface active maghemite nanoparticles.

The increasing presence of arsenic (As), a class I human carcinogen, in groundwater of natural and/or anthropogenic origin represents the main threat to human health and the environment (Smedley and Kinniburgh, 2002). The World Health Organisation provides a guideline value of 10 $\mu\text{g L}^{-1}$ as a maximum acceptable daily intake in drinking water (WHO, 2017).

Arsenic major forms found in water are oxyanions of As^{III} and As^{V} and its speciation is controlled by redox conditions and pH. Conventional treatments including chemical precipitation, coagulation/flocculation, electrochemical processes, ion exchange and biosorption suffer of high operational costs and production of a huge amount of sludge. For these reasons, the development of alternative low-cost remediation methods is of primary concern. The present work investigates on the application of a synthetic maghemite nanoparticle, called SAMN (Surface Active Maghemite Nanoparticle) for the removal of both As^{V} and As^{III} from water. These nanoparticles are superparamagnetic, displayed an excellent colloidal stability without any coating or superficial modification. Moreover, SAMNs were already applied as efficient sorbent nanomaterial for eliminating toxic metals (i.e. Cr^{VI}) in water (Magro et al., 2016).

A detailed investigation about the binding behaviour of arsenic (both As^{III} and As^{V}) to SAMNs under various experimental conditions is proposed. The binding efficiency of As^{III} and As^{V} on SAMNs was demonstrated for very high As concentrations (10 mg L^{-1} , as As) as a function of SAMNs concentration and pH getting, in both cases, to the complete As removal from the solution. A different binding behaviour on SAMN surface emerged between the two species: arsenite binding on SAMNs is faster, displayed a higher stability and a pH independent absorption with respect to arsenate. Conversely, arsenate adsorption on SAMNs progressively decreases as function of pH. These features can be attributed to the different binding mechanism on the iron oxide surface. Noteworthy, besides substantiating the efficiency of SAMNs as competitive option for As removal, an unexpected ability of the nanomaterial to discriminate among arsenite and arsenate was unveiled.

Magro M., Domeneghetti S., Baratella D., Jakubec, P., Salviulo G., Bonaiuto E., Venier P., Malina O., Tuček J., Ranc V., Zoppellaro G., Zbořil R. & Vianello F. (2016) - Colloidal Surface Active Maghemite Nanoparticles for Biologically Safe Cr^{VI} Remediation: from Core-Shell Nanostructures to Pilot Plant Development. *Chem. A. Eur. J.*, 22, 14219–14226.

Smedley P.L. & Kinniburgh D.G. (2002) - A review of the source, behaviour and distribution of arsenic in natural waters. *Appl. Geochemistry*, 17, 517–568.

WHO (2017) - Guidelines for drinking-water quality: Fourth edition incorporating the first addendum.

Effects of zeolite and kaolin foliar application in olive trees on photosynthesis and on drupes oil content

Morrone L.*, Facini O., Mari M. & Rotondi A.

Istituto di Bioeconomia - Consiglio Nazionale delle Ricerche IBE-CNR.

Corresponding email: l.morrone@ibimet.cnr.it

Keywords: zeolite, olive tree, photosynthesis, optical properties.

The reduction of pesticides in agriculture is imperative, so the protection of crop production against plant diseases is a key factor in view of a productive but sustainable agriculture. In this work we evaluated the plant response to foliar application of zeolites and kaolin by measuring physiological parameters, foliar coating through measuring the leaf optical properties (transmittance and reflectance). Plant response to foliar treatments was also evaluated by the biometric index of olive drupes, such as olive weight, water content and oil content. Leaf observations via Environmental Scanning Electron Microscope (ESEM) showed the different three-dimensional structure of zeolites and kaolin and the accumulation during treatments along time. These ESEM results were confirmed by leaf optical characteristics. A decrease in photosynthesis were recorded in plant treated with zeolites and kaolin respect to plant control but this result did not affect the oil content that was greater in olive treated with zeolites. Beyond the effect that these geo-materials can play in reducing the olive diseases, these results help to understand how the film covering the canopy can interfere with the physiology of the olive tree.

Use of geo materials (zeolites) in the rooting phase for the production of olive plant

Morrone L.*, Mari M. & Rotondi A.

Istituto di Bioeconomia - Consiglio Nazionale delle Ricerche IBE-CNR.

Corresponding email: l.morrone@ibimet.cnr.it

Keywords: zeolite, olive, root ability.

In the perspective of protecting and safeguarding biodiversity, many research projects meet the objective of preserving and reintroducing ancient autochthonous olive cultivars to enhance both extra virgin olive oil production and landscape protection. Often the autochthonous cultivars have been abandoned in the course of history also due to their low rooting ability, so the need to study alternative techniques for the improvement of the rooting phase was carried out. Sub apical cuttings belonging to different native cultivars of Emilia Romagna have been rooted in different rooting substrates: test (100% perlite) and zeolite substrate (75% perlite + 25% zeolite). The rooting percentage, the number of roots, their length and the total area of the root system were determined using non-destructive techniques of Video Image Analysis (VIA). The varietal matrix has influenced the rhizogenic activity, in fact some cultivars studied showed an improvement expressed in terms of rooting percentage or root development or both when rooted in the substrate added with zeolite, other cultivars instead did not present any differences between the two rooting substrates.

Environmental remediation of the historical suburban forest Bosco Albergati

Neri L.*, Carriero G., Facini O. & Baraldi R.

Istituto di Bioeconomia, Consiglio Nazionale delle Ricerche, Bologna, Italy.

Corresponding email: neri@ibimet.cnr.it

Keywords: air mitigation, urban forest.

The climate changes recently observed worldwide are the consequence of a progressive global warming caused by the increase in carbon dioxide (CO₂) emissions but also by the presence in the air of particulate matter (PM) and gaseous pollutants such as ozone (O₃), produced by human activities. Emissions derived from vehicular traffic, industries and domestic heating have led to the accumulation of gaseous pollutants, such as sulfur oxides (SO_x), nitrogen oxides (NO_x), carbon monoxide (CO), hydrocarbons and PM in the atmosphere. All these pollutants alter the chemical atmosphere composition and are a hazard for human health. Urban forests not only have hedonic and social effects on the population but play also a pivotal role for air quality and thus for citizen's health. In fact, plants naturally mitigate the atmospheric content of the greenhouse gas CO₂ through photosynthesis, but they also improve air quality intercepting and retaining gaseous pollutants (i.e. O₃, NO₂ and SO₂) and/or particulate (i.e. PM₁₀ and PM_{2.5}).

However, the ability of plants to release in the air volatile organic compounds (VOC) needs to be considered in anthropized environments. In fact VOCs, that are secondary metabolites, species specific, essential for the growth and survival of plants, are extremely reactive and involved in the production/removal of O₃, influencing the chemistry of the atmosphere.

Environmental conditions, and plant species, physiology and morphology influence their capacity to capture atmospheric pollutants. We evaluated the mitigation ability of Bosco Albergati, an historical suburban forest located nearby Castelfranco Emilia, Modena, Northern Italy. Bosco Albergati has an extension of 44 ha, and is characterized by around 1500 trees, mainly belonging to the oak family (*Quercus* spp.) but including as well rare ancient trees and around 1700 shrubs. Using algorithms and the software i-Tree Eco, we estimated the forest ability to: capture and store CO₂; remove the air pollutants O₃ and PM₁₀; release VOCs potentially affecting the tropospheric ozone formation (POF).

In conclusion, the Historical Park of Bosco Albergati stored in its biomass 3451 t of CO₂, and each year captures 215 t of CO₂, removes 196 kg PM₁₀ and produces 110 t of O₂. The contribution of the park to ozone formation resulted irrelevant. Our findings underline the importance of green areas for air quality remediation.

Phytoremediation of contaminated sites: the case study of a petroleum refinery in Mantova, Italy

Neri L.*¹, Monti A. L.², Ottoni S.³, Facini O.¹ & Baraldi R.¹

¹ Istituto di Bioeconomia (IBE), Consiglio Nazionale delle Ricerche (CNR), Bologna, Italy.

² Studio Anna Letizia Monti.

³ Consorzio Vivaisti Europei.

Corresponding email: neri@ibimet.cnr.it

Keywords: soil pollution, phytoremediation.

Industrial development has led to the release into the environment of high quantities of chemical substances, in particular petroleum hydrocarbons, polycyclic aromatic hydrocarbons, halogenated hydrocarbons and metals in the soil, and to the release into the atmosphere of photochemical pollutants and fine dust. The environmental recovery of a polluted and degraded area with sustainable techniques leads to an increase in environmental resilience to climate change, as well as to an improvement in living conditions and human well-being of the nearby population. Green technologies such as phytoremediation have a low environmental impact and high ecological profile, and are well received by the public opinion; phytoremediation involves ecological-friendly techniques such as the use of herbaceous plants, shrubs or trees, and of the associated micro-organisms together with soil amendments to remediate contaminated sites. We are currently setting up a plan to reduce the concentration of toxic contaminants in a site previously occupied by concrete tanks of a petroleum refinery adjacent the city of Mantova, Northern Italy, using the phytoremediation technique. The site resulted polluted mainly by total petroleum hydrocarbons (TPH) including monoaromatic compounds such as benzene, toluene, ethylbenzene and xylene (BTEX), polycyclic aromatic hydrocarbons (PAHs) and aliphatic compounds. Plant species characterized by high remediation and tolerance abilities such as willow (*Salix* spp.), poplar (*Populus* spp.) and tamarisk (*Tamarix* spp.) and ornamental trees and shrubs not previously tested will be employed. Plants will be used alone or in combination with specific microorganisms as well as amendments. Morphological characteristics of the vegetation, pollutants absorption and translocation, and soil composition will be periodically monitored to evaluate plant pollutants tolerance, phytoextraction and soil quality. At the end of the experimental survey, the plants remaining after eradication for data collection will grow as an urban forest *on situ*. Phytoremediation of the site will provide beneficial effects both of soil remediation and air mitigation, and will increase the green areas of an industrial compartment, finally contributing to the health and wellbeing of the nearby population.

Chabazitic-zeolites and Effective Microorganisms for the qualitative improvement and fertilizers reduction in the growth of Aloe plants

Prisa D.*

CREA Research Centre for Vegetable and Ornamental Crops, Council for Agricultural Research and Economics.

Corresponding email: domenico.prisa@crea.gov.it

Keywords: plant quality, ornamental plants, alternative substrates.

Natural Zeolites are a mineral family composed by 54 different species chemically defined as “hydrated allumino-silicates of alkaline and alkaline earth elements” and structurally belonging to the tectosilicates (Passaglia & Sheppard, 2001). Due to their crystal chemistry, zeolites show physical-chemical peculiarities such as high and selective cation exchange capacity (CEC), reversible dehydration, selective molecular absorption, and catalytic behaviour (Armbruster & Gunter, 2001). Therefore, rocks containing more than 50% of zeolites (zeolitites) are widely and profitably utilized in the purification of municipal, zootechnical and industrial wastewaters, as additive in animal nutrition, agriculture and floriculture (Gottardi & Galli, 1985; Galli & Passaglia, 2011). Effective microorganisms (EMs) include a mixture of live cultures of naturally isolated microorganisms from fertile soils that are used during plant cultivation (Olle & Williams, 2015). The main activity of Effective microorganisms is to increase the soil microfauna, leading to an increase in an increase in field production of fruit and vegetables. Photosynthetic bacteria, present in the EM, synergistically with other microorganisms, improve the absorption of nutrients from the soil and reduce the incidence of disease (Condor et al., 2007). EM technology is based on the inoculation of beneficial micro-organisms into the soil to create a favourable environment for plant growth and health. EMs interact with the soil-plant ecosystem by controlling plant pathogens and disease agents, solubilizing minerals, increasing availability of plant energy, stimulating the photosynthetic system, maintaining the microbiological balance of the soil and fixing biological nitrogen (Olle & Williams, 2015). With the aim of improving the growth of plants of *Aloe barbadensis* and *A. arborescens* and improve the content of sugars and minerals, several experiments were conducted replacing chabazitic-zeolites with normal inorganic substrates and adding the effective microorganisms (EM) to assess whether they affected plant development. The experiment on both Aloe species involved three treatments: 1) soil; 2) soil with addition of chabazitic-zeolites; and 3) soil with addition of chabazitic-zeolites and treated with EM. The results showed that the use of zeolites and EM microorganisms increased the quality characteristics of Aloe plants under cultivation; specifically plant growth, root development and production of metabolites useful for nutraceuticals. In addition, the use of chabazite and Em has led to a reduction in the use of fertilisers and water in growing substrates.

Armbruster T. & Gunter M.E. (2001) - Crystal structures of natural zeolites. *Natural Zeolites: Occurrence, Properties, Applications. Reviews in Mineralogy & Geochemistry*, 45, (D.L. Bish & D.W. Ming, eds.). Mineralogical Society of America, Washington, 1-67.

Condor A.F., Gonzalez P. & Lakre C. (2007) - Effective microorganisms: myth or reality? *The Peruvian Journal Biology*, 14, 315-319.

Galli E. & Passaglia E. (2011) - Natural zeolites in environmental engineering. In: H. Holzapfel (Ed.), *Zeolites in Chemical Engineering*, Verlag. Process Eng. Engineering GmbH, Vienna; 392-416.

Gottardi G.E. & Galli E. (1985) - Natural zeolites. *sprinter-verlag, berlin heidelberg*, 409 pp.

Olle M. & Williams I.H. (2015) - The influence of Effective Microorganisms on the growth and Nitrate content of vegetable transplants. *Journal of Advanced Agricultural Technologies*, 2(1), 25-28.

Passaglia E. & Sheppard R.A. (2001) - The crystal chemistry of zeolites. *Natural Zeolites: Occurrence, Properties, Applications. D.L. Bish, D.W. Ming (eds.), Reviews in Mineralogy & Geochemistry. Mineralogical Society of America, Blacksburg, Virginia*, 45, 69-116.

Improvement Quality and Content of Pepper and Chilli Nitrates Influenced by the Effective Microorganisms

Prisa D.*

CREA Research Centre for Vegetable and Ornamental Crops, Council for Agricultural Research and Economics

Corresponding email: domenicoprisa@gmail.com

Keywords: symbiotic bacteria, nitrates, EM.

EM microorganisms include a mixture of live cultures of microorganisms, aerobic and anaerobic naturally isolated from fertile soils, which are used during plant cultivation and can have numerous benefits for humans, animals and the environment (Prisa, 2017; Olle & Williams, 2015). EM microorganisms include lactic acid bacteria, photosynthetic bacteria, yeasts and other soil bacteria. Lactic acid bacteria are *Lactobacillus casei*, *Lactobacillus plantarum* and *Streptococcus lactis*. The photosynthetic bacteria from *Rhodospseudomonas palustris* and *Rhodobacter sphaeroides*. There are also *Saccharomyces cerevisiae*, *Candida utilis*, *Streptomyces albus* and *Streptomyces griseus*, *Pseudomonas* sp., *Aspergillus oryzae*, *Penicillium* sp., *Mucor hiemalis* for a total of 80 different strains that perform different functions in collaboration (Higa, 2012; Mohan, 2008; Prisa, 2016). The products based on Effective Microorganisms, given the microbial multiplicity may contain various organic acids, antioxidants, enzymes and chelates. EM was initially selected as an alternative to agricultural chemicals, but extensive research and field trials allowed its successful application in other sectors, including environmental remediation, composting of organic waste, odour reduction in livestock farming and treatment of polluted water (Prisa & Castronuovo, 2018). EM microorganisms are capable of stimulating plant growth and solubilising the mineral elements present in the soil, in particular Ca, P and Mg. Ca influences many beneficial processes for the plant: a high content of Ca leads to fewer diseases, reduction of attack by insects, better preservation of the product (Ncube & Calistus, 2012). EM microorganisms are able to increase the soil microfauna, leading to an improvement in field production. Photosynthetic bacteria, contained in EM microorganisms, can in fact, in synergy with other microorganisms, improve the absorption of nutrients from the soil and reduce the incidence of disease. The objective of this trial was to evaluate the influence of EM microorganisms on growth and nitrate content on pepper and chilli plants. The treatments carried out were: 1) use of EM microbial selection; 2) plants irrigated with water. In all the experiments carried out, the pepper and chilli plants treated with EM were significantly higher and had larger stems than those treated with water. The use of EM micro-organisms can therefore lead to an increase in production quality and a reduction in nitrate content on pepper and chilli plants.

Higa T. (2012) - "Kyusei Nature arming and environmental management through Effective Microorganisms. The past, present and future". http://www.infric.or.jp/english/KNF_Data_Base_Web/7th_Conf_KP_2.html.

Mohan B. (2008) - "Evaluation of organic growth promoters on yield of dryland vegetable crops in India". *Journal of Organic Systems*, 3, 23-26.

Ncube L. & Calistus B. (2012) - "Effects of the integrated use of effective microorganisms, compost and mineral fertilizer on greenhouse-grown tomato". *African Journal of plant Science*.

Olle M. & Williams I.H. (2015) - "The influence of Effective Microorganisms on the growth and Nitrate content of vegetable transplants". *Journal of Advanced Agricultural Technologies*, 2(1), 25-28.

Prisa D. (2016) - "Trattare la vite con i microrganismi EM". *Bollettino informativo di legislazione vitivinicola* n.20. Prisa,D., 2017."Microrganismi EM e zeolite a chabasite per la coltivazione di ibridi di *Echinopsis*". *Il floricultore*, 48-52.

Prisa D. & Castronuovo G. (2018) - "Xeriscaping: utilizzo di piante succulente e cactacee e di tecniche innovative di coltivazione per il risparmio idrico nei giardini mediterranei". 1 ed., vol.1, Edizioni Lulu, 1-5.

Isolation and selection of bacterial strains for aquifer remediation: a case study in Val d'Agri (Southern Italy)

Rizzo P.*¹, Sanangelantoni A.¹, Iacumin P.¹ & Celico F.¹

¹ Dipartimento di Scienze Chimiche, della Vita e della Sostenibilità Ambientale, Università di Parma.

Corresponding email: pietro.rizzo2@studenti.unipr.it

Keywords: aquifer, bioremediation, hydrocarbons.

The Val d'Agri is a Quaternary NW–SE trending intramountain basin located within the southern Apennines thrust belt (southern Italy). In Val d'Agri is located the biggest onshore oilfield in Europe. Within the Val d'Agri oilfield, some natural hydrocarbon springs are documented since the 19th century in the Tramutola area. Close to these springs several tens of exploration and production wells were drilled in the early 20th century by AGIP (actually ENI). These springs and one of these decommissioned (artesian) wells have been studied for the isolation of new potentially exploitable bacterial strains for bioremediation in anthropic contaminated sites. In order to accomplish this task, several actions were carried out including 3 monitoring campaigns for collecting water and soil samples for: chemical, isotopic, microbiological and metagenomic analyses. Electrical conductivity, temperature and pH measurements were performed *in situ* with a portable equipment (Hanna Instruments 9829). Groundwater samples for stable isotope ($\delta^{18}\text{O}$, $\delta^2\text{H}$), tritium and metagenomic analyses were collected during the discharge measurements. Also, soil samples were collected for the metagenomic and microbiological analyses. The sampling was carried out in springs and at the outflow of the decommissioned artesian well, which is screened only at its bottom. Bacterial DNA was extracted from soil and water samples and its quantity and integrity were evaluated by electrophoresis in agarose gel. To obtain the 16S RNA profiles the samples were analyzed with NGS (Next Generation Sequencing) technique. The isolation of potential bacterial strains was carried out in a liquid and solid selective Bushnell-Haas medium to which an aliquot of diesel was added as the only carbon source. DNA was extracted and sequenced from the isolated bacterial colonies to identify the species.

The discharge of the springs slightly varies over time, with a significant increase in late winter, during rainy periods, therefore suggesting a short delay between rain events and hydraulic head rise. The isotopic data of springs- and ground-waters are well situated along the LMWL, therefore suggesting a complete meteoric origin of the analyzed waters. The microbial communities detected in groundwater samples collected in the well and in the hydrocarbon springs are all characterized by aerobic and mesophilic bacteria. Isolation on selective media revealed the presence of bacterial strains capable of using the hydrocarbons contained in diesel as a carbon source such as *Cupriavidus metallidurans* (Espinoza et al., 2018). Other studies are still ongoing.

Espinoza Tofalos A., Daghio M., González M., Papacchini M., Franzetti A. & Seeger M. (2018) - Toluene degradation by *Cupriavidus metallidurans* CH34 in nitrate-reducing conditions and in Bioelectrochemical Systems. FEMS Microbiology Letters, 365(12). <https://doi.org/10.1093/femsle/fny119>

S15

Geobiology: Biosphere-Earth interactions

CONVENERS AND CHAIRPERSONS

Roberto Barbieri (Università di Bologna)

Cesare Corselli (Università di Milano Bicocca)

***Chamelea gallina* response to a warming Earth: A case study from the Holocene sedimentary succession of the Po-Adriatic system**

Azzarone M.¹, Cheli A.¹, Mancuso A.¹, Stagioni M.¹, Falini G.², Goffredo S.¹ & Scarponi D.*¹

¹ Dipartimento di Scienze Biologiche, Geologiche e Ambientali, Università di Bologna.

² Dipartimento di Chimica “Giacomo Ciamician”, Università di Bologna.

Corresponding email: daniele.scarponi@unibo.it

Keywords: *Chamelea gallina*, Po-Adriatic system, environmental shifts.

This pilot investigation explores skeletal features and growth of the edible bivalve *Chamelea gallina* from the Holocene shoreface deposits of the Po-Adriatic system (Italy). Five horizons rich in *C. gallina*: two from the Early Holocene, when the area was an estuarine system; one from the Middle Holocene, when the area transitioned from a wave-dominated delta, and two from the present-day shoreface settings (ca. 6m depth), south of the modern, and fluvial dominated, Po delta.

Here, we investigated valve skeletal features (height, width, bulk density, micro-density and porosity) in relation to valve length, used as a rough proxy of the animal age. No variation was observed in shell CaCO₃ polymorphism (i.e., 100% aragonite) or in compositional parameters among the analyzed fossil horizons. Across all targeted *C. gallina* levels, juveniles are more porous than adults, suggesting that *C. gallina* promoted an accelerated shell accretion, at the expense of possessing a mechanically weaker shell, in order to quickly attain the size required for sexual maturity. Spearman's rank correlation analyses between alkenone derived sea-surface-temperatures (SSTs), a proxy for different depositional settings and valve micro-skeleton parameters were also performed. Micro-density and bulk density correlated positively with SSTs, whereas porosity correlated negatively. Trace elements analysis show higher presence of metals like chromium (Cr) and nickel (Ni) in valves of modern clams, suggesting that shell trace element ratios can provide useful archive of environmental pollution.

The stratigraphic context in which *C. gallina* assemblages were retrieved, aid understanding the biotic response of this important shellfish species environmental shifts and offers an important baseline for assessing the short- to mid-term impact of anthropogenic activities and climate-driven changes on this important shellfish species.

The precipitation process of the calcium carbonate in *Austromegabalanus Psittacus* and the role of organic matter: a multidisciplinary study

Berton D.¹, Rodriguez Navarro A.², Grenier Romero C.², Roman Martinez R.²,
Rodeghero E.*¹ & Martucci A.¹

¹ Department of Physics and Earth Sciences, University of Ferrara, Italy.

² Department of Mineralogy and Petrology, University of Granada, Spain.

Corresponding email: rdglse@unife.it

Keywords: *Austromegabalanus psittacus*, calcium carbonate precipitation, intramineral organic matter, XRPD.

As well known, biogenic calcite resulted as a nano-composite mineral in which the presence of intracrystalline macromolecules has a role in nucleation and orientation of calcium carbonate crystals during the biomineralization process in different species of bivalves (Towe et al., 1972). In this work a multidisciplinary study (XRD, TG, FT-IR, SEM and vitro crystallization) of the precipitation process of the calcium carbonate in *Austromegabalanus psittacus* (*A. psittacus*) was conducted. Moreover, the possible role of organic matter in the crystals growth has also been considered. FT-IR analysis on both *A. psittacus* whole and decalcified shells highlights the fingers-print of calcium carbonate (1394cm^{-1} , 871cm^{-1} and 712cm^{-1}) for the whole samples, lipids (2960cm^{-1} and 2850cm^{-1}), amides groups (1630cm^{-1} , 1510cm^{-1} and 1230cm^{-1}), sulfate groups (1060cm^{-1}) and polysaccharides (1020cm^{-1}) for decalcified samples. The spectroscopic measurements were also performed increasing temperature up to 400°C in order to observe the behavior of the organic matter included in the analyzed samples. In the $200\text{-}300^\circ\text{C}$ temperature range, FT-IR patterns highlighted an intensity peak loss in the lipids (2960cm^{-1}) and amides groups (1630cm^{-1} , 1510cm^{-1}) regions. Over 400°C , all the peaks ascribable to the components of organic matter undergo a loss of intensity until complete disappearance. These results are in agreement with thermal analysis in which the weight loss and the exothermic reaction in the $250\text{-}450^\circ\text{C}$ range can be associated to the decarbonation process of organic matter. Furthermore, X-ray powder diffraction on the whole shells samples highlights distortion of the calcite lattice related to the intracrystalline components presence. In particular, diffraction study pointed out how the organic matter produced anisotropic lattice distortions more evident along the *c*-axis. This phenomenon, already known in the literature (Pokroy et al., 2004) for other species, had not yet been reported for *A. psittacus*. To better support this relationship, the evolution of structural parameters as a function of increasing temperature was evaluated. These results can well be correlated with the data reported above. Finally, in order to evaluate the effect of organic matter during the calcium carbonate precipitation, batch experiments mixing NaHCO_3 with CaCl_2 and adding the organic matter extracted from *A. psittacus* were carried out. The precipitate analyzed at fixed time intervals (10/30min and 1/2/24/72h) has shown an influence of organic matter on morphology of the precipitated calcite crystals.

Pokroy B., Quintata J., Caspi N., Berner A. & Zolotayabko E. (2004) - Anisotropic lattice distortions in biogenic aragonite. *Nature*, 3, 79-86.

Towe K.M. & Thompson G.R. (1972) - Structure of some bivalve shell carbonates prepared by ion-beam thinning. A comparison study. *Calc. Tiss. Res.*, 10(1), 38-48.

The Cretaceous Oceanic Anoxic Event 2: geochemical constraints from a section of the Atlantic margin

Bonacina G.*¹, Sanfilippo A.¹, Previde Massara E.², Scotti P.², Viaggi P.² & Piva A.²

¹Dipartimento di Scienze della Terra e dell' Ambiente, Univ. of Pavia.

²Eni S.p.A. Upstream Research and Technological Innovation, San Donato Milanese, MI, Italy.

Corresponding email: greta.bonacina01@universitadipavia.it

Keywords: OAE2, Inorganic geochemistry, TOC.

The Cenomanian – Turonian OAE2 (ca 94 Ma) represents the most severe environmental perturbation in Cretaceous time. It is associated to large increase in organic-carbon burial at a global scale and consequently to a positive excursion in $\delta^{13}\text{C}$, global warming, high atmospheric CO_2 , weathering, increased hydrothermal activity, high sea level and changes in oceanic circulation (Takashima et al., 2004; Owens et al., 2013). In this study, we present preliminary geochemical data from a *in situ* sedimentary sequence recovered in a ~1.8 km-thick well located on a passive margin of the Atlantic Ocean. In the interval, from Aptian to Early Campanian, the OAE2 is represented by a ~28 m-thick interval. The event consists of a sedimentary sequence made up of carbonates and organic-rich shales intercalations, with TOC content up to 9 wt%. It is also marked by a noticeable increase in $\delta^{13}\text{C}$, from ~ -27‰ up to ~ -23‰. From a geochemical point of view, the general trend is a covariation between TOC and the redox-sensitive elements (e.g. Mo, U and V). However, during the event the data show a drawdown of these redox-sensitive metals corresponding to a strong increase in total organic carbon. The same variations have been documented in sediments deposited during OAEs (Pearce et al., 2008; Goldberg et al., 2016). The driving factors of this prominent drop are widely debated, probably they are mainly (i) the wide extent of euxinia, (ii) large availability of nutrients into the oceans and therefore high primary production and (iii) partially restricted deep-water circulation (Algeo, 2004; Pearce et al., 2008; Owens et al., 2013; Goldberg et al., 2016). The above-mentioned well, with its long and continuous sedimentary record, permits investigating the environmental perturbations at the onset, during and after the Cenomanian – Turonian Ocean Anoxic Event 2, its causes and effects.

- Algeo T.J. (2004) - Can marine anoxic events draw down the trace element inventory of seawater? *Geology*, 32, 1057-1060.
- Goldberg T., Poulton S.W., Wagner T., Kolonic S.F. & Rehkämper M. (2016) - Molybdenum drawdown during Cretaceous Oceanic Anoxic Event 2. *Earth and Planetary Science Letters*, 440, 81-91.
- Owens J.D., Gill B.C., Jenkyns H.C., Bates S.M., Severmann S., Kuypers M.M.M., Woodfine R.G. & Lyons T. W. (2013) - Sulfur isotopes track the global extent and dynamics of euxinia during Cretaceous Oceanic Anoxic Event 2. *Proceedings of the National Academy of Sciences*, 110, 18407-18412.
- Pearce C.R., Cohen A.S., Coe A.L. & Burton K.W. (2008) - Molybdenum isotope evidence for global ocean anoxia coupled with perturbations to the carbon cycle during the Early Jurassic. *Geology*, 36, 231–234.
- Takashima R., Nishi H., Huber B. T. & Leckie M. (2006) - Greenhouse world and the Mesozoic ocean. *Oceanography*, 19, 82-92.

Taphonomic and diagenetic history of a *Panopea*-rich layer from the Pisco Formation, Peru

Bosio G.*¹, Bracchi V.¹, Malinverno E.¹, Basso D.¹, Collareta A.², Gioncada A.², Coletti G.¹, Di Celma C.³ & Bianucci G.²

¹ Dipartimento di Scienze dell' Ambiente e della Terra, Università degli Studi di Milano-Bicocca.

² Dipartimento di Scienze della Terra, Università di Pisa.

³ Scuola di Scienze e Tecnologie, Università di Camerino.

Corresponding email: valentina.bracchi@unimib.it

Keywords: Taphonomy, East Pisco Basin, *Panopea*.

The East Pisco Basin is a Cenozoic forearc basin placed along the southern Peruvian coast. Its youngest sedimentary unit, the Miocene-Pliocene Pisco Formation, is famous for hosting a globally renowned marine vertebrate fossil-Lagerstätte (Gariboldi et al., 2015). Along the western side of the Ica River, the Pisco Formation is comprised of three allomembers representing three transgressive cycles (Di Celma et al., 2017).

Southeast of the locality of Cerro Colorado, the basal sandstones of the P1 allomember host an unusual invertebrate-rich bed. An abundant mollusk fauna with a peculiar taphonomic and diagenetic history characterizes a 10 cm-thick layer. Only the internal molds are preserved in a variably cemented sandstone. Specimens of *Panopea* cf. *coquimbensis*, an infaunal species living at more than one meter of depth into the seafloor, *Trachycardium* sp. and *Dosinia ponderosa*, which are shallow infaunal species, occur together with barnacles and other epifaunal encrusters. *Panopea* specimens are preserved as internal molds of articulated valves complete with the cast of muscles and pallial line. The molds show serpulids, bryozoans and barnacles encrusting the inner side of the valves, suggesting that the *Panopea* shells were exhumed, exposed at the seafloor and colonized before the successive burial. Microscopical, XRD and XRF analyses reveal that the molds are constituted by terrigenous clasts cemented by ankerite. Gypsum and anhydrite are also present.

We hypothesize that a storm event or strong currents firstly uncovered the *Panopea* specimens and accumulated them after a short transport, allowing articulation to be preserved. After death of the *Panopea* individuals, the inner part of the shell, representing a hard substrate and a sheltered environment, was colonized by different organisms. After the final burial, ankerite precipitated cementing the sediment infill of valves. Finally, secondary circulation of fluids caused the dissolution of the calcite shell and precipitation of gypsum/anhydrite (Gioncada et al., 2018), leaving only the internal molds.

Di Celma C., Malinverno E., Bosio G., Collareta A., Gariboldi K., Gioncada A. & Bianucci G. (2017) - Sequence stratigraphy and paleontology of the upper Miocene Pisco Formation along the western side of the lower Ica valley (Ica Desert, Peru). RIPS, 123, 255-274.

Gariboldi K., Gioncada A., Bosio G., Malinverno E., Di Celma C., Tinelli C. Cantalamessa G., Landini W., Urbina M. & Bianucci G. (2015) - The dolomite nodules enclosing fossil marine vertebrates in the East Pisco Basin, Peru: field and petrographic insights into the Lagerstätte formation. Palaeogeography, Palaeoclimatology, Palaeoecology, 438, 81-95.

Crustose coralline algae: the bioengineers of Mediterranean seafloor at the geological scale

Bracchi V.A.* & Basso D.

Dipartimento di Scienze dell'Ambiente e della Terra, Università degli Studi di Milano-Bicocca.

Corresponding email: valentina.bracchi@unimib.it

Keywords: crustose coralline algae, bioengineers, encrusting activity, algal reef, carbonate production.

One of the most striking interaction between geosphere and biosphere is the phenomenon of coral reef, where hermatypic corals act as marine bioengineers, organisms able to create rigid biostructures at the seafloor (= coral reefs). Their growth not only develops a very special marine habitat, but also drives the sedimentological and geomorphological development of coasts and atolls, modifying the Earth's surface at the geological time scale. Outside the tropics, hermatypic corals disappear, but large areas are still dominated by hard substrates of biological origin. The role of bioengineers is played by other organisms, such as the crustose coralline algae (CCA), sciaphilous algae with skeletal thalli. At the geological time, the continuous encrusting activity of such bioengineer results in the colonization of the seascape and the generation of rigid structure (= algal reefs), referred to as coralligenous in the Mediterranean Sea. Moreover, the Mediterranean Basin hosts an important fossil legacy of coralligenous that formed under contrasting climatic scenarios since Pleistocene resulting in exceptional rocky outcrops completely made by CCA. Some of the main features of algal reefs are strictly linked on the relation of CCA and geological setting, such as availability of suitable substrate, absence of continuous fine sedimentation, no competition with other type of habitat. Only the interacting observation of such phenomenon both in the present-day Mediterranean Sea, and in the fossil record of temperate paleogeographic settings, allow to understand and genetically describe the effect of the interaction of the biosphere (CCA) at the scale of geosphere. CCA are versatile, being able to encrust hard and mobile substrates, or generate new ones. CCA request dim-light conditions, and consequently colonize both shallow water with low level of irradiance, and relatively deep bathymetric interval (circalittoral zone). Coralligenous develops diverse morphotypes, ranging from discrete reliefs, made of small isolated build-ups with a thickness up to 50 cm, up to tabular reliefs, several kilometers large and with a thickness up to 4 m. At the scale of morphotype, Coralligenous develops on sub-horizontal both mobile and hard substrate, although the relation between morphotype and substrate is not linear. The volume of carbonate produced is considerable and makes coralligenous a primary phenomenon for sediment budgets. At the scale of bioengineer, considering the phase of inception of reef, another interesting aspect is that CCA entrap the mobile substrate transforming them in hard substrate during the geological time. Consequently, CCA act as lithifying actor resulting in coralligenous, and they are both able to influence the geological and environmental dynamics over varying spatial and temporal scales.

Human and geological crises of the last millennium in Italy modulated by the episodes of the Little Ice Age

Bragato P.L.*¹

¹ OGS - Istituto Nazionale di Oceanografia e di Geofisica Sperimentale.

Corresponding email: pbragato@inogs.it

Keywords: Little Ice Age, earthquake, pandemic.

The Little Ice Age (LIA) is a broadly defined period of cooling most evident in Europe and Asia between the 17th and the 19th centuries, although in its broader acceptance it embraced the entire northern hemisphere between the 14th century and the first half of the 20th century (Matthews & Briffa, 2005). This wider interpretation is less based on the reconstructed trend of temperature, but, rather, on the evolution of the glaciers in Europe, which took contribution from the combination of temperature and precipitations. From the glacial point of view, the LIA evolved through three main episodes occurred in the 14th, 17th and 19th centuries, respectively. It is well known these episodes had a strong economic and social effect in Europe, inducing famine and economic shocks. In turn, famine, malnutrition and lack of hygiene should have contributed to the widespread of pandemics, like plague in the 14th and 17th centuries and cholera in the 19th century (Alfani & Melegaro, 2011), although some studies have evidenced the role of precipitations in creating favorable biological conditions for the agents of the two diseases (Ben Ari et al., 2010; Righetto et al., 2013). Recent analyses (Bragato, 2019) have shown that the LIA is also correlated with the rate of earthquakes and volcanic eruptions in Italy, with peaks of activity that occurred during the three main glacial phases. These evidences are here presented and discussed. Possible causal relationships between the different natural and social processes are also hypothesized based on the available literature.

Alfani G. & Melegaro A. (2011) - Pandemie d'Italia dalla Peste Nera all'Influenza Suina: l'impatto sulla società. EGEA, Milano.

Ben Ari T., Gershunov A., Tristan R., Cazelles B., Gage K. & Stenseth N.C. (2010) - Interannual variability of human plague occurrence in the western United States explained by tropical and north Pacific ocean climate variability. *The American Journal of Tropical Medicine and Hygiene*, 83, 624–632.

Bragato P.L. & Holzhauser H. (2019) - Observations on the connection between glacial phases, natural catastrophes and economic trends of the last millennium in Italy. *The Holocene*. <https://doi.org/10.1177/0959683619846984>.

Matthews J.A. & Briffa K.R. (2005) - The 'Little Ice Age': re-evaluation of an evolving concept. *Geografiska Annaler*, 87A, 17-36.

Righetto L., Bertuzzo E., Mari L., Schild E., Casagrandi R., Gatto M., Rodriguez-Iturbe I. & Rinaldo A. (2013) - Rainfall mediations in the spreading of epidemic cholera. *Advances in Water Resources*, 60, 34-46.

Characterisation of prokaryotes and eukaryotes in contaminated extreme environments: preliminary results

Consani S. *, Borello A., Vezzulli L. & Carbone C.

Dipartimento di Scienze della Terra, dell'Ambiente e della Vita (DISTAV), Università di Genova.

Corresponding email: sirio.consani@edu.unige.it

Keywords: Acid Mine Drainage, Bacteria, Fungi.

The dissolutive oxidation of Fe sulphides in mining areas leads to the generation of Acid Mine Drainage (AMD). The low pH and high metal concentration of these solutions make AMD and the related precipitates challenging environments for biota. Nonetheless, many prokaryotes (mainly bacteria and archaea) and eukaryotes (mainly fungi) thrive in AMD, and their metabolic activity deeply contributes to the geochemical processes shaping these ecosystems. These extreme environments, such as those observed at the “Rio Tinto” site in Spain, has been intensively studied not only for their environmental importance, but also because they present many similarities towards the Martian surface. In fact, these sites could give clues on the formation of the minerals detected on Mars and on the possibility that such deposits are the result of the activity of life forms.

The Libiola mine (Liguria, NW Italy) has been chosen for this study because it gives the opportunity to sample all the different precipitates related to AMD (Fe-rich, Al-rich, and Cu-rich). In particular, goethite and jarosite, the minerals observed in Fe-rich precipitates, were also detected on Mars surface. The samples of all precipitates were collected both outside and inside the mine adits, in order to test if the different distribution of light and nutrients would impact on the microorganism community. The aim of this work is to characterise the microorganism communities in order to develop a geo-microbiological model of all precipitates.

As a general result, the number of sequences of bacteria and particularly of fungi was higher outside the adits, although the biodiversity (Shannon index) was similar. The main factors controlling the distribution of microorganisms were pH and chemical composition, but also the availability of nutrients was important, as testified by the increase of heterotrophs outside the adits. On the contrary, dissolved elements did not play an important role.

Preliminary results showed that the dominating phylum among bacteria was Proteobacteria (Gammaproteobacteria and Alphaproteobacteria), and among fungi the main phyla were Ascomycota and Basidiomycota. *Acidiphilium*, *Leptospirillum*, *Acidibacter*, and *Thermoplasmataceae* were found to be markers for Fe-rich precipitates, *Gyoefferella* for Al-rich precipitates, whereas *Siphonobacter* were markers for Cu-rich precipitates. *Novosphingobium* and *Tetracladium* were markers for samples collected outside adits.

It was possible to conclude that the great diversity in the environmental conditions among the precipitates led to the generation of specialised autotrophic and heterotrophic microorganism assemblages. The model for the microorganism community involves many different ecological niches, testifying that even in such challenging environments the developing of a complex network took place.

Europlanet 2020 RI has received funding from the European Union's Horizon 2020 research and innovation programme under grant agreement No 654208

Changes in the tree-ring $\delta^{18}\text{O}$ from the Forni Glacier forefield due to glacier stream water inputs and climate change: potential use for environmental and climatic reconstructions

Leonelli G.^{*1-3}, Pelfini M.² & Maggi V.³

¹ Department of Chemistry, Life Sciences and Environmental Sustainability, Università degli Studi di Parma, Parma, Italy.

² Department of Earth Sciences, Università degli Studi di Milano, Milano, Italy.

³ Department of Earth and Environmental Sciences, Università degli Studi di Milano-Bicocca, Milano, Italy.

Corresponding email: giovanni.leonelli@unipr.it

Keywords: Climate change, tree-ring stable isotopes, European Alps.

Tree-ring stable isotopes for reconstructing past climate variability has received an increasing interest in the scientific community in recent years. In fact, climate sensitivity of tree-ring stable isotopes is strictly controlled by environmental conditions impacting tree physiology, and the construction of isotope chronologies opens new opportunities to reconstruct mid- to long-term changes in environmental and climatic factors.

At two forest sites of European larch, located at 2190 m a.s.l. in the Forni Glacier forefield (Italy), one along the glacier stream (GL) and the other towards the valley slope (SL), we constructed four chronologies of tree-ring stable carbon and oxygen isotope with the aim of disentangling climatic and glacier stream signals. We found that at the SL site the $\delta^{18}\text{O}$ of tree-ring cellulose is mainly driven by the $\delta^{18}\text{O}$ of winter snowfall (November to March) and to a lesser extent by the $\delta^{18}\text{O}$ of August precipitation, indicating that these trees during the growing season mostly use the snow melt water of the previous winter. At the GL site, the isotopic signature of the source water is also influenced by glacier meltwaters that mainly drives the tree-ring $\delta^{18}\text{O}$ isotopic signature. Our results show an increasing influence of glacier melt water over the last decade for the GL site, likely due to both higher glacier ablation rates and a larger availability of glacier meltwaters in the forefield under the ongoing climatic changes. By means of an isotope model we could estimate the ^{18}O -depleted glacier melt water inputs (GMWI_ $\delta^{18}\text{O}$), finding that these values are consistent with the mean difference measured between the $\delta^{18}\text{O}$ in the glacier stream and in the precipitation. Moreover, we found that the winter and summer temperature explains up to 37% of the GMWI_ $\delta^{18}\text{O}$ variance. Our analysis highlights the control of winter precipitation isotope signal on cellulose $\delta^{18}\text{O}$ at the SL site and the presence of glacier melt-signals at the GL site, potentially allowing the reconstruction of past $\delta^{18}\text{O}$ of winter precipitation in the European Alps and opening new opportunities to reconstruct changes in water regimes of the glacier streams.

Integrated strategies for quantifying major element contents in modern and fossil bioapatite

Malferrari D.¹, Ferretti A.¹, Mascia M.T.², Medici L.³ & Savioli M.*¹

¹ Dipartimento di Scienze Chimiche e Geologiche, Università di Modena e Reggio Emilia, Italy.

² Dipartimento di Scienze Mediche e Chirurgiche Materno-Infantili e dell'Adulto, Università di Modena e Reggio Emilia, Italy.

³ CNR - Istituto di Metodologie per l'Analisi Ambientale, Tito Scalo (PZ) - Italy.

Corresponding email: daniele.malferrari@unimore.it

Keywords: bioapatite, tooth, diagenesis.

Interactions acting between geosphere and biosphere, regardless of where they take place, can provide important information not only for reflecting past environments, but also for outlining evolutionary events. Several present and fossil organisms have been sharing since Precambrian times the use of bioapatite for the formation of their mineralized structures (e.g., Kallaste & Nemliher, 2005; Pasteris et al., 2008; Ferretti et al., 2017).

From the crystal-chemical point of view, (bio)apatite crystallizes in the hexagonal system and its cell parameters, which are representative of distances between atoms, vary in close correlation with chemical substitutions that can occur in the crystal framework. Likewise, bioapatite crystal growth depends on the presence of biological fluids saturated with phosphate and various major and trace elements that can be incorporated within the frame (Pasteris et al., 2008). When biological contribution is removed, mineral growth occurs only from extracellular fluids, whose composition strictly reflects the surrounding environment. Hence, any investigations aimed at understanding structural variations as well as chemical composition of bioapatite can provide a powerful tool to understand bio-geosphere interactions.

We explored and compared different calibration strategies for quantifying major elements in fossil and living sharks teeth using X-ray fluorescence (XRF), laser ablation inductively coupled mass spectrometry (LA-ICPMS) and optical spectroscopy (ICP-OES). We tested the effectiveness of in-home prepared hydroxyapatite matrix-matched standards used as external calibrating curve. NIST certified standards SRM 1400 and SRM 1486 were used to define laser ablation parameters and, after, as single point calibrator to provide a comparative result.

Percentage data from LA-ICPMS clearly revealed a marked disjunction with respect to percentage data resulting from XRF and ICP-OES. The normalization of the results on the basis of 16 cations allowed to better evaluate the analytical significance of the procedure proposed. Apart from interpretative considerations, our study identified a first reliable tool for chemical characterization by LA-ICPMS on small sized samples (i.e., 50-500 µm, not measurable by XRF and ICP-OES).

This research will be under the contribution of PRIN2017 "Mineral Reactivity, a Key to Understand Large-Scale Processes: from Rock Forming Environments to Solid Waste Recovering/Lithification" Code 2017183s77-004

Ferretti A., Medici L., Malferrari D. & Savioli M. (2017) - Diagenesis does not invent anything new: Precise replication of conodont structures by secondary apatite. *Scientific Reports*, 7(1), 1624.

Kallaste T. & Nemliher J. (2005) - Apatite varieties in extant and fossil vertebrate mineralized tissues. *J. Appl. Cryst.*, 38, 587-594.

Pasteris J.D., Wopenka B. & Valsami-Jones E. (2008) - Bone and tooth mineralization: why apatite? *Elements*, 4(2), 97-104.

Calcareous nannofossils behavior during global warmth intervals of the Neogene

Notaro A.*¹, Garzarella A.¹ & Raffi I.¹

¹ Dipartimento di Ingegneria e Geologia (InGeo), Università degli Studi “G. D’Annunzio” Chieti.

Corresponding email: amalia.notaro@unich.it

Keywords: micropaleontology, calcareous nannofossils, Neogene.

The Neogene time is characterized by high-amplitude climatic variability within the major framework of a global cooling trend. The Miocene Climatic Optimum (MCO; ca. 17 to 14.7 million years ago; e.g. Holbourn et al., 2015) and the early Pliocene warmth (ca. 4.5 to 3 million years ago; e.g. Pagani et al., 2009) are warm intervals extensively studied in recent times due to their similarity to the present-day increasing warm condition.

Here we reports on the “work in progress” of a study of calcareous nannofossils assemblages in deep-sea sediments deposited in the two Neogene time intervals, with the aim of depicting the variability in nannofossil productivity and figuring out if calcareous phytoplankton reacted to changing paleoenvironmental conditions. Semi-quantitative methods of analysis (Backman & Shackleton, 1983) are applied to obtain abundance patterns of major nannofossil taxa in smear slides of high-resolution sampling sets from ODP Site 926 and IODP Site U1338 successions. The dataset is compared to geochemical paleoenvironmental and paleoclimatic proxies (opal accumulation rates, $\delta^{18}\text{O}$ and $\delta^{13}\text{C}$ isotope records) in order to obtain indication of possible control of environmental and climatic changes on nannofossil assemblages.

Backman J. & Shackleton N.J. (1983) - Quantitative biochronology of Pliocene and early Pleistocene calcareous nannofossils from the Atlantic, Indian and Pacific oceans. *Mar. Micropaleont.*, 8, 141–170.

Holbourn A., Kuhnt W., Kochhann K.G.D., Andersen N. & Meier K.J.S. (2015) - Global perturbation of the carbon cycle at the onset of the Miocene Climatic Optimum. *Geology*, 43, 123-126.

Pagani M., Liu Z., LaRiviere J., & Ravelo A.C. (2009) - High Earth-system climate sensitivity determined from Pliocene carbon dioxide concentrations. *Nature Geoscience*, 3, 27-30.

Bio-geosphere interactions in the deep: The important role of cold-water corals

Vertino A.*¹, Savini A.² & Marchese F.²

¹ Department of Geology, Gent University, Belgium.

² Department of Environmental and Earth Science, University of Milano-Bicocca, Italy.

Corresponding email: fabio.marchese1@unimib.it

Keywords: azooxanthellate corals, cold-water corals, ecology, bioconstructions, bio-geosphere interactions.

Like their tropical counterparts, some azooxanthellate coral species can create large bioconstructions that play a crucial role in the biosphere - geosphere dynamics of the deep sea.

During the last two decades the so-called cold-water corals (CWC) and the related deep-sea carbonate mounds have been subject of intensive research. Data collected in hundreds of oceanographic cruises have highly increased our knowledge on the ecology of frame-building deep-sea corals and on the environmental factors that allow them to create large bioconstructions. On the one hand environmental variables, such as hydrodynamics, substrate availability, food supply, temperature and oxygen concentration, highly influence the distribution and reef-building potential of deep-sea coral species. On the other hand, the coral skeletons growing on each other and their baffling and trapping action lead to the formation of extensive carbonate structures that modify through time the physiography of the submarine landscape. CWC are especially able to form or induce the formation of large geomorphological features (diversely named as “reefs”, banks, mounds etc.), up to 300 m high and several kilometers in lateral extension, that in turn influence the local hydrodynamics and sedimentary regime. In addition, the complexity of the 3-dimensional CWC bioconstructions provide niches for many other species, thus enhancing abundance and diversity of benthic life in the deep oceans.

In this study we describe representative modern and past examples of coral bioconstructions that testify long-lasting bio-geosphere interactions in the deep-sea environments of the Mediterranean, since at least the Early Pleistocene.

S16

Planetary evolution: new insights from remote sensing, in-situ, terrestrial analogues and meteorite studies

CONVENERS AND CHAIRPERSONS

Maria Sgavetti (Università di Parma)

Mara Murri (Università di Pavia)

Valentina Galluzzi (IAPS-INAF)

Riccardo Pozzobon (Università di Padova)

Cristian Carli (IAPS-INAF)

InSight, first months on Mars and laboratory experiments to complement planetary observations

Antonangeli D.*¹, Badro J.², Boccato S.¹, Morard G.¹, Rivoldini A.³, Siebert J.², Xu F.¹ & the InSight Science Team

¹ Sorbonne Université, Muséum National d'Histoire Naturelle, UMR CNRS 7590, Institut de Minéralogie, de Physique des Matériaux et de Cosmochimie, IMPMC, Paris, France.

² Université de Paris, Institut de Physique du Globe de Paris, CNRS, Paris, France.

³ Royal Observatory of Belgium, Bruxelles, Belgium.

Corresponding email: daniele.antonangeli@upmc.fr

Keywords: Mars, geophysical observations, high pressure and high temperature experiments.

InSight, short for Interior Exploration using Seismic Investigations, Geodesy and Heat Transport, is a Mars lander dedicated to the study of the deep interior of the planet. The spacecraft successfully landed in Elysium Planitia on November 26th 2018 and, at the time of writing, the entire scientific payload has been deployed and operations are ongoing. The three main experiments are SEIS (Seismic Experiment for Interior Structure), a six-sensor, broad-band seismic instrument to monitor global seismic and impact activity; HP³ (Heat flow and Physical Properties Package) for measuring the ground temperature/gradient, thermal conductivity and mechanical properties from the surface to few meters depth; and RISE (Rotation and Interior Structure Experiment), a geodetic planetary rotation investigation using sub-decimeter-scale precision tracking. These are augmented by APSS (Auxiliary Payload Sensor Suite), an environmental suite comprising a pair of wind and air temperature sensors, a pressure sensor and a magnetometer; and an instrument deployment system, including a robotic arm, a mid-resolution color camera and a wide-angle color camera. The latter two subsystems, included in the mission to support data interpretation of SEIS and HP³, are also providing continuous monitoring of the meteorology and the magnetic environment at the landing site, as well as supporting geological investigations of the lander's surroundings.

In this presentation we will give an overview of the mission status along with a summary of obtained scientific results from the first months of Mars surface operations. Then we will focus on the complementary laboratory activity, presenting high-pressure, high-temperature experiments on (i) phase relations, density and sound velocities of model Martian mantle lithologies, and (ii) melting curve and physical properties of liquid iron alloys expected to comprise the Mars's core, and (iii) core formation and composition models based on metal-silicate partitioning experiments, with direct implications for the nature of Mars' building blocks

The results of these experiments provide critical mineral physics and geochemical constraints required for the interpretation of the InSight observations, which, in turn, will bring unprecedented information on the interior of Mars.

Two possible episodes of karstification in the equatorial layered deposit within Kotido crater, Arabia Terra, Mars

Baioni D.^{*1-2}, Gutierrez F.³, García-Arnay A.³, Luzzi E.⁴, Parenti C.⁵, Sevil J.³ & Nesci O.¹⁻²

¹ Planetary Geology Research Group Università degli Studi di Urbino Carlo Bo, Italy.

² Planetary Geomorphology Working Group Associazione Italiana Geomorfologia (AIGEO), Italy.

³ Departamento de Ciencias de la Tierra, Universidad de Zaragoza, Spain.

⁴ Department of Physics and Earth Sciences, Jacobs University Bremen, Germany.

⁵ Dipartimento di Scienze Chimiche e Geologiche, Università degli Studi di Modena e Reggio Emilia, Italy.

Corresponding email: davide.baioni@uniurb.it

Keywords: Mars, Arabia Terra, karst.

This work describes possible karst landforms observed in evaporite-bearing Equatorial Layered Deposits (ELDs) within Kotido crater, a medium-sized crater centered at 9.1°W and 1°N, and located next to the Martian equator in the Arabia Terra region. A morphological and morphometric study of the landforms developed on the ELDs within Kotido crater was performed integrating Reconnaissance Orbiter (MRO), High Resolution Imaging Science Experiment (HiRISE) and Context Camera (CTX) data. The analysis revealed the presence of numerous closed depressions interpreted as sinkholes related to evaporite dissolution. These topographic basins show similar characteristics to sinkholes documented in karst terrains on Earth, and in other areas of Mars. The detailed analysis performed on 513 closed depressions indicates the presence of two main kinds of depressions that display different features. Smaller depressions display continuous scarp margins and limited sediment accumulation on the floors, while larger depressions have more degraded margins and thick sediment accumulations including well-developed dune systems. These differences between larger and smaller depressions do not appear to be related to spatial variations in aeolian erosion and deposition rates. Instead, we suggest that the differences may be due to variations in age among depressions. Larger depressions may be older and may have been exposed to degradation and aggradation processes for a longer period of time than the smaller and presumably younger depressions. The karst landforms highlight the presence of liquid water in the past. The age differences based on the size and degradation degree of the depressions may suggest that they represent two different episodes of liquid-water availability and karstification during the Amazonian period.

Evidence for direct solid-state quartz-to-coesite transformation in shocked ejecta from the Australasian tektite/microtektite strewn field

Campanale F.^{*1-2}, Mugnaioli E.², Folco L.¹, Gemmi M.², Lee M. R.³, Daly L.³ & Glass B.P.⁴

¹ Dipartimento di Scienze della Terra, Università di Pisa, Pisa, Italy.

² Center for Nanotechnology Innovation@NEST, Istituto Italiano di Tecnologia (IIT), Pisa, Italy.

³ Department of Geographical and Earth Sciences, University of Glasgow, Glasgow, UK.

⁴ Department of Geosciences, University of Delaware, Newark, DE, USA.

Corresponding email: fabrizio.campanale@phd.unipi.it

Keywords: Impact ejecta, shock metamorphism, coesite formation.

Coesite, a high-pressure silica polymorph, is a diagnostic indicator of impact cratering in quartz-bearing target rocks. The formation mechanism of coesite during hypervelocity impacts has been debated since its discovery in the 1960s. In impactites, coesite is preserved as a metastable phase in crystalline rocks that experienced peak shock pressures above ~30-40 GPa (Stöffler & Langenhorst, 1994), and in porous sedimentary rocks shocked at pressures as low as ~10 GPa (Kowitz et al., 2016). There is a general consensus that coesite within impactites originates by crystallization from a dense amorphous phase during shock unloading, when the pressure release path passes through the coesite stability field. Here, we present a combination of TEM-based electron diffraction analyses in order to obtain the necessary high-resolution images and crystallographic data to unravel the spatial and temporal relations of quartz and coesite. Such nanoscale approach revealed evidence for direct solid-state quartz-to-coesite transformation in shocked coesite-bearing quartz ejecta from the Australasian tektite/microtektite strewn field, which is the largest and youngest (~0.8 Myr old) on Earth.

These ejecta consist of a mixture of coesite and quartz in variable proportions, the latter showing planar deformation features (PDFs) with typical {10-11} and {10-12} orientations. Coesite crystals range in size from ~500 nm to few nanometres, with rounded or elongated habit. They show evident twinning and planar disorder along (010) planes. Where quartz and coesite are in contact, no appreciable amorphous or 'glassy' volume was detected. Instead, quartz boundaries are always lobate or sawtooth-like, with euhedral coesite crystals penetrating through the quartz boundaries. Moreover, PDFs in quartz clearly extend in the coesite domains, suggesting that the latter forms directly at the expense of shocked quartz crystals.

Our observations indicate that quartz transforms directly to coesite after PDF formation and through a solid-state process without entering the silica liquid stability field. The recurrent pseudo iso-orientation between the (1-11) vector in quartz and the (010) vector of neighbouring coesite crystals point to a martensitic-like transformation as possible transition mechanism. Arguably, solid-state martensitic-like process could represent the dominant mechanism of coesite formation in a wide range of cratering events, at least for those with porous target rocks like at the Barringer (Kieffer et al., 1976) and Kamil craters (Folco et al., 2018). This implies lower peak impact pressure and temperature conditions for the formation of impact coesite than previously thought.

MIUR-Programma Nazionale delle Ricerche in Antartide, (ID# PNRA16_00029/P.I. LF).

Folco L., Mugnaioli E., Gemelli M., Masotta M., & Campanale F. (2018) - Direct quartz-coesite transformation in shocked porous sandstone from Kamil Crater (Egypt). *Geology*, 46(9), 739-742.

Kieffer S.W., Phakey P.P. & Christie J.M. (1976) - Shock processes in porous quartzite: Transmission electron microscope observations and theory. *Contributions to Mineralogy and Petrology*, 59(1), 41-93.

Kowitz A., Güldemeister N., Schmitt R.T., Reimold W.U., Wünnemann K. & Holzwarth A. (2016) - Revision and recalibration of existing shock classifications for quartzose rocks using low-shock pressure (2.5–20 GPa) recovery experiments and mesoscale numerical modeling. *Meteoritics & Planetary Science*, 51(10), 1741-1761.

Stöffler D. & Langenhorst F. (1994) - Shock metamorphism of quartz in nature and experiment: I. Basic observation and theory. *Meteoritics*, 29(2), 155-181.

VNIR reflectance spectra of iron-bearing Mercury-like glasses

Carli C.^{*1}, Morlok A.², Stojic A.², Weber I.², Renggli C.³, Klemme S.³, Ferrari S.⁴, Pratesi G.⁵, Hiesinger H.² & Capaccioni F.¹

¹ IAPS-INAF, Roma.

² Institut für Planetologie, Universität of Munster.

³ Institut für Mineralogie, Universität of Munster.

⁴ CISAS, Università degli studi di Padova.

⁵ Dipartimento di Scienze della Terra, Università di Firenze.

Corresponding email: cristian.carli@inaf.it

Keywords: Mercury, spectroscopy, glasses.

The MESSENGER mission that orbited Mercury from 2011 to 2015 acquired element distribution data of the planetary surface. This data allowed for retrieving chemical compositions for different terrains. Several studies focused on understanding the geochemical composition of the closest planet to the Sun and on producing reasonable analogue material. In particular, there is evidence for similarity with rocks like komatiite or boninite (e.g. Namur et al., 2016; Vander Kaaden et al., 2017). These hermean compositions show a depletion in iron with respect to volcanic material on other differentiated bodies. In fact, iron is lower than 1-3 wt% (inferred from FeO) (e.g. Weider et al., 2014). We focused on synthetically produced glasses to better understand the spectral properties of such Fe-depleted material. Glasses are expected to be an important component present on a planetary surface characterized by extensive effusive volcanism and a high crater density like Mercury.

Here we used glasses, synthesized under varying oxygen fugacity conditions by Morlok et al. (2017) and (2019) that were already documented in the mid infrared. We acquired bidirectional reflectance spectra with $i=30^\circ$ and $e=0^\circ$ from 0.35 to 2.5 μm for aforementioned glasses from variable grainsize batches. The selected spectral range covers that of the VIHI (SIMBIO-SYS) spectrometer onboard the BepiColombo shuttle, which is complementary to the MERTIS range (7-14 μm , Benkhoff et al., 2010). Spectra show a typical absorption band attributed to the presence of Fe^{2+} with varying intensity. Moreover a slope change in the visible-near infrared can be confirmed up to 0.7 μm . We will retrieve also the optical constant following the approach used in Carli et al. (2016).

Benkhoff J., Van Casteren J., Hayakawa H., Fujimoto M., Laakso H., Novara M., Ferri P. Middleton H.R. & Ziethe R. (2010) - BepiColombo—Comprehensive exploration of Mercury: Mission overview and science goals. *Planetary and Space Science*, 58, 2-20.

Carli C., Roush T.L., Pedrazzi G. & Capaccioni F. (2016) - Visible and Near-Infrared (VNIR) reflectance spectroscopy of glassy igneous material: Spectral variation, retrieving optical constants and particle sizes by Hapke model. *Icarus*, 266, 267-278.

Morlok A., Klemme S., Weber I., Stojic A., Sohn M. & Hiesinger H. (2017) - IR spectroscopy of synthetic glasses with Mercury surface composition: Analogs for remote sensing. *Icarus*, 296, 123-138.

Morlok A., Charlier B., Renggli C., Klemme S., Namur O., Carli C., Sohn M., Reitze M.R., Weber I., Bauch K., Stojic A., Hiesinger H. & Helbert J. (2019) - Infrared spectroscopy of experimental and synthetic planetary analogs for the Bepicolombo mission to Mercury. *LPSC 50th. Abs 2411*.

Namur O., Collinet M., Charlier B., Grove T.L., Holtz F. & McCammon C. (2016) - Melting processes and mantle sources of lavas on Mercury. *Earth and Planetary Science Letters*, 439, 117-128.

Vander Kaaden K.E. McCubbin F.M., Nittler L.R., Peplowski P.N., Weider S.Z., Frank E.A. & McCoy T.J. (2017) - Geochemistry, mineralogy, and petrology of boninitic and komatiitic rocks on the mercurian surface: Insights into the mercurian mantle. *Icarus*, 285, 155-168.

Weider S.Z., Nittler L.R., Starr R.D., McCoy T.J. & Solomon S.C. (2014) - Variations in the abundance of iron on Mercury's surface from MESSENGER X-Ray Spectrometer observations. *Icarus*, 235, 170-186.

Reflectance and emissivity spectroscopy of hydrated salts at different temperature: a method to understand icy planetary bodies surfaces composition

Fastelli M.*¹, Comodi P.¹, Zucchini A.¹, Maturilli A.², Balic-Zunic T.³ & Rossi M.⁴

¹ Dipartimento di Fisica e Geologia, University of Perugia, Italy.

² Planetary Emissivity Laboratory, DLR German Aerospace Center, Berlin, Germany.

³ Department of Geosciences and Natural Resource Management, University of Copenhagen, Denmark.

⁴ Dipartimento di Scienze della Terra, University of Napoli Federico II, Italy.

Corresponding email: maximiliano.fastelli@studenti.unipg.it

Keywords: emissivity, reflectance, hydrated salts.

Jupiter's moons, Europa in particular, are considered as the most promising place to look for an environment suitable for life due to the likely presence of oceans. One way to give a contribution to help understanding this scenario is to describe in detail the surface ice composition through the analysis of existing spacecraft data and telescopic observations compared with an accurate and detailed data base. The composition of Europa's non-ice surface material is assumed to be mixtures of sulfuric acid hydrates, brines, and salt hydrates. In this study, spectra of a selected group of minerals (sulphates, chlorides, alkaline-earth or alkaline sulphates and mixed salts) were collected in reflectance at ambient and low (-80 C°) and in emissivity up to high temperature (500 C°) to investigate the effect of cation and anion substitution as well as the different amount of water molecules in the minerals crystal structure. Fundamental bending and stretching S-O vibration absorption bands occur in the 4-5, and 7-10.4 μm regions. The 1.9 and 1.4 μm bands indicate water molecular and hydroxyl, respectively. Emissivity measurements give us information only about $\nu_{>3}$ absorption band in the spectral range from 600 to 3500 cm^{-1} . Anhydrous sulphates show absorption bands in the 1050–1250 cm^{-1} range corresponding to symmetric stretch of SO_4 . Hydrated sulphates have absorption bands in the $\sim 2500 - 2700 \text{ cm}^{-1}$ range probably due to the presence of water molecules. Unfortunately, the absorption bands, characteristic of the non-water ice materials, are present in the area over 5 μm where the current data from remote sensing mission were not collected. A careful analysis of the depth, area, position, and the FWHM of absorption bands in relation to T was performed. In the emissivity measurement, area and FWHM of the bands have a linear increase with T , whereas the band position does not change with T . In some case cation substitution can affect the wavelength position of SO_4 absorption bands, as observed in BaSO_4 and CaSO_4 . Spectra at high T give information about the dehydration of the minerals and possible phase transitions. For example, hydrous magnesium sulphate after heating shows interesting new anhydrous phases with a $\beta\text{-MgSO}_2$ crystal structure. In reflectance measurements, area and FWHM of the bands showed different temperature dependences. However, on the whole, area and depth of the bands increase as the temperature decreases whereas the FWHM of the bands remains constant. The presented data can give a contribution to the understanding of both the dehydration conditions of these minerals and the change in density which are directly correlated to buoyancy and to the mechanisms of storage/release of water within the planetary bodies.

The near-Earth cosmic dust complex: Perspectives from the unique Transantarctic Mountains micrometeorite collection

Folco L.*

Dipartimento di Scienze della Terra, Università d Pisa, Italy.

Corresponding email: luigi.folco@unipi.it

Keywords: cosmic dust, asteroids, comets.

I evaluate the long-standing contributions to meteoritics and planetary sciences stemming from 16 years of research on cosmic dust recovered from the unique Transantarctic Mountains (TAM) micrometeorite collection. Discovered in 2003, this collection provides a unique opportunity to address outstanding and timely topics in planetary science.

TAM micrometeorites sample the flux of cosmic dust falling to Earth over significant timescales (>1 million years; Rochette et al., 2008; Folco et al., 2008). Such an extraordinarily long collection time has resulted in the accumulation of many thousands of individual particles. This includes an abundance of otherwise rare giant micrometeorites (orders of magnitude larger than previously found in other collections) which are thus suitable for multi-analytical investigations. For example, combining petrographic, bulk compositional and isotopic data on a single particle ensures accurate characterisation and has led to the identification of new micrometeorite types from a range of primitive and evolved parent bodies (Suavet et al., 2010; van Ginneken et al., 2012; Cordier et al., 2018). Additionally, we are able to establish the relative parent body contributions to the modern inner solar system dust complex located at ~1 AU (Cordier & Folco, 2014); whilst also providing information on the micrometeoroid source regions in the solar system – with implications for their orbital evolution (Baecker et al., 2018) and parent body geological processes (Suttle et al., 2018; Nava et al., this meeting; Mugnaioli et al., this meeting).

Looking forward, our ambitious objective is to use the TAM micrometeorite collection to define the composition of the micrometeorites flux to Earth over the last 1 million years (mass, size, compositional type and source bodies in the Solar System), thereby providing a world-class reference dataset for cosmic dust studies. This will serve as a ground-truth resource for future studies into: i) the composition of the dust complex in the inner Solar System; ii) the nature and geology of all the dust producing bodies including asteroids, comets, and perhaps planets and their satellites, which are also the targets of current and future space missions; iii) the dynamical evolution of the interplanetary dust in the zodiacal cloud; iv) the contribution of extraterrestrial matter to our planet's geochemical budget; v) variations in the cosmic dust flux to Earth in the Earth's sedimentary record through time and the break up histories of asteroids and comets in their source regions.

MIUR: PNRA16_00029, PRIN15_20158W4JZ7.

- Baecker B., Ott U., Cordier C., Folco L., Trierloff M., Van Ginneken M., Rochette P. (2018) – Noble gases in micrometeorites from the Transantarctic Mountains. *Geochimica et Cosmochimica Acta*, 242, 266-297.
- Cordier C., Baecker B., Ott U., Folco L. & Trierloff M. (2018) - A new type of oxidized and pre-irradiated micrometeorite. *Geochimica et Cosmochimica Acta*, 233, 135-158.
- Folco L., Rochette P., Perchiazzi N., D'Orazio M., Laurenzi M.A. & Tiepolo M. (2008) - Microtektites from Victoria land transantarctic mountains. *Geology*, 36(4), 291-294.
- Folco L. & Cordier C. (2015) – Micrometeorites. *EMU Notes*, 15:253-297.
- Rochette P., Folco L., Suavet C., Van Ginneken M., Gattacceca J., Perchiazzi N., Braucher R. & Harvey R.P. (2008) - Micrometeorites from the transantarctic mountains. *Proceedings of the National Academy of Sciences*, 105(47), 18206-18211.
- Suttle M.D., Folco L., Genge M.J., Russell S.S., Najorka J. & van Ginneken M. (2019) - Intense aqueous alteration on C-type asteroids: Perspectives from giant fine-grained micrometeorites. *Geochimica et Cosmochimica Acta*, 245, 352-373.
- Suavet, C., Alexandre, A., Franchi, I. A., Gattacceca, J., Sonzogni, C., Greenwood, R. C., Folco L. & Rochette, P. (2010) - Identification of the parent bodies of micrometeorites with high-precision oxygen isotope ratios. *Earth and Planetary Science Letters*, 293(3-4), 313-320.
- Van Ginneken M., Folco L., Cordier C., Rochette P. (2012) - Chondritic micrometeorites from the Transantarctic Mountains. *Meteoritics & Planetary Science*, 47(2), 228-247.

High-Mg region induced stress field in the Victoria quadrangle of Mercury

Galluzzi V.*¹, Ferranti F.², Massironi M.³, Giacomini L.¹, Guzzetta L.¹ & Pasquale P.^{4,1}

¹ INAF, Istituto di Astrofisica e Planetologia Spaziali (IAPS), Roma.

² DiSTAR, Università di Napoli Federico II.

³ Dipartimento di Geoscienze, Università di Padova.

⁴ DST, Università di Napoli Parthenope.

Corresponding email: valentina.galluzzi@inaf.it

Keywords: planetary geology, Mercury (planet), planetary tectonics.

The High-Mg region (HMR) is a large area of Mercury (30-150°W; 25°S-60°N), where the highest Mg/Si ratio is observed (mostly > 0.5) (Weider et al., 2015), and where crustal densities should be higher with respect to the surrounding areas (Namur & Charlier, 2017). The highest Mg/Si ratio and stronger lateral geochemical contrasts with respect to the surrounding terrains are in the H-2 quadrangle of Mercury (0-90°W; 22.5-65°N). This area also encompasses Carnegie Rupes, Victoria Rupes, Endeavour Rupes and Antoniadi Dorsum, some of the major morpho-structures on the planet. We updated the structural mapping of (Galluzzi et al., 2016) and exploited the stratigraphic information of the geological map of the H-2 quadrangle (Galluzzi et al., 2015), and compared it to the existing petrological and geophysical datasets in order to analyze the relationship between faults and the geochemical variations. We used NASA MESSENGER data to perform geomorphological, structural, and timing analyses of fault systems, in order to correlate fault geometry and kinematics to Mercury's crustal properties. Three non-parallel fault systems occur in the Victoria quadrangle of Mercury: the most prominent one trends NNW-SSE (Victoria System, VS); west and northwest of the VS, two additional fault systems with NE-SW (Larrocha System, LS) and NW-SE (Carnegie System, CS) trend are found. Results of the stress inversion and age relationships, together with geometrical and morpho-structural observations suggest that the NE-SW and NW-SE systems were respectively right-transcurrent and left-transpressional at the same time when the computed strain field was active before 3.7 Ga. The HMR highlights a geochemical dichotomy that broadly corresponds to the spatial difference in the distribution of VS versus LS structures. Specifically, whereas LS is mostly found within the HMR, VS form the eastern and the northeastern boundary of the region. It is possible that the lateral geomechanical variations of the crust combined with global contraction processes drove the localization and slip pattern of faults in a kinematically consistent displacement field. The faults have followed previous HMR discontinuities and, in turn, may have deformed the HMR itself.

We gratefully acknowledge funding from the Italian Space Agency (ASI) under ASI-INAF agreement 2017-47-H.0.

Galluzzi V., Di Achille G., Ferranti L., Popa C. & Palumbo P. (2015) - Faulted craters as indicators for thrust motions on Mercury, Geological Society of London, Special Publications, 401, 313–325.

Galluzzi V., Guzzetta L., Ferranti L., Di Achille G., Rothery D.A. & Palumbo P. (2016) - Geology of the Victoria quadrangle (H02), Mercury. Journal of Maps, 12, 227–238.

Namur O. & Charlier B. (2017) - Silicate mineralogy at the surface of Mercury. Nature Geoscience, 10, 9–13.

Weider S.Z., Nittler L.R., Starr R.D., Crapster-Pregont E.J., Peplowski P.N., Denevi B.W., Head J.W., Byrne P.K., Hauck S.A., Denton Ebel S. & Solomon S.C. (2015) - Evidence for geochemical terranes on Mercury: Global mapping of major elements with MESSENGER's X-Ray Spectrometer. Earth and Planetary Science Letters, 416, 109–120.

Geological mapping of the Kuiper (H06) quadrangle of Mercury: Integration between morphologic and spectral characteristics

Giacomini L.*¹, Galluzzi V.¹, Carli C.¹, Zambon F.¹, Massironi M.², Ferranti L.³ & Palumbo P.^{4,1}

¹ INAF, Istituto di Astrofisica e Planetologia Spaziali, Rome, Italy.

² Dipartimento di Geoscienze, Università degli Studi di Padova, Padua, Italy.

³ DISTAR, Università degli Studi di Napoli Federico II, Naples, Italy.

⁴ Dipartimento di Scienze & Tecnologie, Università degli Studi di Napoli 'Parthenope', Naples, Italy.

Corresponding email: lorenza.giacomini@inaf.it

Keywords: Mercury, planetary geology, mapping.

Kuiper quadrangle (H06) is located at the equatorial zone of Mercury and encompasses the area between longitudes 288°E – 360°E and latitudes 22.5°N – 22.5°S. In this contribution we present the results of a detailed geological map (1:3M scale) of the Kuiper quadrangle based on the high resolution MESSENGER data. This geological map will be merged with the adjoining quadrangles and integrated into the global 1:3M geological map of Mercury (Galluzzi et al., 2018), which is being prepared in support to BepiColombo mission.

The main basemap used for H06 mapping is the MDIS (Mercury Dual Imaging System) 166 m/pixel BDR (map-projected Basemap reduced Data Record) mosaic. Additional datasets were also taken into account, such as DLR stereo-DEM of the region (Preusker et al., 2017), mosaics with high-incidence illumination from the east and west, and MDIS global color mosaic (Denevi et al., 2018). The geological map shows that the quadrangle is characterized by a prevalence of crater materials which were distinguished into three classes based on their degradation degree (Galluzzi et al., 2016). Different plain units were also identified and classified as: (i) intercrater, (ii) intermediate, and (iii) smooth plains. Finally, several structures, mainly represented by thrusts, were mapped all over the quadrangle.

Where WAC images at high spatial resolution are available, a more detailed analysis of the spectral behavior of the surfaces was carried out. This allowed us to integrate geomorphological and spectral characteristics of specific areas in order to gain new information about the landforms' origin.

We gratefully acknowledge funding from the Italian Space Agency (ASI) under ASI-INAF agreement 2017-47-H.0. MM, CC, FZ were also supported by European Union's Horizon 2020 research grant agreement No 776276- PLANMAP.

Denevi B.W., Chabot N.L., Murchie S.L., Becker K.J., Blewett D.T., Domingue D.L., Ernst C.M., Hash C.D., Hawkins E.S., Keller M.R., Laslo N.R., Nair H., Robinson M.S., Seelos F.P., Stephens G.K., Turner S.F. & Solomon S.C. (2018) - Calibration, Projection, and Final Image Products of MESSENGER's Mercury Dual Imaging System. *Space. Sci. Rev.*, 214, 2.

Galluzzi V., Guzzetta L., Ferranti L., Di Achille G., Rothery D.A. & Palumbo P. (2016) - Geology of the Victoria quadrangle (H02), Mercury. *Journal of Maps*, 12, 227–238.

Galluzzi et al., 2018. The Making of the 1:3M Geological Map Series of Mercury: Status and Updates. *Mercury: Current and Future Science of the Innermost Planet*. Abstract#6075.

Preusker F., Stark A., Oberst J., Matz K.D., Gwinner K., Roatsch T. & Watters T.R. (2017) - Toward high-resolution global topography of Mercury from MESSENGER orbital stereo imaging: A prototype model for the H6 (Kuiper) quadrangle. *Planetary and Space Sci.*, 142, 26-37.

Hydrothermal iron ooids on Earth as homologues of hematite spherules discovered on Mars

Italiano F.¹, Di Bella M.*¹, Sabatino G.², Barbieri R.³, Cavalazzi B.³⁻⁴, Ferretti A.⁵, Danovaro R.⁶⁻⁷, Romeo T.⁶⁻⁹, Andaloro F.⁶, Esposito V.⁸, Tripodo A.², Scotti G.⁹ & Quartieri S.²

¹ Istituto Nazionale di Geofisica e Vulcanologia (INGV), Sezione di Palermo, Italy.

² Dipartimento di Scienze Matematiche, Informatiche, Fisiche e Scienze della Terra (MIFT), Università di Messina, Italy.

³ Dipartimento di Scienze Biologiche, Geologiche e Ambientali (BiGeA), Università di Bologna, Italy.

⁴ Department of Geology, University of Johannesburg, Johannesburg, South Africa.

⁵ Dipartimento di Scienze Chimiche e Geologiche (DSCG), University di Modena e Reggio Emilia, Italy.

⁶ Stazione Zoologica Anton Dohrn (SZN), Napoli, Italy.

⁷ Università Politecnica delle Marche, Ancona.

⁸ Istituto Nazionale di Oceanografia e di Geofisica Sperimentale (OGS), Trieste, Italy.

⁹ Istituto Superiore per la Protezione e la Ricerca Ambientale (ISPRA), Laboratorio di Milazzo (ME), Italia.

Corresponding email: mdibella@unime.it

Keywords: hydrothermalism, iron ooids, hematite spherules.

A large set of high-resolution images of Mars provided by NASA's rovers have revealed the presence of diffused deposits containing iron-made, spherical particles, similar to the terrestrial ooids. Several hypotheses have been recently proposed in order to explain the formation of these hematite-spherules, including an origin from microbial activity or by meteorite impact. These particles are very similar to nowadays forming hydrothermal iron-ooids recently found in a terrestrial shallow-water volcanic environment, over an active submarine hydrothermal system of the Aeolian Islands (Panarea, Italy). An integrated analysis, carried out by X-ray Powder Diffraction, Environmental Scanning Electron Microscopy, X-ray Fluorescence and Raman spectroscopy, reveals that Panarea ooids are deposited at the seafloor as concentric laminae of primary goethite around existing nuclei. The process is rapid, and driven by hydrothermal fluids as iron source. A sub-spherical, laminated structure resulted from constant agitation and by degassing of CO₂-dominated fluids through seafloor sediments (Di Bella et al., 2019). In this work we investigate the possible role of a hydrothermal-volcanic activity, and in particular, of hydrothermal fluids, in the genesis of the spheroidal Martian grains. The striking similarities observed among the Martian hematite spherules and the hydrothermal iron-ooids from Panarea Island - in terms of host rock composition, sand grain components, physical characteristics of the iron concretions (spheroidal geometry, interior structure, size), mineralogical features - allow us to propose a hydrothermal-related formation mechanism. The ongoing Fe-rich depositions, located at the volcanic seafloor at Panarea, can be considered homologous of the so-called reworked sandstones outcropping as bedrocks on the Martian soils. Moreover, the Martian layered bedrocks could be interpreted as resedimented/reworked hydrothermal deposits triggered by wind systems on the already arid and dried up seabed.

Di Bella M., Sabatino G., Quartieri S., Ferretti A., Cavalazzi B., Barbieri R., Foucher F., Messori F. & Italiano F. (2019) - Modern iron ooids of hydrothermal origin as a proxy for ancient deposits. *Scientific Reports*, 9, 1-9.

From Planetary surface mapping to Planetary subsurface structures

Massironi M.*¹, Pozzobon R.¹, Franceschi M.¹ & Penasa L.²

¹ Dipartimento di Geoscienze Università degli studi di Padova, Padova, Italy.

² Università degli studi di Padova, Padova, Italy.

Corresponding email: matteo.massironi@unipd.it

Keywords: Planetary geological maps, 3D geological models.

To understand the geological evolution of a given planetary or minor body, a planetary geologist must always face the problem of inferring planetary subsurface from remote measurements and observations of their surface. The nowadays available 3D modelling techniques, widely used by oil and, with less extent, mining companies, can be adapted on planetary bodies specifically when stratification is well exposed such as on Inner Layered Deposits (ILD) within craters on Mars (e.g. Pozzobon et al., 2019a), Martian Polar caps (Christian et al., 2013; Foss II et al., 2018); and cometary layered sequences (Penasa et al., 2017). In this cases strata attitudes coupled with geophysical data (when available) turned to be very effective in reaching such a goal and either implicit or explicit 3D geo-models can be accomplished. More difficulties might arise where such subtle stratification is lacking, and alternative solution must be investigated. This is the case for example of wide lava-field on Mars, Moon and Mercury where craters can be used as deep logs under the planetary surfaces to infer possible stratifications (Ernst et al., 2015; Ferrari et al., 2015), fracture and vents distribution can unravel rheological layering of the crust (Pozzobon et al., 2015, 2019b; De Toffoli et al., 2018), deformed craters are key element for retrieving fault attitudes (Galluzzi et al., 2015) and open pits can be used to infer lava tubes depth and development (Sauro et al., 2017).

H2020-PLANMAP project specifically aims at exploring subsurface structures from surface observation and geological maps. By showing key studies that our group have faced on different planetary and minor bodies we will discuss pros and cons of the different approaches and relevant results obtained up to date.

Particular attention will be paid on the implicit modelling of Comet 67P and the explicit one carried out on the deformed layered sequences of Crommelin crater, both successful cases which have returned unexpected results on planetary geological processes such as plastic-brittle deformation during cometary nuclei merging and cratering induced diapirism on Mars.

This project has received funding from the European Union's Horizon 2020 research and innovation programme under grant agreement No 776276-PLANMAP

De Toffoli B., Pozzobon R., Mazzarini F., Orgel C., Massironi M., Giacomini L., Mangold N. & Cremonese, G. (2018).

Estimate of depths of source fluids related to mound fields on Mars. *Planetary and Space Science*, 164, 164-173.

Ernst C.M., Denevi B.W., Barnouin O.S., Klimczak C., Chabot N.L., Head J.W., Murchie S.L., Neumann G.A., Prockter L.M., Robinson M.S., Solomon S.C. Watters T.R. (2015) - Stratigraphy of the Caloris basin, Mercury: Implications for volcanic history and basin impact melt. *Icarus*, 250, 413-429.

Ferrari S., Massironi M., Marchi S., Byrne P.K., Klimczak C., Martellato E. & Cremonese G. (2015) - Age relationships of the Rembrandt basin and Enterprise Rupes, Mercury. *Geological Society, London, Special Publications*, 401(1), 159-172.

Foss F.J., Putzig N.E., Campbell B.A. & Phillips R.J. (2017) - 3D imaging of Mars' polar ice caps using orbital radar data. *The Leading Edge*, 36(1), 43-57.

Galluzzi V., Di Achille G., Ferranti L., Popa C. & Palumbo P. (2015) - Faulted craters as indicators for thrust motions on Mercury. *Geological Society, London, Special Publications*, 401(1), 313-325.

Penasa, L., Massironi, M., Naletto, G., Simioni, E., Ferrari, S., Pajola, M., Scholten F., Jorda I., Gaskell R., Ferri F., Marzari F., Davidsson B., Mottola S., Sierks H., Barbieri C., Lamy P.L., Rodrigo R., Koschny D., Rickman H., Keller H.U., Agarwal J., A'Hearn M.F., Barucci M.A., Bertaux J.L., Bertini I., Cremonese G., Da Deppo V., Debei S., De Cecco M., Deller J., Feller C., Fornasier S., Fratrin E., Fulle M., Groussin O., Gutierrez P.J., Güttler C., Hofmann M., Hviid S.F., Ip W.H., Knollenberg J., Kramm J.R., Kürt E., Küppers M., La Forgia F., Lara L.M., Lazzarin M., Lee J.-C., Lopez Moreno J.J., Oklay N., Shi X., Thomas N., Tubiana C., Vincent J.B. & Gaskell, R. (2017) - A three-dimensional modelling of the layered structure of comet 67P/Churyumov-Gerasimenko. *Monthly Notices of the Royal Astronomical Society*, 469(2), S741-S754.

- Pozzobon R., Mazzarini F., Massironi M. & Marinangeli L. (2015) - Self-similar clustering distribution of structural features on Ascraeus Mons (Mars): implications for magma chamber depth. Geological Society, London, Special Publications, 401(1), 203-218.
- Tomasi I., Massironi M., Meyzen C., Pozzobon R., Penasa L., Sauro F., Santagata T., Tonello M., Martínez-Frías J. & Mateo Medero E. (2019) - How huge lava tubes form? EGU General Assembly.
- Pozzobon R., Mazzarini F., Massironi M., Rossi, A.P., Pondrelli M., Cremonese G. & Marinangeli L. (2019) - Fluids mobilization in Arabia Terra, Mars: Depth of pressurized reservoir from mounds self-similar clustering. *Icarus*, 321, 938-959.

Characterization of the Fe-Si-C system at extreme conditions and application to exoplanets interior

Miozzi F.*¹, Morard G.¹, Antonangeli D.¹, Clark A. N.², Baron M.A.¹, Dorn C.³, Rozel A.⁴, Pakhomova A.⁵, Mezouar M.⁶ & Fiquet G.¹

¹ Institut de Minéralogie, de Physique des Matériaux, et de Cosmochimie (IMPMC), Sorbonne Universités – UPMC, UMR CNRS, 7590, Muséum National d'Histoire Naturelle, F-75005 Paris, France.

² Department of Earth and Planetary Sciences, Northwestern University, Evanston, IL, USA, 60208.

³ University of Zurich, Institute of Computational Sciences, Winterthurerstrasse 109, CH-8057 Zurich.

⁴ Institute of Geophysics, Department of Earth Sciences, ETH Zurich, Sonneggstrasse.

⁵ CH-8092 Zurich, Switzerland ⁵ Deutsches Elektronen-Synchrotron (DESY), Hamburg, Germany.

⁶ European Synchrotron Radiation Facility, Grenoble, France.

Corresponding email: francesca.miozzi@upmc.fr

Keywords: mineral physics, extreme conditions, exoplanets.

The recent search of new habitable planets led to the discovery of more than 3200 exoplanets, orbiting around star with a wide range of chemical compositions. Some in particular display a ratio between carbon and oxygen higher than the threshold dividing oxygen enriched stars from carbon enriched stars. Planets accreting in such conditions might display an “exotic” composition compared to the Earth, enriched in phases such as carbides instead of silicates and oxides (Duffy, 2015).

Exoplanets identification from observation pass through the interpretation of their mass and radius with models of planetary interior determined a priori. Accordingly having reliable models of carbon rich exoplanets interior is fundamental for their identification. Carbon rich exoplanets, initially modelled with the Fe-Si-C system faced the problem of degeneracy (Madhusudhan et al., 2012). More than one mineralogical assemblage resulted in a planet with the same mass and radius. Furthermore, also considering an archetypal end member with a pure Fe core and a SiC mantle, the initial absence of extensive study on SiC at the conditions of planetary interior hampered the possibility of calculating reliable mass radius plots.

In this contribution we will present experimental data regarding two systems: the binary Si-C and the ternary Fe-Si-C, both investigated between 20 and 200 GPa and up to 3500 K. The results provide new insights into the phase stability and properties of SiC at extreme conditions, enabling to calculate precise mass radius plot and make a first estimate on the dynamic of a carbon rich exoplanets. Furthermore, the results on the ternary system unravel how different amount of light element can originate different crystallization processes.

Duffy T. (2015) - Mineralogy of Super-Earth Planets, Treatise on Geophysics. Elsevier B.V. <https://doi.org/10.1016/B978-0-444-53802-4.00053-1>

Madhusudhan N., Lee K.K.M. & Mousis O. (2012) - A possible carbon-rich interior in super-Earth 55 Cancri e. The Astrophysical Journal Letters, 759(2), L40. <https://doi.org/10.1088/2041-8205/759/2/L40>

The 2017 Joint Italian - Iranian Lut desert expedition: compositional and textural features of the meteorites recovered

Moggi Cecchi V.*¹, Pratesi G.², Giuli G.³, Nemati M.⁴, Di Martino M.⁵ & Serra R.⁶

¹ Museo di Storia Naturale dell'Università di Firenze, Firenze, Italy.

² Dipartimento di Scienze della Terra dell'Università di Firenze, Firenze, Italy.

³ Scuola di Scienze e Tecnologia, Università di Camerino, Camerino (MC), Italy.

⁴ Department of Geology, Shahid Bahonar University, Kerman, Iran.

⁵ INAF - OATO, Pino Torinese, Torino, Italy.

⁶ Dipartimento di Fisica, Università di Bologna, Italy.

Corresponding email: vanni.moggicecchi@unifi.it

Keywords: meteorite, Lut Desert, chondrite.

The Lut Desert is a desertic area considered by several authors remarkably suitable for meteorite preservation and recovery (Pourkhorsandi et al., 2016). It is located in the south – eastern part of Iran. It extends for about 270 km in longitude and 190 km in latitude. A joint Italian - Iranian team from the University of Firenze, Italy, and the Shahid Bahonar University of Kerman, Iran, organized a field trip to the Lut Desert from 10 to 25 march 2017. The field trip concentrated in the Kalut desert, which is characterized by the presence of 50-100 meters high ridges consisting of loess deposits, modeled by the action of the wind. The soil surface is consisting of hardened sand, particularly suitable for meteorite recovery. Although several very small black, non- magnetic rounded terrestrial stones are present, larger stones are easy recognizable as meteorites by their external features. In a 10 days campaign 143 fragments belonging to 45 separate specimens of meteorites, ranging from few grams to one kilo and totally weighing 3670 grams, and other doubtful stones have been recovered. A first essay on the fragments density allowed to discriminate terrestrial rocks and to single out three separate clusters in the range 3.2-3.4 g/cm³ for meteorites (Moggi Cecchi et al., 2017). All the samples have been analyzed by means of polarizing optical microscope, both in reflected and transmitted light. A complete textural and compositional survey has been carried out by means of Scanning Electron Microscope for classification purposes. Selected samples have also been analyzed by means of EMPA. Analytical results pointed out remarkable differences between big meteorites and small fragments, although the weathering grade is similar. Analytical data from silicates also suggest a different classification for big samples: while data on most small samples point to a classification as H5 or H6 ordinary chondrite, the presence in big samples of large chondrules of various type (PO, BO, POP) with scarce integration with matrix, together with a slight variation in Fa and Fs mol. %, point a different classification (H4, L5). The common weathering features associated with different textural and compositional data suggest the presence of a strewn field originated from a common rubber-pile meteoroid that broke-up in the lower atmosphere. A report on the complete set of samples has been submitted to the Nomenclature Committee of the Meteoritical Society for the approval with names ranging from Kerman 205 to 249.

Moggi Cecchi V., Cecchi L., Pratesi G., Giuli G., Nemati M., Di Martino M. & Serra R. (2017) - Preliminary Results of the Lut Desert 2017 Joint Italian-Iranian Expedition for Meteorite Recovery. *Meteoritics & Planetary Science*, 52, S1, A239.

Pourkhorsandi H., Mirnejad H., Rochette P. & Hassanzadeh J. (2016) - Lut 009, an H4 (S2, W4) ordinary chondrite meteorite from Lut Desert of Iran. *Journal of the Earth and Space Physics*, 41, 125–130.

3D electron diffraction for the characterization of cryptocrystalline micro-samples: Applications to planetary sciences

Mugnaioli E.*¹, Gemmi M.¹, Campanale F.¹⁻², Suttle M. D.², Folco L.² & Pignatelli I.³

¹ Center for Nanotechnology Innovation@NEST, Istituto Italiano di Tecnologia, Italy.

² Dipartimento di Scienze della Terra, Università di Pisa, Italy.

³ CRPG, CNRS - Université de Lorraine, France.

Corresponding email: enrico.mugnaioli@iit.it

Keywords: electron crystallography, nano-materials, micro-meteorites.

Cutting-edge research topics in Earth and planetary sciences often require the study of small cryptocrystalline polyphasic samples, typically characterized by nano-scale intergrowths, like the products of high-pressure/high-temperature experiments, fast nucleating minerals at non-equilibrium conditions or micro-sized extraterrestrial materials. Conventional optical imaging and X-ray crystallographic tools may be not sufficient for the proper characterization of such samples. The development of efficient probes able to investigate the nanoworld is therefore crucial to further our understanding of the mineralogical and geochemical processes that regulate Earth and extraterrestrial environments. Over the last ten years, electron diffraction (ED) evolved from a qualitative method restricted to few TEM users, to a robust protocol for phase identification and ab-initio structure determination. Such changes have been possible due to the development of automatic and semi-automatic routines for 3D data collection (Mugnaioli & Gemmi, 2018). This methodology is in principle equivalent to single-crystal X-ray diffraction, but can be performed on crystals 10 to 1000 times smaller. In this contribution, we show recent applications of ED in planetary sciences. In particular, how ED allowed the mineralogical screening of the carbonaceous chondrite CM Paris (Pignatelli et al., 2018) and of a hydrated chondritic micrometeorite (CP94-050-052) through the polytypic description of sub-micrometric phyllosilicate grains. Moreover, we will present an extensive petrographic and crystallographic study of quartz-coesite mineralogical association in impact ejecta from Kamil Crater, Egypt (Folco et al., 2018), and from the Australasian tektite strewn field. We believe that the extensive application of modern ED techniques on micro-to-nanometer extraterrestrial samples has the potential for significant breakthroughs in our understanding of the Solar System's formation and evolution. Also, it will allow the thorough exploitation of the evidence already enclosed in the micrometeorite collection recovered within the *Progetto Nazionale Ricerche in Antartide* (PNRA) and in the forthcoming European space missions. ED will also significantly support other sources of information based on remote sensing and spectroscopy and will therefore ensure better constraints in numerical modeling studies.

Folco L., Mugnaioli E., Gemelli M., Masotta M. & Campanale F. (2018) - Direct quartz-coesite transformation in shocked porous sandstone from Kamil Crater (Egypt). *Geology*, 46, 739-742. Mugnaioli E. & Gemmi M. (2018) - Single-crystal analysis of nanodomains by electron diffraction tomography: mineralogy at the order-disorder borderline. *Z. Kristallogr.*, 233, 163-178.

Pignatelli I., Mugnaioli E. & Marrocchi Y. (2018) - Cronstedtite polytypes in the Paris meteorite. *Eur. J. Mineral.*, 30, 349-354.

Laboratory experiments on carbonaceous chondrites: insights into cryovolcanism and hydrothermal alteration on planetary bodies

Nava J.*¹, Maturilli A.², Zambon F.³, Carli C.³, Alemanno G.², Helbert J.², Genovesi S.⁴ & Massironi M.¹

¹ Department of Geosciences, University of Padova, Padova, Italy.

² Institute of Planetary Research, German Aerospace Centre (DLR), Berlin, Germany.

³ IAPS-INAF, Istituto Nazionale di Astrofisica e Planetologia Spaziali, Roma, Italy.

⁴ Università degli Studi di Bologna, Dipartimento di Geologia, Bologna, Italy.

Corresponding email: jacopo.nava@phd.unipd.it

Keywords: Cryovolcanism, carbonaceous chondrites, Hydrothermalism.

Cryovolcanism and hydrothermal alteration are two main processes that characterized the geology of asteroids, dwarf planets and satellites (Krot et al., 1998; Neveu & Desch, 2015). Cryovolcanic-like processes have also been observed on Cometary Nuclei (Belton & Melosh, 2009). Cryovolcanic and hydrothermal processes and related products are still not well understood. For this reason we made some experiments at the PEL DLR laboratory in Berlin with Carbonaceous Chondrites (CCs) and ices to try to recreate a cryovolcanic process as well as heating experiments of CCs mixed with deionized (DD) water and ammoniated (NH₃) water.

The CCs used are: FRO90006, FRO99040, FRO95002 and MCY14014. For the cryovolcanic experiments we mixed FRO99040 with DD-water and FRO90006 and MCY14014 with NH₃-water and froze them at -80°C. Once frozen the mixtures were put into a vacuum chamber equipped with plates capable of heating the samples. Samples were heated up to 100°C. Once the experiments finished we acquired reflectance spectra in the NIR range and compared them with the original samples spectra. During the heating process the samples outgassed fine particles at T~ -40°C. Between ~ -20°C and ~ -5°C samples experienced violent outgassing episodes. The ejected outgassed powders always show absorption bands at 3.4 and 3.5 μm, most likely related to organic matter, while pristine samples and the powders that remained in the sample holder don't show this feature. For the hydrothermal experiments we mixed MCY14014 and FRO95002 with NH₃-water and DD-water respectively. We put the mixtures in two autoclaves that we heated up to 240°C for over a month. Results for MCY14014 are remarkable, showing NIR spectra with absorption bands at 2.7, 3.05 and 4.1 μm not present in the pristine sample spectra. These bands are typical of C-type asteroids (Takir & Emery, 2012). The results of these experiments are unique insights on the interaction between geological processes and composition on planetary icy-water rich bodies of the Solar System.

Europlanet 2020 RI has received funding from the European Union's Horizon 2020 research and innovation programme under grant agreement No 654208. Samples loaned from MNA (Museo Nazionale dell'Antartide, Italy).

Belton M.J.S. & Melosh J. (2009) - Fluidization and multiphase transport of particulate cometary material as an explanation of the smooth terrains and repetitive outburst on 9P/Tempel 1. *Icarus* 200, 280-291.

Krot A.N., Petaev M.I., Scott E.D.R., Choi B-G., Zolensky M.E. & Keil K. (1998) - Progressive alteration in CV3 chondrites: More evidence for asteroidal alteration. *Meteorit. Planet. Sci.*, 33, 1065-1085.

Neveu M. & Desch S.J. (2015) - Geochemistry, thermal evolution and cryovolcanism on Ceres with a muddy ice mantle. *Geophys. Res. Lett.*, 42(10),197-206.

Takir D. & Emery J. (2012) - Outer main belt asteroids: Identification and distribution of four 3-μm spectral groups, 219, 641-654.

Pyroxenes as a proxy for thermal history and water content of asteroid 4 Vesta

Nazzareni S.*¹, Pauselli C.¹, Skogby H.², Murri M.³, Domeneghetti M.C.³, Alvaro M.³, Stalder R.⁴, Petrelli M.¹, De Sanctis M.C.⁵, Formisano M.⁵ & Federico C.⁵

¹ Dipartimento di Fisica e Geologia, Università di Perugia, Perugia, Italy.

² Department of Geosciences, Natural History Museum, Stockholm, Sweden.

³ Dipartimento di Scienze della Terra e dell'Ambiente, Università di Pavia, Pavia, Italy.

⁴ Institute of Mineralogy and Petrography, University of Innsbruck, Innsbruck, Austria.

⁵ INAF, Roma, Italy.

Corresponding email: sabrina.nazzareni@unipg.it

Keywords: HED, pyroxene, NAMs.

Vesta is the only rock body with a differentiated and layered structure of crust-mantle-core type (McSween et al., 2013). Several studies on HED meteorites have been used to constrain Vesta internal models.

To study the role of fluids in Vesta and how they influenced the proposed petrological models we selected pyroxene samples from the Juvinas, Luotolax, Shalka, Bialystok and Stannern HED meteorites from the collection of the Swedish Museum of Natural History (Stockholm) together with the already well characterised Serra de Magè and Kapoeta HED samples (Domeneghetti et al., 1996, Domeneghetti et al., 2000). FTIR spectroscopy was carried out on the HED pyroxenes to calculate the possible water content dissolved in the magma they crystallized from. However, all HED pyroxenes did not show evidence for OH bands in the IR spectra. This “dry” condition may be primary or secondary. During the H-loss process, the associated point defects which have a lower kinetics diffusion rate are retained in the structure, making the process reversible.

The original H content of pyroxene can thus be recovered by thermal annealing experiments. Following this idea, the HED pyroxenes were thermally annealed under hydrogen atmosphere (at 1 atm) in a horizontal glass-tube furnace or in a hydrothermal apparatus at 0.2 GPa and 700°C to evaluate whether they have suffered H loss. FTIR spectra were recorded after each heating step. The IR spectra show no signs of OH-bands, which means that none of the HED pyroxenes has recovered OH after the annealing experiments.

We thus conclude that the HED pyroxenes did not suffer H loss during their geological history, suggesting that they were dry since their crystallisation. These data support the hypothesis that the melt in equilibrium with the studied pyroxenes had a very low water content. These new data will be used to improve the petrological and geophysical model of the internal structure of Vesta.

McSween H.Y., Binzel R.P., DeSanctis M.C., Ammannito E., Prettyman T.H., Beck A.W., Reddy V., Le Corre L., Gaffey M.J., McCord T.B., Raymond C.A. & Russell C.T. (2013) Dawn; the Vesta-HED connection; and the geologic context for eucrites, diogenites, and howardites. *Meteorit. Planet. Sci.*, 48, 2090-2104.

Domeneghetti M.C., Tazzoli V., Boffa Ballaran T. & Molin G.M. (1996) -Orthopyroxene from the Serra de Magé meteorite: a structure refinement procedure for a Pbc phase coexisting with a C2/c exsolved phase. *Am. Mineral.*, 81, 842-846.

Domeneghetti M.C., Molin G.M., Triscari M. & Zema M. (2000) -Orthopyroxene as a geospeedometer: thermal history of Kapoeta, Old Homestead 001 and Hughes 004 howardites. *Meteorit. Planet. Sci.*, 35, 347-354.

Diamonds in ureilites: how did they form?

Nestola F.¹, Barbaro A.*², Morana M.², Christ O.³, Brenker F.E.³, Domeneghetti M.C.², Dalconi M.C.¹,
Alvaro M.², Goodrich C.⁴, Fioretti A.M.⁵, Leoni M.⁶ & Shaddad M.H.⁷

¹ Department of Geological Science, University of Padova, IT.

² Department of Earth and Environmental Sciences, University of Pavia, IT.

³ Geoscience Institute, Goethe-University Frankfurt, Frankfurt, DE.

⁴ Lunar and Planetary Institute, USRA, Houston, TX, USA.

⁵ CNR Institute of Geosciences and Earth Resources (IGG), Padova, IT.

⁶ Department of Civil, Environmental and Mechanical Engineering, University of Trento, IT.

⁷ Department of Physics and Astronomy, University of Khartoum, SU.

Corresponding email: anna.barbaro01@universitadipavia.it

Keywords: ureilites, diamonds, shock event.

Ureilite meteorites often contain significant amounts of interstitial carbon-rich material, which is present as diamond, graphite and its different polytypes, and hydrocarbons.

In this study we investigated diamonds in three ureilitic fragments (AhS 209b, AhS 72 and NWA 7983) by scanning electron microscopy, X-ray diffraction and transmission electron microscopy with the aim to shed light on their origin.

Almahata Sitta (AhS) fragments show a mixture of nano-diamond (with stacking disorder of diamond) and nano-graphite, while in NWA 7983 the simultaneous presence of micro- and nano-diamonds associated with nano-graphite was detected.

Laboratory experiments (Davydov et al., 2004, 2006, 2011, 2014, 2015) demonstrated that graphite, nano-diamonds and micro-diamonds can be produced together from carbon precursors (i.e hydrocarbon-fluorocarbon mixtures) in even less than a few seconds at high pressure and high temperature conditions like those simulating natural impact shock events. These are consistent with the diamond/graphite textures observed, particularly the micro-diamond + nano-diamond assemblage in NWA 7983. Furthermore, this assemblage cannot be a product of high static pressures, which should produce micro-diamonds alone (no nano-diamonds).

The results obtained in our study suggest that the origin of ureilitic diamonds is consistent with a shock event through the conversion of precursor carbon materials and not with a formation under high static pressure conditions in a large planetary body (Nabiei et al., 2018).

The impact event hypothesis is also supported by presence of diamond stacking disorder, which could be formed during an asteroidal impacts event (Németh et al., 2014).

AB, MM, MCD and MA have been funded by the IMPACt project (R164WEJAHH) to M. Alvaro; MCD has been funded by the PNRA 2016 to L. Folco. CG is funded by the NASA EW program.

Davydov V.A. (2004) - Conversion of polycyclic aromatic hydrocarbons to graphite and diamond at high pressures. *Carbon*, 42, 261–269.

Davydov V.A. (2006) - Nanosized carbon forms in the processes of pressure-temperature-induced transformations of hydrocarbons. *Carbon*, 44, 2015–2020.

Davydov V.A. (2011) - Synergistic Effect of Fluorine and Hydrogen on Processes of Graphite and Diamond Formation from Fluorographite-Naphthalene Mixtures at High Pressures. *Phys. Chem.*, 115, 21000–21008.

Davydov V.A. (2014) - Production of Nano and Microdiamonds with Si – V and N – V Luminescent Centers at High Pressures in Systems Based. *JETP Lett.*, 99, 585–589.

Davydov V.A. (2015) - On the nature of simultaneous formation of nano- and micron-size diamond fractions under pressure – temperature-induced transformations of binary mixtures of hydrocarbon and fluorocarbon compounds. *Carbon*, 90, 231–233.

Nabiei F. (2018) - A large planetary body inferred from diamond inclusions in a ureilite meteorite. *Nat. Commun.*, 9, 6–11.

Németh P. (2014) - Lonsdaleite is faulted and twinned cubic diamond and does not exist as a discrete material. *Nat. Commun.*, 1–5.

A new spectroscopic database for silicate glasses: implications for planetary science

Pisello A.^{*1-2}, De Angelis S.², Ferrari M.², Vetere F.P.¹⁻³, Pauselli C.¹, Kueppers U.⁴,
De Sanctis M.C.² & Perugini D.¹

¹ Department of Physics and Geology, University of Perugia, Italy.

² Istituto di Astrofisica e Planetologia Spaziali, Istituto Nazionale di Astrofisica, Rome, Italy.

³ Institute of Mineralogy, Leibniz Universität Hannover.

⁴ Earth and Environmental Sciences, LMU, Munich, Germany.

Corresponding email: alessandro.pisello@studenti.unipg.it

Keywords: spectroscopy, glasses, planets.

In order to interpret spectral data acquired remotely and/or in situ from other planets, an exhaustive database taking into account well-characterized spectra is fundamental. Since spectroscopic techniques were discovered, cutting-edge spectral investigation of wide ranges of minerals has been performed, while glasses and amorphous materials still need deep investigation. Silicate glasses are indeed one of the main constituents of volcanic rocks and a deep knowledge of their spectral response is fundamental in order to be able to characterize volcanic terrains that we can observe on other planets (e.g. Mars or Mercury). For this reason, we propose this study concerning the acquisition of reflectance and Raman spectroscopy on different series of silicate glasses. These glasses were synthesized in order to present wide compositional range relative to different magmatic series: from mafic to felsic, and from subalkaline to peralkaline. Spectral characterization was performed at the Institute for Space Astrophysics and Planetology (IAPS-INAF, Rome), where visible-NIR spectra (spectral range 0.35-2.5 μm) have been acquired in reflectance together with FTIR spectra (spectral range 3-13 μm). Moreover, at the Department for Earth and Environmental Sciences (LMU, Munich): Raman spectra were acquired in order to integrate the spectral characterization.

Results show that in the mid-IR range, spectra shifts towards lower wavelengths. This shift well relates with the silica content, the SCFM factor and/or the degree of polymerization state via the NBO/T: the more evolved is the composition; the more polymerized the structure, the shorter the wavelength at which spectral features are observable. For what concerns near-IR reflectance, it is observed how the spectra are heavily influenced by iron content, iron speciation (Fe III/ Fe tot) and by occurrence of magnetite nanolites. Raman spectroscopy gives us the possibility to parametrize chemical evolution of samples by observing Q speciation (which determines the development of tetrahedral units within structure) and can therefore be correlated with mid-IR spectra. All together, these spectra constitute a unique and novel database for the characterization of volcanic rocks.

Since these spectroscopic techniques will be integrated in different missions regarding exploration of planetary surfaces (e.g. ExoMars, BepiColombo), these results represent an important step forward for the completeness of spectral reference needed for planetary exploration.

HYPPOS, Next generation of a stereo camera

Re C.*¹, Cremonese G.¹, Naletto G.² & Tordi M.³

¹ Osservatorio Astronomico di Padova, INAF.

² Dipartimento di Fisica ed Astronomia, Università di Padova.

³ Eie Space Technologies.

Corresponding email: cristina.re@inaf.it

Keywords: planetary, stereo camera, DTM.

HYPPOS (Hyperspectral Stereo Observing System) is a novel concept of hyperspectral-stereo camera that combines the 3D information attainable by a couple of stereo images, with the fine spectral sampling of a spectrograph. The HYPPOS concept has obtained an Italian patent in 2016 and Planetary remote sensing represents an interesting future application field for the idea in development. The concept at the basis merges two different approaches for studying the surface of a planet: the morphology of any feature analysed by the geologist through the 3D images, and the composition of the same feature, through the hyperspectral data.

Thanks to the integration of these characteristics in a single instrument, with HYPPOS there is no problem of correlating different instrument characteristics, as optical design, resolutions and calibration. In this context, new research themes can be developed concerning the potentialities of the combined use of stereo and multispectral data, with particular interest on the 3D reconstruction but also for feature recognitions and geological classifications. As also described in (Haala et al., 1998), the combination of geometric and radiometric information should improve tasks like DTM generation. Colour images definitely contain more information than grey-scale images. Hence, in the framework of DTM generation the stereo image processing should benefit from the additional use of colour information. Furthermore, according to some pioneering works (Bleyer & Chambon, 2010; Galar, 2013), the DTMs, profiting from additional spectral inputs, may have higher fidelity and resolution. The application of stereo imaging can significantly enhance the ability of the science team to investigate terrain and geology through 3D vision. DTMs and the corresponding texture maps enhance the quantitative analysis of the geomorphology and geology of target areas. The integration of 3D information can therefore supplement the spectral map provided by the imaging system potentially aiding the study of the morphological properties of the target surface. In the case of HYPPOS, the strength is in the possibility to provide a new kind of data, a “4D vision” of the surface, associating the spectral information to every DTM pixel. The high integration of the stereo channels with the spectrograph implies simultaneous acquisition of images with the possibility to generate the DTM accessing directly to the spectra. Generally, the inter-instrument fusion is based on the data-coregistration (i.e., to bring the datasets from different sensors into the same unique coordinate frame) and cross-calibration. This is accomplished with proper geometric and radiometric calibration of each sensor individually and with respect to the platform geometric context. In the case of HYPPOS, the stereo and spectroscopic acquisition are completely integrated and simultaneous, using the same detector and optical path, so a number of data reduction problems are solved.

A unique CO-like micrometeorite hosting an exotic Al-Cu-Fe-bearing assemblage – close affinities with the Khatyrka meteorite

Suttle M.D.*¹, Twegar K.², Nava J.³, Spiess R.³, Spratt J.⁴, Campanale F.¹⁻⁵ & Folco L.¹

¹ Dipartimento di Scienze della Terra, Università di Pisa, Pisa, Italy.

² Department of Chemistry, Istanbul Technological University, Istanbul, Turkey.

³ Dipartimento di Geoscienze, Università di Padova, Padova, Italy.

⁴ Department of Earth Science, The Natural History Museum, London, UK.

⁵ Center for Nanotechnology Innovation@NEST, Istituto Italiano di Tecnologia (IIT), Pisa, Italy.

Corresponding email: martindavid.suttle@dst.unipi.it

Keywords: meteorites, asteroids, quasicrystals.

Micrometeorites are grains of cosmic dust <2mm in diameter which originate from a large and diverse population of solar system small bodies (i.e. asteroids and comets; Genge et al., 2008). The study of micrometeorites provides a wide range of extraterrestrial material; much of which is directly related to existing meteorite groups (Taylor et al., 2012; Suttle et al., 2018) but which also contains new and exotic materials that would otherwise remain unsampled and unstudied.

Here we report the discovery of a unique micrometeorite, containing an exotic Al-Cu-Fe alloy composed of two intermixed phases: khatyrkite (CuAl₂) and stolperite (CuAl) and both containing minor Fe (<1.4wt%). These phases are dendritic and rapidly co-crystallized at the binary system's peritectic (~550°C). The host micrometeorite is an otherwise typical S-type micro-porphyrific cosmic spherule containing relict olivine (Fo76-90, Cr₂O₃: 0.01-0.56wt%, MnO: 0.03-0.32wt% and CaO: 0.09-0.22wt%) and a cumulate layered texture. These properties suggest the micrometeorite is derived from a carbonaceous chondrite (best matched to a CO chondrite) and entered the atmosphere a high speed (~16kms⁻¹), implying an origin from a highly eccentric orbit.

This particle represents the second independent discovery of naturally occurring intermetallic Al-Cu-Fe alloys and is thus similar to the previously reported Khatyrka meteorite - a CV chondrite containing near-identical alloys and the only known example of natural quasicrystals (a form of matter with ordered but non-periodic crystalline structures and forbidden crystal symmetries, Bindi et al., 2009). However, we did not observe quasicrystalline phases in this micrometeorite, likely due to the low amounts of Fe (<2wt%) in the anomalous alloy phase, insufficient to stabilize quasicrystals (which require Fe>10wt%).

The absence of appreciable Cu or Al within the relict olivine crystals demonstrates that these grains grew from a typical chondritic igneous melt and predate the Al-Cu-Fe alloy. Our discovery confirms the existence of Al-Cu-Fe intermetallic alloys on chondritic parent bodies. These unusual phases require a currently unexplained formation process potentially recording the input of exotic interstellar material to the inner solar system via impact delivery.

MIUR: PNRA16_00029 "Meteoriti Antartiche", PRIN15_2015W4JZ7 "Cosmic Dust".

Bindi L., Steinhardt P.J., Yao N. & Lu P.J. (2009) - Natural quasicrystals. *Science*, 324, 1306-1309. <https://doi.org/10.1126/science.1170827>.

Genge, M.J., et al., 2008. The classification of micrometeorites. *MAPS*, <https://doi.org/10.1111/j.1945-5100.2008.tb00668.x>.

Suttle M.D., Folco L., Genge M.J., Russell S.S., Najorka J. & van Ginneken M. (2019) - Intense aqueous alteration on C-type asteroids: Perspectives from giant fine-grained micrometeorites. *Geochimica et cosmochimica acta*, 245, 352-373. <https://doi.org/10.1016/j.gca.2018.11.019>.

Taylor S., Matrajt G. & Guan Y. (2012) - Fine-grained precursors dominate the micrometeorite flux. *Meteoritics & Planetary Science*, 47(4), 550-564.

Genesis and age of clay deposits in Margaritifer Region on Mars using terrestrial soil analogues

Tangari A.C.*¹, Marinangeli L.¹, Scarciglia F.², Pompilio L.¹ & Piluso E.²

¹ DiSPUTer, Università G. d'Annunzio di Chieti-Pescara.

² Dipartimento di Biologia, Ecologia e Scienze della Terra, Università della Calabria.

Corresponding email: a.tangari@unich.it

Keywords: Mars, clay minerals, soil.

We investigate the clay deposits in Margaritifer region on Mars representing the most interesting areas where the weathering processes, due to the strong evidence of past hydrological activity, are prominent. We define the processes formation of the clay deposits and the age of soil in Margaritifer Region using the comparison with Etna and Cerviero soil analogues and reproducing the weathering processes experimentally in the laboratory respectively. The main focus is to understand the climatic conditions required to the clay deposits formation on the Martian surface. We use mineralogical qualitative (CRISM analysis) and quantitative (MESMA tool) analysis for Mars and pedological, mineralogical and chemical analysis for the terrestrial analogues. CRISM data show clays deposits composed by allophane as well as vermiculite, chlorite and smectite in Margaritifer region on Mars. We find good analogies between Etna volcano and Cerviero mount choose, as terrestrial soil profiles analogues and the Martian terrains, in terms of bedrock composition and clay mineralogy. We associate the different clay minerals formation to chemical weathering and hydrothermal alteration. The experimental alteration carried out in the laboratory on alkaline Etnean basalts suggests that acidic conditions (pH values ranged between 3.5 and 5.0) and temperature ranged between 150°C and 175°C promote the clay neof ormation. Therefore, we can hypothesize that in Margaritifer regions, the acidic conditions in a warm humid climate similar to the Mediterranean area on the Earth, may have been responsible for the clay formations, accelerating the time of formation. The amount of clays closes to 50-60% estimated from MESMA analysis in the Margaritifer region is comparable to clay contents of red Mediterranean soils comprised between about 0.5 and 1 Ma, developed during warm and humid climatic conditions of Pleistocene interglacials (Scarciglia et al., 2015) and the red soils in the tropical environments ranged in age from about 40 ka to 200 ka (e.g. Delarmelinda et al., 2017). The iron oxides also obtained from MESMA data (ca. 11 to 16%) are in accordance with the redness rating RR estimated from the NASA rover on Mars that exhibits similar values of Mediterranean and tropical soils. Margaritifer regions on Mars show clear evidence of past water-shaped landforms as suggested by the clay mineralogy, which could have been deposited at centennial to millennial up to million-years timescales.

Delarmelinda E.A., de Souza Júnior V.S., Wadt P.G.S., Deng Y., Campos M.C.C. & Câmara E.R.G. (2017) - Soil-landscape relationship in a chronosequence of the middle Madeira River in southwestern Amazon, Brazil. *Catena* 149, 199-208.

Scarciglia, F., Pelle, T., Pulice, I., & Robustelli, G. (2015) - A comparison of Quaternary soil chronosequences from the Ionian and Tyrrhenian coasts of Calabria, southern Italy: rates of soil development and geomorphic dynamics. *Quat. Int.* 376, 146-162.

Cathodoluminescence and photoluminescence: combined SEM-EDS and Raman to approach the analysis of anorthite in Ca-Al inclusions

Tribaudino M.*¹, Mantovani L.¹, Bersani D.² & Salviati G.³

¹ Dipartimento SCVSA, Università di Parma.

² Dipartimento di Matematica, Fisica e Informatica, Università di Parma.

³ IMEM-CNR, Parma.

Corresponding email: mario.tribaudino@unipr.it

Keywords: Ca-Al inclusions, photo and cathodoluminescence, anorthite.

Cathodoluminescence in the study of meteoritics has been widely used: the highly defective nature of minerals in shocked meteorites promotes the presence of several cathode luminescence centers, which can be related to the crystallization and shock history. Less commonly done is an analysis by Raman spectroscopy, as the highly defective nature of the meteorite, shocked at several points of their history, often results in higher fluorescence and very poor Raman signal. However, the fluorescence signal, once collected in a dedicated run, can provide an alternative to the cathodoluminescence. The lower energy of the laser source in Raman permits to avoid, when suitably chosen, the emission of stronger photoluminescence peaks, and enhance the weaker ones.

Here we present a combined investigation by optical and SEM cathodoluminescence, compared with Raman modulated photoluminescence from a 473 and 632 nm laser emissions on a Ca-Al inclusions in the Renazzo CR2 carbonaceous chondrite. Optical cathodoluminescence, among the several phases present in the Ca-Al inclusion (anorthite, fassaite, spinel, gehlenite, sodalite, albite, and interstitial calcite), was found only in blue in anorthite and in red-orange in calcite. SEM cathodoluminescence confirmed the above emissions, which were modulated in two peaks at 450.0 and 599.9 nm, respectively for anorthite and calcite. Raman fluorescence showed a peak at 690 nm, split in three sub-peaks at 678, 689 and 693 respectively, whereas only a further slight emission at 605 nm, was observed from the blue laser emission. SEM cathodoluminescence failed in showing this feature, which could be possibly a distinctive marker in the investigation of CAI anorthite, as suggested by recent investigation in the Kaba CV3 carbonaceous chondrite (Simonia & Gucsik, 2019).

Mappings by photoluminescence and cathode luminescence are well superimposed for anorthite, showing the detailed distribution of the phase. Luminescence emissions can thus provide an indication on the actual distribution of a given phase complementary to SEM-EDS.

Simonia I. & Gucsik A. (2019) -. Photoluminescence and cathodoluminescence of the solid cometary substance. *Open Astronomy*, 28, 1–12.

Spectral variations across Apollo basin on the Moon

Zambon F.*¹, Carli C.¹, van der Bogert C.H.², Hiesinger H.², Altieri F.¹, Giacomini L.¹ & Massironi M.³⁻⁴

¹ INAF-Istituto di Astrofisica e Planetologia Spaziali, Rome, Italy

² Institut für Planetologie, Westfälische Wilhelms Universität, Münster, Germany

³ Dipartimento di Geoscienze, Padova University, Italy

⁴ INAF - Osservatorio Astronomico di Padova, Italy

Corresponding email: francesca.zambon@inaf.it

Keywords: Moon, Apollo basin, PLANMAP.

Studies, e.g. (Ohtake et al., 2014, Moriarty and Pieters, 2018), reveal that the South-Pole Aitken (SPA) basin is unique, particularly because it is the deepest basin on the Moon and might be expected to expose the lunar mantle (Dhingra et al., 2018). The innermost part of SPA is rich in high Ca-pyroxenes, except for some central crater peaks, where low Ca-pyroxenes dominate. No extensive olivine-rich areas are observed, implying a mantle rich in low Ca-pyroxenes instead of olivine (Ohtake et al., 2014, Dhingra et al., 2018, Melosh et al., 2018). Furthermore, thorium anomalies have been discovered in two craters within Aitken basin (Lawrence et al., 2000). Here, we focus on the spectral analysis of one of the most interesting impact crater inside SPA, the Apollo basin. Recently, Ivanov et al., (2018) published a detailed geological map of the area surrounding Apollo basin (35.69°S, 151.48°W; D~524 km), using morphology, stratigraphy, crater size-frequency distribution measurements, and Clementine spectral data to define the unit. Our work explores data from the M³ imaging spectrometer onboard Chandrayaan-1 (Pieters et al., 2009) for this region. A preliminary analysis of Apollo basin emphasizes a spectral variability between the smooth terrains within the floor and rest of the crater. The smooth terrains appear darker and show a clear compositional variation with respect to the surroundings regions, indicating the presence of other mineralogical phases mixed with pyroxenes, and/or a different geological context.

These study is part of the PLANMAP project, and the integration of the spectroscopical information with the results from Ivanov, et al., (2018) will permit to produce highly informative geological maps of the Moon (<https://www.planmap.eu/>).

This work is funded by the European Union's Horizon 2020 research grant agreement No 776276-PLANMAP.

Ohtake M., Uemoto K., Yokota Y., Morota T., Yamamoto S., Nakamura R., Haruyama J., Iwata T., Matsunaga T. & Ishihara Y. (2014) - Geologic structure generated by large-impact basin formation observed at the South Pole-Aitken basin on the Moon. *Geophysical Research Letters*, 41(8), 2738-2745.

Moriarty D.P. & Pieters C.E. (2018) - The Character of South Pole-Aitken Basin: Patterns of Surface and Subsurface Composition. *Journal of Geophysical Research: Planets*, 123(3), 729-747.

Dhingra D. (2018) - The New Moon: Major Advances in Lunar Science Enabled by Compositional Remote Sensing from Recent Missions. *Geosciences*, 8(12), 498.

Melosh H.J., Kendall J., Horgan B., Johnson B.C., Bowling T., Lucey P.G. & Taylor G.J. (2017) - South Pole-Aitken basin ejecta reveal the Moon's upper mantle. *Geology*, 45(12), 1063-1066.

Lawrence D.J., Feldman W.C., Barraclough B.L., Binder A.B., Elphic R.C., Maurice S., Miller M.C. & Prettyman, T. H. (2000) - Thorium abundances on the lunar surface. *Journal of Geophysical Research*, Volume 105, Issue E8, p. 20307-20332.

Ivanov M.A. (2018) - Geologic History of the Northern Portion of the South Pole-Aitken Basin on the Moon. *Journal of Geophysical Research: Planets*, Volume 123, Issue 10, pp. 2585-2612.

Pieters M.C., Boardman J., Buratti B., Clark R., Combe J.-P., Green R., Head J., Hicks M., Isaacson P., Klima R., Kramer G. & Lundeen S. (2009) - The Moon Mineralogy Mapper (M³) on Chandrayaan-1. *Current Science*. 96(4):500-505.

<https://www.planmap.eu/>

S17.

Unveiling the Antarctica: geological, geophysical and sedimentological approaches to the evolution of Antarctica

CONVENERS AND CHAIRPERSONS

Valerio Olivetti (Università di Padova)

Fabrizio Balsamo (Università di Parma)

Franco Talarico (Univeresità di Siena)

Fabio Florindo (INGV)

Sergio Rocchi (Università di Pisa)

Topography, structural and thermochronological analysis in the Admiralty Block, northern Victoria Land, Antarctica: decoding the Cenozoic evolution of the NE termination of the Transantarctic Mountains

Balestrieri M.L.*¹, Olivetti V.², Rossetti F.³, Gautheron C.⁴ & Zattin M.²

¹ Istituto di Geoscienze e Georisorse, Consiglio Nazionale delle Ricerche, Sede Secondaria Firenze, Italia.

² Dipartimento di Geoscienze, Università di Padova, Padova, Italia.

³ Dipartimento di Scienze, Università degli Studi Roma 3, Roma, Italia.

⁴ GEOPS, Univ. Paris Sud, CNRS Université Paris-Saclay, Orsay, France.

Corresponding email: balestrieri@igg.cnr.it

Keywords: thermochronology, topography, Admiralty Block, uplift/denudation.

The Admiralty Block (AB) constitutes the extreme NE termination of the Transantarctic Mountains (TAMs). The geology of the AB consists of the low-grade volcanic and metasedimentary units of the Neoproterozoic Bowers and Robertson Bay assembly, intruded by the Devonian Admiralty Intrusive suite. The AB shows some peculiar characteristics: (i) larger extent of the uplifted area, (ii) Alpine-style morphological features, and (iii) lack of Permo-Triassic to Jurassic Gondwanian terrestrial sequence at the top of the basement rocks. The AB is also characterized by distributed Cenozoic magmatism along the rift shoulder, defined by an impressive belt of N-S aligned Miocene-Quaternary shield (alkaline) volcanoes. A regional sampling of the Admiralty Intrusives and Robertson Bay Terrane for a thermochronology study (apatite fission-track and (U-Th-Sm)/He) together with a structural and topography analysis were conducted to constrain the Cenozoic spatio-temporal evolution of the uplift/denudation in the region.

The regional pattern of the fission-track ages shows a general tendency to the occurrence of older ages (60-70 Ma) accompanied by shorter mean track-lengths (MTLs) in the interior while the coastal area is characterized by fission-track ages clustering at 35-30 Ma with long MTLs. Differently from other regions of Victoria Land, the younger ages are not confined to the coast but they are found as far as 50-70 km inland. Single grain (U-Th-Sm)/He ages cluster at 50-30 Ma with younger ages found in the coastal domain. Topography analysis reveals that the AB is a region of high local relief, and an area located close to the coast, 180 kms long and 70 kms large, has the highest local relief (>2500m). This area coincides with the area showing the youngest fission-track ages.

Thermal modeling suggests: (i) a rapid cooling between 35 and 20 Ma for the samples collected along the rift shoulder, and (ii) a complex history for the internal domain where a slow cooling or a long persistence within the PAZ predates a moderately rapid cooling. It is noteworthy, that result (i) points to a major exhumation/erosional phase concomitant with the major Cenozoic climate fluctuations during the general descent into icehouse conditions.

The long wave-length of the uplifted area, up to 200 km from the coast, the greater amount of erosion and surface uplift suggest that the uplift of the AB cannot be explained simply by flexural uplift along the TAMs. Moreover, the shape of the area with highest local relief matches the shape of a recently detected (Graw et al., 2016) low velocity zone beneath the northern TAMs, confirming that the high topography of the AB is likely sustained by a mantle thermal anomaly.

Graw J.H., Adams A.N., Hansen S.E., Wiens D.A., Hackworth L. & Park Y. (2016) - Upper mantle shear wave velocity structure beneath northern Victoria Land, Antarctica: Volcanism and uplift in the northern Transantarctic Mountains. *Earth Planet. Sci. Lett.*, 449, 48-60.

High resolution seismo-stratigraphic evidence from the Edisto Inlet fjord, western Ross Sea (Antarctica)

Battaglia F.^{*1-2}, Baradello L.², De Santis L.², Gordini E.², Sauli C.², Kovacevic V.², Morelli D.³, Langone L.⁴, Colleoni F.², Colizza E.³, Rebesco M.² & Accetella D.²

¹ Department of Science and Management of Climate Change, Ca Foscari University of Venice, Italy.

² OGS, National Institute of Oceanography and Applied Geophysics, Trieste, Italy.

³ Department of Mathematics and Earth Sciences University of Trieste, Italy.

⁴ ISMAR CNR, Bologna, Italy.

Corresponding email: fbattaglia@inogs.it

Keywords: Seismo-stratigraphy, sediment drift, Antarctica.

Edisto Inlet, located along the northern Victoria Land coast, is a small fjord about 18 km long and 4 km wide, carved by glacial processes and separated by a sill from the larger Moubray Bay. The bathymetry shows a reversed slope and ranges from 670 m in the innermost sector of the bay to 100 m near the entrance of the bay. The Edisto Inlet is seldom accessible due the presence of persistent sea ice but in 2017 during the PNRA (Programma Nazionale delle Ricerche in Antartide) OGS Explora expedition, exceptional sea-ice free conditions allowed for the first time the acquisition of a wealth of data (including sub-bottom chirp profiles, multibeam swath bathymetry, Acoustic Doppler Current Profiler measurements as well as two gravity cores) inside the fjord. The geophysical dataset combined with previous echo-sounding data collected in the outer sector of the fjord reveal the presence of sediment drifts that are formed under the influence of persistent bottom currents. The sediment drifts are characterized by a very high sedimentation rate and are potential excellent paleoclimatic archives. Paleoclimate records are crucial for understanding current changes taking place in the Antarctica; However, paleoclimate and oceanographic reconstructions, especially from the Antarctic fjords, as well as the circulation and processes impacting their exchange with the shelf and wider ocean, are scarce. The first results of the integrated analysis of the geophysical data and the stratigraphic information from the sediment cores show that during the last glaciation the deposition was influenced by the glaciers that carved the bay. After the last glacial maximum, the glaciers have retreated and never advanced, while during the post-glacial period sedimentation was dominated by bottom currents that allowed the formation of sediment drift, rather than by meltwater fluxes. A laminated and expanded sequence of diatom mud has filled the central part of the Edisto Inlet bay from about 9000 years BP. The cores analysis is still in progress, but a first hypothesis to explain the high accumulation of these muds is that the seasonal sea ice regime that characterizes the fjord has caused a low ventilation on the seafloor which may have allowed the conservation of diatom ooze.

Geology of the Convoy Range and Franklin Island quadrangle, Victoria Land - Antarctica

Capponi G.*¹, Montomoli C.², Casale S.³, Simonetti M.², Musumeci G.³ & Salvatore M.C.³

¹ DISTAV, University of Genoa, Italy.

² Dipartimento di Scienze della Terra, University of Torino, Italy.

³ Dipartimento di Scienze della Terra, University of Pisa, Italy.

Corresponding email: capponi@dipteris.unige.it

Keywords: geological mapping, Convoy Range, Victoria Land, Antarctica.

In the 2017/18 and 2018/19 austral summers (33rd and 34th ItaliAntartide expeditions), a three person team performed geological mapping in Victoria Land (Antarctica), in the area between 76° and 76°30' south. This activity aims to complete 1/250000 geological mapping for Victoria Land, filling the gap between the GIGAMAP maps (Pertusati et al., 2016) to the north and the geological maps by GNS - New Zealand to the south (Pocknall et al., 1994; Cox et al., 2012). The field work was heli-supported, starting from both the Italian Base Mario Zucchelli (2017/18) and from a remote camp at Starr Nunatak (2018/19). Geological observations, collated on the Convoy Range and Franklin Island quadrangles of the USGS 1/250000 topographic base maps, are displayed on this poster. Field activity included geological and glacial-geological field mapping, structural observations and rock sampling. Dolerite sills of the Ferrar Group are prevalent in this area, with limited outcrops of the extrusive correlative, i.e. the Mawson Formation. Sandstones of the Beacon Supergroup are limited to small outcrops and to 100 m-long rafts enclosed in the dolerite. Granites and granodiorites of the Granite Harbour Intrusive Complex constitute the crystalline basement underlying the Gondwana Sequence, only cropping out in the sector close to the Ross Sea coast. Minor enclaves of Wilson Terrane schist are hosted in the Granite Harbour granitoid. Structural data of bedding, fault and fracture attitudes were measured at outcrops. More than 250 rock samples were collected for subsequent laboratory analyses, including samples of glacial deposits to perform surface exposure dating by cosmogenic isotope analysis. Subsequent office-based activity has included: digitization of the new cartographic data, elaboration of structural data, microstructural analyses, mineralo-petrographic analyses of rocks and glacial deposits.

Cox S. C., Turnbull I.M., Isaac M.J., Townsend D.B. & Smith Lyttle B. (2012) - Geology of southern Victoria Land. Institute of Geological & Nuclear Sciences 1:250 000 Geological Map, 22.

Pertusati P.C., Ricci C.A. & Tessensohn F. (2016) - German - Italian Geologic Antarctic Map Programme: Introductory Notes to the Map Case. Terra Antarctica Reports, 15, 1 - 15.

Pocknall D.T., Chinn T.J., Skyes R. & Skinner D.N.B. (1994) - Geology of the Convoy Range, southern Victoria Land, Antarctica. GNS Geological Map, 11.

Deformational structures in Paleozoic sandstones of the Transantarctic Mountains: glacial vs tectonic origin

Cornamusini G.*¹⁻², Zurli L.¹, Perotti M.¹ & Talarico F.M.¹

¹ Dipartimento di Scienze Fisiche, della Terra e dell'Ambiente, Università di Siena.

² Centro di Geotecnologie, Università di Siena.

Corresponding email: cornamusini@unisi.it

Keywords: glaciotectionism, tillite, Paleozoic.

The Transantarctic Mountains (TAM) show a sedimentary cover, Beacon Supergroup, mainly formed of fluvial sandstone, with minor mudstone, gravel and coal, resting unconformably on the crystalline basement of the Ross Orogen. This sedimentary succession is divided in two groups, Devonian and Permian to Early Jurassic in ages, through a major unconformity and the occurrence of a tillite horizon referable to the Late Paleozoic Ice Age (LPIA). This tillite horizon shows differentiate thickness along the TAM, built by a glacial succession formed of diamictite, mudstone with dropstone, sandstone and rare limestone beds and sometimes by a postglacial succession formed of mudstone, conglomerate and sandstone beds. The diamictite represents the most typical glacial deposit, showing massive and stratified lithofacies.

Some outcrops of this diamictite/tillite horizon show a complex stratigraphic architecture and deformational structures, as at Kennar Valley in the Beacon Heights and particularly evident are at Mount Ritchie (Warren Range). Here we have examined preliminarily the structures of this latter. There, we recognize a deformed diamictite enclosing sandstone disrupted beds showing a chaotic texture, lying on to deformed sandstone beds. The diamictite with associated conglomerate on top is delimited upwards by the horizontal lying Permian sandstone beds of the Victoria Group. The deformational structures affecting the below sandstones beds of the ice substrata, show a complex imbricate stacking pattern with reverse and normal faults, sigmoidal shape thrust sheets and folds, involving a horizon some tens of meters thick. Collapsing and pop-up structures have been also recognized, whereas the above diamictite and disrupted sandstone beds lay horizontally and are also partially enclosed between the thrusts.

This typology of structures have been widely showed in glacial settings, due to the pushing and loading of the advancing glacial front on to unlithified deposits, which result to be deformed as thin-skinned thrust sheets.

Such structures are common affecting unlithified deposits as coeval glacial diamictites, but in our opinion they are unlikely affecting rocks, due to the ice dynamic and deformational strength. Furthermore, we think that the wide time-gap between the inferred Devonian age of the substrata sandstones and the Permian age of the tillite, prevents to have unlithified substrata deposit during the glacial event.

Following this reasoning, two explanations are identifiable for the deformational structures: i) they formed during a tectonic phase marking the limit between the two groups, interesting glacial and preglacial deposits; but an early Permian phase has been never identified in the TAM; ii) the below lying and deformed sandstone beds are not ascribable to the Devonian Taylor Group, but could be coeval with the glacial event (Early Permian) to represent an ice retreat pulse during waxing-waning ice masses of the multiphase LPIA.

GeoMAP dataset of the Antarctic Peninsula

Dal Seno N.¹, Lelli L.*¹, Millikin L.², Smith Lyttle B.³, Cox S.C.³, Crispini L.¹ & Burton-Johnson A.⁴

¹ Geology Department, University of Genoa, Italy.

² Colorado College, Colorado Springs, CO, United States.

³ GNS Science, Dunedin, New Zealand.

⁴ British Antarctic Survey, Cambridge, United Kingdom.

Corresponding email: geg.elli@gmail.com

Keywords: Antarctica, GeoMAP, Dataset.

A new geological dataset has been compiled for the Antarctic Peninsula covering the area between 58°S & 74°S using available maps and datasets from BAS (British Antarctic Survey). The dataset was based initially on the Antarctic Digital Dataset (ADD) rock, moraine and lake polygons that were re-located and reshaped (as necessary) using the Landsat Image Mosaic of Antarctica (LIMA). Each polygon was given information on rock types, geological names, age, original mapping sources (author bibliography) and source codes. The GIS database employs international GeoSciML data protocols for feature classification and description of rock and moraine polygons that are attribute-rich and queryable; including links to bibliographic source files for primary literature and maps. All new digital data are linked to the original published work. Many of the early maps left rock outcrops as ‘unclassified’, but recent work (Burton-Johnson & Riley, 2015) provides a regional-scale interpretative framework of major structural units and boundaries. Where polygons were previously mapped “unknown”, the regional interpretation was used to infer geology using a “?” symbol in the unit codes to clearly identify ‘inferred data’ from outcrops that have been visited and/or are better understood. A series of fault lines have been captured, many of which are interpreted and concealed beneath ice, but appear somewhat simplified at 1:250,000 scale. All fault line data contain information on accuracy and exposure, as well as source of information. 1569 structural measurements of bedding, foliation and lineation were also captured, located within areas of rock polygon outcrops they represent. Supraglacial features and glacial till, seasonal water and blue ice, have also been mapped and classified from the LIMA imagery. Data are presently in ArcGIS geodatabases and shapefiles, but can be easily opened in QGIS, or translated into other formats such as google.kml. The work was completed by the first three authors while visiting New Zealand on SCAR-supported student internships. It contributes to the international SCAR GeoMAP initiative to compile a unified geological dataset of Antarctica. Data for the Antarctic Peninsula form one of the larger GeoMAP datasets that will be released at the ISAES XIII conference.

Burton-Johnson A. & Riley T.R. (2015) - Autochthonous v. accreted terrane development of continental margins: a revised in situ tectonic history of the Antarctic Peninsula. *Journal of the Geological Society*, 172, 822-835. <https://doi.org/10.1144/jgs2014-110>.

Continental hydrology and atmospheric circulation during Cenozoic super warm periods

Dallai L.*¹ & Sharp Z.D.²

¹ CNR-IGG Pisa.

² Dept. Earth & Planet. Science, UNM, USA.

Corresponding email: dallai@igg.cnr.it

Keywords: climate, stable isotopes, Antarctica.

During Cenozoic time, diffuse alkaline magmatism related to the rifting in the Ross Sea Embayment intruded the N-E region of the Wilson Terrane, Antarctica, providing the necessary heat source for local hydrothermal systems to develop in the adjacent permeable rocks. Combined stable isotope investigation and A-dating of alkaline intrusives and related hydrothermal systems provide unique evidences to constrain the geological evolution and continental hydrology during the Cenozoic. We use the triple oxygen isotope composition ($^{17}\text{O}/^{16}\text{O}$, $^{18}\text{O}/^{16}\text{O}$) of Cenozoic intrusives and their country rocks to reconstruct the $^{18}\text{O}/^{16}\text{O}$ ratios of ancient meteoric-hydrothermal waters. We combine the obtained $\delta^{18}\text{O}$ values with the δD values measured in hydrosilicate minerals of the same rocks. The D/H ratios of these rocks were buffered by those of meteoric-hydrothermal waters, so that hydrogen isotope composition of meteoric waters feeding hydrothermal systems can be calculated on the basis of the known mineral-water hydrogen fractionation factor. The combined O and H compositions of meteoric waters from distinct Cenozoic ages are used to define the Meteoric Water Line of the geologic time before earth experienced the icehouse to greenhouse transition. More specifically, during the Paleocene-Eocene hyperthermal events, our data indicate atmospheric conditions characterized by highly evaporative processes. Significant amounts of water vapour in Cenozoic atmosphere, in concert with the direct CO_2 forcing, may have provided positive feedbacks to the warming during the Palaeocene–Eocene Thermal Maximum. Atmospheric moisture is a powerful greenhouse gas; thus and a very humid atmosphere may help to explain Paleocene-Eocene high temperatures. Nevertheless, being an internal component of the climate system, moisture can be used to identify possible external forcing mechanisms that produced major temperature changes.

Miocene paleobathymetric reconstruction of the Ross Sea (Antarctica)

De Santis L.*¹, Olivo E.¹, Sorlien C.², Kim S.³, Granot R.⁴, Sauli C.¹, Buseti N.¹, Wardell N.¹, Rui L.¹,
Perez L. F.⁵, Colleoni F.¹, Pochini E.⁶, Wilson D.², Bart O.J.⁷, McKay R.M.⁸,
Kulhanek D.⁹ & IODP Expedition 374 Scientific Party¹⁰

¹ Istituto Nazionale di Oceanografia e di Geofisica Sperimentale.

² University of Santa Barbara, CA, USA2.

³ Korea Polar Research Institute, South Korea.

⁴ University of the Negev, Beer Sheva, Israel.

⁵ British Antarctic Survey, UK.

⁶ Univ. of Trieste, Italy.

⁷ Louisiana State University, LA, USA.

⁸ Antarctic Research Centre, Victoria University, New Zealand.

⁹ Texas AM University, TX, USA.

¹⁰ International Ocean Discovery Program, Texas A&M University, College Station, TX, USA.

Corresponding email: ldesantis@inogs.it

Keywords: ice grounding line, backstripping.

Today the continental shelf of the Ross Sea is overdeepened (average 500 m at the shelf edge), and landward deepening, as the result of erosion by multiple advances of ice streams grounding over the sea bed and deposition of morainal banks at the shelf edge. Conceptual model and data suggest that erosion of the substrate dominate below the ice sheet. The amount and rate of the erosion at the base of ice streams depends on several factors, like the thickness of the ice streams, their flowing velocity, the occurrence of water at the ice stream base, the type of bedrock below the ice stream, the duration of ice flowing, etc. At the grounding line, where the ice streams detach from the substrate and float, the sediment entrained at the base of the ice streams is released and deposited at the sea bed. Multiple glacial erosion of the continental shelf and deposition at the margin, since the onset of glaciations shaped the Ross Sea bed that gradually changed its morphology through time. Reconstructing the sea bed morphology and depth evolution can therefore help inferring ice size and rheology and provides key information to model simulating past ice sheet dynamics.

We present the preliminary results of backstripping modelling applied to depth converted maps of some principal Miocene unconformities obtained from using all the seismic data collected by many nations across the Ross Sea continental margin. The maps are used to reconstruct the Ross Sea paleobathymetry change in the Miocene, that show a gradual deepening and seaward widening of the Ross Sea. The depth maps have been restored after removing sediment load, assuming isostatic compensation, post-rift thermal subsidence and taking into account geological constraints from DSDP leg 28 and IODP Exp 374 sites.

Reconstruction of multiple tectonic events in the Rennick Geodynamic Belt (northern Victoria Land, Antarctica) through inversion of fault slip data

Federico L.*¹, Cianfarra P.², Crispini L.¹, Capponi G.¹, Rossi C.² & Salvini F.²

¹ DISTAV, Università degli Studi di Genova.

² Dipartimento di Scienze, Università degli Studi Roma Tre.

Corresponding email: federico@dipteris.unige.it

Keywords: Rennick Geodynamic Belt, northern Victoria Land, paleostress.

The Rennick Geodynamic Belt (RGB) is a prominent geological feature of East Antarctica. It occurs at the border between the terranes of northern Victoria Land (Wilson, Bowers and Robertson Bay terranes) and the East Antarctic Craton and is characterized by a dense fault network that defines a regionally-sized deformation zone.

The RGB is long known to have been active since Cambrian-Ordovician times up to the upper Cenozoic. This long period of activity produced a great deal of structural complexity, due to superposition and reactivation of faults, and consequently many, sometimes contrasting, tectonic reconstructions. In this contribution we investigate this long-lived tectonic activity by combining inversion of fault-slip data with other field observations (e.g. cross-cutting relationships among faults, fault rock type, coating minerals, syntectonic veins, etc.).

We compute the paleostress tensors from about 400 fault-slip data in 100 measurement stations visited by the Authors during various Italian Antarctic Expeditions in northern Victoria Land (PNRA - Italian National Antarctic Research Program).

Our approach involves the use of different inversion methodologies.

The multiple Monte Carlo convergent method implemented in the Daisy software (free download at <http://host.uniroma3.it/progetti/fralab/Downloads/Programs/>) provides the best orientation of the principal paleostresses with an estimate of the error quantified by the MAD (Mean Angular Deviation) factor, that is the average angular deviation between the measured pitch of the kinematic vector on the fault plane and the predicted one by applying to the fault the computed paleostress. At each step, faults are uniquely associated to the stress tensor that provides the lowest MAD.

The Fsa software (Célérier, 1999) combines a random grid search of the stress tensors following a Monte Carlo approach, with a subsequent check of fulfillment of the frictional constraint (i.e. the fault plane must form with an orientation that satisfies the Mohr-Coulomb yield criterion, i.e. $\tau/\sigma_n = \tan \phi$ with τ = shear stress, σ_n = normal stress and ϕ = angle of internal friction). The software actually allows a direct examination of the reduced Mohr circle of the calculated stress tensors, so that we can select the one with the largest number of faults showing a high τ/σ_n ratio.

The comparison between the results from the two inversion methods gives a more robust portrait of the evolution of the paleostress fields through times and allows to decipher the complex tectonic activity along the RGB in the broader framework of East Antarctica evolution.

In particular, the analyses performed through both methods suggest a superposition of two stress tensors and confirm the prevalent strike-slip kinematics of the RGB faults, characterized by a double reactivation with left-lateral and right-lateral kinematics.

Célérier B. (1999) - Fault Slip and Stress Analysis (Fsa). Available at: <http://www.isteen.univ-montp2.fr/PERSO/celerier/software/fsa.html>.

Crustal architecture of a major pull apart basin in northern Victoria Land, East Antarctica

Ferraccioli F.*¹, Armadillo E.², Crispini L.², Läufer A.³, Ruppel A.³ & Lisker F.⁴

¹ NERC/British Antarctic Survey, Geology and Geophysics, Cambridge, United Kingdom.

² Università di Genova, Dipartimento di Scienze della Terra dell'Ambiente e della Vita, Genova, Italy.

³ Bundesanstalt für Geowissenschaften und Rohstoffe, Polar Geology, Hannover, Germany.

⁴ University of Bremen, Geodynamics of the Polar Regions, Bremen, Germany.

Corresponding email: ffe@bas.ac.uk

Keywords: Northern Victoria Land, intraplate strike-slip fault systems, reactivation processes, pull-apart basin, inherited structural architecture.

Geological and geophysical investigations in Northern Victoria Land (NVL) in East Antarctica indicate that major terrane bounding and intra-terranic fault systems that were active during the early Paleozoic Ross Orogen were in parts reactivated as major Cenozoic intraplate strike-slip fault systems. One of the main structures in NVL that has been inferred to relate to such intraplate reactivation processes is the Rennick Graben (RG), but its age, extent and kinematics have remained both poorly constrained and controversial. In detail, the RG has been previously interpreted either as an extensive left lateral Cretaceous(?) pull-apart basin linked to the early Victoria Land Basin within the proto-West Antarctic Rift System (WARS), or as a much more localised Cenozoic right-lateral basin, seemingly un-connected to the Cenozoic margin of the WARS itself.

Here we present results from a new joint Italian-German and UK geosciences project (REGGAE) that aims to re-investigate the architecture and evolution of the RG by analysing aeromagnetic, aerogravity and land-gravity and bedrock topography images and models, and combine geophysical interpretations with new independent structural and thermochronology constraints.

We show that enhanced aeromagnetic and isostatic residual gravity maps provide new geophysical views of the RG. Our geophysical images reveal the spatial extent of part of a Jurassic Large Igneous Province preferentially preserved within the RG and help define the inherited structural architecture of the underlying Ross-age basement, including for example the more highly magnetic arc basement of the northern part of the Wilson Terrane and a subglacial thrust fault belt located between the western flank of the RG and the eastern margin of Wilkes Subglacial Basin (WSB).

Our geophysical interpretations depict the RG as a right-lateral pull-part basin system that extends from the Oates Coast to the Southern Cross Mountains crustal block, part of the uplifted rift flank of the Ross Sea Rift. The RG appears to be kinematically connected with both the western edge of the WARS and the eastern margin of the WSB. Hence, we conclude that the RG is part of wider and more distributed region of the continental lithosphere of East Antarctica that was affected by evolving Cenozoic transtensional stresses, which ultimately also helped trigger accelerated transform faulting in the oceanic lithosphere between southeastern Australia and Tasmania.

Aerogeophysical imaging unveils the architecture and basement of the Pensacola-Pole subglacial basin in East Antarctica

Ferraccioli F.*¹, Jordan T.A.¹, Forsberg R.², Eagles G.³, Eglinton B.⁴, Kuznir N.⁵, Olesen A.², Matsuoka K.⁶, Casal T.⁷ & Paxman G.⁸

¹ NERC/British Antarctic Survey, Geology and Geophysics, Cambridge, UK.

² DTU National Space Institute, Geodynamics, Lyngby, Denmark.

³ Alfred Wegener Institute, Bremerhaven, Germany.

⁴ University of Saskatchewan, Saskatchewan Isotope Laboratory, Saskatoon, Canada.

⁵ University of Liverpool, Earth, Ocean and Ecological Sciences, UK.

⁶ Norwegian Polar Institute, Tromsø, Norway.

⁷ European Space Agency, ESTEC, Netherlands.

⁸ University of Durham, Geography, UK.

Corresponding email: ffe@bas.ac.uk

Keywords: Aerogeophysics, back-arc, rifts.

Recent continent-wide magnetic and gravity compilations and GOCE satellite gravity gradient data have shed significant new light into the lithospheric architecture and tectonic evolution of interior East Antarctica. However, despite these advancements the South Pole region itself has remained much less well-known, due to the paucity of modern aerogeophysical research in this frontier and the gap in GOCE observations around the South Pole.

Here we present results from the PolarGAP project of ESA that successfully filled the GOCE data void with new reconnaissance aerogeophysical observations, thereby helping unveil both the subglacial topography and the deeper crustal architecture of the South Pole frontier. By combining enhanced aerogravity and aeromagnetic imaging that includes a new compilation with pre-existing datasets, potential field modelling and plate reconstructions, we interpret several major tectonic and magmatic events that affected the region and discuss their broader linkages with plate tectonic evolution, in particular for Jurassic and Cambrian times.

The new bedrock topography map derived from airborne radar images the Pensacola-Pole Basin, demonstrating that it stretches from the Jurassic Weddell Sea Rift System to South Pole, while the new free-air gravity data reveal a system of inferred en-echelon grabens within the basin itself. We interpret these basins as being part of the Jurassic Transantarctic Rift System, and identify several preserved subglacial parts of the Beacon Superbasin within the study region. We further propose that the Jurassic rift basins were superimposed upon a long-lived and originally more distributed strike-slip-dominated plate boundary between East and West Antarctica, which also included several distinct pre-existing microplates/terranes.

High-frequency magnetic anomaly patterns along individual profiles help delineate the remnants of the Jurassic Ferrar Large Igneous province preserved within these subglacial grabens, while longer wavelength magnetic anomalies reflect several distinct uplifted basement blocks. The long-wavelength anomalies reveal the stark contrast between extensive occurrences of early Cambrian rift-related rocks emplaced in an inferred broad back-arc related embayment within the Paleo-Pacific margin of Gondwana and a composite Recovery Block identified further inland. We interpret the latter as a composite Precambrian microplate, which we image as extending from the eastern flank of the Pensacola-Pole Basin to the Shackleton Range, where several distinct Precambrian terranes ranging in age from Archean to Neoproterozoic are relatively well-exposed.

We conclude that the southern edge of this composite microplate, which is tectonically juxtaposed against the so called Queen Maud Terrane, whose existence and degree of allochthoneity is still disputed, exerted significant structural controls on both the back arc region of the early Paleozoic Paleo-Pacific active margin and on parts of the later intracontinental Jurassic rift system, which underlies the Pensacola-Pole Basin.

Subduction-related volatiles involved in the genesis of Cenozoic primary alkaline melts in Northern Victoria Land

Giacomoni P.P.*¹, Coltorti M.¹, Bonadiman C.¹, Ferlito C.², Casetta F.¹, Zanetti A.³ & Ottolini L.³

¹ Department of Physics and Earth Sciences, University of Ferrara, Italy.

² Department of Biological, Geological and Environmental Sciences, University of Catania, Italy.

³ National Research Council, IGG-CNR, Pavia Section, Italy.

Corresponding email: gcmppl@unife.it

Keywords: Melt inclusions, Northern Victoria Land (Antarctica), H₂O content, CO₂ content, primary magmas.

The West Antarctic Rift System (WARS) is an almost unique site where to investigate the complex relationships between the migration of fluid in the mantle wedge after prolonged subduction, the LIP magmatism and the rifting process with related magmatism. It is likely to infer that the last two episodes could be related to the large quantity of volatile introduced into the mantle during the first event. As it is well known, in fact, fluids reduce the solidus temperature allowing a larger melt production.

Major, trace element and volatiles (CO₂, H₂O, F, Cl and S) of olivine-hosted melt inclusions (MI) embedded in Cenozoic basanite and basalt from Northern Victoria Land (NVL) provide us new insights on the composition of primary melts and of the mantle source in the complex framework of the tectonic evolution of this part of Antarctica over the last 500 Ma.

MI comes from Shield Nunatak (Mt. Melbourne), Eldridge Bluff and Handler Ridge and are enclosed in Fo₈₉₋₈₂ olivine. Before being analyzed the inclusion were homogenized at HT (1300°C) and HP (6 kbar). Despite a larger variability, MI are compositionally comparable with the lavas of the West Antarctic Rift System that range from basanite to basalt (41.23-48.64 wt% SiO₂; 7.66-14.15 wt% MgO; 2.78-5.79 wt% Na₂O+K₂O). The MI primary feature is testified by high Mg# and Fo content in host olivine, as well as by observed negative correlations between typical differentiation parameters (SiO₂, MgO and Mg#) and the concentration of highly incompatible element (K₂O; Zr; La), highlighting that chemical heterogeneities are mostly related to melting processes and/or source characteristics.

Primitive mantle normalized trace element diagram show a typical intraplate pattern characterized by positive K, Nb and Ti and negative Pb anomalies.

The H₂O and CO₂ contents range from 0.70 to 2.64 wt% and from 25 to 341 ppm respectively. At a water content of 1.2 wt% few samples show CO₂ values up to 3905 ppm with a H₂O/(H₂O+CO₂) molar ratio down to 0.8, suggesting that many MI underwent CO₂ degassing. Applying this ratio to the MI with the highest water content result in an estimation of a minimum of 8800 ppm of CO₂ in the basanitic melts. F and Cl content varies from 1386 to 10 ppm and from 1336 to 38 ppm respectively. An extensive dataset on volatile and trace element content in MI has been used to constrain the origin of our MI. The comparison are consistent with melt derivation from lithospheric mantle modified by subduction-related fluids.

Thermochronological evolution of Transantarctic Mountains in the Mt Murray area

Guzzo G.*¹, Cattò S.¹, Olivetti V.¹, Zattin M.¹, Balsamo F.², Balestrieri M.L.³ & Rossetti F.⁴

¹ Dipartimento di Geoscienze, Università di Padova ² CNR-IGG, sez Firenze.

² Dipartimento Scienze Chimiche, della Vita e della Sostenibilità Ambientale, Università di Parma

³ CNR, Istituto di Geoscienze e Georisorse, U.O.S. Firenze, Italy.

⁴ Dipartimento di Scienze, Università Roma Tre, Roma, Italy.

Corresponding email: silvia.catto@unipd.it

Keywords: fission track thermochronology, Transantarctic Mountains, Antarctica tectonics.

The Transantarctic Mountains (TAM) are an enigmatic topographic feature considered to be the largest non-compressional mountain range on Earth. The TAM represent the uplifted rift shoulder along the transition between two rheologically different lithosphere structures: a presumably hot, thin, extending continental domain (West Antarctic Rift System) and a cold and thick East Antarctic craton.

Numerous models have been proposed to explain the Cenozoic uplift of the TAM, spanning from different lithospheric flexure model with or without thermal contribution (Stern and Ten Brink, 1989; Wannamaker et al., 2017; Brenn et al., 2017) to lithosphere necking (van der Beek et al., 1994) and collapse of a high elevated plateau (i.e. Bialas et al., 2007).

Each geodynamic model of margin evolution leaves a specific fingerprint in the topography evolution; therefore, the timing and amount of exhumation and the deformation pattern provides diagnostic evidences for different deep seated processes.

Here we present a thermochronological study integrated by structural field data and topographic analysis along an east to west transect of the Prince Albert Mountains, in the northern Victoria Land. Apatite fission track ages span from 50 to 36 Ma with a general correlation with the elevation and with the distance from the coast. The thermochronological ages are consistent with the main phase of exhumation found all over the TAM margin and associated to Eocene-Oligocene rifting (Fitzgerald 2002; Laufer and Lisker, 2013). The regional distribution suggest that Cenozoic exhumation event involved the entire studied area, and points out a differential crustal block uplift.

Bialas R.W., Buck W.R., Studinger M. & Fitzgerald P.G. (2007) - Plateau collapse model for the Transantarctic Mountains– West Antarctic Rift System: insights from numerical experiments. *Geology*, 35(8), 687–690.

Brenn G.R., Hansen S.E. & Park Y. (2017) - Variable thermal loading and flexural uplift along the Transantarctic Mountains, Antarctica. *Geology*, 45(5), 463–466.

Fitzgerald P.G. (2002) - Tectonics and landscape evolution of the Antarctic plate since the breakup of Gondwana, with an emphasis on the West Antarctic Rift System and the Transantarctic Mountains. *R. Soc. N. Z. Bull.*, 35, 453–469.

Lawrence J.F., Wiens D.A., Nyblade A.A., Anandakrishnan S., Shore P.J. & Voigt D. (2006) - Crust and upper mantle structure of the Transantarctic Mountains and surrounding regions from receiver functions, surface waves, and gravity: Implications for uplift models. *Geochemistry, Geophysics, Geosystems*, 7 (10).

Lisker, F., Läufer, A.L., 2013. The Mesozoic Victoria Basin: Vanished link between Antarctica and Australia. *Geology* 41 (10), 1043–1046.

Stern T. & Ten Brink U. (1989) - Flexural uplift of the Transantarctic Mountains. *J. Geophys. Res.*, 94, 10315–10330.

van der Beek P., Cloetingh S. & Andriessen P. (1994) - Mechanisms of extensional basin formation and vertical motions at rift flanks: constraints from tectonic modelling and fission-track thermochronology. *Earth Planet. Sci. Lett.*, 121(3), 417–433.

Wannamaker P., Hill G., Stodt J., Maris V., Ogawa Y., Selway K., Boren G., Bertrand E., Uhlmann D., Ayling B., Green A.M. & Feucht D. (2017) - Uplift of the central Transantarctic mountains. *Nat. Commun.*, 8(1), 1588.

Tectonometamorphic evolution of the Dessent Unit (northern Victoria Land, Antarctica): new data from pseudosection modeling of metasediments

Iaccarino S.*¹, Carosi R.¹, Montomoli C.¹ & Massonne H.-J.²

¹ Dipartimento di Scienze della Terra, Università di Torino, Italy.

² School of Earth Sciences, China University of Geosciences, Wuhan, P.R. China.

Corresponding email: salvatore.iaccarino@unito.it

Keywords: northern Victoria Land, Ross Orogen, high temperature mylonite, pseudosections.

Remnants of the Palaeozoic Ross orogen occur in northern Victoria Land in Antarctica, where three main fault-bounded litho-tectonic units were recognized so far: (i) Wilson Terrane (WT) composed of low- to high-grade metamorphic rocks and Cambro-Ordovician igneous rocks, (ii) Bowers Terrane (BT) dominated by volcanic and sedimentary rocks with a low-grade metamorphic overprint, and (iii) Robertson Bay Terrane with very low-grade turbidites. WT and BT are tectonically juxtaposed by a shear belt, in a transpressional regime, involving also eclogite. The Dessent Unit (DU), mainly composed of amphibolite and metasediment (Capponi et al., 1988), marks this contact in the Mountaineer Range. Very few data on metamorphism are available for the metasediment (Capponi et al., 1988) in contrast to the amphibolite (e.g. Capponi et al., 1988; Palmeri et al., 2012).

In this contribution we present a microstructural and petrological reappraisal of the DU metasediments (collected during Italian Antarctic expeditions). We support that the main regional foliation in the DU is related, at least, to a second deformation phase, since an older foliation is preserved within microlithons and intertectonic porphyroblasts. Evidences of upper amphibolitic to lower granulitic HT mylonitic shearing, later overprinted by a static growth of chlorite (and minor white mica), has been detected for the first time. Pseudosections and mineral compositions indicate that most of the metasediments have equilibrated in the P-T range of 600-650°C and 6.5-8.5 kbar, followed by cooling and decompression, compatible with results from the DU amphibolites (Palmeri et al., 2012). However, some differences exist in the P-T conditions experienced among some samples. Interestingly, relicts of a previous granulitic stage, already recognized in some amphibolite (Scambelluri et al., 2003), have been also identified in one sample. Our results confirm that metasediments shared a common history with the amphibolites, give new constraints on the prograde path and the tectono-metamorphic evolution of the WT-BT suture zone, and support the beginning of shearing still at high T conditions.

Capponi G., Messiga B., Piccardo G.B., Scambelluri M., Traverso G. & Vannucci R. (1988) - Metamorphic assemblages in layered amphibolites and micaschists from the Dessent Formation (Mountaineer range – Antarctica). *Mem. Soc. Geol. It.*, 43, 87-95.

Palmeri R., Sandroni S., Godard G. & Ricci C.A. (2012) - Boninite-derived amphibolites from the Lanterman-Mariner suture (northern Victoria Land, Antarctica): New geochemical and petrological data. *Lithos*, 140-141, 200-223.

Scambelluri M., Messiga B., Vannucci R. & Villa I.M. (2003) - Petrology, geochemistry and geochronology of the Dessent Unit, northern Victoria Land, Antarctica: some constraints on its evolutionary history. *Geol. Jahrb.*, B85, 95–131.

The detrital apatite fission-track signature of post-LGM sediments in the Ross Sea

Li X.*¹, Zattin M.¹ & Olivetti V.¹

¹ Department of Geosciences, University of Padova.

Corresponding email: xia.li@studenti.unipd.it

Keywords: Ross Sea, fission track, Post-LGM.

The Ross Sea is a crucial area to investigate the ice dynamics during the Cenozoic as it records the evolution of both the East Antarctic Ice Sheet (EAIS) and West Antarctic Ice Sheet (WAIS), whose variations are a direct response to climate change. Reconstructions are mainly based on multi-proxy provenance analysis of glacial sediments but so far, a well-established model is not existing (see Licht & Hemming, 2017, for a review).

Our work is based on 32 samples of Quaternary age from 18 piston cores across the Ross Sea that have been processed for apatite fission-track (AFT) analysis. Age data have been modelled with statistical tools (Multidimensional Scaling, MDS) and finally interpreted in terms of thermal evolution by the HeFTy software.

MDS analysis allows to discriminate different groups of samples based on their single grain AFT age distribution. In particular, samples from the central Ross Sea show high similarity and the largest age range, probably due to the confluence of EAIS and WAIS in this area. Peculiar age signatures are present in samples close to the eastern and western coasts, therefore showing a local provenance. Distinctive age markers could be the youngest (230 Ma) AFT age population (related to erosion of East Antarctica regions). They appear in the samples in the western and central Ross Sea, and are absent in the samples in the eastern Ross Sea. Finally, thermal modelling for samples collected in the central and western Ross Sea shows rapid cooling at ca. 30 Ma, therefore matching with the Cenozoic exhumation of the TAM (e.g. Zattin et al., 2014) and a heating phase during the Jurassic. Overall, these data demonstrate once again the complex erosional evolution of the TAM which impacts on the dispersal pattern of the glacial sediments transported across the Ross Sea embayment.

Licht K.J. & Hemming S.R. (2017) - Analysis of Antarctic glacial sediment provenance through geochemical and petrological applications. *Quaternary Science Reviews*, 164, 1-24.

Zattin M., Pace D., Andreucci B., Rossetti F. & Talarico F.M. (2014) - Cenozoic erosion of Transantarctic Mountains: A source-to-sink thermochronological study. *Tectonophysics*, 630, 158-165.

Stratigraphic insights across Permian-Triassic boundary in southern Gondwana: comparison between Victoria Land (Antarctica) and Tasmania (Australia)

Liberato G.P.¹, Cornamusini G.*¹, Zurli L.¹, Conti P.¹, Calver C.², Meffre S.² & Talarico F.M.¹

¹ Dipartimento di Scienze Fisiche, della Terra e dell'Ambiente, Università di Siena.

² University of Tasmania, Hobart.

Corresponding email: cornamusini@unisi.it

Keywords: stratigraphic architecture, Victoria Land, southern Gondwana.

During the Permian-Triassic Transition (PTT), the southern margin of the Gondwana was characterized by backarc, foreland and intracratonic basins, that evolved through different paleotectonic and paleoclimatic phases. The corresponding sedimentary successions record the aforementioned changes. This work, through a multidisciplinary study including logging and facies analysis, aims to face a preliminary stratigraphic comparison between the Victoria Basin (Victoria Land, Antarctica) and the Tasman Basin (Tasmania, Australia), at that time contiguous.

This study focuses with sections of Beacon Supergroup outcropping in Allan Hills for the Victoria Land in Antarctica, where several hundreds of meters of logs, consisting of siliciclastic alluvial/fluvial deposits, have been reconstructed, sampled and interpreted in terms of depositional environments.

From north to south Tasmania, a detailed sedimentological study of approximately 1000 m of Permian-Triassic freshwater siliciclastic sections (Upper Parmeener Supergroup) were measured both in outcrop as well as in core at Mineral Resources Tasmania in Hobart (Australia). Based on sedimentological and stratigraphic features including lithofacies, sand/mud ratio and stacking patterns, the main preliminary results are summarized below:

Permian-Triassic successions are similar in terms of lithologies and of thickness, both siliciclastic with dominant sandstones, but with finer deposits for the Tasman Basin, closed to a greater amount of mudstones, even if the coal seams are much lesser developed than in Victoria Land.

For both the areas the paleoenvironments and fluvial styles across the Permian-Triassic boundary changed. An average sandstone grain-size increase and a fluvial style like sandy-braided are recorded similarly for the two basins in the Early Triassic, whereas it was meandering during Late Permian.

A rise and fall of the base level is clearly evident in Tasmania, in particular also affecting the Lower Parmeener Supergroup (Early Permian), as recorded by these deposits that pass from glacio-marine to shallow marine and freshwater facies at least 2 times during Permian-Triassic. In Antarctica instead, findings of sedimentary structures associated with fluvial tidally influenced zone in Allan Hills (SVL), could be related to these cyclical rise and fall sea level events that interested this portion of the Gondwana.

The stacking pattern frequency of the fluvial systems between Victoria Land and Tasman basins shows a good potential correlation.

From this preliminary study we can understand how useful is the comparison of contiguous backarc foreland/ intracratonic basins along the Southern Gondwana margin. The SVL and Tasman basins show good stratigraphic-sedimentological correspondences, overall in terms of high-resolution facies and stacking pattern analysis, essential discriminant for a better global evolutionary view of the southern Gondwana.

Sandstones provenance study of the Permian-Triassic sequences at Allan Hills (Victoria Land, Antarctica): evidence from petrographic framework

Liberato G.P.¹, Cornamusini G.¹, Zurli L.¹, Woo J.², Corti V.¹, Oh J.-R.² & Talarico F.M.*¹

¹ Università di Siena, Museo Nazionale dell'Antartide, Italy.

² KOPRI, South Korea.

Corresponding email: talarico@unisi.it

Keywords: Antarctica, Permo-triassic evolution, detrital zircon ages.

We present the first results of a multi-proxy study finalized to establish a provenance framework for the Permian-Triassic fluvial sandstones of the Beacon Supergroup of Southern Victoria Land (SVL), along the Transantarctic Mountains (TAM), representing a sector of the southern Gondwana margin. Although several modern data are available for other areas of the TAM, as the Central Transantarctic Mountains (CTAM) and the Northern Victoria Land (NVL), a data-gap exists for the SVL placed between them, particularly regarding the detrital zircon age. The aim of this work is to implement both the data and the knowledge on the composition and provenance of fluvial sediments and understand the evolution basin in relation to the margin of the belt and the cratonic area as well as the interrelations between the sedimentary basins in CTM, SVL and NVL.

The adopted methods include: quantitative analysis of sandstones, heavy mineral (HM) analysis, garnet composition and U/Pb ages of detrital zircon. Sandstone petrology studies reveal shortly as follows: i) Permian sandstones are arkose to subarkose-quartzarenite, with most of the garnets derived from low- and medium-grade metamorphic sources; high phengitic mica composition was found and the HM content prevails in garnet and tourmaline; ii) Lower Triassic sandstones are mainly quartzarenite with subordinate subarkose. Their higher compositional maturity as well as the strongly diminution of garnet and phengitic mica is highlighted. Zircon-Tourmaline-Rutile index is higher than Permian; iii) Middle Triassic sandstones are mostly lithic arkose and feldspathic litharenite with secondary subarkose-sub-litharenite. An increase in garnet, phengitic mica, epidote, rutile and sphene is recorded. Mostly sources of Middle Triassic garnet are higher grade metamorphic rocks than Permian.

Furthermore, here we document about 500 detrital zircons age, mostly unchanged, processed with LA-ICP-MS at Korean Polar Resource Institute (Incheon, Republic of Korea). Through a stratigraphic criterion, detrital zircons were separated by 5 medium-fine-grained sandstones, subdivided as follows: 1 Early-Late? Permian, 2 Early Triassic and 2 Middle Triassic.

During Permian period the broad spectrum of zircons age involves the maximum contribution of all sources available during that time (major peaks 477, 505, 568 Ma and minor to moderate 373, 667, 1085 and 2317 Ma). Craton provenances are for all data >580 while values <580 Ma derive from East margin. The 300-450 Ma range as well as 580-3500 Ma drastically decreases from Permian samples to Early Triassic samples (major peak 496 and moderate peak 991 Ma). Conversely, 450-580 Ma range increases in Early Triassic detrital zircon (major peak 509 Ma). This could be explained by a major paleocurrent change due to paleo-tectonics or more simply from the contribution of fluvial paleo-drainage into the Victoria basin.

From Middle Triassic detrital zircons, the dominant provenance is influenced by Permian-Triassic volcanic activity located in west Antarctica. New data in SVL also indicate significant contributions from Triassic (235 and 238 Ma) rocks; presumably these zircons may represent new support to evidence for extensional backarc volcanism in Gondwana margin. Moreover, 300-450 and 580-700 Ma zircon age ranges show the upturn from middle Triassic samples, very probably also due to the craton and West Antarctica paleo-drainage source contribution in this case.

Ultramafic cumulates from Harrow Peaks, (NVL, Antarctica): the first stages of the Ferrar magmatism

Pelorosso B.*¹, Bonadiman C.¹, Ntaflos T.², Gregoire M.³, Zanetti A.⁴ & Coltorti M.¹

¹ Dipartimento di Fisica e Scienze della Terra, Università di Ferrara, Italy.

² Department of Lithospheric Research, University of Vienna, Austria.

³ GET, Université de Toulouse, CNRS, CNES, IRD, UPS, (Toulouse), France.

⁴ CNR-IGG, Sezione di Pavia, Italy.

Corresponding email: plrbrc@unife.it

Keywords: high-Mg magmatic olivines, orthopyroxenite, Karoo-Ferrar large igneous province.

A group of ultramafic xenoliths hosted in Cenozoic hypabyssal rocks from Harrow Peaks (northern Victoria Land, Antarctica) show textural and geochemical features far been observed in mantle xenoliths of this region and elsewhere in Antarctica (Coltorti et al., 2004; Perinelli et al., 2012; Martin et al., 2015). They consist of spinel bearing lherzolites, harzburgites, with predominant equigranular texture with orthopyroxene modal contents remarkably higher in lherzolites (18 - 26 volume. %) with respect to the harzburgite (13 vol. %), one orthopyroxenite and three composite xenoliths. These latter are formed by olivine-dominant assemblage (olivine > 70 %) crosscut by large monomineralic (clinopyroxene and amphibole) or biminerale (amphibole+clinopyroxene) veins. All this group of rocks contain olivine (Fo_{90.21-82.81}) without any significant compositional correlation with the lithology. They are ascribed to a cumulus phase, and the presence of the orthopyroxenite suggests that the inferred melt/s from which they stemmed, was close to silica saturation. On the basis of major and trace element mineral/melt and mineral/mineral equilibrium modelling, this group of rocks were formed by progressive extraction of olivine from a high magnesium (Mg=72) - high temperature (~1300 °C) melt following a very short fractionation line. Thermo-barometric results indicate the stationing of Harrow Peaks cumulates in the P field of 1.3 ± 0.2 (dunites) – 0.5 ± 0.2 (orthopyroxenite) GPa. These values well constrain the crust/mantle boundary (Moho) of the region. The combined data suggest that Harrow Peaks melts could be related to the initial stage of the Jurassic Ferrar magmatism, which cumulates were subsequently affected by a late stage alkaline metasomatism, sporadically detected in the northern Victoria Land lithosphere and forming the late amphibole /amphibole+clinopyroxene veins.

Perinelli C., Andreozzi G.B., Conte A.M., Oberti R. & Armienti P. (2012) - Redox state of subcontinental lithospheric mantle and relationships with metasomatism: insights from spinel peridotites from northern Victoria Land (Antarctica). *Contrib. Mineral. Petrol.*, 164, 1053 -1067.

Coltorti M., Beccaluva L., Bonadiman C., Faccini B., Ntaflos T. & Siena F. (2004) - Amphibole genesis via metasomatic reaction with clinopyroxene in mantle xenoliths from Victoria Land, Antarctica. *Lithos*, 75, 115-139.

Martin A.P., Price R.C., Cooper A.F. & McCammon C.A. (2015) - Petrogenesis of the Rifted Southern Victoria Land Lithospheric Mantle, Antarctica, Inferred from Petrography, Geochemistry, Thermobarometry and Oxybarometry of Peridotite and Pyroxenite Xenoliths from the Mount Morning Eruptive Centre. *J. Petrol.*, 56, 193–226.

Plutons, dykes and volcanoes as witnesses of lithospheric thinning, faulting and necking in northern Victoria Land, Antarctica

Rocchi S.*¹ & Smellie J.L.²

¹ Dipartimento di Scienze della Terra, Università di Pisa, Italy.

² School of Geography, Geology & the Environment, University of Leicester, UK.

Corresponding email: sergio.rocchi@unipi.it

Keywords: Antarctica, rift, magmatism.

Cenozoic magmatic rocks related to the West Antarctic rift crop out across Antarctica in northern and southern Victoria Land and Marie Byrd Land as well. Northern Victoria Land, located at the north-western tip of the western rift shoulder, is unique in hosting the longest record of the rift igneous activity: plutonic rocks and cogenetic dyke swarms cover the time span from ~50 to ~20 Ma, and volcanic rocks are recorded from 15 Ma to the Present. The origin of the whole igneous suite is debated, nevertheless the combination of geochemical-isotopic data with the regional tectonic history supports at best a model with no role for a mantle plume. The amagmatic Cretaceous extension generated an autometasomatized mantle source that, during the Eocene to Present activity, is producing magma by small degrees of melting induced by the transtensional activity of translithospheric fault systems. The emplacement of Eocene-Oligocene plutons and dyke swarm is focused by the activity of these fault systems. The location of the mid-Miocene to Present volcanoes is governed by the lithospheric necking along the Ross Sea coast for the largest volcanic edifices, while inland, smaller central volcanoes and cinder cones are related to the establishment of magma chambers in thicker crust.

In memory of Pietro Armienti

Rocchi S.*¹, D'Orazio M.¹, Masotta M.¹ & Folco L.¹

¹Dipartimento di Scienze della Terra, Università di Pisa.

Corresponding email: sergio.rocchi@unipi.it

Keywords: Pietro Armienti, Antarctica, obituary.

Pietro Armienti, full professor of Petrology of the University of Pisa and a leading authority on volcanic petrology, died of a heart attack in Pisa on May 16, 2019, after fighting Parkinson's disease for many years. He was 62.

Born in Taranto in 1957, he moved to Pisa in 1975 to study at Scuola Normale, where he graduated in Geology in 1980. Full professor of Petrology since 2001 at the Department of Earth Sciences of the University of Pisa, he also served as a member of the Academic Senate and the Academic administration council.

Pietro's geological research started from the active volcanic systems of the Phlegraean Fields, Etna, Canary Islands to Antarctica. Here, he carried out pioneering work, participating in the very first research campaigns of the Programma Nazionale di Ricerche in Antartide, during which he discovered one of the still unknown active volcanoes on Earth. He devised complex and provocative heterodox models on the distribution of radiogenic elements and isotopes in the Earth's mantle, and developed climate-paleoclimatic models with non-conventional approaches. For him, Antarctica was not only a place of scientific discovery, but also the ideal place in which to read the Divina Commedia.

Pietro's research activity was long focused on quantitative textural analysis of igneous rocks for the thermodynamic interpretation of crystallization kinetics. His scientific attitude was always linked to practical applications, which allowed him to acquire three patents based on Crystal Size Distribution applied to cultural heritage, as well as to design methods for recycling earthquake debris.

This extensive research activity is summarized in more than 120 scientific publications and several funded research projects. To fully appreciate Pietro's eclectic and versatile intelligence, we should note his leaps across disciplinary fences, such as the discovery of the Fibonacci series on the medieval facade of a church in Pisa, and the unveiling of the actual nature of an ancient navigation tool, which others had mistaken for a candelabrum. For these brilliant ideas, the town of Pisa joins the scientific community in acknowledging the Pietro's outstanding work.

These scientific activities pale in the face of how Pietro braved his illness, a great lesson to us all. In everyday life, he used to face serious issues in a frame of fine pleasantness, dissolving them in an unforgettable play of words. We will all have to muse for a long time on the seminal ideas and methods that Pietro Armienti gave us with joy and humor during the too short time we shared with him.

Holocene Antarctic Ice Sheet evolution in the Ross Sea: new evidences from the North-Western Basin

Tolotti R.*¹, Caffau M.², Colizza E.³ & Sauli C.²

¹ DISTAV - Università di Genova.

² Osservatorio Geofisico Sperimentale OGS di Trieste.

³ DISGAM - Università di Trieste.

Corresponding email: raffaella.tolotti@virgilio.it

Keywords: Antarctica, ice-sheet, grounding-line.

The timescale and strength of feedbacks between ice-sheet change and solid Earth deformation is a complicating issue. The cyclic evolution of the Antarctic Ice Sheet reshapes the solid Earth via isostasy and erosion, but the shape and type of the bed exert a fundamental control on ice dynamics and on the position of the grounding line (Whitehouse et al., 2019). During the last OGS/Explora survey within the PNRA Glevors project, two gravity cores, named IT17RS-01 and IT17RS-02, were collected offshore the Borchgrevink coast in the North-Western Ross Sea, at Lat 73.210167S Long 170.323833E, and Lat 73.167833S Long 170.3125E respectively, and at depth range of 350-380 m. The two cores location is on a grounding zone wedge built-up by the inferred Borchgrevink-Mariner valley glaciers draining from the North Victoria Land (NVL), and despite their relative short lengths, they have sampled a sedimentary sequence found to be link to the LGM glaciers retreat. The study area is relevant to better define the grounding line pattern of NVL coastal glaciers and of oscillating southern AIS during and post the LGM recession. In particular Facies 1 (detected in the core from bottom to about 30 cm) suggests a sub-ice/ice marginal diamicton (compound glaciomarine sediments), and is characterized by massive matrix supported diamicton; Facies 2 (from about 30 cm until about 13 cm) testifies a gradual transition from subglacial to sub-ice shelf conditions with retreat of floating ice and the possible presence of iceberg over the site core or in the proximity; Facies 3 (from about 13 cm to the top) represents the open marine/pro-glacial condition, characterized by seasonally open sea ice. The identified planktonic and benthic assemblages testify, in the upper part of core IT17RS-02, the presence of cold paleo currents (HSSW) which were able to provide nutrients enough to support a structured darkness adapted sub ice sheet community. The core IT17RS-01 results lacking the upper part and, due to its channel bottom position, could testify the currents activity that caused sediments removal. These evidences confirm this area as a highly sensitive zone for repeated oscillations/ice grounding events of the glaciers coming from the NVL and highlight the importance, for an environmental analyses, of the planktonic and benthic dataset integration.

Whitehouse P.L., Gomez N., King M.A. & Wiens D.A. (2019). Solid Earth change and the evolution of the Antarctic Ice Sheet. *Nature Communications*, 10(1), 503.

Geochemical, isotopic and geochronological constraints on formation of boninite-type rocks at the Paleopacific margin of Gondwana

Tribuzio R.*¹, Henjes-Kunst F.², Gerdes A.³ & Braga R.⁴

¹ Dipartimento di Scienze della Terra e dell'Ambiente, Università di Pavia.

² Federal Institute for Natural Resources and Geosciences, Hannover (Germany).

³ Goethe University of Frankfurt (Germany).

⁴ Dipartimento di Scienze Biologiche, Geologiche e Ambientali, Università di Bologna.

Corresponding email: tribuzio@crystal.unipv.it

Keywords: northern Victoria Land, U-Pb zircon geochronology, subduction-related magmatism.

We present new geochemical, isotopic and geochronological data for boninite-type rocks exposed in Northern Victoria Land (Antarctica), along the Lanterman-Mariner suture separating the Ross-orogenic inboard Wilson Terrane from the outboard Bowers and Robertson Bay terranes. We considered the boninite-derived mafic-ultramafic intrusion from Niagara Icefalls (Tribuzio et al., 2008), and the boninitic volcanic rocks recrystallized under amphibolite facies conditions from Dessent unit (e.g., Palmeri et al., 2012).

Metaplutonic rocks found as boudins within the Dessent unit metavolcanites were also investigated.

The Niagara Icefalls rocks display major and trace element compositions documenting a cumulate origin, and a wide interval of Nd isotopic compositions, with no correlation between initial ϵ_{Nd} (+5 to -8) and rock-type. Zircon separated from two Niagara Icefalls rocks reveal complex internal structures indicating multiple growth stages. In one of the two samples, zircon domains with igneous microstructures exhibit substantial variations in U-Pb dates (about 540 to 510 Ma) and initial ϵ_{Hf} (-1 to -9). The other sample includes zircons showing an Early Paleozoic age and relatively homogenous initial ϵ_{Hf} (ca. 0).

The Dessent metavolcanites and associated metaplutonic rocks display highly variable major element compositions. The Dessent metavolcanites may be subdivided into two main types. Type 1 metavolcanites show LREE-depleted chondrite-normalized patterns and high initial ϵ_{Nd} (+6 to +7), thereby resembling the fore-arc basalts from the Izu-Bonin-Mariana island arc. Type 2 metavolcanites have: (i) boninitic affinity, (ii) nearly flat to slightly enriched LREE patterns, and (iii) initial ϵ_{Nd} ranging from +2 to +4. The REE and Nd isotopic compositions of Dessent metaplutonic rocks are within the range type 2 metavolcanites, thereby suggesting a comagmatic relationship. Zircons separated from two metaplutonic rocks show U-Pb dates ranging from 520 to 490 Ma and high initial ϵ_{Hf} (ca. +11). Metamorphic overprint of the Dessent unit rocks is dated by a ⁴⁰Ar-³⁹Ar age spectrum for metamorphic amphibole at about 490 Ma.

The mafic-ultramafic Niagara Icefalls intrusion indicates onset of boninitic magmatism in the Early Paleozoic, probably during of rifting and initiation of a subduction system in thinned continental crust at the margin of Gondwana. The Dessent unit likely documents subsequent development of an ocean-island arc system, which was accreted to the active Gondwana margin in the course of the Ross orogeny.

Palmeri R., Sandroni S., Godard G. & Ricci C.A. (2012) - Boninite-derived amphibolites from the Lanterman-Mariner suture (northern Victoria Land, Antarctica): New geochemical and petrological data. *Lithos*, 140-141, 200-223.

Tribuzio R., Tiepolo M. & Fiameni S. (2008) - A mafic-ultramafic cumulate sequence derived from boninite-type melts (Niagara Icefalls, northern Victoria Land, Antarctica). *Contrib. Mineral. Petrol.*, 155, 619-633.

Late Cambrian-Early Ordovician orogenic construction along the paleo-Pacific margin of Gondwana, USARP Mountains, Northern Victoria Land (Antarctica)

Vignaroli G.^{*1}, Rossetti F.², Di Vincenzo G.³, Balsamo F.⁴, Gerdes A.⁵, Theye T.⁶ & Ghezzo C.⁷

¹ Università di Bologna – Dipartimento di Scienze Biologiche, Geologiche e Ambientali – Bologna (Italy).

² Università degli Studi Roma Tre – Dipartimento di Scienze – Roma (Italy).

³ Consiglio Nazionale delle Ricerche – Istituto di Geoscienze e Georisorse – Pisa (Italy).

⁴ Università di Parma – Dipartimento di Scienze Chimiche, della Vita e della Sostenibilità Ambientale – Parma (Italy).

⁵ Goethe Universität – Institute für Geowissenschaften – Frankfurt (Germany).

⁶ Universität Stuttgart, Institut für Mineralogie und Kristallchemie – Stuttgart (Germany).

⁷ Università di Siena – Dipartimento Scienze fisiche, della Terra e dell'ambiente – Siena (Italy).

Corresponding email: gianluca.vignaroli@unibo.it

Keywords: mylonites, orogenic construction, Northern Victoria Land.

The Ross-Delamerian orogeny is a part of a major orogenic cycle developed along the paleo-Pacific margin of the Gondwana supercontinent, which lead to the final continental assembly during Neoproterozoic-Ordovician times. Northern Victoria Land is an integrant part of this orogenic structure, where a long-lasting history of continental accretion and suturing is documented. This work deals with structural fabrics, metamorphic petrology, and geochronology of amphibolite-facies mylonitic shear zones developed across Ross-aged intrusive rocks cropping out in the USARP Mountains (Wilson Terrane), in the region between the Wilson Hills and the Daniels Range. These shear zones correspond to protomylonites and ultramylonites, which are N-S striking and W-dipping in the Wilson Hills, and NW-SE striking and NE-dipping in the Daniels Range. The stretching lineations are mostly dip-parallel and they are provided by Qz+Fsp+Ms±Bt±Sil aggregates, trending from E-W to NE-SW, respectively. Non-coaxial shearing dominates the structural fabrics and kinematic criteria in mylonites point to either top-to-the-ENE (Wilson Hills) or top-to-the-SW (Daniels Range). Mylonitic shearing is also associated with re-crystallisation of U-bearing accessory phases (zircon and monazite), showing oscillatory growth (igneous) domains overgrown by secondary (metamorphic) re-equilibration/alteration textures as documented by CL images. Syn-kinematic monazite growth is also documented. Forward modelling thermo-barometry places the ductile shearing under the amphibolite-facies metamorphic conditions ($T = 570-650$ °C and $P = 0.4-0.6$ GPa), compatible with the occurrence of dynamic re-crystallisation microtextures of quartz and feldspars. Combined U-(Th)-Pb (on syn-kinematic monazite) and $^{40}\text{Ar}-^{39}\text{Ar}$ (on syn-kinematic biotite) data constrain the development of the mylonitic fabric at c. 490-480 Ma. When integrated with the results available from the region, these new findings suggest an along-strike diachronous deformation of the Ross-aged basement and impose a reappraisal of the tectonic scenarios leading to the final continental assembly along the paleo-Pacific margin of East Gondwana.

Stratigraphic comparison between Victoria Land (Antarctica) and Tasmania (Australia) Late-Palaeozoic glaciogenic sequences

Zurli L.*¹, Cornamusini G.¹⁻², Liberato G.P.¹, Talarico F.M.¹⁻³, Woo J.⁴, Conti P.² & Corti V.¹

¹ Department of Physics, Earth and Environmental Sciences, University of Siena, Italy.

² Centre for Geotechnologies, University of Siena, San Giovanni Valdarno (AR), Italy.

³ National Museum of Antarctica, University of Siena, Italy.

⁴ School of Earth and Environmental Sciences, Seoul National University, South Korea.

Corresponding email: luca.zurli@student.unisi.it

Keywords: LPIA, stratigraphy, Antarctica.

During Carboniferous and Permian, the Earth experienced a cold episode known as the Late Palaeozoic Ice Age (LPIA) that left tillite succession across Gondwana. The LPIA view is changing from a single ice sheet covering the entire Gondwana to a series of small and diachronous ice caps widespread through the supercontinent. Stratigraphic studies and facies analysis are key tools for the evaluation of the paleo-environmental depositional setting and, consequently, of the style of glaciation. In this study, 9 detailed stratigraphic logs, from outcrops and drillholes, have been measured: four from Southern Victoria Land (SVL) (Antarctica), three from Northern Victoria Land (NVL) (Antarctica) and two from Tasmania (Australia). For any log, bed-by-bed facies analysis has been done and 19 sedimentary facies have been recognized and grouped in 8 facies associations (FA), indicative of the depositional environment. In SVL, the facies analysis, with the evaluation of the glacio-tectonic structures, indicate that the Metschel Tillite has been deposited in an ice-proximal to sub-glacial subaqueous environment and the deposition recorded at least two phases of ice front advance and related retreat. The glacial interval is delimited at the bottom by an erosive surface delimiting the Devonian Taylor Group and at the top by another erosive surface, above which lay conglomerates grading upward into cross-bedded sandstones of the Weller Coal Measures. In the NVL, the Eisenhower Range diamictites, laying directly the basement, are thin and they present sub-glacial and ice-proximal facies, with a quite different petrographic composition; no glacial features (e.g. clasts with striae) have been recognized and the glacial origin of both these deposits is not certain. Differently, the northern glacial sequences of the Rennick Glacier and Neall Massif are thicker and show a wide facies variety, coherent with a floating ice front in a subaqueous environment; the near glacial sequence in the Lanterman Range shows a glacio-lacustrine origin. Two drillcores in the Tasman Basin have been studied and compared with outcrops of the Wynyard Tillite. Preliminary studies show wide changes in the tillite thickness between the Truro Tillite and the Stockers Tillite; both show an ice-proximal subaqueous depositional environment, with at least two ice front advances. The large-scale view of the LPIA deposits across Victoria Land shows two thick sequences in the SVL and in the northern part of NVL, deposited in a subaqueous environment, separated by thin and scattered deposits related to small ice centres in a basement high in the southern part of NVL.

Provenance study of Late Palaeozoic Ice Age sequences in Victoria Land (Antarctica): petrography and geochronology

Zurli L.*¹, Cornamusini G.^{1,2}, Liberato G.P.¹, Talarico F.M.^{1,3}, Woo J.⁴ & Corti V.¹

¹ Department of Physics, Earth and Environmental Sciences, University of Siena, Italy.

² Centre for Geotechnologies, University of Siena, San Giovanni Valdarno (AR), Italy.

³ National Museum of Antarctica, University of Siena, Italy.

⁴ School of Earth and Environmental Sciences, Seoul National University, Gwanak-gu, Seoul, South Korea.

Corresponding email: luca.zurli@student.unisi.it

Keywords: provenance, LPIA, Antarctica.

The Carboniferous-Permian glacial age, known as the Late-Palaeozoic Ice Age (LPIA), is one of the longest and most extensive cold episodes in the Earth history, which led to the deposition of glaciogenic sequences across the entire Gondwana. In the past, it was believed that during the LPIA a single ice sheet covered the Gondwana, but recent studies demonstrate that small ice caps occupied, diachronically, different portions of Gondwana following the position of the paleo-South Pole; in this scenario, provenance studies can validate the hypothesis of a local source of sediments, rather than the long-distance one. In Antarctica there are discontinuous outcrops of the glaciogenic sequences along the Transantarctic Mountains related to the Stage III of the LPIA; those sequences are known as Metschel Tillite in Southern Victoria Land (SVL) and Lanterman Formation, and its equivalents, in Northern Victoria Land (NVL). Recent studies yielded U/Pb ages from the Central Transantarctic Mountains (CTM) and the Ellsworth Mountains; this work provides new data from Victoria Land, a region of the Transantarctic Mountains where geochronological data from glaciogenic succession are not available. In this study, we present the result of the quantitative petrographic analysis of 42 samples from glacial intervals and pre- and post-glacial formations, the petrographic characterization of the diamictite cobbles to pebbles and the geochronological analysis of 600 zircon detrital grains from four diamictite samples. Samples were collected during XXVIII, XXX and XXXI PNRA expeditions, from the glacial Metschel Tillite in SVL and the Lanterman Formation, and its equivalents, in NVL. Quantitative petrographic data were obtained applying the Gazzi-Dickinson point-counting method; geochronological data were obtained with LA-ICP-MS at the KOPRI laboratory (Incheon – Republic of Korea). U/Pb age populations show wide differences between Southern and Northern Victoria Land samples; while SVL samples are almost similar, with the major population related to the Ross - Pan-African Orogeny (480-600 Ma) and with secondary population related to the Grenville Orogeny (900-1300 Ma), NVL samples show wide differences in the zircon age populations. The petrographic analysis of SVL diamictites show a composition dominated by quartz fragments, both with well-rounded and sub-angular shape, indicating a partial reworking of older deposits; feldspars and/or cordierite are not abundant and strongly weathered. Lithic clasts are made by felsic granitoids, sedimentary and meta-sedimentary rocks and rare volcanic products. NVL diamictites are characterized by the absence of well-rounded quartz grains and the common presence of feldspars, both K-feldspars and plagioclase; lithic clasts are felsic granitoids, meta-sedimentary and metamorphic rocks. The variability in the petrographic composition and in the zircon age populations across Victoria Land indicates the influence of the local basement lithology in the tillite composition and the inference of local paleo-ice flows. Those data are coherent with the forming view of a LPIA characterized by small ice centres across Gondwana, rather than a single ice sheet spreading from Antarctica to Gondwana margins.

Petrographic characterization of gravel size clasts of the IODP_exp374 cores: implication for Miocene ice flows in the Ross Sea region (Antarctica)

Zurli L.¹, Perotti M.¹, Talarico F.M.*¹⁻², Cornamusini G.¹⁻⁶, McKay R.³, De Santis L.⁴, Kulhanek D.K.⁵ & the IODP Expedition 374 Scientists

¹ Department of Physical, Earth and Environmental Sciences, University of Siena, Italy.

² National Museum of Antarctica, University of Siena, Italy.

³ Antarctic Research Centre, Victoria University of Wellington, New Zealand.

⁴ OGS, Sgonico (TS), Italy.

⁵ International Ocean Discovery Program, Texas A&M University, USA.

⁶ Centre of Geotechnologies, University of Siena, San Giovanni Valdarno (AR), Italy.

Corresponding email: talarico@unisi.it

Keywords: Antarctica, Cenozoic evolution, provenance.

The International Ocean Discovery Program (IODP) Expedition 374 drilled five sites from the outer continental shelf to rise in the eastern Ross Sea (Antarctica) to investigate the West Antarctic Ice Sheet evolution during Neogene and Quaternary. The behaviour of Antarctic ice sheets in the past is fundamental for the evaluation of the response of Antarctica to the actual and future climate changes involving the Earth. Detailed petrographic investigation of gravel size clasts is a key tool to identify the source of sediments and consequently the paleo-ice flow shifts during time. In this study, the high resolution clast logging involved the Early-Miocene sequence of the drilling site U1521 in the Pennel Basin and the Late Miocene sequence of the site U1522, located in the Glomar Challenger Basin; more than 26.000 gravel size clasts were macroscopically identified, logged and grouped in seven major lithological groups: igneous rocks, quartz fragments, volcanic rocks, dolerite clasts, sedimentary rocks, meta-sedimentary rocks and metamorphic rocks. Moreover, 220 cobbles and pebbles were sampled for detailed petrographic and minero-geochemical analysis. The number of clasts along the core shows a wide variability, with 0-10 clasts/m in the clast-poor diamictite intervals to 10-47 clasts/m in the clast-rich diamictite, indicating oscillations of the sediment supply at the ice front; furthermore, a reverse proportionality can be observed between clasts number and the presence of mud intraclasts. Four major clasts assemblage changes have been recognized in the westernmost drilling site (U1521). The recognized lithological assemblages, dominated by meta-sedimentary and felsic granitoid rocks, would be consistent with a source in the Transantarctic Mountains basement type; however, a local provenance from basement highs in the Ross Sea can not be excluded. In the easternmost studied site (U1522) the Late-Miocene sequence shows two main lithological assemblage changes, marked by the basalt clasts abundance. The Late Miocene sequence shows a quite different clasts assemblage compared to the Early Miocene assemblage of the site U1521. Further detailed petrographic analyses and the characterization of minero-geochemical composition of mineral phases from granitoid and basalt clasts are needed to better identify the source of clasts.

S18

**Mechanical, chemical and hydraulic interactions in
seismogenic fault zones**

CONVENERS AND CHAIRPERSONS

Silvia Mittempergher (Università di Milano Bicocca)

Michele Fondriest (Università di Padova)

Fabrizio Balsamo (Università di Parma)

Stefano Zanchetta (Università di Milano Bicocca)

Rupture-induced off-fault damage: Laboratory quantification and implications for fault mechanics

Aben F.M.*

Department of Earth Sciences, University College London.

Corresponding email: f.aben@ucl.ac.uk

Keywords: fault mechanism, syn-rupture damage, weakening mechanisms.

The physical properties of damage zone rock surrounding faults strongly affect the mechanics of fault rupture and slip, and influence radiation of seismic waves. During fault rupture, damage zone properties predominantly change by fracturing in response to stress perturbations in the process zone of the rupture. This reduces off-fault elastic moduli, which can be the source of a substantial component of seismic radiation. Further, changes in off-fault properties have an immediate feedback on slip-weakening mechanisms that are active in the wake of the rupture front. It is thus imperative to quantify by how much off-fault properties evolve during rupture and at in situ loading conditions to better understand the feedback that off-fault damage has on slip and seismic radiation. Characterizing off-fault physical properties during dynamic rupture remains difficult because exhumed fault rock contain a complex tectonic record, geophysical measurements do not have the temporal resolution to isolate rupture-related damage from slip-related damage, and data acquisition rates in rock deformation experiments are too low with respect to rupture duration. Here, we perform quasi-static rupture experiments while monitoring syn- and post-rupture damage evolution. We also monitor the post-rupture damage evolution during dynamic rupture experiments. From these data, we assess the syn-rupture damage evolution for a dynamic rupture. The experiments were performed on intact Lanhélin granite in a triaxial loading rig at 100 MPa confining pressure. 3D time-resolved in situ P-wave tomography for quasi-static and dynamic ruptures was obtained from AE aftershocks and ultrasonic surveys, using the FaATSO inversion algorithm. Post-mortem microstructures were analyzed by a semi-automated image analysis code. For quasi-static ruptures, syn-rupture P-wave velocity drops by 25% and elastic moduli by 50% in a localized zone around the fault. We establish that off-fault energy dissipation is 10% of the fracture energy budget G_c , based on the change in elastic moduli around the fault zone. Fracture densities reveal a damage zone width of 20 mm. After dynamic rupture, P-wave velocity dropped by 22% in a localized zone around the fault. The width of the damage zone is 30-40 mm wide, and off-fault energy dissipation by dynamic rupture is twice that of a quasi-static rupture. The data suggests that most off-fault damage is created during rupture and not during slip, and is a function of rupture velocity. This dataset provides a calibration benchmark for dynamic rupture models, and provides input for assessing earthquake source properties. We discuss the effect syn-rupture damage has on slip-weakening mechanisms such as flash heating and thermal pressurization, and on seismic radiation.

Interrelated changes in fluid sources and stress field orientation during the seismic cycle reconstructed for an exhumed analogue of the subduction megathrust shallow portion

Cerchiari A.*¹, Remitti F.¹, Mittempergher S.², Festa A.³, Lugli F.⁴ & Cipriani A.¹⁻⁵

¹ Dipartimento di Scienze Chimiche e Geologiche, Università di Modena e Reggio Emilia.

² Dipartimento di Scienze dell'Ambiente e della Terra, Università di Milano Bicocca.

³ Dipartimento di Scienze della Terra, Università di Torino.

⁴ Dipartimento di Beni Culturali, Università di Bologna.

⁵ Lamont-Doherty Earth Observatory of Columbia University, Palisades NY, USA.

Corresponding email: anna.cerchiari@gmail.com

Keywords: subduction megathrust, fluid source, seismic cycle.

We analysed the tectonic calcite veins of an exhumed thrust fault coming from a field analogue of the shallow portion (Tmax? 100°-150° C) of a subduction megathrust, the Sestola Vidiciatico Tectonic Unit (SVU) in the Northern Apennines of Italy (Vannucchi et al., 2008). Field observations show the cyclical formation of different deformation features with incompatible crosscutting relationships: low-angle thrust faults associated with mixed hybrid-shear- and implosion-breccia-type veins, extensional veins at low-angle to the thrust, and fault-normal extensional veins coupled with thrust-parallel pressure solution cleavage (Mittempergher et al., 2017).

Throughout laser ablation-inductively coupled plasma-mass spectrometry (LA-ICP-MS) analyses, we document differences between REE patterns of extensional and shear veins, suggesting the involvement of different fluid sources during the seismic cycle. In shear veins, a strongly positive Eu²⁺ anomaly suggests an exotic fluid source, while the equilibrium with the fault zone environment of the fluid source of extensional veins, though partly modified by pressure-solution processes, suggests a more local circuit. The coupling of geochemical and structural data thus suggests a cyclical shifting of the principal σ_1 and σ_3 stresses through time, with interrelated changes in permeability, fluid pressure and composition, allowing to define three main seismic cycle phases: (i) a seismic phase, with brittle failure along thrust, crystallization of shear veins from a fluid external to the fault zone and a stress drop, determining the switch to the extensional regime; (ii) a post-seismic phase, with compaction perpendicular to the fault zone and formation of the fault-normal extensional veins from local fluids; (iii) a reloading phase, where the shear stress and the pore pressure are gradually restored, the stress field turns again to compression and fault-parallel extensional veins form, until a new brittle failure occurs.

Beyond Byerlee Friction, Weak Faults and Implications for Slip Behaviour

Collettini C.*¹, Tesei T.², Scuderi M.M.¹, Carpenter B.M.³ & Viti C.⁴

¹ Dipartimento di Scienze della Terra, Sapienza Università di Roma, Italy.

² Department of Earth Sciences, Durham University, Durham, UK.

³ School of Geology and Geophysics, The University of Oklahoma.

⁴ Dipartimento di Scienze Fisiche, della Terra e dell'Ambiente, Università di Siena.

Corresponding email: cristiano.collettini@uniroma1.it

Keywords: Fault, friction, phyllosilicates.

Some faults are considered strong because their strength is consistent with the Coulomb criterion under Byerlee's friction, $0.6 < \mu < 0.85$. In marked contrast, numerous studies have documented significant fault weakening induced by fluid-assisted reaction softening that generally takes place during the long-term evolution of the fault. Reaction softening promotes the replacement of strong minerals with phyllosilicates. Phyllosilicate development within foliated and interconnected fault networks has been documented at different crustal depths, in different tectonic regimes and from a great variety of rock types, nominating fluid-assisted reaction softening as a general weakening mechanism within the seismogenic crust. This weakening originates at the grain-scale and is transmitted to the entire fault zone via the interconnectivity of the phyllosilicate-rich zones resulting in a friction as low as $0.1 < \mu < 0.3$.

Collectively, geological data and results from laboratory experiments provide strong supporting evidence for structural and frictional heterogeneities within crustal faults. In these structures, creep along weak and rate-strengthening fault patches can promote earthquake nucleation within adjacent strong and locked, rate-weakening portions. Some new frontiers on this research topic regard: 1) when and how a seismic rupture nucleating within a strong patch might propagate within a weak velocity strengthening fault portion, and 2) if creep and slow slip can be accurately detected within the earthquake preparatory phase and therefore represent a reliable earthquake precursor.

Fluid-mediated deformation processes along the seismogenic Mt. Morrone fault zone (Central Apennines, Italy)

Coppola M.*¹, Billi A.², Stagno V.¹, Cavallo A.³, Correale A.⁴, Fondriest M.⁵, Nazzari M.⁶, Paonita A.⁴, Romano C.⁷, Viti C.⁸ & Vona A.⁷

¹ Sapienza Università di Roma, Rome, Italy.

² Consiglio Nazionale delle Ricerche, IGAG, Rome, Italy.

³ CERTEMA, Grosseto, Italy.

⁴ Istituto Nazionale di Geofisica e Vulcanologia, Palermo, Italy.

⁵ Università di Padova, Padua, Italy.

⁶ Istituto Nazionale di Geofisica e Vulcanologia, Rome, Italy.

⁷ Università Roma Tre, Rome, Italy.

⁸ Università di Siena, Siena, Italy.

Corresponding email: coppola.martina14@gmail.com

Keywords: faulting, seismic event, fluid-rock interaction.

We present a multidisciplinary study conducted on the principal slip surface of the Mt. Morrone seismogenic normal fault zone (central Apennines, Italy) aimed to investigate the macro- to nano-scale deformation processes related to extensional faulting. The Mt. Morrone fault zone is 25 km long, has a cumulative displacement of about 2 km and its footwall block is estimated to be exhumed from < 2.5 km depth. The studied outcrop consists of a dolostone-hosted NW-SE-striking 25m-long fault surface characterized by reddish branched injections. The footwall includes a fault core (c. 30 cm thick) adjacent to the slip surface and is divided into a proximal and a distal fault core. The proximal fault core (c. 3 cm thick) shows tabular ultracataclasite layers and a fluidized sub-layer with convoluted structures bounded by sharp shear surfaces.

The distal fault core is a cataclasite composed by rounded clasts dispersed in a calcitic matrix, which consists of red and white convoluted bands. Textural and chemical analyses at the micro- and nano-scale supported by optical and field-emission scanning electron microscopy (FE-SEM), cathodoluminescence, electron microprobe (EPMA), and transmission electron microscopy (TEM) show the presence of several features in the proximal fault core like truncated clasts, pulverized dolostone clasts, dolostone micro-clasts rimmed by a Ca-rich rim along fluidized sub-layers, micro-calcite veins within the ultracataclasite layers and along the slip surfaces. In the distal fault core, we observed a strong textural contrast between the red and the white convoluted bands, the former made of a granular texture with nano-calcite spheres and Al-Si-rich minerals occurring as fibrous filaments (nanotubules), whereas the latter are characterized by a monotonous and homogeneous sparry calcite. To provide insights on the possible fluid-rock interaction, we performed Raman spectroscopy on fluid inclusions from calcite veins and trace element analyses of the fine fluidized matrix and clasts by laser ablation (ICP-MS). Raman measurements highlighted the presence of C-H molecules attributable to hydrocarbons of the alkane group, whereas laser ablation measurements revealed an enrichment in REE in the red bands with respect to the white bands. Our preliminary results are interpreted in light of the seismic cycles occurred along the active Mt. Morrone fault. Preliminary results reveal the involvement of circulating fluids with distinct geochemical signature both in the inter- to pre-seismic and in the co-seismic stages.

Structural inheritance, fluid flow and intraplate seismicity along the Samambaia Fault, NE Brazil

Corsi G.*¹, Balsamo F.¹, Bezerra F.H.R.² & Salvioli-Mariani E.¹

¹ University of Parma, Parma, Italy.

² Universidade Federal do Rio Grande do Norte, Natal, Brazil.

Corresponding email: fabrizio.balsamo@unipr.it

Keywords: NE Brazil, Intraplate seismicity, silicified faults.

Understanding the causes of intraplate seismicity is still a challenge and no univocal explanation for intraplate earthquakes exists. Proposed models mainly consider the presence of pre-existing inherited structures, the stress concentration in the lithosphere, and the role of fluids in triggering seismic slip. One of the major difficulties to understand intraplate seismic zones arises from the fact that, due to general low magnitude events, seismic rupture rarely reaches the surface. The present work aims to contribute to the knowledge of intraplate seismicity in the Borborema Province (NE Brazil) by studying the structural framework and cementation pattern in the João Câmara area (Potiguar Basin). In this area, a magnitude 5.1 earthquake occurred on 1986 along the Samambaia Fault, causing buildings collapse and people exodus to neighbouring municipalities. Previous works indicate that the Samambaia Fault consists of three main NE-trending, en-echelon segments with a dextral strike-slip kinematics, and is severely misoriented for reactivation under the present-day stress field. Structural data collected on 36 sites, combined with petrographic and fluid inclusion data on 17 representative samples, indicate that: (i) Precambrian basement rocks have steeply-dipping foliations striking NE-SW, i.e. parallel to the Samambaia Fault; (ii) the epicentral area is characterized by diffuse silicification in the form of 50 m-wide NE-trending veins and silicified breccias; (iii) silicified rocks have up to six generations of cements, some of them occurring in the crystalline basement and others in the sedimentary basin; (iv) the source of fluids responsible for cementation was magmatic with possible metamorphic contamination. By integrating field and laboratory data, we suggest that the Samambaia Fault in the Borborema Province developed by reactivating the pre-existing basement crustal structures in a relatively narrow zone, where the crustal strength was further reduced by transient high fluid pressure. Results obtained in this study suggest that, in intraplate setting, pulses of deep magmatic fluids in foliated basement rocks may promote seismic slip on misoriented faults.

Pseudotachylytes alteration and their loss from the geological record

Fondriest M.*¹, Mecklenburgh J.², Passelegue F.X.³, Artioli G.¹, Nestola F.¹, Spagnuolo E.⁴ & Di Toro G.^{1,4}

¹ Dipartimento di Geoscienze, Università degli Studi di Padova.

² School of Earth and Environmental Sciences, University of Manchester.

³ École polytechnique fédérale de Lausanne.

⁴ Istituto Nazionale di Geofisica e Vulcanologia, Roma.

Corresponding email: michelefondriest@yahoo.it

Keywords: pseudotachylytes, hydrothermal alteration, glass argillification.

Tectonic pseudotachylytes are solidified friction-induced melts produced along faults by seismic slip associated to the propagation of earthquake ruptures. Though pseudotachylytes remain the most convincing marker of seismic ruptures among fault rocks, the report of pseudotachylytes within fault zones is rare if compared with the frequency and distribution of earthquakes in crustal rocks. This observation reinforces the idea that pseudotachylytes are produced only in very dry tectonic settings or at fault asperities sustaining very high shear stresses. However, the ubiquitous production of pseudotachylytes both in dry and wet conditions during laboratory earthquakes indicates frictional melting as a diffuse and efficient fault weakening mechanism. Reconciling such a dispute implies to address a long-lasting question in the earthquake mechanics community: are pseudotachylytes rarely generated or are they only rarely preserved? We addressed this question by performing hydrothermal alteration tests on fresh pseudotachylyte samples. Pseudotachylytes hosted in different lithologies (tonalite, microgabbro, ultramafic gabbro) were produced under vacuum by sliding at seismic slip rates (> 1 m/s) solid rock cylinders using the rotary shear apparatus SHIVA at INGV-Rome. The melt-welded rock samples were then cored along the fault interface to obtain smaller rock cylinders with the experimental pseudotachylyte oriented parallel to the long axis. These samples were finally cooked with water as pore fluid at confining (Pc) and pore pressure (Pp) of 150-200 MPa and temperatures (T) of 300-600°C for 18-35 days using two Nimonic triaxial apparatuses at the Rock Deformation Laboratory of the University of Manchester. The experimental conditions were chosen to be representative of the pressures and temperatures at which natural pseudotachylytes occurred in their host rocks. Detailed microstructural and mineralogical investigations (FE-SEM, EDX, X-ray micro-diffraction, micro-Raman) documented that post alteration pseudotachylytes were very different from the original ones. In particular, altered pseudotachylytes were characterized by a peculiar clastic micro-texture deriving from the intense dissolution of the original glassy to cryptocrystalline matrix. This process determined the formation of a significant amount of porosity and the growth within the matrix of few micrometres in size acicular mineral aggregates with random orientation. In the case of the tonalite-derived pseudotachylyte, the original glassy matrix was K-rich in composition, had no porosity and quartz clasts displayed cusped-lobate boundaries. After hydrothermal alteration, the sample contained only few relics of the original micro-texture embedded within a highly porous matrix depleted in alkali. Preliminary micro-analyses suggest that the acicular aggregates likely were Ca-Mg smectitic clays. This study first demonstrates that the preservation potential of pseudotachylytes is very short (days to months) and is likely to increase only within very dry tectonic settings. The presence of pore fluids instead determines the alteration of the pseudotachylyte matrix and the development of a clastic micro-texture which resembles well the one of other much common fault rocks such as ultracataclasites.

Growth of a sinkhole in a seismic zone of the northern Apennines (Italy)

La Rosa A.^{*1-2}, Pagli C.², Molli G.², Casu F.³, De Luca C.³, Pieroni A.⁴ & D'amato Avanzi G.²

¹ Università di Firenze.

² Università di Pisa.

³ Consiglio Nazionale delle Ricerche - Istituto per il Rilevamento Elettromagnetico dell'Ambiente (IREA-CNR).

⁴ Pro.Geo s.r.l.

Corresponding email: alessandro.larosa@unifi.it

Keywords: Fluid flow, Sinkhole, InSAR.

Sinkholes have been reported along seismically active faults indicating a causal link between sinkhole formation and active tectonics. The processes responsible for their formation may be attributed to fracturing and increased permeability in the fault damage zone, promoting fluid circulation and weathering of soluble rocks at depth. However, the surface deformations and sinkhole evolution are rarely recorded, as these sites are known mainly after a collapse, making the assessment of sinkhole-related hazard challenging. In Italy, a total of 750 sinkholes have been identified and the 40% of them are along active faults. It remains unclear whether seismicity may trigger sinkhole collapses. The sinkhole of Prà di Lama, near the village of Pieve Fosciana (Lucca province, Italy), is a quasi-circular depression filled by a lake. Prà di Lama is located in the seismically active Apennines range of northern Tuscany, at the intersection of two active faults. Here we use a multidisciplinary data set of InSAR, surface mapping and historical records of sinkhole activity to show that the Prà di Lama lake is a long-lived sinkhole that was formed likely in 991 A.D. in an active fault zone and grew through several events of unrest characterized by episodic subsidence, fracturing and lake-level changes, including the two most recent events of unrest in 1996 and 2016. Hot springs are also present at Pieve Fosciana and historical records report bursts of spring water flow and uprising of muddy waters, suggesting that fluids have a deep origin and migrate along the fault planes. Moreover, the InSAR analysis shows that a continuous aseismic subsidence occurred during 2003–2008 on the west edge of the sinkhole. In particular the results highlight a displacement of -4.6 mmyr^{-1} along the vertical direction and 5.4 mmyr^{-1} along the east/west direction, indicating subsidence and contraction centred at the lake. The observed deformation pattern has a quasi-circular shape and partially affects the close urban area of Pieve Fosciana. Earthquakes on the major faults near the sinkhole do not trigger sinkhole activity but low-magnitude earthquakes at 4–12 km depth occurred during sinkhole unrest in 1996 and 2016, indicating that a link between low-magnitude seismicity and sinkhole activity exists. We interpret our observations as evidence of seismic creep at depth causing fracturing and ultimately leading to the formation and growth of the Prà di Lama sinkhole.

Microstructural investigation of a prehnite-epidote bearing detachment horizon in granite (northern Victoria Land, Antarctica): influence of hydrothermal fluids on the fault mechanics

Malatesta C.*¹, Crispini L.¹, Läufer A.², Ildefonse B.³, Federico L.¹ & Scarsi M.¹

¹ University of Genoa, DISTAV, Genoa (Italy).

² Federal Institute for Geosciences and Natural Resources (BGR), Hannover (Germany).

³ CNRS Géosciences Montpellier, Montpellier (France).

Corresponding email: cristina.malatesta@unige.it

Keywords: hydrothermal alteration, prehnite-epidote-deformation, ultracataclasite-pseudotachylyte.

The microstructural and petrologic investigations of exhumed faults and mineralized fault rocks can provide useful information both on the mechanical behavior and the permeability of fault zones, and on their geodynamic history.

This work is focused on the study of a fault zone in paleozoic granite (Granite Harbour Intrusives) of the northern Victoria Land (Antarctica). The fault is part of a ENE-WSW km-scale system of faults with a long lasting history of reactivation from the Paleozoic to the Cenozoic.

The fault zone is characterised by various detachments with epidote and prehnite-bearing fault rocks and pseudotachylytes.

Here we describe the microstructural, mineralogical and petrologic study of a cm-scale detachment horizon and provide new insights into the poorly investigated deformational mechanisms of epidote (ep) and prehnite (prh).

The core of the studied detachment horizon (DC) is characterised by ep and prh-rich ultracataclasites, microveins of calcite or prh+quartz, and pseudotachylyte. The DC is rimmed by an alteration halo where the rock forming minerals of the host-rock (i.e. K-feldspar, plagioclase, biotite and quartz) are partially to completely replaced by albite, chlorite, ep, prh, muscovite and minor sphene, and cut by ep filled microveins.

Optical microscopy, electron microprobe and EBSD investigations revealed that the ultracataclasites consist of clasts of K-feldspar, albite, quartz and calcite replaced either by ep or prh, that cement the matrix of the ultracataclasite. In ep-rich ultracataclasite two generations of ep occur: ep1 records plastic deformation and is rimmed by new undeformed ep2 grains; both have no crystallographic preferred orientation. The prh-rich ultracataclasite includes fragments of ep-rich ultracataclasite and here the matrix is replaced by rare prh1, that records plastic deformation, and by new micron-sized subeuhedral prh2 with no crystallographic preferred orientation.

Relics of mylonitic structures are preserved in mm-wide domains in the ultracataclasites pointing to the existence of a pristine mylonitic shear zone in the granite.

Thin pseudotachylytes occur at the contact between the DC ultracataclasite and the wallrock with sharp limits; they are associated to sub-mm-sized injection veins and wrap sigmoidal clasts of deformed K-feldspar and albite porphyroclasts.

We hypothesize that the studied detachment horizon testifies the occurrence of various slip events, assisted by pulses of metasomatic Ca-CO₂-rich fluids, having varying T (<350°C) and fCO₂ (generally both decreasing). The cataclasis and the grain-size reduction after fault slip were cyclically alternated to the cementation of the ultracataclasite matrix and the filling of microveins by ep, prh and calcite; these processes caused i) the periodic softening and strengthening of the fault core, and ii) the variation of permeability of the fault zone, having strong consequences on fault mechanics and on its aseismic vs seismic behavior.

Fluid-mediated, brittle-ductile cyclicity at seismogenic depth: Fluid record and deformation history of a fault system of the Svecofennian basement in SW Finland

Marchesini B.*¹, Garofalo P.S.¹, Menegon L.², Mattila J.³ & Viola G.¹

¹ Dipartimento di Scienze Biologiche, Geologiche e Ambientali, Università di Bologna, Italy.

² School of Geography, Earth and Environmental Sciences, University of Plymouth, PL48AA Plymouth, UK.

³ Rock Mechanics Consulting Finland.

Corresponding email: barbara.marchesini2@unibo.it

Keywords: brittle-ductile transition, fault reactivation, fluid overpressure.

Crustal deformation and fluid flow at the brittle-ductile transition zone (BDTZ) are closely related and reciprocally dependent during repeating and transient cycles of frictional and viscous deformation. Despite numerous studies documenting in detail seismogenic faults exhumed from the BDTZ, uncertainties remain as to the role of fluids in facilitating broadly coeval brittle and ductile deformation at that structural level. We present the results of a multi-scale and multi-technique study that allowed us to reconstruct the temporal variations in fluid pressure, temperature, and bulk composition of the fluids that mediated deformation and steered strain localization within a strike-slip fault originally active at the BDTZ under overall ductile conditions. The studied fault zone is hosted in the Paleoproterozoic Svecofennian basement of SW Finland. The fault core is characterized by two synkinematic and laterally continuous quartz-chlorite veins formed by two texturally distinct types of quartz – Qtz I and Qtz II, with Qtz I older than Qtz II. Meso- and microstructural analysis combined with fluid compositional data indicate recurrent cycles of mutually overprinting brittle and ductile deformation. Geochemical data from fault-minerals and the fluid inclusion study indicate that the two distinct quartz types precipitated from different fluid batches with a fluid bulk salinity in the 0-11 wt% NaCl_{eq} range. Quartz-chlorite and sphalerite-stannite geothermometry indicates that the temperature of the fluids involved in the deformation evolved through time from > 350 °C during Qtz I precipitation to < 300 °C at the time of Qtz II crystallization. The peak fluid pressure estimates constrain pore pressure oscillations between 80 and 210 MPa during the recorded faulting episodes. Initial, fluid-mediated embrittlement of the crystalline basement at the BDTZ generated a diffuse network of joints and/or hybrid/shear fractures in the damage zone; subsequent strain accommodation led to more localized deformation within the fault core.

Weakening mechanisms and rupture propagation along the Hikurangi margin frontal thrust: preliminary results from high speed friction experiments under controlled fluid pressure

Meneghini F.*¹, Aretusini S.², Spagnuolo E.², Harbord C.² & Di Toro G.³

¹ Dipartimento di Scienze della Terra, Università di Pisa.

² Istituto Nazionale di Geofisica e Vulcanologia INGV, sez. Roma.

³ Dipartimento di Scienze della Terra, Università di Padova.

Corresponding email: francesca.meneghini@unipi.it

Keywords: Hikurangi subduction margin, megathrust earthquakes, high speed experiments.

Subduction thrust faults can fail in a variety of slip styles including steady creep, coseismic slip and everything in between from afterslip, to slow slip events (SSEs), tremor and low-frequency earthquakes. No matter the slip style, there are growing evidences that slip along megathrusts propagate at shallow levels, and/or all the way to the trench.

The shallow megathrust of the Hikurangi subduction margin indeed hosts large repeating SSEs, as well as two, Mw 7.0-7.2 tsunami earthquakes in 1947, that generated 8-10 m high tsunami along the coast of North Island, and had thrust faulting focal mechanisms located near the trench. This margin is therefore a good candidate to unravel the mechanisms of slip propagation along megathrusts.

To this end, we selected samples collected during the International Ocean Drilling Program Expedition 375 across North Hikurangi margin, from a drilled shallow thrust rooting into the plate interface, and located near (possibly within) the rupture area of one tsunami earthquake. On the selected samples from the main fault zone, the hanging wall and the footwall we performed high velocity friction experiments simulating realistic conditions achieved during an earthquake at shallow depth. We imposed 5 MPa effective normal stress, monitored and controlled pore fluid pressure (sub-hydrostatic conditions, $P_p/\sigma_{eff}=0.2$), and applied first a slow slip pulse at 10⁻⁵ m/s and then a fast slip pulse at co-seismic velocity (1 m/s). We used an innovative sample assemblage to control the internal pore fluid pressure and monitor the dynamic evolution of pore fluid pressure inside the simulated fault gouge. Thanks to this experimental set up we infer the relationships between pore pressure and the dynamic decrease of shear strength during earthquake slip.

Texture of tectonised calcite clasts from the San Benedetto-Gioia dei Marsi fault (central Italy)

Merico A.^{1,2}, Giuliani L.*², Iezzi G.^{1,3}, Pace B.², Ferranti L.⁴, Cremona M.⁴, Scafa M.^{1,2}, Nazzari M.³, Colella A.⁴ & Scarlato P.³

¹ Department INGEO, University “G. D’Annunzio”, Chieti, Italy.

² Department DISPUTER, University “G. D’Annunzio”, Chieti, Italy.

³ Istituto Nazionale di Geofisica e Vulcanologia, Rome, Italy.

⁴ Department DISTAR, University Federico II, Naples, Italy.

Corresponding email: gianluca.iezzi@unich.it

Keywords: fault, carbonate, texture.

The San Benedetto-Gioia de Marsi (SBGM) is an active normal fault located along the eastern border of the Fucino basin (central Apennines), and is considered responsible for the large 1915 earthquake (Mw 7.0) that struck central Italy. Moving from the fault plane into the first 100/150 m into the footwall, the shear zone consist of cohesive (principal slip zone and fault core), pulverised and fragmented domain and then fractured carbonate rocks, plus some local and subsidiary fault planes.

Three oriented rock samples were collected from the fault core in the immediate footwall of the SBGM fault, at a mutual distance of few tens of meters going from NW to SE. Mesoscopic and thin sections polished surfaces normal to the fault plane have been analysed with high resolution scanner (HRS), transmission optical microscopy (TOM) and scanning electron microscopy in back-scattered mode (SEM). X-ray powder diffraction (XRPD) data show that only calcite minerals are present in the three samples. Textural features of tectonised calcite crystals have been quantified using image analysis on digitalised photographs at magnifications from 1:1 to 9000:1, unveiling size dimensions of grains from cm down to sub- μm . The distribution of long and short sizes of clasts measured with TOM and SEM in two samples (the north-western and the central ones) at comparable intermediate magnifications is broadly similar. The 2D data have been used to construct grain size distributions, mirroring data obtainable from sieve, sedimentation and/or laser diffraction methods in loose faulted deposits. Both large and sub- μm clasts are more abundant in the NW portion of the SBGM, then both ranges decrease moving towards the SE. The D values provided by best-fit lines through log-log plots of clast sizes vs their number have average values of 1.65 in 2D (equivalent to 2.65 in 3D). These values are on the same order of those measured by previous works in another portion of the fault footwall by sieve methods (Billi, 2007). Importantly, the D values calculated here overlap with those independently obtained by box-counting methods in the same portion of the SBGM fault (Ferraro et al., 2018).

We suggest that the analytical protocols proposed here can appropriately quantify textures of calcite clasts in tectonised and lithified rocks. Similar investigations on surfaces normal to other major faults can shed new lights on the relations between deformation and related textural features.

Roughness, off-fault damage and frictional melt distribution in an exhumed seismogenic fault: quantitative high resolution data from a Digital Outcrop Model study

Mittempergher S.*¹, Bistacchi A.¹, Di Toro G.², Nielsen S.³ & Gukov K.¹

¹ Dipartimento di Scienze dell'Ambiente e della Terra, Università di Milano Bicocca.

² Dipartimento di Geoscienze, Università di Padova.

³ Department of Earth Sciences, Durham University, UK.

Corresponding email: silvia.mittempergher@unimib.it

Keywords: pseudotachylytes, off-fault damage, fault roughness.

The topography of fault surfaces causes significant variations in the near fault stress field, thus controlling fault plane processes such as nucleation, propagation and arrest of earthquake ruptures, off-fault damage and production and redistribution of frictional melts during coseismic slip. All these processes affect the earthquake energy budget and the pattern of the radiated energy. Here, we quantify the 2D relationships between fault surface topography, coseismic off-fault damage and melt distribution on a well-exposed seismogenic fault reproduced in a high-resolution photogrammetric digital outcrop model. The fault surface is about 20 m long along strike and 3 m high, strikes EW and dips of 50° to the South, and is part of a wide fault zone composed of hundreds of fault segments crosscutting the granodiorite of the Avio pluton in the northern Adamello batholith (Italy). The fault experienced dextral transpressive activity, and, since one pseudotachylyte fault vein with average thickness of 3 mm could be identified from field and microstructural observations, it likely hosted only one main seismic rupture. The coseismic offset could not be measured in the field, but, based on a wide dataset of coseismic offsets measured on similar fault strands in the area, it was likely on the order of 1 m. An unknown amount of slip was accumulated at subseismic slip rate before the earthquake propagation, as suggested by the occurrence of a cataclasite layer crosscut by the pseudotachylyte vein. The fault footwall crops out on a recently deglaciated rock cliff and preserves thin patches of hanging wall, where it is possible to measure the thickness of the pseudotachylyte fault vein. The footwall is crosscut by swarms of pseudotachylyte injection veins aligned in direction roughly perpendicular to the slip vector. The digital outcrop model was reconstructed from 2972 photographs by using the VFSM software. The resulting point cloud has sub-millimeter resolution and millimeter accuracy. We extracted several profiles from the point cloud, both parallel and perpendicular to the slip vector, and characterized their topography and roughness by Fourier power spectral analysis. The point cloud was also interpolated to obtain a triangulated mesh, successively textured with selected high-resolution field pictures and used to digitize the relevant structures, i.e., injection vein traces, hanging wall and pseudotachylyte patches. Our preliminary analysis suggests that the fault surface has a self-affine distribution comparable with other fault surface profiles measured in the area. Injection veins are clustered in swarms and located along the releasing sides of asperities with wavelength of around 1m. The thickness of the pseudotachylyte fault vein ranges between less than 1 mm in restraining segments, to more than 1 cm in releasing bands over similar wavelengths. A significant volume of frictional melt, between 1.3 and 1.7 l/m², is drained within injection veins swarms. We therefore propose that the length scale of fault waviness controlling the distribution of macroscopic off-fault damage and the thickness of the coseismic frictional melt layer has a scale comparable with that of the coseismic slip.

Influence of accommodated displacement upon microstructural and petrophysical properties of deformation bands and gouges affecting faulted high-porosity siliciclastic sediments (Rocca di Neto fault zone, Crotona Basin, Italy)

Pizzati M.*¹, Balsamo B.¹ & Storti F.¹

¹ NEXT, Natural and Experimental Tectonics Research Group, Department of Chemistry, Life Sciences, and Environmental Sustainability, University of Parma, Italy.

Corresponding email: mattia.pizzati@studenti.unipr.it

Keywords: subseismic deformation structures, Deformation mechanisms, Petrophysical properties.

Subseismic deformation structures, such as deformation bands and gouges, are known to play an important role in hampering underground fluid migration. Especially in high-porosity siliciclastic rocks and sediments, such deforming elements may act as effective barriers towards fluid flow in fully saturated conditions. Therefore, the study of the petrophysical properties of deformed rocks is crucial to the correct exploitation of petroleum reservoirs, preservation of water reserves and to trace contaminant pathways inside aquifer. Despite the efforts mainly addressed to the comprehensive understanding of the microstructures and deforming mechanism of deformation bands and gouges, there still remain lacks concerning the relationship between petrophysical properties and accommodated displacement.

In order to shed lights upon this open question, we present the results of a study concerning the influence of displacement upon the microstructures and petrophysics characterizing soft-sediment deformation structures developed in a fault zone affecting high-porosity siliciclastic sediments in the Crotona forearc basin. The Rocca di Neto extensional fault zone has a total displacement of 90 m and formed during the tectonic uplift characterizing the basin since Middle Pleistocene. It juxtaposes clayish sediments in the hanging wall to poorly lithified sandstone in the footwall. While the hanging wall side is almost completely covered, the footwall side of the fault zone is well exposed and can be subdivided into 4 distinct structural domains: (1) a ~ 1 m-thick fault core hosting the master fault and subsidiary slip surfaces decorated with gouges; (2) a 2 m-thick mixed zone with pronounced mixing of sediments with different grain size; (3) a 10 m-thick footwall damage zone characterized by a network of conjugate deformation bands, clusters of bands and subsidiary faults; (4) a 50 m-thick low-deformation domain showing a few deformation bands and low-displacement faults. The subseismic deformation elements taken into account have displacement ranging from 0.1 to 20 cm. Microstructural observation combined with image analysis indicate that deforming structures developed by particulate flow during the early stages of faulting, being progressively overprinted by cataclasis after porosity reduction below the 5-6% threshold. The mineralogy of grains controlled the deformation mechanism, with feldspar experiencing severe crushing by intragranular fracturing, while quartz is affected by splitting, abrasion and to lesser extent by intragranular fractures. Permeability of the pristine sandstone ranges from 5.4×10^4 to 1.4×10^5 mD, while deformation bands show a reduction of 1-2 orders of magnitude and gouges reach 3-4 orders of magnitude of permeability drop. With increasing displacement along each deformation features, the grain size becomes finer, sorting diminishes, porosity falls down and as a result the overall permeability is drastically reduced.

Seismicity induced by fluid migration in the Main Ethiopian Rift

Raggiunti M.*¹, Keir D.² & Pagli C.¹

¹ Dipartimento di Scienze della Terra, Università di Pisa.

² Dipartimento di Scienze della Terra, Università di Firenze.

Corresponding email: martina.raggiunti@phd.unipi.it

Keywords: seismicity, fluid-migration, hydrothermal.

Faults can act as preferential degassing pathways for CO₂ and other gasses of deep origin, with the migration of the fluids commonly causing swarms of earthquakes. This process is more evident in areas with intense volcanic and hydrothermal activity. To understand this phenomenon, we studied the spatial, temporal and waveform characteristic of local seismicity data from the northern sector of Main Ethiopian Rift (MER) of East Africa near Fentale and Dofen volcanoes. The seismic database used is from October 2001 to January 2003, and acquired by the Ethiopia Afar Geoscientific Experiment (EAGLE project). The recorded events have been relocated with NLLoc using a new 3D velocity model derived from a wide-angle controlled source experiment. The relocated catalog contains a total of 1543 events with a number of P-wave or S-wave phase recording of ≥ 4 , and magnitude is between 0 and 4. The seismicity is mainly concentrated in two areas: near the border faults of the Ethiopian plateau and within the rift. On the border faults, events mostly occur down to 20 km depth, with an average depth of ~ 12 km. Within the rift, the events mostly happen down to 15 km depth, with an average depth of ~ 9 km. The seismicity is divided into several clusters with direction parallel to the rift direction, and in profile section the clusters are sub-vertical. Analysis of the temporal distribution of earthquakes shows that some of the clusters are strongly clustered in time, and therefore swarm-like. Spatial-temporal distribution of events could be related to fluids migration that could have influenced seismic activity of faults. To understand if the different clusters have been conditioned by fluid migration, a careful analysis of the seismic database has been carried out. For each cluster, we have analyzed the frequency content, release of seismic moment, and b-value of Gutenberg-Richter, to distinguish the nature of these seismic events. The link between earthquakes and fluid migration has also been explored by interpreting the distribution of seismicity using remote sensing mapping of faults, fumaroles and hydrothermal springs. Understanding where and how the fluid migration occurs will aid geothermal exploration efforts in the region, and where linked to seismicity has implications for seismic hazard estimation, very important for this densely and economically active areas.

Understanding the hydro-mechanical interaction in active fault zones by induced seismicity studies

Vadacca L.*¹, Rossi D.¹, Scotti A.¹ & Buttinelli M.²

¹ MOX - Department of Mathematics, Politecnico di Milano, Milan, Italy.

² Istituto Nazionale di Geofisica e Vulcanologia, Department of Seismology and Tectonophysics, Rome, Italy.

Corresponding email: luigi.vadacca@polimi.it

Keywords: fluid-fault interaction, fault reactivation, induced seismicity.

In the last years a large amount of geological, geophysical and seismological data have been produced by induced seismicity studies. These studies have given a great contribute to the understanding of the physical processes triggered by the fluid-structure interaction in active fault zones. Frictional laboratory experiments on fault rock samples have shown that the style of deformation (e.g. stick-slip or aseismic creeping) can change in presence of fluids. In addition, high-precision seismicity locations coupled with the interpretation of high-resolution seismic profiles have allowed to understand the time-spatial evolution of the permeability inside complex fault systems. Here we integrate different data available from the literature to model the stress perturbations induced by wastewater injection in the Val d'Agri oil field by coupled fluid flow and geomechanical numerical simulations. We model the behaviour of main faults involved in the induced seismicity process by frictional contacts in a finite element framework. The permeability into the fault zones are changed in order to understand the role of these structures either as fluid pathways or as efficient compartmentalization barriers for the pore pressure diffusion front associated to wastewater injection. To do this a fault zone model that considers the spatial variation of the hydromechanical properties from the damage zone to the fault core has been implemented in the numerical code. Final aim is to have a more complete picture of the induced seismicity in Val d'Agri oilfield as a consequence of the pore pressure increase as well as its relationship with the deformation style of the fault system and the active stress field.

S19

The interplay between magmatic systems and tectonics: insights from multidisciplinary approaches

CONVENERS AND CHAIRPERSONS

Leonardo Casini (Università di Sassari)

Eugenio Fazio (Università di Catania)

Davide Zanoni (Università di Milano)

Manish A. Mamtani (Università di Kharagpur, India)

Controlled behavior of anatectic melts in the deep crust by regional tectonics and metamorphic conditions

Acquafredda P.¹, Festa V.¹, Fornelli A.*¹, Micheletti F.¹ & Tursi F.¹

¹ Dipartimento di Scienze della Terra e Geoambientali, Università degli Studi di Bari “Aldo Moro”, Bari.

Corresponding email: annamaria.fornelli@uniba.it

Keywords: partial melting in deep crust, sub-spherical and ellipsoidal anatectic granitic pockets.

The lower portion of deep continental crust cropping out in the northern Serre Massif (Calabria, southern Italy) consists of layered metagabbros (Pl+Opx+Amph±Cpx±Bt±Qtz±Grt) with interlayered metric bodies of meta-monzogabbros (Pl+K-feld+Opx+Cpx+Bt±Qtz±Grt) and metabasites (Pl+Opx+Cpx±Bt±Amph±Qtz±Grt), passing in the upper part to felsic granulites and migmatitic metapelites (e.g., Fornelli et al., 2011a).

The magmatic protoliths are Neoproterozoic (about 570 Ma), whereas the granulite-amphibolite facies metamorphism took place from 340 to 280 Ma; the reconstructed P-T-t trajectory shows a late Hercynian thermal peak (at ca. 900°C) under nearly isothermal decompression conditions after the baric peak (at about 11 kb) (Fornelli et al., 2011b).

The meta-monzogabbros show medium grain size and anisotropic texture with different abundances of pyroxenes, garnet, amphibole and biotite, whose flakes are preferentially oriented to give a continuous main foliation. They are characterized by widespread leucocratic pockets (from 2-3 mm to 2-3 cm in size) consisting of single K-feldspar megacrystals or isotropic aggregates of K-feld+Pl+Qtz, the latter showing high temperature deformation effects, such as interlobate grain boundaries. These leucocratic pockets are ellipsoidal in shape, sub-parallel to and draped by the main foliation of the host rock.

The origin of sienogranitic pockets has been connected to first dehydration-partial melting event due to biotite break-down. As the biotite-dehydration melting curve has a positive slope, the physical system changing from solid to solid + silicate melt increases an average its volume. Therefore, the late Hercynian exhumation stage of the deep crust was favored by the new rheological conditions of the melt-bearing weakened crust.

In this scenario, we propose that the change from hydrostatic forces, at higher pressure conditions, to oriented tectonic forces during exhumation, induced the geometric modification of original sub-spherical partially crystallized anatectic melt droplets to ellipsoidal leucocratic pockets. In this context, the different lithologies of the deep crust experiencing incremental partial melting, produced dioritic-trondhjemitic-granitic melts present towards the upper parts of the deep crust as concordant and discordant leucosomes.

Fornelli A., Langone A., Micheletti F. & Piccarreta G. (2011a) - Time and duration of Variscan high-temperature metamorphic processes in the south European Variscides: constraints from U-Pb chronology and trace element chemistry of zircon. *Mineral. Petrol.*, 103(1-4), 101-122.

Fornelli A., Pascazio A. & Piccarreta G. (2011b) - Diachronic and different metamorphic evolution in the fossil Variscan lower crust of Calabria. *Int. J. Earth Sci.*, 101(5), 1191-1210.

Frictional-viscous heating in strong elliptical inclusions during simple shear

Casini L.^{*1}, Maino M.² & Montserrat L.³

¹ Dipartimento di Chimica e Farmacia, Università di Sassari, Italy.

² Dipartimento di Scienze della Terra, dell'Ambiente, Università di Pavia, Italy.

³ Departament de Mineralogia, Petrologia i Geologia Aplicada, Universitat de Barcelona, Martí i Franquès s/n 08028 Barcelona, Spain.

Corresponding email: casini@uniss.it

Keywords: Finite Differences, shear heating, elasto-visco-plastic, partial melting.

This contribution presents the results of numerical modelling of a classical inclusion-in-matrix system. The experiments are formulated in 2D space using an implicit conservative finite difference scheme based on a fully-staggered Eulerian grid and marker-in-cell method that allow to simulate multiphase flow of material with large viscosity contrast (Gerya & Yuen, 2003; Casini & Maino, 2018). The incompressible Stokes, Continuity and heat equations are solved for velocity and pressure. The effective rheology is composite and includes linear elastic response, time- and T-dependent viscosity and plastic deformation. Frictional-viscous shear heating is computed from the inelastic part of stress and strain rate tensors, including both long-term viscous and the effect of instantaneous brittle-plastic deformation through an adaptative implicit timestepping. The experimental setup reproduce a 1 km-thick shear zone composed of a weak layer and multiple inclusions. A free-slip boundary condition is combined to a gradient of horizontal velocity applied to lateral boundaries.

All experiments were conducted for variable shear rates between 1×10^{-12} and 1×10^{-9} m/s until a finite shear $\gamma=5$ was achieved. A persistent feature that come out from many experiments is the development of moderate to strong shear heating (ΔT 10 – 50°C) in the weak matrix around the inclusions. Extreme temperature increments are observed within the largest inclusions in response to localized shear along incipient fault zones.

Casini L. & Maino M. (2018) - 2D-thermo-mechanical modelling of spatial PT variations in heterogeneous shear zones. *Italian Journal of Geosciences*, 137(2), 272-282. <https://doi.org/10.3301/IJG.2018.13>

Gerya T.V. & Yuen D.A. (2003) - Rayleigh–Taylor instabilities from hydration and melting propel ‘cold plumes’ at subduction zones. *Earth and Planetary Science Letters*, 212(1-2), 47-62.

Petrological and geochronological constraints of a shallow intrusion into the Variscan medium-grade metamorphic sequence of the Asinara Island (Sardinia)

Corvo¹ S.*¹, Langone A.², Maino M.¹, Cuccuru S.³, Oggiano G.³ & Seno S.¹

¹ Dipartimento di Scienze della Terra, dell'Ambiente, Università di Pavia, Italy.

² Istituto di Geoscienze e Georisorse, C.N.R., Pavia, Italy.

³ Dipartimento di Scienze della Natura e del Territorio, Università di Sassari, Italy.

Corresponding email: stefania.corvo01@universitadipavia.it

Keywords: Corsica-Sardinia Batholith, Perple-x, U-(Th-)Pb monazite dating.

The Asinara Island, NW Sardinia, is an exceptionally well-preserved segment of medium to high-grade metamorphic Variscan crust. Starting from the pioneering studies (Di Pisa et al., 1993; Del Moro et al., 1996; Carosi et al., 2004) describing the main features of the metamorphic and structural setting, we focus on petrology and geochronology of medium to low-grade metapelites surrounding the largest plutonic body of the island, i.e. the Castellaccio Pluton. The pluton consists of a small sill-shaped granodioritic body emplaced within a late-Variscan shear zone (Cuccuru et al., 2018). In this study, we show preliminary Pressure-Temperature-time (P-T-t) data from both the metapelites and the granodiorites of the Castellaccio Pluton. P-T-t paths are used to characterize the time-dependent thermal evolution of the Variscan upper crust. Close to the contact with granodiorites, the metapelites show HT-LP mineral assemblages (And+Bt+Ms) with local occurrence of fibrolite. Micaschists with cm-sized andalusite porphyroblasts contain also pinitite pseudomorphs after cordierite. A few hundred meter far from the pluton, relicts of the Barrovian HT-MP mineral assemblage (St+Grt) can be still recognised and are partly overprinted by HT-LP mineral assemblages with And+Bt. Integrating petrographic observation, thermo-barometric calculation and thermodynamic modelling (Perple-x) we provide estimations of the metamorphic conditions experienced by the host rocks. U-(Th)Pb ages from zircon and monazite allow to determine the timing of the metamorphic evolution of this crustal segment, as well as to define the emplacement age of the Castellaccio Pluton. Finally, the new data are discussed in the frame of the Variscan evolution of the Corsica-Sardinia massif.

Carosi R., Di Pisa A., Iacopini D., Montomoli C. & Oggiano G. (2004) - The structural evolution of the Asinara Island (NW Sardinia, Italy). *Geodinamica Acta*, 17(5), 309-329.

Cuccuru S., Casini L., Oggiano G. & Simula E.N. (2018) - Structure of the Castellaccio Pluton (Asinara Island, Italy), *Journal of Maps*, 14(2), 293-302.

Del Moro A., Di Pisa A., Oggiano G., Pardini G. (1996) - A syn-collisional variscan granitoid: the Cala d'Oliva Orthogneiss from Asinara island (Sardinia). *Plinius* 16 (1996) 96-98.

Di Pisa A., Oggiano G. & Talarico F. (1993) - Post collisional tectono-metamorphic evolution in the axial zone of the Hercynian belt in Sardinia: the example from the Asinara island. *Orleans, Doc. B.R.G.M.*, 219, 216-217.

Application of *in-situ* gamma-ray spectrometry to mapping intrusive complexes: examples from Sàrrabus igneous massif (SE Sardinia, Italy)

Cuccuru S.*¹, Conte A.M.², Naitza S.³⁻⁴, Oggiano G.¹, Secchi F.¹ & Puccini A.¹

¹ Dipartimento Chimica e Farmacia. Università degli Studi di Sassari, Sassari (Italy).

² IGAG-CNR-Sede Secondaria di Roma. Sapienza, Università degli Studi di Roma. Roma (Italy).

³ Dipartimento di Scienze Chimiche e Geologiche. Università degli Studi di Cagliari, Cagliari (Italy).

⁴ IGAG-CNR-Sede Secondaria di Cagliari. Università degli Studi di Cagliari. Cagliari (Italy).

Corresponding email: scuccuru@uniss.it

Keywords: Late-Variscan magmatism, Anatomy of plutons, Radiological mapping.

The *in-situ* gamma ray spectrometry is a sound and proven technique to map radioelements variations of rocks. Recently this technique has been satisfactorily used in geological surveys of the Variscan basement and late-Variscan plutons belonging to the northern part of the Sardinia batholith, dominated by coalescing intrusions of peraluminous monzogranites, which are hardly distinguishable each other in the field. In addition, at the scale of the entire Sardinia batholith, good contact exposures between intrusive units are often obliterated by the occurrence of colluvium covers and by regolith. This leads to frequent mapping issues, as the geological definition of single intrusive units when common field indicators (e. g. magmatic flow, unconformities and chilled margins), usually used to constrain the anatomy of plutons, are not applicable or conclusive.

The Sàrrabus igneous massif (400 km²) is a multi-pulse, composite intrusive complex recording a complicated history marked by coalescing intrusions dominated by granodiorites, monzogranites and leucogranites. A continuous contribution of mantle pulses is documented by several mafic episodes -predating or coeval to-, granodiorites. Mantle-derived pulses were followed by diffuse diking, which resulted in several generations of mainly NNW mafic dike swarms. Peraluminous character is only recognized for garnet-bearing two mica granites occurring as minor intrusions and NE trending acidic dikes.

In this scenario, some unsolved issues mainly regard the discrimination within different rock-units of similar composition and geological style. The geo-statistical processing of 100 *in-situ* measurements of ⁴⁰K, ²³²Th and ²³⁸U abundances by mean of a gamma-ray spectrometer -equipped with a 1-liter NaI (Tl) scintillator-generated three radionuclides maps, which mirror seven intrusive units improving the previous geological reconstruction. Indeed, the combined geological-petrographical and radiological mapping, allows to better constrain the anatomy and the emplacement sequence of the several intrusions in Sàrrabus massif.

In detail, from older to younger, main intrusive units are:

Burcèi Unit (gabbrotonalites) > Monte Cresia Unit (granodiorites grading to monzogranites) > Cala Regina Unit (granodiorites with mafic septa and monzosyenites) > Monte Maria Unit (peraluminous leucogranites) > Bruncu Nicola Bove Unit (monzogranites grading to leucogranites) > San Priamo Unit (leucogranites) > Monte Sette Fratelli Unit (monzogranites grading to leucogranites).

In this way, an early southward growth model for the Sàrrabus igneous massif can be envisaged for granodioritic intrusions; it seems to be controlled by mixing of different crustal melts and mantle batches, along an E-W crustal shear zone.

Overall, the surveys performed in the Sàrrabus igneous massif has confirmed as the portable gamma-ray spectrometer is a useful tool to improve field surveys when conventional geological discrimination techniques are not conclusive.

A combined petro-structural study assisted by UAV-survey of mafic microgranular enclaves hosted by syn-tectonic tonalites at Rovaglioso outcrop (Calabria-Peloritani Orogen)

Fazio E., Fiannacca P., Lombardo R. *, Tomaselli L., Vilaro F. & Cirrincione R.

Università degli Studi di Catania, Dip. Sc. Biol. Geol. Amb., Catania (Italy).

Corresponding email: rlombardo@unict.it

Keywords: strain analysis, magmatic foliation, 3D virtual outcrop.

The southern Calabria-Peloritani Orogen, in southern Italy, hosts a batholith composed of late Variscan granitoids emplaced at depths ranging from 23 to 6 km (Caggianelli et al., 2000; Fiannacca et al., 2015). The outcrop at Rovaglioso beach (38°21'51.35"N, 15°50'18.85"E) occurring in the southern area of the Palmi shear zone (Fazio et al., 2017) consists of foliated tonalites (Grande et al., 2009) related to the deepest part of batholith; the tonalite is scattered with flattened quartz-dioritic microgranular enclaves, ranging in size from a few cm to several dm. On these enclaves we focused our study. Marine erosion has contributed at this site to offer a multi-perspective view of ellipsoid-shaped enclaves, considered to be good strain markers, by exposing them on different surfaces and then facilitating measurements of the spatial orientation of maximum and minimum axes of 2D ellipses, assisted also by an UAV-aerial survey. The measured enclaves show a mean XY plane of the associated strain ellipsoid averagely WNW-ESE oriented and mostly SW dipping (from 40° to 70°), suggesting an associated maximum stress at 6°/37° (dip direction / dip). The aspect ratio between major and minor axes (R) spans from 3 to 15. As already pointed out by Caggianelli et al. (2000), the deformation event began while the pluton was still hot and at suprasolidus conditions and, to explain such a large range of enclave aspect ratios, we might hypothesize that the injection of the quartz-dioritic melt that formed the enclaves was diachronous. Thus the strain recorded by each enclave would be proportional to the time spent within the crystallizing and cooling tonalites under shear conditions. The outcrop bears also the evidence of subsequent magmatic activity and deformation represented by: a) inter-crossing aplitic and pegmatitic dykes; b) layering produced by fluids permeating through m-spaced fractures and causing mineral alteration, and c) pseudotachylite veins.

- Caggianelli A., Prosser G. & Rottura A. (2000) - Thermal history vs. fabric anisotropy in granitoids emplaced at different crustal levels: an example from Calabria, southern Italy. *Terra Nova*, 12, 109–116.
- Fazio E., Ortolano G. & Cirrincione R. (2017) - Eye-type folds at the Palmi shear zone (Calabria, Italy). *Int. J. Earth Sci.*, 106, 2039-2040.
- Fiannacca P., Cirrincione R., Bonanno F. & Carciotto M.M. (2015) - Source-inherited compositional diversity in granite batholiths: the geochemical message of Late Paleozoic intrusive magmatism in central Calabria (southern Italy). *Lithos*, 236-237, 123–140.
- Grande A., Di Vincenzo G., Prosser G. & Caggianelli A. (2009) - Direct evidence of Middle Oligocene extension in the Calabria–Peloritani terrane from co-seismic faulting: the pseudotachylite-bearing shear zones of Palmi (Southern Calabria, Italy). *Terra Nova*, 21, 293-303.

Interaction between deformation and crustal melt generation at the plastic-brittle transition: a perspective from exhumed pseudotachylyte-bearing mylonites

Fazio E.*¹, Fiannacca P.¹, Lombardo R.¹ & Cirrincione R.¹

¹ Università degli Studi di Catania, Dipartimento di Scienze Biol., Geol. Amb.

Corresponding email: efazio@unict.it

Keywords: pseudotachylytes, mylonites, frictional melting.

The Rovaglioso outcrop of late Variscan foliated tonalites in Calabria (southern Italy), in the southern sector of the Palmi shear zone (Fazio et al., 2017) offers a valid opportunity to study the interactions between host igneous rocks and peculiar crustal melts formed by deformation at very specific conditions, i.e., frictional heating associated with seismic slip. Indeed, the tonalites contain a diffuse network of pseudotachylites, considered to have formed by extensional shearing at c. 33 Ma (Grande et al., 2009). These pseudotachylytes, after diffusively injecting the host tonalites, were involved into subsequent deformational events producing both plastic (mylonites overprinting pseudotachylytes) and brittle typical microstructures (cataclastic shear bands). Association of pseudotachylytes with foliated host rocks may suggest possible cyclic relationships between seismic slip and ductile deformation. Furthermore, the compositional features of these instantaneous crustal melts may help to understand the melting behavior of different rock types at various crustal and tectonic conditions.

Fazio E., Ortolano G. & Cirrincione R. (2017) - Eye-type folds at the Palmi shear zone (Calabria, Italy). *Int. J. Earth Sci. (Geol Rundsch)*, 106, 2039-2040. <https://doi.org/10.1007/s00531-017-1466-9>

Grande A., Di Vincenzo G., Prosser G. & Caggianelli A (2009) - Direct evidence of Middle Oligocene extension in the Calabria–Peloritani terrane from co-seismic faulting: the pseudotachylyte-bearing shear zones of Palmi (Southern Calabria, Italy). *Terra Nova*, 21, 293-303. <https://doi.org/10.1111/j.1365-3121.2009.00884.x>.

A combined petrofabric and AMS approach to reveal the magmatism-tectonics link in a composite batholith: an example from the Serre Massif (Calabria, Italy)

Fazio E.¹, Fiannacca P.¹, Cirrincione R.*¹ & Mamtani M.A.²

¹ Università degli studi di Catania – Dip. Sc. Biol. Geol. Amb. – Sez. Scienze della Terra, Italy.

² Indian Institute of Technology (IIT) - Department of Geology & Geophysics, Kharagpur (West Bengal, India).

Corresponding email: r.cirrincione@unict.it

Keywords: anisotropy of magnetic susceptibility, Serre Massif, plutonic bodies, petrofabric.

AMS (anisotropy of magnetic susceptibility) is a useful technique often adopted when studying plutonic bodies to infer magnetic foliation and/or lineation (Mamtani et al., 2019; Punturo et al., 2017) allowing to deduce, on apparently undeformed rocks, strain induced anisotropies, which otherwise could be very difficult to discern at outcrop scale. In this study we applied such technique to the Serre Batholith (Fiannacca et al., 2015) in order to reveal masked anisotropies and making also correlations with petrofabric and compositional information derived from parallel conducted investigations on the same specimens. Our findings have a good correlation with previously proposed distribution of granitoid rock types in the Serre Massif (Caggianelli et al., 2000). Combined AMS and petrofabric analyses have also allowed us to infer some concealed tectonic alignments as well as to suppose the occurrence of a tectonic phase previously recognized in the hosting metamorphic rocks (Festa et al., 2013).

Caggianelli A., Prosser G. & Del Moro A. (2000) - Cooling and exhumation history of deep-seated and shallow level, late Hercynian granitoids from Calabria. *Geological Journal*, 35, 33-42.

Festa V., Caggianelli A., Langone A. & Prosser G. (2013) - Time-space relationships among structural and metamorphic aureoles related to granite emplacement. A case study from the Serre Massif (Southern Italy). *Geological Magazine*, 150, 441-454.

Fiannacca P., Cirrincione R., Bonanno F., Carciotto M.M. (2015) - Source-inherited compositional diversity in granite batholiths: the geochemical message of Late Paleozoic intrusive magmatism in central Calabria (southern Italy). *Lithos*, 236-237, 123-140.

Fornelli A., Caggianelli A., Del Moro A., Bargossi G.M., Paglionico A., Piccarreta G. & Rottura, A., (1994) - Petrology and evolution of the Central Serre granitoids (Southern Calabria-Italy). *Periodico di Mineralogia* 63, 53-70.

Mamtani M., Bhatt S., Rana V., Sen K. & Mondal T.K. (2019) - Application of anisotropy of magnetic susceptibility (AMS) in understanding regional deformation, fabric development and granite emplacement: examples from Indian cratons. *Geol. Soc. London Spec. Pub.*, 489.

Punturo R., Mamtani M.A., Fazio E., Occhipinti R., Renjith, A.R. & Cirrincione R. (2017) - Seismic and magnetic susceptibility anisotropy of middle-lower continental crust: Insights for their potential relationship from a study of intrusive rocks from the Serre Massif (Calabria, southern Italy). *Tectonophysics*, 712-713, 542-556.

Submagmatic to solid-state shear-related deformation in late Variscan granitoids from a poly-orogenic mountain belt (Peloritani Mountains, southern Italy)

Fiannacca P.*, Fazio E., Russo D., Cirrincione R. & Pezzino A.

¹ Università degli Studi di Catania, Dipartimento di Scienze Biol., Catania, Italy.

Corresponding email: efazio@unict.it

Keywords: deformation microstructures, late Variscan shearing.

Late Variscan granitoid rocks (c. 310-300 Ma) of trondhjemitic and granitic composition, intruded in migmatitic paragneisses in the north-eastern Peloritani Mountains (Fiannacca et al., 2019), exhibit a range of deformation microstructures developed under simple-shear regime at decreasing temperatures, such as sigmoidal feldspar porphyroclasts, mica fish, and asymmetric boudins developed both in muscovite and tiny andalusite crystals. The Peloritani Mountains were involved in three orogenies, i.e. Cadomian, Variscan and Alpine-Apennine, with shear-zone activity so far clearly documented only for the latter (Cirrincione et al., 2015). Nevertheless, some microstructures (e.g. diffuse chessboard pattern in quartz) suggest late Variscan shearing during granitoid cooling, indicating deformation at high-temperature conditions (>650 °C). Submagmatic deformation was extensively superseded by deformation at lower temperatures. Recorded examples of solid state-high temperature deformation-related microstructures (>450°C) include quartz grain boundary migration recrystallization, quartz ribbons and core-and-mantle structures. Low temperature subsolidus microstructures (<450 °C) consist of bulging, subgrain rotation recrystallization, mica kinks and feldspar bending. Subsequent crystallization in sheared micro-domains of undeformed plagioclase from metasomatic fluids likely released by younger late Variscan granitoids (c. 297-292 Ma; Fiannacca et al., 2017), further brackets the shearing event during the latest stages of the Variscan Orogeny in southern Italy.

Cirrincione R., Fazio E., Fiannacca P., Ortolano G., Pezzino A. & Punturo R. (2015) - The Calabria–Peloritani Orogen, a composite terrane in Central Mediterranean; its overall architecture and geodynamic significance for a pre-Alpine scenario around the Tethyan basin. *Period. Mineral.*, 84, 701–749.

Fiannacca P., Williams I.S. & Cirrincione R. (2017) - Timescales and mechanisms of batholith construction: constraints from zircon oxygen isotopes and geochronology of the late Variscan Serre Batholith (Calabria, southern Italy). *Lithos*, 277, 302–314.

Fiannacca P., Basei M.A.S., Cirrincione R., Pezzino A. & Russo D. (2019) - Water-assisted production of late-orogenic trondhjemites at magmatic and subsolidus conditions. *Spec. Pub. Geol. Soc. London*, 491. <https://doi.org/10.1144/SP491-2018-113>.

Structure and petrography of mafic dykes from Val Camonica, Orobic Alps, Italy

Filippi M.^{*1-2}, Pulcini G.¹, Rebay G.³, Zanoni D.¹, Vergani D.³ & Spalla M.I.¹

¹ Dipartimento di Scienze della Terra “A. Desio”, Università degli Studi di Milano

² Géoazur (UMR 7329), Université Côte d’Azur

³ Dipartimento di Scienze della Terra e dell’Ambiente, Università degli Studi di Pavia

Corresponding email: marco.filippi@unimi.it

Keywords: Southalpine domain, Variscan and Alpine structures.

Mafic dykes are widespread within the Southern Alps basement, close to the Tertiary Adamello intrusive stock. Here, Variscan basement rocks are mainly metapelites (*Scisti di Edolo* Auct.), belonging to the Passo Cavalcafciche and Aprica Tectono-Metamorphic Units (Spalla et al., 1999; Gosso et al., 2012; Rebay et al., 2015 and refs therein). The main structure in the basement is the pervasive late-Variscan S2 foliation, developed under greenschist facies conditions and deformed by D3 Alpine folds, which are associated with the thrust and fold structure of the Central Southalpine domain. Alpine structures are mostly non-metamorphic, but locally they record a low-grade metamorphic imprint (Albini et al., 1994).

Form surface maps of key areas are presented here together with results of microstructural and petrologic analyses performed on mafic dykes. Two types of dikes are recognised, both crosscutting the S2 foliation: i) the first comprises amphibole-plagioclase rich rocks of andesitic affinity that crosscut D3 folds and are associated with Tertiary magmatism; ii) the second includes mafic dykes (i.e. *Diabase di Edolo*) whose relationships with the Alpine structures are complex, since they are locally foliated and often parallel to the D3 axial planes. Mafic dykes show an olocrystalline texture, with pyroxene, plagioclase, amphibole and, occasionally, biotite phenocrysts. Opaque minerals are widespread. They attained variable degrees of re-equilibration, with chlorite growing after pyroxene, amphibole and biotite, and sericite after plagioclase. At some places, carbonates replace phenocrysts and fill veins. Pyroxene is diopside or augite, with varying Mg# in different samples, locally with high Ti-content. Amphibole is Mg-hornblende or pargasite, Ti-rich at times. Different trace and major element patterns characterize the whole rock compositions of the two groups of mafic dykes.

Albini S., Battaglia D., Bellini G., Bigoni E., Carminati E., Ceriani S., Forcella F., Gosso G., Guizzetti D., Oliva A., Rebay G., Siletto G.B. & Spalla M.I. (1994) - Alpine deformations and pre-Alpine remnants in the north-eastern Orobic Alps, Southalpine basement. *Quad. Geodin. Alpina e Quaternaria*, 2, 25-39.

Gosso G., Spalla M.I., Siletto G.B., Berr, F., Bini A. & Forcella F. (2012) - Note illustrative della Carta Geologica d’Italia alla scala 1:50.000. Foglio 057, Malonno. ISPRA.

Rebay G., Maroni M., Siletto G.B. & Spalla M.I. (2015) - Superposed syn-metamorphic structures of the Alpine and pre-Alpine convergent cycles in the Southalpine basement of the Orobic Alps (Northern Italy), *J. of Maps*, 11(1), 1-13.

Spalla M.I., Carminati E., Ceriani S., Oliva A. & Battaglia D. (1999) - Influence of deformation partitioning and metamorphic reequilibration on P-T path reconstruction in the pre-Alpine basement of central Southern Alps (Northern Italy). *J. Metam. Geol.*, 17(3), 319-336.

Recent volcano-tectonic evolution of the Ririba rift (southern termination of the Main Ethiopian Rift, East Africa)

Franceschini Z.¹, Cioni R.¹, Corti G.*², Sani F.¹, Scaillet S.³, Isola I.⁴, Mazzarini F.⁴, Erbello A.⁵, Muluneh A.⁶, Keir D.⁷ & Brune S.⁸

¹ Dipartimento di Scienze della Terra, Università degli Studi di Firenze.

² Istituto di Geoscienze e Georisorse, Consiglio Nazionale delle Ricerche.

³ Institut des Sciences de la Terre d'Orléans (ISTO).

⁴ Istituto Nazionale di Geofisica e Vulcanologia.

⁵ School of Applied Natural Sciences, Adama Science and Technology University.

⁶ School of Earth Sciences, Addis Ababa University.

⁷ School of Ocean and Earth Science, University of Southampton.

⁸ German Research Centre for Geosciences GFZ.

Corresponding email: giacomo.corti@igg.cnr.it

Keywords: continental rifting, rift evolution, volcano-tectonics, East Africa.

The Main Ethiopian Rift (East Africa) is a continental rift that records all the different stages of rift evolution and is characterised by significant volcano-tectonic activity spanning from the Oligocene to present. It is therefore an ideal place where to analyse the interplay between tectonics and magmatism during rifting. However, despite these ideal conditions, the knowledge of the volcano-tectonic activity in many rift sectors still remains poorly documented. In this work we provide new constraints on the timing, evolution and characteristics of the poorly documented volcano-tectonic activity of the Ririba rift, at the southern termination of the Main Ethiopian Rift and part of the complex region of interaction with the Kenyan rift in the Turkana depression.

We present geological-structural, geochemical, volcanological and geochronological data which document that the roughly N-S Ririba rift formed from the southward propagation of the Ethiopian rift during the Pliocene. Rift propagation occurred concurrently or shortly after the emplacement of subalkaline basalts forming a widespread lava basement, for which new Ar/Ar dating give ages of ~3.7 Ma. In contrast with previous analysis, our data indicate that activity of the Ririba rift was short-lived and rift-related deformation ceased close to the Pliocene-Pleistocene boundary. Faults are indeed sealed by the basal lava flows of the Hurri Hills volcano (for which old Kr-Ar dating gave ages of 2.3-2.8 Ma) and by more recent alkaline basalts that are associated to several, mainly monogenetic volcanic centres forming the Dilo-Dukana and Mega volcanic fields. For these fields, new Ar/Ar dating indicate ages of 134 ka and Holocene, respectively. Integration of seismicity data with new numerical models indicates that abandonment of the Ririba rift resulted from progressive focusing of the tectonic and magmatic activity in the Turkana depression into an oblique, throughgoing rift zone which directly connects the Ethiopian and Kenyan rifts.

Interestingly, no direct relations are observed between the structures feeding the Quaternary volcanic activity and the major boundary faults of the Ririba rift. Indeed, the alignment of volcanic vents indicates NE-SW feeding structures which cut the roughly N-S major boundary faults of the Ririba rift. This is interpreted as resulting from a major influence exerted by deep, inherited structures on the distribution of the recent volcanic vents under a complex, local stress field resulting from a major episode of reorganization of extensional structures in the region, recording the history of rift propagation and abandonment.

Bimodal felsic-mafic volcano-plutonic magmatism associated to intramontane basins: the late-Variscan geodynamics recorded in North Sardinia (Italy)

Gaggero L.*¹, Maino M.², Cuccuru S.³ & Oggiano G.³

¹ Department of Earth, Environment and Life Sciences (DISTAV), University of Genoa, Genoa, Italy.

² Department of Earth and Environmental Sciences, University of Pavia, Pavia, Italy.

³ Department of Chemistry and Pharmacy, University of Sassari, Sassari, Italy.

Corresponding email: gaggero@dipteris.unige.it

Keywords: strike-slip basins, gabbro, Permian.

The Variscan post-collisional evolution of Sardinia is documented by HT/LP metamorphism, exhumation of core complex, the emplacement of the U2 and U3 intrusive plutons, which form the majority of the Corsica-Sardinia batholith and by a calc-alkaline volcanic activity, mostly confined within Carboniferous-Permian intra-cratonic basins.

Several Permian-Carboniferous basins, filled with sedimentary and volcanic rocks spread from the foreland to the nappe zone. These basins developed in correspondence of structural lows either represented by wide post-nappe synforms, half-grabens bounded by normal growth faults or strike-slip basins

This work addresses a transect across Permian a volcano-sedimentary succession hosted in the Falzu basin and affected by contact metamorphism, related to the Bortigiadas gabbro-diorite intrusion, which is a 10-km² wide, lens shaped, laccolith composed by a gabbroic core variably veined at cm to metre scale, and rimmed by tonalite – granodiorite rocks. The composite intrusion is mostly formed by a medium-fine grained hypidiomorphic Hbl – bearing gabbro associated with fine grained hypidiomorphic Bt-diorite.

The U-Pb LA-ICP-MS dating on zircon separates of the granodiorite yielded a protolith age of 286±4 Ma, which overlaps the U-Pb age of the rhyolitic pyroclastites (275.6±3.4 Ma) at the top of basin infill. Field evidences such as swirling textures of minerals, indicative of turbulence during emplacement, and convolute (i.e. hot) contacts between felsic and mafic melts suggest that the granodiorite is the result of mixing between the gabbro and a more felsic magma. At the mesoscale scale, the contact between intermediate and mafic rocks is lobate and characterized by medium grained facies, suggesting that mutual intrusion occurred at temperature higher than the solidus, associated with convection and possibly active tectonics. The mafic magma also intruded the migmatite that was re-melted into sheeted leucocratic pods.

In the gabbro, the relatively low Σ REE content, the poor La_N / Yb_N fractionation, and the overall low positive Eu / Eu^* indicate a mantle signature. This is confirmed by e_{Sr} between -420,5453694 and -1858,91401, associated with $Sr_{(285)}$ below or equal to 0.705. The e_{Nd} ranges between 8.557 and 11.507 coupled with $Nd_{(285)} = 0.512$: these ratios point to a depleted mantle source, and negligible crustal component, restricted to short range assimilation of the sediments. In fact, structural and stratigraphic constraints, together with pseudosection modelling, point to 2 km as maximum depth of the basin.

To sum up, we propose that the Bortigiadas gabbro intrusion was originated from a depleted mantle source rooted in a major lithospheric discontinuity. The mafic melt channelize along a crustal shear zone mixing with a felsic crustal magma. The mafic melt channelize along a crustal shear zone mixing with a felsic crustal magma. Finally, the composite mafic-felsic melts emplaced at 285 Ma below Permian sediments resulting into UHT-LP metamorphism up to c. 780-800 °C (cordierite+sanidine) in the shallow crust.

Pliocene-Quaternary granitoids in the transfer zone of the Larderello geothermal area (Italy)

Liotta D.^{*1-2}, Brogi A.¹⁻² & Dini A.²

¹ Dipartimento di Scienze della Terra e Geoambientali, Università di Bari.

² IGG-CNR, Pisa.

Corresponding email: domenico.liotta@uniba.it

Keywords: transfer zone, granitoids, geothermal areas.

Transfer zones, due to their internal geometrical complexity, represent ideal structures where the increase of permeability can accommodate magma intrusions, even at shallow levels. When it occurs, if other conditions are favorable, geothermal manifestations result. In this presentation we illustrate the case of the Lago basin, belonging to the Larderello geothermal area, and located within a SW-NE striking transfer zone associated to the extensional tectonics of the inner northern Apennines. In this framework, a key-factor is the regional stress field controlling brittle deformation. In active geothermal areas, this is deduced from local earthquakes, often resulting contradictory and mainly suggesting normal to strike-slip tectonic regime.

This feature has been investigated in the Larderello geothermal area comparing information from field data and available focal mechanisms from the area of the Pliocene-Pleistocene Lago Basin, where the most effective exploitation occurs today. The methodology is based on the classical approach of structural geology, inversion of kinematic data from slip-fault surfaces and comparison with published focal mechanisms of local earthquakes. The analysed dataset is from Pliocene-Quaternary faults. The results indicate strong similarities in the orientation of the main stress axes as obtained from paleo-stress analysis and double couple focal mechanisms solution, thus suggesting the maintenance of the same stress field through time, under the regional NE-oriented stretching direction. In this context, the analysed structures are explained as part of the deformation developed within a NE-oriented transfer zone, affecting the study area. The development of the tectonic depression, giving rise to the Lago Basin, is therefore explained as a pull-apart basin. In this basin, the $^3\text{He}/^4\text{He}$ values and the heat flux indicate a cooling magma at shallow depth (about 4 km). The roof of the intrusion is mimed by the geometry of the local brittle-ductile transition, consistent with the transfer zone geometry. Furthermore, along the study NE-striking transfer zone, older granitoids (from about 3.6 to 1.6 Ma) are located, suggesting the maintenance of the same stress field through time.

Origin and evolution of post-collisional mafic granitoids (Capo Vaticano Promontory, Southern Calabria): geochemical and geochronological constraints

Lombardo R.*¹, Fiannacca P.¹, Basei A.S.² & Cirrincione R.¹

¹ University of Catania, Department of Biological, Geological and Environmental Sciences, Catania, Italy.

² University of São Paulo, Institute of Geosciences, São Paulo, Brazil.

Corresponding email: rlombardo@unict.it

Keywords: isotopic whole rocks, quartz-diorites, tonalites.

Tonalites and minor quartz diorites represent the deepest portion of a composite late-Variscan granitoid batholith, located in the Capo Vaticano Promontory (Calabria, southern Italy), making up the intermediate level of a completely exposed crustal section. Representing the more mafic product of a magmatic sequence, our goal has been to constrain the source contribution (crustal or mantle) and the relative role of melting and differentiation processes in the granitoid genesis. First, Sr-Nd isotopic data rule out an addition of mantle magma, highlighting narrow evolved compositions ($\text{Sr} = 0.7098\text{-}0.7102$) and markedly negative ϵNd values (-7.48 to -6.33). Furthermore, the depicted vertical array is ascribable to partial melting of a slightly heterogeneous, relatively old, crustal source. In fact, comparison with the crustal rocks from southern Calabria reveals ϵNd values and initial Sr and Pb isotopic compositions similar to those of lower crustal metabasites.

Choosing a local amphibolite as a probable source able to generate a tonalitic magma, we obtained a composition close to the assumed parental magma after 30% of partial melting with Pl, Opx, Grt and Qtz as residual phases in batch melting conditions. Major and trace element modelling fits with 40% fractional crystallization of plagioclase, amphibole and biotite from an initial tonalitic magma.

U-Pb zircon data obtained by SHRIMP show an articulate story due to different processes. Older dates ranging from 317 ± 1.8 Ma to 310 ± 3 Ma, possibly related to anatectic conditions, are commonly present in all sample analysed. The magmatic crystallization age ranges from 298 ± 1.1 Ma to 295 ± 0.8 Ma, but sometimes it is completely masked by an ubiquitous zircon recrystallization occurred at c. 290 Ma. A Th/U ratio vs. age diagram highlights a significant clustering of the zircon spots respect to the relative age and the internal texture. Oscillatory zoning zircon matches seamlessly with the emplacement age, as well as CL homogenous dark and bright areas with age ranging from 302 to 295 Ma; a wider age range is instead associated to banded zoning zircon grains. Unzoned overgrowths appear systematically related to late- to post-magmatic recrystallization at c. 290 Ma. The widest Th/U range is showed by the zircon from mafic microgranular enclaves, and by banded zoning zircon crystals in the host granitoids, indicating a more mafic magma. Also, the mean Th/U ratio of mid crystal portions is of about 0.6, while for the edges is 0.5. Additionally, a $T_{\text{mean}} = 783^\circ\text{C}$ was obtained for zircon saturation temperature; little difference between Z_{rsat} and Z_{robs} contents indicates a Zr-saturated and low-temperature magma. Furthermore, negative trends for P_2O_5 , Ba, Zr support differentiation of an I-type magma at relatively low T.

Faults controlling ore deposits distribution in the Las Minas area (Mexico)

Olvera Garcia E.¹, Bastesen E.², Bianco C.¹, Brogi A.¹⁻³, Caggianelli A.¹, Garduño Monroy V.H.⁴, Liotta D.*¹⁻³, Torabi A.², Wheeler W.H.² & Zucchi M.¹

¹ Dipartimento di Scienze della Terra e Geoambientali, Bari.

² Norwegian Research Centre AS, Bergen.

³ Centro Nazionale delle Ricerche – IGG, Pisa.

⁴ Universidad Michoacana de San Nicolás de Hidalgo, Morelia.

Corresponding email: domenico.liotta@uniba.it

Keywords: faults, magma cooling, hydrothermalism.

In the Las Minas area (Central Mexico), hydrothermal mineralization is quite diffuse at the boundary between crystalline and sedimentary rocks and in fault zones. This is a consequence of the interaction between cooling of Miocene felsic magmas and coeval fault activity. We investigated the role of the faults in channeling the hydrothermal fluids by fieldwork and analysis of fractures at outcrops. The field mapping was carried out at 1:10000 scale (60 km²). When possible, kinematic data on recent fault planes influencing the permeability and geothermal fluid paths were collected. This includes information on the main structural trends and the orientation of the intermediate kinematic axis.

Six main units can be recognized in the map: 1) Jurassic-Cretaceous limestone and marble hosting Neogene magmatic rocks; 2) intrusive magmatic complex (Miocene); 3) skarn (Miocene); 4) lacustrine sediments (?Miocene-Pleistocene); 5) magmatic effusive deposits (Pleistocene-Holocene); 6) magmatic dykes (Neogene-Quaternary).

The Jurassic-Cretaceous limestone is affected by contact metamorphism. In detail, the skarn is mainly located (i) along the boundary between the magmatic rocks and the Jurassic-Cretaceous limestone, (ii) along the main faults cataclastic zones, (iii) along the principal foliations affecting the limestone.

Two families of faults have been recognized, NNW-SSE and SW-NE oriented, respectively. The SW-NE trending faults often controlled the emplacement of dykes, indicating that the magmatic fluid was channeled and driven by the faults induced permeability. Nevertheless, fault activity continued even after dykes emplacement, as indicated by the cataclastic zones also involving the magmatic dykes (Miocene). Since faults dissect Pleistocene lacustrine and volcanic units, their activity is at least encompassed between Miocene and Quaternary.

The kinematics of the NNW-SSE trending faults is represented by oblique movement and normal component, the latter always overlapping the former. Whereas, the SW-NE oriented faults encompass a dominant normal component. The kinematic relation between these two fault systems could be explained in an extensional framework, assuming that the NNW-SSE fault system acted as transfer faults. Contemporaneously, the SW-NE faults acted as normal faults, although with a lateral component. The last kinematic event is however characterized by a dominant normal component in both fault systems. This could be explained as a consequence of regional uplift in the Transmexican Volcanic Belt (TMVB), where the preexisting fractured rock-volume, representing weakened sectors, was reactivated as normal faults, in the frame of the NW-SE striking regional extension, that is conserved up to the Present in the TMVB.

Multidisciplinary approach to test the thermal state of Biella pluton country rocks

Roda M.*¹ & Zannoni D.¹

¹ Dipartimento di Scienze della Terra “A. Desio”, Università degli Studi di Milano.

Corresponding email: manuel.roda@unimi.it

Keywords: Alpine Tertiary intrusions, pluton cooling modelling, Sesia-Lanzo zone.

This work contributes to reconstruct the thermal state of HP metamorphic rocks of the Sesia-Lanzo Zone at the time of the intrusion of Biella pluton. We combined field structural data from the pluton margins and thermobarometric estimates on intrusive and country rocks to infer the geometry and depth of emplacement. On the basis of the results, we built a numerical simulation of pluton cooling to get a likely thermal state of the country rock at the time of the intrusion.

The Oligocene Biella pluton comprises a monzonite outer part and a syenite and granite inner part. The intrusion postdates the polyphasic tectono-metamorphic history of surrounding gneisses and schists. The contact metamorphic parageneses overprint the eclogite-facies assemblages dominant at the regional scale and locally overprinted by greenschist-facies parageneses. The amount of contact metamorphic minerals decreases with the distance from the pluton margins. Thermobarometrical estimates referred to the final pluton emplacement, give pressures and temperatures that continuously decrease from NW to SE margins. These estimates are consistent with a post-intrusive southeastward rotation of the pluton and country rocks of about 60°; this result is supported by the analysis on paleomagnetic lineation in Oligocene andesitic dykes intruded in the country rocks. The contact metamorphic peak is constrained at temperatures between 730 and 545 °C as a function of the distance from the pluton.

We develop a 2D thermal model of pluton cooling testing four different thermal gradients (20, 30, 40 e 50°C/Km) affecting the host continental crust. The pre-rotation geometry and emplacement depth are taken from the structural and petrologic analysis of the pluton - country rock system. The intrusion is considered to be 900°C. We compare the extent and the variation in the maximum temperature recorded in the contact aureole with the results of the numerical simulations as a function of the distance from the pluton and the original depth. On this basis the estimated variation of expected maximum temperature and the extent of the mapped contact aureole matches the numerical results. The best fitting thermal gradient for country rocks at the time of intrusion is between 40 and 50°C/km. This gradient is consistent with the intrusion of the Biella pluton during the Alpine collision, after the slab break-off.

The cooling, deformation and exhumation history of the late Miocene syn-tectonic Porto Azzurro pluton in a transfer zone (Elba Island, Italy)

Spiess R.¹, Caggianelli A.², Langone A.³, Stuart F.⁴, Bianco C.², Zucchi M.², Brogi A.^{*2-5} & Liotta D.²⁻⁵

¹ Dipartimento di Geoscienze, Università di Padova.

² Dipartimento di Scienze della Terra e Geoambientali, Università di Bari.

³ CNR-IGG, Pavia.

⁴ Environmental Research Centre, Scottish Universities Edinburgh.

⁵ CNR-IGG, Pisa.

Corresponding email: andrea.brogi@uniba.it

Keywords: magma, extensional tectonics, integrated methods.

In extensional tectonic settings, stretched terrains are often associated to lithosphere partial melting and widespread magmatism with plutons emplaced in the thinned crust. Emplacement of felsic magmas, at upper crustal levels, represents the final stage of the magma transfer from profound to shallow depth. In this framework, a mostly vertical permeability controls the magma uprising migration, as induced by dominant transcurrent crustal structures. Nevertheless, the interplay between extension and prolonged heat transfer favors uplift and progressive exhumation of the magmatic bodies, during their cooling.

In this presentation, we show an example of a felsic magmatic intrusion, the Porto Azzurro pluton (inner northern Apennines), emplaced in an extensional tectonic setting and mainly controlled by a regional transfer zone related to the opening of the Tyrrhenian Basin. This is exposed in the eastern Elba Island (Tuscan Archipelago). The hosting rocks of the Porto Azzurro pluton are mainly represented by micaschist, paragneiss and quartzite, affected by contact metamorphism and intense fluid circulation. We have analysed the structures that assisted the pluton emplacement and the ones that deformed the pluton itself during its cooling, from melt-present to brittle conditions, based on the integration among fieldwork, micro-structural, petrological and EBSD analyses. Furthermore, new U/Pb geochronological data on zircons and (U-Th)/He on apatite fission track refined the age of the pluton emplacement and its cooling, adding new data about the pluton history. Existing petrological analyses of the hosting rocks allowed us to better constrain the time-evolution of the thermal perturbation, permitting to frame the deformation and exhumation history of the Porto Azzurro monzogranite in the context of the Neogene extensional tectonics affecting the inner Northern Apennines.

Semi-automated fabric analysis of strong rheologically contrasting mylonitic rocks: The example from the strike-slip Palmi shear zone

Visalli R.¹, Fazio E.¹, Ortolano G.*¹, Alsop G.I.², Pagano M.¹ & Cirrincione R.¹

¹ Università degli Studi di Catania – Dip. Sc. Biol. Geol. Amb. – Sez. Scienze della Terra, Catania (Italy).

² Aberdeen University – School of Geosciences, Kings College, Aberdeen (UK).

Corresponding email: rvisalli@unict.it

Keywords: Image analysis, paleopiezometry, grain size distribution.

Since the early Paleocene, the complex geodynamic history of the western Mediterranean has been controlled by the activation of several crustal-scale strike-slip shear zones. These shear zones have controlled the early-Alpine drifting of the Kabilo-Calabride crystalline basement, favoring microplate dismembering and accommodating part of the African-verging transport of the more internal sectors of the original southern paleo-Alpine front. One of the best preserved relics of this meso-Alpine geodynamic activity is developed along the north-western part of the Palmi-Line (PL) (Cirrincione et al., 2015; Fazio et al., 2017), which is a WNW-ESE tectonic alignment separating the Serre from the Aspromonte massifs (Southern Calabrian Peloritani Orogen CPO – Italy). On the Tyrrhenian side of the PL can be traced inland for ~1500 m from the Tyrrhenian coast and comprises mylonitic skarns with subordinate mylonitic paragneisses and tonalities. To highlight the kinematics and rheology of the Palmi Shear Zone, we performed a detailed quantitative microstructural study of all of the lithotypes involved in the shear zone. Semi-automated image analysis of mXRF maps combined with high-resolution thin section scans permits the application of new GIS-based tools to structural analysis (e. g. Ortolano et al., 2018). This allows to quantitatively extrapolate microstructural features such as grain-size and -shape distribution, of various minerals, while at the same time storing all the potential derivative mineral-chemical and textural features within a user-friendly database. This procedure applied to mylonitic rocks allows us to collect information that helps constrain the rheology and kinematics of exhumed deep-seated deformation. The outputs obtained permitted us to separate the porphyroclastic domain levels (usually tonalites) from the weakening phase ones (usually calc-silicates rocks and marbles). Image analysis of porphyroclastic domains was useful to estimate the dominant shear-type, with Rigid Grain Analysis indicating a pure shear component of 63% while simple shear constitutes 37%. Grain boundary mapping, associated recrystallization microstructures, and quartz-c axis patterns permits us to estimate shearing temperature at ca. - 430 °C and a preliminary shear strain rate estimation of $1,13E^{-11}$ 1/s, applying the paleopiezometer of Shimizu (2008). Our results allow us to shed new light on the kinematics and rheology of exhumed shear zones, and in particular on this relic of the deep-rooted early-Alpine strike slip tectonics of the western Mediterranean.

Cirrincione R., Fazio E., Fiannacca P., Ortolano G. Pezzino A. & Punturo R. (2015) - The Calabria-Peloritani Orogen, a composite terrane in Central Mediterranean; its overall architecture and geodynamic significance for a pre-Alpine scenario around the Tethyan basin. *Period. Mineral.*, 84(3B), 701-749.

Fazio, E., Ortolano, G. & Cirrincione, R. (2017) - Eye-type folds at the Palmi shear zone (Calabria, Italy). *Int. J. Earth. Sci.*, 106, 2039 - 2040.

Ortolano G., Visalli R., Godard G. & Cirrincione R. (2018) - Quantitative X-ray Map Analyser (Q-XRMA): A new GIS-based statistical approach to Mineral Image Analysis. *Comput. Geosci.*, 115, 56-65.

Shimizu I. (2008) - Theories and applicability of grain size piezometers: The role of dynamic recrystallization mechanisms. *Journal of Structural Geology*, 30(7), 899-917.

Geothermal fluids flow and storage in faulted and folded metasiliciclastics (eastern Elba Island, Italy)

Zucchi M.*¹, Brogi A.¹⁻², Liotta D.¹⁻², Ruggieri G.³, Fregola R.A.¹, Matera P.F.¹, Dini A.², Morelli G.³,
Ventrucci G.¹ & Rimondi V.⁴

¹ Department of Earth and Geoenvironmental Sciences, University of Bari.

² IGG-CNR, Institute of Geosciences and Earth Resources, Pisa.

³ IGG-CNR, Institute of Geosciences and Earth Resources, Florence.

⁴ Department of Earth Sciences, University of Florence.

Corresponding email: martina.zucchi@uniba.it

Keywords: Fe-ore deposits, metasomatism, fluid flow.

The circulation of geothermal fluids in continental and oceanic crust is mainly controlled by fracture networks related to fault zones. In the upper crust, geothermal fluids are mainly channeled within damaged rock volumes associated to extensional settings and also related to magmatism. Fluids storage can occur in permeable stratigraphic levels, overall where permeability is enhanced by chemical aggression of fluids, as it is the case of cataclastic volumes and siliciclastic or carbonatic rocks. In this view, reconstructing the geometry of the geological bodies and the fracture networks formed during the tectonic evolution play an important role to predict the fluids circulation from depth to shallower structural levels, as well as to predict the possible occurrence of traps.

In order to characterize these interactions, we analyzed the case of the exhumed geothermal system exposed in the eastern Elba Island (Tuscan Archipelago, Italy). Here, Fe-ore deposits developed in metasiliciclastics (Verrucano Group) during the circulation of HT (exceeding 300°C) geothermal fluids that were channeled along fault zones and then trapped within folded metasiliciclastic units. The study areas belong to the Rio Marina mining district (Valle Giove, Topinetti and Calendozio) where the ore deposits were exploited for centuries. The detailed fieldwork integrated with mineralogical and fluid inclusions analyses highlight that in the metasiliciclastic rocks, fluid flow was overall controlled by fracture networks. Storage is spatially limited in the surrounding of the feeding channels and controlled by pre-existing fold geometries. Parameters on fault permeability in the range of suitable values have also been obtained by computing fractures array resulting in the range between 10^{-14} and 10^{-16} m². Furthermore, fluid inclusions analyses carried out on hydrothermal minerals (e.g. quartz, calcite, adularia and fluorite) allowed us to reconstruct the evolution and the chemical-physical features of the paleo-geothermal fluids, suggesting the circulation of both high-salinity magmatic derived fluids and low-salinity fluids of meteoric origin.

The research leading to these results has received funding from the European Community's Seventh Framework Programme under grant agreement No. 608553 (Project IMAGE).

S20

**Orogenesis and orogenic wedges: a multiscale and
multitechnique approach**

Conveners and Chairpersons

Francesca Remitti (Università di Modena e Reggio Emilia)

Luca Aldega (Università di Roma)

Stefano Tavani (Università di Napoli)

Giulio Viola (Università di Bologna)

The Calabrian Arc orogenic wedge: a Messinian reconstruction

Argnani A.*¹, Manzi V.², Lugli S.³ & Roveri M.²

¹ Istituto Scienze Marine – CNR, Bologna.

² Dipartimento di Scienze Chimiche, della Vita e della Sostenibilità Ambientale, University of Parma.

³ Dipartimento di Scienze Chimiche e Geologiche, University of Modena e Reggio Emilia, Modena.

Corresponding email: andrea.argnani@ismar.cnr.it

Keywords: Messinian, Calabrian Arc, orogenic wedge.

The Messinian Salinity Crisis represents a short (ca. 0.64 Myr) but remarkable event in the evolution of the Mediterranean region. Detailed field work and analysis of subsurface data have allowed to refine the stratigraphy and the depositional environments during this time interval. Although some details of the stratigraphy are still debated due to the complexity of the lithological relationships and the different scales of observation related to different analytical tools (e.g., field mapping vs geophysical data interpretation), some fundamentally different sedimentary packages have been identified. Moreover, the detailed facies analysis has revealed a variety of depositional environments, in some instance with assigned paleo-water depth. The resulting stratigraphic template and the paleo-water depth of some specific deposits, offer the opportunity to detail the palaeogeography of the late Miocene Calabrian Arc. Messinian deposits are known to occur both at outcrop and in the subsurface all along the Apennines and the Sicilian Mghrebides, including the Calabrian region. In spite of controversial interpretations on the evolution of the Southern Apennines and Sicilian Maghrebides, mostly concerning the nature of the substrate of the more internal units (oceanic vs continental), the integration of geological and geophysical data strongly suggests that the internal basinal units were deposited in an oceanic domain, older than the Alpine Tethys and attributable to the Neotethys, which is currently flooring the Ionian basin. As a consequence, the segment of the Apennine-Maghrebian system that encompasses the Southern Apennines, Calabria and Sicily grew as an accretionary wedge, and during the Neogene opening of the Tyrrhenian backarc basin formed an arcuate belt, with the two limbs undergoing opposite large-scale vertical-axis rotation on either side of Calabria (saloon door-opening). The Calabria sector of the Arc is facing an oceanic corridor (Ionian basin), whereas the accretionary wedge encroached the Adriatic and African continental margins in the Southern Apennines and Sicily, respectively. During the Neogene evolution of the Calabrian Arc the Messinian time represents a critical stage. This contribution aims at using the constraints from the Messinian stratigraphy and sedimentology to address the palaeogeographic evolution of the Calabrian Arc. The resulting reconstructions allow interesting considerations on the relationships occurring between the accretionary wedge and the articulate paleogeographic domains of the lower plate, and offer hints on the sedimentary routes and the depocentres architecture.

The Ganj Ophiolitic Complex reinterpreted as a Late Cretaceous volcanic arc: implications for the geodynamic evolution of the North Makran domain (SE Iran)

Barbero E.*¹, Delavari M.², Dolati A.², Pandolfi L.³⁻⁴, Marroni M.³⁻⁴, Saccani E.¹ & Catanzariti R.⁴

¹ Dipartimento di Fisica e Scienze della Terra, Università di Ferrara.

² Faculty of Earth Sciences, Kharazmi University, Tehran, Iran.

³ Dipartimento di Scienze della Terra, Università di Pisa.

⁴ Istituto di Geoscienze e Georisorse, Consiglio Nazionale delle Ricerche, Pisa.

Corresponding email: edoardo.barbero@unife.it

Keywords: Makran, Neo-Tethys, Late Cretaceous geodynamic.

The Makran accretionary prism (SE Iran) record a Cretaceous – Present day complex geodynamic evolution, resulting from the convergence between the Arabian and Eurasian plates and the subduction of the main Neo-Tethys Ocean and associated minor oceanic branches. The North Makran is the innermost structural domain of this accretionary prism and it consists of an imbricate stack of tectonic units representing deformed remnants of both oceanic and continental margin domains. In turn, the Ganj Complex represents the structurally innermost tectonic unit of the North Makran and it is commonly interpreted in literature as an ophiolitic complex.

We present new structural, stratigraphic, paleontological, and petrological data on the Ganj Complex with the aim of better defining its geological features and its tectonic significance within the Makran accretionary prism. This Complex is dismembered in several tectonic slices bounded by transtensive- to normal- high angle faults; however, its stratigraphic succession can be broadly reconstructed through detailed field and laboratory observations. The succession is more than 3000 m-thick, and it consists (bottom to top) of a sheeted dyke complex showing a transition to a volcano-sedimentary sequence consisting of massive and pillow lava flows with intercalations of sedimentary rocks (mainly arenites). This sequence shows a gradual transition to calcareous turbidites bearing Turonian – Coniacian nannofossil assemblages. The Ganj Complex is unconformably covered by a mainly terrigenous, Eocene – Oligocene stratigraphic succession. Petrographic analysis shows that arenites intercalated in both the volcanic series and its sedimentary cover have an intrabasinal nature. These rocks are characterized by a mixed volcanoclastic-carbonatic framework, where abundant volcanic and sub-volcanic lithic fragments occur along with mudstone and wackestone clasts, as well as bioclastic fragments. Geochemical data indicate that the volcanic and sub-volcanic rocks consist of calc-alkaline and island arc tholeiites bearing subduction-derived chemical imprint, including minor adakite-like components.

Our multidisciplinary study indicates that the Ganj Complex represent a Late Cretaceous volcanic arc, likely built-up in a relatively shallow marine setting along the rim of a continental margin dominated by a carbonate sedimentation. The present-day structural position of this Complex suggests the existence of a volcanic arc onto the southern margin of the Lut continental block during the Late Cretaceous. In particular, the Ganj volcanic arc seems to be related to the subduction of the oceanic lithosphere of the North Makran basin rather than to the subduction of the main Neo-Tethys Ocean. Our results thus provide significant constraints for the geodynamic evolution of the Arabia and Central Iran transect during the Late Cretaceous.

Preliminary stratigraphic and petrological data on the Durkan Complex (Makran accretionary wedge, SE Iran)

Barbero E.*¹, Delavari M.², Dolati A.², Pandolfi L.³⁻⁴, Marroni M.³⁻⁴, Saccani E.¹, Chiari M.⁵,
Luciani V.¹ & Catanzariti R.⁴

¹ Dipartimento di Fisica e Scienze della Terra, Università di Ferrara.

² Faculty of Earth Sciences, Kharazmi University, Tehran, Iran.

³ Dipartimento di Scienze della Terra, Università di Pisa.

⁴ Istituto di Geoscienze e Georisorse, Consiglio Nazionale delle Ricerche, Pisa.

⁵ Istituto di Geoscienze e Georisorse, Florence.

Corresponding email: edoardo.barbero@unife.it

Keywords: Makran, Durkan Complex, Neo-Tethys, Late Cretaceous geodynamic.

The Makran Accretionary Prism (SE of Iran) resulted from the northward subduction of the Neo-Tethys Ocean below the Lut and Afghan continental blocks, associated with the Cretaceous – Present day convergence between the Arabian and Eurasian Plates. The North Makran is the innermost structural domain of this accretionary prism. In the North Makran, the Bajgan and Durkan Complexes consist of a Paleozoic metamorphic basement and its sedimentary cover, respectively, and are thought to represent a continental margin domain. The Durkan Complex is made up of several tectonic units mainly consisting of Early Cretaceous – Paleocene carbonatic and volcanic successions, as well as rare Carboniferous, Permian and Jurassic slices of platform limestone. However, the stratigraphic succession, and the age and geochemistry of the volcanic rocks are poorly known. Nevertheless, such data are necessary for constraining the meaning of the Durkan Complex in the geodynamic evolution of the Makran.

We therefore present preliminary stratigraphic and petrological data on the Durkan Complex in the western sector of the North Makran. Here, it consists of different tectonic slices, which are characterized by hundreds of metres-thick stratigraphic successions whose features range between two end-members. The first type of succession is characterized by pillow and massive lava flows intercalated with silicified limestone, radiolarian chert and shale, as well as alternating volcanoclastic sandstone, shale and minor limestone. The second type of succession is characterized by pillow lava flows, volcanic breccia, as well as volcanoclastic sandstone and coarse-grained limestone, overlain by a carbonatic platform succession consisting of grainstone, recrystallized wackestone, and lenticular bodied of carbonatic breccia. The platform lithofacies are followed by alternating silicified limestone and shale. These first and second end-member successions represent relatively deep and relatively shallow sedimentary deposition, respectively. However, volcanic rocks in all the different successions of the Durkan Complex show very similar geochemistry and overall features. In fact, they mainly consist of alkaline basalt and minor trachybasalt, trachyandesite and trachyte, showing high Nb/Y ratios (0.62 – 4.4) and marked enrichment in LREE compared to HREE. In addition, preliminary biostratigraphic data on the limestone and chert stratigraphically associated with the volcanic rocks show foraminifera and radiolarian assemblages of Late Cretaceous age.

Our preliminary data suggests that a significant alkaline magmatic pulse occurred in the Late Cretaceous in the Makran sector of the Neo-Tethyan Eurasian realm. This volcanism was likely associated with rift activity possibly related, in turn, to mantle plume activity or regional scale mantle heterogeneities. Its tectono-magmatic significance within the Makran geodynamic evolution is then worth to be further investigated in detail.

The Plio-Pleistocene Bradano basin and the Southern Apennine Orogenic Wedge: evidences of accretion collision and segmentation of Apulian continental plate

Basso J.*¹, Artoni A.¹, Torelli L.¹, Polonia A.², Carlini M.³, Gasperini L.² & Mussoni P.^{1,4}

¹ Department of Chemistry, Life Sciences and Environmental Sustainability University of Parma, Italy.

² Institute of Marine Science CNR ISMAR-Bo, Bologna, Italy.

³ Department of Biological, Geological and Environmental Sciences - University of Bologna, Italy.

⁴ ENI S.p.A., E & P Div., San Donato Milanese (MI), Italy.

Corresponding email: andrea.artoni@unipr.it

Keywords: Bradano Basin, Apulian continental plate, orogenic front.

The Pliocene-Pleistocene tectono-stratigraphic evolution of the Bradano Basin in the Gulf of Taranto is investigated by means of multi-scale, high-resolution seismic reflection profiles combined with exploration wells and seafloor bathymetry. Being located between the Ionian Calabrian Margin, to the West, and the Apulian Margin, to the East, the Bradano Basin is the site of pervasive tectonic deformations part of the southward and seaward prolongation of the Southern Apennines orogenic wedge. Within the Gulf of Taranto, five main domains surround the Bradano Basin: the Calabrian Arc, the Calabrian Accretionary Wedge, the Southern Apennines and the subducting Apulian Foreland Ramp. The external fronts of the Calabrian Accretionary Wedge and Southern Apennines progressively migrated toward ESE overriding and colliding with the subducting Apulian lithosphere during the Pliocene-Pleistocene. As previously recognized, this collisional setting has been responsible for the formation of the Pliocene-Pleistocene Bradano Foreland Basins System while the Apulian Foreland Ramp was uplifted and down-flexed toward west but generally considered as an “undeformed” foreland area. The multi-scale analyses of geophysical data reveals active deformation involving the foreland ramp which was affected by different tectonic phases: contraction and transcurrent deformations along E-W trending faults active from the Miocene to recent times; thrusts and thrust-related anticlines even underneath the Southern Apennine fronts; NW-SE and N-S striking thrust-related folds affecting the whole Apulian continental plate, likely inverting inherited Mesozoic-Pliocene extensional faults and gently folding the Pliocene-Recent deposits. Two main transcurrent systems have been recognized to segment the continental margin: the Amendolara Transpressive System and the new Apulian Transpressive System on the foreland ramp never described before this study. The above structures played a major role in the Bradano basin tectonic evolution during two main tectono-stratigraphic events. During middle-upper Pliocene, the Amendolara Transpressive System, a left-lateral strike-slip zone, segmented the Southern Apennine thrust fronts actively moving toward E onto the Apulian plate along a shallow detachment surface. At the end of this stage, the Southern Apennines frontal thrusts could thrust over the Pliocene Bradano Foredeep Basin as well as the underlying western portion of the Apulian Plate. The Apulian Transpressive System was active and, locally, extensional faults were inverted. During the second event (from Pleistocene to Present), the compressional deformations were localized at depths deeper than the subducted Bradano Foredeep Basin. Out-of-sequence thrusting reshaped the Southern Apennines orogenic wedge while, to the east, the Apulian Transpressive System and the inversion of extensional faults were still active. The proposed evolutionary model suggests that Bradano Basin, laying on top of the western margin of Apulian Plate, and the Apulian Foreland ramp are part of the Southern Apennines orogenic wedge whose outermost front can be located in the Apulian Foreland Ramp since Pliocene.

The M. Tancia regional thrust: geometric, kinematic and mechanical characterization within the Structural Geology course at La Sapienza

Berardo G., Bonaccorso L., De Filippis G., Di Carlo L., Di Renzo M. E., Emili E., Gencarelli G., Iammarino C., Lavaroni F., Locchi M. E., Modesti M., Mosconi F., Pardo S., Perrotta V., Pignalberi F., Rinaldi F., Ruggiero G., Solfanelli M., Tedesco C., Valente M., Scuderi M., Curzi M., Marmoni G.M., Mercuri M. & Collettini C.*

Dipartimento di Scienze della Terra, Università La Sapienza, Roma.

Corresponding email: cristiano.collettini@uniroma1.it

Keywords: Fault, friction.

Within the Structural Geology course of the BSC degree at La Sapienza University we have studied the geometry, kinematics and mechanics of a regional thrust fault exposed near Rieti (Lazio) and deformed during the Apenninic compressional phase. The fault is a km-scale displacement structure trending N-S and gently (10-20°) westward dipping. The thrust superposes the Maiolica (Early Cretaceous) over the Scaglia Variegata (Eocene) Formations and it is represented by a 6-8 m thick foliated (SCC' tectonites) shear zone.

Small displacement normal faults showing cataclastic fault rocks, cut the foliated fabric.

We have used SCC' tectonites to characterize the kinematic evolution of the fault zone. We have detected two sets of SCC' fabric: one set shows a top to the east sense of shear that is consistent with the compressional phase, the second set overprints the first one and is characterized by a top the west kinematics likely due to the quaternary extensional phase of the area.

The fault zone is characterized by two main types of fault rocks: principal slipping zones are affected by cataclastic processes, producing grain size reduction and localization; fluid assisted dissolution and precipitation processes promote the development of a distributed foliation within the entire fault zone. During the compressional phase the fault accumulated kilometers of displacement as a well-oriented structure within an Andersonian compressional regime. In the following Quaternary extension, some portions of the shear zone were reactivated via optimally oriented small normal faults, other portions of the fault zone were reactivated as misoriented structures (gently dipping planes) within the Andersonian extensional regime. This misoriented reactivation was likely promoted by clay concentration within the fault planes following pressure-solution processes.

Structural and paleofluid evolution during and after the growth of the Parmelan Anticline, Bornes Massif, Western Alps

Berio L.*¹, Balsamo F.¹, Bistacchi A.², Mitterpergher S.² & Storti F.¹

¹ Dipartimento di Scienze Chimiche, della Vita e della Sostenibilità Ambientale, Università di Parma.

² Dipartimento di Scienze dell'Ambiente e della Terra, Università Milano-Bicocca.

Corresponding email: luigi.berio@gmail.com

Keywords: folding, deformation pattern, carbonates.

In the northern Subalpine massifs and in the Belledonne area, a regional dextral transpression is active since late Neogene times and produced NE-SW en-echelon dextral and NW-SE sinistral faulting. In the Bornes Massif (the northernmost Subalpine massif) and in the neighboring areas (Annecy-Bonneville), well-documented seismic activity (e.g. Grand-Bornand, 1994 and Epagny, 1996 earthquakes) indicates that this strike-slip-dominated stress regime is still active nowadays in this region of the Western Alps. Despite this geodynamic configuration has been investigated in several recently published seismotectonic studies, no geometric and kinematic data were presented to constrain at the mesoscale the complex deformation pattern resulting from the superposition of such transpression-related structural assemblage (formed in response to an E-W-striking σ_1) onto the older deformation pattern developed during a long-lasting, mainly compressional, history (dominated by a NW-SE-striking σ_1). In this contribution, we present the reconstruction of the deformation pattern in the Parmelan anticline, the more external structure of the Bornes Massif. For this purpose, we combined detailed field mapping and structural data with microstructural, petrographic, geochemical (stable carbon and oxygen isotopes) and microthermometric analyses of calcite-filled tectonic veins sampled in the Lower Cretaceous Urgonian Limestones. The NE-SW trending Parmelan anticline is a box fold characterized by steeply dipping limbs separated by a wide flat-lying crestral plateau. Fold limbs were localized by inherited pre-folding extensional fault zones. The oldest structural assemblage includes transversal calcite-filled fibrous veins, frequently forming conjugate en-echelon arrays, and conjugate subsidiary reverse faults with associated horizontal veins, interpreted as part of a well-developed pre-folding deformation pattern formed under NW-SE layer-parallel compression. These calcite-filled veins as well as different sets of syn-folding deformation structures have oxygen isotopic values of $-8\text{‰} < \delta^{18}\text{O V-PDB} < -2\text{‰}$ and carbon isotopic values of $0\text{‰} < \delta^{13}\text{C V-PDB} < +2\text{‰}$ very similar to those displayed by the host-rock, thus suggesting a dissolution-re-precipitation process active in a closed and rock-buffered system. During late-stage transpression, the (re)activation of NNW-SSE and ENE-WSW strike-slip faults produced a pervasive post-folding deformation assemblage including oblique (with respect to the fold axis) E-W veins with associated N-S stylolites. Oxygen isotopic values of $-17\text{‰} < \delta^{18}\text{O V-PDB} < -11\text{‰}$ of vein and fault breccia cements indicate that late-stage fault zones acted as high-permeability pathways for more ^{18}O -depleted mineralizing meteoric fluids, possibly mixed with subsurface waters. According to our microthermometric data and assuming a mineralizing fluid in thermal equilibrium with the host rock, we can speculate that the opening of the paleofluid system, caused by post-folding regional transpression, started under maximum burial temperature (70-90 °C) and progressed during exhumation of the Parmelan anticline.

Validation of structural and depositional models for a reservoir study in southern Apennines: uncertainty quantification by means of discrete geological scenarios

Bitonte R.*¹, Bellentani G.², Dall'Igna M.², Livio F.¹, Ciabbarri F.² & Scaramuzzo E.¹

¹ Università degli Studi dell'Insubria, Como, Italy.

² Edison E&P Spa, Milan, Italy.

Corresponding email: rbitonte@uninsubria.it

Keywords: structural, scenarios, reservoir.

Among the HC Italian provinces, the Southern Apennines Thrust belt and Bradanic Foredeep raised interests in exploration and exploitation since the second half of twentieth century (Holton, 1999; Casero, 2004). Most of the exploited gas field (biogenic gas) sourced by Pliocene-Pleistocene clays in the Bradanic foredeep turbiditic deposits, where our study area is located. The post-Messinian Apennines foredeep, migrated towards the east, through successive deformative phases, during the Pliocene and early Pleistocene. Together with the Murge peripheral forebulge (i.e., the Apulian Foreland), the Bradanic foredeep is the shallow crustal expression of the Adria lithospheric subduction (Lazzari, 2008).

The structural interpretation of a gas field, located in this setting and exploited by Edison S.p.A., is particularly challenging in this sector, despite a huge dataset of subsurface prospecting.

Significant uncertainties come out from the following shortcomings:

- low quality of 2D seismic data;
- difficulties to create an appropriate Velocity Model;
- the complexity of depositional environment and related well correlations;
- the choice of a correct structural paradigm for the interpretation of a poorly-imaged subsurface sector.

These uncertainties lead to generate different interpretative scenarios that have to be validated from a geological point of view (i.e., structural and depositional viability), in order to build reliable 3D reservoir models and to reconstruct the structural and depositional evolution through time (e.g., Bond et al., 2007). Structural validation has been approached performing sequential 2D restoration for different interpreted scenarios.

Structural and stratigraphic scenarios will be combined to create a tree of possible 3D models (i.e., discrete scenarios) that will be populated with reservoir properties and associated uncertainties, obtained from well data analysis. Finally, these alternative discrete scenarios will be the elements for the evaluation and quantification of static and dynamic reservoir uncertainties and possible prospects.

Bond C.E., Gibbs A.D., Shipton Z.K. & Jones S. (2007) - What do you think this is? "Conceptual uncertainty" in geoscience interpretation. *GSA Today*, 17 (11), 4.

Casero P. (2004) - Structural setting of the Petroleum Exploration Plays in Italy. Special Volume of the Italian Geological Society for the IGC 32 Florence-2004

Lazzari M. (2008) - Il comportamento tettonico e sedimentario del bacino d'avanfossa Bradanica durante il Pleistocene inferiore. *Mem. Descr. Carta Geol. d'Italia*, 77, 61–76.

Holton J. (1999) - Oil and Gas Potential – Offshore Southern Italy. *Oil and Gas Journal*, 97(48), 49-51.

Low temperature cyclical switching between brittle and ductile deformation inferred from microstructural analysis of quartz shear veins

Cerchiari A.*¹ & Fagereng A.²

¹ Dipartimento di Scienze Chimiche e Geologiche, Università di Modena e Reggio Emilia, Italia.

² School of Earth and Ocean Sciences, Cardiff University, Wales, UK.

Corresponding email: anna.cerchiari@gmail.com

Keywords: brittle-ductile transition, quartz vein microstructure, subduction thrust fault.

The Mona Complex on Anglesey and Llŷn Peninsula (NW Wales) has been interpreted as a fragment of a ~ 600-500 Ma Pacific-type subduction-accretion complex (Maruyama et al., 2010), built up by imbrication of several units on the NW margin of Avalonia overthrusting the Iapetus Ocean. The oldest rocks belong to the Gwna Group and are interpreted as disrupted and repeated ocean floor stratigraphy, accreted in the early stages of subduction. An accretion-related fault zone crops out in the SW Llŷn Peninsula, where superimposing slivers of dark mudstones with more competent carbonate and chert boudins are cut by subparallel thrust faults with an average inclination of 30°. Quartz shear veins with slickenfibers indicate a mean S-directed thrusting. A well developed foliation dipping 60° to 75° has developed.

In the microstructure, multiple stages of vein opening are recognizable, including early high-angle millimeter-thick extensional veins related to fracture boudinage of competent layers and foliation-parallel or oblique extensional veins, locally deformed by pressure solution. All these structures are cut by crack-and-seal shear veins on thrust surfaces.

All the studied veins are at least locally affected by intracrystalline deformation in quartz to varying extent, as suggested by deformation lamellae, twinning and subgrains, up to initial bulging recrystallization. Older veins appear extensively deformed by ductile mechanisms, while younger shear veins are unevenly affected: some of them have low intracrystalline strain without evidences of recovery, while other show complex recrystallization with fine grained crystals (<100 µm) along microtransforms and larger grains (up to 2 mm) enclosing insoluble fragments. The maximum temperature inferred from the plastic deformation would be around 350 °C (Stipp et al., 2002), if experimental data are extrapolated to a natural strain rate. Anyway, the host rock subgreenschist mineral assemblage without development of a schistose cleavage suggests a lower temperature.

The described microstructure suggests a cyclical shifting from brittle to ductile deformation, mainly controlled by the variation in strain rate coupled with overpressured fluid pulses. Hydrolytic weakening mechanisms and relatively slow strain rate during ductile deformation could have allowed dynamic recrystallization to occur at a temperature lower than 300°C.

Maruyama S., Kawai T. & Windley B.F. (2010) - Ocean plate stratigraphy and its imbrication in an accretionary orogen: the Mona Complex, Anglesey-Llŷn, Wales, UK. In Kusky T.M., Zhai M.G. & Xiao W. (eds): *The Evolving Continents: Understanding Processes of Continental Growth*. Geological Society, London, Special Publications, 338, 55-75.

Stipp M., Stünitz H., Heilbronner R., & Schmid S.M. (2002) - The eastern Tonale fault zone: a “natural laboratory” for crystal plastic deformation of quartz over a temperature range from 270 to 700 °C. *Journal of Structural Geology*, 24, 1861-1884.

Architecture and evolution of an extensionally-inverted thrust (Monte Tancia thrust, central Apennines, Italy): geological, structural, geochemical, and K-Ar geochronological constraints

Curzi M.*¹, Carminati E.¹, Aldega L.¹, Berra F.², Billi A.³, Van der Lelij R.⁴ & Viola G.⁵

¹ Dipartimento di Scienze della Terra, Sapienza Università di Roma (Rome, Italy).

² Dipartimento di Scienze della Terra “Ardito Desio”, Università degli Studi di Milano (Milano, Italy).

³ Consiglio Nazionale delle Ricerche, IGAG (Rome, Italy).

⁴ Geological Survey of Norway (Trondheim, Norway).

⁵ Dipartimento di Scienze Biologiche, Geologiche e Ambientali, Università degli Studi di Bologna (Italy).

Corresponding email: manuel.curzi@uniroma1.it

Keywords: tectonic inversion, deformation mechanisms, K-Ar dating.

Deformation in the upper crust is heterogeneous and mostly localized along brittle faults. Faults and fault rocks may be weak compared to surrounding host rocks and are likely to accommodate repeated slip episodes due to structural reactivation during commonly fluid-assisted faulting events. Thrust fault reactivation by subsequent normal faulting has been commonly documented in orogenic wedges, where extensional tectonics often follows contraction. Fault inversion may lead to variable overprinting of the early tectonic fabrics, which prevents a straightforward interpretation of the complete fault kinematics and deformation history. For this reason, and due to the seismogenic potential of upper crustal faults, much effort has been invested into a better understanding of the architecture of faults, of their deformation mechanisms as well as kinematic evolution through time. In this study, we adopt a multidisciplinary approach to reconstruct the tectonic evolution of the exhumed Monte Tancia Thrust (MTT), central Italy, consisting of a W-dipping thrust fault later inverted into a normal fault. To this goal, we combined: 1) 1:5000 scale geological mapping of an area of about 15 km² and detailed structural analysis both in the hanging wall and in the footwall of the MTT; 2) microstructural analysis of the thrust wall and fault rocks; 3) cathodoluminescence microscopy (CL); 4) X-ray diffraction (XRD) analysis of the clay content of the MTT fault rocks and surrounding undeformed blocks to evaluate their thermal evolution and 5) K-Ar dating of authigenic synkinematic illite. Further geochemical analyses such as stable and clumped isotopes of calcite mineralizations are in progress. The MTT is a 200 m thick shear zone characterized by a pervasive S-CC' fabric associated with contractional top-to-ENE kinematics (S1 foliation). Within the first few metres below the thrust surface, a zone dominated by the partial superimposition of S-CC' fabric showing an extensional top-to-W-SW movement (S2 foliation) on top of the earlier compressional fabric is prominent. Cathodoluminescence suggests that the compressional and extensional deformation stages were facilitated by fluid ingress in the deformation zone, but that the fluid did not undergo significant changes in chemistry. To evaluate the thermal evolution of the MTT and constrain the timing of the tectonic inversion, XRD and K-Ar datings are respectively now in progress. Based on our observation, we speculate that the S1 foliations mainly developed by repeated events of fluid overpressure leading to multiple crack-and-seal events characterized by several veining episodes, followed by pressure-solution creep. S2 foliation characterized by fibrous calcite developed under fluid pressure fluctuations simultaneous with the fault slip in a normal sense.

The superposition of non-coaxial extensional events in rift basins: a case study from the Utsira High

D'Intino N.*¹, Scisciani V.¹ & Esestime P.²

¹ Department of Engineering and Geology, University of Chieti and Pescara, Italy.

² Spectrum Geo Ltd., Dukes Court, Surrey, United Kingdom.

Corresponding email: nico.dintino@unich.it

Keywords: normal faults, seismic reflection, rift systems.

From Devonian to Paleogene the North Sea rift system was affected by several extensional events, which led to the formation of non-collinear arrays of normal faults. During Permo-Triassic times, following the post-orogenic collapse of the Caledonian orogen, a trilate rift system started to open. The zone of junction of these three branches was affected by different sets of fractures which, as they interacted, resulted in a very complex framework. These faults arrays derived both by the growth of new fault segments and by reactivation of pre-existing discontinuities.

The Utsira High, a long-lived basement high, is located close to the zone of convergence of these three rift arms; it is bordered to the west by the Viking Graben and to the east by the Stord Basin, which are approximately NNE-SSW trending. The aim of this work has been to characterize the fault arrays in this area and to reconstruct the complex evolution of the Utsira High, Viking Graben and Stord Basin by the interpretation of a large seismic volume extracted from the Spectrum Seamless multi-survey.

Several key reflectors, from the Paleogene to the Basement, were interpreted and age-constrained by well-tie calibration, using numerous exploration borehole drilled in the area. Seismic attributes, such as similarity and coherence, were extracted from the seismic volume to define the faults patterns. Syn-rift sequence have been defined all over the area, and syn-growth sedimentary wedges in the hanging-walls of the normal faults have been studied and age constrained. Orientation and cross cutting/abutting relationship analysis allowed us to discriminate the faults sets active or reactivated in different times.

In the structural-stratigraphy evolution of the study area, five different stages have been observed: i) a Paleozoic phase, affecting mainly the Stord Basin and a mini-basin in the Utsira High, with NE-SW trending structures; ii) a Triassic-early Jurassic phase, in the Stord Basin and in the Heimdal Terrace, characterized by NNW-SSE trending elements; iii) a late Jurassic-early Cretaceous event, mainly in the Viking Graben and west flank of the Utsira High, with N-S trending faults; iv) a late Cretaceous extension, with evidences in the Stord Basin, Utsira High and Viking Graben with an anomalous E-W trend; v) a final compression during the Paleocene, with a NE-SW trend.

Paleo-depth of fault activity: testing a method based on inversion of fault-slip data

Federico L.*¹, Maino M.², Crispini L.¹ & Capponi G.¹

¹ DISTAV - Università degli Studi di Genova.

² Dipartimento di Scienze della Terra e dell'Ambiente - Università degli Studi di Pavia.

Corresponding email: federico@dipteris.unige.it

Keywords: fault-slip data, depth of fault activity, fault exhumation.

Evaluating the depth of fault activity is a challenging task: we propose a new method that is particularly valuable for inactive, exhumed fault for which seismic data can't be used.

Paleostress calculations using fault-slip data yield the reduced stress tensors, i.e. the orientation of principal stress axes ($\sigma_1 > \sigma_2 > \sigma_3$) and the ratio of the difference between principal stress magnitudes.

The complete stress tensor (defined by six independent variables) can be reconstructed calculating the two remaining unknowns, using the rupture and friction laws (Angelier, 1989).

Then we need some constraints on the pore pressure to infer a depth interval of fault activity. Our method thus consists of four steps:

- 1 - collect fault slip data;
- 2 - calculate the reduced stress tensor through inversion of fault-slip data (we used the FSA software by Célérier, 1999);
- 3 - calculate the complete stress tensor using:
 - 3a) The friction law; the initial friction law is considered linear and intersecting the origin. We need inherited faults, reactivated under the investigated stress field, which correspond to points that should lie on or above the initial friction line and below the failure envelope. As a consequence, the lower boundary of the cloud of points defines the friction line. This operation fixes the abscissa origin of the Mohr diagram.
 - 3b. The rupture law. We use the rupture law of Hoek & Brown (1980):

$$\sigma'_1 = \sigma'_3 + \sigma'_{ci} \left(m \frac{\sigma'_3}{\sigma'_{ci}} + s \right)^{0.5}$$

where σ'_1 and σ'_3 are the major and minor effective principal stresses at failure; σ_{ci} is the uniaxial compressive strength of the intact rock and m and s are material constants.

Moreover, in our fault population, we identified couples of conjugate faults, neofomed by definition. The angle between these faults (2θ angle) fixes a point on the largest Mohr circle, where the rupture law has to be tangent. This defines the scale of the axes, and therefore the values of the principal stresses.

4 - Define paleodepth

The principal stresses closest to vertical represents the vertical stress (σ_v) and therefore the lithostatic load. We can then calculate paleo-depth, assuming the average density of overlying rocks and the hydraulic conditions (i.e. the amount of pore pressure, Pf), using this expression:

$$\sigma'_v = (\rho - \rho_w)gz$$

with ρ = density of the overburden, ρ_w = density of water, g = acceleration gravity (9,81 m/s²), z = depth, and $\sigma'_v = \sigma_v - P_f$, where σ'_v is the effective vertical stress.

We report here our preliminary test of the method in some well-constrained geological occurrences, and show that the calculated depth of fault activity fits well the depth derived from independent, stratigraphic investigations.

Angelier J. (1989) - From orientation to magnitudes in paleostress determinations using fault slip data. J. Struct. Geol., 11, 37-50.

Célérier B. (1999) - Fault Slip and Stress Analysis (FSA).

Hoek E. & Brown E.T. (1980) - Underground Excavations in Rock. London: Institution of Mining and Metallurgy, 527 pp..

Thick-skinned tectonics in orogenic forelands: the external western Alps and the western US Laramide Province case studies

Lacombe O.*

Sorbonne Université.

Corresponding email: olivier.lacombe@sorbonne-universite.fr

Keywords: basement-involved shortening, weakening, Alps, Laramide.

Many fold-and-thrust belts (FTBs) exhibit basement-involved shortening giving birth to large, highly-elevated uplifted basement units. Thick-skinned tectonics usually involves deformation along crustal thrust ramps. It is generally admitted that a key process by which basement becomes involved in shortening is the inversion of pre-existing extensional faults and that basement involvement requires a mechanically weak lithosphere and a significant degree of coupling between the hinterland and the foreland.

I address herein some specific questions related to P-T conditions, mechanisms, timing and sequence of deformation /exhumation of basement units in two different settings : the alpine External Crystalline Massifs (ECMs) formed at the expense of the lower plate in a collision orogen and the Laramide Province that developed within the upper plate of a subduction orogen.

In the ECMs, Cenozoic basement shortening occurred first by distributed shearing or stacking of crustal slices during a long-lasting (~10 Ma) temperature peak (330-400°C) related to burial (10-15 km) under the Penninic nappes, reflecting underplating without orogenic wedge widening, then by frontal accretion/exhumation thanks to localized crustal thrust ramps in a later stage of orogenic wedge widening. Basement shortening and exhumation, as constrained by geo/thermochronometry and by the sedimentary record in the adjacent molassic basin, show a consistent westward sequence. In the Oisans, basement « folding » inferred from the curved cover-basement interface is closely associated with top-to-the-W low-angle brittle-ductile Alpine shear zones. The formation of these distributed shear zones, together with the absence of reactivation of the extensional faults inherited from the Mesozoic Tethyan rifting, reflects an efficient crustal thermal weakening during collisional burial.

The Laramide belt consists of the deformed and disrupted foreland of the former Sevier orogen and formed in response to the long-lasting subduction of the Farallon plate at the expense of the North American cratonic upper plate during late Cretaceous-Paleogene. The belt exhibits a network of anastomosing basement-cored anticlines and uplifts separated by broad basins. The basement arches are bounded by moderate-dipping crustal thrusts, likely resulting from the reactivation of Precambrian normal faults. Basement rocks were mainly brittlely deformed at shallow depth (about 2.5 to 5 km) and at a temperature of about 70–120°C. Laramide cover folding is not related to true basement « folding » but is instead associated with distributed damaging of basement rocks by pervasive fluid-assisted faulting/fracturing and/or cataclasis ahead of the propagating thrust. The arches were exhumed first at slow rate then at higher rate in an overall eastward (cratonward) sequence of deformation, although a westward sequence of uplift is documented in place. This somewhat erratic sequence is probably linked to the heterogeneous and complex stress transmission and accommodation of shortening through the crystalline basement with inherited weaknesses and anisotropies.

In FTBs resulting from inversion of former proximal passive margins (eg, western Alps), basement thrusting therefore requires structural inheritance and/or thermal weakening either inherited from a recent (pre-orogenic) rifting event or resulting from synorogenic underplating and heating. The development of thick-skinned belts within cratons (eg, Laramide) occurs in colder conditions and remains somewhat enigmatic ; it requires specific boundary conditions (strong interplate coupling, such as provided by flat-slab subduction) ensuring efficient transmission of far-field stresses at the crust /lithosphere level, in addition to local structural and/or physical /compositional weakening.

Out-of-sequence thrusting from marine to phreatic conditions in the Gran Sasso Massif, Central Apennines, Italy

Lucca A.¹, Storti F.¹, Balsamo F.¹, Clemenzi L.*¹, Fondriest M.², Burgess R.³ & Di Toro G.^{2,4}

¹ NEXT - Natural and Experimental Tectonics research group, Department of Chemistry, Life Sciences and Environmental Sustainability, University of Parma, Italy.

² Dipartimento di Geoscienze, Università degli Studi di Padova, Italy.

³ School of Earth, Atmospheric and Environmental Sciences, University of Manchester, UK.

⁴ Istituto Nazionale di Geofisica e Vulcanologia, Roma, Italy (Now at ENI S.p.A, Upstream and Technical Services - San Donato Milanese, Italy).

Corresponding email: alessio.lucca@unipr.it

Keywords: out-of-sequence thrusting, stable isotopes, noble gases.

The Gran Sasso Massif arc-shaped fold-thrust stack constitutes the most prominent topographic relief in the Apennine orogenic wedge. It developed in Messinian-Pliocene times in response to the westward subduction of Adria and related slab rollback, which caused in-sequence and out-of-sequence thrusting affecting the Adria passive margin carbonatic sedimentary succession and the siliciclastic foredeep deposits. We performed a multidisciplinary study of the Monte Camicia and Vado di Ferruccio thrusts, at the top of the Gran Sasso thrust stack. Our work includes field mapping, structural analysis, standard and cold cathodoluminescence microscopy, oxygen, carbon, strontium and noble gases stable isotopes. Field mapping and structural data indicate that the thrusts formed in an out-of-sequence fashion resulting in younger-on-older stratigraphic contacts in the Monte Camicia Thrust while the Vado di Ferruccio Thrust cuts fold axes formed during in-sequence thrusting-related deformation. Structural data indicate top to the N and top to NNE for the Monte Camicia and Vado di Ferruccio thrusts, respectively. Microstructural investigations in the thrust zones allowed to discriminate their deformation mechanisms, which are drastically different, being dominated by cataclasis in the Monte Camicia Thrust and by pressure-solution in the Vado di Ferruccio Thrust. In the latter, geochemical analyses indicate that syntectonic dolomitization occurred during circulation of fluids with marine affinity. Conversely, syntectonic cements in the Monte Camicia Thrust crystallized from meteoric phreatic to vadose fluids favouring dolomite calcitization. Moreover, stable isotopes allow us to exclude deep crustal fluid circulation during out-of-sequence thrusting related deformation. Accordingly, Messinian to Pliocene out-of-sequence thrusting in the Gran Sasso thrust stack progressed from submarine to subaerial conditions.

A new geological map of the high Sillaro Valley (Northern Apennines, Italy)

Panini F.¹, Bettelli G.¹, Carlini M.², Fioroni C.¹, Nirta G.³ & Remitti F.*¹

¹ Dipartimento di Scienze Chimiche e Geologiche, Università di Modena e Reggio Emilia.

² Dipartimento di Scienze Biologiche, Geologiche e Ambientali, Università degli Studi di Bologna.

³ Dipartimento di Scienze della Terra, Università di Firenze.

Corresponding email: francesca.remitti@unimore.it

Keywords: Northern Apennines, chaotic rocks, mélange

The “Sillaro Line”, the NE segment of the “Livorno-Sillaro Line”, is one important transverse lineament of the northern Apennines of Italy. In this area, the Ligurian wedge and its sedimentary cover overthrust on the middle Miocene-Pliocene foredeep deposits of the Umbro-Marchean succession, the Marnoso Arenacea formation (MAF). This structural superposition occurred through the interposition of a thick chaotic body, formed by two different sub-units (chaotic unit A and B, Bettelli & Panini, 1992). These chaotic bodies have been recently interpreted as part of the Sestola Vidiciatico tectonic unit (SVU), defined as a tectonic mélange forming the shear zone between the Ligurian wedge and the foredeep deposits of the Adria plate (Vannucchi et al., 2008). The SVU components derive from the frontal part of the Ligurian wedge and its Eocene to Langhian sedimentary cover.

Along the Sillaro line another chaotic body, formerly known (Landuzzi, 2006) as the “Visignano olistostrome” (VIS) forms a large intercalation ~200-300 m thick, within the upper Serravallian-lower Tortonian MAF. Similarly to SVU components, the VIS derive from the frontal part of the Ligurian wedge and its Eocene to Serravallian cover.

We present a new geological map of the area based on: i) a detailed 1:10.000 mapping of key localities and ii) new biostratigraphic data. The detailed investigation of the components of the VIS in relation to the components of the overriding plate and the SVU, here subdivided in SVUa and SVUb, help to better define which was the architecture of the frontal part of the Ligurian wedge at the time of the sealing of the VIS by the younger MAF and to constrain the timing of the deformation phases affecting this portion of the northern Apennines.

The new data suggest that: (i) after the late Serravallian, the SVU no longer represented the northern Apennines interplate shear zone, as suggested by the synsedimentary deformation of the MAF; (ii) before early Serravallian the components of both SVUa and SVUb were not completely underthrust and they formed the frontal part of the Ligurian wedge; (iii) after the emplacement of the VIS, SVUb and the overlying Ligurian wedge were progressively detached from the underlying SVUa by a major shallow-dipping fault characterized by top to the NE kinematics.

Bettelli G. & Panini F. (1992) - Liguridi, mélanges e tettoniti nel complesso caotico lungo la “linea del Sillaro” (Appennino Settentrionale, Province di Firenze e Bologna). Mem. Descr. Carta Geol. d'It., 46, 387–415.

Landuzzi A. (2006) - Syn-depositional emplacement of the Liguride allochthon in the Miocene foredeep of the western Romagna Apennines. In Pasquarè G. & Venturini C. (Eds.): Mapping Geology in Italy: Florence, Italy, Società Elaborazioni Cartografiche, 219–226.

Vannucchi P., Remitti F. & Bettelli G. (2008) - Geological record of fluid flow and seismogenesis along an erosive subducting plate boundary. Nature, 451(7179), 699–703.

Multiproxy Burial and Exhumation Numerical Modelling of the late Miocene succession of the Eastern Romagna Apennines: implications for Messinian salinity crisis-related deposits diagenetic products

Rossi F.P.*¹, Corrado S.²⁻³, Lugli S.⁴, Manzi V.¹, Reghizzi M.¹, Roveri M.¹ & Schito A.²⁻³

¹ Department of Chemistry, Life Science and Environmental Sustainability. University of Parma, Italy.

² Department of Sciences. University of Roma Tre, Italy.

³ Academic Laboratory of Basin Analysis (ALBA), University of Roma Tre, Italy.

⁴ Department of Chemistry and Geological Sciences. University of Modena and Reggio Emilia, Italy.

Corresponding email: francescopaolo.rossi@studenti.unipr.it

Keywords: Eastern Emilia-Romagna, Apennines, Multiproxy Numerical Thermal Modelling.

The Eastern Romagna sector of the Northern Apennine is a key area for studying the Messinian salinity crisis (MSC, 5.971 - 5.33 Ma) deposits that accumulated in both shallow-, e.g. the wedge-top marginal Vena del Gesso basin; VdG, and deep-water environments, e.g. the inner foredeep Giaggiolo-Cella (GCS) and Sapigno (SS) synclines. A robust stratigraphic correlation between these basins, based on detailed facies analysis of the evaporitic and siliciclastic deposits allowed the reconstruction of the geological history of this sector of the Apennines (Roveri et al., 2008 and references therein). However, some uncertainties on burial and exhumation processes affecting the MSC deposits as well as the whole regional Apennines sector, are still present, in terms of timing and sedimentary thickness; this is mainly related to the erosion of mostly of the Plio-Pleistocene succession due to the Apennines uplift (during the last 4 My) and to the discontinuous tectonic activation of the main thrusts fronts.

In order to solve this issue and provide a plausible burial-exhumation scenario, we present here a multiproxy numerical modelling thermal history reconstruction, based on three main constraints: i) high-resolution chronostratigraphic models, ii) Vitrinite Reflectance (Vr%) new dataset and iii) thermal-related evaporite mineralogy. the latter is provided by the gypsum-anhydrite transition temperature ($T_{gat} = 52^{\circ}\text{C}$; Murray, 1964).

In the study area, the formation of anhydrite after gypsum induced by the lithostatic burial thermal heating is limited to those sector that were in deeper conditions during the MSC and is often associated to the formation of diagenetic sulphur derived from bacterial activities (BSR; Machel, 2001).

The main outputs of our thermal modelling point for:

- a present-day heat flow of 35 mW/m^2 for the whole area;
- $Vr < 0.5\%$ suggesting a general thermal immaturity of the organic matter of the late Miocene successions
- a mean burdening thickness of $\sim 800 \text{ m}$ where the gypsum was preserved (VdG basin);
- a mean burdening thickness of $\sim 1300 \text{ (GCS)}$ and $\sim 1900 \text{ m (SS)}$ where gypsum was turned to anhydrite;
- a period of time above T_{gat} necessary for diagenetic gypsum-anhydrite transition shorter than 270 Ka;
- a diagenetic sulphur formation occurrence when the organic-rich deposits laying below the evaporites temperature enter the temperature window of $50^{\circ} - 70^{\circ} \text{ C}$, conditions compatible with the BSR.

Roveri M., Bertini A., Cosentino D., Di Stefano A., Gennari R., Gliozzi E., Grossi F., Iaccarino S.M., Lugli S., Manzi V. & Taviani M. (2008) - A high-resolution stratigraphic framework for the latest Messinian events in the Mediterranean area. *Stratigraphy*, 5, 323-342.

Machel H.G. (2001) - Bacterial and thermochemical sulfate reduction in diagenetic settings - old and new insights. *Sedimentary Geology*, 140, 143-175.

Murray R.C. (1964) - Origin and diagenesis of gypsum and anhydrite. *Journal of Sedimentary Petroleum*, 34, 512-523.

Multidisciplinary study of the Miocene forebulge unconformity in central-southern Apennines

Sabbatino M.*¹, Vitale S.¹, Consorti L.¹, Corradetti A.², Arienzo I.³, Cipriani A.⁴ & Parente M.¹

¹ University of Naples Federico II.

² Texas A&M University at Qatar.

³ National Institute of Geophysics and Volcanology (INGV) - Vesuvius Observatory (OV).

⁴ University of Modena and Reggio Emilia.

Corresponding email: monia.sabbatino@unina.it

Keywords: forebulge, Sr-isotopes, Apennines.

The Miocene foreland of the central-southern Apennine fold-and-thrust belt has experienced pre-thrusting bulging, uplift and erosion caused by the bending of the subducting lithosphere and by the migration of the accretionary wedge. This tectonic stage is evidenced by: (i) a regional unconformity, separating Miocene shallow-water carbonates from underlying Cretaceous to Eocene carbonates, (ii) extensional fracturing and faulting in the uppermost part of the lithosphere, and (iii) the onset of flexural subsidence.

The regional forebulge unconformity in central and southern Apennines is generally represented by a paraconformity at the scale of the outcrop. A sharp surface separates the Miocene syn-orogenic carbonates from underlying pre-orogenic Cretaceous or Eocene carbonates. The Miocene rocks are mostly represented by shallow-water carbonates with red algae, bryozoans, bivalves, echinoids, and benthic Foraminifera. Some areas record also phases of subaerial exposure and non-marine to very proximal marine deposition.

Bed-perpendicular fractures are hosted both in the Cretaceous to Eocene pre-orogenic sequence and in the overlying Miocene syn-orogenic rocks. This early extensional event, characterized by systems parallel and orthogonal to the thrust front, is related to the extensional deformation in the peripheral bulge area, as evidenced by fractures in the pre-orogenic substrate filled and sealed by Miocene calcarenite. Moreover, at the base of the Miocene carbonates there is evidence of syn-sedimentary tectonics. The age of forebulge extension is constrained by sedimentary infilling in fractures associated with the first Miocene transgressive sediments overlying the pre-orogenic passive margin mega-sequence.

In this work, we aim at constraining the migration of the forebulge unconformity through space and time by producing high-resolution ages for the very first syn-orogenic sediments above the unconformity. To overcome the limitations of biostratigraphy of Miocene shallow-water carbonates, which is plagued by low-resolution and poor chronostratigraphic calibration, we used Sr-isotope stratigraphy, which can achieve a resolution of 0.1-0.5 Ma for the Miocene interval.

We carried out a detailed structural and stratigraphic study on the deposits bracketing the forebulge unconformity in many localities of the southern and central Apennines, from Northern Calabria to the Majella massif. The unprecedented high-resolution dating attained by strontium isotope stratigraphy permits to constrain the foreland flexuration and the shortening rate by tracking the migration of the forebulge.

Present-day uplift of the European Alps: mechanisms and relative contributions

Sternai P.*¹

¹ Department of Earth and Environmental Sciences (DISAT), University of Milano-Bicocca, Italy

Corresponding email: pietro.sternai@unimib.it

Keywords: Alps, uplift.

The most updated measurements of surface vertical displacements of the European Alps show widespread rock uplift at rates of up to ~ 2.5 mm/a in the north-western and central Alps and ~ 1 mm/a across a continuous region from the eastern to the south-western Alps. Such uplift rate pattern is at odds with the horizontal strain rate field, characterized by shortening and crustal thickening in the eastern Alps and very limited deformation in the central and western Alps. Proposed climate- or tectonic-controlled mechanisms of uplift include lithospheric adjustment to the deglaciation, erosion and/or detachment of the western Alpine slab, as well as lithospheric and surface deflection due to the sub-Alpine asthenospheric flow. However, integrative quantifications of these contributions to match the currently observed surface vertical motion of the Alpine topography are lacking. Here, I critically resume previous quantifications and present new estimates of the contributions from all potential mechanisms. The lithospheric adjustment to deglaciation and erosion accounts for the majority of the observed surface uplift rate budget in the eastern Alps, which suggests that topographic growth by horizontal shortening and crustal thickening is hampered by subsidence due to the eastern Alpine slab pull or lateral escape of crustal material. In the central and western Alps, the lithospheric adjustment to deglaciation and erosion accounts for roughly half of the uplift rate budget, which points to a noticeable contribution by possible mantle-related processes such as detachment of the European slab and/or asthenospheric upwelling. Although to date it is difficult to constrain even the first order pattern and magnitude of mantle-controlled contributions to ongoing Alpine vertical displacements, cooperative tectonics- and climatic-controlled processes, rather than an individual forcing, best explain current measurements of Alpine uplift.

From layer-parallel shortening and duplexing to fold tightening and strike-slip compartmentalization in the External Dinarides orogenic wedge: the case of platform carbonates folded in the Pag anticline

Succo A.*¹, Mittempergher S.², Lucca A.¹, Bistacchi A.², Meda M.³ & Storti F.¹

¹ NEXT – Natural and Experimental Tectonics research group, University of Parma, Department of Chemistry, Life Sciences and Environmental Sustainability.

² Università degli Studi di Milano Bicocca, Department of Environmental and Earth Sciences, Milano, Italy.

³ ENI Spa, Upstream and Technical Services - San Donato Milanese, Italy.

Corresponding email: andrea.succo@studenti.unipr.it

Keywords: Duplex structures, LPS, platform carbonate, External Dinarides.

Classical fold evolution models are oversimplified in transpressional orogens and the interplay between thrusting and folding at the wedge toe result in deformation patterns and cross-cutting relationship that does not comply with classical templates, which are well-known in literature. The case of Pag anticline (External Dinarides, Croatia) offered us the opportunity, through extensive fieldwork, to document the interaction between folding and faulting from LPS stages to fold tightening, which occurred in a compressional to transpressional tectonic regime, respectively. The Pag anticline involves about one km of Cenomanian to Senonian tight platform carbonates, subdivided into three stratigraphic units (i.e., Gronji Fm., Sveti Duh Fm. and Milna Fm. from top to bottom, respectively), and overlain by an Eocene foreland succession (i.e. Foraminifera Limestone and Dalmatian Flysch). Through a multiscale, field- and laboratory-based (petrographic and microstructural observations, stable isotopes and fluid inclusion data) structural studies, we document fold architecture and timing relationships between deformational structures formed during progressive fold growth. Despite its position near the toe of the Dinaride thrust-belt, the Pag anticline shows a high structural complexity, including high-angle to vertical strike-slip fault zones trending roughly E-W and N-S, respectively. The absence of weak mechanical interlayers in the deformed succession, and the shallow depth environmental deformation conditions, as testified by structural diagenesis data, enhanced bedding-parallel shear accommodated by diffuse bed-parallel veins, conjugate thrust pairs, and duplexing, developed in an early layer-parallel shortening-dominated stage. With increasing contraction, duplexing, fixed-hinge limb rotation, major thrusting and backthrusting occurred, rotating previously-formed deformational structures. Late-stage fold tightening and fold exhumation was mainly accommodated by axial-oblique strike-slip fault zones bounding rotated blocks that compartmentalized fold geometry into sectors with different amounts of tightening. To conclude, our results indicate that progressive fold tightening developed in a dextral transpressive tectonic regime producing folding-related deformation patterns that deviate from classical templates and resulting from the interplay between (i) mechanical properties of the folded and faulted succession and (ii) pre-to syn-folding structural inheritance. This evidence should be taken in consideration in models aimed at understanding folding-related progressive deformations in orogenic wedges.

Geological record of the transition from induced to self-sustained subduction in the Oman Mountains

Tavani S.*¹, Corradetti A.², Sabbatino M.¹ & Mazzoli S.¹

¹ University of Naples “Federico II”, Naples, Italy.

² Department of Petroleum Engineering, Texas A&M University at Qatar.

Corresponding email: stefano.tavani@unina.it

Keywords: Slab-pull, Oman, Early-orogenic deformation.

Plate tectonics is driven by the negative buoyancy of the oceanic slab that pulls the lower plate toward the trench. Bending and offscraping of the lower plate are processes occurring at subduction zones and playing against plate motions. These localised dissipative processes cause extensional deformation in the bulge-foredeep region and thrusting and folding in the thrust wedge, respectively. Within this framework, widespread early orogenic extensional structures affecting pre-orogenic rocks of the lower plate of fossil subduction systems are commonly interpreted as induced by extension occurring in the forebulge-foredeep area. Slab pull is to date poorly considered as a potential causative process when interpreting basin-scale pre-shortening extensional structures. The problem of distinguishing slab-pull and foreland flexuring induced extensional structures relies in the fact that for most belts, slab pull and forebulge-foredeep flexuring are expected to produce extension roughly in the same direction (i.e. parallel to the foredeep-belt system) and, when syn-kinematic strata are not available, discriminating between these two processes is arduous. In this work we present a field investigation of basin-scale extensional faults from the lower plate of the Oman Mts. fossil subduction system. Syn-kinematic strata indicate that normal faults development largely anticipated extension in the bulge-foredeep region. In fact, it occurred during the transition from induced to self-sustained subduction, i.e. when the negative buoyancy of the slab started to exceed the resisting forces and the lower plate began to be pulled toward the trench. We propose that the documented faults record the onset of extension in the lower plate in response to slab pull initiation and, thus, that the reorganisation of forces acting on the lower plate during the transition from induced to self-sustained subduction can be invoked as a process able to produce extensional deformation.

U-Pb detrital zircon geochronology of Cretaceous-Eocene flysch basins of the N-E Adria plate

Velicogna M.*¹, Princivalle F.¹, Petrelli M.², Venier M.¹ & Lenaz D.¹

¹ Dipartimento di Matematica e Geoscienze, Università degli Studi di Trieste.

² Dipartimento di Fisica e Geologia, Università degli Studi di Perugia.

Corresponding email: matteoveli87@gmail.com

Keywords: geochronology, zircon, Adria Plate.

Detrital zircon geochronology is often used for having constraints about the relative old positions of tectonic plates and how they have moved-united-separated throughout times. An excellent zircon container are the flysch basins, which are filled by a huge quantity of material derived by orogenic tectonics. This contribution will study several narrow elongated turbidic basins (i.e. Julian, Brkini, Istrian and Zara basins) formed during the end of the Cretaceous and the entire Paleogene in the northeastern part of the Adria Plate. These basins suffered a mixed sediment supply due to the alternation of several triggering events that comprehend tectonic movements of the region and eustatic sea level changes. The mixed carbonatic and siliciclastic sediments supplies are supposed to belong to the Adriatic Carbonatic platform that are well represented in all the north eastern part of the Adria Plate and the ophiolitic-crystalline rocks outcropping mainly in the Dinarides (i.e. Lenaz et al., 2000, 2018; Tunis & Venturini, 1997). The rock samples have been crushed with a jaw grinder and mechanically sieved to obtain a grain size between 63 and 250 μm . Then magnetic and heavy liquid separation with tetrabromothane (2.97 g/cm^3) have been applied to isolate the non magnetic-heavy mineral fraction. Finally, optical microscope have been used for the mineralogical identification. Zircon abundance and dimensions (about 65-150 μm) resulted to vary among the basins, suggesting that the provenance area/s and the source/s changed through time. The aim of this work is to individuate the terranes involved in the supply of the flysch basins belonging to the north eastern part of the Adria Plate, comparing the different basins each other to understand if there were different line of supply and if possible to give constraints about the source rocks.

Lenaz D., Kamenetsky V.S., Crawford A.J. & Princivalle F. (2000) - Melt inclusion in detrital spinel from SE Alps (Italy-Slovenia): a new approach to provenance studies of sedimentary basins. *Contribution to Mineralogy and Petrology*, 139, 748-758.

Lenaz D., Mazzoli C., Velicogna M. & Princivalle F. (2018) - Trace and Rare Earth Elements chemistry of detrital garnets in the SE Alps and Outer Dinarides flysch basins: An important tool to better define the source areas of sandstones. *Marine and Petroleum Geology*, 98, 653-661.

Tunis G. & Uchman A. (1997) - Trace fossils and facies changes in Cretaceous-Eocene flysch deposits of the Julia Prealps (Italy and Slovenia): Consequences of regional and world-wide changes. *Ichnos, An international Journal for Plant and Animal Traces*, 4(3), 169-190.

S21

**Active tectonics and seismotectonics between Northern
Apennines and Southern Alps as a complex thrust belt -
foredeep system**

Conveners and Chairpersons

Riccardo Caputo (Università di Ferrara)

Emanuela Falcucci (INGV)

Maria Eliana Pioli (Università di Udine)

Francesco Emanuele Maesano (INGV)

A multidisciplinary approach to the structural setting and morphotectonics of the Eastern Monferrato Arc: new constraints to the seismic hazard assessment of a slowly deforming area

Bonadeo L.*¹⁻², Frigerio C.², Ferrario M.F.², Livio F.², Michetti A.M.², Bitonte R.², Scaramuzzo E.², Zerboni A.³, Porat N.⁴, Fioraso G.⁵, Irace A.⁵, Catanzariti R.⁵, Da Prato S.⁵, Ellero A.⁵ & Ottria G.⁵

¹ Istituto Nazionale di Geofisica e Vulcanologia.

² Dipartimento di Scienza e Alta Tecnologia, Università degli Studi dell'Insubria.

³ Dipartimento di Scienze della Terra "A. Desio", Università degli Studi di Milano.

⁴ Geological Survey of Israel.

⁵ CNR, Istituto di Geoscienze e Georisorse.

Corresponding email: livio.bonadeo@ingv.it

Keywords: Monferrato Arc, seismic risk, OSL dating.

The Monferrato Arc is the westernmost of the 3 frontal arcs pertaining to the N Apennine domain, locally buried beneath the thick alluvial cover of the Po Plain. Even if it is generally considered less active than the easternmost arcs, the Monferrato Arc has been recently incorporated in the INGV Database of Seismogenic Sources (DISS Working Group, 2018), including the tectonic structures classified as potential sources for earthquakes larger than Mw 5.5.

Extensive stratigraphic, geomorphological and seismic data were gathered in the 70s and 80s, in the framework of the National Nuclear Plan of Italy introduced in 1975. Recently, new reconstructions of the Late Pleistocene to Holocene evolution (e.g., Giraudi, 2015, 2016), and repeated recent earthquake surface faulting (Frigerio et al., 2017), has been documented in the E Monferrato Arc.

Nevertheless, our understanding of the active tectonics along the Monferrato Arc is hampered by the absence of detailed chronostratigraphic markers in the hilly sector, which indeed are more widespread in the Po Plain, to the North, and in the Alessandria Plain, to the South.

We performed some investigations in the eastern Monferrato, including: i) a brand new geological survey; ii) original stratigraphic and structural field surveys; iii) OSL and TT-OSL dating of 9 samples of fluvial and aeolian sediments; and iv) digitization and re-interpretation of deep seismic reflection surveys performed in the last decades and never published to date.

Our multidisciplinary approach allows to depict an updated reconstruction of the Late Quaternary evolution of the Alessandria and Valenza plateau. New chronological constraints provide the missing information to link the deformation rates and the geological evolution.

Despite the low seismicity of the Monferrato Arc its structural setting and its seismogenic potential suggest that the seismic risk of the area might be underestimated, due to the high exposure in terms of critical facilities, infrastructures and economic assets.

DISS Working Group 2018. Database of Individual Seismogenic Sources (DISS), Version 3.2.1: A compilation of potential sources for earthquakes larger than M 5.5 in Italy and surrounding areas, <http://diss.rm.ingv.it/diss/>

Frigerio C., Bonadeo L., Zerboni A., Livio F., Ferrario M.F., Fioraso G., Irace A., Brunamonte F. & Michetti A.M. (2017) - First evidence for Late Pleistocene to Holocene earthquake surface faulting in the Eastern Monferrato Arc (Northern Italy): Geology, pedomorphology and structural study of the Pecetto di Valenza site. *Quaternary International*, 451, 143-164.

Giraudi C. (2015) - Quaternary evolution of the plain between Casale Monferrato and Valenza: implications for the tectonics of the Monferrato Thrust Front (Piedmont, NW Italy). *Alpine and Mediterranean Quaternary*, 28(1), 71-92.

Giraudi C. (2016) - The evolution of the northernmost Apennine Front (Piedmont, Italy): Plio-Pleistocene sedimentation and deformation in the Po basin and Monferrato Hills. *Alpine and Mediterranean Quaternary*, 29(1), 45-65.

Tectonic cycles over a human lifetime: multi-decadal periodicity of strong seismicity in Italy (Alps-Apennines system)

Bragato P.L.*¹

¹ OGS - Istituto Nazionale di Oceanografia e di Geofisica Sperimentale.

Corresponding email: pbragato@inogs.it

Keywords: synchronous seismicity, seismic transient, periodicity.

It is generally assumed that geological processes act at a time scale much longer than the human lifetime. It is the case of earthquakes on a given fault, with return periods lasting from centuries to millennia. Differently from this common view, according to the catalogues of earthquakes available for the last millennium, the seismicity of Italy has been characterized by abrupt changes and almost regular cycles that took place at the country level within a few decades. In particular, these processes have led to the synchronization of the earthquake rates between the Alps and the Apennines, both in a compressional and extensional environment. Two features of the Italian seismicity are taken in consideration. The first one is a transient of increased activity that occurred between the 17th and the 20th centuries, that is apparently concluding in the last decades (Bragato, 2017a). Within the transient, it is possible to recognize the time clustering of the earthquakes with a periodicity of about 50 years (Bragato, 2017b). In particular, the last three clusters occurred at the beginning of the 20th century (earthquakes of Calabria, 1905; Messina, 1908; Marsica, 1915; Garfagnana, 1920); around 1970 (earthquakes of Belice, 1968; Friuli, 1976, and Irpinia, 1980) and in the last decade (L'Aquila, 2009; Emilia, 2012; Centro Italia, 2016). The aim of the present work is to describe the data set that is at the basis of the observations as well as to illustrate the considerations and the statistical tests that support the significance of the previous time features.

Bragato P.L. (2017a) - A statistical investigation on a seismic transient occurred in Italy between the 17th and the 20th centuries. *Pure and Applied Geophysics*, 174, 907-923.

Bragato P.L. (2017b) - Periodicity of strong seismicity in Italy: Schuster spectrum analysis extended to the destructive earthquakes of 2016. *Pure and Applied Geophysics*, 174, 3725-3735.

The effects of the Cenozoic Dinaric and Alpine orogenies in the Gulf of Trieste (North Adriatic Sea)

Busetti M.*¹, Zgur F.¹, Dal Cin M.¹, Vrabc M.², Baradello L.¹, Böhm G.¹, Brancatelli G.¹, Caffau M.¹,
Furlani S.³, Picotti S.¹ & Zampa L.S.¹

¹ Istituto Nazionale di Oceanografia e di Geofisica Sperimentale.

² Faculty of Natural Sciences and Engineering, University of Ljubljana, (Slovenija).

³ Dipartimento di Matematica e Geoscience, Università degli Studi di Trieste.

Corresponding email: mbusetti@inogs.it

Keywords: Gulf of Trieste, Adriatic Sea, Cenozoic orogenies.

The Gulf of Trieste (north-eastern Adriatic Sea), is a semi-enclosed shallow marine basin, that despite its small extension (about 40 x 20 km), presents a complex geological setting derived by its location in an area affected by both Dinaric and Alpine orogenies. The area was investigated during several geophysical surveys in the last decade acquiring multichannel and single channel seismic data.

During the Early Cenozoic Dinaric compression phase, the gulf represented the frontal part of the SW-ward advancing External Dinaric thrust system, and was initially buried by foredeep flysch sediments of Eocene age, then dissected by thrusts in the final stage of Dinaric deformation. As results, the Dinaric main structure is the Karst Thrust located at the eastern coast with more than 1600 meter of vertical displacement that is the southern prosecution of the Palmanova and Panzano thrusts buried below the Friuli Plain (Busetti et al., 2010; Dal Cin, 2018).

During the Alpine chain building, the Gulf of Trieste, located in the distal foreland area, was affected by northward tectonic tilting, and draped by sediment coming mainly from the northern relieves.

The Messinian and middle Pleistocene regressional events provided a unique regional unconformity in the westernmost part of the gulf that is an important marker also for dating the tectonic activity. In fact, fault strands belonging to the north-west/south-east fault system (Cenozoic Dinaric or Mesozoic extensional) have been displaced by some tens of meter the Messinian-middle Pliocene Unconformity with a transpressional kinematic, indicating a Late Cenozoic activity (Busetti et al., 2010). In the easternmost part of gulf, the Late Quaternary marine ingressions produced a coastal system of slopes and terraces. This system is presently buried from tens to hundreds meters, providing a further evidence of tectonic subsidence of the area (Zampa, 2016).

The main NW-SE tectonic structures crossing the gulf correlated with those occurring in the northern coast of the Istria peninsula, and those buried below the Friuli Plain, providing further information about geometries and timing of the onland/offshore tectonic.

Busetti M., Volpi V., Nicolich R., Barison E., Romeo R., Baradello L., Brancatelli G., Giustiniani M., Marchi M., Zanolla C., Wardell N., Nieto D. & Ramella R. (2010) - Dinaric tectonic features in the Gulf of Trieste (Northern Adriatic). *Boll. Geof. Teor. Appl.*, 51(2-3), 117-128.

Dal Cin M. (2018) - 3D velocity depth model in the Gulf of Trieste by means of tomographic analysis from multichannel seismic reflection data. PhD Thesis, University of Trieste, OGS & ICTP. 212 pp.

Zampa L.S. (2014) - Evidenze di subsidenza tettonica nel sistema di scarpata e terrazzi tardo-pleistocenici nel Golfo di Trieste. Tesi in Scienze Geologiche, Università degli Studi di Trieste, 63 pp.

Active seismotectonics of the Northern Apennines: insights from the 2012 Emilia earthquake sequence

Cheloni D.*¹, Giuliani R.², D'Agostino N.¹, Mattone M.², Bonano M.³, Fornaro G.³, Lanari R.³,
Reale D.³ & Atzori S.¹

¹ Osservatorio Nazionale Terremoti, INGV - Roma.

² Ufficio Rischio Sismico e Vulcanico, DPC - Roma.

³ Istituto per il Rilevamento Elettromagnetico dell'Ambiente, CNR - Napoli.

Corresponding email: daniele.cheloni@ingv.it

Keywords: northern Apennines, thrust, dislocation modeling.

The Northern Apennines thrust belt borders the southern edge of the Po Plain Quaternary alluvial plain, that is a densely populated region of the Northern Italy, hosting also significant productive activities and important historical centers. Although the external fold-and-thrust system of the Northern Apennines is buried under a thick cover of Plio-Quaternary sediments, evidence of its activity includes few moderate historical (Rovida et al., 2016) and instrumental (Selvaggi et al., 2001) earthquakes, the 2012 Emilia seismic sequence (Chiarabba et al., 2014), as well as recent GPS measurements which show motion in a N-S direction consistent with 1-2 mm/yr of active shortening accommodated along the external front of the Northern Apennines (Devoti et al., 2011). In this context of low tectonic strain, buried active seismogenic sources and sparse seismicity, dense geodetic surface displacements are therefore of fundamental importance to unravel the behavior of the seismogenic faults for a better seismic hazard estimation.

The 2012 Emilia earthquake sequence, which represents the largest Italian seismic sequence occurring in a continental active compressive regime that has been observed with modern geodetic measurements, provides valuable insights into fault activation and stress transfer between the continental thrusts that border the Po Plain to the south. Using dislocation modeling, we estimate the geometries and the distributions of slip during and after the two major events of the sequence and investigate the interaction between coseismic slip, aftershocks, and estimated patches of afterslip as well as the possibility of triggering of a pulse of aseismic slip on an adjacent fault segment during the 2012 Emilia sequence. Our results suggest that among continental en echelon thrusts, stress transfer and interaction between earthquakes and aseismic slip may play an important role in the way they activate during a seismic sequence.

Chiarabba C., De Gori P., Improta L., Lucente F.P., Moretti M., Govoni A., Di Bona M., Margheriti L., Marchetti A. & Nardi A. (2014) - Frontal compression along the Apennines thrust system: The Emilia 2012 example from seismicity to crustal structure. *J. Geodyn.*, 82, 98-109. <https://doi.org/10.106/j.jog.2014.09.003>.

Devoti R., Esposito A., Pietrantonio G., Pisani A.R. & Riguzzi F. (2011) - Evidence of large scale deformation patterns from GPS data in the Italian subduction boundary. *Earth Planet. Sci. Lett.*, 311, 230-241. <https://doi.org/10.1016/j.epsl.2011.09.034>.

Rovida A.N. Locati M. Camassi R.D. Lolli B. & Gasperini P. (2016) - CPTI15, the 2015 version of the Parametric Catalogue of Italian Earthquakes. Istituto Nazionale di Geofisica e Vulcanologia. <https://doi.org/10.6092/INGV:IT-CPTI15>.

Selvaggi G. et al., 2001. The Mw = 5.4 Reggio Emilia 1996 earthquake: Active compressional tectonics in the Po Plain, Italy. *Geophys. J. Int.*, 144, 1-13.

3D velocity depth model and seismic imaging of geological structures in the Gulf of Trieste (North Adriatic Sea), at the south-western edge of Dinarides and Alps

Dal Cin M.*¹, Busetti M.¹, Böhm G.¹, Picotti S.¹, Zgur F.¹ & Camerlenghi A.¹

¹ Istituto Nazionale di Oceanografia e di Geofisica Sperimentale.

Corresponding email: mdalcin@inogs.it

Keywords: Gulf of Trieste, 3D velocity depth model, depth seismic imaging.

The Gulf of Trieste is located in northern Adriatic, it represents the south-western foredeep of the NW-SE and E-W trending External Dinarides and South-Eastern Alps, respectively. Its sedimentary sequence consists of the Mesozoic-Paleogene Friuli-Dinaric Carbonate Platform, the Eocene turbiditic flysch, the Plio-Quaternary continental and marine sediments covering the Messinian Unconformity, which becomes Early-Pliocene in the eastern part (Busetti et al., 2010). In the Mesozoic, extensional regime generated NE-SW normal faults, allowing the aggradation of the carbonate platform. Late Cretaceous-Paleogene Dinaric orogeny gradually developed SW, deflecting the carbonate platform E-ward and depicting the north-eastern gulf shoreline with the Karst Thrust. This expresses the main frontal ramp of the External Dinarides, separating the Karst highland (hanging-wall) from the footwall buried under the gulf. In the Oligocene-Miocene, the S-ward verging Southern Alpine orogeny caused N-ward deepening of the platform and reactivated the Meso-Cenozoic structures with a dextral transpression. Evidence of neotectonics is given by presence of fluids, migrating from the carbonates to the seafloor (Busetti et al., 2013).

Advanced seismic tomography techniques were applied on part of a large multichannel seismic reflection dataset recently acquired. Traveltime tomography allowed resolution of vertical and lateral velocity gradients, by means of a procedure based on ray tracing and simultaneous iterative reconstruction technique (SIRT), that minimize the difference between the modelled and measured traveltimes (Carrion et al., 1993). The velocity field was refined in an iterative imaging technique through pre-stack depth migration, residual move-out analysis and grid tomography (Yilmaz, 2001).

The results provide a 3D velocity depth model and imaging of the flysch and carbonates units and their top surfaces. The top platform lies at a maximum depth of around 1600 ± 30 m below sea level, at about 2 km offshore the city of Trieste. This indicates that Karst Thrust is responsible for a vertical displacement of about 1600-1800 m.

Busetti M., Volpi V., Nicolich R., Barison E., Romeo R., Baradello L., Brancatelli G., Giustiniani M., Marchi M., Zanolla C., Wardell N., Nieto D. & Ramella R. (2010) - Dinaric tectonic features in the Gulf of Trieste (Northern Adriatic). *Boll. Geof. Teor. Appl.*, 51(2-3), 117-128.

Busetti M., Zgur F., Vrabec M., Facchin L., Pelos C., Romeo R., Sormani L., Slavec P., Tomini I., Visnovich G. & Zerial A. (2013) - Neotectonic reactivation of Meso-Cenozoic structures in the Gulf of Trieste and its relationship with fluid seepings. *Proc. 32nd GNGTS*, 3, 29-34.

Carrion P., Böhm G., Marchetti A., Pettenati F., Vesnaver A. (1993) - Reconstruction of lateral gradients from reflection tomography. *J. of Seismic Expl.*, 2, 55-67.

Yilmaz O. (2001) - *Seismic Data Analysis: Processing, Inversion and Interpretation of Seismic Data*. SEG, Tulsa.

Evidence of surface ruptures along the Norcia fault during the Mt. Vettore fault earthquake. Passive activation induced by Coulomb stress change?

Galderisi A.^{*1-2}, Galli P.²⁻³ & Trotta O.⁴

¹ University of Chieti-Pescara - Department InGeo, Italy.

² IGAG-CNR, Rome, Italy.

³ Dipartimento Protezione Civile, Rome, Italy.

⁴ Freelance geologist, Laurino (SA), Italy.

Corresponding email: a.galderisi92@gmail.com

Keywords: Active faults, Coulomb stress change, kinematic indicators.

The Monte Vettore Fault System (MVFS) ruptured at surface over 30 km during the October 30th, 2016 earthquake (Mw 6.5), with vertical offset exceeding 2 m. Evidence of superficial faulting along the 10-km-far Norcia Fault System (NFS) was also observed for a length of 2.5 km (~15 cm maximum vertical offset: Galli et al., 2018). This represents an unusual circumstance, as no seismic events were caused by this fault (Improta et al., 2019), meaning that it did not rupture at depth. According to the theory of Coulomb stress change, following a seismic event part of the static stress can be transferred to neighbouring faults (King et al., 1994). Mainly, this theory is applied to the identification of lateral interactions between systems of strike-slip faults. In this case, we hypothesize that part of the Coulomb stress is transferred frontally from the MVFS to the NFS. To support this idea, we calculated the Coulomb stress changes generated on October 30th by the MVFS by using the Coulomb 3.4 software. We observed the formation of a positive stress lobe in the upper 2 km of the MVFS hanging-wall, matching the surficial portion of some splays of the NFS. According to InSAR data (Brignani et al., 2018), the Norcia basin area was also affected by an anomalous uplift in response to the MVFS faulting. Now, whereas the existing striae analysed on the NFS rock planes show left oblique kinematics (i.e., compatible with the Apennine direction of extension), the slip-vector deriving from the coseismic ruptures measured in the Norcia basin indicate dip-slip kinematics. Therefore, we hypothesize that the sudden increase of the Coulomb stress induced by the MVFS rupture, coupled to the abrupt uplift of the Norcia basin, might have caused the passive gravity-slip of some splays of the Norcia fault, along the plane of maximum dip.

Bignami C., Valerio E., Carminati E., Doglioni C., Tizzani P. & Riccardo Lanari R. (2019) - Volume unbalance on the 2016 Amatrice - Norcia (Central Italy) seismic sequence and insights on normal fault earthquake mechanism. *Scientific Reports*, 9, 42-50.

Galli P., Galderisi A., Ilardo I., Piscitelli S., Scionti V., Bellanova J. & Calzoni F. (2018) - Holocene paleoseismology of the Norcia fault system (Central Italy). *Tectonophysics*, 745, pp. 154–169.

Improta L., Latorre D., Margheriti L., Nardi A., Marchetti A., Lombardi A. M., Castello B., Villani F., Ciaccio M.G., Mele F.M., Moretti M. & The Bollettino Sismico Italiano Working Group (2019) - Multi-segment rupture of the 2016 Amatrice-Visso-Norcia seismic sequence (central Italy) constrained by the first high-quality catalog of Early Aftershocks. *Scientific reports*, 9(1), 6921.

King, G.C.P., R.S. Stein, and J. Lin (1994) - Static stress changes and the triggering of earthquakes, *Bull. Seismol. Soc. Amer.*, 84 (3), 935-953.

Seismo-stratigraphic model of the Po Plain (Italy)

Mascandola C.*¹, Massa M.¹, Barani S.², Albarello D.³, Lovati S.¹, Martelli L.⁴, Poggi V.⁵ & Morasca P.¹

¹ Istituto Nazionale di Geofisica e Vulcanologia (INGV), Milano, Italy.

² Università degli Studi di Genova, Dipartimento di Scienze della Terra, dell'Ambiente e della Vita, Genova, Italy.

³ Università degli Studi di Siena, Dipartimento di scienze fisiche, della terra e dell'ambiente, Siena, Italy.

⁴ Regione Emilia-Romagna, Servizio Geologico, Sismico e dei Suoli, Bologna, Italy.

⁵ Istituto Nazionale di Oceanografia e Geofisica Sperimentale (OGS), Udine, Italy.

Corresponding email: claudia.mascandola@ingv.it

Keywords: seismo-stratigraphic model, seismic bedrock, Po Plain.

The aim of this study is to provide a seismo-stratigraphic model of the Po Plain sedimentary basin (Northern Italy), to be implemented in soil hazard studies at regional scale. The proposed model characterizes the subsoil up to the seismic bedrock depth. Mascandola et al. (2018) identifies the seismic bedrock of the Po Plain in correspondence with a marked increase in the mechanical properties of the subsoil materials, which produces a measurable resonance effect at the surface in the medium-to-long-period range.

To map the seismic bedrock depth we rely on an extensive collection of both existing and newly acquired ambient vibration measurements, with the aim of defining the soil resonance frequencies and the shear-wave velocity gradients within the soft sediments above seismic bedrock. Based on the collected data, an empirical regression model that relates the thickness of the soil deposits above the seismic bedrock to their resonant frequency is defined and applied to map the seismic bedrock depth in the Po Plain area. The resultant seismic bedrock map is correlated with depth of the main unconformities recognized inside the Quaternary succession (Regione Emilia-Romagna, ENI-AGIP, 1998; Regione Lombardia, Eni Divisione Agip, 2002).

The shear-wave velocity model above seismic bedrock is derived through the interpolation of 51 S-wave velocity profiles selected after a quality check on the available data. The velocity gradients highlights two different zones inside the study area: one at Northwest and another at East-Southeast with higher and lower velocity gradients respectively. To compute the soil amplification functions, the velocity model is discretized into a grid. For each grid node, a 1D soil model is defined and a numerical ground response analysis is carried out. The gridded soil amplification model is checked at those sites with both borehole and surface seismic sensors by comparing the theoretical and empirical soil amplification functions. These results will be included in regional seismic hazard studies, to account for soil amplification in seismic hazard estimates.

Mascandola C., Massa M., Barani S., Albarello D., Lovati S., Martelli L., & Poggi V. (2019) - Mapping the Seismic Bedrock of the Po Plain (Italy) through Ambient-Vibration Monitoring. *Bulletin of the Seismological Society of America*, 109 (1), 164-177, <https://doi.org/10.1785/0120180193>.

Regione Emilia-Romagna, ENI-AGIP (1998) - Riserve idriche sotterranee della Regione Emilia-Romagna, a cura di Di Dio, G. (Editor), S.EL.CA., Florence, Italy (in Italian).

Regione Lombardia, Eni Divisione Agip (2002) - Geologia degli acquiferi Padani della Regione Lombardia, Carcano, C. and A. Piccin (Editors), S.EL.CA., Florence, Italy (in Italian).

Geophysical imaging of a buried faulted anticline: the San Colombano hill, southern Po Plain of Lombardy (Northern Italy)

Mele M.*¹, Zuffetti C.¹, Aliverti Piuri E.¹, Bersezio R.¹, Giudici M.¹, Comunian A.¹ & Contini D.¹

¹ Dipartimento di Scienze della Terra “Ardito Desio”, Università degli Studi di Milano.

Corresponding email: mauro.mele@unimi.it

Keywords: San Colombano hill, geophysics, Po plain.

A geophysical survey, consisting in Vertical Resistivity Soundings (VES) and seismic profiling with Horizontal-to-Vertical Spectral Ratio (HVSr), was conducted in the San Colombano hill area, at the Po plain – Northern Apennines border (Lombardy, Italy).

The hill develops above one of the buried frontal arcs of the Northern Apennine thrust belt and represents a key-sector to understand the Quaternary evolution at the Northern Apennine-Po Plain border.

Here we present the results of the resistivity and seismic imaging obtained by Vertical Electrical Soundings (VES) and Horizontal-to-Vertical Spectral Ratio passive seismic (HVSr). 14 VES were acquired with Schlumberger array (maximum half-spacing 500 m); 8 HVSr were acquired in free-field conditions with a 3D land geophone. The results were compared to previous surface and subsurface stratigraphic and geophysical reconstructions (Bersezio et al., 2016; Mele et al., 2018; Zuffetti et al., 2018a; Zuffetti et al., 2018b).

Oriented VES cross-sections allowed to draw the electrostratigraphic picture of the uppermost 300 m of the subsurface, from the shallow Late Pleistocene alluvial synthem down to the Miocene open shelf formations; HVSr passive seismic profiling helped to portray the local uplift of the pre-Quaternary seismic basement.

Electrostratigraphy shows the most relevant stratigraphic and tectonic features at the San Colombano hill area, comprising the frontal salient of the northern Apennines, represented by a thrust-propagation anticline related to N-wards propagation of the Pavia – Casteggio lateral ramp. The structure uplifts low-resistivity electrostratigraphic units, plausibly corresponding to the Miocene-Pliocene–Calabrian marine succession, containing the saltwater and brackish–freshwater interfaces. It also deforms the high-resistivity alluvial Quaternary deposits and their lateral terminations onto the folded marine substratum, revealed by HVSr interpretation.

This work shows how such a cost-efficient, integrated geophysical approach allowed to depict the geological complexity of the subsurface of this part of the Po basin by comparing geophysical data with the available surface and direct subsurface geological reconstructions of the alluvial stratigraphy.

Bersezio R., Zuffetti C., Cavalli E., Baio M., Cantone M., Inzoli S., Mele M., Pavia F., Rigato V., Rusnighi Y., Rodondi C. & Sozzi S. (2016) - The Quaternary N-Apennine tectonics recorded in the Po Basin: stratigraphic and geomorphological evidences along a NS traverse in Lombardy (Italy). EGU General Assembly.

Mele M., Bersezio R. & Giudici M. (2018) - An electrostratigraphic cross-section across the central Po plain: bearings on subsurface geology and hydrostratigraphy. *Int. J. Earth. Sci.*, 107(8), 2787-2802.

Zuffetti C., Bersezio R., Contini D., & Petrizzo, M.R. (2018a) - Geology of the San Colombano hill, a Quaternary isolated tectonic relief in the Po Plain of Lombardy (Northern Italy). *J. of Maps* 14(2), 199-211.

Zuffetti C., Trombino L., Zembo I. & Bersezio R. (2018) - Soil evolution and origin of landscape in a late Quaternary tectonically mobile setting: The Po Plain-Northern Apennines border in Lombardy (Italy). *Catena*, 171, 376-397.

Active normal faulting in the Garfagnana and Lunigiana basins. New geomorphic and geological constraints

Nirta G.*¹, Piccardi L.¹, Bonini M.¹, Corti G.¹, Montanari D.¹, Moratti G.¹ & Sani F.²

¹ Consiglio Nazionale delle Ricerche, Istituto di Geoscienze e Georisorse, Sede di Firenze.

² Università degli Studi di Firenze, Dipartimento di Scienze della Terra.

Corresponding email: giuseppe.nirta@gmail.com

Keywords: active tectonics, capable faulting.

The Garfagnana and Lunigiana depressions are the northernmost intermontane basins of the Northern Apennines. Both basins are bounded by ca. NW-SE-trending normal fault systems on the northeastern and southwestern margins. These basins experienced the most destructive seismic event ever recorded in the Northern Apennine (i.e., the Mw = 6.5 earthquake of 1920), as well as other devastating seismic events, particularly the earthquakes of 1834 (Mw~5.9), 1837 (Mw~5.9) and 1481 (Mw~5,6). At a map-view scale, the northeastern fault systems are in rough continuity across the two basins, whereas the southwestern fault systems are separated by a ca. NE-trending right-lateral transfer zone known as North Apuan Fault zone.

Fault activity started in the early Pliocene and evolved throughout the Pleistocene until present. Coarse grained continental sedimentation events documented the main phases of tectonic activity testifying and initial faulting along the southwestern border of the basins followed by the activation of the northeastern and southwest-dipping fault systems. However, the geometrical and chronological relationships between the fault systems (i.e., master fault vs. antithetic fault) in both basins along with their seismogenic role is still matter of debate.

Field evidence of Quaternary faulting combined with quantitative geomorphology elaborations allowed us to derive the averaged rates of fault motion for the main fault systems located on both basin margins, as well as on the North Apuan Fault zone. Furthermore, geomorphological and field structural analyses have shed light on the overall architecture and kinematic history of the analyzed fault systems, allowing us to speculate about their structural role and seismogenic potential.

Seismotectonic characterization of active faults in the LGM plain between Udine and Pozzuolo (Friuli, NE Italy)

Patricelli G.*¹⁻² & Poli M.E.¹

¹ Dipartimento di Scienze Agroalimentari, Ambientali e Animali, Università di Udine.

² Dipartimento di Scienze della Vita, Università di Trieste.

Corresponding email: giulia.patricelli@phd.units.it

Keywords: seismogenic potential, Udine plain, seismic hazard.

The seismogenic potential of LGM Udine plain was investigated through a multidisciplinary approach, considering geophysical, geological, morphotectonic, seismological and geodetic data. The study area is located between eastern Friuli Venezia Giulia region and western Slovenia, where at present, according to GPS data and focal mechanisms of the main seismic events, two different deformational systems accommodate the N-ward indentation and the CCL rotation of Adria microplate:

the central-western Friuli compressional domain, characterized by reverse activity on WSW-ENE oriented thrusts

the NE-Friuli/western Slovenia domain, where strike-slip tectonics on high angle NW-SE oriented faults prevails.

Both domains are subjected to an about N-S oriented compression, with velocities of the order of 2-3mm/yr, causing a slip partitioning between transpressive/transcurrent structures.

Historical seismicity reveals that the study area is an active region. At least three $M_w > 6$ struck the area in 1348 (M_w 6.63), 1511 (M_w 6.32) and 1976 (M_w 6.45) (Rovida et al, 2016). Moreover, even if sparse, recent instrumental seismicity supports this issue.

With the aim to define the seismogenic potential of Friuli Plain under Udine, 2D and 3D-geometries of the Quaternary active faults was reconstructed by means of ENI seismic lines interpretation through 3D-Move software. Moreover, the integration with seismological data, compared with GPS velocities, allowed us to investigate the seismic behaviour of the detected faults that show clear evidence of Quaternary activity.

Rovida A., Locati M., Camassi R., Lolli B., Gasperini P. (2016) - CPTI15, the 2015 version of the Parametric Catalogue of Italian Earthquakes. Istituto Nazionale di Geofisica e Vulcanologia.

The Montello thrust image obtained with a dense, high-quality seismic network (Southeastern Alps, Italy)

Romano M.A.*¹, Peruzza L.¹, Garbin M.¹, Priolo E.¹ & Picotti V.²

¹ Centro Ricerche Sismologiche, Istituto Nazionale di Oceanografia e di Geofisica Sperimentale, Trieste and Udine.

² Geological Institute, Department of Earth Sciences, ETH, Zurich.

Corresponding email: aromano@inogs.it

Keywords: microseismicity, Montello thrust, Collalto Seismic Network.

An underground gas-storage operates in the anticline at the hanging-wall of the Montello thrust, in the complex system of the active southeastern front of the Alps in northeastern Italy. A dense, high quality seismic network, the Collalto Seismic Network (Rete Sismica di Collalto, RSC), has been specifically designed to monitor both the induced microseismicity and natural earthquakes around this storage (Priolo et al., 2015). The analysis of the first 6-year seismic catalog clearly depicts the aligned seismicity pattern of the Montello thrust as a ~1000 km² plane, gently dipping to NW and locally interrupted by high-angle faults nearly perpendicular to the main plane (Romano et al., 2019). From the analysis of the observed seismicity we suggest a mainly creeping behavior of the main thrust at seismogenic depth (5-13 km), with local re-orientation of stress-axes supported by focal mechanisms. This investigation cannot exclude the possibility that some parts of the system that are not microseismically active might be locked and under loading stress condition. Finally, we do not reckon a space-time correlation between the microseismicity and the activity carried out at the reservoir.

Priolo E., Romanelli M., Plasencia Linares M.P., Garbin M., Peruzza L., Romano M.A., Marotta P., Bernardi P., Moratto L., Zuliani D. & Fabris P. (2015) - Seismic monitoring of an underground natural gas storage facility: The Collalto Seismic Network. *Seismol. Res. Lett.* 86(1), 109–123. <https://doi.org/10.1785/0220140087>.

Romano M.A., Peruzza L., Garbin M., Priolo E. & Picotti V. (2019) - Microseismic Portrait of the Montello Thrust (Southeastern Alps, Italy) from a Dense High-Quality Seismic Network. *Seismol. Res. Lett.*, in press. <https://doi.org/10.1785/0220180387>

A new approach to estimate the depth of historical earthquakes: seismotectonic implications for the Northern Apennines and the southern Po Plain

Sbarra P.¹, Burrato P.*¹, Tosi P.¹, Vannoli P.¹, De Rubeis V.¹ & Valensise G.¹

¹ Istituto Nazionale di Geofisica e Vulcanologia.

Corresponding email: pierfrancesco.burrato@ingv.it

Keywords: seismogenic sources, macroseismic intensities, earthquake parameters.

The parameters of large earthquakes of the pre-instrumental era are a crucial piece of information for the seismotectonic characterisation of active regions and for the assessment of the associated hazard. Knowing their hypocentral depth, even when this parameter is only approximated, may help constraining their causative source, especially where active faults are spatially overlapped and occur at different depths. To this end we analysed seismicity of an area that includes the NE-verging Northern Apennines fold-and-thrust belt and its foredeep/foreland basin in the southern Po Plain, where earthquakes exhibit largely variable depth, ranging from very shallow (< 10 km) to deep (> 100 km).

We started analysing crowdsourced macroseismic data from the HSIT database (<http://www.haisentitoilterremoto.it/>), relating to instrumental earthquakes that occurred in the study area during the past 12 years and are characterised by a wide range of hypocentral depth. We found a correlation between the depth of these earthquakes and the slope of the attenuation curve describing the decay of macroseismic intensity within 50 km of the epicenter, regardless of their magnitude. Starting from this observation we calculated the absolute value of the slope for the attenuation curve of each earthquake of our learning set and plotted it against the hypocentral depth. We found that the data points are well fitted by a logarithmic function.

We then used such logarithmic function as a modern “Rosetta Stone” to infer the plausible hypocentral depth range of selected pre-instrumental earthquakes. Our statistics shows that the entire approach is independent of the magnitude of the earthquake being considered but depends only on its focal depth.

Once the expected depth was estimated, we calculated the expected magnitude for all the earthquakes of the analysed set. We show that for the deeper earthquakes (i.e. depth larger than 30 km) the revised magnitudes are larger than those calculated using traditional methods based on intensity alone.

We analysed and calculated new parameters for 20 pre- and early-instrumental earthquakes ranging in age from the 1570 “Ferrara” to the 1972 “Appennino settentrionale” events and with a magnitude range of 4.9 to 6.5. The analysed set includes earthquakes generated in the different tectonic regimes that characterise the study area and hence by different faulting styles. Here we show examples referred to selected events and discuss the seismotectonic implication.

Our methodology may help highlighting the existence and seismic potential of a class of deeper and less known seismogenic sources and may have an impact on the calculation of the annual earthquake rates, and hence on the assessment of the seismic hazard, particularly in areas of low strain rates and infrequent seismicity.

Crustal wedge structure in the Mt. Campo dei Fiori Area (Lugano - Lake Maggiore area): foredeep implication

Scaramuzzo E.*¹, Livio F.¹, Di Capua A.¹⁻² & Bitonte R.¹

¹ Università degli Studi dell'Insubria, Como, Italy.

² CNR – Institute for the Dynamics of the Environmental Processes, Milan, Italy.

Corresponding email: emanuele.scaramuzzo@gmail.com

Keywords: Alpine tectonic, wedge structure.

The geodynamic evolution of the Western (Ivrea – Verbano Zone) and Central (Orobic Alps) part of the South Alpine thrust system have been subjected to deep investigations through years to unravel the deformation and kinematic history of this part of the Alpine Chain (e.g. Brack et al., 2010; D'Adda et al., 2010; Zanchetta et al., 2011; Schmid et al., 2017). Nevertheless, studies on the evolution of their geological knot, the Lake Maggiore – Lugano area, have never been carried out, although it has been the source area of the most part of the synorogenic detritus in the first clastic pulses recorded in the Adriatic Foredeep (Di Capua et al., 2016). This investigational gap created a mismatch between the theoretical models and the buried terminations of the Southern Alps below the Po Plain at the boundary between the chain and the Po Plain.

Our study area is focused on the Mt. Campo dei Fiori range, between Lake Maggiore, to the west, and the Mesozoic Generoso basin, to the east.

The range is structured into an ENE-WSW striking asymmetric anticline, whose upright northern flank closes against the subparallel and high-dipping Marzio Fault. The latter experienced polyphasic reactivation since the Carboniferous (?) – Permian (Casati, 1978), during the Mesozoic extension and, finally, during the Alpine orogeny. This regional and deeply rooted structure directly lies along the easternmost tip of the Cremosina line, a well-known dextral lineament.

Our cross-sections, based on geological mapping and extrapolated at depth thanks to published geophysical data, show that the Mt. Campo dei Fiori Anticline and Marzio Fault are a crustal-rooted break-through fault-propagation fold, connected at depth to a crustal wedge. This interpretation leads to solve this sector in thick-skinned view, assuming a fixed-axis fault-propagation folds model (Jamison, 1987; Suppe & Medwedeff, 1990). Conversely, different interpretations have been previously proposed since the 90's for this area: from a pure thin-skinned style (Roeder, 1992), to a basement-involved thin-skinned sheet (Schumacher, 1997; Pfiffner, 2016).

The proposed indentation of a crustal wedge could provide a kinematic model to interpret both the retrovergence of the Mt. Campo dei Fiori Anticline and the inception of the shallower Gonfolite back-thrusting, interpreted as mainly active during Burdigalian to Tortonian (Bernoulli et al., 1989).

Bernoulli D., Bertotti G. & Zingg A. (1989) - Northward thrusting of the Gonfolite Lombarda ("South-Alpine Molasse") onto the Mesozoic sequence of the Lombardian Alps: implications for the deformation history of the Southern Alps. *Eclogae Geol. Helv.*, 82, 841-856.

Brack P., Ulmer P. & Schmid S. (2010) - A crustal magmatic system from the Earth mantle to the Permian surface: Field trip to the area of lower Valsesia and Val d'Ossola (massiccio dei Laghi, Southern Alps, Northern Italy), *Swiss Bull. Angew. Geol.*, 15, 3-21.

Casati P. (1978) - Tettonismo e sedimentazione nel settore occidentale delle Alpi Meridionali durante il tardo Paleozoico, il Triassico e il Giurassico. *Riv. Ital. Paleontol. Strat.*, 84, 313-326.

D'Adda P., Zanchi A., Bergomi M., Berra F., Malusà M.G., Tunesi A. & Zanchetta S. (2010) - Polyphase thrusting and dyke emplacement in the central Southern Alps (Northern Italy). *Int. J. Earth Sci.*, 100(5), 1095-1113.

Di Capua A., Vezzoli G., Cavallo A. & Gropelli G. (2016) - Clastic sedimentation in the Late Oligocene Southalpine Foredeep: from tectonically controlled melting to tectonically driven erosion. *Geol. J.*, 51, 338-353.

Jamison W.R. (1987) - Geometric analysis of fold development in overthrust terranes. *J. Struct. Geol.*, 9, 207-219.

Pfiffner A. (2016) - Basement-involved thin-skinned and thick-skinned tectonics in the Alps. *Geol. Mag.*, 153, 5-6.

Roeder D. (1992) - Thrusting and wedge growth, Southern Alps of Lombardia (Italy). *Tectonophysics*, 207, 199-243.

Schmid S.M., Kissling E., Diehl T., van Hinsbergen D.J.J. & Molli G. (2017) - Ivrea mantle wedge, arc of the Western Alps, and kinematic evolution of the Alps–Apennines orogenic system. *Swiss J. Geosci.*, 110, 581-612.

- Schumacher M. 1997. Geological interpretation of the seismic profiles through the Southern Alps (lines S1-S7 and C3-south). In: Pfiffner A., Lehner P., Heitzmann P., Mueller S. & Steck A. Deep Structure of the Swiss Alps: Results of NRP 20, 101-14: Birkhäuser Verlag, Basel.
- Suppe J. & Medwedeff A. 1990. Geometry and kinematics of fault-propagation folding. *Eclogae Geol Helv.*, 83, 409-454.
- Zanchetta S., D'Adda P., Zanchi A., Barberini V. & Villa I.M. 2011. Cretaceous-Eocene compression in the central Southern Alps (N Italy) inferred from $^{40}\text{Ar}/^{39}\text{Ar}$ dating of pseudotachylytes along regional thrust faults. *J. Geodyn.*, 51(4), 245-263.

Kinematics and seismic potential of the Eastern Southern Alps from space geodetic data

Serpelloni E.^{*1}, Anderlini L.², Pintori F.¹, Vannucci G.², Tolomei C.¹, De Martini P.M.³ & Pezzo G.¹

¹ Istituto Nazionale di Geofisica e Vulcanologia, Osservatorio Nazionale Terremoti.

² Istituto Nazionale di Geofisica e Vulcanologia, Sezione di Bologna.

³ Istituto Nazionale di Geofisica e Vulcanologia, Sezione Roma 1.

Corresponding email: enrico.serpelloni@ingv.it

Keywords: Southern Alps, space geodesy, active tectonics.

Space geodetic data provide precise measurements of horizontal and vertical ground displacements over the great Alpine area. In northeastern Italy horizontal GPS velocities well describe the present-day kinematics of the Adria microplate, providing measurements of tectonic shortening rates, which are of the order of 1-1.5 mm/yr across the mountain front in Veneto and Friuli Venezia Giulia. In particular, GPS velocities show that the higher strain-rates are localized across the Montello and Cansiglio segments of the Eastern Southern Alps (ESA) thrust belt. Here, seismic and geodetic moment release rates show a significant discrepancy, which has been interpreted as due to an aseismic component of deformation, as suggested by GPS-constrained kinematic models providing indications of limited interseismic coupling for the Montello and Cansiglio faults (Serpelloni et al., 2016). Consequently, despite geological and geomorphological evidence of Quaternary deformation, the identification of the seismogenic faults, responsible for the M>6 historical earthquakes, remains unclear in the Venetian sector of the ESA. The same area is interested by non-tectonic deformation transients associated with the hydrological cycle in karst areas, which are well tracked in space and time by continuous GPS stations (Serpelloni et al., 2018). These transient signals, which affect the horizontal components of ground displacements along the same direction of the tectonic shortening, make the estimate of the long-term tectonic deformation rates from geodesy more challenging and less accurate. For this reason we use vertical ground velocities obtained from GPS, InSAR and leveling measurements to provide additional constraints on the interseismic deformation and seismogenic potential across the Montello and Bassano-Valdobbiadene faults. Here a positive vertical velocity gradient, with uplift rates of the order of ~1.5 mm/yr in the Belluno Valley, cannot be explained only by isostatic and hydrological processes. A simple interseismic dislocation model, whose geometry is constrained by subsurface geological reconstructions and newly acquired instrumental seismicity, suggests a higher seismogenic potential for the Bassano-Valdobbiadene thrust than the Montello thrust.

Serpelloni E., Vannucci G., Anderlini L. & Bennett R.A. (2016) - Kinematics, seismotectonics and seismic potential of the eastern sector of the European Alps from GPS and seismic deformation data. *Tectonophysics*, 688, 157–181. <https://doi.org/10.1016/j.tecto.2016.09.026>

Serpelloni E., Pintori F., Gualandi A., Scoccimarro E., Cavaliere A., Anderlini L., Belardinelli M.E. & Todesco M. 2018. Hydrologically-induced karst deformation: insights from GPS measurements in the Adria-Eurasia plate boundary zone. *J. Geophys. Res.*, 85, 457. <https://doi.org/10.1002/2017jb015252>.

Seismogenic structures in the onshore-offshore Padano-Adriatic foothills between Emilia Romagna and Marche: a tentative modelling for the evaluation of risks in seismically quiet areas

Teloni S.¹, Invernizzi C.*¹, Costa M.² & Pierantoni P.P.¹

¹ School of Science and Technology, Geology Division, University of Camerino, Italy.

² Independent Researcher.

Corresponding email: chiara.invernizzi@unicam.it

Keywords: seismogenic structures, modelling, risks reduction.

In the last decade two seismic sequences, the Emilia 2012 earthquakes (maximum magnitude Mw 6.1) and the 2016-2017 Amatrice-Norcia-Visso earthquakes (maximum magnitude Mw=6.5), severally affected the Northern-central Italy. For this reason, nearby potentially seismic active areas have received particular attention by researchers and governmental institutions for emergency planning management. Seismogenic faults between Emilia Romagna and Marche regions represent the main target of this study, in fact, several significantly destructive earthquakes hit this area: i.e., Fabriano 1741 (Mw= 6.2), Cagli 1781 (Mw= 6.4), Senigallia 1930 (Mw= 5.8) and Rimini 1875 – 1916 (respectively Mw= 5.7 and 5.8).

Increasing availability of digital multi-scale geological dataset coupled with a deep geological and geophysical knowledge of the study area allowed building reliable geological models depending upon the distribution of the seismicity of the area.

This work is based on a collection of the seismic events occurred from 1985 to 2019, characterised by magnitude $M \geq 2$ (INGV data), coupled with interpreted seismic sections (SW-NE oriented) and structural maps (Chicco et al., 2019; Pierantoni et al., in press). With these input data, a 3D geological model was created by means of Move™ software licenced by Midland Valley Ltd. The hypocentres of seismic events have been compared with deep and shallow geological structures, in order to identify any correlation among them.

Results showed that seismic events tend to cluster in the proximity of some of the main faults at variable depths particularly approaching the faults affecting the Quaternary-Holocene deposits with an evidence of recent activity. More in detail, while in the Po Plain area vigorous seismicity testifies to active frontal thrusting, the seismotectonic setting of the Adriatic domain is characterized by the occurrence of active crustal strike-slip faults dissecting the thrust belt (Mazzoli et al., 2014).

The present study is aimed to evaluate the seismic risk in potentially active areas, which is considered as an essential tool to define strategic urban and emergency planning management actions. This could lead civil protection and governmental institutions to a strategic emergency preparedness and to a substantial reduction of seismic risks.

Chicco J., Pierantoni P.P., Costa M. & Invernizzi C. (2019) - Plio-Quaternary tectonics from seismic interpretation and its potential relation with deep geothermal fluids in the Marche (Central Italy). *Tectonophysics*, 775, 21-34.

Mazzoli S., Macchiavelli C. & Ascione A. (2014) - The 2013 Marche off-shore earthquakes: new insights into the active tectonic setting of the outer-northern Apennines. *Journal of Geological Society*, 171, 457-460.

Pierantoni P.P., Chicco J., Costa M. & Invernizzi C. (2019) - Plio-Quaternary transpressive tectonics: a key factor for the structural evolution of the outer Apennine-Adriatic system (Italy). *J. Geol. Soc. London*, accepted manuscript; <https://doi.org/10.1144/jgs2018-199>

Geometry and kinematics of the Umbro-Marchean Apennines in the Adriatic foreland

Tirincanti E.*¹, Roccheggiani M.¹ & Menichetti M.¹

¹ Department of Pure and Applied Sciences, Urbino (PU), Italy.

Corresponding email: emanuela.tirincanti@uniurb.it

Keywords: balanced geological cross-sections, Apennine foreland, deformation style.

The external portion of the Neogene foreland thrust belt of the umbro-marchean Apennines is buried by a thick clastic sequence pertaining to the Adriatic foredeep. The Adriatic offshore is characterized by an arcuate system of NE verging thrust sheets with at least two foredeep basins. Since Upper Oligocene, the nappes-troughs system of the Northern Apennines migrated discontinuously from West to East. During the Pliocene, this system reached the Adriatic area and originated, and differentiated at several depth, major foredeep basins. These basins were progressively filled by silicoclastic sequences mainly came from NW, with maximum subsidence more than 6000 m in the Pliocene. The geophysical data were used to extrapolate in depth the main structures, define their deformation style and verify spatial and temporal relationships between them. The geological data have been integrated with subsurface data coming from reinterpreted seismic profiles (ViDEPI project), to create some on-offshore seriate geological cross-section integrating geometries, deformation styles and calibrated with thicknesses derived from wells data. The deep structures described in the seismic reflection profiles mainly vary from thin-skinned to thick-skinned deformation style which means the existence of both styles of deformation. The deepest detachment, in the Triassic anhydrites located at 6-10 km of depth, is the main control factor of the formation of the largest anticlines, separated by wide synclines. The shallower detachment in the Messinian evaporites is one of the control factors of the development of minor structures in the foredeep, affecting the thickness distribution of the Plio-Pleistocene sediments. These cross-sections were balanced and restored with an average shortening that can reach 30%. In this area there are anticlines with a large thickness of Plio-Pleistocene sediments in the footwall-synclinal of the thrust. In few structures, the presence of important backthrusts can be noticed. They interest especially the Neogene layers, associated with the main thrusts. Well highlighted is the progressive migration of the structures to the east/northeast from northernmost sections to those further South. These cross-sections are useful to get a new 3D structural picture of the area which can contribute to define its seismotectonics. Reconstruction of the geodynamic evolution of this portion of the Northern Apennines chain is also important to better define the seismotectonics of the offshore area, where low to moderate earthquakes occur.

The Schio-Vicenza fault system: field and seismological evidences and open questions

Zampieri D.*¹, Burrato P.² & Vannoli P.²

¹ Dipartimento di Geoscienze, Università degli Studi di Padova.

² Istituto Nazionale di Geofisica e Vulcanologia.

Corresponding email: dario.zampieri@unipd.it

Keywords: Adria, eastern Southern Alps, Schio-Vicenza line.

Within the Adriatic domain, the Schio-Vicenza Fault System (SVFS) has a significant imprint in the landscape across the Southern Alps and the Venetian Po Plain. It can be divided into a northern segment, extending north of Schio, and a southern one, the Schio-Vicenza Line (SVL) proper. The latter borders to the east the Lessini, Berici and Euganei Mts block, separating this foreland structural high from the Veneto-Friuli foredeep, and continuing towards SE beneath the recent sediments of the plain via the Conselve-Pomposa fault. The SVL has been active with different tectonic phases and different kinematics at least since the Mesozoic, with a long-term dip-slip component of faulting well defined and the horizontal component of the movement not well constrained (Pola et al., 2014a).

As a whole, there is little evidence to constrain the recent activity of SVFS. Although its kinematics is still largely unknown, we observe that it interrupts the continuity of the Southern Alps thrust front in the Veneto sector, suggesting that it played a passive role in controlling the geometry of the active fault system and possibly the current distribution of seismic release. In this context the SVL has always been referred to as a sinistral strike-slip boundary of the northeastern Adriatic indenter. This kinematics would be confirmed by the recent deformation of a travertine mound close to the Euganei Mts. (Pola et al., 2014b).

On the contrary, the moderate seismicity along the northern segment point to a dextral strike-slip activity (e.g. 13 September 1989, Mw 4.9, depth 40 km), which is also corroborated by the field analysis of a synthetic Riedel of the fault cropping out just north of the Borcola Pass (Fondriest et al., 2012). These apparently conflicting data can be reconciled in the sinistral opening “zipper” model (Passchier and Platt, 2017), where intersecting pairs of simultaneously active faults with different sense of shear merge into a single fault via a zippered section (extraction fault).

Fondriest M., Smith S.A.F., Di Toro G., Zampieri D. & Mitterpergher S. (2012) - Fault zone structure and seismic slip localization in dolostones, an example from the Southern Alps, Italy. *J. Struct. Geol.*, 45, 52-67.

Passchier C.W. & Platt J.P. (2017) - Shear zone junctions: Of zippers and freeways. *J. Struct. Geol.*, 95, 188-202.

Pola M., Ricciato A., Fantoni R., Fabbri P. & Zampieri D. (2014 a) - Architecture of the western margin of the North Adriatic foreland: the Schio-Vicenza fault system. *Ital. J. Geosci.*, 133, 2, 223-234.

Pola M., Gandin A., Tuccimei P., Soligo M., Deiana R., Fabbri P. & Zampieri D. (2014 b) - A multidisciplinary approach to understanding carbonate deposition under tectonically controlled hydrothermal circulation: A case study from a recent travertine mound in the Euganean Hydrothermal System, northern Italy. *Sedimentology*, 61, 172199.

The Holocene deformed succession of Montodine (Cremona, Italy): evidence of recent tectonic activity?

Zanchi A.*¹, Deaddis M.², De Amicis M.¹, Marchetti M.³, Ravazzi C.² & Vezzoli G.¹

¹ University of Milano – Bicocca, Department of Environmental and Earth Sciences, Milano, Italy.

² CNR – Institute for the Dynamics of Environmental Processes (IDPA), Milano, Italy.

³ University of Modena and Reggio Emilia, Dept. of Education and Humanities, Reggio Emilia, Italy.

Corresponding email: andrea.zanchi@unimib.it

Keywords: Po Plain, recent faulting, seismotectonics.

A possible evidence of surface faulting was discovered close to Montodine, Cremona, Italy, along the western bank of River Serio during 2008. The outcrop was analysed by us 10 years ago during summer 2009 and was successively covered with an artificial embankment, which completely hides the studied exposure.

The study area is located in an actively deforming area, laying above the buried thrust front of the North Apennines, where Apennine structures interact with the frontal portion of the central Southern Alps. In addition, the well-known Soncino earthquake occurred about two hundred years ago testify to the recent seismic activity of the area.

The outcrop showed well-bedded sandy-clay thin layers including compressed peat beds related to a palustrine to fluvial environment. Liquefaction structures possibly due to seismic wave shaking occur in the upper part of succession. The described unit covers Lateglacial coarse -grained fluvial deposits and is covered on top by recent loose gravels related to the Serio River, which can be ascribed to the end of the Middle age. The fine-grained portion of the outcrop is crosscut by a low-angle reverse fault, showing a net displacement of the succession between 0.5 and 1 meter. The hangingwall shows a marked thickening of the succession accompanied by gentle folding with an open syncline with a metric wavelength, and shows secondary reverse faults forming a small backtrust, whereas the footwall is almost undeformed. We performed ¹⁴C radiocarbon dating on the deformed peat deposits, which gave ages ranging around 10 ka. Younger ages of about 5ka cal BP were obtained for wood fragments stretched along the fault plane. The outcrop also shows several logs of Bronze Age related to pile dwellings, which were constructed on top of the fine-grained succession and which seem to postdate fault motions.

The present contribution aims to discuss the possible origin of the deformation structures, which can be alternatively ascribed to anthropic, gravitational or tectonic processes.

Late Quaternary sedimentation and tectonics in the Po Basin: field evidences at the Po Plain-Apennines border (Lombardy)

Zuffetti C.*¹ & Bersezio R.¹

¹ Dipartimento di Scienze della Terra “A. Desio”, Università degli Studi di Milano.

Corresponding email: chiara.zuffetti@unimi.it

Keywords: Po Plain, Quaternary, San Colombano hill.

Topographic reliefs and terraced landscapes represent key-sectors to constrain recent geological evolution and subsurface stratigraphy in almost flat landscapes like the Quaternary Po Plain. Aiming to investigate the role of Late Quaternary tectonics on the complexity of stratigraphic and geomorphological features exposed at the Po Plain-Apennines border in Lombardy, we focus on a structural culmination of the Emilia salient, the San Colombano Hill ramp anticline.

Geological and geomorphological mapping at 1:10.000 scale, stratigraphic, sedimentological, paleontological, petrographic and morpho-structural analyses, complemented by C¹⁴ and OSL age determinations, show the incremental tectonic imprints on the Quaternary stratigraphy originating the present-day palimpsest landscape. Location of unconformable stratigraphic vs. conformable morphological boundaries, pinch-out and cross-cut relationships among alluvial sedimentary bodies, uplifted paleovalley fills, cannibalism of pre-existing alluvial clastics, colluvial wedges and sediment deformation structures highlight how, where and when tectonic-driven processes controlled the evolution of the Hill and the adjacent plain.

The S. Colombano ramp anticline underwent Early-Middle Pleistocene thrusting, which uplifted and folded the Gelasian regional unconformity between littoral Calabrian and deep-marine Miocene formations. Late Pleistocene, alpine-sourced alluvial and glacio-fluvial units, terraced the deformed marine succession through the composite Late Pleistocene unconformity. The mapped synthem progressively wedge, thin and amalgamate S-wards, suggesting the syn-sedimentary confinement by an uplifting mild relief ancestor of the present-day Hill. Relicts of syn-tectonic paleo-valley fills testify the first drainage pattern of this proto-hill, where also polycyclic loess-soil aggraded during early Late Pleistocene.

The S. Colombano structure underwent dissection since latest Pleistocene along three fault systems, while LGM glacio-fluvial and alluvial units prograded from the NW. Evidences of Latest Pleistocene fault activity are observed as thickness variations of the LGM synthem, offset of the Late Pleistocene unconformity, paleosol reworking in colluvial wedges on the fault-block hangingwalls, marked by triangular facets and abrupt diversions of the river network. A late-LGM muddy flood plain developed N of the hill, owing to tectonic-induced subsidence. This was cross-cut by the meandering tributaries of the paleo-Po River during the Late Glacial. The post-glacial-Holocene entrenchment of the river network and river anomalies suggest an eventual latest phase of uplift and transtension of the San Colombano structure, plausibly related to the ongoing N-wards propagation of the Emilia salient. The progressing research is integrating the surface and subsurface field geological and evolutionary constraints into 3D(4D) geological models, as the basis for hydrogeological and geohazard applications.

S22

**From seismic source to fault using multidisciplinary
approaches: the central and southern Apennines as natural
laboratory**

CONVENERS AND CHAIRPERSONS

Massimiliano Porreca (Università di Perugia)

Debora Presti (Università di Messina)

Rita de Nardis (Università di Chieti)

Fault pattern and seismotectonic potential at the south-western edge of the Ionian Subduction system (southern Italy): new field and geophysical constraints

Barreca G.¹⁻², Scarfi L.³, Gross F.⁴, Monaco C.*¹⁻² & De Guidi G.¹⁻²

¹ Dipartimento di Scienze Biologiche Geologiche e Ambientali, Università di Catania.

² CRUST - Centro interUniversitario per l'analisi SismoTettonica tridimensionale con applicazioni territoriali.

³ INGV-Osservatorio Etneo, Catania.

⁴ Institute of Geosciences, Geophysics, Christian-Albrechts-University Kiel, Germany.

Corresponding email: cmonaco@unict.it

Keywords: Subduction, Calabrian Arc, active faulting, seismic profiling.

The south-western edge of the Calabrian Arc in southern Italy has been investigated throughout a joint analysis of field, marine and geophysical data which provided constraints on the fault pattern and on the seismotectonic potential. The study was focused on a poorly known sector of a larger belt of seismically active faults slicing across the NE corner of Sicily, the so-called Aeolian-Tindari-Letojanni Fault System. Our data pointed out that the investigated area, including the mainland and the Ionian offshore, is deformed by oblique faulting with a general NW-SE tectonic trend. Earthquake distribution and seismic profiles pointed out active deformation in the offshore while the mainland is characterized by the occurrence of a more than 20 km-long NW-SE structural belt. However, scarce seismicity has been recorded in the last 30 years alongside this structure, accounting for a possible silent segment of this larger fault system. Tomographic images revealed that the Moho discontinuity is deformed by a NE-dipping lithospheric tectonic structure which has been here retained the main mode of deformation and responsible for coseismic displacement in the area. As a whole, field and geophysical data agree with a general NW-SE trend segmented pattern of active faults which have the potentiality of generating magnitude 6.5-7 earthquakes. The orientation and transtensional kinematics of the fault segments are consistent with those of large faults found in the deep Ionian Sea.

Mainshock anticipated by intra-sequence ground deformations: insights from multiscale field and SAR interferometric measurements

Brozzetti F.*¹, Mondini A.C.², Pauselli C.³, Mancinelli P.³, Cirillo D.¹, Guzzetti F.² & Lavecchia G.¹

¹ CRUST – DiSPUTer Università G. d'Annunzio, Chieti, Italy.

² CNR – IRPI, Perugia, Italy.

³ Dipartimento di Fisica e Geologia, Università degli Studi di Perugia, Italy.

Corresponding email: f.brozzetti@unich.it

Keywords: 2016 central Italy earthquake, coseismic and intra-sequence ground deformations, comparison of DinSAR and field data.

Integrating DInSAR analysis with fieldwork, we studied the ground deformation caused by the 2016 Central Italy seismic sequence along the Vettore-Bove Fault (VBF). In particular, we delineated the patterns and measured the Intra Sequence Ground Deformations (IGD) occurred between the 24 August Mw 6.0 and the 26 October, Mw 5.9 foreshocks.

To study IGD, we developed individual interferograms using ESA Sentinel-1 images at the Level-1, Single Look Complex (SLC) processing level.

We considered three periods: (i) a 30-day period (T1) from 27 August to 26 September, (ii) a 24-day period (T2) from 2 to 26 October (before the occurrence of the Mw 5.9 event) and (iii) a 60-day period from 27 August to 26 October (T1+T2).

The observation that, since the T1 period, and even more during the T2 period, the IGD was largely independent of the coseismic deformation caused by the 24 August foreshock, suggested that it cannot be merely attributed to after-slip following the earthquake.

Our temporal analysis highlighted that during the considered periods, the ground was continuously deformed and the obtained deformation pattern outlined the pattern caused by the 30 October, Mw 6.5 mainshock.

Immediately after the 24 August earthquake, although the deformation was more intense in the southern part of the VBF causative fault, it soon expanded northwards and westwards. After about two month, before the mainshock occurred, the length of the ground deformation, measured along the fault strike, ranged between 28.7 and 36.3 km. It extended to the whole portion of the hanging wall that was later affected by surface faulting, during the 26 and 30 October events.

Assuming the intra-sequence length of the deforming ground (i.e. the fault parallel length of the surface deformation that occurred during the T1+T2 period) to be a proxy for the expected (=coseismic) surface rupture length and using scaling dependencies that link fault rupture area to the earthquake magnitude, we calculate $6.4 < Mw < 6.7$ for the imminent earthquake, in good agreement with the magnitude of the mainshock.

We propose that if, after a severe seismic event, the deformation expands outside the initial coseismically deformed area, a new earthquake with a magnitude comparable to or larger than the foreshock should be expected.

The impact of high structural complexity on seismotectonics: hints and lessons learned in the areas of the 2016-2018 central Italy seismic sequence in the framework of the RETRACE-3D project

Buttinelli M.*¹, Petracchini L.², Maesano F.E.¹, Scrocca D.², D'Ambrogi C.³, Di Bucci D.⁴, Marino M.³, Capotorti F.³, Cavinato G.², Bigi S.⁵ & RETRACE-3D working group 1,2,3,4

¹ Istituto Nazionale di Geofisica e Vulcanologia.

² Consiglio Nazionale delle Ricerche, Istituto di Geologia Ambientale e Geoingegneria.

³ Istituto Superiore per la Protezione e la Ricerca Ambientale.

⁴ Dipartimento della Protezione Civile della Presidenza del Consiglio dei Ministri.

⁵ Università degli Studi di Roma La Sapienza.

Corresponding email: mauro.buttinelli@ingv.it

Keywords: Seismotectonics, Central Apennines, RETRACE-3D.

Young and tectonically active mountain chains like the Central Apennines (Italy) represent challenging areas where to investigate the relationship between fault development and seismotectonics.

Those areas are fashioned by a very complex patterns of seismicity, which have been associated both to single fault or complex fault systems activation.

The high structural complexity and repeated cycles of tectonic phases can be clearly recognized even from surface geology, especially when supported by highly detailed stratigraphic constraints. Nevertheless, the overprint of subsequent deformational stages must be taken into careful account since geological observations made at the surface might mask different structural architecture at depth, with consequent important implication for seismotectonics.

The RETRACE-3D project focused on the review of a large set of underground data acquired for hydrocarbons explorations in the area struck by the 2016-2018 Central Apennines seismic sequence, integrated with surface geological information, to build a robust and comprehensive 3D geological model to be related to observed seismicity.

Results primarily show that, at least for the shallow crust, the general architecture of the chain is still dominated by large-scale compressional structures associated to the build-up phase of the Central Apennines. We generally found widespread evidence of fault segmentation, reactivation of faults, as well as the recent generation of new sets of extensional faults. For these latter in particular, the surface expression and their evolution are conditioned by the presence of previous structures at depth.

This contribution would open new points of discussion regarding a more realistic estimate of seismic hazard of complex areas such as the Central Apennines.

A time dependent model of elastic stress in the Central Apennines, Italy

Caporali A. *, Zurutuza J. & Bertocco M.

Department of Geosciences, University of Padova Italy

Corresponding email: alessandro.caporali@unipd.it

Keywords: GNSS Geodesy, stress and strain, Coulomb Failure.

Seismicity in the Central Apennines is characterized by normal faulting with dip NE-SW near 45°. If the stress at the hypocenter of the 2016 Norcia (Mw=6.5) and 2009 L'Aquila (Mw=6.3 on the Paganica fault) earthquakes originated only from stress transfer from previous historical events, the orientation of the principal stress axes would have been inconsistent with the observed tensional regime. The additional contribution of a regional stress is thus required, but GNSS geodesy provides only stress rates. We empirically estimate a time multiplier for the regional stress rate, computed with a dense GNSS network, such that the principal stress axes resulting from the sum of the stress transferred by previous events and the regional stress rate multiplied by the empirical temporal scale are consistent with normal faulting, both at the L'Aquila and Norcia hypocenters. Based on a Catalogue of 36 events of magnitude larger than 5.6 we estimate the total Coulomb stress at depths and along planes parallel to those of L'Aquila and Norcia. We provide evidence of an asymmetry of the Coulomb stress leading to a stress concentration near the hypocenter of the two events just prior of the 2009 and 2016 earthquakes. This stress anomaly disappeared after the two events. Similar stress patterns are observed for earlier events which took place in 1461 at L'Aquila, 1703 on the Montereale plain and in 1703 at Norcia/Valnerina. The 1997 sequence of Colfiorito exhibits a similar, anisotropic Coulomb stress pattern. Other areas with a similar stress anisotropy could be seismic gaps.

Multidisciplinary approach for 3D fault geometry reconstruction: an example from Calabrian-Lucanian boundary in the Mt. Pollino area (Southern Apennines-Italy)

Cirillo D.*¹, Brozzetti F.¹, de Nardis R.¹, Lavecchia G.¹, Orecchio B.², Presti D.² & Totaro C.²

¹ CRUST, DiSPUTer - Università G. d'Annunzio, Chieti, Italy.

² Dipartimento di Scienze Matematiche e Informatiche, Scienze Fisiche e Scienze della Terra - Università di Messina, Italy.

Corresponding email: d.cirillo@unich.it

Keywords: Pollino earthquakes, Calabria extensional faults, Quaternary normal faults.

We present a tridimensional model of a Quaternary and active normal faults system, located in the southern Apennines extensional belt (Brozzetti et al., 2017a, 2017b), reconstructed integrating field and seismological data.

The fault system is located in the Mt Pollino area which, from 2010 to 2014, was affected by long lasting seismic activity including three major events occurred in May 2012 (Mw 4.2), October 2012 (Mw 5.0) and June 2014 (Mw 4.0) and ~3000 other earthquakes with 1

The 3D geometry of the Seismogenic sources activated during the aforesaid sequence was reconstructed by integrating high quality earthquake locations with the surface geometry of the active faults defined, in the epicentral areas, through detailed structural and morpho-tectonic survey.

The 3D geometry of the faults at depth was constrained using high-resolution hypocenter distributions, after an accurate selection and re-location performed by HypoDD method.

The hypocenters were managed through the Move v.2018.2.1 PetEx software package and plotted on a closely spaced grid of sections, striking SW-NE, SE-NW, N-S and E-W, (half-width 2 km) that is oriented orthogonal, transversal and parallel to the elongation of the epicentral clusters. This spatial orientation is in fact the most useful to better highlight the seismogenic patches on the faults at depth.

Further, our multidisciplinary approach allowed to determine the geometry, the kinematics, the cross-cutting relationships and the slip rates of the inferred active fault segments within and near the epicentral area.

The reconstructed fault system is markedly asymmetrical, characterized by low-angle, E and NNE-dipping faults, and high-angle, SW- to WSW-dipping seismogenic antithetic faults.

The East-dipping faults, which include low-angle structures, are interpreted as synthetic to a basal detachment. The antithetic W-dipping faults, although less important in terms of long-term deformation, are however significant in controlling the Pollino 2010-2014 seismic activity.

Some of the detected faults were substantially unknown or were not considered active, thus their recognition is of considerable importance for the definition of the seismic hazard of the Calabria-Lucania border.

Brozzetti F., Cirillo D., de Nardis R., Cardinali M., Lavecchia G., Orecchio B., Presti D. & Totaro C. (2017) - Newly identified active faults in the Pollino seismic gap, southern Italy, and their seismotectonic significance. *Journal Structural Geology*, 94, 13-31.

Brozzetti F., Cirillo D., Liberi F., Piluso E., Faraca E., De Nardis R. & Lavecchia G. (2017) - Structural style of quaternary extension in the Crati valley (calabrian arc): Evidence in support of an east-dipping detachment fault. *Italian Journal of Geosciences*, 136, 434-453.

Structural architecture and microstructural properties of the seismogenic Monte Marine fault zone, central Apennines (Italy)

Cortinovis S.*¹, Balsamo F.¹, Fondriest M.², La Valle F.² & Di Toro G.^{2,3}

¹ NEXT- Natural and Experimental Tectonics research group, Dipartimento di Scienze Chimiche, della Vita e della Sostenibilità Ambientale, Università di Parma, Italy.

² Dipartimento di Geoscienze, Università degli Studi di Padova, Italy.

³ Istituto Nazionale di Geofisica e Vulcanologia (INGV), Roma, Italy.

Corresponding email: silvia.cortinovis@studenti.unipr.it

Keywords: faults, fault rocks properties, fault zone architecture.

The Central Apennines of Italy are characterized by a complex array of seismogenic extensional faults causing destructive earthquakes with $M_w \leq 7.0$ (e.g., L'Aquila Mw 6.1, 2009; Amatrice-Norcia Mw 6.0-6.6 during 2016). The NW-SE-trending Monte Marine Fault Zone (MMFZ) is an extensional seismogenic fault located NW of the L'Aquila town, which was activated during the 1703 AD seismic sequence (Galli et al., 2011). The MMFZ consists of two near-parallel hard-linked major fault strands which crop out for ~8 km from the village of Barete (to the Northwest) to the village of Arischia (to the Southeast) and cut through Jurassic dolostones in the footwall block. The interaction between the two fault strands occurs within a step-over region near the Pizzoli village. To study the fault zone architecture and the fault rock properties, different sectors of the MMFZ were mapped at 1:500 and 1:5000 scale, and two detailed geological cross sections were constructed. Field data show that the exposed footwall of the MMFZ consists of (i) a 3-5 m wide cataclastic fault core, (ii) a transition zone with variable thickness of loose highly fragmented protocataclasites and breccias, and (iii) a fractured damage zone. The loose highly fragmented rocks represent the most significant structural unit in terms of volume within the fault zone, are exposed within bad-land areas, and show variable thickness with maximum values up to several hundreds of meters within the step-over region. These fault rocks seem to have been shattered in situ and share textural similarities with "pulverized rocks" described in other settings (Fondriest et al., 2015; Schröckenfuchs et al., 2015). Furthermore, in this step-over region, NW-SE-trending extensional faults cutting both reverse and minor strike-slip faults suggest the important role played by inherited structures in shaping the MMFZ architecture. Based on the spatial distribution and quantitative analysis of cataclastic and highly fragmented fault rocks (e.g. grain size and shape distributions) we discuss the main factors involved in the formation and evolution of fault rocks in seismogenic carbonate faults.

Fondriest M., Aretusini S., Di Toro G. & Smith S.A.F. (2015) - Fracturing and rock pulverization along an exhumed seismogenic fault zone in dolostones: The Foiana Fault Zone (Southern Alps, Italy). *Tectonophysics*, 654, 56–74. <https://doi.org/10.1016/j.tecto.2015.04.015/>

Galli P.A.C., Giaccio B., Messina P., Peronace E. & Zuppi G.M. (2011) - Palaeoseismology of the L'Aquila faults (central Italy, 2009, Mw 6.3 earthquake): Implications for active fault linkage. *Geophysical Journal International*, 187, 1119–1134. <https://doi.org/10.1111/j.1365-246X.2011.05233.x>

Schröckenfuchs T., Bauer H., Grasemann B. & Decker K. (2015) - Rock pulverization and localization of a strike-slip fault zone in dolomite rocks (Salzach-Ennstal-Mariazell-Puchberg fault, Austria). *Journal of Structural Geology*, 78, 67–85. <https://doi.org/10.1016/j.jsg.2015.06.009>

Multidisciplinary survey methods of the Fiandaca-Pennisi fault zone reactivated during the 26th December 2018 coseismic and postseismic event

De Guidi G.^{*1-2}, Barreca G.¹⁻², Bella D.⁵, Brighenti F.¹⁻², Carnemolla F.¹⁻², Figlioli A.⁶, Menichetti M.³⁻⁴, Roccheggiani M.³⁻⁴ & Monaco C.¹⁻²

¹ Dipartimento di Scienze Biologiche, Geologiche ed Ambientali, Università di Catania.

² CRUST, UR-UniCT, Catania, Italy.

³ Dipartimento di Scienze Pure e Applicate (DiSPeA), Università degli Studi di Urbino Carlo Bo.

⁴ CRUST, UR-Chieti, Italy.

⁵ Geologo libero professionista.

⁶ Studente UNICT.

Corresponding email: deguidi@unict.it

Keywords: Geo-structural investigations, geodetic monitoring, Mt. Etna.

Geo-structural investigations and geodetic monitoring have been performed along the Fiandaca-Pennisi fault, an active volcano-tectonics shear zone on the eastern flank of Mt. Etna. On December 26, 2018 a seismic swarm nucleated alongside this structure that slipped in response to the intrusion, at the Etna summit area, of a large dike preceding the December 24th 2018 eruptive event. The main shock ($M=4.8$) occurred at 3.19 am (UTC) and produced severe damaging on the villages surrounding the seismogenic fault. Damages were primarily related to the propagation of co-seismic fractures field across the urban areas. Topographic and aero-photogrammetric techniques were firstly adopted to map the earthquakes associated fractures whereas kinematics has been obtained by geo-structural measurements and local GNSS velocity field which has consisted in the implementation of the UNICT_NET, with the installation of 4 new benchmarks along the sides of the seimogenic fault, 48 hours after the seismic event. Aerial photographs and field displacement on several man-made structures (concrete walls, roads etc.) allow to obtain the geometric pattern and the kinematic of tectonic structures. They form a wide deformation zone which include NW-SE trending oblique (right-lateral) fault segments and associated N-S trending, én-echelon arranged extensional (T) cracks mainly developed at the NW tip of the structure. Interferometric methods (SAR) were further used to support previous investigations and to better define geometric and dynamic parameters of the deformation zone. The high-resolution interferograms were obtained by Observation of Progressive Scans (TOPS) mode from the Sentinel-1 satellite, which provide high-quality Synthetic Aperture Radar images illuminating the shear zone in a time range straddling the seismic event.

High-sampling of multi-layered crust-scale seismogenic deformation in Central-Eastern Italy

de Nardis R.¹, Pandolfi C.*¹, Monachesi G.², Cattaneo M.², Marzorati S.², Cirillo D.¹, Ferrarini F.¹, Brozzetti F.¹ & Lavecchia G.¹

¹ CRUST, DiSPUTer, Università “G. d’Annunzio”, Chieti Scalo.

² Istituto Nazionale di Geofisica e Vulcanologia, Ancona.

Corresponding email: rita.denardis@unich.it

Keywords: fault plane solutions, crust-scale seismogenic deformation, Central-Eastern Italy.

The geometric-kinematics pattern of active deformation in Central-Eastern Italy is up to now poorly constrained due to the lack of high quality seismological data full integrated with the geological information. In this work, thanks to a dense seismometric network in Central-Eastern Italy, managed by the INGV – Ancona (Monachesi et al., 2012 and 2013), it was possible to perform a detailed analysis of multi-layered crust-scale seismogenic deformation. After a highly selective process of the available seismic locations and focal mechanisms, we gained a good quality final dataset of 141965 earthquakes, with $0.5 \leq ML \leq 4.8$, and 254 new focal mechanisms. Such data were opportunely integrated with 63 focal solutions retrieved from catalogues RCMT and TDMT (<http://rcmt2.bo.ingv.it/>, <http://cnt.rm.ingv.it/tdmt>) and detailed papers for the time period from 1967-to-2009. The study area was investigated starting from 72 radial cross-section, with a half-width of 2.5 km, where we plotted the huge number of hypocentral data and well constrained at depth focal solutions. The high-quality analysis and selection allowed us to detect seismogenic volumes at different layers of depth and to study the kinematics and the deformation pattern with the aim to define a good correspondence between the identified geometries and the associated kinematics. The principal geometries characterize an upper crust-middle crust west-dipping structure corresponding to the already known Adriatic Basal Thrust (ABT) (Lavecchia et al., 2003) and unveil a middle crust-upper mantle west-dipping shear zone, here referred to as Incipient Thrust (IT). The focal mechanisms associated to the ABT and the IT show a P-trend that is near perpendicular to the Adriatic frontal thrust and rotates in direction from NE-SW to E-W. The map of the Sh_{max} computed with this new data set shows a more defined stress field in the study area.

Lavecchia G., Boncio P. & Creati N. (2003) - A lithospheric-scale seismogenic thrust in central Italy. *J. Geodyn.*, 36, 79-94.

Monachesi G., Marzorati S., Ladina C., Cattaneo M., Frapiccini M., D’Alema E. & Carannante S. (2012) - Beach Balls dell’Italia Centro Orientale, una raccolta di meccanismi focali dei terremoti registrati dal 2009 dalle stazioni della Rete Sismometrica Integrata dell’Italia Centro Orientale (ReSiICO). Istituto Nazionale di Geofisica e Vulcanologia. <http://ingvan.protezionecivile.marche.it/BB/home.html>

Monachesi G., Cattaneo M., Ladina C., Marzorati S., D’Alema E., Frapiccini M., Carannante S., Ferretti M., Sebastianelli M., Delladio A. & Selvaggi G. (2013) - Esperienze di monitoraggio integrato: il caso della Rete Sismometrica dell’Italia Centro Orientale e dei suoi servizi. *Quaderni di Geofisica*, 106.

Multi-temporal tectonic evolution of Capo 1 Granitola and Sciacca foreland transcurrent faults (Sicily channel)

Ferranti L.¹⁻²⁻³, Pepe F.⁴, Barreca G.²⁻⁵, Meccariello M.¹⁻² & Monaco C.^{*2-5}

¹ Dipartimento di Scienze della Terra, dell'Ambiente e delle Risorse, Università di Napoli "Federico II", Napoli.

² CRUST - Centro interUniversitario per l'analisi SismoTettonica tridimensionale con applicazioni territoriali.

³ INGV-Sezione Roma 1.

⁴ Dipartimento di Scienze della Terra e del Mare (DISTEM), Università di Palermo, Palermo.

⁵ Dipartimento di Scienze Biologiche, Geologiche e Ambientali, Università di Catania, Catania.

Corresponding email: cmonaco@unict.it

Keywords: strike-slip faults, fold growth rates, Pelagian foreland.

Joint analysis of high-penetration multi-channel and high-resolution single-channel seismic reflection profiles, calibrated by deep well boreholes, allowed a detailed reconstruction of the Late Miocene to Recent tectonic history of the Capo Granitola and Sciacca fault systems offshore southwestern Sicily. These two fault arrays are part of a regional system of transcurrent faults that dissect the foreland block in front of the Neogene Sicilian fold and thrust belt. The Capo Granitola and Sciacca faults are thought to reactivate inherited Mesozoic to Miocene normal faults developed on the northern continental margin of Africa. During Latest Miocene-Pliocene, the two ~NNE-SSW striking faults were active in left transpression, which inverted Late Miocene extensional half-grabens and created push up ridges along both systems. Tectonic activity decreased during the Pleistocene, but transpressional folds deform Middle-Late Pleistocene sediments as well, suggesting that the two fault systems are active. The ~40-50 km long longitudinal amplitude 24 profile of 1st order folds (Capo Granitola and Sciacca anticlines) shows ~10-30 km bell-shaped undulations that represents 2nd 26 order folds. The length of these undulations together with the map pattern of faults allowed to divide the CGFS and SFS into two segments, northern and southern, respectively. Total uplift of the Sciacca Anticline is twice than the uplift of the Capo Granitola Anticline. Incremental fold growth rates decreased during time from 0.22 mm/yr (Capo Granitola Anticline) and 0.44 mm/yr (Sciacca Anticline) in the Pliocene, to 0.07 and 0.22 mm/yr, respectively, during the last ~1.8 Ma.

Recent and active tectonics in the Campanian Plain based on integration of fault kinematics and seismological data: preliminary results

Forlano S.*¹, Ferranti L.¹ & Milano G.²

¹ Dipartimento di Scienze della Terra, delle Risorse e dell'Ambiente, Università Federico II, Napoli.

² Istituto Nazionale di Geofisica e Vulcanologia, Osservatorio Vesuviano, Napoli.

Corresponding email: serena.forlano@unina.it

Keywords: seismotectonics, Campanian Plains, Southern Apennines.

The Campanian Plain is a sector of Quaternary extension and subsidence on the Tyrrhenian margin of the Southern Apennines. Extension was chiefly accommodated by E-W to NE-SW striking, listric-shaped normal faults, which caused domino-block faulting and growth of up to ~3.5 km deep extensional basins segmented by buried ridges. Although extension is thought to have been rapid during the Pleistocene, the plain exhibits a low-energy historical and instrumental seismicity.

So far, very few fault structural data were available to unravel the kinematic evolution of the plain. Similarly, no complete assessment of the instrumental seismicity outside the Neapolitan volcanic area was ever performed. Our multidisciplinary approach integrates geological-structural data and instrumental seismicity to link the long-term kinematics evolution and the seismogenic deformation. The study is focused on the tectonic borders of the plain where faults are exposed, and tectonic seismicity is present.

Structural and fault-slip data have been collected on ~250 major to minor fault planes exposed along the flanks of the plain and specifically along three of the main border ridges (Caserta, Avella and Sarno ridges). The analysis revealed the existence of two sets of differently oriented slip lineations on the major faults, which we relate to two different kinematics regimes and related deformation events. A first set is associated to right-transensional slip on NE-SW faults and minor left-transensional slip on NW-SE E-W striking faults and defines a T axis whose trend progressively switch from NNE-SSW to NNW-SSE moving from east to west. Based on morphostructural criteria, this first was the major episode of slip recorded on the studied faults. A second set of lineations developed primarily on NW-SE striking faults that had a normal to right-transensional slip with a T axis that trends from ~NE-SW to ~E-W.

The preliminary results on the relocated background seismicity that occurred in the last 12 years in and around the Campanian Plain show temporally and spatially isolated events with magnitudes <2.5. The few events with epicenter inside the plain are located in the north-western sector and a concentration of seismic events is noticeable along the Avella ridge. Relatively to this cluster, the seismicity is constituted by low magnitude single events ($M_L \leq 2.0$), and by a low magnitude seismic swarm ($M_{Lmax} < 3.5$) that occurred in 2005.

The fault plane solutions of few low magnitude events localized beneath the eastern flank of the plain show kinematics that changes from normal to slightly transensional moving from north to south. These events have a trend of the T axis similar to that associated to the second set of fault-slip lineations (from ~NE-SW to ~E-W), and both are consistent with the current extension axis documented by geological data and large-magnitude seismicity along the Apennines.

Three-dimensional pattern of lithospheric compression in central Italy – Geodynamic implication

Lavecchia G.*¹, de Nardis R.¹, Pandolfi C.¹, Monachesi G.², Cattaneo M.², Marzorati S.², Cirillo D.¹, Ferrarini F.¹ & Brozzetti F.¹

¹ CRUST, DiSPUTer, Università “G. d’Annunzio”, Chieti Scalo.

² Istituto Nazionale di Geofisica e Vulcanologia, Ancona.

Corresponding email: glavecchia@unich.it

Keywords: continental lithosphere shear zones, active thrusting, Central Italy.

The geodynamic context of Central-Eastern Italy has always been controversial (Lavecchia et al., 2003 and references therein). To better enlighten this scenario, we used new high-quality earthquake data (hypocenters and focal solutions) obtained for the 2009-2017-time interval by recordings from a dense seismometric network in Central Italy. Such a new dataset updates the previous one by Carannante et al. (2013). By integrating earthquake data with structural-geological constraints, a realistic and curvi-planar 3D fault model of the compressional system active from upper crust to upper mantle depths in eastern Central Italy was built. Geometric and kinematic results highlight two well distinct individual shear zones, one corresponding to the down-dip prosecution of the Adriatic frontal thrust and the other to a hidden and up to now unrevealed independent SW-dipping structure, referred to as Incipient Thrust (IT). IT is well evident at depth between 25 and 60 km, for an along -strike extent of at least 250 km. Tomographic results and related Vp velocities shows that both shear zones dislocate the bottom of Adriatic crust and penetrate across the underlying continental lithosphere. A lack of intermediate depth earthquake (depth >70 km) is highlighted, and no compatibility of P- and T-axes trend with subduction models is observed. In turn, no signature of ongoing subduction is found, but rather an ongoing process of intra-lithosphere compression observed. Shmax trajectories, built at a dense grid of measure nodes, show a kinematic compatibility between the IT and the Adriatic thrust, with a common outward-diverging P-axes radial pattern, possibly reproducing the basal drag of the stretched and outward migrating Tuscan-Tyrrhenian mantle.

Lavecchia G., Boncio P. & Creati N. (2003) - A lithospheric-scale seismogenic thrust in Central Italy. *Journal of Geodynamics*, 36, 79-94.

Carannante S., Monachesi G., Cattaneo M., Amato A. & Chiarabba C. (2013) - Deep structure and tectonics of the northern-central Apennines as seen by regional-scale tomography and 3-D located earthquakes, *J. Geophys. Res. Solid Earth*, 118, 391-5403.

Ultra-shallow imaging of a surface rupture fault of the 30 October 2016 Mw 6.5 central Italy earthquake from multidisciplinary geophysical approach

Maraio S.*¹, Villani F.², Serri L.¹, Sapia V.², Improta L.² & Bruno P.P.³

¹ Centro di Geotecnologie, Università di Siena – Italy.

² Istituto Nazionale di Geofisica e Vulcanologia – Italy.

³ Khalifa University - UAE.

Corresponding email: stefano.maraio@unisi.it

Keywords: high-resolution seismic fault

The Pian Grande di Castelluccio (PGC) basin is a ~20 km² wide intramontane depression located eastwards of the Norcia area, in the hangingwall of the Vettore-Bove normal fault-system (VBFS). The VBFS contributed significantly to the total moment release during the 30 October 2016 Mw 6.5 Norcia Earthquake that provoked coseismic surface faulting through the basin. In this work we present the results of multidisciplinary geophysical investigation across one of the surface-rupturing faults within the PGC, previously described in 2003 by Galadini & Galli through paleoseismological trenches and later analyzed by Villani and Sapia (2017) using multi-scale electrical resistivity data. We have recorded a 190 m long high-resolution seismic profile WSW-ENE trending, oriented perpendicular to the surface fault scarp, with a multi-fold wide-aperture geometry in order to obtain complementary velocity and reflectivity images of the shallow structure of the activated fault. The seismic profile exactly overlaps the electrical survey made by Villani and Sapia in 2017; this permits a precise comparison and integration between the results from two different geophysical methods. Seismic data were collected using two adjacent linear arrays made respectively of 96 vertical geophones with a 4.5 Hz eigenfrequency 2m spaced and 48 horizontal geophones 4 m spaced, to record both P and Rayleigh waves. The seismic source was a 5 kg sledgehammer; source move-up was 2 meters and at each point we stacked three blows, to increase the signal-to-ambient-noise ratio. We proceeded to first-arrival picking that provided data for traveltimes tomography; the P-wave velocity model was achieved by means of an iterative tomographic approach based on the SIRT image reconstruction technique. Reflection processing was performed using a standard flow used in deep exploration seismology; the processing flow sequence and the parameters was designed to enhance the shallowest reflections and the reflected events from dipping reflectors, such as fault planes. To process the dispersion curve of Rayleigh waves we used the approach of multichannel analysis of surface waves (MASW), considering both vertical and horizontal components. The 1D Vs profiles were calculated each 10 meters and then interpolated to have a 2D model. The meaningful comparison of the results provided by seismic reflection, seismic tomography images and Vs model, combined with the electrical resistivity data, allowed a detailed image of the ultra-shallow (< 100 m deep) fault structure. Disrupted shallow reflectors suggest fault throw in the order of 30 m, in accordance with previous results by Villani and Sapia (2017).

Galadini F. & Galli P. (2003) - Paleoseismology of silent faults in the Central Apennines (Italy): the Mt. Vettore and Laga Mts. Faults. *Ann. Geophys.*, 46 (5), 815-836.

Villani F., & Sapia V. (2017) - The shallow structure of a surface-rupturing fault in unconsolidated deposits from multi-scale electrical resistivity data: The 30 October 2016 Mw 6.5 central Italy earthquake case study. *Tectonophysics*, 717(16), 628–644.

Earthquake ruptures geometries as tools for seismic hazard assessment

Menichetti M.*, Tirincanti E. & Roccheggiani M.

Dipartimento di Scienze Pure e Applicate, Università di Urbino.

Corresponding email: marco.menichetti@uniurb.it

Keywords: seismotectonics, coseismic ruptures, seismic hazard.

The survey of the geometries of the earthquake ruptures is central to define the kinematic and dynamic relationships of the active faults structures and the regional seismic hazard. Earthquake events that produce coseismic surface deformation that reach the Earth's surface generate offset in the landforms linked to the kinematics and the magnitude of the seismic event. Despite their importance in assessing the hazard and risk of earthquakes and in the developing hazard reduction procedure, the accurate morphologies and geometries of the ground ruptures, remain uncertain. The scarps can result from a single earthquake or from the cumulative effects of several events over the geological timescale. Their geometrical features are a function of the topographic gradient of the region. Morphostructural quantitative parameters of the forming scarps, such as length, displacements permit to characterize the historical activity the fault. Generally, calculus of the displacements across surface ruptures, in the different tectonic scenario, are performed on single faults segments collect with a local ground-based field survey often with the aid of GNSS devices. Consequently, the frame of the whole structure and the characteristics of off-fault deformation and the parameters that control it remain poorly understood. Precise and more accurate displacements across coseismic ruptures can be acquired using recent available remote sensing platforms. Satellite images for scientific purpose, like Google (Digital Globe) and Pleiades (CNES) can reach at least at a resolution of 0.5 m where is limited to detect the offset related to the medium size earthquake ground ruptures. Both methods, however, either fail to capture patterns of near-field coseismic surface deformation. High-resolution mapping based on an Unmanned Aerial Vehicle (UAV) represents an opportunity to gather three-dimensional high-resolution topographic datasets. Images with centimeter resolution obtained via SfM photogrammetry permits to mapping in 3D the details of the vertical and horizontal displacement and constraining the spatial geometrical characteristics of active faults. The analysis of different coseismic ruptures in tectonic and volcanic contest show that about 40% of the total surface displacement occurred as off-fault deformation, over a mean deformation width of a few hundred meters. The rupture zone fabric and the off-fault deformation is mostly controlled by the structural complexity of the fault system, with a more weak correlation with the rheology of the ruptures materials.

The shallow crust in Central Italy depicted by geophysical deep well logs

Montone P.* & Mariucci M.T.

INGV Istituto Nazionale di Geofisica e Vulcanologia, Roma, Italy.

Corresponding email: mariateresa.mariucci@ingv.it

Keywords: Sonic log, P-wave velocity, density.

In order to better define seismic properties of the crust in the area affected by the 2016-2018 central Italy seismic sequence, we have selected the deepest wells with available sonic logs of the Apennine belt and related Adriatic foredeep. These data contribute to better characterize the shallow crust and to build detailed crustal velocity models in a tectonically complex region.

Most exploration wells have a set of geophysical logs that provide valuable information on the in situ conditions of the shallow crust. Sonic log data are among the most important measurements of rock properties and provide a reliable image of in situ conditions at depth, despite their limits mainly due to the investigated rock volume. The borehole sonic tool is a string with one or more transmitters that emit high-frequency acoustic waves, and two or more receivers that record full waveforms. The differences in the arrival times of the wave trains travelling through the formations from the transmitters to the receivers are used to determine the sonic velocities.

We have analysed 21 sonic logs, compared to the borehole stratigraphic profiles, in order to infer P-wave velocity of each single unit (e.g. Massiccio Formation) and the lithostratigraphic groups defined in this work (e.g. “Eocene-Miocene”). Most of the wells in central Italy have been analysed in the framework of the RETRACE-3D project (centRAL italy EarThquakes integRAted Crustal model) which aims to build a new 3D model of the area struck by the 2016-2018 seismic sequence, with the multi-disciplinary skills of a large community of researchers. Moreover, we have used P-velocities to estimate rock density values, following an empirical relationship between sonic velocity and density in sedimentary rocks. In situ measurements of stress magnitudes are still undefined almost everywhere, in this area we have estimated vertical stress magnitude from density data - down to 7 km depth - between the inner Apennine belt and the Adriatic foredeep. Results show large spatial differences within a small area moving from the belt to the foredeep, mainly with depth, and a lithostatic gradient from ~26 to ~22 MPa/km. Finally, petrophysical parameters inferred from geophysical logs help 3D reconstruction of the shallow crust evidencing both the main tectonic setting and the small local characters. These results contribute to a better interpretation of physical conditions at depth and provide data useful for more realistic models.

A multi-method approach to characterize the geometry of the Paganica and Matese seismogenetic faults (Central-Southern Apennines, Italy).

Nappi R.*¹, Paoletti V.², Gaudiosi G.¹, Luiso P.⁴, Cella F.³, Florio G.² & Fedi M.²

¹ Istituto Nazionale di Geofisica e Vulcanologia, Sezione Osservatorio Vesuviano, Naples.

² Department of Earth, Environment and Resources Science, University of Naples Federico II.

³ Department of Biology, Ecology and Earth Sciences, University of Calabria.

⁴ SOCOTEC, Avellino.

Corresponding email: rosa.nappi@ingv.it

Keywords: Central-Southern Apennines, multi-method approach, Multiscale Derivative Analysis.

The Abruzzo and Molise regions (Central-Southern Apennines) are characterized by the occurrence of the strongest seismic activity of Italian Apennines. The seismogenetic sources of Abruzzo and Molise, responsible for destructive historical events ($M_w > 6$) are located along the Apennine chain, along NW–SE faults, with hypocenters focused within the upper 10–20 km of the crust. Structural observations on the Pleistocene faults suggest normal to sinistral movements for the NW–SE faults and normal to dextral movements for the NE–SW structures. The focal mechanisms of the largest events show normal solutions consistent with a NE–SW extension of the chain. The last earthquake that struck the Abruzzo region, occurred on April 6, 2009 ($M_w = 6.3$), killing 309 people. The epicenter was located close to the L’Aquila town, along the Paganica fault belonging to the Paganica-San Demetrio fault system. This earthquake was followed by a long seismic crisis including four events with $5.1 < M_w < 5.6$.

After the 1980 Irpinia large earthquake, the release of seismic energy in Southern Apennines was characterized by the occurrence of moderate energy sequences ($M_w < 5$) mainly of shock-aftershocks type and with swarm-type activity, along NW–SE and NE–SW systems of fault. A moderate seismic sequence ($M_{max} = 5.1$) struck the Molise region, in the Matese area, from December 29, 2013 (Ferranti et al., 2015).

Our study consists of a multiparametric analysis carried out by merging tectonic, seismic and gravimetric data in GIS environment, with the aim of constraining the geometry of Paganica and Matese seismogenetic faults, both at the surface and at depth. The *Multiscale Derivative Analysis* (MDA) data of the gravity field, whose maxima define the structural lineaments characterized by density contrast, were compared with earthquakes epicentral distribution and faults from literature. Moreover, 2D seismic hypocentral distribution was correlated with the *DEXP* (*Depth from Extreme Points*; Fedi and Pilkington, 2012) gravity imaging, to estimate the fault systems parameters (strike, dip direction and dip angle) at depth.

This multi-parametric approach was already applied to the seismically active region of the Central Apennines (Luiso et al., 2018), hit by the 2016–2017 Amatrice-Visso-Norcia seismic sequence.

Fedi M., & Pilkington M. (2012) - Understanding imaging methods for potential field data. *Geophysics*, 77, G13-G24.

Ferranti L., Milano G., Burrato P., Palano M. & Cannavo F. (2015) - The seismogenic structure of the 2013–2014 Matese seismic sequence, Southern Italy: implication for the geometry of the Apennines active extensional belt. *Geophys. J. Int.*, 201(2), 823–837.

Luiso P., Paoletti V., Nappi R., Gaudiosi G., Cella F. & Fedi M. (2018) - Testing the value of a multi/scale gravimetric analysis in characterizing active fault geometry at hypocentral depths: the 2016/2017 central Italy seismic sequence. *Annals of Geophysics*, 61(5), 558–571.

3D reconstruction of the M. Vettore seismogenic fault system (Central Apennines, Italy): cross-cutting relationship with the M. Sibillini Thrust

Porreca M.*¹, Fabbrizzi A.², Azzaro S.¹, Pucci S.³, Del Rio L.⁴, Pierantoni P.P.⁵, Giorgetti C.¹,
Roberts G.⁶ & Barchi M.R.¹

¹ Dipartimento di Fisica e Geologia, Università di Perugia, Italy (CRUST Member, Centro interUniversitario per l'analisi SismoTettonica tridimensionale con applicazioni territoriali).

² University of South Florida, USF Tampa, USA.

³ Istituto Nazionale di Geofisica e Vulcanologia, Rome, Italy.

⁴ Dipartimento di Geoscienze, Università di Padova, Italy.

⁵ Scuola di Scienze e Tecnologie, Università di Camerino, Camerino (MC), Italy.

⁶ Department of Earth and Planetary Sciences, University of London, UK.

Corresponding email: massimiliano.porreca@unipg.it

Keywords: 2016-2017 Central Italy earthquake, cross-cutting fault, 3D structural model.

The 2016-2017 Amatrice-Norcia seismic sequence was triggered by the reactivation of a complex NNW-SSE trending, WSW-dipping fault system cross-cutting the Umbria-Marche fold and thrust belt. This fault system produced important co-seismic ruptures in the hangingwall of the M. Sibillini thrust, whereas less evident or absent ruptures were observed in the footwall. A strong controversy exists in the literature about the geometry of the seismogenic faults, their relationships with pre-existing thrusts, and the location of normal-faulting rupture tips. In this work we present a 3D geological model of the M. Vettore area located between the Castelluccio basin and the outcrop of the M. Sibillini thrust, where the most evident co-seismic ruptures have been observed. The model shows the relationship between the ruptured normal faults and the M. Sibillini thrust, and was constructed using a grid of 14 geological cross-sections parallel and orthogonal to the main structural elements (i.e. normal faults and thrusts) down to a depth of 3 km. The model was constructed using reference structural surfaces, such as the top of Lower Cretaceous Maiolica Fm, the M. Sibillini thrust and the main seismogenic normal faults belonging to the M. Vettore fault system. The 3D model shows the vertical cumulative throw distribution for the M. Vettore normal faults. The cumulative geological throw of more than 1300 m across the normal faults in the proximity of the M. Sibillini thrust, suggests that the seismogenic fault system continues into the footwall of the thrust, displacing it in the sub-surface. The results of this study provide important constraints on the cross-cutting relationships between active normal and old compressional structures in a seismic active area, contributing to a better definition of the faults segmentation, and thus of the related seismic hazard.

Evolution of an active fault system in an extensional context: the case of the Mt. Vettore system in the central Apennines and insights in its segmentation pattern

Puliti I.*¹, Pizzi A.¹, Benedetti L.², Di Domenica A.¹ & Fleury J.²

¹ Dipartimento InGeo, Università di Chieti-Pescara, Chieti, Italy.

² Aix-Marseille Université, CEREGE CNRS-IRD UMR 34, Aix-en-Provence, France.

Corresponding email: irene.puliti@unich.it

Keywords: Mt. Vettore - Mt. Bove normal fault system, active faults, Aug-Oct 2016 earthquakes.

The morphotectonic and structural geology of the Mt. Vettore - Mt. Bove normal fault system (VBFS) in the central Apennines is studied to unravel its evolution over time. In Aug-Oct 2016, this normal fault system broke during three earthquakes (Mw6.0, Mw5.9, and Mw6.5) associated with clear coseismic ruptures. Based on topographical, geological and high-resolution satellite images, as well as original field observations integrated with the available surface rupture maps (e.g., Villani et al., 2018), we identify three types of faults: 1) Active faults with 2016 surface ruptures and morphological evidence of Late Quaternary activity; (2) Probably active faults with only morphological evidence; (3) faults without morphological and coseismic evidence.

From seven geological cross-sections leveled across the fault system, using published geological maps (Pierantoni et al., 2013) and original field geological surveys, we derived the geological offsets on both active fault segments (types 1 and 2) and on normal faults with no evidence of recent activity (type 3). The cumulative morphological offset is instead assessed on each fault portion exhibiting evidence of activity by using topographic profiles extracted from a high-resolution DEM (derived from Pleiades images acquired after the 2016 earthquakes, DEM resolution is 2 m). Those 102 offsets measurements yield the distribution of the last post-glacial cumulative throw over the 22 km-long studied portion, between Mt. Vettore and Mt. Bove. The maximum throw is observed along the southern portion of the fault system, on the Mt. Vettore segment, where it reaches 25 m and progressively decreases northward.

The 2016 coseismic ruptures concentrate just on those segments that have recorded Late Quaternary activity. In particular, faults at the southern tip of the system seem to have experienced, over the last 18 kyr, the same rupturing pattern and surface displacement during each seismic event, like the one observed in 2016.

We recognize in this feature the surface effect of a significant segment boundary ruled by the deep WNW-dipping listric structure attributable to the inherited Mt. Sibillini thrust ramp. The largest slip observed at the surface along the VBFS is located in an area corresponding to the presence of a major asperity at depth (Manighetti et al., 2005), along the barrier between the VBFS and the southern Laga Fault.

Manighetti I., Campillo M., Sammis C., Mai P. M. & King G. (2005) - Evidence for self-similar, triangular slip distributions on earthquakes: Implications for earthquake and fault mechanics. *Journal of Geophysical Research: Solid -Earth*, 110(B5).

Pierantoni P., Deiana G. & Galdenzi S. (2013) - Stratigraphic and structural features of the Sibillini mountains (Umbria-Marche Apennines, Italy). *Italian Journal of Geosciences*, 132(3), 497-520.

Villani F., Civico R., Pucci S., Pizzimenti L., Nappi R., De Martini P. M. & Amoroso S. (2018) - A database of the coseismic effects following the 30 October 2016 Norcia earthquake in Central Italy. *Scientific data*, 5, 180049.

The southern Italy 1980 earthquake and the rupture processes of large earthquakes in Italy

Scarpa R.*

Dipartimento di Fisica “E.R.Caianello”, Università di Salerno.

Corresponding email: rscarpa@unisa.it

Keywords: seismotectonics, earthquake mechanisms.

A detailed reconstruction of the rupture mechanism of the 1980 Campania–Lucania (southern Italy) earthquake is presented. Relocation of the main hypocenters and the estimation of fault-plane solutions of the aftershocks, through P-wave velocity inversion models provide an overall comprehensive picture of the source mechanism. The analysis of available data suggests a complex rupture mechanism, as already identified by many previous studies, which consists of three separate events. The present work provides however a convincing evidence of almost simultaneous activation of a synthetic-antithetic normal fault couple as characterizing rupture source process of this earthquake. The first event activated the northern SW-NE striking segment of a large (~40-km-long), high-angle, E-dipping, master fault. With the second event the rupture propagated southward along the fault strike and activated the southern WNW-ESE striking segment (~15-km-long) of the same master fault. Conversely, the third rupture occurred along a SW-dipping normal fault antithetic to the master fault northern segment. No foreshocks occurred but the first large rupture triggered the delayed sequence of large events. Then the sequence is followed by a series of aftershocks which are still occurring along the asperities not broken during the main sequence, similar to the Messina, 1908 event, which seems to present similar rupture triggering phenomena along a graben like structure.

Seismic velocity variations of carbonates across the Apennines

Trippetta F.*¹, Barchi M.R.², Borromeo O.³, Mastellone D.³, Rosset G.² & De Paola N.⁴

¹ Sapienza University of Rome.

² University of Perugia.

³ Eni E&P.

⁴ Durham University (UK).

Corresponding email: fabio.trippetta@uniroma1.it

Keywords: seismic velocity, carbonates, Apennines.

Modelling seismic source, co-seismic strain and displacement and geometry of seismogenic faults relies on the estimation of seismic velocities, which strongly depend on the physical properties of the involved rocks. Seismic velocities are severely influenced by lithological contrasts and by changing environmental conditions, such as for example state of stress, depth and fracturing. In this work, we analyse and compare an extensive seismic-wave velocity dataset of the Apennines carbonates since in recent years, the moderate to large magnitude earthquakes that struck Italy nucleated and propagated through carbonate rocks. We thus focused on the most representative (thicker) carbonate formations of the Apennines: massive pure limestone (Calcare Massiccio, CM), layered pure limestone (Maiolica, MA), and layered marly limestone (Calcareous Scaglia, SC). We compared seismic-velocity dataset obtained from different acquisition methodologies applied at a wide range of scales, including down-hole in situ measurements (sonic logs and interval velocities) and laboratory experiments on cm-scale rock cores. The different acquisition-methodologies give comparable results where the most common recorded V_p is 6.1 km/s for CM, 5.7 km/s for MA and 5.8 km/s for SC. We observed that laboratory measurements (performed on cm-scale core samples) are mostly sensitive to mineralogical variations, with lower V_p where the clay content is high and faster V_p where dolomitization is widespread. Laboratory measurements at increasing confining pressure indicate that velocities are mostly pressure (depth) independent. Conversely, sonic and interval velocity, are depth-influenced where SC is significantly influenced, MA is only slightly influenced, and CM is not influenced. Moreover, our results on sonic and interval velocity highlight a strong control exercised by the structural position where a larger average velocity is observed in the mountain range (where formations are deeper-buried and more fractured), respect to the foreland (where formation are shallower and less fractured). We thus suggest that the burial history, i.e. the maximum experienced lithostatic load, exerts a key-role in controlling V_p for carbonates, in particular for stratified formations MA and SC whilst fracturing seems to have a minor role in controlling average velocities. The observed difference can be quite large (about 1 km/s for SC) highlighting that, the mechanical properties of the involved rocks can be defined only through the construction of detailed, laterally variable velocity models. We then suggest that this conclusion can be extended to other tectonically complex region around the World.

High-resolution seismic profiling in the Castelluccio basin: new constraints on the shallow subsurface of the 30 October 2016 Mw 6.5 Norcia earthquake fault (central Italy)

Villani F.*¹, Maraio S.², Bruno P.P.³, Improta L.¹, Wood K.⁴, Civico R.¹, Baccheschi P.¹, Sapia V.¹, Pucci S.¹, Brunori C.A.¹, De Martini P.M.¹, Pantosti P.M.¹, Conti P.² & Doglioni C.¹

¹ Istituto Nazionale di Geofisica e Vulcanologia – Italy.

² Centro di Geotecnologie, Università di Siena - Italy.

³ Khalifa University - UAE.

⁴ Université Montpellier - France.

Corresponding email: fabio.villani@ingv.it

Keywords: high-resolution seismic profiling, fault, Norcia earthquake.

Following the 30 October 2016 Mw 6.5 Norcia earthquake in central Italy, in order to understand the complex kinematics and geometry of the mainshock causative normal fault-system and its effects at the surface, many seismological, geodetic, geophysical and geological data have been collected. The Vettore-Bove fault-system (VBFS), renowned as one of the major seismogenic sources in the central Apennines, contributed significantly to the total moment release during the Norcia mainshock. The VBFS hosts in its hangingwall a wide intramontane depression, the Castelluccio basin. This basin is settled in a key structural position, matching the locus of the largest long-term displacement of the VBFS and it was affected by surface faulting during the Norcia earthquake. Yet, details on the shallow subsurface structural setting of this basin are still lacking, hampering the accurate knowledge of the shallow architecture of the fault system and the estimate of the Quaternary activity of the VBFS.

During the Fall 2017, we acquired three high-resolution seismic profiles within the basin with a multi-fold wide-aperture acquisition geometry that allows collecting simultaneously reflection and refraction data in a wide offset range. The first profile is 2600 m-long, trends WNW, and crosses nearly orthogonal the 2016 surface ruptures as well as an important splay of the VBFS. The second profile is 2000 m-long, trends WNW, and intercepts one of the basin-bounding faults to the south. This profile is tied at both ends to two boreholes reaching the pre-Quaternary limestone bedrock. The third profile is 3000 m-long, trends NNE, and connects the first two lines. We deployed a linear array of 240 vertical geophones 5-m spaced and controlled by ten 24-bit seismometers using a roll-along technique to cover the overall profiles length. We used a 6-tons vibroseis (Minivib of IVI©) as a powerful yet safe energy source, with average 5-m spacing. We collected > 1200 shot-gathers, for a total of > 280,000 seismic traces. We handpicked first-arrival traveltimes in order to perform a non-linear tomographic inversion using a multi-scale imaging strategy. The obtained P-wave velocity models illuminate the basin structure down to 350-400 m depth along the three key sections. The limestone bedrock is imaged as a high-velocity region (V_p 4500-5000 m/s) showing a complex geometry due to the presence of a large number of subsurface faults defined by abrupt lateral V_p changes. We apply an advanced processing flow to the reflection data taking advantage of the high fold and large offset range of the CMP gathers that show reflections with an overall good signal-to-noise ratio and coherency. The obtained time-migrated stack sections show details of the depositional architecture down to 0.5 sec TWT, characterized by alternating coarse clastics and thin-bedded lacustrine deposit. These data put constraints on the location and geometry of several subsurface faults.

Roughness evaluation of the Monte Vettoreto active fault after the massive 2016 seismic sequence of Central Apennines, Italy

Zambrano M.*¹, Corradetti A.², Tavani S.³, Pitts A.¹, Seers T.D.² & Tondi E.¹

¹ School of Science and Technology, Geology Division, University of Camerino, (MC), Italy.

² Department of Petroleum Engineering, Texas A&M University at Qatar.

³ DiSTAR, Università di Napoli Federico II, Italy.

Corresponding email: miller.zambrano@unicam.it

Keywords: photogrammetry, fault roughness, active faults, FFT power spectrum.

It is well recognized from both experimental and simulation studies that small-scale asperities on fault planes (i.e. fault roughness) can act as stress concentrators, affecting the fault frictional behavior and the dynamics of rupture propagation. The acquisition of highly accurate and detailed datasets of fault surface topographies represent the primary datasets used in the assessment of fault roughness. Typically, this involves the use of field-based LiDAR stations to cover observations at larger scales (> few centimeters) or laboratory-based investigations using laser profilometers and white light interferometers for smaller scale roughness studies (e.g. sub-mm to nanoscale).

In this study, we have applied structure from motion-multiview stereo (SfM-MVS) photogrammetry to reproduce decimeter-sized patches of the topography of the Monte Vettoreto active fault (Central Apennines, Italy), in order to explore the potential use of field-based photogrammetric methods for the assessment of fault roughness. Such methods are presently underexplored, and offer the potential to provide detailed fault plane profilometry data directly in the field. The photo survey presented in this study was performed on the freshly exposed surface of the fault after few days of the main Mw 6.5 shock that hit the area on the 30th October 2016.

The methodology used herein comprises of field-based high-resolution SfM-MVS photogrammetric reconstruction of the fault surface, with fault roughness assessed by means of a power spectral density (PSD) frequency domain analysis. Fault patch surface models were aligned and processed using Agisoft PhotoScan Pro, generating high vertex density point clouds. Further processing consisted of (i) removing the artificial trend of the surface, (ii) surface interpolation, and (ii) sampling vertex data into a regular grid. A complete description of the fracture roughness is given by the specification of two functions: the probability density function (depending on the media and standard deviation) for asperity heights and the Power Spectral Density (PSD) using Fast Fourier Transform (FFT) analysis. The FFT analysis was made on the surfaces along the direction of slip and perpendicular to it using a 1-D FFT approach, deployed via a bespoke Matlab script.

Our results show that, by means of field-based photogrammetry, we were able to fill the resolution gap existing between field-based LiDAR and laboratory-based techniques for fault plane profilometry data acquisition. The use of the SfM-MVS photogrammetry is especially useful towards the evaluation of fault surface roughness after major seismic events, where the portability and accuracy of photogrammetric survey tools (i.e. consumer grade cameras) are advantageous. Results of the FFT analysis are in overall agreement with published works using proven methods. These encouraging results demonstrate the utility of photogrammetric methods for future fault roughness studies, particularly those involving field-based data acquisition, where established techniques have limitations.

S23

**Analogue and numerical modelling of geological processes:
linking observation, interpretation and prediction**

CONVENERS AND CHAIRPERSONS

Marco Bonini (CNR-IGG)

Giacomo Corti (CNR-IGG)

Francesca Funicello (Università di Roma Tre)

Antonello Provenzale (CNR-IGG)

Pietro Sternai (Università di Milano Bicocca)

An attempt at modelling the lithosphere of Sardinia block and surroundings: relationships among isostatic disequilibrium, geomorphic features and neotectonics

Cocco F.*¹ & Funedda A.¹

¹ Dipartimento di Scienze Chimiche e Geologiche, Università degli Studi di Cagliari.

Corresponding email: fabrcocco@gmail.com

Keywords: elevation, geoid anomaly, thermal analysis.

We present a model of the lithospheric structure beneath Sardinia and surroundings, in an area that extends from Balearic to Tyrrhenian basins. The method allows to map crustal and lithospheric thicknesses using elevation, geoid anomaly and thermal analysis (Fullea et al., 2007).

Our results highlight four main domains each one characterized by different lithospheric structure. The areas where the crust has been thinned more are the Balearic and Tyrrhenian basins, although they differ each other because the mantle lithosphere is thinner in the Balearic Basin. Sardinian lithosphere has a mantle lithosphere thinned as much as that of Tyrrhenian Basin and a crust roughly of normal thickness. NE Sicily and part of the Sardinian Channel show the highest lithospheric thickness in the study area.

Our model fits quite well with previous lithospheric structure defined by geophysical methods. The differences are more important in the mantle lithosphere than in the crustal thickness, especially in the Balearic and Tyrrhenian basins. The best fitting is with lithosphere beneath Sardinia.

To investigate where and if isostatic equilibrium has been reached in the model, we follow two different approaches: we computed (i) the crustal roots and the anti-roots by means of Airy-Heiskanen isostasy model and (ii) the elevation that there should be in the study area considering in isostatic equilibrium the lithospheric structure achieved from our model. The crustal roots and anti-roots throughout the model are deeper by roughly 7 km than Moho depth inferred by the model. This evidence indicates that the area investigated is slightly undercompensated. However, considering the contribution of the whole lithosphere and not only of the crust, overcompensation seems to affect Balearic and Tyrrhenian basins whereas Sardinia Channel and Sardinia are undercompensated. Undercompensation means that Sardinia is currently uplifted, explaining several geomorphic features as rugged morphology, relief inversions and deep river incisions that characterize the Island. The still lasting isostatic disequilibrium might have led to vertical movements that, reactivating previous structures, gave rise to neotectonic structures as the Pleistocene Campidano Basin, as well as rare and low-magnitude earthquakes recorder in the Island. Finally, also the Plio-Pleistocene volcanic complex is probably closely related to the lithospheric structure.

The relationships between the current lithospheric structure in western Mediterranean and its Cenozoic geodynamic evolution are still debated. Our findings suggest that the Balearic and Tyrrhenian basins lithosphere is affected mainly by extension, whereas Sardinian lithosphere by thermal thinning.

Fullea J., Fernández M., Zeyen H. & Vergés J. (2007) - A rapid method to map the crustal and lithospheric thickness using elevation, geoid anomaly and thermal analysis. Application to the Gibraltar Arc System and adjacent zones. *Tectonophysics*, 430, 97–117.

Improving subduction megathrusts seismic hazard assessment: a proof of concept based on analog modelling and machine learning.

Corbi F.*

Univ. Roma Tre - Dip. Scienze - Sez. Geologia.

Corresponding email: fabio.corbi3@gmail.com

Keywords: analog modelling, megathrust seismicity, machine learning.

Subduction zones are complex dynamic systems hosting two of the most dangerous geo-hazards: mega-earthquakes and tsunamis. Despite the growing spatio-temporal density of geophysical observations at subduction zones, our understanding of the megathrust earthquake cycle continues to be limited by a series of factors. Among the others the short observation time compared to mega-earthquake recurrence and the partial spatial coverage of geodetic data. Here, I contribute to improving this understanding by simulating dozens of seismic cycles in a laboratory-scale analogue model of subduction. The model creates analog earthquakes of magnitude M_w 6.2–8.3, with a coefficient of variation in recurrence intervals of 0.5, similar to real subduction megathrusts. Using a digital image correlation technique, I measure coseismic and interseismic deformation with high accuracy (few tens of μm) and resolution (few mm). This is equivalent to having a very dense geodetic network homogeneously distributed over the whole margin, including the generally offshore seismogenic zone. I show that the common procedure of estimating the next earthquake size from slip-deficit is unreliable, even in the case of an ideally designed monitoring network. On the contrary, machine learning predicts well the timing and size of laboratory earthquakes by reconstructing and properly interpreting the spatiotemporally complex loading history of the system. I conclude showing future research paths for exporting this method to real subduction zones and demonstrating the contribute of this method for designing an efficient geodetic network. These results promise substantial progress insubduction megathrusts seismic hazard assessment.

Modelling the influence of pre-existing brittle fabrics on the development and architecture pull-apart basins

Corti G.*¹, Nencini R.² & Skyttä P.³

¹ Istituto di Geoscienze e Georisorse, Consiglio Nazionale delle Ricerche.

² Dipartimento di Scienze della Terra, Università degli Studi di Firenze.

³ Department of Geography and Geology, Geology Section, University of Turku.

Corresponding email: giacomo.corti@igg.cnr.it

Keywords: pull-apart basins, analogue modelling, pre-existing structures.

Pull-apart basins form as a result of local extension generated by the interaction between major segments of strike-slip faults. Much of the current knowledge on the development of these basins comes from the results of analogue models that simulate the deformation of a homogeneous crust or lithosphere. In this work, we improve these previous analyses by considering the development of pull-apart basins in an upper crust characterized by the presence of pre-existing discrete fabrics.

To this aim, we used new $1g$ analogue models to analyze the conditions under which these pre-existing structures are reactivated, and to investigate their influence on the development of pull-aparts. The set-up of the experiments was the same used in the majority of normal gravity models: the movement between two crustal blocks was simulated through the lateral movement of basal rigid plates. Local extension allowing the formation of a pull-apart basin was produced by the presence of an offset area between the two basal plates: as in previous modelling works, we reproduced conditions of neutral, overlapping and underlapping master faults. The model upper crust, reproduced by a sand mixture, was characterized by the presence of pre-existing structures (modelled as an artificial dilation zone in the sand cake) with different orientations with respect to the trend of the main strike-slip faults. For comparison, models with a homogenous upper crust were also performed.

The evolution of homogenous models was similar to that described in previous works: deformation and basin subsidence were initially accommodated by border fault systems, followed by cross-basin faults linking the major strike-slip fault segments. In agreement with previous findings, the offset angle between the main transcurrent faults had the most important influence on the pull-apart geometry: the basins were Z-shaped, rhomboidal-shaped or lozenge-shaped in case of neutral, overlapping and underlapping master faults, respectively. Comparison among models with fabrics and homogeneous ones allows to highlight that -in specific conditions- reactivation of the pre-existing structures can occur both within and at the margins of the pull-apart basins. Inside the basin, reactivation occurs when the pre-existing structures are orthogonal or sub-orthogonal to the local extension direction. In this case, the reactivated pre-existing fabrics delay the development and linking of cross-basin faults and increase the complexity of the basin architecture by giving rise to a new set of faults characterized by an atypical trend. At the margins of the pull-apart, reactivation occurs if the fabrics spatially coincides with the margins of the area undergoing deformation. In these conditions, reactivation allows a faster development of the border faults, which are less segmented than in the homogenous models; this also results in a more regular final geometry of the pull-apart.

Unveiling the engine of mid-term deformations at Ischia resurgent caldera (Italy) using remote sensing and in situ data

Lanzi C.*¹, Trasatti E.² & Battaglia M.¹

¹ Dipartimento Scienze della Terra, Università La Sapienza di Roma.

² Istituto Nazionale di Geofisica e Vulcanologia, Roma.

Corresponding email: chiaralanzi94@libero.it

Keywords: surface deformation, Ischia, InSAR, numerical model.

In this work, we model the surface deformation of Ischia (Campi Flegrei / Vesuvius volcanic region, Naples, Southern Italy) measured in the 1987–2010 time period. Our analysis shows that simple analytical models cannot properly describe the observed deformation and stress the need of employing numerical models which can help us to take into consideration the topography forces and local geology. A quantitative analysis of InSAR, levelling and GPS data allow us to define two localized zones of subsidence, one in the NW of the island (max values of -24 cm) and the other on the southern slope of Mt. Epomeo (max value of -16 cm). Moving towards the coastline, outside the central zone of the island characterized by the resurgent block (culminating with Mt. Epomeo at the center of the island), the deformation shows little or no displacement. We employ the Finite Element Method to evaluate the influence of two different sources: one simulating the deformation along a fault located in the NW rim of the resurgent block of the island and the second simulating the island-scale deformation due to the magmatic source (about 2 km beneath Mt. Epomeo). The three models employed are: 1) a flat-surface domain with the deformation controlled only by gravity, 2) deformation forces by gravity but controlled by the topographic relief and 3) the influence of local geology (i.e., the island hydrothermal system) in forcing the sliding long existing faults. The first two attempts allow us to discard the hypothesis that the deformation is controlled by gravity alone (e.g., the weight of the topographic relief of Mt. Epomeo). In the final model, with the adding of a force on the fault to simulate the depressurization of the local hydrothermal system, the achieved result shows a good agreement with the deformation data. Our interpretation of the mechanism controlling the subsidence is the volume variation at the island-scale source, due to depressurization. This causes the localized deformation at the NW portion of the island along direct faults located at the rim of the resurgent block, on the northern flank of Mt. Epomeo.

Collapsed calderas vs inherited fabrics: insights from analogue modelling

Maestrelli D.*¹, Bonini M.¹, Corti G.¹, Montanari D.¹ & Moratti G.¹

¹ CNR-IGG, Consiglio Nazionale delle Ricerche, Istituto di Geoscienze e Georisorse.

Corresponding email: daniele.maestrelli@gmail.com

Keywords: analogue modelling, caldera collapse, inherited structures.

Caldera collapse is a complex geological process that, due to its quasi-instantaneous nature, remains difficult and elusive to investigate. Because of this, several numerical and analogue modelling experiments have been used to analyse this process during the last decades (e.g., Geyer & Martí, 2014, and reference therein): these approaches are indeed of great importance because they allow to monitor the progressive evolution and the architecture of deformation resulting from caldera collapse. In particular, analogue models available in literature, show different processes for ring-fault formation and propagation, especially focusing on the interactions between outward-dipping reverse faults and inward-dipping normal faults. If a general agreement is shared regarding the first-order processes leading to collapsed edifices (e.g. Acocella, 2007), some aspects are still barely known and need to be investigated, such as the role of inherited structures and their interaction with caldera collapse processes. To address this issue, in the frame of the GEMex Europe-Mexico cooperation project (Horizon 2020 Programme, grant agreement No. 727550), we have performed a series of analogue models investigating the influence of pre-existing faults on caldera deformation pattern resulting from evacuation of a magmatic chamber in the upper crust. In our modelling, we have induced caldera collapse by draining out an analogue magma (polyglycerine-3, PG3; see Montanari et al., 2017) from an analogue magma chamber, emplaced below a brittle sedimentary cover (simulated by a multi-layered sand mixture). Pre-existing faults have been placed either at the caldera margin(s) and/or above the caldera depression. In particular, the shape of the magma chamber was varied by imposing straight sides, simulating pre-existing fault discontinuities, and in some models the sand pack was pre-deformed by introducing artificial dilation zones in different positions to simulate inherited fabrics within the brittle crust. Our models show that discontinuities may induce caldera ring-faults to deviate from standard evolution (i.e., initial inward dipping reverse-faults followed by outward-dipping normal faults). The inherited fabric may influence significantly the deformation pattern, modifying and/or inhibiting the formation of specific collapsed caldera structures.

Acocella V. (2007) - Understanding caldera structure and development: An overview of analogue models compared to natural calderas. *Earth-Science Reviews*, 85(3-4), 125-160.

Geyer A. & Martí J. (2014) - A short review of our current understanding of the development of ring faults during collapse caldera formation. *Frontiers in Earth Science*, 2, 22.

Interplay between rift propagation and inherited crustal fabrics: a case study from the Trans-Mexican Volcanic Belt (Mexico)

Maestrelli D.*¹, Bonini M.¹, Corti G.¹, Montanari D.¹ & Moratti G.¹

¹ CNR-IGG, Consiglio Nazionale delle Ricerche, Istituto di Geoscienze e Georisorse.

Corresponding email: daniele.maestrelli@gmail.com

Keywords: analogue modelling, rift propagation, inherited structures.

The Trans-Mexican Volcanic Belt (TMVB) is a large-scale, NW to SE trending volcano-tectonic feature extending through central Mexico for a length of more than 2000 km. Its genesis is strictly related to the interaction between the subducting Rivera and Cocos plates and the North America plate, as the eastward propagation of volcanism is considered to be associated with slab detachment, and consequent asthenospheric upwelling (e.g., Ferrari, 2004). The progressive SE-directed tearing of the slab and the consequent detachment are hypothesised to cause crustal extension propagating in the same direction. In this context, the TMVB developed several large scale volcanoes and calderas, some of which are the target of geothermal exploration. In the frame of the GEMex Europe-Mexico cooperation project (Horizon 2020 Programme, grant agreement No. 727550), we aim to investigate the interplay between the hypothesized propagating rift and inherited crustal fabrics. Particularly, in the easternmost part of the TMVB, where the GEMex Project is focusing its investigation, the inherited fabric is represented by ca. NE-SW and NW-SE regional faults (Campos-Enriquez & Garduño-Monroy, 1987). These structures may have played a role in the localization of volcanic centres, thus being important players in the geothermal investigation processes. We have addressed this issue through analogue models, which have reproduced continental-scale rift propagation in order to evaluate if and how the inherited structures may interact or reactivate during the rifting. In our models, rift propagation was simulated using a deformation apparatus represented by two basal moving plate hinged at their topmost side, allowing for rotational opening. Extensional deformation was distributed using a rubber sheet overlaid by a PDMS-corundum mixture reproducing the lower crust. The upper crust was instead simulated by a Qz- and K-feldspar sand mixture (80%-20% proportion in weight). Artificial dilation zones trending at various angles to the rift axis (which coincides with the direction of rift propagation) have been introduced within the analogue brittle crust to simulate inherited fabrics. Our modelling results highlight that a propagating rift may reactivate the inherited fabrics as extensional structures or transfer zones (depending on their orientation) for angles $\leq 45^\circ$ to the rift axis. These results also suggest that the intersection between rift faults and reactivated structures may represent a favourable site for magma emplacement, and ultimately for geothermal exploration.

Campos-Enriquez J. & Garduño-Monroy V.H. (1987) - The shallow structure of Los Humeros and Las Derrumbadas geothermal fields, Mexico. *Geothermics*, 16(5-6), 539-554.

Ferrari L. (2004) - Slab detachment control on mafic volcanic pulse and mantle heterogeneity in central Mexico. *Geology*, 32(1), 77-80.

New Granular Rock-Analogue Materials (GRAM) for simulation of multi-scale fault and fracture processes

Massaro L.*¹, Adam J.¹ & Jonade E.¹

¹ Department of Earth Sciences, Royal Holloway University of London, United Kingdom.

Corresponding email: Luigi.Massaro.2018@live.rhul.ac.uk

Keywords: analogue modelling, granular materials, rock mechanics.

Faults and fractures represent the most common geological structures in the brittle Earth's crust, occurring from the regional scale of fault systems to the meso-scale fracture networks and micro cracks. Although fault-fracture processes have been intensely studied, the prediction of their spatial distribution and the understanding of the underlying fundamental processes still represent major scientific challenges. At the sample scale, rock mechanical tests highlight the complex rock behaviour under different stress conditions, characterised by contrasting deformation processes such as elastic deformation, plastic deformation with softening and hardening, strain-dependent strength, transient deformation mechanisms, frictional sliding, cataclastic flow and tensile, compressional or shear failure. Scaled analogue experiments allow to simulate brittle geological deformation processes and their geometric and kinematic evolution, investigated by a detailed time and space analysis. Granular cohesion-less silica sands are commonly applied as rock-analogue materials, showing a geometrical scaling, 1 mm in the model corresponding to 100 m in nature, ideal to simulate regional fault-scale processes in lab-scale experiment but not suitable to resolve small-scale fracture processes. In order to bridge the gap between mechanical fracture tests and regional fault models in scaled analogue experiments with cohesion-less sand material, this study proposes the development of new Granular Rock-Analogue Materials (GRAM), with mechanical properties geometrically scaled to natural brittle rocks, into a range between the field and the outcrop scale. GRAM must be capable to show tensile and shear failure under different stress conditions and requires a geometric scaling suitable for the simulation of simultaneous fault and fracture processes in lab-scaled experiments. Silica sand is considered an ideal rock-analogue material to simulate fault systems under natural gravity conditions. The comparable mechanical behaviour and rheology of granular flow and brittle deformation processes permit geometric, kinematic and dynamic similarity between analogue and prototype. Therefore, GRAM development is based on silica sand. To achieve the required experiment resolution (1 mm in the model corresponding to 1 - 10 m in nature), GRAM must have a much smaller geometrical scaling factor ($L^* = L_{\text{prototype}}/L_{\text{model}}$), ranging from $L^* = 10^4 - 10^3$, than sandbox experiments ($L^* = 10^5 - 10^6$). Our GRAM design is using sand aggregates which are cemented with gypsum powder. Mixing ratios and preparation workflows are tested to adjust the key material properties, such as shear, compressional and tensile strength, Young modulus and Poisson ratio. The new GRAM can provide a new application of lab-scaled analogue experiments, allowing the investigation of fault and fracture processes and their interaction in fault zones and damage zones during different stages of fault evolution.

How many subductions in the Variscan orogeny? Insights from numerical models

Regorda A.*¹, Lardeaux J.-M.², Roda M.¹, Marotta A.M.¹ & Spalla M.I.¹

¹ Dipartimento di Scienze della Terra, Università degli Studi di Milano.

² UMR Geoazur, Université Nice Sophia-Antipolis.

Corresponding email: alessandro.regorda@unimi.it

Keywords: double subduction, numerical modelling, Variscan orogeny.

The debate on the number of oceans and subduction systems that have been active during the Variscan orogeny is still open (Franke et al., 2017). The Variscan belt results from the successive collision of Armorican terranes and Gondwana against Laurussia and Avalonia during Devonian-Carboniferous times (e.g., Matte, 2001; von Raumer et al., 2003; Cocks & Torsvik, 2011; Edel et al., 2013). Armorica is not defined precisely on the basis of palaeomagnetic data, but it has been interpreted as a small continent between the northern Teplà and Rhenohercynian suture and the southern Galicia-southern Brittany sutures. However, the width and the duration of the Galicia-Southern Brittany oceanic domain are debated, due to the discrepancies between metamorphic and paleo-geographic data. Two scenarios concerning the geodynamic evolution of the Variscan orogeny have been proposed, monocyclic and polycyclic. Models of double subduction, characterised by two ocean/continent subduction systems with opposite vergence, have been developed for the first time and here proposed to verify if such a scenario better fit with Variscan P-T evolutions from different sectors of the chain. From the comparison between model predictions and natural Variscan P-T-t estimates from the Alps and the French Central Massif (FCM) results that data from the Alps with high P/T ratios and accurate radiometric ages, compatible with a younger subduction event, show a better fit with the double subduction model, supporting that a polycyclic scenario is more suitable for the Variscan orogeny. On the other hand, data of the FCM with high P/T ratios that fit with both single and double subduction models have poorly constrained geological ages and, therefore, are not suitable to discriminate between mono- and polycyclic scenarios. Moreover, considering the FCM, the predictions of the models open to the possibility that rocks of the Upper Gneiss Unit could derive from tectonic erosion of the upper plate and not only from the ocean-continent transition of the lower plate.

Cocks L.R.M. & Torsvik T.H. (2011) - The Palaeozoic geography of Laurentia and western Laurussia: A stable craton with mobile margins. *Earth-Science Reviews*, 106, 1-51.

Edel J.B., Schulmann K., Skrzypek E. & Cocherie A. (2013) - Tectonic evolution of the European Variscan belt constrained by palaeomagnetic, structural and anisotropy of magnetic susceptibility data from the Northern Vosges magmatic arc (eastern France). *Journal of the Geological Society*, 170(5), 785-804.

Franke W., Cocks L.R.M. & Torsvik T.H. (2017) - The Palaeozoic Variscan oceans revisited. *Gondwana Research*, 48, 257-284.

Matte P. (2001) - The Variscan collage and orogeny (480-290 Ma) and the tectonic definition of the Armorica microplate: A review. *Terra Nova*, 13(2), 122-128.

von Raumer J.F., Stampfli G.M. & Bussy F. (2003) - Gondwana-derived microcontinents-the constituents of the Variscan and Alpine collisional orogens. *Tectonophysics*, 365, 7-22.

Combining analogue experiments with ground deformation from space to study volcano tectonic processes

Ruch J.*

Department of Earth Sciences, University of Geneva.

Corresponding email: joel.ruch@unige.ch

Keywords: volcano tectonic processes, analogue experiments, ground deformations, InSAR.

In the past 20 years, analogue experiments became a key tool to analyze volcano tectonic processes, such as dike intrusions, caldera collapses and rift structures evolution. Recent laboratory techniques, such as digital image correlation and 3D mapping of the model surface deformation go toward new quantitative tools. In the same direction, ground deformation analysis from space via satellite radar data (InSAR) provides since the 1990's a new vision on ground deformation processes. However, in some cases, interpretation of laboratory experiment and/or geophysical data alone can lead to biased understanding of volcano tectonic processes. Here I propose to review a few examples where analogue experiments integrated with geophysical observations and numerical modeling can be merged to have a better understanding of volcano tectonic processes. I will show some examples of rifting events detected from space (Dabbahu in Ethiopia and Bardarbunga in Iceland) that show a clear contribution of magma in shaping rift zones. These results can be used to ameliorate analogue experiment setups of rift zones and our understanding of the structural evolution and related morphologies found in graben related to dike injection. I will then show how analogue experiments combined with numerical modeling can help to better appreciate complex ground deformation detected at subsiding calderas observed with InSAR. Integrated analogue and numerical modeling highlight the key role played by ring faulting in explaining overlapping ground deformation observed by InSAR at calderas that are usually explained by multiple magmatic sources without ring faulting. There is a real need to merge laboratory experiments with geophysical data to fully appreciate the complexity of volcano tectonic processes. This approach can be extended to broader geological processes, such as e.g. fault rupture processes.

Rock-slope failure after deglaciation: rapid response or progressive long-term evolution? Insights from numerical modelling

Spreafico M.C.*, Sternai P. & Agliardi F.

Dipartimento di Scienze dell'Ambiente e della Terra, Università di Milano Bicocca.

Corresponding email: margherita.spreafico@unimib.it

Keywords: rock slope instability, deglaciation, modelling.

Glacial and paraglacial processes have a major influence on rock slope stability in alpine environments (McColl, 2012). Deglaciation of oversteepened valley slopes and associated debuitting and hydro-mechanical perturbation promote progressive failure processes, resulting in rock mass damage, increased permeability and eventual development of deep-seated failures, that can evolve slowly for thousands of years before failing catastrophically (Ballantyne et al., 2014; Riva et al., 2018).

Rock slope instability was documented soon after ice downstage or while the glacier was still melting (e.g. Aletsch glacier area, Kos et al., 2016) while other slope deformations occurred long after deglaciation (e.g. Prager et al 2008), involving a phase of progressive rock failure and damage propagation which can continue for thousands of years.

To investigate the factors that control the mechanisms and timing of deep-seated instability-development in paraglacial environments we modify the time-dependent 2D FEM model DaDyn-RS (Riva et al., 2018), which integrates damage and time-to-failure laws. The model is forced by realistic deglaciation time histories, based on Stokes solutions of the ice flow that rely on the shallow ice approximation, derived from the ICE-CASCADE model (Sternai et al., 2013).

We performed a parametric study to evaluate the effects of initial ice thickness, deglaciation timing, slope strength and valley shape on the time lag between the end of deglaciation and the development of instability. Results allowed constraining the range of conditions in which rapid failures or delayed slow deformations occur, which we compared to measured slope instability timing and mechanisms from natural Alpine case studies.

- Ballantyne C. K., Sandeman G. F., Stone J. O., & Wilson P. (2014) - Rock-slope failure following Late Pleistocene deglaciation on tectonically stable mountainous terrain. *Quaternary Science Reviews*, 86, 144-157.
- Kos A., Amann F., Strozzi T., Delaloye R., Ruetten J., & Springman S. (2016) - Contemporary glacier retreat triggers a rapid landslide response, Great Aletsch Glacier, Switzerland. *Geophysical Research Letters*, 43, 24.
- McColl S.T. (2012) - Paraglacial rock-slope stability. *Geomorphology*, 153, 1-16.
- Prager C., Zangerl C., Patzelt G. & Brandner R. (2008) - Age distribution of fossil landslides in the Tyrol (Austria) and its surrounding areas. *Natural Hazards and Earth System Sciences*, 8, 377-407.
- Riva F., Agliardi F., Amitrano D. & Crosta G.B. (2018) - Damage-Based Time-Dependent Modeling of Paraglacial to Postglacial Progressive Failure of Large Rock Slopes. *Journal of Geophysical Research: Earth Surface*, 123(1), 124-141.
- Sternai P., Herman F., Valla P.G. & Champagnac J.D. (2013) - Spatial and temporal variations of glacial erosion in the Rhône valley (Swiss Alps): Insights from numerical modeling. *Earth and Planetary Science Letters*, 368, 119-131.

Factors controlling the structural architecture of continental rift margins: insights from analogue centrifuge models

Zwaan F.¹, Corti G.², Keir D.¹ & Sani F.*¹

¹ Dipartimento di Scienze della Terra, Firenze, Italy.

² Consiglio Nazionale delle Ricerche (CNR), Istituto di Geoscienze e Georisorse, Firenze, Italy.

Corresponding email: federico.sani@unifi.it

Keywords: rifted margin, flexure, faulting style.

Continental rift margins are generally associated with large-scale synthetic (i.e. basinward dipping) rift boundary faults that accommodate subsidence and mark the transition between rift shoulders and the rift valley floor (e.g. the Rhine Graben). Yet in parts of the Main Ethiopian Rift and the adjacent Afar Depression, the transition from rift shoulders to rift floor is instead characterized by crustal flexure, pervasive antithetic faulting (i.e. dipping away from the basin) and in some cases marginal grabens hugging the rift shoulders. These observations suggest that the development of rift basins can be complex and for a better understanding of the processes involved more investigation is needed.

In order to assess the factors that govern the structural architecture and evolution of rift margins, we ran a series of brittle-viscous analogue centrifuge models at the Tectonic Modelling Lab of the CNR-IGG and the University of Florence. Our models are inspired by the situation in Afar and involve a viscous lower crustal analogue. This 10 mm thick layer is stronger below the rift shoulder and weaker below the future rift basin, simulating the thermal weakening of the Afar lithosphere by the establishment of a mantle plume and associated magma intrusion. A thin layer of strong viscous material overlays this lower crust analogue, reducing strength contrasts between the weak and strong domains. Finally, a cover of fine K-feldspar sand mimics the behaviour of the brittle upper crust. During a model run, we asymmetrically extend the model, causing the weak lower crustal analogue to collapse leading to subsidence and the formation of a rift margin and associated structures.

Varying sand thicknesses have an important effect on our modelled rift margins: we observe dominant flexure and little faulting when the brittle layer is thin (6 mm) versus the development of a rift boundary fault and marginal graben structure when the sand layer is thicker (10-15 mm), and a double marginal graben structure when the sand is 20 mm thick. In models without a thin viscous layer between the lower crustal analogue and the sand cover (i.e., with a higher strength contrast), structures are more localized; a marginal graben developed even with a thin sand cover (6 mm). A 15 mm sand cover initially leads to an early double marginal graben structure, which later on evolves in a distributed fault zone.

Our results thus show how variations in brittle cover thickness and strength contrasts in the lower crust can have important effects on the development of rift margins, leading to more localized or distributed faults. In the future, analogue models based on observations from Afar we will explore the effects of sedimentary (or magmatic) loading, as well as margin obliquity.

S24

Geology-hydrogeology of karst environments and modeling of preferential flow in variably saturated fractures

CONVENERS AND CHAIRPERSONS

Maria Clementina Caputo (CNR-IRSA)

Giorgio Cassiani (Università di Padova)

Costantino Masciopinto (CNR-IRSA)

Mario Parise (Università di Bari)

Structural control on karst system in folded layered carbonates, Potiguar basin, NE Brazil

Arcari A.*¹, Dall'Aglio M.¹, Balsamo F.¹, Menezes D.², Bagni F.² & Bezerra F.H.R.²

¹ University of Parma, Parma, Italy.

² Universidade Federal do Rio Grande do Norte, Natal, Brazil.

Corresponding email: fabrizio.balsamo@unipr.it

Keywords: fractures, karst, mechanical stratigraphy.

During the last decades, the geological and speleological communities have investigated the relationship between tectonics and karst, demonstrating that karst terrains are good recorders of brittle deformation and, in turn, that tectonics may control the main directions and alignment of karst systems. Despite the numerous researches on this topic, the relationship between fracture intensity and the development of karst features in layered carbonates (e.g., sinkholes, caves systems, selectively dissolved layers, tufa deposits) has not fully investigated. This study, funded by Petrobras oil company and the *Universidade Federal do Rio Grande do Norte* (Brazil) and the Overworld student program from University of Parma (Italy), focused on karstified fractured carbonates of the Cretaceous Jandaira Formation in the Potiguar Basin (NE Brazil) where a broad range of karst features are superbly exposed in pavements along the Rio Apodi river. In particular, this study was aimed to understand the possible structural control on sinkhole and karst features development by combining detailed field mapping of fracture pattern on drone imagery with deformation intensity quantification via linear scanlines (in the field) and circular scanlines (on mapped drone images). Furthermore, petrographic observations and mercury-intrusion porosity analysis were integrated with fracture pattern dataset to characterize matrix porosity of host and karstified carbonates. In the study area, host carbonates have total porosity of 2-5%, whereas in m-thick karstified layers and tufa deposits the total porosity reaches 25-30%. Sinkholes locally occur as isolated structures with 15-25 m in diameter. Structural analysis indicates that carbonates are invariably characterized by the presence of N-S veins and E-W stylolites, whose cross cutting relationships indicate they are contemporaneous and developed during a N-S-oriented compression. Further, a NE-SW joint set overprints the previous structural fabric, consistently with the broad NE-trending regional-scale fold (Apodi fold). Fracture pattern quantification indicates that, in studied layered carbonates, fracture density (P_{20}) and intensity (P_{21}) increase approaching the sinkholes and the karstified m-thick layers. Moreover, the development of sinkholes produce a 5-10 m-wide sinkhole-related "damage zone" with concentric fractures. This work indicates that regional scale folding and local variations in fracture intensity (controlled by the mechanical stratigraphy) may control the spatial distributions of sinkholes, caves, and m-thick porous and permeable layers. This study has implications for water management in heterogeneous karst settings, as well as for exploration and exploitation of carbonate hydrocarbon reservoirs.

Modeling hydraulic conductivities of an infiltration trench

Berardi M., Vurro M & Portoghese I.*

IRSA - CNR Bari.

Corresponding email: marco.berardi@ba.irsas.cnr.it

Keywords: infiltration trench, hydraulic conductivity assessment, mathematical modelling.

This study takes a cue from the research and monitoring activities held in the infiltration trenches downstream of waste water treatment plant of Castellana (Puglia). The goal of this approach is modeling the variation in time of hydraulic head in a infiltration trench of Castellana plant: in such a way, the saturated hydraulic conductivities will be estimated. As a first approximation, we will assume that the saturated hydraulic conductivity is equal in each spatial direction, and that the infiltration occurs mainly by the bottom of the trench: the infiltration from the vertical sides are neglected. Secondly, we will consider infiltration also by the vertical sides of the trench, both assuming the same conductivity and, secondarily, assuming a different saturated hydraulic conductivity in the horizontal and in the vertical direction, say K_x and K_z . We start considering the very basic mass conservation law: $dV/dt=Q_{in}-Q_{out}$ (1) Where Q_{in} is the inflow rate, given in input, and Q_{out} is the outflow rate, computed assuming that a certain proportionality holds with the hydraulic head h . Considering the abovementioned hypothesis, for which the infiltration occurs only from the bottom, we first assume that the outflow is related to the hydraulic head by the following law: $Q_{out} = \alpha h^n$, where α and n are assessed by fitting the available observed data. The model can be further complicated by assuming a different filtration rate from the bottom and from the lateral sides. This means that Q_{out} takes into account both a vertical filtration, say αh^n , and a horizontal one, let say, in general, βh^m . For example, several commercial codes, like Feflow, assume as default setting that the vertical conductivity is one tenth of the horizontal one. In line with such hypothesis, the filtration from the lateral sides is considered: in such a case, the lateral surface is considered too, therefore $Q_{out} = [Q_{out}]_B + [Q_{out}]_L$ where $[Q_{out}]_B$ is the flow-rate through the bottom, whereas $[Q_{out}]_L$ is the flow-rate through the lateral sides. Denoting by A the bottom surface, equation (1) reads now as $A dh/dt = Q_{in} - ([A K]_z + [p h K]_x)$ (2).

For sake of simplicity, similarly to several commercial codes, like Feflow, let us assume that the two hydraulic conductivities are proportional each other, i.e. $K_z = [\alpha K]_x$, therefore $dh/dt = Q_{in}/A - K_x (\alpha + p/A)$. These models are compared and the fitted head values will be used to assess the saturated hydraulic conductivity.

Detailed analysis of soil-atmosphere interactions in two sample sites in Oltrepò Pavese

Bordoni M.¹, Valentino R.*², Meisina C.¹ & Bittelli M.³

¹ Università di Pavia.

² Università di Parma.

³ Università di Bologna.

Corresponding email: roberto.valentino@unipr.it

Keywords: field measurements, soil water retention curve, wetting-drying cycles.

Large-scale quantitative assessment of water resources is generally carried out using models that take into account the soil-atmosphere interaction and hydraulic behaviour of an unsaturated soil.

Volumetric water content and pore water pressure are the main basic characteristics to be considered when assessing the hydraulic behaviour of the soil in relation to rainfall events. These quantities are very useful because they constitute input data in different types of water balance models.

Some models require knowledge of water retention curves that indicate a sort of “biunivocal” link between water content and pore water pressure. Most of these models include a single hysteresis, due to in situ wetting-drying processes to which soils are subjected under natural conditions (Bordoni et al., 2017).

Experimental evidence shows that the “biunivocal” relationship between the quantities considered does not allow to adequately reproduce the real behaviour of un saturated soils. In the modelling chain, this mismatch can lead to an inappropriate estimate of water resources, in relation to the amount of rain.

This note reports a detailed description of the interaction between soil and atmosphere in a specific area in Northern Italy. Data from continuous monitoring of two sample sites in Oltrepò Pavese, namely Montuè and Costa Cavalieri, representing two different geological contexts, were used (Bordoni et al., 2015). Different time spans have been considered, even those including single rainy events. Field measurements of both water content and pore pressure allow to clearly identify not only the seasonal fluctuations of the hydraulic properties of the soil, but also the hysteresis cycles that characterize the hydraulic behaviour of the unsaturated soil in correspondence of single rain events. In order to achieve this objective, the data recorded over a long period of time were processed and graphs representing the link between pore pressure and water content were obtained. The trends were also compared with the data on precipitation and air temperature.

Analysis of the data shows that the dynamics characterising variations in water content and pore pressure at both test sites are closely linked to the alternation of wet and dry periods. However, the response is different in the two sample sites because it depends on the geological context and on the type of shallow soil. It seems that the response is also affected by the presence of preferential flow paths, especially in cracked clayey soil.

In general, it can be observed that in winter and spring months, after rain events followed by a prolonged drying period, the response of soil layers up to 0.6 m from ground level is faster than that of the underlying layers. In fact, by increasing depth, the interaction between soil and atmosphere is delayed. Moreover, it is evident that the soil behaviour is not characterized by a single wetting-drying hysteresis, but by numerous cycles that correspond to different isolated rainy events.

Bordoni M., Bittelli M., Valentino R., Chersich S. & Meisina C. (2017) - Improving the estimation of complete field soil water characteristic curves through field monitoring data. *Journal of Hydrology*, 552, 283-305.

Bordoni M., Meisina C., Valentino R., Lu N., Bittelli M. & Chersich S. (2015) - Hydrological factors affecting rainfall-induced shallow landslides: from the field monitoring to a simplified slope stability analysis. *Engineering Geology*, 193, 19-37.

Characterization of Episodic Recharge in a Fractured and Karst Coastal Aquifer by Episodic Master Recession Analysis

Caputo M.C.*¹, Nimmo J.R.² & Perkins K.S.²

¹ CNR National Research Council, IRSA Water Research Institute, Bari, Italy.

² U. S. Geological Survey, CA, USA.

Corresponding email: maria.caputo@ba.irsas.cnr.it

Keywords: ground water, unsaturated flow, fractured aquifer.

In the Puglia region of southern Italy, water for various human needs is mainly sourced from carbonatic and fractured rocks affected by karst process. We hypothesize that precipitation water infiltrates through preferential pathways and accumulates in the aquifer leaving very few surficial water sources. For this reason, it is very important for strategic water resources planning and management to be able to quantify ground water recharge. Considering that preferential flow cannot be simulated with the same laws that describe flow in porous rock and that ground water recharge cannot be directly measured using field techniques, new methods have been developed for simulating episodic recharge that commonly occurs through fractured unsaturated zones. In this study the Episodic Master Recession method (EMR) (Nimmo & Perkins, 2018) was applied to a fractured and karst coastal aquifer system to estimate recharge from individual precipitation events. This technique allows the understanding of how factors such as precipitation intensity and seasonality impacts the response of the water table to preferential flow through the unsaturated zone. Two different wells designed CNR-IRSA and BA22, 5 km away from each other, were used for EMR analysis. The wells are completed in the same aquifer, which is characterized by a thin layer of soil at land surface underlain by Plio-Pleistocene Calcarenite over fractured Cretaceous limestone within which the water table fluctuates. For the EMR analysis we utilized hourly water level data from 2008 to 2011 from the CNR-IRSA well and from 2010 to 2011 from the BA22 well along with local precipitation data.

The results of the EMR analysis give distinct recharge episodes associated with precipitation events and for each episode characteristics such as start, duration and peak of precipitation, recharge amount, and recharge/precipitation ratio are calculated. The analysis of these characteristics in different combinations, allows examination of the behaviour of the ground water in response to different precipitation inputs. In both of the studied wells, results show that the recharge is directly proportional to the precipitation duration, and weakly correlated to the maximum precipitation intensity. The EMR calculated recharge shows the same direct proportionality to the average precipitation intensity and total amount of precipitation input but only for the CNR-IRSA well, which shows a bimodal trend. In fact, for average precipitation intensity values lower than 20 mm/d recharge increases with the average precipitation intensity much more than with higher values. This could mean that with high precipitation intensity runoff is initiated, likely because preferential pathways are fully saturated and cannot accommodate the additional infiltration. The same behaviour was observed in term of recharge vs total amount of precipitation for each episode. The bimodal trend was not apparent for well BA22 likely due to the shorter period of data availability compared to CNR-IRSA. This work shows the EMR method is very useful for characterizing the behaviour of the coastal aquifer in response to individual precipitation events allowing the evaluation of the episodic recharge and other factors that may influence aquifer storage such as storm duration or intensity.

Nimmo J.R. & Perkins K. (2018) - Episodic Master Recession Evaluation of Groundwater and Streamflow Hydrographs for Water-Resource Estimation. *Vadose Zone Journal*, 17, 180050. <https://doi.org/10.2136/vzj2018.03.0050>.

Combined approaches to provide evidence of preferential flow in a layered vadose zone during artificial rainfall

Caputo M.C.¹, De Carlo L.*¹, Masciale R.¹, Perkins K.² & Turturro A.C.¹

¹ Water Research Institute, National Research Council, Bari (Italy).

² US Geological Survey, 345, Menlo Park, CA, USA.

Corresponding email: lorenzo.decarlo@ba.irsra.cnr.it

Keywords: preferential flow, artificial rainfall, field test.

Preferential flow is a mechanism by which water flows through the vadose zone in a rapid, non-uniform pattern. Preferential pathways associated with subsurface geologic discontinuities have been shown to have strong impacts on flow and transport dynamics with consequences relevant to agricultural practices, environmental protection, and water management. In fact, during infiltration processes, it is very important to evaluate changes in storage of water in the vadose zone for several reasons including to supply a sufficient amount of water required by roots during crop irrigation, to prevent transport of contaminants to groundwater and to estimate aquifer recharge. Understanding and predicting flow through preferential pathways is a crucial issue and it requires a multidisciplinary approach due to the heterogeneity of the subsurface. In a test site located in Bari, Southern Italy, during an artificial rainfall event, we used a combined approach of sprinkling infiltration with electrical resistivity tomography to detect preferential flow in the fractured vadose zone. The experimental site is equipped with five monitoring wells, one placed in a central position and the other four 10 m apart oriented along the cardinal directions. A rainfall event was simulated by placing a network of sprinklers at the soil surface uniformly distributed over an area of 7 m x 7m. Electrodes for electrical resistivity measurements were also placed in a grid pattern within the plot. A pipe system connected to the sprinklers provided 2 m³ of brackish water (2.26 mS/cm) in 5 hours with a constant flow rate for 5 irrigation cycles, each in a day for 5 days. Brackish water was used to simulate the rainfall in order to enhance the resistivity changes due to the infiltration in the vadose zone. During the artificial rainfall event, direct and non-direct measurements were performed to evaluate the water movement in the unsaturated zone. Electrical conductivity, temperature and water level measurements were collected in the monitoring wells every 2 hours by means of multi-parametric probes. Simultaneously, non-invasive time-lapse geophysical surveys were carried out in order to monitor the movement of the infiltrated water in the vadose zone. The time-lapse geophysical survey was performed at different spatial scales in order to detect with high spatio-temporal resolution the small water content variations. The distribution of the groundwater physico-chemical parameters collected in the monitoring wells indicates preferential pathways along the northeast direction, as confirmed by the time-lapse geophysical results.

Occurrence of flash floods in the karst environment of Apulia (Southern Italy)

Gentile P., Iaia C., Liso I.S.* & Parise M.

Università Aldo Moro, Dipartimento di Scienze della Terra e Geoambientali, Bari.

Corresponding email: isabella.liso@uniba.it

Keywords: floods, hazards, karst.

Floods in karst environment are among the most frequent and damaging geological hazards, due to hydraulic and hydrogeological peculiarities of the karst terrains. Since absence of water at the surface is one of the main features characterizing karst, the occurrence of floods in consequence of prolonged rainfall, or of concentrated and intense rainstorms, may often result in severe damage to human activities and infrastructures, threatening lives as well.

Apulia, the south-eastern sector of Italy, almost entirely consisting of soluble rocks intensely affected by karst processes, is not an exception at this regard. Flash floods have repeatedly characterized the history of many Apulian towns, and the number of events, with consequences on the society, has increased in the last decades, due to expansion of the urbanized and industrial areas. This was often carried out without considering the peculiarity of karst, and the possibility of occurrence of flash floods. Therefore, the effects have often been devastating, in terms of both casualties and economic losses.

Through description of a series of events, that have hit different sectors of the region, this article presents a documented chronology of the events occurred in Apulia, in the attempt to contribute to build a deeper knowledge about the areas inundated by floods, their triggering conditions, and the relationships with human activities. The Apulian sectors that will be dealt with are: the Gargano Promontory, where, at the beginning of September 2014, severe rainstorms caused many types of geohazards, including floods, and claimed some casualties; the town of Bisceglie, north of Bari, where the system of temporary water courses (locally named *lame*) work as the main water flow way during floods; the sector comprising Putignano and Castellana-Grotte, in the Low Murge, where an high number of swallow holes had been closed in recent decades; the coastal area downhill from Ostuni, where several tourist resorts are located; the town of Ginosa, where two different flood events in 2013 sadly resulted in 4 victims; and the Salento peninsula, where many urban centers are interested by floods and inundations, even in consequence of not significant rainfall events. In addition, to analyse the pluviometric events causing the floods, the role of the geological and morphological features in karst will be examined, also as regards the transport of solid materials by the flowing water, that may significantly contribute to the registered damage.

Micro-climatic aspects at the karst system of Vora Bosco (Salento, Southern Italy)

Liso I.S.* & Parise M.

Department of Earth and Environmental Sciences, University Aldo Moro, Bari, Italy.

Corresponding email: isabella.liso@uniba.it

Keywords: karst cave, temperature, monitoring.

Apulia Region (Southern Italy) presents a very high percentage of soluble (carbonate) outcropping rocks. Karst phenomena are therefore widespread, and mark the territory with typical landforms and features. Among these, the Vora Bosco swallow hole, located in Salento, is one of the two sites in the region that allow man to move within a cave system, eventually reaching the groundwater. Interception of the water table, at a depth of – 60 m below the ground (altitude of the cave entrance: 64 m a.s.l.), makes Vora Bosco one of the most important caves to directly study the complex hydrogeological dynamics in the Apulian karst. The underground environment is characterized by very narrow passages, and the system is almost entirely developed inside calcarenitic formations (Plio/Pleistocene – Miocene), with only the few last meters within the Cretaceous limestones. The *Vora Bosco* plan, realized by speleological surveys, draws a predominant E-W elongation direction of the cave system. Numerous monitoring actions have been started since October 2017 inside the karst system and in the surrounding superficial areas, in order to collect geological, hydrogeological and biological data from both surface and subsoil.

Among the informations collected so far (internal and external meteorological data, water level, temperature and electrical conductivity, petrological and structural data) the processing and analysis of the cave climate values has revealed extremely interesting. Karst scientists typically consider the cave environment quite stable, with a temperature about equal to the mean external temperature value at the access of the cave. However, in at least two cases, during February 2018, the *Vora Bosco* temperature fell down very quickly. The three HOBO sensors, installed along the cave pathway to register temperature and humidity data, with a pace of one measure per hour, detected significant and sudden temperature values decreases (about 10 °C in 24 h), through the whole cave system. In addition, such a decrease in temperature is accompanied by a correspondent lowering in the groundwater temperature, and by a significant rise in the groundwater level, following intense rainfall.

This behavior could be explained considering that *Vora Bosco* is a shallow karst system that, since it develops prevalently within porous calcarenites, rapidly drains the rainfall towards the deepest sectors of the cave. The cold water remains inside the rock mass pores, thus influencing the HOBO temperature records. In addition, the turbulent flux of rainwater, which disappears within the subsoil crossing the cave entrance, produces a cold spray, adding its effect to the previous one. Analysis of these events, and of the related micro-climate changes, is still going on, aimed at quantifying the time required by the *Vora Bosco* karst system to return to steady state conditions (that is, to the situation present before the rainstorm).

Hydrogeological model to study natural water flow in karstified and fractured aquifers

Liso I.S.¹, Masciopinto C.² & Parise M.*¹

¹ Dipartimento Scienze della Terra e Geoambientali, Università Aldo Moro, Bari.

² CNR IRSA, Bari.

Corresponding email: mario.parise@uniba.it

Keywords: karst caves, groundwater, hydrogeological model.

Many studies deal with the evolution of karst processes in fractures and conduits within the epikarst, the vadose zone and the phreatic zone of karstified limestone rock masses. Details about the geo-structural setting and the underground conduit pathways and connections can be obtained from the integration of geological/speleological surveys and tracer tests. These methods are aimed to collect geomorphological, geo-structural, stratigraphic and petrological data at the surface and inside the cave systems, to combine with information derived from tracer tests (i.e. δO^{18} - $\delta^{13}\text{C}$ stable isotopes).

Whatever the approach, the choice of the best hydrogeological model, i.e. the best way to simulate the water flow through a karstified aquifer, is a very complex problem due to the difficulties to gather detailed geological and hydrological data. The lack of information often leads to several uncertainties on the assumptions of the starting model, namely as regards the underground water movements, the delimitation of the hydrogeological catchment, and the thickness of the saturated zone.

The final goal of this research is to build the most suitable conceptual hydrological model, which may allow implementing a realistic simulation of the karstified and fractured groundwater flow. This aim will be obtained by a detailed investigation of the cave systems and the surrounding superficial areas, merging classical geological surveys and speleological investigations.

So far, we are able to present the exploration results of the Apulian cave “Inghiottitoio di Masseria Rotolo”, located in the Canale di Pirro polje (Low Murge - Monopoli, Italy). It has been discovered in 2012 and totally develops inside Cretaceous limestones belonging to Apulian Carbonate Platform. The cave reaches water table at the depth of - 264 meters below the ground; diving explorations, carried out during 2018, have brought the total depth of the karst system at - 324 m, making it the deepest cave in Apulia. Inghiottitoio di Masseria Rotolo is a remarkable cave system, characterized by very large passages, including very impressive vertical shafts, with presence also of extremely rich in speleothems rooms.

This extraordinary situation represents a real natural, hydrogeological, field-scale laboratory, to direct study both the groundwater and karst conduits outflows, giving the opportunity to collect precious data to better support the hydrogeological conceptual and mathematical model of the Cretaceous limestone rock mass.

Influence of tectonic CO₂ degassing on the occurrence of earthquake precursors

Martinelli G.*¹ & Tamburello G.²

¹ ARPA Emilia-Romagna.

² INGV-sez. Bologna.

Corresponding email: giovanni.martinelli15@gmail.com

Keywords: Underground fluids, CO₂ degassing, earthquake precursors.

Underground fluids play a crucial role in precursory non-seismometric earthquake phenomena. Here we map and compare the global distribution of the main CO₂-rich gas discharges with earthquake precursors obtained from an updated compilation. We integrate these datasets with supplementary geological and geophysical parameters like faults, volcanism, heat flow, crustal velocities and depth of seismic events. Possible relations among tectonic CO₂ degassing and the occurrence of fluid-related earthquake precursors are considered and discussed

Preferential flow dynamics in unsaturated zone hydrology

Nimmo J.R. & Perkins K.S.*

United States Geological Survey.

Corresponding email: kperkins@usgs.gov

Keywords: preferential flow, unsaturated zone.

There are two major ways that water travels through the unsaturated zone, preferential flow and diffuse flow, and in general, both of these are hydrologically important. Diffuse flow occurs all the time, but is slow. Preferential flow occurs seldom and briefly, but is fast and supports high fluxes of water and its mobile constituents. Nearly all natural subsurface media sometimes conduct preferential flow. Thus unsaturated zone hydrology needs to treat preferential as well as diffuse flow.

Diffuse and preferential flow proceed by different physical processes. Diffuse flow is the result of surface tension (capillary) and viscous forces acting within a network of many small pores. Preferential flow, especially in the typical form of macropore flow, results from rapid application of large quantities of water and is driven through the unsaturated zone by gravity.

Diffuse unsaturated flow has a well-established, widely-accepted theory, based on surface-tension/viscous-flow principles, embodied in Richards' equation. Preferential flow does not. Currently, most quantitative treatment of preferential flow use Richards' equation with little modification. This usage is inappropriate for several reasons, for example that capillarity plays a major role in Richards' equation but has little or no influence on preferential flow. More realistic alternatives are available, based on such concepts as film flow, kinematic waves, and transfer functions, but none of these is widely accepted yet. For practical applications the choice of models must be made with awareness of the shortcomings and limitations of each.

Estimation of Preferential Flow Contributions to Aquifer Recharge Based on Hydrograph Analysis

Perkins K.S.* & Nimmo J.R.

United States Geological Survey.

Corresponding email: kperkins@usgs.gov

Keywords: preferential flow, aquifer recharge, unsaturated zone.

In many locations, a major portion of episodic aquifer recharge is conveyed through unsaturated zone preferential flow paths. Some commonly used recharge estimation techniques do not adequately represent this important component of recharge. Hydrograph analysis tools employing a master recession curve (MRC) are useful for the quantification of episodic aquifer recharge especially where preferential flow through the unsaturated zone is an important mechanism. An MRC is the relation between the value of a measured response, such as water levels within a well, and its rate of change with time occurring on the falling limb of the hydrograph when there is no water input source. We have developed MRC and hydrograph-evaluation methods for multiple purposes, utilizing both water table and streamflow data. The determination of a parameterized MRC through a structured procedure provides a basis for quantification of hydrologic variables and characteristics that can be compared among different events, sites, and periods of time. Application of the MRC to needed hydrologic quantifications is done with the Episodic Master Recession (EMR) method. Our algorithms partition a time series hydrograph data into discrete recharge episodes. Each recharge episode or stormflow event is associated with a specific interval of rainfall, so storm characteristics such as intensity and duration can be associated with the amount of recharge or stormflow that results. The iterative procedures requiring hydrologic judgement are used to quantify parameters needed in applying the MRC and EMR methods to a given site. This structured iterative approach allows estimation of recharge attributable to preferential flow using procedures that can be quantified and documented.

Hydrodynamic of karst springs in metamorphic carbonate rocks: the case of Apuan Alps (Tuscany, Italy)

Piccini L.^{*1-2} & Poggetti E.²⁻³

¹ Department of Earth Science – Università degli Studi di Firenze.

² Commissione Scientifica – Federazione Speleologica Toscana.

³ Gruppo Speleologico Maremmano CAI.

Corresponding email: leonardo.piccini@unifi.it

Keywords: karst hydrogeology, hydrogeochemical monitoring, karst system.

Apuan Alps, in north-western Tuscany (Italy), are famous worldwide for its marbles used since several centuries as ornamental stone. Apuan marbles are made of almost pure calcite and so are affected by dissolution processes due to meteoric water infiltration. Marbles along with meta-dolostone and cherty metamorphic limestones have a total area of about 140 km² forming one of the most important karst areas in Italy. Metamorphic carbonate aquifers have specific hydrogeological features, due to the development of underground karst that determine a high infiltration rate and the occurrence of a high conductivity, underground network of conduits (Piccini, 2002; Doveri et al., 2017). Major karst springs are located along the borders of the Apuan massif, mainly on the seaward side. The most important one is the Forno spring, whose average flow rate is about 1.6 m³/s. On the opposite side it is Pollaccia spring with a mean flow rate of about 0.9 m³/s. At the extreme northern side, the Equi springs, whose total discharge is about 0.9 m³/s in average, are located. At least a dozen other springs have flow rates between 0.4 and 0.1 m³/s and many others have discharge more than 10 L/s. The total average discharge of karst aquifers is about 6 m³/s. The responses of the major spring in respect of precipitation is rather fast, within a few hours, but they show a complex pattern probably linked to different infiltration times in the various sectors of recharge areas. Temperature shows significant variations during the year ranging between 8.5 to 10.5 °C. The minimum temperatures are due to cold meltwater and occur usually in spring, while in the middle of winter, in the absence of precipitation and melting, the temperature increases. Electrical conductivity usually ranges between 200 to 240 mS/cm. The average conductivity is about 190 mS/cm, but the values are subject to rapid changes during floods. In most of the cases, an important increase in electric conductivity is not registered during floods. Only certain conditions you can have slight conductivity and temperature increases, which are probably attributable to a local “piston effect” in the waterfilled segment close to the springs. In conclusion, groundwater drainage networks in metamorphic carbonates aquifers have a very low fissure porosity, reducing the storage of water underground very much and enhancing short term responses to infiltration events (Doveri et al., 2018).

Piccini L. (2002) - Acquiferi carbonatici e sorgenti carsiche delle Alpi Apuane. Atti Conv. “Le risorse idriche sotterranee delle Alpi Apuane: conoscenze attuali e prospettive di utilizzo” Forno (MS), 22 giugno 2002, 41-76.

Doveri M., Piccini L., Menichini M. (2018) - Hydrodynamic and Geochemical Features of Metamorphic Carbonate Aquifers and Implications for Water Management: The Apuan Alps (NW Tuscany, Italy) Case Study. In Younos T., Schreiber M. & Kosič Ficco K. (eds.), Karst Water Environment, The Handbook of Environmental Chemistry 68, 209-249.

Water storage changes and crustal deformation in karst regions: examples from the Venetian Southern Alps

Pintori F.*¹, Serpelloni E.¹, Longuevergne L.², Belardinelli M.E.³, Gualandi A.⁴ & Scoccimarro E.⁵

¹ Istituto Nazionale di Geofisica e Vulcanologia, Osservatorio Nazionale Terremoti.

² Geosciences Rennes, UMR CNRS 6118, Université de Rennes 1, Rennes, France.

³ Università di Bologna, Dipartimento di Fisica e Astronomia, Settore di Geofisica.

⁴ Jet Propulsion Laboratory, NASA, Pasadena, CA, USA.

⁵ Fondazione Centro euro-Mediterraneo sui Cambiamenti Climatici - CMCC, Bologna.

Corresponding email: francesco.pintori@ingv.it

Keywords: karst aquifers, crustal deformation, hydrogeodesy.

Continuous GPS measurements allow tracking ground deformation associated with hydrological processes at different spatial scales. Accounting for these signals is mandatory for improving the accuracies of tectonic deformation rates and for detecting small tectonic transient deformation, eventually preceding or following major earthquakes. While surface hydrological loading, acting at regional and continental scale, maps mainly into seasonal deformation in the vertical components, increasing evidence of horizontal non-seasonal deformation associated with groundwater level changes in karst aquifers have been recently provided by dense GPS networks in the Alps and in the Apennines.

Here we present the results obtained from the analysis of ground GPS displacements time-series integrated by hydrological and numerical modeling in the Eastern Southern Alps. The area hosts active seismogenic faults, belonging to the south-verging South Alpine belt, which are monitored by a dense continuous GPS network. Serpelloni et al. (2018) found that non-seasonal transient deformation are present in three karst areas of the Southern Alps and Northern Dinarides: the Lessini mountains, the M.te Grappa-Col Visentin mountain range, the Cansiglio plateau and the Classic Karst in Friuli and Slovenia. In these areas GPS stations move at opposite directions, inverting the sense of motion through time, thus causing a succession of horizontal extensions and contractions, occurring about normal to natural fractures. An hydrological forcing of this transient deformation signal has been proposed by Serpelloni et al. (2018), based on the analysis of precipitation data. In this work we better investigate the link between ground deformation and hydrological processes, focusing on the Piave river basin and the area surrounding the Belluno Valley.

We used the GR5J model to estimate water storage changes in the hydrological basins, finding a strong correlation between the temporal evolution of the water storage and the ten-year-long temporal evolution of the geodetic deformation signal. This suggests that geodetic techniques could be used for indirect measurements of water resources. The relation between water redistribution and ground displacements has been described through a 2D numerical model, accounting for the geological features of the study area. We found that water pressure changes caused by water level variations in the fractured area corresponding to the backthrust of the Bassano-Valdobbiadene fault, a major thrust of the seismogenic Venetian fold-and-thrust belt, is the most likely source of deformation that allows best reproducing the displacements obtained from the geodetic analysis.

Serpelloni E., Pintori F., Gualandi A., Scoccimarro E., Cavaliere A., Anderlini L., Belardinelli M.E. & Todesco M. (2018) - Hydrologically-induced karst deformation: insights from GPS measurements in the Adria-Eurasia plate boundary zone. *J. Geophys. Res.*, 85, 457. <https://doi.org/10.1002/2017jb015252>.

Evidence of No Preferential Flow in Porous Rock by Testing the Validity of the Darcy-Buckingham Law in a Centrifugal Field

Turturro A.C.*¹, Nimmo J.R.², Perkins K.S.² & Caputo M.C.¹

¹ CNR National Research Council, IRSA Water Research Institute, Bari, Italy.

² U. S. Geological Survey, Menlo Park, CA, USA.

Corresponding email: celeste.turturro@ba.irsa.cnr.it

Keywords: preferential flow, unsaturated flow, porous rock.

Diffuse water movement in unsaturated porous media is commonly formulated according to the classical Darcy-Buckingham law and Richards' equation. Instead, preferential flow, observed in soils with macropores and in fractured rocks, limits the applicability of those standard flow models and it suggests other conceptual approaches such as free-surface film flow, source responsive model, dual-porosity model, kinematic waves, dual-permeability model, etc. This work aims to see whether preferential flow occurs in unsaturated porous rocks under centrifugation by testing the validity of the Darcy-Buckingham law that states the flux density, q (LT⁻¹), through an unsaturated porous medium is directly proportional to the force, F , driving the water flow. This implies that the ratio q/F , or simply the unsaturated hydraulic conductivity, $K(\theta)$, remains constant for a constant value of water content, θ . Measured q values plotted against different amounts of force used in their measurements, must depict a straight line passing through the origin if θ is the same for each force/flux combination. However, certain physical conditions that may be associated with preferential flow can make this law inapplicable. These conditions include: particular flow regimes such as free-surface film flow, partially filled macropores, high fluid velocities, altered air-water interface configuration due to centrifugal force possibly affecting K . In this study the experimental method used to test the Darcy-Buckingham law is the Quasi-Steady Centrifuge (QSC) method. The tests were conducted on rock core samples, designated as C and M lithotypes, extracted from Canosa di Puglia and Massafra quarries respectively, both in the southeastern Italy. The samples belong to the Calcarene di Gravina Formation, a sedimentary carbonatic rock of marine origin and Plio-Pleistocene age. This material could be subject to preferential flow in the form of films driven through pores larger than the film thickness, or in the form of fingered flow. The QSC method tested the law's validity in a centrifugal field, giving the measurements of q and θ for different centrifugal forces. This method allows large changes in force and flux without substantial variation in θ . The Darcy-Buckingham law was verified for the tested conditions, as measured fluxes at a water content were found to vary in direct proportion to driving force. The tested conditions include a range of K of 9.7E-09 to 1.8E-06 m/s, θ between 0.34 and 0.21, and force between 136 and 685 times earth gravity, exhibiting R^2 between 0.912 and 0.998. The validity and applicability of the Darcy-Buckingham law suggests that preferential flow did not occur in tested rocks. In consideration that until now only for few materials has been tested, all represented from granular media and unconsolidated rock, we can assert that the Darcy-Buckingham law can be verified also on consolidated porous rock under conditions similar to those of our experiments.

Conceptual models related to underground circulation in carbonate aquifers¹

Vigna B.¹ & Fiorucci A.*¹

¹ Dipartimento di Ingegneria dell'Ambiente, del Territorio e delle Infrastrutture, Politecnico di Torino, Torino.

Corresponding email: adriano.fiorucci@polito.it

Keywords: karst aquifers, conceptual models, monitoring.

On the basis of many years of studies concerning aquifers set in fractured and/or karst carbonate aquifers, it has been possible to recognize three different conceptual models related to the circulation of groundwater: *Systems with dominant drainage*, *Systems with interconnected drainage*, *Systems with dispersive circulation*.

Systems with dominant drainage are characterized by a high permeability of the aquifer, which is related to a remarkable karstification of the rock mass. The outflow network is well organized with a series of main collectors and secondary drains which quickly discharge the incoming infiltration water. There is no phreatic zone or a somewhat reduced one. The geochemistry of the groundwater shows sudden decrease in the mineralization values during important infiltration events. This happens when the neo-filtration water reaches the emergences and quickly replaces the water circulating in the system (*prevalent substitution*).

Systems with interconnected drainage are found in fractured and karstified rock masses that have different drainage pathways. The phreatic zone can be very extensive, with a channel and fracture network that can be karstified to a different degree and interconnected. The rapid increases in the flow that can be observed in the spring are not connected to the arrival of the neo-filtration water, but to the effect of the transmission of the hydraulic pressures in the fractures or in the high flood channels. The hydrogeochemical values show temporary increases in the mineralization and temperature values of the water during flooding after *piston flow* phenomena.

Systems with dispersive circulation are present in aquifers that are characterized by a rather reduced permeability and which are set in a micro-fractured network with numerous interconnected discontinuity families with extremely reduced karstification. These systems have an extensive phreatic zone and are characterized by rather reduced speeds of water flows. The physical-chemical parameters of the groundwater show a remarkable temporal constancy of the values, with modest variations of a seasonal nature (*chemical signal homogenization* phenomena).

In general, groundwater circulation in carbonate aquifers is more complex than that summarized in these three conceptual models with intermediate situations where different types of drainage network can be coexisted, developed both vertically and horizontally. In any case it is always possible to refer to one of the three conceptual models, since the hydrodynamic and hydrogeochemical characteristics are strongly linked to the type of main flow. The recognition of an aquifer system therefore passes through the acquisition of monitoring data that must be carried out at the sources by installing multi-parameter probes (flow rate data, temperature and electrical conductivity of the water), sampling and related chemical analyzes (in different hydrodynamic conditions of the system) and interpretation of the tracer test.

Numerical models of karst processes

Wang X.* & Jourde H.

Hydrosciences Montpellier UMR 5569 CNRS-IRD-UM.

Corresponding email: x.wang0127@gmail.com

Keywords: karst hydrodynamics, numerical modelling, integrated approach.

Karstified carbonates represent an important element of the Critical Zone as they contain important aquifers and reservoirs, which offer essential resources for the survival and prosperous of humanity. Karst aquifers are highly dynamic hydrosystems that subject constantly to prominent influences from natural (e.g. geological or meteorological forcings) and anthropogenic (e.g. climate change, land use change, agriculture and industrial pollutions, extraction of subsurface energy resources) factors. The characterization and utilization of these hydrosystems are very challenging and far more complex than that contained in any other type of geological media. The main reasons are 1) the major pathways for the transport of water, mass and energy consist of hierarchically organized conduits with strong heterogeneity in their hydraulic properties and 2) a wide range of physico-chemical processes and flow regimes simultaneously occur, and the interactions between them are significantly strong.

To achieve a quantitative prediction of the response of karst hydrosystems to changes in global and local forcing parameters, it is crucial to acquire a deeper understanding of dominant hydrogeological processes and develop reliable modeling tools to predict interactions in the short and long terms between target aquifers and adjacent hydrosystems in the Critical Zone. In this talk, a review of the main modelling methods applied in each specific research domain (including hydrogeology, engineering geology, environmental engineering, petroleum engineering etc.) will be provided first. A critical comparison between various models will be offered. The emphasis is placed on the integration of various modeling schemes and techniques. The consequence of the integrated modeling approach on the understanding of the whole process of karst genesis and functioning will also be discussed.

The influence of the dolomitization process on texture and porosity of carbonates

Zucchini A.*¹, Cirilli S.¹, Comodi P.¹, Mitillo N.¹, Lanzafame G.² & Frondini F.¹

¹ Dipartimento di Fisica e Geologia, Università di Perugia.

² Elettra - Sincrotrone Trieste S.C.p.A., Basovizza (Trieste).

Corresponding email: azzurra.zucchini@unipg.it

Keywords: carbonate reservoirs, dolomitization, Synchrotron X-ray phase-contrast microtomography.

The porosity features of carbonate rocks are fundamental parameters influencing their aptitude as reservoirs for fluids (water, oils, gasses). Carbonate reservoirs can be both limestones and dolostones and their potentiality is strictly controlled by sedimentary and diagenetic processes. Most dolomite arises from “dolomitization” processes where the Ca to Mg substitution in calcite mineral structure occurs due to Mg-rich fluid (mainly water) circulating within calcite horizons. “Dolomitization” can occur either during early or late (burial) diagenesis. However, the pores spatial distribution and interconnection play a fundamental role in the dolostone ability for transmitting fluids. The present work is devoted to study the influence of dolomitization degree and dolomite textures on the porosity features of different carbonate rocks. An integrated study based on Synchrotron X-ray phase-contrast microtomography (micro-CT) analyses and sedimentary petrology was used. Experiments were performed at the SYRMEP beamline (Elettra Synchrotron, Trieste, Italy) on samples coming from early Jurassic carbonates cropping out in the Castel Manfrino Area (Montagna dei Fiori, Central Apennines, Italy) and from a well provided by Eni. The analyzed samples are characterized by different primary porosity and sedimentary textures, replaced by dolostone. The studied succession includes the peritidal cycles of Calcare Massiccio Fm (CM) and the overlying thin bedded muddy limestone of Corniola Fm (C). In particular, six dolomitized samples, two partially dolomitized and two undolomitized samples were analyzed. The dolostone textures span from Planar E to Planar S and the pattern distribution results to be controlled by the original carbonate textures. Synchrotron X-ray micro-CT data were acquired at spatial resolution of 2 $\mu\text{m}/\text{pixel}$. The collected data were analyzed by using the Pore3D software library developed at Elettra. Results showed that among the dolomitized samples, those featuring NON-Planar deformations have the lowest total porosity. The total porosity increases as planar S and planar E textures occur. As regards both the undolomitized samples and the partial replaced ones, the total porosity has the same order of magnitude of the NON-planar textures (0.1 vol.% for CM and 2.3 vol.% for C) being approximately 0.3 vol.% and 2.1 vol.% for the partial replaced CM and C, respectively. By the above-mentioned results, a quite important influence of both dolomitization degree and dolomite textural features was observed on the total porosity of the carbonate rocks. The detailed pore size distribution analysis gave a fundamental contribution to study the 3D textural characteristics of dolomitic reservoir rocks and their porosity, taking into account the physical properties of the voids (dimensions and spatial distribution) and the interconnection between them.

The authors thank Eni Management for permission to study the subsurface core samples.

S25

**Geosciences for disaster risk reduction: problems, solutions
and perspective**

CONVENERS AND CHAIRPERSONS

Fausto Guzzetti (CNR-IRPI)

Warner Marzocchi (Università di Napoli)

The importance of integrated monitoring approach: the case study of Arzeno (Graveglia Valley - Ligurian Apennine, Italy)

Allasia P.*¹, Godone D.¹, Wrzesniak A.¹, Notti D.¹, Baldo M.¹, Faccini F.², Elter F.M.² & Poggi F.³

¹CNR-IRPI.

² Dipartimento di Scienze della Terra dell' Ambiente e della Vita, Università di Genova.

³ Dipartimento Ambiente e Assetto del Territorio, Regione Liguria.

Corresponding email: paolo.allasia@irpi.cnr.it

Keywords: geoscience, monitoring, deep seated displacements.

The impact of large slope instabilities on local communities cannot be always resolved using remedial interventions. If the landslide evolution during the years is compatible with the life of buildings and infrastructures, often the best long-term strategy is coexistence with the landslide coupled with adequate and strict monitoring activities. Currently, surface monitoring approaches are preferred due to various technological advances especially in the field of remote sensing. However, the surface monitoring cannot provide with certainty the deep behavior of the landslide, especially in cases of a complex and slow phenomena. The integration of surface and deep monitoring systems allows obtaining a robust method to evaluate the landslide activity for risk mitigation and coexistence with local community. In this paper, the Arzeno landslide case study is presented. Arzeno is a hamlet of Ne Municipality in Genova province. This landslide affects the entire slope, where Arzeno is located, covering approximately 2.6 km² area. Since decades, there have been reports of instability phenomena in Arzeno and neighboring villages that are outlined by several kinematic indicators. In 2015, drilling activities were performed to identify the stratigraphic sequence and to set up the monitoring network in the frame of regional program for yearly geo-hydrological risk mitigation works funded by Liguria Region. In 2017, after an extensive geophysical survey a second geognostic survey was carried out featuring 6 boreholes (2 inclinometer and 4 piezometric cases were installed). Robotized Inclinometric System (AIS) was installed in one of inclinometric case. The AIS measurements (twice a day) have shown a cumulative displacement of 2.6 cm since 26/10/18 and a main sliding surface at 17 m depth. The measurements performed manually in the second inclinometric case have shown approximately the same cumulative displacement but a sliding surface at 50m depth. Additionally, one weather station and three GPS benchmarks (for crosschecking of the displacement) were installed. The activities also included the definition of damage degree of buildings by means of crack measurements in the facades, and the analysis of the PSInSARTM displacement rate data delivered by the National Environmental Remote Sensing Project. Recently, an aerial LiDAR survey for geomorphological analysis and numerical modeling purposes was performed. The field surveys and monitoring activities showed a complex situation for the studied area. A large slope instability was recognized with several sub-sectors representing different kinematics and hydrogeological behavior. Thanks to the integrated surface/deep monitoring approach, it was possible to significantly improve the interpretation of the landslide kinematics that is different from the one based on the PSInSARTM data.

Automatic delineation of slope units and terrain classification of Italy

Alvioli M.*, Guzzetti F. & Marchesini I.

Istituto di Ricerca per la Protezione Idrogeologica, Consiglio Nazionale delle Ricerche, Perugia, Italy.

Corresponding email: massimiliano.alvioli@irpi.cnr.it

Keywords: slope units, geomorphology, Terrain Classification.

Automatic subdivision of landscapes into terrain units, in large areas and with homogeneous criteria, remains a challenge. Slope units (SUs) are irregular terrain units bounded by drainage and divide lines, with the requirement of maximizing geomorphological homogeneity within a single unit and heterogeneity between different ones (Guzzetti et al., 1999). SUs are suitable to describe a variety of processes: to assess different natural hazards, for hydrological and erosion modelling, for geo-environmental, ecological, forestry, agriculture, and in general for studies requiring the identification of homogeneous terrain domains facing distinct directions. Nevertheless, their use has been hampered because of the lack of reliable software for their automatic delineation.

For a given digital landscape, no unique SU partition exists. Any such partition is characterized by a granularity i.e., the size distribution of the SUs. Granularity varies in different landscapes and for different purpose of the terrain partition. We recently developed the *r.slopeunits* software (Alvioli et al., 2016) for GRASS GIS, which can draw SU polygons on a digital surface. It provides an unambiguous and reproducible delineation of SUs based on quantitative hydrologic and topographic criteria, allowing for a flexible yet well-defined SU delineation through an adaptive algorithm. The code is designed to quickly produce results on large areas. It requires a digital elevation model and a few input parameters, whose values must be optimized in a sound way, by means of multiple software runs and a proper objective function to be maximized.

We propose a parameter-free SU map of the entire Italian territory, containing about 330,000 SU polygons. We optimized the map considering only objective morphometric quantities. To assess the validity of the nationwide SU partition, we classified the whole of Italy into different categories using a clustering procedure, initialized using only morphometric properties of the SUs. We compared the classification form clustering with zonal statistics of independent quantities: terrain elevation and slope, drainage density and lithology. The analysis confirmed that the SU partition was geo-morphologically sound, suggesting that the proposed method is effective for a general-purpose SU delineation of a large, complex and heterogeneous landscape. The whole SU map is available for download (CNR-IRPI URL).

Alvioli M., Marchesini I., Reichenbach P., Rossi M., Ardizzone F., Fiorucci F. & Guzzetti F. (2016) - Automatic delineation of geomorphological slope units with *r.slopeunits* v1.0 and their optimization for landslide susceptibility modeling. *Geosci. Model Devel.*, 9, 3975–3991.

Guzzetti F., Carrara A., Cardinali M. & Reichenbach P. (1999) - Landslide hazard evaluation: a review of current techniques and their application in a multi-scale study, Central Italy, *Geomorphology*, 31, 181–216.

CNR-IRPI URL: <http://geomorphology.irpi.cnr.it/tools/slope-units>

Regional landslide early warning systems in Italy

Brunetti M.T.*, Peruccacci S., Rossi M., Marchesini I., Denti B., Solimano M., Martinotti M.E.,
Balducci V. & Guzzetti F.

CNR IRPI, Perugia, Italy.

Corresponding email: maria.teresa.brunetti@irpi.cnr.it

Keywords: landslides, early-warning systems, regional.

In Italy, landslides pose a recurrent hazard to human life and livelihood every year. For this reason, with the support of the Italian National Department for Civil Protection (DPC) we have developed a landslide early warning system named SANF (an Italian acronym for national early warning system for rainfall-induced landslides) to forecast the possible occurrence of rainfall-induced landslides in Italy (Rossi et al., 2012). The system uses (i) rainfall measurements from a network of about 3000 rain gauges, (ii) rainfall forecasts at different time intervals, (iii) probabilistic rainfall thresholds (Brunetti et al., 2010; Peruccacci et al., 2017), and (iv) a susceptibility map derived at national scale. Since 2008 the system has been running at national scale. Following the request of regional civil protection authorities of Liguria, Sardinia and Apulia, new SANF versions were developed at regional scale (SARF). While maintaining the structure of the system and the same approach in the calculation of the landslide occurrence probability, each SARF has been customized to cope with the specific user requirements. As an example, for the Liguria region SARF uses regional rainfall thresholds and an ensemble of forecasted rainfall models issued daily by the local environmental protection agency (ARPAL). Differently, the local agency of the Sardinia region (ARPAS) provides us the BOLAM rainfall forecast. After a proper running and validation period, SARF systems are expected to become a valid support for decision makers in forecasting rainfall-induced landslides at regional scale.

Rossi M., Peruccacci S., Brunetti M.T., Marchesini I., Luciani S., Ardizzone F., Balducci V., Bianchi C., Cardinali M., Fiorucci F., Mondini A.C., Reichenbach P., Salvati P., Santangelo M., Bartolini D., Gariano S.L., Palladino M., Vessia G., Viero A., Antronico L., Borselli L., Deganutti A.M., Iovine G., Luino F., Parise M., Polemio M., Guzzetti F. & Tonelli G. (2012) - SANF: National Warning System for Rainfall-Induced Landslides in Italy. *Landslides and Engineered Slopes: Protecting Society through Improved Understanding*, 2, 1895–1899.

Brunetti M.T., Peruccacci S., Rossi M., Luciani S., Valigi D. & Guzzetti F. (2010) - Rainfall thresholds for the possible occurrence of landslides in Italy. *Nat. Hazards Earth Syst. Sci.*, 10, 447–458.

Peruccacci S., Brunetti M.T., Gariano S.L., Melillo M., Rossi M. & Guzzetti F. (2017) - Rainfall thresholds for possible landslide occurrence in Italy. *Geomorphology*, 290, 39–57.

Ischia Island: a model for sustainable development and natural risk mitigation

Buondonno E.¹, Cubellis E.*², Delizia I.¹, Luongo G.²⁻³ & Ricci F.⁴

¹ DiARC, Università di Napoli “Federico II”.

² Osservatorio Vesuviano – Sezione di Napoli dell’Istituto Nazionale di Geofisica e Vulcanologia (INGV).

³ Emerito Università di Napoli “Federico II”.

⁴ Architetto Professionista, Esperto vulnerabilità edifici e agibilità post sisma.

Corresponding email: elena.cubellis@ingv.it

Keywords: natural risk assessment, Ischia Island, sustainable development

The island of Ischia has a land area of 46.3 square kilometers and a population of 64.115 inhabitants by 2019. The territorial density is 1,385 inhabitants per square kilometer. The environmental sustainability of Ischia is about 22 thousand inhabitants. In the year 2017 there were about 2.3 million tourists.

The remarkable expansion of historical settlements on the Island in recent decades, without adequate planning that would pay attention to the geological hazard, has produced an exponential increase in risk, as it was shown by the disastrous earthquake that occurred in Casamicciola on 21 August 2017. The underestimation of volcanic, seismic and hydrogeological risks on the Island is incomprehensible due to the catastrophes that occurred with the historic eruption of 1302, the strong earthquakes of 1881 and 1883 and the disastrous flood of 1910.

The historical data and the most recent ones produced through the monitoring of the Island allow to obtain the maps of the hazard of the territory. These maps are the basic tools for defining acceptable risk and structural interventions to reach this level. The entire Island is exposed to volcanic risk because its structure is an active volcanic field affected by the collapse of the Green Tuff Caldera, an area considered active. In the last 10 Ka eruptive activity developed mainly between the eastern edge of Mt. Epomeo and the eastern coast of the Island. The area with the greatest seismic risk develops on the northern edge of the Mt. Epomeo massif. The hydrogeological instability invests Mt. Epomeo and the floods develop both on the southern and northern side of the Island.

The territory is divided into six Municipalities: Ischia, Casamicciola Terme, and Lacco Ameno to the north, Barano d’Ischia, Serrara Fontana and Forio to the south, but none of the six municipalities has an urban Plan and an inter-municipal Plan is missing. The government of the Island territory, characterized by valuable environmental elements and high risks, has to provide for a unitary action such as to allow the conservation of environmental parameters through the evaluation of environmental sustainability to the anthropic impact and the mitigation of risks. The model for such an intervention foresees:

- Map of volcanic, seismic and hydrogeological risks;
- Definition of Homogeneous Territorial Zone on the basis of the maximum expected damage - any measures to reduce the density of housing and construction;
- Destination of land use - Apply the Landscape Plan;
- Evaluation of the vulnerability of buildings and seismic adaptation of existing buildings;
- Realize an efficient infrastructural system of road and path networks to enhance escape routes;
- Develop equipment and public thermal resources activities.

In this context of natural risks and extraordinary environmental resources it would be appropriate to set up an Advanced Research Center to be placed in an area destined for a Scientific-Naturalistic and Archaeological Park.

Assessing lava flow risk at Etna volcano

Cappello A.*¹, Ganci G.¹, Bilotta G.¹, Corradino C.¹, Hérault A.^{1,2} & Del Negro C.¹

¹ Istituto Nazionale di Geofisica e Vulcanologia, Osservatorio Etneo, Sezione di Catania, Italy.

² Conservatoire National des Arts et Métiers, Laboratoire Modélisation Mathématique et Numérique, Paris, France.

Corresponding email: annalisa.cappello@ingv.it

Keywords: lava flow hazard, elements at risk, multi-criteria evaluation.

Lava flows represent by far the greatest threat to exposed population and infrastructure on Mt Etna. The increasing exposure of a larger population, which has almost tripled in the area around Mt Etna during the last 150 years, is often derived from a poor assessment of the volcanic hazard, allowing inappropriate land use in vulnerable areas. Lack of information about the risk appears to be a major constraint to providing improved mitigation actions that reduce the adverse effects of effusive eruption disasters. A detailed map showing areas that are likely to be inundated by future lava flows is extremely useful, allowing people living nearby to judge for themselves the relation between potentially dangerous areas and their daily lives. Here we quantify the lava flow risk at Etna volcano using a GIS-based approach that integrates the hazard with the exposure of elements at stake. The hazard, showing the long-term probability related to lava flow inundation, is obtained combining three different kinds of information: the spatiotemporal probability for the future opening of new eruptive vents, the event probability associated with classes of expected eruptions, and the overlapping of lava flow paths simulated by the MAGFLOW model. Data including all elements at stake were gathered from institutional web portals and high-resolution satellite imagery, and organized in four thematic layers: population, buildings, service networks, and land use. The total exposure is given by a weighted linear combination of the four thematic layers, where weights are calculated using the Analytic Hierarchy Process (AHP). The resulting risk map shows the likely damage caused by a lava flow eruption, allowing rapidly visualizing the areas in which there would be the greatest amount of losses if a flank eruption occurred at Etna.

Seismic site effects in the area of Tortora (Northern Calabria)

Chiappetta G.D.*¹, Gervasi A.^{1,2}, Festa R.L.¹ & La Rocca M.¹

¹ Università della Calabria.

² Istituto Nazionale di Geofisica e Vulcanologia.

Corresponding email: giuseppe.d.chiappetta@gmail.com

Keywords: site effects, local amplification, HVSR.

Seismic noise and earthquakes recorded at more than 70 sites in an area of about 50 km² have been used to investigate site effects at Tortora (Northern Calabria - CS). The aim of this work is the evaluation of the seismic response in various morphological context. In fact, the investigated area includes coastal plain, marine terraces, alluvial fans, fluvial environments and reliefs. Our efforts were focused to estimate the seismic resonance of the shallow geological structure through the HVSR analysis performed on seismic noise and, in some cases, even on earthquakes. In about 30 cases the HVSR curves are characterized by significant peaks in the frequency range from 1 Hz to 3 Hz. This type of result, which is observed at any sites along the coastal plain, has been interpreted as representative of a local seismic resonance. In other cases the results show quite flat HVSR curves, usually at bedrock sites. Some unclear results, e.g. HVSR curves without clear peaks but not flat, have also been found. While the most of seismic noise recordings lasted only about 1 hour, in five sites continuous recordings from many days to a couple of months were acquired. Tens of local and regional earthquakes were recorded at these sites. The HVSR analysis have been applied also to earthquake recordings, and results have been compared with those obtained from seismic noise. Results are very similar for sites on sediments, while they appear quite different at the sites on bedrock. The continuous recordings allowed for studying the relationship between HVSR curves and the properties of the noise wavefield, such as rms and polarization, as they may change in time depending on weather conditions. Results of this analysis show that the height of the resonance peak depends on both signal amplitude and polarization. On the other hand, sites on bedrock that are characterized by flat HVSR curve in good weather conditions, show the presence of HVSR peaks in case of strong wind and rough sea. This result is well correlated with the hill slope, therefore we interpret it as a topographical effect. During many weeks continuous signals were recorded by two instruments at two different sites, one near the coast on sediments, and another one upon the hill on the bedrock. The spectral ratio between earthquakes recorded at sites on sediments and at sites on bedrock gives an estimation of the local amplification of ground motion as a function of frequency. From this analysis we found that the local amplification is frequency dependent, with the maximum at the resonance frequency found from the HVSR analysis.

The 2016 Central Italy Seismic Sequence: emergency and post-emergency activities

Fiorucci F.^{*1}, Ardizzone F.¹, Santangelo M.¹, Bucci F.¹, Allasia P.², Alvioli M.¹, Baldo M.², Bianchi C.¹, Brunetti M.T.¹, Cavalli M.³, Clerissi F.¹, Crema S.³, Donnini M.¹, Giordan D.², Guzzetti F.¹, Marchesini I.¹, Marchi L.³, Melillo M.¹, Mondini A.C.¹, Peruccacci S.¹, Reichenbach P.¹, Rossi M.¹, Salvati P.¹ & Cardinali M.¹

¹ IRPI-CNR, Perugia.

² IRPI-CNR, Torino.

³ IRPI-CNR, Padova.

Corresponding email: federica.fiorucci@irpi.cnr.it

Keywords: earthquake, Central Italy, civil protection.

On August 24, a seismic sequence started in Central Italy. Four main shocks with Mw between 5.5 and 6.5 (August 24, October 26, October 30, and January 18) and more than 90,000 aftershocks were recorded. The seismic events have caused 299 casualties and more than 20,000 homeless, and major damage mostly to buildings and architectural heritage of the Abruzzo, Lazio, Marche and Umbria regions. The main shocks and some of the most severe aftershocks triggered landslides, chiefly rock falls and minor rock slides that caused damage to the transportation network. Since the immediate aftermath of the event, and during the emergency and post-emergency phases, we assisted the Italian National Department for Civil Protection in the evaluation of local landslide and hydrological risk conditions. Technical and scientific activities focused on: (i) evaluating and selecting sites for locating residential and productive temporary settlements, through an assessment of the local geomorphological and hydrological conditions; (ii) evaluating rock fall hazard on roads, (iii) developing a methodological approach aimed at identifying suitable and safe areas for the relocation of villages and hamlets destroyed by the earthquake. To execute these activities, we exploited a wide range of methods, techniques, and technologies. In particular, we performed a systematic preliminary interpretation of historical stereoscopic aerial photographs and Google Earth™, detailed field surveys, helicopter reconnaissance flights in wide and/or inaccessible areas. We also carried out models to evaluate landslide susceptibility and the exposure of roads to potential trajectories of rock fall and debris flows. Furthermore, we developed and deployed an integrated modelling and heuristic approach for the evaluation of the suitable areas to relocate entire villages. This experience has shown that applied geomorphology can help addressing problems at different scales and in different phases of the emergency management. The integrated methodological approach can be effective not only for emergency and post-emergency decision support, but also in ordinary urban planning.

Analyzing flood risk perception to connect forecasting and alert agencies with the community: the case of the life primes project

Gioia E.*¹ & Marincioni F.¹

¹ Department of Life and Environmental Sciences, Università Politecnica delle Marche, Italy.

Corresponding email: e.gioia@staff.univpm.it

Keywords: flood, risk perception, community.

One of the main problems faced by scientists working on the prediction of geological phenomena is the effective communication of the expected impacts both to the population and to those that locally manage the risk. In fact, for the forecasting system to be functional to risk management, it is necessary to have (a) a strategy for passing accurate information around the local authorities and technical officers, and (b) a population willing to listen to institutions for activating correct behaviors (Lombardi, 2005). The reasoning that effectively connect forecasting and alert agencies with the community pertain to the social dimension of risk management. Hence, it is necessary to consider how individuals judge the characteristics and severity of the risks they face, namely the risk perception.

The present study proposes a flood risk perception analysis of citizens and municipal civil protection technicians, focusing on: (i) knowledge of the flood hazard and risk; (ii) awareness of the local flood risk; (iii) perception of climate change; (iv) knowledge of the alerting tools; (v) accessibility and reliability of flood risk information; (vi) trust in institutions. The cases of 10 municipalities, belonging to the Emilia Romagna Marche and Abruzzo regions (central Italy), participant to the European Life PRIMES project, were analyzed. The municipalities were chosen because subject to an increasing number of floods, especially in autumn and spring (ARPAE-SIMC, 2016).

Results show that both technician and citizens have a good knowledge of the flood causes but are mostly not aware of the actual hazard in their territory, particularly in spring. However, they all admit the possibility of widespread material and psychological damages, especially to vulnerable categories and in the light of the current climate change. Conversely, technicians consider alerts well spread, timely, but often wrong, while citizens are generally more uncertain. Citizens also declared to not have received any information about floods and what to do in an emergency, as opposed to the answer of the technicians, but they all agree that civil protection should oversee the risk communication. Finally, in contrast to technicians, citizens do not consider institutions efficient for the management of flood risk, particularly concerning the description of the alert systems and the return to normal conditions after the emergency.

ARPAE-SIMC (ed) (2016) - Report B1: Summary of data and state of the art about hydraulic risk observed in the three Regions. Report of the PRIMES Project: Action A1, 1-12.

Lombardi M. (ed) (2005) - La comunicazione dei rischi naturali. un confronto internazionale. Vita e Pensiero, Milano, 1-228.

A comparison between empirical landslide predictive models applied to the Marche region (Central Italy)

Gioia E.*¹ & Marincioni F.¹

¹ Department of Life and Environmental Sciences, Università Politecnica delle Marche, Italy.

Corresponding email: e.gioia@staff.univpm.it

Keywords: landslide, empirical predictive models, central Italy.

This research contributes to the landslide forecast debate, analyzing the relationship between rainfall and slope failures in the eastward section of the Esino river basin, located in the Marche region (central Italy). Post-orogenic quaternary sediments, prone to rainfall-induced shallow landslides, characterize this 550 km² wide area. Based on the review of historical landslides, the study area was affected by 234 landslides over the period 1953 to 2012.

In order to determine rainfall thresholds for the possible occurrence of landslides, an approach that consider 3 empirical (statistical) methods have been applied: (i) the cumulative event rainfall– duration (ED) method, (ii) the intensity – duration (ID) method, and (iii) the Bayesian probabilistic method (one-dimensional and two-dimensional). These methods were applied for the same landslides and rainfall databases and for the same zone, which is characterized by comparable hydrogeological properties.

The ED and ID method allowed the definition of local rainfall thresholds which, even if showing general consistency with the trends of the literature thresholds, highlight the need of considering limited areas with similar lithological settings. Moreover, it was possible to associate different ranges of ED or ID with the corresponding number of landslides expected, from rainfall events that could trigger 1 landslide to rainfall events that could trigger more than 10 landslides.

On the other hand, the Bayesian method allowed to consider in a probabilistic framework all the past rainfall events, whether they resulted in landslides or not, and thus to select the critical rainfall parameters for the area of investigation. Results of this analysis show that the most significant rainfall variables in explaining the initiation of landslides are: cumulative event rainfall (E), daily rainfall (R), and five days antecedent rainfall (A5) only if coupled with daily rainfall.

Finally, all the considered models were tested during a recent rainfall event that affected the study area on 2-4 May 2014 and triggered several landslides.

The encouraging results obtained in this research have shown the benefits of applying a diversified methodological approach to study a complex problem as the landslide hazard in the Marche region.

Seismic microzonation and analysis of the Emergency Limit Condition - Useful tools for the seismic risk mitigation

Giuffrè M.*¹, Benigni M.S.¹, Coltella M.¹, Martelli L.², Pietrosante A.¹ & Romani M.³

¹ Istituto di Geologia Ambientale e Geoingegneria - Consiglio Nazionale delle Ricerche, Roma.

² Regione Emilia-Romagna – Direzione Generale Cura del Territorio e dell’Ambiente - Servizio Geologico, Sismico e dei Suoli.

³ Regione Emilia-Romagna – Agenzia Regionale per la Ricostruzione Sisma 2012 - Servizio per la gestione tecnica degli interventi di ricostruzione e per la gestione dei contratti e del contenzioso.

Corresponding email: margherita.giuffre@igag.cnr.it

Keywords: seismic risk mitigation, seismic microzonation, Emergency Limit Condition.

Following the earthquake of 2009 in L’Aquila, with the enactment of Law 77/2009 and the “National Plan for the Prevention of Seismic Risk” the Italian Parliament aimed at promoting studies and interventions for seismic risk prevention across Italy. This national program financed both the Seismic Microzonation studies (MS) and the Emergency Limit Condition analysis (CLE) involving municipalities with medium to high seismic risk. MS studies are highly useful tools for local seismic hazard assessment; its purpose is to identify and to map areas of the territory (microzones) characterized by homogeneous seismic behavior. These studies may be carried out at various levels of growing complexity (from Level 1 to level 3), showing and classifying the territory according to 3 categories: stable zones, stable zones prone to local amplifications, zones prone to instability. The study of the earthquake behavior in urban settlements is based on the CLE analysis, which represents the condition by which, in the wake of a seismic event, the entirety of an urban settlement loses all its functions (physical and functional, including residential system), but it conserves the use of the majority of its strategic functions for emergency management, together with its accessibility and connections with the surrounding territory. The “National Plan for the Prevention of Seismic Risk” is carried out by the assumption that the knowledge of seismic local response, according to the analysis of the behavior under earthquake of urban settlements, can provide useful indications and decision-making criteria for land use management during the post-event phase in areas subject to risk. The conjugate approach of the MS and the CLE allows to associate geological information with the strategic functions for emergency management. By overlaying the CLE elements and the microzones, it’s possible to define criteria and land use guidelines. Despite the fact that all the Italian Regions have been explicitly urged to adopt and incorporate these studies in dedicated legislative measures into planning systems, nowadays only few cases verify these conditions, maintaining a clear separation between the different studies and disciplines. It is particularly important to overcome the traditional concept of seismic risk as something unexpected (which is managed with emergency policies) by referring to an approach of regional planning policies rather than technical and administrative acts. The cases studies of Emilia Romagna Region go in this direction, showing those municipalities which have adopted an integrated approach in urban planning, between MS studies and CLE analysis.

AA.VV. (2013) - Strategie di mitigazione del rischio sismico e pianificazione – CLE Condizione Limite per l’Emergenza. Urbanistica dossier, INU Edizioni, Roma.

Gruppo di lavoro MS (2008) - Indirizzi e criteri per la microzonazione sismica. Conferenza delle Regioni e delle Province autonome - Dipartimento della protezione civile, Roma.

Seismic- and Meteo-induced Landslides in Emilia Romagna

Grezio A.*¹, Ardizzone F.², Bucci F.², Guzzetti F.² & Marzocchi W.³

¹ Istituto Nazionale di Geofisica e Vulcanologia, sezione di Bologna, Italy.

² Consiglio Nazionale delle Ricerche, Istituto di Ricerca per la Protezione Idrogeologica, Perugia, Italia.

³ University of Naples, Federico II, Dept. of Earth, Environmental, and Resources Sciences, Italy.

Corresponding email: anita.grezio@ingv.it

Keywords: multi-hazards, seismic activity, meteorological events.

Understanding interactions among different natural hazards is taking a great relevance to evaluate the risk posed by natural events. The development of multi-hazard approaches is widely encouraged in key government and intergovernmental initiatives and agencies and further investigations are mandatory. The identification of all possible and spatially related hazards is important in a full multi-hazard analysis. Triggering factors represents a key point towards the definition of a multi-hazard and consequently a multi-risk assessment. Here we consider the case of earthquake and landslide interaction. Seismic sequences and earthquakes, not necessarily of medium-high magnitudes, could trigger other hazardous events and produce destructive ground effects. One of the potential consequences of the seismicity is the modification of the slope stability that favours the occurrence of multiple landslides caused by other different triggering factors, such as the meteorological events. For the purpose we present a preliminary analysis of the landslides induced by both seismic activity and meteorological conditions in the Emilia Romagna region. The scope of the study is the investigations of the shaking effects on the slope failures, concomitant or not with long lasting rainfalls or snow melt or other intense meteorological conditions, both in the short- and long-term. We examined more than 800 landslide records selected from a digital archive of landslide events occurred in the period from February 2007 to March 2018. The investigation time window was chosen to include the 20th May 2012 earthquake (Terremoto Emilia, magnitude 5.9). In the correspondent decade we extracted the daily precipitation data from the National Oceanic and Atmospheric Administration (NOAA) to evaluate the general trend of the precipitation intensity in the area. For the same period and for the two antecedent years we selected the magnitudes and the locations of the earthquakes from the Italian Seismological Instrumental and Parametric Data-Base (ISIDE) to analyse the seismic events and sequences occurred in the study region.

A statistical procedure used for the flood hazard zonation at national scale

Marchesini I.*¹, Salvati P.¹, Rossi M.¹, Donnini M.¹, Guzzetti F.¹, Sterlacchini S.², Zazzeri M.², Cappellini G.² & Voltolina D.²

¹ CNR IRPI.

² CNR IDPA.

Corresponding email: ivan.marchesini@irpi.cnr.it

Keywords: flood, zonation, statistical approach.

Floods occur frequently in Italy and produce extensive damage to the public and private sector. The delineation of the flood prone areas is mandatory for an effective environmental planning and to limit the damage and the costs related to the inundations. Currently, in Italy, an inhomogeneous flood hazard zonation of the territory is available. It is the result of several process-based modelling approaches, used by the different basin units of management for the preparation of the flood hazard maps and flood risk management plans, as required by the e EU Flood Directive. Here we present a tool, named FLOOD-SHE (Flood Statistical Hazard Evaluation), which was used to delineate the potential flooded areas, at national scale, according to different return periods. The procedure is based on a statistical approach and is finalised to extend the flood hazard zonation to the portion of the river network where process-based models were not still applied. The proposed tool is based on a multivariate classification algorithm calibrated and validated using the existing process-based flood hazard maps available for the river basin districts. The tool is made by a complex processing chain implemented using Open Source software and libraries and was developed for the GNU-Linux OS. The classification algorithm is based on the usage of morphometric variables derived from the Tinitay DTM at 10 meters resolution. As a consequence, the delineated flood-prone areas only depend on the geomorphological settings of the territory and are poorly affected by the presence of small levees or other types of flood mitigations works. Fair performances were obtained from the application of the tool both in calibration and validation phases. The outputs of the FLOOD-SHE tool were used to generate water-depth maps, in the potential flood-prone areas, for different return periods. This information, which represents a proxy of the flood magnitude, can be used to perform ex ante evaluation of the potential damage and the related costs.

Local indexes, based on a nationwide threshold, for rainfall-induced landslides

Martinotti M.E.*¹, Marchesini I.¹, Rossi M.¹, Peruccacci S.¹ & Guzzetti F.¹

¹ CNR IRPI, Perugia, Italy

Corresponding email: maria.elena.martinotti@irpi.cnr.it

Keywords: rainfall-induced landslides, probability.

The Italian territory is affected by rainfall-induced landslides, which can result in loss of lives and widespread damage. Empirical rainfall thresholds are widely used for predicting the occurrence of failures triggered by intense or prolonged rainfall at national and regional scale, even if they have empirical limitations for small geographical areas. These limitations depend on the size of the landslide catalogue available for the definition of statistically robust rainfall threshold over small areas (Peruccacci et al., 2012). Martinotti et al. (2017) theorized, designed and tested the Ensemble-Non-Exceedance Probability (E-NEP) algorithm, which exploits standard rainfall records obtained from rain gauges and a given rainfall threshold to quantitatively assess the landslide occurrence probability over time. Using the rainfall threshold defined by Peruccacci et al. (2017) for the entire Italian territory, they applied the E-NEP algorithm to analyse the landslides triggered during a time period of torrential rain between 1 and 6 September 2014 in the Gargano Promontory (Puglia) and found that the E-NEP metrics provided better diagnostics than the single metrics often used for landslide forecasting.

Here, we show that a nation wide rainfall threshold can be tailored to specific sub-region where only a small catalog of rainfall-induced landslides is available. For this purpose, we created empirical local indexes based on the regular metrics produced by the E-NEP algorithm and a nation wide rainfall threshold (Peruccacci et al., 2017). The local indexes could be used in place of or combined with the regular E-NEP metrics to improve the forecasting capability of rainfall-induced landslides at local scales. The indexes performances are calibrated and validated exploiting a catalogue of rainfall-induced landslides occurred in the Liguria region. Being particularly sensitive to the rainfall intensity, the indexes are able to better isolate the rainfall condition responsible for the failures, thus reducing locally the number of false alarms.

Martinotti M.E., Pisano L., Marchesini I., Rossi M., Peruccacci S., Brunetti M.T., Melillo M., Amoroso G., Loiacono P., Vennari C., Vessia G., Trabace M., Parise M. & Guzzetti F. (2017) - Landslides, floods and sinkholes in a karst environment: the 1–6 September 2014 Gargano event, southern Italy. *Natural Hazards and Earth System Sciences Discussions*, 17, 467–480.

Peruccacci S., Brunetti M.T., Luciani S., Vennari C. & Guzzetti F. (2012) - Lithological and seasonal control of rainfall thresholds for the possible initiation of landslides in central Italy. *Geomorphology* 139–140, 79–90.

Peruccacci S., Brunetti M.T., Gariano S.L., Melillo M., Rossi M. & Guzzetti F. (2017) - Rainfall thresholds for possible landslide occurrence in Italy. *Geomorphology*, 290, 39–57.

Progresses and challenges for Operational Earthquake Forecasting in Italy

Marzocchi W.^{*1-2}, Falcone G.² & Taroni M.²

¹ DiSTAR Università di Napoli Federico II.

² Seismic Hazard Center INGV.

Corresponding email: warner.marzocchi@unina.it

Keywords: Earthquake forecasting, seismic risk.

Tracking the time evolution of seismic hazard in time windows shorter than the usual 50-years of long-term hazard models may offer additional opportunities to reduce the seismic risk. This is the target of operational earthquake forecasting (OEF) as it has been defined by the International commission on earthquake forecasting (ICEF) appointed by the Italian Government after the L'Aquila earthquake in 2009. In this talk we describe the current OEF development in Italy – carried out by the seismic hazard center of the Istituto Nazionale di Geofisica e Vulcanologia – and the challenges that we met, some of them purely scientific and others related to the practical interface of science with society. As regards the implementation, we describe the liaison with the Collaboratory for the Study of Earthquake Predictability (CSEP) activities, and the prospective forecasts made during the recent destructive Amatrice-Norcia sequence in 2016-2017, which has been characterized by several bursts of seismicity and a significant deviation from the Omori law. Specifically, we show that the current OEF system in Italy issued statistically reliable and skillful space-time-magnitude forecasts of the largest earthquakes of the sequence. Finally we discuss the challenges encountered and how we are handling them. In particular, we focus our attention on the non-scientific issues that range from the usefulness of OEF information, its importance in terms of seismic risk, and the difficulties in communicating low-probability/high-impact events like the occurrence of large earthquakes during a seismic sequence.

MPS19: the updated seismic hazard model of Italy as an example of state-of-the-art in PSHA

Meletti C.*¹, Marzocchi W.², D'Amico V.¹, Luzi L.¹, Martinelli F.¹, Pace B.³, Rovida A.¹,
Visini F.¹ & MPS16 Working Group¹

¹ Istituto Nazionale di Geofisica e Vulcanologia.

² University of Naples Federico II.

³ University of Chieti-Pescara.

Corresponding email: carlo.meletti@ingv.it

Keywords: seismic hazard, building code, Italy.

In 2015 the Centro Pericolosità Sismica (CPS) of the INGV was commissioned to coordinate the national scientific community (about 150 people from different institutions) with the aim of elaborating a new reference seismic hazard model. The main requirements were defined together with experts in earthquake engineering that will then participate to the revision of the building code. The CPS outlined a roadmap to release a significantly renewed PSHA model, with regard to both the updated input elements and the strategies to be followed.

CPS fixed some key constraints that had to be respected in order to guarantee a large participation and consensus: (i) the use of international standards for PSHA; (ii) open and transparent procedures that totally guarantee reproducible outcomes; (iii) the involvement of a large Italian scientific community when proposing data, models and approaches; (iv) a full exploration and representation of the epistemic uncertainty in the final seismic hazard model; (v) the implementation of a robust testing phase, in addition to the elicitation session with national and international independent experts.

The activities were organized in 6 tasks: T1) project management, T2) input data, T3) seismicity models, T4) ground motion and intensity predictive equations (GMPEs and IPEs), T5) computation and rendering, T6) testing.

T1 planned the activities and managed the other 5 tasks to ensure the achievement of the Project scopes.

T2 selected the most updated information about historical and instrumental seismicity, seismogenic faults, and deformation.

T3 elaborated the seismicity models in terms of classic source areas, fault sources and gridded seismicity based on different approaches, with associated seismicity rates. Moreover, modellers had to explore the epistemic uncertainty related to their model; this step is crucial to estimate an overall epistemic uncertainty of the final model.

T4 selected the most recent models accounting for their tectonic suitability and forecasting performance. The forecasting performance of each GMPE has been evaluated through the comparison with accelerometric records available in the Italian (itaca.mi.ingv.it) and European (esm.mi.ingv.it) strong-motion databases. In this way, each GMPE has been ranked according to different specific metrics, so that the best performing GMPEs can be identified.

T5 identified the code OpenQuake (www.openquake.org) for calculation. It is an open source software, therefore we had a large interaction with the developing team in order to integrate the code with new, dedicated functions.

T6 performed statistical procedures to test, with the available data, the whole seismic hazard models, and single components such as the seismicity models and the GMPEs. T6 also organised the elicitation session and finally weighted the different models.

Finally, the MPS19 model was implemented also according to the suggestions of a revision panel (composed of 5 Italian experts selected by DPC).

Differential Synthetic Aperture Radar Experiments over the Ocean-Reclaimed Lands of Shanghai: Long-term flood Hazard Modeling and Urban Infrastructure Monitoring

Pepe A.*¹, Zhao Q.², Kubanek J.³, Falabella F.¹⁻⁴, Yin J.², Yu D.², Lin N.³, Ma G.² & Liu M.²

¹ IREA-CNR, National Council Research of Italy, Napoli.

² East China Normal University, Shanghai.

³ ESTEC, ESA, The Netherlands.

⁴ University of Basilicata, Potenza, Italy.

Corresponding email: pepe.a@irea.cnr.it

Keywords: deformation, flood, DInSAR.

The growing demand of new lands in populated areas for urban development has been faced in many coastal areas by reclaiming the lands from the sea. This is the case of the ocean-reclaimed lands of Lingang New City, Shanghai, where a complex reclamation procedure has started in the 90s' and is still active. The area, being almost flat with a low-lying topography, is subject to severe floods from the ocean, also emphasized by the mean sea level rise that has reached an average rate of 3.8 mm/a. Human activities have also greatly modified the coastal topography in the past decades. Natural compaction of loose sediments and self-weight consolidation of dredger fill caused significant land subsidence in this area.

The changes of the Earth's surface can be monitored through the use of satellite-based remote sensing approaches. In particular, the DInSAR technique (Massonet and Feigl, 1998) is widely used to retrieve ground displacements. Difficulties arise in the coastal area of Shanghai due to the significant decorrelation of the different SAR scenes acquired by the satellites over time, and the lack of regular acquisitions over the investigated area in the last two decades. These technological challenges require the development of new multi-temporal DInSAR approaches that allow improving our ability to observe the temporal evolution of the on-going, time-varying phenomena.

This study is two-folded. On one hand, some new recent DInSAR developments to increase the density of detectable pixels subject to deformation in moderate-to-low coherent areas are presented. On the other hand, this study presents the results of a long-term coastal flood risk analysis obtained by considering 100- and 1000-year coastal flood return periods, local sea-level rise projections, and long-term ground subsidence projections. Predictions on the future coastal flood inundations have been obtained by using a flood inundation model for different time-periods of analysis (Yin et al., 2019). Our results suggest that the sea-level rise, together with land subsidence, could result in minor but non-linear impacts on coastal inundation over time, and that an increased flood risk would be primarily determined by future exposure and vulnerability of population and property in the floodplain.

Massonet D. & Feigl K.L. (1998) - Radar interferometry and its application to changes in the Earth's surface. *Rev. Geophys.*, 36, 441–500.

Jie Yin, Qing Zhao, Dapeng Yu, Ning Lin, Julia Kubanek, Guanyu Ma, Min Liu, Antonio Pepe (2019) - Long-term flood-hazard modeling for coastal areas using InSAR measurements and a hydrodynamic model: The case study of Lingang New City, Shanghai. *Journal of Hydrology*, 571, 593-604.

National and regional empirical rainfall thresholds for possible shallow landslide occurrence in Italy

Peruccacci S.*¹, Brunetti M.T.¹, Gariano S.L.¹, Melillo M.¹, Rossi M.¹ & Guzzetti F.¹

¹ CNR IRPI, Perugia, Italy.

Corresponding email: silvia.peruccacci@irpi.cnr.it

Keywords: shallow landslides, rainfall thresholds, environmental domains.

The Italian territory is highly prone to shallow rainfall-induced landslides. Moreover, a large physiographic, geological and climatic variability characterizes the national landscape. For these reasons - and for the abundance of available rainfall measurements - Italy is an ideal test site to investigate how rainfall conditions that induced shallow landslides may vary in different environmental settings.

Since 2007, we have been building a catalogue of rainfall events responsible for the triggering of landslides in Italy. Using accurate landslide information and hourly rainfall data recorded by a network of 2228 rain gauges, we reconstructed 2309 rainfall events that induced 2819 (mostly) shallow landslides in Italy in the period January 1996 - February 2014. We calculated the rainfall duration D (in hours) and the cumulated event rainfall E (in mm) presumably responsible for each failure.

Using a well-established frequentist method, we calculated empirical cumulated event rainfall–rainfall duration (ED) thresholds at different non-exceedance probabilities and the uncertainties associated with their parameters. Using the entire dataset, we determined a national threshold representing the rainfall conditions that can likely result in landslides in Italy. By considering six environmental subdivisions based on topography, lithology, soil regions, land cover, climate, and precipitation regime, we defined 26 regional thresholds identifying the rainfall conditions responsible for landslide triggering in different environmental settings in Italy.

Overall, the resulting national and environmental thresholds are similar, and cover a small part of the possible DE domain. Nevertheless, thresholds for meteorological domains, which are classified according to the mean annual precipitation (MAP) become higher at increasing values of the MAP. This confirms the idea that the landscape adjusts to the regional meteorological conditions. We also observed that the national threshold at 20% non-exceedance probability was capable of predicting all the rainfall-induced landslides that caused casualties between 1996 and 2014. We suggest that this threshold can be used as lower limit to forecast fatal rainfall-induced landslides in Italy.

The findings encourage the use of empirical rainfall thresholds for landslide forecasting in Italy, but poses an empirical limitation to the possibility of defining accurate thresholds for small geographical areas, with insufficient datasets.

Between ethics and territorial planning: the value of the ESI-2007 scale

Porfido S.^{1,2}, Nappi R.*¹, Gaudiosi G.¹, Alessio G.¹ & Michetti A.M.³

¹ INGV-Osservatorio Vesuviano Napoli.

² CNR-ISA Avellino.

³ Univ. degli Studi Insubria.

Corresponding email: rosa.nappi@ingv.it

Keywords: ESI-2007 scale, ethics, seismic hazard.

A modern approach to the assessment of seismic hazard cannot disregard the study of effects induced by earthquakes in the natural environment. The knowledge and mapping of seismic-induced effects represents the basis for providing a more reliable and realistic scenario in territorial planning. In recent years this has been dramatically demonstrated by large subduction events (Indonesia 2004, Japan 2011, Ecuador 2016, Mexico 2017, etc.), but also, and remarkably, by moderate to small earthquakes which affected Italy (Emilia Romagna 2012, Casamicciola (Ischia) 2017, Fleri-Pennisi (Sicily) 2019). The introduction of the new ESI 2007 macroseismic scale (Michetti et al., 2007), has been fundamental in pursuing this ethically and scientifically comprehensive approach for evaluation of seismic hazard. The assessment of intensity based only on environmental effects is applicable everywhere in the world, regardless of quality of the built environment, and therefore ethically more correct, being not influenced by the socio-economic conditions that affect the urban development of the various countries. The ESI scale integrates the traditional macroseismic scales, of which it represents the evolution, allowing to assess the intensity parameter also where buildings are absent or damage-based diagnostics saturate. For this purpose, we revisit three representative case histories from very different tectonic environments: the reverse faulting of the 2012 Emilia sequence (May 20, $M_w = 5.8$; and May 29, $M_w = 5.6$; Di Manna et al., 2012) in the Po Plain foredeep environment of N Italy; the normal faulting of August 21, 2017 Casamicciola earthquake ($M_d = 4.0$; Nappi et al., 2018) in the Ischia volcanic island, S Italy; and the devastating February 4, 1976, Guatemala earthquake ($M = 7.5$; Porfido et al., 2015), along the left-lateral Motagua Fault at the boundary between the N America and Caribbean plates.

The macroseismic study of these earthquakes with ESI 2007 scale has contributed to define more realistic seismic scenarios in terms of intensity. We show that this methodology is essential for seismic hazard evaluation, and a fundamental step towards appropriate post-seismic reconstruction.

Di Manna P., Guerrieri L., Piccardi L., Vittori E., Castaldini D., Berlusconi A., Bondaleo L., Comerci V., Ferrario F., Gambillara R., Livio F., Lucarini M. & Michetti A.M. (2012) - Ground effects induced by the 2012 seismic sequence in Emilia: implications for seismic hazard assessment in the Po Plain. *Ann. Geoph.*, 55(4), <https://doi.org/10.4401/ag-6143>

Michetti A.M., Esposito E., Guerrieri L., Porfido S., Serva L., Tatevossian R., Vittori E., Audemard F., Azuma T., Clague J., Comerci V., Gurbinar A., Mc Calpin J., Mohammadioun B., Morner N.A. Ota Y. & Roghazin E. (2007) - Intensity Scale ESI 2007, *Mem. Descr. Carta Geologica d'Italia*, Roma, 74, 53 pp.

Nappi R., Alessio G., Gaudiosi G., Nave R., Marotta R.E., Siniscalchi V., Civico R., Pizzimenti L., Peluso R., Belviso P. & Porfido S. (2018) - The 21 August 2017 M_d 4.0 Casamicciola earthquake: First evidence of coseismic normal surface faulting at the Ischia volcanic island. *Seism. Res. Lett.*, 89(4), 1323–1334. <https://doi.org/10.1785/0220180063>.

Porfido S., Esposito E., Spiga E., Sacchi M., Molisso F. & Mazzola S. (2015) - Impact of Ground Effects for an Appropriate Mitigation Strategy in Seismic Area: The Example of Guatemala 1976 Earthquake. In Lollino G., Giordan D., Crosta G.B., Corominas J., Azzam R., Wasowski J. & Sciarra N. (eds.): *Engineering Geology for Society and Territory – Vol. 2*. Springer, Cham.

Modelling societal landslide risk in Italy

Rossi M.*¹, Guzzetti F.¹, Salvati P.¹, Donnini M.¹, Napolitano E.² & Bianchi C.¹

¹ CNR IRPI, Perugia, Italy.

² Private consultant. Formerly CNR IRPI, Perugia, Italy.

Corresponding email: mauro.rossi@irpi.cnr.it

Keywords: landslide, fatalities, societal risk.

Landslides cause every year worldwide severe damages to the population. A quantitative knowledge of the impact of landsliding phenomena on the society is fundamental for a proper and accurate assessment of the risk posed by such natural hazards. In this work, a novel approach is proposed to evaluate the spatial and the temporal distribution of societal landslide risk from historical, sparse, point information on fatal landslides and their direct human consequences (Rossi et al., Accepted). The approach was tested in Italy, using a detailed catalogue listing 5571 fatalities caused by 1017 landslides at 958 sites across Italy, in the 155-year period 1861 – 2015. The model adopting a Zipf distribution to evaluate societal landslide risk for the whole of Italy, and for seven physiographic and 20 administrative subdivisions of Italy. The model is able to provide estimates of the frequency (and the probability) of fatal landslides, based on the parameters, namely (i) the largest magnitude landslide F , (ii) the number of fatal events E , and (iii) the scaling exponent of the Zipf distribution s , which controls the relative proportion of low vs. large magnitude landslides. Different grid spacings, g and circular kernel sizes, r were tested finally adopting $g = 10$ km and $r = 55$ km. Using such geometrical model configuration, the values of the F , E and s parameters were derived for each grid cells revealing the complexity of landslide risk in Italy, which cannot be described properly with a single set of such parameters. Based on such modeling configuration. This model configuration allowed to estimate different risk scenarios for landslides of increasing magnitudes, which were validated checking the anticipated return period of the fatal events against information on 130 fatal landslides between 1000 and 1860, and eleven fatal landslides between January 2016 and August 2018. Despite incompleteness in the old part of the record for the low magnitude landslides, and the short length and limited number of events in the recent period 2016 – 2018, the anticipated return periods are in good agreement with the occurrence of fatal landslides in both validation periods. Despite the known difficulty in modelling sparse datasets, the proposed approach was able to provide a coherent and realistic representation and new insight on the spatial and temporal variations of societal landslide risk in Italy.

Rossi M., Guzzetti F., Salvati P., Donnini M., Napolitano E. & Bianchi C. (Accepted for publication) - A predictive model of societal landslide risk in Italy. *Earth-Science Reviews*.

Landslide early warning: lessons learned after 10-year experience in Italy

Rossi M.*¹, Marchesini I.¹, Martinotti M.E.¹, Brunetti M.T.¹, Peruccacci S.¹, Balducci V.¹ & Guzzetti F.¹

¹ CNR IRPI, Perugia, Italy.

Corresponding email: mauro.rossi@irpi.cnr.it

Keywords: landslides, early-warning systems, rainfall.

As prioritized by the Sendai Framework, enhancing disaster preparedness is fundamental for the effective response, for taking actions in anticipation of events, and to ensure that the appropriate capacities are in place for effective response and recovery at all levels. Under this view early warning systems can be seen as irreplaceable tools to supporting the Civil Protection authorities in the preparedness and response phases. This is particularly relevant for the case of rainfall-induced slope failures that occur worldwide every year, claiming lives and causing severe economic disruption. Implementing early warning systems to forecast the occurrence of such geo-hydrological phenomena is difficult and challenging both from the scientific and technological side. Here we present a framework developed in Italy (Rossi et al., 2012) for the operation forecasting of rainfall induce landslides over large areas, which includes (i) criteria, tools and technological supports for the collection of rainfall induced landslide occurrences; (ii) scientific methods and tools for the analysis of the relation between rainfall and landslides occurrences and for the landslide rainfall threshold definition; (iii) operational early warning system procedures and technological supports for the rainfall induced landslide forecasting; (iv) interfaces for the query and analysis of the early warning system outputs; (v) criteria, tools and technological supports for the validation of the early warning system outputs. The main lessons learned in the last decade and the most critical issues experienced implementing such framework for the entire Italian territory (SANF system) and for different regions both in Italy and India (SARF systems, LANDSLIP LEWS system) are highlighted and discussed.

Rossi M., Peruccacci S., Brunetti M.T., Marchesini I., Luciani S., Ardizzone F., Balducci V., Bianchi C., Cardinali M., Fiorucci F., Mondini A.C., Reichenbach P., Salvati P., Santangelo M., Bartolini D., Gariano S.L., Palladino M., Vessia G., Viero A., Antronico L., Borselli L., Deganutti A.M., Iovine G., Luino F., Parise M., Polemio M., Guzzetti F. & Tonelli G. (2012) - SANF: National Warning System for Rainfall-Induced Landslides in Italy'. *Landslides and Engineered Slopes: Protecting Society through Improved Understanding* 2, 1895–1899.

A GIS-based application to support decision makers in preparedness and response to flood-related risks

Sterlacchini S.*¹, Zazzeri M.¹, Cappellini G.¹, Voltolina D.¹, Marchesini I.², Salvati P.², Rossi M.²,
Donnini M.² & Guzzetti F.²

¹ Istituto per la Dinamica dei Processi Ambientali (CNR-IDPA, Milano).

² Istituto di Ricerca per la Protezione Idrogeologica (CNR-IRPI, Perugia).

Corresponding email: simone.sterlacchini@cnr.it

Keywords: flood, impact, risk scenarios.

Planning in advance to prepare for and respond to hydro-meteorological hazard-induced emergencies is a key-action that allows decision makers to mitigate unexpected impacts and potential damage.

This study presents an open source GIS-based application (**BLINKS** - Building Loss estimation iN risk analysiS) designed and implemented to support local/regional decision makers in preparedness and response to flood-related risks and, in so doing, mitigate the expected impacts and potential damage. **BLINKS** allows spatial planners and risk managers to access and analyze relevant distributed, authoritative and multi-source spatial data useful to support decision making process aimed at reducing flood risks and building a stronger communities' resilience.

This aim is achieved by processing available institutional and research-based information to identify areas where a significant flood risk exists. Input data consist of expert-driven or model-based flood hazard maps, high resolution digital elevation models (DEM), census tracts, real-estate market values and construction/reconstruction costs. **BLINKS** returns, for each unit area used in the analysis, the expected number of vulnerable elements potentially exposed as well as the expected degree of direct loss. Concerning the exposure, **BLINKS** provides the number of people potentially exposed and endangered and the number and economic value of different building types (expressed in monetary terms referring to their market values and construction/reconstruction costs). Concerning the expected degree of loss, **BLINKS** provides three hydraulic risk scenarios for three different water height values (< 0.5 m; between 0.5 and 1.0 m; and > 1.0 m) by analyzing the expected level of damage for each functional and structural building component (wiring, hydro-thermo-sanitary system, frames and fixtures, etc.). The analysis can be performed at micro-scale (i.e., the scale of the single affected building as portrayed by a cadastral map) and meso-scale (i.e., spatially census-based aggregate information provided by the Italian National Institute of Statistics).

An overview of the **BLINKS** architecture and the different GIS-based functions embedded will be presented as well as results from an application of **BLINKS** concerning the flood event occurred in the city of Olbia (Sardinia Island, Italy) in November 2013.

Laboratory tests on pyroclastic soil to simulate the infiltration processes responsible of landslide trigger

Versace P., Capparelli G., Spolverino G.* & Galasso L.

Dipartimento di Ingegneria Informatica, Modellistica, Elettronica e Sistemistica, Università della Calabria.

Corresponding email: g.spolverino@dimes.unical.it

Keywords: flume test, landslides, physical model.

We propose some tests performed with the physical slope scaled-model. The model consists of two connected channels of 1 meter wide and 3 meters in length each. It is well equipped by many sensors as tensiometers, pressure transducers, TDRs and laser-displacement transducers. Furthermore, the physical model is equipped with a PIV scan device, with high-resolution cameras to determine surface displacement fields and with a remote controlled rainfall system. Some experimental tests were conducted, using pyroclastic soil from Sarno area (Southern Italy - near the volcano Vesuvio), affected by landslide events on 5 May 1998. In particular, tests considering both homogeneous volcanic ash and stratified deposits of ash and pumice were carried out, during which we have observed water infiltration processes and failure processes characteristics and highlighted the role of pumice layers in the instability occurrences.

People's vulnerability to floods: the EVIL model

Versace P.*, Capparelli G., Biondi D., Cruscomagno F., Vacha D. & Galasso L.

Dipartimento di Ingegneria Informatica, Modellistica, Elettronica e Sistemistica, Università della Calabria.

Corresponding email: g.spolverino@dimes.unical.it

Keywords: EVIL model, People's vulnerability, floods.

Estimating the vulnerability of the exposed elements (human lives, economic assets, properties, infrastructures) to natural hazards like floods, is essential in quantitative risk analysis that aims to represent the expected damage over a certain area as a combination of hazard, vulnerability and exposure. Moreover, the European Flood directive 2007/60/CE considers hydraulic risk maps as fundamental tools for land use and emergency planning. Nevertheless, very often, the vulnerability component is neglected by implicitly attributing the maximum value equal to 1, i.e. considering only the exposure and the frequency of the events in the estimation of flow effects on a target.

The mentioned simplifications should not be applied to maps for flood emergency plans that, instead, must highlight endangered areas where the vulnerability of people is greater and therefore require greater timeliness of interventions.

The EVIL (Evaluation of Vulnerability to Inundations and Landslides) model, developed by CAMILab of the University of Calabria, is aimed at estimating the individual vulnerability index IVI (Individual Vulnerability Index). Only floods will be considered here. EVIL requires the identification of some basic elements: 1) a flood event scenario, which defines the extent of the floodplains, the time-space evolution of the main hydraulic quantities (as water depth and velocity); 2) the spatial scale of the objects - buildings, blocks, districts, streets, railways, etc.- to be analyzed, i.e. the minimum territorial elements at risk for which IVI is estimated; 3) factors F_i that concur to determine the vulnerability of a person in each object; 4) attributes to be used to assign a value to the factors.

Specifically, depending on the object being investigated, IVI is based on different sets of factors related to flood scenario, socioeconomic, demographic and built environment characteristics that are considered to influence individual vulnerability during extreme flooding.

IVI is, thus, estimated as

$$IVI = \sum_i \alpha_i F_i W_i \quad (1)$$

where W_i is the weight attributed to the i -th factor F_i .

Each factor is calculated as the weighted sum of its attributes A_{ij} ($j = 1, \dots, n_i$):

$$F_i = \sum_j \alpha_{ij} A_{ij} w_{ij} \quad (2)$$

IVI is comprised between 0 and 1, and this leads to factor and attribute values being classified between 0 and 1. Weights are positive and their sum must be equal to one 1.

For instance, to estimate the factor related to "individual characteristics" attributes like "age", "disability", "non-Italian speaking", "rate of awareness" are considered suitable.

For each object, the number of people potentially damaged as a consequence of the flood scenario is estimated by multiplying the estimated IVI by a coefficient N_p which represents a crowding index, i.e. the average number of people in that object.

In order to assess the feasibility of the proposed model, EVIL has been tested on several case studies. The outlet of the Esaro River in Calabria, running through the city of Crotona, was selected for this research. The investigated area comprises 6797 objects and the population is estimated at about 170000.

S26

**Approaches for evaluation and protection of groundwater
resources**

CONVENERS AND CHAIRPERSONS

Daniela Ducci (Università di Napoli)

Emma Petrella (Università di Parma)

Stefania Stevenazzi (Università di Milano)

Natural polluted waters in Calabria Region (Italy): preliminary data on arsenic contamination and treatment

Apollaro C.*¹, Fuoco I.¹, De Rosa R.¹, Vespasiano G.¹, Gabriele B.³, Mancuso R.³, Criscuoli A.² & Figoli A.²

¹ DiBEST – University of Calabria, Arcavacata di Rende (CS) Italy.

² Institute on Membrane Technology (ITM-CNR), Arcavacata di Rende (CS) Italy.

³ LISOC Group, Department of Chemistry and Chemical Tecnologie, University of Calabria, Arcavacata di Rende (CS), Italy.

Corresponding email: apollaro@unical.it

Keywords: contaminated waters, arsenic, nanofiltration membranes treating.

In the water systems, potentially harmful elements such as arsenic (As), can reach high concentrations, becoming extremely dangerous for environment and human health. To limit the proved negative effects on the human health of this element, the World Health Organization (WHO, 2001) has set the drinking water guideline values of As to 10 µg/L. The abundance of dangerous elements in water systems mainly depends on their availability into bedrocks and on geochemical conditions during water-rock interaction process. In water systems, As can occur mainly as oxyanions of trivalent (As³⁺) and pentavalent (As⁵⁺) inorganic forms (Smedley & Kinniburgh, 2002) as the result of water-arsenic minerals interaction. These minerals are mainly sulphides: arsenopyrite (FeAsS), orpiment (As₂S₃), realgar (As₂S₂) and arsenian (As-rich) pyrite (Fe(As,S)₂). In this regard, a thorough bibliographic research has been performed to create a database of all the waters of Calabria Region and some anomalies have been identified. In response to these preliminary data it was planned a geochemical prospection in the areas where anomalies were found and many springs, river waters and wells were sampled and analyzed.

New data have shown high concentration of As in the southern Sila Massif where Hercynian and pre-Hercynian gneiss, granite and metapelite belonging to Calabride complex, outcrop.

Subsequently, preliminary tests of treatment on As contaminated groundwater were performed using membranes technology (Figoli et al., 2016). Four types of membrane modules named HL (polyamide), DK (proprietary thin-film), CK (cellulose acetate) and NP030P (polyethersulfone) were used through a nanofiltration (NF) laboratory pilot unit.

The results have shown that all the membranes, except NP030P, are able to reject As very well and As concentrations after the treatment were below 10 µg/L (WHO limit). The application of this technique could allow the use of water resource in the studied contaminated area.

The work has been supported by the project “AsSe” n. CUP: J28I17000030006, cofunded by Fondo FESR POR Calabria FESR FSE 2014-2020-Azione 1.2.2.

Figoli A., Hoinkis J., Bundschuh J. (eds.) (2016) - Membrane Technology for Water Treatment, Removal of toxic trace elements with emphasis on arsenic, fluoride and uranium, CRC Press.

Smedley P.L. & Kinniburgh D.G. (2002) - A Review of the Source, Behaviour and Distribution of Arsenic in Natural Waters. Appl. Geochem., 17, 517-568.

World Health Organization (2001) - Guideline for drinking-water quality: Arsenic in drinking water. Fact Sheet No. 210.

3-Dimensional geological reconstruction of the Maltese archipelago geology as a tool for a better understanding on the main Maltese groundwater bodies

Barbagli A.*¹, Guastaldi E.¹⁻²⁻³, Giannuzzi M.¹, Borsi I.⁴, Lotti F.⁴, Basile P.⁵, Schembri M.⁶ & Sapiano M.⁶

¹ Centro di Geotecnologie - Università di Siena.

² CGT SpinOff Srl.

³ GeoExplorer Srl.

⁴ Tea Sistemi SpA.

⁵ STEAM Srl.

⁶ EWA - Energy and Water Agency - Malta.

Corresponding email: barbagli@cgt-spinoff.it

Keywords: 3D geological model, aquifer geometry, Malta groundwater bodies.

Represent the real world in a numerical groundwater flow model is always a challenging experience, starting from the solid data input (eg. aquifer geometries and properties) to the analysis of the results.

In this case studies, we are going to focus on how prepare the aquifer geometry input for a numerical model by presenting a geological 3D model realized on a regional level and including the main island of the Maltese archipelago (Malta, Gozo and Comino) used as a tool for a better understanding the Maltese main groundwater bodies geometries and properties. The implementation of the geological model started from the existing official geological map (Oil Exploration Directorate, Office of the Prime Minister, Malta, 1993) by realizing 23 geological cross-sections drawn according to the main geological features in order to intercept all the main structural features and crossing through Comino and all the archipelago main islands. The geological cross-sections were then overlapped with the a spatially referenced profile (extracted by the intersection of the DEM and the cross-section profiles) and digitalized on CAD to reconstruct the geological boundaries of each formation and members (as identified by Pedley et al., 1976; and Pedley et al., 1978) on a 3D georeferenced space. The outcrops boundaries were also use by selecting the real formational boundaries and projecting them in a 3D space by draping them on the DEM. All the 3D georeferenced polylines obtained were transformed in points (with a density of 10 m) and merged with borehole stratigraphic data, collected from various sources (national Maltese boreholes database and reports, shared by the Energy and Water Authority of Malta) and previously screened in order to detect the reliable data and discard the data presenting inconsistencies within the boreholes data itself or with the geological map. Since the complex geological structure of the Maltese archipelago, characterized by a dense net of faults (oriented SW-NE) and a subsequent horst and graben structure, to interpolate the surfaces representing the geological boundaries a “spline with barrier” was selected as interpolator, with the barrier are representing the main faults.

As a final result, the 3d model was used to generate input surfaces for numerical models of the studied aquifers and obtain a mode detailed quantification of stored groundwater resource for each of the main groundwater bodies.

Oil Exploration Directorate, Office of the Prime Minister (1993) - Geological Map of the Maltese Islands: Sheet 1- Malta; Sheet 2 - Gozo and Comino.

Pedley H.M., House M.R. & Waugh B. (1976) - The Geology of Malta and Gozo. Proc. Geol. Ass., 87(3),325-341.

Pedley H.M., House M.R. & Waugh B. (1978) - The geology of the Pelagian block: the Maltese Islands. In Nairn A.E.M., Kanes W.H. & Stehli F.G. (eds.): The ocean basins and margins - 4B, the Western Mediterranean. Plenum Press, New York: 417-433.

A new thermal model of the shallow aquifer by statistical temperature distribution in the Piedmont Po Plain (NW Italy)

Barbero D.^{*1}, Bucci A.², De Luca D.A.³, Forno M.G.³ & Lasagna M.³

¹ Studio Geologico, Geotecnico e Geofisico Dott. Diego Barbero, San Martino Alfieri (AT).

² Geodata Engineering S.p.A., Turin.

³ Department of Earth Sciences, University of Turin.

Corresponding email: diego-barbero@libero.it

Keywords: statistical temperature distribution, underground thermal model, Piedmont Po Plain.

Various conceptual models are available about heat transfer in the shallow subsurface depending on the geological contexts. These models are supported by analytical solutions in order to determine the hydro-physical and thermodynamic parameters of the aquifers.

This study of underground thermal data was conducted by means of aquifer thermal profiles, derived from temperature data collection in boreholes, and allowed to perform a new conceptual thermal model of the shallow aquifer of the Piedmont Po Plain (NW Italy). Boreholes exclusively cross the Quaternary fluvial and outwash deposits. These sediments, consisting of cross bedded coarse gravel and sand with subordinate silty-clayey intercalations, host a shallow aquifer with thickness of 20 up to 50 meters and high hydraulic conductivity ($k=10^{-4}$ - 10^{-3} m s⁻¹).

Experimental evidence suggests the presence of two different thermal zones with different features that can be distinguished in aquifer by typical temperature profiles. Starting from ground level up to generally 25 meters, temperature is strongly influenced by the air temperature fluctuation with amplitude decreasing with depth: this depth range is here identified as “*heterothermic zone*”. Below this depth and up to 50 meters b.g.l., the temperature profiles commonly show a constant temperature, suggesting that the temperature is uniform in space and constant in time; this depth range detects the “*homoeothermic zone*”. The depth separating the *heterothermic and homoeothermic zones* is defined as “*homoeothermic depth*”.

The analysis of thermal logs recorded in deep boreholes shows that temperature increases with depth according to the local geothermal gradient at depth higher than 50 m from ground level.

Finally, solutions of heat diffusion equation were developed to describe the time-averaged distribution of the temperature in the Piedmont Po Plain, providing a statistical evaluation with an uncertainty of $\pm 1.00^\circ\text{C}$ of the expected value of the groundwater temperature at different depths in the “*heterothermic zone*”. For greater depths (>25 meters b.g.l.), solutions are compatible with a constant value of temperature according to the presence of the “*homoeothermic depth*”.

In conclusion, the experimental methodology proposed can be useful for preliminary investigations for the exploitation of subsoil by means of low enthalpy geothermal systems.

Thermal data as a tool for groundwater flow velocity determination in aquifer recharge areas

Barbero D.*¹, Bucci A.², De Luca D.A.³, Forno M.G.³ & Lasagna M.³

¹ Studio Geologico, Geotecnico e Geofisico Dott. Diego Barbero, San Martino Alfieri (AT).

² Geodata Engineering S.p.A., Turin.

³ Department of Earth Sciences, University of Turin.

Corresponding email: diego-barbero@libero.it

Keywords: Temperature profiles, Aquifer recharge areas, Groundwater flow velocity.

The groundwater flow velocity is a significant parameter to estimate the time of recharge of deep aquifers for drinking water supply. In recharge areas, temperature profiles measured along the water column in boreholes show a typical pattern: concave upward, because the seepage of cooler water causes an anomalous low gradient, and elongated in depth, because of the downward flow of cooler water.

The Turin Town drinking water (in the western Piedmont Po Plain) is essentially supplied by the fluvial sediments forming the wide Alpine fans. The Lanzo Fan, comprised in the recharge area, is a terraced alluvial fan, with an extension of about 300 km², drained by the Stura di Lanzo River. Groundwater flow is directed from the recharge area to the final receptor, represented by the Po River. The piezometric surface of the shallow aquifer, that follows the topographic surface, shows hydraulic gradient varying from 1%, in the proximity of the apex of the fan, to 0.1%, in the distal areas.

This research, in order to estimate the groundwater vertical velocity of the aquifer, was conducted by: a) the development of a geo-hydrogeological and physical model of heat transfer in a porous media of the Lanzo Fan aquifer through a particular solution of heat transport equation by conduction and advection, with stationary boundary conditions; b) the collection of temperature data in boreholes; c) the selection of temperature profiles showing the typical recharge areas pattern; d) the processing of temperature data with a statistical analysis in order to determine the groundwater vertical velocity.

The depth of the boreholes used in this study ranges between 30 and 50 meters. The measures were obtained by the use of probes equipped with sensors of temperature and depth, with an accuracy of $\pm 0.2^\circ\text{C}$ and a resolution of 0.1°C for temperature.

The temperature profiles show a common trend characterized, in the first meters of depth, by temperature fluctuations linked to seasonal oscillations. Below this zone the profiles become concave with a gradually higher radius of curvature due to the aquifer supply. The application of statistical analysis on temperature dataset, according to the physical model developed, returns a vertical velocity of about $10^{-9} \text{ m}\cdot\text{s}^{-1}$.

Geophysical and hydrological model of “Barcellona-Milazzo plain” groundwater body

Capizzi P.*^{1,2}, Martorana R.¹, Favara R.², Albano L.², Bonfardeci A.², Costa N.² & Gagliano A.L.²

¹ Istituto Nazionale di Geofisica e Vulcanologia, Palermo.

² DiSTeM department, University of Palermo.

Corresponding email: patrizia.capizzi76@gmail.com

Keywords: groundwater body, geophysical surveys.

The “Barcellona-Milazzo plain” groundwater body in the northern Sicily, was analysed in detail, through numerous geophysical measurements that were integrated with stratigraphic data in order to reconstruct the hydrological model.

The “Barcellona-Milazzo plain” (BMP) groundwater body has been identified within the coastal sector between the village of Oliveri, to the west, and Capo Rasocolmo, to the east. It also includes several rivers that rise further south in correspondence with the Peloritani ridge and flow into the wide Barcellona-Milazzo alluvial plain.

On the basis of several geophysical and geological data analysis and interpretation have been used to reconstruct the composition and thickness of the marine and alluvial deposits to construct the conceptual model of groundwater circulation in the Barcellona-Milazzo plain.

For the reconstruction of the subsurface model of the water body, 466 vertical electric surveys and 72 refraction seismic sections acquired in the 70s and 80s (CASMEZ surveys reports) have been reprocessed and reinterpreted. These data have been integrated with 50 HVSR surveys and 85 geognostic boreholes.

All collected vertical electrical surveys (VES) were inverted using the ZondIP1D software. The inversions were performed trying to limit the lateral heterogeneities and using bore-hole stratigraphic data as constraints, where possible. The 1D inverse models of electrical resistivity were interpolated, using the Voxler software (Golden Software), to obtain a 3D representations of electrical resistivity, limited above by the D.E.M. of the investigated zone and inferiorly by the depth of investigation reached. In the areas characterized by almost regular geological trends, a 1.5D inversion algorithm was used, in which the deepest layer the subsurface section is considered almost-horizontal, while the top part of the section admits more sharp lateral variations. Finally, the geological interpretation of each VES, joined to HVSR and refraction seismic sections have been integrated with 85 stratigraphic boreholes to obtain the two-dimensional maps depth of the most important stratigraphic levels. In particular, the surface of the floods in contact with the clayey substrate has been reconstructed, which delimits in depth the groundwater body. This allowed us to have an estimate of the volume of the water body equal to $1.13 \cdot 10^{10} \text{ m}^3$ and to calculate the hydrological model using MODFLOW software.

The role of snow melting and rainfall on the discharge and physico-chemical characteristics of springs: a statistical analysis in Central Apennines

Chiaudani A.¹, Di Curzio D.¹ & Rusi S.*¹

¹ Dipartimento InGeo Università “d’Annunzio” Chieti-Pescara.

Corresponding email: sergio.rusi@unich.it

Keywords: groundwater, multiparameter time-series, snow melt.

In this study, the statistical relations between meteorological recharge and hydrodynamic and hydrochemical behavior of the Verde spring, the main discharge of the Majella Carbonate aquifer system (central Apennine) exploited for drinking and hydroelectric purposes, were synthesized.

The results allowed to identify several flow paths, characterized by different sizes, hydraulic conductivities, and distances from the spring, that get activated depending on the type (rain or snowmelt) and the amount of the inflow.

In order to get a deeper insight on the Majella system groundwater flow, multiparameter daily time-series were considered, all related to the same time period (1803 days; about 5 years between 1997 and 2002) and collected in different monitoring point all over the Majella aquifer. In detail, they were analyzed: the snow cover thickness, the rainfall data, the Verde spring discharge, the electrical conductivity and temperature of the Verde spring.

The raw and residual multiparameter time-series were then analyzed by the Autocorrelation Function (ACF) and Cross-Correlation Function (CCF), to investigate how the spring parameters react to the different inflows.

The results obtained by the ACF and the raw and residual CCFs, together with the knowledge of the hydrogeological features of the Majella aquifer, allowed to implement a refined conceptual model.

The Autocorrelation analysis showed that the variability of the spring discharge and Electrical conductivity time-series can be accounted by the combined effect of both rainfall (i.e. random component) and snowmelt (i.e. systematic component) recharge.

The results obtained clearly demonstrated that the snowmelt contribution is predominant with respect to the rainfall one. The travel times in the unsaturated and saturated zones of the water moving toward the Verde spring and the aquifer recharge modes depend on the different inflows (i.e. snowmelt and rainfall), their distribution in the recharge areas, their intensity and distribution in time. In detail, the multiparameter time-series analyses allowed to identify several recharge modes related to different flow paths, that are characterized by different sizes, hydraulic conductivities and distances from the spring, in both the unsaturated and saturated zones.

The level of detail obtained by the multiparameter time-series analyses is high, although below the one provided by tracer tests. In fact, this methodological approach allowed to account for small changes in the spring parameters, such as the electrical conductivity (about ± 15 mS/cm) and temperature (about $\pm 0.1^\circ$ C), that are considered meaningless.

The study demonstrated that the multiparameter hydrodynamic and hydrochemical time-series analyses, related to heterogenous fractured and/or partially karst aquifer systems, can provide more detailed information about the groundwater flow and the recharge modes, without using tracer tests.

The well fields of the Maggiore e Tifata mountains (Campania Region): new hydrochemical and isotopic data

Corniello A.¹, Del Gaudio E.², Ducci D.*¹ & Stellato L.³

¹ Department of Civil, Architectural and Environmental Engineering, DICEA. Università degli Studi di Napoli Federico II, Naples, Italy.

² Interdepartmental Center for Environmental Research - C.I.R.A.M. Università degli Studi di Napoli Federico II, Naples, Italy.

³ Center for Isotopic Research on Culturale and Environmental heritage - CIRCE. Università Luigi Vanvitelli, Caserta, Italy.

Corresponding email: daniela@unina.it

Keywords: groundwater resources, hydrogeochemistry, isotopic composition of groundwater.

The groundwater exploitation imposes a deep knowledge of the characteristics of the aquifers and of the possible relationships between groundwater and surface waters, also considering the probability of an over-exploitation of the groundwater resources.

The area of the study concerns the wide valley crossed by the Volturno River located in southern Italy. In the northern sector, the valley is bounded by carbonate slopes of the Maggiore Mountain and of the Tifata Mountain (to the south). The tectonic relationships between the Maggiore Mountain and the Tifata Mountain are very complex and not yet completely defined. In the valley, at the base of the carbonate slopes, pyroclastic deposits are associated to alluvial deposits linked to the Volturno's expansions. These sediments form the shallow aquifer of the valley; on the contrary, the main aquifer of the plain corresponds to the carbonate substratum, found at variable depth below the alluvial-pyroclastic deposits.

Along the southern sector of the valley, quite close to the river and at the base of the Tifata Mountain, there are two well fields ($Q_{tot} \approx 37 \times 10^6 \text{ m}^3/\text{y}$); another well field (with 20 wells) is located at the foot of the Maggiore Mountain ($Q_{tot} \approx 31 \times 10^6 \text{ m}^3/\text{y}$).

A Mediterranean rainfall regime characterizes this area with a single maximum in winter (November) and a dry summer (August). The average rainfall is about 1200 mm/y. The temperature in the valley ranges from 9°C in January to 25°C in July, while on the mountains ranges from 3°C in winter to 20°C in summer.

The interpretation of the groundwater flowpath in the valley and of the chemical and isotopic (D, ¹⁸O) characteristics of the Volturno River and of the groundwater tapped by wells allowed a better understanding of the relationships between the carbonate groundwater bodies of the Maggiore and Tifata mountains and between these groundwater resources and the Volturno River.

Rare earth element speciation in volcanic groundwater: the Mount Vulture aquifer (Southern Italy)

Deluca F.*¹, Mongelli G.¹, Paternoster M.¹, Sinisi R.¹ & Zhu Y.²

¹ Dipartimento di Scienze, Università degli Studi della Basilicata.

² National Metrology Institute of Japan (NMIJ), National Institute of Advanced Industrial Science and Technology (AIST), Tsukuba, Japan.

Corresponding email: ferdinando.deluca@unibas.it

Keywords: REEs, speciation, groundwater.

The distribution of Rare Earth Elements (REEs) in the aquatic environment has gained growing attention, also as a consequence to the improvement of analysis accuracy, due to its capability to unroof water-rock interactions, water physico-chemical conditions, and groundwater flow paths and mixing (e.g. Munemoto et al., 2015, Liu et al., 2016). Here, we report for the first time the REEs' concentration in groundwater of the Mt. Vulture volcanic aquifer. Mt. Vulture is a Pleistocene composite volcano located at the easternmost border of the Apennine compressive front whose aquifer core is mainly composed of pyroclastics and subordinate lava flow of different permeability, which give rise to distinct aquifer layers. The collected water samples were cold and slightly acidic with electrical conductivity (EC) that varies over a wide range of value. The water samples, due to the high variability of some physical-chemical parameters, can be divided into a high salinity subset (HSS, EC > 800 $\mu\text{s}/\text{cm}$) with low Eh values and a low salinity subset (LSS, EC < 800 $\mu\text{s}/\text{cm}$) characterized by higher Eh values. The concentration of dissolved REEs in groundwater shows a slightly positive correlation with water temperature and a slightly negative correlation with the dissolved oxygen (DO); relationships with EC, pH and Eh are not observed. Further, in the $\log a\text{SiO}_{2(\text{aq})}$ vs $\log a(\text{Na}^+/\text{H}^+)$ activity diagram the most of the samples are in equilibrium with kaolinite although some HSS samples, due to higher Na contents, fall in the stability field of a 2:1 clay mineral. As for the REEs, the HSS Post-Archean Australian Shales normalized patterns generally show LREE/HREE fractionation and moderate Ce_N^* and Eu_N^* anomaly whereas the LSS is characterized by minor LREE/HREE fractionation and relevant Eu_N^* anomaly. In both the subsets the dominant aqueous specie is generally LnCO_3^+ although, in some samples, dissolved LREE can exist as the free ion Ln_3^+ and, subordinately, as LnSO_4^+ . This likely suggests that REEs form progressively stronger carbonate complexes with increasing atomic number which, in turn, accounts for the MREE and HREE increase relatively to LREE as a function of pH and/or carbonate ion activity (Noack et al., 2014, and references therein).

Liu H., Guo H., Xing L., Zhan Y., Li F., Shao J., Liang X., Li C. & Niu H. (2016) - Geochemical behaviors of rare earth elements in groundwater along a Low path in the North China Plain. *Journal of Asian Earth Sciences*, 117, 33-51.

Munemoto T., Ohmori K. & Iwatsuki T. (2015) - Rare earth elements (REE) in deep groundwater from granite and fracture-filling calcite in the Tono area, central Japan: Prediction of REE fractionation in paleo- to present-day groundwater. *Chemical Geology*, 417, 58-67.

Noack C.W., Dzombak D.A. & Karamalidis A.K. (2014) -Rare Earth Element Distributions and Trends in Natural Waters with a Focus on Groundwater, *Environmental Science and Technology*, 48, 4317-4326.

Stationary and non-stationary geostatistics to model 3-D hydraulic conductivity distribution: a case study in the southern Po river plain

Di Curzio D.*¹ & Rusi S.¹

¹ Dipartimento di Ingegneria e Geologia (InGeo), Università degli Studi “G. d’Annunzio” di Chieti-Pescara.

Corresponding email: diego.dicurzio@unich.it

Keywords: hydraulic conductivity, geostatistics, groundwater.

Groundwater numerical modeling has become one of the most important up-to-date water resource management tools because it allows reproducing the aquifer behavior, that is vital in sustainable water resource exploitation, contamination fate assessment, and remediation scheme design and efficiency evaluation. During numerical model implementation, besides the hydrogeological boundary conditions, the hydraulic conductivity (K) of the considered aquifer is a key parameter to be defined. In general, this parameter is assigned to each hydrogeological complex, relying on values obtained by point permeability tests (e.g. pumping tests, slug tests, etc.). Although the obtained experimental K values could be representative of a portion of the whole aquifer volume, its intrinsic heterogeneities cannot be detected, especially when the considered aquifer is very complex (Bianchi & Pedretti, 2017).

For this reason, the main objective of the research is to draw a physically based 3-D hydraulic conductivity model by both stationary (i.e. Ordinary Kriging, OK) and non-stationary (Intrinsic Random Function theory, IRF-k) geostatistical methods, applying these techniques to 182 Cone Penetration Test (CPT) profiles of the tip (q_c) and shaft (f_s) resistances, collected by the Emilia Romagna Regional Geological Survey. The obtained 3-D q_c and f_s models were combined by equations present in literature (Robertson, 1990; Lunne et al., 1997) to obtain the lithology index (Ic) and the K models.

The selected study area is in the southern part of the Po plain and is characterized by mainly alluvial deposits made up of undifferentiated fine silty-sandy deposits, with coarser (i.e. sandy gravelly alluvial fans and sandy paleo-channels) and finer (i.e. silty clayey lacustrine lenses) geological inclusions.

As a result, the OK and IRF-k method allowed to estimate the K values in a 3-D model, starting from CPT data. The obtained models reproduce as closely as possible the actual geological and hydrogeological features, not neglecting the multi-scale heterogeneity. The proposed methodological approach provides a detailed physically based 3-D hydraulic conductivity model. The obtained 3-D K model can represent a useful starting point for hydrogeological numerical modeling and/or a constraint for model calibration, especially when the intrinsic deposit heterogeneity could affect substantially the groundwater flow and contaminant transport in the aquifer.

Bianchi M. & Pedretti D. (2017) - Geological entropy and solute transport in heterogeneous porous media. *Water Resources Research*, 53, 4691-4708.

Lunne T., Robertson P.K. & Powell J.J.M. (1997) - *Cone Penetration Testing in Geotechnical Practice*, Blackie Academic, EF Spon/Routledge Publication, New York.

Robertson P.K. (1990) - Soil classification using the cone penetration test. *Canadian Geotechnical Journal*, 27(1), 151-158.

A Modified AVI Model to Map Groundwater Vulnerability to Contamination: case studies in Southern Italy

Ducci D.* & Sellerino M.

Department of Civil, Architectural and Environmental Engineering, Università degli Studi di Napoli Federico II,
Naples, Italy.

Corresponding email: daniela@unina.it

Keywords: groundwater contamination vulnerability, AVI method, WFD 2000/60/EC, GIS, Campania, Italy.

The WFD (Water Framework Directive 2000/60/EC), with the aim of protecting groundwater and surface water, is devoted to the achievement of environmental objectives. To meet these objectives, the aquifer vulnerability maps are of crucial significance.

Many methods for assessing groundwater vulnerability maps have been developed in the past four decades, especially using GIS. These maps are planned to recognize areas of highest potential for groundwater contamination, mainly based on the hydrogeological setting. However, if aquifer vulnerability concept is well defined and the methods have been constantly tested and compared, the problem of the choice of the best method, remains. The choice of the method depends on a series of factors, including the scale of the problem, the hydrogeological characteristics of the area and the data availability.

The most widely used groundwater vulnerability mapping method is the DRASTIC empirical model (Aller et al., 1987), based on seven hydrogeological factors. Among the methods, the AVI (Aquifer Vulnerability Index) method (Van Stempvoort et al., 1992) has been the first explicitly promoting the use of GIS. Moreover, it presents the advantage of use only two physical parameters, The AVI Index represents the hydraulic resistance of an aquifer to the vertical flow, as ratio between the thickness of each sedimentary unit above the uppermost aquifer (D, length) and the estimated hydraulic conductivity (K, length/time) of each of these layers. The AVI index has a time dimension and it is divided into five classes in terms of years. In this study for avoiding a widespread and often found presence of the higher vulnerability classes, especially in shallow aquifers, the AVI classification has been modified, also using statistical methods (Bonfanti et al., 2016).

Moreover, the study reports applications of the modified AVI method to three study areas in southern Italy, in porous alluvial aquifers, highlighting the limitations of the method and the differences with the DRASTIC method. The modified AVI method results more reliable for alluvial shallow aquifers when compared with the DRASTIC method.

The final aim of the study is the standardization of the methods, also in order to the WFD application, to permit a worldwide application, not only by researchers but also by environmental technicians.

Aller L., Bennett T., Lehr JH., Petty RJ. & Hackett G. (1987) - DRASTIC: A standardized system for evaluating ground water pollution potential using hydrogeologic settings. US Environmental Protection Agency, Report 600/2-85/018, Washington

Bonfanti M., Ducci D., Masetti M., Sellerino M. & Stevenazzi S. (2016) - Using statistical analyses for improving rating methods for groundwater vulnerability in contamination maps. *Environmental Earth Sciences*, 75(12), 1003.

Van Stempvoort D., Ewert L., Wassenaar L. (1993) - Aquifer vulnerability index (AVI): a GIS compatible method for groundwater vulnerability mapping. *Can. Water Res. J.*, 18, 25-37.

Spatial and statistical analysis of factors influencing groundwater vulnerability on the study area of the Gömör-Torna Karst (Hungary and Slovakia)

Iván V.¹, Masetti M.², Mádl-Szőnyi J.¹, Pollicino L.C.² & Stevenazzi S.*²

¹ Eötvös Loránd University, Department of Geology, Budapest, Hungary.

² Università degli Studi di Milano, Dipartimento di Scienze della Terra “A. Desio”, Milan, Italy.

Corresponding email: stefania.stevenazzi@unimi.it

Keywords: karst spring, statistical method, vulnerability.

The Gömör-Torna Karst (known also as Aggtelek Karst and Slovak Karst) is an unconfined transboundary aquifer located on the border of Hungary and Slovakia. Thanks to its complex natural heritage, which includes surface karst forms, caves and sinkholes, the region is under the protection of the Aggtelek National Park and the Slovak Karst National Park. The aquifer consists of karstified Triassic carbonates, partially covered with Quaternary clayey sediments. The karst springs provide the drinking water for the inhabitants of the area. The high sensitivity of these resources thus requires an effective and accurate protection strategy.

In the past decades, the Gömör-Torna Karst was in the focus of numerous studies, including hydrogeological investigations and local-scale groundwater vulnerability assessments (Iván & Mádl-Szőnyi, 2017). For the significant springs of the area records of long term daily observations (1964-1993) are available (Maucha, 1998). This detailed hydrometeorological database provides an appropriate base for data-driven analysis of the factors influencing groundwater vulnerability.

The Weights of Evidence (WofE) technique is a well-known spatial statistical method successfully applied for mineral exploration, landslide hazard zonation, groundwater productivity potential or vulnerability assessment (Bonham-Carter, 1994). WofE is a method based on the Bayesian conditional probability, which enables observations of the individual role and the combined effect of different geological, geophysical or geochemical features to assess the spatial distribution of a natural phenomenon.

Here, we attempt to apply the WofE technique for: i) the evaluation of factors influencing the spring distribution in the karst area and ii) the assessment of a reliable groundwater vulnerability map. The spatial statistical analysis can provide a reliable support in the evaluation of geological and hydrogeological factors influencing groundwater vulnerability in the karst system.

This result is part of a project that has received funding from the European Union's Horizon 2020 research and innovation programme under grant agreement No 810980.

Bonham-Carter G.F. (1994) - Geographic Information Systems for Geoscientists: modelling with GIS. Pergamon Press, New York.

Iván V. & Mádl-Szőnyi J. (2017) - Vulnerability assessment and its validation: the Gömör-Torna Karst, Hungary and Slovakia: Geological Society, London, Special Publications, 466, 261-273.

Maucha L. (1998) - Az Aggteleki-hegység karszthidrológiai kutatási eredményei és zavartalan hidrológiai adatsorai. 1958–1993 [Results and undisturbed data of karsthydrological researches on Aggtelek Hills]. VITUKI Rt. Hidrológiai kiadványa, 414 [in Hungarian].

Hydrogeological and isotopic characterization of an ophiolite aquifer (Monte Zirone, Northern Apennines, Italy)

Petrella E.*¹, Chiari A.¹, Segadelli S.² & Celico F.¹

¹ Department of Chemical Sciences, Life and Environmental Sustainability, University of Parma, Italy.

² Geological Survey, Emilia-Romagna Region Administration, Bologna, Italy.

Corresponding email: emma.petrella@unipr.it

Keywords: Ophiolite aquifer, Northern Apennines.

The ophiolites are retained as one of the main aquifers within the northern Apennines, but few hydrogeological studies have been carried out worldwide to understand the behaviour of such aquifers. The main aim of this study is to characterize the hydrogeological behaviour of the Mt. Zirone ultramafic massif in the northern Apennines, using hydrogeological and chemical-isotopic investigations.

The investigation were carried out from April 2016 to March 2017. The monitoring net consists in 2 piezometers, 10 springs and 2 rainwater samplers. The hydraulic heads were monitored on an hourly basis and the discharge on a bi-weekly basis. Samples for physico-chemical parameters and for stable isotope analysis were carried out in all monitoring water points on a bi-weekly basis. Major and minor (CrVI) elements and Tritium contents were analysed twice, during low- and high-flow periods.

In Mt. Zirone aquifer, the groundwater flows mainly from SW to NE toward several seasonal springs and only two perennial springs. This two springs are the outflow of two different sub-basins (SB-a and SB-b). The analysis of the hydraulic head fluctuations over time shows a different behaviour: SB-a responds very quickly to the rainfall events, instead SB-b react to the precipitation only when the in the SB-a the groundwater level rise more than 1,5m. Moreover, the SB-a shows a hydraulic gradient (10%) lower than the SB-b (24%), emphasizing also the difference in terms of permeability of the medium. The tritium content shows the same age for the two sub-basins, but the EC and isotopic values shows a very complex groundwater flowpath highlighting a great heterogeneity of the medium. No perched groundwater was found in the case study, differently from another ophiolite aquifer, Mt. Prinzera, located no more than 5km to the north-east from Mt. Zirone. The CrVI concentration is not always negligible and in some cases is higher (9.5µg/l) than the admissible concentration for drinking water ($\leq 5\mu\text{g/l}$, D.L. 152/2006). Its distribution and evolution is quite complex and correlated with infiltration processes.

In conclusion, Mt. Zirone ophiolite aquifer is characterised by a discontinuous heterogeneity that determines a different groundwater flowpath and great variability in terms of groundwater quality. The proposed conceptual model, based on field data, could be of primary interest for managing the groundwater resource of peridotite aquifers.

Infiltration ponds adopted for treated wastewater disposal: a risk-assessment approach in the Apulia region

Portoghese I.*¹, Demichele F.², Fidelibus D.² & Vurro M.¹

¹ Istituto di Ricerca sulle Acque del CNR (CNR-IRSA), Bari, Italy.

² Politecnico di Bari (DICATECh), Bari, Italy.

Corresponding email: ivan.portoghese@cnr.it

Keywords: wastewater infiltration ponds, artificial groundwater recharge, risk assessment.

The lack of rivers and lakes in most of the Apulia region, a karst region of southern Italy, and the forbidden discharge of treated wastewater (TWW) in injection wells and sinkholes occurred 1999 (Decree n.152/99), challenged the local government to find solutions for wastewater disposal for 92 out of 180 existing treatment plants. For these reasons, a treatment upgrade programme was launched, while injection wells and sinkholes were replaced by surface infiltration ponds and trenches mostly dug into limestone and sandstone formations, with unsaturated zone permeability varying from minimal (massive carbonates) to high values. Nowadays 32 surface infiltration facilities are operated with an average discharge per plant of 3000 m³/d and infiltration volume of more than 30 Mm³/yr. Furthermore, effluents from other 60 treatment plants, currently disposed into karst ephemeral streams, mostly infiltrate (with average discharge per plant of 4000 m³/d and infiltration volume of more than 85 Mm³/yr). This indirect groundwater recharge practice, though positive for the quantitative state of highly exploited groundwater bodies, is rising concerns due to potential sanitary and environmental risks.

In such context, water quality and discharge measurement from the treatment plants were considered in combination with local groundwater vulnerability setting. For all TWW infiltration ponds potential benefits and threats of artificial recharge were summarized using two specific indices useful to design more efficient GW monitoring strategies for risk assessment. In particular, the water reuse index, WRI, represents the potential indirect reuse (benefit) of the annual infiltration volumes for crop irrigation, expressed as ratio between annual irrigation demand around the infiltration facility and TWW infiltration volume, while the pollution vulnerability index, PVI, uses the pollution dose concept applied to basic chemical parameters (yearly doses are given multiplying pollutant concentrations by the yearly volumes of infiltrated water). Each dose provides an evaluation of the maximum amount of pollutants to be diluted by the groundwater flow at the local scale. Intrinsic aquifer vulnerability and biodegradation potential of the unsaturated zone are respectively considered in the PVI as maximizing or dampening factors of groundwater pollution risk. Setting aside possible attenuation processes in the vadose and saturated zone, the evaluation of annual chemical doses provide an overall measure of the infiltration pollution load at the local scale. The combined use of the WRI and PVI indices allowed mapping the most critical conditions in the study region in terms of opportunities and potential risks connected to the existing infiltration facilities. A preliminary risk assessment against contamination of drinking water wells was undertaken in the most critical hydrogeological conditions recognized in the study region.

Hydrogeological and isotopic investigation to define the hydrological behaviour of a complex landslide: a case study in the Northern Apennines (Italy)

Raimondo M.*¹, Chelli A.¹, Celico F.¹, Iacumin P.¹ & Petrella E.¹

¹ Department of Chemical Sciences, Life and Environmental Sustainability, University of Parma.

Corresponding email: melinda.raimondo@studenti.unipr.it

Keywords: landslide hydrology, multilevel groundwater-monitoring system, water isotopes.

The aim of this research is to define a specific monitoring system in order to investigate the hydrogeological behaviour of a low permeability heterogeneous medium in a complex landslide. Case Pennetta active landslide is caused by roto-translational slides and complex active earth slides-earth flows and mainly involves sandstones and clays.

Piezometric levels were monitored, over two hydrogeological years, by two multilevel well systems. Discharge and physico-chemical parameters were monitored in several springs and artificial drains to understand the hydrogeological setting and its evolution over time. Mixing processes between groundwater and neo-filtration water were investigated by EC logs performed in the boreholes. In addition, isotopic analyses of $\delta^{18}\text{O}$ and δD were carried out to define the recharge areas, and ^3H analyses allowed to investigate the mean transit times.

Results showed the coexistence of different flowpaths within the saturated zones at the slope scale. A shallow one, rapid and reactive to the rainfall regime is characterized by fast circuit, that shows EC values of less than 1000 $\mu\text{S}/\text{cm}$ in high flow and up to 3700 $\mu\text{S}/\text{cm}$ in depletion phase, according to local infiltration processes. The isotopic values also show a great variability over time ($\delta^{18}\text{O}$: $-7,86 \div -6,95\text{‰}$) and this variation is also observed in artificial drains and springs, according to a very shallow flowpaths. ^3H content values are indicative of a mixture between sub-modern and neo-infiltration water (mean value 2,95 UT).

Due to the heterogeneity of the medium, a deep, local and more conductive flowpaths were found. This circuit shows smoother hydrograph, higher EC values (from 2500 up to 4200 $\mu\text{S}/\text{cm}$ without any influence by depletion/recharge phases) and more depleted isotope values with less variation. ^3H content values underlines long transit times (mean value 0,34 UT).

The monitoring system developed in this study allowed a better understanding of the hydrogeological behaviour in this type of movement, where the heterogeneity of the material involved influences the groundwater dynamics.

Evidences of diffuse water and nitrate input via river-groundwater interactions in a regulated river: flood irrigation as main driver?

Severini E.*¹, Pinardi M.², Racchetti E.¹, Celico F.¹ & Bartoli M.¹

¹ Department. of Chemistry, Life Sciences and Environmental Sustainability, University of Parma ² IREA - CNR Milan.

Corresponding email: edoardo.severini@unipr.it

Keywords: river-groundwater interactions, nitrate, irrigation.

Total N inputs to agro-ecosystems of the Mincio basin are estimated in over 26,000 t N in 2000, composed mainly of manure spreading (42% of total, increased to 56% in 2010) and synthetic fertilizers (32% of the total, decreased to 18% in 2010). Such inputs largely exceed outputs, resulting in excess N in the cultivated soil (Pinardi et al., 2018). In the Mincio river catchment, the main type of irrigation is flood irrigation, that mobilizes large water volume and soluble compounds as nitrate. Soil N excess and flood irrigation are likely drivers of high NO₃⁻ concentrations measured in surface- and ground-water. Nitrate represents on average 95% of the dissolved nitrogen forms and 75% of TN in the Mincio River. The ARPA dataset showed that NO₃⁻ concentrations in the Mincio river increase from Peschiera del Garda (0.31 mg L⁻¹) to Goito (7.97 mg L⁻¹), whereas they tend to decrease downstream the Mantua Lakes. Nitrate increase in the upstream sector exceeds expected outcomes from river modelling (nitrification) and suggests diffuse input from the watershed (Pinardi et al., 2018).

Preliminary results suggest river-groundwater interaction in the central-norther sector of the river and we expect this interaction to vary seasonally and to be regulated by irrigation. During summer, the steep increase of nitrates concentrations in upstream reaches of the Mincio river, supports the hypothesis of groundwater to river nitrate exchange. The underlying mechanisms seems driven by the *irrigation loop*: flooding permeable soils causes percolation of nitrate-rich waters, which feed shallow groundwater and supply the riverbed.

Pinardi M., Soana E., Laini A., Bresciani M. & Bartoli M. (2018) - Soil system budgets of N, Si and P in an agricultural irrigated watershed: surplus, differential export and underlying mechanisms. *Biogeochemistry*, 140, 175-197.

Multi-disciplinary study to characterize groundwater flow processes and quality in an agriculture impacted volcanic-sedimentary coastal aquifer in the archaeological site of Cumae (Phlegraean Fields, southern Italy)

Stellato L.*¹, Allocca V.², Arienzo M.³, Coda S.², De Vita P.², Di Rienzo B.¹, D'Onofrio A.¹, Ferrara L.³, Marzaioli F.¹ & Trifuoggi M.³

¹ Centre for Isotopic Research on Cultural and Environmental Heritage(CIRCE), Dipartimento di Matematica e Fisica, Università degli Studi della Campania Luigi Vanvitelli, Caserta.

² Dipartimento di Scienze della Terra, dell' Ambiente e delle Risorse, Università degli Studi di Napoli Federico II, Napoli.

³ Dipartimento di Scienze Chimiche, Università degli Studi di Napoli Federico II, Napoli.

Corresponding email: luisa.stellato@unicampania.it

Keywords: sedimentary coastal aquifer, isotopic methodologies, archaeological site.

The Cumae archaeological site extends for about 3.0 km² along the Tyrrhenian coast of the southern Italy, north-west of the active volcanic system of Phlegraean Fields, about 20 km north of Naples bay. The coastal plain of the *Cumae* archaeological site is an area of relevant environmental and archaeological interest. The ancient city of *Cumae*, in the Naples Province, was the first Greek colony, named Kyme, founded in mainland southern Italy along the Tyrrhenian coast in the 730 B.C., and remained continuously occupied until the 1207 A.D. During the Holocene epoch the coastal plain has changed significantly, due to endogenous and exogenous phenomena, such as volcanic eruption, bradyseismic crises, eustatic sea-level variations, shoreline changes and formation of lake environments and palustrine wetlands. As a result of these natural processes, the coastal plain is characterized by a complex volcanic-sedimentary sequence formed by sands, silts, silty clays and volcanoclastic sediments, resting on a substrate of yellow tuff and trachytic lavas, outcropping in the surrounding reliefs.

Land use of this coastal area is mainly characterized by intensive irrigated agriculture, with use of pesticide and organic fertilizers.

In the last years, the coastal plain of the *Cumae* archaeological site is affected by rising of groundwater, causing groundwater flooding phenomena of several archaeological artefacts and a sharp slowdown of archaeological researches.

This paper documents a well-designed hydrological, hydrogeological, chemical and isotopic monitoring program carried out for the first time in an experimental site within the coastal plain of the *Cumae* archaeological site, having an extension of approximately 1 km², during the period from December 2013 to February 2015 in thirteen domestic and agricultural wells (six shallow, up to 15 m, and 7 deep wells, up to 80 m) on a monthly basis.

Based on a detailed stratigraphic model of the study area, multidisciplinary investigations (hydrological monitoring, piezometric measurements, field parameters determinations, isotopic and hydrochemical water analyses) were conducted to characterise: i) groundwater flow and quality, ii) natural and anthropogenic processes affecting the hydrochemical and isotopic composition of groundwater in the coastal volcanic-sedimentary aquifer, iii) and spatial and temporal variations of the contamination sources by anthropic activities of the coastal aquifer in order to collect information to prevent the damage of archaeological artefacts and buildings by salinized groundwater.

Groundwater samples were analysed to characterize physico-chemical, hydrochemical and isotopic parameters: temperature, pH, electrical conductivity, total dissolved solids, major ions and trace elements, $\delta^{18}\text{O}$, $\delta^2\text{H}$, ^{222}Rn , $\delta^{15}\text{N-NO}_3$, $\delta^{18}\text{O-NO}_3$ and $\delta^{11}\text{B}$.

Hydrostratigraphic data and piezometric monitoring confirm the presence of a multi-layered coastal aquifer, whereas all the hydrochemical and isotopic observations show that the groundwater quality is affected mainly by: i) aquifer lithologies and localised rise of deep magmatic fluids highly mineralized, ii) freshwater-saltwater interactions (induced by groundwater pumping), and iii) contamination from non-point agricultural sources.

Hydrogeochemical, isotopic and geological characterization of the thermal areas in the Calabria region

Vespasiano G.^{1,2}, Apollaro C.¹, Muto F.¹, Tripodi V.¹, Fuoco I.*¹, Dotsika E.³ & De Rosa R.¹

¹ Dept. of Biology, Ecology and Earth Sciences (DIBEST), University of Calabria, Arcavacata di Rende, CS, Italy.

² EalCUBO (Environment, Earth, Engineering) start-up soc. Coop., Italy.

³ National Center for Scientific Research “Demokritos”, Athens, Greece.

Corresponding email: ilaria.fuoco@unical.it

Keywords: thermal areas, geothermometric functions, isotopic analysis.

The thermal springs of the Calabria region (Southern Italy) have been the subject of several geochemical investigations. The first studies (Italiano et al., 2010 and therein) adopted a “*regional*” approach and were focused on the chemistry of thermal waters and related gases and isotopic variables. Since these data were insufficient for constraining the conceptual model of the Calabrian thermal circuits, new geological-geochemical surveys were performed by the DIBEST UNICAL geochemical team on the thermal sites of Calabria adopting a “*local*” detailed approach. In these new geological-geochemical surveys: (i) new structural data were acquired and (ii) chemical, geothermometric and isotopic analysis ($\delta^{34}\text{S}$, $\delta^{18}\text{O}$ and $\delta^2\text{H}$) were carried out. At the same time, the isotope-elevation relationship was investigated and established for the meteoric waters of Northern Calabria adopting the small springs method. All this made possible to reconstruct the conceptual geothermal model of the Sibarite Spa, Luigiane Spa, Grotta delle Ninfe, Caronte Spa, Spezzano Albanese Spa, Ponte Coniglio, Galatro Spa and Antonimina Spa (Vespasiano, 2015).

Through the hydro-geochemical and isotopic approach it has been ascertained that the Mesozoic carbonate or evaporate-carbonate units (Pollino Unit and Lungro-Verbicaro Unit) host the main geothermal reservoirs of northern Calabria whereas, the crystalline-metamorphic basement represents the main aquifer for southern Calabria.

From a chemical point of view, the Calabrian thermal systems showed considerable differences in composition and salinity, mainly due to the interaction with different lithotypes. The interaction with the rocks of the Mesozoic carbonate-evaporitic sequences gives the waters compositions from Na-Cl-SO₄ to Ca-SO₄ to Ca-SO₄ (HCO₃) whereas, the interaction with the rocks of the crystalline basement instead determines a Na (Ca)-Cl composition.

The geothermometric functions provided reservoir temperature comprised between 60 °C (Guardia Piemontese) and 33 °C (Cassano allo Ionio) for the systems hosted in the carbonate or evaporate-carbonate units whereas, system linked to the crystalline-metamorphic units showed wider range from 55 °C to ~110 °C. Depending on the reservoir temperatures and adopting the average terrestrial geothermal gradient, 33 °C/km, the depth of the geothermal reservoir, in the areas examined, is generally between 0.6 and 1.5 km. The only exceptions were identified for Ponte Coniglio and Galatro systems, whose deepest parts would extend to a depth of 3.1 km and 2.5 km respectively.

Italiano F., Bonfanti P., Pizzino L. & Quattrocchi F. (2010) - Geochemistry of fluids discharged over the seismic area of the Southern Apennines (Calabria region, Southern Italy): implications for fluid-fault relationships. *Appl. Geochem.*, 25, 540–554.

Vespasiano G. (2015) - Hydrogeochemical Isotopic and Geological Characterization of the Thermal Areas of Northern Calabria. (Ph.D. Thesis). University of Calabria.

S27

**Geologic and geothematic mapping in a dynamic country:
maps, database and data dissemination**

CONVENERS AND CHAIRPERSONS

Fabrizio Berra (Università di Milano)

Chiara D'Ambrogi (ISPRA Roma)

Effect of types of Atmospheric corrections on Hyperspectral processing in lithology mapping, Case study of Iranian S-E Ophiolitic lithology

Bahrambeygi B.¹, Moeinzadeh H.¹ & Alavipanah SK.^{*2}

¹ Department of Geology, Faculty of science, Shahid Bahonar University of Kerman, Iran.

² Department of Remote Sensing and GIS, Faculty of Geography, University of Tehran, Iran.

Corresponding email: b.bahram@sci.uk.ac.ir

Keywords: Ophiolite, Hyperion, Atmospheric corrections.

Hyperspectral images of Hyperion sensor is a rich source of information with 242 narrow contiguous spectral bands (Alavipanah, 2004). Among these, there are a number of atmospheric agents which contaminate the content of various information bands. Therefore to obtain the complete advantage of a Hyperspectral image in optimum condition, atmospheric correction is an inevitable process. Atmospheric corrections may be conducted by two methods, namely data based, and image based. In the image based methods, spectral anomalies are detected and corrected by using self-image spectral information processing without a field information requirement (Moeinzadeh, 2015). In this study, two images based atmospheric correction method of Quick Atmospheric Correction (QUAC) and Internal Average Relative Reflectance (IARR) were examined on Hyperion image of Ophiolite units of Darepahn area in Iran. To evaluate the results of these two images based methods, the results of field spectroscopy and data based empirical line method were used. X-ray diffraction and spectral analysis of selected samples were determined through the SAM method, illustrated Serpentine pattern as index mineral of Serpentinite zone. In order to compare the results obtained from different atmospherically corrected images quantitatively, maximum probability pixels obtained from the SAM method were evaluated for each corrected images in classified information format. After drawing the accuracy matrix for classified pixels and sampled and investigated pixels in the field and laboratory studies, the accuracy coefficients were calculated for the favorable districts of the corrected images by two images based methods and ELM method. Examination results display the producer accuracy of 78.32 percent for IARR corrected images and a producer accuracy of 53.39 percent for QUAC corrected image; whereas the ELM data based correction method despite using field spectrometry data shows the producer accuracy of 81.51 percent. Therefore in lithology mapping in semi-arid regions, IARR atmospheric correction method is considered as a suitable and affordable preprocessing method to retrieve Hyperspectral information.

Alavipanah S.K. (2004) - Application of thermal remote sensing in the environmental studies. *Journal of Environmental Studies*, 30, 29-38.

Geological mapping and first level seismic microzonation in Abruzzo: case studies in the Aventino basin (southern Abruzzo)

Berti D.*¹, Basi M.², Bonomo R.¹, Marino M.¹, Pampaloni M.L.¹, Ricci V.¹, Rossi M.¹,
Silvestri S.¹ & Urbani A.²

¹ ISPRA - Dipartimento per il Servizio Geologico d'Italia

² Regione Abruzzo - Servizio di Prevenzione dei rischi di Protezione Civile, Ufficio Rischio Sismico

Corresponding email: domenico.berti@isprambiente.it

Keywords: Abruzzo, seismic microzonation, geological mapping.

Starting from 2009, thanks to National Civil Protection funds, the Abruzzo Regional Council has planned the execution of first level seismic microzonation studies (MS₁), entrusted to professionals of the regional Geologic Order. The products of the studies are validated by the Technical Table for Seismic Microzonation, composed by regional experts, researchers and university professors, researchers of INGV and of the Geological Survey of Italy (ISPRA). Among the products of the MS₁ products, the technical geological map has a primary target; it is produced on the basis of the official Geological Map of Italy 1:50000 scale (CARG Project), where available, or from the elaboration of recent publication, and after new field surveys. Here we examine the experience made up in the Gessopalena municipality, which is located in the Aventino basin (Chieti province). Due to the lack of a updated official geological map, the intervention of the Geological Survey of Italy was requested, aimed to the production and validation of new cartographic data for the MS₁. These activities and relevant products provided the starting point for further studies in the context of an agreement between ISPRA and the Abruzzo Regional Council. Thus a field and sampling survey was carried out aimed to the production of new geological maps at 1:10.000 scale extended to the entire Aventino river basin, made according to the guidelines of CARG Project. More recent geological maps of the area were produced by Vezzani et al. (2004), Accotto et al. (2014), and those made available by the PhD thesis of D'Ambrogi (1999). Based on this cartography, the field survey on the pre-continental Quaternary substrate was mainly aimed to the mapping of the lithofacies of the different formations and the definition of their chronostratigraphic range. Moreover, in some cases the type of the contacts among various stratigraphic units was redefined, both for those of structural type (faults, thrusts, detachments) and for those of sedimentary type (type of stratigraphic boundaries). The first results of this study provide an up-to-date geological mapping and possibly further data for the definition of the main structural units of the area. It is hoped that this project will continue and find a further finalization for the realization of a new portion of the Official Geological Map of Italy.

Accotto C., Coscarelli F., Malerba E., Palazzin G. & Festa A. (2014) - Geological map of the Aventino River Valley (Eastern Majella, Central Italy). Scala 1:25.000. Journal of Maps, 10.

D'Ambrogi C. (1999) - Evoluzione geologica e geomorfologica plio-pleistocenica del settore dell'area periadriatica compresa tra il fiume Pescara e il fiume Sangro. Dottorato di ricerca XI° Ciclo. Università degli Studi di Roma "La Sapienza", Dipartimento di Scienze della Terra.

Vezzani L., Festa A. & Ghisetti F. (2004) - Carta geologica del Molise. SELCA, Firenze.

The Lithological Database of the CARG Project

Carta R. *, Muraro C., Bonomo R., D'Angelo S., Martarelli L., Papasodaro F., Ricci V. & Vita L.

Dipartimento per il Servizio Geologico d'Italia - ISPRA.

Corresponding email: roberta.carta@isprambiente.it

Keywords: Carg project, GIS.

The Project for the construction of the Lithological Database, at 1: 25,000 scale, consists of a reasoned synthesis work of the contents of the Database and of the Geological Map of Italy, at a 1: 50,000 scale, of the National Cartography CARG Project. The objective is to be able to characterize from a lithological point of view the lithostratigraphic units of the geological sheet through the elaboration of the numerous information recorded in the different cartographic and computer products (Database, Geological sheet, Legend, Profiles, Geological schemes, Explanatory Notes).

The first step of this work was the development of a Lithological Legend organized in hierarchical classes. The model adopted is not only the result of an elaboration of different international lithological classifications (BGS Rock Classification, INSPIRE Glossary, CGI Simple Lithology Categories 2014) but has also taken into account the model of the lithological map 1: 100,000 of the Italian Geological Service and the contents of the Geological map, at 1: 50,000 scale, of the CARG Project. Furthermore, in order to obtain a certain level of detail and homogeneity, we tried to keep the same hierarchical rank as much as possible for the different types of sediments and rocks. The Lithological Legend presents four levels of information that go from the most generic to the most detailed (for example: 1- Sedimentary rocks; 2- Clastic sedimentary rocks, 3- Rudites, 4- Breccias).

We started from the information contained in the CARG database, focusing our attention on the level of information with regard to the geological polygons and the tables of content related to this Layer, which show the data on the Legend Units of the geological sheet and on the textures of the Quaternary units.

The lithostratigraphic units (formation, member, lithofacies, unconformity bounded stratigraphic units), indicated in the chart of the sheet associated with the polygonal geological layer, were analyzed and classified to define a Lithologic Type Value up to a maximum of three (LITO1, LITO2, LITO3). For each of them was indicated the Composition Part Role Value (prevalent, subordinated, alternation, etc.) and many different codified attributes (bedding, texture, structure, composition, etc.). In addition for every single geological unit are also reported the age and the thickness.

In the GIS environment the lithological data have been linked, through the related table, to the geological polygons of the Data Base of the Geological Sheet. In the next phase, we proceeded with the unification of the neighboring databases in order to create a territorial Lithological Map. This work has highlighted a series of problems in the contact between the sheets that have been solved, when possible, through a process of elaboration and homogenization of the data.

The state of the art consists so far in the realization the territorial lithological maps of Marche, Sardinia and Valle d'Aosta regions.

Geological map of the Italian Northern Apennines (Emilia-Romagna, Marche, Tuscany, Umbria regions) at 1:250.000 scale, with GIS vector data

Conti P.*, Cornamusini G. & Carmignani L.

Centro di GeoTecnologie - Dipartimento di Scienze Fisiche, della Terra e dell'Ambiente, Università di Siena, Italy.

Corresponding email: conti@unisi.it

Keywords: Northern Apennines, tectonics, stratigraphy.

In the year 2012 the administrations of the Emilia-Romagna, Marche, Tuscany and Umbria regions (central Italy) started a still ongoing project aimed to compile a common geological map for their territories. The map should be based on the previously available data, delivered in vector format using a common GIS database, have a single geological legend, and have no discontinuities at regional boundaries. The first step of this project is deliver a 1:250,000 map of the whole area as printed paper copy and as vector GIS data. The Center for Geotechnologies of the University of Siena (Italy) is charged for the realization of the Map, here presented.

The Map cover the territories of the Emilia-Romagna, Marche, Tuscany and Umbria regions and part of the adjoining areas, the Map is compiled starting from the 1:10,000 geological databases produced by the involved Regions in the past years.

The lithostratigraphic units are grouped in domains, tectonic units, successions, and a special effort was made to correlate similar lithostratigraphic units across the area. The Map distinguish tectonic units derived from: a) Ligurian domain (Internal and External Ligurian domains); b) Subligurian domain; c) Tuscan domain (Tuscan Nappe, Tuscan metamorphic units, Cervarola-Falterona unit, Modino unit, Rentella unit, Pseudoverrucano unit); Umbria-Marche domain. Are mapped tectonic units derived from regional shear zones (Sestola-Vidiciatico unit), and units affected by HP metamorphism in the Tuscan Archipelago and southern Tuscany. Have been distinguished younger successions as: a) Epiligurian succession; b) Miocene-Pleistocene succession of the Tyrrhenian margin; c) Miocene-Pleistocene succession of the Po Plain and Adriatic margin. Are moreover mapped main outcrops of magmatic rocks (Miocene-Pleistocene in age) and Quaternary alluvial, continental and coastal deposits.

Main tectonic contacts (high angle normal faults, main thrust and low-angle normal faults) are indicated.

This 1:250,000 Geological Map of the Northern Apennines will be shortly available also as raster and GIS vector data from: <http://www.geological-map.it>

The Piemonte Ornamental Stones geodatabase compliant with the “GeoPiemonte Map” web-GIS service

d’Atri A.^{*1-2}, Barale L.², Borghi A.¹, Dino G.¹, Favero-Longo S.E.³, Gambino F.¹, Giardino M.¹, Lombardo V.⁴, Martire L.¹, Perotti L.¹ & Piana F.²

¹ Dipartimento di Scienze della Terra, Università di Torino.

² CNR-IGG, Istituto di Geoscienze e Georisorse, Torino.

³ Dipartimento di Scienze della Vita e biologia dei sistemi, Università di Torino.

⁴ Dipartimento di informatica, Università di Torino.

Corresponding email: anna.datri@unito.it

Keywords: Piemonte ornamental stones, geodatabase, GeoPiemonte Map.

The Piemonte region shows an extraordinary variety of ornamental stones, as more than 50 lithotypes are employed in the Historical and Modern Architecture Heritage. The aim of this study consists in the creation of a petrographic geodatabase of the ornamental stones, derived from Alpine rocks, used in historical buildings of the Piemonte region. The petrographic geodatabase relies on the data model of the GeoPiemonte Map (Piana et al., 2017). The GeoPiemonte Map and geodatabase derive from a thorough revision of existing geological maps and papers and it is presently available on a WebGIS application as an interactive scalable map (<http://arpapiemonte.maps.arcgis.com/apps/webappviewer/index.html?id=fff173266afa4f6fa206be53a77f6321>).

The geological features represented on the map are described following shared concepts and vocabularies, consistent with IUGS descriptive standards for the geosciences.

The Piemonte Ornamental Stones geodatabase has been thus implemented in a way compliant with some authoritative standard for the geosciences, namely the “Earth material” and the “Simple lithology” controlled vocabularies. A detailed census of historical and contemporary stones quarried in Piemonte and used in art and architecture was implemented. The stone materials were classified by lithology and provenance, also identifying the historic quarries, and defining their geological properties and main use. The database includes the commercial and scientific name of the rock, the quarry location, the petrographic description, the physical and mechanical properties, and their main uses in Piemonte. Patterns of interaction of lithobiontic (micro-) organisms with the different lithologies, and their impact on surface durability (biodegradation vs. bioprotection), are also considered and addressed to conservation issues.

Five important historical buildings were chosen and described to represent the ornamental stone diversity of the region. The Piemonte Ornamental Stones geodatabase provides the knowledge base for the realization of a lithological map of Piemonte tailored to the representation of the main ornamental stones quarried in Piemonte.

This work was carried out in the framework of the GeoDIVE research project concerning the geodiversity of the Piemonte region, “from rocks to stones, from landforms to landscapes”, funded by Compagnia di San Paolo and University of Torino.

Mapping a HP belt and its sedimentary cover: interplay between tectonics and sedimentation (Ligurian Alps, Italy)

Federico L., Scarsi M., Crispini L., Piazza M. & Capponi G.*

DISTAV, University of Genoa, Italy.

Corresponding email: capponi@dipteris.unige.it

Keywords: Ligurian Alps, late-orogenic tectonics, tectonics and sedimentation.

This geological map covers an area of about 200 km² in Liguria (NW Italy) and it provides an insight into the relationships between an exhumed orogenic belt (Ligurian Alps) and its syn- to post-tectonic cover.

This map results from a detailed field mapping (1:10000 scale) and gives new information on the relationships between the sediments of the Tertiary Piedmont Basin (TPB) and its HP (High Pressure) metamorphic substratum. This substratum is composed of a complex pile of tectonic units either of oceanic or continental affinity, with peak metamorphic conditions ranging from eclogite to blueschist facies; such units are tectonically coupled during different steps of the exhumation history of the belt.

In this area the TPB succession starts with the Molare Formation, chiefly consisting of Oligocene sandstones and conglomerates, attesting to fast exhumation of the underlying Eocene eclogites (Federico et al., 2005; Rubatto & Scambelluri, 2003), and their exposure at the surface by that time. The Molare Formation is overlain mainly by silty marls and sandstones of Oligocene to Lower Miocene age, recording a complex Oligo-Miocene syntectonic sedimentation controlled by a network of strike-slip, reverse and normal faults.

The TPB sediments and their substratum show different types of contacts (Federico et al., 2015): stratigraphic contacts are represented by unconformities between the metamorphic rocks of the substratum and the TPB deposits. Such contacts are locally folded and occur along the steeply dipping short limbs of asymmetric folds, related to the late-alpine/apennine tectonics.

Structural contacts are related to both the late-alpine/apennine tectonics (thrust faults) and to Plio-Quaternary extensional/transensional faulting. Such contacts are often decorated by thick, continuous layers of cataclasites and fault breccias.

Federico L., Capponi G., Crispini L., Scambelluri M. & Villa I.M. (2005) - ³⁹Ar/⁴⁰Ar dating of high-pressure rocks from the Ligurian Alps: Evidence for a continuous subduction–exhumation cycle, *Earth Planetary Science Letters*, 240, 668-680.

Federico L., Crispini L., Dabove G.M., Piazza M. & Capponi G. (2015) - Stratigraphic vs structural contacts in a late orogenic basin: the case of the Tertiary Piedmont Basin in the Sassello area (Ligurian Alps, Italy), *Journal of Maps*, 12(5), 959-967. <http://doi.org/10.1080/17445647.2015.1100561>

Rubatto D. & Scambelluri M. (2003) - U-Pb dating of magmatic zircon and metamorphic baddeleyite in the Ligurian eclogites (Voltri Massif, Western Alps), *Contributions to Mineralogy and Petrology*, 146(3), 341-355.

SuoliBo-HD: preliminary results of the high-density magnetic mapping of the Bologna topsoils from the public green and other outcropping urban soils

Funari V.¹, Rizzieri A.*¹ & Dinelli E.¹

¹ Dipartimento di Scienze Biologiche Geologiche e Ambientali (BiGeA), Università di Bologna, Bologna, Italy.

Corresponding email: alessio.rizzieri@gmail.com

Keywords: urban topsoil, magnetic susceptibility, iron oxides.

Here we present the preliminary results of the project “SuoliBo-HD: high density magnetic monitoring of urban topsoils from the Bologna municipality” which has the objective of evaluating the anthropic impacts in the urban area using a combination of geochemical and magnetic methods. We collected 70 samples of topsoil (up to 20 cm depth) from the public green and outcropping soils of different origin according to a strategic grid of sampling where 2 km²-wide squares and three macrozones (city centre, inner ring, and outer ring) are used.

The magnetic measurements can provide unique information on magnetic mineral assemblages (e.g., magnetite vs hematite content, magnetic sulphides) and magnetic grain sizes according to the fundamental magnetic domains (e.g., single domain SD, multidomain MD, pseudo-single domain PSD, superparamagnetic SP). We will provide interpolation maps of magnetic properties at room-temperature for the Bologna municipality area as well as a comparison with the available geochemical data, stressing the role of magnetic minerals. An emphasis is given to magnetic susceptibility and hysteresis properties such as isothermal remanent magnetization (IRM), anhysteretic remanent magnetization (ARM), and coercivity.

This study can help to identify the magnetic signatures of anthropic activity and inform further research on urban land management, exposition risk to anthropogenic pollution, protection and conservation of natural resources.

Geological-Structural map of the Late Carboniferous – Early Permian Orobic basin in the upper Brembana Valley (Orobic Alps, N Italy)

Montepeloso M.¹, Zanchetta S.*¹, Berio L.¹⁻² & Zanchi A.¹

¹ Dipartimento di Scienze dell'Ambiente e della Terra, Università degli Studi di Milano Bicocca.

² Dipartimento di Scienze Chimiche, della Vita e della Sostenibilità Ambientale, Università di Parma.

Corresponding email: stefano.zanchetta@unimib.it

Keywords: Orobic Basin, Permian Low-Angle Normal Fault, Alpine tectonics.

The Upper Carboniferous – Lower Permian deposits of the central Southern Alps consist of thick (up to 1000 m in the study area) succession of volcanic and volcanoclastic units grading upward to siliciclastic continental sediments, mainly of alluvial and lacustrine origin. All these units make together the Laghi Gemelli Group, which records the volcanic and sedimentary evolution of the Permian extensional basins that dissected the collapsed Variscan orogen. The Permian successions are characterized by great variability in terms of volume, geometry, facies, and stacking patterns. All these features suggest a strong tectonic control on the evolution of these basins. This is also testified by the widespread occurrence of synsedimentary tectonic structures that were recognized in the Upper Brembana valley, within the upper portion of the succession in the Aga Conglomerate and the Pizzo del Diavolo Formation. Synsedimentary deformation is mainly related to the activity of high-angle faults that root into low-angle normal faults (LANFs) which have been interpreted to represent the master structures that accommodated the opening of the basin. The main LANF extends along all the boundary of the basin and the fault zone is marked by cataclasites frequently transformed in tourmalinites after fluid infiltration and related metasomatism. The contemporaneous activity of high-angle faults and LANFs configured the asymmetric architecture of the Orobic Basin in this area, with a progressive thickness increase of the succession from North to South, accompanied by sharp lateral facies changes and transition from coarse-grained conglomerates to lacustrine black shales and volcanoclastic sandstones.

The original sedimentary and tectonic structures of the basin are still well-preserved, despite the Alpine deformation and related shortening. Finite strain partitioning in the different sectors of the basin resulted in different deformation style and amount of shortening during the Alpine compression. Permian normal faults are either partially inverted (Cigola-Longo Fault, Fregaborgia Fault) or preserve their original features (Aga-Vedello and Masoni LANFs). Also, Alpine related folding is strongly heterogeneous, with gentle folds developed in the hangingwall of the Aga-Vedello LANF that contrasts with upright nearly isoclinal folds mainly developed in volcanoclastic sandstones and slates just to the North of the Fregaborgia fault.

All the described features are depicted in the geological-structural map of the Upper Brembana valley. Stereographic projections of attitudes of geological-structural elements (bedding, faults, cleavage and folds) together with geological cross sections traced through different sectors of the area, allow to reconstruct the present-day architecture of the partially inverted Orobic basin.

Defining the potential of Ground Source Heat Exchanger (GSHE) through a geological-based thermal modelling: a GIS approach applied to Fano Municipality (Marche region, Italy)

Taussi M.^{*1}, Borghi W.², Gliaschera M.², Del Moro S.³, Di Gregorio A.⁴ & Renzulli A.¹⁻³

¹ Dipartimento di Scienze Pure e Applicate, Università degli Studi di Urbino, Urbino, Italy.

² Studio geologico associato GEOCON, Fano, Italy.

³ Spin Off “Geo.In.Tech. srl”, Università degli Studi di Urbino, Urbino, Italy.

⁴ Centro di Ricerca Interuniversitario in Economia del Territorio (CRIET), Università di Milano Bicocca.

Corresponding email: m.taussi@campus.uniurb.it

Keywords: low-enthalpy, direct use, Ground Source Heat Exchange.

Low-enthalpy geothermal energy represents a virtuous almost carbon-free alternative energy source capable of satisfying the energy demand for domestic heating and cooling. Ground Source Heat Exchanger (GSHE) coupled with heat pump is a widespread type of air conditioning system that can be developed anywhere and anytime with a very low environmental impact. GSHE can be related to two different types of systems: i) a closed system (Borehole Heat Exchanger), and ii) an open system (Groundwater Heat Exchanger).

The purpose of this study is to identify promising areas for the development of this renewable energy throughout the territory of Fano, a medium (122 km²; ~60.000 inhabitants) municipality in the Marche region (Italy). In order to plan future GSHE small plants at the local scale and to drive new investments in this environment friendly heating and cooling system, it should be very useful, for a Municipality, having a map which defines the most promising areas where the heat exchange with the shallow ground (50-200 metres) is maximized in terms of potential watts per metres of depth.

In this on-going work the shallow geothermal potential and the economic feasibility of both BHE and GWHE will be evaluated using a GIS-related methodology, already used in other geological contexts (e.g. Muñoz et al., 2015). Being the efficiency of the GSHE dependent on the ability of the ground and the groundwater to exchange heat, the thermal properties of the stratigraphic sequence and the physical hydrogeological parameters need to be studied in detail.

The studied area is characterized by two main geographical zones, represented by the fluvial valleys of the Metauro and Arzilla rivers and the surrounding hilly areas, respectively. The bedrocks outcropping in the hilly area is mainly represented by the “Argille Azzurre”, a sandy-clayey Pliocene Formation. The sedimentary infill in the fluvial areas is mainly alluvial, fluvial and colluvial, but beach pebbles and sand facies are also present along the shoreline. Its thickness varies between 5 to up to 50 m, while the aquifer, located above the impermeable bedrocks, has variable thickness ranging from < 5 up to 25 m.

Seismic microzonation studies, made available by the Civil Protection of the Marche region, the “Archivio nazionale delle indagini nel sottosuolo” data, made accessible by ISPRA, together with new piezometric and temperature data of the aquifer and new field observations, will provide information of paramount importance in order to reconstruct the geological and hydrogeological model of the studied area. Finally, in order to test our results in terms of heat exchange efficiency, numerical modelling through COMSOL Multiphysics® software will be involved.

Muñoz M., Garat P., Flores-Aqueveque V., Vargas G., Rebolledo S., Sepúlveda S., Daniele L., Morata D. & Parada M.A. (2015) - Estimating low-enthalpy geothermal energy potential for district heating in Santiago basin-Chile (33.5 °S). *Renew. En.*, 76, 186-195.

A regional geodatabase on landslide, flood and sinkholes for civil protection application

Vennari C.*¹, Casarano D.¹, Marchesini I.², Salvati P.², Parise M.³ & Lollino P.¹

¹ Italian National Research Council (CNR), Research Institute for Geo-Hydrological Protection (IRPI), Bari, Italy.

² Italian National Research Council (CNR), Research Institute for Geo-Hydrological Protection (IRPI), Perugia, Italy.

³ University Aldo Moro, Bari, Italy.

Corresponding email: c.vennari@ba.irpi.cnr.it

Keywords: geodatabase, geohydrological phenomena.

The analysis of the existing Italian databases of geo-hydrological hazards reveals that (i) most of them deal with a single phenomenon, (ii) they usually do not distinguish the location of phenomena and damages (which are rarely represented using different types of geometries), (iii) information on spatial and temporal accuracy are uncommon, (iv) some of the data structures are not compliant with the EC INSPIRE and Flood Directives. Most of these phenomena depends on single meteorological or seismic trigger, but this heterogeneity of information hampers the possibility to derive comprehensive vision about the consequences in terms of number of phenomena, damages and costs.

To overcome this limitations a new geodatabase structure has been designed and developed by the CNR IRPI (Napolitano et al., 2018), and recently implemented and optimized: LAND-deFeND 1.1, a geodatabase structure able to record, organize and manage non homogeneous information on geo-hydrological events occurred in the past.

The database structure can be described with a conceptual, a logical and a physical model (Napolitano et al., 2018). It allows to collect information on landslides, floods and sinkholes, about their location and to record additional data concerning damage, mitigation works and the related costs. Data entry is made using QGIS® software or a dedicated web interface.

The main upgraded features of the 1.1 version concern the inclusion, at the phenomena level, of the sinkholes, in addition to landslides and floods. Others tables have been added, that we consider of great interest for civil protection issues: a table dedicated to the rainfall events responsible for landslide triggering, a table for the critical levels issued by the Civil Protection authorities during and before the occurrence of geo-hydrological hazards. As regard damage classification, the new structure meets the needs of the Regional Civil Protection agencies to comply with specific databases (e.g. Floodcat) and to be interoperable at the international level (Flood Directive).

The database structure, physically implemented in a PostgreSQL RDBMS, was recently compiled, as part of a research project funded by the Civil Protection of Apulia Region. In order to collect the largest number of accurate data, since 1992 to nowadays, we consulted several information source: i) online newspaper archives, ii) technical reports provided by Regional Civil Protection concerning severe geo-hydrological events, for which a State of Emergency was declared, iii) studies performed and technical reports collected by IRPI-CNR, iv) technical reports, provided by local fire brigades, concerning rescue interventions resulting from geo-hydrological events.

Data entry is still in progress but, so far, the registered data (more than 300 different phenomena) allowed to validate the database structure which is expected to represent a reliable management tool for civil protection authorities at different geographical scales.

Napolitano E., Marchesini I., Salvati P., Donnini M., Bianchi C. & Guzzetti F. (2018) - LAND-deFeND—An innovative database structure for landslides and floods and their consequences. *Journal of environmental management*, 207, 203-218.

S28

Geomorphological Hazards and Cartography

CONVENERS AND CHAIRPERSONS

Alessandro Chelli (Università di Parma)

Edoardo Rotigliano (Università di Palermo)

Massimiliano Bordoni (Università di Pavia)

The negative space: a geological journey into an open pit quarry

Bonomo A.E.*¹, Prosser G.¹, Rizzo G.¹, Bentivenga M.¹ & Acito A.M.²

¹ Department of Science, University of Basilicata, Potenza, Italy.

² Studio Acito & Partners S.R.L., Matera, Italy.

Corresponding email: agnese.bonomo@unibas.it

Keywords: cultural heritage, geomorphological evolution, soft limestone.

The old district of Matera, the Sassi (Southern Italy), is one of the oldest well-preserved cities in the world. It is an UNESCO site since 1992 and represents an example of human rock settlements completely integrated in the geological and geomorphological landscape. During millennia the urban and natural landscape have harmoniously undergone a continuous evolution. The development of rock civilizations was favoured in the Murgia thanks to the presence of the Calcarene di Gravina, a workable and easy available building stone. The Sasso Barisano, Sasso Caveoso and Civita, district of Sassi, were built within the Pleistocene Calcarene di Gravina, just above the contact with the underlying Cretaceous limestone, whereas the Piano district coincides with the upper flat area of the Sassi and is not located at a specific geological boundary. This latter district was built during the maximum urbanistic development of Matera using the calcarenite quarried in the neighbourhood of the town. In this sense mining activity controlled the evolution of the landscape within and outside the town.

Calcarene di Gravina is a Pleistocene poorly lithified limestone overlapping a large area of the Apulian foreland in southern Italy, in an area known as Murgia Materana, where people used to carve their houses within this soft calcarenite. The Murgia Materana represents the western edge of the Apulian Murge, with limestone bedrock that forms a gentle hilly landscape, reflecting the long history of sea-level changes, tectonic activity, erosion and weathering processes in addition to anthropogenic activities. The latter represent an important factor in the landscape evolution of the area. Numerous open pit quarries have been opened to excavate the building material needed for the urban growth and, huge negative spaces remained in the area surrounding the town. The high quarry walls represent preferential sections for the observation of the geological and litho-stratigraphic features of the Calcarene di Gravina. Moreover, quarry landscape is very suggestive and unique with respect to the extraction techniques, originally manual and later assisted by mechanical tools. Aim of this work is to analyse the geomorphological changes related to mining activities in the Parco della Murgia Materana, an area which is deeply modified by human activities, and to promote the old quarries as starting point for geotourisms. We first describe the main old quarries in La Vaglia locality, North of Matera, where the first evidence of mining activity is known. Among them, la Palomba quarry is a 40 m deep open pit quarry, involving an area of 20.000 m². In this quarry it was possible to estimate an excavated volume of about 800.000 m³ of calcarenite. The extraction activity started in the 1950s and ended in the 1970s, when calcarenite was no longer used as building stone. Now it is possible to walk on the bottom of the Gravina Calcarene Formation on a cemented bioclastic layer rich in foraminifera and small calcitic shell fragments. Looking around it is possible to describe the transgressive and regressive depositional cycles of the Calcarenites, the erosional surface of an old channel and the basal contact with the Cretaceous limestone at the bottom. It is perfect for observing the complete stratigraphic succession of the calcarenite. In addition, textural and compositional characterization of the calcarenite allows to define the main fossil association of the original depositional environment. The idea is to turn the mining area into a "Talking Park", through active preservation and sustainable architecture projects, aiming to attracting visitors in order to increase the cultural and scientific understanding of the natural and anthropic landscape. This will also allow the geoconservation of the area, which can be defined as a geosite.

Reconstruction of lithotechnical terrain units for the assessment of shallow landslides hazard in Oltrepò Pavese (northern Italy)

Bordoni M. *, Lucchelli L., Corradini B. & Meisina C.

Dipartimento di Scienze della Terra e dell' Ambiente, Università di Pavia.

Corresponding email: massimiliano.bordoni@unipv.it

Keywords: lithotechnical units, shallow landslides, Apennines.

The prediction of the areas prone to rainfall-induced shallow landslides needs of terrain units which represent the basis for the susceptibility and the hazard zonation of the territory. Terrain units correspond generally to sub-sections of catchments, distinguishes each other by slope angle, altitude and hydrological parameters. Instead, the proneness of a hillslope towards shallow landsliding is strictly related also to the lithotechnical features of the superficial soils, which are affected by these slope instabilities. Thus, the distinction of the terrain units across a catchment should consider also these soil properties. This work has the objective to develop and apply a methodology for the definition of the main litho-technical terrain units across a particular area, aiming to represent an input predictor for the assessment of shallow landslides susceptibility and hazard. The methodology was tested in the Oltrepò Pavese area (Lombardy region, northern Italy), that corresponds to the northern termination of the Italian Apennines and is characterized by a significant predisposition towards shallow failures events as a consequence of severe rainfalls. The following parameters are measured as basic input for defining the terrain units: 1) soil lithotechnical profile, determined through the field evaluation of soil density, porosity, carbonate content, resistance to the penetration; 2) grain size distribution and Atterberg limits of the levels identified in a soil profile; 3) thickness of the soil profile. These parameters were measured in more than 200 points, corresponding to field surveys realized in an area of about 250 km². Soil profiles with similar features were, then, grouped through a cluster analysis, which allowed to identify soil groups characterized by similar lithotechnical properties. A map of distribution of these lithotechnical terrain units were obtained, linking the features of the soil profiles with the distribution of the bedrock materials with geological features similar to those ones of the reconstructed terrain units. The terrain unit distribution were compared with the shallow landslides inventory map of Oltrepò Pavese area, in order to identify the most prone lithotechnical terrain units by means of a knowledge-driven technique based on the Frequency Ratio methodology. These results could represent the basis for a future implementation of other methodologies (deterministic or data-driven models) for the assessment of shallow landslides susceptibility and hazard at regional scale, that could take into account also for this terrain units. This work was made in the frame of the ANDROMEDA project, funded by Fondazione Cariplo.

Using web-based applications to enhance traditional geomorphic mapping: a case study of the Upper Mkhomazi River basin, KwaZulu-Natal, South Africa

Bosino A.*¹, Bernini A.¹, Botha G.², Omran A.^{3,4}, Pellegrini L.¹ & Maerker M.¹

¹ Department of Earth and Environmental Sciences, University of Pavia.

² Council for Geoscience, Pietermaritzburg, - South Africa.

³ Department of Geography, Tübingen University, Tübingen, Germany.

⁴ Department of Science and Mathematical Engineering, Faculty of Petroleum and Mining Engineering, Suez University, Egypt.

Corresponding email: alberto.bosino01@universitadipavia.it

Keywords: Geomorphological map, Web-based applications, KwaZulu Natal (RSA).

We present a 1:50,000 scale geomorphological map of the Upper Mkhomazi River basin in western Kwazulu-Natal, (RSA). The study area is characterised by hilly topography and a range of soil erosion forms and features like rill/inter-rill erosion and gullying that are causing severe soil loss. The bedrock geology of the study area comprises sedimentary rocks of the Permo-Triassic Beaufort Group intruded by Jurassic dolerite sills and dykes. Some lower slopes are mantled by unconsolidated Masotcheni Formation colluvial deposits and a series of alluvial terraces of late Pleistocene age. These stratified silty clay sediments include interbedded paleosols. The soil associations are dominated by Solonetz, Stagnosols and Ferralsols developed in sheetwash sediment. The geomorphological evolution of the area is driven by the near horizontal attitude of the sedimentary bedrock and thick intrusive dolerite sills that are deeply incised by the river valley, creating a characteristic plateau morphology. The erosional landforms were mapped using orthophotos and Google Earth imagery, complimented by field survey and verification. In the study area 279 gullies and 133 areas of sheet erosion were identified. Based on a high resolution (12m cell size) Digital Elevation Model (DEM) from the Tandem X satellite platform provided by Deutsches Zentrum für Luft- und Raumfahrt (DLR), a set of four river terrace levels were identified and mapped. These geomorphological features, derived by classic field mapping methods and remote sensing applications, were combined to generate a 1:50,000 map using the QGIS platform. We provide the map via a web-based platform that allows to add important information layers that normally are not reported in classic geomorphological maps, including; i) processes susceptibilities (gullying and sheet erosion), ii) field data that describes the 3D substrates morphology derived using electro magnetometer (EMP) data; iii) additional remotely sensed data such as NDVI or mineralogy derived using a handheld spectrometer. The digital map is generated using common web applications based on Open Source Software Environments. In conclusion, through a web-based geomorphological map it is possible to represent and assess the geomorphological hazards in relation to a wide range of additional information. This enhances geomorphological research with data that are usually not represented in a traditional geomorphological map.

Seismic-induced rockfalls: Correlations between the slope aspect and seismic source

Cafiso F.¹, Cappadonia C.*¹, Rotigliano E.¹ & Sulli A.¹

Dipartimento di Scienze della Terra e del Mare (DiSTeM) - Università degli Studi di Palermo.

Corresponding email: chiara.cappadonia@unipa.it

Keywords: Seismic-induced landslides, Startegic urban area, Seismic forcing.

The northern urban area of Palermo (Sicily) is affected by several rockfall events that represent a relevant risk of people, structures and infrastructures. The study area develops in the western sector of the northern Sicily continental margin (NSCM), characterized by a relevant seismic activity. An archive of landslides and the associated spatial database with different information about the inventoried landslides has been implemented and also other thematic maps deriving from the factors layers including the seismic history of the area. The latter is strong linked to the adjacent offshore area where the morphobathimetric and seismic data evidenced the main tectonic trends recognized along NNW-SSE and ENE-WSW fault systems respectively. These trends are in agreement with the main clusters of the high magnitude events in this Tyrrhenian sector. In the framework of the assessment of rockfall susceptibility at different scale a research focused to identify new layers which taking into account the action of the seismic forcing was carried out by relating the aspect of the source slopes of rockfall and the main direction of the seismic events which occurred just before the landslides phenomena. These layers are necessary to define these correlations and consist of information about regional geological and structural setting, active and seismogenic faults in the area, the earthquakes list containing all technical information concerning the seismic events, landslides and detailed physiographic characteristics of the study area such as geomorphology, geology, structures. In this study we present the first results of the analysis and also indicate a procedural scheme of the methodology that may be used in other areas at regional scale.

Gully erosion susceptibility maps in Sicily through data mining techniques

Conoscenti C., Martinello C., Agnesi V. & Rotigliano E.*

Dipartimento di Scienze della Terra e del Mare - Università degli Studi di Palermo.

Corresponding email: edoardo.rotigliano@unipa.it

Keywords: gully erosion, susceptibility maps, Sicily.

Gully erosion causes land degradation in a wide range of environmental conditions. The development of gullies in agricultural watersheds may induce high soil loss and reduction of water availability, leading to a significant decrease of soil quality and crop yield.

Gully erosion is mainly controlled by rainfall, topography, soil, lithology and land use. Recently, accurate predictions of gully locations have been achieved by using statistical modeling and data mining techniques such as logistic regression, classification and regression trees, multivariate adaptive regression splines, stochastic gradient treeboost, artificial neural network, random forest, maximum entropy, etc. (e.g., Gómez-Gutiérrez et al., 2009; Conoscenti et al., 2013, 2014, 2018; Angileri et al., 2016).

In this study, a set of topographic indices was employed to predict the spatial distribution of gullies. These indices are given by different combinations of primary topographic attributes, including catchment area, slope angle, plan curvature and convergence index. The latter were derived from 2-m grid digital elevation models.

Gully erosion susceptibility maps were prepared by exploiting data mining techniques such as logistic regression (LR; Hosmer & Lemeshow, 2000) and multivariate adaptive regression splines (MARS; Friedman, 1991) for two catchments in Sicily, Italy. LR and MARS models were prepared by using a set of predictors including primary topographic attributes, such as catchment area, slope angle, plan curvature and convergence index, derived from 2-m grid digital elevation models. Models were calibrated and validated by using 100 random samples of grid cells extracted from each catchment. Validation was performed both internally, by using k-fold cross-validation, and externally, by transferring the models trained in one catchment to another catchment. The predictive performance was evaluated by preparing receiver operating characteristic (ROC) curves and by calculating the area under the ROC curve (AUROC). Furthermore, once optimal cut-off values of gully occurrence probability were identified, cut-off dependent performance statistics such as Cohen's kappa index κ , sensitivity and specificity, were also calculated, to further evaluate the ability of topographic indices and data mining techniques to predict the locations of gullies in the studied catchments.

The results show that the two techniques are suitable for producing high performing gully erosion susceptibility maps.

- Angileri S.E., Conoscenti C., Hochschild V., Märker M., Rotigliano E. & Agnesi V. (2016) - Water erosion susceptibility mapping by applying stochastic gradient treeboost to the Imera Meridionale River basin (Sicily, Italy). *Geomorphology*, 262, 61–76.
- Conoscenti C., Agnesi V., Angileri S., Cappadonia C., Rotigliano E. & Märker M. (2013) - A GIS-based approach for gully erosion susceptibility modelling: a test in Sicily, Italy. *Environ. Earth Sci.* 70, 1179–1195.
- Conoscenti C., Agnesi V., Cama M., Caraballo-Arias N.A. & Rotigliano E. (2018) - Assessment of Gully Erosion Susceptibility Using Multivariate Adaptive Regression Splines and Accounting for Terrain Connectivity. *L. Degrad. Dev.*, 29, 724–736.
- Conoscenti C., Angileri S., Cappadonia C., Rotigliano E., Agnesi V. & Märker M. (2014) - Gully erosion susceptibility assessment by means of GIS-based logistic regression: a case of Sicily (Italy). *Geomorphology*, 204, 399–411.
- Hosmer D.W. & Lemeshow S. (2000) - Applied logistic regression, Wiley Series in Probability and Statistics, Wiley series in probability and statistics: Texts and references section. Wiley. <https://doi.org/10.1198/tech.2002.s650>
- Friedman J.H. (1991) - Multivariate adaptive regression splines. *Ann. Stat.* 19, 1–141.

Historical maps as source of information on temporal distribution of landslide events in the Northern Apennines

Gemignani C.A.¹, Giacomelli S.², Leonelli G.² & Chelli A.*²

¹ Dipartimento di Discipline Umanistiche, Sociali e delle Imprese Culturali, Università di Parma.

² Dipartimento di Scienze Chimiche, della Vita e della Sostenibilità Ambientale, Università di Parma.

Corresponding email: alessandro.chelli@unipr.it

Keywords: historical map, landslide inventory, landslide hazard.

Landslide inventories are crucial elements to support investigations of where and when landslides have happened and may occur in the future. There is a need of information, both at the global and local scales, on the historical occurrence of landslides. Deepening knowledge on the temporal distribution of landslide activity means the passage from landslide susceptibility to landslide hazards maps. In general, several sources of data are employed to compile landslide inventories. As a function of the inventory map typology, the most common sources that can be involved are: aerial photos and other remotely sensed products, newspaper reports, scientific papers and technical notes, and other sources. Historical maps are an important source of data and information on the occurrence of landslides and on the evolution of the territory through time. Nevertheless, the information from historical maps is not of immediate use because, often, their usefulness depends on the knowledge of the evolution (change) through time of the cartographic perspective of the man on the territory. Indeed, the point of view of the historical geographer, and a correct philological approach to the sources (placing them in their proper archival context), are crucial to understand the representation and to extract territorial information from it.

A landslide inventory map in the Northern Apennines was implemented mainly thank to the use of newspaper reports, scientific papers and aerial photos. Some case studies in which the use of historical maps allowed to acquire and improve the knowledge about the temporal distribution of landslide activity are here presented.

A SRTM-based geomorphometric analysis aimed at (neo)tectonics activity detection: a case study from an intracratonic area (Mato Grosso, Brazil)

Giacomelli S.*¹, Lammoglia T.² & Sgavetti M.¹

¹ Dipartimento di Scienze Chimiche, della Vita e della Sostenibilità Ambientale, Università di Parma.

² Petrobras, Rio De Janeiro, Brazil.

Corresponding email: serena.giacomelli@unipr.it

Keywords: SRTM-DEM, geomorphometry, neotectonics.

Morphometric analyses are usually involved in tectonic studies of different geological settings as attested by the existing abundant literature on the subject (El Hamdouni et al., 2008; Font et al., 2010; Giaconia et al., 2012; Raj, 2012; Scotti et al., 2013; Dominguez-Gonzalez et al., 2015; Santos et al., 2019, etc.). In the last decades, the wide availability of open-access remote sensing (RS) data and the increasing employment of Geographical Information System (GIS) have even more promoted the use of geomorphometry in morphotectonic studies making it an essential reliable tool, both at regional and local scales.

Here it is presented the geomorphometric analysis of a portion of the Parecis Basin (Mato Grosso, Brazil) carried out, in GIS environment, on a STRM DEM (Shuttle Topographic Mission Digital Elevation Model) with a geometric resolution of 90m, to find out morphologic evidences of possible (neo)tectonic influence on the study area that belongs to an intracratonic region.

The analysis has consisted on the definition of the principal topographic features and on the determination of the drainage network characteristics, from a qualitative-quantitative point of view.

After defining the basic properties of the basin, such as aspect, slope and after highlighting the main morphologic features through a “hillshade” representation of its topographic surface (DEM), the drainage network was extracted and the higher order (*sensu* Strahler, 1957) watersheds were outlined.

Several fundamental geomorphometric indices dealing with streams network characteristics and watersheds properties were then calculated, such as “Stream order”, “Bifurcation ratio”, “Local Relief”, “Form Factor”, “Hypsometric curve and integral”, etc. The longitudinal rivers’ profile analysis was carried out, defining “Steepness” and “Concavity” indices, as well, for many rivers of the study area.

The “Stream Length Gradient” index (SL index, Strahler, 1957) was calculated for most of the rivers and a SL values map was interpolated to study SL variation across the drainage basin.

The “Isobase” map (Filosofov, 1960) was also extracted to outline the most recent erosional surface affecting the study area.

Among the geomorphometric indices calculated, longitudinal rivers’ profiles together with SL and Isobase revealed to be the most meaningful tools for the area of interest analysis. The overlap of these indices and their integration with the geological map, indeed, pointed out some regions within the study area characterized by morphometric “anomalies” that likely suggest a recent tectonic influence in such an area.

Dominguez-Gonzalez L., Andreani L., Stanek K.P. & Gloaugen R. (2015) - Geomorpho-tectonic evolution of the Jamaican restraining bend. *Geomorphology*, 228, 320-334.

El Hamdouni R., Irigaray C., Fernández T., Chacón J. & Keller E.A. (2008) - Assessment of relative active tectonics, southwest border of the Sierra Nevada (southern Spain). *Geomorphology*, 96, 150–173.

Filosofov V.P (1960) - Brief Guide to Morphometric Methods in Search of Tectonic Features. Saratov University Publishing House, Saratov, Russia (in Russian).

Font M., Amorese D. & Lagarde J.L. (2010) - DEM and GIS analysis of the stream gradient index to evaluate effects of tectonics: the Normandy intraplate area (NW France). *Geomorphology*, 119, 172-180.

Giaconia F., Booth-Rea G., Martínez-Martínez J.M., Azañón J.M., Pérez-Peña J.V., Pérez-Romero & J. Villegas I. (2012) - Geomorphologic evidence of active tectonics in Sierra Alhamilla (eastern Betics, SE Spain). *Geomorphology*, 145-146, 90-106.

Raj R. (2012) - Active tectonics of NE Gujarat (India) by morphometric and morpho-structural studies of Vatrak River basin. *J. of Asian Earth Sci.*, 50, 66-78

Scotti V., Molin P., Faccenna C., Soligo M. & Casas-Sainz A. (2014) - The influence of surface and tectonic processes on landscape evolution of the Iberian Chain (Spain): Quantitative geomorphological analysis and geochronology. *Geomorphology*, 206, 37-57.

- Santos J.M., Salamuni E., Silva C.L., Sanches E., Gimenez V. B. & Nascimento E.R. (2019) - Morphotectonics in the Central-East Region of South Brazil: Implications for Catchments of the Lava-Tudo and Pelotas Rivers, State of Santa Catarina. *Geomorphology*, 328, 138-156.
- Strahler A.N. (1957) - Quantitative analysis of watershed geomorphology. *Trans. Am. Geophys. Union* 38, 913–920.

Integrated use of geomorphological and open-access remote sensing data: examples from different case studies

Giacomelli S.*¹, Sgavetti M.¹, Bertoni D.², Rossi V.³, Lammoglia T.⁴, Leonelli G.¹ & Chelli A.¹

¹Dipartimento di Scienze Chimiche, della Vita e della Sostenibilità Ambientale, Università di Parma.

² Dipartimento di Scienze della Terra, Università di Pisa.

³ Dipartimento di Scienze Biologiche, Geologiche e Ambientali, Università di Bologna.

⁴ Petrobras, Rio De Janeiro, Brazil.

Corresponding email: serena.giacomelli@unipr.it

Keywords: remote sensing, digital cartography, open-access data.

The growing availability of open-access remote sensing (RS) data such as satellite/airborne radar and multispectral optical images, and the increasing distribution of dedicated software for their analysis (e.g., ENVI, ERDAS, GIS) promote their widespread use in many scientific fields (agriculture, forestry, forecast, geology, etc.) with different purposes (analysis, monitoring, mapping, etc). In geology RS data have become indispensable, especially in the last few decades with the introduction of digital cartography essentially based on them. Here, some case studies concerning the use of open-access RS data with different geological purposes are presented.

A SRTM DTM (Shuttle Radar Topographic Mission Digital Terrain Model) was acquired and processed to perform a geomorphometric analysis of a portion of a sedimentary basin (and its drainage network) belonging to the intra-craton region of Mato Grosso (Brazil). The resulting data suggest possible (neo)tectonic influence on such an area.

A LiDAR DTM was analyzed to map in detail geomorphologic features characterizing a densely vegetated fluvial delta area (Arno river, Tuscany), providing significant information for its late- Holocene palaeogeographic reconstruction.

Multispectral optical satellite images (Landsat 7 ETM+, Landsat 8 OLI, Sentinel 2a) were integrated with a LiDAR DTM enabling the detection and mapping of a buried tidally-influenced paleo-drainage system in the Mezzano lowland (Po delta, Emilia-Romagna Region) that furnished new insights in the reconstruction of the Po delta dynamics during the mid-late Holocene period.

A dataset of multispectral optical images (Landsat 7 ETM+) were processed and analysed to map coastline variations and sedimentary rivers' plume dispersion in the sea (i.e., Serchio and Arno rivers), providing useful information about the erosion-accretion dynamic of the Pisa coastal plain.

PSInSAR (Permanent Scatterers-Interferometric Synthetic Aperture Radar) data from GEOscopio (Tuscany webGIS) were examined to integrate and update the geomorphologic map of the Patigno landslide (Province of Massa, Tuscany), providing detailed differential displacements data and deformation velocity (mm/yr) ranges affecting the area over time (i.e., several years).

Cases listed above are just some examples about open-access RS data potential in facing geological matters. Depending on the data (e.g., DTM, optical image, etc) and based on their geometric resolution with respect to the target, RS data can be exploited in "preliminary" phase to efficiently address further analysis and investigations on an issue (e.g., coring areas with geomorphologic anomalies) and integrated with other data to enhance information on a subject (e.g., quantitative estimation of spatial displacement for a mapped landslide) or used by themselves to get information not otherwise obtainable (e.g., data from remote places or densely vegetated), with the advantage of no money/time charge for their acquisition.

Landslides in the Sibillini Mountains National Park (Central Apennines, Italy)

Guarino P.M.*, Amanti M., Chiessi V., Fiano V., Guarneri E.M., Marasciulo T., Olivetta L., Pistocchi L., Roma M., Serafini R. & Vitale V.

Dipartimento per il Servizio Geologico d'Italia - ISPRA.

Corresponding email: paolomaria.guarino@isprambiente.it

Keywords: Central Apennines, coseismic effects, landslide.

Between August 2016 and January 2017 a wide area of Central Apennines, one of the most seismically active in Italy, experienced a severe and prolonged seismic sequence, whose mainshocks reached many times a magnitude greater or close to Mw6.

The mainshocks caused the death of more than 300 people and several hundreds of injured, and led to the onset of many hundreds of ground deformation-coseismic effects, the most part represented by landslides of different types and volumes.

Landslides which interfered with villages or caused the interruption of road connections have been subjected to remediation work in the months following the seismic sequence, but those which interested the inner areas of the territory were never surveyed and for this reason never subjected to remediation.

In the framework of the initiatives and policies aimed at ensuring the safety of the population and the environment and to foster the recovery of the areas affected by seismic events, a two-year research agreement, funded by Italian Ministry for Environment, Land and Sea Protection, between ISPRA and Mts. Sibillini National Park was signed in 2018.

The objectives of this project were to verify the hazard conditions along the park's network of paths never investigated before and suggest, accordingly, possible remediation works.

In this work, first results are shown.

From a geological point of view, the study area belongs to the Apennine Range, a thrust and fold structure formed during Upper Miocene-Quaternary, when a Triassic-Miocene pre-orogenic sedimentary succession thrust on Mio-Pliocene syn-orogenic sediments, affected by a extensional tectonics during the Pliocene and the Quaternary.

Firstly, in selected areas, geological and geomorphological surveys have been carried out, matched with photointerpretation of aerial photos.

Many of the landslides studied are classified as rock slides, rock falls and avalanches, sometimes not directly seismically induced, but as we verified, induced by seismic shaking, which made slopes susceptible to debris flow during subsequent rainfall events.

Lithology units involved in the landslides are primarily marine carbonate shelf domain successions aged Lower Jurassic and Middle Liassic-Lower Miocene stratified marine pelagic sediments.

Due to the morphological characteristics of the territory (many of the landslides are located at altitude above 1100 – 1300 m a.s.l.) an extensive use of drone surveys has been made.

Data acquired by drones allowed the elaboration and reconstruction of 3D and DTM models, in turn used to define the evolutive morphological scenarios.

Geomorphological cartography in urban coastal settlements: the Rimini town case history (Emilia-Romagna, Italy)

Guerra C.¹, Guerra V.*² & Nesci O.²

¹ Department of Civil, Chemical, Environmental, and Materials Engineering, University of Bologna, Italy.

² Department of Pure and Applied Sciences, University of Urbino, Italy.

Corresponding email: veronicaguerra@live.com

Keywords: urban geomorphology, climate deterioration, geoarchaeology.

The town of Rimini is located at the southernmost end of the Po Plain, in the Emilia-Romagna region. The geomorphology of the site mainly depends on the action of the Marecchia River, coupled with marine processes in Holocene times. Rimini rests above the Marecchia alluvial fan that extends for almost 100 km² with a thickness up to over 300 m (40% below the modern Adriatic Sea), and experienced multiple growth stages spanning several glacial-interglacial cycles in mid-late Quaternary times. By creating a detailed geomorphological map of the area, we propose to highlight the geomorphological factors that influenced the historical evolution of the city, relating them to anthropic factors, with acmes in natural changes probably matching periods of climate deterioration. Between the first and third centuries, AD Rimini was located amid the Marecchia and Ausa rivers, in proximity to the shoreline that ran close to the city walls following the so-called “Roman” wave-cut scarp (Elmi et al., 2001). When reconstructing geomorphological environments of Roman times, the location of major monuments can be helpful. Many clues suggest that the Marecchia and Ausa river patterns changed frequently and drastically during the climate deterioration of the Early Middle Ages, when the river name changed from Ariminus to Maricula, meaning “little sea”. At this time, from the Riparotta to the Roman mouth, the land was swampy and the river channels filled up and frequently changed their course. In the early 1400s, canalization supported by the Malatesta family forced the terminal reach of the Marecchia River within an artificial riverbed, exploiting it as the city harbour, which is a position and function that were maintained until 1938. During the climate deterioration of the L.I.A. and until the early 20th century, the Marecchia River frequently aggraded and overflowed, flooding the town centre. The urban geomorphological map, implemented according to the criteria of the official ISPRA cartography, allowed us to point out those geomorphological elements so useful in reconstructing the evolution of the city but which are now almost completely hidden by urbanization.

Elmi C., Colantoni P., Gabbianelli G. & Nesci O. (2001) - Holocene shorelines along the central adriatic coast (Italy). *GeoActa*, 1, 27-36.

Historic and pre-historic landslide activity along the lake Garda - Brenta Group channel area (NE Italy)

Ivy-Ochs S.¹, Martin S.*², Viganò A.³, Campedel P.³, Rossato S.², Vockenhuber C.¹ & Rigo M.²

¹ ETH, Zurich, Switzerland.

² Università degli Studi di Padova, Padova, Italy.

³ Servizio Geologico, Provincia Autonoma di Trento, Trento, Italy.

Corresponding email: silvana.martin@unipd.it

Keywords: Pre-historic and historic landslides, Southern Alps, Trentino, 36Cl exposure dating.

The mountainous slopes in the Lake Garda - Brenta Group area (Southern Alps of Trentino, NE Italy) bear evidence of numerous deep-seated catastrophic rock-slope failures located along a line stretching from the Mt. Baldo ridge to the Brenta Group within sedimentary rocks. Many of these evolved into long-runout rock avalanches with volumes of several 100 Mm³. This includes some of the most famous and spectacular rock avalanches: Nago-Torbole (260 Mm³), Marocche di Dro (1000 Mm³) in the Sarca valley; Molveno (500 Mm³) and Tovel (300 Mm³) in the Brenta Dolomites. Many of these colossal events once thought to have occurred between 17,000 and 12,000 years ago are now shown by 36Cl dating to have failed much more recently, even within historical times (Martin et al., 2014; Ivy-Ochs et al., 2017). To date the events, we use cosmogenic 36Cl dating of limestone and dolomite boulders in the deposits. In this part of the Southern Alps, three periods during the Holocene of enhanced rock-slope failure activity have been evidenced: 10-9 ka, 6-3 ka and 2-1 ka (Zerathe et al., 2014). Activity at the sites we study fall within the latter two. Usually, in the same site, we observe a repetition of the landslide events: some pre-historic and some others historic, concentrated in these two time periods. At the sites studied, detachment was favored by fault and pervasive fracture systems that are closely related to the Alpine tectonics along the Giudicarie fault system (Viganò et al., 2015), which seems to have been the main controller of the landslide activity in this “channel area”. Results are interpreted in the framework of detailed geomorphological and structural field mapping, remote image analysis and runout modelling. Overall 36Cl ages show excellent coherence where independent dating (for example historical records) is available.

Martin S., Campedel P., Ivy-Ochs S., Viganò A., Alfimov V., Vockenhuber C., Andreotti E., Carugati G., Pasqual D. & Rigo M. (2014) - Lavini di Marco (Trentino, Italy): 36Cl exposure dating of a polyphase rock avalanche. *Quaternary Geochronology*, 19, 106-116.

Ivy-Ochs S., Martin S., Campedel P., Hippe K., Alfimov V., Vockenhuber C., Andreotti E., Carugati G., Pasqual D., Rigo M. & Viganò, A. (2017) - Geomorphology and age of the Marocche di Dro rock avalanches (Trentino, Italy). *Quaternary Science Reviews*, 169, 188-205.

Viganò A., Scafidi D., Ranalli G., Martin S., Della Vedova B. & Spallarossa D. (2015) - Earthquake relocations, crustal rheology, and active deformation in the central-eastern Alps (N Italy). *Tectonophysics*, 661, 81-98.

Zerathe S., Lebourg T., Braucher R. & Bourlès D. (2014) - Mid-Holocene cluster of large-scale landslides revealed in the Southwestern Alps by 36Cl dating. Insight on an Alpine-scale landslide activity. *Quaternary Science Reviews*, 90, 106-127.

Integrating GIS and tree-ring techniques for characterizing surface movements of landslides in the Northern Apennines: challenges, strengths and limitations at the Carobbio study site

Leonelli G.*, Celico F., Petrella E., Francese R. & Chelli A.

Department of Chemistry, Life Sciences and Environmental Sustainability, Università degli Studi di Parma, Italy.

Corresponding email: giovanni.leonelli@unipr.it

Keywords: landslide, Apennine, dendrochronology.

Landslide activity strongly characterizes the landscape of the Northern Apennines, often impacting roads, infrastructures and real-estate assets. The province of Parma is particularly impacted by such instabilities that find their origins in the lithological composition, stratigraphy, fractures, geological and hydrogeological characteristics, and the climate. The inner areas towards the Apennine ridge, at higher altitudes and with steeper slope-inclinations, during the Pleistocene glaciations directly experienced the morphological activities of glaciers, and in this belt also the cryo-nival processes of rock degradation were widespread. These past conditions are now witnessed by landforms such as cirques and glacial deposits often causing instabilities. Current instabilities are also widespread in the median belt that is at lower altitudes and is characterized by flysch rocks and clayey formations. Both the inner and the median belts are also facing land abandonment, an additional factor contributing to landscape degradation.

In the median belt, the integration of GIS and tree-ring techniques have been planned at the toe of a large, mainly dormant, landslide in the Val Parma, the Carobbio landslide. This landslide presents some smaller portions often reactivating also in recent times, with planar and rotational movements. West of the Carobbio town, one of these smaller landslides bordering the main body underwent a gravitational movement approximately four years ago involving an area of approximately 4 ha, delimited at the toe by the Parma River and in the upper portion by its crown that is currently at 100 m from a private house. The landslide surface presents a dense vegetation cover of broadleaf trees that are now tilted or falling, thus representing a suitable place where testing an integrated approach of GIS and tree-ring techniques. Tree age in Apennine environments is surely a limitation for dendrochronological approaches aiming at long-term reconstructions and the assessment of the events frequency. However, classical dendrogeomorphological techniques as well as advanced ones (e.g., based on tree-ring stable isotope analysis), can allow the assessment of times and areas of recent surface movements or of possible changes in soil and ground waters occurred in the landslide body. Tree rings in this environment may thus mainly contribute to the reconstruction of the spatio-temporal distribution of recent instability signals and of the type of landslide movement.

Investigation of prediction errors in the landslide susceptibility statistical models through multiple nested MARS analyzes: application in the Caldera area of Ilopango (El Salvador, C.A.)

Martinello C.*¹, Rotigliano E.¹, Conoscenti C.¹ & Agnesi V.¹

Dipartimento di Scienze della Terra e del Mare, Università degli Studi di Palermo, Italy.

Corresponding email: chiara.martinello@unipa.it

Keywords: landslide susceptibility, prediction errors, MARS.

In the evaluation of landslide susceptibility through statistical modelling, the correct definition of the prediction errors is of great importance. Indeed, these have different weight in the assessment of landslide susceptibility. The aim of this research was to identify a method capable to analyze the prediction errors and, therefore, to allow a better definition. MARS (Multivariate Adaptive Regression Splines)-based susceptibility models were prepared in the Caldera Ilopango area (El Salvador), using a set of predictors and a landslides inventory, remotely recognized at 2003. The archive includes 1503 shallow debris flows activated by the rainfall season in 2003. The twelve physical-environmental predictors were selected according to their expected influence on slope instability and to their control on slope failure mechanisms. LIP (Landslide Identification Point) and a 10m pixel structure were adopted as diagnostic areas and mapping unit partitioning, respectively. Three different model building procedures (mod-A, mod-B and mod-C) were applied, based on the preparation of 100 replicates and in averaging the optimized regression coefficients to obtain a generalized final model, whose predictive performance was evaluated by means of confusion matrixes. For mod-A, each of the 100 replicate included all the positives and a different randomly extracted subset of negatives. By applying a Youden-index based cut-off, the validation indices (TP_A -True Positive, FP_A -False Positive, FN_A -False Negative and TN_A -True Negative of mod-A) were obtained. For mod-B, whose purpose is to investigate type-II errors, each replicate included all FN_A and a same number of TN_A like as positives and negatives, respectively. A generalized mod-B was obtained and, by applying a Youden-index based cut-off, the new validation indices calculated. Finally, to analyze the type-I errors, a generalized mod-C was built by averaging the regression coefficients of replicates obtained including all TP_A and a same number of FP_A like as positives and negatives, respectively. Again, by applying a Youden-index based cut-off, the validation indices were calculated. The validation indices show that the 21% of positives and the 30% of negative are missed by the mod-A, FN_A and FP_A , respectively. However, Mod-B correctly provides ~90% of FN_A , as TN, whilst the ~40% of TN_A still was defined as FP. The 10% of FN_A and 60% of TN_A remain FN and TN in mod-B, respectively. The mod-C allow to correctly define the ~70% of FP_A and only the 30% remains FP. The 66% of TP_A rests TP in mod-C but the 34% of TP is now predicted as negative. The test suggests preparing sub-models to investigate false prediction as a promising tool for discriminating inside the false cases, future activations from errors.

Site-specific to large-scale landslides susceptibility assessment in Rwanda

Nsengiyumva J.B.¹, Valentino R.*², Sobio Y.³, Mizero J.³, Nsengiyumva F.³, Bordoni M.⁴ & Meisina C.⁴

¹ Chinese Academy of Sciences, China.

² University of Parma, Italy.

³ Institut d'Enseignement Supérieur INES-Ruhengeri, Rwanda.

⁴ University of Pavia, Italy.

Corresponding email: roberto.valentino@unipr.it

Keywords: Susceptibility Assessment, Rwanda, Multi-scale Approach.

This note deals with a pilot study that intends connecting the landslide susceptibility analysis at large scale with the slope stability analysis at single slope scale in the Rwandan context. The suggested methodology aims at putting together analyses at different scales, in order to better validate models at large scale on the basis of both field and laboratory geotechnical data at local scale. This approach, that has been already applied in other contexts such as Italy (Bordoni et al., 2015), will be applied for the first time in Rwanda.

Landslides in Rwanda are very common in slopes close to urbanized areas and main roads. For this reason, they can cause significant damage to cultivation, structures and infrastructures and sometimes cause human losses. It appears extremely urgent to conduct a detailed landslide susceptibility study for Rwanda in order to overcome losses and curb the impacts. Efforts, therefore, must be in highlighting unstable zones by using suitable methodologies since it can provide sustainable response and protect lives and properties. In this perspective, landslide susceptibility study can deliver valuable information useful for hazard mitigation through appropriate planning (Nsengiyumva et al., 2018).

In this work, a methodology that aims at linking field observations and laboratory tests on some sample slopes with distributed slope stability analyses at large scale is presented. To assess the occurrence of rainfall-induced landslides in a certain area, three main aspects can be considered to be of paramount importance: (1) a detailed description of the physical– mechanical triggering mechanism in relation to the site specific characteristics of the involved soils and stratigraphy; (2) the choice of the more suited slope stability model to be applied at the local scale; and (3) the definition of a reliable methodology to extend the model from the site-specific to large scale. On the other hand, it is well known that landslide triggering mechanisms are strictly linked to rainfall events. For this reason, even typical rainfall pattern in Rwanda should be taken into account.

The proposed working scheme includes the implementation of well-established models and aims at finding a potential methodology for extending the analysis from site-specific to a wider area. This work gives some indications about the influence of the type of mapping unit chosen for the homogenization of the soil parameters, which are required as input data for the model's application at large scale. The analysis of the role played by mapping units described in this research aims at identifying which zoning can be more representative of the distribution of the soil's properties over the study area and evaluate the differences in the assessment of susceptible areas considering different types of soil mapping units.

Bordoni M., Meisina C., Valentino R., Bittelli M., Chersich S. (2015) - Site-specific to local-scale shallow landslides triggering zones assessment using TRIGRS. *Nat. Hazards Earth Syst. Sci.*, 15, 1025–1050.

Nsengiyumva J.B., Luo G., Nahayo L., Huang X., Cai P. (2018) - Landslide Susceptibility Assessment Using Spatial Multi-Criteria Evaluation Model in Rwanda, *Int. J. Environ. Res. Public Health*, 15, 243.

Composite landslide susceptibility maps

Rossi M.*¹, Santangelo M.¹, Alvioli M.¹, Marchesini I.¹, Cardinali M.¹, Bucci F. & Fiorucci F.¹

IRPI - CNR, Perugia.

Corresponding email: michele.santangelo@irpi.cnr.it

Keywords: landslide, composite susceptibility, multiple modelling approach.

Landslides are heterogeneous natural processes. Given the significant variability of the different landslide types and in particular of their dimensional characteristics, style of movement and triggering mechanisms, multiple models and approaches have been developed in the literature. At present, no single model or modelling approach is applicable to all the different landslide types. This also limits the prediction of the spatial occurrence of landslides achieved through susceptibility models which aims at estimating the probability of the spatial landslide occurrence. Such models divide and classify a territory on the basis of its propensity to specific landslide types, using relationships linking the occurrence of landslides with their conditioning factors. In this work, we identify and apply a methodology for the combined modelling of susceptibility posed by different landslide types. The methodology initially envisages the modelling of the susceptibility for the individual landslide types using differentiated approaches, calibration, evaluation and application phases and subsequently their combination. In the modelling, the pixel is used as the base mapping unit, while the slope unit is used as a mapping unit for a subsequent spatial susceptibility aggregation. The result maps, here defined as “composite susceptibility maps”, subdivide a territory according to its propensity to failure of one or more landslide types. The proposed model was applied as part of the Project “Paesaggi Sicuri”, funded by the Italian Ministry of Cultural Heritages and Activities (MIBACT), in a portion of the UNESCO site “Porto Venere, Cinque Terre e Isole” characterized by the occurrence of different landslides types, namely slides, falls and flows. The derived composite susceptibility map allowed a more realistic analysis of the geo-hydrological vulnerability being able to consider jointly the different landslides types occurring in the study area.

Integrating pixel analysis into slope units landslide susceptibility mapping: an application to the Imera river basin

Rotigliano E.¹, Martinello C.*¹, Cappadonia C.¹ & Agnesi V.¹

Dipartimento di Scienze della Terra e del Mare, Università degli Studi di Palermo, Palermo, Italy.

Corresponding email: chiara.martinello@unipa.it

Keywords: landslide susceptibility, slope units, grid cell units.

In this work, the different efficiency of mapping unit partitioning in evaluation of landslide susceptibility was tested. In particular, this test is designed to compare the most commonly used grid cell units (CLUs, in this research corresponding to the 8m pixel structure of DEM) and a new type of slope units: LCL_SLU (Landform Classification Slope Units). The latter were obtained by dividing the SLU (Slope Units delimited by applying the Grass r.watershed function to DEM) according to the classes of LCL (Landform Classification).

The study area was the Imera basin, in the north sector of Sicily (Italy). A systematic landslide inventory was produced by using Google Earth's aerial imagery from 2013: 1551 slides have been identified through LIPs (Landslide Identification Points) as diagnostic areas. A set of eleven physical-environmental predictors was selected according to their expected influence on slope instability and to their control on slope failure mechanisms. MARS (Multivariate Adaptive Regression Splines)-based susceptibility statistical models were prepared by defining 100 replicates of balanced datasets, made of positive mapping units (pixels or LCL_SLU with at least one LIP) and an equal number of randomly selected negatives (pixels or LCL_SLU without LIP).

A random partition technique was applied by multiple random splitting (75%, for calibration, 25% for validation) of the source balanced dataset for testing the goodness of models and their predictive performances evaluated through both cutoff-dependent and -independent metrics (ROC-curve analysis and confusion matrixes).

Firstly, pixels-based MARS statistical models were developed. By averaging the regression coefficients, a generalized pixels-based model and the related landslide susceptibility map were obtained. By zoning the obtained pixel landslide susceptibility values in the LCL_SLU, mean (MN), max (MX) and mean + standard deviation (MS) of the included pixels in each LCL_SLU were obtained and then adopted as new predictors for a subsequent LCL_SLU-based modelling.

The results show that excellent Area Under Curve (AUC) values are obtained for both models (equal to 0.89 for the pixel-based model and 0.83 for the other one). However, there is a greater Sensitivity for the LCL_SLU-based model (0.86 versus 0.83) although there is a heavy lowering of the Specificity (0.68 versus 0.78).

This test seems to show that by integrating the classical pixel-based modelling on the LCL_SLU-based model it is possible to optimize the results of the landslide susceptibility evaluation obtained with statistical methods. In particular, it is believed that this approach and the susceptibility maps thus obtained (divided by territories and no longer by pixels) are more suitable for administrations in land management and therefore in identifying those areas that may be affected by landslides in the future.

Advantages of innovative automatic inclinometers applied to landslides monitoring for early warning activities

Valletta A.*¹, Cavalca E.¹, Savi R.¹ & Segalini A.¹

¹ Dipartimento di Ingegneria e Architettura, Università di Parma.

Corresponding email: alessandro.valletta@unipr.it

Keywords: landslides, monitoring, Early Warning Systems.

Geotechnical monitoring is one of the most important activities aimed to study and understand the evolution of a landslide. Traditionally, surveys have been performed by using different devices specifically developed to measure a parameter of interest. Inclinometers are some of the most commonly used and well-known tools, designed to monitor slope displacements at different depths. These instruments present a series of features typical of the so-called “traditional” approach, including the need for an operator on-site to perform all the passages required to obtain monitoring data, and a sampling rate typically ranging from some day to weeks depending of several factors, including site accessibility and operator’s availability. While these characteristics do not affect the tool’s ability to perform as a survey system, they represent a relevant limitation to their application for early warning purposes. In fact, in a context where it is essential to acquire timely information on the evolution of a critical event, it should be required to provide a monitoring system able to provide a continuous description of the ongoing phenomenon. In particular, features like automatic data acquisition, high sampling frequency and remote control of the on-site instrumentation are typical of monitoring systems designed for early warning applications. The need for tools able to meet these requirements has led to several upgrades of classical inclinometers, resulting into the development of new contact-based tools. These innovative systems include the possibility to integrate different devices typologies (e.g. inclinometers, piezometers and thermometers) creating a single, multi-parametric array of sensors. The exploited technologies allow for the implementation of automatic procedures for data sampling, elaboration and visualization, which can greatly contribute to the design of alert systems for instability phenomena. In particular, larger datasets achievable by these tools are suitable for a more reliable application of failure forecasting models, which are a key component in the development of early warning activities. In order to provide an example of the importance of these considerations, a case study is presented where both traditional and innovative inclinometers were installed on-site. While the monitoring plan was intended as a geotechnical survey activity, the innovative system allowed to identify a series of critical events which interested the monitored area. Thanks to the innovative procedures implemented, it was possible to obtain a good representation of the final collapse of the landslide, which irreversibly damaged all the traditional inclinometer casings and, ultimately, broke the automatic array. Nonetheless, the dataset recorded before the system failure allowed the application of forecasting models, which correctly predicted the landslide collapse several hours before its occurrence.

S29

**Recent advances in fluid geochemistry in active volcanic and
geothermal areas: following Mariano Valenza**

CONVENERS AND CHAIRPERSONS

Alessandro Aiuppa (Università di Palermo)

Sergio Gurrieri (INGV)

Franco Tassi (Università di Firenze)

Jacopo Cabassi (Università di Firenze)

Carlo Cardellini (Università di Perugia)

Global trends in volcanic gas composition

Aiuppa A.*¹

¹ DiSTeM, Università di Palermo.

Corresponding email: alessandro.aiuppa@unipa.it

Keywords: volcanic gases, carbon, sulfur.

The chemical composition of volcanic gases has been extensively studied since the mid-1900s, thanks to efforts of a small number of pioneer geochemists including the highly missed Mariano Valenza. The last 20 years, in particular, have seen major advances in our ability to real-time measuring volcanic gas compositions and fluxes, both in-situ and remotely. The emerging, more complete volcanic gas catalogues (Aiuppa et al., 2017, 2019) now allow exploring the global variability of H₂O-CO₂-S volcanic gas compositions, and to more fully constrain the origin of these magmatic volatiles in different volcano contexts. Here, I review and extend recent work (Aiuppa et al., 2017, 2019) that attempts at understanding the source processes governing the global variability of volcanic gas compositions, with a focus on the CO₂-S system. By using a global catalogue of > 70 mafic volcanoes for which high-temperature (> 450 °C) gas data are available, I initially characterise the global relationship between volatile (volcanic gas CO₂/S ratios) and non-volatile (trace elements) tracers in arc magmas. I show that volcanic arc gas CO₂/S ratios are globally linked to Ba/La and Sr/Nd ratios in the source magmas (from whole-rock analysis), and I use these global associations to resolve the mantle vs. slab vs. crustal contributions to arc gas budgets. Results demonstrate higher carbon output (higher volcanic gas CO₂/S ratios) in arcs where carbonate sediment subducts on the seafloor. From this, I model the global gas vs. trace element relationships as due to spatially variable additions of slab-sediment melts (variably enriched in C) to the mantle wedge. An additional crustal carbon contribution, from limestone assimilation in the crust, is eventually locally over-imposed on the slab-mantle mixing relationship in some arc segments (e.g., Indonesia, Mexico and perhaps in the Mediterranean region). Within-plate and/or rift related volcanoes similarly exhibit globally linked volcanic gas (CO₂/S ratios) compositions and trace elements tracers (e.g., Sr/Nd) in magmas, which I suggest is caused by variable additions of C-rich (carbonatitic or carbonated silicate) melts rising from the deep mantle to a shallow (depleted) mantle source.

Aiuppa A., Fischer T.P., Plank T. & Bani P. (2019) - CO₂ flux emissions from the Earth's most actively degassing volcanoes, 2005–2015. *Scientific Reports*, 9 (1), art. no. 5442.

Aiuppa A., Fischer T.P., Plank T., Robidoux P. & Di Napoli R. (2017) - Along-arc, inter-arc and arc-to-arc variations in volcanic gas CO₂/S_T ratios reveal dual source of carbon in arc volcanism. *Earth-Science Reviews*, 168, 24-47.

Estimating the energetic budget of hydrothermal systems using diffuse emission of CO₂: the case of Nisyros (Greece)

Bini G.*¹, Chiodini G.², Cardellini C.³, Vougioukalakis G.E.⁴ & Bachmann O.¹

¹ Department of Earth Sciences, ETH Zurich.

² INGV, Bologna.

³ Dipartimento di Fisica e Geologia, Università di Perugia.

⁴ IGME, Athens.

Corresponding email: giulio.bini@erdw.ethz.ch

Keywords: Nisyros caldera, CO₂ diffuse degassing, thermal energy.

Since the '1990s, diffuse emissions of CO₂ from soil were measured to predict changes in the plumbing systems of active volcanoes. Lately, the accumulation chamber method has also found useful applications in geothermal exploration, for example to estimate the thermal energy released from hydrothermal systems. The availability of CO₂ flux data (1999-2001 period; Caliro et al., 2005) and the accessibility of several diffuse degassing structures (DDSs), make Nisyros caldera the ideal site to test those techniques. The CO₂ efflux from the soil of the south east sector of the caldera (Lakki Plain) has been measured during a new detailed survey (~1400 soil CO₂ flux measurements) performed in October 2018. The gas emissions are fed by hydrothermal sources and in minor amount by the soil biogenic activity, whose mean CO₂ flux (4 g m⁻²d⁻¹) has been estimated for the first time. The outgassing of deep carbon occurs from nine DDSs, whose origin is strongly controlled by the regional tectonics (NE-SW and NW-SE trending lineaments) or by the volcanic-hydrothermal activity (hydrothermal craters and domes). The total amount of hydrothermal CO₂ released in atmosphere is 92 ± 8 t/d, accounting for an increase in emissions of ~24 % for two decades – considering the previous estimation based on the same method applied to 1999-2001 data (from Caliro et al., 2005), i.e. 74 ± 7 t/d.

Although the CO₂ output is not particularly high at Nisyros (close to the median of CO₂ emissions measured in volcanoes worldwide), the energy released by deep fluids circulation is remarkable. We computed the energetic budget involved in a convective model, where the CO₂ currently emitted at Lakki Plain is originally dissolved in the deep hydrothermal liquids and released during their ascent, depressurization and boiling. The separated steam which approach the surface, discharge ~60 MW through shallow condensation in the DDSs, while the total thermal energy involved in the convective rising of the deep liquids carrying CO₂ account for 134-270 MW. This large flux of energy could dramatically increase during future earthquakes by addition of heat and mass from a deep hydrothermal reservoir, potentially triggering hydrothermal explosions, as it happened several times in the past few centuries.

Caliro S., Chiodini G., Galluzzo D., Granieri D., La Rocca M. & Ventura G. (2005) - Recent activity of Nisyros volcano (Greece) inferred from structural, geochemical and seismological data. Bull. Volcanol., 67, 358–369.

The impact of Mt. Etna's ash plume on the chemical composition of meteoric deposition

Brugnone F.*¹, Calabrese S.¹⁻², D'Alessandro W.², Li Vigni L.² & Parello F.¹

¹ University of Palermo, Italy.

² Istituto Nazionale di Geofisica e Vulcanologia, Palermo, Italy.

Corresponding email: brugnonefilippo92@gmail.com

Keywords: volcanic gases, trace elements, environmental volcanology.

Mt. Etna, in eastern coast of Sicily (Italy), is one of the most active and most intensely monitored volcanoes of the planet. It is the biggest volcanic point source of volcanic gases and particles to the troposphere in the Mediterranean basin. On the morning of December 24th 2018, a new lateral eruption of the Mount Etna started. This eruption was related to an intrusion of a magmatic dike on the high eastern flank of the volcano, which a two kilometers long fracture in the NNW - SSE direction. At the same time, the summit craters also produced a continuous strombolian activity generating a very dense dark ash plume, dispersed by the wind into the south-eastern direction. This volcanic event well record from the atmospheric precipitations. During the period from June 2018 to May 2019, atmospheric precipitations were collected in the area of Priolo, eighty kilometer far SSE from Mt. Etna. The sampling and analytical protocols were chosen following the guidelines published by the main international agency involved in the monitoring of atmospheric precipitation. The rain gauges were open during the entire exposure time, collecting both wet and dry deposition (bulk collectors). All the collected water samples were analysed for major ion contents and for a large number of trace elements. The atmospheric precipitation of the period straddling the eruptive event is characterized by high concentration of major ions, such as Fluoride (up to 0.88 mg/l), Chloride (up to 124 mg/l) and Sulphate (23.1 mg/l). These derive mainly from the emitted volcanic gases (HF, HCl and SO₂). On the another hand, an enrichment of some trace elements is also presented, such as Aluminum (up to 152 µg/l), Thallium (0.16 µg/l), Tellurium (0.025 µg/l). While Tl and Te are highly volatile elements typically enriched in volcanic emissions, Al is a refractory element that is probably correlated to the dissolution of the emitted volcanic ashes.

Water and dissolved gas geochemistry at Coatepeque, Ilopango and Chanmico volcanic lakes (El Salvador, Central America)

Cabassi J.¹⁻², Capecchiacci F.¹⁻², Magi F.^{*1-3}, Vaselli O.¹⁻², Tassi F.¹⁻², Montalvo F.⁴, Esquivel I.⁴, Grassa F.⁵ & Caprai A.⁶

¹ Dipartimento di Scienze della Terra, University of Florence, Florence (Italy).

² CNR – Istituto di Geoscienze e Georisorse, Florence (Italy).

³ Dipartimento di Scienze della Terra, University of Pisa, Pisa (Italy).

⁴ Ministerio de Medio Ambiente y Recursos Naturales, San Salvador (El Salvador).

⁵ Istituto Nazionale di Geofisica e Vulcanologia, Sezione di Palermo (Italy).

⁶ CNR – Istituto di Geoscienze e Georisorse, Pisa (Italy).

Corresponding email: jacopo.cabassi@unifi.it

Keywords: volcanic lakes, water and dissolved gas geochemistry, unusual chemical compositions.

In November 2016, a geochemical survey based on water and dissolved gas chemistry was carried out at Coatepeque (on the E slope of Santa Ana Volcano), Ilopango (inside Ilopango Caldera) and Chanmico (associated with San Salvador Volcano) volcanic lakes in El Salvador, a land characterized by complex fault systems and related volcanism. The three lakes showed a thermocline at a relatively shallow depth (from 30 to 40 m, from 20 to 40 m and from 5 to 15 m depth, respectively) and anoxic conditions below 33, 24 and 4 m depth, respectively. Along the vertical water columns, increasing salinity and decreasing pH were measured. The Na⁺-Cl⁻ composition of the Coatepeque and Ilopango lakes, displaying TDS values up to 1,226 and 1,216 mg/L, respectively, is likely due to hydrothermal fluids that feed these two lakes, as also confirmed by Cl⁻/Br⁻ molar ratios ≤ 650 , high As, B, Li and Si contents and Cl⁻/SO₄²⁻ ratio > 1 . The Mg²⁺-HCO₃⁻ water composition of Lake Chanmico, whose TDS values were between 566 and 856 mg/L, suggests water-rock interaction processes with mafic/ultramafic rocks variably affected by serpentinization processes, which produced high Mg²⁺, Si and B concentrations. Waters at depth were characterized by the presence of CO₂ with a likely hydrothermal signature based on the $\delta^{13}\text{C-CO}_2$ values, albeit this gas was found in smaller quantities when compared to those recorded in other meromictic lakes hosted in quiescent volcanic systems (e.g. Lake Kivu in DRC, Monticchio, Albano and Averno lakes in Italy, Hule and Rio Cuarto lakes in Costa Rica, Lake Pavin in France). The occurrence of CH₄, whose concentrations in Lake Chanmico were up to two orders of magnitude higher than those recorded in Coatepeque and Ilopango lakes, suggests bacterial methanogenesis. Further surveys aimed at determining both the isotopic signature of helium and methane ($\delta^{13}\text{C-CH}_4$ and $\delta\text{D-CH}_4$ values) and microbiological data are needed to support such hypothesis and investigate the complex biogeochemical processes acting in these lakes.

The precious “scientific heritage” of Mariano Valenza: the unknown history of Ludovico Sicardi and the birth of the modern volcanology

Calabrese S.*¹⁻², Li Vigni L.², Brugnone F.¹ & Capasso G.²

¹ Università degli Studi di Palermo, Dipartimento di Scienze della Terra e del Mare (DiSTeM), Palermo, Italy.

² Istituto Nazionale di Geofisica e Vulcanologia, sezione di Palermo, Italy.

Corresponding email: sergio.calabrese@gmail.com

Keywords: Vulcano island, Valenza, fumarolic field.

Mariano Valenza was an important scientific figure of the geochemical community and a person characterized by his great intellect, diplomacy and human qualities. Sadly, he passed away in July of 2018, leaving a great void. He left us a precious treasure for all the geochemists involved in volcanology: the story and the memory of Ludovico Sicardi. Indeed, Valenza carefully preserved in his office, for a long time, four boxes containing the scientific material belonged to Ludovico Sicardi. As often happens, a little by chance, the precious material returned to light thirty-five years later, on the 20th of April 2018, and was donated to the Museum of Mineralogy of Palermo. It is nowadays subject of study and cataloging by the volunteers of the Associazione Naturalistica Geode. The “scientific treasure” consists of the personal field-equipment of Sicardi, glassware, copies of the scientific articles, many old maps of volcanic areas, several historical photos of Vulcano and Solfatara. Among all these findings, several manuscript notes and three important unpublished researches about Vulcano, Vesuvio and Campi Flegrei.

Who was Ludovico Sicardi? Sicardi was a chemist and a pharmacist, who was passionate about volcanoes and, in particular, enraptured by the island of Vulcano (Eolie - Sicily). During his several field trips in Vulcano, he observed and described the fumarolic field on systematic basis, measuring the temperatures and recording their variations over time (Sicardi, 1973). He was the first to perform chemical analysis of fluids emitted by fumaroles in Vulcano Island and Solfatara. Furthermore, he was the former to suppose the coexistence of SO₂ and H₂S in fumarolic discharges, which by that time was considered to be impossible. Also, he succeeded in measuring their ratio by developing an in situ method that chemically separate the S-gaseous species. This method was based on the sampling of fumarolic fluids using a glass flask that contained a NH₄OH-AgNO₃ solution, with the aim to absorb the soluble acid gases (CO₂, SO₂ and HCl) and precipitate H₂S as an insoluble Ag₂S (Sicardi, 1955). Based on his remarkable scientific production, Sicardi can be considered as a precursor of the modern Volcanology and a pioneer of the volcanic monitoring techniques. We are extremely grateful to Mariano Valenza for giving us this fascinating story.

Sicardi L. (1955) - Captazione ed analisi chimica dei gas della esalazione solfidrico-solforosa dei vulcani in fase solfatarica. Bull. Volcanologique, 17(1), 107-112.

Sicardi L. 1973. The thermal oscillations of the fumaroles of the Island of Vulcano from 1913 to 1970. Stromboli, 13, 65-68.

Carbon dioxide diffuse emission in volcanic and hydrothermal areas: monitoring volcanic activity and impact on carbon global emissions

Cardellini C.*¹, Chiodini G.², Frondini F.¹, Caliro S.³, Avino R.³, Bagnato E.³, Beddini G.¹ & Rosiello A.¹

¹ Dipartimento di Fisica e Geologia, Università di Perugia.

² INGV-Bologna.

³ INGV-Napoli.

Corresponding email: carlo.cardellini@unipg.it

Keywords: carbon dioxide, diffuse degassing, volcanoes.

Volcanoes emit volatiles through active plumes, fumarolic vents and zones of diffuse soil degassing. Emitted volatiles may represent the surface manifestation of magma degassing providing useful information for assessing the state of activity of a volcano. Diffuse CO₂ degassing may represent the dominant mode of volcano degassing especially at calderas and volcanoes with hydrothermal activity. The monitoring of CO₂ diffuse emissions can provide important clues in understanding the evolution of volcanic activity especially at calderas where the interpretation of unrest signals is often complex. For example the analysis of soil CO₂ fluxes data resulting from the long term monitoring of Solfatara of Pozzuoli revealed that, starting from 2003, the area releasing deep-sourced CO₂ tripled its extent during the unrest phases. This expansion was accompanied by an increase of the background CO₂ flux caused by contributions from the non-biogenic CO₂ source. Concurrently, the amount of diffusively released CO₂ increased up to values typical of persistently degassing active volcanoes (up to 3000 t/d) (Cardellini et al., 2017). These variations resulted consistent with the increase in the flux of magmatic fluids injected into the Solfatara hydrothermal system. Diffuse CO₂ emissions constitutes also a contribution to the global emissions of carbon in atmosphere, however this was frequently neglected in most global carbon budget estimates. In order to estimate the total amount of the CO₂ diffuse emission a global dataset was retrieved from MaGa database (www.magadb.net). The compilation includes data from more than one hundred of soil diffuse degassing areas and lakes. The data set is not homogeneous in terms of field strategies and method used to estimate the CO₂ emission, furthermore, in many cases the CO₂ flux estimates include the contribution from the biogenic source. For this reasons data statistical analysis was applied to define a reasonable maximum threshold for the specific flux sustained by the biogenic source to limit the over estimation of volcanogenic CO₂ emission. In order to estimate the global CO₂ emission, the “typical” CO₂ emission of a Diffuse Degassing Structure was defined and coupled with a reasonable number for degassing volcanoes hosting diffuse emissions. The global CO₂ emission from diffuse degassing resulted globally significant, in the order or higher than the estimate emission by volcanic plumes. However, data analysis pointed out that a larger number of ad-hoc and reliable investigations of diffuse degassing are necessary to reduce estimate uncertainty.

Cardellini C., Chiodini G., Frondini F., Avino R., Bagnato E., Caliro S., Lelli M. & Rosiello A. (2017) - Monitoring diffuse volcanic degassing during volcanic unrests: the case of Campi Flegrei (Italy). *Sci. Rep.*, 7, 6757

Magma degassing episodes at volcanoes in hydrothermal activity

Chiodini G.*¹ & Caliro S.¹

¹ INGV

Corresponding email: giovanni.chiodini@ingv.it

Keywords: Campi Flegrei, Vulcano, Vesuvio, Panarea, Nisyros, Mammoth Mt., magma degassing, geochemical anomalies.

Here we discuss time series of fumarolic composition collected in the last 40 years at various volcanoes including Campi Flegrei, Vulcano, Vesuvio, Panarea, Nisyros and Mammoth Mt. Anomalous peaks of CO₂/CH₄ and He/CH₄ (or CO₂/H₂O) fumarolic ratios were observed to follow clustered seismicity and/or pulses of ground deformation. In principle, the fumarolic ratio among CO₂ and He, gas species of main magmatic origin, with CH₄, that is formed in the hydrothermal environment results as a powerful indicator of the arrival at the surface of the deep magmatic component (Chiodini, 2009). The observed correspondence between the geochemical anomalies and the geophysical signals are thus interpreted as a signal of the occurrence at depth of a magma degassing episode (MDE). The longest time series are available for Campi Flegrei and Vulcano: at Campi Flegrei 16 MDEs were detected in 1982-2017 (Chiodini et al., 2016, and unpublished data) while 6 MDEs occurred at Vulcano in 1979-2005 (Granieri et al., 2005). Similar episodes are documented also at Vesuvio, at Nisyros, at Panarea and at Mammoth Mt (California).

It is relevant that: (i) MDEs shows the same sequence of events, the geophysical signals preceding the geochemical anomalies of tens to hundreds days, a lag that, in our interpretation, corresponds to the time necessary for the transferring of the gas to from depth to the fumarolic effluents; (ii) the geochemical anomalies shows similar shapes that can be modeled as the result of the injection at depth of large amounts of magmatic fluids (Chiodini et al., 2003). The sudden release of magmatic fluids causes pressurization and heating of the hydrothermal systems and in turn earthquakes and ground deformations complicating the interpretation of volcanic unrests.

Chiodini G. 2009. CO₂/CH₄ ratio in fumaroles a powerful tool to detect magma degassing episodes at quiescent volcanoes.

Geophysical Research Letters, 36, L02302. <https://doi.org/10.1029/2008GL036347>

Chiodini G., Todesco M., Caliro S., Del Gaudio C., Macedonio G. & Russo M. (2003) - Magma degassing as a trigger of bradyseismic events; the case of Phlegrean Fields (Italy): Geophysical Research Letters, 30, 1434, <https://doi.org/10.1029/2002GL016790>.

Chiodini G., Paonita A., Aiuppa A., Costa A., Caliro S., De Martino P. & Vandemeulebrouck J. (2016) - Magmas near the critical degassing pressure drive volcanic unrest towards a critical state. Nature Communications, 7, 13,712. <https://doi.org/10.1038/ncomms13712>

Granieri D., Carapezza M.L., Chiodini G., Avino R., Caliro S., Ranaldi M., Ricci T. & Tarchini L. (2006) - Correlated increase in CO₂ fumarolic content and diffuse emission from la Fossa crater (Vulcano, Italy): Evidence of volcanic unrest or increasing gas release from a stationary deep magma body? Geophysical Research Letters, 33 (13), art. no. L13316.

Measuring and interpreting CO₂ and advective heat fluxes at regional scale: the case of Apennines, Italy

Chiodini G.*¹, Beddini G.², Caliro S.¹, Cardellini C.², Frondini F.² & Rosiello A.²

¹ INGV.

² Dipartimento di Fisica e Geologia, Perugia University.

Corresponding email: giovanni.chiodini@ingv.it

Keywords: CO₂, carbon dioxide degassing, Apennines, regional aquifers carbon balance.

Tectonically active regions are often characterised by a large amounts of carbon dioxide degassing, and estimation of the total CO₂ discharged to the atmosphere from tectonic structures, hydrothermal systems and inactive volcanic areas is crucial for the definition of present-day global Earth degassing. The carbon balance of regional aquifers is a powerful tool to quantify the diffuse degassing of deep inorganic carbon sources because the method integrates the CO₂ flux over large areas. In the last 20 years, the method, based on the isotopic composition of the inorganic carbon dissolved in the groundwater, has been systematically applied to the largest springs from the carbonate aquifers of the Apennines. The region results affected by specific CO₂ fluxes higher than the baseline determined for the geothermal regions of the world. Furthermore, the measured amount of endogenous CO₂ discharged through diffuse regional degassing in the peninsular Italy ($\sim 2.1 \times 10^{11}$ mol yr⁻¹) is the major component of the geological CO₂ budget of Italy, prevailing over the CO₂ discharged by Italian active volcanoes and volcanoes in hydrothermal activity.

The database of the largest springs of central Italy, originally produced for the carbon balance computations, has been successively used to compute the enthalpy balance of the aquifers. Practically, the geothermal heat flux affecting the aquifers was estimated starting from the temperature difference between recharge water and springs highlighting a relevant thermal anomaly in the Apennine. Italy is a historical geothermal region, but our researches have highlighted there are gaps in our knowledge of the real geothermal heat flux. The thermal gradients of the deep wells, which are the basis of the current heat flux map in Italy, are not significant in areas affected by important circulation of groundwater, such as the Apennines. In these zones most of the heat is transported by the groundwaters and is released by the springs. Furthermore, we have found a spectacular positive correlation between the geothermal heat and deep CO₂ dissolved in the groundwater. The results demonstrate that (i) the geothermal heat is transported into the aquifers by the same hot CO₂ rich fluids causing the Italian CO₂ anomaly and (ii) the advective heat flow is the dominant form of heat transfer of the region.

The monitoring of hydrogen and carbon dioxide at Stromboli volcano

Di Martino R.M.R.*¹, Camarda M.¹ & Gurrieri S.¹

¹ Istituto Nazionale di Geofisica e Vulcanologia, sezione di Palermo, Italy.

Corresponding email: roberto.dimartino@ingv.it

Keywords: Soil gases, Carbon dioxide, Hydrogen.

The monitoring of soil gases is a powerful tool for volcano surveillance, for investigating the subsurface magma dynamics and for gas hazard assessment in volcanic areas. High level of understanding of the processes affecting the gas emissions at the surface can be achieved by investigating the chemistry of the volcanic gases and the budget of gases discharged from a volcano. Several species have been targeted as tracers of volcanic activity. Among them, the carbon dioxide (CO₂) has been studied with great detail because a large amount of CO₂ may be escaping through the volcanic edifice during the volcanic crisis and the quiescent periods as well. The volcanic gas monitoring involves the use of electrochemical sensors deployed in the field. These systems can measure simultaneously the concentration of multiple gas species. Hydrogen (H₂) in the volcanic gases has a strong dependence from the temperature and the water dissolution equilibrium in the magmatic system. The monitoring of H₂ with the CO₂ has been effectively used to investigate the connection between volcanic gases and magmatic processes.

The CO₂ flux measurement is a routine technique for volcano monitoring purposes, because of CO₂ is the second-abundant component of the gas phase in silicate magmas, attaining saturation at the mantle to deep crustal level. The H₂ concentration has provided indications concerning the oxygen fugacity of magmatic gases, a parameter that changes over a wide range, and affects the redox state of multivalent elements.

This study reports on the use of a tailor-made automatic system developed for continuous monitoring of H₂ concentration and CO₂ flux in the summit area of Stromboli volcano (Aeolian islands). The automatic device consists of an electrochemical sensor H₂-selective, and two IR-spectrophotometers for measuring the CO₂ flux in agreement with the dynamic concentration method.

The data collected by the automatic system deployed at Stromboli from May 2009 to December 2010 are presented herein. The data indicate that the variations exhibited by CO₂ and H₂ are correlated with the eruptive activity of Stromboli, typically changing on time scale of hours or days. Furthermore, the investigation of the relationships between CO₂ flux and H₂ concentration provides an evaluation of the depth of the degassing source, which is an estimate of the depth from which the gases (CO₂-H₂-bearing mixture) start to move toward the surface following an advective-diffusive transport process. Our data suggest that the depth of that degassing source ranges between 2 and 4 km in the volcano plumbing system, in agreement with the magma storage zone that has been proposed by other geochemical, volcanological, petrological and geophysical investigations.

The on-field measurements of $^{13}\text{C}/^{12}\text{C}$ of the CO_2 improve the consolidated practices of volcano monitoring

Di Martino R.M.R.*¹, Capasso G.¹ & Camarda M.¹

¹ Istituto Nazionale di Geofisica e Vulcanologia, sezione di Palermo, Italy.

Corresponding email: roberto.dimartino@ingv.it

Keywords: Carbon dioxide, Stable isotopes, Carbon isotopes.

The monitoring of soil gases is a powerful tool for volcano surveillance, for investigating the subsurface magma dynamics and for gas hazard assessment in volcanic areas. High level of understanding of the processes affecting the gas emissions at the surface can be achieved by investigating the chemistry of the volcanic gases and the budget of gases discharged from a volcano. Several species have been targeted as tracers of volcanic activity. Among them, the carbon dioxide (CO_2) has been studied with great detail because a large amount of CO_2 may be escaping through the volcanic edifice during the volcanic crisis and the quiescent periods as well. The volcanic gas monitoring involves the use of electrochemical sensors deployed in the field. These systems can measure simultaneously the concentration of multiple gas species. Hydrogen (H_2) in the volcanic gases has a strong dependence from the temperature and the water dissolution equilibrium in the magmatic system. The monitoring of H_2 with the CO_2 has been effectively used to investigate the connection between volcanic gases and magmatic processes.

The CO_2 flux measurement is a routine technique for volcano monitoring purposes, because of CO_2 is the second-abundant component of the gas phase in silicate magmas, attaining saturation at the mantle to deep crustal level. The H_2 concentration has provided indications concerning the oxygen fugacity of magmatic gases, a parameter that changes over a wide range, and affects the redox state of multivalent elements.

This study reports on the use of a tailor-made automatic system developed for continuous monitoring of H_2 concentration and CO_2 flux in the summit area of Stromboli volcano (Aeolian islands). The automatic device consists of an electrochemical sensor H_2 -selective, and two IR-spectrophotometers for measuring the CO_2 flux in agreement with the dynamic concentration method.

The data collected by the automatic system deployed at Stromboli from May 2009 to December 2010 are presented herein. The data indicate that the variations exhibited by CO_2 and H_2 are correlated with the eruptive activity of Stromboli, typically changing on time scale of hours or days. Furthermore, the investigation of the relationships between CO_2 flux and H_2 concentration provides an evaluation of the depth of the degassing source, which is an estimate of the depth from which the gases (CO_2 - H_2 -bearing mixture) start to move toward the surface following an advective-diffusive transport process. Our data suggest that the depth of that degassing source ranges between 2 and 4 km in the volcano plumbing system, in agreement with the magma storage zone that has been proposed by other geochemical, volcanological, petrological and geophysical investigations.

Geochemistry of trace metals and REE in low temperature hydrothermal areas in Vulcano Island (Aeolian Islands, Italy)

Falcone E.E.*¹, Federico C.¹, Boudoire G.¹, Brusca L.¹, Bellomo S.¹ & Saiano F.²

¹ Istituto Nazionale di Geofisica e Vulcanologia, Sezione di Palermo.

² Dipartimento Scienze Agrarie, Alimentari e Forestali, Università di Palermo.

Corresponding email: eddaelisa.falcone@gmail.com

Keywords: Rare Earth Elements, Trace metals, Volcanic-hydrothermal system.

Effects of submarine hydrothermal venting on the balance of chemicals in seawater are known since the mid-1970s (German et al., 2002 and references therein). The present study provides insights upon geochemical processes involving trace metals and REE (Rare Earth Elements) discharged by submarine hydrothermal vents in the Levante Bay of Vulcano (Aeolian Islands). Samples were collected on July 2012 and October 2013 from several submarine vents, small natural pools and one thermal well, and analyzed for Fe, Mn, Cr, Ti, V, Se, Zn, Cs, Sr, Ba, As, and REE, besides major ions. The REE concentrations were measured by ICP-MS after co-precipitation onto newly-forming Fe(OH)₃ (Raso et al., 2013). Analytical data were compared with the results of equilibrium and reaction path modeling. The very reactive volcanic fluids undergo chemical modification during ascent, upon cooling and extensive water-rock interaction. When these fluids are emitted in submarine environment, dissolved metals undergo oxidative scavenging onto suspended particulate matter (SPM). Competitive equilibria between the aqueous complexes and SPM drive the fate of chemicals and affect their concentrations as result of fractionation mechanisms. The contamination of ambient seawater by hydrothermal fluids can be recognized by the pattern of normalized REE. Where acidic vapor is emitted from submarine vents, it likely remobilizes metals and REE from local sediments, thus increasing their mobility. The Y/Ho ratio is widely used to ascertain the competitive role of complexation and the precipitation of secondary minerals in controlling the fate of chemicals in seawater. The highest REE contents were measured in the bubbling pools and show near- or sub-chondritic Y/Ho ratios ($43 < Y/Ho < 51$), due to the isochemical leaching of local volcanic rock, driven by the H₂S-rich hydrothermal vapor. The higher than chondritic Y/Ho ratio in seawater has been attributed to the differential scavenging of Y and Ho in the SPM, having Ho a larger affinity for Fe-oxyhydroxides. The results of the equilibrium and reaction-path modeling show that the contents of chemicals are controlled by both the contamination of deep fluids and the processes of oxidation and co-precipitation in seawater. The modeling shows that, when acidic and reducing fluids interact with seawater, REE are scavenged by the newly forming solid carbonates, fluorite or Fe-oxyhydroxides, while they are also increasingly complexed in solution and the interplay between these two processes differs from an element to another.

German C.R., Colley S., Palmer M.R., Khripounoff A. & Klinkhammer G.P. (2002) - Hydrothermal plume-particle fluxes at 13 N on the East Pacific Rise. *Deep Sea Research Part I: Oceanographic Research Papers*, 49(11), 1921-1940.

Raso M., Censi P. & Saiano F. (2013) - Simultaneous determinations of zirconium, hafnium, yttrium and lanthanides in seawater according to a co-precipitation technique onto iron-hydroxide. *Talanta*, 116, 1085-1090.

The microbial community structure in a meromictic volcanic lake (Lake Averno, Italy)

Fazi S.^{*1}, Tassi F.²⁻³, Rossetti S.¹, Pratesi P.², Ceccotti M.¹, Cabassi J.²⁻³, Capecchiacci F.², Venturi S.²⁻³ & Vaselli O.²⁻³

¹ IRSA-CNR Water Research Institute, National Research Council of Italy, Monterotondo, Rome, Italy.

² Department of Earth Sciences, University of Florence, Italy.

³ IGG-CNR Institute of Geosciences and Earth Resources, National Research Council of Italy, Florence, Italy.

Corresponding email: fazi@irsa.cnr.it

Keywords: Lake Averno, volcanic lakes, microbial community, greenhouse gases.

Volcanic lakes are characterized by physicochemical favorable conditions for the development of reservoirs of greenhouse gases that can be dispersed to air during occasional rollover events. By combining a microbiological and geochemical approach, we showed that the chemistry of the CO₂- and CH₄-rich gas reservoir hosted within the meromictic Lake Averno (Campi Flegrei, southern Italy) are related to the microbial niche differentiation along the vertical water column. The simultaneous occurrence of diverse functional groups of microbes operating under different conditions suggests that these habitats harbor complex microbial consortia that impact on the production and consumption of greenhouse gases. In the epilimnion, the activity of aerobic methanotrophic bacteria and photosynthetic biota, together with CO₂ dissolution at relatively high pH, enhanced CO₂- and CH₄ consumption. At Lake Averno, the chemical, isotopic and microbiological data consistently indicate a strong inter-dependence between the chemical features of the dissolved gas reservoir and the microbial community structure along the vertical water column

Bioavailability of trace and ultratrace elements in soils in the Mt. Etna volcanic area: the role of the emission source and insights on their mobility in the interstitial solution

Federico C.*¹, Bellomo S.¹, Brusca L.¹, Calabrese S.², D'Alessandro W.¹, Falcone E.E.¹ & Longo M.¹

¹ Istituto Nazionale di Geofisica e Vulcanologia, Sezione di Palermo.

² DISTEM Department, University of Palermo.

Corresponding email: cinzia.federico@ingv.it

Keywords: rare earth elements, trace metals, volcanic soil.

Although trace and ultratrace elements are essential for living beings, they can become toxic at high concentrations and their potential toxicity is related principally to the bioavailability in the environment. Furthermore, the application of some ultratrace elements (rare earth elements, REE) in the high technology has raised their interest as potential emerging pollutants. Volcanoes are important natural chemical emitters and they can deeply affect the quality of air, water and soils, as well as the human health.

We report on the first data combining the rainfall trace metal contents in three different areas of Mt Etna, variably fumigated by the volcanic plume, and the trace and ultratrace element contents in soil, collected over the whole volcano. We analyzed separately the labile fraction of soil samples, considered the fraction bioavailable to plants and soil organisms living in. The complexing media used to extract the bioavailable fraction simulates the growth environment of plant roots.

Rainfall samples were collected from three rain gauges placed at different elevation on the Eastern flank of the volcano, the most exposed to airborne chemicals, and analyzed for Fe, Cr, Co, Ni, Se, Zn, Cu, Sr, Ba, Cd and As, besides major ions. Soil samples were collected at various elevations along the flanks of the volcano, and treated for the analysis of the pseudototal and bioavailable fractions. Major ions, transition metals (V, Mn, Fe, Co, Ni, Cu, Zn), As, Se and Tl, and REY were measured in both fractions.

The rainfall samples collected at close distance from the summit craters (less than 6 km) show the lowest pH values and highest concentrations for all analyzed elements. Analyzed samples are primarily enriched in metals leached from the airborne volcanic ash and few elements directly emitted by volcanic plume and transported by acidic gases (SO₂, HCl, HF). This is confirmed by the results of reaction-path modeling.

The trace and ultratrace contents of soil samples show peculiar patterns, apparently unrelated to the plume fumigation. The transition metal content in the bioavailable fraction account for less than 6 % of the pseudototal fraction and the highest contents were measured in soil samples less acidic and farthest from the summit craters. In particular, high Fe, Mn, Co, Ni, Pb, Zn, Cd contents are paralleled by high organic carbon contents, which increase downwind the summit vents. Two elements, Se and Tl, are enriched in soil samples collected at closer distance from the summit vents. Their origin is probably more directly related to the plume deposition. Concerning REY elements, their abundance in the bioavailable fraction is related to the Al contents and, therefore, to the Al-bearing secondary phases.

It is thus evident that the accessibility of plants to potentially harmful trace and ultratrace elements present in the soil is not simply related to the exposure to pollutants, but also to their fate in the pedogenetic environment.

Chemical weathering rates and CO₂ consumption in the eastern sector of Sila Massif (Calabria, Italy) inferred from riverine water chemistry

Fuoco I.*¹, Apollaro C.¹, Vespasiano G.¹, Timpano A.¹, Cundari F.¹ & De Rosa R.¹

¹ DiBEST – University of Calabria, Arcavacata di Rende (CS) Italy.

Corresponding email: ilaria.fuoco@unical.it

Keywords: chemical weathering, atmospheric CO₂ consumption, riverine water chemistry.

Chemical composition of river waters is the result of several contributes like atmospheric input, anthropogenic input and chemical weathering of different rocks. Carbonate and silicates weathering require atmospheric and soil CO₂ to occur, becoming a short-term and long-term sink to CO₂, respectively. Instead, evaporite weathering doesn't need of CO₂ attendance but this process provides a marked imprint on water chemistry. In this regard, the knowledge of the dissolved loads transported by rivers, allows an evaluation of weathering rates and an indirect estimation of the atmospheric CO₂ consumed by weathering (Donnini et al., 2016). In this paper the eastern sector of Sila Massif was studied considering the following main basins: Alli, Corace, Crocchio, Fiumarella, Neto, Simeri, Tacina e Trionto. For each river were selected the sampling sites where it was measured the river flow rate and water samples were collected and subsequently analyzed in laboratory for major compounds. Starting from rain composition, atmospheric and anthropogenic inputs were subtracted to total dissolved load allowing the estimation of silicates (SWR), carbonates (CWR) and evaporites (EWR) weathering rates (Li et al., 2016 and references in therein).

Considering the obtained results for each studied river, the total weathering rates are the following: (i) SWR= 73.3 t/km²a, (ii) CWR= 82.23 t/km²a, (iii) EWR = 212.53 t/km²a. Although evaporites outcrops are less abundant and they don't crop up in all basins, the weathering rates of these rocks is the highest in the studied area in that their dissolution is much faster than carbonate and silicate. In the same time, carbonate weathering (that include carbonate rocks s.s., carbonate cements and small carbonate minerals as dolomite and calcite that could be present as veins in silicate rocks) is easier than silicate one. On the basis of these results, an indirect estimation of CO₂ moles consumed was performed stating from reaction stoichiometry for silicate (CO₂_{sil}) and carbonate (CO₂_{carb}) weathering process, respectively. The results showed that the consumption of CO₂_{sil} is equal to 2.2x10⁶ mol/Km² a, whereas the consumption of CO₂_{carb} is equal to 1.3x10⁶ mol/Km² a, considering the eight main rivers that drain the studied area.

Donnini M., Frondini F., Probst J.L., Probst A., Cardellini C., Marchesini I. & Guzzetti F. (2016) - Chemical weathering and consumption of atmospheric carbon dioxide in the Alpine region. *Global and planetary change*, 136, 65-81.

Li J., Yuan G.L., Deng X.R., Jing X.M., Sun T.H., Lan, X X. & Wang G.H. (2016) - Major ion geochemistry of the Nansihu Lake basin rivers, North China: chemical weathering and anthropogenic load under intensive industrialization. *Environmental Earth Sciences*, 75(6), 453.

New perspectives in geothermal CH₄ output estimation

Gagliano A.L.*¹, Daskalopoulou K.² & D'Alessandro W.¹

¹ INGV sez. Palermo, Palermo, Italy.

² GFZ, Postdam, Germany.

Corresponding email: lisagagliano86@gmail.com

Keywords: methane flux, methanotrophs, hydrothermal activity.

Magmatic gases during their ascent to the surface may interact with hydrothermal systems. So, fluids initially rich in CO₂, SO₂, HCl and many others undergo scrubbing processes, mixing with other fluids and change in composition before they are released to the surface. Studies of these gases allow to rebuild their original composition in such way to assess variation on the volcanic and hydrothermal activity. Output estimations are also important in assessing their environmental impact. Such studies are quite complex and often a multidisciplinary approach is necessary, also considering microbes thriving in the degassing soils.

Here we show the results of a multidisciplinary campaign carried on at Nisyros Island (Greece), a quiescent but active volcanic system with strong hydrothermal activity, aiming at the estimation of its CH₄ output. CH₄ flux values ranging from -3.4 to 1420 mg/m² day were measured by using the accumulation chamber at 130 sites. Soils were sampled at 10 sites with different T (27-70 °C), pH (1.4-3.7) and gas composition (e.g. H₂S 0.3-3.6%). Soils were incubated in a CH₄-enriched atmosphere to measure CH₄ consumption. Values were in a range from 5 to 40 ng/g/h, with higher values in samples with milder environmental conditions (lower temperature and H₂S contents and higher pH).

The total estimated CH₄ output of the geothermal system is about 1.4 t/a, more than one order of magnitude lower than the previous estimation (54 t/a - Etiope et al., 2007). The latter was made by cross-correlating CO₂ output data with the CO₂/CH₄ ratios of its gaseous manifestations. On one hand, the great variability in space of the CO₂/CH₄ ratios of the fumarole emissions at Nisyros introduces a great uncertainty in the CO₂/CH₄ ratio used for the estimation; on the other hand, as previously evidenced (D'Alessandro et al., 2009, 2011), the difference can also be attributed to the disregarding of methanotrophic activity within the soils. Microbial activity has the potential to oxidize great quantities of CH₄ also within the soils of geothermal areas (Gagliano et al., 2014).

These results can be compared with those found at Pantelleria Island (Italy) and Sousaki (Greece) where the assessment of high methanotrophic activity evidenced an over-estimation of the CH₄ output and confirmed the efficiency of the soil to act as natural filter for greenhouse gases (D'Alessandro et al., 2009, 2011; Gagliano et al., 2014). Notwithstanding, the hydrothermal areas are a significant source of CH₄ but probably their contribution has been overestimated. A lot has still to be done to better constrain the global hydrothermal CH₄ burden but the importance of direct CH₄ flux measurements has to be underscored.

D'Alessandro W., Bellomo S., Brusca L., Fiebig J., Longo M., Martelli M., Pecoraino G. & Salerno F. (2009) - Hydrothermal methane fluxes from the soil at Pantelleria island (Italy). *Journal of Volcanology and Geothermal Research*, 187(3-4), 147-157.

D'Alessandro W., Brusca L., Kyriakopoulos K., Martelli M., Michas G., Papadakis G. & Salerno F. (2011) - Diffuse hydrothermal methane output and evidence of methanotrophic activity within the soils at Sousaki (Greece). *Geofluids*, 11(1), 97-107.

Etiope G., Fridriksson T., Italiano F., Winiwarter W. & Theloke J. (2007) - Natural emissions of methane from geothermal and volcanic sources in Europe. *Journal of Volcanology and Geothermal Research*, 165(1-2), 76-86.

Gagliano A.L., D'Alessandro W., Tagliavia M., Parello F. & Quatrini P. (2014) - Methanotrophic activity and diversity of methanotrophs in volcanic geothermal soils at Pantelleria (Italy). *Biogeosciences*, 11(20), 5865-5875.

Modelling the dynamics of volcanic lakes: Nyos Lake (Cameroon) and Albano Lake (Italy)

Grezio A.*¹, Costa A.¹, Rouwet D.¹ & Chiodini G.¹

¹ Istituto Nazionale di Geofisica e Vulcanologia.

Corresponding email: anita.grezio@ingv.it

Keywords: limnic eruptions, Nyos Lake, Albano Lake.

Limnic eruptions caused by excessive accumulation of magmatic CO₂ in crater lakes are rare but devastating. The present study aims to model the dynamics of volcanic lakes with the use of a three-dimensional primitive equation numerical model (Princeton Ocean Model). It contains an imbedded second moment turbulence closure schema for the vertical mixing coefficients. It is a sigma coordinate model with the vertical coordinate scaled on the water column depth and a free surface. Two case studies are considered: the Nyos Lake (Cameroon) where a gas disaster took place in 1986 and the Albano Lake (Italy) where anomalous degassing of likely magmatic origin is present. Averaged profiles of temperature and CO₂ recorded during different seasons and years are used as initial conditions in the numerical model for both lakes. The simulations were performed until the lake conditions reached the steady state (about 2-3 years in both case studies). Then horizontal winds are included to investigate the dynamics of the lakes, the variations in the vertical stratifications of the fluid and the potential overturning driven by the deepest layers with high content of CO₂. Scenarios of different stratifications and degassing improve the comprehension of the water mixing processes during the limnic eruptions to reduce the hazard of the volcanic lakes.

Relationships between CO₂ soil degassing and regional/local fault systems in the Kiejo-Mbaka geothermal prospect (Tanzania)

Lelli M.*¹, Taramaeli M.², Ariph K.², Sadock J.², Pisani P.³, Pasqua C.³, Principe C.¹, Mnzava F.², Armadillo E.⁴, Rizzello D.⁵ & Mkangala A.²

¹ IGG-CNR, Pisa.

² Tanzania Geothermal Development Company Limited (TGDC), Dar es Salaam, Tanzania.

³ ELC-Electroconsult, Milano, Italy.

⁴ DISTAV, University of Genova.

⁵ Tellus s.a.s., Italy.

Corresponding email: m.elli@igg.cnr.it

Keywords: CO₂ diffuse degassing, Volcano-tectonics, Fluid flow-path.

The Kiejo-Mbaka geothermal prospect in the Mbeya region of SW Tanzania was surveyed for geothermal exploration in a recent study co-financed by the Ministry for Foreign Affairs in Iceland and by the Nordic Development Fund (NDF) and implemented by the Tanzania Geothermal Development Company Limited (TGDC). A multidisciplinary approach was adopted, including geological, geochemical and geophysical surveys. The prospect falls within the southern sector of the Rungwe Volcanic Province (RVP), which is situated at the triple junction of the Rukwa, Usangu and Karonga basins of the East Africa Rift System.

Recent volcanism is concentrated in the northern sector of the RVP, whereas recent eruptions were sustained by small magma batches derived from deep sources in the prospect area. Local stratigraphy is mainly characterized by Pre-Cambrian rocks of the metamorphic-intrusive complex covered by Pleistocene volcanic products (basalts and ignimbrites) with a thickness never exceeding 200 m. Several fault systems are present, among which the most important trends are oriented NW-SE and N-S. The main tectonic feature is the NW-SE-trending Mbaka fault, which controls the local emergence of hot waters at Ilwalilo and Kilambo-Kajala (maximum discharge temperature of 64°C), delimits to the W the Mbaka ridge, and is associated with a series of parallel structures extending in the plain. Both the gravimetric and the electromagnetic surveys concur in identifying the existence of a block corresponding to the above mentioned Mbaka ridge and characterized by a pronounced positive Bouguer anomaly and by high resistivity, due to the proximity of basement rocks. NS and NNW/SSE faulting has been also detected. At Kiejo, Ikama, and Lufundo there are gas vents emitting CO₂-rich gases, which are captured by drilled wells in the first two sites.

Since the Kiejo-Mbaka prospect is classified as an extensional domain, in which flow-paths of geothermal fluids are fault-controlled, part of the geochemical survey was addressed to identify and define the relationships between fluid flow and structures at local scale, in selected hydrothermal areas including Kilambo-Kajala, Ilwalilo and Kiejo. Considering the regional faults distribution and the preliminary results obtained during the geological and geochemical field surveys, also other areas were included in the investigation (i.e. Lufundo, Itende and Kikusya). A total of 598 soil CO₂ flux and temperature measurements (~1 m depth) were carried out. Total output was estimated and iso-flux maps were elaborated for each investigated sector. In general, CO₂ fluxes appear to be controlled by NW-SE and N-S trending faults and fractures. The former prevails at Kiejo, Kilambo-Kajala and Ilwalilo, which is not surprising for Kilambo-Kajala and Ilwalilo, since the hot springs are positioned along the Mbaka fault. In contrast, the N-S trend dominates in Lufundo area.

Preliminary study on geogenic degassing through the big karstic aquifers of Greece

Li Vigni L.*¹, D'Alessandro W.¹, Cardellini C.², Daskalopoulou K.³, Calabrese S.¹⁻³ & Brugnone F.³

¹ Istituto Nazionale di Geofisica e Vulcanologia, sezione di Palermo.

² Dipartimento di Fisica e Geologia, Università di Perugia.

³ Dipartimento delle Scienze della Terra e del Mare, Università di Palermo.

Corresponding email: livignilorenza@gmail.com

Keywords: CO₂ degassing, carbon cycle, karst aquifers.

Non-volcanic degassing contributes to the C-cycle by providing on a global scale a significant amount of CO₂ emitted through diffuse earth degassing processes (Kerrick et al., 1995). Due to the elevated solubility of the CO₂ in water, in the areas where high CO₂ fluxes directly affect regional aquifers, most of it can be dissolved, transported and released by groundwaters. Therefore, quantification of this contribution to the atmosphere has a substantial implication for modeling the global carbon cycle. According to Chiodini et al. (2000), total dissolved inorganic carbon (TDIC) concentrations and $\delta^{13}\text{C}_{\text{TDIC}}$ values of groundwaters are useful tools to both quantify the geogenic degassing and distinguish the different carbon sources. This approach was proved to be valid for central Italy and can possibly work for continental Greece; due to similar geodynamic history. Greece is considered one of the most geodynamically active regions and is characterized by intense geogenic degassing. The main source of degassing in the Hellenic area is concentrated on hydrothermal and volcanic environments (Daskalopoulou et al., 2019), however, the impact of geogenic CO₂ released by tectonically active areas shouldn't be disregarded. Aim of this work is to quantify the CO₂ degassing through aquifers hosted in the carbonate successions in the Hellenic region.

95 karst, thermal and cold waters were collected in the northern and central part of Greece with some of which being characterized by bubbling of CO₂-rich gases. Results show that karst waters have a typical Ca-HCO₃ composition. Thermal and cold waters show two different compositions: some samples are characterized by Ca-HCO₃ composition suggesting the presence of a carbonate basement, whilst others have a prevailing Na-HCO₃ composition. On the basis of TDIC concentrations and $\delta^{13}\text{C}_{\text{TDIC}}$ values, the springs are divided into two groups. The first group includes karst waters and some of thermal waters and is characterized by low TDIC concentrations and negative $\delta^{13}\text{C}_{\text{TDIC}}$ values. This group shows no evidence of deep CO₂ contributions, whereas the carbon of these waters derives from dissolution of carbonate minerals by organic derived CO₂. Remaining samples belong to the second group and present intermediate to high TDIC concentrations and $\delta^{13}\text{C}_{\text{TDIC}}$ values, indicating a possible input of inorganic CO₂. Some of these springs are characterized by gas bubbling at discharge, suggesting an extensive degassing.

Chiodini G., Frondini F., Cardellini C., Parello F. & Peruzzi L. (2000) - Rate of diffuse carbon dioxide Earth degassing estimated from carbon balance of regional aquifers: The case of central Apennine, Italy. *Journal of Geophysical Research: Solid Earth*, 105(B4), 8423-8434.

Daskalopoulou K., Calabrese S., Gagliano A.L. & D'Alessandro W. (2019) - Estimation of the geogenic carbon degassing of Greece. *Applied Geochemistry*.

Kerrick D.M., McKibben M.A., Seward T.M. & Caldeira K. (1995) - Convective hydrothermal CO₂ emission from high heat flow regions. *Chemical Geology*, 121(1-4), 285-293.

Travertine masses from western Central Italy and natural Earth degassing: an approach to evaluate the geogenic CO₂ flux

Mancini A.*¹⁻⁵, Frondini F.¹, Capezzuoli E.², Galvez Mejia E.¹, Lezzi G.¹, Matarazzi D.¹, Brogi A.³⁻⁴ & Swennen R.⁵

¹ Department of Physics and Geology, University of Perugia.

² Department of Earth Sciences, University of Florence.

³ Department of Earth and Geoenvironmental Sciences, University of Bari “Aldo Moro”.

⁴ IGG-CNR, Institute of Geosciences and Earth Resources, Pisa.

⁵ Department of Geology, Earth and Environmental Sciences, Heverlee, Belgium.

Corresponding email: alemancini84@yahoo.it

Keywords: Travertines, CO₂ flux, Central Apennine.

Understanding the global geological carbon cycle is an important target to better quantify the carbon fluxes between solid Earth and its atmosphere. In general, the most important CO₂ contributors are related to metamorphic and/or magmatic-mantle processes, in relation to active and quiescent volcanoes, fault zones in seismic and geothermal areas, CO₂ rich groundwater, etc.

We propose a simple method to evaluate the CO₂ fluxes in areas characterized by travertine deposition and where travertine masses deposited in the past. Such a method has been applied in western Central Italy for the broadest travertine deposits: Rapolano Terme, Canino and Tivoli. Here the travertine deposition is (and was) driven by CO₂ degassing of hydrothermal fluids circulating in deep carbonate-evaporite reservoirs, which finally discharged at the surface being tectonically controlled. Based on volume and age of the travertine masses it is possible to evaluate the amount of CO₂ discharged over time.

The results obtained show that the study areas, since Middle Pleistocene, are characterized, by diffuse CO₂ degassing processes with CO₂ fluxes ranging between $1.24 \pm 0.12 \times 10^6 \text{ mol y}^{-1} \text{ km}^{-2}$ and $1.38 \pm 0.42 \times 10^6 \text{ mol y}^{-1} \text{ km}^{-2}$. The values obtained are of the same order of magnitude of carbon dioxide fluxes measured by different methods in western central Italy. Moreover, these values are higher than the global baseline CO₂ flux from high heat flow regions.

Taking into account the widespread occurrence of travertine deposits worldwide, the reported approach can be used as a reliable tool to characterize the CO₂ flux in different geodynamic settings within system Earth.

Geochemical features of the shallow aquifer in the former mining area of Abbadia San Salvatore (Tuscany, central Italy)

Meloni F.*¹, Vaselli O.¹⁻², Nisi B.³, Rappuoli D.⁴, Cabassi J.¹⁻² & Bianchi F.⁵

¹ Dept. Earth Science, Florence, Italy.

² CNR-IGG, Florence, Italy.

³ CNR-IGG, Pisa, Italy.

⁴ Unione dei Comuni Amiata-Val D'Orcia, Castiglion d'Orcia, Siena, Italy.

⁵ S.B.C. Geologi Associati, Florence, Italy.

Corresponding email: chiccafede95@gmail.com

Keywords: Mt. Amiata, water, Mercury.

The geochemical characteristics of groundwater samples from the former mining area of Abbadia San Salvatore (Mt. Amiata, Siena, central Italy) were examined. In January 2017, 41 waters were collected and analyzed by acidimetric titration, colorimetry and ion chromatography (main and minor solutes) and ICP-MS (As, Sb, and Hg). The recorded temperatures matched those related to the sampling period while the pH values were generally close to neutrality, while those of electrical conductivity did not exceed 2,000 mS/cm. The water composition was characterized by two geochemical facies: Ca-SO₄ and Ca-HCO₃, likely related to dissolution processes mainly involving carbonate and sulfate minerals. Generally speaking, the concentrations of As and Sb were mostly lower than those defined by Italian law (Leg. Decree 152/2006), whereas those of Hg were very often higher than the permissible concentration limit (PCL) for water consumption (>1 mg/L) and industrial waters (5 mg/L). Nevertheless, it is worth to mention that waters collected downstream showed Hg contents lower than PCL. By comparing specific dot-maps that were built for As, Hg and Sb with those obtained in the 2013-2014 period, a significant decrease was observed. This decrease was possibly due to the construction of a bypass channel that cuts the whole mining area, allowing to recover the surface waters in order to minimize the water-rock interaction processes between meteoric waters and the terrains, which are mostly consisting of material associated with the mineral production processes. Periodic geochemical surveys of the shallow aquifer system can likely provide useful information to understand how to proceed for the reclamation phase that is expected to start early 2020.

A geochemical reappraisal of the hydrothermal system of La Soufrière of Guadeloupe (French West Indies) with implications for unrest

Moretti R.^{*1-2}, Moune S.¹⁻²⁻³, Robert V.¹⁻², Bonifacie M.¹⁻², Jessop D.¹⁻²⁻³ & Komorowski JC.¹⁻²

¹ Université de Paris, Institut de Physique du Globe de Paris, CNRS, Paris, France.

² Observatoire Volcanologique et Sismologique de Guadeloupe, Institut de Physique du Globe de Paris, Gourbeyre, France.

³ Université Clermont Auvergne, CNRS, IRD, OPGC, Laboratoire Magmas et Volcans, Clermont-Ferrand, France.

Corresponding email: moretti@ipgp.fr

Keywords: unrest, phreatic eruption, hydrothermal system.

We have re-assessed the main physicochemical features of the hydrothermal system of La Soufrière of Guadeloupe (FWI) andesitic volcano. A careful analysis of different techniques adopted historically for gas sampling and analysis by OVSG has allowed us to extend the use of our modeling and of gas thermobarometers as back as possible to the last 20 years, also including data from the 1976-77 phreatic eruption. We then tracked the evolution of P-T conditions of the gas equilibrium zone within the hydrothermal system, often reaching or exceeding critical point conditions. Our results show that long-term P-T fluctuations characterize the behavior of the hydrothermal system in relation to injections of more magmatic deeper-sourced fluid into the hydrothermal system. This is also corroborated by concomitant fluctuations of halogen species recently determined in alkaline samples as well as condensates. Whether such long-term P-T increases reflect an oscillating behavior of the deep source injecting fluids upward, or are due to the modulation determined by the volcano structure via the many structures dissecting the edifice and relaxing the accumulated tensions, is matter of the ongoing investigations. Nevertheless, available data show that the recent unrest phase recorded between February and the end of April 2018 (Moretti et al., submitted; see also OVSG-IPGP reports) was due to the temperature increase and pressure build-up of the hydrothermal system, which originated a rapidly occurring (in the order of days) but sharp peak in monitored geochemical quantities. Therefore, scenarios that could lead to the sudden decompression of critical fluids must be considered in monitoring strategies and risk analysis.

Unravelling hypogean mineralizing fluids from the geochemistry of epigean travertines: insights from central-southern Tuscan (Italy)

Nicodemi L.*¹, Brogi A.²⁻³, Capezzuoli E.⁴, D'Orazio M.¹, Fulignati P.¹ & Zanchetta G.¹

¹ Dipartimento di Scienze della Terra, Università di Pisa.

² Dipartimento di Scienze della Terra e Geambientali, Università di Bari.

³ IGG-CNR, Pisa.

⁴ Dipartimento di Scienze della Terra, Università di Firenze.

Corresponding email: andrea.brogi@uniba.it

Keywords: travertine, hydrothermal fluids, southern Tuscany.

Southern Tuscany was one of the most important mining regions of Italy: pyrite, iron oxides, base metals, mercury, antimony and silver were mined since the Etruscan age up until the early '90s of the XX century. The region is interested by post-apenninic extensional tectonics progressively migrating eastwards. This extension caused Neogene-Quaternary magmatism that acted as heat source for a widespread hydrothermal activity, often leading to the formation of mineral deposits. Starting from the mid '80s of the XX century, some carbonate-hosted Sb-Hg (and minor Au) mineralizations belonging to the so-called Carlin type were identified in southern Tuscany, mainly at the edges of Larderello and Mt. Amiata geothermal fields. This type of deposit is genetically linked to sustained hydrothermal circulation and jasperoid alteration at depth.

Travertine can be considered a notable paleo-surface expression of these fossil hydrothermal systems. It is a continental limestone that forms where hydrothermal waters emerge. Another kind of continental chemically-precipitated limestone is cold-water travertine, also known as tufa.

The goal of this study is to verify if travertine and tufa composition can act as geochemical pathfinder for the occurrence of mineralization at depth. This will be done looking for relationships between secondary chemical features (such as trace elements abundances, REE partitioning and C, O and Sr isotope composition) of these rocks, their thermal affinity and the presence of associated epithermal mineralization.

This research has been carried out on many samples collected in central and southern Tuscany. The collected samples come both from mineralized (Sb-Hg ± Au) and unmineralized areas for comparison. Tufa and travertine samples were investigated by optical microscopy and back-scattered imaging with SEM-EDS, and analyzed for trace elements (Li, Be, V, Cr, Co, Cu, Zn, Ga, Rb, Sr, Y, Zr, Nb, Mo, Ag, Sn, Cd, Sb, Cs, Ba, La, Ce, Pr, Nd, Sm, Eu, Gd, Tb, Dy, Ho, Er, Tm, Yb, Lu, Hf, Ta, W, Tl, Pb, Bi, Th, U with ICP-MS, Hg with DMA-80). Stable ($\delta^{18}\text{O}$ and $\delta^{13}\text{C}$) and radiogenic ($^{87}\text{Sr}/^{86}\text{Sr}$) isotopes were also determined.

The results allow discriminating between the epigenetic and hypogenic origin of parent fluids. The metal contents vary, with the majority of samples showing both positive and negative anomalies, which could be related with the fluids origin, their temperature and the lithologies they passed through.

If the results show consistent correlation, this study will not only strengthen the role of travertine analyses as geochemical indirect methodology for mineral exploration in certain contexts but could also imply other uses, such as getting insights on potentially toxic elements natural occurrences or helping to model the underlying hydrologic reservoir lithologies where the fluids passed through.

Does the anthropogenic lake Ex-Snia, in the centre of Rome, simulate the characteristics of a volcanic lake?

Procesi M.*¹, Cinti D.¹, Cabassi J.², Capecchiacci F.¹, Caracausi A.¹, Pizzino L.¹, Fazi S.³ & Casentini B.³

¹ Istituto Nazionale di Geofisica e Vulcanologia, Roma, Italy.

² Università degli Studi di Firenze, Dipartimento Scienze della Terra, Italy.

³ IRSA-CNR, Monterotondo, Roma, Italy.

Corresponding email: monia.procesi@ingv.it

Keywords: anthropogenic lake, Rome, degassing.

Lago Ex-Snia is a small lake in the eastern sector of the urban area of Rome. It has an anthropogenic origin related to a great urban speculation of the '90s that, in the attempt to illegally build a shopping center, brought the underlying aquifer to be intercepted, giving rise to a mirror of water: Lago Ex-Snia.

The lake is 10.000 mq large, around 7 meters deep and it is hosted in the distal deposits of the Colli Albani Volcanic Complex. In particular, it is located in an area named "Acqua Bullicante" (i.e. Bubbling Water) since degassing phenomena were historically recognised. Unfortunately today, these phenomena are not recognizable due to the huge overbuilding.

In this framework, Lago Ex-Snia could represent a natural laboratory to investigate potential degassing processes and analogies with volcanic lakes. Thus, a preliminary geochemical and microbial sampling survey was carried out. Conductivity, pH, and temperature were measured along a vertical profile of the lake from the surface to the maximum depth (7 meters) with a sampling interval of 1 meter. Samples for major, minor, trace elements, dissolved gases and stable isotopes were also collected at each sampling depth.

Preliminary results and the comparison with geochemical data from neighboring wells suggest an origin of the lake's water from the shallow aquifer hosted in the volcanic deposits. Dissolved gases and, carbon and helium isotopic data do not show any magmatic/mantle input.

Although no "volcanic" input is recognized, the accidental birth of the Lago Ex-Snia gave as the opportunity to study the fluid geochemical in a strongly urbanized environment as Rome. Moreover, the characterization of the Lago Ex-Snia from a geochemical point of view has represented the first step for the official ratification of the site as natural protected area.

Fluid geochemistry and CO₂ output in the southern Apennine (Italy): Preliminary results

Randazzo P.*¹, Caracausi A.², Apollaro C.³, Cardellini C.⁴, Chiodini G.⁵, Paternoster M.⁶,
Rosiello A.⁴ & Aiuppa A.¹

¹ Dipartimento di Scienza della Terra e del Mare, Università degli Studi di Palermo.

² Istituto Nazionale di Geofisica e Vulcanologia- sez. di Palermo.

³ Dipartimento di Biologia, Ecologia e Scienze della Terra, Università della Calabria.

⁴ Dipartimento di Fisica e Geologia, Università degli Studi di Perugia.

⁵ Istituto Nazionale di Geofisica e Vulcanologia- sez. di Bologna.

⁶ Dipartimento di Scienze, Università degli Studi della Basilicata.

Corresponding email: paolo.randazzo@unipa.it

Keywords: carbon dioxide, degassing, Helium.

Although central to our understanding of planetary evolution over geological time, past and present natural CO₂ fluxes are poorly quantified. This limited knowledge is caused by CO₂ being emitted from the Earth's interior in different geodynamical contexts, in different modes and at different rates. Mantle degassing and CO₂ emissions from the Earth's mainly occur in volcanic regions, in young oceanic lithosphere setting, but an active and robust CO₂ degassing also occurs in seismically/tectonically active regions, that are punctuated by CO₂-rich manifestations, including cold gas vents, degassing soils and CO₂-rich springs. These manifestations are clear hints for anomalous transport of deep CO₂ toward the surface through faults systems.

Regional aquifers, in particular, can dissolve large amounts of CO₂ providing geochemical evidences for deep degassing processes at regional scale. Studying regional aquifers and their main springs is thus key to establishing regional CO₂ budgets. Here we present preliminary results of a geochemical study on CO₂ degassing in the southern Italy (Basilicata-Calabria area). The investigated area is a tectonically active region, where historical and recent earthquakes have been recorded (magnitude up to 5.2). We collected and analysed 45 samples, both cold and thermal groundwaters, with the aim of defining the origin of the dissolved gases, quantifying the CO₂ output at regional scale and understanding the origin for regional thermalism. In this contest, helium has been used as the key tracer for recognizing the contributions of crustal and mantle components and the associated heat. The collected water have been divided in 3 groups on the basis of their major element chemistry: Ca(Mg)-HCO₃, Mg(Ca)-HCO₃ and Ca(Na)-SO₄. The δ¹⁸O and δD isotopic signature of groundwaters falls close the Eastern Mediterranean Meteoric Water Line (EMMWL) indicating its meteoric origin. Helium and neon isotopes indicate our samples fall in the field of ASW (Air Saturated Water), with the exception of the thermal waters. The latter identify mixing between atmospheric and a radiogenic end members, but these also exhibit trace mantle contributions. Coupling Total Dissolved Inorganic Carbon (TDIC) and δ¹³C compositions we identified 2 groups of waters (i) infiltrating waters, with low δ¹³C_{TDIC}, and (ii) a group of samples with more positives δ¹³C_{TDIC} and higher TDIC, indicative of outgassing of deeply sourced CO₂. By applying the carbon mass balance approach proposed by Chiodini et al. (2000) and considering the hydrogeological parameters of the studied springs, a first estimate of the deep CO₂ flux has been attempted.

Chiodini G., Frondini F., Cardellini C., Parello F. & Peruzzi L. (2000) - Rate of diffuse carbon dioxide Earth degassing estimated from carbon balance of regional aquifers: The case of central Apennine, Italy. *J. Geophys. Res.*, 105(B4), 8423-8434.

CO₂ Earth Degassing in Southern Italy: quantification and source identification of the main regional aquifers of the Southern Apennines and Gargano Promontory

Rosiello A. *, Cardellini C., Chiodini G., Frondini F. & Caliro S.

Dipartimento di Fisica e Geologia, Università degli studi di Perugia.

Corresponding email: geol.angelo.rosiello@gmail.com

Keywords: CO₂, hydrogeochemistry, Southern Italy.

In this work we present an evaluation of the carbon fluxes of some hydrogeological system of Southern Italy, to improve our knowledge about the CO₂ Earth degassing in non volcanic areas with an active tectonic. Although it seems unequivocal that the impact of anthropogenic CO₂ emissions are playing an important role in the acceleration of the climate change, it's still incomplete our understanding about natural processes that determine the input of greenhouse gases into the atmosphere. So, it's necessary to increase the number of studies to better describe the processes that transfer CO₂ into the atmosphere from Earth interior, oceans and biosphere and to quantify the carbon fluxes for improving the future climate projections and the evolution of the global carbon cycle in geological times. The first studies that started to highlight the evidence of earth degassing processes in non volcanic areas were made for central and part of the southern Italy, that finally produced the edition of the first regional map of CO₂ Earth Degassing (Chiodini et al., 2004), quantifying the CO₂ dissolved in the main regional aquifers of central Apennines through the isotopic mass balance of the dissolved inorganic carbon. Large portion of the Italian peninsula are still not investigating and the main objective of this work is to extend the study area to the southern Italy. It was investigated the main regional aquifers hosted in the carbonatic hydrogeological units of Southern Apennines (Campano-Lucana Carbonatic Platform), the Gargano Promontory and the aquifers of the calcareous-siliceous sequence of the Lagonegro basin. Furthermore it was investigated some gas emission springs located in the study area and included into the gas emission's catalogues (<http://www.magadb.net>). For each hydrogeological structure the main springs were sampled selecting those of large flow rate. The produced dataset includes physical and chemical parameters of the water, major ions concentrations, waters isotopes composition, isotopic composition of the Total Dissolved Inorganic Carbon and the concentrations of dissolved gas. These data were used for the geochemical classification of the groundwaters, for the definition of the recharging areas combining hydrogeological data with isotopic composition of the sampled waters and to quantify the dissolved CO₂ released by the springs through the isotope-mass balance of the dissolved inorganic carbon. Finally, for each investigated aquifer the CO₂ degassing mean rate was estimated, combining hydrogeological and geochemical data.

Chiodini G., Cardellini C., Amato A., Boschi E., Caliro S., Frondini F. & Ventura G. (2004) - Carbon dioxide Earth Degassing and seismogenesis in central and southern Italy. *Geophysical Research Letters*, 31, 1-4.

Resuming volcanic surveillance at Lake Albano: updates on the dissolved gas content and vertical temperature profiles

Rouwet D.*¹, Tamburello G.¹, Procesi M.², Venturi S.³, Santi A.³, Chiodini G.¹, Pecoraino G.⁴, Ricci T.², Cabassi J.³ & Tassi F.³

¹ Istituto Nazionale di Geofisica e Vulcanologia, Sezione di Bologna, Italy.

² Istituto Nazionale di Geofisica e Vulcanologia, Sezione di Roma 1, Italy.

³ Department of Earth Sciences, University of Florence, Italy.

⁴ Istituto Nazionale di Geofisica e Vulcanologia, Sezione di Palermo, Italy.

Corresponding email: dmitri.rouwet@ingv.it

Keywords: Lake Albano, CO₂ degassing, monitoring.

In April 2019, in the framework of the FISR-2016 CALAPA project, Lake Albano (Colli Albani volcanic complex, Rome, Italy) was the target of a geochemical sampling and measurement campaign, the first one of this kind since May 2010 (Chiodini et al., 2012). Conductivity, pH, and temperature were measured along the vertical profile of the lake, until a maximum depth of about 160 m. An evident thermocline is observed near 10 m depth, showing a T drop from 13.1°C at the surface to 9.9°C near 20 m depth. This thermocline has remained stable with respect to May 2010: a T drop from 16 to 10°C in May 2010 for the same depth interval. Temperature further dropped till 9.2°C between 20 m depth and the bottom. The 95 m thermocline, as observed in May 2010, was less evident in April 2019, probably due to the fact that a lower bottom temperature was detected in May 2010 (8.7°C). pH dropped from 9.1 at the surface to 7.6 near the bottom. These pH values fit the increasing pH trend as observed between 1989 and 2010. Alkalinity follows a long-term decreasing trend. The degassing model for Lake Albano proposed by Chiodini et al. (2012) is revised based on the full chemical composition (dissolved gases, major, minor and trace elements, He-C isotope systematics of dissolved gases). Apparently, partial CO₂ degassing during density driven winter roll-over events is a fact, but not a factor to explain the alkalinity drop on the long-term. Temperature loggers were installed at six different depths (at 2, 8, 23, 43, 73 and 153 m depth) to track seasonal variations in lake water temperatures. This will enable to better understand thermal lake stratification, lake stability and its relation to CO₂ degassing from Lake Albano, and to better constrain the geochemical evolution shown by the lake during the last 30 years.

Chiodini G., Tassi F., Caliro S., Chiarabba C., Vaselli O. & Rouwet D. (2012) - Time-dependent CO₂ variations in Lake Albano associated with seismic activity. *Bullertin of Volcanology*, 74, 861-871.

The synthesis of fluid inclusions: from the lab to geothermal wells

Ruggieri G.¹, Orlando A.*¹ & Borrini D.²

¹ CNR IGG Firenze.

² Dipartimento di Scienze della Terra UNI FI.

Corresponding email: orlando@igg.cnr.it

Keywords: synthetic fluid inclusions, geothermal area, experiments.

The synthesis of fluid inclusions has classically several applications (i.e. solubility studies, P-V-T studies) and it is commonly run in lab through experimental apparatus. The synthesis is commonly obtained inserting pre-fractured quartz chips, aqueous fluid and SiO₂ powder in gold capsule which is subjected to P-T conditions pertaining to upper crustal conditions through cold seal vessel. The observation and microthermometric determinations of so produced fluid inclusions are useful to better interpret natural fluid inclusions commonly found in minerals.

The combination of suitable experimental apparatus in Experimental Mineralogy and Petrology Lab (CNR-IGG, DST-UNIFI) with microthermometric heating/freezing stage (CNR-IGG) encouraged us to synthesize fluid inclusions and to explore their application in geothermic issues.

Firstly, different sets of fluid inclusions were produced in lab with the aim to explore the feasibility of this technique up to 540 °C and 0.16 GPa. This technique, if run using a wide spectra of aqueous salinities could be useful to calibrate cold seal vessel and thus diminishing experimental uncertainty of P-T values.

Then, once expertise has been attained as regards also the time necessary to develop fluid inclusions, a method was elaborated aimed to the production of synthetic fluid inclusions in an apparatus that is then lowered in geothermal wells. This apparatus consists of a stain steel vessel (micro-reactor) partially filled with an amount of distilled water such that the P-T conditions in the micro-reactor will follow the liquid-vapour curve of H₂O and critical isochore of H₂O (characterized by a density of 0.322 g/cm³) above the critical point of H₂O. The gold capsule contains an alkaline and saline solution (~10 wt.% NaCl) that will be trapped in micro fractures of quartz chips. A set of experiments have been performed in the lab by placing the micro-reactor in a furnace. Experiments demonstrated that fluid inclusions form within a relatively short time (even in 48 hours) and their trapping temperatures give a good estimate of the experimental temperatures. Thus, two tests were performed in geothermal wells of Krafla (Iceland) and Larderello (Italy). Both tests show that synthetic fluid inclusions easily formed and that their trapping temperature (up to 343 °C) closely approach the measured temperature by using conventional methods, such as mechanical temperature and pressure gauges (Kuster device) and electronic devices.

The proposed method can be potentially used to measure the temperature in relatively high-temperature (>380°C) geothermal wells, such as those in super-hot geothermal systems. In fact, the measurement of temperature in the hottest areas of these geothermal wells could be very difficult and onerous through the application of conventional measurement methods. The method here proposed, based upon the synthesis of fluid inclusions could represent a valid alternative, deserving to be widely explored.

Distribution of the thermal springs in the world in relation to active volcanic and tectonic areas

Tamburello G.*¹ & Carbonara N.²

¹ Istituto Nazionale di Geofisica e Vulcanologia, sezione di Bologna

² Università degli Studi di Bologna, Dipartimento BiGeA

Corresponding email: giancarlo.tamburello@ingv.it

Keywords: thermal springs, volcanoes, tectonics.

Here we present a work-in-progress inventory of the thermal springs of the world obtained by the digitization of the manuscript “Thermal springs of the United States and other countries of the world; a summary” of Gerald A. Waring (1965). We provide the geographic coordinates of ~6500 thermal springs for 180 areas/countries, and we attempt to investigate, for the first time, their correlation with active volcanism and tectonics. Other supplementary information (e.g. temperature, flow) still needs to be derived from the previous work of Waring. Despite the current data set is merely spatial, it will offer considerable promise for future studies at a global scale of geodynamic-related processes such as the estimation of the crustal heat flow.

Past and present of geochemical investigations on meromictic volcanic lakes: hints for the next future

Tassi F.*

Dipartimento Scienze della Terra. Università di Firenze.

Corresponding email: franco.tassi@unifi.it

Keywords: volcanic lake, geochemistry, interdisciplinary investigation.

Volcanic lakes represent a common feature of active and quiescent volcanoes. Notwithstanding, the scientific community demonstrated a particular attention for their peculiar geochemical features only after the dramatic “limnic” event occurred at Nyos and Monoun lakes (Cameroun) three decades ago. Since then, a number of studies aimed to evaluate the hazard for further limnic eruptions has been carried out. At Nyos, the intervention of the local government in collaboration with an international scientific team, allowed the installation of a relatively simple system, consisting of tubing placed at depth, that allows the control of the gas recharge rate in the lake reservoir, efficiently preventing further events. Other meromictic volcanic lakes worldwide distributed have been investigated, evidencing different dynamics regulating the development of their dissolved gas reservoirs. Meromictic volcanic lakes in Europe (Italy, France, Germany, Portugal) as well as in Central America (Costa Rica, Nicaragua) and Africa (DRC) were deeply investigated by scientific groups, including geologists, botanists, limnologists, ecologists and microbiologists. The results of these studies clearly showed that the evolution of dissolved gas reservoirs is regulated by a complex balance between (i) CO₂-rich sub-lacustrine springs, adding deep-originated fluids to the lake system, and (ii) biogeochemical processes that mostly occur within the bottom sediments and in the monimolimnion. In these lakes, recently classified as *bio-activity* lakes, the Carbon cycle is intimately related not only to the fate of CO₂ but also to the role played by the activity of microbial communities able to interact with the external fluid source(s), resulting in consumption/production processes of methane. In such a complex environment, a multidisciplinary approach is to be regarded as the most promising method of investigation to assess the limnic hazard, as well as to investigate the microbial structure and behaviour at the anomalous conditions dictated by the occurrence of volcanic gases.

Preliminary geochemical investigation of the Colpitas hydrothermal system, northern Chile

Tassi F.*¹⁻², Inostroza M.³⁻⁴, Sepúlveda J.⁵, Capecchiacci F.⁶ & Aguilera F.⁵

¹ Dipartimento Scienze della Terra, Università di Firenze, Italia.

² CNR-IGG, Florencia, Italia.

³ Programa de Doctorado en Ciencias, mención Geología, Universidad Católica del Norte, Antofagasta, Chile.

⁴ Núcleo de Investigación en Riesgo Volcánico CKELAR, Universidad Católica del Norte, Antofagasta, Chile.

⁵ Departamento de Ciencias Geológicas, Universidad Católica del Norte, Antofagasta, Chile.

⁶ INGV sez. Napoli, Italia.

Corresponding email: franco.tassi@unifi.it

Keywords: Colpitas, Central Andean Volcanic Zone, hydrothermal fluid circulation.

The hydrothermal area of Colpitas is located in northern Chile, at a distance of 28 km from Putre village and 15 km W of the border with Bolivia. Two volcanoes, pertaining to the Central Andean Volcanic Zone (CAVZ), are located in the proximity, Taapaca and Lexone, although no information about their volcanic activity is available. The development of geothermal resources has recently raised the attention of the Chilean government, aimed to differentiate the sources for energy supply of the country, traditionally produced from Carbon. In agreement with this new policy, the study zone, where hydrothermal manifestations and altered terrains were historically recognized, was recently investigated to provide a preliminary geological and geophysical information, although after this initiative no further prospecting activity has been carried out. The present study, based on the geochemical analysis of fluids, is aimed to construct a conceptual model of hydrothermal fluid circulation, evaluate the fluid reservoir temperature and investigate the possible relationship with the near volcanoes. The hydrothermal area, about 4 km², is characterized by the occurrence of a number of thermal springs (>50 °C) with bubbling gases. Thermal waters, slightly acidic (pH 5-6) have a Na-Cl composition, typical of geothermal waters, and Cl concentrations up to 8,500 mg/L. Springs having lower outlet temperature (20-30 °C) have more acidic (pH 3-4) and show a Ca-SO₄ composition, likely due to the interaction of a shallow aquifer with the uprising gases. The gas phase is dominated by CO₂, followed by N₂ and CH₄, as commonly observed in hydrothermal gases. H₂S and H₂ were also present although at relatively low concentrations (<0.05 and 0.006% by vol., respectively). Geothermometric calculations in the H₂O-H₂-CO₂-CH₄-CO system suggests equilibrium temperatures of about 150 °C at R_H values of 3.4. At such redox conditions, the propane-propene pair indicates similar temperatures. The δ¹³C-CO₂ values are consistent with those of the mantle, but the R/Ra values indicate a He mantle contribution <20% and the CO₂/³He ratios are 1-2 orders of magnitude higher than that of the mantle, indicating a dominant CO₂ crustal source. Consistently, the δ¹³C-CH₄ values are typical of thermogenic gases. Further isotopic (e.g. water isotopes) and chemical (trace elements) analysis are still ongoing. Such a preliminary picture clearly evidences the occurrence of an anomalous geothermal gradient, whose cause(s) are to be deeply investigate adopting a multidisciplinary approach, also including geological observations and geophysical measurements in order to assess the geotectonic setting as well as the dimensions of the geothermal reservoir.

Mechanisms regulating CO₂ and CH₄ dynamics in the Azorean volcanic lakes (São Miguel Island, Portugal)

Tassi F.¹⁻², Cabassi J.*², Andrade C.³, Callieri C.⁴, Silva C.³⁻⁵, Viveiros F.³, Corno G.⁴, Vaselli O.¹⁻², Selmo E.⁶, Gallorini A.¹, Ricci A.¹, Giannini L.¹⁻² & Cruz J.V.³

¹ Department of Earth Sciences, University of Florence, Italy.

² Institute of Geosciences and Earth Resources, National Research Council of Italy, Florence, Italy.

³ Instituto de Investigação em Vulcanologia e Avaliação de Riscos, Universidade dos Açores, Portugal.

⁴ Institute of Ecosystem Study, National Research Council of Italy, Verbania, Italy.

⁵ Centro de Informação e Vigilância Sismovulcânica dos Açores, Universidade dos Açores, Portugal.

⁶ Department of Chemistry, Life Sciences and Environmental Sustainability, University of Parma, Italy.

Corresponding email: franco.tassi@unifi.it

Keywords: methane paradox, dissolved gas reservoir, microbiological activity.

Chemical and isotopic vertical profiles from the volcanic lakes of Sete Cidades, Santiago, Fogo, Congro and Furnas (Island of São Miguel, Azores Archipelago, Portugal) were studied to investigate the biogeochemical processes acting at different depths, with a focus on the CO₂ and CH₄ dynamics. These lakes are fed by meteoric water affected by seawater spray and interacting with volcanic rocks at a relatively low extent. In addition to volcanogenic gas inputs, the biogeochemical processes are influenced by microbial activities since the lakes offer specialized ecological niches for oxic and anoxic metabolism. The lakes were sampled in two extreme conditions of (partial) mixing (winter) and stratification (summer), respectively. The seasonal thermal stratification favored the development of anaerobic hypolimnia, showing relatively high concentrations of NH₄⁺, NO₃⁻, P and other minor species (Fe, Mn, Zn, As) controlled by microbial activity and mineralogical processes occurring within the lake sediments. The strongly negative δ¹³C-TDIC values measured in almost all the studied lakes suggest dominant contribution of organic carbon. Dissolved gases were mostly consisting of atmospheric compounds with significant concentrations of CO₂ and CH₄. The δ¹³C-CO₂ values were intermediate between those measured in the hydrothermal fluids and those typical of biogenic CO₂. Dissolved CH₄, which was the most abundant extra-atmospheric gas in the anoxic waters, was measured at significant concentrations even in the aerobic layers, especially in the winter season. This unexpected feature may tentatively be explained by admitting (i) convective mixing of shallow and deep waters, and/or (ii) aerobic CH₄ production. Further investigations, focusing on the recognition of microbial populations able to produce CH₄ at different redox conditions, may be useful to corroborate these intriguing hypotheses.

Tropical saline-alkaline lakes as a major source of greenhouse gases: evidence from lake Sonachi, Kenya

Venturi S.^{*1-2}, Cabassi J.¹⁻², Butturini A.³, Vazquez E.³, Pacini N.⁴, Tassi F.¹⁻², Vaselli O.¹⁻², Amalfitano S.⁵, Crognale S.⁵, Rossetti S.⁵, Harper D.M.⁶⁻⁷, Capecchiacci F.⁸ & Fazi S.⁵

¹ Department of Earth Sciences, University of Florence.

² Institute of Geosciences and Earth Resources, National Research Council (IGG-CNR), Firenze.

³ Department of Evolutionary Biology, Ecology and Environmental Sciences, University of Barcelona.

⁴ Department of Environmental and Chemical Engineering, University of Calabria.

⁵ Water Research Institute, National Research Council (IRSA-CNR), Roma.

⁶ Department of Geography, University of Leicester.

⁷ Freshwater Biological Association, Far Sawry, Ambleside, Cumbria.

⁸ INGV Istituto Nazionale di Geofisica e Vulcanologia – Osservatorio Vesuviano, Napoli.

Corresponding email: stefania.venturi@unifi.it

Keywords: soda lakes, biogeochemistry, greenhouse gases.

Lake Sonachi is a small (0.18 km²), endorheic, crater soda lake located within the Eastern Rift Valley, 90 km NW of Nairobi (central Kenya). It lacks surface inflows or outflows; its water balance is maintained by local precipitation in the crater catchment (~680 mm annual average) and subsurface inflow from the nearby freshwater Lake Naivasha, with water losses only due to evaporation (~1,870 mm per year). Despite its shallowness (5 m depth), the lake is meromictic, being characterized by (i) an upper water layer (mixolimnion; TDS around 8.6 g L⁻¹), affected by diel stratification and mixing, and (ii) a deep and persistent layer (monimolimnion; TDS up to 19 g L⁻¹) that does not participate in vertical mixing. The mixolimnion and monimolimnion are separated by a chemocline at 3.5-4 m depth. The relatively high amount of dissolved organic carbon in the monimolimnion (up to 500 ppm), resulting from the degradation of abundant organic matter stored in the bottom sediments, contributes to the chemical stratification of the water column (*biogenic meromixis*). The balance between photosynthetic production and microbial consumption largely regulates the dissolved gas concentrations in the water column. Microbial respiration in the anoxic deep layer leads to a significant storage of CH₄ (up to 615 μmol L⁻¹; δ¹³C-CH₄ values ≤ -60 ‰ vs. V-PDB), as well as CO₂. In the mixolimnion, aerobic metabolism consumes oxygen. The occurrence of biogenic CH₄ production, even at shallow oxic conditions, was indicated by large CH₄ concentrations (~150 μmol L⁻¹), associated with δ¹³C-CH₄ values down to -57 ‰ vs. V-PDB, measured in the shallowest water layers. Epilimnetic waters were undersaturated with CO₂ as a consequence and strikingly oversaturated with CH₄. Lake Sonachi thus behaves as a sink of CO₂, rather than an emitter (as commonly observed for active volcanic lakes), while it can be regarded as a huge emitter of CH₄ relative to freshwaters. The estimated water-air CH₄ exchange flux (up to ~3.65 g C m⁻² d⁻¹), calculated according to the thin boundary layer (TBL) model, is, to the best of our knowledge, the largest diffusive flux ever measured from a lake. The high CH₄ emission from Lake Sonachi was probably caused by its shallowness and high perimeter to volume ratio, favoring microbial respiration and resulting in limited CH₄ oxidation efficiency. It is worth noting that our estimation is probably conservative, as loss of CH₄ through bubbling was not estimated. However, our theoretical simulations indicate that ebullition along the water column might increasingly contribute to CH₄ emissions from the lake as a consequence of current and future temperature increases.

S30

Legacy and new applications of stable-isotope geochemistry

CONVENERS AND CHAIRPERSONS

Riccardo Petrini (Università di Pisa)

Lisa Ghezzi (Università di Pisa)

Maddalena Pennisi (IGG-CNR)

The link between groundwater and milk in the Parmigiano-Reggiano cheese production area: validation with the isotopic analysis for food traceability

Boito M.*¹, Iacumin P.¹ & Ogrinc N.²

¹ Department of Chemistry, Life Sciences and Environmental Sustainability, University of Parma.

² Jožef Stefan Institute, Ljubljana, Slovenia.

Corresponding email: marta.boito@studenti.unipr.it

Keywords: stable isotopes, Parmigiano Reggiano, origin.

Determination of the geographical origin of foodstuffs is becoming of increasing interest to consumers and producers, since it may be used as a criterion for certifying quality and authenticity. The Protected Designation of Origin (PDO) trademark has been assigned to numerous local products based on their area of origin. In order to obtain this designation, the raw materials must have been produced and processed in the specific region from which the product gets its name (Sacco et al., 2009; Dotsika et al., 2017). For traceability study the stable isotopes ratios ($^{13}\text{C}/^{12}\text{C}$, $^{15}\text{N}/^{14}\text{N}$, $^{87}\text{Sr}/^{86}\text{Sr}$, $^{18}\text{O}/^{16}\text{O}$, $^2\text{H}/^1\text{H}$) of animal feed (hay and fodder), groundwater and milk have been monthly investigated. The samples are from ten cattle-shed belonging to the “Consorzio del Parmigiano Reggiano” over a period of one year. The main aim of the investigation is the evaluation of the dependence of the isotopic composition of milk on food and water ingested by the cow and define the isotopic fractionation of water ingested/milk produced and milk produced/food supplied. The $^{18}\text{O}/^{16}\text{O}$ and $^2\text{H}/^1\text{H}$ isotope ratios of groundwater and local food are indicators of the area of the milk origin being affected by the climatic and geological factors. From the first results obtained it is possible to differentiate between plain and mountain milk. There is a correlation between water and milk values belonging to the same cattle-shed. Even, the hay produced locally by breeders is different compared to the one purchased by import indicating a geographic dependence. Overall, the results of the present study can be used to verify the possibility of discriminating the milk produced in different places on the basis of isotopic ratios, and develop a model for traceability (Camin & Bontempo, 2010).

Sacco D., Brescia M.A., Sgaramella A., Casiello G., Buccolieri A., Ogrinc N. & Sacco A. (2009) - Discrimination between Southern Italy and foreign milk samples using spectroscopic and analytical data. *Food Chemistry*, 114, 1559–1563.

Dotsika E., Bulleri E., Brunella R., Nudda A., Mele M., Battaglini R., Poutoukis D. & Chantzi P. (2017) - Fingerprinting the origin of sheep milk products based on H-O-C-N isotopes. *Integrative Food, Nutrition and Metabolism*.

Camin F. & Bontempo L. (2010) - Pascoli e Formaggi d'Alpe. *Atti del Convegno conclusivo del Progetto FISIR Pro-Alpe*. Torino, 65.

Inter-measurement determination of the isotopic composition of Sr (II)

Cavazzini G.*

CNR Istituto di Geoscienze e Georisorse.

Corresponding email: giancarlo.cavazzini@igg.cnr.it

Keywords: Rayleigh's distillation, isotopic composition, strontium.

Instrumental isotopic fractionation in mass spectrometer source can be interpreted in terms of Rayleigh' distillation process. The observed changes in measured values of isotopic ratios during spectrometric runs are quantitatively interpreted in terms of change in sample mass fraction, and of vapor/residue distribution coefficients (Ds) which values are different over the mass range of the isotopes of the element. (Cavazzini, 2009).

In different spectrometric runs of a same sample, in general, the $D=D(m)$ function is not reproduced. This irreproducibility can explain the observed change in the geometry of distributions of measured values isotopic ratios from run to run.

$\ln x$ vs. $\ln y$ distributions (x, y = measured values of isotopic ratios of the element) are linear distributions, theoretically, and, in practice, these distributions can be really linearly fitted with a very good success. Parameters of linear best-fit of a distribution (slope S and intercept I) are related to the true values of the isotopic ratios x_0, y_0 , and to ratios and differences between the values of the distribution coefficients of the isotopes that define the two ratios. They change from run to run, due to changes in the $D=D(m)$ function.

From a theoretical point of view, intra-run geometrical parameters S and I are fixed, and pairs (S, I) from distributions obtained in different spectrometric runs of a sample are not, in general, inter-run linearly correlated because of the change in the $D=D(m)$ curve from run to run.

However, if the isotopic ratios x, y are characterized by an equivalent mass difference between the mass at the numerator and the mass at the denominator, some quantities can be neglected, and pairs (S, I) from different runs are expected to be strictly linearly correlated. The true values of the isotopic ratios are expected to be the parameters of the correlation, so that we expect that the true values of the isotopic ratios can be determined by fitting a straight line through a set of pairs (S, I) from different runs of a sample (Cavazzini and Roccato, 2017).

In the case of two isotopic ratios x, y characterized by an equivalent mass difference between the isotope at the numerator and the isotope at the denominator, the change in the value of the ratio y/x is very small during run, even if the range of isotopic fractionation is large. This means that we know the value of quantity y/x with a certain good precision (note that is impossible for any of the isotopic ratios of the sample). We show that this quantity can be used as a useful constraint to calculate the true values of the isotopic ratios of the sample.

Cavazzini G. (2009) - Rayleigh's distillation law and linear hypothesis of isotope fractionation in thermal ionization mass spectrometry. *International Journal Mass Spectrometry*, 288, 84-91.

Cavazzini G. & Roccato D. (2017) - Inter-measurements determination of isotopic composition of Strontium (Abstract) in *Geosciences* "a tool in a changing world, Pisa, 4-6 Settembre.

First isotopic analyses in fluid samples using MC-ICP-MS (NEPTUNE PLUS™): results on Boron-poor fluvial and rain water (Adige basin)

Dordoni M.¹, Pennisi M.*¹, Agostini S.¹, Dini A.¹, Di Giuseppe P.¹, Rielli A.¹, Provenzale A.¹, Bianchini G.², Natali C.³, Marchina C.⁴ & Cidu R.⁵

¹ Istituto di Geoscienze e Georisorse, (IGG) CNR, Pisa, Italy.

² Dipartimento di Fisica e Scienze della Terra, Università di Ferrara, Ferrara, Italy.

³ Dipartimento di Scienze della Terra, Università degli Studi di Firenze, Firenze, Italy.

⁴ Dipartimento Territorio e Sistemi Agro-Forestali, Università di Padova, Legnaro, Italy.

⁵ Università degli Studi di Cagliari, Dipartimento di Scienze Chimiche e Geologiche, Monserrato (CA), Italy.

Corresponding email: m.pennisi@igg.cnr.it

Keywords: MC-ICP-MS, Boron isotope, Adige waters.

The advent of a last generation of instruments coupling mass spectrometers with a plasma source (MC-ICP-MS) allowed significant improvements in the analysis of B isotopes, such as an increased sensitivity, reduced mass bias and increased efficiency compared to PTIMS, while maintaining a comparable precision and accuracy. The impact of MC-ICP-MS in environmental research was even stronger than in other traditional disciplines of Earth Sciences. Indeed, these studies usually involve complex open systems, and a significant number of data needed, to constrain and trace sources and processes.

Since the mid-80s B isotopes have become increasingly important in hydrology, where are used to trace the processes controlling exchanges between different reservoirs and to distinguish the geogenic versus anthropogenic sources of contaminants. The B-poor water (<0.1 mg/L), and in particular rainwaters, where B is generally in the order of 1-50 ppb, suffers of significant analytical difficulties using TIMS, because of samples size (liter of samples needed) and a time consuming sample preparation. The use of MC-ICP-MS, performing analyses in the 10-15 ppb B range, have thus opened to the new investigation of meteoric, mountain and glacial waters.

We present here the first results of boron isotopic composition of fluid samples determined by MC-ICP-MS (Neptune PLUS™) at the IGG-CNR of Pisa (Pennisi et al., this Symposium). We have validated our new methodology with an intercalibration exercise using the IAEA standards B1 (sea water), B2 and B3 (groundwaters; Gonfiantini et al., 2003) together with a set of well-characterized samples (volcanic, thermal and geothermal fluids), and with a wide range of B concentration and isotopic composition ($-21.4\text{‰} < \delta^{11}\text{B} < +46.3\text{‰}$).

We determined boron isotopic composition of fluvial and rain waters from the Adige basin (Natali et al., 2016), characterized by B concentrations ranging from 3.0 ppb to 8.3 ppb for fluvial samples, and below 1.0 ppb for meteoric waters. The rainfall component ($+7.4\text{‰} < \delta^{11}\text{B} < +24.3\text{‰}$) generally matches the B isotopic signature of the river ($+4.5\text{‰} < \delta^{11}\text{B} < +9.4\text{‰}$) but cannot be considered as the main source of B in the system because of the higher B contents in the river waters. The comparison between $\delta^{11}\text{B}$ and nitrates in the river waters suggests that the anthropic input, if present, is subordinated.

Boron isotopic composition of fluvial waters of the Adige river finally appears to be mainly controlled by a meteoric and a geogenic component. The anthropogenic source of boron in the basin, if present, is subordinated.

We estimated a mean value for the isotopic composition of boron for the Adige river water ($\delta^{11}\text{B} = 7.3\text{‰} \pm 1.6$). This result will help assessing any future change in the B source/s of the Adige river system.

Natali C., Bianchini G., Marchina C. & Knöller K. (2016) - Geochemistry of the Adige River water from the Eastern Alps to the Adriatic Sea (Italy): evidences for distinct hydrological components and water-rock interactions. *Environmental Science and Pollution Research*, 23(12), 11677-11694.

Gonfiantini R., Tonarini S., Gröning M., Adorni-Braccesi A., Al-Ammar A.S., Astner M., Bachler S., Barnes R.M., Bassett R.L., Cocherie A., Deyhle A., Dini A., Ferrara G., Gaillardet J., Grimm J., Guerrot C., Krahenbuhl U., Layne G., Lemarchand D., Meixner A., Northington D.J., Pennisi M., Reitzenerová E., Rodushkin I., Sugiura N., Surberg R., Tonn S., Wiedenbeck M., Wunderli S., Xiao Y. & Zack T. (2003) - Intercomparison of boron isotope and concentration measurements. Part II: evaluation of results. *Geostandards Newsletter*, 27(1), 41-57.

Characteristics of hydrogen and oxygen stable isotopes in water from an area impacted by past-mining activity in southern Apuan Alps (Italy)

Doveri M.¹, Stenni B.², Giannecchini R.³, Petrini R.^{*3}, Ghezzi L.³, Dreossi G.⁴ & Menichini M.¹

¹ IGG-CNR, Pisa.

² Dipartimento di Scienze Ambientali, Informatica e Statistica, Università Ca' Foscari Venezia.

³ Dipartimento di Scienze della Terra, Università di Pisa.

⁴ IDPA-CNR, Venezia.

Corresponding email: riccardo.petrini@unipi.it

Keywords: hydrogen and oxygen isotopes, AMD-impacted waters, past-mining legacy.

The major environmental impact in past-mining areas is represented by acid drainages (AMD) and by the release of potentially toxic elements (PTE) produced by sulfide oxidation and their by-products. The oxidative reaction pathways of sulfide minerals and the fate of PTE are driven by the meteorological and hydrological regime throughout variations in the infiltration rate of oxygenated meteoric waters. Indeed, within the hydrologic system of post-mining workings, AMDs are generated continuously during the groundwater flow in channels and open voids, and the quantity and quality of acid water is dependent on recharge of the aquifer that is hydrologically connected to the mine. In this scenario, the interconnections between acidic water outflow fluxes and recharge of groundwater systems can represent a major environmental hazard. The ⁸O/¹⁶O and D/H ratios of water molecule, expressed through the $\delta^{18}\text{O}$ and δD values, act as conservative tracers in low-temperature water-rock interactions. This implies that changes in stable oxygen and hydrogen isotopic abundances reflect the variation in time and space in precipitations at recharge areas and physical processes during the fluid flow. However, it has been demonstrated that water is the primary source of oxygen in sulfide (pyrite) abiotic and biotic oxidation, yielding sulfate-water-oxygen fractionation.

The southern sector of the Apuan Alps chain (Tuscany Region, Italy) is characterized by the occurrence of sulfide-bearing mineral deposits since long exploited. Mine closure occurred at the beginning of 1990's, leaving the legacy of abandoned tunnels and mine waste residuals that introduce acidity and PTE outflows into the surface waters of the Baccatoio stream. Oxygen and hydrogen isotopic data were obtained on acid effluents, drippings in tunnels, stream water, springs and groundwater tapped by wells during different surveys in 2015. In addition, an isotopic local precipitation line (LMWL) was built by collecting monthly rainwater between 2014 and 2018. The LMWL is: $\delta\text{D}=7.02\pm 0.35\times\delta^{18}\text{O}+8.54\pm 2.89$. The data indicate that waters from different recharge areas enter the mine workings. The isotopic data are also consistent with the hypothesis that is the groundwater hosted in the aquifer systems, not the directly infiltrating rainwater, that enters the mine tunnel network, interacts with mineralization and contaminate. In addition, an isotopic shift towards heavier compositions is observed in drippings, possibly reflecting fractionation during pyrite oxidation/ferric iron hydrolysis. The isotopic data on stream water indicates that during storm events the runoff may affect episodically the stream flow, indicating contrasting infiltration regimes. The possible interconnections between groundwater pathways, interaction with mineralization and mixing with contaminated water bodies as revealed by the O-H isotopic data require a monitoring program for springs used as drinking water supply to be established.

Trace element composition and Sr-isotope ratio in wine, must and soil from a high-altitude vineyard in the Apuan Alps UNESCO Global Geopark (Italy)

Ghezzi L.*¹, Petrini R.¹, Castorina F.², Scotti C.³, Ottria G.⁴ & Bartelletti A.⁵

¹ Dipartimento Scienze della Terra, Università di Pisa.

² Dipartimento Scienze della Terra, Università "Sapienza" Roma.

³ I.TER, Bologna.

⁴ CNR, Istituto di Geoscienze e Georisorse, Pisa ⁵ Ente Parco Regionale delle Alpi Apuane, Lucca.

Corresponding email: lisa.ghezzi@unipi.it

Keywords: trace element, Sr-isotopes, Unesco Global Geopark, Bosa Farm Apuan Alps, high-altitude vineyard.

The control of wine geographic origin is currently one of the most challenging topics related to authenticity. The wine characteristics are essentially due to the geographical and geo-pedological environment where vines grow. Indeed, the geology of the vineyard substrate and rock-weathering processes influence the wine character, providing inorganic nutrients for vine growth and determining the content of metals in wine. High-altitude vineyards distinguish from their flatland counterparts for the exposure to climate contrasts, temperature shifts, exceeding winds, snow cover, higher solar radiation and light intensity. Field observations indicate that, for the same lithology, the physical erosion generally becomes the dominant process with respect to chemical weathering as increasing altitude. Indeed, at high altitude, the mineral dissolution rates are lowered and more selective, and solely the most reactive minerals contribute to the plant available pool.

The Sr isotopic systematics has been demonstrated to have high potential for the traceability and authentication of wine, and the metal content of wine samples is also related to the specific production area. This study presents the results obtained from the first step in traceability and geochemical characterization of the Bosa wine. The Bosa Geopark Farm vineyard (Merlot) is located in the Apuan Alps UNESCO Global Geopark (www.apuanegeopark.it), at an altitude of 850 m (a.s.l.) representing one of the highest vineyard of Italy. The soil is closely related to the geological substratum of the Scaglia Toscana Formation, developing directly from the parental material through beginning processes of pedogenesis. Trace elements in the 2015 harvest wine show a characteristic pattern that mimics parental rocks, suggesting a minor role of bedrock chemical weathering in developing the soil profile. The Sr isotopic composition in wine and must [$^{87}\text{Sr}/^{86}\text{Sr} = 0.70843(1)$ and $0.70846(1)$, respectively] approaches the NH_4OAc extractable Sr from soil [$^{87}\text{Sr}/^{86}\text{Sr} = 0.70847(1)$]. However, the Sr-isotope data on grape juice collected in different vines show a small-scale vineyard variability indicating that the root system explores heterogeneous soil resources for nutrient uptake. Grape seeds and stems from one single vine both show a significantly lower $^{87}\text{Sr}/^{86}\text{Sr}$ ratio with respect to corresponding juice, possibly reflecting the uptake from isotopically different reservoir during the evolved dynamic of vine and fruit development.

Chromium-isotope systematics, new insights from a contaminated area in the Friuli Venezia-Giulia Region

Lutman A.¹, Petrini R.*² & Ghezzi L.²

¹ Friuli Venezia Giulia Region, Directorate for Environment and Energy, Trieste, Italy.

² Department of Earth Sciences, University of Pisa, Italy.

Corresponding email: riccardo.petrini@unipi.it

Keywords: Chromium isotopes, chromium-isotope fractionation, industrial contamination.

The Cr(VI) contamination of natural waters represents an environmental and health threat affecting many sites in the EU. Regulations pose a threshold for Cr(VI) concentration in groundwater of 5 µg/L; in Italy, the DM November 14, 2018 introduced the upper concentration limit of 10 µg/L in drinking water to be achieved within December 31, 2019. Cr(VI) may be released to the environment by anthropogenic activities and/or by lithogenic sources. Cr mostly occurs in natural environments in two stable oxidation states: Cr(III) and Cr(VI). Cr(III) is considered essential for human beings, although this belief was questioned in recent studies. On the contrary, Cr(VI) is classified toxic in the Group 1. In natural ecosystems, Cr(VI) has the tendency to be reduced to the sparingly water soluble Cr(III) by several abiotic and biotic reductants. Depending on the redox and pH conditions, the chromate reduction by S²⁻ and Fe²⁺ in aquatic reducing environments can be very fast, while the reduction by organic matter in sediments is generally much slower. Cr(III) can, in turn, be oxidized to Cr(VI) by various naturally occurring oxidizing agents, in particular Mn(IV) and Mn(III). In addition, the oxidation of Cr(III) to Cr(VI) occurs during drinking water treatments that use chlorine as oxidant. These oxidation pathways extend the potential threats of Cr(VI) contamination. The Cr-isotope systematics, expressed by the ⁵³Cr/⁵²Cr ratio through the δ⁵³Cr notation, has been demonstrated to be effective in assessing the fate of Cr(VI) in the water-sediment system. In the present study, new insights are reported for the origin of a resurgent hexavalent chromium contamination in groundwater from a phreatic aquifer in the Friuli Venezia Giulia Region using Cr isotopic data. The area underwent a severe Cr(VI) contamination by industrial effluents in 1997. In subsequent years the contamination naturally attenuated, totally disappearing in 2003. A renewal of water contamination was observed in 2008, Cr(VI) exceeding 1500 µg/L. The δ⁵³Cr value in groundwater and extracts from sediments measured in 2009-2011 surveys ranges in the large span between -3.21 and +0.21‰ and between -4.71 and +1.26‰, respectively. Due to the lack of geogenic Cr-sources, these data have been interpreted as evidence of the subsequent oxidation through Mn-oxides of the Cr(III) hosted in the aquifer and originated by the reduction of the original industrial chromates. Cr(III) is characterized by negative δ⁵³Cr, starting from the δ⁵³Cr value around zero of Cr(VI) in industrial effluents. Oxidation liberates soluble Cr(VI) which is transported by groundwater and permeated soils. The complex Cr-isotopic vs. concentration distribution reflects both the new Cr(VI) reduction and dilution processes in the aquifer system. From an environmental point of view, the data raise concerns regarding the potential impact of past Cr(VI)-contamination.

Heavy metals in surface waters and suspended solids from the Usciana River (Tuscany, central Italy)

Maccelli C.*¹, Avanzinelli R.¹, Casalini M.¹, Nisi B.², Vaselli O.^{1,2} & Mason P.³

¹ Department of Earth Sciences, Florence (Italy).

² CNR-Institute of Geosciences and Earth Resource, Florence (Italy).

³ Department of Earth Sciences, Utrecht University (Netherlands).

Corresponding email: chiara.maccelli@gmail.com

Keywords: Usciana River, Heavy metals, radiogenic isotopes.

The Usciana River (Tuscany central Italy) is an artificial channel built in 1934 to reclaim and control the swamping waters of Padule di Fucecchio, which is located in the lower reaches of the Nievole River Valley, before it flows into the Arno River. During the last decades, an important tanning district developed in the surrounding of the Usciana River, which acts a significant anthropogenic pressure equivalent to about 2,250,000 inhabitants (Autorità di Bacino, 1998; Nisi et al., 2008). During the years, the Usciana River waters have been spoiled as testified by numerous events of fish die-off since 2001 (Pucci, 2001), the last one occurring in 2015 (Sabia, 2015). In 2003, the Regional Agency for the Environmental Protection has been started an ecological and chemical survey in order to monitor the status of the river waters (Bresciani et al., 2008), whose results indicated an extremely low quality of the surface waters, particularly related to the presence of large amounts of nutrients caused by urban and industrial wastes (Vannini et al., 2017). To evaluate the anthropogenic and natural contribution in the surface waters and suspended solids, original chemical and isotopic data from 13 sampling sites distributed along the Usciana River and before and after the confluence of the Arno River are presented. Trace and ultra-trace elements were determined by ICP-OES and ICP-MS at the Utrecht University (Netherlands) while Sr and Pb isotope ratios were measured by TIMS at the University of Study of Florence (Italy).

Autorità di Bacino del Fiume Arno (1998) - Piano di bacino del Fiume Arno: Qualità delle acque. Sintesi del piano stralcio. Quaderno 8. Felici Ed., Ospedaletto, Pisa.

Bresciani O., Cavalieri S., Franchi A., Giovannelli L., Menichetti S. & Tricarico V. (2008) - Quattro anni di monitoraggio sui fiumi toscani prima del recepimento della direttiva europea (2003-2006). Direzione Tecnica ARPAT – STEPPAS, 202 pp.

Nisi B., Vaselli O., Buccianti A., Minissale A., Delgrado Huertas A., Tassi F. & Montegrossi G. (2008) - Indagine geochemica ed isotopica del carico disciolto nelle acque di scorrimento superficiale della valle dell'Arno: valutazione del contributo naturale ed antropico. Mem. Soc. Geol. It., 79, 13-21.

Pucci P. (2001) - Moria di pesci nell'Usciana. Le cause sono misteriose, scatta l'indagine dell'Arpat. Il Tirreno, sezione Pontedera.

Sabia M. (2015) - Moria di pesci a Torre, nel canale Usciana solo scarichi. Il Tirreno, sezione Empoli, Agosto 14, 2015.

Vannini J., Bigagli V., Bartaletti S., Beglioni V., Mancini P. & Poggi A. (2017) - Analisi della qualità dei corpi idrici superficiali ed evoluzione dell'impatto del sistema depurativo in Valdinievole – anno 2017. Dipartimento provinciale ARPAT di Pistoia.

Paleoclimate reconstruction using freshwater organisms from prehistoric shell midden

Macri A.*¹ & Iacumin P.¹

¹ Dipartimento di Scienze Chimiche, della Vita e della Sostenibilità Ambientale, Università di Parma, (Italia).

Corresponding email: antonella.macri@studenti.unipr.it

Keywords: carbon and oxygen stable isotopes, *Pila wernei*, palaeoclimatic reconstruction.

Shell midden is an archaeological feature formed by the accumulation of domestic refuses consisting primarily of mollusk shells. Many species of gastropods have been used in isotopic investigation to reconstruct environmental conditions (Leng & Lewis, 2016) while other species are not ubiquitous and poorly studied, such as *Pila wernei*. Large accumulations of mainly *Pila wernei* shells are present at Al Khiday in a well-preserved deposit, spanning nearly one millennium, from 7000 to 6100 cal BC. The archaeological site Al Khiday is situated in Central Sudan, about 20 km south of the confluence of the White and Blue Nile. A pioneer carbon and oxygen stable isotope investigation on the aragonitic shells of *Pila wernei* was performed to improve our knowledge of the paleo-environmental conditions of the wetlands along the White Nile during Mesolithic period. A paleo-environmental interpretation of isotope data firstly requires an assessment of the relationship between modern shells and the water in which they form. For this reason, modern specimens of *Pila wernei* and water were collected during a field trip to Jebel Awlia (twenty-five km south of Al Khiday) from a catching fish canal connected to the main water system. Our results suggest that the oxygen isotope composition of modern shells is in isotopic equilibrium with water. In order to obtain more information about freshwater system, isotopic analysis of fish bones ($\delta^{13}\text{C}_{\text{apatite}}$ of the bone and $\delta^{18}\text{O}$ of both the carbonate and phosphate group) from Al Khiday midden was performed. The gastropods that inhabit river-connected swamps, floodplains and other stagnant water can give a record of environmental changes over most of a year of flood season while fishes with their own ecological niches integrate environmental condition of river over substantial time period. The $\delta^{18}\text{O}$ values for aragonite and bone bioapatite of different organisms clearly indicate a past hydrological budget of the Nile river with less evaporation than today. The wetter climate would have supported seasonally flooded grassy plain and therefore more resources for Mesolithic people (Williams et al., 2015)

Leng M.J. & Lewis J.P. (2016) - Oxygen isotopes in Molluscan shell: Applications in environmental archaeology. *Environmental Archaeology*, 21, 295-306.

Williams M.A.J., Usai D., Salvatori S., Williams F.M., Zerboni A., Maritan L. & Linseele V. (2015) - Late Quaternary environments and prehistoric occupation in the lower White Nile valley, central Sudan, 130, 72-88.

Boron isotopic analyses in fluid samples: PTIMS *VERSUS* MC-ICP-MS (Neptune PLUSTM)

Pennisi M.*¹, Agostini S.¹, Dini A.¹, Dordoni M.¹, Di Giuseppe P.¹, Rielli A.¹, Provenzale A.¹
& Rodushkin I.²

¹ Istituto di Geoscienze e Georisorse, (IGG) CNR, Pisa, Italy.

² ALS Scandinavia LAB and Lulea University of Technology, Lulea, Sweden.

Corresponding email: m.pennisi@igg.cnr.it

Keywords: MC-ICP-MS, Boron isotope, fluids.

In the frame of the CNR project Nextdata major renovation occurred at the former Thermal Ionization Mass Spectrometers (TIMS) laboratory of the *Istituto di Geoscienze e Georisorse* (IGG-CNR, Pisa), through the installation of a Multi Collector-High Resolution-Inductively Coupled Plasma-Mass Spectrometer (MC-HR-ICP-MS). In the last two decades, the most significant contribution to the isotope revolution was the introduction of this last-generation mass spectrometer, which started as complementary tool of the TIMS, but gradually are substituting it.

We present the first results of boron isotopic composition of fluid samples determined by MC-ICP-MS (Neptune PLUSTM) at the IGG-CNR of Pisa. This machine has been recently installed (October 2017) and has substituted the VG54E PTIMS previously used for boron isotopes analysis at IGG. We have validated our new methodology with an intercalibration exercise using the IAEA standards B1 (sea water), B2 and B3 (groundwaters; Gonfiantini et al., 2003) together with a set of well-characterized samples (volcanic, thermal and geothermal fluids), and with a wide range of B concentration and isotopic composition ($-21.4\text{‰} < \delta^{11}\text{B} < +46.3\text{‰}$).

Samples were processed in a 100-1000 class clean room laboratory, using B-free consumables and reagents. B was separated from the sample matrix using ion exchange resins and the eluted was diluted to 25 ppb in 2% HNO₃. Samples were then analyzed using the bracketing method with a 25 ppb B solution of the 951 NBS standard. For the analysis we used nickel cones, a 100 $\mu\text{l}/\text{min}$ PFA Nebulizer, 10¹² Ω resistors and tuned the machine for stable mass fractionation. Our results obtained by MC-ICP-MS were compared with those obtained using another MC-ICP-MS (NeptuneTM) at the Lulea University and by PTIMS at the IGG-CNR of Pisa.

The results of the intercalibration exercise show that there is a linear correlation ($R^2 = 0.998$; $n = 16$) between $\delta^{11}\text{B}$ values obtained with the two different MC-ICP-MS (IGG-CNR, Pisa and University of Lulea) and PTIMS (IGG-CNR, Pisa). This indicates that our new methodology allows precise and accurate analyses over a wide range of chemical compositions and boron contents. As case study, we have determined for the first time the B isotopic composition of riverine and meteoric waters from the Adige basin of Northern Italy, which are characterized by low B concentrations (as low as < 1 ppb).

Our new methodology allows the accurate and precise analysis of B isotopes by MC-ICP-MS in water samples with B concentration lower than 1 ppb. We determined boron isotopic composition of fluvial and rain waters from the Adige basin characterized by B concentrations ranging from 3.0 ppb to 8.3 ppb for fluvial samples, and below 1.0 ppb for meteoric waters (Dordoni et al., this Symposium).

This advance opens to new possibilities in the field of isotopes hydrology, allowing the study of B isotopic composition of B-poor hydrological environments.

Gonfiantini R., Tonarini S., Gröning M., Adorni-Braccesi A., Al-Amman A.S., Astner M., Bachler S., Barnes R.M., Bassett R.L., Cocherie A., Deyhle A., Dini A., Ferrara G., Gaillardet J., Grimm J., Guerrot C., Krahenbuhl U., Layne G., Lemarchand D., Meixner A., Northington D.J., Pennisi M., Reitzenerová E., Rodushkin I., Sugiura N., Surberg R., Tonn S., Wiedenbeck M., Wunderli S., Xiao Y. & Zack T. (2003) - Intercomparison of boron isotope and concentration measurements. Part II: evaluation of results. *Geostandards Newsletter*, 27(1), 41-57.

Dordoni M., Pennisi M., Agostini S., Dini A., Di Giuseppe P., Rielli A., Provenzale A., Bianchini G., Natali C., Marchina C. & Cidu R. (2019) - First isotopic analyses in fluid samples using MC-ICP-MS (NEPTUNE PLUSTM): results on Boron-poor fluvial and rain water (Adige basin)

Hydrological significance of $\delta^{18}\text{O}$ composition of speleothems and lakes carbonates from Apennine sites (Italy): a coherent hydrological framework for the Last Interglacial period

Regattieri E.^{*1-2}, Zanchetta G.¹, Drysdale R.N.³, Giaccio B.⁴, Isola I.⁵, Mannella G.¹, Nomade S.⁶ & Hellstrom J.C.⁷

¹ Dipartimento di Scienze della Terra, Università di Pisa, Italy.

² Istituto di Geoscienze e Georisorse, IGG-CNR, Pisa, Italy.

³ Department of Resource Management and Geography, University of Melbourne, Australia.

⁴ Istituto di Geologia Ambientale e Geoingegneria, IGAG-CNR, Rome, Italy.

⁵ Istituto Nazionale di Geofisica e Vulcanologia, INGV, Pisa, Italy.

⁶ Laboratoire des Sciences du Climat et de l'Environnement, IPSL, CEA/CNRS/UVSQ, Gif-Sur-Yvette, France.

⁷ School of Earth Sciences, University of Melbourne, Victoria 3010 Australia.

Corresponding email: eleonora.regattieri@unipi.it

Keywords: stable isotope, paleoclimate, carbonates.

Continental carbonate successions (speleothems and lake sediments) from central Mediterranean are powerful archives of environmental and hydrological variability. The stable oxygen isotope composition ($\delta^{18}\text{O}$) of these deposits is considered a proxy for precipitation amount and seasonality, whereas other geochemical properties reflect environmental processes operating at the catchment-scale. Here we present a comparison between multiproxy, highly resolved, well-dated continental records from a N-S transect over the Apennines (Italy), covering the Last Interglacial period (ca. 130-90 ka). Records comprise speleothems from Apuan Alps (northern Italy; Tzedakis et al., 2018; Regattieri et al., 2016) and paleo-lacustrine succession from the intermontane basins in Abruzzo (Mannella et al., 2019; Regattieri et al., 2017). All records are independently dated by means of U/Th dating for speleothems and by $^{40}\text{Ar}/^{39}\text{Ar}$ dating and tephrostratigraphy for volcanic ash layers interbedded to the lake sediment. The variability of the $\delta^{18}\text{O}$ records is consistent among most sites, indicating a spatial and temporal coherent hydrological pattern over the Apennines during the investigated period. The environmental evolution inferred by properties other than $\delta^{18}\text{O}$ supports the hydrological interpretation of the $\delta^{18}\text{O}$ signal. The climatic evolution reconstructed from central Italy records can be tracked in marine records from the Mediterranean and the North-Atlantic, shedding light on the links between Mediterranean precipitation variability and oceanic and atmospheric changes occurring at regional and extra-regional scale.

Mannella, G., Giaccio, B., Zanchetta, G., Regattieri, E., Niespolo, E. M., Pereira, A., Renne P.R., Nomade S., Leicher N., Perchiazzi N. & Wagner B. (2019) - Palaeoenvironmental and palaeohydrological variability of mountain areas in the central Mediterranean region: A 190 ka-long chronicle from the independently dated Fucino palaeolake record (central Italy). *Quat. Sci. Rev.*, 210, 190-210.

Regattieri E., Zanchetta G., Drysdale R.N., J.D. Woodhead, Hellstrom J., Giaccio B., Isola I., Greig A. & Baneschi. (2016) - Environmental variability between the penultimate deglaciation and the mid Eemian: insights from Tana che Urla (central Italy) speleothem trace element record". *Quat. Sci. Rev.*, 152, 80-92.

Regattieri E., Giaccio B., Zanchetta G., Nomade S., Francke A., Vogel H., Drysdale R.N., Perchiazzi N., Wagner B., Gemelli M., Mazzini I. & Boschi C. (2017) - A Last Interglacial record of environmental changes from the Sulmona basin (Central Italy), *Palaeogeogr. Palaeoclimatol. Palaeoecol.*, 472, 51-66.

Tzedakis P. C., Drysdale R.N., Margari V., Skinner L.C., Menviel L., Rhodes R.H., Taschetto A.S., Hodell D., Crowhurst S.J., Hellstrom J.C., Fallick A.E., Grimalt J.O., McManus J.F., Martrat B., Mokkedem Z., Parrenin F., Regattieri E., Roe K., Zanchetta G. (2018) - Enhanced climate instability in the North Atlantic and southern Europe during the Last Interglacial. *Nature Comm.*, 9(1), 4235.

Novel application of MC-ICP-MS for stable isotope measurements

Rodushkin I.*¹⁻², Pallavicin N.² & Engström E.¹⁻²

¹ Division of Geosciences, Luleå University of Technology, Luleå, Sweden.

² ALS Laboratory Group, ALS Scandinavia AB, Luleå, Sweden.

Corresponding email: ilia.rodushkin@alsglobal.com

Keywords: MC-ICP-MS, unconventional stable isotopes, trace elements.

High precision isotope ratio measurements by MC-ICP-MS found increasing applications in various scientific fields allowing tracing sources and processes using stable and radiogenic isotope signatures. The usefulness of such approach can be limited by analytical challenges in obtaining reliable isotope information (especially for elements present at trace levels relevant for uncontaminated environmental matrices or in situations where available sample size is limited) and by natural variability of isotope compositions. This challenges will be discussed on example of case study focusing on assessment of variability for several isotope systems (Cr, Fe, Cu, Zn, Ag, Cd, and Tl) and in various environmental samples (soil profiles, lysimetric water, leaves, needles, mushroom, lichen, mosses) from Northern Sweden.

Use of lead isotopic fingerprint in human scalp hair to identify potential sources of pollution in industrial Sicilian sites (Italy)

Varrica D.*¹, Tamburo E.¹, Alaimo M.G.¹, Losno R.² & Monna F.³

¹ Dipartimento di Scienze della Terra e del Mare (DiSTeM), Palermo, Italy.

² Institut de Physique du Globe de Paris Sorbonne Paris Cité, Univ Paris Diderot, Paris, France.

³ UMR 6298, ArTeHiS, Université de Bourgogne - CNRS - Culture, Dijon, France.

Corresponding email: daniela.varrica@unipa.it

Keywords: Lead isotope ratios, environmental geochemistry, human biomonitoring, industrial areas

Petrochemical industries represent a controversial, although important, the economic resource. They offer numerous job opportunities, which in turn contribute to the economic development of the city. People living in towns close to industrial plants are particularly exposed to severe environmental decline, which involves the deterioration of the quality of air, water, soil, and food. The municipalities of Augusta (SR), Gela (CL) and Pace del Mela (ME) host large oil refineries, together with several important chemical and petrochemical industries. The main goal of this study is to evaluate if stable lead isotope ratios measured in the biological matrix can be used as pollution fingerprints. Total lead concentrations in 354 human scalp hair samples from adolescents (11–13 years old) belonging to both genders, along with 16 lead isotope analyses in hair samples from Augusta (6 samples), Gela (6 samples) and Pace del Mela (4 samples) are discussed here. Pb concentrations of adolescents living at Pace del Mela resulted higher than those of adolescents living at Augusta and Gela (median values Pb_{PM} : 1.13 $\mu\text{g/g}$, Pb_{AU} : 0.36 $\mu\text{g/g}$ and Pb_{GL} : 0.43 $\mu\text{g/g}$, respectively). Hair from adolescent living in the three industrial sites exhibited lead isotope ratios in the ranges 1.138–1.171 (average 1.157) for $^{206}\text{Pb}/^{207}\text{Pb}$ and 2.093–2.122 (average 2.108) for $^{208}\text{Pb}/^{206}\text{Pb}$. These values pointed to a multi-source mixing between bedrock parent material and industrial ash. In general, the results obtained confirm that the towns of Augusta, Gela and Pace del Mela are heavily affected by industrial emissions. Moreover, the data endorse that the lead isotope method remains a powerful technique to identify potential sources of environmental contamination.

Geochemical and isotopic investigation on underground waters affected by high sulfate contents

Vaselli O.¹⁻², Tarchiani U.³, Nisi B.*⁴ & Cabassi J.¹⁻²

¹ Dept. Earth Science, Florence, Italy.

² CNR-IGG, Florence, Italy.

³ Studio Associato Tecnologie Ambientali, Barberino di Mugello, Florence, Italy.

⁴ CNR-IGG, Pisa, Italy.

Corresponding email: barbara.nisi@unifi.it

Keywords: dissolved sulphate, groundwater, Prato, Sulfur isotopes.

A couple years ago, relatively high contents of sulphate were recorded in the shallow aquifer at Prato (Tuscany, central Italy), located below an area used for storage and treatment purposes of geological material derived by the excavation of tunnels for a highway by-pass and managed by a private company. According to the requirements by the local environmental agency, periodical geochemical surveys of the shallow aquifer along with water level measurements were adopted by the company using pre-existing wells and new-drilled piezometers, to verify whether the interaction between the stored material and the meteoric waters was affecting the groundwater system. It has to be pointed out that no previous geochemical analyses of the shallow aquifer in this area were available. Strikingly, the geochemical data evidenced that the sulphate contents were up to 500 mg/L, i.e. well above the recommended value of 250 mg/L, suggesting a potential contamination of the shallow aquifer due to the working activities at the surface operated by the private company. Leaching tests of the stored and core drilled down material, the latter being collected down to the depth of the shallow aquifer, did not evidence any appreciable content of sulphate. However, the presence of almost intact plant leaves and authigenic pyrite in the deepest part of the drillings (about 6 m) suggested the possible presence of oxidation processes that could have favoured the formation of the relatively high contents of sulfate in the oxygenated shallow aquifer. An extensive study of sulfur isotopes in the dissolved sulphate measured in the underground and leaching waters and those of waters interacting with the stored material suggested a supergenic origin of sulphate from oxidation of relatively large amounts of sulphides contained in the geological layers interacting with the shallow aquifer and not from the interaction of the stored material with the meteoric waters.

S31

**Geochemistry of mercury: from noble metal to global
pollutant**

CONVENERS AND CHAIRPERSONS

Stefano Covelli (Università di Trieste)

Orlando Vaselli (Università di Firenze)

Barbara Nisi (IGG-CNR)

Mercury distribution and speciation in soils contaminated by historically mining activity: The Isonzo River plain (NE Italy)

Acquavita A.*¹, Brandolin D.¹, Felluga A.¹, Maddaleni P.¹, Meloni C.¹, Poli L.¹, Skert N.¹ & Zanella A.¹

¹ ARPA FVG - Agenzia Regionale Protezione Ambiente Friuli Venezia Giulia, Palmanova -Udine

Corresponding email: alessandro.acquavita@arpa.fvg.it

Keywords: Mercury, Isonzo River, speciation.

The secular mining of cinnabar (HgS) and native Hg ore exploited at Idrija (NW Slovenia) impacted the environment of the whole Isonzo/Soča River basin with the contamination of soil, water and river sediment (Gosar & Teršič, 2012). Due to the risk for health and to fulfil the gap of knowledge, a relevant number of soil samples (n=262) were evaluated for Hg level and distribution in surface and subsurface levels, and, to assess the potential risk, for chemical speciation and atmospheric contents. Total Hg concentration varied from <0.06 to 41.0 mg kg⁻¹ and was higher in surface than subsurface levels (7.36 ± 0.84 and 3.64 ± 0.58 mg kg⁻¹, respectively). Mean contents were large different from the median because a restrict a number of samples contributed to the high degree of contamination: these were found close to the Isonzo River banks especially in the upper area investigated. The calculated index of geoaccumulation (Igeo) (Kowalska et al., 2018) ranged from -0.58 to 8.8 with 28% of samples classified as “slightly to moderate contaminated” and 60% as “highly to extremely contaminated”. Mercury speciation was performed to distinguish mobile, organic and strongly bound species (Bloom et al., 2003). The compounds with very low solubility (mineral-bound) prevailed (89% of the whole set samples), whereas organo-complexed and strongly-complexed forms were significantly lower and the presence of bioaccessible forms was almost negligible. This behaviour was common to all the area considered, thus testifying the common origin of contamination and the absence of industrial point sources. The concentration of gaseous elemental mercury (GEM) was, on average, lower than 3.0 ng m⁻³, which is close to the background reported for the Mediterranean basin (Wangberg et al., 2008) and, if the threshold set by the WHO is considered (WHO, 2000), suggests the absence of risk for local inhabitants.

- Bloom N.S., Preus E., Katon J. & Hiltner M. (2003) - Selective extractions to assess biogeochemically relevant fraction of inorganic mercury in sediments and soils. *Anal Chim Acta*, 479, 233–248.
- Gosar M. & Teršič T. (2012) - Environmental geochemistry studies in the area of Idrija mercury mine, Slovenia. *Environ. Geochem. Health*, 34, 27-41.
- Kowalska J.B., Mazurek R., Gašiorek M. & Zaleski T. (2018) - Pollution indices as useful tools for the comprehensive evaluation of the degree of soil contamination—A review. *Environ. Geochem. Health*, 40, 2395–2420.
- Wangberg I., Munthe J., Pirrone N., Iverfeldt A., Bahlman E., Costa P., Ebinghaus R., Feng X., Ferrara R., Gardfeldt K., Kock H., Lanzillotta E., Mamane Y., Mas F., Melamed E., Osnat Y., Prestbo E., Sommar J., Spain G., Sprovieri F. & Tuncel G. (2001) - Atmospheric mercury distribution in Northern Europe and in the Mediterranean Region. *Atmos Environ*, 35, 3019-3025.
- WHO (2000) - Air quality guidelines for Europe. WHO Regional Publications European Series 91, World Health Organization Regional Office for Europe, Copenhagen, 288 pp.

Distribution of mercury, antimony and arsenic in the terrains from the former mining area of Abbadia San Salvatore (Siena, central Italy)

Bianchi F.*¹, Rappuoli D.², Vaselli O.^{3,4}, Nisi B.⁴ & Esposito A.²

¹ SBC Geologi Associati, Florence, Italy.

² Unione dei Comuni Amiata-Val D'Orcia, Castiglion d'Orcia, Siena, Italy.

³ Dept. Earth Science, Florence, Italy.

⁴ CNR-IGG, Florence, Italy.

Corresponding email: frank.bianchi@tiscali.it

Keywords: Abbadia San Salvatore, terrain characterization, mercury, antimony, arsenic.

The contaminated site of Abbadia San Salvatore mercury mine covers an area of 15 ha and includes the mining complex, mostly underground mine, mine waste piles, and the metallurgical plant for elemental mercury refinement, beginning from ore drying machineries, roasting furnaces and condensing lines, ending with slag waste piles (low temperature burned ore). Reclamation targets are covering contaminated terrains, clean up of buildings and plants since the final destination is that to establish a mining park. Setting aside the hydrocarbon contaminated materials and asbestos-bearing materials, the aim is that to manage the excavated terrains in-situ.

The reclamation plan required a characterization of the terrain to be pre-excavated in order to differentiate each parcel of terrain on the basis of hazard levels.

It has to mention that the site is located in an area with the occurrence of widely distributed mineralizations, which is therefore characterized by exceedances of regulations thresholds (CTV: contamination threshold values) for a site where the designated use as a mining park is assimilated to type A site, i.e. residential and public park area. The CTVs are defined in Table 1, Appendix 5, Title V, Part I Tab.1, Appendix 5, Title V, Part IVa, as reported in the Legislative Decree 152/2006. These exceedances are widespread and ubiquitously distributed for a few metals, especially for those that are related of epithermal mineral association, i.e. Antimony, Arsenic and Mercury. In order to proceed with the reclamation and clean-up operations of all buildings in the former mining site and remodeling of bordering slopes and covering and waterproofing technology of all waste piles, a characterization of the down 1 m depth ground was carried, following a sampling plan based on a square grid of 25 m².

The sampling grid was adapted to follow the subdivision of reclamation operations in two phases, allowing to set-up of a managing plan of the excavated ground. The terrain sampling was performed by collected 5 aliquots from each site with a wide bucket backhoe. The material was then homogenized and sieved at 2 cm. Finally, the resulting material was quartered to until when about 1 kg of sample was obtained.

Each sample (47) was dried at 40 °C and then, sieved at 2 mm. As, Hg and Sb were analyzed by ICP-MS by using two different procedures: i) dissolution with aqua regia and ii) leaching with CO₂-saturated MilliQ water. The analytical results evidenced relatively high contents of mercury particularly for those samples collected close to the area where the edifice hosting Gould furnaces is located and that bordering the condensing plant and adduction system to the chimneys of smoke exhaust chimneys.

100 years of high GEM concentration in the Central Italian Herbarium and Tropical Herbarium Studies Centre (Florence, Italy)

Cabassi J.*¹⁻², Rimondi V.¹⁻², Yeqing Z.¹, Vacca A.¹, Vaselli O.¹⁻², Buccianti A.¹ & Costagliola P.¹⁻²

¹ Department of Earth Sciences, University of Florence.

² CNR – Institute of Geosciences and Earth Resources, Florence.

Corresponding email: jacopo.cabassi@unifi.it

Keywords: gaseous elemental mercury (GEM), Mercuric chloride, Herbaria.

Herbaria represent unique archives for botanists, hence the stored specimens need to be properly preserved through physical or chemical treatments. Up to 1980s, the most used preservative and biocide was mercuric chloride (HgCl₂), sublimating at ambient air conditions; in herbaria, ionic Hg reduces to Hg⁰ (i.e. gaseous elemental mercury, GEM) and easily diffuses throughout the poor ventilated environment. Recent studies recognized that high GEM levels may indeed persist for decades, representing a health hazard for humans. A key question concerns how long high GEM levels could be recognized from the last HgCl₂ treatment. In this study, we present new original GEM data in the Central Italian Herbarium (Natural History Museum) and Tropical Herbarium Studies Centre of the Botanical Department of the University of Florence (Italy), located in the same building at the first and second floor, respectively. These herbaria host one of the largest plants collection in the world. Here, HgCl₂ was documented as a plant preservative up to the 1920s. GEM surveys, carried out by Lumex[®], were conducted in July 2013 and repeated in July and December 2017, to account for temporal and seasonal variations.

Herbaria show GEM concentrations well above those measured in the external locations. Peak levels of GEM were recorded within specimen storage cabinets, exceeding the instrumental detection limit (50,000 ng/m³). GEM concentrations up to ~7,800 ng/m³ were observed at the Central Italian Herbarium, where the most ancient collections are stored and no ventilation is active. On the contrary, lower GEM concentrations were observed at the first floor in all surveys. Here, lower and more homogeneously distributed GEM concentrations were measured in 2017 than in 2013 since the air-conditioning system was updated in early 2017.

GEM concentrations were in the range of those of other herbaria worldwide and lower than Italian permissible exposure limit of 20,000 ng/m³ (8-hour working day). Our results indicate that after about a century from the latest HgCl₂ treatment GEM concentration are still high in the herbaria leading to the conclusion that the treatment itself may be considered almost irreversible. Air conditioning and renewing is probably the less expensive and more effective method for GEM lowering in herbaria.

Gaseous Elemental Mercury (GEM) fluxes from the soil of the hydrothermal area of Monterotondo Marittimo (Grosseto, Central Italy)

Cabassi J.¹⁻², Di Bennardo F.¹, Venturi S.*¹⁻², Tassi F.¹⁻², Nisi B.⁴, Magi F.¹⁻³, Ricci A.⁵, Picchi G.¹ & Vaselli O.¹⁻²

¹ Department of Earth Sciences, University of Florence, Italy.

² CNR-IGG Institute of Geosciences and Earth Resources, Florence, Italy.

³ Department of Earth Sciences, University of Pisa, Italy.

⁴ CNR-IGG Institute of Geosciences and Earth Resources, Pisa, Italy.

⁵ Department of Biological, Geological and Environmental Sciences, University of Bologna, Italy.

Corresponding email: jacopo.cabassi@unifi.it

Keywords: GEM fluxes, diffuse soil degassing, air contaminant.

Measurements of diffuse fluxes of gaseous elemental mercury (GEM) from the soil of the hydrothermal area of Monterotondo Marittimo (Central Italy), known for the presence of the geosite “*Le Biancane*”, were performed by the combined use of a static closed chamber (SCC) and a Lumex® RA-915M portable analyzer. At the 89 GEM fluxes measurement points, CO₂ fluxes using the accumulation chamber method, as well as temperature at the soil - air interface using a thermocouple, were also measured. The dataset was implemented with CO₂/N₂ concentration ratios of interstitial gases and soil temperature measured at the depth of interstitial gas sampling. The main aims were to i) investigate the geochemical behaviour of GEM with respect to CO₂, soil temperature and soil permeability and ii) estimate the output of GEM and CO₂ from the area. The data show that: i) GEM and CO₂, despite having a common hydrothermal origin, tend to decouple due to secondary processes (scrubbing) occurring at relatively low depth up to the soil surface; ii) high GEM and low CO₂ fluxes were caused by strong soil fracturing favouring air circulation and, consequently, dilution of the major gaseous species (CO₂); iii) soil temperatures, although showing a good correlation with the CO₂ fluxes, seem not to control the GEM fluxes. The gas output estimations suggest that the diffuse degassing from the area (20,000 m²) represents a significant natural source of air contaminants: i) 0.335 tons a day of CO₂ and ii) 2.01×10^{-7} tons a day of GEM. The GEM output was in agreement with previous investigations in other active degassing hydrothermal areas (e.g. Solfatara Crater, Southern Italy) and has important implications for air quality at a local scale, despite it only represents a portion of the total output of Monterotondo Marittimo area. Consequently, GEM flux measurements can be of strategic support to monitoring programs aimed to control the impact of this air contaminant, especially in areas where hydrothermal gas emissions are combined with those related to the cultivation and exploitation of geothermal fluids.

Spatial and temporal distribution of mercury in the recent sediments of the Adriatic Sea

Covelli S.*¹, Langone L.², Petranich E.¹, Acquavita A.³, Giordano P.² & Giani M.⁴

¹ Dipartimento di Matematica e Geoscienze, Università degli Studi di Trieste, Trieste, Italy.

² CNR, Istituto di Scienze Marine (ISMAR), Bologna, Italy.

³ ARPA FVG, Palmanova, Udine, Italy.

⁴ Istituto Nazionale di Oceanografia e di Geofisica Sperimentale (OGS), Trieste, Italy.

Corresponding email: covelli@units.it

Keywords: mercury, sediments, core profiles.

Several sources of anthropogenic mercury (Hg), which date back to the sixteenth century, have been identified in the Adriatic Sea making this basin one of the most contaminated marine areas with regard to duration and amount of metal accumulated. Taking into account 2 complementary datasets, the distribution of total Hg was investigated in surface sediments (0.003-16.940 $\mu\text{g g}^{-1}$; avg. $0.715 \pm 1.929 \mu\text{g g}^{-1}$; median $0.102 \mu\text{g g}^{-1}$, $n=162$) and in 7 short cores collected from the Po River delta to the Strait of Otranto (0.002-0.963 $\mu\text{g g}^{-1}$; avg. $0.171 \pm 0.226 \mu\text{g g}^{-1}$; median $0.077 \mu\text{g g}^{-1}$, $n=189$). The objectives of our research were to integrate the two datasets in a distribution map to identify anomalies and potential sources at basin scale, and to reconstruct the recent history of sediment contamination. Results show that the coastal sediments of the northern sector are particularly enriched in Hg compared to the area extending from the Po delta to the Otranto Strait. This is due to the presence of multiple sources of contamination, the main one identifiable in the Gulf of Trieste at the north-easternmost side of the basin. Even now the Isonzo River supplies significant quantities of Hg to the sea, mainly in mineral form (cinnabar) as a result of mining activity that was operating at Idrija (Slovenia) for 500 years (Covelli et al., 2001). The nearby Marano and Grado Lagoon is another prominent area of metal accumulation by sources which include but are not restricted to mining (Acquavita et al., 2012). Part of Hg contamination is also associated with the past activity of a chlor-alkali plant whose effluents were deliberately discharged into the lagoon system. The “industrial” Hg was dispersed in this environment mixing with Hg from Idrija mine. Similarly, other sources can be recognised in the Venice Lagoon (the Porto Marghera industrial site) and Po River drainage basin. As we proceed southwards along the Italian coast, the concentrations of Hg decrease showing a significant negative gradient with increasing distances from the emission sources. The sedimentary profiles of Hg show decreasing trends in concentration and flux over the last 20-30 years indicating the beginning of a “recovery” period. The only exception is the core collected offshore Otranto, which still shows a weak increasing trend probably due to a delay in transferring the contamination signal of Hg coming from the northern sector of the basin.

Acquavita A., Covelli S., Emili A., Berto D., Faganeli J., Giani M., Horvat M., Koron N. & Rampazzo F. (2012) - Mercury in the sediments of the Marano and Grado Lagoon (Northern Adriatic Sea): sources, distribution and speciation. *Estuarine, Coast. Shelf Sci.*, 13, 20-31.

Covelli S., Faganeli J., Horvat M. & Brambati A. (2001) - Mercury contamination of coastal sediments as the result of a long-term cinnabar mining activity (Gulf of Trieste, Northern Adriatic Sea). *Appl. Geochem.*, 16, 541-558.

First investigation of atmospheric mercury pollution around the chlor-alkali plant of Pieve Vergonte (Italian central Alps)

Fantozzi L.*¹, Marziali L.², Valsecchi L.², Schiavon A.², Orrù A.¹ & Guerrieri N.¹

¹ IRSA - CNR Verbania.

² IRSA - CNR Brugherio.

Corresponding email: laura.fantozzi@cnr.it

Keywords: atmospheric mercury pollution, bioaccumulation, lichens.

In this study, the gaseous elemental mercury (Hg^0) in air and its bioaccumulation in lichens were investigated in a case study located in the Ossola valley, close to the town of Pieve Vergonte (Italian central Alps), which is heavily polluted by chlor-alkali industrial activity operating since 1915. Atmospheric Hg^0 was measured by means of a portable mercury analyzer (Lumex RA-915+) during car surveys and at fixed locations in autumn 2018 and winter 2019. Surveys covered an area of about 10 km², including the chlor-alkali plant external area and the town of Pieve Vergonte. Results highlight Hg^0 concentrations in air always above the typical terrestrial background concentration in the Northern Hemisphere (~1.5-1.7 ng m⁻³). Maximum values observed are two order of magnitude higher than the background levels and were always measured in the vicinity of the chlor-alkali plant. Samples of lichens were collected around the same area to evaluate the long-term dispersion pattern of atmospheric Hg. Total Hg concentrations in lichens were measured using an Automated Mercury Analyzer (AMA254, FKV, Italy). Results show a North-South gradient of Hg accumulation along the Ossola valley, where northerly winds prevail. Hg concentrations range from 0.143 mg kg⁻¹ d.w. in lichens collected North of the chlor-alkali plant to 0.624 mg kg⁻¹ d.w in lichens collected South of the chlor-alkali plant.

Mercury in groundwater from the Mt. Amiata area (central Italy)

Magi F.^{*1-3}, Cabassi J.²⁻⁴, Capecchiacci F.⁴⁻⁵, Giannini L.⁴, Nisi B.³, Pandeli E.²⁻⁴, Rappuoli D.⁶, Tassi F.²⁻⁴, Venturi S.²⁻⁴ & Vaselli O.²⁻⁴

¹ Dipartimento di Scienze della Terra - Università di Pisa (Italy).

² Dipartimento di Scienze della Terra - Università di Firenze (Italy).

³ CNR-IGG, Sezione di Pisa (Italy).

⁴ CNR-IGG, Sezione di Firenze (Italy).

⁵ INGV – Osservatorio Vesuviano, Napoli (Italy).

⁶ Unione dei Comuni Amiata-Val D'Orcia, Gallina, Castiglion d'Orcia (Siena), Italy.

Corresponding email: francesco.magi@dst.unipi.it

Keywords: mercury, fluid geochemistry, water-rock interaction.

The Mt. Amiata geothermal area is well-known for the presence of the (homonymous) extinct Quaternary volcano and its residual hydrothermal activity. Additionally, several epithermal Hg-ore bodies are widely distributed in the area and are prevalently represented by *stockworks* and *mantos* depositional structures, whose genesis is intimately linked to the volcano-geothermal setting of this province. These peculiar features made this site the fourth largest and most important mining district worldwide (World Class Deposit) for mercury exploitation where the operations started around the mid-'800s and officially ended at Abbadia San Salvatore mine (ASSM) in 1982. The industrial exploitation was based on two main exploitation and production sites, ASSM and Siele mines, respectively, and in other minor "satellite" centers (e.g. Solforate, Abetina (Argus), Morone, Cornacchino, Pietrineri, Cortevicchia, Montebuono). Metallic mercury, also called "quicksilver", was used in agricultural practices, medical purposes, thermometric devices, cosmetics, weapon industry and as a pigment.

Through the last decades, several geochemical studies dealing with mercury metallogeny and environmental issues related to the past mining activities have been performed. Currently, monitoring and remediation programs, started in 2009, are still going on at the ASSM site.

In the framework of collaboration with the local water management company, aimed at better definition of the hydro-geochemical characteristics of the main groundwater bodies hosted in the Mt. Amiata area, over 130 spring water samples (including thermal waters and waters discharging from some dismissed mine drainage tunnels) were collected and analyzed for water chemistry.

Among the analyzed (by ICP-MS) trace species, Hg is here considered for discussion along with the detected concentrations of other heavy metals such as As and Sb. Another goal of this research was indeed that to support the local authorities with useful hints on the most appropriate strategy to adopt (in terms of both availability and quality assessments) for the management of freshwater resources in the area.

The detected mercury concentrations were ranging between <0.1 and 11 mg/L. The average values of Hg measured in water samples from the cold Mt. Amiata aquifer (volume of about 55*10⁶ m³, hosted in the Quaternary volcanics) were around 0.2-0.3 mg/L, whereas concentrations up to 2.5 mg/L were occasionally found in correspondence to the outlets of some hypothermal springs from the area. Locally, higher mercury concentrations were recorded in other springs discharging from different portions of the regional carbonate aquifer cropping out in the close surroundings of the volcanic edifice. Water chemistry appeared to be mainly governed by water-(mineralized)rock and gas-water interactions, although secondary processes are also likely.

Long-term monitoring and modeling of gaseous mercury concentrations around the abandoned mine of Abbadia San Salvatore: the potential of passive sampling for detecting variation patterns and effects of emission-reduction associated with remediation works

Monaci F.*¹, McLagan D.S.², Rappuoli D.³, Huang H.⁴, Lei Y. D.⁴, Mitchell C.P.J.⁴ & Wania F.⁴

¹ Dept. of Life Science, University of Siena, Italy.

² Institute of Geoecology, Technische Universität Braunschweig, Germany.

³ Unione dei Comuni Amiata-Val d'Orcia, Siena, Italy.

⁴ Dept. of Physical and Environmental Sciences, University of Toronto Scarborough, Canada.

Corresponding email: fabrizio.monaci@unisi.it

Keywords: Gaseous mercury, Point source monitoring, Passive sampling.

Thirty six years after the cessation of mining and metallurgical activities and despite recent partial remediation works, the mine of Abbadia San Salvatore (Mt. Amiata, Central Italy) still remains a major source of atmospheric mercury (Hg) at both local and global scale. Recently, a detailed characterization and quantification of this source was obtained using a passive sampler (PAS) developed at the University of Toronto (McLagan et al., 2019). The intrinsic advantages of the passive sampling approach (limited costs, spatial resolution, long-term deployments) and the specific features of the adopted system (high analytical accuracy and precision, applicability over a wide range of concentrations) permitted a concurrent, high-spatially resolved mapping assessment of time-averaged (weekly to seasonal) gaseous Hg concentrations in and around the mine site. This allowed an unprecedented visualization of the spatio-temporal patterns of gaseous Hg dispersal at the site and, in combination with meteorological data and other relevant urban spatial data (e.g. residential areas, topographic attributes), facilitated the identification of potential chronic-exposure pathways to gaseous Hg for the local populace.

There is interest to further improve the knowledge on the extent of gaseous Hg contamination at the Abbadia San Salvatore mine site, which is about to undergo additional remediation works. A main guiding principle of a follow-up study supported by the Unione dei Comuni Amiata-Val d'Orcia is maintaining the comparability with the previous data set while taking advantage of the high adaptability of the passive sampling methodology to design experimental applications of specific temporal and spatial scale. By producing a long-term averaged dataset of spatially defined concentrations of gaseous Hg, the follow-up study is aimed at:

- determining temporal trends throughout the different phases of the envisaged reclamation process (before, during and after the remediation/mitigation measures);
- contributing to ascertain the effective attainment of the remediation objectives with respect to currently available legal limits or regional guideline values for gaseous Hg;
- supporting human exposure control and risk mitigation with respect to the chronic inhalation exposure for workers and residents living close to the mining area.

So far, the PAS-based approach has proven to be effective and low cost for reliably estimating emissions and quantifying gaseous Hg concentrations in complex environments, such as that of Abbadia San Salvatore. The focus of the ongoing research at this site is on expanding potential applications of this versatile technique, in particular its use in supporting effective emission reduction efforts in contaminated land management.

McLagan D. S., Monaci F., Huang H., Lei Y. D., Mitchell C. P. J. & Wania F. (2019) - Characterization and Quantification of Atmospheric Mercury Sources Using Passive Air Samplers. *J. Geophys Res.*, 2351–2362.

New insight into Hg origin in the Orbetello lagoon (Tuscany, Italy)

Pasquetti F.¹, Zanchetta G.¹, Vaselli O.², Nisi B.*³, Bianchi S.⁴, Mirri S.⁵ & Nannucci S.M.⁵

¹ Dipartimento di Scienze della Terra, Università di Pisa.

² Dipartimento di Scienze della Terra, Università di Firenze.

³ IGG-CNR, Pisa.

⁴ Studio Tecnico di Geologia e Arte Mineraria, Follonica.

⁵ Regione Toscana, Firenze.

Corresponding email: barbara.nisi@igg.cnr.it

Keywords: Mercury, Orbetello, GIS database.

In the last years several studies have highlighted the presence of anomalous concentrations of Hg and other trace elements such as As, Cd, Mn, Pb, Cu and Zn in the sediments of the Orbetello lagoon (Focardi, 2003; Focardi, 2005; AA.VV., 2008; ISPRA, 2009a,b), which is located along the coast of southern Tuscany (Grosseto, Italy). Among these metals, the attention of public institutions has focused on mercury due to its peculiar distribution which significantly differs from that of the other elements. This probably means that Hg has a different origin with respect to that of the other metals, likely associated with past human activities located around the lagoon (ISPRA, 2009a). The whole area is currently involved in a reclamation process. Understanding the reasons that led to the presence of mercury in the lagoon sediments is important for both properly managing of the site remediation and preserving the area for the future.

Therefore, the first step was aimed at producing a comprehensive assessment of the site that was including current and historical analyses of the site and the surrounding area and the collection of previous scientific and technical investigation reports carried out on different environmental matrices of the area. Subsequently, the acquisition of new targeted data was planned.

Most hydrogeological and geochemical data available for the Orbetello area were provided by the authorities of the Tuscany Region. During the collection, all the available data were stored in a GIS to build a comprehensive database from which distribution maps of mercury for the lagoon and the surrounding area can be visualized.

AA.VV. (2008) - Piano di indagini finalizzato alla bonifica ed al risanamento ambientale della Laguna di Orbetello. ICRAM e Università degli Studi di Siena. Relazione finale, 1° Stralcio attuativo, Giugno 2008. CII-TO-OR-04.01-1°Stralcio.

Focardi S. (2003) - Caratterizzazione ecotossicologica dei sedimenti e degli organismi della Laguna di Orbetello. Università degli Studi di Siena. Relazione finale anno 2003.

Focardi S. (2005) - Relazione tecnico scientifica relativa alla caratterizzazione ambientale dell'area ex-Sitoco perimetrazione a mare. Università degli Studi di Siena. Relazione scientifica 6 Agosto 2005.

ISPRA (2009a) - Interventi per il risanamento delle aree lagunari di Orbetello - Laguna di Levante. Premesse di progetto, Maggio 2009. Bol-Pr-TO-OR-Laguna Levante-01.01.

ISPRA. (2009b) - Interventi per il risanamento delle aree lagunari di Orbetello – Laguna di Ponente. Premesse di progetto, Dicembre 2009. Bol-Pr-TO-OR-Laguna Ponente-01.01-Premesse progetto.

Mercury mobility in harbour sediments: evidence from selective sequential extraction and short-term microcosm resuspension experiments (northern Adriatic Sea, Italy)

Petranich E.*¹, Pavoni E.¹⁻², Signore S.³ & Covelli S.¹

¹ Dipartimento di Matematica e Geoscienze, Università degli Studi di Trieste, Italy.

² Dipartimento di Scienze Chimiche e Farmaceutiche, Università degli Studi di Trieste, Italy.

³ Azienda Speciale per il Porto di Monfalcone (ASPM), Gorizia, Italy.

Corresponding email: epetranich@units.it

Keywords: mercury, harbour sediments, resuspension.

The coastal sediments of the Gulf of Trieste have been historically contaminated by mercury (Hg) due to mining activity in Idrija (Slovenia). Several research activities have taken place investigating Hg in this area (e.g. Covelli et al., 2001) but no information has thus far been available to evaluate the possible impact on the water column of the contaminated sediments as a consequence of dredging operations. Sixteen surface sediment samples were collected along the main channel approaching the Port of Monfalcone, which is used for commercial and industrial activities. The channel is expected to be deepened by 1 meter in the near future. From sixteen surface sediment samples analysed for Hg concentrations, selective sequential chemical extraction (SSE, Bloom et al., 2003) was applied to selected samples. The effects of sediment resuspension on the fate of the Hg species were evaluated in the laboratory using a short-term small-reactor system. The experiment was conducted with sediments taken from two sites following the same approach which had already been successfully executed in a previous study. The six sediment samples subjected to the SSE procedure were characterised by Hg mainly related to poorly soluble or insoluble compounds (98.7%), such as sulphides. This was confirmed by the results obtained from experiments conducted in the laboratory over a period of 24 h, where the first 10 cm of the sediments were resuspended in the overlying water (approximately 15 cm). After resuspension, dissolved Hg (DHg) and methylmercury (DMeHg), were detected in only one of the two selected sites. DHg showed concentrations comparable to those observed at the beginning of the experiments (pre-resuspension), varying in a narrow range (2.72-8.17 ng L⁻¹). DMeHg concentrations were < lod (limit of detection) over time and were only occasionally observed (up to 809 pg L⁻¹). In addition, the high values of the partitioning coefficient ($K_D = [Hg]_{\text{solid}}/[Hg]_{\text{dissolved}}$) confirmed the high affinity of Hg to the suspended sediment particles rather than to the dissolved phase. The consequences of a resuspension event which takes place over a limited time period can be considered of negligible impact due to the scarce mobility of Hg from sediments and to the dilution of Hg species present in the porewaters.

Bloom N.S., Preus E., Katon J. & Hiltner M. (2003) - Selective extractions to assess the biogeochemically relevant fractionation of inorganic mercury in sediments and soils. *Anal. Chim. Acta*, 479, 233–248.

Covelli S., Faganeli J., Horvat M. & Brambati M. (2001) - Mercury contamination of coastal sediments as the result of long-term cinnabar mining activity (Gulf of Trieste, northern Adriatic sea). *Appl. Geochem.*, 16, 541–558.

What are the major challenges that should be taken on board in supporting nations in the implementation of the Minamata convention on mercury

Pirrone N.*

CNR – Institute of Atmospheric Pollution Research, Rende, Italy.

Corresponding email: nicola.pirrone@iia.cnr.it

Keywords: anthropogenic mercury emissions, Minamata convention.

The second UN Conference of the Parties (COP) for the Minamata Convention on Mercury (MCM), met in Geneva in November 2018 to further the Convention's objective "*to protect human health and the environment from anthropogenic emissions and releases of mercury and mercury compounds*". Thus far, over 100 countries (with the U.S. being the first) have ratified the Convention, which entered into force in August 2017. Yet much more mercury work to reduce mercury emissions is needed, because according to an upcoming UN report (Global Mercury Assessment 2018 for the COP3 that will be held in Geneva on 25-29 November 2019), global mercury emissions rose by 20% between 2010 and 2015. During the last two decades a number of international programmes and initiatives have been developed for better understanding major patterns of mercury fate in the global environment and elaborate possible strategies for reducing its impact on human health and ecosystems. The GEO Work Programme (2016-2025) has launched the Global Observation System for Mercury (GOS4M) (www.gos4m.org) as a Flagship, which is aimed to support all interested Parties in the implementation of the MCM by providing a Knowledge Hub to support policy makers and stakeholders in the evaluation of the effectiveness of measures implemented under the convention. The ERA-PLANET (www.era-planet.eu) programme has launched two projects, namely iGOSP (Integrated Global Observing Systems for Persistent Pollutants) and iCUPE (Integrative Comprehensive Understanding on Polar Environment) to support the development and implementation for the Minamata Knowledge Hub. This lecture is aimed to provide a highlight on major progress and future challenges in our understanding of mercury fate in the global environment and ongoing policy development.

Mercury contamination in soils of an urban setting and the pathways of dispersion

Valerio M.*¹, Ghezzi L.¹ & Petrini R.¹

¹ Dipartimento di Scienze della Terra.

Corresponding email: martavalerio94@gmail.com

Keywords: mercury contamination, rhizosphere, taraxacum officinale.

The full characterization of mercury contamination in an ecosystem requires the analysis of several environmental matrices and the study of different geochemical processes. Indeed, the chemical form of mercury in the environment is crucial for long-term mobilization and uptake by the biota, since mercury may occur in the context of the ecosystem in different inorganic and organic forms. In general, the cycle of mercury in the environment, on a global scale, is dominated by the transport of mercury Hg(0) in the vapor phase through the atmosphere. Hg(0) may oxidize to mercuric ions Hg(II). The solubility of Hg(II) in the aqueous phase is mostly related to the occurrence of the compounds that mercury may form with chloride and to the presence of organic forms generated by microorganisms, forming methylmercury (MeHg). In contaminated soils and sediments, mercury may be partly transformed into MeHg or stable (HgS) and metastable (β -HgS) sulfides, with strong implications on its mobility and bio-availability. In this work the results of preliminary surveys after the discovery of mercury contamination in an urban soil and shallow groundwater are reported, including data on the exchange of mercury between atmosphere and vegetation. Analysis were performed using a Milestone DMA-80 triple cell direct mercury analyzer. The total mercury (THg) content in topsoil is in the range between 0.5 - 17 mg/kg; THg at 50 cm depth reaches the maximum value exceeding 300 mg/kg, possibly representing remnants of backfill material, while at depth higher than 1 m the concentration of mercury is below the threshold imposed by law (1 mg/kg). THg in the rhizosphere, root system and leaves of a locally diffuse plant (*Taraxacum officinale*) is in the range between 0.2 - 172 mg/kg, 0.01 - 0.03 mg/kg and 0.1 - 1.5 mg/kg, respectively. No univocal relationships are observed with the Hg content in soil and plants, and the data indicate that the Hg taken up by plants through root exudates and translocated to the aerial parts of plants is limited. The Hg volatile component measured in open air ant at the soil surface using a mercury vapor analyzer instrument (Lumex, RA 915 M) range between 20 – 85 ng/m³, well below the threshold of 200 ng/m³ imposed by regulations. Experiments indicate that a measurable amount of mercury in plant leaves is taken through air. The Hg content in shallow groundwater (actually representing an aquitard) is less than 0.5 μ g/l, indicating the lack of significant soil-water exchanges. However, the occurrence of bacterial populations leaves open the possibility of Hg(II) methylation or HgS precipitation. This important aspect is under investigation. Despite preliminary, these data represent the basis for planning remediation activities in the site.

Discontinuous monitoring of Gaseous Elemental Mercury in the former mining area of Abbadia San Salvatore (Siena, central Italy)

Vaselli O.*¹⁻², Nisi B.³, Rappuoli D.⁴, Cabassi J.², Esposito A.⁴ & Tassi F.¹⁻²

¹ Dept. Earth Science, Florence, Italy.

² CNR-IGG, Florence, Italy.

³ CNR-IGG, Pisa, Italy.

⁴ Unione dei Comuni Amiata-Val D'Orcia, Castiglion d'Orcia, Siena, Italy.

Corresponding email: orlando.vaselli@unifi.it

Keywords: mercury, abandoned mining areas, Central Italy, Gaseous Elemental Mercury.

Mercury exploitation in the Mt. Amiata area (Italy) lasted about 130 years (1847-1974) and affected the local economic conditions. About 100,000 tons of mercury were produced from roasted cinnabar. The mining complex covers about 65 ha and contains mining structures and workers' edifices. Since 2010, efforts by the local authorities were done to increase the knowledge about the environmental issue. In this work, in-door and out-door Gaseous Elemental Mercury (GEM) concentrations were discontinuously determined in the buildings and structures where liquid mercury was bottled and pigments were prepared. Criticalities and perspectives for the remediation process are presented, the ultimate goal being to recover the area as a mining museum. The environmental impact was evaluated according to the most recent regulatory laws. GEM (July 2011-November 2018) showed strong spatial and temporal variability, depending on the distance from the mining structures and ambient temperature, respectively. Surveys in summertime (June to September) showed high GEM concentrations ($>50,000 \text{ ng m}^{-3}$). To understand whether mercury was adsorbed in natural and anthropogenic materials (paints, plasters, roof tiles, concretes, metals, dust, wood structures and soils), total and leached mercury concentrations were measured. Strikingly high contents of mercury (up to $46,580 \text{ mg kg}^{-1}$ and $4,470 \text{ mg L}^{-1}$) were recorded. Such a geochemical characterization has relevant interest for the operational cleanings during the reclamation activities.

S32

**New developments and challenges in volcanology: insights
from experimental, analytical and field studies**

CONVENERS AND CHAIRPERSONS

Alessandro Vona (Università di Roma Tre)

Laura Spina (INGV)

Daniele Morgavi (Università di Perugia)

Stefania Sicola (Università di Roma Tre)

Eugenio Nicotra (Università della Calabria)

Eruptive dynamics during violent strombolian Vesuvius 1906 eruption

Cubellis E.¹, Pappalardo L.*¹ & Petrosino P.²

¹ Istituto Nazionale di Geofisica e Vulcanologia, Osservatorio Vesuviano, Italy.

² Università degli Studi di Napoli Federico II, Dipartimento di Scienze della Terra, dell'Ambiente e delle Risorse, Italy.

Corresponding email: lucia.pappalardo@ingv.it

Keywords: strombolian eruption, Somma Vesuvius.

About 600,000 people live around Mt. Vesuvius, where the risk associated with an explosive eruption is very high. Violent strombolian events have occurred in the most recent history of the volcano and this kind of events is considered to have a high probability of occurrence in the next future. Combining new volcanological analyses with historical observations, we reconstructed the eruptive dynamics during the violent strombolian 1906 event. The 1906 Vesuvius eruption began on the 4th of April with the opening of numerous vents at the base of the Gran Cono and the flowing of conspicuous lava flows towards the South side of the volcano including the villages of Boscotrecase and Torre Annunziata. This effusive phase was followed by explosive activity (from the 8th of April) with the development of a volcanic plume and the accumulation a fallout deposit (pumice and ash) on a wide territory extending eastward.

Raffaele Vittorio Matteucci (1862-1909) and Giuseppe Mercalli (1850-1914), Directors at Observatory between 1903-1909 and 1911-1914 respectively, followed the eruption and collected ash samples accumulated at the historical building of Vesuvius Observatory. In particular, Matteucci collected systematically ash during the various eruptive stages (now belonging to the ash collection of the Vesuvius Observatory Museum) and described step-by-step volcanic activity in daily bulletins that he sent to the authorities for risk assessment and defense of people that lived around volcano.

In this study we performed geochemical and textural analyses for the first time on the ash samples of 1906 eruption collected by Matteucci at the time of the eruption. Preliminary results are compared with the description of the volcanic activity reported in the Matteucci's daily bulletins, to identify correlation between geochemical and textural features and eruptive dynamics. Moreover, this information furnishes a picture of the response of the Vesuvian communities to the volcanic eruptions and of the relationship between scientists, governments apparatus and population exposed to risk.

The results of this study will contribute to evaluate trigger mechanisms and spatial-temporal evolution of this kind of eruption, useful for risk assessment in Vesuvian area.

Investigating the behaviour of volcanic ash using controlled laboratory experiments

Del Bello E.*¹, Taddeucci J.¹ & Scarlato P.¹

¹ Istituto Nazionale di Geofisica e Vulcanologia, Sezione di Roma I.

Corresponding email: elisabetta.delbello@ingv.it

Keywords: hazards, Ash settling, ash remobilization, ash aggregation.

Volcanic ash particles are magma fragments that are emitted in large quantity into the atmosphere during explosive volcanic eruptions. After injection, ash particles are transported into the atmosphere until settling on the ground forms loose deposits that are eventually re-suspended by winds. Mitigating the impact of volcanic ash in the earth system is a major task, and requires the formulation of models that need accurate inputs of volcanic ash properties in order to provide reliable hazard scenarios. To this end, laboratory experiments illuminate some of the complex aspects of the volcanic plume-atmospheric systems through their simulation in controlled and simplified conditions. Here we summarise some experimental studies undertaken by our team in the recent years investigating some key physical processes characterising the lifecycle of volcanic ash: i) particle settling velocity, ii) inter-particle and particle-fluid interactions, ii) aggregation, ii) resuspension. These aspects are recognized as important factors in the dispersal and final distribution of deposits, and thus need to be accounted for when computing hazard-oriented models. Our experimental approach includes the use of custom-designed facilities, controlled conditions and high-speed imaging equipment that allows reaching an unparalleled temporal and spatial resolution of particles and flow dynamics. The scope is to quantify how key parameters describing the above physical processes depend upon volcanic ash particles properties such as size, shape, surface features, porosity and chemical composition, to ultimately provide empirical relations that can be used to simulate eruptive scenarios that are calibrated on the specific conditions of a particular volcano.

The role of new magma recharges and crystal-mush interaction in the Campanian Ignimbrite activity, revealed by geochemical and isotope micro-analyses

Di Salvo S.*¹, Avanzinelli R.¹, Isaia R.², Druitt T.H.³ & Francalanci L.¹

¹ Dipartimento di Scienze della Terra, Università degli Studi di Firenze, Italy.

² Osservatorio Vesuviano, INGV sezione di Napoli, Italy.

³ Université Clermont Auvergne, Clermont-Ferrand, France.

Corresponding email: sara.disalvo@unifi.it

Keywords: crystal-mush, Campanian Ignimbrite, micro-analyses.

The Campanian Ignimbrite (CI) eruption (Campi Flegrei, Italy) is associated to a voluminous pyroclastic sequence of trachytic to phonolitic magma emplaced in southern-central Italy, around 39 ka ago. Its proximal deposits are made up by a basal pumice plinian fallout, followed by several distinct crystal-poor ignimbritic flow units and the topmost crystal-rich Upper Pumice Flow Unit (UPFU). We have applied a geochemical and isotopic micro-analytical approach to study in detail matrix glass and crystal compositions of the juvenile components from the proximal-CI deposits, to assess how the distinct components interact with each others and with the crystal-mush of the resident magmatic reservoir. The scale of the observation were reduced down to analyse different areas of matrix glass inside single clasts in order to recognise the possible presence of geochemical (major and trace elements) and Sr and Nd-isotope heterogeneities in the magma components of the CI plumbing system. Moreover, zoning of feldspar and clinopyroxene were also characterised for major and trace elements and micro-Sr isotopes, to reveal the possible presence of solid/liquid geochemical and isotopic disequilibria. Samples from all units, with the notable exception of the last erupted UPFU, have *i*) low crystal content, *ii*) evolved matrix glasses, *iii*) negative Eu anomalies (0.2-0.6), *iv*) strong micro-scale geochemical and isotope heterogeneities and *v*) phenocrysts mostly showing disequilibrium textures. On the other hand, the UPFU shows significant differences with respect to the products of the previously erupted units, namely *i*) a marked higher phenocryst content, *ii*) less evolved matrix glass compositions, *iii*) positive Eu anomalies (1.0-1.4), *iv*) less Sr- and Nd-radiogenic signatures and *v*) high-Or₈₃₋₈₇ sanidine with equilibrium textures. This micro-analytical study adds new and important constraints to the structure and evolution of the reservoir of a large explosive eruption such as the CI. In this light, an extremely complex scenario is depicted, where the arrival of new batches of fresh “mafic” melt thermally re-activated the crystal-poor evolved magmas stored within the CI resident reservoir. Sr- and Nd-isotope data suggest that this new incoming magma is significantly involved in the eruption, directly interacting with the cumulate crystal-mush at the base of the reservoir. Moreover, geochemical and isotope data from the UPFU matrix glasses can be explained by a complex evolution process involving 1) mixing between the entering “mafic” magma and mush-derived melts made up by *i*) a large proportion (about 80%) of high-degree melts of sanidine hosted in the crystal mush and *ii*) a lower amount (about 20%) of interstitial melt hosted within the crystal mush, but also 2) a minor but significant amount of sanidine crystallisation induced by cooling of the “mafic” magma during partial melts of mush components.

Rheology of particle-bearing suspensions: preliminary results

Frontoni A.^{*1}, Costa A.², Vona A.¹, Pistone M.³ & Romano C.¹

¹ Dipartimento di Scienze, Università degli Studi Roma Tre, Roma, Italy.

² Istituto Nazionale di Geofisica e Vulcanologia – Sezione di Bologna, Italy.

³ University of Lausanne | UNIL · Institute of Earth Sciences (ISTE), Lausanne, Svizzera.

Corresponding email: alessandro.frontoni@uniroma3.it

Keywords: magma viscosity, modeling, rheological behaviour.

The viscosity of a magmatic system plays a primary role in forecasting volcanic hazard in active systems. This physical parameter is controlled mainly by the chemical composition, temperature (T), strain rate and vesicle and crystal contents, including the aspect ratio (A.R.) of the crystals. To date, scientific community is not completely able to model magma viscosities, though several studies have been performed in this attempt. In this work, we present some preliminary results aimed at modelling the viscosity of round-shaped (A.R. 1) crystal-bearing magmas, on the basis of the semi-empirical formula describing the effective relative viscosity as a function of crystal fraction and strain rate, developed by “Costa et al., 2009”. The model has been applied to a dataset including most of literature rheological papers, providing a wider variation of the fitting parameters from the equation of “Costa et al., 2009”. This allows us to forecast the rheological behaviour of crystal-bearing magmatic systems, covering a wide range of crystal content (1-80%) and under different strain rates (between 10^{-7} and 10^2 s⁻¹). One step forward will consist in modelling magmatic suspensions with crystals having an A.R.>1, which is currently in progress.

Clastogenic lava flow: the case study from Mount Etna

Frontoni A.*¹, Vona A.¹, Giordano G.¹, Viccaro M.²⁻³ & Romano C.¹

¹ Dipartimento di Scienze, Università degli Studi Roma Tre, Italy.

² Dipartimento di Scienze Biologiche Geologiche e Ambientali, Università di Catania, Italy.

³ Istituto Nazionale di Geofisica e Vulcanologia – Sezione di Catania, Osservatorio Etneo, Italy.

Corresponding email: alessandro.frontoni@uniroma3.it

Keywords: Mount Etna, lava flows, rheological behaviour.

On the 18th May 2016 a lava-fountaining episode occurred on Mount Etna filled the summit craters creating a clastogenic lava flow. This work describes the rheological behaviour of the pyroclasts and the flow, on the basis of a suite of high-temperature (1050 to 1100 °C), uniaxial deformation experiments (strain rate 10^{-4} s^{-1}) on crystal- and vesicle-bearing natural samples, collected both along the lava flow (channel and lateral levees) and along a vertical profile. A progressive change in the rheological behaviour has been recognized in agreement with the progressive increase in the vesicle content, which shows a maximum value for pyroclasts (56%) and varies from the inner part to the upper part (18-25%), reaching a minimum value in the intermediate portion (10%) of the lava flow. No correlation has been observed as a function of increasing crystal content. Rheological results of experiments performed at 3 different experimental temperatures and constant strain rate of 10^{-4} s^{-1} , show deformation both within the brittle and the ductile regime, depending on the increase in vesicle content and temperature: samples with high vesicle content maintain their brittle behaviour, whereas in denser samples and as the temperature increases, the ductile deformation dominates. Field observations of the 2016 clastogenic lava flow are confirmed by the combined textural and rheological data. A marked decrease in vesicle content from the pyroclasts to the overflowing zone due to sintering and compaction promoted lava viscous flow. Subsequently, the down flow porosity increase favoured the brittle behaviour and autobreccia formation.

Monitoring of lava flow hazards: The December 24, 2018 Mt. Etna eruption

Ganci G.¹, Cappello A.*¹, Bilotta G.¹, Corradino C.¹, Hérault A.^{1,2} & Del Negro C.¹

¹ Istituto Nazionale di Geofisica e Vulcanologia, Osservatorio Etneo, Sezione di Catania, Italy.

² Conservatoire National des Arts et Métiers, Laboratoire Modélisation Mathématique et Numérique, Paris, France.

Corresponding email: annalisa.cappello@ingv.it

Keywords: satellite images, Digital Elevation Model, volcanic hazard.

Quantifying lava flow hazards by combining field observations, satellite data and numerical modeling has immediate applications to the real time monitoring of effusive eruptions. By monitoring, we mean here both following the manifestations of the eruption once it has started, as well as forecasting the areas potentially threatened by lava in an effusive scenario. The strategy implemented in the Lav@hazard web-GIS framework for the assessment of lava flow inundation hazards integrates the HOTSAT satellite monitoring system to analyze multispectral images and determine hotspot location, lava thermal flux, and effusion rate estimation, and the physics-based MAGFLOW model to simulate the spatial and temporal evolution of lava flow fields. The satellite-derived TADR (Time Averaged Discharge Rate, i.e. an estimation of the effusion rate) provided by HOTSAT is used to drive MAGFLOW simulations in order to obtain updated lava flow scenarios in near real time. Recently the HOTSAT system, initially designed for low to moderate spatial resolution data (e.g. MODIS, AVHRR, SEVIRI) has been extended to ingest recent data from SLSTR instrument (Sentinel-3 mission) and higher spatial resolution satellite data (e.g. ASTER, Landsat-8, Sentinel-2) particularly precious to retrieve detailed thermal maps of the lava flow field. These thermal maps are then compared with the eruptive scenarios simulated by MAGFLOW for iterative validation. This new satellite-driven modelling strategy represents an operational monitoring system that should give during an eruption: (i) the current state of the effusive activity; (ii) the probable evolution of the lava flow field; (iii) the potential impact of lava flows. Here, we will describe and demonstrate the operation of this system during the most recent flank eruption occurred at Etna volcano on December 24, 2018.

Textural variations along a vertical section of a distal portion of an Etnean lava flow

Giuliani L.*¹, Iezzi G.¹⁻², Casarin A.¹, Piattelli V.¹, Lanzafame G.¹⁻⁴, Nazzari M.², Ferlito C.³, Mollo S.², Scarlato P.², Trabucco F.¹ & Colò M.¹

¹ Dipartimento di Ingegneria e Geologia, Università “G. D’Annunzio”, Chieti.

² Istituto Nazionale di Geofisica e Vulcanologia, Roma.

³ Dipartimento di scienze biologiche, geologiche e ambientali, Università di Catania.

⁴ Elettra-Sincrotrone Trieste S.C.p.A., Basovizza (Trieste).

Corresponding email: letizia.giuliani@unich.it

Keywords: Etnean lava, texture, bubbles.

The textures of bubbles and minerals in a distal portion (~ 3 km from the vent) of an Etnean lava flow have been investigated. Nine oriented rock samples with a volume of about 10³ cm³ have been collected each ~20 cm along the vertical stratigraphy, from the crust down to ~180 cm below. The nine samples (from LV1 to LV9 moving from the bottom to the top, respectively) were cut and polished such to expose the surfaces containing the flow and vertical directions.

High-resolution scanner (HRS) was used to quantify all bubbles ≥ 1 mm on the mesoscopic polished planes, while optical microscopy (TOM) and electron scanning microscope (SEM) were used to analyze crystals and bubbles < 1 mm on thin sections.

From the top to the bottom, large and coalesced bubbles are 30 to 20 area% (LV9, LV8 and LV7), then they decrease to around 15 area% (LV6, LV5 and LV4) and finally became equal or even lower than 10 area% (LV3, LV2 and LV1). These three latter and deepest samples host many sub-mm bubbles, LV4 shows vertical pipe-like bubble channels, while from LV5 to LV9 the bubbles increase in size (mm to cm) and decrease in number per area (1/mm² or mm⁻²). On the whole, from LV1 to LV9 the bubbles content (area%) and their number per area linearly increase and roughly decrease, respectively.

The lava hosts the following minerals: clinopyroxene (cpx), plagioclase (plg), olivine (ol) and spinel (sp). From LV1 to LV9, the area% of sp does not show evident changes. From LV1 to LV7, the amount of cpx slightly decreases and then suddenly increases from LV7 to LV8 and LV9. Plg follows an opposite trend. The number of cpx and plg per area is almost constant and close to 1-2 mm⁻², while it changes for sp from 2 to 18 mm⁻². The crystal size of cpx, plg and sp slightly changes along the vertical section and reach maximum values of 10, 2, and 0.5 mm, respectively.

In 2D, the long side of crystals aligns along the flow direction, normal to the vertical section, whereas bubbles are poorly oriented along a preferential direction, except for LV4 which displays vertical degassing channels.

The outcomes indicate that at several km away from vent bubbles still degassing, ascend and coalesce. Indeed, these bubble dynamics are possible only in a poor viscous suspension; in turn, this lava was at high temperature and with low amount of crystals. A second consequence is that a significant portion of cpx and plg crystallized during flowage in response of distal release of volatiles and cooling kinetics. The gentle increase of plg content coupled with the slight decrease of cpx crystals from LV1 to LV7 can be ascribed to distal degassing. Conversely, the further increase of cpx content accompanied by the decreasing of plg in LV8 and LV9 can be due to high cooling conditions in proximity of the lava crust.

Diffusive fractionation of trace elements between mixing melts: the experimental approach

González-García D.*¹, Petrelli M.², Behrens H.³, Vetere F.², Morgavi D.², Giordano D.^{1,4} & Perugini D.²

¹ Dipartimento di Scienze della Terra, Università degli Studi di Torino.

² Dipartimento di Fisica e Geologia, Università degli Studi di Perugia.

³ Institut für Mineralogie, Leibniz Universität Hannover.

⁴ IGG-CNR, Pisa.

Corresponding email: diego.gonzalezgarcia@unito.it

Keywords: trace elements, diffusion, magma mixing.

During the interaction between compositionally distinct magmas, the evolution of the system is controlled by the interplay between chemical diffusion and advection/mingling, in a way that these two processes enhance each other. In consequence, to understand the chemical evolution of magma mixing events and unravel their timescales, a good knowledge of chemical diffusion is necessary. Particularly, trace elements are of crucial importance since they exhibit a higher variability in behaviour than major elements, which are often subject to strong coupling.

Since the diffusive behaviour of trace elements can be influenced by their starting concentrations, it is of crucial importance in any experimental work to use melts of natural composition. We carried out a series of diffusion couple experiments using natural shoshonitic and rhyolitic melts from Vulcano (Aeolian Islands, Italy) at high pressure and temperature and varying water contents, from 0.3 to 1.9 wt.% H₂O (González-García et al., 2018). Experiments were run in an IHPV apparatus and trace elements were analysed using LA-ICP-MS. Results show that two distinct trace element groups can be distinguished according to their diffusive behaviour: (I) elements showing a normal diffusive behaviour, mostly LILE and transitional elements (e.g. Rb, Ba, Sr, V) plus Eu; and (II) elements with strongly non-ideal behaviour (uphill diffusion), comprising HFS (Y, Zr, Nb, Pb) and, more strikingly, all trivalent-only REE (La to Sm and Gd to Lu).

Elements in group I can be modelled by using a simple concentration-dependent approach. However, elements in group II show strongly asymmetric profiles in the form of deep minima in the rhyolitic side coupled to wide maxima in the shoshonitic side. These profiles can be modelled by a modified effective binary diffusion model (Zhang, 1993) in which activity gradients control diffusion, instead of concentration gradients. This results in a melt-melt transient partitioning towards the less polymerized melt (shoshonite), superimposed to normal diffusion. These results show that group II elements can potentially fractionate quickly to one of the magmas in the early stages of a mixing event, effectively increasing their compositional variability instead of evolving towards the hybrid composition.

González-García D., Petrelli M., Behrens H., Vetere F., Fischer L.A., Morgavi D. & Perugini D. (2018) - Diffusive exchange of trace elements between alkaline melts: implications of element fractionation and timescale estimation during magma mixing. *Geochimica et Cosmochimica Acta*, 233, 95-114.

Zhang Y. (1993) - A modified effective binary diffusion model. *Journal of Geophysical Research*, 98, 11901-11920.

An experimental overview on the role of decompression on bubble formation in trachytic magma

Kazarian A.*¹, Cáceres F.², Scheu B.², Vona A.¹, Misiti V.³, Dingwell D.B.² & Romano C.¹

¹ Dipartimento di Scienze, Università degli studi Roma Tre.

² Earth & Environmental Sciences, Ludwig-Maximilians-Universität, Munich, Germany.

³ INGV, Rome.

Corresponding email: anush.kazarian@uniroma3.it

Keywords: decompression experiment, degassing.

Rapid decompression of magma represents an important trigger for the fragmentation mechanisms and explosive eruptions. During the ascent path of magma in the conduit, the drop of the confining pressure leads to nucleation and growth of bubbles (e.g., decrease of volatile solubility). This process can develop a certain overpressure of bubbles and, concurrently, an accelerating ascent rate. The development of overpressure in the magmatic system plays a key role during the magma ascent driving the fragmentation processes and the eruptive styles.

In this regard, the investigation of the degassing processes in magmas represents a powerful tool to better understand and quantify the fragmentation mechanisms and eruptive behavior of different compositions.

This study investigates the influence of the physical state of trachytic magma from the Agnano Monte Spina eruption (Phlegrean Fields) (e.g., volatile content, bubble content, and shape) and the decompression style (rapid, one-step, multi-step decompression and decompression rate) on the degassing process. We performed isothermal decompression experiments at liquidus state with a shock-tube apparatus at 750-850°C, resembling the temperatures conditions in the shallow conduit prior to fragmentation. Three hydrous homogeneous glasses with different water contents (0.35 wt.%, 0.5 wt.%, and 1.77 wt.%, respectively) were decompressed starting from undersaturated conditions (pressure ranging from 22 MPa to 6 MPa) to oversaturated pressure conditions.

According to previous studies from literature, our experimental results are discussed in terms of textural features of the degassed samples in order to identify and discriminate the effect of the decompression style (e.g., decompression rates, annealing time) and of the initial water content. Compared to literature data for different melt composition, the results showed good consistency.

Our preliminary results show how the experimental strategy is consistent with previous studies from literature, and future analyses will improve the investigation on the different degassing styles of trachytes via vesiculation and water diffusivity, as well as their influence on the rheology of magmas in the conduit and on the AMS eruption dynamics (e.g., fragmentation threshold and explosive dynamics).

Early explosive activity at Vico volcano, central Italy: a new perspective from proximal and distal sedimentary archives

Monaco L.*¹, Giaccio B.², Palladino D. M.¹, Gaeta M.¹, Sottili G.¹, Marra F.³, Castorina F.¹, Nomade S.⁴, Pereira A.⁴⁻⁵ & Albert P.G.⁶

¹ Dipartimento di Scienze della Terra, Università degli Studi di ROMA “La Sapienza”, Rome, Italy.

² Istituto di Geologia Ambientale e Geoingegneria, CNR, Monterotondo, Rome, Italy.

³ Istituto Nazionale di Geofisica e Vulcanologia, Rome, Italy.

⁴ Laboratoire des Sciences du Climat et de L’Environnement (CEA-CNRS-UVSQ), and Université de Paris-Saclay, France.

⁵ Ecole française de Rome, Rome, Italy.

⁶ Research Laboratory for Archaeology and the History of Art, School of Archaeology, University of Oxford, UK.

Corresponding email: lorenzo.monaco@uniroma1.it

Keywords: Vico, Tephrostratigraphy, Distal Archives.

Explosive volcanism is commonly reconstructed thanks to near-vent deposits, where geological records can provide fundamental insights for evaluating depositional processes, eruptive dynamics and evolution of the volcanic edifice. However, due to the intense volcano-tectonic and sedimentary processes occurring close to the volcano, proximal outcrops are most of the time lacunose and incomplete (Giaccio et al., 2014). In contrast, distal archives can continuously record sedimentation of ash layers, providing useful integrative information for reconstructing history and dynamics of the explosive activity (Albert et al., 2019).

In this study, we have stratigraphically and geochemically characterised proximal and distal deposits belonging to the early activity (425-400 ka) of Vico volcano, central Italy. Specifically, we analysed tephra layers hosted in the lacustrine successions of Fucino and Sulmona intermountain basins as well as Rome’s near-coastal aggradational successions, spanning the ca. 430-365 ka interval. A series of chemically-zoned, rhyolitic to trachytic-phonolitic tephra were analysed and, based on stratigraphical, geochemical and geochronological data, were attributed to Vico explosive activity. In addition to the two major eruptive units, known as Vico a and Vico b (Cioni et al., 1987), a series of “minor” events were recognised in distal settings, documenting a much more complex volcanic history and eruptive behaviour (e.g. eruption frequency and intensities, periods of quiescence) than previously thought. Furthermore, new ⁴⁰Ar/³⁹Ar dates based on distal and mid-distal tephra deposits allowed to propose more precise and accurate geochronological constraints for the two main explosive eruptions of Vico (i.e. a and b), dated at 414.5 ± 1.1 ka and 406.6 ± 1.0 ka (2s analytical uncertainty), respectively.

Our results highlight how a multidisciplinary approach, which integrates data from distal and near-source sedimentary records, is pivotal to better constrain magnitude, eruptive mechanisms and time history of explosive volcanism. In this perspective, a systematic future application of this approach to other volcanoes is fundamental to improve hazard assessment and risk mitigation.

Albert P.G., Giaccio B., Isaia R., Costa A., Niespolo E. M., Nomade S., Pereira A., Renne P.R., Hinchliffe A., Mark D.F., Brown R. J. & Smith V.C. (2019) - Evidence for a large-magnitude eruption from Campi Flegrei caldera (Italy) at 29 ka. *Geology*, <https://doi.org/10.1130/G45805.1>

Cioni R., Sbrana A., Bertagnini A., Buonasorte G., Landi P., Rossi U. & Salvati L. (1987) - Tephrostratigraphic correlations in the Vulcini, Vico and Sabatini volcanic successions. *Per. Mineral.*, 56, 137-155.

Giaccio B., Galli P., Peronace E., Arienzo I., Nomade S., Cavinato G. P., Mancini M., Messina P. & Sottili G. (2014) - A 560–440 ka tephra record from the Mercure Basin, southern Italy: volcanological and tephrostratigraphic implications. *J. Quat. Sci.*, 29, 232-248.

AEOLUS: a laboratory to study bubble-bearing flow dynamics and geophysical signals through analogue volcanic eruption

Morgavi D.*¹, Spina L.², Cannata A.³, Musu A.¹, Campeggi C.¹ & Perugini D.¹

¹ Department of Physics and Geology, University of Perugia, Italy.

² Istituto Nazionale di Geofisica e Vulcanologia, Sezione di Roma1, Roma, Italy.

³ Dipartimento di Scienze Biologiche, Geologiche e Ambientali, Università di Catania, Italy.

Corresponding email: daniele.morgavi@unipg.it

Keywords: Experiments, degassing dynamics.

Basaltic volcanoes represent a very large portion of active volcanism and exhibit a wide variability in their eruptive style. The basaltic eruptive activity in fact shows either a purely effusive behavior or an explosive character, which can, rarely, also turn into violent Plinian eruptions. The most characteristic explosive activities of basaltic magmatism are represented by Strombolian eruptions and lava fountains. The study of the relationship that exists between the pre-eruptive dynamics (e.g. fractional crystallization, mixing, degassing), the chemical-physical variations of the magma in the volcanic feeding system and the related outcomes (in terms of eruptive style and geophysical markers) at the surface has been, in the last decades, reason of numerous studies. Nonetheless, the complexity of the volcanic system and its inaccessibility to direct observations still makes it difficult to reconstruct the dynamics of the magmatic system, basing on surface observations of the eruptive activity. A challenging objective of modern volcanology is to quantitatively characterize eruptive/degassing regimes from geophysical signals (in particular seismic and infrasonic), for both research and monitoring purposes. The outcomes of the attempts made so far are still considered very uncertain because volcanoes remain inaccessible when deriving quantitative information on crucial parameters such as plumbing system geometry and magma viscosity. Therefore the realization of laboratory made by several devices, capable to scale and reproduce in a controlled way the degassing dynamics of volcanic systems and measure the relative elastic markers (seismic and acoustic), is an indispensable tool to identify reliable quantitative relationships between the geophysical signals and the related eruptive and outgassing parameters. With the Aeolus project we build an experimental laboratory for the study of degassing dynamics through analogue volcanic eruptions. In particular the laboratory is capable of 1) investigate the relationship between degassing processes and the relative seismo-acoustic signals; 2) study the effect of different degrees of irregularity (i.e. roughness of the internal surface) of volcanic conduits on the eruptive style and/or the associated seismic-acoustic signals; 3) unravel the timescales of cyclic activity at basaltic volcanoes, reproducing the foam collapse model of Jaupart and Vergnolle (1988, 1989), which explains the transition between different explosive terms of the basaltic system (e.g. Strombolian activity and lava fountains), in a range of dimensionless parameters close to the volcanic system.

Lava fountaining activity: the Collapsing Foam Layer Model applied to the 2000 – 2013 South-East Crater eruptive period (Mt. Etna, Italy)

Musu A.*¹, Morgavi D.¹, Spina L.², Corsaro R.A.³ & Perugini D.¹

¹ Department of Physics and Geology, University of Perugia, Italy.

² Istituto Nazionale di Geofisica e Vulcanologia, Sezione di Roma1, Roma, Italy.

³ Istituto Nazionale di Geofisica e Vulcanologia, Osservatorio Etneo-Sezione di Catania, Italy.

Corresponding email: alessandro.musu.9@gmail.com

Keywords: volcanology, experimental, Mt. Etna.

Basaltic volcanoes constitute a big portion of the active volcanoes worldwide and their explosive activity, generally accompanied by eruptive columns formation and pyroclastic fallouts, produced, in the last decades, several damages on human's life with great economical and aviation impact (Scollo et al., 2009; Bonaccorso et al., 2011). Is therefore not surprising the flourishing number of studies devoted to the investigation of the link between plumbing system dynamics and eruptive style. Basaltic eruptive activity may range in a widespread spectrum from lava effusion up to rare violent Plinian eruptions. However, the most iconic explosive activities of basaltic volcanoes are represented by Strombolian explosions and lava fountains.

From 2000 to 2013 several were the episodic lava fountain eruptions taking place at South-East Crater and New South-East Crater (SEC and NSEC – Mt. Etna, Italy –) and a similar eruptive pattern (with gradual increase in explosivity marked by the passage from strombolian to fountain activity) was observed in almost all explosive events. To justify the onset, periodicity and the transition between the above-mentioned eruptive styles, different hypothesis on the degassing dynamics have been made. Here, we make use of a laboratory volcano, Mt. Etna, to test the validity of these assumptions and to calculate different volcanological parameters (e.g. erupted volume and gas flux in the plumbing system). In particular, we applied the Collapsing Foam layer (CF) model (Jaupart and Vergnolle, 1989) to the episodic lava-fountains eruptions occurred at the SEC-NSEC volcanic system between 2000 and 2013. First, we test the validity of CF model by studying the exceptional series of lava fountains observed in 2000 at SEC, with a multi-parametric approach and by assuming the CF model as the reference source model for this eruption, looking for the best parameters that allows to fit the observed pattern and eruptive behavior (e.g. intermittence time, erupted volume of lavas etc.). Secondly, we apply the CF model to three selected eruptions that took place at Mt. Etna south-eastern vents between 2000 and 2013 (the 2000, 2007-08 and 2011-13 eruptions).

Scollo S., Prestifilippo M., Spata G., D'Agostino M. & Coltelli M. (2009) - Forecasting and monitoring Etna volcanic plumes. *Nat. Hazards Earth Syst. Sci.*, 9, 1573-1585.

Bonaccorso A., Caltabiano T., Currenti G., Del Negro C., Gambino S., Ganci G., Giammarco S., Greco F., Pistorio A., Salerno G., Spampinato S. & Boschi E. (2011) - Dynamics of a lava fountain revealed by geophysical, geochemical and thermal satellite measurements: The case of the 10 April 2011 Mt Etna eruption. *Geophysical Research Letters*, 38(24).

Volcanic plumbing system dynamics: unravelling rates and timescales of magma transfer, storage, and eruption

Petrelli M.*¹ & Zellmer G.²

¹ Dipartimento di Fisica e Geologia, Università degli Studi di Perugia.

² Volcanic Risk Solutions, Massey University.

Corresponding email: maurizio.petrelli@unipg.it

Keywords: volcano plumbing system dynamics, timescales of magmatic systems, ephemeral magma chambers.

Unravelling the rates and timescales of crustal magma transfer, storage, emplacement, and eruption is of paramount importance to better understand subvolcanic processes, characterizing volcanic hazards, and developing mitigation strategies. Here, we review the most relevant open questions in this field. Results highlight long storage timescales in deep (i.e., ~20-30 km) crustal hot zones. Estimated ascent velocities from deep reservoirs to shallower systems span a range of ~10 orders of magnitude, being a function of the thermo-physical parameters of the ascending magma (e.g., density, viscosity, and overpressures in the reservoirs) and the host rocks. At mid- to upper crustal levels (i.e., <15-20 km), we elucidate the paradigm of cold storage of magma mushes, which can be unlocked during short-term events to form ephemeral magma chambers.

Unlocking timescale estimates range from minutes to kyrs, indicating a variability of about ~8 to ~10 orders of magnitude. This large variation results from the interplay among many processes, often non-linearly coupled, occurring before an eruption. For example, exsolved volatile species have a significant role in controlling pre-eruptive dynamics and relative timescales. They increase the buoyancy of magmas, affect phase equilibria, promote convective dynamics, and may ultimately trigger eruptive events. As a consequence, understanding the role of volatiles in subvolcanic magmatic processes, including ascent rates, storage mechanisms, and relative timescales, will be paramount for future studies.

Viscosity of ultramafic melts during cooling: insights for emplacement of Martian lava flows

Pisello A.^{*1-2}, Vetere F.P.¹⁻³, Murri M.⁴, Alvaro M.⁴, Rossi S.¹, Holtz F.³ & Perugini D.¹

¹ Department of Physics and Geology, University of Perugia, Italy.

² Istituto di Astrofisica e Planetologia Spaziali, Istituto Nazionale di Astrofisica, Rome, Italy.

³ Institute of Mineralogy, Leibniz Universität Hannover, Germany.

⁴ Dept. of Earth and Environmental Sciences, University of Pavia, Italy.

Corresponding email: alessandropisello@studenti.unipg.it

Keywords: rheology, ultramafic, viscosity.

The study of rheology of magmas under dynamic conditions is possible to be performed with state-of-the-art tools, which allow us to understand dynamics of emplacement of magmatic flows, as well as intraconduit behavior of magmas. In particular, investigating rheological response of mafic and ultramafic magmas is key point to understand and explain very long lava flows that can be observed on terrestrial planets of the solar system, in order to make hypotheses about the geodynamics that determines the superficial manifestation of endogenous processes.

For this reason, new viscosity experiments have been performed, starting from isothermal measurements at superliquidus (>1650 K) and subsequent measurements during cooling down the system at different rates. These measurements were performed on extremely mafic melts whose composition can be correlated to the ones of Martian lava flows. In particular, two melts were synthesized and analysed: one melt whose composition was relatable to the 120m thick pyroxenitic layer of Theo's flow (Abitibi Greenstone belt, Ontario, Canada) an ancient (2.7 Ga) outcrop which has been recognized as a possible Martian analogue; and another melt having the same bulk composition of Martian metoerites (Nakhlites). Results show how these compositions are extremely fluid as measured viscosity ranges between ca. 2 and 8 Pa*s in the temperature range 1650-1520 K. These values can determine the onset of turbulent regime flow, and this might explain the occurrence of extremely long lava flows on Mars as well as features interpreted as volcanic channels in the Kasei Valles on Mars.

This study integrates the scarce but growing number of studies concerning the observation of viscosity variation during cooling, with insights on applications to planetary science. However, investigating non-equilibrium rheology for a wide range of compositions is generally important to understand dynamics occurring in different types of volcanic scenarios.

Rheological behavior of lava flows from Ischia Island (Campania, Italy)

Primerano P.*¹, Giordano G.¹, Vona A.¹, De Vita S.² & Morgavi D.³

¹ Dipartimento di Scienze, Università degli Studi Roma Tre.

² Istituto Nazionale di Geofisica e Vulcanologia - Osservatorio Vesuviano Napoli.

³ Dipartimento di Fisica e Geologia, Università di Perugia.

Corresponding email: paolo.primerano@uniroma3.it

Keywords: hazard, lava, rheology.

Ischia island is a densely inhabited active volcano, hosting a permanent population of about 50'000 people which increases during summer. Nonetheless, the risk associated with lava flows in case of renewal of activity is relatively understudied.

The first analysis in this work is the description and the distribution of both effusive and explosive eruptions volumes during the last 10 kyrs.

Starting from the characterization of the last period of history of the island, we have chosen two end-member lava flows, in order to produce a rheological model on which to base a potential scenario. A textural analysis and a rheological study of natural and partially-crystallized magma from the Arso Lavas (1302 A.D) and Zaro Lava domes and flows (6 ± 2.2 ka) have been performed. The present work aims at investigating the role of the high crystal cargo (up to 75% for Arso and 87% for Zaro) in the rheological behavior of these lava flows. Three gaussian-shaped peaks observed in both CSDs can be interpreted as the magma chamber crystallization phase with rise of magma to surface in at least one stage. The syn-emplacement conditions have been established by removing the microcrystal population in a temperature-controlled furnace. The rheological properties are determined by a series of high-temperature deformation experiments in a uniaxial press.

One of the important targets for this work is the relationship between the velocity of the lava flows and the ground slope. All the data necessary to apply the Jeffreys equation, relative to the environment and to the area of emplacement, like position, geometry and slope of the channel, have been evaluated by a GIS analysis. The rheological model will be improved with analogue experiments, aimed to mimic lava flow dynamics, performed on reconstructed paleomorphology by 3D printing. The eruption duration of Arso Lavas is known because it is the last eruption at Ischia, which occurred in 1302 A.D. This information makes it possible to constrain a rheological model that can be extended to estimate the impact parameters of other similar lava flows on the island.

Basalt-rhyolite interaction timescales in the caldera-forming Halarauður eruption (Krafla, Iceland) constrained by chaotic mixing experiments

Rooyackers S.¹, Morgavi D.*², Perugini D.², Petrelli M.², Vetere F.², Stix J.¹, Berlo K.¹,
Barker S.³ & Charlier B.³

¹ Department of Earth and Planetary Sciences, McGill University, Montreal, Canada.

² Dipartimento di Fisica e Geologia, Università Degli Studi di Perugia, Perugia, Italy.

³ School of Geography, Environment and Earth Sciences, Victoria University of Wellington, Wellington, New Zealand.

Corresponding email: shane.rooyackers@mail.mcgill.ca

Keywords: Magma mixing, eruption trigger.

Interactions between mafic and felsic magmas are common, and their influence on the timing and dynamics of small eruptions, including many historic examples, is well-studied. However, less is known about these interactions in caldera-forming eruptions (magma volumes > several km³), which have scarcely been observed historically. Further studies are needed to better constrain the role magma mixing processes may play in priming, triggering and modulating these large events.

Ignimbrite from the ~110 ka caldera-forming Halarauður eruption of Krafla volcano, Iceland (magma volume ~2-5 km³), preserves physical and chemical evidence for magma mixing. Millimetre-scale quenched mafic enclaves are ubiquitous in felsic pumice erupted in the earliest phase, and record initial interaction of mafic magma with felsic compositions near the chamber roof. Later-erupted spatter-rich welded ignimbrites preserve fluidal steaks and blebs of diverse composition at outcrop- to thin section-scale, reflecting chaotic mixing of sub-equal volumes of basalt and rhyolite in a liquid state at deeper levels. Juvenile whole-rock compositions span a continuous range from rhyolite (74.6 wt% SiO₂, 0.2 wt% MgO) to basalt (50 wt% SiO₂, 5 wt% MgO) and become more mafic on average up-section. The uppermost units are uniformly basaltic, and reflect tapping of the deepest levels of the chamber.

Correlations between whole-rock major oxide concentrations, and between concentrations of trace elements with similar properties (e.g. rare earth or high field strength elements), are strongly linear ($R^2 > 0.8$). Other pairs of trace elements show weaker correlations, reflecting the diffusive fractionation of elements with differing mobilities that homogenise at different rates during chaotic mixing (Perugini et al., 2006). This diffusive fractionation process acts as a 'geochemical clock', and can be used to constrain mixing timescales if the different rates of element homogenisation are known. Recent studies have shown that chaotic mixing experiments, performed at magmatic temperatures using natural samples, can effectively constrain these rates empirically and unravel mixing timescales. Towards this objective, we have performed a time series of chaotic mixing experiments with the Chaotic Magma Mixing Apparatus (COMMA) at the University of Perugia, using natural Halarauður endmember compositions. The experimental mixing protocol produced filaments that are structurally similar to those in our natural samples, and major and trace element compositional transects across these filaments reveal a diversity of hybrid compositions produced by diffusive fractionation. Our preliminary results suggest that mixing timescales were short (hours to a few tens of hours), and imply that the eruption was triggered by basaltic recharge.

Perugini D., Petrelli M. & Poli G. (2006) - Diffusive fractionation of trace elements by chaotic mixing of magmas. *Earth Planet. Sci. Lett.*, 243, 669-680.

Role of magma mixing in the pre-eruptive dynamics of the Aeolian Islands volcanoes (Southern Tyrrhenian Sea, Italy)

Rossi S.*¹, Petrelli M.¹, Morgavi D.¹, Vetere F.P.¹, Almeev R.R.², Astbury R.L.¹ & Perugini D.¹

¹ Dipartimento di Fisica e Geologia, Università degli Studi di Perugia.

² Institut für Mineralogie, Leibniz Universität Hannover.

Corresponding email: stefano.rossi1@studenti.unipg.it

Keywords: magma mixing, time series experiments, eruption timescales.

In this work, we combined literature and experimental data to investigate the role of magma mixing in the pre-eruptive dynamics of the Aeolian Islands volcanoes. First, we reviewed the evidence supporting the hypothesis of mixing-triggered eruptions in the Aeolian archipelago, providing textural, chemical, and rheological constraints. Literature data highlighted significant occurrences of magma mixing dynamics in many eruptive events throughout the entire archipelago. Examples include the Upper Pollara and Porri volcano eruptions at Salina, the Monte Guardia and the AD 1230 Monte Pilato eruption at Lipari, and the present-day volcanic activity at Stromboli. We then focused our attention on Vulcano Island, chosen as a case study as it represents one of the volcanoes posing the highest risk in the Aeolian region. Here, we studied the role of magma mixing in the AD 1739 and 1888–90 eruptions. Thereafter, we investigated mixing-to-eruption timescales for the AD 1739 eruption, performing magma mixing experiments and then evaluating the progressive decay of the chemical concentration variance with time. Our estimates pointed to mixing-to-eruption timescales of the order of 29 ± 9 hours and magma ascent rates ranging between 3×10^2 and 5×10^2 m s⁻¹. Finally, we emphasized the potential implications of the presented results in the context of volcanic hazard mitigation and planning of emergency activities.

SO₂ flux and eruptive activity at Mt. Etna between the 2015 and 2016

Sacco G.*¹, Caltabiano T.², Salerno G.² & Viccaro M.^{1,2}

¹ Dipartimento di Scienze Biologiche, Geologiche e Ambientali.

² Istituto Nazionale di Geofisica e Vulcanologia – Sezione di Catania, Osservatorio Etneo.

Corresponding email: gaiasacco176@gmail.com

Keywords: SO₂-flux, eruptive activity, magma budget.

Between March 2015 and May 2016, Mt Etna experienced an intense sequence of explosive activity which ranged from weak Strombolian to extremely vigorous lava fountaining from the New South East Crater and the Voragine (Cannata et al., 2018; Corsaro et al., 2017). Throughout the 14 months, the degassing regime of the volcano was regularly observed by measuring the bulk SO₂ flux from the summit craters. Data indicates values typical of quiescence and below 5,000 tons/day (t/d) for most of the period during March 2015 – May 2016, except for some increases with values up to 9,500 t/d that marked especially the onset of eruptive activity. By integrating the SO₂ emission rates with petrological data, we inverted the volume of degassed magma that stated for $\sim 1.4 \times 10^5 \text{ m}^3$ and $\sim 2.6 \times 10^5 \text{ m}^3$ at 1 March 2015 and 31 May 2016, respectively. The total average erupted volumes during the three main eruptive episodes were of $\sim 3.9 \times 10^6 \text{ m}^3$ for the May 2015, $\sim 9.7 \times 10^6 \text{ m}^3$ for December 2015 and of $\sim 5.6 - 8.8 \times 10^6 \text{ m}^3$ for the event occurred on May 2016 (Corsaro et al., 2017; Branca, personal communication). This leads to a total average volume of erupted magma of about $\sim 2.0 \times 10^7 \text{ m}^3$ over the considered period. Considering the total volume of degassed magma on 31 May 2016 of $\sim 1.2 \times 10^8 \text{ m}^3$, the balance between the degassed and erupted magma yields a volumetric ratio of about 6:1, which imply a volume of intruded and not erupted magma of about $\sim 1.0 \times 10^8 \text{ m}^3$. Results achieved in this study, underline a close relationship between the SO₂ emission rates and the eruptive activity in both magnitude and temporal scale. The observed disequilibrium between degassed and erupted magmas volume, implies two scenarios in which (i) the intruded magma remains stored at depth within the crust undergoing continuous degassing, and/or might be potentially remobilized upward through recharge from depth by new gas-rich magma injections, or (ii) gas flushing processes.

- Cannata A, Di Grazia G., Giuffrida M., Gresta S., Palano M., Sciotto M., Viccaro M. & Zuccarello F. (2018) - Space-time evolution of magma storage and transfer at Mt. Etna volcano (Italy): The 2015-2016 reawakening of Voragine crater. *Geochemistry, Geophysics, Geosystems*, 19, 471-495. <https://doi.org/10.1002/2017GC007296>
- Corsaro R.A., Andronico D., Behncke B., Branca S., Caltabiano T., Ciancitto F., Cristaldi A., De Beni E., La Spina A., Lodato L., Miraglia L., Neri M., Salerno G., Scollo S. & Spata G. (2017) - Monitoring the December 2015 summit eruptions of Mt. Etna (Italy): Implications on eruptive dynamics. *J. Volcanol. Geotherm. Res.*, 341, 53-69. <https://doi.org/10.1016/j.jvolgeores.2017.04.018>.

Infrared thermography of pyroclast cooling across the glass transition temperature: effect of clast composition, porosity and dimension

Scarani A.*¹, Silleni A.¹, Vona A.¹, Romano C.¹ & Giordano G.¹

¹ Dipartimento di Scienze, Università degli Studi Roma Tre.

Corresponding email: alex.scarani@uniroma3.it

Keywords: cooling, tg.

Understanding the thermal evolution of explosive eruptive events such as volcanic plumes and pyroclastic density currents (PDCs) is of paramount importance to model and anticipate the dynamics of volcanic eruption. For instance, the temperature of a PDC directly influences its total run out distance and ultimately determines the characteristic of the volcanic deposit. Most of our knowledge about pyroclasts cooling stems on physical and mathematical models, where tephra particles are usually assumed to be spherical and homogeneous.

In order to evaluate the complexities of natural volcanic material, a suite of cooling experiments was carried out with a thermal camera FLIR T 1030 on selected pyroclasts of variable porosity, dimension, and composition. Investigated samples include pumices and scoriae from the 4.1 ka Agnano Monte Spina (AMS, Campi Flegrei, alkali-trachyte) and 472 CE Pollena (PO, Vesuvius, phono-tephrite) eruptions. Samples were machined to have a fixed cubic shape (1.5 x 1.5 cm and 0.9 x 0.9 cm) and a porosity (ϕ) ranging from 53-63% (PO) to 82-88% (AMS). Pyroclasts were heated up to 800°C (above the glass transition temperature, T_g) and temperature decay was recorded during natural cooling in air with a thermal camera and with two thermocouples placed inside the sample and next to its surface (used as external calibration temperatures).

Temperature-time plots describe a different cooling path above and below the glass transition temperature (T_g). Cooling curves are well modeled using a combination of two exponential decay functions, describing the clast thermal evolution at T > T_g and T.

Cooling behavior of investigated scoriae and pumices is strongly affected by clast dimension and porosity. In general, cooling efficiency increases with decreasing size and increasing porosity of the clasts. Moreover, the influence of dimension seems to be more important for low porosity clasts, compared to high porosity ones where higher air entrainment allows more efficient cooling.

These preliminary results indicate that further experimental work is needed to constrain and model systematically the cooling of juvenile component, contributing to improve our understanding of volcanic plumes and PDCs dynamics.

The effects of interclast viscosity contrast in the welding ability of pyroclastic deposits

Silleni A.*¹, Ryan A.G.², Russell J.K.², Vona A.¹, Giordano G.¹, Ort M.³ & Romano C.¹

¹ Dipartimento di Scienze, Università di Roma Tre.

² Volcanology and Petrology Laboratory, Department of Earth and Ocean Sciences, University of British Columbia.

³ SES, Box 4099, Northern Arizona University.

Corresponding email: aurora.silleni@uniroma3.it

Keywords: welding, viscosity, pyroclastic deposits.

The rheological behaviour of pyroclastic deposits during welding is incompletely understood and is based on a small number of experimental studies. In order to understand the effect of interclast viscosity contrast, during the welding process, high-temperature experiments were done with two different dimension classes: ash and lapilli.

The experiments are performed with a uniaxial compression load apparatus using a constant displacement rate to simulate the increasing load during the deposition (≤ 1.1 MPa), at elevated temperature above the glass transition (600-800°C). Powder (0.64-2 mm) was inserted in cylindrical alumina sleeves (3.8 cm diameter, ~ 6 cm length). In addition to ash, in the experiments were introduced lapilli to evaluate the strain dissipation between the different sizes and to reproduce the fiamme formation in the natural deposits.

The rheological model provides new understanding of the welding process and welding degree with different size material and in particular the emplacement condition of the pyroclastic density currents. An example of this is represented by the Campanian Ignimbrite (CI), the largest caldera-forming eruption of the Campi Flegrei. As a matter of fact, the main units of the pyroclastic flow generated during the eruption show different welding degree, ranging from partially welded with the presence of fiamme in the proximal area to widely unwelded in the distal location.

Experimental investigations on degassing behavior and related seismo-acoustic markers: the effect of complex conduit geometries

Spina L.*¹, Morgavi D.², Cannata A.³⁻⁴ & Perugini D.²

¹ Istituto Nazionale di Geofisica e Vulcanologia, Sezione di Roma1, Rome, Italy.

² Department of Physics and Geology, University of Perugia, Italy.

³ Istituto Nazionale di Geofisica e Vulcanologia, Osservatorio Etneo, Sezione di Catania, Italy.

⁴ Dipartimento di Scienze Biologiche, Geologiche e Ambientali, Università di Catania, Italy.

Corresponding email: laura.spina@ingv.it

Keywords: analogue experiments, fractal conduits, seismic tremor.

One of the main challenge in monitoring active volcanoes is understanding gas-magma dynamics in volcanic conduits and relating them with their geophysical markers at the surface. Accordingly, we combine here two main approaches used to investigate conduit dynamics via indirect observations, i.e. analogue laboratory experiments and seismo-acoustic measurements, and address a crucial, yet unexplored, subject: the irregularity (i.e. the departure from an ideal smooth cylindrical shape) of the conduit surface. To this aim, we developed a protocol to assemble epoxy conduits with different fractal dimensions (D_c ; i.e. irregularity) of the internal surface, and used silicone oil as a proxy for magma. We investigated different degassing patterns, from bubbly to slug and churn-annular flow, by varying systematically: 1) injected gas flux (5 to 180×10^{-3} l/s); 2) analogue magma viscosity (10 to 1000 Pas); 3) fractal dimension (D_c) of the conduit surface (i.e. $D_c=2$, $D_c=2.18$ and $D_c=2.99$). The experiments were monitored by tracking the temporal evolution of sample expansion and outgassing periodicity through a video-camera and investigating the relative seismo-acoustic fingerprint by means of a set of dedicated sensors (i.e. microphone, piezo-films, accelerometer). Results show that viscosity strongly influences the transition among degassing patterns and the frequency of slug bursts at the surface. Furthermore, we noticed an increase of the exponent of the power law equation linking squared seismic amplitude to gas flow rate with conduit roughness; whereas the opposite trend was observed increasing the viscosity of the liquid phase. These results have fundamental implications for linking eruption source parameters such as the volume discharge rate to seismic data (i.e. volcanic tremor) at different volcanoes or for investigating their temporal evolution at a single vent.

S33

Geosciences at school 2019

CONVENERS AND CHAIRPERSONS

Elena Bonaccorsi (Università di Pisa)

Francesca Cifelli (Università di Roma Tre)

Rosolino Cirrincione (Università di Catania)

Eleonora Paris (Università di Camerino)

Manuela Pelfini (Università di Milano)

Design and experimentation of educational activities on Water resources in the underground: development of an experimental protocol to analyze the dynamics of infiltration, accumulation and exploitation processes in incoherent deposits

Antiga R.*¹, Cabella R.², Elter F.M.² & Massa A.²

¹ Ufficio Regionale III USR Liguria - Genova.

² Dipartimento di Scienze della Terra, dell'Ambiente e della Vita - Università di Genova.

Corresponding email: antiga.roberto@libero.it

Keywords: educational activities, water resources, teaching methodology.

The didactic activity constitutes a vertical laboratory path (from the 1st and 2nd cycle of education) related to the water infiltration processes in incoherent deposits. The educational segment, tested in the IA class of the lower school of the ISA "Carducci Mazzini" in La Spezia, represents a series of experiences aimed at making the dynamics of the processes of accumulation and exploitation of the deep water resource understood. Moreover, experimental protocols have been activated to stimulate students' reflection on the concept of aquifer vulnerability and on gravitational processes, with slipping dynamics due to the accumulation of infiltration water at the interface between permeable and waterproof sedimentary layers. The aim of the course is to activate and / or enhance different complementary skills: on the one hand the ability to stimulate and / or refine the critical observation of a simplified model of reality, identifying the variables involved and the relationships that they exist between them, on the other hand the ability to extend these reflections to the real context to understand the causes and dynamics of natural phenomena. The teaching methodology, is based on the design of laboratory activities fusing simple resources. It aims at stimulating the students' activity and direct interaction with the objects and ideas involved in observations, experiments and study - dedicating ample space for discussion, dialogue, confrontation (cooperative learning), reflection on what one does, problem / solving, in order to construct "logical structures of thought".

The evaluation of the effectiveness of the teaching / learning processes, carried out also through in-out tests, has shown progress at the level of application of a correct use of the scientific methodology, an improvement of the sectoral language, distinguishing it from the common language and in researching / identifying / constrain the system variables in order to assess the objectivity of the data collected and their degree of reliability. Specifically, the students have extrapolated, from the macroscopic observations at the simplified model level, the variables underlying the infiltration, circulation, accumulation and exploitation of the deep water resource; this is essential for an understanding of the dynamics of natural processes.

**To know the hydrogeological instability - study methods and its awareness:
the case of Val Graveglia - Genova - Eastern Liguria**

Antiga R.¹, Cabella R.², Coniglio L.³, Carpanese M.G.³, Elter F.M.*², Lodi C.³, Massa A.², Parola C.³, Tarella G.³ & Tsakarisianos M.D.⁴

¹ Ufficio Regionale III USR Liguria - Genova.

² Dipartimento di Scienze della Terra, dell'Ambiente e della Vita - Università di Genova.

³ Scuola Secondaria I grado Don Gnocchi - Lavagna (Ge).

⁴ Scuola Secondaria I grado Villaggio del Ragazzo - Cogorno (Ge).

Corresponding email: elter@dipteris.unige.it

Keywords: hydrological instability, Secondary First Level school.

From 2017 as part of the PLS-GEO (at DISTAV, University of Genoa), the topic concerning the Hydrogeological instability in Liguria was addressed. This project was aimed both at Secondary First Level School and at Secondary Second Level School. In particular the project was carried out with the First Level School Don Gnocchi of Lavagna (Ge) with their teachers. Liguria is characterized by a wide process of instability. A sample area was chosen, located in Val Graveglia - Municipality of Nè - (Ge), where since 2015 the DISTAV monitors one of the largest landslide in the Ligurian region. This event involves three housing fractions with heavy social repercussions. The project was divided into three parts: the first part dedicated to frontal lessons in school, addressed to the acquisition of the basic concepts of instability in geology and to the presentation of the geological framework of the chosen area; during this step, an anonymous test was presented to define the level of knowledge on the concept of instability. The second part addressed to the acquisition of data on the area, which consists in the measurement of the fractures on buildings, the measurement of the water level using a digital caliper and a phreatimeter; the third and last part related to the data processing by means calculating data collected and their discussion. During the second step of the project, the acquisition of data by the students was filmed by local television channel and presented in the local newcasts. The third part of project targets the drafting of the damage map of building and the geological repercussion on the local and the downstream environment. At the end of the data interpretation the students involved were presented with an anonymous exit test designed to define the level of acquisition of the project. The result has led at least 90% of students have become aware of what the instability means at a technical and social level.

Virtual geomorpholabs: simple games for geomorphorisk education

Artoni C.*¹, Bollati I.M.¹ & Pelfini M.¹

¹ Dipartimento di Scienze della Terra “A. Desio”, Università degli Studi di Milano.

Corresponding email: claudio.arto@fastwebnet.it

Keywords: geomorphology, risk, education.

Geomorphological risk education is a key point in getting awareness about dynamic environment as the high mountain one, and to better understand the landscape evolution in sensitive areas. The wide spreading of mountain lifts and cableways allows many people to easily reach high altitudes and get in direct contact with dynamic and fast changing landscapes. Here, also the impact of climatic changes is evident as high mountains can be considered sentinels of global climate trend. A general destabilization of mountain slopes, changes in geomorphological processes and related hazard scenarios with consequences on the human sphere are becoming even more common. For this reason, it is important for the general public, and moreover for new generations, to get awareness on the role of geomorphological processes and how these processes may impact on risk scenarios. Virtual experiences may help both to train students before the outdoor experience and to consolidate the concepts acquired on the field. With these aims, it is fundamental to develop specific tools. Some examples have been recently proposed to primary and secondary schools: i) web-based games to analyse the dynamics of the debris covered glaciers, the related geomorphic hazards and the connected vegetations dynamics, ii) laboratory activities to be performed in classrooms, based on board games within is important to correctly respond to general questions on physical geography. The proposal of an online platform called “HIGH-MOUNTAIN EDUCATIONAL LAB”, could collect a variety of activities supporting young students in Geosciences educational project. These approaches, allowing to reproduce the outdoor experience in indoor conditions, overcomes problems dealing with high mountain environments such as distances, costs, accessibility, seasonality.

Sustainable city: work together for a more sustainable life style

Beccaceci A.*¹, Stacchiotti L.¹ & Paris E.¹

¹ School of Science and Technology, University of Camerino, Italy.

Corresponding email: alessandra.beccaceci@unicam.it

Keywords: georesources, sustainability, multidisciplinary.

The Sustainable City project (SUSTACITY) aims to introduce students to the themes of the exploitation and utilisation of georesources and, in general, to the need of adopting a more sustainable life style. SUSTACITY has been created in the frame of the Agenda 2030, to allow treatment of topics including clean water and energy, responsible consumption and production, actions for climate, sustainable cities and communities.

The multidisciplinary approach of the project allows to involve teachers of many disciplines, and should be especially useful in Middle School classes (ages 11-14), where time for laboratories is always limited and the teaching of Geosciences and Environmental Education always penalized due to lack of time. Instead, this project shows how using a combination of geoscience topics and environmental problems, with inputs from other disciplines (both sciences and humanities) can allow students to acquire valuable geoscience knowledge as well as developing skills of active citizenship and increased environmental awareness.

The first initiative of the project is an engaging ludic activity carried out using a table game, to be played in teams, planned for 11-14 years old students. This activity will be soon adapted to be used with younger and older students (aged 10 and 15) as an activity related to the vertical curriculum. Each team has an itinerary to follow in steps, with the aim to reach the heart of a sustainable city, starting from a conventional city. The itinerary includes multiple answer quizzes, open tests, mimic and word games. The topics proposed deal with the definition of georesources, their distribution and uses, the pollution, the concept of renewable and non-renewable resources. The questions posed offer also the possibility to reflect about simple but effective actions to take in the everyday life to increase environmental sustainability. In this way the students can become protagonists of the game and translate what they learn to their everyday life, involving the school mates and also their families in the process. The multidisciplinary approach allows proposing questions in the game, where topics of history, geography, science, math and technology are closely connected, also offering links to literature, foreign languages and art.

The first experimentation has been carried out in May 2019 in 2 classes and the preliminary results are very satisfying in terms of involvement of students as well as teachers. It is important to mention that other teachers have already declared to be interested in participating in the project and the experimentation. Expected results include: a) learning new concepts related to geosciences and the Agenda 2030; b) acquiring key competences of active citizenship for more sustainable life styles; c) helping the students' mind to assimilate new content/information and modes of thinking in non-traditional ways; d) developing problem-solving skills.

ICA-LAB: un laboratorio di ricerca interdisciplinare nel Lagerstätte del deserto costiero di Ica (Perù)

Belluzzo A.¹, Bronzo L.¹, Citron S.², Di Stefano G.¹, Favaroni A.*¹, Gazzola R.¹, Gazzurra G.¹, Giacomini P.¹, Martella A.¹, Merella M.¹, Nicodemi L.¹, Porta L.¹, Bianucci G.¹, Bosio G.³, Collareta A.¹, Gioncada A.¹, Landini W.¹, Molli G.¹, Sarti G.¹ & Borghini A.^{1,4}

¹ Dipartimento di Scienze della Terra, Università di Pisa.

² Dipartimento di Biologia, Università di Pisa.

³ Dipartimento di Scienze dell'Ambiente e della Terra, Università degli Studi di Milano-Bicocca.

⁴ Dottorato Regionale in Scienze della Terra Pegaso.

Corresponding email: a.favaroni@studenti.unipi.it

Keywords: Bacino di Pisco, Fossil-Lagerstätte.

Il deserto di Ica, esteso lungo la costa meridionale del Perù, è sede di una successione di sedimenti marini depositi in quella che è oggi la parte emersa di uno dei bacini di avanzamento peruviani: il bacino di Pisco. Tale successione si caratterizza per la straordinaria ricchezza in fossili eccezionalmente conservati di vertebrati marini che ne fanno un vero e proprio Fossil-Lagerstätte. Questa straordinaria associazione fossile è spesso associata all'alta produttività del bacino, a sua volta controllata dall'interazione di dinamiche climatiche, oceanografiche, orogenetiche e vulcaniche in un contesto complesso quale il margine andino dell'Oceano Pacifico. Dal 2006, in questo quadro d'eccezione, un team scientifico internazionale comprendente ricercatori dell'Università di Pisa si è focalizzato sullo studio sistematico dei vertebrati fossili. A partire dal 2014, lo stesso gruppo di ricerca è stato affiancato da esperti in stratigrafia, tettonica, micropaleontologia, vulcanologia, petrologia e geochimica in una serie di progetti di ricerca che hanno visto la partecipazione costante di giovani ricercatori e l'irrobustirsi di una prassi di lavoro sul campo fortemente improntata alla multidisciplinarietà.

Nel mese di gennaio 2019, nell'ambito dei "progetti didattici speciali" promossi dall'Università di Pisa, si è svolto l'ICA-LAB: un campo geo-paleontologico nel deserto costiero di Ica, concepito come un vero e proprio laboratorio di ricerca interdisciplinare nell'ambito delle geoscienze. Tale campo scuola, della durata di 12 giorni, ha visto la partecipazione di 12 studenti di laurea magistrale. Nel corso di questo campo scuola gli studenti hanno potuto avvicinarsi ed interagire con diverse discipline delle geoscienze, apparentemente molto distanti tra loro, quali la paleontologia, la stratigrafia, la tettonica, la geochimica e la vulcanologia. Nel dettaglio, gli studenti hanno fatto esperienza in prima persona di un contesto geologico d'eccezione quale il bacino orientale di Pisco, svolgendo, sotto la guida dei docenti accompagnatori, le seguenti attività:

1. cartografia geologica ed analisi sedimentologico-paleoambientale di sezioni stratigrafiche di dettaglio;
2. analisi delle strutture geologiche associate alle principali fasi tettoniche andine come registrate nel bacino di Pisco-Ica;
3. campionamento della successione sedimentaria e dei tefra ad essa intercalati per analisi geochimiche, radiocronologiche e biostratigrafiche;
4. georeferenziazione e mappatura dei vertebrati fossili;
5. osservazioni tafonomiche/paleoecologiche/sistematiche sui vertebrati fossili;
6. campionamento di vertebrati e macro-invertebrati fossili e di depositi fosforitici per analisi geochimiche, istologiche e mineralogico-petrografiche.

In questo poster i protagonisti dell'ICA-LAB – studenti e docenti – raccontano la propria esperienza, rievocando i tanti aspetti del deserto in cui hanno vissuto e lavorato insieme nel corso di una "lezione fuori sede" davvero speciale.

The good, the bad and the ugly: a movie around the geoscience textbooks

Bonaccorsi E.¹⁻², Borghini A.*¹⁻³, Gioncada A.¹ & Pieraccioni F.¹

¹ Earth Science Department University of Pisa.

² Natural History Museum University of Pisa.

³ PhD Tuscany School - Earth Science.

Corresponding email: alessandra.borghini@phd.unipi.it

Keywords: geoscience, textbooks, misconceptions.

The results of both international and local surveys indicate a worrying and frequent presence of misconceptions about many geoscience topics, expressed by students of any age. The reasons of such phenomenon are complex and involve the whole learning process. The scientific literature points up that, whereas it may be a challenging task to modify the previous, non-scientific, alternative conceptions of the students, it is quite common to maintain them through careless or inappropriate teaching methods and instruments. In this research, we focus on high school textbooks to examine how they present some basic geoscience concepts. Textbooks, according to our knowledge, represent the main tool for most of high school science teachers, widely used for their instructional activities and lessons. The relevance of the geoscience textbooks is amplified for science teachers without a specific training in geology, who often rely on a strictly transmissive approach to the matter, exclusively based on the textbook.

We examine 12 geoscience textbooks, chosen among those adopted in the local high schools. On the basis of a previous survey on the geoscience knowledge at the end of high school and of the scientific literature, we list the most common alternative conceptions that are observed among students, as regards basic Earth science concepts. Afterwards, a form is built through which each textbook is checked for the following five features: (1) if the specific topic of the list is present in the textbook; (2) if there are errors or oversimplifications; (3) the presence of clear definitions; (4) the clarity and correctness of images and labels; (5) the sequence of the arguments.

We will show the preliminary data of this research, in which we may individuate at least two different levels of criticality: (1) errors and/or oversimplifications occur in several parts of the text and (2) the images, which should help students to grasp the meaning of the scientific text, are confuse or wrong. It is worth noting that the latter is not simply an “aesthetic” issue. By comparing our list of students’ alternative conceptions to the corresponding misrepresenting images, in fact, we find that the two sets are closely related. It is probable that the textbooks’ misrepresentations act as a confirmation of pre-existing non-scientific alternative concepts, making more difficult for the students to build correct concepts of the processes that involve our planet.

The virtual trip of Darwin, the geologist

Boniello A.^{*1-2} & Paris E.²⁻³

¹ IC Nettuno I.

² UnicamEarth group – University of Camerino.

³ School of Science and Technology, Geology division.

Corresponding email: annalisa.boniello@unicam.it

Keywords: virtual worlds, geoscience education, immersive education.

Virtual Worlds (VWs) can offer learning environments for geoscience education, giving the students a feeling of “being there”. In fact, VWs are immersive environments that enable situated and constructivist learning, according to the Vygotsky theory, because the learner is inside an “imaginary” world context. In this environment activities and experiences can take place with scaffolding, cooperative learning, peer to peer and peer evaluation, coaching, scientific inquiry.

The research was focused on two questions: 1) Can VWs be effective in improving the acquisition of literacy and skills in geosciences topics? 2) Can an immersive VWs experience motivate students to learn geosciences?

The experience takes place in a virtual island, the UnicamEarth Island (Boniello & Paris, 2014) (<http://d7.unicam.it/unicamearthisland/>) built for this research project at University of Camerino with the software Open Sim (www.opensimulator.org). UnicamEarth Island is a virtual platform where students and science teachers can study, collaborate and create activities on geosciences. Among the available paths, ‘The trip of Darwin, the geologist’, taken from “The Voyage of the Beagle” has been experimented in Middle and High schools in the Napoli area (Italy).

An avatar, Charles Darwin, is built by retrieving data on his actual appearance in young years, to engage the students imagining Darwin, close to their age, as a young scientist. Original pieces from Darwin’s book have been used as a “diary” to read during the virtual journey. Other documents (maps, satellite images, drawings) are available in the path. In their role-play as Darwin, the students can look, move, investigate, operate, access docs and read from the diary. Landscapes as well as the ‘Beagle’ have been virtually re-built in details to recreate a realistic immersive environment, to engage the students in the virtual trip.

Three stops introduce the students to geoscience topics: the city of Concepción, the Andes and an atoll. In the first stop, Concepción is destroyed by earthquakes and tsunami and the students can read in the diary what Darwin wrote about his direct experience. In the Andes the Darwin avatar moves in the mountains and interacts with rocks and maps, images and texts, with the purpose to get acquainted with the different lithologies, their characteristics and environments of formation. In the third stop there is the virtual reconstruction of an atoll, which the students explore in details and read an explanation of the Darwin theory on their formation. The path allows to make interdisciplinary connections as well as introduce subjects like climate change or marine biology.

Questionnaires, observations and interviews have been used to collect data and test the virtual paths. The results suggest that virtual worlds are very effective in education and can be useful to enhance learning outcomes in Earth science learning.

Boniello A. & Paris E. (2014) - Geosciences in virtual worlds: A path in the volcanic area of the Phlegraean Fields. <https://doi.org/10.3301/ROL.2016.64>

What are the students' mental models of the Earth's inner structure?

Borghini A.*¹⁻², Pieraccioni F.¹, Gioncada A.¹ & Bonaccorsi E.¹⁻³

¹ Earth Science Department University of Pisa.

² PhD Tuscany School - Earth Science.

³ Natural History Museum University of Pisa.

Corresponding email: alessandra.borghini@phd.unipi.it

Keywords: misconceptions, Earth's internal structure, secondary school.

According to international scientific literature, misconceptions about Earth's internal structure are common in secondary school students. These alternative ideas mostly concern the layering and the physical state of Earth's layers (e.g. the idea of a liquid mantle is widespread among non-geologists).

A good comprehension of Earth's structure is crucial for further understanding of Earth dynamics (including earthquakes, volcanic activity and plate tectonics). For this reason learning activities should lead students to the construction of a scientifically correct mental model of Earth's interior. This is not an easy task mainly because it is hard for young students to visualize the real dimensions of the Earth and to figure the physical state of rocks at very high temperature and pressure, and also because it is not possible to experience its interior through direct observations.

A pilot teaching sequence was tested on over 130 students 11 to 14 years old from two schools in central Italy. The activities were carried out using different approaches: reading a text, class discussion and the construction of a concrete model to represent the Earth's inner structure.

In this work we discuss the data collected at the beginning of the learning sequence (Earth's interior drawings) and after the teaching intervention (answers to both closed and open-ended questions), with the aim to collect information on how teaching the Earth's internal structure can be improved. The results of the study help to find out which of the misconceptions present in literature we find in Italian secondary school students and what are the main difficulties that students encounter in learning this topic.

Project “What a show! Create a geological corner in your high school”

Caironi V.¹, Regazzola V.², Lorenzetti S.C.¹, Berra G.², Coltro G.² & Fumagalli P.*¹

¹ Dipartimento di Scienze della Terra A.Desio, Università degli Studi, Milano.

² Istituto Orsoline S.Carlo, Milano.

Corresponding email: valeria.caironi@unimi.it

Keywords: School-Work Alternance, geologic exhibition, transversal skills.

The experiences of “Alternanza Scuola–Lavoro (School-Work Alternation) have been organically inserted as an obligatory integral part in the educational offer of all the study addresses of the secondary school (Licei and Technical Institutes) with the law 13 July 2015, n.107 (the so-called “Buona Scuola”). The 2019 Budget Law then changed the name in “Paths for transversal skills and orientation”, also reducing the number of hours required by the previous legislation.

In that frame, the Department of Earth Sciences A. Desio of the University of Milan offers to schools several projects. One of them, entitled “What a show! Create a geological corner in your high school”, was held between February and May 2019 with the Liceo Orsoline San Carlo in Milan. The project was attended by 22 students of the IV class of Liceo Artistico, address Architecture, and the V class of the Liceo Scientifico.

Taking inspiration from the discovery, during renovations of the Institute, of a large number of samples of minerals and rocks, it was decided to have the students set up a small Museum of Earth Sciences.

The work consisted in a first observation and quick identification of the samples, followed by a selection and proper classification of the most interesting ones. Subsequently the participants discussed together the themes to be illustrated, choosing the most suitable samples, the style and the type of exhibition. For the selected samples, identification labels and descriptive sheets with the main mineralogic or petrographic characters were prepared, accompanied by general information on the use of minerals and rocks, with a particular focus on industrial minerals and on lithotypes used in architecture, especially in the urban area of Milan. The students of the Liceo Scientifico mainly worked on the scientific and historical information, while those of the Liceo Artistico mainly focused on the relationship between the use of rocks in different artistic styles and took care of the graphic aspects and the exhibition layout, with the coordination of the Graphic and Design teachers.

The project allowed to increase specific disciplinary knowledge and to exercise and refine observation and classification skills. Furthermore, transversal skills on visual communication, scientific dissemination and the use of computer techniques have been developed.

The exhibition prepared by the students is permanently hosted in the school and is also an enrichment of its heritage, remaining available to future students.

Exploring the moon, using Earth's rocks and fossils: an earth science module

Ferretti M.¹, Invernizzi C.*¹, Mazzoli S.² & Carroll M.R.¹

¹ Università di Camerino, Scuola di Scienze e Tecnologie – Sezione Geologia.

² Università di Napoli Federico II, Dipartimento di Scienze della Terra.

Corresponding email: chiara.invernizzi@unicam.it

Keywords: Moon, interdisciplinary teaching, rock, fossils.

Among the science subjects taught in the Italian secondary schools, Earth sciences is the one that probably suffered the most from the changes introduced by the recent reformation of the National curricula, with chemistry and biology becoming predominant in terms of teaching time, especially in the terminal classes. Despite this, Earth science still represents one of the most diverse branches of the natural sciences, linking astronomy to geology, life sciences and economics, as well as using/applying basic chemistry, physics and math to the natural world. For this reason, geoscience topics allow the development of interdisciplinary teaching units, so much invoked in the new guidelines of the Italian secondary schools.

We present here an Earth Science Module for grade 11 students, designed to engage students in simple hands-on activity to understand how the Earth-Moon relationship can be investigated, by using terrestrial rocks and fossils. The 50th Anniversary of Apollo 11 Moon Landing will represent the starting point of this activity, that should trigger the interest of the students to know why and how the moon is relevant to them.

The activity is focused on two aspect of the Earth-Moon relationship: the origin of the moon (and thus its composition, evidenced by observable dichotomy between dark mare and lighter colored highlands) and the tidal effect of the moon. This latter point is addressed by analysing how lunar tidal forces influence coral growth in both living and fossil examples.

After an introduction to magmatic rocks and the biology of coral growth, students will search information in order to compare terrestrial and lunar rocks, as well as the influence of astronomical cycles on the rhythmic growth of the coral skeletons.

The main goal is to make students understand what evidence exists in support of present hypotheses about the origin of the moon and its main surface structures (as craters, mare, and lunar highlands) and the paleontological data that indicate the gradual slowing of the Earth rotation, thus affecting the number of days in a year.

From Physics to Geology: exploring the time and space”, an outreach and successful project to understand the Earth system and the earthquakes, through the use of the *Quakecaster*, awarded by Gran Sasso National Laboratory (LNGS), INFN (National Institute for Nuclear Physics), contest “Anch’io Scienziato 2019”

Garzarella A.^{*1-3}, Valentini A.², Pace B.², Liguori A.³, Michelangeli M.A.³ & Middle School Class 3B³

¹ Dipartimento InGeo, Università degli Studi “G. d’Annunzio” Chieti.

² DiSPUTER, Università degli Studi “G. d’Annunzio”.

³ Istituto Comprensivo 3 “V. Antonelli”, Chieti.

Corresponding email: a.garzarella@unich.it

Keywords: outreach, quakecaster, earthquake.

In collaboration with the Department DiSPUTER (University of Chieti, Italy), the middle school class 3B from “V. Antonelli” School of Chieti took part to the contest “*Anch’io scienziato 2019*”, organized by the Gran Sasso National Laboratory (LNGS), INFN (National Institute for Nuclear Physics). The competition, open to classes, groups or individual students, consisted of the realization of scientific works on a free theme. The works could relate to projects, machines, images, experiences or results of experiments and be accompanied by a report in typewritten or multimedia format and a bibliography. The Class 3B project focused on the knowledge of the seismic behaviour of the lithosphere and the mechanism triggering earthquakes, through the use of the tool “*QuakeCaster*”, at first developed by USGS. *QuakeCaster* is an interactive teaching model that simulates earthquakes and their interactions along a plate-boundary fault. It contains the minimum number of physical processes needed to demonstrate most observable earthquake features: a winch to steadily reel in a line simulates the steady plate tectonic motions far from the plate boundaries; a granite slider in frictional contact with a nonskid rock-like surface simulates a fault at a plate boundary; a rubber band connecting the line to the slider simulates the elastic character of the Earth’s crust. By stacking and unstacking sliders and cranking in the winch, one can see the results of changing the shear stress and the clamping stress on a fault. By placing sliders in series with rubber bands between them, one can simulate the interaction of earthquakes along a fault, such as cascading or toggling shocks (Linton & Stein 2015). A classroom training meeting was held by the researchers to explain the Earth system, seismic processes and laws, and to show the *QuakeCaster*. The students recorded a set of measures related to the simulation of earthquakes. With a stopwatch and a ruler, they measured the timing and slip distance of earthquakes, transcribed the data in an Excel file sheet and plotted them. The whole data set were analysed and discussed and shown it through a PPT presentation. The project was awarded during the Open day 2019 ceremony, at the Gran Sasso National Laboratory (LNGS), INFN (National Institute for Nuclear Physics), Assergi (Aq).

Linton K. & Stein R.S. (2015) - How to build and teach with *QuakeCaster* - An earthquake demonstration and exploration tool (ver. 1.1, March 2015): U.S.G.S. Open-File Rep. 2011–1158. <https://www.lngs.infn.it/it/concorsi-per-scuole>

Climate education in the deep time perspective: working with teachers and students

Lozar F.* & Tonon M.D.

Dipartimento di Scienze della Terra. Università di Torino.

Corresponding email: francesca.lozar@unito.it

Keywords: geoscience education, climate change, thermal maxima.

Climate science is a complex interdisciplinary field of knowledge, to which many scientists from different fields can contribute (physics, chemistry, mathematics, engineering, social sciences, economics...). Among these, Earth sciences can contribute to climate science, and in particular to the understanding of thermal maxima in Earth history, since sedimentary rocks can record valuable information about past environment, climate, and biota just before, during and after the perturbation. The geological record offers a unique approach, not shared by other sciences, that allow to understand how the biota responded to climate change and how they coped in past high CO₂ worlds. After the establishment of the Intergovernmental Panel on Climate Change in 1988 and the United Nation Rio de Janeiro Earth Summit, held in 1992, both governments and scientists are working to address the subject of climate change. This subject has been a matter of exclusively scientific and political debate for long time, but recently has become a very common concern among the public, and more so in the last year, since the beginning of the movement Fridays For Future, that asks governments to respect the 2015 Paris agreements on keeping the temperature rise below 2 degrees and stop increasing greenhouse gas emissions as soon as possible. As for other scientific subjects impacting everyday life (such as volcanic and seismic risks), it is very common to come across scientific misconceptions when interacting with the general public, mainly due to the very limited scientific literacy of the people. We applied the geological approach to the subject of climate change with teachers and students, in order to eliminate misconceptions and overcome the cognitive obstacles related to the time scale at which the process of climate change takes place and to the amplitude of its impact. First we held a class for teachers only, on how to communicate and teach the subject of climate change. We used geological examples useful to understand the time frame of the change (e.g. the Paleocene/Eocene thermal maximum, climate change at the precessional scale, such as Mediterranean sapropels formation), and prepared lab and field exercises that can be reproduce by the teachers alone with their students. The lab exercises have been designed to encourage reflection on the geological time scale of the change, both studying data on fossil populations and on the depositional regime. The field exercise held with the students were useful to reinforce the concept of the time scale of the change and the extent of the impact (even a small change has an important impact). The outcome of the project is to improve the scientific literacy of both teachers and students, stimulating the reflection on the difference between geological and man-made climate change, and boost virtuous behaviour that can diminish the human impact on the current climate change.

“HAVE YOU GOT A GREEN THUMB?” Hands-on experiences of kids’ and teens’ earth science education by inquiry-based methods

Moroni B.*

Istituto di Istruzione Superiore “Ciuffelli-Einaudi”, Todi (PG) - Dipartimento di Chimica Biologia e Biotecnologie, Università di Perugia

Corresponding email: beatrice.moroni1@istruzione.it

Keywords: IBSE, soil texture, soil permeability.

Inquiry-Based Science Education (IBSE; Olson & Loucks-Horsley, 2000) is a form of science education that gives the students the opportunity to explore the world around them by means of hands-on experiments, to ask questions and to develop responses based on reasoning and critical reflection. It has been proven to be a very powerful tool to stimulate students’ interest in scientific disciplines and the development of a critical thinking.

Hands-on activities play a crucial role in all four levels of inquiry-based learning in science education: confirmation inquiry, structured inquiry, guided inquiry and, finally, open inquiry which is the highest level of inquiry and the closest to the “real” scientific research. It is not easy to transform science content into the form of IBSE, and the main task for the teacher is to adequately support the pupils during the different phases of an IBSE project, such as formulating a proper research question and designing and conducting an investigation. This study presents a particular example of hands-on activities on the same topic involving two distinct groups of students at different level of enquiry.

The topic of investigation was the relationship between texture and water permeability of soil. This topic was proposed by the same teacher to a class of 6-year pupils at the beginning of the primary school, and to a class of 16-year students of a secondary school of agriculture, both in Todi (Central Italy). This was made possible due to the presence of an educational farm (open to students of all ages from three years onwards) and a school of agriculture in the same place with the same teacher as the “guide” of inquiry.

Starting from the same engagement situation (“Have you got a green thumb?”) two distinct IBSE projects were conceived. In the 6-year class the project was designed as a confirmation inquiry in which the pupils were asked to confirm the principle (“soils of different textures have different water permeability”) through an experimental guided procedure whose results are known in advance. The goal in this case was to introduce the children to experimental and inquiry skills. In the 16-year class the same project was designed as a guided inquiry in which the students investigated a research question provided by the teacher (“how does the soil texture influence the soil water permeability?”) using procedures designed or selected by the students themselves. The goal in this case was to improve inquiry skills in students already quite experienced in planning experiments and analysing data.

The results of the dual project revealed a clear improvement in competence, knowledge and, especially, in participation, interest and motivation of the students after the hands-on activities. The prominent role of the teacher as a promoter, a guide and a tutor triggering meaningful learning situations and supporting students with sympathy and appreciation, was also evidenced.

Olson S. & Loucks-Horsley S. (2000) - Inquiry and the National Science Education Standards: a guide for teaching and learning. The National Academies Press

Earth Science in Opensim-based virtual worlds

Occhioni M.*

Istituto Comprensivo di San Cesario di Lecce, San Cesario di Lecce (LE).

Corresponding email: michelina.occhioni@gmail.com

Keywords: Opensimulator, VW, Techland.

3D virtual worlds are typical constructivist platforms offering valid opportunities for teaching and learning. One of the main software that allow the setting of 3D environments is Opensimulator (<http://opensimulator.org>).

Techland is one of the hundreds OpenSim-based virtual worlds. It is an archipelago of about 25 educational and service islands centered on math, earth science, chemistry and biology, and it is suitable for K6 – K8 degree students, using the IBL methodology.

Techland has been owned and managed by the author since 2010 and it can be visited by other students and teachers, coming from other similar virtual worlds. People can access Techland as avatars using a user graphical interface simply called viewer (Techland loginURI <http://techlandgrid.it:8002>).

To simplify abstract scientific concepts the user interface (viewer) can provide tools for modeling and scripting objects in-world.

Properly scripted, objects built by teachers or students can perform animations (change in color, size, position and transparency), providing information and showing the related scientific property in real time and in a dynamic way (as natural phenomena, chemical reactions, experiments). So Techland is a sort of giant 3D book where students/avatars can hang around and interact by clicking with scripted objects (3D paragraphs) or simply watching the animation.

Using the camera tools students can have a “first person” or a “third person” view of the objects and can be “immersed” in phenomena and scenarios.

Earthland is one of the Techland’s island focused on Geoscience, where is possible to find many fields of natural science related to the planet Earth. At the ground level the water cycle is explained adding to transparent objects particular scripts called particles that produce awesome graphic effects as rain, snow, clouds, fog. Rotating textures on sculpted objects simulate rivers. In air, at different levels there are platforms with other topics (atmosphere and Earth layers, volcanism and so on).

Some topics related to Chemistry (rocks and minerals, radon...) are placed at Chemland.

Students can also add their multimedia presentation in special sliders.

Techland contents and island can be remodeled depending of the students’ needs. Students approach scientific matters in an informal way, develop creativity and logical thinking, are able working in a team and can acquire specific technical and digital skills that can be reused in different contexts and fields of application (video and photoediting, coding, use of 3D CAD, digital storytelling...).

Occhioni M. (2013) - Techland, a virtual world for math and science, Proceedings of the 3th European Immersive Education Summit, 94-99, London.

Occhioni M. (2017) - Techland: math and Science in a virtual world, In Panconesi G. & Guida M. (Eds.): Handbook of Research on Collaborative Teaching Practice in Virtual Learning Environments, 407-426. IGI Global.

A PBL approach to enhance the sensitivity of students towards natural risks and hazards, in italian schools

Occhipinti S.*¹

¹ School principal - PhD in Teaching Earth Science, coordinator of IESO and IGEO for Italy , Chair of European Chapter for EGU and IGEO, member of the educational commission of the Italian Geological Society

Corresponding email: Susocchip@gmail.com

Keywords: PBL, Natural risks and hazards.

The goal of this research is to contribute in spreading a greater awareness of the dangers derived from natural phenomena, in Italian schools. The different steps are to raise awareness of the dynamics of the territory in which one lives, through a geological and historical analysis of the context, the understanding of the natural and inevitable evolution of the territory, the speed and frequency with which they can occur, the surface that can be affected by different natural phenomena and the transformations into risks factors. Finally, awareness that their knowledge is the basis for preventing and reducing risk in vulnerable contexts is needed. Since it is experienced that the usual transmissive approach of this content is not proving effective, a PBL approach was experimented. The target were secondary school students. The employed path has been defined with disciplinary objectives and specific skills to be developed and monitored. These applied, investigative and hands-on activities have shown an interesting growth of skills and competences in the involved students. The double result of a greater awareness of environmental dynamics and risks and of greater skills, technical, such as knowing how to observe or recognize relationships, and of citizenship, seem to have been achieved.

A EGU-IGEO European chapter to promote the teaching learning of Earth science in all schools

Occhipinti S.*¹

¹ Geologist - School principal - PhD in Teaching Earth Science, coordinator of IESO and IGEO for Italy, Chair of European Chapter for EGU and IGEO, member of the educational commission of the Italian Geological Society

Corresponding email: susocchip@gmail.com

Keywords: EGU-IGEO European Chapter.

On the initiative of EGU-European Geological Organization and IGEO, international geological education organization, a European Chapter was established in Coimbra, Portugal, on Aprile 2019, on the model of the one already activated in South America. The purpose of the Chapter is to organize a network that gathers European Earth Science teachers, to promote the teaching learning of this discipline in schools of every order in the European countries. Its main goals are:

- To promote Geoscience knowledge not only among teachers and students, but also for the general public
- To improve the teaching of Earth science among teachers, especially young teachers
- To collaborate among our institutions in order to promote exchange of ideas and teachers
- To build a common strategy in order to make agreements with the different educational authorities about the future Earth science curriculums
- Design and share strategies to make Earth science an increasingly attractive subject

The need to promote greater sensitivity towards environmental problems, towards hydrogeological instability, large and small natural hazards and the risks that derive from it is evident: environmental and geological emergencies are on the agenda. EGU and IGEO, through the EGU contact person prof. Chris King and the representatives of IGEO, prof. Roberto Greco and Shankar, invited the presidents of national Associations of teachers of Earth sciences and geography to collaborate for these purposes. At the moment

- the Associação Portuguesa de Professores de Biologia e Geologia - APPBG
- The Asociación Española para la Enseñanza de las Ciencias de la Tierra - AEPECT
- The Associazione Nazionale Insegnanti di Scienze Naturali – ANISN- Italy
- The Earth Science Teachers' Association – ESTA- United Kingdom
- Association des Professeurs de Biologie et de Géologie – APBG- France

have joined. Others countries have been contacted and we hope they can grow the network. The chairs of the European Chapter for the next two years will be Susanna Occhipinti (ANISN Italy) and Marc Jubault (APBG)

Il terremoto: impariamo a conoscerlo. The earthquake: let's get to know it

Pauselli C.*, Musu A., Mancinelli P., Ercoli M., Porreca M., Azzaro S., Carboni F., Samperi L., Giorgetti C., Mirabella F., Barchi M., Minelli G., Moriconi A. & Martorana S.

¹ Dipartimento di Fisica e Geologia, Università degli studi di Perugia CRUST - Interuniversity Center for 3D Seismotectonics with territorial applications.

² Educational Innovation Office & E-learning Lab, Educational Area, Università degli Studi di Perugia

Corresponding email: cristina.pauselli@unipg.it

Keywords: earthquake culture, seminars.

The recent destructive seismic events that affected central Italy further highlighted the importance of spreading a greater seminar. The sequence of events, while on the one hand awakened in the conscience of all the need to coexist with this type of events, on the other highlighted a lack of “earthquake education” on various levels, highlighting the persistence of unfounded ideas and extravagant, extremely amplified by the mass media and social networks.

It follows the need to provide simple answers to complex questions, which are framed on a solid scientific basis. In a society that is increasingly computerized, but no longer informed, the responsibility for conscious management and safeguarding the territory will fall on the new generations.

The knowledge of a natural phenomenon that affects a fragile territory due to its geological characteristics, represents an indispensable cultural base to the prevention and mitigation of risk.

Increasing the level of awareness is a fundamental prevention tool: the project therefore aims to increase knowledge about earthquakes, seen as a natural phenomenon to live with and from which to learn to defend themselves. The main objective of the project, co-financed by the Fondazione Cassa di Risparmio di Perugia, will be to increase the seismic culture of the community starting from the new generations.

To reach this goal, cycles of lessons to explain in a simple but complete and correct way the meaning of earthquake and its relationship with the territory, have been created. The seminars themselves have been recorded with the support of Educational Innovation Office & E-learning Lab, (University of Perugia) and will be made available on the online platform. In this way, starting from the students who will be the first to experiment the platform, through verification tests and self-evaluation, which will allow the students to monitor the learning. These students will inevitably become “carriers”, bringing back the experience they had, in family or with friends via social media. In this way, the platform, once consolidated and established, could become a point of access to information for the whole population, also helping to limit disinformation in the topic.

At the end of this cycle, among the results an increase is expected in:

- the knowledge of the seismic phenomenon and its relationship with the territory,
- the awareness of the need to coexist with the earthquake (historical memory),
- the knowledge of the attitudes to be taken during an event and away from events (risk prevention and mitigation),
- the interest in this topic by those who feel they can contribute (generations of future of researchers).

How to exploit geodiversity in geoscience education activities?

Pelfini M.*¹, Apuani T.¹, Artoni C.¹, Conforto A.¹ & Bollati I.¹

¹ Dipartimento di Scienze della Terra “A.Desio” Università degli Studi di Milano.

Corresponding email: manuela.pelfini@unimi.it

Keywords: geodiversity, geoeducation, fieldwork.

Geodiversity constitutes the foundation for Biodiversity and for Geoheritage identification. Being it represented by all the components of the Geosphere (e.g., minerals, rocks, landforms), it could be an interesting starting point in Geoeducation. Indeed, Geodiversity can be easily observed both in natural and anthropic sites and in restricted or extended areas, allowing multi-spatial and -temporal observations. In this research, starting from previous experiences (Pelfini et al., 2016; Bollati et al., 2018), the different characteristics and roles of Geodiversity are delineated through simple educational activities, in order to discuss opportunities and criticisms. It emerges a strategical role of urban itineraries (Pelfini et al., 2018) and natural sites equipped for sport activities (Bollati et al., 2018), where also virtual experiences, based on multimedia tools can be realized. Here, the preliminary results of a classwork and a fieldwork realized with a secondary school of first level, based on geodiversity evaluation and experimentation, are presented. Working on Geodiversity demonstrates to be useful for better understanding the role of geological and geomorphological processes in controlling the landscape shaping, in driving human settlements and artefacts creation, and, more simply, in helping student to recognize the main rock types of their own territory, being it natural or strongly human impacted.

Bollati I., Gatti C., Pelfini M.P., Speciale L., Maffeo L. & Pelfini M. (2018) - Climbing walls in Earth Sciences education: an interdisciplinary approach for the secondary school (1st level) *Rend. Online Soc. Geol. It.*, 44, 134-142.

Pelfini M., Bollati I., Pellegrini L. & Zucali M. (2016) - Earth Sciences on the field: educational applications for the comprehension of landscape evolution, *Rend. Online Soc. Geol. It.*, 40, 56-66.

Pelfini M., Bollati I., Giudici M., Pedrazzini T., Sturani M. & Zucali M. (2018) - Urban geoheritage as a resource for Earth Sciences education: examples from Milan metropolitan area. *Rend. Online Soc. Geol. It.*, 45, 83-88.

Alps in a box

Pelorosso B.^{*1-2}, Brombin V.¹⁻², Bertagnon A.²⁻³, Calore E.²⁻⁴, Forastieri F.¹⁻², Polastri L.²,
Rolando V.² & Vinciguerra E.²

¹ Department of Physics and Earth Sciences, University of Ferrara, Italy.

² NOVA A.P.S., Ferrara, Italy.

³ Department of Engineering, University of Ferrara, Italy.

⁴ INFN, Ferrara, Italy.

Corresponding email: plrbrc@unife.it

Keywords: scientific divulgation, Earth Science, Alps.

Teaching Geology to secondary and high schools' students is not a simple task, as in classrooms are clearly missing some essential elements of this science (i.e. outcrops, mountains, rocks, rivers, volcanoes). A team of PhD and Master Graduated from the University of Ferrara (Italy) promotes divulgation activities and teaching courses in secondary schools, with the aim to promote and disseminate STEAM (Science, Technology, Engineering, Arts, Mathematics) disciplines, including Earth Sciences. Seminars on geology, hydrogeology, paleontology, petrography, volcanology, and natural hazard aim to spread knowledge and increase participation in Planet preservation. These "lessons" are performed in class or during public events, using multimedia materials supported by demonstrations and practicals. Among the several activities proposed, this Group presents also structural modeling, performed using a deformation sandbox, as described by Castello & Cook (2007), which is suitable for reproducing geological processes such as folding and faulting. Recently, the same methodology has been developed to reconstruct the origin and the evolution of the Alpine chain. The aim of this activity is to mimic the evolution model of the Alps proposed by Bosellini (2005), the simplest and most intuitive reconstruction of the Alpine orogenesis. Using different daily-use materials (box, paper, flour, corn flour, and colored sand), the students are invited to recreate and discuss the main Alpine (Eoalpine-Mesoalpine-Neoalpine) phases, from the initial stage of Eurasia-Africa plates convergence through the continental collision and subsequent closure of the Ligure-Piemontese ocean and formation of the orogen. During the experiment, students report their own observations for each phase with sketches and descriptions in a simple activity-report form.

This laboratory allows to introduce some basic geological notions of (i) plate tectonics, (ii) structural geology, (iii) regional geology, and (iv) physical and chemical properties of coherent and incoherent daily materials miming the rheology of the rocks. This experience has been successfully tested in public divulgation events.

Bosellini A. (2005). Storia Geologica d'Italia-Gli ultimi 200 milioni di anni. Zanichelli

Castello M.D. & Cooke M. (2008) - Watch Faults Grow Before Your Very Eyes in a Deformational Sandbox. Journal of Geoscience Education, 56, 324-333.

Social Emotional Learning (SEL) and earthquake: teaching through emotions meets Geoscience

Piangiamore G.L.*¹, Trolese P.², Frione A.² & Cortopassi P.³

¹ Istituto Nazionale di Geofisica e Vulcanologia (INGV), Roma 2 - Sede di Portovenere.

² Comando dei Vigili del Fuoco di La Spezia.

³ Regione Toscana, Settore Sismica - Ufficio di Massa.

Corresponding email: giovanna.piangiamore@ingv.it

Keywords: Social Emotional Learning, Earthquake, Risk Communication.

Building transformational learning paths is the ambitious goal of the natural risk education projects by the Istituto Nazionale di Geofisica e Vulcanologia in collaboration with local authorities, Civil Protection Service, Provincial Fire Brigade Department and State Forest Rangers Corps. Every initiative implemented is not a simple outreach science venue, but an opportunity for *active learning* to promote good practices and to trigger a process of self-awareness (*long life learning*). The *ScienzAperta2019* by INGV of Portovenere in memory of the 2009 L'Aquila earthquake involved about 300 secondary school students in *Social Emotional Learning (SEL)* activities. The focus is on the consequences on society ten years after the earthquake occurred throughout the emotions aroused by the catastrophic event. We let the ancient feelings experienced working on the seismic disaster rise again with the aim to face fear and not be caught unprepared when the earthquake will hit again. *SEL* promotes the overall development of the person and it is associated with the knowledge of cooperation, loyalty, respect for others and the ability to better manage our behavior in case of hazard. Our learning path of meetings promotes the growth in resilience without ever losing hope, to become active citizens in collective choices. The cognitive contents are storytelling through images, videos, testimony readings to give voice to those who lived the destruction, the rubble and the tent city experience. Our know-how vibrates with emotions, transmitting to students and teachers what the rescuers, seismologists, geologists and emergency communicators feel when a natural disaster occurs. And the emotions become learning while the images flow while the fire brigades tell or read by the book "Sarnano in the province of Macerata... free thoughts of a fireman" (Trolese P., 2017) and "Angels in the rubble" (Federici M., 2009). Then the tent city fairytale initiative storytelling dampens the tension, just as it has brought a little distraction and ripped a smile with its talking puppets to the children in central Italy ten years ago. And so the video "L'Aquila Earthquake ten years later: the temporary is forever" focus the attention on the places symbol and delays of the city that does not give up. The researcher conveys his personal experience and invites students to watch at home the video "Don't call me Earthquake" (*EDURISK* project) on a girl their age from L'Aquila at the time of the 2009 earthquake. Different roles, but emotions, moods, feelings, similar identity perceptions united by the common will to support and help those who have suffered the disaster: a training course not only formative for the recipients, but also for the trainers themselves. Our message is well received by young students who have written beautiful essays collected by their teachers after *ScienzAperta* experience.

We thank the commander of the La Spezia Fire Brigade Leonardo Bruni for intervening.

Trolese P. (2017) - Sarnano, in provincia di Macerata...liberi pensieri di pompieri.

Federici M. (2009) - Angeli tra le macerie.

<https://www.ilfattoquotidiano.it/2019/04/02/terremoto-laquila-10-anni-dopo-il-provvisorio-e-per-sempre-luoghi-simbolo-e-ritardi-di-una-citta-che-non-si-arrende-videoracconto/5074323/>

<https://www.youtube.com/watch?v=Ny12bhH3zDw>

Il Piano Lauree Scientifiche come strumento di didattica inclusiva: il contributo delle geoscienze

Placuzzi E.*¹, Barbieri G.², Berti M.², Gasparotto G.², Giura E.¹, Rossi V.², Squarzoni G.², Vaiani S.C.² & gli studenti del Liceo E. Ferrari, Cesenatico¹

¹ Istituto Statale d'Istruzione Superiore "L. da Vinci" / Liceo Enzo Ferrari Cesenatico (FC).

² Dipartimento di Scienze Biologiche, Geologiche e Ambientali, Università di Bologna.

Corresponding email: ernestina.placuzzi@gmail.com

Keywords: laboratorio PLS, geologia, didattica inclusiva.

Nell'ambito del Piano nazionale Lauree Scientifiche Geologia (PLS 2014-2016) dell'Università di Bologna è stato progettato assieme ai docenti di scienze un laboratorio didattico della durata di circa 15 ore per un gruppo di 20 studenti appartenenti a diverse classi del triennio del liceo E. Ferrari di Cesenatico (FC). Il laboratorio è stato svolto in classe e in campo, presso il parco geologico della Cava del Monticino (Brisighella, RA) e la frana di Casola Valsenio (RA). La scelta è ricaduta su questi siti al fine di coinvolgere gli studenti attivamente sul terreno in un contesto geologico tipico dell'Appennino romagnolo e stimolare la conoscenza del territorio, dei processi geologici che lo governano e dei possibili georischi.

Sono state effettuate le seguenti attività:

- osservazione e riconoscimento delle principali formazioni del versante padano dell'Appennino romagnolo (Marnoso-Arenacea, Vena del Gesso e Argille Azzurre);
- analisi macroscopica e microscopica, anche tramite stereoscopi portati in loco, di campioni raccolti dagli studenti per osservazioni mineralogiche e paleontologiche. In particolare, il gesso è stato esaminato dal punto di vista strutturale, per gli usi, per il contenuto fossile e per quello che la sua storia geologica ci racconta;
- studio della frana di Casola Valsenio tramite l'osservazione degli elementi principali di questo grande scorrimento traslativo in roccia, riconoscendone le caratteristiche peculiari e ricostruendone la dinamica di attivazione;
- elaborazione dei dati raccolti per la progettazione e la realizzazione in formato digitale di un poster, al fine di promuovere lo scambio di conoscenze entro il gruppo e divulgarle agli altri studenti della scuola.

Tali attività hanno consentito di mettere gli studenti a contatto con la geologia in modo pratico, valutandone alcune applicazioni nel campo delle risorse e dei rischi connessi all'uso del territorio, nonché di sviluppare una didattica inclusiva, olistica e fortemente propensa allo sviluppo di competenze tramite modalità di apprendimento contestualizzato. Il lavoro di gruppo, in campo e in classe tramite la realizzazione del poster, ha migliorato le loro capacità di studio delle geoscienze, ovvero hanno imparato ad imparare sviluppando uno spirito d'iniziativa collettivo per la gestione efficace degli incarichi e dei tempi di lavoro, in accordo con le competenze chiave richieste dalle direttive europee.

Inoltre, come evidenziato dai docenti della scuola, questo approccio didattico così incentrato sull'attività di terreno, tipica delle geoscienze, ha favorito una proficua integrazione di studenti con varie tipologie di BES (Bisogni Educativi Speciali). Collaborando fra pari, essi possono utilizzare in modo libero le loro capacità di osservazione del territorio ed interpretazione dei dati, fruire dello scambio di competenze informatiche e apprendere dai compagni la gestione dello spazio di lavoro (foglio), il rispetto dei tempi e dei modi espressivi più consoni al compito da svolgere.

The Floristella-Grottacalda Mineral Park (Sicily): a geological trip that becomes history, literature and memory of a territory

Punturo R., Fazio E., Fiannacca P., Ortolano G. & Cirrincione R.*

Università di Catania.

Corresponding email: r.cirrincione@unict.it

Keywords: Floristella-Grottacalda Mineral Park, Sicily, Rocca di Cerere Unesco Global Geopark.

The Floristella – Grottacalda sulfur mines represent an excellent site which combines geology with history with social as well as cultural elements of the central Sicily territory. For this reason, they have been added to “Rocca di Cerere” Unesco Global Geopark and are listed in the European geoparks network. Today, the remnants of the extraction devices and instruments as well as tunnels and wells spanning from early XIX to late XX century are gathered in the former mine sites and visitable. The proposed educational activity starting as the geological interpretation of the territory, develops then to a multidisciplinary level since it comprises the technological and economical aspects together with the history of the Sicilian population. The proposed itinerary comprises the geological aspects represented by Messinian evaporitic rocks which crop out, and the evolution of the exploitation plants and the extraction sites over almost two hundred years. Finally, the visit of the main building shows the power of the former landowners. Therefore, the park becomes not only an industrial-geological example, but also testifies the social organization in Sicily during the XIX and XX centuries.

New opportunities for teacher professional development in Earth sciences: EGU Geoscience Fieldwork Officers Project

Realdon G.*¹ & Gravina T. ²

¹ University of Camerino - Geology Section, UNICAMearth group.

² Guglielmo Marconi University, Rome.

Corresponding email: giulia.realdon@unicam.it

Keywords: EGU, earth sciences teaching, professional development.

Despite being present in all Italian primary and secondary school curricula, Earth Sciences receive the least attention within Natural Science teaching and are mostly taught by teachers with poor academic background in this field (Realdon et al., 2016). This situation, common in many other European countries (King, 2013), is worsened in Italy by the scarcity of professional development opportunities available to teachers in the field of geosciences.

A new initiative promoted by European Geoscience Union (EGU) to “inspire, update and support geoscience teachers and educators” in Europe, could help to address this long standing problem. EGU, a non-profit international union of scientists, was established in 2002 and is “dedicated to the pursuit of excellence in the Earth, planetary, and space sciences”. One of its purposes is to support geoscience education from school to university level through a Committee on Education (CoE). Since 2003 CoE has been running an annual Geosciences Information for Teachers (GIFT) workshop, a two-and-a-half-day training event held in conjunction with EGU annual General Assembly.

In order to reach a wider number of European geoscience educators, in 2018 CoE proposed to enhance its activity for teachers professional development with a pilot project that includes the appointment of Geoscience Education Fieldwork Officers. Four school and university teachers from different EU countries (France, Italy, Portugal and Spain) and two from non-EU countries were trained to offer interactive workshops for “teachers of science or geography with some geoscience in their teaching, who have weak geoscience backgrounds”. Financially supported by CoE, Fieldwork Officers are running these workshops in their countries, building on the experience of Earth Science Education Unit (originally at Keele University) in the training of nearly 40,000 UK teachers.

EGU Officer’ workshops are characterized by being:

- given in national languages;
- focused on appropriate topics according to official curricula and syllabi;
- based on practical experiences to be implemented in the classroom with low-cost accessible materials and easily replicable by teachers;
- aimed at empowering teachers by promoting self-efficacy in addressing Earth sciences offered for free (within a certain number funded by EGU)

The aim of this abstract is to present the activity of the Italian Fieldwork Officer and underline the relevance of conferences to promote the workshops as an opportunity for teacher professional development and for the sharing of best practices.

King C. (2013) - Geoscience education across the globe - results of the IUGS-COGE/IGEO survey. *Episodes*, 36(1), 19-30.

Realdon G., Paris E. & Invernizzi M.C. (2016) - Teaching Earth Sciences in Italian liceo high schools following the 2010 reform: a survey. *Rend. Online Soc. Geol. It.*, 40, 71-79.

Esperienze didattiche attorno a Valentina, balena fossile di 3.5 milioni di anni

Scacchetti M.*¹ & Chicchi S.²

¹ Società Reggiana di Scienze Naturali e Scuola secondaria di 1° grado “Manzoni” Reggio Emilia.

² Musei Civici di Reggio Emilia.

Corresponding email: mauscacchetti@alice.it

Keywords: balena, fossile, attività laboratoriali.

Sono passati circa 20 anni da quando, nella fascia pedecollinare reggiana, è stato scoperto, scavato e trasportato ai Musei Civici di Reggio Emilia lo scheletro fossile di una balena pliocenica, denominata “Valentina” dalla località di rinvenimento, San Valentino di Castellarano. Si tratta del maggior esemplare di cetaceo fossile ritrovato finora nell’Appennino reggiano. I resti constano dei due mandibolari, di buona parte della cassa toracica, di numerose vertebre e di alcune parti degli arti anteriori, nonché di una scapola. Lo scheletro apparteneva ad un adulto di circa 10 metri di lunghezza. (Musei Civici di Reggio Emilia, 2003)

La presenza dell’eccezionale reperto ha dato impulso alle attività didattiche che i Musei Civici di Reggio Emilia offrono alle scuole del territorio provinciale in ambito paleontologico. I percorsi sono rivolti con modalità differenziate a scuola dell’infanzia, primaria e secondaria di primo grado. Partendo da alcune domande chiave e con il supporto e di attività laboratoriali e osservazione di reperti, l’intento è di condurre gli studenti alla comprensione dei diversi apporti che i fossili offrono alla ricostruzione della linea del tempo, allo studio dell’evoluzione dei viventi, alla ricostruzione della storia paleogeografica e paleoclimatica di un territorio, al crocevia tra insegnamento della storia, delle scienze, della geografia.

Un monitoraggio, effettuato tramite la somministrazione di questionari mirati, ha testimoniato l’incremento delle conoscenze dei ragazzi, uno stimolo all’interesse scientifico, una migliore percezione dei musei come luoghi di apprendimento.

Musei Civici di Reggio Emilia (2003) - Valentina balena fossile del mare padano. Comune di Reggio Emilia.

La circolazione oceanica

Scapellato B.*

¹liceo scientifico IISS Paciolo-D'Annunzio, Fidenza (PR).

Corresponding email: barbarascapellato@gmail.com

Keywords: IBSE, oceano, plastica.

L'inquinamento da plastica e microplastica delle acque marine è considerato, attualmente, una delle emergenze ambientali più gravi insieme ai cambiamenti climatici, all'acidificazione degli oceani e alla perdita di biodiversità. Per fare avvicinare gli studenti ad un problema così complesso è necessario partire dal far comprendere che una delle caratteristiche peculiari del nostro pianeta è proprio la presenza di un unico grande oceano, un sistema connesso su scala globale, fondamentale per la vita sulla Terra. L'oceano, infatti, fornisce ossigeno, assorbe anidride carbonica, è fonte di cibo, regola il clima e supporta la grande abbondanza di vita sulla Terra. Studiare il sistema oceano significa, quindi, arrivare a comprendere che oceano e uomo sono interconnessi in modo inestricabile (College of Exploration, 2005. Ocean literacy—The essential principles of ocean sciences K–12). L'inquiry-based science education (IBSE) è un approccio didattico centrato sullo studente, che lo coinvolge attivamente e a livello personale, promuovendo un apprendimento delle scienze profondo, significativo e persistente (European Commission, 2007). Viene qui proposto un percorso inquiry-based, sviluppato con il modello delle 5E (Bybee, 2015), che guiderà lo studente nell'esplorazione delle diverse caratteristiche del nostro unico grande oceano. Con le attività proposte gli studenti investigano i fattori che determinano e influenzano il movimento dell'acqua dell'oceano in superficie e in profondità, l'effetto della circolazione oceanica sul sistema climatico e sulla biosfera e come l'inquinamento da plastica sia una minaccia non solo per la biodiversità ma per l'uomo stesso. Attraverso questo percorso, adatto a classi di prima superiore, gli studenti hanno anche modo di comprendere che le scienze della Terra consentono di interpretare la realtà in cui viviamo per poter essere in grado di prendere decisioni consapevoli e informate anche nella vita oltre la scuola.

College of Exploration (2005) - Ocean literacy—The essential principles of ocean sciences K–12. <https://www.coexploration.org/oceanliteracy/documents/OceanLitChart.pdf>

European Commission (2007) - Science Education Now: A New Pedagogy for the Future of Europe. Office for Official Publications of the European Communities.

https://ec.europa.eu/research/science-society/document_library/pdf_06/report-rocard-on-science-education_en.pdf

Bybee R.W. (2015) - The BSCS 5E instructional model – creating teachable moments. NSTA Press, National Science Teachers Association.

Geosciences and museum: new frontiers in didactic for high school students

Scopesi C.*¹, Belmonte D.², Briguglio A.², Cabella R.², Carbone C.², Forchielli A.¹ & Doria G.³

¹ Associazione Didattica Museale.

² DISTAV, Università degli Studi di Genova.

³ Museo Civico di Storia Naturale G. Doria.

Corresponding email: genova@assodidatticamuseale.it

Keywords: Natural history museum G. Doria, education, geosciences.

The Natural history museum G. Doria (Genova, It.), hosts a notable scientific collection, of around 4 million specimens from all over the world. Among these collections mostly are zoological, but there are also botanical, mineralogical and paleontological ones.

Since 2008, ADM (Associazione Didattica Museale) has been in charge of the outreach and education aspects focusing on both schools and general public.

Over the years, the museum has established a number of international and national collaborations. In most recent times, thanks to the PLS project (Progetto Lauree Scientifiche) of geological science, the museum has become a waypoint between research and didactic as visible from the joint projects of the last two academic years.

The program “Orientiamoci all’Università”, a collaboration between the museum, ADM and the geological science department of University of Genoa, is active since 2017. This is a didactic offer, targeting high school students, with a twofold educational offer: a scientific talk hold by a faculty and a didactic activity (including laboratory) hold by ADM staff in the museum.

Since the beginning of the program, two refresher courses for teachers have been organized: a mineralogical and a paleontological one.

Strengthening of didactic (practical and laboratory) activities thanks to scientific and technical support from the university.

Renewal of the mineral exhibit in 2015 (Project “MINERABILIA”), funded by the Ministero dell’Istruzione, dell’Università e della Ricerca (MIUR), Law n.6/2000 for the dissemination of scientific culture

We have engaged more than 30 classes (with around 600 students) and 50 teachers, not only from Genova municipality but also from all over Liguria.

The museum has become an experiential tool/space for student to get involved in natural wonders, to be fascinated by mineralogical collections and passionate about the geological processes that rule our planet. The museum become a waypoint between experiential place and an occasion of cognitive development and scientific curiosity.

Geoscience laboratory for primary school: an attempt for engaging young people in Earth Sciences

Seno S.*¹ & Lupi C.¹

¹Department of Earth and Environmental Sciences, University of Pavia.

Corresponding email: silvio.seno@unipv.it

Keywords: Geoscience Education, discovery- and inquiry-based learning, 2030 Global Agenda.

In 2015, the United Nations approved the “2030 Global Agenda for Sustainable Development” identifying 17 Goals. The “Geoscience laboratory” here presented aims to provide quality, inclusive and stimulating scientific training in the Science area, with particular emphasis for geosciences, in compliance with the Goal 4 of the Agenda: “Ensure inclusive and equitable quality education and promote lifelong learning opportunities for all”. The philosophy is to carry out cooperative and collaborative activities “with scientists as scientists” for primary school students.

The geosciences provide a natural window on the world of science and children display an innate curiosity about the physical world. To be effective, education in science must begin early and take advantage of this curiosity before it is lost. In Italy, geoscience education activities are not usually focused on pre- and K-12 education, however the quality of students entering college, their knowledge base, their ability to solve problems and present results, their intellectual self-confidence, and their open-yet-skeptical habits of mind are formed at that time.

With the goal to develop new strategies and new materials for engaging young people in Earth Sciences, in October 2018 we organized the “Geoscience laboratory” for four primary schools from the city of Pavia. The laboratory has been financially supported by the Cariplo Foundation and carried out at the University of Pavia: it was part of the “Planet Earth Week” program, the Italian Geoscience festival with events all over the country. The 175 students involved, 9-10 years old, have been divided into small groups and they attended a wide range of hand-on activities through discovery- and inquiry-based learning.

The groups participated in short workshops with micro and macroscopic observation of rocks, minerals, fossils, 3D vision of images collected by drone, experimental hands-on activities, orienteering exercises and easy games on the key words of Geology and on the differences between scientists of Science, Technology, Engineering and Mathematics areas. The style adopted for the design and development of the laboratory followed a transversal approach for learning scientific subjects through innovation, creativity and motivation and giving inputs to make children curious on Geosciences. In particular, a “learning by doing” approach has been favored by emphasizing the scientific method used by researchers in describing and interpreting the Earth History signals recorded in rocks. In this way, children have thus become active subjects of the learning path.

The scientific method between geology and history

Stacchiotti L.*¹, Beccaceci A.² & Paris E.²

¹ IC “Beltrami” - Filottrano (AN).

² Scuola di Scienze e Tecnologie, Sezione di Geologia-Università degli Studi di Camerino.

Corresponding email: lucia.stachys@gmail.com

Keywords: scientific method, geoscience, Soil.

The aim of this activity is to improve students' interest about science history and the application of scientific method through a simple experiment. The activity was carried out by researchers belonging to Unicamearth group and it was addressed to 13-years-old students (75 pupils) during “Science days” at UNICAM.

The engage phase consisted of a “Guess who?” game: a sequence of scientists' images was showed to them. Pupils were focused on discovering the true scientists' identity. They had to follow the given clues through story-telling about scientists' scientific path. The purpose of this activity was to highlight that scientists are not unusual or extraordinary people: conversely they are creative and curious men or women who investigated phenomena. The scientists asked questions and finally found the right answers by applying the scientific method.

In the second part, students carried out experiments about soil, using operational sheets and following the scientific method, step by step. The first one was the observation of the same amount of two different soil samples: sample A - a clayey soil - and sample B - a rich in organic matter soil. Students carefully observed the samples' differences (e.g. their color, volumes, structures and so on). Then, they formulated hypotheses about the research questions: “What will happen if we put the same amount of water in sample A? What about sample B? Write an explanation of your hypothesis”. Each student wrote his own hypothesis and explanation on the operational sheet and all the hypotheses were discussed with other students. Each group carried out an experiment in order to verify the shared hypothesis: students transferred the samples in two plastic pierced bottles and then they poured a known amount of water (150 ml) on sample A and on sample B. Pupils observed the amount of filtered water in each sample and the different response of the two kinds of soil to a set of repeated pouring water. In this way, each group wrote scientifically correct conclusions about what they observed. Furthermore, they were able to correct their previous wrong hypotheses. Pupils repeated the same procedure using sample A, sample B and polluted water (simulated with a solution made of water and food coloring), in order to compare results from the two experiments (what's happening in both samples with water versus what's happening with water and food coloring).

Then researchers introduced the issue of soil pollution, its effects on groundwater and then the consequences on everybody's health. Finally, researchers showed a video “Let's talk about soil”, also available in English. This video might be a chance for future interdisciplinary CLIL lessons at school. Pupils were actively involved in this laboratory experience, showing deep interest and motivation. Teachers were satisfied and enthusiastic about this activity because researchers gave them useful suggestions, ready-to-use materials and work procedures.

The aesthetic approach to teaching geosciences and sustainable education

Tonon M.D.* & Caretto A.

Dipartimento di Scienze della Terra, Università di Torino.

Corresponding email: marco.tonon@unito.it

Keywords: sustainable education, primary teachers, georesources.

Since the last century, loss of natural areas, growing process of urbanization and environmental degradation have distanced us from ecological systems on which, however, we continue to depend, though less awareness. Although our lifestyle makes it increasingly difficult to perceive the indissoluble links with resources of a finite planet and material processing time and recycling. These processes are often not compatible with the frenetic extraction and use of raw materials, the socio-environmental crisis is more than obvious, so as to represent for some of us an urgency that requires new educational aims and a radical renewal of all education system (Sterling, 2006). For over 16 years, our work within the Degree Course of Primary Sciences Education of Turin University provides teachings and workshops dealing with fundamental Geosciences concepts that we lead with the belief that initial training of Primary teachers must take responsibility for promoting a socio-cultural model based on the values of sustainability contributing to developing a strong and awareness *ecological identity* (Tomashow, 1996). Cognitive and emotional spheres must be integrated in order to achieve a science education that leads at environment respect, through a sense of interdependent relationship that is essential to develop environmental behaviours, sense of responsibility and awareness. The emotions experienced in engaging activities are correlated with significant learning of scientific concepts. Our research focuses on the testing of learning models to develop a deep awareness of the relationships that connect humans to the environment. The failure to perceive the indissoluble connections with nature convinced us to develop transdisciplinary proposals for to life some esthetical experiences in contact with the environment. In some innovative workshops, we privilege introspective aspect and autobiographical storytelling, suggesting theatrical activities whose stage is natural environment. Other our proposals favouring instead manual activities, to complete works of artistic expression or to create some artefacts made with collected raw materials (Ingold, 2013). In our activities the integration between cognitive, perceptual-motor and emotional-relational spheres produces significant effects on multiple levels (Tonon M.D., Perazzone A. e Caretto A., 2017).

Ingold T. (2013) - *Making: Anthropology, Archaeology, Art and Architecture*. Routledge, London.

Sterling S. (2006) - *Educazione sostenibile*. Anima Mundi Editrice.

Tomashow M. (1996) - *Ecological identity*. The MIT Press, Cambridge (USA).

Tonon M.D., Perazzone A. & Caretto A. (2017) - Dal golem di argilla agli haiku in natura: alla ricerca di una nuova identità ecologica. In: Kanizsa, Oltre il fare. I laboratori nella formazione degli insegnanti, S.Junior Ed., Reggio Emilia, 107-115.

Pollution from magnetic minerals in leaves: an “Alternanza Scuola Lavoro” project in secondary schools in Parma and Torino

Zaccara Bertolini P.*¹, Foglia C.¹, Classe IVF¹, Groppi E.², Classe IIIH², Mantovani L.³, Tribaudino M.³,
Artesi T.³ & Solzi M.⁴

¹ Liceo Scientifico P. Gobetti Torino.

² Liceo Scientifico G. Ulivi Parma.

³ Dipartimento SCVSA Università di Parma.

⁴ Dipartimento di Matematica Fisica e Informatica Università di Parma.

Corresponding email: p.zaccara@liceogobetti.it

Keywords: air pollution, alternanza scuola lavoro, magnetic minerals.

In the Northern Italy cities of the Padan plain a major problem, which strikes most in the driest winter months, is airborne pollution. Here we present a project developed in the framework of the “alternanza scuola lavoro” (ASL) between two classes in the cities of Parma and Torino, namely an 3th year class from the Liceo Scientifico Ulivi (Parma) and a 4th year class from the Liceo Scientifico Gobetti-Segrè (Torino), and the University of Parma. Over a period of 7 weeks, between February and March, we collected leaves samples from *Parietaria officinalis*, *Hedera helix*, and *Rubus caesius* three evergreen (so they always have got leaves) plants that are easy to find in every period of the year both in different areas both in Parma and Torino. The aim is to verify whether, through the mass magnetic susceptibility of the minerals which are deposited on the leaves, as an effect mostly of vehicular traffic, the leaves can be a suitable marker of the winter-side pollution. In the PMs there are magnetic minerals, mainly magnetite and maghemite, that stuck on leaves surfaces, which change leaves mass susceptibility; so we expect that the susceptibility is proportional to pollution and if we measure this variation we can understand if the area is polluted or not.

The samples were collected in Parma, in the University Campus, at different distance from the urban highway (tangenziale di Parma) and in Torino from Lungo Po Machiavelli, near the river Po, from C.so Casale, a very congested street, and at the entrance of school court. After we collected the samples, we dried them, crumbled them and packed them up with a marking label.

Once we went to the University of Parma we measured the magnetic susceptibility of the deposited minerals. The results, which will be discussed in a companion contribution, showed us that all the examined samples show a signal, related to vehicular pollution, well beyond the error. Moreover, we observed that *Parietaria officinalis* and *Rubus caesius* are better indicators than *Hedera helix*. The highest pollution was found near the congested Corso Casale, Turin, but also in the apparently unspoiled location at Lungo Po Machiavelli, the susceptibility is not different from that found at the side of the urban highway in Parma. The susceptibility in the campus in Parma is in general lower than in Turin, but we can observe a significant increase in samples as we approach the urban highway.

The outcome in the ASL activity was twofold: 1) to get in touch of how an environmental investigation has to be done, how simple sampling procedures have to be planned carefully, and how to treat results on natural samples, which need specific representation and statistical analysis; 2) to understand how pollution affects our living towns, and how it can be tracked by environmental proxies, in order to gain attention to the issues in policies to contain pollution.

Abad I.	119	Andreozzi G.B.	45, 54, 261
Aben F.M.	425	Andujar J.	204
Abudureheman A.	123, 178	Angel R.J	42, 44, 46, 52, 209, 216, 221
Accetella D.	400	Angiboust S.	252
Acito A.M.	607	Antiga R.	709, 710
Acquafredda P.	338, 441	Antonangeli D.	375, 386
Acquavita A.	673, 677	Antonelli F.	160
Adam J.	530	Antongirolami V.	178
Agard P.	252, 50	Antonicelli M.	262
Ager Vázquez F. J.	173	Apollaro C.	578, 594, 639, 649
Aghazadeh M.	255	Appiah H.	207
Agliardi F.	533	Apuani T.	726
Agnesi V.	611, 620, 623	Aquino A.	82, 108
Agnini C.	235	Aradi L.E.	210
Agostini S.	245, 250, 252, 277, 329, 661, 667	Arcari A.	536
Agrosi G.	41, 59	Ardit M.	83, 180
Ague J.J.	224	Ardizzone F.	560, 564
Aguilera F.	655	Aretusini S.	434
Ahmadipour H.	260	Argnani A.	460
Aiuppa A.	626, 649	Arienzo I.	475
Alaimo M.G.	670	Arienzo M.	593
Alavipanh SK.	596	Ariph K.	642
Albano L.	582	Arletti R.	71, 94, 117
Albarello D.	487	Armadillo E.	407, 642
Albert P.G.	696	Armandola S.	306
Aldega L.	468	Artesi T.	738
Alemanno G.	389	Artioli G.	343, 430, 463
Alessio G.	571	Artoni C.	711, 726
Alipour R.	260	Arzilli F.	191, 196, 206
Alisi C.	150	Assanelli M.	291
Aliverti Piuri E.	488	Astbury R.L.	703
Alkmim A.	254	Atwood R.	191
Allasia P.	554, 560	Atzori S.	484
Allegretta I.	41	Audra P.	67
Allocca V.	593	Avanzinelli R.	246, 249, 665, 689
Almeev R.R.	703	Avataneo C.	131
Alsop G.I.	457	Avino R.	631
Altieri F.	397	Azzaro S.	517, 725
Alvaro M.	42, 44, 47, 49, 51, 52, 53, 209, 216, 339, 390, 391, 700	Azzarone M.	363
Alvioli M.	555, 560, 622	Baccheschi P.	521
Amalfitano S.	657	Bachmann O.	627
Amanti M.	616	Badro J.	375
Amisano M.F.	134	Badrzadeh Z.	255
Andaloro F.	383	Bagnato E.	631
Anderlini L.	495	Bagni F.	536
Andersen M.	251	Bahrambeygi B.	596
Andersen N.	57	Baioni D.	376
Anderson M.	323	Balassone G.	119
Andersson J.	325	Baldo M.	554, 560
Andò S.	60	Balducci V.	556, 573
Andrade C.	656	Balestrieri M.L.	399, 410
		Balestro G.	241

Balic-Zunic T.	379	Beltrame C.	160
Balsamo B.	437	Beltrami G.	84, 129
Balsamo F.	410, 420, 429, 465, 472, 507, 536	Belviso C.	130, 141, 148
Bamber E.	191	Belviso S.	130
Baneschi I.	85	Benà E.	315
Baradello L.	400, 483	Benedetti L.	518
Baraldi R.	357, 358	Benigni M.S.	563
Barale L.	103, 131, 172, 600	Bensaid I.A.A.	278
Barani S.	487	Bentaleb I.	67
Baratella D.	354	Bentivenga M.	607
Baratelli L.	203	Benvenuti M.	173, 189
Barbagli A.	579	Berardi M.	537
Barbaro A.	391	Berardo G.	464
Barbero D.	580, 581	Berio L.	465, 603
Barbero E.	461, 462	Berlo K.	702
Barbieri G.	729	Bernabale M.	161
Barbieri R.	383	Bernardi M.I.	274
Barca D.	166	Bernardini F.	278
Barchi M.	725	Bernini A.	609
Barchi M.R.	517, 520	Bernini F.	350
Bargossi G.M.	238	Berra F.	468
Barker S.	702	Berra G.	717
Baron M.A.	386	Bersani D.	60, 90, 201, 266, 307, 396
Barone G.	90, 98, 99, 114, 186, 502, 508, 510	Bersezio R.	488, 500
Bart O.J.	405	Bertagnon A.	727
Bartelletti A.	663	Berti D.	597
Bartoli M.	592	Berti M.	729
Bartoli O.	210, 211, 314	Berto D.	343
Basch V.	292	Bertocco M.	505
Basei A.S.	453	Bertok C.	103
Basi M.	597	Berton D.	364
Basile P.	579	Bertoni D.	615
Basso D.	366, 367	Bertotto G.W.	274
Basso J.	463	Bettelli G.	473
Bastesen E.	454	Beyssac O.	327
Battaglia F.	400	Bezerra F.H.R.	429, 536
Battaglia M.	527	Biagioni C.	61, 62, 74
Beccaceci A.	712, 736	Bianchi C.	560, 572
Becker H.	306	Bianchi F.	645, 674
Beddini G.	631, 633	Bianchi S.	681
Behrens H.	694	Bianchini G.	78, 102, 180, 255, 661
Belardinelli M.E.	548	Bianco C.	454, 456
Bella D.	508	Bianucci G.	366, 713
Bellentani G.	466	Bighi B.	350
Bellieni G.	228	Bigi S.	267, 504
Bello M.	123	Bignozzi M.C.	115
Bellomo S.	636, 638	Bigot J.-Y.0	67
Belluso E.	132, 136	Billi A.	428, 468
Belluzzo A.	713	Bilotta G.	558, 692
Belmonte D.	43, 280, 286, 289, 734	Bindi L.	62, 63, 65, 72, 77
Beltenev V.E.	124	Bini G.	627
		Biondi D.	576
		Bistacchi A.	436, 465, 477

Bitonte R.	466, 481, 493	Bracchi V.	366
Bittelli M.	538	Bracchi V.A.	367
Boccatto S.	375	Brack P.	227
Boero R.	88	Braga R.	266, 419
Böhm G.	483, 485	Bragagni A.	246
Boito M.	659	Bragato P.L.	368, 482
Bollati I.	726	Branatelli G.	483
Bollati I.M.	711	Brandolin D.	673
Bonaccorsi E.	64, 714, 716	Braschi E.	255, 329
Bonaccorso L.	464	Brenker F.E.	391
Bonacina G.	365	Brenna M.	269
Bonadeo L.	481	Briais A.	295
Bonadiman C.	78, 107, 118, 180, 228, 231, 263, 265, 268, 271, 283, 284, 409, 415	Brigatti M.F.	350
Bonano M.	484	Briggs R.	269
Bonatti E.	282, 293, 295, 301, 312	Brighenti F.	508
Bonazzi M.	42, 316	Briguglio A.	734
Bonazzi P.	65	Brogi A.	85, 237, 329, 452, 454, 456, 458, 644, 647
Bonfardeci A.	582	Brombin V.	228, 242, 727
Boni M.	89, 119	Bronzo L.	713
Boniello A.	715	Brooker R.A.	191
Bonifacie M.	646	Brozzetti F.	503, 506, 509, 512
Bonini M.	85, 309, 489, 528, 529	Brugnone F.	628, 630, 643
Bonomo A.E.	607	Bruguier O.	234
Bonomo R.	597, 598	Brune S.	450
Bordoni M.	538, 608, 621	Brunelli D.	274, 282, 295, 301, 312
Borello A.	369	Brunetti M.T.	556, 560, 570, 573
Borghia A.	162, 241, 600	Bruno P.P.	513, 521
Borghia S.	185	Brunori C.A.	521
Borghia W.	604	Brusca L.	636, 638
Borghini A.	713, 714, 716	Bucci A.	580, 581
Borghini G.	205, 264, 270, 292, 294, 298	Bucci F.	560, 564, 622
Borrini D.	97, 652	Buccianti A.	675
Borromeo O.	520	Buccieri F.	102
Borsari M.	350	Buondonno E.	557
Borsi I.	579	Buono G.	192
Bosch D.	234, 29, 304	Burgess R.	472
Boschetti T.	307	Burrato P.	492, 498
Boschi A.O.	95	Burton M.	196
Boschi C.	85, 329	Burton M.R.	191
Bosi F.	45, 61, 260, 261	Burton-Johnson A.	403
Bosino A.	609	Busetti M.	483, 485, 405
Bosio G.	366, 713	Bussolesi M.	66
Bosman A.	267	Buttinelli M.	439, 504
Botha G.	609	Buttitta D.	193
Botta S.	131	Butturini A.	657
Botter R.	116	Byrne P.	133
Botticelli M.	174	Cabassi J.	629, 637, 645, 648, 651, 656, 657, 671, 675, 676, 679, 685
Boudoire G.	636	Cabella R.	87, 116, 184, 185, 709, 710, 734
Boukili B.	69	Cáceres F.	695
Boumehdi M.A.	278		

Caddick M.J.	225	Caprai A.	629
Caffau M.	418, 483	Caputo M.C.	539, 540, 549
Cafiso F.	610	Caracausi A.	193, 648, 649
Caggianelli A.	237, 335, 454, 456	Carbonara N.	653
Caggiani M.C.	41	Carbone C.	67, 68, 116, 369, 734
Caggiati M.	230, 233, 239	Carboni F.	725
Cai B.	191	Cardellini C.	627, 631, 633, 643, 649, 650
Cailhol D.	67	Cardinale A.M.	68
Caironi V.	717	Cardinali M.	560, 622
Calabrese S.	628, 630, 638, 643	Caretto A.	737
Calandrini E.	79	Cariddi B.	194
Caldeira R.	278	Caridei F.	349
Caliro S.	631, 632, 633, 650	Carli C.	378, 382, 389, 397
Callegaro S.	228	Carlini M.	463, 473
Callieri C.	656	Carlomagno I.	143
Calore E.	727	Carmignani L.	599
Caltabiano T.	704	Carminati E.	233, 468
Calver C.	413	Carnemolla F.	508
Camara F.	72	Carosi R.	317, 318, 324, 328, 330, 333, 334, 336, 337, 411
Cámara F.	43	Carpanese M.G.	710
Camarda M.	634, 635	Carpenter B.M.	427
Cambi C.	93	Carriero G.	357
Camerlenghi A.	485	Carroll M.	202
Campanale F.	377, 388, 394	Carroll M.R.	123, 206, 207, 718
Campedel P.	618	Carta R.	86, 598
Campeggi C.	697	Caruso V.	163
Campione M.	49	Carvalho B.B.	210
Campobasso C.	168	Casal T.	408
Campomenosi N.	44	Casale S.	401
Campos T.	295	Casalini M.	249, 665
Cangemi M.	135	Casarano D.	605
Cangiotti M.	142	Casarin A.	102, 693
Cannaò E.	195, 247, 248	Casentini B.	648
Cannata A.	697, 707	Casetta F.	231, 232, 265, 269, 276, 409
Cantaluppi M.	163	Casini L.	303, 319, 442
Cantisani E.	82, 169	Casiraghi G.	195
Capacci F.	136	Castagnotto E.	87, 164
Capaccioni F.	378	Castelli S.	107
Capasso G.	630, 635	Castellini E.	350
Capecchiacci F.	629, 648, 655, 657, 679, 637	Castorina F.	267, 663, 696
Capella S.	132, 136	Casu F.	431
Capezzuoli E.	237, 644, 647	Catalli F.	167
Capizzi L.S.	45	Catanzariti R.	461, 462, 481
Capizzi P.	582	Catizzone E.	104
Caporali A.	505	Cattaneo C.	163
Capotorti F.	504	Cattaneo M.	509, 512
Cappadonia C.	610, 623	Cattò S.	410
Capparelli G.	575, 576	Cavalaglio G.	93
Cappelletti P.	119, 170, 181, 111	Cavalazzi B.	383
Cappellini G.	565, 574	Cavalca E.	624
Cappello A.	558, 692	Cavalcante F.	130, 141, 148
Capponi G.	401, 406, 470, 601	Cavalli M.	560

Cavallo A.	140, 428	Clemenzi L.	472
Cavazzini G.	660	Clerissi F.	560
Caviglia C.	88	Cluzel D.	297
Cavinato G.	504	CNR Committee	
Ceccotti M.	637	“ECORD-IODP and ICDP”	38
Celico F.	361, 589, 591, 592, 619	Coccatto A.	90, 99, 114, 186
Cella F.	516	Cocco F.	524
Cerchiari A.	426, 467	Coda S.	593
Cesare B.	210, 211	Colella A.	435
Cesenatico	729	Coletti C.	165
Cestelli-Guidi M.	41, 281	Coletti G.	366
Ceuleneer G.	295	Colizza E.	400, 418
Charlier B.	702	Collareta A.	366, 713
Cheli A.	363, 591, 612, 615, 619	Colleoni F.	400, 405
Cheloni D.	484	Collettini C.	427, 464
Chen S.	251	Collings I.E.	104
Chenet T.	129	Colò M.	693
Cherchi M.	187	Coltella M.	563
Chiappetta G.D.	559	Coltorti M.	228, 231, 232, 263, 265, 268, 269, 271, 276, 345, 346, 347, 409, 415
Chiari A.	589	Coltro G.	717
Chiari M.,	462	Columbu S.	91
Chiaudani A.	583	Comboni D.	73, 91, 92, 104, 203
Chicchi S.	732	Comodi P.	80, 93, 379, 552, 137
Chiessi V.	616	Compagnoni R.	131, 172
Chilleri E.	133	Comparelli R.	351
Chinn I.	55	Comunian A.	488
Chiodini G.	627, 631, 632, 633, 641, 649, 650, 651	Confalonieri G.	88, 94
Chirico R.	89	Conforto A.	726
Christ O.	391	Coniglio L.	710
Chroňáková A.	67	Conoscenti C.	611, 620
Chu X.	224	Consani S.	68, 369
Churakov S.	139	Consorti L.	475
Ciabbari F.	466	Consuma G.	266
Cianfarra P.	406	Conte A.	69
Cibin G.	217	Conte A.M.	261, 267, 444
Cidu R.	151, 661	Conte S.	95, 96, 127
Cinosi J.,	102	Conti A.	267
Cinquini I.	327	Conti P.	413, 521, 599, 421
Cinti D.	648	Conticelli S.	245, 246, 249, 250, 255
Cioni R.	249, 450	Contini D.	488
Cipriani A.	236, 272, 273, 274, 282, 295, 312, 426, 475	Cook N.J.	61
Cirilli S.	552	Coppola M.	428
Cirillo D.	503, 506, 509, 512	Corbi F.	525
Cirrincione R.	331, 332, 445, 446, 447, 448, 453, 457, 730	Cordier P.	36
Citron S.	713	Cornamusini G.	402, 413, 414, 421, 422, 423, 599
Ciuffi B.	136	Corniello A.	584
Civico R.	521	Corno G.	656
Clark A. N.	386	Corradetti A.	475, 478, 522
Classe IIIH	738	Corradini B.	608
Classe IVF	738	Corradino C.	558, 692

Corrado S.	474	Dabrowski M.	57
Correale A.	268, 428	Daković A.	155
Corsaro R.A.	698	Dal Cin M.	483, 485
Corsi G.	429	Dal Seno N.	403
Corti G.	300, 309, 450, 489, 526, 528, 529, 534	Dalconi M.C.	343, 391
Corti L.	212, 213	Dall'Aglio M.	536
Corti V.	414, 421, 422	Dall'Igna M.	466
Cortinovis S.	507	Dallai L.	243, 282, 405
Cortopassi P.	728	Daly L.	377
Corvo' S.	319, 320, 443	Danovaro R.	383
Cossio R.	131	Darling J.	323
Costa A.	138, 641, 690	Darling R.	215
Costa M.	496	Daskalopoulou K.	640, 643
Costa N.	582	Davis M.	200
Costagliola P.	133, 189, 675	De Amicis M.	499
Costamagna L. G.	194	De Angelis S.	392
Cotana F.	93	De Bonis A.	181
Covelli S.	677, 682	De Bonis A.	170
Cox S.C.	403	de Brito J.	102
Crema S.	560	De Carlo L.	540
Cremona M.	435	De Caroli S.	241
Cremonese G.	393	de Castro E.I.	105
Criscuoli A.	578	De Cristofaro S.P.	196
Crispini L.	137, 403, 406, 432, 470, 601, 407	De Filippis G.	464
Croce A.	134, 214	De Francesco A.M.	166
Crognale S.	657	de Gennaro B.	155
Cruciani G.	321, 322	De Giudici G.	143, 150, 151
Cruscomagno F.	576	De Giudici G.B.	110
Cruz J.V.	656	De Guidi G.	502, 508
Cubellis E.	557, 687	de Ignacio C.	278
Cuccuru S.	261, 443, 444, 451	De Luca C.	431
Cuffaro M.	267, 295, 301	De Luca D.A.	580, 581
Cundari F.	639	De Martini P.M.	495, 521
Curetti N.	149, 263	De Min A.	242, 278
Curri M.L.	351	de Nardis R.	506, 509, 512
Curzi M.	233, 464, 468	De Paola N.	520
D'Agostino G.	331	De Rosa R.	578, 594, 639
D'Agostino N.	484	De Rubeis V.	492
D'Aleo R.	135	De Sanctis M.C.	390, 392
D'Alessandro W.	638, 640, 643, 628	De Santis L.	400, 405, 423
D'amato Avanzi G.	431	De Vecchi Gp.	228
D'Ambrogi C.	504	De Vita P.	593
D'Amico V.	568	De Vita S.	182, 701
D'Angeli I.M.	67	De Vito C.	161, 167, 174
D'Angelo S.	598	De Waele J.	67
D'Atri A.	103, 162, 600	Deaddis M.	499
D'Intino N.	469	Del Bello E.	688
D'Onofrio A.	593	Del Gaudio E.	584
D'Orazio M.	417, 647	Del Moro S.	604
Da Pelo S.	146	Del Negro C.	558, 692
Da Prato S.	481	Del Rio L.	517
		Del Vecchio A.	112, 281
		Delavari M.	461, 462

Delizia I.	557	Domeneghetti M.C.	390, 391
Dell'Aquilano M.	182	Donahue R.E.	179
Della Ventura G.	69, 70, 211	Dondi M.	83, 95, 96, 127
Della Ventura G.C.	41	Donnini M.	560, 565, 572, 574
Dellarole E.	316	Dordoni M.	661, 667
Delleani F.	213	Dore E.	151
Deloule E.	248	Doria G.	734
Deltedesco E.	344, 346	Dorn C.	386
Deluca F.	585	Dotsika E.	594
Demichele F.	590	Doveri M.	662
Denti B.	556	Dreossi G.	662
Dentoni V.	146	Druitt T.H.	689
Deraco M.	296	Drysdale R.N.	668
Destefanis E.	88, 149	Ducci D.	584, 587
Di Bella M.	383	Eagles G.	408
Di Benedetto C.	181	Eglington B.	408
Di Benedetto F.	136, 189	El Moutouakkil N.	69
Di Bennardo F.	676	Elbrecht A.L.	200
Di Bonaventura G.	105	Ellero A.	481
Di Bucci D.	504	Elliott T.	251
Di Capua A.	493	Elter F.M.	554, 709, 710
Di Carlo I.	204	Emili E.	464
Di Carlo L.	464	Emiliani R.	349
Di Celma C.	366	Engström E.	669
Di Curzio D.	583, 586	Eramo G.	176
Di Domenica A.	518	Erbello A.	450
Di Fazio M.	167	Ercoli M.	725
Di Fiore F.	197	Ercoli R.	97
Di Genova D.	191, 192, 198, 201	Erickson T.	211
Di Giuseppe D.	345, 142	Erra S.	134
Di Giuseppe P.	245, 250, 661, 667	Esestime P.	469
Di Gregorio A.	97, 120, 604	Esposito A.	674, 685
Di Lorenzo F.	139	Esposito R.	170
Di Martino M.	387	Esposito R.	181
Di Martino R.M.R.	634	Esposito V.	383
Di Martino R.M.R.	635	Esquivel I.	629
Di Martire D.	170	Fabbiani M.	71, 94, 117
di Renzo F.	71, 94, 117	Fabbrizzi A.	517
Di Renzo M. E.	464	Faccini B.	269, 271, 276, 345, 346, 347
Di Rienzo B.	593	Faccini F.	554
Di Salvo S.	689	Facini O.	355, 357, 358
Di Stefano G.	713	Fagereng A.	467
Di Toro G.	430, 434, 436, 472, 507	Falabella F.	569
Di Vincenzo G.	267, 330, 420	Falcone E.E.	638, 636
Diella V.	163	Falcone G.	567
Dinelli E.	100, 602	Falini G.	363
Dingwell D.B.	201, 695	Fanara S.	192, 196, 199
Dini A.	85, 452, 458, 661, 667	Fancello D.	150
Dino G.	600	Fantini R.	71
Doglioni C.	245, 521	Fantoni R.	37
Dolati A.	461, 462	Fantozzi L.	678
Doménech-Carbó A.	167	Farina F.	254
Doménech-Carbó M.T.	167	Fastelli M.	379

Favara R.	135, 582	Fois E.	94
Favaroni A.	713	Folco L.	377, 380, 388, 394, 417
Favero-Longo S.E.	600	Fondriest M.	428, 430, 472, 507
Fazi S.	637, 648, 657	Forastieri F.	727
Fazio E.	332, 445, 446, 447, 448, 457, 730	Forchielli A.	734
Federico C.	390, 636, 638	Foresta Martin F.	182
Federico L.	406, 432, 470, 601, 50	Forlano S.	511
Fedi M.	516	Formisano M.	390
Felici A.C.	167	Fornaro G.	484
Felluga A.	673	Fornasaro S.	137
Ferlito C.	265, 271, 409, 693	Fornasini L.	60, 201, 90
Ferraccioli F.	407, 408	Fornelli A.	338, 441
Ferrando C.	292	Forno M.G.	580, 581
Ferrando S.	201	Forsberg R.	408
Ferranti F.	381	Forti F.	349
Ferranti L.	382, 435, 510, 511	Francalanci L.	689
Ferrara L.	593	Franceschelli M.	321, 322
Ferrari E.	108, 109, 234, 297	Franceschi M.	384
Ferrari M.	392	Franceschini Z.	450
Ferrari S.	378	Francese R.	619
Ferrarini F.	509, 512	Fratini F.	82, 169
Ferrario M.F.	481	Frau F.	151
Ferrero S.	46, 215	Frau I.	151
Ferretti A.	371, 383	Fregola R.A.	458
Ferretti G.	345, 346, 347	Freyruth H.	251
Ferretti M.	101, 164, 718, 87	Frigerio C.	481
Ferretti V.	78	Frione A.	728
Ferri F.	210	Froncini F.	80, 93, 552, 631, 633, 644, 650
Festa A.	241, 426	Frontoni A.	690, 691
Festa F.	338	Fugazzotto M.	99, 114, 186, 90
Festa R.L.	559	Fulignati P.	647
Festa V.	441	Fumagalli P.	195, 205, 264, 270, 294, 298, 717
Fiannacca P.	331, 332, 445, 446, 447, 448, 453, 730	Fumanti F.	86
Fiano V.	616	Funari V.	100, 106, 138, 602
Fidelibus D.	590	Funedda A.	110, 146, 524
Figlioli A.	508	Fuoco I.	578, 594, 639
Figoli A.	578	Furlani S.	483
Filippi M.	449	Gabriele B.	578
Filippini M.	349	Gaeta M.	260, 696
Finocchiaro C.	98, 99, 114, 90	Gaggero L.	101, 144, 164, 451
Fioraso G.	481	Gagliano A.L.	582, 640
Fiore S.	141	Gagni S.	349
Fioretti A.M.	391	Gain S.E.M.	72
Fioretti G.	168	Galamini G.	345, 346, 347
Fioroni C.	473	Galasso L.	575, 576
Fiorucci A.	550	Galderisi A.	102, 486
Fiorucci F.	560, 622	Galli E.	67, 486
Fiquet G.	386	Gallorini A.	656
Fleury J.	518	Galluzzi V.	381, 382
Florio G.	516	Galvez Mejia E.	644
Foglia C.	738	Gamberi F.	120

Gambino F.	162, 185, 600	Giardino M.	600
Ganci G.	558, 692	Gilio M.	216, 252
Garabeiti E.	135	Gill B.C.	225
Garbin M.	491	Gimeno D.	112, 111
García-Arnay A.	376	Gioia E.	561, 562
Garduño Monroy V.H.	454	Gioncada A.	177, 366, 713, 714, 716
Gargini A.	349	Giordan D.	560
Gariano S.L.	570	Giordani M.	139, 142
Garofalo P.S.	220, 433	Giordano D.	196, 201, 694
Garzarella A.	372, 719	Giordano G.	104, 691, 701, 705, 706
Garzonio C.A.	249	Giordano P.	677
Gasparotto G.	238, 729	Giorgetti C.	517, 725
Gasperini L.	463	Giorno M.	103
Gatta D.	91	Giovanardi T.	236, 243, 266, 272, 273, 274, 316
Gatta G.D.	73, 92, 104	Gioventù E.	189
Gaudiosi G.	516, 571	Girani A.	52
Gautheron C.	399	Girardi V.A.V.	272
Gazzola R.	713	Giudici M.	488, 563
Gazzurra G.	713	Giuli G.	68, 77, 202, 217, 387, 79
Geddo Z.	47	Giuliani L.	200, 435, 693
Gemignani C.A.	612	Giuliani R.	484
Gemmi M.	76, 377, 388	Giuntoli F.	218, 323
Gencarelli G.	464	Giura E.	729
Genovesi S.	389	Giura P.	79
Gentile P.	60, 541	Giustetto R.	172
George L.L.	61	Glass B.P.	377
Gerdes A.	419, 420	gli studenti del Liceo E. Ferrari	729
Germinario C.	155, 170	Gliaschera M.	604
Germinario L.	171	Gò E.	343
Gervasi A.	559	Godard G.	56, 332
Gerya T.	222	Godard M.	252
Ghezzi L.	663, 664, 684, 662	Godone D.	554
Ghezzi C.	420	Goffredo S.	363
Giaccherini A.	136	Gola G.	85
Giaccio B.	668, 696	González-García D.	196, 201, 694
Giacomelli S.	612, 613, 615	González-Partida E.	329
Giacomini L.	381, 382, 397	Goodrich C.	391
Giacomini P.	713	Gordini E.	400
Giacomoni P.	268	Gorfer M.	346
Giacomoni P.P.	231, 232, 265, 271, 409	Grammatica M.	298
Giamello M.	82	Grandinetti V.	115
Giani M.	677	Granot R.	405
Giannandrea P.	193	Grassa F.	629
Giannantonio R.	351	Gravina T.	731
Giannattasio B.M.	184, 185	Graziano S.F.	111, 119, 181
Giannecchini R.	662	Gregoire M.	415
Giannini C.	351	Gregory E.	295
Giannini L.	656, 679	Grenier Romero C.	364
Giannuzzi M.	579	Grezio A.	564, 641
Gianola O.	210	Grieco G.	66, 140
Gianolla P.	230, 233	Grifa C.	155, 170
Gianolla P.	239	Griffin W.L.	72
Giansante C.	351		

Groppi E.	738	Iadanza A.	38
Gross F.	502	Iaia C.	541
Grosso F.	134	Iammarino C.	464
Gualandi A.	548	Ickert R.B.	231
Gualtieri A.F.	142	Iezzi G.	102, 200, 435, 693
Guarini G.	96	Ildefonse B.	303, 432
Guarini G.	127	Improta L.	513, 521
Guarino P.M.	616	Inostroza M.	655
Guarino V.	181, 194	Invernizzi C.	496, 718
Guarneri E.M.	616	IODP Expedition Scientific Party	405
Guastaldi E.	579	Ionca V.	148
Guerini S.	299	Irace A.	481
Guerra C.	617	Isaia R.	689
Guerra V.	617	Isola I.	450, 668
Guerrieri N.	678	Italiano F.	268, 276, 383
Gukov K.	436	Iván V.	588
Günter C.	215	Ivy-Ochs S.	618
Günther D.	220	Izzo F.	155
Gurrieri S.	634	Jacob D.E.	55
Gutierrez F.	376	Jahn S.	48
Guzzetta L.	381	Jain A.K.	324
Guzzetti F.	503, 555, 556, 560, 564, 565, 566, 570, 572, 573, 574	Jamtveit B.	57
Guzzo G.	410	Janasi V.	196
Haines J.	94	Jbara R.	295
Hålenius U.	62	Jerais A.	296
Hamelin C.	295	Jessop D.	646
Hanfland M.	92, 104	John T.	225
Harbord C.	434	Johnson T.	211
Harigane Y.	308	Jonade E.	530
Harper D.M.	657	Jordan T.A.	408
Harris J.W.	55, 54	Joseph B.	43
Hartley M.	191	Jourdan F.	228
Hattendorf B.	220	Jourde H.	551
Hawthorne F.C.	70	Kaczmarek M.-A.	295
Heidy M.	191	Kazarian A.	695
Helbert J.	389	Keiblinger K.M.	344, 346, 347, 348, 352, 353
Hellstrom J.C.	668	Keir D.	300, 438, 450, 534
Hemond C.	243, 312, 274	Khosravi M.	122
Henjes-Kunst F.	419	Kiénast J.R.	56
Hérault A.	558, 692	Kim S.	405
Hermann J.	44	Klemme S.	270, 378
Hernández-Sánchez M.Y.	95	Komorowski J.C.	646
Herrington R.	121	Konzett J.	266
Hiesinger H.	378, 397	Kovacevic V.	400
Hin R.	251	Kral R.M.	348, 352, 353
Hippeli T.	200	Krištúfek V.	67
Holtz F.	700	Kubanek J.	569
Huang H.	680	Kueppers U.	392
Hutchison M.T.	41	Kulhanek D.	405
Iaccarino S.	317, 324, 328, 330, 411	Kulhanek D.K.	423
Iacovino K.	202	Kusznir N.	408
Iacumin P.	361, 591, 659, 666	La Fortezza M.	49

La Maestra S.	144	Liguori A.	719
La Rocca M.	559	Lin N.	569
La Rosa A.	300	Liotta D.	85, 329, 452, 454, 456, 458, 237
La Rosa A.	431	Liotta M.	204
La Spina G.	191	Lisker F.	407
La Valle F.	507	Liso I.S.	541, 542, 543
Lacalamita M.	59, 75	Liu C.Z.	305
Lacombe O.	471	Liu M.	569
Lammoglia T.	613, 615	Liu T.	262
Lana C.	254	Livio F.	466, 481, 493
Lanari R.	484	Llewellyn E.	191
Landini W.	713	Lo Monaco A.	349
Langella A.	155	Locardi F.	101, 164, 87
Langenhorst F.	219	Locatelli M.	252, 50
Langone A.	109, 118, 234, 243, 273, 275, 296, 316, 320, 335, 339, 443, 456, 338	Locchi M. E.	464
Langone L.	400, 677	Lodi C.	710
Lanzafame G.	552, 693	Logvinova A.M.	54
Lanzi C.	527	Loi A.	110, 146
Lardeaux J.-M.	531	Lollino P.	605
Lasagna M.	580, 581	Lombardi F.	295
Lattanzi P.	133, 151	Lombardo R.	445, 446, 453
Läufer A.	407, 432	Lombardo V.	600
Laurent O.	215	Longo M.	638
Laurita S.	75	Longo V.	187
Lavagnino G.	144	Longuevergne L.	548
Lavaroni F.	464	Lorenzetti A.	51, 54
Lavecchia G.	503, 506, 509, 512	Lorenzetti S.C.	717
Lazzara G.	147	Lorenzon S.	51
Lazzarini L.	160	Losno R.	670
Le Gall N.	191	Lotti F.	579
Lee M. R.	377	Lotti P.	43, 73, 92, 104, 203
Lee P.	191	Lottici P.P.	60, 201
Lee-Thorp J.A.	179	Lovati S.	487
Lei Y. D.	680	Lozar F.	720
Leiss B.	330	Lucca A.	472, 477
Lelli L.	403	Lucchelli L.	608
Lelli M.	85, 642	Lucci F.	69
Lenaz D.	278, 479, 54	Luciani V.	462
Leoncini C.	349	Lugli F.	266, 426
Leonelli C.	98	Lugli S.	474, 460
Leonelli G.	370, 612, 615, 619	Luguet A.	39
Leoni M.	391	Luiso P.	516
Lettino A.	141	Luongo G.	557
Lezzerini M.	82	Luoni P.	291, 302
Lezzi G.	644	Lupi C.	735
Li J.	225	Lustrino M.	277
Li P.	282	Lutman A.	664
Li Vigni L.	630, 643, 628	Luzi L.	568
Li X.	412	Luzzi E.	376
Liberato G.P.	413, 414, 421, 422	M. Alvaro M.	221
Ligi M.	282, 295, 301, 296, 312	Ma G.	569
		Maccelli C.	665

Macri A.	666	Marescotti P.	137
Macrini D.	102	Mari M.	355, 356
Maczurad M.	119	Marinangeli L.	395
Maddaleni P.	673	Marincioni F.	561, 562
Mádl-Szőnyi J.	588	Marino M.	504, 597
Madonia G.	67	Marinoni N.	163
Madonia P.	135	Maritan L.	165
Maerker M.	609	Mariucci M.T.	515
Maesano F.E.	504	Mark D.F.	231
Maestrelli D.	528, 529	Marmoni G.M.	464
Maftukhah R.	348, 353	Marotta A.M.	240, 531
Maggi V.	370	Marra F.	696
Magi F.	629, 676, 679	Marras P.A.	151
Magnani L.	108	Marroni M.	461, 462
Magro M.	354	Martarelli L.	598
Maia M.	295	Martella A.	713
Maino M.	303, 319, 320, 442, 443, 451, 470	Martelli L.	487, 563
Mair V.	238	Martin S.	235, 315, 618
Makovicky E.	61	Martinelli A.	68
Malaspina N.	49, 219, 253, 275	Martinelli F.	568
Malatesta C.	137, 432	Martinelli G.	544
Malferrari D.	350, 371	Martinello C.	611, 620, 623
Malinverno E.	366	Martini M.	326, 340
Mameli P.	187	Martinotti M.E.	556, 566, 573
Mamtani M.A.	447	Martire L.	103, 162, 600
Manca R.	173	Martorana R.	582
Mancinelli M.	105	Martorana S.	725
Mancinelli P.	503, 725	Martorelli E.	267
Mancini A.	644	Martra G.	71, 94, 117
Mancini L.	212	Martucci A.	78, 105, 107, 118, 129, 180, 364
Mancuso A.	363	Marzaioli F.	593
Mancuso R.	578	Marziali L.	678
Mandrone G.	88	Marzocchi W.	564, 567, 568
Manetti P.	245, 250	Marzoli A.	228, 278, 315
Manfriani C.	173	Marzorati S.	509, 512
Mangone A.	41	Mascandola C.	487
Mannella G.	668	Mascia M.T.	371
Mantovani L.	100, 106, 157, 396, 738	Masciale R.	540
Manzella A.	85	Masciopinto C.	543
Manzi S.	115	Mascolo G.	351
Manzi V.	474, 460	Masetti M.	588
Maraio S.	513, 521	Mason P.	665
Marani M.	120	Masotta M.	196, 417
Marasciulo T.	616	Masoudi F.	277
Marcelli I.	131	Massa A.	709, 710
Marchese F.	373	Massa M.	487
Marchesini B.	220, 433	Massaro L.	530
Marchesini I.	555, 556, 560, 565, 566, 573, 574, 605, 622	Massironi M.	381, 382, 384, 389, 397
Marchetti M.	499	Massonne H.-J.	321, 324, 411
Marchi L.	560	Mastellone D.	520
Marchina C.	661	Mastroianni F.	246
		Mata J.	278

Matarazzi D.	644	Merlini M.	43, 92, 104, 163, 203, 205
Matera P.F.	458	Merlino S.	64
Matsuoka K.	408	Mesto E.	59, 75
Matteucci F.	351	Mezouar M.	386
Mattila J.	220, 433	Michelangeli M.A.	719
Mattioli M.	120, 139, 142	Micheletti F.	338, 441
Mattone M.	484	Michetti A.M.	481, 571
Maturilli A.	379, 389	Middle School Class B	719
Maurice J.	203	Migliori M.	104
Mauro D.	62, 74	Mignardi S.	174
Mazzari C.	106	Mihailova B.	44, 70
Mazzarini F.	450	Mihailova B.D.	209
Mazzoleni P.	98, 99, 114, 186, 90	Milanese M.	187
Mazzoli C.	165, 315	Milani S.	55, 104, 203
Mazzoli S.	478, 718	Milano G.	511
Mazzucchelli M.	236, 243, 266, 272, 273, 274, 316	Milioto S.	147
Mazzucchelli M.L.	47, 221, 54	Militello G.M.	144
McCammon C.	80	Millikin L.	403
McKay R.	423	Minelli G.	725
McKay R.M.	405	Miozzi F.	386
McLagan D.S.	680	Mirabella F.	725
Meccariello M.	510	Mirri S.	681
Mecklenburgh J.	430	Misiti V.	281, 695
Meda M.	477	Mitchell C.P.J.	680
Medas D.	143, 150, 151	Mitillo N.	552
Medeghini L.	174	Mittempergher S.	223, 426, 436, 465, 477
Medici L.	371	Mizero J.	621
Meffre S.	413	Mkangala A.	642
Meisina C.	538, 608, 621	Mnzava F.	642
Melchiades F.G.	95	Modesti M.	464
Mele D.	41	Moeinzadeh H.	260, 596
Mele M.	488	Moëlo Y.	61
Melekestseva I. Yu.	124	Moggi Cecchi V.	387
Meletti C.	568	Molinari C.	96, 127
Melillo M.	560, 570	Molinari S.	354
Melluso L.	194	Möller C.	325
Meloni C.	673	Molli G.	237, 327, 713, 431
Meloni F.	645	Mollo S.	197, 200, 693
Meloni M.A.	110, 146	Monachesi G.	509, 512
Menant A.	222	Monaci F.	680
Meneghini C.	143	Monaco C.	502, 508, 510
Meneghini F.	434	Monaco L.	696
Menegon L.	218, 220, 323, 433	Mondillo N.	89, 119
Menezes D.	536	Mondini A.C.	503, 560
Menichetti M.	497, 508, 514	Mongelli G.	75, 122, 585
Menichini M.	662	Monna F.	670
Mentler A.	347, 348, 352, 353	Montalvo F.	629
Mercuri M.	464	Montanari D.	85, 489, 528, 529
Mercurio M.	155	Montanini A.	219, 297, 304, 307
Merella M.	713	Montegrossi G.	85, 136
Merico A.	435	Montemagni C.	324, 328
Merli M.	147, 263, 283, 284	Montepeloso M.	603

Monti A. L.	358	Nannucci S.M.	681
Montomoli C.	317, 324, 328, 330, 333, 334, 336, 337, 401, 411	Napolitano E.	572
Montone P.	515	Nappi R.	516, 571
Montorfano C.	235	Nardini N.	232
Montserrat L.	442	Narduzzi F.	254
Morana M.	391, 52	Natali C.	78, 180, 255, 661
Morandi S.	71	Nava J.	389, 394
Morard G.	375, 386	Nazzareni S.	77, 79, 390
Morasca P.	487	Nazzari M.	45, 200, 428, 435, 693
Moratti G.	309, 489, 528, 529	Nemati M.	387
Moreira S.	295	Németh P.	76
Morelli C.	238	Nencini R.	526
Morelli D.	400	Neri L.	357, 358
Morelli G.	329, 458	Nesci O.	376, 617
Moretti A.	238	Nestola F.41, 55, 77, 211, 391, 430, 51, 54	
Moretti R.	285, 646	Ngadisih	348, 353
Moretti S.	189	Nicodemi L.	647, 713
Morganti S.	221	Nicolini A.	93
Morgavi D.	694, 697, 698, 701, 702, 703, 707	Nielsen S.	436
Moriconi A.	725	Nigro L.	161, 174
Morishita T.	243	Nimis P.	41, 55, 124, 235, 51, 54
Morlok A.	378	Nimmo J.R.	539, 545, 546, 549
Moro D.	125, 126, 145, 158, 175	Nirta G.	473, 489
Moroni B.	721	Nisi B.	645, 665, 671, 674, 676, 679, 681, 685
Moroni M.	108, 109, 110, 235	Nobécourt J.-C.	67
Morra V.	170, 181, 194	Nobre A.	118
Morrone L.	355, 356	Nomade S.	668, 696
Mosconi A.	305	Nonni S.	191
Mosconi F.	464	Norelli F.	85
Mougel B.	295	Notaro A.	372
Moune S.	646	Notti D.	554
Mousavi Aghdam M.	146	Novembre D.	111, 112
MPS Working Group	568	Nsengiyumva F.	621
Mucci A.	350	Nsengiyumva J.B.	621
Mugnaioli E.	76, 211, 377, 388	Ntaflos T.	231, 276, 415
Muluneh A.	450	O'Brien P.	215
Münker C.	246	O'Brien P.J.	46
Muntoni I.M.	176	O'Reilly S.Y.	72
Muraro C.	598	Oberto M.	113
Murri M.	53, 209, 390, 700, 52	Occhioni M.	722
Murtiningrum	348, 353	Occhipinti R.	99, 114, 186, 90
Musiyachenko K.	53	Occhipinti S.	723, 724
Mussoni P.	463	Oggiano G.	108, 110, 443, 444, 451
Musu A.	697, 698, 725	Ogrinc N.	659
Musumeci G.	321, 401	Oguchi C.T.	171
Muto F.	594	Oh J.-R.	414
Naitza S.	108, 110, 261, 444	Ohara Y.	308
Najorka J.	119	Olesen A.	408
Naletto G.	393	Oliveira B.	55
Nalini Jr H.A.	254	Olivetta L.	616
Nania L.	330	Olivetti V.	399, 410, 412
		Olivo E.	405

Olvera Garcia E.	454	Pascucci S.	148
Omran A.	609	Pasero M.	61, 62, 64, 74
Onnis P.	133	Pasqua C.	642
Orecchio B.	506	Pasquale P.-	381
Orlando A.	85, 97, 652	Pasqualetto L.	55, 54
Orrù A.	678	Pasquetti F.	681
Ort M.	706	Passelegue F.X.	430
Ortega Feliu I.	173	Pastero L.	88, 149
Ortenzi M.A.	149	Pasti L.	105, 129
Ortolano G.	331, 332, 457, 730	Paternoster M.	193, 585, 649
Osculati A.	132	Patricelli G.	490
Ottaviani M.F.	142	Pauselli C.	390, 392, 503, 725
Ottner F.	352	Pavese A.	88, 149, 263, 283, 284
Ottolini L.	271, 409	Pavoni E.	682
Ottonello G.	286, 289	Paxman G.	408
Ottoni S.	358	Pecchioni E.	82, 169, 189
Ottria G.	481	Pecoraino G.	651
Ottria G.	663	Pecorari M.	239
Pace B.	435, 568, 719	Pedrotti J.J.	105
Pacheco J.	77	Pelfini M.	370, 711, 726
Pacini N.	657	Pellegrini L.	609
Padovan S.	172	Pellegrini M.	179
Paganin P.	150	Pellegrino L.	275
Pagano M.	457	Pelorosso B.	263, 268, 415, 727
Pagli C.	300, 438, 431	Penasa L.	384
Pagliaro F.	43, 104	Pennisi M.	661, 667
Pagnetti A.	97	Pepe A.	569
Pakhomova A.	386	Pepe F.	510
Palladino D.M.	696, 192, 199	Pereira A.	696
Pallavicin N.	669	Perez L. F.	405
Palombo A.	148	Perinelli C.	260, 267
Palumbo P.-	382	Periotto B.	54
Pampaloni M.L.	597	Perkins K.	540
Pancani D.	177	Perkins K.S.	539, 545, 546, 549
Pandeli E.	679	Peroni V.	116
Pandolfi C.	509, 512	Perotti L.	162, 600
Pandolfi L.	461, 462	Perotti M.	402, 423
Panini F.	473	Perri F.	122
Pantosti P.M.	521	Perritt S.	55
Paoletti V.	516	Perrotta V.	464
Paonita A.	428	Peruccacci S.	556, 560, 566, 570, 573
Papale P.	287	Perugini D.	392, 694, 697, 698, 700, 702, 703, 707
Papasodaro F.	598	Peruzza L.	491, 211, 343
Pappalardo L.	192, 687	Petracchini L.	295, 504
Pardo S.	464	Petranich E.	677, 682
Parello F.	628	Petrella E.	589, 591, 619
Parente M.	475	Petrelli M.	390, 479, 694, 699, 702, 703
Parenti C.	376	Petriglieri J.R.	307
Paris E.	97, 102, 115, 123, 178, 206, 217, 712, 715, 736	Petrini R.	662, 663, 664, 684
Parise M.	541, 542, 543, 605	Petroccia A.	333, 334
Parisi F.	147	Petroff M.	225
Parola C.	710		

Petrosino P.	192, 687	Poli S.	248
Pettke P.	50	Polisi M.	117
Pettke T.	252	Pollicino L.C.	588
Peyve A.	288	Polo L.	196
Pezzino A.	332, 448	Polonia A.	463
Pezzo G.	495	Pompilio A.	105
Piana F.	103, 600, 131	Pompilio L.	395
Piangiamore G.L.	728	Ponce A.D.	274
Piatteli V.	102	Porat N.	481
Piattelli V.	693	Porfido S.	571
Piazolo S.	320	Porreca M.	517, 725
Piazza M.	601	Porta L.	713
Piccardi L.	489	Portoghese I.	537, 590
Picchi G.	676, 238	Posee D.	300
Piccini L.	547	Pozzobon R.	384
Piccoli F.	224	Prando F.	220
Picotti S.	483, 485	Pratesi G.	217, 378, 387
Picotti V.	491	Pratesi P.	637
Pieraccioni F.	714, 716	Precisvalle N.	78, 118, 180
Pierantoni P.P.	496, 517	Prencipe M.	209, 53
Pieroni A.	431	Presti D.	506
Pietrosante A.	563	Previde Massara E.	365
Pigazzi E.	214	Primerano P.	701
Pignalberi F.	464	Principe C.	642
Pignatelli I.	388	Principalle F.	147, 278, 479, 54
Pignatti S.	148	Priolo E.	491
Piluso E.	395	Prisa D.	359, 360
Pinardi M.	592	Procesi M.	648, 651
Pintori F.	495, 548	Prosperi L.	51
Pirrone N.	683	Prosser G.	335, 607
Pisani P.	642	Provenzale A.	661, 667
Pisello A.	392, 700	Pucci S.	517
Pistis M.	146	Pucci S.	521
Pistocchi L.	616	Puccini A.	444
Pistone M.	690	Pulcini G.	449
Pitts A.	522	Puliti I.	518
Piva A.	365	Punturo P.	332, 730
Pizzati M.	437	Pusceddu C.	143
Pizzi A.	518	Putzolu F.	119, 121
Pizzino L.	648	Puzenat V.	295
Placitu S.	150	Quartieri S.	71, 94, 117, 383
Placuzzi E.	729	Racchetti E.	592
Pochini E.	405	Raco B.	85
Podda F.	151	Radica F.	217
Poe B.T.	281	Raffi I.	372
Poggetti E.	547	Raggiunti M.	438
Poggi F.	554	Ragone P.	130
Poggi V.	487	Rahimzadeh B.	277
Polacci M.	191, 196	Raimondo M.	591
Polastri L.	727	Rampone E.	264, 270, 292
Poli L.	673	Randaccio P.	146
Poli M.E.	490	Randazzo P.	649
Poli S.	205	Raneri S.	177, 201

Rappuoli D.	645, 674, 679, 680, 685	Roman Martinez R.	364
Rasul N.	296	Romanelli M.	136
Ravazzi C.	499	Romani M.	563
Re C.	393	Romano C.	197, 428, 690, 691, 695, 705, 706
Realdon G.	731	Romano M.A.	491
Reale D.	484	Romano P.	204
Rebay G.	56, 291, 302, 325, 449	Romeo T.	383
Rebesco M.	400	Rooyackers S.	702
Regattieri E.	668	Rosatelli G.	105
Regazzola V.	717	Rosiello A.	631, 633, 649, 650
Reghizzi M.	474	Rossato S.	618
Regorda A.	240	Rosset G.	520
Regorda A.	531	Rossetti F.	399, 410, 420
Reichenbach P.	560	Rossetti P.	103, 108, 113
Remitti F.	426, 473	Rossetti S.	637, 657
Renggli C.	378	Rossi C.	406
Renna M.	107	Rossi D.	439
Renna M.R.	306, 335	Rossi F.P.	474
Renzulli A.	97, 120, 182, 188, 604	Rossi G.	120
Rescic S.	169	Rossi M.	102, 379, 556, 560, 565, 566, 570, 572, 573, 574, 597, 622
Respaldiza M.A.	173	Rossi S.	700, 703
RETRACED working group	504	Rossi V.	615, 729
Revillon S.	295	Rossignol S.	98
Riberti R.	349	Rotigliano E.	610, 611, 620, 623
Ricci A.	656, 676	Rotolo S.G.	204
Ricci F.	557	Rotondi A.	355, 356
Ricci T.	651	Rouwet D.	641, 651
Ricci V.	597, 598	Roveri M.	474, 460
Rielli A.	85, 661, 667	Rovida A.	568
Rigo M.	618	Rozel A.	386
Rigonat N.	151	Rubatto D.	44
Rimondi V.	133, 458, 675	Ruch J.	532
Rinaldi F.	464	Ruggieri G.	85, 108, 329, 458, 652
Rinaudo C.	134, 214	Ruggiero G.	464
Rispoli C.	170, 181	Rui L.	405
Risso L.	116	Rull F.	67
Rivoldini A.	375	Ruppel A.	407
Rizzello D.	642	Rusi S.	583, 586
Rizzieri A.	602	Russell J.K.	201, 706
Rizzo A.L.	193, 268, 276	Russo D.	448
Rizzo G.	75, 152, 193, 607	Ryan A.G.	706
Rizzo P.	361	Sabatino G.	383
Robert V.	646	Sabatino S.	106
Roberts G.	517	Sabbatino M.	475, 478
Roccheggiani M.	497, 508, 514	Saccani E.	461, 462
Rocchi S.	416, 417	Sacchi E.	153, 154
Roda M.	240, 302, 455, 531	Sacco G.	704
Rodeghero E.	107, 364	Sacco V.	332
Rodriguez Navarro A.	364	Sadock J.	642
Rodushkin I.	667, 669	Saiano F.	636
Roghi G.	228	Salari G.	277
Rolando V.	727		
Roma M.	616		

Salerno G.	704	Scarponi D.	363
Salters V.	305	Scarsi M.	432, 601
Salters V.J.M.	288	Schannor M.	254
Salvadego F.	51	Schembri M.	579
Salvati P.	560	Schenker F.	319, 320
Salvati P.	565, 572, 574, 605	Schettino D.	102
Salvatore M.C.	401	Scheu B.	695
Salviati G.	396	Schiavi F.	195
Salvini F.	406	Schiavon A.	678
Salvioli-Mariani E.	60, 307, 429	Schiavoni M.	149
Salviulo G.	354	Schingaro E.	59, 75
Samperi L.	725	Schito A.	474
Sanangelantoni A.	361	Schmidt B.C	199, 192
Sanfilippo A.	288, 296, 303, 305, 306, 308, 365	Schmidt P.K.	220
Sanguineti E.	144	Schwarz G.	220
Sani C.	308	Schwarzenbach E.M.	225
Sani F.	300, 309, 450, 489, 534	Sciarroni G.	178
Santangelo M.	560, 622	Sciascia L.	147
Santi A.	651	Scisciani V.	469
Santi P.	182, 188	Scoccimarro E.	548
Santilano A.	85	Scopelliti G.	67
Santini F.	148	Scopesi C.	734
Santone S.	102	Scotti A.	439
Santoro L.	119, 121	Scotti C.	663
Santoro M.	94	Scotti G.	383
Sanz-Arranz A.	67	Scotti P.	365
Sapia V.	513, 521	Scricciolo E.	77, 79
Sapiano M.	579	Scrivano S.	164, 184, 185, 173
Sarti G.	713	Scrocca D.	504
Sassi R.	315	Scuderi M.	464
Sauli C.	400, 405, 418	Scuderi M.M.	427
Savascin M.Y.	245, 250	Sebastianelli L.	350
Savelli C.	183, 310	Secchi F.	108, 110, 444
Savi R.	624	Secchiari A.	297, 304
Savini A.	373	Secco L.	235, 54
Savioli M.	371	Sedea R.	228
Sayab M.	212	Seers T.D.	522
Sbarra P.	492	Segadelli S.	589
Scacchetti M.	732	Segalini A.	624
Scafa M.	435	Sejkora J.	61
Scaillet B.	204	Sellerino M.	587
Scaillet S.	450	Selmo E.	656
Scambelluri M.	44, 49, 216, 247, 252, 339	Seno S.	319, 320, 443, 735
Scapellato B.	733	Sepúlveda J.	655
Scaramuzza E.	466, 481, 493	Serafini R.	616
Scarani A.	705	Serpelloni E.	495, 548
Scarciglia F.	395	Serra R.	387
Scarfi L.	502	Serri L.	513
Scarlato P.	45, 200, 435, 688, 693	Sessa G.	109, 248
Scarpa R.	519	Severini E.	592
Scarpelli R.	166	Sevil J.	376
		Seyler M.	295
		Sgavetti M.	613, 615

Shaddad M.H.	391	Sternai P.	222, 311, 476, 533
Sharp Z.D.	405	Stevenazzi S.	588
Siebert J.	375	Stevens G.	254
Signore S.	682	Stix J.	702
Silleni A.	705, 706	Stojic A.	378
Silva C.	656	Storti F.	437, 465, 472, 477
Silvestri S.	597	Stracke A.	288, 99, 114, 186, 90
Simonetti M.	333, 334, 336, 337, 401	Stuart F.	456
Sinisi R.	75, 122, 152, 585	Succo A.	241, 477
Sinojmeri A.	140	Sulli A.	610
Sitzia F.	91	Sulpizio R.	197
Skert N.	673	Susta U.	93
Skogby H.	390	Suttle M.D.	388, 394
Skyttä P.	526	Swennen R.	644
Smellie J.L.	416	Tabacchi G.	94
Smiljanić D.	155	Tacchetto T.	210
Smith Lyttle B.	403	Taddeucci J.	688
Snow J.	308	Talamo P.	170
Sobio Y.	621	Talarico F.M.	402, 413, 414, 421, 422, 423
Sobolev N.V.	54	Talavera C.	69
Sokolov S.	288	Tallone S.	131
Soldati R.	96, 127	Talozzi D.	188
Solfanelli M.	464	Tamburello G.	256, 544, 651, 653
Solimano M.	556	Tamburo E.	670
Soltanmohammadi A.	295	Tangari A.C.	395
Solzi M.	157, 738	Taramaeli M.	642
Somma R.	156	Tarantino S.C.	97
Sorlien C.	405	Tarchiani U.	671
Sottili G.	192, 199, 696	Tarella G.	710
Spagnuolo E.	430, 434	Taroni M.	567
Spalla M.I.	213, 240, 291, 302, 449, 531	Tartarotti P.	108, 299
Spartà D.	205	Tassi F.	97, 629, 637, 651, 654, 655, 656, 657, 676, 679, 685
Spasojević M.	155	Tasso F.	150
Spatafora F.	182	Tateo F.	343
Speziale S.	135	Taussi M.	604
Spiess R.	338, 394, 456	Tavani S.	478, 522
Spina A.	237	Tedesco C.	464
Spina L.	697, 698, 707	Teixeira W.	272
Spolverino G.	575	Teixera L.	254
Spratt J.	394	Teloni S.	496
Spreafico M.C.	533	Temovski M.	67
Sprocati A.R.	150	Tempesta G.	41, 59
Squarzoni G.	729	Tesei T.	427
Stabile P.	115, 123, 206, 207, 217	Testone V.	187
Stacchiotti L.	712, 736	Tharowi A.	296
Stagioni M.	363	the InSight Science Team	375
Stagno V.	45, 428	the IODP Expedition Scientists	423
Stalder R.	390	Theye T.	420
Stangarone C.	209	Thomas J.	42
Stanley C.J.	61	Thomassot E.	51
Stellato L.	584, 593	Tiepolo M.	195, 247, 248
Stenni B.	662		
Sterlacchini S.	565, 574		

Timpano A.	639	Vadacca L.	439
Tirincanti E.	497, 514	Vaggelli G.	162
Toffolo L.	124, 235	Vaiani S.C.	729
Toledo V.	72	Valdrè G.	125, 126, 145, 158, 175
Toller S.	138	Valensise G.	492
Tolomei C.	495	Valente M.	464
Tolotti R.	418	Valentini A.	719
Tomaselli L.	445	Valentini L.	142
Tommasini S.	249	Valentino D.	162
Tondi E.	522	Valentino R.	538, 621
Tonelli G.	188	Valerio M.	684
Tonon M.D.	720, 737	Valletta A.	624
Torabi A.	454	Valsecchi L.	678
Tordi M.	393	van der Bogert C.H.	397
Torelli L.	463	Van der Lelij R.	468
Torre M.	176	Van Schrojenstein Lantman H.W.	339
Toscani L.	307	Vanara N.	67
Tosi P.	492	Vannoli P.	492, 498
Totaro C.	506	Vannucci G.	495
Trabucco F.	693	Varrica D.	670
Tramontana M.	188	Vaselli O.	97, 629, 637, 645, 656, 657, 665, 671, 674, 675, 676, 679, 681, 685
Trapananti A.	68	Vattano M.	67
Trasatti E.	527	Vazquez E.	657
Trentini T.	238	Velicogna M.	242, 479
Tret'yakov G.A.	124	Veneri F.	188
Tribaudino M.	100, 106, 157, 396, 738	Venier M.	242, 278, 479
Tribuzio R.	38, 234, 262, 304, 305, 306, 419	Vennari C.	605
Trifuoggi M.	593	Ventruiti G.	329, 458
Tripodi V.	594	Venturi S.	637, 651, 657, 676, 679
Tripodo A.	383	Vergani D.	449
Trippetta F.	520	Verhoest L.	295, 312
Trivellato T.	295	Verlaguet A.	50
Trolese P.	728	Verrucchi M.	189
Trombino L.	163	Versace P.	575, 576
Tropper P.	266	Vertino A.	373
Trotta O.	486	Vespasiano G.	578, 594, 639
Trumpy E.	85	Vetere F.	200, 694, 702
Tsakarisianos M.D.	710	Vetere F.P.	392
Tucci A.	166	Vetere F.P.	700
Tumiati S.	42, 109, 235, 253, 257, 258, 275	Vetere F.P.	703
Turci F.	131	Vettori S.	189
Turnau K.	150	Vetuschi Zuccolini M.	286, 289
Tursi F.	338, 441	Vezzalini G.	71, 94, 117
Turturro A.C.	540, 549	Vezzoli G.	499
Twegar K.	394	Vezzulli L.	369
Tzamos E.	66	Viaggi P.	365
Ulian G.	125, 126, 145, 158, 175	Vianello F.	354
Unterfrauner H.	344	Viccaro M.	704, 691
Urbani A.	597	Viganò A.	618
Vacca A.	675	Vigliotti L.	100, 296
Vacha D.	576	Vigna B.	550

Vignaroli G.	420	Xu F.	375
Vilardo F.	445	Yamahshita H.	308
Villa I.M.	328	Yeqing Z.	675
Villani F.	513, 521	Yin J.	569
Vinciguerra E.	727	Youbi N.	278
Viola G.	220, 433	Yu D.	569
Viola G.	468	Yus González A.	144
Virgili S.	178	Zaccara Bertolini P.	738
Visalli R.	212, 331, 332, 457	Zaccara P.	157
Visini F.	568	Zaccarini F.	66, 74
Visonà D.	324, 328, 317	Zaffiro G.	54
Visonà S.	132	Zambon F.	382, 389, 397
Vita L.	598	Zambrano M.	522
Vitale Brovarone A.	218, 327, 224	Zampa L.S.	483
Vitale S.	475	Zampieri D.	498
Vitale V.	616	Zanatta M.	77
Viti C.	211, 427, 428	Zanchetta G.	647, 668, 681
Vivani R.	93	Zanchetta S.	275, 328, 603
Viveiros F.	656	Zanchi A.	499, 603
Vo N.	191	Zanelli C.	95, 96, 127
Vockenhuber C.	618	Zanello A.	673
Voltolina D.	565, 574	Zanetti A.	243, 271, 273, 274, 292, 296, 305, 316, 409, 415
Vona A.	197, 428, 690, 691, 695, 701, 705, 706	Zanon V.	77
Vougioukalakis G.E.	627	Zanoni A.	60
Vrabec M.	483	Zanoni D.	213, 302, 449, 455
Vurro M.	537, 590	Zappaterra O.	107
Waesermann N.	70	Zattin M.	315, 399, 410, 412
Wang H.	300	Zazzeri M.	565, 574
Wang X.	551	Zechmeister-Boltenstern S.	346, 347
Wang Z.	295, 306	Zehetner F.	344
Wania F.	680	Zellmer G.	699
Wannhoff I.	215	Zepeda-Martínez M.	326, 340
Wardell N.	405	Zerboni A.	481
Warren C.	323	Zgur F.	483, 485
Webb L.W.	228	Zhao Q.	569
Weber I.	378	Zhong X.	57
Welch M.D.	61	Zhu Y.	585
Wheeler W.H.	454	Zibra I.	237
White J.C.	204	Ziemann M.A.	215
Wilson D.	405	Zoleo A.	136
Woo J.	414, 421, 422	Zucali M.	212, 213, 214
Wood K.	521	Zucchi M.	329, 341, 454, 456, 458
Wriessnig K.	352	Zucchini A.	80, 93, 137, 379, 552
Wrzesniak A.	554	Zuffetti C.	488, 500
Wu F.Y.	262	Zurli L.	402, 413, 414, 421, 422, 423
Wunder B.	46, 215	Zurutuza J.	505
Xia Q.-K.	282	Zwaan F.	534

SPONSOR

PLATINUM



GOLD



SILVER



BRONZE



PATROCINI



9 788894 022797